Spring 2014

Rhodium-catalyzed asymmetric amination of trichloroacetimidates with application to nitrogen heterocycle synthesis

Jeffrey Scott Arnold
University of Iowa

RHODIUM-CATALYZED ASYMMETRIC AMINATION OF TRICHLOROACETIMIDATES WITH APPLICATION TO NITROGEN HETEROCYCLE SYNTHESIS

by

Jeffrey Scott Arnold

A thesis submitted in partial fulfillment
of the requirements for the Doctor of
Philosophy degree in Chemistry
in the Graduate College of
The University of Iowa

May 2014

Thesis Supervisor: Associate Professor Hien M. Nguyen

Graduate College
The University of Iowa
Iowa City, Iowa

CERTIFICATE OF APPROVAL

PH.D. THESIS

This is to certify that the Ph.D. thesis of

Jeffrey Scott Arnold

has been approved by the Examining Committee
for the thesis requirement for the Doctor of Philosophy
degree in Chemistry at the May 2014 graduation.

Thesis Committee:

Hien M. Nguyen, Thesis Supervisor

Mark A. Arnold

Gregory K. Friestad

F. Christopher Pigge

Horacio F. Olivo

To my wife Barbara, and my children Maggie and Cal

ACKNOWLEDGEMENTS

This work would not have been possible without the numerous contributions from others. First, I would like to thank my research advisor, Professor Hien Nguyen for his guidance, helpful discussions and support throughout the last six years. In addition, the success of this project was very dependent on the exchange of ideas and support of many, including group members, graduate students and faculty at Montana State University and the University of Iowa. I would especially like to thank Dr. Joe Topczewski and Professor Tom Livinghouse in this regard. I need to recognize Dr. Dale Swenson for X-ray crystallographic analysis and Dr. Lynn Teesch and Vic Parcell for mass spectrometry results. Their friendly demeanor, helpful suggestions and prompt response were invaluable to moving this project forward.

This work was not possible without financial support. The move to the University of Iowa and startup funding was critical to accelerated screening and development of this work. Continued assistance was acquired through National Science Foundation (NSF) and National Institutes of Health (NIH) grant funding. Thank you to the University of Iowa for a summer graduate research fellowship.

Lastly and most importantly, I thank my loving wife Barb and my two wonderful children who have supported my dream to earn my doctorate. Barb selflessly put her career as a school administrator on hold and works very hard to support the family financially and in day-to-day activities. Maggie and Cal have had to endure the stress of leaving friends and family during two moves and have not had the time with their father that they deserve. I thank them for their sacrifices and look forward to spending more time with them.

ABSTRACT

Chiral quaternary centers possessing a bond to nitrogen are an important class of amine compounds, however, methods for their enantioselective preparation remain sparse. The focus of my graduate research described herein has been the development of a novel rhodium-catalyzed regio- and enantioselective allylic aryl amination of tertiary trichloroacetimidates for the synthesis of amine-bearing quaternary centers (also termed α,α-disubstituted amines). Prior to our work, allylic carbonates and acetates had been successfully utilized in transition-metal catalyzed substitution reactions with anilines for the asymmetric synthesis of tertiary centers. In contrast, these electrophiles have not proven useful in dynamic kinetic asymmetric transformations (DYKAT) that yield enantioenriched amine products, and no reports describing the asymmetric preparation of α,α-disubstituted allylic aryl amines via allylic substitution are noted.

Many of the ideas for development of our rhodium-catalyzed amination method were based upon the findings of Overman where linear allylic trichloroacetimidates are utilized in [3,3]-sigmatropic rearrangements and substitution reactions by oxygen nucleophiles under palladium (II) catalysis. Our method diverges from this previous work by application of branched allylic trichloroacetimidates where the olefin component is mono-substituted, and the use of a transition-metal complex capable of facile oxidative addition to an intermediate organometallic complex. We hypothesized that bidentate chelation of these substrates at the imidate nitrogen and the relatively unimpeded olefin by a rhodium (I) complex would lead to rapid ionization to an activated complex and competent electrophile for substitution by neutral aniline nucleophiles. This premise was supported by many control studies and resulted in the development of a highly regioselective amination of branched allylic trichloroacetimidates for the operationally simple synthesis of α-substituted and α,α-disubstituted allylic aryl amines. Work followed utilizing chiral diene ligands that rendered the reaction enantioselective for

preparation of enantioenriched tertiary and quaternary amine-containing centers. A highlight of these studies is the first example of DYKAT using a tertiary electrophile and an aryl amine nucleophile. The reaction is of broad substrate scope, is tolerant of varied functionality and substitution patterns on the nucleophilic partner, and solves regioselectivity issues often encountered with some substrate and aniline classes. I end by showing the synthetic utility of our rhodium-catalyzed reaction by applying this method to the synthesis of enantioenriched amino acids and construction of 7-membered nitrogen-containing heterocycles by a 2-step DYKAT amination and olefin hydroacylation sequence.

TABLE OF CONTENTS

LIST OF TABLES viii

LIST OF FIGURES x

LIST OF SCHEMES xxvi

LIST OF ABBREVIATIONS xxix

CHAPTER

I. THE SYNTHETIC UTILITY OF ALLYLIC TRICHLOROACETIMIDATES 1

1.1. Introduction 1
1.2 Synthesis and Properties of Trichloroacetimidates 2
1.3 Allylic Trichloroacetimidate Applications in Synthesis 8
1.3.1 The Overman Rearrangement 8
1.3.2 [3,3]-Rearrangements of Propargyl Trichloroacetimidates 18
1.3.3 [1,3]-Rearrangement of Allylic Trichloroacetimidates 19
1.3.4 Oxazolines Via Intramolecular Addition 20
1.3.5 Allylic Substitution Reactions with Oxygen Nucleophiles 21
1.4 Conclusion 36

II. RHODIUM (I)-CATALYZED REGIOSELECTIVE AMINATION OF TRICHLOROACETIMIDATES 37

2.1 Secondary Allylic Trichloroacetimidates: Rhodium-Catalyzed Preparation of α-substituted Amines 37
2.1.1 Background 37
2.1.2 Results and Discussion 46
2.1.3 Conclusion 56
2.2 Tertiary Allylic Trichloroacetimidates: Rhodium-Catalyzed Preparation of α,α-disubstituted Amines 57
2.2.1 Background 57
2.2.2 Results and Discussion 59
2.2.3 Conclusion 67

III. DYNAMIC KINETIC ASYMMETRIC TRANSFORMATIONS OF RACEMIC TRICHLOROACETIMIDATES 69

3.1 The Regio- and Enantioselective Preparation of α,α-disubstituted Allylic Aryl Amines 69
3.1.1 Background 69
3.1.2 Results and Discussion 76
3.1.3 Conclusion 85
3.2 The Regio- and Enantioselective Preparation of α-substituted Allylic Aryl Amines
3.2.1 Background 86
3.2.2 Results and Discussion 87
3.2.3 Conclusion 97

IV. SEQUENTIAL ASYMMETRIC AMINATION AND OLEFIN HYDROACYLATION 100
4.1 Background…… 100
4.2 Results and Discussion 108
4.3 Conclusion 116

V. CONCLUSIONS AND FUTURE DIRECTIONS.....118

VI. EXPERIMENTAL SECTION.....124
5.1 Methods, Reagents and Instrumentation.....124
5.2 General Procedure for Preparation of Secondary Trichloroacetimidates 125
5.3 General Procedure for Amination of Secondary Trichloroacetimidates with 1 mol% $[RhCl(ethylene)_2]_2$/ $P(OPh)_3$ 130
5.4 General Procedure for Amination of Secondary Trichloroacetimidates with 5 mol% $[RhCl(ethylene)_2]_2$/ $P(OPh)_3$ 148
5.5 General Procedure for Preparation of Tertiary Allylic Trichloroacetimidates .....159 and 195
5.6 General Procedure for the Regioselective Amination of Tertiary Allylic Trichloroacetimidates with $[RhCl(norboradiene)]_2$ 162
5.7 General Procedure for Preparation of Reverse Prenylated Indoles ...187
5.8 Procedure for the Preparation of (1*S*,4*S*)-2,5-Diarylbicyclo[2.2.2]octa-2,5-dienes 189
5.9 General Procedure for the Preparation of Mono-protected Allylic Diols 193
5.10 General Procedure for Regio- and Enantioselective Amination of Racemic Tertiary Allylic Trichloroacetimidates with $[RhCl(ethylene)]_2$/ **L7** 199
5.11 General Procedure for Regio- and Enantioselective Amination of Racemic Secondary Allylic Trichloroacetimidates with $[RhCl(ethylene)]_2$/ **L1** 216
5.12 General Procedure for Preparation of *N*-methyl Homophenylalanine Derivatives 230
5.13 Additional DYKAT Amination Products of Secondary Racemic Trichloroacetimidates 236
5.14 Preparation of Allylic Trichloroacetimidate **377** 245
5.15 General Procedure for Asymmetric Amination of Branched Allylic Trichloroacetimidates with 2-Aminobenzaldehyde **183z** 246
5.16 General Procedure for Intramolecular Hydroacylation of Allylic Aryamines Containing *ortho*-Aldehyde Functionality ...258
5.17 Hydroacylations for 6-membered rings performed with 5 mol% $[Rh(COD)_2]OTf$ 269

APPENDIX A: NMR SPECTRAL DATA 271

APPENDIX B: X-RAY CRYSTALLOGRAPHIC DATA FOR TFA-SALT **152** 673

BIBLIOGRAPHY.....789

LIST OF TABLES

Table 1.1 Imidate Resonance Forms, Bond Orders and Lengths 4

Table 1.2 Asymmetric Esterification of (*Z*)-Acetimidates 24

Table 1.3 Enantioselective Aryl Etherification of (*Z*)-Allylic Trichloroacetimidates.....31

Table 1.4 Enantioselective Aryl Etherification of (*E*)-Allylic Trichloroacetimidates.....33

Table 1.5 Intramolecular Enantioselective Etherification of (*E*)-Allylic Imidates.....34

Table 2.1 Hartwig's Regio- and Enantioselective Amination of Allylic Carbonates.....43

Table 2.2 Evan's Regio- and Stereospecific Amination of Branched Carbonates 44

Table 2.3 Optimization for Regioselective Amination 47

Table 2.4 Rhodium-catalyzed Amination of Trichloroacetimidates with **183a** – **f** 49

Table 2.5 Rhodium-catalyzed Amination of β-substituted Imidates **228** – **230** 50

Table 2.6 Amination Reaction Optimization of α-Branching Imidate **231** 51

Table 2.7 Rhodium-catalyzed Amination of α-substituted Imidates **231** – **233** 52

Table 2.8 Lewis Acid and Rhodium-catalyzed Amination of Imidates.....54

Table 2.9 Optimization Studies of Tertiary Trichloroacetimidate **253**.....60

Table 2.10 Survey of Various Anilines with Tertiary Trichloroacetimidate **253** 61

Table 2.11 Survey of Tertiary Allylic Trichloroacetimidates.....63

Table 3.1 DYKAT Optimization of Tertiary Trichloroacetimidate **255**.....77

Table 3.2 ^{13}C Data of Rhodium-Ligated Diene **L4**, **L5** and **L7** 80

Table 3.3 Survey of Aniline Nucleophiles in DYKAT.....81

Table 3.4 Substrate Scope of DYKAT Amination 83

Table 3.5 Optimization of DYKAT of **229** with *N*-methylamine **183f** 89

Table 3.6 Survey of *N*-methylamine Nucleophiles in DYKAT Amination.....90

Table 3.7 Survey of Allylic Trichloroacetimidates with *N*-methylamines…...……92

Table 3.8 Survey of Anilines and Secondary Trichloroacetimidates in DYKAT 95

Table 4.1 Optimization of DYKATwith Aniline **183y**.....109

Table 4.2 Hydroacylation Optimization of Amine **227y** 111

Table 4.3 Scope of sequential DYKAT Amination and Hydroacylation 113

Table B1 Crystal Data and Structure Refinement for **152** 674

Table B2 Atomic coordinates (x 10^4) and equivalent isotropic displacement 675
parameters (A^2 x 10^3) for **152**

Table B3 Selected bond lengths [A] and angles [deg] for **152** 678

Table B4 Bond lengths [A] and angles [deg] for **152** 683

Table B5 Anisotropic displacement parameters (A^2 x 10^3) for **152** 694

Table B6 Hydrogen coordinates (x 10^4) and isotropic.....697
displacement parameters (A^2 x 10^3) for **152**

Table B7 Torsion angles [deg] for **152** 698

Table B8 Hydrogen bonds for **152** [A and deg.] 701

Table B9 Observed and calculated structure factors for **152** 706

LIST OF FIGURES

Figure 1.1 pKa of Common Leaving Groups in Allylic Substitution Reactions 5

Figure 1.2 pKas of Protonated Carbonyls, Trichloroacetamides and Imidates 7

Figure 1.3 Palladium (II) Complexes for Asymmetric Overman Rearrangement.....11

Figure 1.4 Cyclic Intermediates in COP-catalyzed Rearrangement 14

Figure 2.1 Potential Use of Branched Imidates in TM-catalyzed Substitution 40

Figure 3.1 Natural and Synthetic Compounds Containing α,α-disubstituted Amines.....69

Figure 3.2 Modification of Ligand Substituents 78

Figure 3.3 ORTEP Diagram of TFA salt **152** Dimer.....85

Figure 4.1 Minimizing Decarbonylation in Hydroacylation Reactions.....103

Figure A1 400 MHz 1H NMR ($CDCl_3$) Spectra of Compound **223**.....272

Figure A2 100 MHz 13C NMR ($CDCl_3$) Spectra of Compound **223**.....273

Figure A3 400 MHz 1H NMR ($CDCl_3$) Spectra of Compound **226**.....274

Figure A4 100 MHz 13C NMR ($CDCl_3$) Spectra of Compound **226**.....275

Figure A5 400 MHz 1H NMR ($CDCl_3$) Spectra of Compound **227**.....276

Figure A6 100 MHz 13C NMR ($CDCl_3$) Spectra of Compound **227**.....277

Figure A7 400 MHz 1H NMR ($CDCl_3$) Spectra of Compound **228**.....278

Figure A8 100 MHz 13C NMR ($CDCl_3$) Spectra of Compound **228**.....279

Figure A9 400 MHz 1H NMR ($CDCl_3$) Spectra of Compound **229**.....280

Figure A10 100 MHz 13C NMR ($CDCl_3$) Spectra of Compound **229**.....281

Figure A11 400 MHz 1H NMR ($CDCl_3$) Spectra of Compound **230**.....282

Figure A12 100 MHz 13C NMR ($CDCl_3$) Spectra of Compound **230**.....283

Figure A13 400 MHz 1H NMR ($CDCl_3$) Spectra of Compound **231**.....284

Figure A14 100 MHz 13C NMR ($CDCl_3$) Spectra of Compound **231**.....285

Figure A15 400 MHz 1H NMR ($CDCl_3$) Spectra of Compound **232**.....286

Figure A16 100 MHz 13C NMR ($CDCl_3$) Spectra of Compound **232**.....287

Figure A17 400 MHz 1H NMR ($CDCl_3$) Spectra of Compound **233**.....288
Figure A18 100 MHz 13C NMR ($CDCl_3$) Spectra of Compound **233**.....289
Figure A19 400 MHz 1H NMR ($CDCl_3$) Spectra of Compound **224**.....290
Figure A20 100 MHz 13C NMR ($CDCl_3$) Spectra of Compound **224**.....291
Figure A21 400 MHz 1H NMR ($CDCl_3$) Spectra of Compound **225**.....292
Figure A22 100 MHz 13C NMR ($CDCl_3$) Spectra of Compound **225**.....293
Figure A23 400 MHz 1H NMR ($CDCl_3$) Spectra of Compound **223b** 294
Figure A24 100 MHz 13C NMR ($CDCl_3$) Spectra of Compound **223b**.....295
Figure A25 400 MHz 1H NMR ($CDCl_3$) Spectra of Compound **223c**.....296
Figure A26 100 MHz 13C NMR ($CDCl_3$) Spectra of Compound **223c** 297
Figure A27 400 MHz 1H NMR ($CDCl_3$) Spectra of Compound **223d** 298
Figure A28 100 MHz 13C NMR ($CDCl_3$) Spectra of Compound **223d**.....299
Figure A29 400 MHz 1H NMR ($CDCl_3$) Spectra of Compound **223e**.....300
Figure A30 100 MHz 13C NMR ($CDCl_3$) Spectra of Compound **223e** 301
Figure A31 400 MHz 1H NMR ($CDCl_3$) Spectra of Compound **223f** 302
Figure A32 100 MHz 13C NMR ($CDCl_3$) Spectra of Compound **223f** 303
Figure A33 400 MHz 1H NMR ($CDCl_3$) Spectra of Compound **226a**.....304
Figure A34 100 MHz 13C NMR ($CDCl_3$) Spectra of Compound **226a**.....305
Figure A35 400 MHz 1H NMR ($CDCl_3$) Spectra of Compound **226b** 306
Figure A36 100 MHz 13C NMR ($CDCl_3$) Spectra of Compound **226b**.....307
Figure A37 400 MHz 1H NMR ($CDCl_3$) Spectra of Compound **226c**.....308
Figure A38 100 MHz 13C NMR ($CDCl_3$) Spectra of Compound **226c** 309
Figure A39 400 MHz 1H NMR ($CDCl_3$) Spectra of Compound **226d** 310
Figure A40 100 MHz 13C NMR ($CDCl_3$) Spectra of Compound **226d**.....311
Figure A41 400 MHz 1H NMR ($CDCl_3$) Spectra of Compound **226e**.....312
Figure A42 100 MHz 13C NMR ($CDCl_3$) Spectra of Compound **226e** 313
Figure A43 400 MHz 1H NMR ($CDCl_3$) Spectra of Compound **226f** 314

Figure A44 100 MHz 13C NMR ($CDCl_3$) Spectra of Compound **226f** 315
Figure A45 400 MHz 1H NMR ($CDCl_3$) Spectra of Compound **227a**.....316
Figure A46 100 MHz 13C NMR ($CDCl_3$) Spectra of Compound **227a**.....317
Figure A47 400 MHz 1H NMR ($CDCl_3$) Spectra of Compound **227b** 318
Figure A48 100 MHz 13C NMR ($CDCl_3$) Spectra of Compound **227b**.....319
Figure A49 400 MHz 1H NMR ($CDCl_3$) Spectra of Compound **227c**.....320
Figure A50 100 MHz 13C NMR ($CDCl_3$) Spectra of Compound **227c** 321
Figure A51 400 MHz 1H NMR ($CDCl_3$) Spectra of Compound **227d** 322
Figure A52 100 MHz 13C NMR ($CDCl_3$) Spectra of Compound **227d**.....323
Figure A53 400 MHz 1H NMR ($CDCl_3$) Spectra of Compound **227e**.....324
Figure A54 100 MHz 13C NMR ($CDCl_3$) Spectra of Compound **227e** 325
Figure A55 400 MHz 1H NMR ($CDCl_3$) Spectra of Compound **227f** 326
Figure A56 100 MHz 13C NMR ($CDCl_3$) Spectra of Compound **227f** 327
Figure A57 400 MHz 1H NMR ($CDCl_3$) Spectra of Compound **228a**.....328
Figure A58 100 MHz 13C NMR ($CDCl_3$) Spectra of Compound **228a**.....329
Figure A59 400 MHz 1H NMR ($CDCl_3$) Spectra of Compound **228b** 330
Figure A60 100 MHz 13C NMR ($CDCl_3$) Spectra of Compound **228b**.....331
Figure A61 400 MHz 1H NMR ($CDCl_3$) Spectra of Compound **228c**.....332
Figure A62 100 MHz 13C NMR ($CDCl_3$) Spectra of Compound **228c** 333
Figure A63 400 MHz 1H NMR ($CDCl_3$) Spectra of Compound **228d** 334
Figure A64 100 MHz 13C NMR ($CDCl_3$) Spectra of Compound **228d**.....335
Figure A65 400 MHz 1H NMR ($CDCl_3$) Spectra of Compound **228e**.....336
Figure A66 100 MHz 13C NMR ($CDCl_3$) Spectra of Compound **228e** 337
Figure A67 400 MHz 1H NMR ($CDCl_3$) Spectra of Compound **228f** 338
Figure A68 100 MHz 13C NMR ($CDCl_3$) Spectra of Compound **228f** 339
Figure A69 400 MHz 1H NMR ($CDCl_3$) Spectra of Compound **229a**.....340
Figure A70 100 MHz 13C NMR ($CDCl_3$) Spectra of Compound **229a**.....341

Figure A71 400 MHz 1H NMR ($CDCl_3$) Spectra of Compound **229b** 342
Figure A72 100 MHz 13C NMR ($CDCl_3$) Spectra of Compound **229b**.....343
Figure A73 400 MHz 1H NMR ($CDCl_3$) Spectra of Compound **229c**.....344
Figure A74 100 MHz 13C NMR ($CDCl_3$) Spectra of Compound **229c**.....345
Figure A75 400 MHz 1H NMR ($CDCl_3$) Spectra of Compound **229d** 346
Figure A76 100 MHz 13C NMR ($CDCl_3$) Spectra of Compound **229d**.....347
Figure A77 400 MHz 1H NMR ($CDCl_3$) Spectra of Compound **229e**.....348
Figure A78 100 MHz 13C NMR ($CDCl_3$) Spectra of Compound **229e**.....349
Figure A79 400 MHz 1H NMR ($CDCl_3$) Spectra of Compound **229f**.....350
Figure A80 100 MHz 13C NMR ($CDCl_3$) Spectra of Compound **229f** 351
Figure A81 400 MHz 1H NMR ($CDCl_3$) Spectra of Compound **230a**.....352
Figure A82 100 MHz 13C NMR ($CDCl_3$) Spectra of Compound **230a**.....353
Figure A83 400 MHz 1H NMR ($CDCl_3$) Spectra of Compound **230b** 354
Figure A84 100 MHz 13C NMR ($CDCl_3$) Spectra of Compound **230b**.....355
Figure A85 400 MHz 1H NMR ($CDCl_3$) Spectra of Compound **230c**.....356
Figure A86 100 MHz 13C NMR ($CDCl_3$) Spectra of Compound **230c**.....357
Figure A87 400 MHz 1H NMR ($CDCl_3$) Spectra of Compound **230d** 358
Figure A88 100 MHz 13C NMR ($CDCl_3$) Spectra of Compound **230d**.....359
Figure A89 400 MHz 1H NMR ($CDCl_3$) Spectra of Compound **230e**.....360
Figure A90 100 MHz 13C NMR ($CDCl_3$) Spectra of Compound **230e**.....361
Figure A91 400 MHz 1H NMR ($CDCl_3$) Spectra of Compound **230f**.....362
Figure A92 100 MHz 13C NMR ($CDCl_3$) Spectra of Compound **230f** 363
Figure A93 400 MHz 1H NMR ($CDCl_3$) Spectra of Compound **231a**.....364
Figure A94 100 MHz 13C NMR ($CDCl_3$) Spectra of Compound **231a**.....365
Figure A95 400 MHz 1H NMR ($CDCl_3$) Spectra of Compound **231b** 366
Figure A96 100 MHz 13C NMR ($CDCl_3$) Spectra of Compound **231b**.....367
Figure A97 400 MHz 1H NMR ($CDCl_3$) Spectra of Compound **231c**.....368

Figure A98 100 MHz 13C NMR ($CDCl_3$) Spectra of Compound **231c** 369
Figure A99 400 MHz 1H NMR ($CDCl_3$) Spectra of Compound **231d** 370
Figure A100 100 MHz 13C NMR ($CDCl_3$) Spectra of Compound **231d**.....371
Figure A101 400 MHz 1H NMR ($CDCl_3$) Spectra of Compound **231e**.....372
Figure A102 100 MHz 13C NMR ($CDCl_3$) Spectra of Compound **231e**.....373
Figure A103 400 MHz 1H NMR ($CDCl_3$) Spectra of Compound **232a**.....374
Figure A104 100 MHz 13C NMR ($CDCl_3$) Spectra of Compound **232a**.....375
Figure A105 400 MHz 1H NMR ($CDCl_3$) Spectra of Compound **232b** 376
Figure A106 100 MHz 13C NMR ($CDCl_3$) Spectra of Compound **232b**.....377
Figure A107 400 MHz 1H NMR ($CDCl_3$) Spectra of Compound **232c**.....378
Figure A108 100 MHz 13C NMR ($CDCl_3$) Spectra of Compound **232c**.....379
Figure A109 400 MHz 1H NMR ($CDCl_3$) Spectra of Compound **232d** 380
Figure A110 100 MHz 13C NMR ($CDCl_3$) Spectra of Compound **232d**.....381
Figure A111 400 MHz 1H NMR ($CDCl_3$) Spectra of Compound **233a**.....382
Figure A112 100 MHz 13C NMR ($CDCl_3$) Spectra of Compound **233a**.....383
Figure A113 400 MHz 1H NMR ($CDCl_3$) Spectra of Compound **233b** 384
Figure A114 100 MHz 13C NMR ($CDCl_3$) Spectra of Compound **233b**.....385
Figure A115 400 MHz 1H NMR ($CDCl_3$) Spectra of Compound **233c**.....386
Figure A116 100 MHz 13C NMR ($CDCl_3$) Spectra of Compound **233c**.....387
Figure A117 400 MHz 1H NMR ($CDCl_3$) Spectra of Compound **242**.....388
Figure A118 100 MHz 13C NMR ($CDCl_3$) Spectra of Compound **242**.....389
Figure A119 400 MHz 1H NMR ($CDCl_3$) Spectra of Compound **253**.....390
Figure A120 100 MHz 13C NMR ($CDCl_3$) Spectra of Compound **253**.....391
Figure A121 400 MHz 1H NMR ($CDCl_3$) Spectra of Compound **254**.....392
Figure A122 100 MHz 13C NMR ($CDCl_3$) Spectra of Compound **254**.....393
Figure A123 400 MHz 1H NMR ($CDCl_3$) Spectra of Compound **255**.....394
Figure A124 100 MHz 13C NMR ($CDCl_3$) Spectra of Compound **255**.....395

Figure A125 400 MHz 1H NMR ($CDCl_3$) Spectra of Compound **256**.....396
Figure A126 100 MHz 13C NMR ($CDCl_3$) Spectra of Compound **256**.....397
Figure A127 400 MHz 1H NMR ($CDCl_3$) Spectra of Compound **257**.....398
Figure A128 100 MHz 13C NMR ($CDCl_3$) Spectra of Compound **257**.....399
Figure A129 400 MHz 1H NMR ($CDCl_3$) Spectra of Compound **175**.....400
Figure A130 100 MHz 13C NMR ($CDCl_3$) Spectra of Compound **175**.....401
Figure A131 400 MHz 1H NMR ($CDCl_3$) Spectra of Compound **253b** 402
Figure A132 100 MHz 13C NMR ($CDCl_3$) Spectra of Compound **253b**.....403
Figure A133 400 MHz 1H NMR ($CDCl_3$) Spectra of Compound **253c**.....404
Figure A134 100 MHz 13C NMR ($CDCl_3$) Spectra of Compound **253c** 405
Figure A135 400 MHz 1H NMR ($CDCl_3$) Spectra of Compound **253d** 406
Figure A136 100 MHz 13C NMR ($CDCl_3$) Spectra of Compound **253d**.....407
Figure A137 400 MHz 1H NMR ($CDCl_3$) Spectra of Compound **253f** 408
Figure A138 100 MHz 13C NMR ($CDCl_3$) Spectra of Compound **253f** 409
Figure A139 400 MHz 1H NMR ($CDCl_3$) Spectra of Compound **253g**.....410
Figure A140 100 MHz 13C NMR ($CDCl_3$) Spectra of Compound **253g**.....411
Figure A141 400 MHz 1H NMR ($CDCl_3$) Spectra of Compound **253h** 412
Figure A142 100 MHz 13C NMR ($CDCl_3$) Spectra of Compound **253h**.....413
Figure A143 400 MHz 1H NMR ($CDCl_3$) Spectra of Compound **253i** 414
Figure A144 100 MHz 13C NMR ($CDCl_3$) Spectra of Compound **253i**.....415
Figure A145 400 MHz 1H NMR ($CDCl_3$) Spectra of Compound **253j** 416
Figure A146 100 MHz 13C NMR ($CDCl_3$) Spectra of Compound **253j** 417
Figure A147 400 MHz 1H NMR ($CDCl_3$) Spectra of Compound **253k** 418
Figure A148 100 MHz 13C NMR ($CDCl_3$) Spectra of Compound **253k**.....419
Figure A149 400 MHz 1H NMR ($CDCl_3$) Spectra of Compound **253l** 420
Figure A150 100 MHz 13C NMR ($CDCl_3$) Spectra of Compound **253l**.....421
Figure A151 400 MHz 1H NMR ($CDCl_3$) Spectra of Compound **253m** 422

Figure A152 100 MHz 13C NMR ($CDCl_3$) Spectra of Compound **253m** 423
Figure A153 400 MHz 1H NMR ($CDCl_3$) Spectra of Compound **253n** 424
Figure A154 100 MHz 13C NMR ($CDCl_3$) Spectra of Compound **253n**.....425
Figure A155 400 MHz 1H NMR ($CDCl_3$) Spectra of Compound **253o**.....426
Figure A156 100 MHz 13C NMR ($CDCl_3$) Spectra of Compound **253o**.....427
Figure A157 400 MHz 1H NMR ($CDCl_3$) Spectra of Compound **254a**.....428
Figure A158 100 MHz 13C NMR ($CDCl_3$) Spectra of Compound **254a**.....429
Figure A159 400 MHz 1H NMR ($CDCl_3$) Spectra of Compound **254b** 430
Figure A160 100 MHz 13C NMR ($CDCl_3$) Spectra of Compound **254b**.....431
Figure A161 400 MHz 1H NMR ($CDCl_3$) Spectra of Compound **254c**.....432
Figure A162 100 MHz 13C NMR ($CDCl_3$) Spectra of Compound **254c**.....433
Figure A163 400 MHz 1H NMR ($CDCl_3$) Spectra of Compound **254d** 434
Figure A164 100 MHz 13C NMR ($CDCl_3$) Spectra of Compound **254d**.....435
Figure A165 400 MHz 1H NMR ($CDCl_3$) Spectra of Compound **254f** 436
Figure A166 100 MHz 13C NMR ($CDCl_3$) Spectra of Compound **254f** 437
Figure A167 400 MHz 1H NMR ($CDCl_3$) Spectra of Compound **254h** 438
Figure A168 100 MHz 13C NMR ($CDCl_3$) Spectra of Compound **254h**.....439
Figure A169 400 MHz 1H NMR ($CDCl_3$) Spectra of Compound **254j** 440
Figure A170 100 MHz 13C NMR ($CDCl_3$) Spectra of Compound **254j** 441
Figure A171 400 MHz 1H NMR ($CDCl_3$) Spectra of Compound **254k** 442
Figure A172 100 MHz 13C NMR ($CDCl_3$) Spectra of Compound **254k**.....443
Figure A173 400 MHz 1H NMR ($CDCl_3$) Spectra of Compound **254m** 444
Figure A174 100 MHz 13C NMR ($CDCl_3$) Spectra of Compound **254m** 445
Figure A175 400 MHz 1H NMR ($CDCl_3$) Spectra of Compound **254o**.....446
Figure A176 100 MHz 13C NMR ($CDCl_3$) Spectra of Compound **254o**.....447
Figure A177 400 MHz 1H NMR ($CDCl_3$) Spectra of Compound **255a**.....448
Figure A178 100 MHz 13C NMR ($CDCl_3$) Spectra of Compound **255a**.....449

Figure A179 400 MHz 1H NMR ($CDCl_3$) Spectra of Compound **255b** 450
Figure A180 100 MHz 13C NMR ($CDCl_3$) Spectra of Compound **255b**.....451
Figure A181 400 MHz 1H NMR ($CDCl_3$) Spectra of Compound **255c**.....452
Figure A182 100 MHz 13C NMR ($CDCl_3$) Spectra of Compound **255c**.....453
Figure A183 400 MHz 1H NMR ($CDCl_3$) Spectra of Compound **255d** 454
Figure A184 100 MHz 13C NMR ($CDCl_3$) Spectra of Compound **255d**.....455
Figure A185 400 MHz 1H NMR ($CDCl_3$) Spectra of Compound **255h** 456
Figure A186 100 MHz 13C NMR ($CDCl_3$) Spectra of Compound **255h**.....457
Figure A187 400 MHz 1H NMR ($CDCl_3$) Spectra of Compound **255j** 458
Figure A188 100 MHz 13C NMR ($CDCl_3$) Spectra of Compound **255j** 459
Figure A189 400 MHz 1H NMR ($CDCl_3$) Spectra of Compound **255k** 460
Figure A190 100 MHz 13C NMR ($CDCl_3$) Spectra of Compound **255k**.....461
Figure A191 400 MHz 1H NMR ($CDCl_3$) Spectra of Compound **255m** 462
Figure A192 100 MHz 13C NMR ($CDCl_3$) Spectra of Compound **255m** 463
Figure A193 400 MHz 1H NMR ($CDCl_3$) Spectra of Compound **255o**.....464
Figure A194 100 MHz 13C NMR ($CDCl_3$) Spectra of Compound **255o**.....465
Figure A195 400 MHz 1H NMR ($CDCl_3$) Spectra of Compound **256a**.....466
Figure A196 100 MHz 13C NMR ($CDCl_3$) Spectra of Compound **256a**.....467
Figure A197 400 MHz 1H NMR ($CDCl_3$) Spectra of Compound **256b** 468
Figure A198 100 MHz 13C NMR ($CDCl_3$) Spectra of Compound **256b**.....469
Figure A199 400 MHz 1H NMR ($CDCl_3$) Spectra of Compound **256c**.....470
Figure A200 100 MHz 13C NMR ($CDCl_3$) Spectra of Compound **256c**.....471
Figure A201 400 MHz 1H NMR ($CDCl_3$) Spectra of Compound **257a**.....472
Figure A202 100 MHz 13C NMR ($CDCl_3$) Spectra of Compound **257a**.....473
Figure A203 400 MHz 1H NMR ($CDCl_3$) Spectra of Compound **257b** 474
Figure A204 100 MHz 13C NMR ($CDCl_3$) Spectra of Compound **257b**.....475
Figure A205 400 MHz 1H NMR ($CDCl_3$) Spectra of Compound **257c**.....476

Figure A206 100 MHz 13C NMR ($CDCl_3$) Spectra of Compound **257c** 477
Figure A207 400 MHz 1H NMR ($CDCl_3$) Spectra of Compound **257h** 478
Figure A208 100 MHz 13C NMR ($CDCl_3$) Spectra of Compound **257h**.....479
Figure A209 400 MHz 1H NMR ($CDCl_3$) Spectra of Compound **257j** 480
Figure A210 100 MHz 13C NMR ($CDCl_3$) Spectra of Compound **257j** 481
Figure A211 400 MHz 1H NMR ($CDCl_3$) Spectra of Compound **257k** 482
Figure A212 100 MHz 13C NMR ($CDCl_3$) Spectra of Compound **257k**.....483
Figure A213 400 MHz 1H NMR ($CDCl_3$) Spectra of Compound **258**.....484
Figure A214 100 MHz 13C NMR ($CDCl_3$) Spectra of Compound **258**.....485
Figure A215 400 MHz 1H NMR ($CDCl_3$) Spectra of Compound **259**.....486
Figure A216 100 MHz 13C NMR ($CDCl_3$) Spectra of Compound **259**.....487
Figure A217 400 MHz 1H NMR ($CDCl_3$) Spectra of Compound **260**.....488
Figure A218 100 MHz 13C NMR ($CDCl_3$) Spectra of Compound **260**.....489
Figure A219 400 MHz 1H NMR ($CDCl_3$) Spectra of Compound **L7**.....490
Figure A220 100 MHz 13C NMR ($CDCl_3$) Spectra of Compound **L7** 491
Figure A221 376 MHz 19F ($CDCl_3$) Spectra of Compound **L7**.....492
Figure A222 400 MHz 1H NMR ($CDCl_3$) Spectra of Compound **L5**.....493
Figure A223 100 MHz 13C NMR ($CDCl_3$) Spectra of Compound **L5** 494
Figure A224 400 MHz 1H NMR ($CDCl_3$) Spectra of Compound **L6**.....495
Figure A225 100 MHz 13C NMR ($CDCl_3$) Spectra of Compound **L6** 496
Figure A226 400 MHz 1H NMR ($CDCl_3$) Spectra of Compound **L8**.....497
Figure A227 100 MHz 13C NMR ($CDCl_3$) Spectra of Compound **L8** 498
Figure A228 376 MHz 19F ($CDCl_3$) Spectra of Compound **L8**.....499
Figure A229 400 MHz 1H NMR ($CDCl_3$) Spectra of Compound **L9**.....500
Figure A230 100 MHz 13C NMR ($CDCl_3$) Spectra of Compound **L9** 501
Figure A231 376 MHz 19F ($CDCl_3$) Spectra of Compound **L9**.....502
Figure A232 400 MHz 1H NMR ($CDCl_3$) Spectra of Compound **299**.....503

Figure A233 100 MHz 13C NMR ($CDCl_3$) Spectra of Compound **299**.....504
Figure A234 400 MHz 1H NMR ($CDCl_3$) Spectra of Compound **300**.....505
Figure A235 100 MHz 13C NMR ($CDCl_3$) Spectra of Compound **300**.....506
Figure A236 400 MHz 1H NMR ($CDCl_3$) Spectra of Compound **301**.....507
Figure A237 100 MHz 13C NMR ($CDCl_3$) Spectra of Compound **301**.....508
Figure A238 400 MHz 1H NMR ($CDCl_3$) Spectra of Compound **302**.....509
Figure A239 100 MHz 13C NMR ($CDCl_3$) Spectra of Compound **302**.....510
Figure A240 400 MHz 1H NMR ($CDCl_3$) Spectra of Compound **303**.....511
Figure A241 100 MHz 13C NMR ($CDCl_3$) Spectra of Compound **303**.....512
Figure A242 400 MHz 1H NMR ($CDCl_3$) Spectra of Compound **304**.....513
Figure A243 100 MHz 13C NMR ($CDCl_3$) Spectra of Compound **304**.....514
Figure A244 400 MHz 1H NMR ($CDCl_3$) Spectra of Compound **305**.....515
Figure A245 100 MHz 13C NMR ($CDCl_3$) Spectra of Compound **305**.....516
Figure A246 400 MHz 1H NMR ($CDCl_3$) Spectra of Compound **255i** 517
Figure A247 100 MHz 13C NMR ($CDCl_3$) Spectra of Compound **255i**.....518
Figure A248 400 MHz 1H NMR ($CDCl_3$) Spectra of Compound **255l** 519
Figure A249 100 MHz 13C NMR ($CDCl_3$) Spectra of Compound **255l**.....520
Figure A250 400 MHz 1H NMR ($CDCl_3$) Spectra of Compound **255p** 521
Figure A251 100 MHz 13C NMR ($CDCl_3$) Spectra of Compound **255p**.....522
Figure A252 400 MHz 1H NMR ($CDCl_3$) Spectra of Compound **255q** 523
Figure A253 100 MHz 13C NMR ($CDCl_3$) Spectra of Compound **255q**.....524
Figure A254 400 MHz 1H NMR ($CDCl_3$) Spectra of Compound **299b** 525
Figure A255 100 MHz 13C NMR ($CDCl_3$) Spectra of Compound **299b**.....526
Figure A256 400 MHz 1H NMR ($CDCl_3$) Spectra of Compound **300b** 527
Figure A257 100 MHz 13C NMR ($CDCl_3$) Spectra of Compound **300b**.....528
Figure A258 400 MHz 1H NMR ($CDCl_3$) Spectra of Compound **301b** 529
Figure A259 100 MHz 13C NMR ($CDCl_3$) Spectra of Compound **301b**.....530

Figure A260 400 MHz 1H NMR ($CDCl_3$) Spectra of Compound **302b** 531
Figure A261 100 MHz 13C NMR ($CDCl_3$) Spectra of Compound **302b**.....532
Figure A262 400 MHz 1H NMR ($CDCl_3$) Spectra of Compound **303b** 533
Figure A263 100 MHz 13C NMR ($CDCl_3$) Spectra of Compound **303b**.....534
Figure A264 400 MHz 1H NMR ($CDCl_3$) Spectra of Compound **304b** 535
Figure A265 100 MHz 13C NMR ($CDCl_3$) Spectra of Compound **304b**.....536
Figure A266 400 MHz 1H NMR ($CDCl_3$) Spectra of Compound **305d** 537
Figure A267 100 MHz 13C NMR ($CDCl_3$) Spectra of Compound **305d**.....538
Figure A268 400 MHz 1H NMR ($CDCl_3$) Spectra of Compound **308**.....539
Figure A269 100 MHz 13C NMR ($CDCl_3$) Spectra of Compound **308**.....540
Figure A270 400 MHz 1H NMR ($CDCl_3$) Spectra of Compound **309**.....541
Figure A271 400 MHz 1H NMR ($CDCl_3$) Spectra of Compound **310**.....542
Figure A272 100 MHz 13C NMR ($CDCl_3$) Spectra of Compound **310**.....543
Figure A273 400 MHz 1H NMR ($CDCl_3$) Spectra of Compound **311**.....544
Figure A274 100 MHz 13C NMR ($CDCl_3$) Spectra of Compound **311**.....545
Figure A275 400 MHz 1H NMR ($CDCl_3$) Spectra of Compound **312**.....546
Figure A276 100 MHz 13C NMR ($CDCl_3$) Spectra of Compound **312**.....547
Figure A277 400 MHz 1H NMR ($CDCl_3$) Spectra of Compound **313**.....548
Figure A278 100 MHz 13C NMR ($CDCl_3$) Spectra of Compound **313**.....549
Figure A279 400 MHz 1H NMR ($CDCl_3$) Spectra of Compound **229r**.....550
Figure A280 100 MHz 13C NMR ($CDCl_3$) Spectra of Compound **229r**.....551
Figure A281 400 MHz 1H NMR ($CDCl_3$) Spectra of Compound **229s**.....552
Figure A282 100 MHz 13C NMR ($CDCl_3$) Spectra of Compound **229s** 553
Figure A283 400 MHz 1H NMR ($CDCl_3$) Spectra of Compound **229t** 554
Figure A284 100 MHz 13C NMR ($CDCl_3$) Spectra of Compound **229t** 555
Figure A285 400 MHz 1H NMR ($CDCl_3$) Spectra of Compound **229u** 556
Figure A286 100 MHz 13C NMR ($CDCl_3$) Spectra of Compound **229u**.....557

Figure A287 400 MHz 1H NMR ($CDCl_3$) Spectra of Compound **229v**.....558
Figure A288 100 MHz 13C NMR ($CDCl_3$) Spectra of Compound **229v**.....559
Figure A289 400 MHz 1H NMR ($CDCl_3$) Spectra of Compound **229w**.....560
Figure A290 100 MHz 13C NMR ($CDCl_3$) Spectra of Compound **229w**.....561
Figure A291 400 MHz 1H NMR ($CDCl_3$) Spectra of Compound **229x**.....562
Figure A292 100 MHz 13C NMR ($CDCl_3$) Spectra of Compound **229x**.....563
Figure A293 400 MHz 1H NMR ($CDCl_3$) Spectra of Compound **308r**.....564
Figure A294 100 MHz 13C NMR ($CDCl_3$) Spectra of Compound **308r**.....565
Figure A295 400 MHz 1H NMR ($CDCl_3$) Spectra of Compound **309r**.....566
Figure A296 100 MHz 13C NMR ($CDCl_3$) Spectra of Compound **309r**.....567
Figure A297 400 MHz 1H NMR ($CDCl_3$) Spectra of Compound **310t**.....568
Figure A298 100 MHz 13C NMR ($CDCl_3$) Spectra of Compound **310t**.....569
Figure A299 400 MHz 1H NMR ($CDCl_3$) Spectra of Compound **223t**.....570
Figure A300 100 MHz 13C NMR ($CDCl_3$) Spectra of Compound **223t**.....571
Figure A301 400 MHz 1H NMR ($CDCl_3$) Spectra of Compound **311q**.....572
Figure A302 100 MHz 13C NMR ($CDCl_3$) Spectra of Compound **311q**.....573
Figure A303 400 MHz 1H NMR ($CDCl_3$) Spectra of Compound **312q**.....574
Figure A304 100 MHz 13C NMR ($CDCl_3$) Spectra of Compound **312q**.....575
Figure A305 400 MHz 1H NMR ($CDCl_3$) Spectra of Compound **231q**.....576
Figure A306 100 MHz 13C NMR ($CDCl_3$) Spectra of Compound **231q**.....577
Figure A307 400 MHz 1H NMR ($CDCl_3$) Spectra of Compound **232q**.....578
Figure A308 100 MHz 13C NMR ($CDCl_3$) Spectra of Compound **232q**.....579
Figure A309 400 MHz 1H NMR ($CDCl_3$) Spectra of Compound **233q**.....580
Figure A310 100 MHz 13C NMR ($CDCl_3$) Spectra of Compound **233q**.....581
Figure A311 400 MHz 1H NMR ($CDCl_3$) Spectra of Compound **313q**.....582
Figure A312 100 MHz 13C NMR ($CDCl_3$) Spectra of Compound **313q**.....583
Figure A313 400 MHz 1H NMR ($CDCl_3$) Spectra of Compound **227q**.....584

Figure A314 100 MHz 13C NMR ($CDCl_3$) Spectra of Compound **227q**.....585
Figure A315 400 MHz 1H NMR ($CDCl_3$) Spectra of Compound **314**.....586
Figure A316 100 MHz 13C NMR ($CDCl_3$) Spectra of Compound **314**.....587
Figure A317 400 MHz 1H NMR ($CDCl_3$) Spectra of Compound **314-OAc** 588
Figure A318 100 MHz 13C NMR ($CDCl_3$) Spectra of Compound **314-OAc**.....589
Figure A319 400 MHz 1H NMR ($CDCl_3$) Spectra of Compound **314-Boc**.....590
Figure A320 100 MHz 13C NMR ($CDCl_3$) Spectra of Compound **314-Boc**.....591
Figure A321 400 MHz 1H NMR ($CDCl_3$) Spectra of Compound **315**.....592
Figure A322 100 MHz 13C NMR ($CDCl_3$) Spectra of Compound **315**.....593
Figure A323 400 MHz 1H NMR ($CDCl_3$) Spectra of Compound **316**.....594
Figure A324 100 MHz 13C NMR ($CDCl_3$) Spectra of Compound **316**.....595
Figure A325 400 MHz 1H NMR ($CDCl_3$) Spectra of Compound **317**.....596
Figure A326 100 MHz 13C NMR ($CDCl_3$) Spectra of Compound **317**.....597
Figure A327 400 MHz 1H NMR ($CDCl_3$) Spectra of Compound **227r**.....598
Figure A328 100 MHz 13C NMR ($CDCl_3$) Spectra of Compound **227r**.....599
Figure A329 400 MHz 1H NMR ($CDCl_3$) Spectra of Compound **229q** 600
Figure A330 100 MHz 13C NMR ($CDCl_3$) Spectra of Compound **229q**.....601
Figure A331 400 MHz 1H NMR ($CDCl_3$) Spectra of Compound **229y**.....602
Figure A332 100 MHz 13C NMR ($CDCl_3$) Spectra of Compound **229y**.....603
Figure A333 400 MHz 1H NMR ($CDCl_3$) Spectra of Compound **227y**.....604
Figure A334 100 MHz 13C NMR ($CDCl_3$) Spectra of Compound **227y**.....605
Figure A335 400 MHz 1H NMR ($CDCl_3$) Spectra of Compound **231y**.....606
Figure A336 100 MHz 13C NMR ($CDCl_3$) Spectra of Compound **231y**.....607
Figure A337 400 MHz 1H NMR ($CDCl_3$) Spectra of Compound **377**.....608
Figure A338 100 MHz 13C NMR ($CDCl_3$) Spectra of Compound **377**.....609
Figure A339 400 MHz 1H NMR ($CDCl_3$) Spectra of Compound **227z** 610
Figure A340 100 MHz 13C NMR ($CDCl_3$) Spectra of Compound **227z**.....611

Figure A341 400 MHz 1H NMR ($CDCl_3$) Spectra of Compound **310z**.....612
Figure A342 100 MHz 13C NMR ($CDCl_3$) Spectra of Compound **310z**.....613
Figure A343 400 MHz 1H NMR ($CDCl_3$) Spectra of Compound **223z**.....614
Figure A344 100 MHz 13C NMR ($CDCl_3$) Spectra of Compound **223z**.....615
Figure A345 400 MHz 1H NMR ($CDCl_3$) Spectra of Compound **229z**.....616
Figure A346 100 MHz 13C NMR ($CDCl_3$) Spectra of Compound **229z**.....617
Figure A347 400 MHz 1H NMR ($CDCl_3$) Spectra of Compound **375z**.....618
Figure A348 100 MHz 13C NMR ($CDCl_3$) Spectra of Compound **375z**.....619
Figure A349 400 MHz 1H NMR ($CDCl_3$) Spectra of Compound **230z**.....620
Figure A350 100 MHz 13C NMR ($CDCl_3$) Spectra of Compound **230z**.....621
Figure A351 400 MHz 1H NMR ($CDCl_3$) Spectra of Compound **311z**.....622
Figure A352 100 MHz 13C NMR ($CDCl_3$) Spectra of Compound **311z**.....623
Figure A353 400 MHz 1H NMR ($CDCl_3$) Spectra of Compound **231z**.....624
Figure A354 100 MHz 13C NMR ($CDCl_3$) Spectra of Compound **231z**.....625
Figure A355 400 MHz 1H NMR ($CDCl_3$) Spectra of Compound **230za**.....626
Figure A356 100 MHz 13C NMR ($CDCl_3$) Spectra of Compound **230za**.....627
Figure A357 400 MHz 1H NMR ($CDCl_3$) Spectra of Compound **376za**.....628
Figure A358 100 MHz 13C NMR ($CDCl_3$) Spectra of Compound **376za**.....629
Figure A359 400 MHz 1H NMR ($CDCl_3$) Spectra of Compound **310zb** 630
Figure A360 100 MHz 13C NMR ($CDCl_3$) Spectra of Compound **310zb**.....631
Figure A361 400 MHz 1H NMR ($CDCl_3$) Spectra of Compound **229zc**.....632
Figure A362 100 MHz 13C NMR ($CDCl_3$) Spectra of Compound **229zc**.....633
Figure A363 400 MHz 1H NMR ($CDCl_3$) Spectra of Compound **377za**.....634
Figure A364 100 MHz 13C NMR ($CDCl_3$) Spectra of Compound **377za**.....635
Figure A365 400 MHz 1H NMR ($CDCl_3$) Spectra of Compound **390**.....636
Figure A366 100 MHz 13C NMR ($CDCl_3$) Spectra of Compound **390**.....637
Figure A367 400 MHz 1H NMR ($CDCl_3$) Spectra of Compound **371**.....638

Figure A368 100 MHz 13C NMR ($CDCl_3$) Spectra of Compound **371**.....639
Figure A369 400 MHz 1H NMR ($CDCl_3$) Spectra of Compound **372**.....640
Figure A370 100 MHz 13C NMR ($CDCl_3$) Spectra of Compound **372**.....641
Figure A371 400 MHz 1H NMR ($CDCl_3$) Spectra of Compound **378**.....642
Figure A372 100 MHz 13C NMR ($CDCl_3$) Spectra of Compound **378**.....643
Figure A373 400 MHz 1H NMR ($CDCl_3$) Spectra of Compound **379**.....644
Figure A374 100 MHz 13C NMR ($CDCl_3$) Spectra of Compound **379**.....645
Figure A375 400 MHz 1H NMR ($CDCl_3$) Spectra of Compound **380**.....646
Figure A376 100 MHz 13C NMR ($CDCl_3$) Spectra of Compound **380**.....647
Figure A377 400 MHz 1H NMR ($CDCl_3$) Spectra of Compound **381**.....648
Figure A378 100 MHz 13C NMR ($CDCl_3$) Spectra of Compound **381**.....649
Figure A379 400 MHz 1H NMR ($CDCl_3$) Spectra of Compound **382**.....650
Figure A380 100 MHz 13C NMR ($CDCl_3$) Spectra of Compound **382**.....651
Figure A381 400 MHz 1H NMR ($CDCl_3$) Spectra of Compound **383**.....652
Figure A382 100 MHz 13C NMR ($CDCl_3$) Spectra of Compound **383**.....653
Figure A383 400 MHz 1H NMR ($CDCl_3$) Spectra of Compound **384**.....654
Figure A384 100 MHz 13C NMR ($CDCl_3$) Spectra of Compound **384**.....655
Figure A385 400 MHz 1H NMR ($CDCl_3$) Spectra of Compound **385**.....656
Figure A386 100 MHz 13C NMR ($CDCl_3$) Spectra of Compound **385**.....657
Figure A387 400 MHz 1H NMR ($CDCl_3$) Spectra of Compound **386**.....658
Figure A388 100 MHz 13C NMR ($CDCl_3$) Spectra of Compound **386**.....659
Figure A389 400 MHz 1H NMR ($CDCl_3$) Spectra of Compound **387**.....660
Figure A390 100 MHz 13C NMR ($CDCl_3$) Spectra of Compound **387**.....661
Figure A391 400 MHz 1H NMR ($CDCl_3$) Spectra of Compound **388**.....662
Figure A392 100 MHz 13C NMR ($CDCl_3$) Spectra of Compound **388**.....663
Figure A393 400 MHz 1H NMR ($CDCl_3$) Spectra of Compound **389**.....664
Figure A394 100 MHz 13C NMR ($CDCl_3$) Spectra of Compound **389**.....665

Figure A395 400 MHz 1H NMR ($CDCl_3$) Spectra of Compound **391**.....666
Figure A396 100 MHz 13C NMR ($CDCl_3$) Spectra of Compound **391**.....667
Figure A397 400 MHz 1H NMR ($CDCl_3$) Spectra of Compound **373**.....668
Figure A398 100 MHz 13C NMR ($CDCl_3$) Spectra of Compound **373**.....669
Figure A399 1H COSY NMR ($CDCl_3$) Spectra of Compound **373**.....670
Figure A400 400 MHz 1H NMR ($CDCl_3$) Spectra of Compound **374**.....671
Figure A401 100 MHz 13C NMR ($CDCl_3$) Spectra of Compound **374**.....672
Figure B1 Monomer A **152** Structure.....702
Figure B2 Monomer B **152** Structure.....703
Figure B3 TFA-Salt Structures.....704
Figure B4 TFA-Salt Bridged Structural Dimer of **152**.....705

LIST OF SCHEMES

Scheme 1.1 Utilization of Trichloroacetimidates in Chemical Synthesis.....1

Scheme 1.2 Pinner Imidate Salt Preparation and Competing Side Reactions 2

Scheme 1.3 Cramer Base-catalyzed Preparation Trichloroacetimidates 3

Scheme 1.4 Imidic Acid-Amide Tautomerization 6

Scheme 1.5 Heats of Methylation and Enthalpy Determination.....6

Scheme 1.6 [3,3]-Sigmatropic Rearrangement Through Chair-like Transition States.....8

Scheme 1.7 Transfer of Chirality in Thermal [3,3]-Sigmatropic Rearrangements.....10

Scheme 1.8 Mercury (II) Catalyzed [3,3]-Sigmatropic Rearrangement.....11

Scheme 1.9 COP-Cl Asymmetric Rearrangement of Trichloroacetimidates 13

Scheme 1.10 β-amino Acid Synthesis Utilizing Overman Rearrangement.....15

Scheme 1.11 Chida Synthesis of Anti-influenza agent A-315675 16

Scheme 1.12 Synthesis of broussonetine F.....16

Scheme 1.13 Sutherland One-pot Three-step Synthesis of Bicyclic γ-lactams.....17

Scheme 1.14 Ether-directed Diastereoselective [3,3]-Sigmatropic Rearrangement.....17

Scheme 1.15 *N*-Acylamido 1,3-Diene Preparation by [3,3]-Rearrangement 18

Scheme 1.16 Propargylic Rearrangement Products in Diels-Alder Cycloadditions.....19

Scheme 1.17 Cinchona-catalyzed [1,3]-Rearrangement.....19

Scheme 1.18 1,2-*cis* oxazoline Formation by Conjugate Addition 20

Scheme 1.19 Palladium-catalyzed Synthesis of (*E*)-4-vinyloxazolines **49** 21

Scheme 1.20 Galactoside Synthesis by Ferrier Rearrangement 22

Scheme 1.21 Discovery of Asymmetric Allylic Esterification.....22

Scheme 1.22 Catalytic Cycle for Pd (II)-Mediated Allylic Esterification.....26

Scheme 1.23 Stereochemical Course of Antarafacial S_N2' Displacement.....27

Scheme 1.24 Kirsch Synthesis of (+)-chloriolide Via Asymmetric Esterification.....29

Scheme 1.25 Iterative Approach to Stereoselective Synthesis of 1,3-Polyols 29

Scheme 1.26 Synthesis of Polyketide-class of Natural Products.....30

Scheme 1.27 [COP-NHCOCCl$_3$]$_2$ Catalyst for Etherfication.....32

Scheme 1.28 Synthesis of 2-Vinyl-1,4-benzodioxanes and 2-Vinyl-1,4-Benzoxazines ...35

Scheme 2.1 Pd(II) Reaction By-products of Branched and Hindered Imidates 39

Scheme 2.2 Pd°-catalyzed Aryl Aminations of Allylic Electrophiles 41

Scheme 2.3 Rhodium-catalyzed Amination Via *Enyl* Intermediates.....45

Scheme 2.4 Proposed Strategy for Regioselective Amination 46

Scheme 2.5 Studies with Allylic Carbonates and Acetates 55

Scheme 2.6 Enantiospecific Study with Enantioenriched (*S*)-**239** 56

Scheme 2.7 Proposed Mechanism for Racemization of (*S*)-**239** 56

Scheme 2.8 TM-Catalyzed Synthesis of α,α-disubstituted Arylamines 58

Scheme 2.9 Proposed Regioselective Amination of Tertiary Trichloroacetimidates 59

Scheme 2.10 Preparation of Isoprenylated Indoles.....65

Scheme 2.11 Control Studies with Tertiary Electrophiles.....66

Scheme 3.1 Enantioselective Synthesis of α,α-Disubstituted Amines 70

Scheme 3.2 Proposed Mechanism for Racemization of **273** 72

Scheme 3.3 Strategy for DYKAT of Tertiary Allylic Imidates.....73

Scheme 3.4 Equilibration of π-Allyl Rhodium Complexes.....74

Scheme 3.5 Resolution of Racemic Electrophiles in Allylic Aminations 75

Scheme 3.6 Preparation of TFA salt **306** for X-ray Analysis.....84

Scheme 3.7 DYKAT Amination of *N*-Methyl Anilines 87

Scheme 3.8 *N*-methyl Homophenylalanine Derivatives via DYKAT..... 93

Scheme 3.9 Steric and Electronic Control of Regioselectivity..... 97

Scheme 4.1 DYKAT Amination for *N*-Methyl Manzacidin C Synthesis.....101

Scheme 4.2 Mechanism of Hydroacylation Reaction of Olefins.....102

Scheme 4.3 Intramolecular Hydroacylation for Medium-sized Ring Enones 104

Scheme 4.4 Chelating Strategies in Intramolecular Hydroacylation 105

Scheme 4.5 Nitrogen-directed Rhodium-Catalyzed Hydroacylation 107

Scheme 4.6 Strategy for Sequential DYKAT Amination and Hydroacylation 108

Scheme 4.7 Six-Membered Ring Formation with $[Rh(COD)_2]OTf$ Catalyst.....112

Scheme 4.8 Sequential DYKAT and Hydroacylation with Tertiary Imidate **255** 116

Scheme 5.1 Rhodium-catalyzed Amination of Vinyl Acetates and Applications.....122

LIST OF ABBREVIATIONS

acac	acetylacetone
BF_3	boron trifluoride
Bn	benzyl
Boc	*tert*-butyloxycarbonyl
calcd	calculated
$CDCl_3$	deuterated chloroform
CH_2Cl_2	dichloromethane
CHO	aldehyde
CIR	cyclization-induced rearrangment
COD	cyclooctadiene
COP	cobalt oxazoline palladacycle
COSY	2-D ^{1}H-^{1}H NMR coupling experiment
CPME	cyclopropylmethyl ether
DABCO	1,4-diazabicyclo[2.2.2]octane
DBU	1,8-diazabicycloundec-7-ene
DDQ	2,3–dichloro–5,6–dicyano–1,4–benzoquinone
DFT	density functional theory
DIBAL	diisobutylaluminum hydride
DMF	dimethylformamide
dppb	1,2-Bis(diphenylphosphino)butane
dppe	1,2-Bis(diphenylphosphino)ethane
dppp	1,2-Bis(diphenylphosphino)propane
dr	diastereomeric ratio
DYKAT	dynamic kinetic asymmetric transformation
ee	enantiomeric excess

equiv	equivalents
ESI	electrospray ionization
Et_2O	ethyl ether
EtOAc	ethyl acetate
EtOH	ethanol
GC	gas chromatography
Hex	hexanes
Hg	mercury
HMDS	hexamethyldisilazide
HPLC	high pressure liquid chromatography
Ir	iridium
*i*pr	isopropyl
Mbs	methoxybenzylsulfonyl
Me	methyl
MeCN	acetonitrile
MOM	methoxymethyl
MTBE	methyl –*tert*-butyl ether
NBD	norbornadiene
NMR	nuclear magnetic resonance
Pd	palladium
Ph	phenyl
PMB	*para*-methoxybenzyl
PMP	*para*-methoxyphenyl
RCM	ring-closing Metathesis
Rh	rhodium
TBS	*tert*-butyldimethylsilyl
TBDPS	*tert*-butyldiphenylsilyl

TFA	trifluoroacetic acid
THF	tetrahydrofuran
TM	transition-metal
TMS	trimethylsilyl
Tf	trifluoromethyl sulfonyl

CHAPTER I
THE SYNTHETIC UTILITY OF ALLYLIC TRICHLOROACETIMIDATES

1.1 Introduction

The efficient and selective incorporation of heteroatoms into the carbon framework of synthetic targets continues to be of paramount importance in chemical research. The persistent efforts by synthetic chemists towards difficult problems often provides new mechanistic understanding that expands our capabilities and inspires new approaches to bond construction. Reliance on the findings of the scientific community helps drive our endeavors, with intense areas of investigation often stemming from a few novel and pioneering works. One example and the central premise of this thesis is the introduction and utility of trichloroacetimidates in synthesis. Many laboratories have utilized this functional group in carbon-heteroatom bond-forming methods, the majority of which are built upon Overman's highly selective [3,3]-sigmatropic rearrangement of trichloroacetimidates for the preparation of allylic amines (Scheme 1.1a).[1, 2] Schmidt

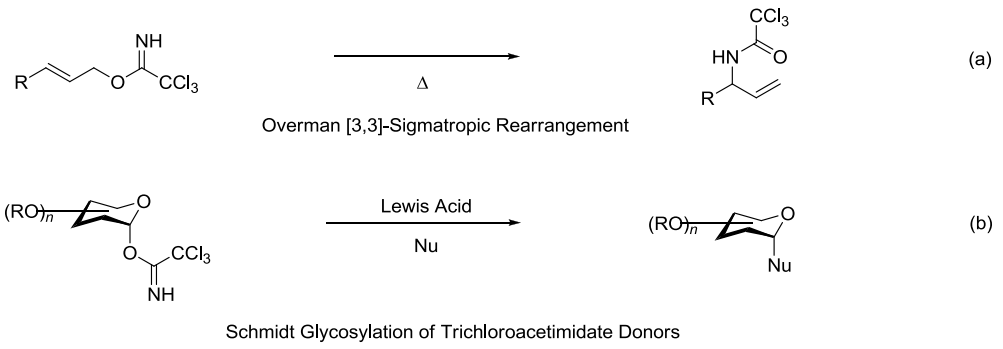

Scheme 1.1 Utilization of Trichloroacetimidates in Chemical Synthesis

followed by popularizing this functionality as an effective and highly-utilized anomeric leaving group in glycosylation methodologies (Scheme 1.1b).[3] Although the contributions

of Schmidt are of great importance and have had a major impact in the field of carbohydrate synthesis, this chapter will focus on transformations of trichloroacetimidates in unsaturated environments. It is these developments, and lessons learned therein that inspired our development of an amination reaction that uses branched allylic trichloroacetimidates as competent electrophiles in a transition-metal catalyzed substitution reaction.

1.2 Synthesis and Properties of Trichloroacetimidates

A hallmark of reactions that are commonly utilized to effect a given transformation is the ease with which the starting materials can be prepared. Imidates, referred to as imino ethers or imidic acid esters, were first synthesized by the acid catalyzed condensation of a nitrile with a primary or secondary alcohol or phenol (Scheme 1.2).[4, 5] This method, known as the Pinner reaction or synthesis was reported by Adolf Pinner in 1877.[6] In the reaction, alkyl or aryl nitriles and alcohols are combined in dichloromethane, chloroform or benzene in the presence of HCl. The resulting imidate products are called Pinner salts.

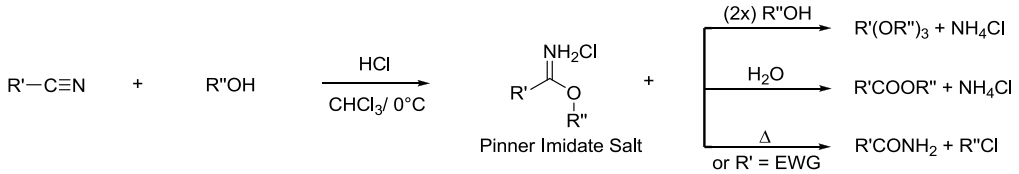

Scheme 1.2 Pinner Imidate Salt Preparation and Competing Side Reactions

The yields of imidate by the Pinner method is often affected by competing side reactions (Scheme 1.2).[4, 5] Anhydrous reaction conditions are important as the resulting hydrochloride salts are prone to hydrolysis to resultant esters. Care must be taken to ensure moisture-free storage conditions. The salts can be converted to the free base in an additional step to increase stability and enhance shelf-life. The yields of the desired

product may be lowered due to efforts employed to increase reaction progress. For example, in the presence of excess alcohol reagent and extended reaction times, competing *ortho*-ester formation can occur, and at elevated temperatures, the imidate salts decompose to the more stable amides due to attack on the alkyl ether by choride ion (Scheme 1.2). These by-products are kept to a minimum by using stoichiometric amounts of the alcohol and running the reaction at 0 - 5°C. A major limitation of this method is that it fails to produce acceptable yields of the Pinner salt when strong electron-withdrawing nitriles are used, including trichloroacetonitrile for preparation of trichloroacetimidates.[4, 5] In these reactions, amide products result as described previously (Scheme 1.2) or by Ritter reaction.[2]

The aforementioned limitations and the search for milder procedures for preparation of imidates led to the development of base-catalyzed methods. The first general synthesis of this type was described by Cramer using trichloroacetonitrile and alkoxide nucleophiles (Scheme 1.3).[7] The reaction was later expanded to a range of

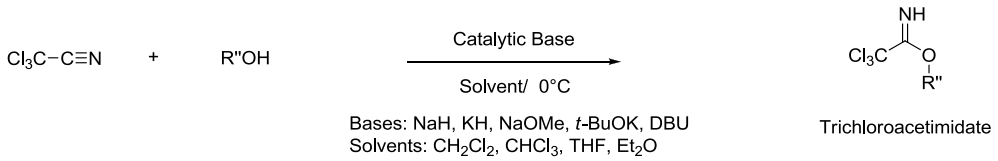

Scheme 1.3 Cramer Base-catalyzed Preparation Trichloroacetimidates

electron-deficient nitriles and alcohols by Schaefer and Peters in the presence of catalytic sodium methoxide.[8] Primary, secondary and some tertiary alcohols are now commonly derivatized to trichloroacetimidates in dichloromethane at 0°C in the presence of excess trichloroacetonitrile and catalytic DBU.[9] Hindered secondary and tertiary substrates often require more forcing conditions using substoichiometric sodium or potassium hydride in ethereal solvents.[10, 11] Many of the product trichloroacetimidates are liquids that can be

distilled, but care must be taken to minimize [3,3]-rearrangement at elevated temperatures in unsaturated systems.[1, 10] Alternatively, base-catalyzed products that are sufficiently stable have been purified by normal-phase chromatography. Primary and secondary allylic trichloroacetimidates are generally stable to silica gel while tertiary and some secondary imidates may require addition of an amine base to the eluent to prevent acid-catalyzed ionization.[12, 13] Overall, basic reaction conditions provide excellent yields of free trichloroacetimidates that that are less-prone to hydrolysis compared with the salt-forms. The acidic and basic methods for preparation of imidates complement each other as electron-poor nitriles are good substrates for synthesis under basic conditions and electron-rich nitriles are more amenable to the Pinner reaction.[4]

Trichloroacetimidates possess chemical and structural properties that have been utilized to provide varied and novel chemistries. The 1,3-arrangement of nitrogen and oxygen is a unique feature of imidates that imparts spatial and electronic requirements to function as a leaving group and to rearrange in transposition methods. In these transformations, a planar arrangement along the O-C-N backbone would allow effective

Table 1.1 Imidate Resonance Forms, Bond Orders and Lengths

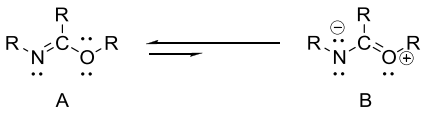

	π-Bond Order	Bond Length, Å
Imidates A/B	C-N 0.828 C-O 0.437	C-N 1.282 C-O 1.304
Amides	C-N 0.463 C-O 0.827	C-N 1.369 C-O 1.219

Source: G. Häfelinger, 1975, *The Chemistry of Imidates*, New York, John Wiley & Sons, Table 9, pg. 27.

overlap of p-orbitals for product formation. Indeed, two resonance forms of imidates are possible (Table 1.1, A and B) that delocalizes double bond character over the triad. HMO calculations for imidates place π-bonds primarily between carbon and nitrogen with partial sp^2 character between carbon and oxygen (Table 1.1).[4] In addition, calculated bond lengths

between carbon and nitrogen (1.282Å) and carbon and oxygen (1.304Å) are shorter than typical sp^3 bonding arrangements (C-N, 1.465Å and C-O, 1.416Å),[14] supporting p-orbital overlap over three centers. The calculated data for typical amides have been included (Table 1.1) and show reversed bonding orders and lengths in comparison to imidates.[4] Imidates display IR frequencies in the range of 1670-1646 cm^{-1} which is very similar to unconjugated imines.[4] This supports HMO calculation findings that structure A (Table 1.1) is the predominant resonance contributor, and the more accurately reflects the chemistry of imidates.

Trichloroacetimidates have been utilized as leaving groups in glycosylation[3] and alkylation reactions, particularly in the benzylation and allylation of alcohols.[15] Inspection of pKa values for the conjugate acids of common leaving groups used in allylic substitution methodologies (Figure 1.1) shows that trichloroacetimidate should be a relatively poor leaving group. The inductive effect of the trichloromethyl substituent lowers the pKa of trichloroacetamide to 12.42[16] versus common amides (pKa 15-16), but clearly other factors contribute to the leaving group ability of trichloroacetimidates.

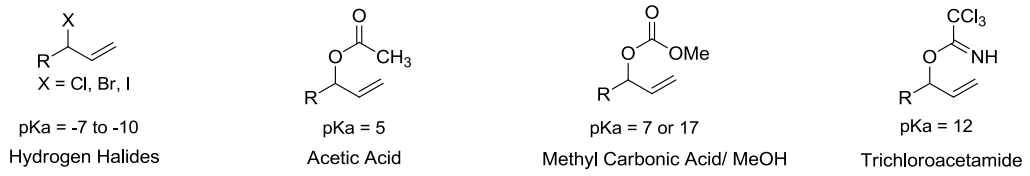

Figure 1.1 pKa of Common Leaving Groups in Allylic Substitution Reactions

Thermodynamic parameters provide the driving force making carbonates and trichloroacetimidates effective leaving groups. The degradation of methyl carbonate anion into one part methoxide ion and one part CO_2 gas results in large increases in entropy (Figure 1.1), and the conversion of an imidate to an amide is exothermic and driven by the enthalpic term. Imidic acids (imidols) and amides have been described as tautomeric pairs

in equilibrium (Scheme 1.4).[4, 17] This equilibrium lies almost exclusively on the amide side of the equation although isolated examples including imidol forms in extended conjugation have been observed. Although these protomeric pairs can potentially tautomerize, alkylmeric (imidates) cannot. However, imidates can accept charge as a leaving group with heterolytic C-O bond cleavage and in a related manner, rearrange forming amide products. The Chapman rearrangement involving aryl or alkyl migration from an imidate

Scheme 1.4 Imidic Acid-Amide Tautomerization

oxygen to nitrogen most closely resembles the tautomerization of imidols and amides.[18] The energetics of these amide-imidate transforming reactions have been investigated by Beak (Scheme 1.5).[19, 20] By measuring the separate heats of methylation of the amide and

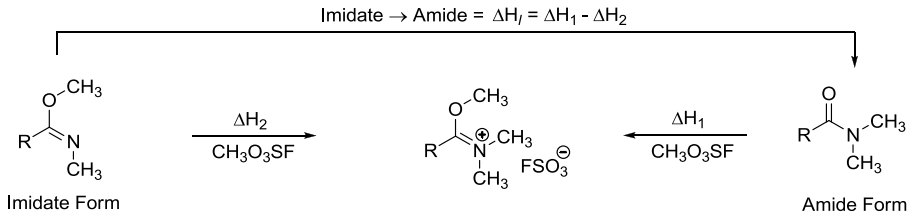

Scheme 1.5 Heats of Methylation and Enthalpy Determination

imidate forms, the difference in enthalpy in the liquid-phase for these transformations was determined to be -17 kcal/mol. Gas phase ΔH_g is in agreement at -16 kcal/mol using the the heats of vaporization of these isomeric compounds. Overall, the highly exothermic nature of the transformation from imidate to amide makes trichloroacetimidates good

leaving groups in substitution methods and provides ample driving force when utilized in rearrangement reactions.

Since a variety of alcohols derivatized as trichloroacetimidates are generally stable compounds under common purification and storage conditions, an energetic barrier precludes conversion to amides at ambient temperature. However, facile conversion to amides is accomplished by activation of trichloroacetimidates with a variety of Brønsted and Lewis Acids including TfOH, acidic resins, TMSOTf, $BF_3 \cdot OEt_2$, and $LiClO_4$, and by strong chelation to transition-metals as we shall see shortly.[21] These mildly acidic or neutral conditions are advantageous because a given reaction can proceed in the presence of acid-labile functionality. Activation occurs at the imidate nitrogen, the primary site responsible for the unique and varied chemisty of trichloroacetimidates. In comparison to the pKa of -6 to -7 for protonated carbonyls (Figure 1.2), protonated trichloroacetimidates are much less acidic and are readily activated with a pKa around 1.[22, 23] In the transformation of trichloroacetimidate substrates, the resultant amide formed by rearrangement or as a free by-product is less basic than the starting imidate with its conjugate acid having a pKa between -4 and -5 (Figure 1.2).[24] This is an important aspect of reactions catalyzed by substoichiometric quantities of metal-catalysts, enabling product release and catalytic turnover.

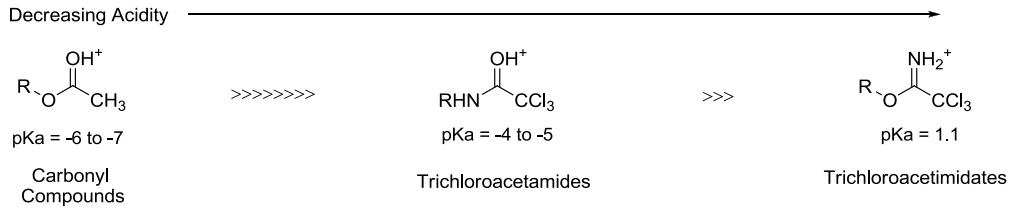

Figure 1.2 pKas of Protonated Carbonyls, Trichloroacetamides and Imidates

1.3 Allylic Trichloroacetimidate Applications in Synthesis

1.3.1 The Overman Rearrangement

In order to provide backgound that led to the development of our rhodium-catalyzed amination reaction, I will review a number methods that apply allylic trichloroacetimidates to the construction of carbon-heteroatom bonds, highlighting the basic and nucleophilic nature of the imidate nitrogen. The use of this substrate class for all practical purposes is due to the major contributions of Larry Overman. In 1974, Overman reported the first practical thermal [3,3]-sigmatropic rearrangement involving the 1,3 interchange of the nitrogen and oxygen functionality in allylic trichloroacetimidates (Scheme 1.6).[1] This aza-Claisen, now named the Overman rearrangement, was significant because it provided access to allylic amines from more easily prepared allylic alcohols derivatized as trichloroacetimidates. The first thermal rearrangement of an allylic imidate was described

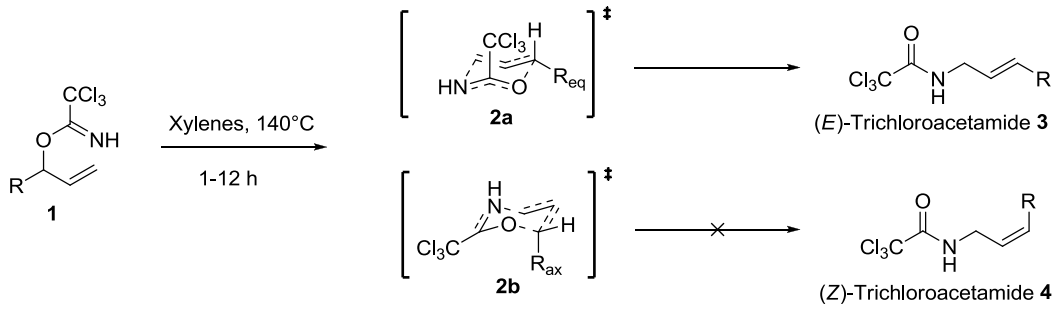

Scheme 1.6 [3,3]-Sigmatropic Rearrangement Through Chair-like Transition-States

by Mumm and Möller in1937.[25] However, early rearrangement methods were of low synthetic utility due to poor yields in the preparation of the starting imidates, and the requirement of temperatures above 200°C for the rearrangements of *N*-phenylimidates.[1, 2, 10] Overman addressed these issues by first showing the utility of the base-catalyzed method

developed by Cramer for efficient preparation of primary, secondary and tertiary trichloroacetimidates in nearly quantitative yields,[7, 26] and subsequently subjecting these substrates to facile rearrangement at lower temperatures.

The thermal rearrangement of allylic trichloroacetimidates **1** is a powerful and operationally simple C-N bond-forming transformation that typically is conducted in refluxing xylenes at ~140°C (Scheme 1.6). The reaction is applicable to primary, secondary and tertiary imidates, with predictable stereochemical outcomes arising from a concerted pericyclic mechanism with chair-like transition states (Scheme 1.6). There is a substantial amount of evidence supporting this suprafacial [3,3]-concerted process.[1, 2, 10, 27] First, intermediates are not detected and the reaction proceeds without generating [1,3]-rearrangement products. A stepwise mechanism would generate an anionic imidate and allyl cation pair of intermediates making [1,3]-product formation more favorable due to the prevalence of the more stable secondary cation. Large negative entropies are observed in Overman, Cope, and Claisen rearrangements which is indicative of a highly ordered transition state and consistent with a concerted mechanism. There is however, evidence for charge-separation in the transition state which is observed in an increased rate of reaction by changing the solvent from xylene to more polar nitrobenzene, and by appending electron donating groups (R-group imidate **1**, Scheme 1.6) on the imidate-bearing carbon, presumably stabilizing developing positive charge. Additional evidence of a [3,3]-concerted process is provided by the observed rigid transfer of chirality from starting imidate to the rearrangement products, and high ratios of (*E*)-olefin configuration in the amide products. High selectivity for *E*-olefin products can be attributed to chair-like transition states that place bulky substituents equatorial (Scheme 1.6, **2a** versus **2b**). This selectivity decreases with increasing numbers of substituents. Scheme 1.7 demonstrates transfer of chirality, and a strategy to prepare both (*E*)-configured amide enantiomers **6** and **8** from enantiopure (*E*)- and (*Z*)-trichloroacetimidates **5** and **7**.

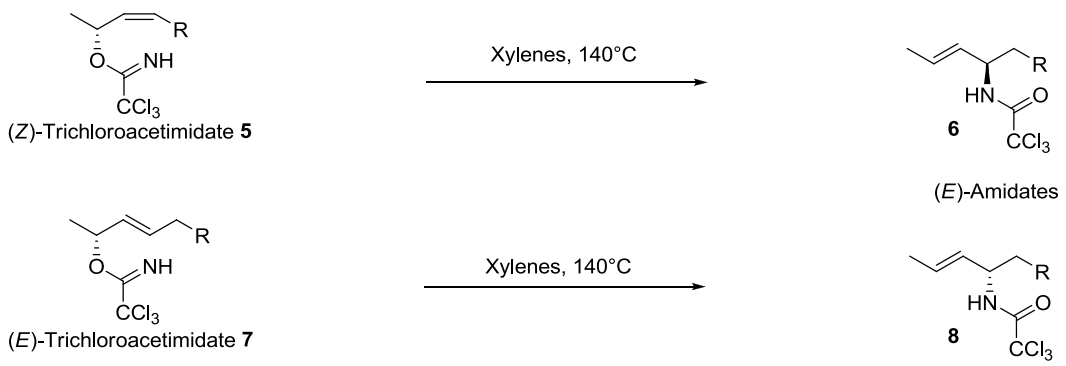

Scheme 1.7 Transfer of Chirality in Thermal [3,3]-Sigmatropic Rearrangements

In addition to the thermal rearrangement, Overman's initial report described the first metal catalyzed [3,3]-sigmatropic rearrangement of allylic trichloroacetimidates.[1] Catalytic loadings of mercury (II) salts including $Hg(O_2CCF_3)_2$ and $Hg(NO_3)_2$ dramatically increase the rate of the rearrangement in comparison to the thermally induced reaction, allowing efficient transformation to amide products at ambient temperatures. Reports followed showing that soluble palladium (II) complexes are superior catalysts and have become the metal of choice in these rearrangements.[28] The metal-catalyzed reaction is very clean and selective providing high ratios of *trans*-olefins with excellent transfer of chirality. However, the scope of the reaction is limited mainly to primary *trans*-disubstituted olefin substrates, because metal chelation to the basic imidate nitrogen leads to competitive ionization and elimination with less-reactive substrates.

Pd(II) and Hg(II) catalyzed aza-Claisen rearrangements are proposed to operate by a cyclization-induced rearrangement mechanism (CIR)[2, 29]. In the mercury-catalyzed reaction (Scheme 1.8), initial mercurinium ion formation activates the olefin towards intramolecular 6-*endo* cyclization between the nucleophilic imidate nitrogen and C-3. The organomercury adduct **10b** can revert back to the starting allylic trichloroacetimidate **9**, or undergo an irreversible deoxymercuration to the allylic amide product **11** which is favored

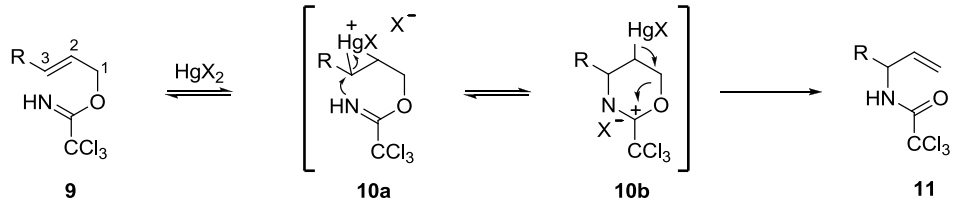

Scheme 1.8 Mercury (II) Catalyzed [3,3]-Sigmatropic Rearrangement

thermodynamically. Likewise in the Pd(II) catalyzed reaction, coordination by palladium activates the olefin to attack by the basic imidate nitrogen forming a comparable cyclic sigma-bound palladium intermediate, which undergoes deoxypalladation to rearrangement product **11**. The CIR mechanism is supported by several experimental results. Again exclusive regioselectivity for [3,3] products is observed in the metal-catalyzed reaction. By-products of allylic cation and imidate formation via ionization and isolable π-allyl complexes are not observed in the Pd(II)-catalyzed reaction, thereby preventing [1,3]-rearrangement products.[27] In addition, the resulting selectivities in metal-catalyzed rearrangements mirror thermal rearrangements. A CIR pathway is also supported based on the effects that substituents on the olefin have on reaction the outcome. Terminal olefins

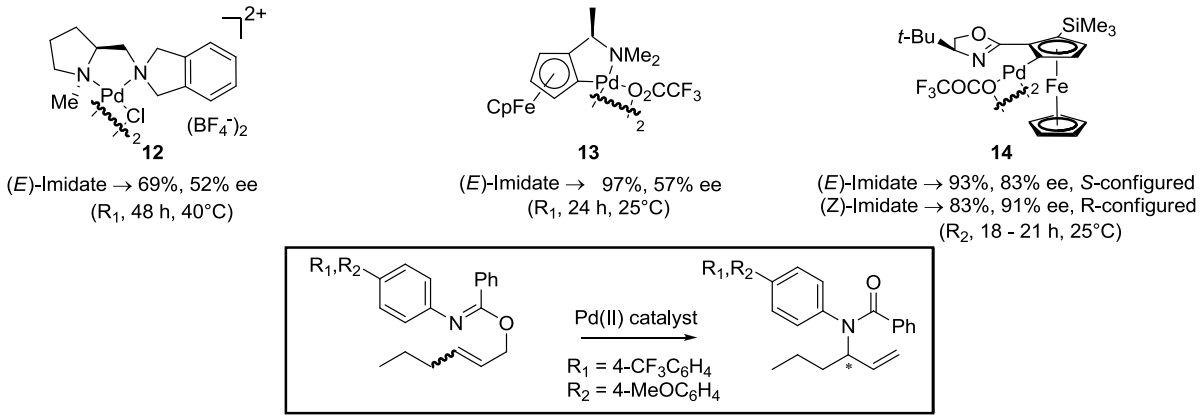

Figure 1.3 Palladium (II) Complexes for Asymmetric Overman Rearrangement

where R = H (Scheme 1.8) favor 5-*exo* attack at C-2 forming the kinetic metalation product at primary position C-3, and the rate of rearrangement decreases when C-2 is substituted, presumably due to difficulty forming a tertiary metal-bound carbon center.

The development an efficient metal-catalyzed transposition of imidate functionality prompted investigations toward an enantioselective variant of the reaction.[30] Work began with the development of cationic Pd(II) complexes containing chiral oxazolines[31] and diamines[32] (Figure 1.3, complex **12**) ligands. These first generation complexes provided the [3,3]rearrangement products of primary *N*-aryl benzimidates in moderate yields and enantioselectivities (Figure 1.3). A major limitation of cationic palladium-catalyzed reactions was competing ionization of the starting imidate, resulting in elimination and [1,3] rearrangement products. As a result, studies targeting softer neutral Pd(II) complexes ensued.[30] Neutral cyclopalladated amine dimers greatly improved reaction efficiency, but the products were obtained with low enantiopurity. Enantioselectivities returned to levels obtained with cationic complexes when neutral ferrocenyl palladacycles (i.e. **13**) possessing increased steric bulk above and below the coordination-plane were employed.[33,34] Oxazoline ferrocenyl palladacycle **14** (Figure 1.3) was most impressive in the rearrangement reaction providing high yields and stereoinduction from starting (*E*)- and (*Z*)- primary *N*-aryl benzimidates.[35,36]

Although an optimized asymmetric aza-Claisen transformation using ferrocenyl palladacycles had been developed, this method was not applicable to trichloroacetimidates which are more useful building-blocks for synthesis of complex targets. For example, acidic treatment of trichloroacetamides provides the amine·HCl salt and reduction converts the amide to an acetyl group. In 2003, Overman reported that chiral cobalt oxazoline palladacycles **15** (Scheme 1.9) cleanly and efficiently catalyze the rearrangement of primary (*E*)-trichloroacetimidates in high yield and with excellent selectivities.[37, 38] In contrast to early chiral palladium-catalysts where *N*-aryl benzimidate (*E*)- and (*Z*)-configured olefins were efficiently rearranged in high yields to *R* and *S*-configured

enantiomers, cobalt complexes catalyze the rearrangement of (*Z*)-trichloroacetimidates at diminished rates in comparison to the *trans*-configured olefin substrates (Scheme 1.9). As we shall see, this is a feature that has been advantageous to the development of new chemistries utilizing allylic trichloroacetimidates.

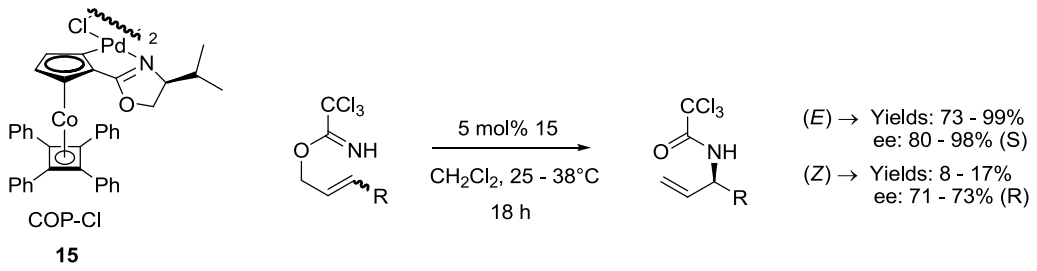

Scheme 1.9 COP-Cl Asymmetric Rearrangement of Trichloroacetimidates

Overman and coworkers conducted kinetic and computational model studies of the COP-Cl-catalyzed rearrangement that supports the cyclization-induced rearrangement (CIR) mechanism that was proposed for Hg(II) and Pd(II) catalysts.[39] Kinetic studies provide evidence for an initial and reversible binding event between the Pd(II) catalyst and the substrate, most likely at the imidate nitrogen rather than the olefin. Under high concentrations of imidate, the relative binding constants for trichloroacetimidates, (*E*)-olefins and (*Z*)-olefins were determined to be 2.2 x 10^{-4} mM^{-1}, 5.4 x 10^{-8} mM^{-1} and 2.5 x 10^{-5} mM^{-1} respectively, more than 10^4 greater binding affinity of the imidate nitrogen to palladium than an (*E*)-configured olefin.[39] Since η^2-coordination of the olefin by palladium was presumed critical for activation towards attack by the imidate nitrogen, it was unclear if this nitrogen-bound palladium species is a "non-productive" complex or a "productive" and necessary step for intramolecular transfer of palladium to the olefin. Kinetic simulations were unable to rule out either of these possibilities.

Regardless of the mode of reversible binding between the allylic trichloroacetimidate substrate and the palladium catalyst, activation of the olefin does not appear to be rate-limiting. DFT calculations show that the CIR mechanism is energetically viable and the formation of a discrete Pd-bound cyclic intermediate is the rate and enantiodetermining step in the catalytic cycle.[39] The difference in the reactivity of *N*-aryl benzimidates versus trichloroacetimidates with *cis* and *trans* olefin substrates can be attributed to the rates of nucleophilic attack forming the cyclic intermediates in each case. The more electron-rich *N*-aryl benzimidates react at a faster rate with ferrocenyl palladacycles on both double-bond isomers forming cyclic intermediates comparable to **16** and **17** (Figure 1.4), perhaps making palladium-olefin coordination rate-determining in these reactions. The COP-catalyzed reaction of electron-deficient trichloroacetimidates however, react a slower rate and realize a significant barrier to formation of cyclic structure **17** that by necessity places a substituent axial when *Z*-olefin substrates are utilized. Calculations for a model of enantioinduction in the COP-catalyzed reactions support favorable coordination of the allylic imidate *trans* to the oxazoline component of the complex, making the planar chirality of the COP ligand, rather than chirality present in the oxazoline ring a more important factor for enantioselectivity. The cyclopentadienyl and tetraphenylcyclobutadiene components of the COP ligand destabilize unfavorable steric interactions with the bound allylic imidate leading to elevated enantioselectivity that is set with formation of the cyclic palladium-bound intermediate.

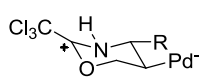

16 Cyclic intermediate from an (*E*)-olefin

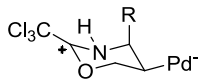

17 Cyclic intermediate from an (*Z*)-olefin

Figure 1.4 Cyclic Intermediates in COP-catalyzed Rearrangement

The Overman rearrangement is a powerful transformation that has been incorporated into the synthesis of many bio-active natural products and medicinal agents containing chiral amine functionality.[40, 41] Due to the ready availability of chiral alcohol starting materials and methods for generation of enantiopure allylic alcohols, the thermally induced rearrangement is most often employed in synthetic strategies. Chiral amino acid synthesis has benefited from the use of Overman rearrangements in synthetic sequences.[42,43] As an example, Walsh developed a strategy to unsaturated β-amino acids (Scheme 1.10), important intermediates for β-lactam and β-peptide synthesis.[44] The method relies on an enantioselective vinylzinc addition to benzaldehydes that was previously described in their laboratory to provide allylic alcohol **19**, which undergoes facile thermal rearrangement to amine **20** with high selectivity. A one-pot deprotection and oxidation furnished β-amino acid **21**.

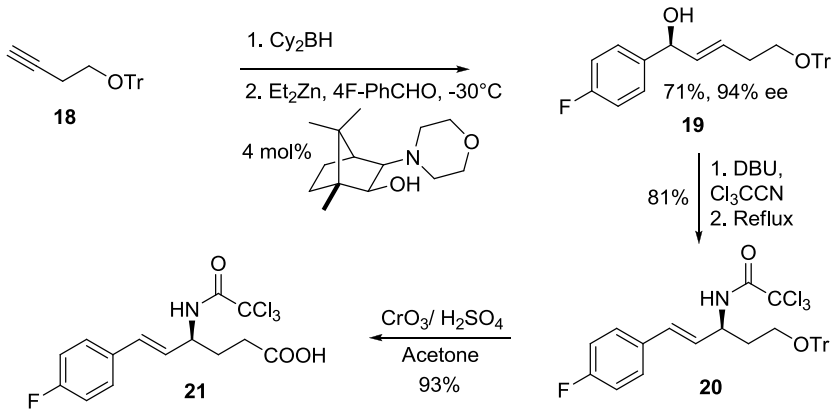

Scheme 1.10 β-amino Acid Synthesis Utilizing Overman Rearrangement

Chida reported the asymmetric synthesis of anti-influenza agent A-315675 developed by Abbott (Scheme 1.11).[45] The route is interesting in that it incorporates a sequential Overman rearrangement of bis-trichloroacetimidate **22** that was prepared from

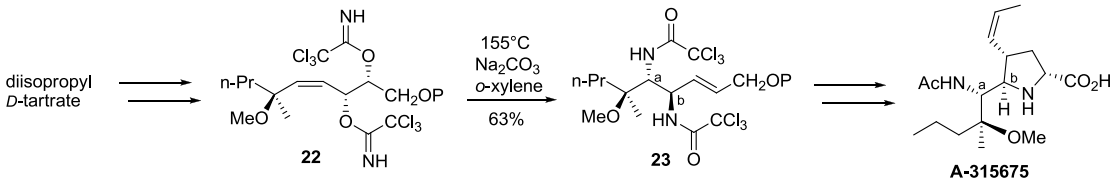

Scheme 1.11 Chida Synthesis of Anti-influenza agent A-315675

D-tartrate in ten steps. The transformation required (*Z*)-configured olefin **22** for the initial rearrangement and the resulting transfer of stereochemistry. The second rearrangement onto the intermediate (*E*)-configured allylic imidate provided 1,2-*trans* diamine **23** as a single isomer in 63% overall yield. The synthesis of A-315675 was completed in nine additional steps from compound **23**. Chida utilized the similar strategy for the synthesis of (-)-Agelastatin A.[46]

In another report, Chida uses a *syn*-diol prepared from *L*-tartrate and develops conditions for selective preparation of *ortho*-amide **24** (Scheme 1.12).[47] Imidate rearrangement provided amino alcohol **25**, obviating the need for additional protection. The 1,4-arrangement of the nitrogen and alcohol functionality in **25** are utilized towards formation of the pyrrolidine core of broussonetine F.

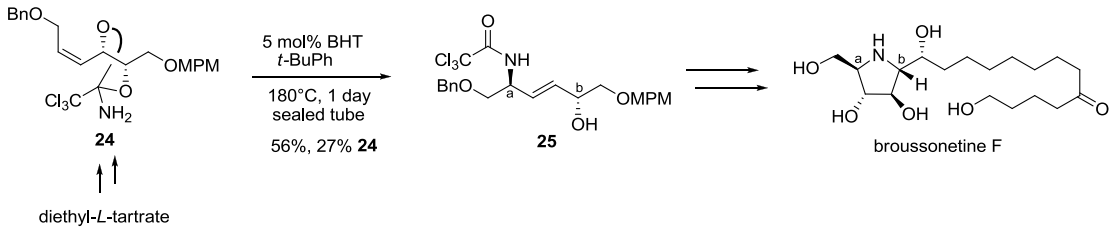

Scheme 1.12 Synthesis of broussonetine F

Sutherland has reported a number natural product and building block syntheses that utilize aza-Claisen rearrangements in enantiodetermining steps. An asymmetric example

is utilized in the preparation of bicyclic γ-lactams (Scheme 1.13). A one-pot process was developed that relied on a COP-Cl enantioselective rearrangement to set the stereochemistry. Grubbs I catalyzed RCM provided cyclohexene intermediate **28** that underwent subsequent Ru(II)-mediated Kharasch cyclization resulting in lactam **29** in 70% overall yield and with 89% ee.[48] Sutherland prepared hydroxylated 3-aminoazepanes with a similar strategy.[49]

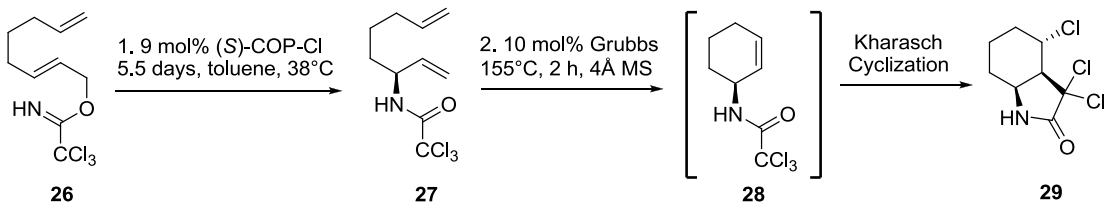

Scheme 1.13 Sutherland One-pot Three-step Synthesis of Bicyclic γ-lactams

A more recent development in palladium (II) catalyzed Overman rearrangements has been the integration of chiral centers bearing heteroatoms capable of directing diastereoselectivity in these transformations (Scheme 1.14).[50] The use of MOM ethers provides the highest diastereoselectivity presumably due to an additional point of chelation.

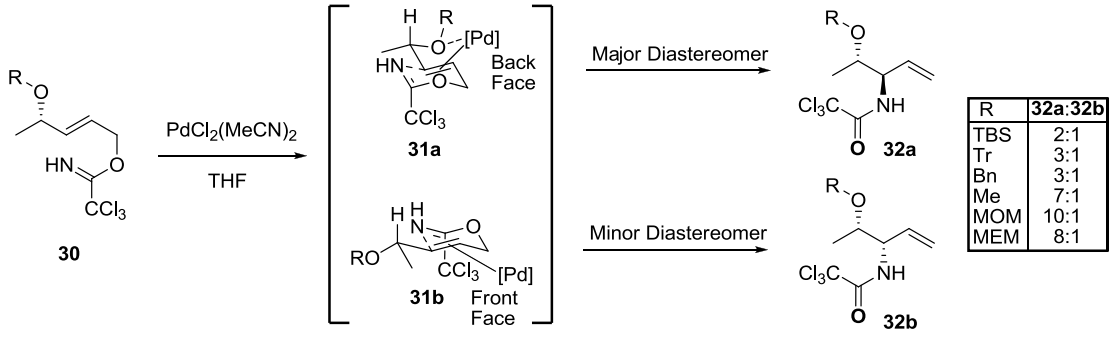

R	32a:32b
TBS	2:1
Tr	3:1
Bn	3:1
Me	7:1
MOM	10:1
MEM	8:1

Scheme 1.14 Ether Directed Diastereoselective [3,3]-Sigmatropic Rearrangement

Chelation of the tethered oxygen to the metal center results in directed coordination to the back face of the olefin and chair conformation **31a** possessing the least amount of 1,3-allylic strain. This MOM-ether directed rearrangement has been utilized by Sutherland to prepare *anti*-1,2 amino alcohols for the synthesis of guanidine alkaloid (+)-monanchorin,[51] clavainol A, C and H,[52] and a variety of sphingosines.[53]

1.3.2 [3,3]-Rearrangements of Propargyl Trichloroacetimidates

In addition to the vast body of work encompassing the rearrangement of allylic trichloroacetimidates, Overman found that propargylic trichloroacetimidates also undergo thermal [3,3]-sigmatropic rearrangement.[54, 55] The reaction is run in refluxing xylene for 4 – 12 hours (Scheme 1.15) providing (1*Z*, 3*E*) configured *N*-acylamido dienes in 14- 92% yield.[55] The transformation proceeds with initial formation of allene **34a**, followed by a [1,5]-sigmatropic hydrogen migration from structure **34b**.[17, 55] (1*Z*, 3*E*)-diene selectivity in **35** appears to arise from a kinetic preference for tautomer **34b** and subsequent geometry for facile hydrogen migration.

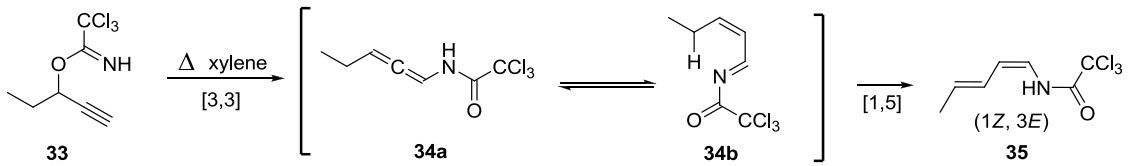

Scheme 1.15 *N*-Acylamido 1,3-Diene Preparation by [3,3]-Rearrangement

The product *N*-Acylamino 1,3-dienes from the thermal rearrangement of propargylic trichloroacetimidates have proven to be useful substrates in Diels-Alder reactions.[17, 54] The required (1*E*, 3*E*)-configured olefins **36,** easily accessed by isomerization of product **35** with TEA in refluxing xylene, and are competent dienophiles

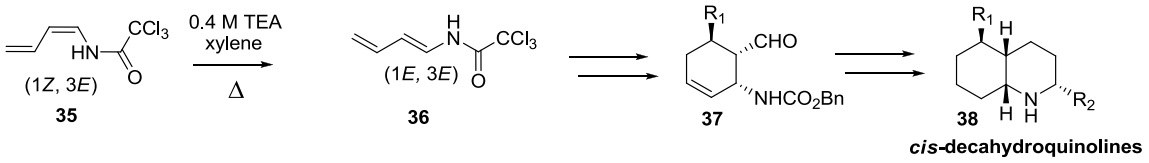

Scheme 1.16 Propargylic Rearrangement Products in Diels-Alder Cycloaddition

in these cycloadditions. Overman and his colleagues applied this strategy to the racemic synthesis of the neurotoxin alkaloids *dl*-pumiliotoxin-C[56] and *dl*-perhydrogephyrotoxin,[57] possessing *cis*-decahydroquinoline structures (Scheme 1.16).

1.3.3 [1,3]-Rearrangement of Allylic Trichloroacetimidates

Although thermal and metal-catalyzed [3,3]-sigmatropic rearrangements are designed to produce minimal [1,3]-products, alternative methodologies have been reported for their exclusive formation. In 2008, Jørgensen and coworkers reported the first organocatalyzed enantioselective [1,3]-rearrangement of allylic trichloroacetimidates utilizing dimeric cinchona alkaloid catalysts (Scheme 1.17).[58] 20 mol% of the organocatalyst $[DHQD]_2PHAL$ in dioxane provided [1,3]-rearranged allylic trichloroacetimidates in good yields and enantioselectivity. DFT studies of the reaction

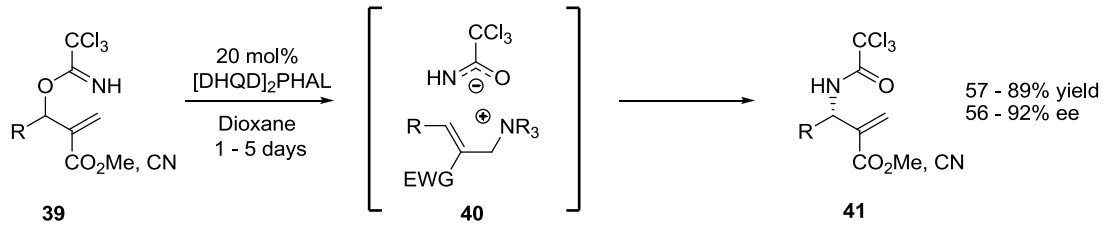

Scheme 1.17 Cinchona-catalyzed [1,3]-Rearrangement

support a mechanism involving two S_N2' steps, each involving lower energy *syn* addition of the nucleophile.[59] In the first of these steps, addition of cinchona alkaloid is favored by 5.4 kcal/mol versus Overman rearrangement, thus providing a favorable pathway towards chiral ion pair **40**. The lowest energy alignment of ion-pair **40** orients it for a second S_N2' displacement by the anionic trichloroacetimidate fragment. The overall transformation was found to be exothermic by 17.4 kcal/mol,[59] in agreement with previously reported values.[20]

1.3.4 Oxazolines Via Intramolecular Addition

The prevalence of 1,2-amino alcohols moieties in natural products and drug candidates have prompted studies for selective attack by the imidate nitrogen at the α-position for preparation of oxazolines. Early examples provided 1,2-*cis* amino alcohol functionality by nucleophilic epoxide opening[60] and activation of terminal olefins with electrophilic iodine[61] and mercury (II) salts,[62] with 1,3-oxazines forming as expected from internal olefin substrates.[1, 63] Conjugate addition has recently been employed to effect this transformation.[64] Nishimura utilized this strategy in the synthesis of *L*-iduronic acid-type inhibitors of tumor metastasis (Scheme 1.18).[65] In this method, Michael addition of *in situ* generated allylic trichloroacetimide **43** onto the α,β-unsaturated ester provided *cis*-oxazoline **44** in 76% yield.

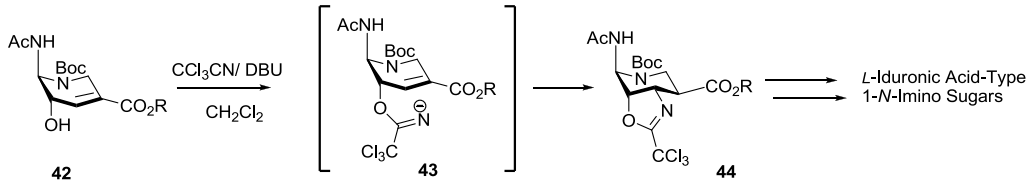

Scheme 1.18 1,2-*cis*-oxazoline Formation by Conjugate Addition

In 2009 Jirgensons reported a palladium(II)-catalyzed method for preparation of 4-vinyloxazolines from (*Z*)-configured allylic trichloroacetimidates **45** (Scheme 1.19) possessing a secondary or tertiary δ-oxy acetyl, TBS or Boc protected leaving group.[66] The reaction is high yielding and selective producing exclusive formation of (*E*)-4-vinyloxazolines **49** with low competitive Overman rearrangement due to required axial placement of a substituent in the 6-*endo* aminopalladation transition state (see Figure 1.4, structure **17**). Again, the configuration of the olefin is critical for efficient reaction as (*E*)-trichloroacetimidate substrates in the reaction suffer decreased yields due to competitive Overman rearrangement. High transfer of chirality is also observed in this oxazoline forming reaction (Scheme 1.19). The authors postulate a mechanism where 5-*exo* aminopalladation occurs reversibly and stereospecifically forming oxazolinium intermediates **46** and **48** followed by rate-determining deoxypalladation (Scheme 1.19). Both the aminopalladation and deoxypalladation are predicted to occur with *anti*-orientation leading predominately to (*E*)-*R* product **49**.

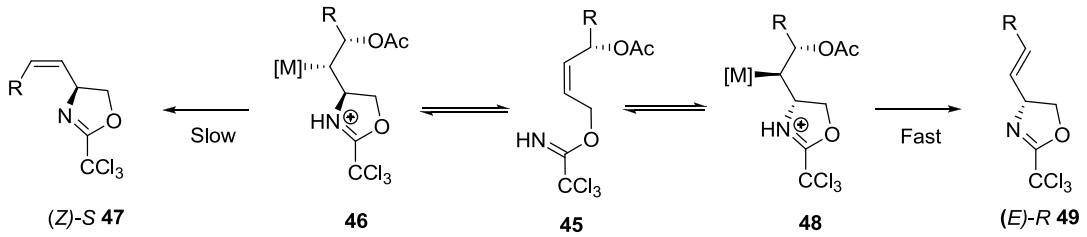

Scheme 1.19 Palladium-catalyzed Synthesis of (*E*)-4-vinyloxazolines **49**

1.3.5 Allylic Substitution Reactions with Oxygen Nucleophiles

Given the fact that trichloroacetimidates are competent leaving groups under mildly acidic alkylation and glycosylation conditions, it is not surprising that this functionality has been utilized for carbon-heteroatom bond formation in allylic systems. An example was

first reported by Schmidt for diastereoselective pseudogalactal glycoside synthesis of **52** (Scheme 1.20) where TMSOTf activates trichloroacetimidate galactal donor **50** for Ferrier rearrangement with acceptor glucopyranose **51**.[67]

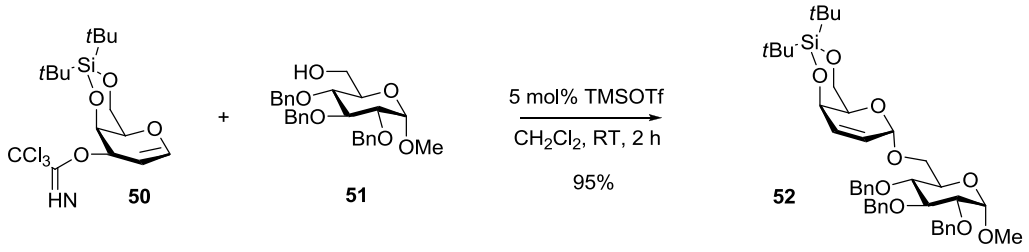

Scheme 1.20 Galactoside Synthesis by Ferrier Rearrangement

In 2005, the Overman group was expanding the scope of their COP-catalyzed intramolecular aminopalladation reaction for preparation of 4-vinyloxazolines by utilizing a trichloroacetimidate substrate as the tethered nucleophilic amine source.[68] When (*Z*)-

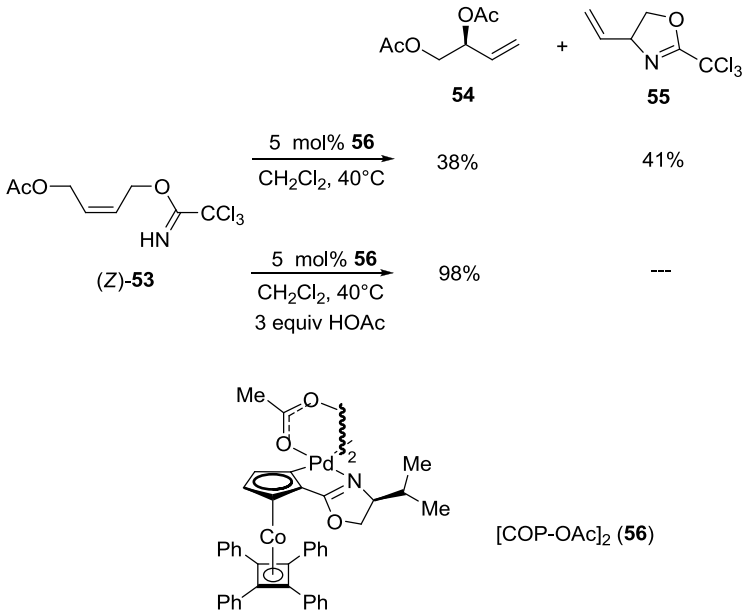

Scheme 1.21 Discovery of Asymmetric Allylic Esterification

olefin **53** was subjected to aminopalladation conditions a 1:1 mixture of the desired 4-vinyl oxazoline **55** and diacetate **54** was observed in the reaction (Scheme 1.21).[69, 70] This experiment suggested that S_N2' displacement of (*Z*)-allylic imidate **53** with acetic acid to form diacetate **54** was competing with intramolecular attack of the imidate nitrogen to afford the desired oxazoline product **55**. To suppress the amino-cyclization pathway, 3 equivalents of acetic acid was employed in the reaction, and complete conversion to the diacetate product **54** was observed (Scheme 1.21). This finding initiated development of the first asymmetric allylic esterification reaction of (*Z*)-allylic trichloroacetimidates with carboxylic acid nucleophiles.[71]

Early optimization studies determined that COP-OAc dimer **56** (Scheme 1.21) provided the best balance of yield and enantioselectivity in the esterification reaction with acetic acid nucleophile.[70] Optimal yields of allylic ester product were obtained in dichloromethane while running the reaction at room temperature provided the highest enantioinduction. For slow reactions, the reaction temperature could be increased leading to elevated yields but diminished enantioselectivity. In reactions where acetate salts were substituted for acetic acid, no reaction was observed indicating that a proton source is required to neutralize the anionic imidate leaving group. The importance of the trichloroacetimidate group in the $[COP\text{-}OAc]_2$ catalyzed esterification reaction is evidenced by the failure of (*Z*)-allylic *N*-arylimidates and trifluoroacetimidates to react with acetic acid. Again, olefin geometry in the starting acetimidate is critical, with (*E*)-olefins providing 82% of the enantiomeric ester product with 66% *ee* and 10% of the [3,3]-rearrangement product.[70]

Table 1.2 summarizes Overman's investigations of the allylic esterification of a number of (*Z*)-trichloroacetimidate substrates with acetic acid (entries 1 - 6), aryl acids (entries 7 – 13) and aliphatic carboxylic acids (entries 14 – 19). The reaction is very general for formation of branched allylic esters **53** – **75** in moderate to high yields and with excellent enantiomeric purity.[70, 71] The reactions forming enantioenriched allylic acetates

Table 1.2 Asymmetric Esterification of (*Z*)-Acetimidates

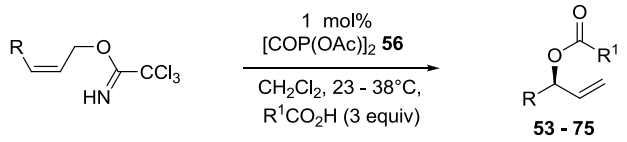

entry	imidates (R)	R^1	time (h)	temp (h)	allylic ester	yield (%)	*ee* (%)
1	**57a** *i*-pr	Me	14	23	**58**	96	93
2	**57b** Cyclohexyl	Me	48	23	**59**	45	90
3	**57c** CH_2OH	Me	17	23	**60**	92	97
4	**53** CH_2OAc	Me	8	23	**54**	90	99
5	**57d** CH_2OPMB	Me	16	23	**61**	93	99
6	**57e** $(CH_2)_3OTBS$	Me	17	23	**62**	98	93
7	**57f** $(CH_2)_2Ph$	C_6H_5	17	23	**63**	85	93
8	**57f**	4-Me-C_6H_4	17	38	**64**	85	93
9	**57f**	4-MeO-C_6H_4	22	23	**65**	79	86
10	**57f**	4-Ph-C_6H_4	19	38	**66**	95	97
11	**57f**	4-Cl-C_6H_4	16	38	**67**	86	97
12	**57f**	4-NO_2-C_6H_4	22	38	**68**	65	87
13	**57f**	2-Cl-C_6H_4	18	38	**69**	24	53
14	**57g** *n*-pr	CH_2Ph	20	23	**70**	90	91
15	**57g**	*i*-Pr	21	23	**71**	89	92
16	**57f**	*t*-Bu	48	38	**72**	95	94
17	**57f**	1-adamantyl	48	38	**73**	68	86
18	**57f**	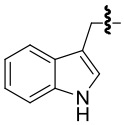	17	38	**74**	65	96
19	**57f**	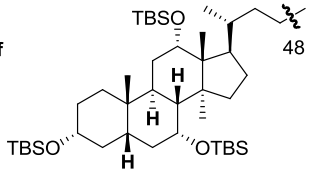	48	38	**75**	91	91

54 – **62** shows a high degree of functional group tolerance present in the starting substrates (Table 1.2, entries 1 – 7). A free hydroxyl group was compatible under the reaction conditions, providing ester **60** in 92% yield with 97% *ee*. Ester **53**, ether **57d**, and silyl ether **57e** (entries 4 – 6) also were compatible imidate substrates in the esterification

reaction. Bulky imidate **57b** bearing a vinylic cyclohexyl group provided **59** with 90% *ee* but only in 45% yield (entry 2).

Esterification with a number of aromatic carboxylic acids were evaluated with allylic imidate **57f** (Table 1.2, entries 8 - 13). In the reactions, electron-rich, neutral and electron-poor benzoic acids provide the corresponding allylic esters **63** - **69** in 65–95% yield and with excellent enantioselectivity (86– 97% *ee*). Only the *ortho*-substituted 2-chlorobenzoic acid (entry 13) resulted in a diminished yield and enantioselectivity (24%, 53% *ee*) presumably due to additional sterics present in the nucleophile.

Aliphatic carboxylic acids were also successfully utilized as nucleophiles in the $[COP\text{-}OAc]_2$-catalyzed reaction with *n*-propyl (*Z*)-allylic imidate **57g** and phenethyl **57h**, resulting in good yields (65 – 95%) and enantioselectivities (86 – 96% *ee*) in the product esters **70** – **75** (Table 1.2, entries 14 – 19).[70] Sterically encumbered *t*-butyl and adamantyl carboxylic acids (entries 16 and 17) and less soluble carboxylic acids (entries 18 and 19) effectively reacted at 38 ^{o}C, giving the corresponding allylic esters in good yields and with excellent levels of asymmetric induction.

With the successful development of the $[COP\text{-}OAc]_2$-catalyzed method for preparation of a variety of allylic esters in high yields and with excellent enantiopurity, the Overman group focused on gaining mechanistic understanding involved in this transformation.[22] The proposed catalytic cycle based on a combination of experimental and computational data sets is shown in Scheme 1.22. NMR studies confirmed the presence of a mixture of acetate, carboxylic acid and amidate homo- and heterodimers in the reaction mixtures (Scheme 1.22, **76** – **78**), with no correlation found between equilibrium values of these complexes, the rate of the reaction and the pKas of the carboxylic acid nucleophiles. The fact there was no correlation between the rate of the reaction and the relative nucleophilicity of the carboxylic acid, and negligable change in % *ee* as the reaction progresses and more trichloroacetamide is produced, suggested that a monomeric imidate substrate complex **80** is the entry point into the catalytic cycle.[22]

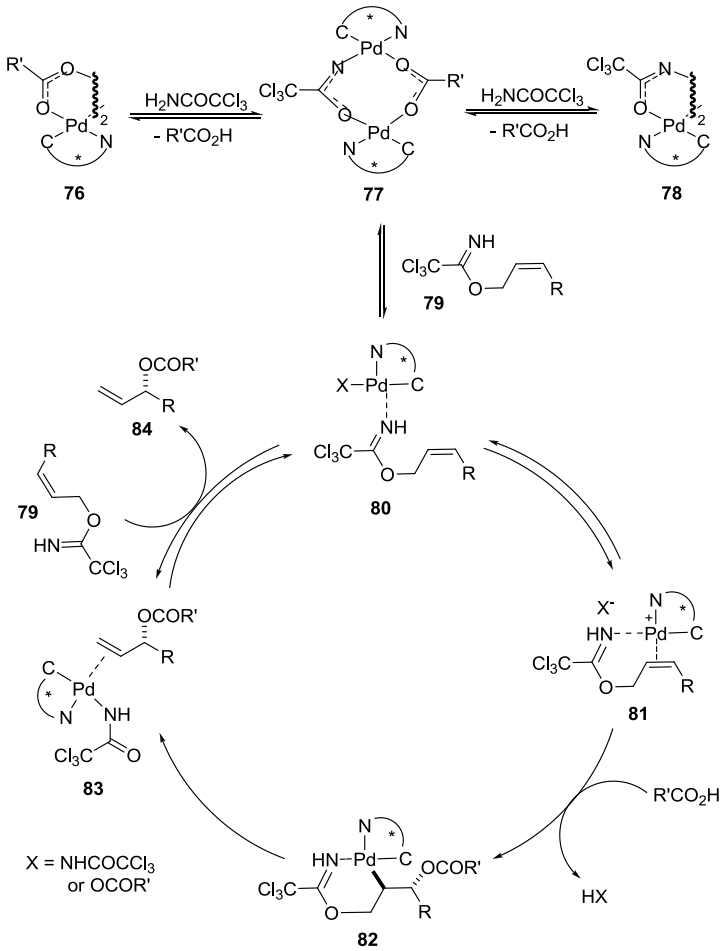

Scheme 1.22 Catalytic Cycle for Pd (II)-Mediated Allylic Esterification

Bidentate chelation of the imidate nitrogen to palladium forming complex **81** (Scheme 1.22) is a critical step for the selective C-O forming transformation. This hypothesis was initially based on a few experimental observations and later gained support through DFT calculations. As mentioned earlier, *N*-aryl imidates and allylic esters are not effective substrates in the reaction, suggesting that participation of a basic imidate nitrogen is required for efficient reactivity. The regioselectivities observed in these reactions are very high, with branched to linear ratios approaching 800:1.[71] It is highly unlikely that this level of selectivity could result from monodentate chelation of the substrate or through a palladium π-allyl intermediate, but could arise from a rigid cyclic metal-bound

intermediate. When enantioenriched deuterated imidates **85** were subjected to the esterification reaction, it was observed that nucleophilic addition and loss of the trichloroacetimidate leaving group occurred in an antarafacial manner forming ester product **90** (Scheme 1.23). This result would require *syn*-addition of the nucleophile and palladium followed by *anti*-elimination of imidate and palladium or the reverse process, *anti*-oxypalladation and *syn*-deoxypalladation. The relative energies of *syn*- and *anti*-palladium-bound complexes **86** – **89** primed for oxypalladation (Scheme 1.23) were calculated, and a reaction coordinate diagram was calculated for each of these starting complexes in the S_N2' displacement mechanism. Cationic palladium-complex **86**, bound to the substrate imidate nitrogen and the olefin, although intermediate in energy to starting complexes **87** -**89**, resulted in lower transition-states in each of the 2 steps by 6.2 and 7.4 kcal/mol, supporting *anti*-oxypalladation of **86** followed by *syn*-deoxypalladation. Because

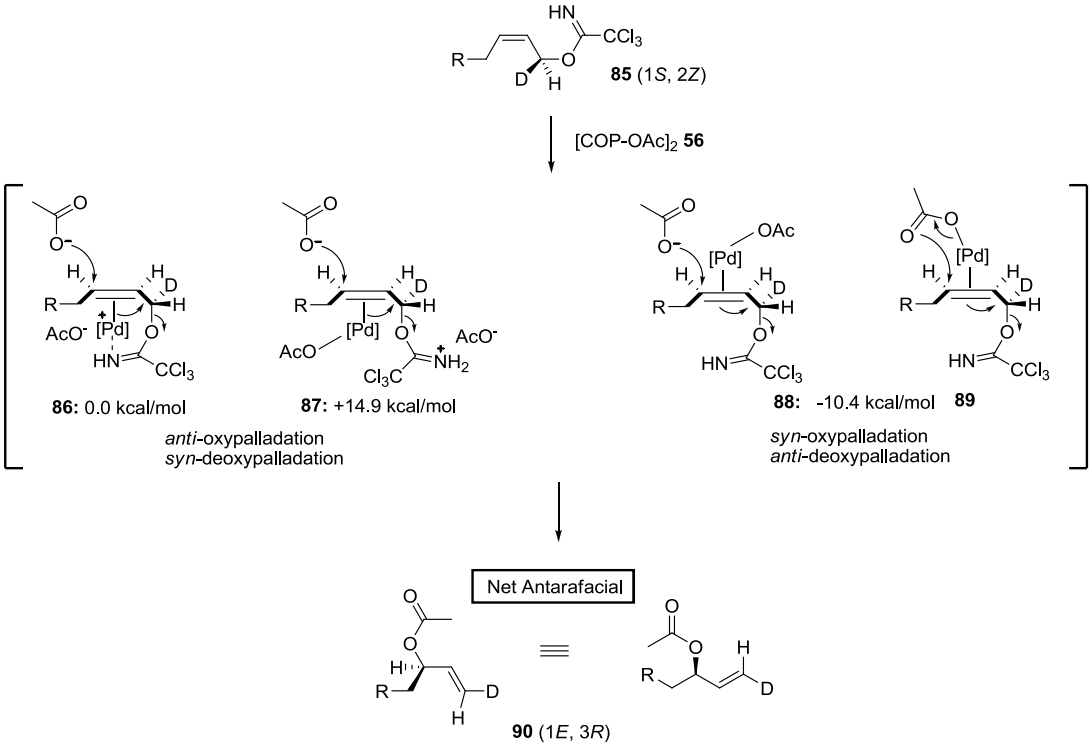

Scheme 1.23 Stereochemical Course of Antarafacial S_N2' Displacement

complex **86** has intermediate stability, the mechanism would require that palladium-bound imidate is a reversible process. Favorable chelation at the imidate nitrogen[39] provides complex **80** (Scheme 1.21) that directs the metal-center to the olefin. With binding of palladium to the olefin and loss of acetate, cationic bidentate complex **81** results, that is activated towards nucleophilic attack by external carboxylic acid. The path from **80** to activated complex **81** is reversible and enantiodetermining, setting the stage for formation of *anti*-oxypalladated intermediate **82** and *syn*-deoxypalladated complex **83**. Displacement of branched ester product **84** by imidate **79** completes the catalytic cycle.

The asymmetric [COP-OAc]$_2$-catalyzed esterification of (*Z*)-configured olefin trichlorochloroacetimidates is a powerful tool that has been utilized towards the synthesis of natural products and chiral oxygenated scaffolds, primarily 1,3-polyol structural motifs. For example, in 2010 Kirsch and Haug reported the synthesis of the polyketide derived fungal macrolide (+)-chloriolide.[72, 73] Their strategy utilized Overman's method to prepare two enantioenriched allylic alcohol fragments **93** and **97** (Scheme 1.24) that when joined end to end provided the required stereochemistry at C4 and C7 of (+)-chloriolide **101**. In the synthesis of fragment **93**, asymmetric esterification of acetimidate **91** (Scheme 1.24) provided benzoate **92** in 95% yield and with 96% ee. Protecting group interchanges and Wittig olefination provided **93** in six steps. Enantioselective [COP-OAc]$_2$-catalyzed reaction of trichloroacetimidate **95** and aliphatic PMBO$(CH_2)_3$COOH nucleophile delivered ester **96** in 83% yield and with dr > 99:1. The use of this unusual carboxylic acid allowed selective removal in the presence of the terminal acetate group.[72] Oxidative removal of the PMB group resulted in intramolecular lactonization and free allylic alcohol **97**. From allylic alcohol fragments **93** and **97**, (+)-chloriolide **101** was assembled in eight linear steps.

Kirsch has been instrumental in developing routes to 1,3-polyol structures which are the main structural feature of many polyketide-derived natural products.[74-76] The central premise of this strategy is to set the stereochemistry with Overman's esterification

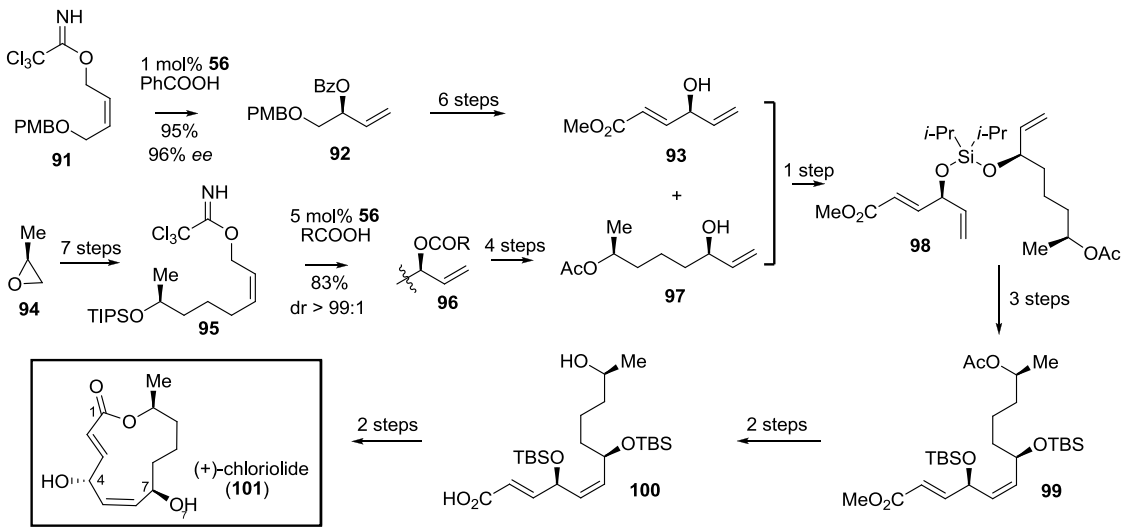

Scheme 1.24 Kirsch Synthesis of (+)-chloriolide Via Asymmetric Esterification

reaction and functionalize the resulting allylic alcohol for the next iteration of asymmetric esterification, thus building a 1,3-polyol chain. Scheme 1.25 shows three enantioselective esterifications forming triol **108** in 13% overall yield and >95:5 dr. 1 mol% of (+)-[COP-OAc]$_2$ catalyst **56** in the esterification reaction of **102** with benzoic acid resulted in 93% yield of benzoate **103** with 92% *ee*.[74] DIBAL reduction, carbodiimide esterification with vinyl acetic acid, Grubbs II ring-closing metathesis and DBU-catalyzed isomerization of the cyclic olefin provided α,β-unsaturated lactone **104** in 72% yield. Luche reduction, bis-

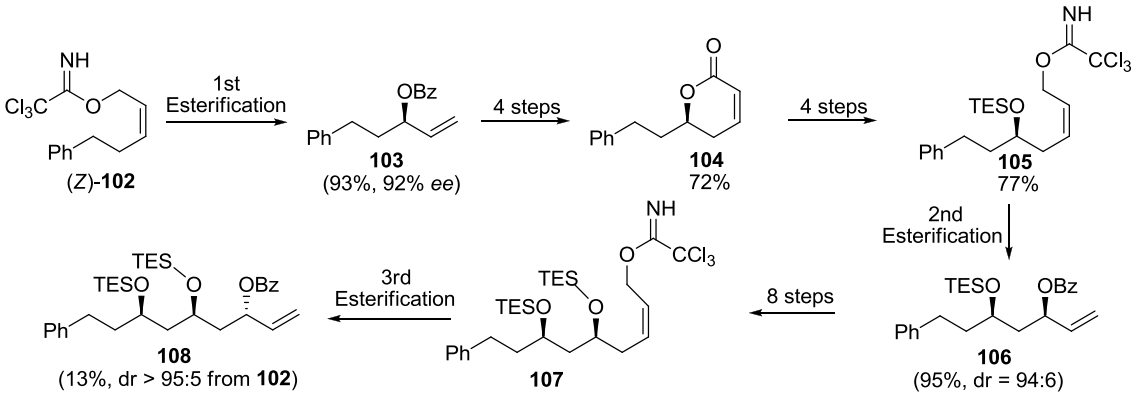

Scheme 1.25 Iterative Approach to Stereoselective Synthesis of 1,3-Polyols

silylation, selective removal of the primary TES group, and treatment with trichloroacetonitrile and catalytic DBU provided (*Z*)-allylic trichloroacetimidate **105** in 77% yield. **105** was then subjected to the second esterification reaction in the sequence using the same (+)-[COP-OAc]$_2$ catalyst **56** forming **106** in 95% yield and dr = 94:6. It is important to note that the catalyst controls the stereochemistry in the reaction, not existing chirality in the substrate. Using the same sequence, **107** was prepared and subjected to a third esterification with (-)-[COP-OAc]$_2$ resulting in **108** with dr >95:5 and of opposite configuration at the newly formed center. Kirsch and coworkers highlighted the utility of this strategy by preparing natural products (+)-solistatin,[74] polyrhacitides A and B,[75] and rugulactone[76] (Scheme 1.26).

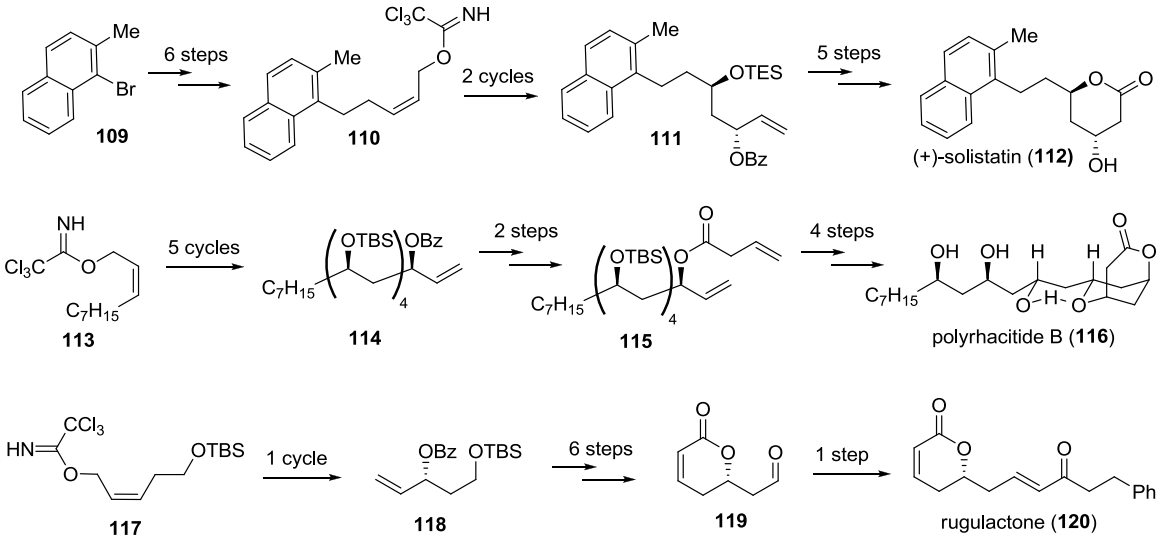

Scheme 1.26 Synthesis of Polyketide-class of Natural Products

In 2007, Overman showed that phenols make viable nucleophiles in the palladium catalyzed substitution reaction of (*Z*)-configured allylic trichloroacetimidates forming branched aryl ethers.[77] Although a highly regio- and enantioselective iridium-catalyzed method had been developed using phenoxide nucleophiles[78, 79], Overman's method was

advantageous because it allowed preparation of enantioenriched aryl ethers using neutral phenols. Optimal conditions utilized 1 mol% of $[COP\text{-}OAc]_2$ **56** catalyst, 3 equivalents of phenol nucleophile in dichloromethane at 38°C (Table 1.3). As expected, the reaction of phenols with (*Z*)-imidates was slower than carboxylic acid nucleophiles, requiring extended reaction times at 38°C. However, excellent yields and enantioselectivites are achieved in 24 – 96 hours with unprecedented branched to linear ratios. Table 1.3 shows

Table 1.3 Enantioselective Aryl Etherification of (*Z*)-Allylic Trichloroacetimidates

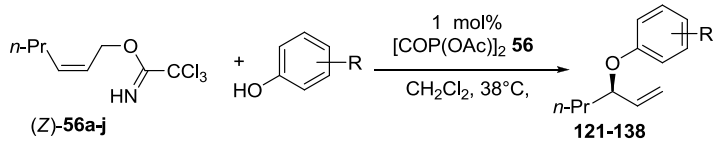

entry	imidates (R)	R	time (h)	allylic ether	yield (%)	*ee* (%)
1	**56a** *i*-pr	H	36	**121**	86	92
2	**56a**	4-Me	96	**122**	79	90
3	**56a**	4-OMe	96	**123**	63	90
4	**56a**	4-Cl	36	**124**	96	91
5	**56a**	2-Br	24	**125**	87	90
6	**56a**	4-OAc	36	**126**	93	94
7	**56a**	2-OAc	36	**127**	90	90
8	**56a**	3-OAc	36	**128**	91	92
9	**56a**	3-CHO	72	**129**	90	94
10	**56a**	3-NO_2	72	**130**	90	65
11	**56h** CH_2OTBS	4-Me	96	**131**	70	97
12	**56h**	4-OAc	36	**132**	97	96
13	**56h**	2,6-F	36	**133**	97	90
14	**56h**	3-OMe	96	**134**	80	97
15	**56i** $(CH_2)_2OTBS$	4-OAc	24	**135**	97	92
16	**56f** $(CH_2)_2Ph$	4-OAc	36	**136**	97	92
17	**56j** $(CH_2)_2OAc$	4-OAc	48	**137**	93	96
18	**56b** Cyclohexyl	4-OAc	96	**138**	30	90

the results of asymmetric ether forming reactions with various phenol nucleophiles and (*Z*)-imidate substrates. Electron-rich, poor and neutral phenols (entries 1 – 10) with

differing substitution patterns resulted overall in moderate to high yields (63 – 96%) and asymmetric induction (65 – 94% ee) with alkyl imidate **56a**. It is notable that many types of functionality are tolerated, including 3-formyl phenol that provided aryl ether **129** in 94% yield and with 94% *ee* (Table 1.3, entry 9). Silyl ether acetimidates **56h** and **56i** and acetate **56j** (entries 11 – 15 and 17) were viable substrates in the etherification reaction providing high yields and levels of enantioselectivity in the products. The bulky vinyl cyclohexyl imidate **56b** resulted in low yield (30%) of ether **138** in 96 hours however with 90% *ee*.

The [COP-OAc]$_2$-catalyzed reactions of (*Z*)-2-alkene-1-trichloroacetimidates result in high yields and selectivities for branched allylic aryl ethers, however comparable (*E*)-stereoisomer substrates result in high levels of competing [3,3]-sigmatropic rearrangement products. Overman and coworkers prepared new amidate catalyst **142** that

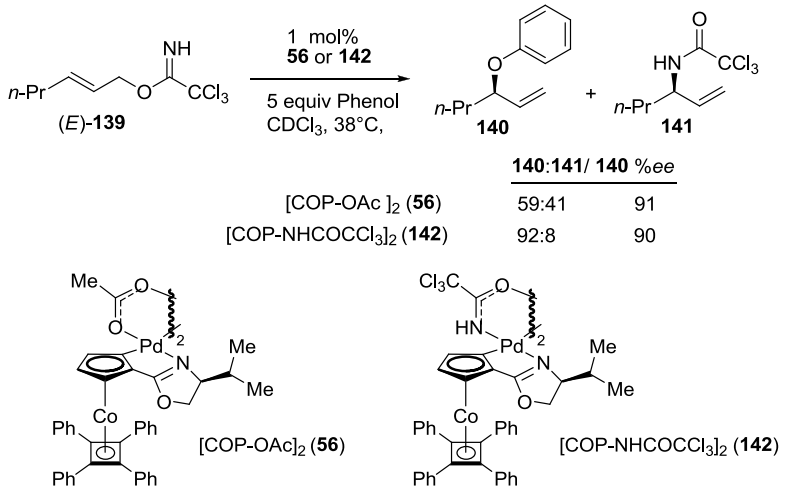

Scheme 1.27 [COP-NHCOCCl$_3$]$_2$ Catalyst for Etherfication

provided low levels of amide products under rearrangement reaction conditions (Scheme 1.27).[80] With these results, the [COP-NHCOCCl$_3$]$_2$ complex **142** was tested in the ether forming reaction utilizing (*E*)-configured imidate **139** which resulted in a 92:8 ratio of

branched ether **140** to rearranged amide product **141**. In addition, ether product **140** was obtained with 90% *ee*. Excited by these results, the scope of phenol nucleophiles and (*E*)-olefin substrates were investigated.

The asymmetric synthesis of aryl ethers with (*E*)-olefin trichloroacetimidates in combination with 1 mol% of [COP-NHCOCCl$_3$]$_2$ complex **142** or *ent*-**142** and phenol nucleophiles is shown in Table 1.4.[80] Allylic aryl ethers are prepared in acceptable yield and enantioselectivity in an average of 60 h at 38°C. The reaction of (*E*)-**139** with an electronically and sterically diverse set of phenol nucleophiles provided allylic ethers **146** – **155** in 45 – 78% yield and with 25 – 93% *ee*. The lowest enantioselectivity resulted from

Table 1.4 Enantioselective Aryl Etherification of (*E*)-Allylic Trichloroacetimidates **139 - 145**

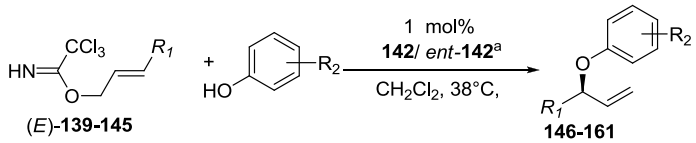

(*E*)-**139-145** **146-161**

entry	imidates (R_1)	R_2	time (h)	allylic ether	yield (%)	*ee* (%)
1	**139** *i*-pr	H	60	**146**	75	91
2	**139**	4-Me	96	**147**	62	93
3	**139**	4-OMe	96	**148**	45	92
4	**139**	4-Cl	16	**149**	78	86
5	**139**	2-Br	96	**150**	72	85
6	**139**	4-OAc	48	**151**	53[a]	92[a]
7	**139**	2-OAc	48	**152**	57[a]	93[a]
8	**139**	3-OAc	48	**153**	71[a]	93[a]
9	**139**	3-CHO	96	**154**	51[a]	90[a]
10	**139**	3-NO_2	96	**155**	48[a]	25[a]
11	**143** $(CH_2)_2Ph$	H	48	**156**	77[a]	95[a]
12	**143**	4-Cl	16	**157**	83[a]	90[a]
13	**144** $(CH_2)_3NBn(Boc)$	H	48	**158**	61[a]	98[a]
14	**144**	4-Cl	16	**159**	88[a]	96[a]
15	**145** $(CH_2)_3(CO)CH_3$	H	96	**160**	59	78
16	**145**	4-Cl	18	**161**	86	80

electron-deficient 3-nitrophenol (48% yield and 25% *ee*, entry 10) while the lowest yielding reaction resulted from electron-rich 4-methoxyphenol (45% yield and 92% *ee*, entry 3). In addition, the scope of the reaction was investigated with (*E*)-imidates bearing different functional groups (Table 1.4, entries 11 – 16). Protected amine substrate **144** and ketone **145** were well tolerated in the reaction delivering ether products **158** – **161** in 61 – 88% yield and with 78 – 98% *ee*. Importantly, both enantiomers of ether products can be prepared by selecting the appropriate [COP-NHCOCCl$_3$]$_2$ catalyst **142** or *ent*-**142**.

Overman provided one more version of the asymmetric etherfication of allylic trichloroacetimidates by investigating an intramolecular variant of the reaction.[81] In these studies, *ortho*-tethered (*E*)- and (*Z*)-allylic imidates **162a** – **c** were prepared and subjected to asymmetric ring-closure using [COP-OAc]$_2$ **56** and [COP-NHCOCCl$_3$]$_2$ **142** catalysts (Table 1.5). (*Z*)-configured starting imidates resulted in 92% of 2-vinyl chromane **163a**, however enantioselectivity was very low at only 9% *ee*.[81] In contrast, reactions of (*E*)-configured substrates catalyzed by **56** and **142** were high yielding and enantioselective.

Table 1.5 Intramolecular Enantioselective Etherification of (*E*)-Allylic Trichloroacetimidates **162a -c**

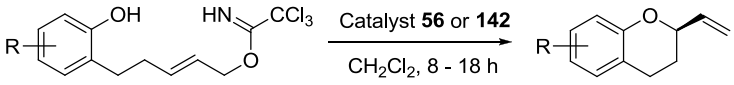

162a-c **163a-c**

entry	imidates	catalyst	loading (mol%)	temp (h)	yield **163** (%)	*ee* ***163*** (%)
1	**162a** R = H	**56**	2	38	86	89
2	**162a** R = H	**142**	2	38	81	87
3	**162a** R = H	**56**	0.5	23	91	94
4	**162b** R = 4-Br	**56**	0.5	23	94	90
5	**162c** R = 4-OMe	**56**	0.5	23	92	91

Using 2 mol% catalyst loadings at 38°C, 81 – 86% yields and 87 – 89% *ees* of product **163a** resulted (entries 1-2), with amidate catalyst **142** performing less efficiently in each category and in addition yielded 13% of the undesired rearrangement product (entry 2). Entries 4-5 using COP-OAc **56** show that electron deficient and electron-rich phenols work equally well in the reaction providing **163b** – **d** in high yields and with excellent asymmetric induction.

The intramolecular method was also amenable to imidate substrates bearing *ortho* oxygen or nitrogen substituents on the phenol ring (substrates **162d** – **e**, Scheme 1.28) for enantioselective formation of 2-vinyl-1,4-benzodioxane **163d** and 2,3-dihydro-2-vinyl-2*H*-1,4-benzodioxazine **163e**. The reactions forming these products were high yielding (90 – 98%) with impressive asymmetric induction (94 – 98% *ee*). Unfortunately sulfur-containing imidate **162f** did not provide product **163f**, presumably due to catalyst poisoning by the substrate.

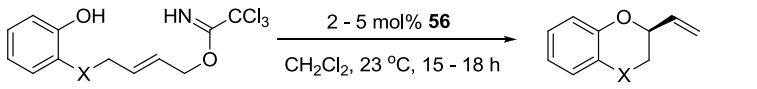

162d X = O
162e X = NTs
162f X = S

163d X = O 90%, 94% *ee*
163e X = NTs 98%, 98% *ee*
163f X = S 0%

Scheme 1.28 Synthesis of 2-Vinyl-1,4-benzodioxanes and 2-Vinyl-1,4-Benzoxazines

Deuterium-labeling studies of the intramolecular transformation were conducted that confirmed that the overall S_N2' reaction occurs with antarafacial geometry like earlier studies of the intermolecular reactions of (*Z*)-acetimidates and carboxylic acid nucleophiles.[22, 81] DFT calculations also supported the same *anti*-oxypalladation/ *syn*-deoxypalladation sequence that was found for esterification reactions. In addition, DFT experiments calculated the difference in transition state energies leading to the *anti*-

oxypalladation step which is rate and enantiodetermining, for the possible bidentate binding arrangements of the COP-catalyst, the imidate nitrogen and olefin *Re* and *Si* faces for both (*E*)- and (*Z*)-imidates. The difference in transition state energies for (*E*)-substrates was calculated to be $\Delta\Delta E^{\ddagger}$ 3.7 kcal/mol, while (*Z*)-substrates was 0.8 kcal/mol, consistent with low enantioselectivities resulting from (*Z*)-trichloroacetimidates in the reaction.

1.4 Conclusion

Allylic trichloroacetimidates are versatile substrates of broad utility for the synthesis of carbon-heteroatom bonds. Overman's pioneering work and pursuit of mechanistic understanding in rearrangements of primary allylic acetimidates has inspired the development of new methodologies for regio- and enantioselective constructions of C-N, C-O, and C-F[82] connectivity in good yields and with excellent selectivity. In many cases, the introduction of trichloroacetimidate functionality to allylic systems has improved or provided access to bonding arrangements that were previously unmet. Enantioenriched amines can be prepared by [3,3]- or [1,3]-rearrangements of trichloroacetimidates, and the use of this motif has had a major impact on stereo-controlled amino acid, 1,2-amino alcohol and 1,3-polyol synthesis prevalent in many natural products. Although allylic trichloracetimidates can be sensitive to acidic conditions, the ease of preparation and relative stability have found application in an increasing number of synthetic strategies. Based on the general availability of these constructs and their use towards difficult chemistries, methods utilizing trichloroacetimidates in unsaturated environments will continue to expand in novel ways into the future and will impact strategies for preparation of biologically relevant natural products and pharmaceuticals. The pages that follow describe the next application of allylic trichloroacetimidates to synthetic methodology for the regioselective and enantioselective preparation of α-substituted and α,α-disubstituted allylic aryl amines.

CHAPTER II
RHODIUM (I)-CATALYZED REGIOSELECTIVE AMINATION OF TRICHLOROACETIMIDATES

2.1 Secondary Allylic Trichloroacetimidates: Rhodium-Catalyzed Preparation of α-substituted Amines

2.1.1 Background

Our interest in regio- and enantioselective aminations of allylic electrophiles had roots in methods that were developed in our laboratory towards difficult problems encountered in carbohydrate chemistry. The Nguyen group had been utilizing transition-metals to effect rearrangements of trichloroacetimidate glycals[41, 83] and to direct anomeric selectivity in glycosylation reactions of trichloroacetimidate donors.[84] An important attribute that that was exploited in these methods was that transition-metals will chelate available Lewis basic sites, and in doing so activate the starting acetimidates and template the stereochemical outcome in these reactions. These ideas were based largely on Overman's studies where primary (*E*)-configured olefin trichloroacetimidates were effective substrates in [3,3]-sigmatropic rearrangements,[1, 38] (*Z*)- trichloroacetimidates for asymmetric esterification[71] with carboxylic acids and (*Z*)- and (*E*)-olefin electrophiles in ether forming reactions with phenol nucleophiles.[77, 80] These investigations showed that the basic imidate nitrogen does bind to palladium complexes and is intimately involved in directing and enantiodetermining steps of these reaction mechanisms. Ultimately, the course of these Pd(II)-catalyzed reactions are dependant on the configuration of the olefin and the nature of the catalyst. For example, (*Z*)-configured olefins undergo rearrangement very slowly in the presence of COP-OAc dimers allowing substitution by carboxylic acids and phenols to predominate. The COP-trichloroamidate dimer only slowly catalyzes the [3,3]-rearrangement of (*E*)-configured trichloroacetimidates but cleanly and efficiently catalyzes the substitution by phenols.[80] Given these findings and our experience using

transition-metals with carbohydrates, we wanted to expand our research interests by applying branched trichloroacetimidate electrophiles to allylic substitution methodologies.

We became interested in developing an allylic substitution method that utilized terminal branched trichloroacetimidates **164** (Scheme 2.1) for a number of reasons. First, this area of organic synthesis is dominated by methods that utilize primary and secondary halide, acetate and carbonate leaving groups, so there was opportunity to explore alternate electrophiles in these reactions. The efficient and successful synthesis of complex molecules depends on the methods and options available for construction. Investigating transition-metal catalyzed allylic substitutions of branched trichloroacetimidates could lead to new and useful chemistry. A benefit of these substrates is that they are easily introduced during a synthetic sequence. The allylic alcohol precursors are prepared by addition of a vinyl Grignard to aldehydes and ketones, which can be protected as required and efficiently derivatized as trichloroacetimidates.[1, 2] Another advantage of terminal olefins is they are more reactive than linear counterparts in transition-metal catalyzed reactions,[85, 86] due to less steric bulk around the terminal double bond. A more reactive electrophile avoids elevated reaction temperatures and extended reaction times for effective transformation which would decrease competing elimination and rearrangement side-reactions, increasing overall efficiency. In addition, utilization of racemic imidates have potential in kinetic or dynamic kinetic asymmetric transformation (DYKAT) type resolutions,[87]providing new avenues to prepare enantioenriched products from racemic starting materials.

Overman's Pd(II)-catalyzed methods for the enantioselective synthesis of branched amines, esters and phenols does have limitations. These reactions cannot utilize branched allylic trichloroacetimidates **164** as effective substrates (Scheme 2.1a). Previous rearrangement experiments in his laboratory showed that this olefin-type resulted in 5-*exo* attack by the imidate nitrogen on the double-bond and terminally palladated intermediates **165**.[1, 10] Basic hydrolysis of the reaction product provides evidence of this mode of reactivity by releasing 2-amino alcohols **166** (Scheme 2.1a).[2] The reaction of branched

terminal olefins lacking (*Z*)-geometry that slowly undergoes the competing CIR would presumably follow the same 5-*exo* pathway in COP-mediated substitution reactions with carboxylic acid and phenol nucleophiles. Another limiting aspect of Pd(II)-catalyzed asymmetric reactions is that the substrate scope is confined primarily to unhindered electrophiles for synthesis of tertiary carbon centers bearing a heteroatom. The reactions

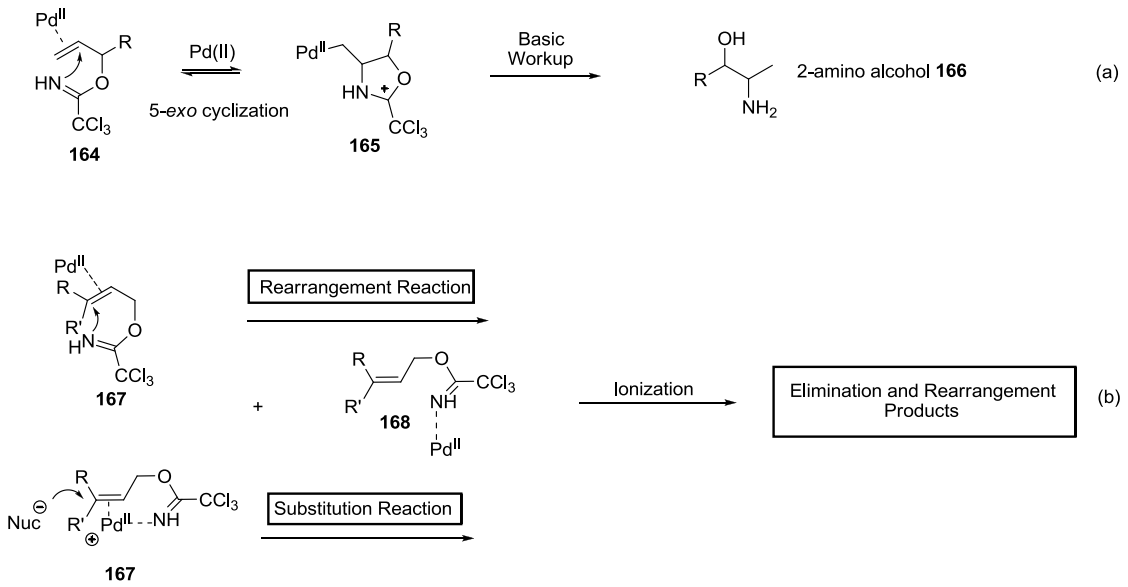

Scheme 2.1 Pd(II)-catalyzed Reaction By-products of Terminal Branched and Hindered Trichloroacetimidates

of sterically encumbered substrates result in low yields of the desired products and increased levels of byproducts due to slow rates of addition and elevated ionization of the trichloroacetimidate starting material (Scheme 2.1b). Early on in our studies we were interested in targeting these difficult structures, so this fact combined with a lack of allylic substitution methods that provide quaternary centers was additional motivation to explore the use of branched allylic trichloroacetimidate electrophiles in these reactions.

We proposed a new mode of reactivity for trichloroacetimidates in transition-metal catalyzed allylic substitution methodologies. What if ionization of the starting substrates

is not a pathway that is suppressed and avoided but rather a facile and necessary step in the reaction? We wondered if organometallic complex **170** (Figure 2.1) could result from oxidative addtion of an appropriate transition-metal complex with an allylic trichloroacetimidate electrophile. Would complex **170** make an effective activated complex providing high yields and selectivity for the branched substitution products **171a** (Figure 2.1)? Or would this strategy result in the competing linear isomer **171b**, elimination **172** or rearrangement products **173**?

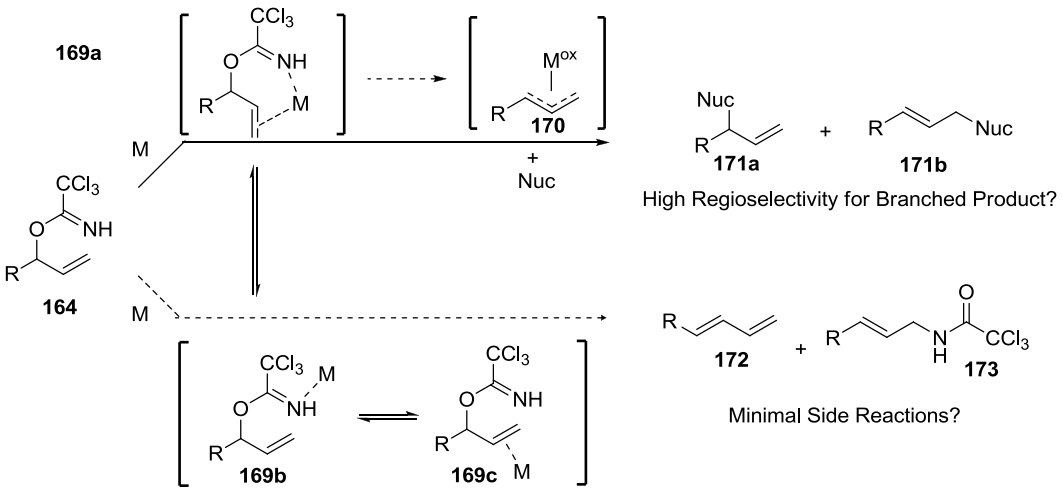

Figure 2.1 Proposed Use of Branched Imidates in TM-catalyzed Substitution

We began with the hypothesis that ionization of branched allylic trichloroacetimidates **164** to organometallic intermediate **170** would be faster than routes to elimination and rearrangement in the presence of a transition-metal capable of oxidative addition. Prior studies with linear imidates provided evidence for initial coordination of Pd(II) to the imidate nitrogen (**169b**) followed by intramolecular rearrangement to olefin-bound Pd (**169c**) and entry into the [3,3]-rearrangement pathway,[39] or formation of bidentate chelation complex **169a** and substitution by an external nucleophile.[22] We knew

that terminal branched electrophiles are more reactive than the corresponding linear structures in transition-metal catalyzed reactions,[85, 86] and therefore would enable rapid bidentate chelation to a metal center forming complex **169a** followed by facile ionization to organometallic intermediate **170**. An easily accessed and ionized electrophile may play an important role in efficient substitutions of tertiary trichloroacetimidates.

In order to draw some comparison to reported transition-metal catalyzed substitution reactions, [77, 78, 80, 88] we began our investigations using phenol nucleophiles. Although we had some success, implementation of aniline nucleophiles had more potential in allylic substitution reactions of branched allylic trichloroacetimidates. In addition, we decided to use aniline nucleophiles because of the high importance of this structural motif. *N*-arylamines are present in a number of bioactive natural products, are important synthons for the preparation of catalysts and materials, and have become increasingly common in pharmacophores present in drugs and agrochemicals.[89, 90]

Several approaches to the preparation of *N*-arylamines have been investigated with allylic carbonates and acetates employing transition-metal catalysts.[91] The use of palladium catalysts in allylic amination of unsymmetrical allylic acetates with amines tends to favor the thermodynamic linear product. The kinetic branched isomer, however, can be isolated

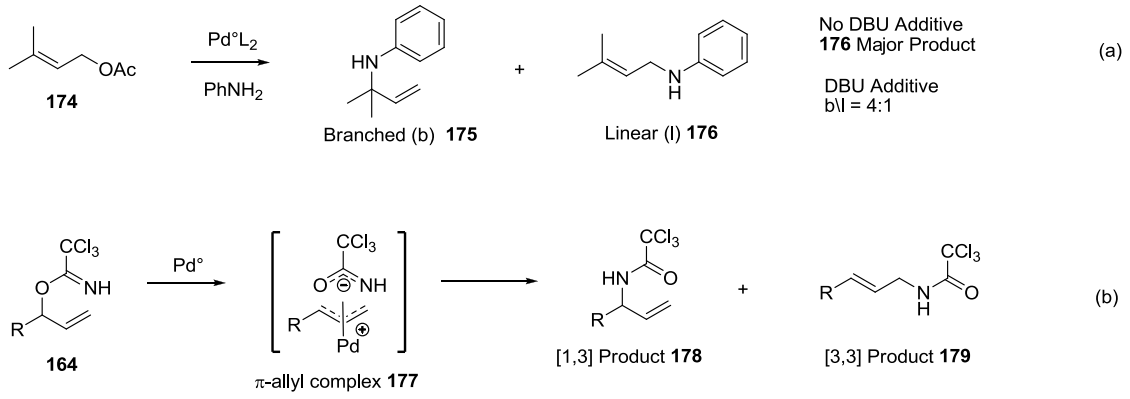

Scheme 2.2 Pd°-catalyzed Aryl Aminations of Allylic Electrophiles

as the major product when DBU is employed to suppress product isomerization (Scheme 2.2a).[92-94] In reactions of allylic acetates, this isomerization is the result of acetic acid byproduct generation which protonates and activates the branched amine product **175** for another ionization and aniline substitution cycle. The amination of branched allylic trichloroacetimidates would avoid this issue because the pKa of the trichloroacetamidate byproduct is similar to DBU at ~12.[16] However, a different issue could arise. Ionization by oxidative addition forms Pd^{II} π-allyl trichloroacetamidate salt **177** (Scheme2.2b). If attack by a neutral unactivated aniline nucleophile (pKa 17 – 24) on the palladium π-allyl complex is slower than attack by the anionic component of the salt, competing [1,3]- and [3,3]-trichloroacetamide rearrangement products could arise (Scheme 2.2b).[27] This could make the d^9 metals iridium and rhodium a better option with trichloroacetimidate electrophiles because they may possibly react via neutral oxidative addition complexes.

Hartwig reported a powerful strategy for preparing branched *N*-arylamines via iridium-catalyzed amination of allylic carbonates **180 - 181** with unactivated anilines (Table 2.1).[95] At the start, this method was the benchmark for our studies as it is applicable to a number of different substrates and aniline nucleophiles providing excellent regio- and enantioselectivity. The method utilizes linear allylic carbonates, neutral anilines and 1 mol% of chiral cyclometalated phosphoramidite catalyst in THF at ambient temperature. 10 mol% of DABCO is required in the reaction for in situ formation of the active iridium catalyst. Electron-deficient, rich and sterically encumbered aniline nucleophiles efficiently react with high yields and selectivities in 2 – 10 h. For example, 4-fluoroaniline **183b** (entry 1) and 4-chloroaniline **183g** (entry 4) resulted in 89 – 90% yield of branched amines **186** and **189** with high regioselectivity (49:1 b/l) and enantioselectivity (94 – 96% *ee*). The reaction of electron-rich aniline **183c** provided similar results (entry 2) with the exception that the reaction was complete in 4 h rather compared with 10 h for electron-deficient anilines **183b** and **183c**. The bulky 2,4,6-trimethylaniline **183e** (entry 5) very efficiently

provided allylic amine **190** in 82% yield, 32:1 b/l ratio and 96% *ee* within 2 h, while *ortho*-bromoaniline (entry 6) only resulted in 66% yield of the desired product **191** in 16 h. The reaction is also amenable to 1-naphthylamine **184** and the secondary cyclic tetrahydroquinoline **185** (entrys 8-9) providing branched amine products in 83 – 89% yield,

Table 2.1 Hartwig's Regio- and Enantioselective Amination of Allylic Carbonates with Anilines

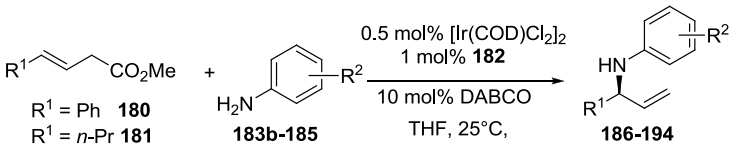

entry	imidates (R^1)	Aniline R^2	time (h)	allylic amine	yield (%)	b/l	*ee* (%)
1	**180**	**183b** 4-F	10	**186**	90	49:1	94
2	**180**	**183c** 4-OMe	4	**187**	91	49:1	95
3	**181**	**183c**	2	**188**	95	19:1	95
4	**180**	**183g** 4-Cl	10	**189**	89	49:1	96
5	**180**	**183e** 2,4,6-Me	2	**190**	82	32:1	96
6	**180**	**183m** 2-Br	16	**191**	66	13:1	94
7	**180**	**183f** N-Me,R^2 = H	--	**192**	–	1:1-4:1	--
8	**180**	**184**	10	**193**	83	32:1	95
9	**180**	**185**	2	**194**	89	32:1	96

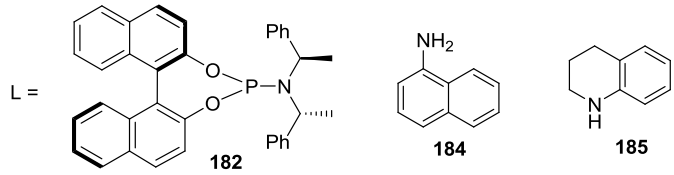

32:1 b/l ratios and 95 – 96% *ee*. On the other hand, Hartwig reports that secondary acyclic *N*-methylaniline **183f** in the iridium-catalyzed reaction provides low ratios (1:1 – 4:1 b/l) of the branched product **192** (entry 7), and therefore does not report yields or enantioselectivity in these reactions.

P. Andrew Evans developed a rhodium-catalyzed amination of branched allylic carbonates that is regioselective and enantiospecific (Table 2.2).[96-98] The method utilizes

Wilkinson's catalyst in combination with trimethyl phosphite as the active complex that delivers good yields of branched allylic aryl amines. The method however, is limited to activated and stabilized anionic nucleophiles, requiring a stabilizing group and a lithiated nitrogen in order to balance nucleophilicity and basicity. The use of neutral aniline in Evan's method provided 10:1 regioselectivity for branched products but in poor to moderate yields.[96] Base treatment of aniline provided a more reactive and basic nucleophile that was poor yielding due attack on rhodium and elimination of organorhodium intermediates. Attenuation of basicity was accomplished by addition of sulfonylphenyl group to the deprotonated aniline nucleophile.

Table 2.2 Evan's Regio- and Stereospecific Allylic Amination of Branched Carbonates

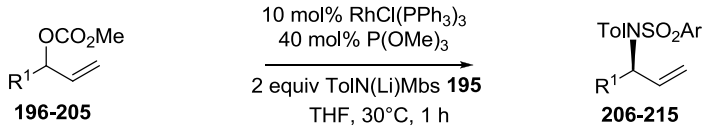

entry	Carbonates (R^1)	allylic amine	yield (%)	b/l
1	**196** Me	**206**	96	>99:1
2	**197** $CH_2{=}CH(CH_2)_3$	**207**	91	46:1
3	**198** $(CH_3)_2CHCH_2$	**208**	94	12:1
4	**199** $(CH_3)_2CH(CH_2)_2$	**209**	89	27:1
5	**200** $PhCH_2$	**210**	86	20:1
6	**201** $PhCH_2CH_2$	**211**	93	90:1
7	**202** $TBSOCH_2$	**212**	83	23:1
8	**203** $BnOCH_2$	**213**	85	8:1
9	**204** Ph	**214**	94	47:1
10	**205** $(CH_3)_2CH$	**215**	---	1:2

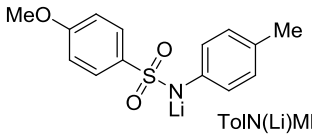

TolN(Li)Mbs **195**

In the reaction, Wilkinson's catalyst and trimethyl phosphite are stirred for 20 min in THF at 30°C. In a separate flask the lithiated **195** is prepared by addition of LiHMDS to *N*-4-methoxybenzenesulfonyltoluidine in a THF/DMF mixture at 30°C for 15 min. The two flasks are then combined via canula and the methyl carbonate electrophile is added via syringe and stirred at 30°C for 1 h. The reaction efficiently provides high yields and regioselectivities of a number of branched allylic amines **206** – **214** (Table 2.2, entries 1 – 9). Aliphatic carbonates **196** – **201** differing in appended substituents and chain lengths were high yielding 86 93% and regioselective (12:1 - >99:1). Even terminal olefin **197** resulted in 91% yield of allylic amine **207** with 46:1 b/l ratio. β-oxy substrates **202** – **203** were effective in the method (entries 7 – 8) as was α-phenyl **204** providing amine **214** in 94% yield and with excellent regioselectivity (Table 2.2, entry 9). The reaction is not compatible with substrates bearing α-branching such as substrate **105** (entry 10), which result predominately in the linear isomer (1:2 b/l).

An important property of Evan's rhodium-catalyzed aryl amination reaction is that it is enantiospecific and not enantioselective. Overall retention of configuration is observed in the products and is thought to proceed via a double inversion process with *enyl* organorhodium intermediates (or a distorted π-allyl) **217** (Scheme 2.3).[99] For example,

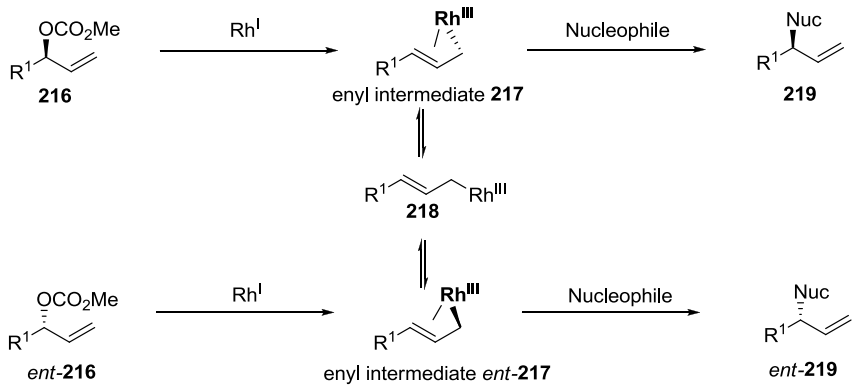

Scheme 2.3 Rhodium-catalyzed Amination Via *Enyl* Intermediates

branched branched carbonate **216** would be displaced with inversion to its respective *enyl* intermediate **217** by rhodium. If isomerization of *enyl* intermediates **217** and *ent*-**217** via linear isomer **218** is sufficiently slow compared to the rate of nucleophilic addition, S_N2' displacement of rhodium by backside attack of the nucleophile would again occur with inversion and exclusive **219** formation. The proposed mechanism is based on studies that compare the reactivity of linear and branched allylic carbonates.[99] If the reaction proceeds through a π-allyl intermediate, the same regioselectivity should be observed regardless of utilization of the branched or linear isomer. However, opposite regioselectivities result suggesting the involvement of different intermediates that template regio- and enantiospecificities in these reactions. This occurs even in the presence of unsymmetrical substitution on the starting carbonates that should favor one isomer over another.

Based on the possible challenges that could be encountered with palladium catalysts and branched allylic trichloroacetimidates and an existing regio- and enantioselective Ir-catalyzed amination using neutral anilines, we selected rhodium metal as catalyst in our investigation. We initiated our studies with branched allylic trichloroacetimidates, Rh(I) catalysts, phosphite ligands and neutral anilines (Scheme 2.4) for the branched selective synthesis of allylic aryl amines.[12]

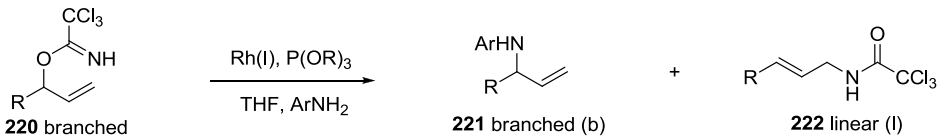

Scheme 2.4 Proposed Strategy for Regioselective Amination

2.1.2 Results and Discussion

The Rh-catalyzed regioselective amination reaction was optimized by changing the rhodium source, the phosphite ligands employed and catalyst loadings (Table 2.3). Utilizing 10 mol % of Wilkinson's catalyst modified with trimethyl phosphite ligand (20 mol %) in the presence of aniline nucleophile **183a** (3 equiv.) at 40 ^{0}C provided the corresponding *N*-arylamines **224** - **225** in a combined 13% yield, with 5:1 regioselectivity

Table 2.3 Optimization for Regioselective Amination

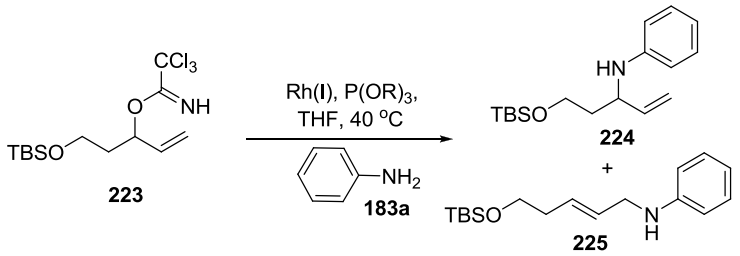

Entry	Rh Source	Rh (mol %)	P(OR)$_3$	P(OR)$_3$ (mol %)	Time (h)	Yield[a]	**224/225** Ratio[b]
1	$RhCl(PPh_3)_3$	10	$P(OMe)_3$	20	24	13 %	5:1
2	$[RhCl(cyclooct)_2]_2$	5	$P(OMe)_3$	20	24	37 %	4:1
3	$[RhCl(COD)_2]_2$	5	$P(OMe)_3$	20	24	39 %	41:1
4	$[RhCl(ethylene)_2]_2$	5	$P(OMe)_3$	20	7	84 %	65:1
5	$[RhCl(ethylene)_2]_2$	5	P(O*i*Pr)$_3$	20	24	23 %	10:1
6	$[RhCl(ethylene)_2]_2$	5	$P(OPh)_3$	20	0.5	95 %	>99:1
7	$[RhCl(ethylene)_2]_2$	2	$P(OPh)_3$	8	0.5	95 %	>99:1
8	$[RhCl(ethylene)_2]_2$	1	$P(OPh)_3$	4	0.5	96 %	>99:1
9	$[RhCl(ethylene)_2]_2$	1	None	-	12	11 %	10:1

[a] Reported based on GC purity of isolated products.

[b] The ratio was determined by GC in the crude reaction mixture.

favoring the branched product **224** (entry 1). The branched product **224** was obtained in higher yield and regioselectivity (65:1) in the presence of 5 mol% of and 20 mol % of $P(OMe)_3$ (entry 4). The use of a more sterically hindered ligand, P(O*i*Pr)$_3$, was detrimental to the reaction (entry 5), while use of a more electron withdrawing ligand, $P(OPh)_3$, significantly shortened the reaction time and improved both the yield (84% → 95%) and

regioselectivity (65:1 → 99:1) (entry 6). Lowering the metal and ligand loadings further did not diminish the yield or the regioselectivity (entries 7 - 8). Omission of phosphite ligand resulted in low regioselectivity and yield over 12 hours (entry 9). Compared to other systems, this chemistry provides the branched product such as **224** with higher regioselectivity. For instance, reaction of allylic carbonate with **183a** in the presence of the Wilkinson's catalyst provided the branched product in poor yield and with 10:1 regioselectivity.[96] Under iridium conditions, reaction of allylic carbonate with **183a** provided the products with 13:1 regioselectivity.[100]

With the initial optimal conditions in hand, a variety of aniline derivatives **183a - f** were investigated with allylic trichloroacetimidates **223, 226,** and **227** (Table 2.4). Branched *N*-arylamines were obtained in good yield and with excellent regioselectivity. Importantly, the Overman rearrangement products were not observed in these reactions. The observed reaction time for electron-rich aniline **183c** was longer than more electron-deficient nucleophiles in the allylic amination reaction (entry 2). This is likely due to the binding of rhodium metal to both the nitrogen and oxygen groups of the products **223c** and **227c**, resulting in slow turnover rates of the rhodium catalyst. The larger *t*-butyldiphenylsilyl group in product **226c** blocks chelation by rhodium at oxygen resulting in shorter time to completion. The current method is also feasible with sterically hindered anilines **183d - f** (entries 4 - 6). Reaction of **223** with secondary aniline **183f** provided the *N*-arylamine **223f** with 60:1 regioselectivity (entry 6). Under iridium conditions, reaction of allylic carbonates with secondary anilines such as **183f** provided the products with poor regioselectivities (1:1 → 4:1).[95]

The Rh-catalyzed regioselective allylic amination also works well with β-substituted allylic trichloroacetimidates **228-230** (Table 2.5). In the presence of anilines **183a - f**, the desired products **228 – 230 a - f** were formed with excellent regioselectivity (entries 1 - 6). As expected, reaction of **228** and **229**, containing the OTBS and OBn at the β- position provided the products **228c** and **229c** in much lower yields (entry 3). These

Table 2.4 Rhodium-catalyzed Amination of Allylic Trichloroacetimidates with Anilines **183a - f**

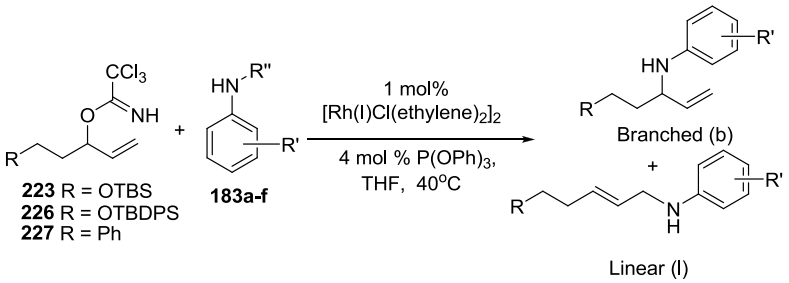

	Anilines	Products		Time (h)	Yield[a]	b/l Ratio[b]
1	**183a**	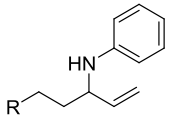	**226a** R = OTBDPS	0.5	94%	>99:1
			227a R = Ph	0.5	97%	>99:1
2	**183b**	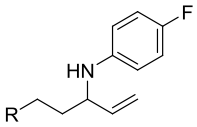	**223b** R = OTBS	3.5	96%	>99:1
			226b R = OTBDPS	2	99%	>99:1
			227b R = Ph	0.5	94%	>99:1
3	**183c**	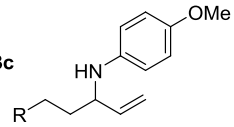	**223c** R = OTBS	9	72%	>99:1
			226c R = OTBDPS	0.5	93%	>99:1
			227c R = Ph	3	93%	>99:1
4	**183d**	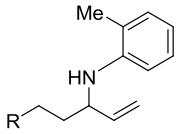	**223d** R = OTBS	4	94%	>99:1
			226d R = OTBDPS	4	83%	>99:1
			227d R = Ph	7	80%	>99:1
5	**183e**	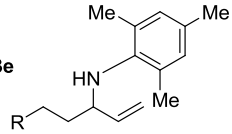	**223e** R = OTBS	4	85%	70:1
			226e R = OTBDPS	4[c]	83%[c]	90:1[c]
			227e R = Ph	1[c]	83%[c]	91:1[c]
6	**183f**	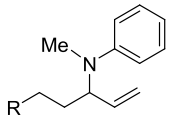	**223f** R = OTBS	9	86%	60:1
			226f R = OTBDPS	4[c]	70%[c]	>99:1[c]
			227f R = Ph	1[c]	99%[c]	83:1[c]

[a] Reported based on GC purity of isolated products.

[b] The ratio was determined by GC in the crude reaction mixture.

[c] The reaction with 5 mol% $[RhCl(ethylene)_2]_2$ and 20 mol% $P(OPh)_3$ at 25 °C.

Table 2.5 Rhodium-catalyzed Amination of β-substituted Imidates **228 - 230**

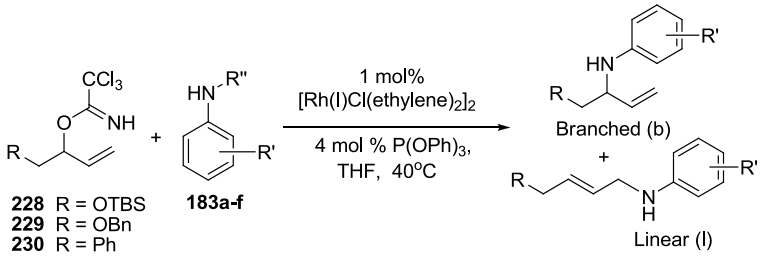

Entry	Anilines	Products		Time (h)	Yield[a]	b/l Ratio[b]
1	**183a**	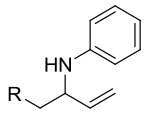	**228a** R = OTBS	1	95%	>99:1
			229a R = OBn	0.5	99%	>99:1
			230a R = Ph	2	94%	>99:1
2	**183b**	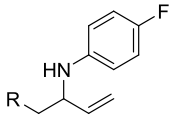	**228b** R = OTBS	1	91%	>99:1
			229b R = OBn	0.5	96%	>99:1
			230b R = Ph	2	92%	>99:1
3	**183c**	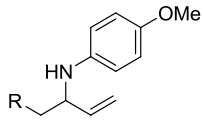	**228c** R = OTBS	8	20%	>99:1
			229c R = OBn	6	47%	>99:1
			230c R = Ph	2	80%	>99:1
4	**183d**	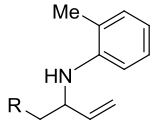	**228d** R = OTBS	2	94%	>99:1
			229d R = OBn	3	97%	>99:1
			230d R = Ph	3	87%[c]	> 99:1[c]
5	**183e**	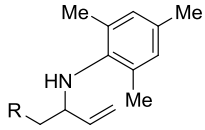	**228e** R = OTBS	2	94%	>99:1
			229e R = OBn	3	87%	>99:1
			230e R = Ph	1[c]	93%[c]	80:1[c]
6	**183f**	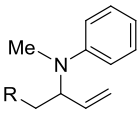	**228f** R = OTBS	2	94%	>99:1
			229f R = OBn	3	99%	32:1
			230f R = Ph	1[c]	98%[c]	30:1[c]

[a]Reported based on GC purity of isolated products.

[b] The ratio was determined by GC in the crude reaction mixture.

[c] The reaction with 5 mol% $[RhCl(ethylene)_2]_2$ and 20 mol% $P(OPh)_3$ at 25 °C.

results are consistent with what had been observed with substrate **223** (Table 2.4). Reaction of β-phenyl allylic trichloroacetimidate **230** with sterically demanding anilines **183e - f** required higher catalyst loading (entries 5-6). Overall, our reaction is more regioselective than other systems. For instance the reaction of the allylic carbonate derivative of **228** (**202**, Table 2.2) with TolN(Li)Mbs provided the amination product with 23:1 regioselectivity. Similarly, reaction **200** and **203** (Table 2.2), carbonate derivatives of **230** and **229** provided the amination products with regioselectivity of 20:1 and 8:1, respectively.[97]

Allylic carbonates containing substitutents at the β-position with respect to the carbonate leaving group are known to be challenging substrates, and they often provide amination products with poor regioselectivity in favor of linear products. [96, 97] Subjecting β-branched cyclohexyl imidate **231** to optimized reaction conditions with aniline **183a**

Table 2.6 Amination Reaction Optimization of β-Branching Imidate **231**

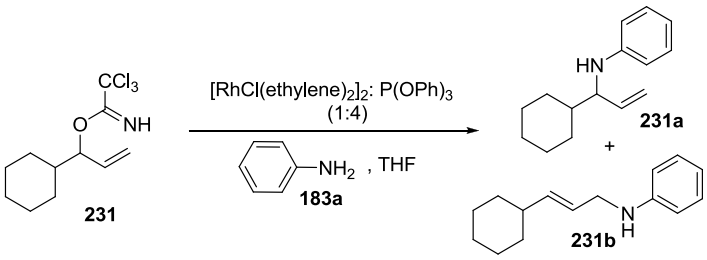

Entry	Mol% [Rh]	Time (h)	Temperature	Conversion[a]	**231a/b** Ratio[b]
1	1	4	40 °C	33%	1:1
2	2	3	40 °C	70%	5:1
3	5	2	40 °C	>99%	18:1
4	5	4	25 °C	>99%	53:1
5	5	21	0 °C	>99%	73:1

[a] Reported based on GC conversion.

[b] The ratio was determined by GC in the crude reaction mixture.

resulted in 33% conversion and a 1:1 mixture of branched aniline product **231a** and linear aniline product **231b** (entry 1, Table 2.6). Increasing the catalyst loadings at 40°C (entries 2 and 3) resulted in complete conversion and b/l ratios of 18:1. Lowering the reaction temperatures to 25°C (entry 4) and 0°C (entry 5) increased the time for complete conversion and resulted in higher regioselectivities (b/l = 18:1 and 73:1 respectively). Nucleophilic attack on hindered substrate **231** may be rate-limiting. At extended reaction

Table 2.7 Rhodium-catalyzed Amination of α-substituted Imidates **231-233**

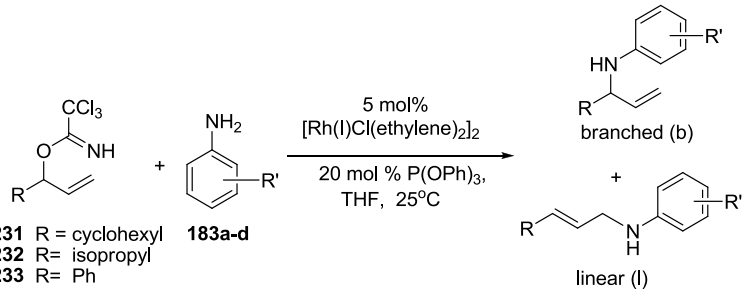

Entry	Anilines	Products		Time (h)	Yield[a]	b/l Ratio[b]
1	**183a**	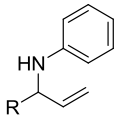	**231a** R = Cyclohexyl	4	96%	53:1
			232a R = Isopropyl	4	94%	31:1
			233a R = Ph	6	75%	90:1
2	**183b**	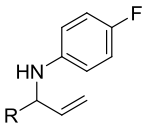	**231b** R = Cyclohexyl	4	91%	42:1
			232b R = Isopropyl	3	94%	36:1
			233a R =Ph	6	85%	19:1
3	**183c**	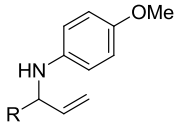	**231c** R = Cyclohexyl	4	93%	42:1
			232c R = Isopropyl	4	88%	45:1
			233a R = Ph	1	84%	39:1
4	**183d**	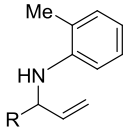	**231d** R = Cyclohexyl	4	70%	12:1
			232d R = Isopropyl	7	73%	14:1

[a] Reported based on GC purity of isolated products.

[b] The ratio was determined by GC in the crude reaction mixture.

times and with lower catalyst loadings, functional catalyst may be consumed resulting in low yields and decreased regioselectivity for branched product due to increases in the uncatalyzed background reaction. At lower temperatures, either the rate of the background reaction or the rate of attack at the terminus of an equilibrating organorhodium intermediate decreases.

With optimized conditions in hand, α-substituted allylic trichloroacetimidates **231** - **233** were aminated with anilines **183a** - **d** in the presence of 5 mol % $[RhCl(ethylene)_2]_2$ and 20 mol % $P(OPh)_3$ at 25 ºC, providing the branched products as the major isomers (Table 2.7). The regioselectivity decreased as the aniline became more sterically hindered (entry 4). Under the Wilkinson's catalyst modified with trimethyl phosphite conditions, reaction of isopropyl allylic carbonate **205** (Table 2.2) derivative of **232** with TolN(Li)Mbs provided the linear product as the major isomer.[96, 97]

Trichloroacetimidate donors are widely used in carbohydrate chemistry and trichoroacetimidate electrophiles have become popular alkylating agents. They are generally activated with Lewis acids such as BF_3-OEt_2, TMSOTf, TBSOTf, and Tf_2O. To determine if rhodium acts as a Lewis acid to activate the trichloroacetimidate group, we investigated reaction of secondary trichloroacetimidate **223** with aniline **183a** in the presence of 2 mol % of BF_3-OEt_2 at 40 ºC (Table 2.8). At 15 h, GC analysis showed that the reaction reached 99% conversion with a 1:1 mixture of the branched product **224** and the linear product **225**, a stark difference when compared to the rhodium-catalyzed reaction. In addition, linear (*E*)-imidate **235** and linear (*Z*)-imidate **236** were subjected to rhodium and lewis acid catalyzed amination reactions. Under lewis acid mediation, mainly the (*Z*)-linear isomer **234** was observed after complete conversion (b/l = 1:5 – 1:9). After 21 hours at 40°C in the presence of rhodium, linear imidates **235** and **236** reached 65 – 79% conversion and again resulted in the (*Z*)-linear **234** as the major product. Some comments should be made here. First, the vast difference in reactivity of the Lewis acid and metal-catalyzed reactions of branched imidate **223** suggests that rhodium is not acting

Table 2.8 Lewis Acid and Rhodium-catalyzed Amination of Imidates

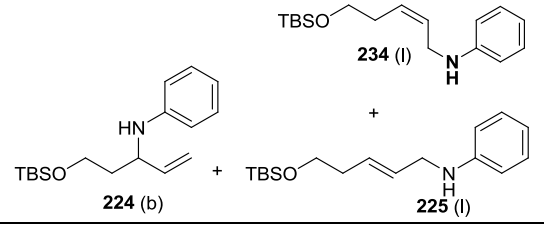

		Branched (b)		Linear (l)
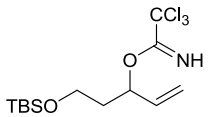 **223**	Lewis Acid Conditions 15h, 99% (GC)	1	:	1 (**225**/**234** = >99:1)
	Rhodium (I) Conditions 0.5h, 96%	>99	:	1 (**225**/**234** = >99:1)
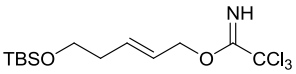 (*E*)-Linear **235**	Lewis Acid Conditions 6h, 99% (GC)	1	:	5 (**225**/**234** = 1:28
	Rhodium (I) Conditions 21h, 79% (GC)	1	:	14 (**225**/**234** = 1:2)
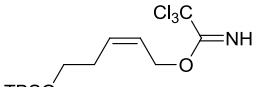 (*Z*)-Linear **236**	Lewis Acid Conditions 8h, 99% (GC)	1	:	9 (**225**/**234** = 1:29)
	Rhodium (I) Conditions 21h, 65% (GC)	1	:	17 (**225**/**234** = 1:3)

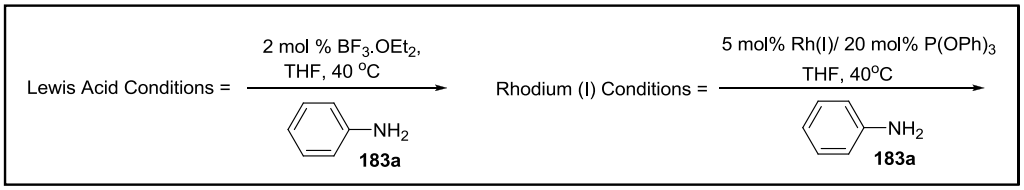

primarily as a Lewis acid. Second, the reaction of linear trichloroacetimidates react very differently in the rhodium-catalyzed reaction. The fact that the reactions of linear imidates are slower and primarily result in linear products supports our initial hypothesis that branched imidates are more accessible for rapid ionization. Similar product ratios under $BF_3 \cdot OEt_2$ and rhodium-catalyzed control suggest that rhodium may act as a Lewis acid when linear imidates are utilized.

To compare branched allylic trichloroacetimidates versus commonly employed electrophiles under our rhodium conditions, reactions of allylic methyl carbonate **237** and

acetate **238** were attempted with aniline **183a** (Scheme 2.5). The amination products were not observed in these control experiments even if the reactions had been stirring at 40 °C for 12 h, suggesting that both allylic carbonate **237** and acetate **238** are less reactive than secondary allylic trichloroacetimidate **223**.

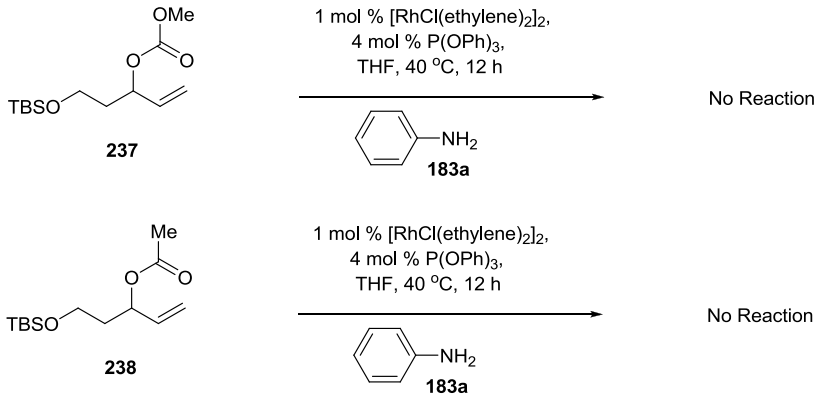

Scheme 2.5 Studies with Allylic Carbonates and Acetates

In a pivotal control study, an enantiomerically enriched trichloroacetimidate (*S*)-**239** was subjected to reaction conditions to gain understanding into the stereochemical outcome and perhaps some mechanistic insight regarding our newly developed rhodium-catalyzed amination (Scheme 2.6). The reaction of (*S*)-**239** did not progress enantiospecifically, instead resulting in nearly racemic product **242** (Scheme 2.6).[12] This result is opposite to other transition-metal catalyzed allylic substitution methodologies, which provide products with net retention of stereochemistry.[96-98, 101, 102]

The outcome of the experiment illustrated in Scheme 2.6 can be rationalized by comparing the relative rates of equilibration of organorhodium complexes **241** and *ent*-**241** and nucleophilic attack by aniline nucleophile (Scheme 2.7). The rhodium catalyst coordinates to both the imidate nitrogen and the alkene of (*S*)-**239** forming rhodium-olefin complex **240**, which subsequently undergoes ionization to generate π-allylrhodium **241**.

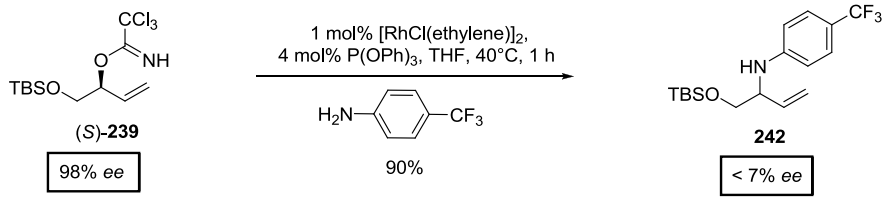

Scheme 2.6 Enantiospecific Study with Enantioenriched (*S*)-**239**

Nucleophilic attack of the aniline nucleophile onto the organorhodium intermediate **241** at the internal more substituted carbon, provides the desired amination product (*R*)-**242**. We propose that the rate of aniline substitution (k_1 and k_2) is much slower than that of π-σ-π interconversion, resulting in racemization in the amine product **242**.

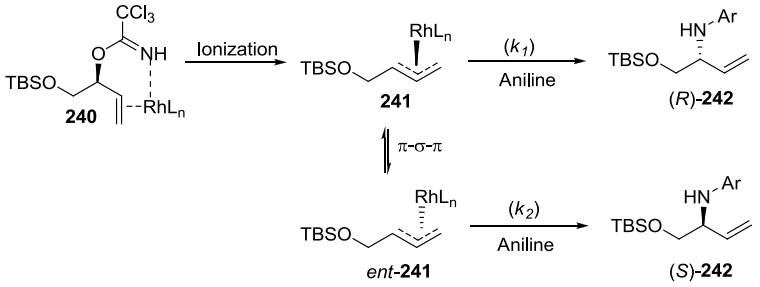

Scheme 2.7 Proposed Mechanism for Racemization of (*S*)-**239**

The results of this study set the stage for development of a regioselective and enantioselective amination reaction.[103, 104] The hypotheses that led to this discovery and the outcomes of this work are described in detail in chapters 3 and 4.

2.1.3 Conclusion

In summary, a rhodium-phosphite complex was found to be an efficient catalyst for the regioselective amination of secondary allylic trichloroacetimidates with unactivated,

neutral primary and secondary anilines providing *N*-arylamines in high yield and with excellent regioselectivity for branched products.[12] This amination reaction is applicable to acyclic secondary aniline and β-branching allylic trichloroacetimidates, reactions that resulted in low regioselectivity with previously reported methods.[96, 97] Control studies show that our rhodium-catalyzed amination method is unique. Allylic acetates and carbonates are unreactive, and linear imidates are less reactive and provide primarily linear amination products. These studies support the requirement of the chelating imidate nitrogen and an accessible olefin for rapid ionization. Distinct from other amination methods where the reaction proceeds with overall retention, this reaction proceeds with a significant amount of racemization.

2.2 Tertiary Allylic Trichloroacetimidates: Rhodium-Catalyzed Preparation of α,α-disubstituted Amines

2.2.1 Background

With the development of a highly regioselective amination method for secondary trichloroacetimidate substrates with a variety of aniline nucleophiles, we set out to apply this reaction to tertiary trichloroacetimidates for the regioselective preparation of α,α-disubstituted allylic aryl amines.[13] Approaches for synthesis of α,α-disubstituted amines are limited, usually involving the addition of organometallic reagents to ketamines[105-108] or the Pd^{II}-catalyzed Overman rearrangement of more nucleophilic *N*-PMP trihaloacetimidates.[109] Transition-metal catalyzed amination of allylic carbonates or acetates has been utilized to prepare α,α-disubstituted allylic amines. Palladium catalysts in combination with 1,1-dimethyl-1-propenyl acetate and alkyl amines selectively favor the thermodynamically formed linear products.[92, 93, 110] As discussed earlier, branched products, α,α-disubstituted amines, can be formed as the major isomer when DBU (1 equiv)

is used to suppress product isomerization (Scheme 2.8a).[93] Iridium catalysis of allylic acetates with alkyl amines also provides α,α-disubstituted amines in high yield and regioselectivity.[100] In these palladium and iridium amination methods (Scheme 2.8a - b), the only aryl amine nucleophile reported is aniline. A more general method for use of aryl amine nucleophiles is the iron-catalyzed allylic amination reaction reported by Plietker (Scheme 2.8c).[111] The method works with *para*- and *meta*-substituted anilines, providing α,α-disubstituted allylic aryl amines in good yield and with excellent levels of regioselectivity. *Ortho*-substituted anilines are not tolerated in the iron-catalyzed method and do not result in the desired allylic amine products.[111]

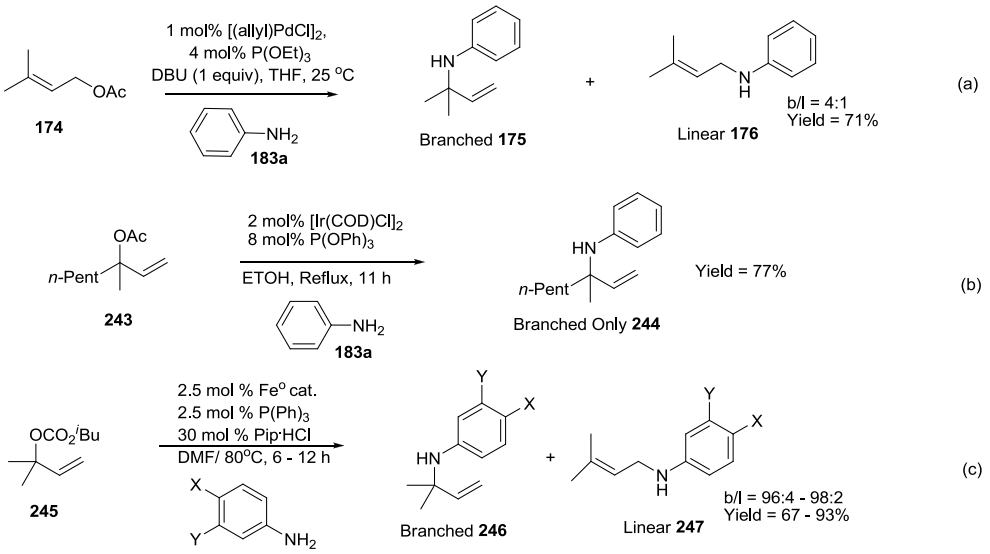

Scheme 2.8 TM-Catalyzed Synthesis of α,α-disubstituted Arylamines

Due to limited reports detailing transition-metal catalyzed preparation of α,α-disubstituted allylic aryl amines, we were excited to apply our method to this application. However, we anticipated some potential challenges because tertiary trichloroacetimidates are more prone to undergo Overman rearrangement to generate trichloroacetamide **252** and

ionize more readily leading to increased elimination forming diene **251** compared to secondary allylic trichloroacetimidates (Scheme 2.9).

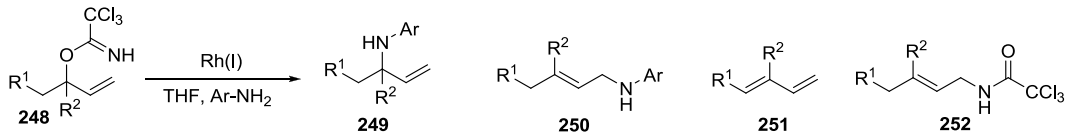

Scheme 2.9 Proposed Regioselective Amination of Tertiary Trichloroacetimidates

2.2.2 Results and Discussion

We commenced by investigating the amination reaction of tertiary allylic trichloroacetimidate **253** with aniline **183a** (Table 2.9).[13] Under previous rhodium optimal conditions, α,α-disubstituted aryl amine **175** was isolated in moderate yield and with 14:1 regioselectivity (entry 1). Increasing the catalyst loading improved both yield and regioselectivity (entries 2 and 3). Switching to a more electron withdrawing phosphite ligand (entry 4), $(4\text{-F-PhO})_3P$, improved both yield (69% → 86%) and regioselectivity (18:1 → 31:1). Although diene ligands were inefficient in the rhodium catalyzed amination reactions with the secondary allylic trichloroacetimidates, cyclooctadiene and norbornadiene rhodium dimers efficiently catalyze the allylic amination of tertiary trichloracetimidate **253** (entries 5-9) within 30 min to provide α,α-disubstituted aryl amine **175** in high yield (84% - 90%) and regioselectivity (50:1 - 62:1). Under these conditions, both rearrangement and elimination products (e.g. **252** and **251**, Scheme 2.9) were not observed.

Compared to other methods, our approach provides allylic aryl amine **175** with higher regioselectivity. For instance, reaction of allylic acetate with **174** (Scheme 2.8) in the presence of $[(\text{allyl})\text{PdCl}]_2\text{-P(OEt)}_3$ complex provided **175** with 4:1 regioselectivity.[93] In

another case, reactions of both branched and linear allylic alcohols with **183a** and $Pd(acac)_2$-PPh_3 complex provided linear aryl amine **176** as the major product.[112]

Table 2.9 Rhodium-catalyzed Amination Optimization Studies of Tertiary Trichloroacetimidate **253**[a]

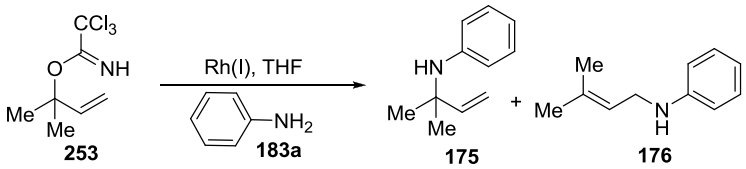

Entry	Rh Catalyst	Loading (mol %)	Temp (°C)	Time (h)	Yield[b] (%)	**175**/**176**[c] Ratio
1	$RhCl(P(PhO)_3)_3$	2	40	6	45	14:1
2	$RhCl(P(PhO)_3)_3$	4	40	4	60	13:1
3	$RhCl(P(PhO)_3)_3$	10	40	2	69	18:1
4	$RhCl(P(F\text{-}4\text{-}PhO)_3)_3$	10	40	2	86	31:1
5	$[RhCl(COD)_2]_2$	5	40	0.5	84	54:1
6	$[RhCl(NBD)]_2$[d]	5	40	0.5	89	50:1
7	$[RhCl(NBD)]_2$[d]	5	25	0.5	87	62:1
8	$[RhCl(NBD)]_2$[d]	2.5	25	0.5	90	62:1
9	$[RhCl(NBD)]_2$[d]	1	25	0.5	87	56:1

[a] All reactions were conducted at 0.2 M in THF with 1 equiv of **253** and 3 equiv of **183a**.

[b] Isolated yields.

[c] The ratio was determined by GC in the crude reaction mixture.

[d] NBD = Norbornadiene

With optimized reaction conditions in place, the scope was examined with a wide range of aromatic amines **183b - n** (Table 2.10). Good to excellent yields and regioselectivities (77 – 88%, 55:1 - >99:1 b/l) were obtained with both the electron-rich *para*-methoxyaniline **183c** (entry 2) and the electron-withdrawing 4-substituted anilines including 4-fluoro **183b**, 4-chloro **183g**, 4-pinacol boronate ester **183h** and 4-acetyl **183i** (entries 1-4). Aryl amines **183j - k** bearing *meta*-carbonyl functionality also provided α,α-disubstituted allylic amines **253j - k** (entries 5 and 6) in good yield (87% and 84%) and

Table 2.10 Survey of Various Anilines with Tertiary Trichloroacetimidate **253**

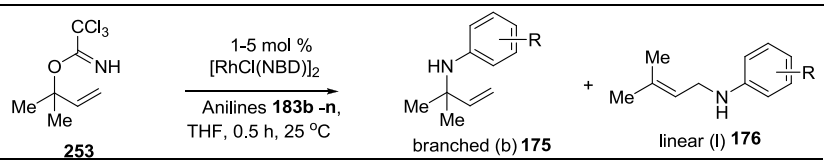

Entry	Anilines	Products	Yield(%)[b]	b/l[c]
1	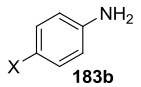 **183b** **183g**	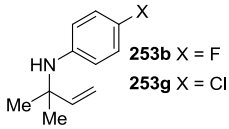 **253b** X = F **253g** X = Cl	81 85	86:1 >99:1
2	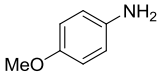 **183c**	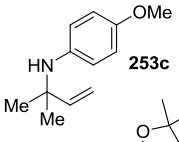 **253c**	84	66:1
3	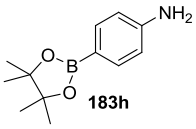 **183h**	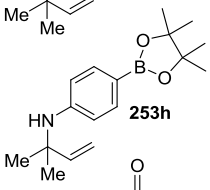 **253h**	77	90:1
4	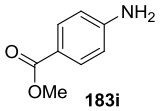 **183i**	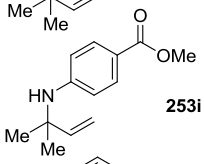 **253i**	88	55:1
5	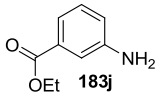 **183j**	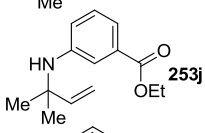 **253j**	87	98:1
6	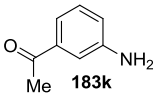 **183k**	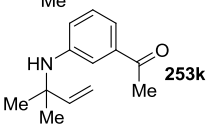 **253k**	84	>99:1
7	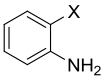 **183d** X =Me **183l** X = isopropyl	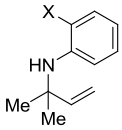 **253d** X = Me **253l** X = *i*pr	95 86	>99:1 34:1
8	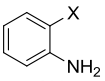 **183m** X = Br **183n** X = CO_2Me	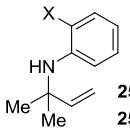 **253m** X = Br **253n** X = CO_2Me	67 63	24:1 33:1
9	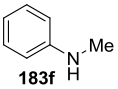 **183f**	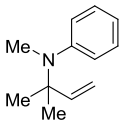 **253f**	85	15:1

[a]All reactions were conducted with 1-5 mol% $[RhCl(NBD)]_2$, 0.2 M in THF.

[b] Isolated yields.

[c] b/l ratio determined by GC.

regioselectivity (b/l = 98:1 and >99:1). The reaction catalyzed by $[RhCl(NBD)]_2$ is very tolerant of *ortho*-substitution on the aniline nucleophiles (entries 7 and 8), with bromo, methyl ester, methyl and even isopropyl functionality providing 63 – 95% yields of 2-substituted aniline amines with high regioselectivities (24:1 - >99:1). This class of aniline nucleophile does not result in allylic aniline products under iron-catalyzed conditions.[111] Notably, this method is also feasible with challenging secondary aniline **183f** (Table 2.10, entry 9), and the corresponding allylic amine **253f** was isolated in 85% yield and with 15:1 regioselectivity. Here we are used a tertiary electrophile with a sterically encumbered secondary acyclic aniline nucleophile, and recall that this resulted in low regioselectivity with secondary carbonates (1:1 – 4:1 b/l) in a previous report.[95]

Next, we broadened the scope and showed that tertiary allylic imidates **254** - **257** (Table 2.11) are suitable substrates under rhodium reaction conditions, generating α,α-disubstituted allylic aryl amines in good yields and with excellent levels of regioselectivity. These tertiary allylic trichloroacetimidates are of three types. **254** and **255** contain a β-oxygen substituent with respect to the newly formed quaternary center. Trichloroacetimidates **256** and **257** do not possess an ethereal oxygen but monoterpenoid substrate **257** does contain an additional olefin that potentially could bind to the rhodium catalyst. Reactions of aniline **183a**, 4-fluoroaniline **183b** and anisidine **183c** provided 72–96% yields and moderate to high regioselectivities (11:1 - >99:1) for the branched amine products with all substrates (Table 2.11, entries 1 – 3). Importantly, the presence of an additional olefin in **257** did not slow or alter the course of the reaction. Aniline nucleophile **183h** with *para*-boronic acid ester substitution also resulted in good yields (63 – 81%) and moderate to high b/l ratios (entry 4) for all substrate types, although the product could not be isolated cleanly in the reaction of phenyl imidate **256**. Tertiary substrates **255** and **256** possessing β-oxygen functionality reacted efficiently with electron-rich anisidine **183c** (72 - 92%, >99:1 b/l) whereas the comparable secondary trichloroacetimidates **228** and **229** (Table 2.5) provided low yields of the branched amines (20 -47%, >99:1). In the amination

Table 2.11 Survey of Tertiary Allylic Acetimidates

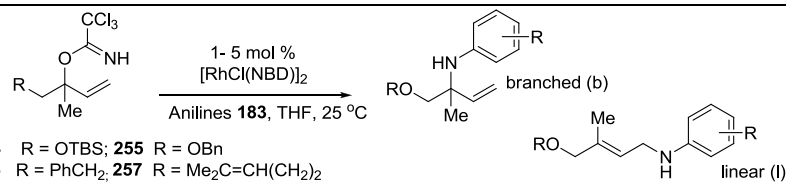

254 R = OTBS; **255** R = OBn
256 R = $PhCH_2$; **257** R = $Me_2C{=}CH(CH_2)_2$

Entry	Anilines	Products	Yield(%)[b]	b/l[c]
1	**183a** 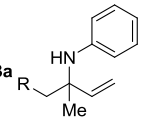	**254a** R = OTBS **255a** R = OBn **256a** R = $PhCH_2$ **257a** R = $Me_2C{=}CHCH_2$	95 90 84 95	>99:1 >99:1 11:1 14:1
2	**95b** 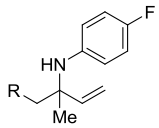	**254b** R = OTBS **255b** R = OBn **256b** R = $PhCH_2$ **257b** R = $Me_2C{=}CHCH_2$	90 87 96 85	>99:1 >99:1 12:1 18:1
3	**183c** 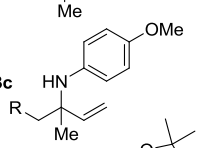	**254c** R = OTBS **255c** R = OBn **256c** R = $PhCH_2$ **257c** R = $Me_2C{=}CHCH_2$	92 72 95 73	>99:1 >99:1 12:1 25:1
4	**183h** 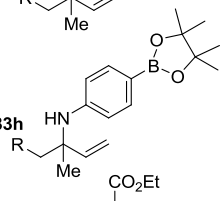	**254h** R = OTBS **255h** R = OBn **257h** R = $Me_2C{=}CHCH_2$	81 63 81	>99:1 >99:1 23:1
5	**183j** 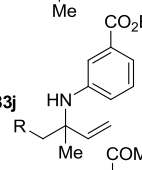	**254j** R = OTBS **255j** R = OBn **257j** R = $Me_2C{=}CHCH_2$	90 71 93	>99:1 62:1 72:1
6	**183k** 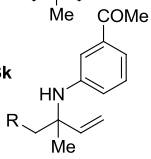	**254k** R = OTBS **255k** R = OBn **257k** R = $Me_2C{=}CHCH_2$	94 64 95	>99:1 61:1 52:1
7	**183d** 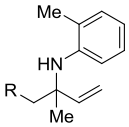	**254d** R = OTBS **255d** R = OBn	90 88	>99:1 >99:1
8	**183m** 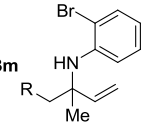	**254m** R = OTBS **255m** R = OBn	69 95	>99:1 64:1
9	**183f** 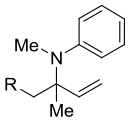	**254f** R = OTBS	78	62:1

[a] All reactions were conducted at 25 °C at 0.2 M in THF, 1 equiv of allylic imidate and 3 equiv of aniline.

[b] Yields are isolated values.

[c] The b/l ratio was determined by GC

reactions of tertiary imidates, bidentate chelation of the product by rhodium near a bulky quaternary center is presumably less feasible, allowing ample catalyst turnover. It is also notable that allylic amination reactions of tertiary imidates **254** and **255** bearing an oxygen substituent at the β-position results in higher branched to linear ratios compared to tertiary imidates **256** and **257**, suggesting that the proximal ether oxygen provides additional chelation control for increased regioselectivity. For example, the benzyl and TBS protected alcohol imidates in entries 1 – 4 (Table 2.11) provide products in >99:1 regioselectivity, but the products of **256** and **257** are isolated with 12:1 – 25:1 b/l ratios. It is interesting that the regioselectivities in reactions using *meta*-substituted ethyl ester **183j** and acetyl **183k** anilines (Table 2.11, entries 4 and 5) are not as dependant on the substrate, where benzyloxy products **255j** and **k** were isolated in 64 – 71% yield and 61:1 – 62:1 b/l ratio and monoterpenoid **257j** and **k** were prepared in 93 – 95% yield and with 52:1 – 72:1 regioselectivity.

The generality of the rhodium-catalyzed amination method was demonstrated with *ortho*-substituted and secondary acyclic *N*-methylanilines. Again these are challenging nucleophiles that have failed to provide satisfactory results in previous reports.[95, 111] In our reaction, *ortho*-toluidine **183d** and 2-bromoaniline **183m** are effective nucleophiles with β-TBSO and BnO substrates providing aniline products in 69 – 95% yield and with 64: -->99:1 b/l ratios (Table 2.11, entries 7 and 8). The reaction of sterically hindered *N*-methylaniline **183f** with tertiary allylic imidate **254** (Table 2.11, entry 9), containing OTBS at the β-position resulted in 78% yield of a b/l ratio of 62:1. Conversely, the reaction of 1,1-dimethyl-2-propenyl imidate **253** (Table 2.10, entry 9) with the same nucleophile was isolated with 15:1 regioselectivity, highlighting the importance of β-oxygen functionality in the reaction of sterically encumbered anilines and substrates. Importantly, in all of these studies with tertiary trichloroacetimidates rearrangement products are not observed.

The *N*-1,1-dimethyl-2-propenyl indoles and derivatives are structural motifs found in biologically active natural products.[113] These compounds are commonly prepared via a

multi-step sequence involving *N*-propargylation of indoline, oxidation to indole and partial hydrogenation of alkyne to the alkene.[113] A direct reverse isoprenylation of indole using large excess of reagents has been described.[114] Transition-metal catalyzed ring closure of

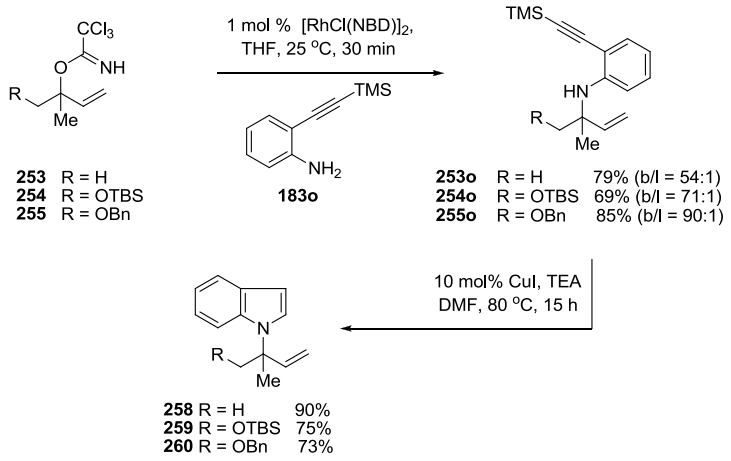

Scheme 2.10 Preparation of Isoprenylated Indoles

2-alkynyl anilines could potentially provide access to 1,1-disubstituted indoles;[115] thus we reasoned that allylic amination of tertiary trichloroacetimidates (Scheme 2.10) in the presence of 2-((trimethylsilyl)ethynyl) aniline and subsequent ring closure would result in an efficient 2-step synthesis of varied reverse prenylated indoles. Aniline **183o** possessing an *ortho*-alkynyl group could prove to be problematic in the amination step due to hinderance and/or introduction of another coordination site for the rhodium metal catalyst. Although there were these potential challenges, tertiary trichloroacetimidates **253**, **254** and **255** (Scheme 2.10) were subjected to optimized amination conditions with aniline **183o** resulting in the allylic aryl amine products **253o**, **254o** and **255o**, respectively, in good yield (69% - 85%) and with excellent levels of regioselectivity (54:1 - 90:1). These branched aryl amine products subsequently cyclized to the corresponding reverse prenylated indoles **258**, **259**, and **260** (Scheme 2.10) in high yield after treatment with CuI at 80^0C for 15 h.[13]

Having successfully applied our rhodium-catalyzed amination method to tertiary trichloroacetimidate electrophiles for the synthesis of α,α-disubstituted allylic aryl amines, I conducted a few more studies to gain understanding of the mechanism. Tertiary electrophiles are more easily ionized so we wanted to determine if reactivity would parallel previous control studies with secondary trichloroacetimidates (Table 2.8 and Scheme 2.5).[12] A Lewis acid study in the presence of aniline nucleophile was conducted with imidate **253** (Scheme 2.11a). As expected, the reaction was much faster (1 h) than the comparable reaction with secondary trichloroacetimidates (15 – 21 h, Table 2.8) and products **175** and **176** were prepared with low regioselectivity (1:3 b/l), again providing

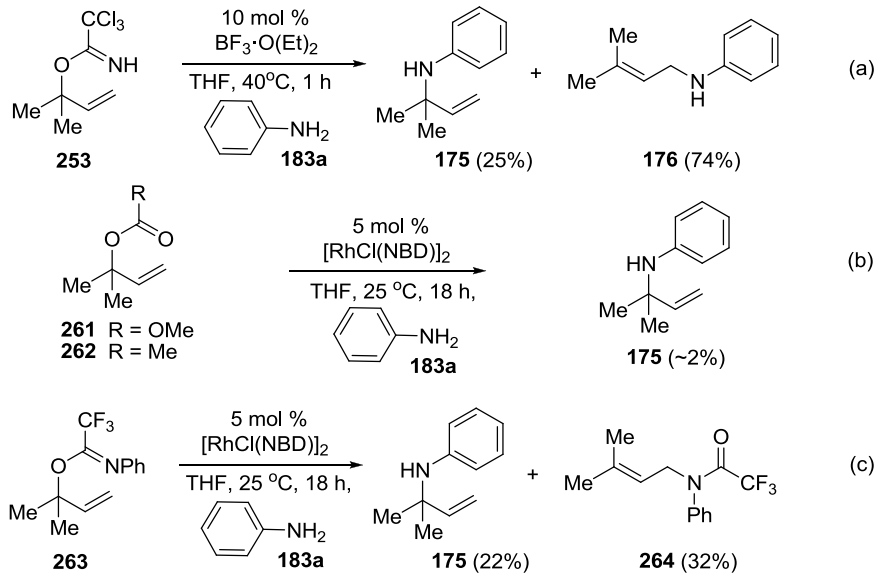

Scheme 2.11 Control Studies with Tertiary Electrophiles

evidence that the rhodium catalyst is not simply acting as a Lewis acid. Allylic carbonate **261** and acetate **262** (Scheme 2.11a) derivatives of trichloroacetimidate **253** were prepared and subjected to our reaction conditions (Scheme 2.11b). Although the starting materials were completely consumed in this case, less than 2% yield of the desired allylic amination

product **175** was isolated after 18 h. In a new experiment, the less basic *N*-phenyl trifluoroacetimidate derivative **263** (Scheme 2.11c) was prepared and subjected to rhodium conditions. This reaction resulted in only 22% yield of the desired branched allylic amine product **175** and for the first time in our studies, 32% of the rearrangement product **264**. In accordance with our previous studies,[12] these three studies suggest that the strongly coordinating nitrogen atom of the trichloroacetimidate leaving group is a required component for bidentate chelation by the rhodium catalyst for efficient allylic amination.

2.2.3 Conclusion

In summary, we have sucessfully applied our rhodium-catalyzed reaction to tertiary allylic trichloroacetimidate electrophiles. Optimized conditions consisting of 1-5 mol% of NBD dimer catalyst at ambient temperature, provides the desired α,α-disubstituted allylic amines in good yields and with excellent levels of regioselectivity. As observed with secondary trichloroacetimidates,[12] the reaction is amenable to a variety of aromatic amines and tertiary imidates, with the exception that substrates lacking a β-oxygen substituent result in lower regioselectivities. This work now provides a more general transition-metal catalyzed allylic amination method with a wide palette of tolerable neutral aniline nucleophiles and substrates for preparation of these quaternary centers. The method is amenable to synthetic applications as demonstrated in the facile two-step preparation of isoprenylated indoles that are present in a number of natural products.

During development of our methodology, we continued to conduct studies to try to probe the important aspects related to reaction mechanism. Experiments using secondary and tertiary electrophiles continue to support our initial hypothesis that a more reactive branched allylic trichloroacetimidate should ionize rapidly forming an oxidized transition-metal complex that is activated for attack by an external nucleophile. Our studies confirm the requirement of the basic imidate nitrogen, and a reaction pathway more involved than

Lewis acid activation of the imidate. Our critical findings that diene-ligated rhodium is an efficient catalyst for regioselective amination and the fact that the amination is not enantiospecific sets the stage for development of an enantioselective reaction in chapter

CHAPTER III
DYNAMIC KINETIC ASYMMETRIC TRANSFORMATIONS OF RACEMIC TRICHLOROACETIMIDATES

3.1 The Regio- and Enantioselective Preparation of α,α-disubstituted Allylic Aryl Amines

3.1.1 Background

The enantioselective synthesis of target compounds from racemic sources continues to be an area of intense focus in organic synthesis. Increases and advancement of efficient methodologies for asymmetric synthesis have become commonplace, appearing daily in top peer reviewed journals. Although seemingly trivial, there are new applications and difficult challenges that require development or improvement of existing methods for enantioselective synthesis. One such example is the asymmetric synthesis of α,α-disubstituted amines.[89, 116, 117] These chiral amines are structural moieties present in bioactive natural and non-natural products (Figure 3.1), and methods to prepare these amine-bearing quaternary centers are relatively sparse. One approach to the synthesis of chiral α,α-disubstituted amines is the palladium-catalyzed aza-Claisen rearrangements of

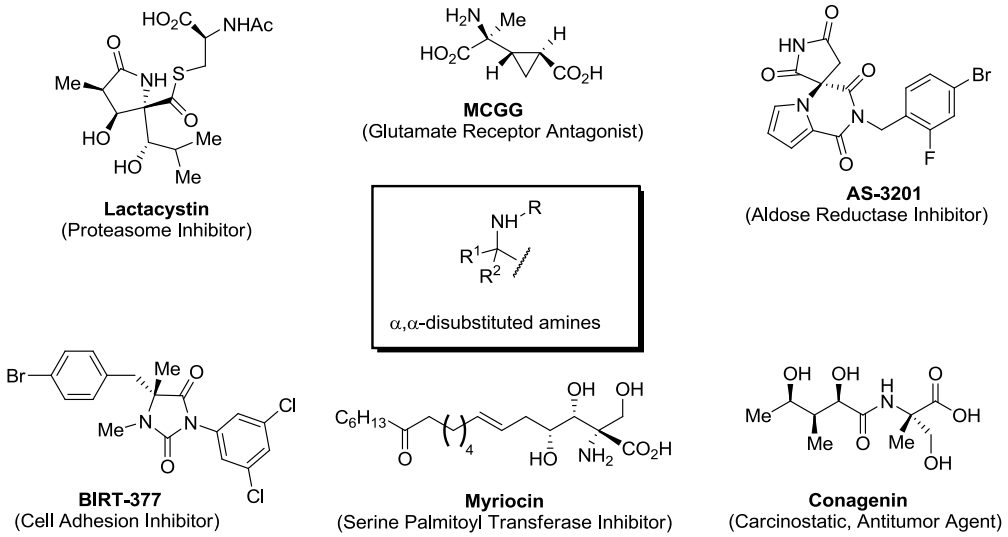

Figure 3.1 Natural and Synthetic Compounds Containing α,α-disubstitued Amines

linear allylic *N*-aryl trihaloacetimidates (Scheme 3.1a).[109] Although allylic amines are formed in good yields and with excellent enantioselectivity in the rearrangement, full conversion necessitates 50°C over 2.5 - 10 days. In addition, this method requires in situ preparation of the cationic ferrocenyl imidazoline palladacycle (FIP-X) **264** with close to 4 equivalents (based on the catalyst) of AgTFA. A problem that is encountered is large amounts of elimination product is formed due to the introduction of trifluoroacetic acid

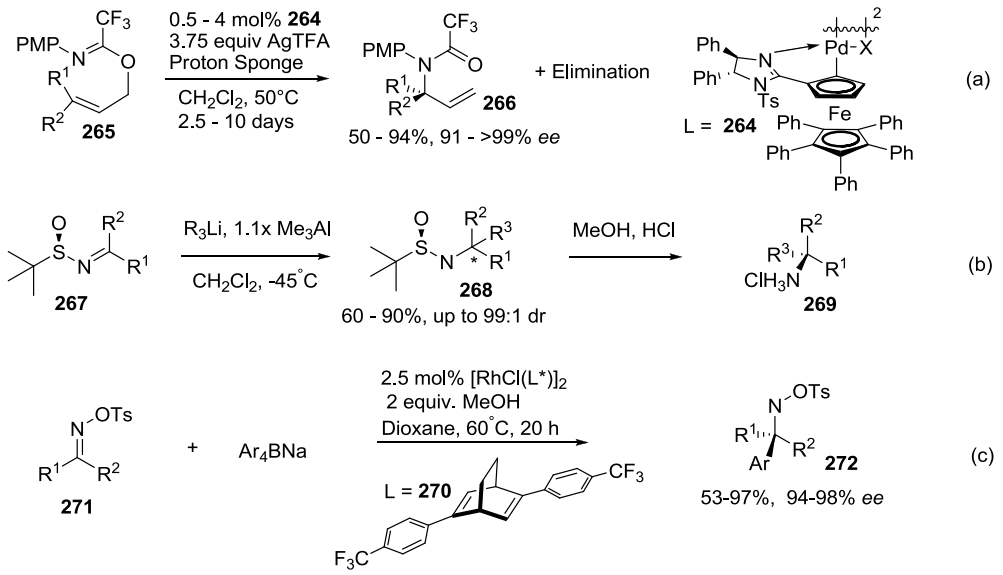

Scheme 3.1 Enantioselective Synthesis of α,α-Disubstituted Amines

during preparation of the active catalyst. Inclusion of a proton sponge can suppress formation of this byproduct, however, catalyst **264** also activates acetimidates for elimination. A more common approach to α,α-disubstituted amines involves addition of organometallic reagents to ketimines (Scheme 3.1b).[105, 106, 117, 118] Several challenges can emerge using this approach. First, the addition to ketimines containing an α-hydrogen is problematic because imines have the propensity to enolize.[106] Second, stereoselectivity is often moderate because the ketimine component (i. e. **267**, Figure 3.1b) can be difficult to

prepare with high selectivity for the desired *E*- or *Z*-isomer. High stereoselectivity in the addition step can also be difficult because differentiation of enantiotopic faces of the ketimine is often limited.[106] Third, ketimines are significantly less reactive than aldimines and require activation by the addition of a Lewis acid (Scheme 3.1b). While aromatic ketimines react with high yield and stereoselectivity, aliphatic ketimines remain problematic. In response to these challenges, Hayashi reported that rhodium-chiral diene complexes effectively catalyze the addition of sodium tetraarylborates to *N*-tosyl ketimines (Scheme 3.1c).[107] Although this reaction has greatly improved the addition reaction to ketimines, it still requires extended reaction times and elevated temperatures.

As discussed in chapter 2, the transition-metal catalyzed substitution of primary and secondary allylic carbonates and acetates has been utilized for the enantiospecific[96, 97] and enantioselective preparation of α-substituted *N*-aryl amines.[91, 95, 119] These useful and powerful methods deliver high yields of amine building blocks with excellent enantiopurity. I also described transition-metal mediated substitutions of tertiary electrophiles for the regioselective synthesis of α,α-disubstituted *N*-aryl amines. [93, 100, 111] These methods now include our newly developed rhodium-catalyzed substitution reaction of tertiary allylic trichloroacetimidates with neutral aniline nucleophiles.[13] Our method is tolerant of a much wider range of anilines and substrates providing some of the highest regioselectivities in these reactions to date. At this point however, there were no examples of a regioselective and enantioselective allylic substitution reaction catalyzed by a transition-metal that furnished α,α-disubstituted *N*-aryl amines with high enantiopurity.

Our early studies led to some important findings that ultimately provided a path towards the first DYKAT of a tertiary electrophile and an aniline nucleophile.[103] First, we had developed an allylic amination from branched imidates that results in high regioselectivity for the desired branched products, and additional studies showed that the branched amine products do not isomerize to linear products under our reaction conditions. Second, although rhodium dimers containing diene ligands such as

[RhCl(cyclooctadiene)]$_2$ and [RhCl(cyclooctene)$_2$]$_2$ do not promote high yielding and regioselective reactions with secondary imidates under our conditions (Table 2.3, entries 2 and 3),[12] [RhCl(norbornadiene)]$_2$ is an efficient catalyst for the amination of secondary and tertiary trichloroacetimidates.[13] This should make it feasible to develop a chiral diene-ligated rhodium catalyst for an asymmetric version of the reaction based on a norbornadiene or bicyclo[2.2.2]octadiene scaffold. The most significant finding was the control study using enantiopure trichloroacetimidate (*S*)-**239** (Scheme 2.6) where the resulting amine product **242** was isolated in racemic form, indicating that our rhodium-catalyzed amination of branched allylic trichloroacetimidates is not enantiospecific. This unusual outcome can be rationalized by the proposed mechanism outlined in Scheme 3.2

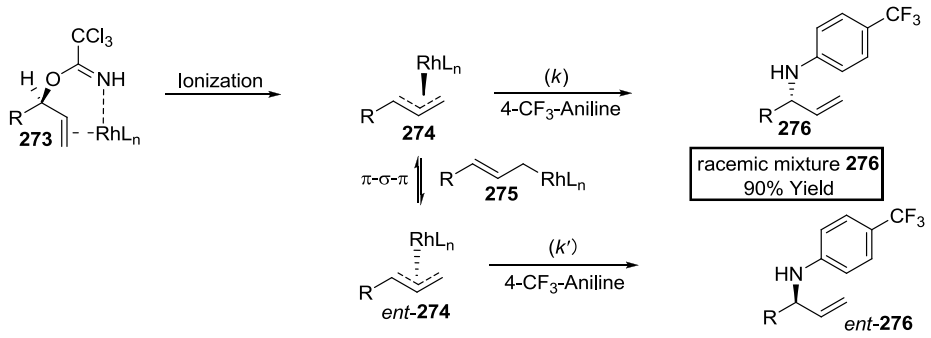

Scheme 3.2 Proposed Mechanism for Racemization of **273**

(and Scheme 2.7). To review, ionization of **273** would result in π-allyl organorhodium complex **274**. This η3-complex **274** is in equilibrium with its sigma-bonded η^1-derivative **275** and could interconvert to π-allyl complex *ent*-**274** by a process described shortly. If the rate of substitution by the aniline nucleophile (*k* and *k'*) is sufficiently slow versus the equilibration of **274** and *ent*-**274**, a racemic mixture of amination product **276** will result.

Our strategy for an enantioselective version of our rhodium-catalyzed allylic amination reaction with aniline nucleophiles hinged on the results of the enantiospecific

study (Scheme 2.6) and the proposed mechanism for racemization (Scheme 3.2). We hypothesized that a dynamic kinetic asymmetric transformation (DYKAT)[87] of a racemic mixture of trichloroacetimidates (**273** and *ent*-**273**) could be possible if chiral ligands were ligated to the rhodium metal center. Ionization of **273** and *ent*-**273** would provide two diastereomeric π-allyl rhodium complexes **274** and *ent*-**274**, respectively (Scheme 3.3). We reasoned that the asymmetric environment provided by the chiral ligands would slow down the rate of nucleophilic attack by anilines and increase the time allowed for rapid π-σ-π interconversion of complexes **274** and *ent*-**274**. The lower energy transition-state (matched pathway, *k*) to amination products would lead to preferential formation of enantiomer **277**.

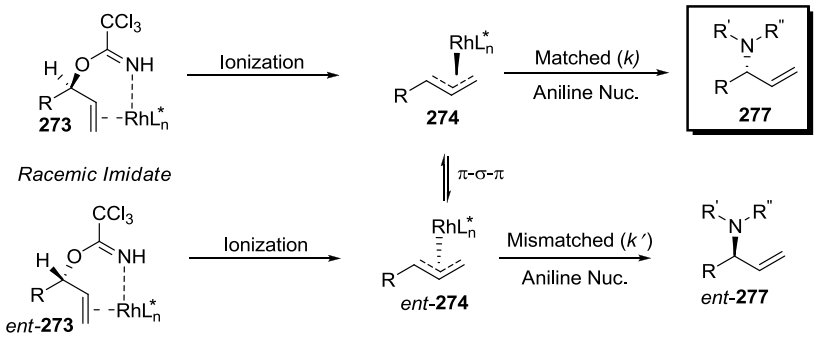

Scheme 3.3 Strategy for DYKAT of Tertiary Allylic Imidates

The π-σ-π interconversion of π-*syn* **274** and π-*syn* *ent*-**274** can occur from each complex by two different pathways, all in equilibrium (Scheme 3.4).[91, 120] The interconversions proceed through the terminally bound σ-rhodium complexes **278** and **278'**, and internally bound complexes **279** and **279'**. Each of these η^1-rhodium complexes can rotate 180° about the rhodium-carbon σ-bond and slip into η^3-complexes, thereby providing pathways for π-σ-π interconversion. In palladium π-allyl complexes, the energy barrier to complexes **279** and **279'** is much larger than terminally bound σ-complexes **278** and**278'** because there is substantial steric interaction between substituents on the substrate

and the ligands on palladium.[91, 120, 121] In addition, π-anti complexes (**280** and **280'**) are generally less stable than π-syn complexes (**278** and **278'**) due to $A^{1,3}$ strain in the former complexes (Scheme 3.4). In the studies of iridium (I) allylic substitution reactions, terminal branched and linear (*E*)-allylic acetates do not form (*Z*)-products, which are the major products from (*Z*)-configured acetates. (*E*)-configured products derive from *syn* π-allyl complexes and (*Z*)-products from *anti*-π-allyl complexes suggesting high barriers and slow interconversion of these complexes.[85] Considering these facts, we proposed that isomerization of the complexes π-*syn* **274** and π-*syn ent*-**274** will predominate leading to enantioenriched amine products.

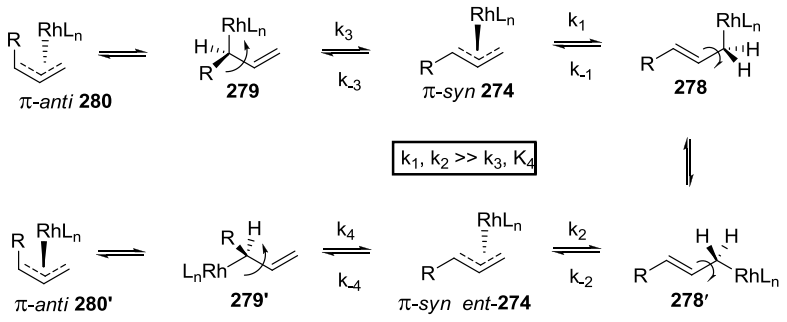

Scheme 3.4 Equilibration of π-Allyl Rhodium Complexes

At the onset of our studies, few resolutions of unsymmetrical acyclic racemic substrates in amination reactions had been described, and no reports using an aryl amine as the nucleophile (Scheme 3.5).[102, 122-124] Kinetic resolutions of secondary racemic carbonates[122] and benzoates[102] catalyzed by chiral rhodium and iridium complexes were reported that prepare branched amines **284** and **287** in ≤ 50% yield and with high enantioselectivity (Scheme 3.5a and b). Dai and coworkers developed a palladium-catalyzed DYKAT method that utilizes secondary allylic acetates, benzylamine as the nucleophile and a novel ferrocene-based *P*,*N* ligand **288** that provides amine prducts in 76

– 94% yield and with 94 – 98% ee (Scheme 3.5c).[123] A very powerful DYKAT method that delivers primary allylic amines **294** in 44 – 89% yield and with 66 – 99% *ee* from racemic allylic alcohols was recently reported by Carreira (Scheme 3.5d).[124] The only amination involving resolution of a tertiary substrate was reported by Trost using phthalimide in DYKAT ring opening of a vinyl epoxide (Scheme 3.5e).[125]

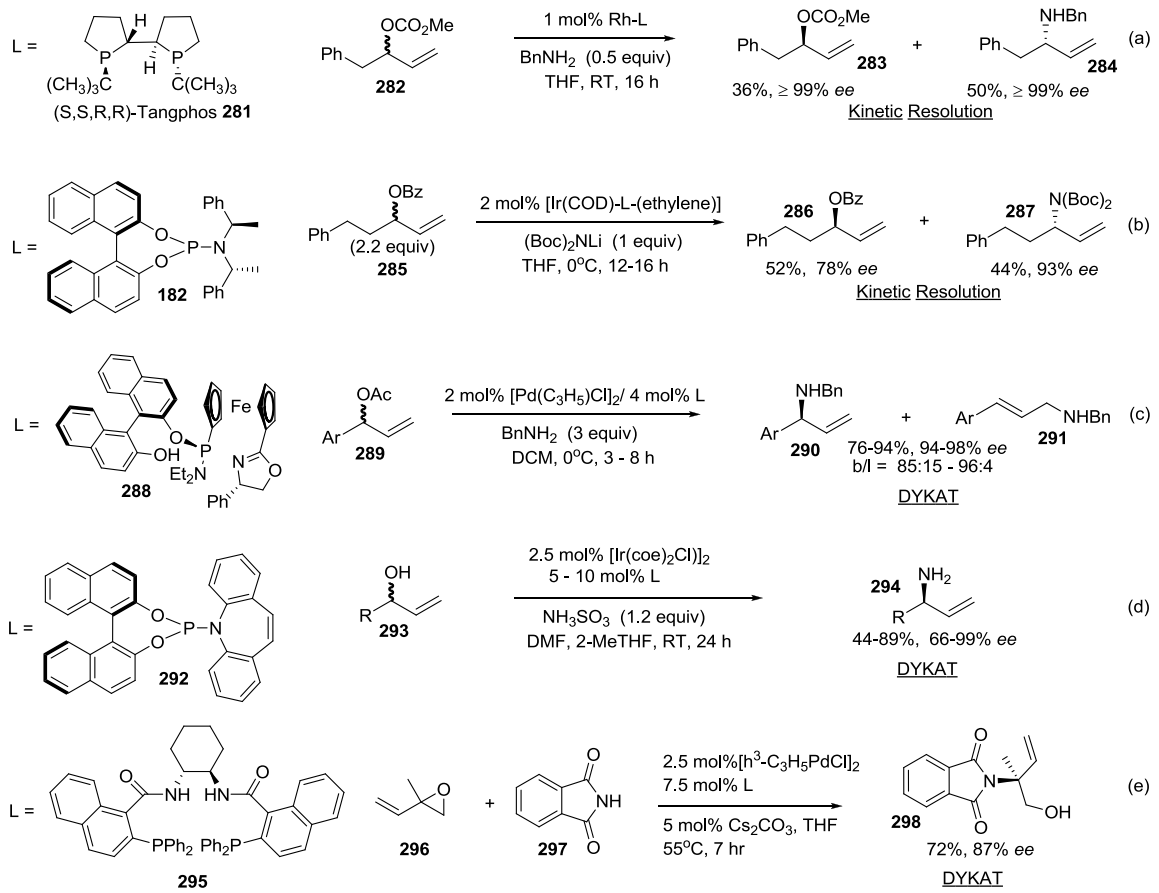

Scheme 3.5 Resolution of Racemic Electrophiles in Allylic Aminations

We decided to begin our DYKAT investigations with tertiary allylic trichloroacetimidates for a few reasons. First, we felt that there was a greater need and opportunity to persue an amination reaction of this type. The single example for preparation of non-racemic α,α-disubstituted amines (Scheme 3.5e) involves vinyl epoxide

ring-opening rather than an allylic leaving group. An allylic trichloroacetimidate would allow a wider range of substrate types that could be utilized. In general, enantioselective preparation of quaternary centers is a difficult problem with few available methods. To date, tertiary allylic carbonates and acetates have not been suitable electrophiles in enantioselective allylic aminations. The prospect that development of an asymmetric method to construct this motif via the first dynamic kinetic resolution of an allylic tertiary electrophile and an aniline nucleophile was certainly alluring. Second, we postulated that the use of tertiary imidates may have a greater chance of success in a rhodium-catalyzed DYKAT of racemic trichloroacetimidates. Our proposed mechanism requires that nucleophilic attack by the aniline nucleophile is slow versus the interconversion of intermediate organorhodium π-allyl complexes (**274** and *ent*-**274**, Scheme 3.3). Tertiary trichloroacetimidates should be more readily ionized and attack by aniline at a more sterically congested center should be slow in comparison to secondary imidates.

3.1.2 Results and Discussion

To test our hypothesis, we set out to explore the effects of a number of commercially available chiral diene ligands,[126] **L1**-**L4** (Table 3.1) on enantioselectivity in the amination reaction of racemic tertiary allylic trichloroacetimidate **255** with aniline **183a**. Lin ligand **L1**[127] (entry 1) and Hayashi ligand **L2**[128] (entry 2) resulted in a near-racemic product **255a**. Carreira ligand **L3**[129] (entry 3) gave measurable enantioselectivity (26% *ee*) for the process. Hayashi ligand **L4**[130] (entry 4) was the most active and enantioselective at 40°C, providing α,α-disubstituted amine **255a** as a single regioisomer in 72% yield and with good enantioselectivity (73% *ee*). Lowering the reaction temperature to 25°C (entry 5) resulted in significant enhancement in enantioselectively (84% *ee*). With tertiary substrates, this most likely results from a lowered rate of nucleophilic attack by aniline versus the rate of interconversion of the organorhodium complexes (**274** and *ent*-**274**, Scheme 3.3).

Table 3.1 DYKAT Optimization of Tertiary Trichloroacetimidate **255**[a]

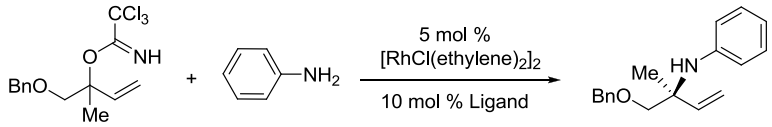

255 (racemic) **183a** **255a**

entry	ligand	aniline (equiv)	solvent	temp (°C)	time (h)	yield[b] (%)	% *ee*[c]
1	**L1**	3	THF	40	4	14	-2
2	**L2**	3	THF	40	1	59	-1
3	**L3**	3	THF	40	1	71	-26
4	**L4**	3	THF	40	1	72	73
5	**L4**	3	THF	25	1	77	84
6	**L4**	3	THF	0	1	77	83
7	**L4**	3	Et_2O	25	1	72	76
8	**L4**	3	CH_2Cl_2	25	1	43	68
9	**L4**	3	Acetone	25	1	66	61
10	**L4**	3	Dioxane	25	1	73	78
11	**L4**	3	Toluene	25	1	71	82
12	**L4**	3	MTBE	25	1	78	86
13	**L4**	1.5	MTBE	25	1	69	89

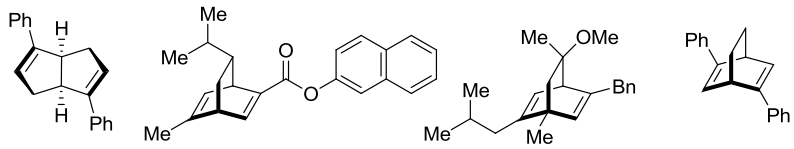

L1 **L2** **L3** **L4**

[a] All reactions were conducted at 0.2 M with 1 equiv. of tertiary allylic imidate.

[b] Yields are isolated values

[c] *ee*'s were determined by chiral HPLC.

Conversely, lowering the reaction temperature may make destabilizing interactions in the transition state leading to the minor enantiomer more prohibitive. Reduction of the catalyst loading to 1 mol% at 25°C for 4 hours lowered the yield to 41% and enantioselectivity to 77% (not shown in Table 3.1) Reducing the reaction temperature further to 0°C (entry 6) did not impact the results. A number of solvents (entries 7– 12) were screened, with *t*-butyl methyl ether (MTBE) inducing the highest enantioselectivity providing **255a** with 86% *ee* (entry 12). Decreasing the equivalents of aniline **183a** resulted

in conditions that afforded 89% *ee* with good yield (69%) and complete regioselectivity (entry 13). Again, lower yields and increases in enantioselectivity may reflect a lower rate of addition by aniline.

Having established bicyclo[2,2,2]-octadiene **L4** as the optimal chiral ligand, I examined the steric and electronic nature of substituents on the phenyl rings by preparing dienes **L5**-**L9** (Figure 3.2) and utilizing these ligands in the enantioselective amination of **255** with aniline **183a**. The electron-rich 4-methoxyphenyl substituted diene **L5** resulted in a substantial drop in enantioselectivity and yield (60%, 71% *ee*, Figure 3.2). Amination using *t*-butyl derivative **L6** provided yields and *ee*s that are intermediate between methoxy derivative **L5** and the commercially available Hayashi **L4**. Because the results follow the donating ability of the substitutents on the phenyl rings suggests that the electronic nature

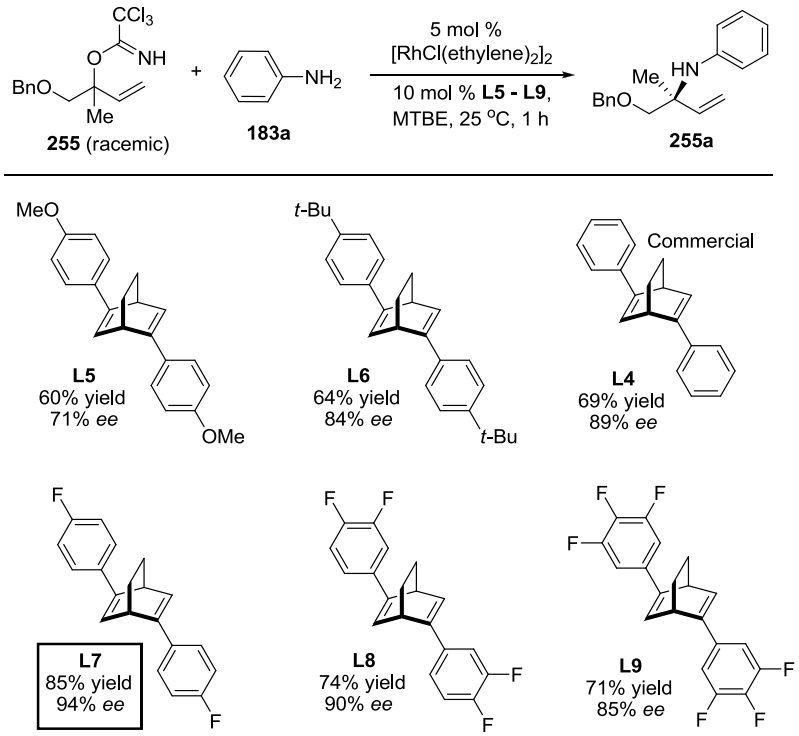

Figure 3.2 Modification of Ligand Substitutents

of the ligand is a more important factor determining reaction outcome. I continued to modify the electronics of the ligands by making electron-poor fluorinated Hayashi ligand derivatives **L7** to **L9** (Figure 3.2). The electron-deficient 4-fluorophenyl group **L7** significantly improved both yield and enantioselectivity (85% yield, 94% *ee*). The more electron-deficient ligands 3,4-difluoro **L8** and 3,4,5-trifluoro **L9** did not show further improvement, rather yields and enantioselectivity decreased as fluorine substitution increased.

The trend that is observed with respect to ligand electronics and the resulting yields and enantioselectivities is quite interesting. As the ligands progress from the most electron-donating **L5** to the withdrawing 4-fluoro derivative **L7**, the yields and enantioselectivities increase, then taper off with more electron-withdrawing groups **L8** and **L9**. To gain some insight regarding these results, I conducted a few ^{13}C NMR studies where free ligand and the rhodium-bound ligand were individually monitored and the difference in chemical shift was observed (Table 3.2). It is generally accepted that electron-deficient olefins provide more stable transition-metal complexes in comparison to electron-rich olefins due to increased backbonding from the metal center into the π^* antibonding molecular orbital of the olefin.[126, 131, 132] This weakens the π-bond, shifting hybridization of the olefin from sp^2 to more sp^3 character, and is evidenced by large upfield shifts of the olefinic carbons to the sp^3 region of the ^{13}C spectrum.[131] Stability is conferred by increasing pyramidalization of the olefin to the metal.[126, 133] For example, electron-withdrawing ligand **L7** has a larger coordination shift than electron-donating diene ligand **L5**, possibly suggesting a more stable rhodium- **L7** complex. The magnitude of the $^{103}Rh–^{13}C$ coupling constant of 10.6−12 Hz (Table 3.2) suggests that there is considerable s-character in these rhodium−chiral diene complexes.[131] As we prepare new ligands for asymmetric transformations we will continue to conduct these ligation NMR studies to determine if it can be used as a predictive tool for ligand design and selection.

Table 3.2 ^{13}C Data of Rhodium-Ligated Dienes **L4**, **L5** and **L7**

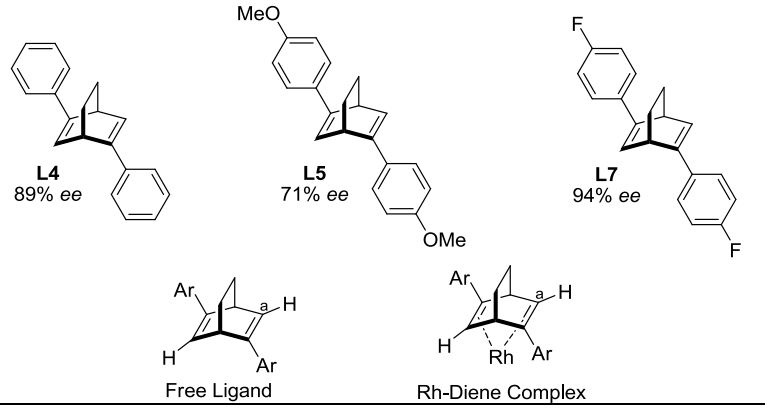

Ligand	$^{13}C_a$free δ(ppm)	$^{13}C_a$ complex δ(ppm)	Δ = ($\delta_{complex}$-δ_{free}) $^{13}C_a$	J(^{103}Rh- $^{13}C_a$) (Hz)
L4	129.7772	45.3250	-84.4522	10.8
L5	127.3815	44.0943	-83.2872	12.0
L7	129.5563	45.4043	-84.1520	10.6

Having optimized the reaction with respect to equivalents of aniline, temperature, solvent and chiral ligand for efficient enantioselective amination of tertiary benzyloxy trichloroacetimidate **255** with aniline **183a**, the scope of the allylic amination reaction was investigated with a number of anilines **183b** – **q** (Table 3.3) that differ in electronics, sterics and substitution patterns on the aromatic ring. Electron-rich and electron-deficient *para*-substituted anilines (entries 1 – 5) were found to be suitable nucleophiles, giving rise to α,α-disubstituted allylic amines in moderate to good yields (51 – 82%) and good to high enantioselectivity (85 – 96% *ee*). In each of these examples it is worth noting that all reactions proceeded with excellent regioselectivity (33:1 - >99:1). The reaction product **255c** (entry 3) prepared using the electron-rich 4-methoxyaniline **183c** was isolated in somewhat lower yield (77%) and selectivity (33:1 b/l, 90% *ee*) compared to electron-poor products **255b** and **255p** (entries 1 and 2) that were isolated in 82 – 86% yields, >99:1 b/l ratio and 91- 96% *ee*. The lower yield may be due in part to some product inhibition of the catalyst with an accessible β-oxygen. The same results were observed in the regioselective

Table 3.3 Survey of Aniline Nucleophiles in DYKAT[a]

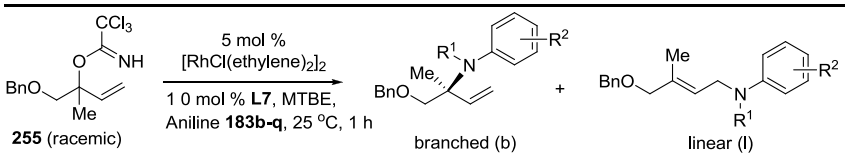

entry	anilines	products	% yield	b/l ratio	% *ee*
1	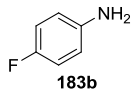 **183b**	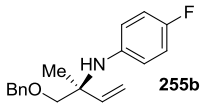 **255b**	82	>99:1	96
2	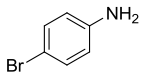 **183p**	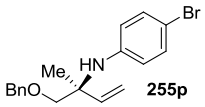 **255p**	86[b]	>99:1[b]	91[b]
3	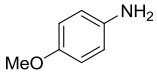 **183c**	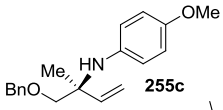 **255c**	77	33:1	90
4	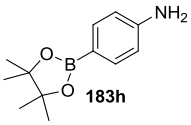 **183h**	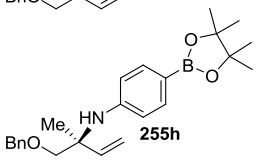 **255h**	54	>99:1	91
5	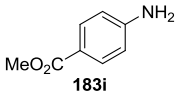 **183i**	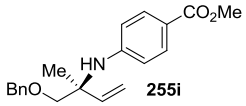 **255i**	51	>99:1	85
6	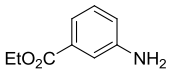 **183j**	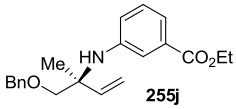 **255j**	79	>99:1	94
7	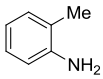 **183d**	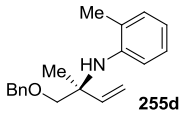 **255d**	69	51:1	89
8	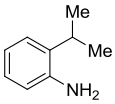 **183l**	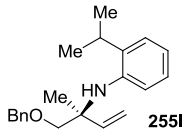 **255l**	74	48:1	94
9	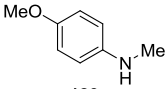 **183q**	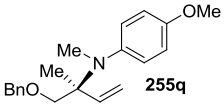 **255q**	70	30:1	93

[a]All reactions were conducted with 1 equiv of allylic imidate and 1.5 equiv of aniline. Yields are isolated values; *ee*'s were determined by chiral HPLC and b/l ratio by GC.

[b] 0.5g scale.

amination reaction product (Table 2.11, entries 1 and 2) where **255c** was isolated in 72% yield versus 87% yield for **255b**. The lower selectivities may result from increased background reaction or a more nucleophilic aniline. The moderate yield (51%) of **255i** (entry 5) in the reaction of trichloroacetimidate **255** with 4-ester substituted aniline **183i** may simply reflect a less nucleophilic aniline because 4-nitroaniline (unpublished results) fails to provide the desired product under our reaction conditions. In contrast, the more basic aniline **183j**, containing ester functionality at the *meta*-position, provided product **255j** (entry 6) as a single regioisomer in good yield (79%) and with high levels of enantioselectivity (94% *ee*). We were very excited to see that this method also works with *ortho*-substituted anilines **183d-l** (entry 7 and 8), and allylic amines were isolated with high enantioselectivity (89 – 94% *ee*) and regioselectivity (b/l = 48:1 – 51:1). Our previous report[13] had delivered the first highly regioselective allylic amination of tertiary electrophiles that is compatible with o*rtho*-substituted aniline nucleophiles and now we had rendered the reaction enantioselective as well. As a result, we sought to extend this catalytic method to a challenging acyclic secondary aniline **95f** (entry 9), which is known to provide the products with poor regioselectivity in the aminination reaction of primary allylic carbonates.[95] The reaction of tertiary imidate **255** and *N*-methyl anisidine **183q** proceeded smoothly under our optimized conditions, and amine **255q** (entry 9) was isolated in 70% yield and with excellent selectivity (b/l = 30:1, 93% *ee*).

Next I proceeded to examine the substrate scope of the reaction using the reactive 4-fluoroaniline nucleophile**183b** (Table 3.4). Based on previous experience using tertiary trichloroacetimidates in regioselective reactions, the functional-group tolerance of the rhodium-**L7** catalyst was first evaluated with a number of branched imidates containing different β-protected alcohols (entries 1 – 7). Both electron-rich and electron-deficient benzyl ether derivatives **299** and **300** (entries 1 and 2) provided the amination products **299b** and **300b** in 61 – 76% yield, >99:1 b/l ratios and with comparable enantioselectivity (~93% *ee*) to that of benzyl ether **255** (96% *ee*, Table 3.3). Phenyl, methyl and MOM

Table 3.4 Substrate Scope of DYKAT Amination[a]

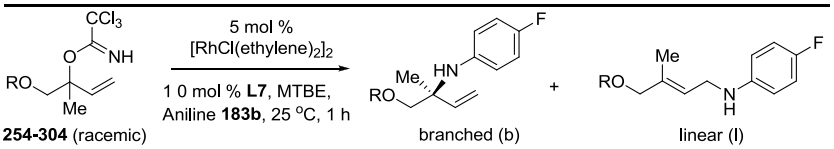

entry	Imidates	Products	% yield	b/l ratio	% *ee*
1	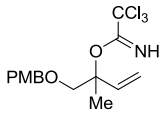 **299**	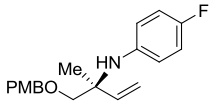 **299b**	76	>99:1	93
2	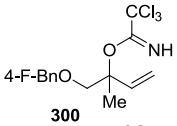 **300**	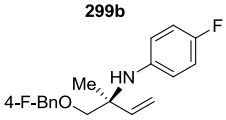 **300b**	61	>99:1	92
3	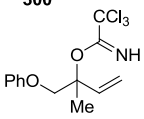 **301**	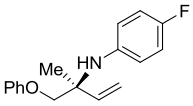 **301b**	84	>99:1	80
4	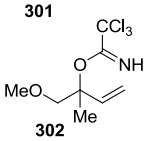 **302**	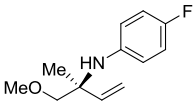 **302b**	57	>99:1	86
5	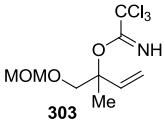 **303**	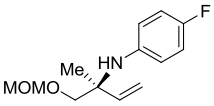 **303b**	62	>99:1	89
6	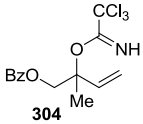 **304**	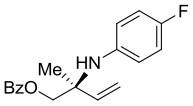 **304b**	53	>99:1	59
7	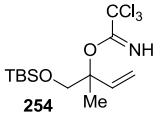 **254**	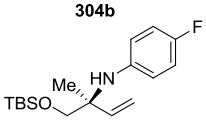 **254b**	92	90:1	76
8	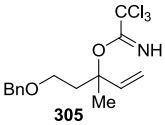 **305**	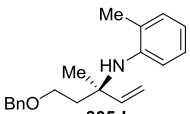 **305d**	70	5:1	56
9	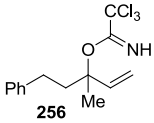 **256**	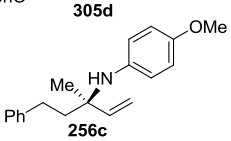 **256c**	68	7:1	52

[a]All reactions were conducted with 1 equiv. of allylic imidate and 1.5 equiv of aniline. Yields are isolated values; *ee*'s were determined by chiral HPLC and b/l ratio by GC.

protected ethers **301** – **303** (entries 3 – 5) also resulted in good yields, excellent regioselectivities and 80 – 89% *ee* in the reaction. The ester group was not suitable for this system, and benzoyl allylic amine **304 b** (entry 6) was isolated in 53% yield and with 59% *ee*. As the functional group becomes more bulky (i.e. TBS **254**, entry 7), a significant drop in enantioselectivity was observed (76% *ee*). In addition, substrates **305** and **256** that lack a β-oxygen substituent were subjected to DYKAT amination with aniline **183b** (entries 8 and 9). Although 68 – 70% yield of the amine products **305d** and **256c** were prepared, the regioselectivites (b/l = 5:1 – 7:1) and enantioselectivities (52 – 56% *ee*) were lower than entries 1 – 5 (Table 3.4) and entries 3 and 7 (Table 3.3) using comparable nucleophiles. This is in agreement with our previous studies, where yields and selectivities drop with substrates lacking a β-oxygen substituent.[13] This is also evident, but to a lesser degree with imidates possessing inaccessible β-oxygen functionality (entries 6 and 7, Table 3.4). Again this suggests that additional chelation control is provided by available β-oxygen lone-pairs and is necessary for high selectivity in the amination reaction of tertiary substrates.

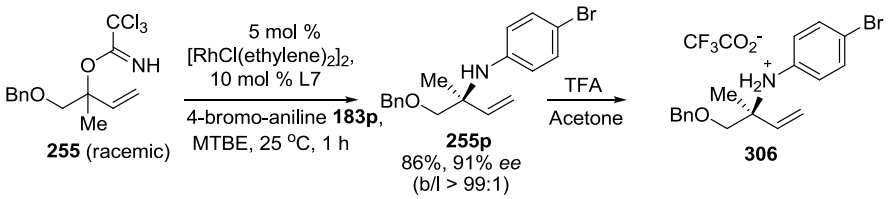

Scheme 3.6 Preparation of TFA salt **306** for X-ray Analysis

To establish the absolute stereochemistry of the product, allylic imidate **255** was subjected to our rhodium conditions in the presence of *para*-bromoaniline **183p** (Scheme 3.6). The reaction was performed on a half-gram scale to give amine **255p** in 86% yield and with 91% *ee*. Surprizingly, very few of the allylic aryl amine products that we have prepared are solids. Most of these products are isolated as clear to light brown oils. After

a number of trials and various conditions, I obtained crystalline product **255p** as a TFA salt. The absolute stereochemistry of amine-TFA salt **306** was determined to be (*S*) by X-ray crystallographic analysis (Figure 3.3). The solid-state structure of **306** shows that it exists as two independent cation-anion pairs through hydrogen bonding. The amine cations have the same configuration but different conformations (Figure 3.3).

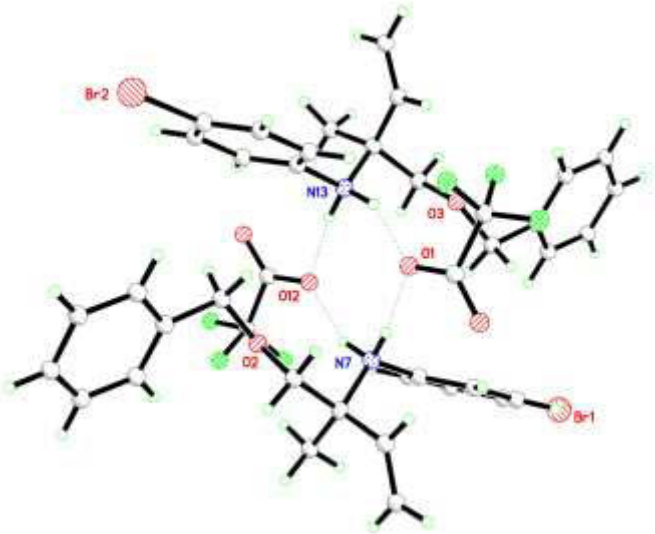

Figure 3.3 ORTEP Diagram of TFA salt **306** Dimer

3.1.3 Conclusion

In summary, we have successfully applied chiral Hayashi-type bicyclo[2.2.2]octadiene ligands to our rhodium-catalyzed amination reaction which has resulted in the first reported dynamic kinetic asymmetric transformation (DYKAT) of racemic tertiary electrophiles with unactivated anilines. The method is operationally simple and efficient, providing a new method for synthesis of α,α-disubstituted allylic *N*-aryl amines in moderate to good yields and with good to excellent regio- and enantioselectivity. The method is successful because it deviates from conventional

methods that utilize allylic carbonates and acetates and instead uses a branched trichloroacetimidate leaving group possessing two points of accessible chelation. In the next section I describe the expansion of our DYKAT reaction to secondary trichloroacetimidates for the enantioselective preparation of α-substituted allylic aryl amines.

3.2 The Regio- and Enantioselective Preparation of α-substituted Allylic Aryl Amines

3.2.1 Background

Our catalytic amination reaction is a powerful tool that allows for the similtaneous regio- and enantioselective synthesis of nitrogen-containing quaternary centers. In large part, this achievement is an adaptation of Overman's novel work with primary allylic trichloroacetimidates. By applying branched trichloroacetimidates to transition-metal catalyzed allylic substitution reactions, we now have options to bond constructions that were problematic with allylic acetates and carbonates. Issues of low regioselectivity with α-dibranched substrates, *ortho*-substituted and secondary acylic anilines, and no reports of DYKAT amination using aniline nucleophiles are a few examples. The development of new methodologies can provide increased efficiency or selectivity, or complement existing procedures by providing alternative routes for synthetic construction.

Hartwig's Ir(I)-catalyzed amination of prochiral linear carbonates with aniline nucleophiles is an excellent choice for enantioselective synthesis of α-substituted allylic aryl amines and is the benchmark for such amination methodologies (Table 2.1).[95] We noted one limitation of Hartwig's method. Acyclic secondary anilines react with poor regioselectivity (branched/linear = 1:1 – 4:1) in the enantioselective method and we had utilized *N*-methyl anilines with good regio- and enantioselectivity in previous studies.[12, 13, 103] Thus, we decided first to extend our amination method to secondary

allylic trichloroacetimidates **220** with acyclic secondary anilines to generate allylic *N*-methyl aryl amines **307** (Scheme 3.5).[134]

We initiated our DYKAT studies with tertiary trichloroacetimidates because we proposed that these substrates may have a better chance of success where nucleophilic addition occurs on a more substituted carbon center. It was critical to our proposal that nucleophilic attack is slow relative to the rate of interconversion of π-allyl organorhodium intermediates **274** and *ent*-**274** (Scheme 3.3). We wondered if the DYKAT reaction could be applied to secondary trichloroacetimidates since the rate of addition on a less-sterically encumbered carbon may approach the rate of interconversion. This concern, combined with the fact that poor regioselectivity had been reported in the asymmetric method with *N*-methyl aniline could make this strategy problematic.

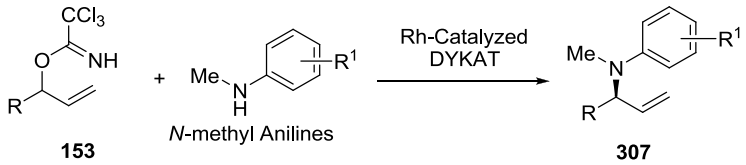

Scheme 3.7 DYKAT Amination with *N*-Methyl Anilines

3.2.2 Results and Discussion

We began our investigation using benzyloxy allylic trichloroacetimidate **229** and *N*-methyl aniline **183f** as the standard substrate and nucleophile in a series of optimization reactions where commercially available Hayashi ligand **L4** and derivatives **L5–L7** (Table 3.5) were investigated after ligation to rhodium dimer.[134] Initial amination conditions were performed with 5 mol% $[RhCl(ethylene)_2]_2$, 10 mol% of ligand **L4**, 3 equivalents of aniline **183f** and 1 equivalent of imidate **229** in THF. In 1 h at room temperature, the reaction providing branched *N*-methyl amine product **229f** was complete and resulted in 83% yield

and 55% *ee* (Table 3.5, entry 1). To our excitement, the undesired linear product was not detected in the reaction. Increasing the reaction temperature to 40°C (entry 2) and lowering the equivalents of *N*-methyl aniline **183f** (entry 3) both resulted in higher enantioselectivity (72 and 80% *ee*). Continuing to increase the temperature to 60 °C (entry 4) had an adverse effect on the enantioselectivity (69% *ee*). We reason that increasing the reaction temperature leads to faster interconversion of rhodium π-allyl complexes and accelerates nucleophilic attack which lowers enantioselectivity (Scheme 3.3). Running the reaction at 40°C with secondary trichloroacetimidates may be optimal for interconversion without detrimental increases in nucleophilicity. As we had observed earlier, temperature presumably affects aniline nucleophilicity more than interconversion in the reaction of tertiary imidates. Optimization continued by reducing the Rh catalyst loading to 2 mol% (entry 5), which did not affect the reaction efficiency. A number of solvents were subsequently screened including methyl t-butyl ether (MTBE), cyclopropyl methyl ether (CPME), toluene and dioxane (entries 6 – 9). Dioxane (entry 9) was established as the optimal solvent, providing **229f** in 99% yield and with 85% *ee*.

Next, we studied the steric and electronic bias of the substituents on the phenyl ring of the diene ligands (**L5 – L7**) in the DYKAT reaction. These chiral ligands (Table 3.5, entries 10 – 12) are less enantioselective than the parent diene **L4** (entry 9). When the amination reaction was scaled utilizing 0.5 g of imidate **229** using diene **L4** (entry 13) and required concentration with catalyst prior to purification, significant isomerization from the branched amine **229f** to the linear isomer was observed. To avoid isomerization, the crude product was filtered through a pad of silica prior to concentration to remove the rhodium catalyst. Product **229f** from the larger scale reaction was isolated in 99% yield, 87% *ee* and 23:1 b/l ratio (entry 13). Configuration of **229f** is assigned based on our previous report with tertiary allylic imidates.[103]

With optimized amination conditions in hand, we proceeded to explore the reaction scope with a variety of *N*-methyl anilines and secondary trichloroacetimidate

Table 3.5 Optimization of DYKAT of **229** with *N*-methylamine **183f**

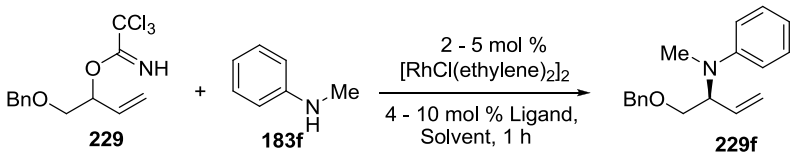

entry	ligand	Rh loading (mol%)	aniline (equiv)	solvent	temp (°C)	yield (%)[a]	% *ee*[b]
1	**L4**	5	3	THF	25	83	55
2	**L4**	5	3	THF	40	80	72
3	**L4**	5	1.5	THF	40	89	80
4	**L4**	5	1.5	THF	60	83	69
5	**L4**	2	1.5	THF	40	87	80
6	**L4**	2	1.5	MTBE	40	80	75
7	**L4**	2	1.5	CPME	40	83	82
8	**L4**	2	1.5	Toluene	40	80	79
9	**L4**	2	1.5	Dioxane	40	99	85
10	**L5**	5	1.5	Dioxane	40	88	72
11	**L6**	2	1.5	Dioxane	40	55	49
12	**L7**	2	1.5	Dioxane	40	88	68
13	**L4**[c]	2	1.5	Dioxane	40	99	87

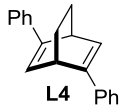

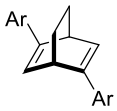

L5: Ar = 4-MeO-Ph
L6: Ar = 4-*t*-Bu-Ph
L7: Ar = 4-F-Ph

[a] Yields are isolated values

[b] The *ee*'s were determined by chiral HPLC and b/l ratios of the isolated products by GC (b/l = 84:1 – >99:1).

[c] 0.5 g scale amination of **229** (b/l > 23:1).

229 (Table 3.6).[134] For most substrates, optimal yields, regioselectivity and enantiomeric excesses were obtained using 2 mol% $[RhCl(ethylene)_2]_2$ and 4 mol% **L4** in dioxane at 40 °C for 1 h. As shown in Table 3.6, a range of *ortho*-, *meta*-, and *para*-substituted *N*-methyl anilines **229r - x** undergo allylic amination with a branched to linear (b/l) ratio in the range of 22:1 – 88:1 to provide allylic *N*-methyl arylamines 229**r - x** in good yields (72 – 92%) and with good to excellent levels of enantioselectivity (83 – 93% *ee*). It is quite noteworthy that the mild reaction conditions are tolerant of such a varied set of substituted *N*-methyl aniline nucleophiles,

Table 3.6 Survey of *N*-methylamine Nucleophiles in DYKAT Amination

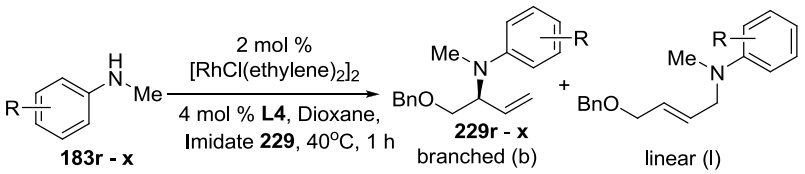

entry	anilines	products	% yield[a]	b/l ratio[b]	% *ee*[c]
1	**183r:** R = 4-CF_3	**229r**	72	30:1	93
2	**183s:** R = 4-Br	**229s**	78	74:1	83
3	**183t:** R = 2,4-F	**229t**	86	26:1	91
4	**183u:** R = 3-Br	**229u**	92	88:1	89
5	**183v:** R = 2-Me	**229v**	87	42:1	89
6	**183w:** R = 2-OMe	**229w**	86	22:1	85
7	**183x:** R = 2-F	**229x**	78	22:1	91

[a] Yields are isolated values.

[b] The b/l ratios were determined by GC.

[c] The *ee*'s were determined by chiral HPLC.

and highlights the uniqueness of our rhodium-catalyzed method. For example, electron-deficient 4-trifluoromethyl aniline **183r** could be utilized as a nucleophile in the asymmetric reaction resulting in amine **229r** in 72% yield, 30:1 regioselectivity and with 93% *ee* (entry 1). Under the same reaction conditions the sterically encumbered and electron-rich 2-methoxyaniline **183w** (entry 6) provided **229w** in 86% yield, 22:1 b/l ratio and 85% ee. Anilines **183s** and **183u** possessing *para*- and *meta*-bromo functional groups were also effective nucleophiles. These anilines reacted to provide high yielding and selective products **229s** and **229u**, which could be very useful chiral amine intermediates for further functionalization. The more sterically hindered *N*-methyl-2-toluidine (Table 3.6, entry 5) possessing an ortho methyl group also reacted efficiently in the amination reaction. Fluorinated *N*-methyl arylamines **183t** and **183x** could be desirable building blocks in medicinal chemistry applications where addition

of fluorine to bioactive agents introduces desirable properties (entries 3 and 7). In these reactions, enantioenriched **229t** and **229x** were prepared in good yields (78 – 86%) and with excellent regioselectivity (b/l = 22:1 – 26:1) and enantioselectivity (91% *ee*).

We continued application of this transformation to a wide variety of racemic secondary allylic trichloroacetimidates (Table 3.7).[134] The results show a high degree of functional group tolerance that are present in substrates. With this collection of substrates, the highest combination of regio- and enantioselectivity were obtained employing 5 mol% $[RhCl(ethylene)_2]_2$ and 10 mol% **L4** at room temperature. We often employ higher catalyst loadings and lower temperatures with sterically encumbered nucleophiles and/or substrates in order to increase regioselectivity, sometimes at the expense of some enantioselectivity. Like our previous report with tertiary allylic imidates,[103] substrates **308** and **309** (entries 1 and 2) bearing the β-oxygen substituent afforded the amination products **308r** and **309r**, respectively, in 57 – 80% yields and with high regioselectivity (b/l = 27:1 – 46:1) and enantioselectivity (89– 94% *ee*). The lower yielding reaction with trichloroacetimidate **309** may be due to competitive binding of the alkynyl group present in the substrate to rhodium. However, 57% yield and the resulting selectivities make the reaction synthetically useful. In contrast to tertiary allylic imidates, substrates **310**, **223**, **311** and**312** (entries 3 – 6) lacking the β–ether substituents still provided aminination products with good regioselectivity (b/l ratio = 9:1 – 69:1) and enantioselectivity (87 – 91% *ee*). It has been established that secondary allylic carbonates containing β-branching substituents react with poor regioselectivity in favor of linear products.[96, 97] Under our reaction conditions β-branching cyclohexyl allylic imidates **231** and isopropyl imidate **232** (entries 7 and 8) with *N*-methyl *p*-anisidine (**183q**) provided allylic *N*-methyl amines **231q** and **232q**, respectively, in good yield (88%) and with excellent regioselectivity (b/l= 11:1 – 14:1) and enantioselectivity (95 – 96% *ee*). The scope of allylic substitution is also suitable with respect to the α-substituted aromatic allylic imidates **233** and **313** (entries 9 and

Table 3.7 Survey of Allylic Trichloroacetimidates with *N*-methylamines

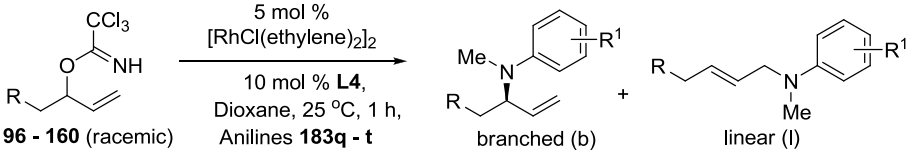

entry	imidates	anilines	products	% yield[a]	b/l ratio[b]	% *ee*[c]
1	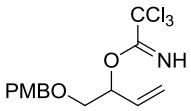 **308**	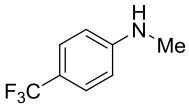 **183r**	**308r**	80	46:1	94
2	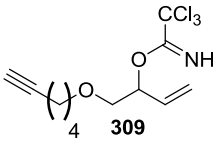 **309**	**183r**	**309r**	57	27:1	89
3	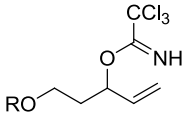 **310:** R = Bn	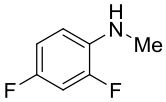 **183t**	**310t**	82	9:1	88
4	**223:** R = TBS	**183t**	**223t**	80	19:1	87
5	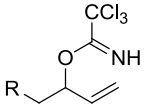 **311:** R = *i*-Pr	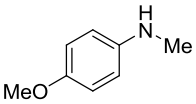 **183q**	**311q**	78	35:1	91
6	**312:** R = 4-MeO-Ph	**183q**	**312q**	92	69:1	87
7	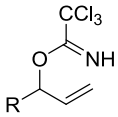 **231:** R = Cyclohexyl	**183q**	**231q**	88	11:1	96
8	**232:** R = *i*-Pr	**183q**	**232q**	88	14:1	95
9	**233:** R = Ph	**183q**	**233q**	87	7:1	93
10	**313:** R = 4-Br-Ph	**183q**	**313q**	95	12:1	86

[a] Yields are isolated values.

[b] The b/l ratios were determined by GC.

[c] The *ee*'s were determined by chiral HPLC

10). Because the leaving group is both allylic and benzylic, these substrates have a high propensity to undergo Overman's rearrangement.[2] However, under room temperature conditions **233q** and **313q** were formed in excellent yield (87 – 95%), high regioselectivity (b/l = 7:1 – 12:1) and high enantiomeric excesses (86 – 93% *ee*), with no rearrangement products observed in the reaction.

To demonstrate the utility of rhodium-catalyzed DYKAT of *N*-methyl anilines with racemic secondary allylic imidates, I prepared *N*-methyl homophenylalanine derivatives **315** - **317** (Scheme 3.8).[134] This motif is present in the structure of antillatoxin B, a secondary-metabolite of the marine algae antillatoxin and a potent activator of voltage-sensitive sodium-ion channels.[135] Amination of **227** with *N*-methyl 4-methoxyaniline **183q** provided allylic *N*-methyl arylamine **227q** in 92% yield and with b/l = 19:1 and 85% *ee*. After various failed attempts to oxidatively cleave the

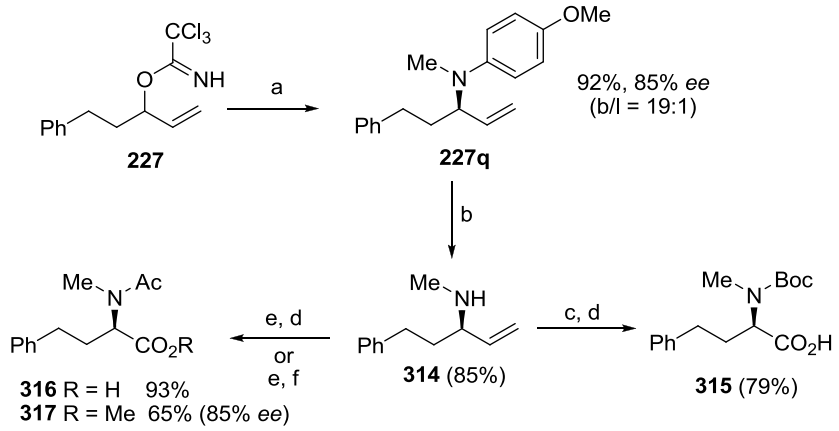

Reagents and conditions: (a) N-methyl *p*-anisidine **183q**, dioxane, 5 mol% $[RhCl(ethylene)_2]_2$ and 10 mol% **L1**, 40°C, 1h; (b) CAN, CH_3CN and H_2O, 15 min; (c) Boc_2O, K_2CO_3, THF/H2O (1:1); (d) $RuCl_3$, $NaIO_4$; (e) Ac_2O, pyridine; (f) O_3, NaOH, MeOH

Scheme 3.8 *N*-methyl Homophenylalanine Derivatives via DYKAT

olefin in **227q**, I determined that the PMP group needed to be replaced by a more inductive protecting group. Removal of the PMP group with ceric ammonium nitrate

afforded secondary amine **314** in 85% yield. Subsequent Boc-protection followed by oxidative cleavage of the olefin with ruthenium chloride and sodium periodate provided *N*-methyl-α-amino acid **315** (Scheme 3.8) in 79% yield over 2 steps. Alternatively, acetylation of **314**, followed by oxidative cleavage of the olefin, afforded amino acid **316** in 93% yield over 2 steps. On the other hand, subjecting the acetylated product to ozonolysis in basic methanol provided the methyl ester **317**. HPLC enantiomeric excess analysis revealed that the enantiopurity had not eroded during transformation steps from amination product **227q** to *N*-methyl homophenylalanine derivative **317**, and should prove useful for the asymmetric synthesis of a variety of chiral amino acids.

To further expand the substrate scope of the DYKAT process with secondary trichloroacetimidates, I investigated a broad spectrum of aniline and benzylamine nucleophiles with three substrates of differing class (Table 3.8).[104] Substrate **229** possesses a β-oxygen substituent that may provide additional chelation control along the reaction coordinate. Allylic imidates **227** and **231** lack an ether oxygen. In addition, substrate **231**, which contains the β-branching cyclohexyl group, has been reported to result in low regioselectivity in amination reactions.[96, 97] Overall, elevated temperatures (40°C) improve the yield and enantioselectivity in this study, but regioselectivity tends to be higher at room temperature. Therefore reactions using bulky cyclohexyl imidate **103** were run at ambient temperature for better regioselectivity. As shown in Table 3.8, electron-poor and rich primary anilines **183b** and **183c** (entries 1 and 2) provided allylic amination products in good yield (82 – 92%) and with excellent regioselectivity (b/l = 20:1 – >99:1) as well as enantioselectivity (80 – 95% *ee*). Even *ortho*-methyl substituted aniline **183d** (entry 3) delivered *N*-arylamines products with high regioselectivity and enantiomeric excess, highlighting the efficacy of our rhodium-catalyzed methodology with sterically challenging nucleophiles. Entries 4 and 5 clearly illustrate the electronic effects of the *para*-substituents on the aryl rings of *N*-methylanilines **183r** and **183q**. For instance, benzyloxy imidate **229** reacts efficiently with electron-poor aniline **183r**, providing allylic

Table 3.8 Survey of Anilines and Secondary Trichloroacetimidates in DYKAT

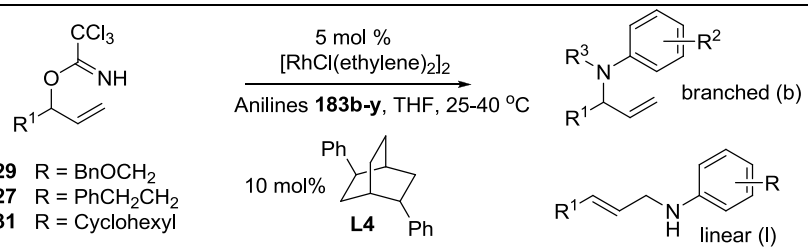

Entry	Anilines	Products	Temp (°C)	Time (h)	Yield[a] (%)	b/l[b] Ratio	ee[c] (%)
1	**183b** 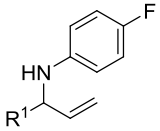	**229b** R = $BnOCH_2$	40	1	90	>99:1	87
		227b R = $PhCH_2CH_2$	40	1	92	>99:1	93
		231b R = Cyclohexyl	25	1	82	20:1	90
2	**183c** 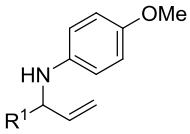	**229c** R = $BnOCH_2$	40	1	86	28:1	80
		227c R = $PhCH_2CH_2$	40	1	83	>99:1	89
		231c R = Cyclohexyl	25	2	82	>99:1	95
3	**183d** 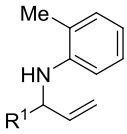	**229d** R = $BnOCH_2$	40	1	75	>99:1	90
		227d R = $PhCH_2CH_2$	40	1	81	90:1	96
		231d R = Cyclohexyl	25	22	44	79:1	82
4	**183r** 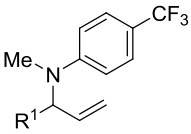	**229r** R = $BnOCH_2$	40	1	72	30:1	93
		227r R = $PhCH_2CH_2$	40	20	42	2:1	57
		231r R = Cyclohexyl	25	22	0	-----	----
5	**183q** 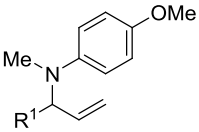	**229q** R = $BnOCH_2$	40	1	88	52:1	56
		227q R = $PhCH_2CH_2$	40	1	92	19:1	85
		231q R = Cyclohexyl	25	2	88	11:1	96
6	**183y** 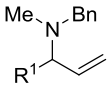	**229y** R = $BnOCH_2$	40	22	51	8:1	34
		227y R = $PhCH_2CH_2$	25	24	59	5:1	53
		231y R = Cyclohexyl	25	22	67	18:1	66

[a]Isolated Yield.

[b]Determined by GC.

[c]Determined by HPLC Analysis.

amine **229r** in 72% yield, good regioselectivity (b/l = 30:1) and 93% *ee* (entry 4). However, reaction of imidate **227** with this nucleophile was low yielding (42%) and low in selectivity (b/l 2:1, 57% *ee*). No amination product was observed with β-branching cyclohexyl substrate **231** (entry 4). A drastic difference in reactivity is observed in the reaction of electron-rich *N*-methyl 4-methoxyaniline **183q** (entry 5) with imidate **229**. Although the product **229q** was isolated in high yield, enantioselectivity is much lower (56% *ee*, entry 5) than that with electron-poor aniline **183r** (93% *ee*, entry 4). This outcome can be rationalized by the competitive rates between nucleophilic substitution and π-σ-π interconversion (Scheme 3.3). In contrast, when imidate **227** was reacted with aniline **183q**, the amination product **227q** was isolated in higher yield (92%) and selectivity (b/l = 19:1, 85% *ee*) than when paired with electron-withdrawing aniline **183r** (42%, 57% *ee*, and b/l=2:1). Cyclohexyl imidate **231** and electron-rich aniline **183q** provided amination product **231q** in 88% yield, 11:1 b/l ratio and impressive 96% *ee*, presumably a good balance of nucleophilicity and rate of interconversion. To our excitement, the DYKAT process is also applicable to alkyl amines (entry 6). For instance, using *N*-methyl benzylamine **183y** in the amination provided N-methyl allylic benylamines in moderate yields, regioselectivities, and enantiomeric excess.

One aspect that has not been discussed is the origin of branched selectivity in our amination reaction. In the stereospecific rhodium-catalyzed amination of branched allylic carbonates with anionic aniline nucleophiles, Evan's ascribes the observed regioselectivity to formation of *enyl*-type organorhodium intermediates that have both σ- and π-bond components (Scheme 2.3).[99] This positions σ-bound rhodium at the less-substituted terminus of the olefin, thereby obstructing nucleophilic attack and limiting the formation of the linear product. At the other extreme, organorhodium intermediates in our method could be true η^3-bound π-allyl complexes **318**, which are commonly observed Pd^{II} species (Scheme 3.9). In palladium π-allyl complexes, factors that influence regioselectivity are thought to arise from both steric and electronic characteristics of the palladium-ligand

complex.[120, 136] In general, palladium catalyzed allylic substitution reactions favour linear product formation. The use of bulky ligands (Scheme 3.9a) increases the steric interaction between the substrate R-group and the bound palladium complex resulting in increased selectivity for the branched substitution products. Utilization of π-acids including the diene-class of ligand increases the cationic character of the π-allyl fragment (Scheme 3.9b). Development of positive charge is favored at the more stable substituted carbon **319** leading to nucleophilic addition at this position. In contrast, small ligands and poor π-acids do not favor branched selectivity, therefore elevated levels of linear products result. Future mechanistic studies and attempts to isolate and analyze a crystalline organorhodium intermediate will hopefully clarify the controlling factors for high regioselectivity observed using our amination method.

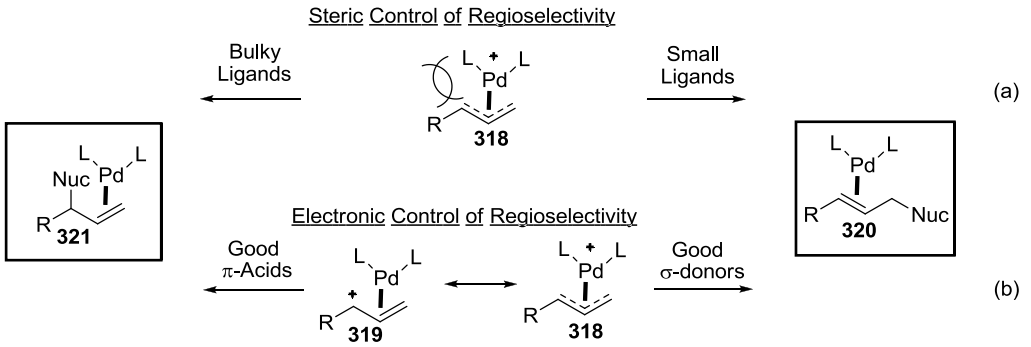

Scheme 3.9 Steric and Electronic Control of Regioselectivity

3.2.3 Conclusion

In summary, we have applied our method to the development of a highly versatile rhodium-catalyzed DYKAT of racemic secondary trichloroacetimidates with a wide variety of anilines, *N*-methylanilines, and benzylamines. At the outset, we were concerned that DYKAT may be problematic with less-hindered secondary electrophiles because

nucleophilic addition may be competitive with the rate of organorhodium complex interconversion. This was not the case, however, and reaction parameters could be modulated by choice of ligand, catalyst loadings and temperature.[104, 134] The reaction is operationally simple and displays broad functional group tolerance, providing a number of nitrogen containing tertiary centers in high yield, regio- and enantioselectivity. The utility of the method to prepare enantioenriched amino acids was demonstrated with the expedient synthesis of *N*-methyl homophenylalanine derivatives.

Application of our asymmetric method to the synthesis of tertiary allylic aryl amines now allows comparison with previous reports. Evans method using Wilkinson's catalyst and branched allylic carbonates generally provides high yields (83 – 96%) and moderate to high regioselectivities (8:1 - >99:1 b/l).[96-98] Our method delivers enantioenriched products in slightly lower average yield but with higher regioselectivity. Our DYKAT method is superior because it is enantioselective, is not limited to a few lithiated and stabilized aniline nucleophiles, and is applicable to β-dibranched substrates. Hartwig's iridium-catalyzed amination of primary allylic carbonates provides good to high yields of aryl amine products (72 – 95%) with good regioselectivities (11:1 – 99:1) and excellent enantiopurities (90 – 97% *ee*).[95] The iridium method achieves higher enantioselectivity, however our method provides higher regioselectivity and comparable yields. Side by side, our reaction accels in terms of substrate scope. Hartwig reports only aryl and alkyl substrates with the exception of methoxy groups on the aryl rings, while we have described the amination of ether, ester, and alkyne containing trichloroacetimidates. On the other hand, the two methods are equally tolerant of varied functionality on the neutral aniline nucleophiles with few exceptions. The iridium method efficiently catalyzes the reaction of secondary cyclic anilines such as tetrahydroquinoline and rhodium does not, and rhodium-catalyzes the amination of trichloroacetimidates with a number of *N*-methylanilines in high yield, regio- and stereoselectivity while iridium delivers these products with low regioselectivity. In terms of an asymmetric reaction for preparation of

tertiary allylic aryl amines, these methods should be considered complementary, giving the organic chemist options for introduction of this moiety into synthetic targets.

CHAPTER IV
SEQUENTIAL ASYMMETRIC AMINATION AND INTRAMOLECULAR OLEFIN HYDROACYLATION

4.1 Background

Efficient methods for preparation of enantioenriched amine-containing materials continues to be of paramount importance for amino acid, natural product and pharmaceutical synthesis. Our development of a highly regio- and enantioselective amination of racemic trichloroacetimidates for preparation of α-substituted[104, 134] and α,α-disubstituted[103] allylic aryl amines is one example. This catalytic method does not require additives[93, 95] or preparation of the aniline nucleophile[96, 97], only solvent, substrate, aniline and catalyst delivering products at 25-40°C under 3 hours. We had utilized our method towards facile preparation of *N*-methyl amino acids,[134] and were looking for further applications including the synthesis of nitrogen-containing heterocycles. Our strategy was to utilize our DYKAT method to set the required stereochemistry at the chiral amine-bearing centers and use these intermediates for subsequent transformation into enantioenriched aza-heterocycles.

Initially, we searched the literature for a synthetic target that would be applicable to our DYKAT amination and attainable prior to completion of my graduate career. We found the bioactive Manzacidin family of compounds isolated from marine sponges and decided that they would make excellent targets showcasing our method.[137, 138] In particular, we pursued the enantioselective synthesis of *N*-methyl Manzacidin C (Scheme 4.1)[138] because of the functionality present in the structure. This included an oxygen substituent beta to a chiral methylated nitrogen-containing quaternary center, a tertiary nitrogen-bearing center, and a *N*-methyl amine. The strategy was to utilize our DYKAT method to provide the quaternary center in high enantiopurity, functionalize the alkene and use the introduced chirality to direct diastereoselectivity during formation of the tertiary center. Synthesis of the quaternary center was accomplished using *N*-methylanisidine **183q** and

N-methyl benzylamine **183y** in good yield and with high selectivities (Scheme 4.1). Unfortunately, the basic nitrogen in both of the allylic aryl compounds **255q** and **322y** was problematic, just as we had observed in the amino acid synthetic strategy (Scheme 3.6). This would require additional deprotection and protective manipulations in order complete the synthesis Although these changes would allow me to finish the project, it would be accomplished at the expense of overall yield and efficiency making route less desirable. At this point we decided to set the synthesis aside and focus on another project. This was

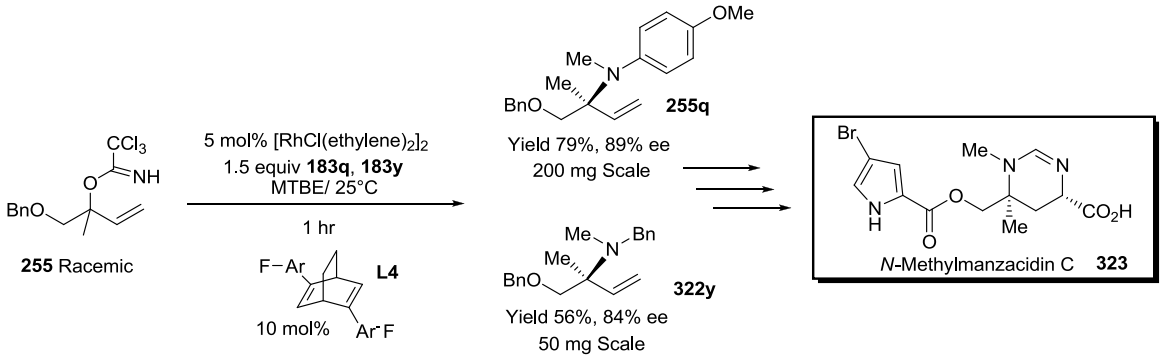

Scheme 4.1 DYKAT Amination for *N*-Methyl Manzacidin C Synthesis

a good experience though, because this work inspired new ideas and possible applications of the amination method that could be implemented in future synthetic efforts. These ideas will be presented in chapter 5.

With the synthesis of *N*-methyl Manzacidin C on hold, we directed our attention towards utilization of our DYKAT method to prepare enantioenriched alkenal substrates for intramolecular hydroacylation reactions. These transformations are highly efficient and atom-economical C-H activation reactions for preparation of five to eight-membered cycloketones.[139, 140] In these reactions, phosphine complexes of Rh, Co, Ru oxidatively add into the C-H bond of an aldehyde forming an acyl-metal hydride intermediate **325** that

subsequently inserts across the tethered olefin (Scheme 4.2). Reductive elimination furnishes the cycloketone product and regenerates the catalyst. The first intramolecular

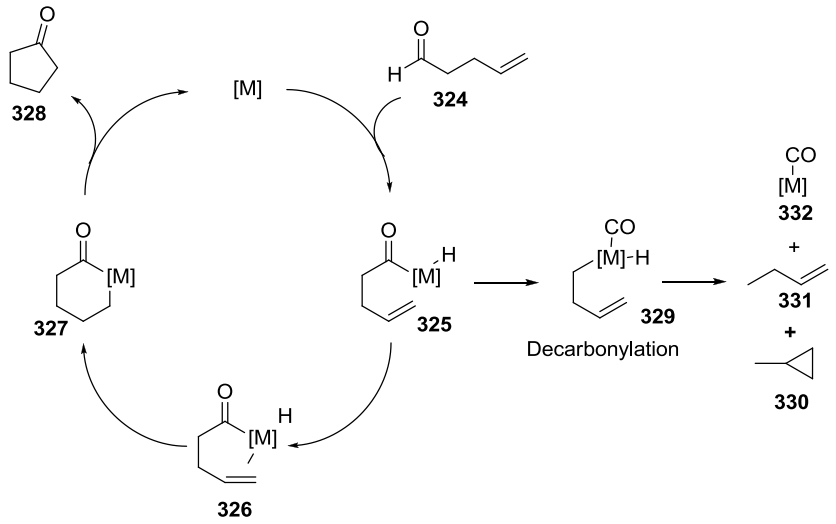

Scheme 4.2 Mechanism of Hydroacylation Reaction of Olefins

hydroacylation was reported by Sakai for preparation of 2,3-disubstituted cyclopentanones in prostaglandin synthesis.[141] In this report, stoichiometric Wilkinson's catalyst was used to prepare 30% of the desired cyclopentanone from 4-pentenal along with ~30% of the decarbonylation by-product methylcyclopropane **330** (Scheme 4.2).

Decarbonylation is the major competitive pathway due to the instability of acyl-metallic intermediates **325**.[142] Most improvements in transition-metal hydroacylation methodologies have involved strategies to stabilize these intermediates, thereby minimizing decarbonylation. Many improvements have been made by adding points of chelation.[139, 143, 144] For example, this competing side-reaction was reduced in Sakai's cyclopentanone forming method by saturating the reaction medium with ethylene (Figure 4.1). This provides a more stable acyl intermediate **334** although several hydroacylation products were isolated in low yield due the addition of ethylene.[145] Bosnich made a major

improvement in intramolecular hydroacylation reactions by applying cationic rhodium catalysts bearing bidentate diphoshine ligands.[146] These complexes exist as bridged arene dimers in non-coordinating solvents and catalyze these reaction at 10^3 the rate of Wilkinson's catalyst. This was a breakthrough because reaction could now be run with catalytic loadings of rhodium, whereas [$RhCl(PPh_3)_3$] was only slightly catalytic. In the presence of 4-pentenal, the cationic dimer dissociates forming a monomeric rhodium-substrate complex that with oxidative addition forms complex **335** (Figure 4.1). Elevated reaction rates and lower levels of decarbonylation is thought to derive from additional coordination sites on the acyl-rhodium hydride intermediate that allow immediate chelation to the olefin. In contrast, acyl-rhodium hydride complex **333** using $RhCl(PPh_3)_3$ catalyst that must first undergo ligand exchange to arrive at this complex which is required for migratory insertion. Another strategy to promote insertion versus decarbonylation is the incorporation of appropriately positioned heteroatoms including oxygen, sulfur, nitrogen and phosphorous. Aldehydes **336** – **339** shown in Figure 4.1 are examples of effective modulators of reactivity in intermolecular hydroacylations. (Figure 4.1).[144, 147]

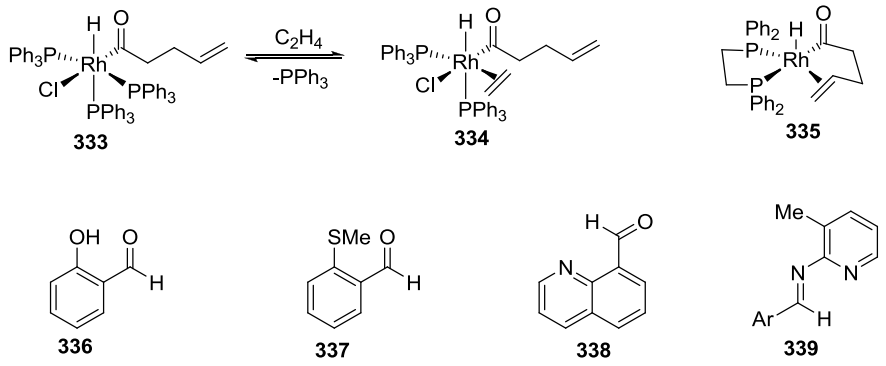

Figure 4.1 Minimizing Decarbonylation in Hydroacylation Reactions

Ring systems larger than cyclopentanone have been more difficult to prepare by hydroacylation because these reactions progress at slower rates making decarbonylation

more prominent and the kinetic five-membered ketones will form over larger rings if a suitable path is available.[139] For example, when 5-hexenal is subjected to rhodium-catalyzed intramolecular hydroacylation, no cyclohexanone results, only exclusive formation of methyl-cyclopentanone.[148] In response, medium-sized rings prepared by intramolecular hydroacylation were developed that include functionality in the starting material favoring larger ring formation. Mori reported the formation of seven-membered

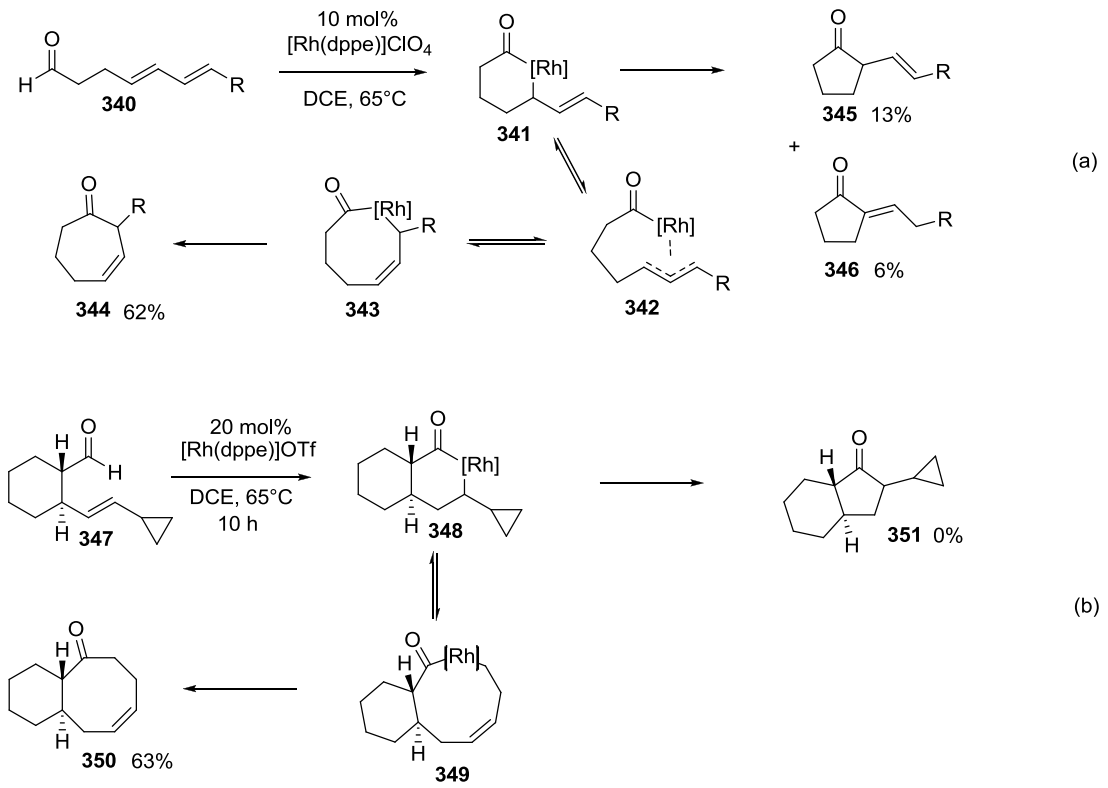

Scheme 4.3 Intramolecular Hydroacylation for Medium-sized Ring Enones

ring enones **344** from linear dienals **340** via intramolecular hydroacylation (Scheme 4.3a).[149] Oxidative addition and insertion resulted in 6-membered rhodacycle **341** which could undergo reductive elimination to cyclopentanone **345** or, stabilized by the exocyclic olefin, reversibly slip to π-allyl complex **342** and rhodacycle **343** leading to **344**. Mori

reported 62% yield of cyclic enone **344** along with 19% yield of cyclopentanones **345** and **346**. In a similar way, Shair treated vinyl cyclopropane substrates **347** to hydroacylation conditions (Scheme 4.3b).[150] Intermediate **348** could undergo reductive elimination or insertion into the appended cyclopropane ring forming cyclic **349** and cyclooctenone **350**. In the reaction, 63% yield of the desired product and none of five-membered ring product was observed.

Heteroatoms including oxygen,[151-153] sulfur,[152, 154] and recently nitrogen[155, 156] have been introduced to the framework of the starting substrate for synthesis of medium-sized heterocycles. The first report of this type was developed by Bendorf using Wilkinson's catalyst and sulfur as a tethered chelating group in alkenal **352** (Scheme 4.4a).[154] The

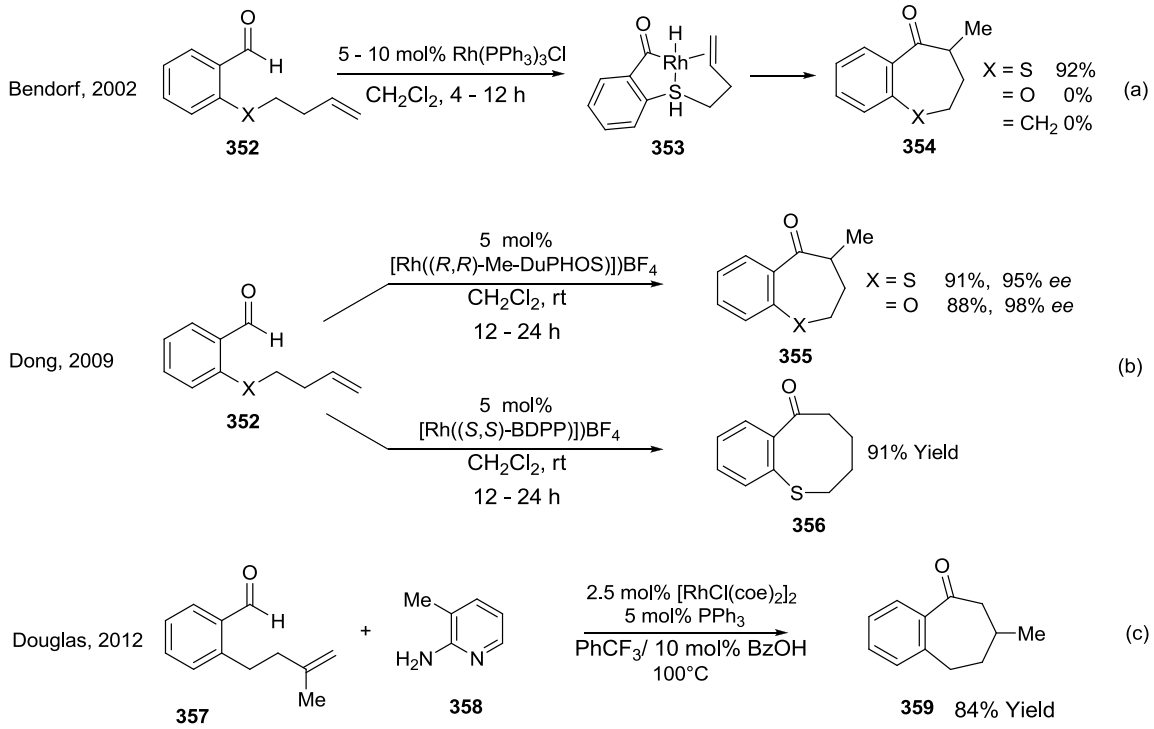

Scheme 4.4 Chelating Strategies in Intramolecular Hydroacylation

presence and position of sulfur was critical to formation of hydroacylation product **355** in 92% yield. The sulfur atom presumably chelates to rhodium, which helps facilitate oxidative addition, provides stabilization of acyl-rhodium hydride intermediate **353**, and helps position the olefin for coordination and migratory insertion. Oxygen and carbon tethers were ineffective in these reactions. In 2012, Dong and coworkers reported an asymmetric intramolecular hydroacylation of sulfur and oxygen-containing alkenals (Scheme 4.4b) using cationic rhodium chiral bisphosphine complexes.[152] The reaction is high yielding and enantioselective at room temperature in 12 to 24 h. In contrast to Bendorf's work, the tether lengths of sulfur substrates could be modified for seven- and eight-membered ring formation. In an interesting discovery, changing the ligand modulates seven-membered **355** formation versus eight-membered **358** in the reaction of substrate **352** (Scheme 4.4b). In an recent example (Scheme 4.4c), Douglas applied the work of Suggs[157] and Jun[144] where addition of 2-amino-3-picoline **358** forms transient aldimines that possesses a chelating pyridyl nitrogen for efficient hydroacylation.[158] Cyclic ketones **359** could be prepared in high yield, however, use of chiral ligands achieved only low to moderate enantioselectivities.

Dong and coworkers reported the first example of rhodium-catalyzed amine-directed hydroacylation of ketones for the enantioselective synthesis of seven- and eight-membered aza-lactones (Scheme 4.5a).[156] Electron-withdrawing groups on the nitrogen were unreactive, but a methyl group **360** provided optimal Lewis basicity in the hydroacylation reaction resulting in high yielding and enantioselective heterocyclic products **362**, with no decarbonylation products observed. Under optimized conditions using model substrate **360** where n = 1 and R = phenyl (Scheme 4.5a), reaction of the nitrogen substrate was very efficient and complete in 5 min versus 2 h for sulfur and 36% conversion in 48 h for the oxygen derivative. Bendorf subsequently showed the feasibility of amine-directed intramolecular hydroacylation of olefins, providing racemic seven- and eight-membered ring ketones (Scheme4.5b).[155] In contrast to Dong's findings,[152] the use

of Wilkinson's catalyst is significantly slower with nitrogen versus sulfur tethers, requiring reflux in acetonitrile for efficient hydroacylation reaction. Yields and reaction times are optimal when an allyl group is present on nitrogen **363**, with methyl and homoallyl groups providing only 11 and 35% yields respectively of the aza-ketone seven-membered ring. This suggests that the *N*-allyl group provides additional chelation to the rhodium-center in the intramolecular hydroacylation reaction.

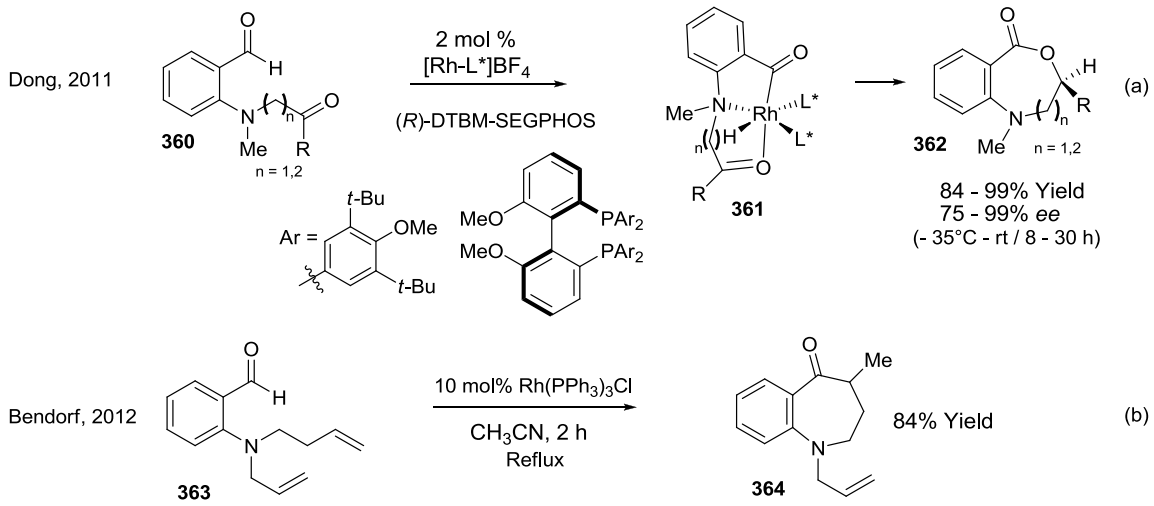

Scheme 4.5 Nitrogen-directed Rhodium-Catalyzed Hydroacylation

After reviewing these reports, we began to think about the potential use of our DYKAT reaction to prepare enantioenriched alkenal substrates for intramolecular hydroacylation (Scheme 4.6) . At this point we had conducted a number of studies with a variety of aniline nucleophiles possessing varied electronics, sterics and substitution patterns. However, our reaction had not been evaluated with anilines bearing an *ortho*-aldehyde group. This could be a challenging since the rhodium(I) catalyst utilized in the amination reaction that could potentially undergo oxidative addition with benzaldehyde **365** or DYKAT product **366** forming rhodium(III) acyl-intermediates that could proceed

to decarbonylation products **367** and **370** (Scheme 4.6). This process would likely be more facile due to chelation by the aniline nitrogen.[152, 155] Could a benzaldehyde nucleophile be utilized in the DYKAT of racemic trichloroacetimidates and result in high selectivities of branched enantioenriched alkenals, or would decarbonylation predominate? If the amination reaction was successful, would these products make suitable substrates for intramolecular hydroacylation and retain enantiopurity? If successful, this 2-step strategy would yield enantioenriched nitrogen-containing heterocycles **368** or **369**. This approach differs from Dong's work because asymmetric induction would be controlled during the amination step, not during hydroacylation.[156]

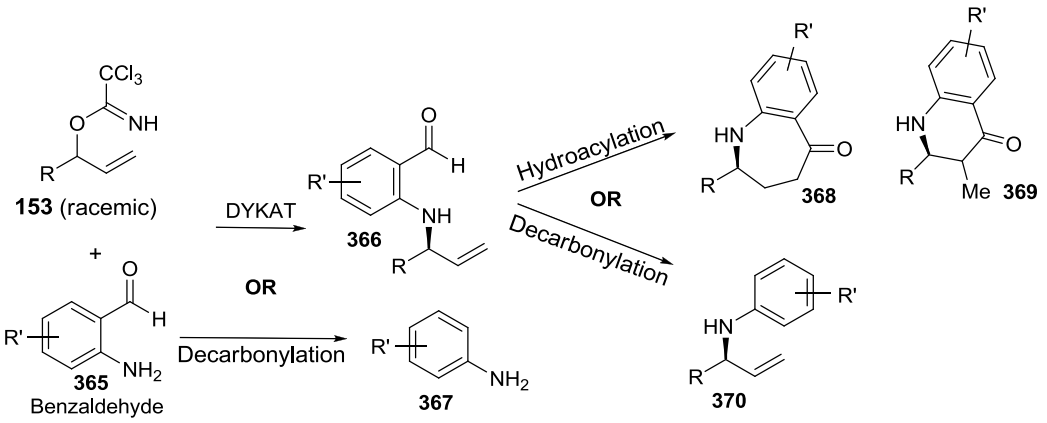

Scheme 4.6 Strategy for Sequential DYKAT Amination and Hydroacylation

4.2 Results and Discussion

We began our studies of the sequential 2-step process by investigating the racemic amination of trichloroacetimidate **227** with benzaldehyde nucleophile **183z** (Table 4.1). The neutral rhodium catalyst $[RhCl(COD]_2$ was much more effective (entry 3) than cationic rhodium catalysts (entries 2 –3) resulting in 77% yield of the amination product **227z** with >99:1 b/l selectivity. In these reactions we did not observe decarbonylation or

Table 4.1 Optimization of DYKAT with Aniline **183z**

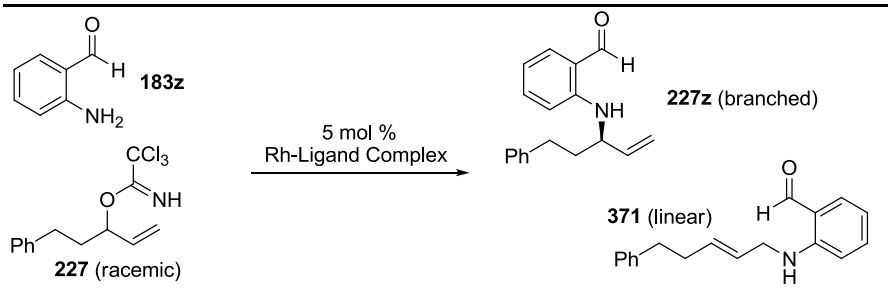

entry	Rh-Ligand complex	solvent	temp (°C)	time (h)	yield (%)[b]	b:l[c]	**227z** % ee[d]
1	$[Rh(COD)_2]OTf$	THF	25	3	66	10:1	-
2	$[Rh(COD)_2]BF_4$	THF	25	3	59	6:1	-
3	$[RhCl(COD)]_2$	THF	25	3	77	>99:1	-
4	$[RhCl(ethylene)_2]_2$/**L4**	Dioxane	40	22	14	2:1	29
5	$[RhCl(ethylene)_2]_2$/**L4**	Dioxane	25	22	11	29:1	67
6	$[RhCl(ethylene)_2]_2$/**L4**	THF	25	22	44	82:1	71
7	$[RhCl(ethylene)_2]_2$/**L4**	Toluene	25	22	22	30:1	53
8	$[RhCl(ethylene)_2]_2$/**L4**	MTBE	25	22	61	29:1	67
9	$[RhCl(ethylene)_2]_2$/**L10**	MTBE	25	22	34	26:1	59
10	$[RhCl(ethylene)_2]_2$/**L7**	MTBE	25	22	35	20:1	70
11	$[RhCl(ethylene)_2]_2$/**L8**	MTBE	25	22	46	53:1	65
12	$[RhCl(ethylene)_2]_2$/**L9**	MTBE	25	22	64	>99:1	84
13	$[RhCl(ethylene)_2]_2$/**L11**	MTBE	25	22	59	6:1	62

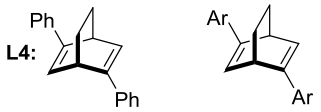

L7: Ar = 4-F-Ph
L8: Ar = 3,4-F-Ph
L9: Ar = 3,4,5-F-Ph
L10: Ar = 2-Napth
L11: Ar = 3,5-CF_3-Ph

[a] All reactions were conducted at 0.2 M with 1 equiv. of imidate **227**.

[b] Isolated yields.

[c] The branched to linear ratio (b:l) was determined by ^{1}H NMR.

[d] Determined by chiral HPLC.

hydroacylation products. Next, the DYKAT amination was investigated utilizing previously optimized conditions[134] (entry 4) which provided the amination product in low yield and selectivities (14%, b/l = 2:1, 29% *ee*). Reducing the temperature from 40°C to room temperature had little effect on the yield but the regioselectivity and enantioselectivity increased substantially (entry 5, b/l = 29:1, 67% *ee*). When various

solvents were screened (entries 5 – 8), MTBE provided the best result with 61% yield, b/l = 29:1, and enantioselectivity at 67% *ee* (entry 8). As we had done in previous optimization studies, a number of Hayashi[130] chiral diene derivatives of varying electronic properties were tested in the DYKAT amination of **227** with **183z**. The 3,4,5-trifluoro derivative **L9** (entry 12) provided the highest combination of yield (64%), regio- and enantioselectivity (b/l = >99:1, 84% *ee*) and was utilized for hydroacylation going forward.

Next we focused on the rhodium-catalyzed intramolecular hydroacylation of allylic amine **227z**. Based on Dong's previous reports,[153, 156] we knew that ligand bite angle plays an important role in the rates of intramolecular hydroacylation. Thus we investigated cationic rhodium bis-phenylphosphine complexes prepared by hydrogenation of $[Rh(NBD)_2]BF_4$ in the presence of dppe, dppp, and dppb.[153] The efficiency of cyclization to prepare **372** decreased (96% vs. 72%, entries 1 and 2) as the bite angle of the bis-phosphine ligands becomes smaller, which is consistent Dong's report for rhodium-catalyzed enantioselective intramolecular ketone hydroacylation. The dppp ligand seems optimal in these reactions and the yield drops slightly with dppb ligand (82% versus 96% yield, entries 2 and 3). The solvent choice did not affect the hydroacylation yields or reaction times at 105°C. Although these rhodium-bisphosphine complexes performed well

in the cyclization, preparation prior to use detracts from their desirability as hydroacylation catalysts (entries 1–5). We found that commercially available $[Rh(COD)(dppb)]BF_4$ was equally effective, affording seven-membered ring aza-ketone **372** in 99% yield (Table 4.2, entry 6). Cyclization to form seven-membered ring product **372** progressed slowly at 70 °C (entry 9) with 32% conversion after 1 h, and full conversion was observed after 20 h. To our excitement, HPLC enantiopurity analysis of nitrogen-containing heterocycle **372** revealed that the cyclization reaction results in complete transfer of stereochemistry in all cases, and no decarbonylation products have been observed. Hydroacylation of the olefin can proceed via 2 different pathways forming 6- or 7-membered ring products. With these catalysts however, exclusive formation of the larger

7-membered product suggests that insertion into the terminal position of the olefin is favorable. Importantly, our results illustrate that cyclization can effectively take place in the absence of additional substituents on the nitrogen atom of allylic amine **227z**, which were unsuitable substrates under Bendorf's conditions.[155]

Table 4.2 Hydroacylation Optimization of Amine **227z**

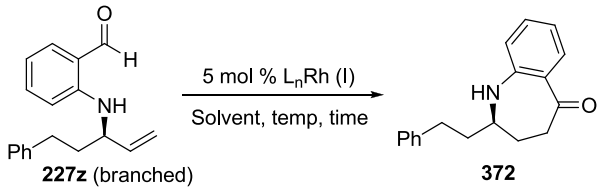

227z (branched) **372**

entry	Rh(I) cat.	solvent	temp (°C)	time (h)	yield (%)[b]	*ee* (%)[c]
1	$[Rh(dppe)_2]BF_4$	$PhCF_3$	105	1	72	84
2	$[Rh(dppp)_2]BF_4$	$PhCF_3$	105	1	96	84
3	$[Rh(dppb)_2]BF_4$	$PhCF_3$	105	1	82	84
4	$[Rh(dppp)_2]BF_4$	Toluene	105	1	99	84
5	$[Rh(dppp)_2]BF_4$	Dioxane	105	1	99	84
6	$[RhCOD(dppb)]BF_4$	Dioxane	105	1	99	84
7	$[RhCOD(dppb)]BF_4$	Dioxane	70	20	99	84

[a] All reactions were conducted at 0.2 M.

[b] Isolated yield.

[c] Determined by chiral HPLC

We were interested to know if minor linear amination product **371** would undergo hydroacylation in the presence of cationic rhodium catalysts (Scheme 4.7). Under $[Rh(COD)(dppb)]BF_4$ conditions utilized for cyclization of **227z** (Table 4.2), the corresponding linear isomer **371** was unreactive. However, use of the rhodium triflate complex, $[Rh(COD)_2]OTf$, provided the corresponding six-membered aza-heterocycle **373** in 58% yield (Scheme 4.7). Interested by this result, we then subjected branched **227z** to $[Rh(COD)_2]OTf$. Again we obtained a 6-membered aza-ketone, and **374** was obtained in

high yield but with low diastereoselectivity (Scheme 4.7, 84%, dr = 1.8:1). This is not new observation, as Dong and Bendorf report different outcomes depending on the metal complex used in the reaction.[152, 155]

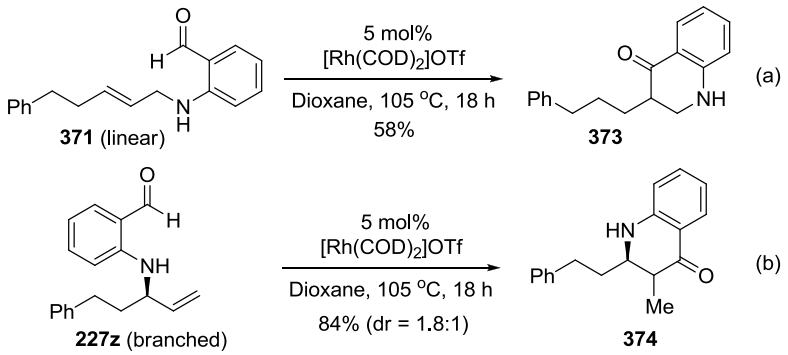

Scheme 4.7 Six-Membered Ring Formation with [Rh(COD)$_2$]OTf Catalyst

With optimized DYKAT amination and hydroacylation reactions in hand, a number of one-pot reaction reactions without isolating the intermediate branched alkenyl aldehyde **227z** were explored. Unfortunately, the desired intramolecular hydroacylation product **372** resulted in poor yield in all cases. These experiments showed that it is imperative to isolate the allylic amine product prior to cyclization.

To illustrate the scope of the sequential process, we turned our attention to assessing the rhodium-catalyzed asymmetric amination with a diverse set of racemic secondary allylic imidates (Table 4.3). The starting trichloroacetimidates used in entries 1 – 7 containing several functional groups were suitable reaction partners with 2-amino benzaldehyde **183z**. The corresponding allylic amines were isolated in 40–95% yield, 80–92% *ee* and with high selectivity for the branched isomer. Notably, α-substituted cyclohexyl imidate **231** (entry 7) reacted to afford allylic amine **231z** with low 41% yield, but with 80% *ee* and with high regioselectivity, which has been reported to give amination

Table 4.3. Scope of Sequential DYKAT Amination and Hydroacylation[a]

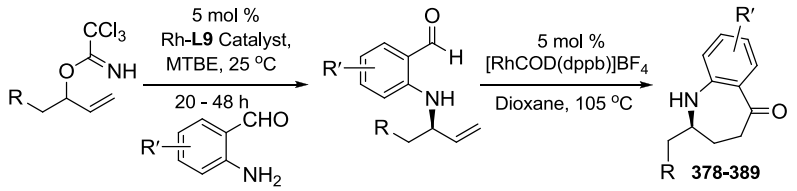

Entry	Imidates	Allylic Amines (yield,[b] *ee*[c])	Aza-Ketones (yield,[b] *ee*[c])
	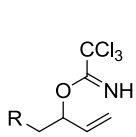	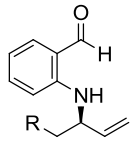	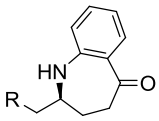
1	**310:** R = $BnOCH_2$	**310z:** 95%, 87% *ee*	**378:** 99%, 89% *ee*
2	**223:** R = $TBSOCH_2$	**223z:** 67%, 83% *ee*	**379:** 90%, 83% *ee*
3	**229:** R = BnO	**229z:** 81%, 86% *ee*	**380:** 99%, 86% *ee*
4	**375:** R = 4-F-PhO	**375z:** 77%, 80% *ee*	**381:** 99%, 80% *ee*
5	**230:** R = Ph	**230z:** 59%, 92% *ee*	**382:** 95%, 92% *ee*
6	**311:** R = $(CH_3)_2CH$	**311z:** 40%, 80% *ee*[e]	**383:** 96%, 78% *ee*
7	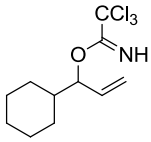 **231**	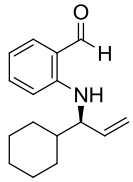 **231z:** 41%, 80% *ee*[e]	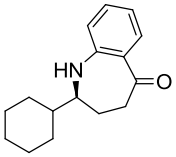 **384:** 99%, 80% *ee*
8	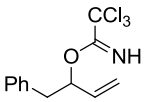 **230**	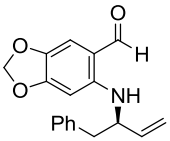 **230za:** 91%, 94% *ee*	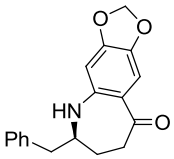 **385:** 92%, 95% *ee*
9	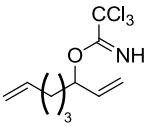 **376**	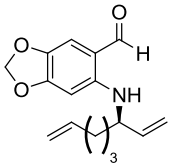 **376za:** 61%, 84% *ee*	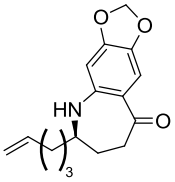 **386:** 50%, 86% *ee*[d]
10	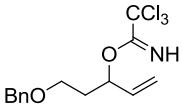 **310**	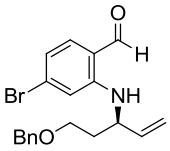 **310zb:** 64%, 93% *ee*[e]	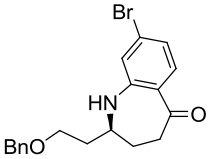 **387:** 62%, 94% *ee*[f]

Table 4.3 Continued

11	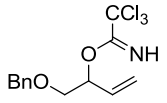 **229**	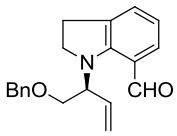 **229zc:** 83%, 88% *ee*	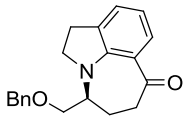 **388:** 66%, 84% *ee*[g]
12	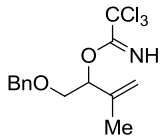 **377**	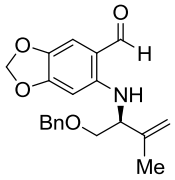 **377za:** 10%, 13% *ee*[e]	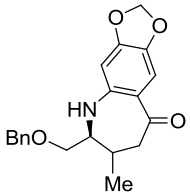 **389:** 99%, dr = 4:1

[a] Reactions conducted with 1 equiv. of allylic imidate and 1.5 equiv.of 2-amino arylaldehyde.

[b] Isolated yields.

[c] Determined by chiral HPLC.

[d] 70 °C, 18 h.

[e] 7.5 mol% Rh-**L9** complex at 40 °C.

[f] 10 mol% [RhCOD(dppb)]BF_4, 24 h.

[g] 5 mol% [RhCOD(dppb)]BF_4, 24 h.

products with low regioselectively.[96, 97] Furthermore, the amination reaction is compatible with electron-donating **183za** and electron-deficient **183zb** 2-amino arylaldehydes (entries 8–10), giving access to a range of aryl alkenals in 61% – 91% with excellent enantioselectivity (84 – 94% *ee*). Cyclic aniline nucleophile **183zc** (entry 11) is also amendable to provide the allylic amine product **229zc** in 83% yield with 88% *ee*. To establish the generality of the process, we examined the amination with disubstituted olefin **377** (entry 12), a substrate type which has never been explored under our our DYKAT conditions. This imidate presents an additional challenge in that both *syn* and *anti* α-allylrhodium intermediates need to be considered.[121] While the 2-methyl group on the α-allyl destabilizes the *syn*-isomer through 1,2-steric interaction, the *anti*-isomer suffers

A(1,3)-interaction. As we expected, allylic arylamine **377za** was isolated in 10% yield with 13% *ee* (entry 12). This low selectivity suggests that Rh-**L9** complex was not effective at controlling the relative population of these two *syn*- and *anti*-isomers.[121] Overall, Table 4.3 illustrates the generality of the DYKAT method with 2-amino arylaldehydes.

With alkenyl aldehydes in hand, we subsequently subjected these amination products to the intramolecular olefin hydroacylation conditions consisting of 5 mol% [RhCOD(dppb)]BF_4 at 105 ^oC for 1 h (Table 4.3). Cyclization of alkenals (entries 1 – 12) proceeded smoothly to afford seven-membered aza-heteroccyles **378 - 389** in good yields (50 – 99%) without any observable racemization. A range of functional groups are tolerated in the β-substituted alkenals. Notably, the α-substituted cyclohexyl alkenal **231z** (entry 7) efficiently underwent cyclization to provide seven-membered ring aza-ketone **384** in nearly quantitative yield. For substrate **376za** (entry 9), we observed that hydroacylation preferentially occurred at the allyl position to provide nitrogen-containing heterocycle, with simultaneous isomerization of the γ -vinyl substituent as a 2:1 mixture of *E*:*Z* isomers at 105 ^oC. On the other hand, cyclization of amine **376za** at 70 ^oC provided the desired aza-ketone **386** (entry 9) and the exclusive *Z*-isomerization product as a 1:1 inseparable mixture of isomers. Electron-deficient alkenal **310zb** (entry 10) significantly slowed down the cyclization process. Even after 24 h, only 62% yield of aza-heterocycle **387** (entry 10) was obtained in the reaction. Cyclization of alkenyl aldehyde **229zc** (entry 11), bearing secondary aniline functionality, also reacted sluggishly and took 24 h to reach completion. Seven-membered ring product **388** was obtained in only 66% yield. Interestingly, hydroacylation of challenging allylic arylamine **377za** (entry 12) proceeded smoothly to afford aza-heterocyle **389** in 99% yield with dr = 4:1 and without racemization. While the major diastereomer of **389** was isolated with 15% *ee*, the minor isomer was 11% *ee*.

As a further demonstration of the robust nature and operational simplicity of the sequential catalytic events, the enantioselective amination of tertiary allylic trichloroacetimidate **255** (Scheme 4.8) was attempted. Under standard conditions, the

reaction proceeded slowly to provide nitrogen-containing quaternary center **390** with poor yield. Increasing catalyst loading (5 →7.5 mol%) and reaction temperature (25 → 40 °C)

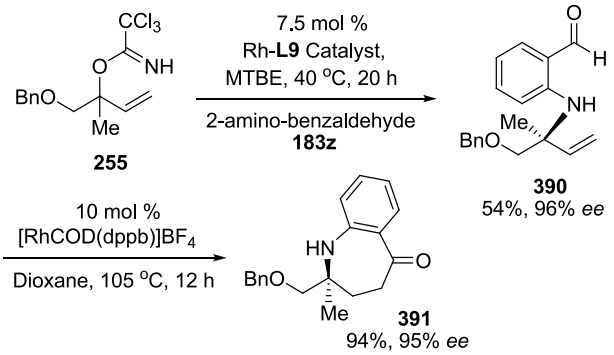

Scheme 4.8 Sequential DYKAT and Hydroacylation with Tertiary Trichloroacetimidate **255**

provided amine **390** in 54% yield with 96% *ee*. Subsequent cyclization of **390** with 10 mol % [RhCOD(dppb)]BF_4 at 105 °C for 12 h afforded seven-membered aza-heterocycle **391** in 94% yield without observable racemization (95% *ee*).

4.3 Conclusion

In summary, we were able to develop a successful application of our rhodium-diene ligated DYKAT methodolgy to the enantioselective synthesis of nitrogen-containing heterocycles. In this sequential method, asymmetric amination using a variety of allylic trichloroacetimidate electrophiles with aniline nucleophiles possessing an *ortho*-formyl group provide a number of enantioenriched alkenal substrates that readily undergo intramolecular olefin hydroacylation cyclization using cationic rhodium-catalysis. This is a departure for previous reports that prepare medium-sized ring heterocycles where enantioselectivity is achieved during the hydroacylation step. Overall, the 2-step process readily provides enantioenriched 2-alkyl-benzoazepin-5-ones in high yield with retention

of enantioselectivity from the DYKAT amination step, with no decarbonylation observed throughout the sequence. Electron-rich and deficient anilines, as well as tertiary trichloroacetimidates are tolerated providing an efficient route to the constructs We anticipate that the method will have potential impact on the strategies used for the preparation of bioactive natural products and potential pharmaceutical agents containing these aza-ketone ring systems.

CHAPTER V
CONCLUSION AND FUTURE DIRECTIONS

As I look back at the start of my graduate research, it is quite amazing how far this project has come and could not be happier with the way it all unfolded. We began with an idea, based on observations in Overman's research and developments that followed, that the basic nitrogen and less-hindered terminal olefin of branched allylic trichloroacetimidates should rapidly ionize forming activated complexes for substitution by a nucleophile using an appropriate transition-metal catalyst. We set out to develop a reaction using these imidate substrates and phenol nucleophiles, trying a number of transition-metal catalysts, ligand types, and reaction conditions. There was some early success, and persistence paid off when one day in October of 2009 I tried a few aniline nucleophiles under my best reaction conditions. These were exciting days in my graduate career, preparing and utilizing as many secondary trichloroacetimidate types as I could with any number of anilines that could be found in the Sigma-Aldrich catalog. Thus began the development of this highly regioselective rhodium-catalyzed aryl amination method.

Along the way, we found that our method could address shortcomings described in earlier reports including low regioselectivity using α-dibranched substrates and *N*-methyl anilines in the aminations of allylic acetates and carbonates.[95-97] We were always looking for these problematic areas to apply our method. Prior to any of our studies, the literature provided few examples of substitution reactions catalyzed by transition-metals using tertiary electrophiles and anilines. While working on the regioselective amination of secondary trichloroacetimidates, our sights were already on tertiary electrophiles. We worked feverishly on the tertiary version, and submitted the manuscript to *The Journal of the American Chemical Society* only to be rejected. This turned out to be a very positive and perhaps lucky happening. Prior to submission, we had discovered that the commercially available chloronorbornadiene rhodium(I) dimer very efficiently and reproducibly catalyzes these reactions at room temperature and with higher

regioselectivities compared to phosphite complexes of rhodium. We completely overhauled this paper and resubmitted to *Organic Letters* in 2012, and I am very proud of this work. It is a robust method that undergraduate and graduate students can set up for the first time and prepare allylic aryl amine products with yields and regioselectivities as reported. We haven't used phosphite ligands since, which were a component that added some variability to our reaction results. In addition, revision of this paper solidified chiral dienes as the best ligand choice for DYKAT reactions because of the efficiency of these reactions and the fact that numerous chiral phosphite ligands that I was preparing were not delivering any level of asymmetric induction. In all, this amination is the most general allylic substitution using aniline nucleophiles for the regioselective preparation of quaternary amine-bearing centers. This is demonstrated by the wide range of imidate and aniline functionality that is compatible in the reaction, and now provides a means to aryl amine products bearing *ortho*-substituents.

The control experiments that were conducted support our original hypothesis that the trichloroacetimidate nitrogen and branched allylic substrates are of critical importance to our amination method. Electrophiles such as acetates and carbonates using our rhodium conditions do not provide amination products (Scheme 2.5), and primary linear imidates which are effective in transformations mediated by Pd(II), react sluggishly and mainly provide linear products (Table 2.8). The amination reactions of all classes of allylic imidates with boron trifluoride dietherate (Table 2.8) require extended reaction times (6 – 21 h) for completion and result in low levels of regioselectivity (1:1 – 1:9 b/l ratios). In comparison, the reaction of same trichloroacetimidate under rhodium-catalyzed conditions is complete in 30 min and provides >99:1 regioselectivity for the branched aryl amine product, a markedly different result.

We had early aspirations of an asymmetric amination method for the synthesis of α,α-disubstituted allylic amines and we were aware that this might be acheivable when experimental data showed that our reaction was not enantiospecific. This was reported in

my first graduate school publication, and although one reviewer failed to see the point of a new method that was not enantiospecific, we felt as though the clock was running thinking a few lights might turn on in the synthetic community. I worked very diligently on this project which resulted in the first DYKAT of tertiary electrophiles with an aniline nucleophile, a real triumph. Our work continued by developing a niche application of the DYKAT reaction where *N*-methylanilines are efficient nucleophiles with secondary trichloroacetimidates for the regio- and enantioselective preparation α-substituted allylic amines. And finally, I highlighted the utility of our method by preparing enantioenriched *N*-methyl homophenylalanine amino acids and by developing a DYKAT amination and hydroacylation sequence for the asymmetric synthesis of 7-membered aza-heterocycles, completing my graduate work at the University of Iowa.

My work is done but of course many studies and applications of the DYKAT reaction remain. There is a lot of room to improve the scope of our enantioselective substitution reaction. There were some nucleophiles that performed well in the regioselective amination that did not work well in the DYKAT reaction and should be revisited. 2-((Trimethylsilyl)ethynyl) aniline **183o** utilized for racemic preparation of isoprenylated indoles (Scheme 2.10) does not react efficiently in the enantioselective reaction and likewise 2-bromoaniline **183m** is a good nucleophile with tertiary substrates under $[RhCl(NBD]_2$ catalysis but not using chiral diene ligands. Both of these amine products would be quite useful building blocks and would be a great addition to the large number of anilines that can be utilized. Another aniline nucleophile that has not provided acceptable results in the enantioselective reaction is tetrahydroquinoline **185** (Table 2.1). This cyclic secondary aniline is an excellent nucleophile under Hartwig's reaction conditions.[95] Perhaps this nucleophile would have to be used under iridium conditions just as secondary acylic *N*-methyl anilines are only efficient under rhodium conditions. I have conducted a few experiments using amine sources other than anilines and *N*-methyl benzylamines including sulfonamides and indoles, and some attempts with phenols in the

DYKAT reaction. Although these reactions were not successful, perhaps a more intensive investigation and optimization is needed in each case. In addition to scope of the nucleophilic partner, much could be expanded regarding the scope of tertiary substrates that could be subjected to enantioselective rhodium conditions. Tertiary electrophiles utilized to this point have a methyl substituent at the resulting quaternary center. Many natural products possess this feature, and we selected these substrates because they are easy to prepare by Grignard addition to methyl ketones. What if functionality other than methyl was required at this center? Expanding the diversity of accessible groups at this position would make this method more versatile, and it would be interesting to see how these electrophiles perform under rhodium-catalysis. So far we have been limited by the ability to prepare new substrates. Again, much more attention is required because the time I dedicated to this endeavor was in response to reviewer comments under a timeframe. I attempted to prepare the ethyl derivative but could not functionalize the tertiary alcohol as the trichloroacetimidate, which was presumably too hindered. All attempts to prepare imidates from a number of alcohols bearing aromatic groups were too unstable and could not be isolated. Perhaps addition of electron-withdrawing groups at the center possessing the leaving group that is both allylic and benzylic could boost stability of these substrates.

Another area of substrate expansion that only recently has been explored is substitution of the olefin component. Although we had originally proposed that a less-hindered terminal olefin was required for efficient ionization to organorhodium intermediates, we wanted to test this hypothesis. We revisited this idea during my *N*-methyl Manzacidin C synthesis project. While encountering many failures to functionalize the olefin of the allylic amination product, we thought it would be advantageous if the DYKAT reaction could be run with a terminal vinyl acetate or comparable group already installed on imidate **392** (Scheme 5.1). If this were possible, the enantioselective synthesis of members of the Manzacidin family could be rapidly be accessed. Another thought and application that stemmed from this idea involves DYKAT amination followed by a second

palladium or iridium substitution of the remaining allylic acetate, possibly forming another stereogenic center **394b** (Scheme 5.1). We had already demonstrated that allylic acetates and carbonates are stable to our rhodium reaction conditions. Perhaps this could be a one-pot or sequential-type reaction in the future. Unfortunately, early attempts utilizing vinyl acetates provides products with low enantioselectivity, suggesting slower rates of interconversion of organorhodium intermediates due to the congested terminus. Recent work in our laboratory however, has shown that the amination of enantioenriched **392** is enantiospecific using the racemic rhodium NBD catalyst. This would allow access to the Manzacidins and a 2-step substitution sequence which I look forward to seeing in the future. I discussed another olefin modification in chapter 4 where DYKAT amination of trichloroacetimidate **377** (Table 4.3) possessing a 2-methyl group on the allyl fragment led to low yields and enantioselectivity. Again, the chiral ligands were inadequate to differentiate populations of *syn*- and *anti*- conformers and the unfavorable interactions that result. Efforts should continue to investigate various classes of substrates and nucleophilic partners in the reaction which will provide mechanistic understanding and elucidate the boundaries of this methodology

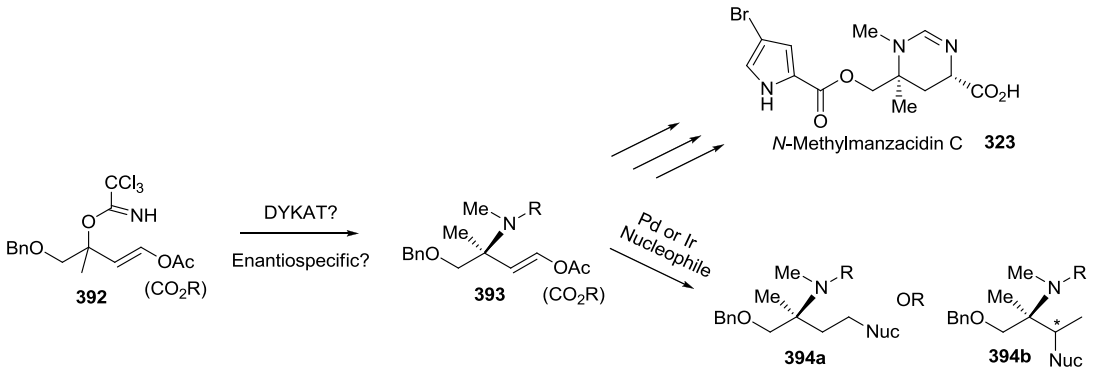

Scheme 5.1 Rhodium-catalyzed Amination of Vinyl Acetates for Synthetic Application

Investigations that have commenced in our laboratory to solve the issues of low yield, regioselectivity and or enantioselectivity associated with tertiary trichloroacetimidates lacking an accessible β-oxygen group. This has largely involved the the synthesis of a new ligand design. Preliminary results show major improvements in enantioselectivity but much lower yielding reactions. I am confident that continued efforts will result in a catalyst complex that provides a good balance of yield and enantioselectivity which would greatly improve the value and usefulness of our DYKAT reaction.

And lastly, it is time to conduct in-depth mechanistic studies. Studies that probe the inner-workings our our amination method would futher our ability to design ligands for increased efficiency, selectivity and scope. Initially these studies should start by trying to isolate substrate bound intermediates or designing and testing presumed catalytic intermediates. There have been minimal attempts to isolate intermediates in our laboratory and again more effort is needed. Additionally, expanded NMR studies, kinetic and computational work would greatly improve our mechanistic understanding of this reaction. What is the rate-limiting in our amination? What is the catalytic-turnover? What makes anilines favorable in our reaction while other substitution reactions catalyzed by iridium and rhodium are amenable to a wider range of nucleophiles. Clearly, there are substantial mechanistic differences between rhodium(I) catalyzed allylic substitution reactions of branched trichloroacetimidates using π-acidic diene and phosphite ligands versus Evan's work with branched carbonates and a mixture of donor phosphine and π-acidic phosphite ligands.[96] When trichloroacetimidate **223** was subjected to amination with Wilkinson's catalyst and trimethyl phosphite only 13% of the desired product was isolated with 5:1 regioselectivity (Table 2.1). Conversly, there is no amination reaction of carbonate electrophiles using our catalyst system.[12, 13] We need to unravel the reasons that this combination of ligands and branched allylic trichloroacetimidate electrophiles result in an efficient DYKAT reaction while other methods fail. I hope that these investigation are undertaken and would look forward to seeing the results in the future.

CHAPTER VI
EXPERIMENTAL

5.1 Methods, Reagents and Instrumentation

All reactions were performed in oven-dried Schlenk flasks fitted with glass stoppers under positive nitrogen pressure. Organic solutions were concentrated by rotary evaporation below 40 ^{o}C at 25 torr. Analytical thin-layer chromatography (TLC) and gas chromatography (GC) were routinely used to monitor the progress of the reactions. TLC was performed using pre-coated glass plates with 230-400 mesh silica gel impregnated with a fluorescent indicator (250 nm). Visualization was accomplished using UV light, potassium permanganate, or phosphomolybdic acid. Dry solvents were obtained from a SG Waters solvent system utilizing activated alumina columns under an argon pressure or purchased from Sigma-Aldrich in sure-seal bottles. The rhodium catalysts and chiral diene ligands were handled and transferred to Schlenk flasks within a glove box under a nitrogen atmosphere. All chemicals and reagents were obtained from commercial vendors and used without further purification.

Monitoring by GC was performed on an Agilent 6850 with autosampler using an HP-1 (30m x 0.320mm) column and temperature gradient of 100-250°C over 10 min. Flash chromatography was performed on a Teledyne Isco CombiFlash R_f system utilizing normal phase pre-column cartridges and gold high performance columns. The *ee*'s were determined on an Agilent 1200 series HPLC using a Diacel Chiralcel 4.6 x 250 mm OD-H or Diacel Chiralcel OJ-3 4.6 x 150 mm column fitted with guard columns with flow rates and mobile phases as indicated. All proton (^{1}H) nuclear magnetic resonance spectra were recorded on a 400 MHz spectrometer. All carbon (^{13}C) nuclear magnetic resonance spectra were recorded on a 100 MHz NMR spectrometer. Chemical shifts are expressed in parts per million (δ scale) and are referenced to residual $CHCl_3$ (^{1}H: δ 7.24 ppm, ^{13}C: δ 77.23 ppm) in the NMR solvent. Data are presented as follows: chemical shift,

multiplicity (s = singlet, d = doublet, t = triplet, q = quartet, m = multiplet, and bs = broad singlet), integration, and coupling constant (*J*) in hertz (Hz). Infrared (IR) spectra were reported in cm^{-1} on a Jasco 4100 FT/IR. Optical rotations were measured on a Jasco P-2000 polarimeter at RT. High resolution TOF mass spectrometry utilizing electrospray ionization in positive mode was performed on a Water QTOF Premier instrument to confirm the identity of the compounds.

5.2 General Procedure for the Preparation of Secondary Trichloroacetimidates

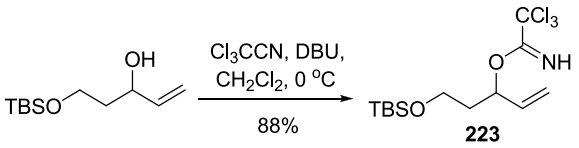

A 100 mL oven-dried Schlenk flask was charged with the allylic alcohol (1.94 g, 8.96 mmol, 1 equiv) and dry dichoromethane (50 mL). Trichloroacetonitrile (2.70 mL, 26.9 mmol, 3 equiv) was added. The resulting solution was cooled to $0^{O}C$, and DBU was added (0.33 mL, 2.24 mmol, 0.25 equiv). The reaction mixture was allowed to warm to room temperature and stir overnight. The mixture was concentrated *in vacuo*, and the resulting residue was purified by silica gel flash chromatography (30/1 hexane/ethyl acetate + 1% triethylamine) to provide **223** (2.84 g, 88%) as a clear oil.

Compound **223**:

^{1}H NMR ($CDCl_3$, 400 MHz): δ = 8.29 (s, NH), 5.91-5.83 (m, 1H), 5.54-5.49 (m, 1H), 5.34 (dt, *J* = 17.0, 2.4 Hz, 1H), 5.19 (dt, *J* = 10.6, 1.2 Hz, 1H), 3.74-3.70 (m, 2H), 2.03-1.87 (m, 2H), 0.86 (s, 9H), 0.03 (s, 6H).

^{13}C NMR ($CDCl_3$, 100 MHz): δ = 161.9, 135.8, 116.7, 76.5, 59.1, 37.7, 26.1, 18.5, -5.2.

IR (film, cm^{-1}): ν = 3349, 2955, 2929, 2857, 1664, 1471, 1286, 1255, 1100, 980, 832, 795, 776, 647.

HRMS (TOF ESI+): calc. for $C_{13}H_{24}Cl_3NO_2SiNa$ $(M+Na)^+$: 382.0543; found: 382.0542.

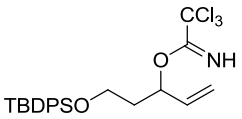

226

Compound **226**:

^{1}H NMR ($CDCl_3$, 400 MHz): δ = 8.30 (s, NH), 7.65-7.62 (m, 4H), 7.42-7.32 (m, 6H), 5.92-5.84 (m, 1H), 5.66-5.61 (m, 1H), 5.34 (dt, *J* = 17.3, 1.3 Hz, 1H), 5.19 (dt, *J* = 10.6, 1.2 Hz, 1H), 3.83-3.72 (m, 2H), 2.07-1.93 (m, 2H), 1.02 (s, 9H).

^{13}C NMR ($CDCl_3$, 100 MHz): δ = 161.9, 135.8, 135.7, 133.9, 133.8, 129.8, 127.8, 116.7, 76.5, 59.9, 37.5, 27.0, 19.4.

IR (film, cm^{-1}): ν = 3344, 3071, 2958, 2930, 2857, 1663, 1472, 1427, 1298, 1286, 1111, 1091, 979, 823, 795, 737, 702, 647.

HRMS (TOF ESI+): calc. for $C_{23}H_{28}Cl_3NO_2SiNa$ $(M+Na)^+$: 506.0853; found: 506.0859.

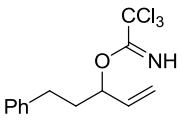

227

Compound **227**:

^{1}H NMR ($CDCl_3$, 400 MHz): δ = 8.30 (s, NH), 7.29-7.25 (m, 2H), 7.20-7.16 (m, 3H), 5.92-5.84 (m, 1H), 5.40-5.35 (m, 1H), 5.37 (dt, *J* = 17.3, 1.3 Hz, 1H), 5.23 (dt, *J* = 10.6, 1.2 Hz, 1H), 2.82-2.67 (m, 2H), 2.17-1.97 (m, 2H).

^{13}C NMR ($CDCl_3$, 100 MHz): δ = 162.0, 141.5, 135.6, 128.7, 128.6, 126.2, 117.2, 78.8, 36.2, 31.5.

IR (film, cm^{-1}): ν = 3343, 3085, 3026, 2928, 2861, 1661, 1496, 1455, 1285, 1074, 974, 928, 884, 824, 793, 748, 697.

HRMS (TOF ESI+): calc. for $C_{13}H_{14}Cl_3NONa$ $(M+Na)^+$: 306.0219 ; found: 306.0225.

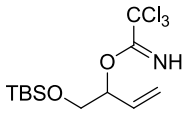

228

Compound **228**:

^{1}H NMR ($CDCl_3$, 400 MHz): δ = 8.31 (s, NH), 5.93-5.84 (m, 1H), 5.43-5.40 (m, 1H), 5.41 (dt, *J* = 17.4, 1.3 Hz, 1H), 5.26 (dt, *J* = 10.7, 1.2 Hz, 1H), 3.83-3.74 (m, 2H), 0.86 (s, 9H), 0.05 (s, 3H), 0.04 (s, 3H).

^{13}C NMR ($CDCl_3$, 100 MHz): δ = 162.2, 133.0, 118.1, 80.0, 64.6, 26.0, 18.5, -5.1, -5.2.

IR (film, cm^{-1}): ν = 3349, 2954, 2929, 2858, 1664, 1471, 1462, 1287, 1255, 1130, 1078, 993, 933, 835, 795, 777.

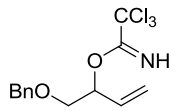

229

Compound **229**:

^{1}H NMR ($CDCl_3$, 400 MHz): δ = 8.35 (s, NH), 7.34-7.30 (m, 4H), 7.30-7.25 (m, 1H), 5.95-5.85 (m, 1H), 5.66-5.58 (m, 1H), 5.44 (dt, *J* = 17.3, 1.3 Hz, 1H), 5.28 (dt, *J* = 10.7, 1.2 Hz, 1H), 4.60 (s, 2H), 3.72-3.69 (m, 2H).

^{13}C NMR ($CDCl_3$, 100 MHz): δ = 162.1, 138.2, 132.7, 128.6, 127.9, 127.8, 118.3, 78.3, 73.5, 71.3.

IR (film, cm^{-1}): ν = 3342, 3088, 3064, 3030, 2897, 2861, 1664, 1496, 1454, 1362, 1286, 1205, 1075, 987, 930, 873, 793, 735, 697.

HRMS (TOF ESI+): calc. for $C_{12}H_{22}Cl_3NO_2SiNa$ $(M+Na)^+$: 343.9988; found: 343.9984

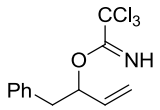

230

Compound **230**:

^{1}H NMR ($CDCl_3$, 400 MHz): δ = 8.26 (s, NH), 7.30-7.25 (m, 4H), 7.22-7.18 (m, 1H), 5.91-5.83 (m, 1H), 5.60-5.55 (m, 1H), 5.32 (dt, *J* = 17.2, 1.3 Hz, 1H), 5.20 (dt, *J* = 10.6, 1.2 Hz, 1H), 3.11 (dd, *J* = 13.9, 7.4 Hz, 1H), 2.99 (dd, 13.9, 5.8 Hz, 1H).

^{13}C NMR ($CDCl_3$, 100 MHz): δ = 161.9, 136.9, 135.1, 129.9, 128.4, 126.8, 117.3, 80.0, 40.8.

IR (film, cm^{-1}): ν = 3342, 3087, 3064, 3029, 2948, 2925, 1661, 1496, 1455, 1343, 1301, 1285, 1073, 984, 930, 859, 837, 793, 751, 698.

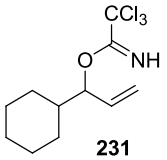

231

Compound **231**:

^{1}H NMR ($CDCl_3$, 400 MHz): δ = 8.21 (s, NH), 5.84-5.75 (m, 1H), 5.30 (dt, *J* = 17.3, 1.2 Hz, 1H), 5.22 (dt, *J* = 10.6, 1.2 Hz, 1H), 5.15 (t, *J* = 6.3 Hz, 1H), 1.88-1.62 (m, 6H), 1.27-1.02 (m, 5H).

^{13}C NMR ($CDCl_3$, 100 MHz): δ = 162.2, 134.4, 117.7, 92.2, 83.7, 42.0, 28.8, 28.3, 26.6, 26.2, 26.1.

IR (film, cm^{-1}): ν = 3346, 2926, 2853, 1661, 1450, 1340, 1302, 1286, 1073, 980, 930, 933, 889, 824, 792.

HRMS (TOF ESI+): calc. for $C_{11}H_{17}Cl_3NO$ $(M+H)^+$: 284.0376; found 284.0383

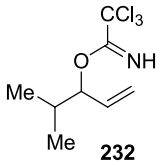

Compound **232**:

^{1}H NMR ($CDCl_3$, 400 MHz): δ = 8.23 (s, NH), 5.86-5.77 (m, 1H), 5.33 (dt, *J* = 17.2, 1.4 Hz, 1H), 5.24 (dt, *J* = 10.6, 1.4 Hz, 1H), 5.16 (t, *J* = 6.0 Hz, 1H), 2.07-1.95 (m, 1H), 0.99 (d, *J* = 7.0 Hz, 3H), 0.97 (d, *J* = 7.0 Hz, 3H).

^{13}C NMR ($CDCl_3$, 100 MHz): δ = 162.3, 134.1, 117.8, 84.2, 32.3, 18.4, 17.9.

IR (film, cm^{-1}): ν = 3347, 2965, 2934, 2876, 1662, 1469, 1303, 1287, 1076, 984, 926, 826, 794.

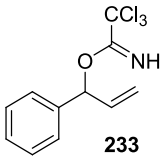

Compound **233**:

^{1}H NMR ($CDCl_3$, 400 MHz): δ = 8.36 (s, NH), 7.43-7.28 (m, 5H), 6.35 (d, *J* = 5.7 Hz, 1H), 6.10-6.02 (m, 1H), 5.40 (dt, *J* = 15.8, 1.4 Hz, 1H), 5.28 (dt, *J* = 10.5, 1.3 Hz, 1H).

^{13}C NMR ($CDCl_3$, 100 MHz): δ = 161.4, 138.6, 135.9, 128.7, 128.4, 127.0, 117.3, 91.7, 80.7.

IR (film, cm^{-1}): ν = 3346, 2926, 2853, 1661, 1450, 1340, 1302, 1286, 1073, 980, 930, 933, 889, 824, 792.

HRMS (TOF ESI+): calc. for $C_{11}H_{11}Cl_3NO$ $(M+H)^+$: 277.9925; found: 277.9906

5.3 General Procedure for Amination of Secondary Trichloroacetimidates with 1 mol% $[RhCl(ethylene)_2]_2$/ $P(OPh)_3$

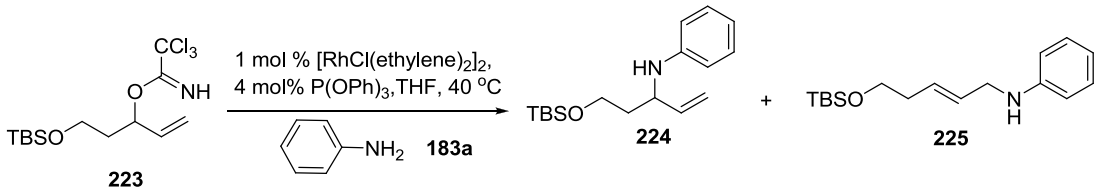

A 10 mL Schlenk flask was charged with $[RhCl(ethylene)_2]_2$ (0.54 mg, 1.4 μmol, 1 mol%) in a glove box. The flask was sealed and removed from the glove box, and THF (0.35 mL) was added to the Schlenk under argon followed by triphenylphosphite (1.5 μL, 5.5 μmol, 4 mol%). The rhodium-phosphite complex solution was allowed to stir at 25 °C for 15 min. A separate 10 mL Schlenk flask was charged with **223** (50 mg, 0.14mmol, 1 equiv), THF (0.35 mL) and aniline **183a** (38 μL, 0.42 mmol, 3 equiv). The rhodium catalyst solution was then added to the flask containing the **223** and **183a** solution. The reaction mixture was stirred at 40°C under argon. Reaction progress was monitored by GC. After 30 min, the crude reaction was concentrated *in vacuo*, loaded in dichloromethane onto an ISCO load cartridge, and dried under vacuum. Elution onto an

ISCO 12g silica column (0 → 2.5% ethyl acetate/hexane) provided **224** and **225** (40 mg, 96%, **224**/**225** >99:1) as pale yellow oil.

Compound **224**:

^{1}H NMR ($CDCl_3$, 400 MHz): δ = 7.13 (dd, *J* = 7.3, 2.0 Hz, 1H), 7.11 (dd, *J* = 7.3, 1.9 Hz, 1H), 6.63 (t, *J* = 7.3 Hz, 1H), 6.58 (d, *J* = 1.0 Hz, 1H), 6.56 (d, *J* = 0.96 Hz, 1H), 5.80-5.72 (m, 1H), 5.21 (dt, *J* = 17.2, 1.4 Hz, 1H), 5.12 (dt, *J* = 10.3, 1.4 Hz, 1H), 4.34 (s, NH), 4.03-3.99 (m, 1H), 3.82-3.77 (m, 1H), 3.74-3.68 (m, 1H), 1.88-1.73 (m, 2H), 0.90 (s, 9H), -0.04 (s, 6H).

^{13}C NMR ($CDCl_3$, 100 MHz): δ = 148.0, 139.7, 129.2, 117.0, 115.5, 113.4, 60.6, 54.3, 38.0, 26.1, 18.4, -5.2.

IR (film, cm^{-1}): ν = 3340, 3085, 3061, 3024, 2941, 2860, 2812, 1663, 1597, 1503, 1453, 1378, 1348, 1306, 1211, 1193, 1076, 1031, 990, 922, 796, 746, 692.

HRMS (ESI): calc. for $C_{17}H_{30}NOSi$ (M+H): 292.2103; found: 292.2097

Compound **225**:

^{1}H NMR ($CDCl_3$, 400 MHz): δ = 7.18 (dd, *J* = 7.4, 2.1 Hz, 1H), 7.15 (dd, *J* = 7.3, 2.0 Hz, 1H), 6.69 (t, *J* = 7.3 Hz, 1H), 6.61 (d, *J* = 1.1 Hz, 1H), 6.59 (d, *J* = 0.96 Hz, 1H), 5.67-5.54 (m, 2H), 3.75 (d, *J* = 5.8 Hz, 2H), 3.65 (t, *J* = 6.6 Hz, 2H), 2.34 (q, *J* = 6.6 Hz, 2H), 0.89 (s, 9H), -0.05 (s, 6H).

^{13}C NMR ($CDCl_3$, 100 MHz): δ = 148.4, 129.6, 129.4, 128.8, 117.7, 113.2, 62.8, 41.4, 31.5, 26.2, 18.6, -5.0.

IR (film, cm^{-1}): ν = 3401, 3052, 3020, 2954, 2928, 2885, 2856, 1727, 1604, 1505, 1314, 1255, 1096, 929, 836, 777, 748, 691.

HRMS (ESI): calc. for $C_{17}H_{30}NOSi$ (M+H): 292.2103; found: 292.2097

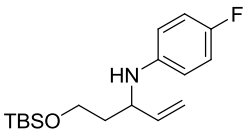

223b

Compound **223b**:

^{1}H NMR ($CDCl_3$, 400 MHz): δ = 6.82 (t, *J* = 8.8 Hz, 2H), 6.49 (dd, *J* = 9.0, 4.5 Hz, 2H), 5.77-5.69 (m, 1H), 5.21 (dt, *J* = 17.2 Hz, 1.4 Hz, 1H), 5.12 (dt, *J* = 10.3 Hz, 1.3 Hz, 1H), 4.25 (s, NH), 3.95-3.91 (m, 1H), 3.82-3.77 (m, 1H), 3.74-3.68 (m, 1H), 1.87-1.72 (m, 2H), 0.90 (s, 9H), 0.04 (s, 6H).

^{13}C NMR ($CDCl_3$, 100 MHz): δ = 156.8, 144.2, 139.7, 115.7, 115.5, 114.2, 60.6, 55.1, 38.0, 26.1, 18.4, -5.2.

IR (film, cm^{-1}): ν = 3405, 2953, 2929, 2857, 1509, 1471, 1255, 1220, 1096, 918, 835, 816, 775.

HRMS (ESI): calc. for $C_{17}H_{29}NOSiF$ (M+H): 310.2002; found: 310.2000.

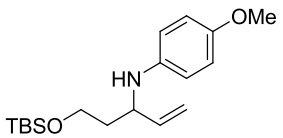

223c

Compound **223c**:

^{1}H NMR ($CDCl_3$, 400 MHz): δ = 6.73 (d, *J* = 9.0 Hz, 2H), 6.54 (d, *J* = 8.9 Hz, 2H), 5.78-5.70 (m, 1H), 5.20 (dt, *J* = 17.2 Hz, 1.4 Hz, 1H), 5.10 (dt, *J* = 10.3 Hz, 1.2 Hz, 1H), 4.01 (s, NH), 3.94-3.89 (m, 1H), 3.81-3.76 (m, 1H), 3.73-3.68 (m, 1H), 3.71 (s, 3H), 1.85-1.72 (m, 2H), 0.89 (s, 9H), 0.04 (s, 6H).

^{13}C NMR ($CDCl_3$, 100 MHz): δ = 151.9, 142.2, 140.3, 115.3, 114.9, 114.7, 60.6, 56.0, 55.2, 38.2, 26.1, 18.4, -5.2.

IR (film, cm^{-1}): ν = 3397, 2952, 2929, 2856, 1510, 1470, 1236, 1094, 1041, 916, 835, 816, 775.

HRMS (ESI): calc. for $C_{18}H_{32}NO_2Si$ (M+H): 322.2202; found: 322.2198.

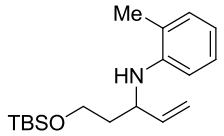

223d

Compound **223d**:

^{1}H NMR ($CDCl_3$, 400 MHz): δ = 7.07-7.00 (m, 2H), 6.61-6.57 (m, 2H), 5.81-5.73 (m, 1H), 5.20 (dt, *J* = 17.2 Hz, 1.2 Hz, 1H), 5.11 (dt, *J* = 10.2 Hz, 1.1 Hz, 1H), 4.07-4.05 (m, 1H), 4.00 (s, NH), 3.83-3.79 (m, 1H), 3.76-3.70 (m, 1H), 2.13 (s, 3H), 1.90-1.80 (m, 2H), 0.88 (s, 9H), 0.03 (s, 6H).

^{13}C NMR ($CDCl_3$, 100 MHz): δ = 147.9, 139.7, 129.2, 117.0, 115.4, 113.3, 60.5, 54.3, 38.0, 26.1, 18.4, -5.2.

IR (film, cm^{-1}): ν = 3423, 2953, 2928, 2856, 1606, 1587, 1512, 1471, 1449, 1315, 1255, 991, 916, 834, 776, 744.

HRMS (ESI): calc. for $C_{18}H_{32}NOSi$ (M+H): 306.2253; found: 306.2249.

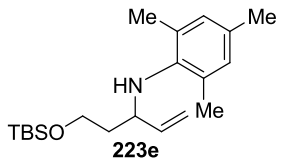

223e

Compound **223e**:

^{1}H NMR ($CDCl_3$, 400 MHz): δ = 6.76 (s, 2H), 5.70-5.61 (m, 1H), 4.95-4.94 (m, 1H), 4.92-4.90 (m, 1H), 3.79-3.64 (m, 3H), 2.97 (s, NH), 2.19 (s, 6H), 2.18 (s, 3H), 1.90-1.82 (m, 1H), 1.75-1.67 (m, 1H), 0.87 (s, 9H), 0.01 (s, 6H).

^{13}C NMR ($CDCl_3$, 100 MHz): δ = 142.4, 140.5, 130.8, 129.5, 115.4, 60.1, 57.5, 39.2, 26.2, 20.8, 19.2, 18.4, -5.2.

IR (film, cm^{-1}): ν = 3386, 3077, 2952, 2928, 2897, 2856, 1482, 1472, 1253, 1231, 1095, 989, 916, 835, 774.

HRMS (ESI): calc. for $C_{20}H_{36}NOSi$ (M+H): 334.2566; found: 334.2562.

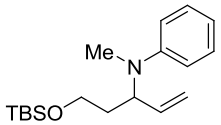

223f

Compound **223f**:

^{1}H NMR ($CDCl_3$, 400 MHz): δ = 7.20-7.14 (m, 2H), 6.81-6.79 (m, 2H), 6.66 (tt, *J* = 7.2, 1.0 Hz, 1H), 5.86-5.77 (m, 1H), 5.14-5.07 (m, 2H), 4.56-4.51 (m, 1H), 3.64-3.56 (m, 2H), 2.72 (s, 3H), 1.94-1.79 (m, 2H), 0.86 (s, 9H), 0.02 (s, 6H).

^{13}C NMR ($CDCl_3$, 100 MHz): δ = 150.8, 137.5, 129.2, 116.6, 115.8, 113.4, 60.1, 56.6, 34.7, 31.8, 26.1, 18.4, -5.2.

IR (film, cm^{-1}): ν = 2953, 2928, 2884, 2857, 1598, 1504, 1471, 1253, 1095, 990, 835, 775, 747.

HRMS (ESI): calc. for $C_{18}H_{32}NOSi$ (M+H): 306.2253; found: 306.2250.

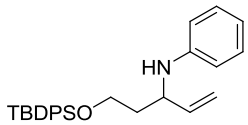

226a

Compound **226a**:

^{1}H NMR ($CDCl_3$, 400 MHz): δ = 7.67-7.62 (m, 4H), 7.41-7.29 (m, 6H), 7.13 (dd, *J* = 8.5, 7.3 Hz, 2H), 6.65 (tt, *J* = 7.3, 1.0 Hz, 1H), 6.58 (dd, *J* = 8.6, 1.0 Hz, 2H), 5.79-5.71 (m, 1H), 5.22 (dt, *J* = 17.1, 1.4 Hz, 1H), 5.11 (dt, *J* = 10.3, 1.3 Hz, 1H), 4.21 (s, NH),

4.15-4.07 (m, 1H), 3.87-3.81 (m, 1H), 3.76-3.71 (m, 1H), 1.90-1.87 (m, 1H), 1.86-1.79 (m, 1H), 1.06 (s, 9H).

^{13}C NMR ($CDCl_3$, 100 MHz): δ = 147.9, 139.8, 135.8, 133.6, 129.8, 129.2, 127.9, 117.1, 115.3, 113.4, 61.4, 53.9, 38.1, 27.1, 19.3.

IR (film, cm^{-1}): ν = 3409, 2952, 2930, 2857, 1601, 1505, 1427, 1316, 1105, 1092, 822, 743, 700.

HRMS (ESI): calc. for $C_{27}H_{34}NOSi$ (M+H): 416.2410; found: 416.2404.

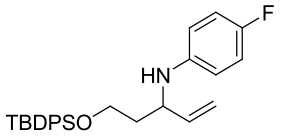

226b

Compound **226b**:

^{1}H NMR ($CDCl_3$, 400 MHz): δ = 7.66-7.61 (m, 4H), 7.43-7.29 (m, 6H), 6.83 (t, *J* = 8.8 Hz, 2H), 6.49 (dd, *J* = 9.0, 4.4 Hz, 2H), 5.77-5.68 (m, 1H), 5.20 (dt, *J* = 17.2, 1.4 Hz, 1H), 5.11 (dt, *J* = 10.3, 1.3 Hz, 1H), 4.11 (s, NH), 4.04-4.02 (m, 1H), 3.87-3.81 (m, 1H), 3.76-3.71 (m, 1H), 1.88-1.85 (m, 1H), 1.82-1.78 (m, 1H), 1.05 (s, 9H).

^{13}C NMR ($CDCl_3$, 100 MHz): δ = 144.1, 139.7, 135.7, 133.6, 133.5, 129.8, 127.9, 115.7, 115.5, 114.2, 61.3, 54.6, 38.1, 27.1, 19.3.

IR (film, cm^{-1}): ν = 3409, 2930, 2889, 2857, 1509, 1427, 1220, 818, 775, 736, 700, 688.

HRMS (ESI): calc. for $C_{27}H_{33}NOFSi$ (M+H): 434.2315; found: 434.2317.

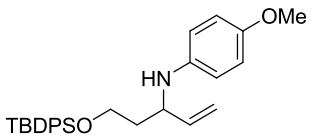

226c

Compound **226c**:

^{1}H NMR ($CDCl_3$, 400 MHz): δ = 7.66-7.61 (m, 4H), 7.43-7.29 (m, 6H), 6.73 (d, *J* = 9.0 Hz, 2H), 6.53 (d, *J* = 9.0 Hz, 2H), 5.77-5.69 (m, 1H), 5.20 (dt, *J* = 17.2, 1.3 Hz, 1H), 5.09 (dt, *J* = 10.3, 1.1 Hz, 1H), 4.04-4.00 (m, 1H), 3.91 (s, NH), 3.86-3.80 (m, 1H), 3.76-3.71 (m, 1H), 3.72 (s, 3H), 1.85-1.79 (m, 2H), 1.05 (s, 9H).

^{13}C NMR ($CDCl_3$, 100 MHz): δ = 151.9, 142.1, 140.2, 135.7, 133.7, 133.5, 129.8, 127.8, 115.4, 115.0, 114.8, 61.5, 55.9, 54.7, 38.2, 26.9, 19.4.

IR (film, cm^{-1}): ν = 3399, 2930, 2896, 2857, 1509, 1471, 1463, 1427, 1236, 1108, 1040, 819, 737, 701, 688.

HRMS (ESI): calc. for $C_{28}H_{36}NO_2Si$ (M+H): 446.2511; found: 446.2515.

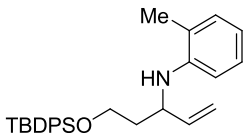

226d

Compound **226d**:

^{1}H NMR ($CDCl_3$, 400 MHz): δ = 7.67-7.62 (m, 4H), 7.45-7.29 (m, 6H), 7.15-7.0 (m, 2H), 6.70-6.60 (m, 2H), 5.84-5.75 (m, 1H), 5.22 (dt, *J* = 17.2, 1.4 Hz, 1H), 5.12 (dt, *J* = 10.3, 1.3 Hz, 1H), 4.25-4.21 (m, 1H), 3.89-3.85 (m, 1H), 3.83-3.76 (m, 1H), 3.6 (s, NH), 2.08 (s, 3H), 1.95-1.86 (m, 2H), 1.07 (s, 9H).

^{13}C NMR ($CDCl_3$, 100 MHz): δ = 145.6, 140.0, 135.7, 133.9, 133.7, 130.2, 129.8, 127.8, 127.1, 121.9, 116.8, 115.2, 111.0, 61.0, 52.9, 38.7, 27.1, 19.4, 17.8.

IR (film, cm^{-1}): ν = 3427, 2956, 2930, 2892, 2856, 1605, 1587, 1510, 1427, 1105, 821, 739, 700, 687.

HRMS (ESI): calc. for $C_{28}H_{36}NOSi$ (M+H): 430.2566; found: 430.2565.

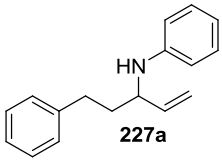

227a

Compound **227a**:

^{1}H NMR ($CDCl_3$, 400 MHz): δ = 7.29-7.25 (m, 2H), 7.20-7.10 (m, 5H), 6.66 (t, *J* = 7.2 Hz, 1H), 6.55 (dd, *J* = 8.6, 1.0 Hz, 2H), 5.80-5.72 (m, 1H), 5.21 (dt, *J* = 17.2, 1.3 Hz, 1H), 5.14 (dt, *J* = 10.3, 1.2 Hz, 1H), 3.83 (bs, 1H), 3.61 (s, NH), 2.74 (t, *J* = 7.6 Hz, 2H), 1.93-1.87 (m, 2H).

^{13}C NMR ($CDCl_3$, 100 MHz): δ = 147.7, 141.8, 139.8, 129.3, 128.7, 128.6, 126.1, 117.4, 115.6, 113.5, 55.5, 37.4, 32.3.

IR (film, cm^{-1}): ν = 3403, 3083, 3052, 3024, 2977, 2921, 2856, 1599, 1503, 1454, 1428, 1315, 1254, 992, 918, 746, 691.

HRMS (ESI): calc. for $C_{17}H_{20}NO$ (M+H): 238.1596; found: 238.1599.

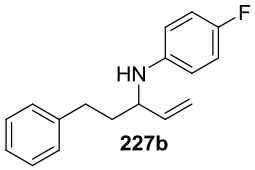

227b

Compound **227b**:

^{1}H NMR ($CDCl_3$, 400 MHz): δ = 7.29-7.24 (m, 2H), 7.20-7.15 (m, 3H), 6.83 (t, *J* = 8.8 Hz, 2H), 6.45 (dd, *J* = 9.0, 4.4 Hz, 2H), 5.76-5.68 (m, 1H), 5.18 (dt, *J* = 17.2, 1.3 Hz, 1H), 5.14 (dt, *J* = 10.3, 1.2 Hz, 1H), 3.74 (q, *J* = 6.1 Hz, 1H), 3.49 (s, NH), 2.73 (t, *J* = 6.9 Hz, 2H), 1.91-1.85 (m, 2H).

^{13}C NMR (CDCl$_3$, 100 MHz): δ = 141.7, 139.8, 128.6, 126.2, 115.9, 115.5, 114.4, 103.7, 56.1, 37.4, 32.5.

IR (film, cm^{-1}): ν = 3412, 3083, 3061, 3026, 3003, 2977, 2922, 2857, 1507, 1454, 1313, 1218, 992, 920, 817, 778, 749, 699.

HRMS (ESI): calc. for $C_{17}H_{19}NF$ (M+H): 256.1502; found: 256. 500.

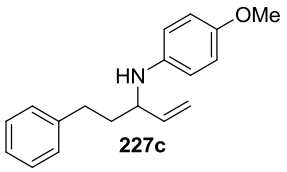

227c

Compound **227c**:

^{1}H NMR (CDCl$_3$, 400 MHz): δ = 7.29-7.25 (m, 2H), 7.20-7.16 (m, 3H), 6.73 (d, *J* = 8.8 Hz, 2H), 6.51 (d, *J* = 8.8 Hz, 2H), 5.78-5.69 (m, 1H), 5.20 (d, *J* = 17.2 Hz, 1H), 5.13 (d, *J* = 10.3 Hz, 1H), 3.75 (q, *J* = 6.7 Hz, 1H), 3.73 (s, 3H), 3.36 (s, NH), 2.73 (t, *J* = 7.7 Hz, 2H), 1.91-1.85 (m, 2H).

^{13}C NMR (CDCl$_3$, 100 MHz): δ = 152.1, 141.9, 141.7, 140.2, 128.7, 128.6, 126.1, 115.7, 115.0, 114.9, 56.4, 55.9, 37.5, 32.3.

IR (film, cm^{-1}): ν = 3395, 3081, 3061, 3025, 2998, 2932, 2856, 2830, 1602, 1508, 1463, 1453, 1441, 1231, 1178, 1036, 992, 817, 816, 747, 699.

HRMS (ESI): calc. for $C_{18}H_{22}NO$ (M+H): 268.1701; found: 268.1694.

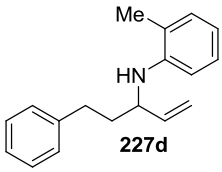

227d

Compound **227d**:

^{1}H NMR ($CDCl_3$, 400 MHz): δ = 7.30-7.26 (m, 2H), 7.21-7.17 (m, 3H), 7.08-7.03 (m, 2H), 6.62 (td, *J* = 7.4, 1.0 Hz, 1H), 6.52 (d, *J* = 7.9 Hz, 1H), 5.84-5.75 (m, 1H), 5.21 (dt, *J* = 17.2, 1.4 Hz, 1H), 5.13 (dt, *J* = 10.3, 1.2 Hz, 1H), 3.90 (q, *J* = 6.5 Hz, 1H), 3.47 (s, NH), 2.73 (t, *J* = 7.5 Hz, 2H), 2,11 (s, 3H), 1.98-1.94 (m, 2H).

^{13}C NMR ($CDCl_3$, 100 MHz): δ = 145.4, 141.8, 140.2, 130.2, 128.6, 127.1, 126.2, 121.8, 116.9, 115.5, 110.8, 55.3, 37.6, 32.4, 17.7.

IR (film, cm^{-1}): ν = 3434, 3025, 2920, 2854, 1605, 1586, 1509, 1497, 1478, 1447, 1314, 1257, 990, 916, 744, 698, 682.

HRMS (ESI): calc. for $C_{18}H_{22}N$ (M+H): 252.1752; found: 252.1746.

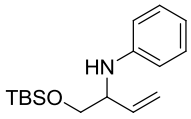

228a

Compound **228a**:

^{1}H NMR ($CDCl_3$, 400 MHz): δ = 7.15 (dd, *J* = 7.8, 6.6 Hz, 2H), 6.69 (tt, *J* = 7.3, 1.0 Hz, 1H), 6.38 (dd, *J* = 10.6, 1.1 Hz, 2H), 5.86-5.77 (m, 1H), 5.31 (dt, *J* = 17.3, 1.4 Hz, 1H), 5.19 (dt, *J* = 10.3, 1.3 Hz, 1H), 4.19 (s, NH), 3.87 (bs, 1H), 3.75 (dd, *J* = 9.9, 4.5 Hz, 1H), 3.64 (dd, *J* = 9.9, 6.0 Hz, 1H), 0.90 (s, 9H), 0.06 (s, 3H), 0.05 (s, 3H).

^{13}C NMR ($CDCl_3$, 100 MHz): δ = 148.0, 137.8, 129.2, 117.0, 116.7, 114.0, 65.9, 57.9, 26.1, 18.5, -5.1, -5.2.

IR (film, cm^{-1}): ν = 3397, 2953, 2928, 2884, 2857, 1602, 1503, 1471, 1316, 1254, 1101, 992, 835, 812, 776, 747, 690.

HRMS (ESI): calc. for $C_{16}H_{28}NOSi$ (M+H): 278.1940; found: 278.1944.

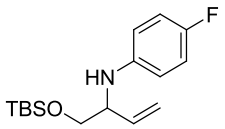

228b

Compound **228b**:

^{1}H NMR ($CDCl_3$, 400 MHz): δ = 6.84 (t, *J* = 8.9, 2H), 6.57 (dd, *J* = 9.1, 4.5 Hz, 2H), 5.82-5.74 (m, 1H), 5.29 (dt, *J* = 17.3, 1.4 Hz, 1H), 5.18 (dt, *J* = 10.3, 1.3 Hz, 1H), 4.02 (s, NH), 3.81-3.77 (m, 1H), 3.74 (dd, *J* = 9.7, 4.3 Hz, 1H), 3.61 (dd, *J* = 9.8, 6.1 Hz, 1H), 0.89 (s, 9H), 0.06 (s, 3H), 0.05 (s, 3H).

^{13}C NMR ($CDCl_3$, 100 MHz): δ = 157.3, 154.9, 144.4, 137.8, 116.9, 115.7, 115.5, 115.1, 115.0, 65.8, 58.7, 26.0, 18.5, -5.1.

IR (film, cm^{-1}): ν = 3394, 2953, 2929, 2884, 2857, 1509, 1471, 1463, 1255, 1220, 1097, 835, 818, 776.

HRMS (ESI): calc. for $C_{16}H_{27}NOFSi$ (M+H): 296.1846; found: 296.1854.

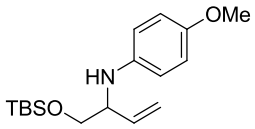

228c

Compound **228c**:

^{1}H NMR ($CDCl_3$, 400 MHz): δ = 6.73 (d, *J* = 9.0, 2H), 6.61 (d, *J* = 9.0 Hz, 2H), 5.83-5.74 (m, 1H), 5.28 (dt, *J* = 17.3, 1.4 Hz, 1H), 5.16 (dt, *J* = 10.3, 1.3 Hz, 1H), 3.79-3.75 (m, 1H), 3.73 (dd, *J* = 11.1, 1.2 Hz, 1H), 3.72 (s, 3H), 3.59 (dd, *J* = 9.8, 6.2 Hz, 1H), 2.14 (s, NH), 0.88 (s, 9H), 0.05 (s, 3H), 0.04 (s, 3H).

^{13}C NMR ($CDCl_3$, 100 MHz): δ = 152.4, 142.2, 138.2, 116.7, 115.6, 114.8, 65.9, 59.1, 55.9, 26.1, 18.5, -5.1, -5.2.

IR (film, cm^{-1}): ν = 3385, 2952, 2929, 2898, 2857, 2831, 1510, 1470, 1463, 1243, 1232, 1100, 1041, 835, 819, 777.

HRMS (ESI): calc. for $C_{17}H_{30}NO_2Si$ (M+H): 308.2046; found: 308.2053.

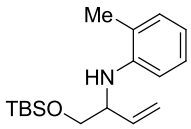

228d

Compound **228d**:

^{1}H NMR ($CDCl_3$, 400 MHz): δ = 7.09-7.04 (m, 2H), 6.67-6.62 (m, 2H), 5.87-5.78 (m, 1H), 5.31 (dt, *J* = 17.3, 1.4 Hz, 1H), 5.20 (dt, *J* = 10.3, 1.3 Hz, 1H), 3.95-3.90 (m, 1H), 3.79 (dd, *J* = 9.8, 4.4 Hz, 1H), 3.68 (dd, *J* = 9.8, 6.1 Hz, 1H), 2.17 (s, 3H), 0.91 (s, 9H), 0.08 (s, 3H), 0.07 (s, 3H).

^{13}C NMR ($CDCl_3$, 100 MHz): δ = 146.0, 138.1, 130.2, 127.0, 122.7, 117.2, 116.7, 111.5, 66.0, 57.7, 26.0, 18.4, 17.7, -5.2.

IR (film, cm^{-1}): ν = 3402, 2953, 2928, 2884, 2857, 1606, 1586, 1509, 1471, 1462, 1313, 1254, 1102, 918, 834, 812, 776, 744.

HRMS (ESI): calc. for $C_{17}H_{30}NOSi$ (M+H): 292.2097; found: 292.2098.

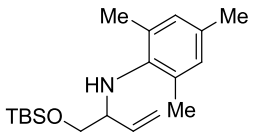

228e

Compound **228e**:

^{1}H NMR ($CDCl_3$, 400 MHz): δ = 6.77 (s, 2H), 5.91-5.83 (m, 1H), 5.12 (dt, *J* = 17.2, 1.7 Hz, 1H), 5.02 (dt, *J* = 10.3, 1.1 Hz, 1H), 3.79 (dd, *J* = 9.7, 3.7 Hz, 1H), 3.67 (dd, *J* = 9.7, 2.9 Hz, 1H), 3.63-3.59 (m, 1H), 2.22 (s, 6H), 2.20 (s, 3H), 0.91 (s, 9H), 0.06 (s, 3H), 0.05 (s, 3H).

^{13}C NMR ($CDCl_3$, 100 MHz): δ = 142.2, 138.5, 130.8, 129.7, 129.5, 115.8, 66.0, 61.3, 26.0, 20.7, 18.9, 18.5, -5.1, -5.2.

IR (film, cm^{-1}): ν = 2953, 2928, 2857, 1483, 1471, 1462, 1443, 1251, 1098, 992, 952, 833, 812, 775.

HRMS (ESI): calc. for $C_{19}H_{34}NOSi$ (M+H): 320.2410; found: 320.2413.

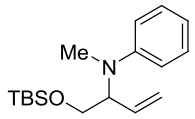

228f

Compound **228f**:

^{1}H NMR ($CDCl_3$, 400 MHz): δ = 7.24-7.18 (m, 2H), 6.80-6.77 (m, 2H), 6.69 (tt, *J* = 7.2, 1.0 Hz, 1H), 5.93-5.85 (m, 1H), 5.23 (d, *J* = 1.8 Hz, 1H), 5.19 (dt, *J* = 7.0, 1.8 Hz, 1H), 4.43-4.38 (m, 1H), 3.84-3.76 (m, 2H), 2.82 (s, 3H), 0.84 (s, 9H), 0.02 (s, 3H), 0.01 (s, 3H).

^{13}C NMR ($CDCl_3$, 100 MHz): δ = 150.7, 135.1, 129.2, 116.8, 116.6, 113.2, 63.6, 62.4, 32.8, 25.9, 18.3, -5.4.

IR (film, cm^{-1}): ν = 2952, 2928, 2884, 2856, 1597, 1503, 1471, 1462, 1108, 835, 814, 774, 746, 690.

HRMS (ESI): calc. for $C_{17}H_{30}NOSi$ (M+H): 292.2097; found: 292.2099.

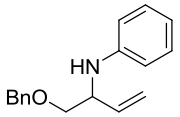

229a

Compound **229a**:

^{1}H NMR (CDCl$_3$, 400 MHz): δ = 7.39-7.29 (m, 5H), 7.17 (dd, *J* = 13.9, 7.3 Hz, 2H), 6.71 (t, *J* = 7.3 Hz, 1H), 6.64 (dd, *J* = 7.6, 1.9 Hz, 2H), 5.91-5.83 (m, 1H), 5.34 (dt, *J* = 17.3, 1.3 Hz, 1H), 5.22 (dt, *J* = 10.3, 1.2 Hz, 1H), 4.59 (d, *J* = 12.1 Hz, 1H), 4.55 (d, *J* = 12.1 Hz, 1H), 4.16 (s, NH), 4.09-4.05 (m, 1H), 3.63 (dd, *J* = 9.5, 4.5 Hz, 1H), 3.57 (dd, *J* = 9.6, 6.2 Hz, 1H).

^{13}C NMR (CDCl$_3$, 100 MHz): δ = 147.8, 138.2, 137.6, 129.2, 128.6, 127.9, 127.8, 117.8, 116.7, 114.0, 73.4, 72.7, 56.0.

IR (film, cm^{-1}): ν = 3396, 3085, 3051, 3026, 2897, 2857, 1600, 1503, 1453, 1431, 1360, 1100, 1076, 1027, 992, 922, 870, 747, 692.

HRMS (ESI): calc. for $C_{17}H_{20}NO$ (M+H): 254.1545; found: 254.1545.

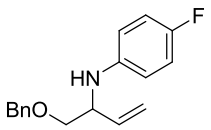

229b

Compound **229b**:

^{1}H NMR (CDCl$_3$, 400 MHz): δ = 7.39-7.29 (m, 5H), 6.86 (t, *J* = 6.7 Hz, 2H), 6.59-6.54 (m, 2H), 5.87-5.78 (m,

1H), 5.32 (dt, *J* = 17.3, 1.3 Hz, 1H), 5.21 (dt, *J* = 10.3, 1.2 Hz, 1H), 4.58 (d, *J* = 12.1 Hz, 1H), 4.53 (d, *J* = 12.1 Hz, 1H), 4.07 (s, NH), 3.99-3.95 (m, 1H), 3.63 (dd, *J* = 9.6, 4.3 Hz, 1H), 3.53 (dd, *J* = 9.6, 6.5 Hz, 1H).

^{13}C NMR ($CDCl_3$, 100 MHz): δ = 157.3, 155.0, 144.1, 138.1, 137.5, 128.6, 128.0, 127.9, 116.9, 115.7, 115.5, 115.0, 114.9, 73.4, 72.7, 56.8.

IR (film, cm^{-1}): ν = 3398, 2898, 2858, 1602, 1508, 1453, 1360, 1313, 1215, 1095, 1076, 1027, 992, 922, 819736, 696.

HRMS (ESI): calc. for $C_{17}H_{19}$FNO (M+H): 272.1458; found: 272.1451.

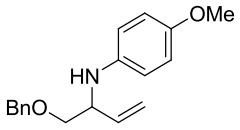

229c

Compound **229c**:

^{1}H NMR ($CDCl_3$, 400 MHz): δ = 7.36-7.27 (m, 5H), 6.74 (d, *J* = 9.0 Hz, 2H), 6.60 (d, *J* = 9.0 Hz, 2H), 5.87-5.79 (m, 1H), 5.31 (dt, *J* = 17.3, 1.3 Hz, 1H), 5.18 (dt, *J* = 10.3, 1.2 Hz, 1H), 4.56 (d, *J* = 12.0 Hz, 1H), 4.52 (d, *J* = 12.0 Hz, 1H), 3.98-3.94 (m, 1H), 3.72 (s, 3H), 3.60 (dd, *J* = 9.5, 4.5 Hz, 1H), 3.53 (dd, *J* = 9.5, 6.4 Hz, 1H).

^{13}C NMR ($CDCl_3$, 100 MHz): δ = 152.7, 141.8, 138.2, 137.9, 128.6, 128.0, 127.9, 116.9, 115.7, 115.0, 114.9, 73.4, 72.8, 57.2, 56.0.

IR (film, cm^{-1}): ν = 3387, 2931, 2902, 2857, 2832, 1601, 1509, 1463, 1453, 1233, 1178, 1097, 1036, 992, 818, 736, 697.

HRMS (ESI): calc. for $C_{18}H_{22}NO_2$ (M+H): 284.1651; found: 284.1657.

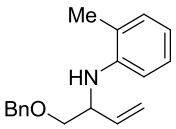

229d

Compound **229d**:

^{1}H NMR ($CDCl_3$, 400 MHz): δ = 7.38-7.29 (m, 5H), 7.10-7.05 (m, 2H), 6.69-6.62 (m, 2H), 5.93-5.84 (m, 1H), 5.35 (d, *J* = 17.3 Hz, 1H), 5.23 (d, *J* = 10.4 Hz, 1H), 4.60 (d, *J* = 12.0 Hz, 1H), 4.58 (d, *J* = 12.0 Hz, 1H), 4.12-4.09 (m, 1H), 3.68-3.60 (m, 2H).

^{13}C NMR ($CDCl_3$, 100 MHz): δ = 145.8, 138.2, 137.8, 130.2, 128.6, 127.9, 127.8, 127.0, 122.6, 118.8, 117.4, 116.7, 111.4, 73.3, 72.7, 55.9, 17.7.

IR (film, cm^{-1}): ν = 3405, 2895, 2857, 1605, 1586, 1508, 1477, 1448, 1359, 1313, 1262, 1102, 1050, 1026, 989, 920, 744, 715, 697.

HRMS (ESI): calc. for $C_{18}H_{22}NO$ (M+H): 268.1701; found: 268.1706.

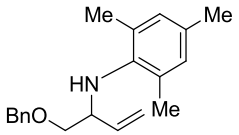

229e

Compound **229e**:

^{1}H NMR ($CDCl_3$, 400 MHz): δ = 7.37-7.27 (m, 5H), 6.80 (s, 2H), 6.01-5.92 (m, 1H), 5.21 (dt, *J* = 17.3, 1.3 Hz, 1H), 5.10 (dt, *J* = 10.3, 1.2 Hz, 1H), 4.59 (d, *J* = 12.1 Hz, 1H), 4.53 (d, *J* = 12.1 Hz, 1H), 3.77-3.74 (m, 1H), 3.63-3.56 (m, 2H), 3.50 (s, 1H), 2.23 (s, 9H).

^{13}C NMR ($CDCl_3$, 100 MHz): δ = 142.2, 138.4, 131.0, 129.8, 129.6, 128.5, 127.7, 115.8, 73.6, 73.2, 60.0, 20.7, 18.8.

IR (film, cm^{-1}): ν = 3380, 3004, 2939, 2913, 2856, 1508, 1482, 1452, 1357, 1233, 1099, 1038, 1027, 1012, 991, 852, 733, 696.

HRMS (ESI): calc. for $C_{20}H_{26}NO$ (M+H): 296.2014; found: 296.2024.

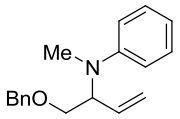

229f

Compound **229f**:

^{1}H NMR ($CDCl_3$, 400 MHz): δ = 7.35-7.21 (m, 7H), 6.81 (d, *J* = 8.7 Hz, 2H), 6.73 (t, *J* = 7.2 Hz, 1H), 5.94-5.86 (m, 1H), 5.26 (d, *J* = 1.8 Hz, 1H), 5.22 (dt, *J* = 7.5, 1.6 Hz, 1H), 4.61-4.57 (m, 1H), 4.55 (d, *J* = 12.3 Hz, 1H), 4.51 (d, *J* = 12.3 Hz, 1H), 3.74-3.66 (m, 2H), 3.50 (s, 1H), 2.83 (s, 9H).

^{13}C NMR ($CDCl_3$, 100 MHz): δ = 150.5, 138.4, 135.1, 129.2, 128.5, 127.8, 127.8, 117.1, 113.5, 73.3, 70.5, 60.3, 32.7.

IR (film, cm^{-1}): ν = 2858, 2815, 1596, 1503, 1453, 1359, 1312, 1289, 1209, 1094, 1028, 990, 921, 745, 712, 691.

HRMS (ESI): calc. for $C_{18}H_{22}NO$ (M+H): 268.1701; found: 268.1699.

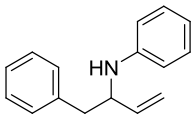

230a

Compound **230a**:

^{1}H NMR ($CDCl_3$, 400 MHz): δ = 7.32-7.28 (m, 2H), 7.23-7.20 (m, 3H), 7.16-7.12 (m, 2H), 6.68 (tt, *J* = 7.3, 1.0 Hz, 1H), 6.59 (dd, *J* = 7.8, 1.0 Hz, 2H), 5.85-5.77 (m, 1H), 5.19 (dt, *J* = 17.2, 1.4 Hz, 1H), 5.12 (dt, *J* = 10.3, 1.3 Hz, 1H), 4.15-4.12 (m, 1H),, 3.70 (s, NH), 2.92 (d, *J* = 6.6 Hz, 2H).

^{13}C NMR ($CDCl_3$, 100 MHz): δ = 147.5, 139.4, 137.8, 129.6, 129.3, 128.6, 126.7, 117.6, 115.6, 113.7, 56.7, 42.1.

IR (film, cm^{-1}): ν = 3406, 3083, 3052, 3025, 2978, 2919, 2851, 1599, 1503, 1453, 1429, 1315, 1287, 1252, 992, 919, 747, 692.

HRMS (ESI): calc. for $C_{16}H_{18}N$ (M+H): 224.1439; found: 224.1445.

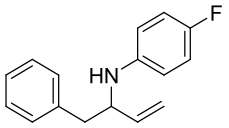

230b

Compound **230b**:

^{1}H NMR (CDCl$_3$, 400 MHz): δ = 7.32-7.28 (m, 2H), 7.25-7.19 (m, 3H), 6.84 (t, *J* = 8.8 Hz, 2H), 6.50 (dd, *J* = 9.0, 4.4 Hz, 2H), 5.83-5.74 (m, 1H), 5.16 (dt, *J* = 17.2, 1.4 Hz, 1H), 5.12 (dt, *J* = 10.3, 1.3 Hz, 1H), 4.06-4.04 (m, 1H),, 3.57 (s, NH), 2.92 (dd, *J* = 13.7, 6.4 Hz, 1H), 2.88 (dd, *J* = 9.5, 2.6 Hz, 1H).

^{13}C NMR (CDCl$_3$, 100 MHz): δ = 157.2, 154.8, 143.8, 139.4, 137.7, 129.6, 128.6, 126.8, 115.8, 115.7, 115.6, 114.7, 114.6, 57.5, 42.1.

IR (film, cm^{-1}): ν = 3409, 1506, 1454, 1217, 991, 921, 817, 766, 751, 699.

HRMS (ESI): calc. for $C_{16}H_{17}NF$ (M+H): 242.1345; found: 242.1347.

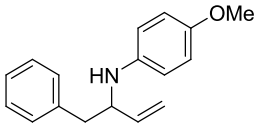

230c

Compound **230c**:

^{1}H NMR (CDCl$_3$, 400 MHz): δ = 7.31-7.27 (m, 2H), 7.24-7.19 (m, 3H), 6.75 (d, *J* = 9.0 Hz, 2H), 6.56 (d, *J* = 9.0 Hz, 2H), 5.84-5.75 (m, 1H), 5.17 (dt, *J* = 17.2, 1.4 Hz, 1H), 5.11

(dt, J = 10.3, 1.3 Hz, 1H), 4.04 (q, J = 6.6 Hz, 1H), 3.72 (s, 3H), 3.45 (s, NH), 2.90 (d, J = 6.6 Hz, 2H).

^{13}C NMR ($CDCl_3$, 100 MHz): δ = 152.3, 141.6, 139.8, 138.0, 129.6, 128.6, 126.7, 115.6, 115.3, 114.9, 57.8, 55.9, 42.1.

IR (film, cm^{-1}): ν = 3396, 1508, 1463, 1453, 1233, 1178, 1036, 992, 919, 817, 749, 700.

HRMS (ESI): calc. for $C_{17}H_{20}NO$ (M+H): 254.1545; found: 254.1550.

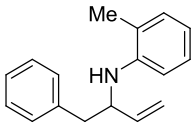

230d

Compound **230d**:

^{1}H NMR ($CDCl_3$, 400 MHz): δ = 7.32-7.28 (m, 2H), 7.24-7.21 (m, 3H), 7.07 (t, J = 7.8 Hz, 2H), 7.02-6.99 (m, 1H), 6.64-6.60 (m, 2H), 5.90-5.82 (m, 1H), 5.21 (dt, J = 17.2, 1.4 Hz, 1H), 5.14 (dt, J = 10.3, 1.3 Hz, 1H), 4.15 (s, 1H), 3.57 (s, NH), 3.01 (dd, J = 13.7, 6.2 Hz, 1H), 2.92 (dd, J = 13.6, 7.2 Hz, 1H), 2.01 (s, 3H).

^{13}C NMR ($CDCl_3$, 100 MHz): δ = 145.5, 139.8, 137.8, 130.2, 129.6, 128.6, 127.1, 126.8, 122.3, 117.1, 115.4, 111.2, 56.8, 42.3, 17.6.

IR (film, cm^{-1}): ν = 3423, 1604, 1586, 1509, 1478, 1447, 1313, 1258, 1051, 989, 918, 744, 699.

HRMS (ESI): calc. for $C_{17}H_{20}N$ (M+H): 238.1596; found: 238.1607.

5.4 General Procedure for Amination of Secondary Allylic Trichloroacetimidates with 5 mol% $[RhCl(ethylene)_2]_2$/ $P(OPh)_3$

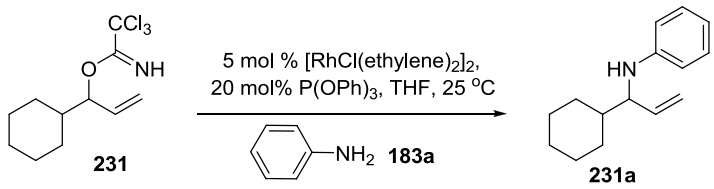

A 10 mL Schlenk flask was charged with $[RhCl(ethylene)_2]_2$ (2.7 mg, 7.0 μmol, 5 mol%) in a glove box. The flask was sealed and removed from the glove box, and THF (0.35 mL) was added to the Schlenk under argon followed by triphenylphosphite (7.4 μL, 28.0 μmol, 20 mol%). The rhodium-phosphite complex solution was allowed to stir at 25 ºC for 15 min. A separate 10 mL Schlenk flask was charged with **231** (40 mg, 0.14mmol, 1 equiv), THF (0.35 mL) and aniline **183a** (38 μL, 0.42 mmol, 3 equiv). The rhodium catalyst solution was then added to the flask containing **231** and **183a** solution. The reaction mixture was stirred at 25 ºC under argon. Reaction progress was monitored by GC. After 30 min, the crude reaction was concentrated *in vacuo*, loaded in dichloromethane onto an ISCO load cartridge, and dried under vacuum. Elution onto an ISCO 24g silica column (0 → 40% ethyl acetate/hexane) provided **231a** (30 mg, 96%, branched/linear >53:1) as pale yellow oil.

Compound **231a**:

^{1}H NMR ($CDCl_3$, 400 MHz): δ = 7.13 (dd, *J* = 7.3, 2.2 Hz, 1H), 7.11 (dd, *J* = 7.3, 2.2 Hz, 1H), 6.64 (t, *J* = 6.3 Hz, 1H), 6.58 (d, *J* = 1.0 Hz, 1H), 6.56 (d, *J* = 0.92 Hz, 1H), 5.74-5.66 (m, 1H), 5.15 (dt, *J* = 14.9, 1.4 Hz, 1H), 5.12 (dt, *J* = 9.0, 1.4 Hz, 1H), 3.67-3.61 (m, 1H, NH), 1.85-1.65 (m, 5H), 1.53-1.44 (m, 1H), 1.29-1.01 (m, 5H).

^{13}C NMR ($CDCl_3$, 100 MHz): δ = 148.1, 138.5, 129.3, 117.1, 116.0, 113.4, 61.2, 42.9, 29.7, 29.5, 26.7, 26.6, 26.5.

IR (film, cm^{-1}): ν = 3314, 3081, 3051, 3018, 2922, 2850, 1725, 1600, 1502, 1503, 1448, 1429, 1317, 1251, 1065, 992, 916, 745, 690.

HRMS (ESI): calc. for $C_{15}H_{22}N$ $(M+H)^+$: 216.1752; found: 216.1751.

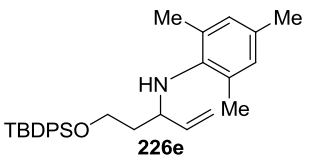

226e

Compound **226e**:

^{1}H NMR ($CDCl_3$, 400 MHz): δ = 7.69-7.65 (m, 4H), 7.45-7.35 (m, 6H), 6.80 (s, 2H), 5.70-5.61 (m, 1H), 4.97-4.95 (m, 1H), 4.93 (bs, 1H), 3.89-3.81 (m, 2H), 3.77-3.71 (m, 1H), 2.89 (s, NH), 2.22 (s, 9H), 2.01-1.91 (m, 1H), 1.77-1.69 (m, 1H), 1.06 (s, 9H).

^{13}C NMR ($CDCl_3$, 100 MHz): δ = 142.2, 140.3, 135.8, 134.0, 130.8, 129.7, 129.6, 129.5, 127.8, 115.4, 61.1, 57.3, 39.1, 27.0, 20.7, 19.3, 19.2.

IR (film, cm^{-1}): ν = 2930, 2895, 2857, 1482, 1472, 1427, 1107, 1090, 917, 822, 737, 700, 687.

HRMS (ESI): calc. for $C_{30}H_{40}NOSi$ (M+H): 458.2879; found: 458.2877.

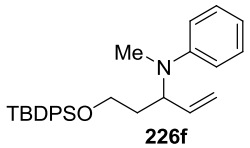

226f

Compound **226f**:

^{1}H NMR ($CDCl_3$, 400 MHz): δ = 7.77-7.67 (m, 2H), 7.59-7.57 (m, 2H), 7.46-7.30 (m, 6H), 7.26-7.21 (m, 2H), 6.89-6.86 (m, 2H), 6.76-6.70 (m, 1H), 5.90-5.82 (m, 1H), 5.18-5.10 (m, 2H), 4.75-4.70 (m, 1H), 3.75-3.65 (m, 2H), 2.71 (s, 3H), 1.98-1.88 (m, 2H), 1.07 (s, 9H).

^{13}C NMR ($CDCl_3$, 100 MHz): δ = 150.7, 137.5, 135.7, 133.9, 133.8, 129.8, 129.7, 129.2, 127.9, 127.8, 116.7, 115.7, 113.5, 60.8, 56.6, 34.5, 31.8, 27.0, 19.3.

IR (film, cm^{-1}): ν = 2953, 2930, 2887, 2856, 1597, 1574, 1503, 1471, 1427, 1106, 1087, 822, 742, 700, 688.

HRMS (ESI): calc. for $C_{28}H_{36}NOSi$ (M+H): 430.2566; found: 430.2561.

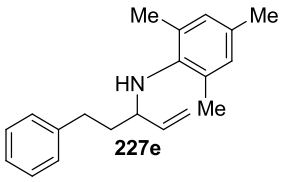

227e

Compound **227e**:

^{1}H NMR (CDCl$_3$, 400 MHz): δ = 7.30-7.26 (m, 2H), 7.20-7.17 (m, 3H), 6.78 (s, 2H), 5.75-5.67 (m, 1H), 5.03-4.96 (m, 2H), 3.55 (q, *J* = 7.8 Hz, 1H), 2.88 (s, NH), 2.75-2.71 (m, 2H), 2.21 (s, 3H), 2.18 (s, 6H), 2.03-1.96 (m, 1H), 1.87-1.83 (m, 1H).

^{13}C NMR (CDCl$_3$, 100 MHz): δ = 142.2, 142.1, 140.4, 130.9, 129.6, 129.4, 128.6, 128.5, 126.0, 115.7, 60.0, 37.9, 32.6, 20.7, 19.1.

IR (film, cm^{-1}): ν = 3062, 3025, 2939, 2916, 2856, 1482, 1453, 1230, 1011, 989, 916, 853, 743, 698.

HRMS (ESI): calc. for $C_{20}H_{26}N$ (M+H): 280.2065; found: 280.2063.

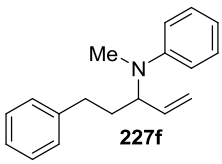

227f

Compound **227f**:

^{1}H NMR (CDCl$_3$, 400 MHz): δ = 7.29-7.14 (m, 7H), 6.78-6.70 (m, 3H), 5.89-5.80 (m, 1H), 5.19-5.11 (m, 2H), 4.34 (m, 1H), 2.81 (s, 3H), 2.70-2.59 (m, 2H), 2.08-1.96 (m, 2H).

^{13}C NMR (CDCl$_3$, 100 MHz): δ = 150.7, 142.0, 137.3, 129.2, 128.6, 128.5, 126.0, 116.7, 115.9, 113.3, 59.6, 33.9, 33.0, 31.6.

IR (film, cm^{-1}): ν = 3083, 3060, 3024, 3003, 2941, 2863, 2811, 1596, 1502, 1453, 9990, 919, 745, 691.

HRMS (ESI): calc. for $C_{18}H_{22}N$ (M+H): 252.1752; found: 252.1759.

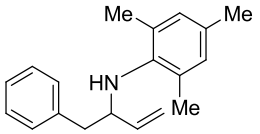

230e

Compound **230e**:

^{1}H NMR ($CDCl_3$, 400 MHz): δ = 7.30-7.26 (m, 2H), 7.22-7.19 (m, 3H), 6.78 (s, 2H), 5.74-5.65 (m, 1H), 4.93-4.87 (m, 2H), 3.83 (q, *J* = 7.7 Hz, 1H), 3.01 (dd, *J* = 13.2, 5.4 Hz, 1H), 2.96 (s, NH), 2.79 (dd, *J* = 13.2, 7.9 Hz, 1H), 2.20 (s, 3H), 2.15 (s, 6H).

^{13}C NMR ($CDCl_3$, 100 MHz): δ = 141.9, 139.7, 138.6, 131.2, 129.8, 129.6, 128.4, 126.4, 115.5, 61.5, 42.7, 20.8, 19.1.

IR (film, cm^{-1}): ν = 3371, 3026, 2939, 2915, 1482, 1453, 1373, 1300, 1230, 1156, 990, 917, 853, 737, 698.

HRMS (ESI): calc. for $C_{19}H_{24}N$ (M+H): 266.1909; found: 266.1924.

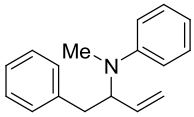

230f

Compound **230f**:

^{1}H NMR ($CDCl_3$, 400 MHz): δ = 7.28-7.15 (m, 7H), 6.76-6.67 (m, 3H), 5.92-5.84 (m, 1H), 5.17-5.09 (m, 2H), 4.61-4.56 (m, 1H), 3.05-2.91 (m, 2H), 2.82 (s, 3H).

^{13}C NMR ($CDCl_3$, 100 MHz): δ = 150.4, 139.1, 136.6, 129.3, 129.2, 128.5, 126.3, 116.9, 116.3, 113.5, 62.3, 38.3, 32.3.

IR (film, cm^{-1}): ν = 3084, 3061, 3024, 3002, 2979, 2938, 1595, 1573, 1502, 1453, 1118, 1097, 1030, 990, 920, 745, 691.

HRMS (ESI): calc. for $C_{17}H_{20}N$ (M+H): 238.1596; found: 239.1608.

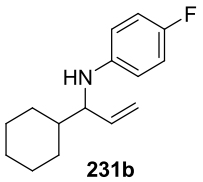

231b

Compound **231b**:

^{1}H NMR ($CDCl_3$, 400 MHz): δ = 6.82 (t, *J* = 8.8 Hz, 1H), 6.49 (dd, *J* = 9.1, 4.4 Hz, 1H), 5.75-5.62 (m, 1H), 5.14 (d, *J* = 2.0 Hz, 1H), 5.11 (dd, *J* = 3.8, 1.5 Hz, 1H), 3.53 (bs, 2H), 1.84-1.62 (m, 5H), 1.48-1.44 (m, 1H), 1.25-1.03 (m, 5H).

^{13}C NMR ($CDCl_3$, 100 MHz): δ = 156.9, 154.5, 144.4, 116.1, 115.7, 115.5, 114.3, 114.2, 62.0, 42.9, 29.7, 29.5, 26.7, 26.5, 26.4.

IR (film, cm^{-1}): ν = 3422, 2923, 2851, 1507, 1449, 1315, 1289, 993, 917, 816.

HRMS (ESI): calc. for $C_{15}H_{21}NF$ $(M+H)^+$: 234.1658; found: 234.1655.

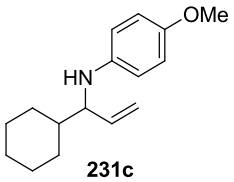

231c

Compound **231c**:

^{1}H NMR ($CDCl_3$, 400 MHz): δ = 6.73 (d, *J* = 8.8 Hz, 2H), 6.53 (d, *J* = 8.8 Hz, 2H), 5.72-5.64 (m, 1H), 5.15-5.10 (m, 2H), 3.71 (s, 3H), 3.53 (t, *J* = 6.5 Hz, 1H), 3.41 (s, NH), 1.85-1.64 (m, 5H), 1.51-1.44 (m, 1H), 1.28-1.00 (m, 5H).

^{13}C NMR ($CDCl_3$, 100 MHz): δ = 151.9, 142.4, 138.9, 115.9, 115.0, 114.8, 62.3, 55.9, 42.9, 29.7, 29.5, 26.7, 26.6, 26.5.

IR (film, cm^{-1}): ν = 3405, 2922, 2850, 2831, 1509, 1481, 1463, 1448, 1232, 1178, 1038, 994, 915, 815.

HRMS (ESI): calc. for $C_{16}H_{24}NO$ $(M+H)^+$: 246.1858; found: 246.1855.

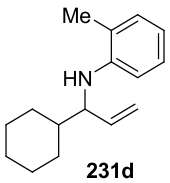

231d

Compound **231d**:

^{1}H NMR ($CDCl_3$, 400 MHz): δ = 7.08-7.01 (m, 2H), 6.61-6.54 (m, 2H), 5.77-5.68 (m, 1H), 5.15 (d, *J* = 9.2, 1.5 Hz, 1H), 5.13-5.11 (m, 1H), 3.70 (s, 1H), 3.56 (bs, NH) 2.14 (s, 3H), 1.88-1.74 (m, 5H), 1.69-1.55 (m, 1H), 1.27-1.05 (m, 5H).

^{13}C NMR ($CDCl_3$, 100 MHz): δ = 145.8, 138.6, 130.2, 127.1, 121.7, 116.5, 115.8, 110.7, 60.8, 42.9, 29.6, 26.7, 26.6, 26.5, 17.8.

IR (film, cm^{-1}): ν = 3442, 2922, 1605, 1586, 1509, 1477, 1447, 1315, 1302, 1288, 1254, 1051, 984, 916, 794, 743, 713.

HRMS (ESI): calc. for $C_{16}H_{24}N$ $(M+H)^+$: 230.1909; found: 230.1910

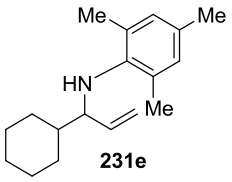

231e

Compound **231e**:

^{1}H NMR ($CDCl_3$, 400 MHz): δ = 6.75 (s, 2H), 5.63-5.54 (m, 1H), 4.87 (dd, *J* = 10.2, 1.8 Hz, 1H), 4.77 (dd, *J* = 16.9, 1.8 Hz, 1H), 3.33 (dd, *J* = 8.4, 5.9 Hz, 1H), 2.18 (s, 9H) 1.95-1.65 (m, 5H), 1.49-1.45 (m, 1H), 1.31-1.01 (m, 5H).

^{13}C NMR ($CDCl_3$, 100 MHz): δ = 142.5, 138.7, 130.5, 129.6, 129.2, 115.8, 65.7, 43.2, 30.4, 29.3, 26.9, 26.6, 20.7, 19.3.

IR (film, cm^{-1}): ν = 3349, 2921, 2851, 1483, 1301, 1246, 1231, 1152, 989, 976, 914, 852.

HRMS (ESI): calc. for $C_{18}H_{28}N$ $(M+H)^+$: 258.2222; found: 258.2226.

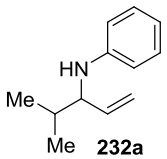

232a

Compound **232a**:

^{1}H NMR ($CDCl_3$, 400 MHz): δ = 7.16-7.11 (m, 2H), 6.67-6.63 (m, 1H), 6.60-6.57 (m, 2H), 5.76-5.67 (m, 1H), 5.15 (td, *J* = 15.7, 1.4 Hz, 2H), 3.69-3.62 (m, 2H), 1.90-1.82 (m, 1H), 0.99 (d, *J* = 6.8 Hz, 3H), 0.96 (d, *J* = 6.8 Hz, 3H),

^{13}C NMR ($CDCl_3$, 100 MHz): δ = 148.1, 138.1, 129.3, 117.2, 116.2, 113.5, 61.6, 32.6, 19.0, 18.7.

IR (film, cm^{-1}): ν = 3416, 2959, 2940, 2929, 2902, 2872, 1600, 1503, 1428, 1317, 1272, 1178, 1154, 916, 866, 746, 690.

HRMS (ESI): calc. for $C_{12}H_{18}N$ $(M+H)^+$: 176.1439; found: 176.1438.

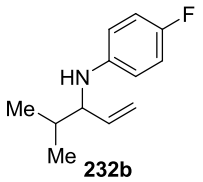

232b

Compound **232b**:

^{1}H NMR ($CDCl_3$, 400 MHz): δ = 6.86-6.80 (m, 2H), 6.53-6.48 (m, 1H), 5.72-5.64 (m, 1H), 5.17 (d, *J* = 3.0 Hz, 1H), 5.13 (dd, *J* = 2.8, 1.6 Hz, 1H), 3.55-3.53 (m, 2H), 1.87-1.79 (m, 1H), 0.97 (d, *J* = 6.8 Hz, 3H), 0.94 (d, *J* = 6.8 Hz, 3H),

^{13}C NMR ($CDCl_3$, 100 MHz): δ = 156.8, 154.6, 144.4, 138.0, 116.4, 115.8, 115.6, 114.3, 114.2, 62.4, 32.7, 19.0, 18.7.

IR (film, cm^{-1}): ν = 3424, 2960, 2873, 1507, 1466, 1315, 1218, 994, 918, 816, 773, 749.

HRMS (ESI): calc. for $C_{12}H_{17}NF$ $(M+H)^+$: 194.1345; found: 194.1341.

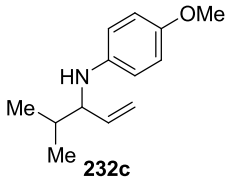

232c

Compound **232c**:

^{1}H NMR ($CDCl_3$, 400 MHz): δ = 6.76-6.72 (m, 2H), 6.57-6.53 (m, 1H), 5.73-5.65 (m, 1H), 5.17 (t, *J* = 1.6 Hz, 1H), 5.15-5.12 (m, 1H), 3.71 (s, 3H), 3.54 (t, *J* = 5.4 Hz, 1H), 3.40 (s, NH), 1.88-1.79 (m, 1H), 0.98 (d, *J* = 6.8 Hz, 3H), 0.94 (d, *J* = 6.8 Hz, 3H),

^{13}C NMR ($CDCl_3$, 100 MHz): δ = 152.0, 142.3, 138.4, 116.2, 115.0, 114.8, 62.6, 56.0, 32.6, 19.1, 18.7.

IR (film, cm^{-1}): ν = 3404, 2932, 1509, 1463, 1229, 1178, 1038, 994, 916, 815, 756.

HRMS (ESI): calc. for $C_{13}H_{20}NO$ $(M+H)^+$: 206.1545; found: 206.1547.

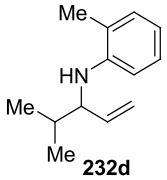

232d

Compound **232d**:

^{1}H NMR ($CDCl_3$, 400 MHz): δ = 7.09-7.03 (m, 2H), 6.62-6.55 (m, 2H), 5.79-5.71 (m, 1H), 5.20 (t, *J* = 1.6 Hz, 1H), 5.17-5.14 (m, 1H), 3.74-3.69 (m, 1H), 3.55 (s, NH), 2.16 (s, 3H), 1.95-1.87 (m, 1H), 1.01 (d, *J* = 6.8 Hz, 3H), 0.97 (d, *J* = 6.8 Hz, 3H),

^{13}C NMR ($CDCl_3$, 100 MHz): δ = 145.8, 138.2, 130.2, 127.2, 121.8, 116.7, 116.1, 110.8, 61.2, 32.7, 19.0, 18.8, 17.7.

IR (film, cm^{-1}): ν = 3442, 2958, 1605, 1586, 1510, 1477, 1464, 1446, 1315, 1303, 1252, 1051, 992, 917, 744, 714.

HRMS (ESI): calc. for $C_{13}H_{20}N$ $(M+H)^+$: 190.1596; found: 190.1589.

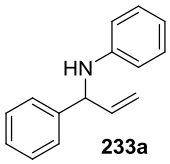

233a

Compound **233a**:

^{1}H NMR ($CDCl_3$, 400 MHz): δ = 7.35-7.21 (m, 5H), 7.11-7.06 (m, 2H), 6.64 (t, *J* = 7.3 Hz, 1H), 6.56 (d, *J* = 8.6 Hz, 2H), 6.07-5.98 (m, 1H), 5.28 (bs, 1H), 5.24-5.19 (m, 1H), 4.91 (t, *J* = 4.4 Hz, 1H), 4.02 (bs, NH),

^{13}C NMR ($CDCl_3$, 100 MHz): δ = 147.4, 142.0, 139.2, 129.3, 128.9, 127.6, 127.3, 117.8, 116.2, 113.7, 61.0.

IR (film, cm^{-1}): ν = 3409, 3082, 3051, 3024, 1599, 1500, 1451, 1428, 1313, 1266, 1243, 1179, 1028, 991, 923, 746, 690.

HRMS (ESI): calc. for $C_{15}H_{16}N$ $(M+H)^+$: 210.1288; found: 210.1283

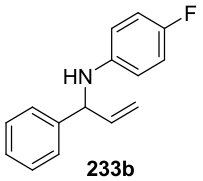

233b

Compound **233b**:

^{1}H NMR ($CDCl_3$, 400 MHz): δ = 7.35-7.25 (m, 5H), 6.82 (t, *J* = 8.8 Hz, 2H), 6.50 (dd, *J* = 8.7, 4.4 Hz, 2H), 6.01-5.96 (m, 1H), 5.27 (dt, *J* = 18.8, 1.4 Hz, 1H), 5.21 (dt, *J* = 10.2, 1.3 Hz, 1H), 4.84 (d, *J* = 5.9 Hz, 1H), 3.95 (bs, NH),

^{13}C NMR ($CDCl_3$, 100 MHz): δ = 157.2, 154.9, 143.7, 141.9, 139.2, 128.9, 127.7, 127.3, 116.3, 115.8, 115.6, 114.6, 114.5, 61.6.

IR (film, cm^{-1}): ν = 3413, 1508, 1452, 1402, 1312, 1218, 927, 818, 780, 749, 700.

HRMS (ESI): calc. for $C_{15}H_{15}NF$ $(M+H)^+$: 228.1193; found: 228.1189.

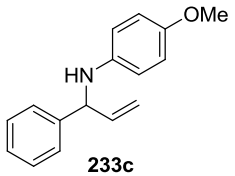

233c

Compound **233c**:

^{1}H NMR ($CDCl_3$, 400 MHz): δ = 7.39-7.24 (m, 5H), 6.73 (D, *J* = 9.0 Hz, 2H), 6.55 (d, *J* = 8.9 Hz, 2H), 6.06-5.98 (m, 1H), 5.26 (dt, *J* = 17.1, 1.4 Hz, 1H), 5.20 (dt, *J* = 10.2, 1.3 Hz, 1H), 4.85 (d, *J* = 6.0 Hz, 1H), 3.80 (bs, NH), 3.71 (s, 3H).

^{13}C NMR ($CDCl_3$, 100 MHz): δ = 152.2, 142.3, 141.6, 139.6, 128.9, 127.6, 127.3, 116.1, 115.0, 114.8, 61.9, 55.9.

IR (film, cm^{-1}): ν = 3396, 2830, 1509, 1463, 1452, 1405, 1240, 1230, 1178, 1036, 992, 924, 817, 764, 746, 700.

HRMS (ESI): calc. for $C_{16}H_{18}NO$ $(M+H)^+$: 240.1389; found: 240.1388.

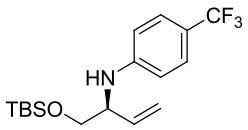

242

Compound **242**:

^{1}H NMR ($CDCl_3$, 400 MHz): δ = 7.35 (d, *J* = 8.5, 2H), 6.61 (d, *J* = 8.5 Hz, 2H), 5.81-5.76 (m, 1H), 5.27 (dt, *J* = 17.3, 1.4 Hz, 1H), 5.20 (dt, *J* = 10.4, 1.3 Hz, 1H), 4.51 (d, *J* = 5.8 Hz, NH), 3.92-3.86 (m, 1H), 3.77 (dd, *J* = 10.4, 4.4 Hz, 1H), 3.63 (dd, *J* = 10.0, 5.8 Hz, 1H), 0.88 (s, 9H), 0.06 (s, 3H), 0.05 (s, 3H).

^{13}C NMR ($CDCl_3$, 100 MHz): δ = 150.5, 136.8, 126.7, 119.2, 118.9, 117.2, 113.0, 65.7, 57.5, 26.0, 18.5, -5.1, -5.2.

IR (film, cm^{-1}): ν = 3421, 2954, 2931, 2884, 2858, 1617, 1531, 1483, 1472, 1325, 1257, 1186, 1159, 1107, 1066, 835, 825, 778.

HRMS (ESI): calc. for $C_{17}H_{27}NOF_3Si$ (M+H): 346.1819; found: 346.1814.

5.5 General Procedure for the Preparation of Tertiary Allylic Trichloroacetimidates

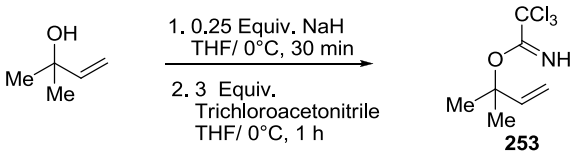

A 25 mL oven-dried Schlenk flask was charged with NaH (60% dispersion in oil, washed 5x with hexanes and dried under vacuum, 0.23 g, 5.8 mmol, 0.25 equiv) and dry THF (6 mL) and cooled to 0°C. 2-methyl-3-buten-2-ol (2.4 mL, 23 mmol) was added dropwise and the resulting mixture allowed to stir for 30 minutes. Trichloroacetonitrile (7.0 mL, 70 mmol, 3.0 equiv) and THF (6 mL) were added to a separate oven-dried Schlenk flask and cooled to 0°C. The alcohol/alkoxide solution was transferred slowly to the trichloroacetonitrile solution via cannula. The reaction mixture was stirred at 0°C for 1 hour, quenched with MeOH (0.7 mL) and loaded directly onto a RediSep load cartridge containing pre-equilibrated and dried silica. Purification by silica gel flash column

chromatography (pre-equilibrated 80g RediSep column, 20% ethyl acetate/Hexane + 1% triethylamine) resulted in **253** (3.6 g, 67%) as a brown oil.

Compound **253**:

^{1}H NMR ($CDCl_3$, 400 MHz): δ = 8.24 (s, NH), 6.13 (dd, *J* = 17.5, 10.9, 1H), 5.25 (dd, *J* = 17.5, 0.8, 1H), 5.11 (dd, *J* = 10.9, 0.8, 1H), 1.62 (s, 6H).

^{13}C NMR ($CDCl_3$, 100 MHz): δ = 160.4, 142.2, 116.2, 113.4, 84.4, 26.2.

IR (film, cm^{-1}): ν = 3337, 2983,1698, 1662, 1512, 1319, 1084, 865, 820, 794.

HRMS (TOF ES+): calc. for $C_7H_{10}Cl_3NONa$ $(M + Na)^+$: 251.9726; found: 251.9740.

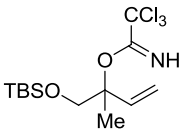

254

Compound **254**:

^{1}H **NMR ($CDCl_3$, 400 MHz):** δ = 8.25 (s, NH), 6.00 (dd, *J* = 17.6, 11.1 Hz, 1H), 5.27 (d, *J* = 17.6 Hz, 1H), 5.21 (d, *J* = 11.1 Hz, 1H), 3.87 (d, *J* = 10.2 Hz, 1H), 3.69 (d, *J* = 10.2 Hz, 1H), 1.64 (s, 3H), 0.86 (s, 9H), 0.03 (s, 6H).

^{13}C NMR ($CDCl_3$, 100 MHz): δ = 160.3, 138.9, 115.4, 86.4, 69.4, 68.3, 26.0, 19.8, 18.4, -5.2, -5.3.

IR (film, cm^{-1}): ν = 3341, 2929, 1664, 1471, 1319, 1252, 1082, 834, 774, 667.

HRMS (TOF ES+): calc. for $C_{13}H_{25}Cl_3NO_2Si$ $(M + H)^+$: 360.0720; found: 360.0735.

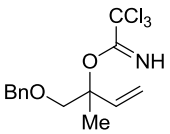

255

Compound **255**:

^{1}H NMR ($CDCl_3$, 400 MHz): δ = 8.30 (s, NH), 7.34-7.27 (m, 5H), 6.10 (dd, *J* = 17.6, 11.0 Hz, 1H), 5.33 (dd, *J* = 17.6, 0.7 Hz, 1H), 5.24 (dd, *J* = 11.0, 0.8 Hz, 1H), 4.64 (d, *J* = 12.3 Hz, 1H), 4.61 (d, *J* = 12.3 Hz, 1H), 3.78 (d, *J* = 10.4 Hz, 1H), 3.71 (d, *J* = 10.4 Hz, 1H), 1.70 (s, 3H).

^{13}C NMR ($CDCl_3$, 100 MHz): δ = 160.1, 138.8, 138.6, 128.5, 127.7, 1276, 115.5, 85.9, 75.2, 73.7, 20.4.

IR (film, cm^{-1}): ν = 3334, 2860, 1663, 1453, 1317, 1078, 793, 734, 696.

HRMS (TOF ES+): calc. for $C_{14}H_{16}Cl_3NO_2Na$ $(M+Na)^+$: 358.0144; found: 358.0143.

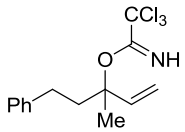

256

Compound **256**:

^{1}H NMR ($CDCl_3$, 400 MHz): δ = 8.34 (s, NH), 7.30-7.26 (m, 2H), 7.20-7.16 (m, 3H), 6.09 (dd, *J* = 17.5, 11.0 Hz, 1H), 5.34 (dd, *J* = 17.5, 0.8 Hz, 1H), 5.24 (dd, *J* = 11.0, 0.9 Hz, 1H), 2.72 (m, 2H), 2.37 (m, 1H), 2.16 (m, 1H), 1.73 (s, 3H).

^{13}C NMR ($CDCl_3$, 100 MHz): δ = 160.1, 142.2, 141.2, 128.60, 128.56, 128.52, 126.0, 114.2, 86.3, 42.0, 30.1, 23.1.

IR (film, cm^{-1}): ν = 3334, 3027, 2976, 1704, 1662, 1496, 1454, 1319, 1083, 819, 794, 745, 698.

HRMS (TOF ES+): calc. for $C_{14}H_{17}Cl_3NO$ $(M+H)^+$: 320.0376; found: 320.0384.

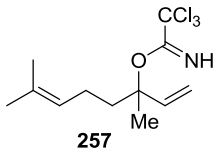

257

Compound **257**:

^{1}H NMR ($CDCl_3$, 400 MHz): δ = 8.23 (s, NH), 6.02 (dd, *J* = 17.5, 11.0 Hz, 1H), 5.24 (dd, *J* = 17.5, 0.8 Hz, 1H), 5.15 (dd, *J* = 11.0, 0.8 Hz, 1H), 5.09 (m, 1H), 2.06 (m, 2H), 1.98 (m, 1H), 1.83 (m, 1H), 1.64 (s, 6H), 1.56 (s, 3H).

^{13}C NMR ($CDCl_3$, 100 MHz): δ = 160.1, 141.3, 132.1, 123.9, 113.8, 86.5, 40.1, 25.8, 22.9, 22.4, 17.7.

IR (film, cm^{-1}): ν = 3337, 2969, 2915, 1701, 1663, 1516, 1448, 1319, 1247, 963, 821, 793, 739, 682.

HRMS (TOF ES+): calc. for $C_{12}H_{18}Cl_3NONa$ $(M+Na)^+$: 320.0352; found: 320.0353.

5.6 General Procedure for Regioselective Amination of Tertiary Allylic Trichloroacetimidates with $[RhCl(norbornadiene)]_2$

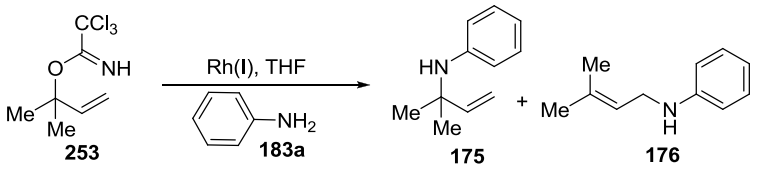

A 10 mL Schlenk flask was charged with $[RhCl(norbornadiene)]_2$ (0.64 mg, 1.4 μmol, 1 mol%) in a glove box. The flask was sealed, removed from the glove box, and THF (0.35 mL) was added to the Schlenk and stirred to homogeneity under argon for 5 minutes. A separate 10 mL Schlenk flask was charged with **253** (32 mg, 0.14 mmol, 1 equiv), THF (0.35 mL) and aniline **183a** (38 μL, 0.42 mmol, 3 equiv). The rhodium catalyst solution was then added to the flask containing the **253** and **183a** solution. The mixture was stirred at RT under argon and the reaction progress was monitored by GC at 30 minutes. The crude reaction was purified by adsorbing directly onto a dry 5g Teledyne Isco silica cartridge using vacuum followed by elution onto a pre-equilibrated 24g silica flash

column (0 → 10% diethyl ether/Hexane + 1 % triethylamine) providing **175** and **176** (21 mg, 87%, **175**/**176** 56:1) as pale yellow oil.

Compound **175**:

^{1}H NMR ($CDCl_3$, 400 MHz): δ = 7.11-7.07 (m, 2H), 6.69-6.67 (m, 3H), 6.00 (dd, *J* = 17.5, 10.7 Hz, 1H), 5.17 (dd, *J* = 17.5, 1.1 Hz, 1H), 5.09 (dd, *J* = 10.6, 1.1 Hz, 1H), 3.67 (bs, NH), 1.37 (s, 6H).

^{13}C NMR ($CDCl_3$, 100 MHz): δ = 146.8, 146.4, 128.9, 117.6, 115.9, 112.9, 54.8, 28.5.

IR (film, cm^{-1}): ν = 3413, 2978, 2926, 1602, 1503, 1317, 1260, 1191, 996, 914, 747, 694.

HRMS (TOF ES+): calc. for $C_{11}H_{16}N$ $(M+H)^+$: 162.1275; found: 162.1283.

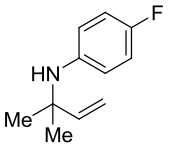

253b

Compound **253b**:

^{1}H NMR ($CDCl_3$, 400 MHz): 7.11-7.07 (m, 2H), 6.69-6.65 (m, 2H), 6.00 (dd, *J* = 17.5, 10.7 Hz, 1H), 5.17 (dd, *J* = 17.5, 1.1 Hz, 1H), 5.09 (dd, *J* = 10.6, 1.1 Hz, 1H), 3.67 (bs, NH), 1.37 (s, 6H).

^{13}C NMR ($CDCl_3$, 100 MHz): δ = 157.6, 146.4, 117.8, 115.4, 115.2, 113.0, 55.2, 28.4.

IR (film, cm^{-1}): ν = 3413, 2978, 1508, 1216, 916, 822.

HRMS (TOF ES+): calc. for $C_{11}H_{15}FN$ $(M+H)^+$: 180.1190; found: 180.1189.

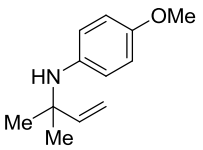

253c

Compound **253c**:

^{1}H NMR ($CDCl_3$, 400 MHz): δ = 6.70 (s, 4H), 5.99 (dd, *J* = 17.5, 10.6 Hz, 1H), 5.12 (dd, *J* = 17.5, 1.0 Hz, 1H), 5.06 (dd, *J* = 10.7, 1.1 Hz, 1H), 3.72 (s, 3H), 1.31 (s, 6H).

^{13}C NMR ($CDCl_3$, 100 MHz): δ = 153.2, 146.8, 140.4, 119.3, 114.4, 112.6, 55.8, 55.4, 28.3.

IR (film, cm^{-1}): ν = 3387, 2976, 2831, 1507, 1299, 1234, 1176, 1038, 967, 916, 822, 763.

HRMS (TOF ES+): calc. for $C_{12}H_{18}NO$ $(M+H)^+$: 192.1381; found: 192.1388.

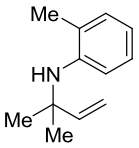

253d

Compound **253d**:

^{1}H NMR ($CDCl_3$, 400 MHz): δ = 7.04-6.98 (m, 2H), 6.82 (dd, *J* = 8.1, 1.2, 1H), 6.60 (td, *J* = 7.3, 1.1 Hz, 1H), 6.02 (dd, *J* = 17.5, 10.7 Hz, 1H), 5.18 (dd, *J* = 17.5, 1.1 Hz, 1H), 5.11 (dd, *J* = 10.7, 1.1 Hz, 1H), 3.57 (bs, NH), 2.13 (s, 3H), 1.42 (s, 6H).

^{13}C NMR ($CDCl_3$, 100 MHz): δ = 146.6, 144.7, 130.3, 126.5, 122.7, 116.9, 113.7, 112.9, 54.6, 28.7, 18.1.

IR (film, cm^{-1}): ν = 3435, 2979, 1605, 1587, 1510, 1444, 1315, 1262, 1180, 1053, 991, 916, 745, 696.

HRMS (TOF ES+): calc. for $C_{12}H_{18}N$ $(M+H)^+$: 176.1461; found: 176.1439.

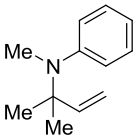

253f

Compound **253f**:

^{1}H NMR ($CDCl_3$, 400 MHz): δ = 7.24-7.19 (m, 2H), 7.14-7.11 (m, 2H), 7.04 (tt, *J* = 7.2, 1.2 Hz, 1H), 5.97 (dd, *J* = 17.5, 10.8 Hz, 1H), 5.05 (dd, *J* = 10.8, 1.2 Hz, 1H), 5.03 (dd, *J* = 17.5, 1.2 Hz, 1H), 2.73 (s, 3H), 1.19 (s, 6H).

^{13}C NMR ($CDCl_3$, 100 MHz): δ = 150.5, 145.5, 128.0, 127.2, 123.8, 112.4, 59.2, 37.4, 25.3.

IR (film, cm^{-1}): ν = 2976, 1596, 1491, 1131, 914, 772, 700.

HRMS (TOF ES+): calc. for $C_{12}H_{18}N$ $(M+H)^+$: 176.1434; found: 176.1439.

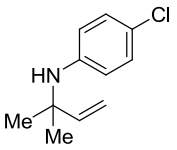

253g

Compound **253g**:

^{1}H NMR ($CDCl_3$, 400 MHz): 7.04-7.02 (m, 2H), 6.61-6.58 (m, 2H), 5.95 (dd, *J* = 17.6, 10.6 Hz, 1H), 5.16 (dd, *J* = 17.6, 1.0 Hz, 1H), 5.10 (dd, *J* = 10.6, 1.0 Hz, 1H), 1.35 (s, 6H).

^{13}C NMR ($CDCl_3$, 100 MHz): δ = 145.9, 145.4, 128.7, 122.3, 116.9, 113.2, 54.9, 28.4.

IR (film, cm^{-1}): ν = 3565, 2973, 2860, 1065, 1029.

HRMS (TOF ES+): calc. for $C_{11}H_{15}NCl$ $(M+H)^+$: 196.0898; found: 196.0893.

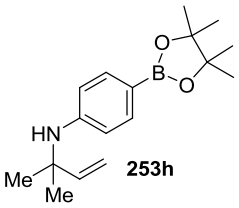

253h

Compound **253h**:

^{1}H NMR ($CDCl_3$, 400 MHz): δ = 7.56-7.53 (m, 2H), 6.64-6.60 (m, 2H), 5.95 (dd, *J* = 17.5, 10.7 Hz, 1H), 5.15 (dd, *J* = 17.5, 1.0 Hz, 1H), 5.08 (dd, *J* = 10.6, 1.0 Hz, 1H), 1.37 (s, 6H), 1.28 (s, 12H).

^{13}C NMR ($CDCl_3$, 100 MHz): δ = 149.5, 145.6, 136.0, 114.5, 113.2, 83.3, 54.7, 28.5, 25.0.

IR (film, cm^{-1}): ν = 3423, 3372, 2977, 1602, 1355, 1324, 1313, 1255, 1183, 1139.

HRMS (TOF ES+): calc. for $C_{17}H_{27}BNO_2$ $(M+H)^+$: 288.2155; found: 288.2135.

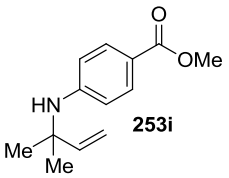

253i

Compound **253i**:

^{1}H NMR ($CDCl_3$, 400 MHz): δ = 7.78-7.75 (m, 2H), 6.62-6.58 (m, 2H), 5.94 (dd, *J* = 17.5, 10.6 Hz, 1H), 5.18 (dd, *J* = 17.5, 1.0 Hz, 1H), 5.13 (dd, *J* = 10.7, 1.0 Hz, 1H), 4.21 (bs, NH), 3.01 (s, 3H), 1.40 (s, 6H).

^{13}C NMR ($CDCl_3$, 100 MHz): δ = 167.6, 150.8, 145.1, 131.2, 118.2, 113.9, 113.6, 54.9, 51.7, 28.5.

IR (film, cm^{-1}): ν = 3379, 2980, 2948, 1693, 1602, 1520, 1434, 1339, 1271, 1173, 1108, 994, 840, 821.

HRMS (TOF ES+): calc. for $C_{13}H_{18}NO_2$ $(M+H)^+$: 202.1338 ; found: 202.1348.

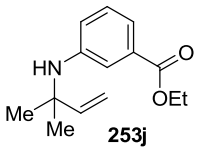

253j

Compound **253j**:

^{1}H NMR ($CDCl_3$, 400 MHz): δ = 7.36-7.32 (m, 2H), 7.15 (t, *J* = 8.0 Hz, 1H), 6.85 (dd, *J* = 8.1, 2.4 Hz, 1H), 5.97 (dd, *J* = 17.5, 10.6 Hz, 1H), 5.18 (d, *J* = 17.5 Hz, 1H), 5.12 (d, *J* = 10.6 Hz, 1H), 4.31 (q, *J* = 7.1 Hz, 2H), 1.38 (s, 6H), 1.34 (t, *J* = 7.1 Hz, 3H).

^{13}C NMR ($CDCl_3$, 100 MHz): δ = 167.2, 146.8, 145.8, 131.1, 128.8, 119.8, 118.6, 116.7, 113.3, 60.9, 54.9, 28.4, 14.5.

IR (film, cm^{-1}): ν = 3392, 2978, 2931, 2971, 1708, 1604, 1598, 1587, 1509, 1487, 1365, 1277, 1236, 1190, 1106, 1026, 999, 917, 823, 753, 686.

HRMS (TOF ES+): calc. for $C_{14}H_{20}NO_2$ $(M+H)^+$: 234.1494; found: 234.1495.

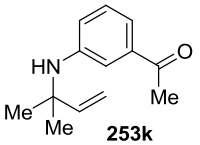

253k

Compound **253k**:

^{1}H NMR ($CDCl_3$, 400 MHz): δ = 7.26-7.21 (m, 2H), 7.16 (t, *J* = 7.9, 1H), 6.86 (ddd, *J* = 8.0, 2.5, 1.1 Hz, 1H), 5.97 (dd, *J* = 17.5, 10.6 Hz, 1H), 5.19 (dd, *J* = 17.5, 1.0 Hz, 1H), 5.13 (dd, *J* = 10.6, 1.0 Hz, 1H), 2.51 (s, 3H), 1.38 (s, 6H).

^{13}C NMR ($CDCl_3$, 100 MHz): δ = 198.8, 147.0, 145.8, 138.0, 129.0, 120.1, 117.7, 115.0, 113.3, 54.9, 28.4, 26.9.

IR (film, cm^{-1}): ν = 3385, 2977, 1676, 1601, 1485, 1426, 1357, 1330, 1274, 1232, 1189, 1090, 999, 960, 919, 779, 689.

HRMS (TOF ES+): calc. for $C_{13}H_{18}NO$ $(M+H)^+$: 204.1384; found: 204.1388.

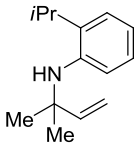

253l

Compound **253l**:

^{1}H NMR ($CDCl_3$, 400 MHz): δ = 7.11 (dd, *J* = 7.6, 1.5 Hz, 1H), 7.01-6.97 (m, 1H), 6.85 (dd, *J* = 8.2, 1.2 Hz, 1H), 6.69 (td, *J* = 7.3, 1.2 Hz, 1H), 6.02 (dd, *J* = 17.5, 10.7 Hz, 1H), 5.18 (dd, *J* = 17.6, 1.1 Hz, 1H), 5.10 (dd, *J* = 10.7, 1.1 Hz, 1H), 3.76 (bs, NH), 2.85 (sept., *J* = 6.8 Hz, 1H), 1.41 (s, 6H), 1.25 (d, *J* = 6.8 Hz, 6H).

^{13}C NMR ($CDCl_3$, 100 MHz): δ = 146.8, 143.4, 133.1, 126.0, 125.1, 117.4, 114.8, 112.8, 54.7, 28.8, 27.6, 22.6.

IR (film, cm^{-1}): ν = 3446, 2961, 2869, 1747, 1603, 1585, 1508, 1465, 1449, 1410, 1360, 1311, 1258, 1186, 1039, 993, 915.

HRMS (TOF ES+): calc. for $C_{14}H_{22}N$ $(M+H)^+$: 204.1752; found: 204.1744.

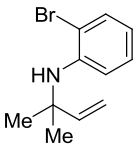

253m

Compound **253m**:

^{1}H NMR ($CDCl_3$, 400 MHz): δ = 7.39 (dd, *J* = 7.9, 1.5 Hz, 1H), 7.04 (m, 1H), 6.86 (dd, *J* = 8.3, 1.5 Hz, 1H), 6.50 (m, 1H), 5.98 (dd, *J* = 17.5, 10.6 Hz, 1H), 5.18 (dd, *J* = 17.5, 1.0 Hz, 1H), 5.12 (dd, *J* = 10.7, 1.0 Hz, 1H), 1.42 (s, 6H).

^{13}C NMR ($CDCl_3$, 100 MHz): δ = 146.8, 143.7, 132.6, 127.8, 117.8, 115.0, 113.3, 111.1, 55.0, 28.5.

IR (film, cm^{-1}): ν = 3407, 2980, 2143, 1744, 1593, 1508, 1461, 1321, 1187, 1018, 918, 864, 841, 740, 696.

HRMS (TOF ES+): calc. for $C_{11}H_{15}NBr$ $(M+H)^+$: 240.0388; found: 240.0372.

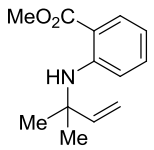

253n

Compound **253n**:

^{1}H NMR ($CDCl_3$, 400 MHz): δ = 8.06 (bs, NH), 7.87 (dd, *J* = 8.1, 1.6 Hz, 1H), 7.24-7.19 (m, 1H), 6.85 (dd, *J* = 8.6, 0.9 Hz, 1H), 6.54-6.50 (m, 1H), 5.98 (dd, *J* = 17.6, 10.7 Hz, 1H), 5.17 (dd, *J* = 17.6, 1.0 Hz, 1H), 5.11 (dd, *J* = 10.7, 1.0 Hz, 1H), 3.83 (s, 3H), 1.45 (s, 6H).

^{13}C NMR ($CDCl_3$, 100 MHz): δ = 169.6, 150.4, 146.0, 133.7, 131.9, 114.8, 114.4, 113.1, 110.5, 54.4, 51.7, 28.5.

IR (film, cm^{-1}): ν = 3342, 2979, 2951, 1683, 1605, 1586, 1519, 1456, 1437, 1330, 1248, 1221, 1187, 1165, 1085, 964, 918, 839.

HRMS (TOF ES+): calc. for $C_{13}H_{18}NO_2$ $(M+H)^+$: 202.1338; found: 202.1339.

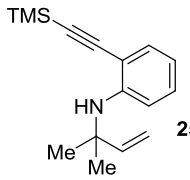

253o

Compound **253o**:

^{1}H NMR ($CDCl_3$, 400 MHz): δ = 7.24 (dd, *J* = 7.6, 1.6 Hz, 1H), 7.03 (m, 1H), 6.76 (d, *J* = 8.4 Hz, 1H), 6.52 (td, *J* = 7.5, 1.0 Hz, 1H), 5.97 (dd, *J* = 17.5, 10.7 Hz, 1H), 5.17 (dd, *J* = 17.5, 1.0 Hz, 1H), 5.10 (dd, *J* = 10.6, 1.0 Hz, 1H), 1.40 (s, 6H), -0.24 (s, 9H).

^{13}C NMR ($CDCl_3$, 100 MHz): δ = 148.4, 145.9, 132.1, 129.4, 116.1, 113.2, 113.0, 108.4, 100.5, 54.7, 28.3, 0.3.

IR (film, cm^{-1}): ν = 3394, 2960, 2143, 1600, 1576, 1510, 1457, 1324, 1249, 916, 865, 746, 698.

HRMS (TOF ES+): calc. for $C_{16}H_{24}NSi$ $(M+H)^+$: 258.1678; found: 258.1678.

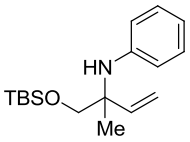

254a

Compound **254a**:

^{1}H NMR ($CDCl_3$, 400 MHz): δ = 7.13-7.09 (m, 2H), 6.73-6.70 (m, 3H), 5.98 (dd, *J* = 17.6, 10.7 Hz, 1H), 5.26 (dd, *J* = 17.6, 1.1 Hz, 1H), 5.22 (dd, *J* = 10.7, 1.1 Hz, 1H), 4.35 (bs, NH), 3.52 (d, *J* = 9.2 Hz, 1H), 3.36 (d, *J* = 9.4 Hz, 1H), 1.38 (s, 3H), 0.93 (s, 9H), 0.07 (s, 6H).

^{13}C NMR ($CDCl_3$, 100 MHz): δ = 147.1, 143.0, 128.9, 117.9, 116.4, 115.7, 70.6, 58.7, 26.0, 19.9, 18.5, -5.3.

IR (film, cm^{-1}): ν = 3385, 2954, 2929, 2857, 1602, 1504, 1499, 1255, 1084, 836, 777, 748.

HRMS (TOF ES+): calc. for $C_{17}H_{30}NOSi$ $(M+H)^+$: 292.2087; found: 292.2097.

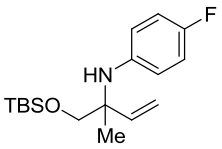

254b

Compound **254b**:

^{1}H NMR ($CDCl_3$, 400 MHz): δ = 6.82-6.78 (m, 2H), 6.68-6.65 (m, 2H), 5.94 (dd, *J* = 17.5, 10.9 Hz, 1H), 5.22 (dd, *J* = 17.5, 1.1 Hz, 1H), 5.21 (dd, *J* = 11.0, 1.1 Hz, 1H), 4.19 (bs, NH), 3.48 (d, *J* = 9.4 Hz, 1H), 3.33 (d, *J* = 9.4 Hz, 1H), 1.30 (s, 3H), 0.91 (s, 9H), 0.05 (s, 6H).

^{13}C NMR ($CDCl_3$, 100 MHz): δ = 157.7, 155.4, 143.3, 143.2, 143.0, 118.1, 118.0, 115.8, 115.4, 115.2, 70.2, 59.1, 26.0, 19.9, 18.5, -5.3.

IR (film, cm^{-1}): ν = 3384, 2954, 2929, 2857, 1508, 1254, 1216, 1086, 923, 835, 776, 668.

HRMS (TOF ES+): calc. for $C_{17}H_{29}FNOSi$ $(M+H)^+$: 310.1985; found: 310.2002.

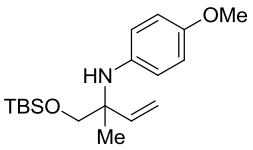

254c

Compound **254c**:

^{1}H NMR ($CDCl_3$, 400 MHz): δ = 6.71 (d, *J* = 1.0 Hz, 4H), 5.97 (dd, *J* = 17.6, 10.8 Hz, 1H), 5.20 (dd, *J* = 17.7, 1.2 Hz, 1H), 5.18 (dd, *J* = 10.8, 1.2 Hz, 1H), 4.03 (bs, NH), 3.72 (s, 3H), 3.47 (d, *J* = 9.4 Hz, 1H), 3.33 (d, *J* = 9.4 Hz, 1H), 1.28 (s, 3H), 0.92 (s, 9H), 0.05 (s, 6H).

^{13}C NMR ($CDCl_3$, 100 MHz): δ = 153.1, 143.4, 140.7, 119.3, 115.4, 114.4, 70.2, 59.2, 55.8, 26.1, 20.1, 18.5, -5.3.

IR (film, cm^{-1}): ν = 3387, 2953, 2930, 2857, 1509, 1463, 1253, 1088, 921, 837, 764, 750, 670.

HRMS (TOF ES+): calc. for $C_{18}H_{32}NO_2Si$ $(M+H)^+$: 322.2218; found: 322.2202.

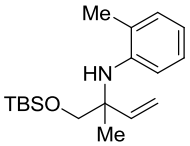

254d

Compound **254d**:

^{1}H NMR ($CDCl_3$, 400 MHz): δ = 7.05-6.99 (m, 2H), 6.84 (dd, *J* = 8.1, 0.9 Hz, 1H), 6.62 (td, *J* = 7.3, 1.0 Hz, 1H), 6.00 (dd, *J* = 17.6, 10.8 Hz, 1H), 5.27 (dd, *J* = 17.7, 1.1 Hz, 1H), 5.25 (dd, *J* = 10.8, 1.1Hz, 1H), 4.46 (bs, NH), 3.56 (d, *J* = 9.3 Hz, 1H), 3.38 (d, *J* = 9.3 Hz, 1H), 2.16 (s, 3H), 1.41 (s, 3H), 0.94 (s, 9H), 0.09 (s, 6H).

^{13}C NMR ($CDCl_3$, 100 MHz): δ = 145.1, 143.3, 130.4, 126.5, 123.5, 117.1, 115.7, 114.0, 71.3, 58.5, 26.0, 19.4, 18.4, 18.0, -5.3.

IR (film, cm^{-1}): ν = 3404, 2954, 2928, 2857, 1607, 1587, 1510, 1258, 1082, 920, 837, 816, 776, 746, 674.

HRMS (TOF ES+): calc. for $C_{18}H_{32}NOSi$ $(M+H)^+$: 306.2252; found: 306.2253.

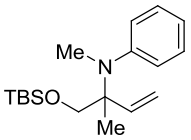

254f

Compound **254f**:

^{1}H NMR ($CDCl_3$, 400 MHz): δ = 7.22-7.14 (m, 4H), 6.99 (tt, *J* = 8.5, 1.4 Hz, 1H), 5.95 (dd, *J* = 17.7, 10.9 Hz, 1H), 5.16 (dd, *J* = 11.0, 1.4 Hz, 1H), 5.10 (dd, *J* = 17.7, 1.4 Hz, 1H), 3.54 (s, 2H), 2.81 (s, 3H), 1.20 (s, 3H), 0.87 (s, 9H), 0.01 (s, 6H).

^{13}C NMR ($CDCl_3$, 100 MHz): δ = 150.5, 142.4, 128.1, 126.1, 122.9, 114.4, 69.0, 63.2, 37.6, 26.1, 19.1, 18.5, -5.3.

IR (film, cm^{-1}): ν = 2954, 2928, 2856, 1598, 1492, 1255, 1006, 917, 836, 773, 701.

HRMS (TOF ES+): calc. for $C_{18}H_{32}NOSi$ $(M+H)^+$: 306.2253; found: 306.2246.

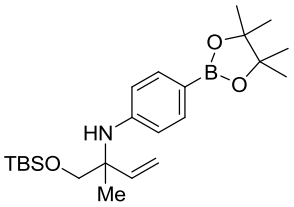

254h

Compound **254h**:

^{1}H NMR ($CDCl_3$, 400 MHz): δ = 7.55 (dd, *J* = 6.8, 1.6 Hz, 2H), 6.65 (dd, *J* = 6.7, 1.8 Hz, 2H), 5.92 (dd, *J* = 17.6, 10.8 Hz, 1H), 5.23 (dd, *J* = 17.6, 1.1 Hz, 1H), 5.21 (dd, *J* = 10.8, 1.0 Hz, 1H), 4.57 (bs, 1H), 3.47 (d, *J* = 9.5 Hz, 1H), 3.36 (d, *J* = 9.5 Hz, 1H), 1.37 (s, 3H), 1.29 (s, 12H), 0.91 (s, 9H), 0.05 (s, 6H).

^{13}C NMR ($CDCl_3$, 100 MHz): 149.8, 142.3, 136.0, 116.0, 115.0, 83.3, 70.7, 58.6, 26.1, 25.1, 25.0, 19.9, 18.4, -5.3.

IR (film, cm^{-1}): ν = 3397, 2929, 2857, 1605, 1471, 1396, 1357, 1315, 1253, 1143, 1089, 923, 835, 776, 737, 671.

HRMS (TOF ES+): calc. for $C_{23}H_{41}BNO_3Si$ $(M+H)^+$: 418.2959; found: 418.2949.

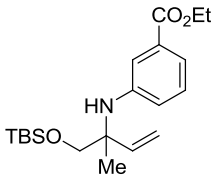

254j

Compound **254j**:

^{1}H NMR ($CDCl_3$, 400 MHz): δ = 7.38 (m, 1H), 7.34 (dt, *J* = 8.0, 1.0 Hz, 1H), 7.13 (t, *J* = 7.9, 1H), 6.87 (ddd, *J* = 8.1, 2.5, 1.0 Hz, 1H), 5.95 (dd, *J* = 17.6, 10.8 Hz, 1H), 5.26 (dd, *J* = 17.7, 1.1 Hz, 1H), 5.24 (dd, *J* = 10.7, 1.1 Hz, 1H), 4.40 (bs, NH), 4.32 (q, *J* = 7.1

Hz, 2H), 3.50 (d, J = 9.5 Hz, 1H), 3.36 (d, J = 9.4 Hz), 1.36 (s, 3H), 1.34 (t, J = 7.1 Hz, 3H), 0.94 (s, 9H), 0.05 (s, 6H).

^{13}C NMR ($CDCl_3$, 100 MHz): δ = 167.2, 147.1, 142.4, 131.1, 128.8, 120.4, 118.9, 117.1, 116.0, 70.5, 60.9, 58.7, 26.1, 19.9, 18.5, 14.5, -5.3.

IR (film, cm^{-1}): ν = 3393, 2953, 2929, 2857, 1718, 1605, 1485, 1277, 1238, 1104, 1081, 1028, 1001, 836, 776, 752, 684.

HRMS (TOF ES+): calc. for $C_{20}H_{34}NO_3Si$ $(M+H)^+$: 364.2308; found: 364.2295.

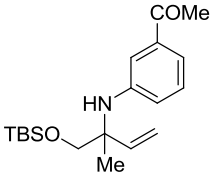

254k

Compound **254k**:

^{1}H NMR ($CDCl_3$, 400 MHz): δ = 7.29-7.28 (m, 1H), 7.24 (dt, J = 7.7, 1.0 Hz, 1H), 7.16 (t, J = 7.9 Hz, 1H), 6.88 (ddd, J = 8.0, 2.4, 1.0 Hz, 1H), 5.94 (dd, J = 17.5, 10.9 Hz, 1H), 5.26 (dd, J = 18.2, 1.0 Hz, 1H), 5.25 (dd, J = 11.1, 1.0 Hz, 1H), 4.50 (bs, NH), 3.50 (d, J = 9.5 Hz, 1H), 3.36 (d, J = 9.5 Hz, 1H), 2.51 (s, 3H), 1.36 (s, 3H), 0.91 (s, 9H), 0.05 (s, 6H).

^{13}C NMR ($CDCl_3$, 100 MHz): δ = 198.8, 147.3, 142.4, 138.0, 129.0, 120.7, 118.0, 116.1, 115.4, 70.5, 58.7, 26.9, 26.0, 19.8, 18.5, -5.3.

IR (film, cm^{-1}): ν = 3385, 2953, 2928, 2857, 1682, 1601, 1471, 1356, 1256, 1175, 1085, 835, 775, 687.

HRMS (TOF ES+): calc. for $C_{19}H_{32}N0_2Si$ $(M+H)^+$: 334.2202; found: 334.2196.

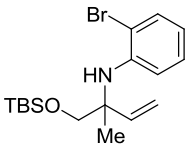

254m

Compound **254m**:

^{1}H NMR (CDCl$_3$, 400 MHz): δ = 7.39 (dd, *J* = 7.9, 1.5 Hz, 1H), 7.02 (td, *J* = 7.3, 1.5 Hz, 1H), 6.87 (dd, *J* = 8.3, 1.5 Hz, 1H), 6.50 (td, *J* = 7.9, 1.5 Hz, 1H), 5.95 (dd, *J* = 17.5, 10.9 Hz, 1H), 5.25 (dd, *J* = 17.4, 1.0 Hz, 1H), 5.24 (dd, *J* = 11.0, 1.0 Hz, 1H), 5.21 (bs, NH), 3.55 (d, *J* = 9.4 Hz, 1H), 3.36 (d, *J* = 9.4 Hz, 1H), 1.39 (s, 3H), 0.92 (s, 9H), 0.08 (s, 6H).

^{13}C NMR (CDCl$_3$, 100 MHz): δ = 144.1, 142.5, 132.7, 127.7, 117.8, 116.2, 115.1, 111.6, 71.0, 58.9, 26.1, 19.4, 18.4, -5.3.

IR (film, cm^{-1}): ν = 3368, 2954, 2928, 2857, 1594, 1507, 1463, 1252, 1085, 923, 836, 776, 740, 670.

HRMS (TOF ES+): calc. for $C_{17}H_{28}NOSiBr$ $(M+H)^+$: 370.1202; found: 370.1202.

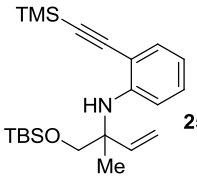

254o

Compound **254o**:

^{1}H NMR (CDCl$_3$, 400 MHz): δ = 7.26 (dd, *J* = 7.6, 1.6 Hz, 1H), 7.04- 7.00 (m, 1H), 6.75 (d, *J* = 8.4 Hz, 1H), 6.53 (dd, *J* = 7.5, 1.0 Hz, 1H), 5.95 (dd, *J* = 17.7, 10.8 Hz, 1H), 5.23 (dd, *J*= 17.7, 1.1 Hz, 1H), 5.21 (dd, *J* = 10.8, 1.1 Hz, 1H), 5.16 (s, NH), 1.39 (s, 3H), 0.88 (s, 9H), 0.24 (s, 9H), 0.01 (s, 3H), -0.03 (s, 3H).

^{13}C NMR ($CDCl_3$, 100 MHz): δ = 148.1, 142.3, 132.9, 129.2, 116.1, 115.5, 113.4, 108.8, 102.8, 100.1, 69.2, 58.8, 26.2, 22.1, 18.6, 0.4, -5.2, -5.3.

IR (film, cm^{-1}): ν = 3379, 2955, 2929, 2857, 2144, 1599, 1575, 1508, 1248, 1089, 866, 775, 757.

HRMS (TOF ES+): calc. for $C_{22}H_{38}NOSi_2$ $(M+H)^+$: 388.2492; found: 388.2487.

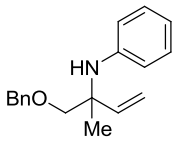

255a

Compound **255a**:

^{1}H NMR ($CDCl_3$, 400 MHz): δ = 7.38-7.30 (m, 5H), 7.13-7.09 (m, 2H), 6.74-6.70 (m, 3H), 6.01 (dd, *J* = 17.6, 10.7 Hz, 1H), 5.26 (dd, *J* = 17.7, 1.1 Hz, 1H), 5.23 (dd, *J* = 10.8, 1.1 Hz, 1H), 4.59 (d, *J* = 12.2 Hz, 1H), 4.54 (d, *J* = 12.3 Hz, 1H), 4.33 (bs, NH), 3.43 (d, *J* = 8.8 Hz, 1H), 3.32 (d, *J* = 8.8 Hz, 1H), 1.44 (s, 3H).

^{13}C NMR ($CDCl_3$, 100 MHz): δ = 146.8, 142.9, 138.3, 128.9, 128.6, 127.9, 127.7, 118.0, 116.5, 115.6, 77.3, 73.5, 58.1, 21.0.

IR (film, cm^{-1}): ν = 3393, 2977, 2860, 1600, 1497, 1315, 1296, 1090, 1077, 1028, 996, 921, 746, 693.

HRMS (TOF ES+): calc. for $C_{18}H_{22}NO$ $(M+H)^+$: 268.1698; found: 268.1701.

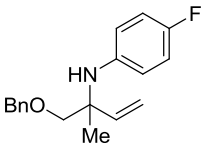

255b

Compound **255b**:

^{1}H NMR ($CDCl_3$, 400 MHz): δ = 7.37-7.30 (m, 5H), 6.83-6.78 (m, 2H), 6.70-6.66 (m, 2H), 5.97 (dd, *J* = 17.6, 10.8 Hz, 1H), 5.23 (dd, *J* = 17.6, 1.0 Hz, 1H), 5.21 (dd, *J* = 10.8, 1.1 Hz, 1H), 4.56 (d, *J* = 12.2 Hz, 1H), 4.53 (d, *J* = 12.2 Hz, 1H), 4.16 (bs, NH), 3.40 (d, *J* = 8.9 Hz, 1H), 3.29 (d, *J* = 8.8 Hz, 1H), 1.37 (s, 3H).

^{13}C NMR ($CDCl_3$, 100 MHz): δ = 157.8, 155.5, 142.9, 138.2, 128.9, 128.6, 127.9, 127.8, 118.4, 118.3, 115.6, 115.4, 115.2, 100.2, 77.0, 73.6, 58.5, 21.1.

IR (film, cm^{-1}): ν = 3387, 2977, 2858, 1506, 1454, 1303, 1212, 1092, 1077, 1027, 923, 791, 735, 695.

HRMS (TOF ES+): calc. for $C_{18}H_{21}FNO$ $(M+H)^+$: 286.1626; found: 286.1607.

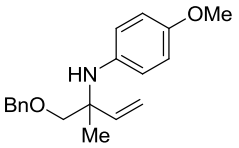

255c

Compound **255c**:

^{1}H NMR ($CDCl_3$, 400 MHz): δ = 7.35-7.29 (m, 5H), 6.76-6.70 (m, 4H), 6.00 (dd, *J* = 17.6, 10.9 Hz, 1H), 5.20 (dd, *J* = 17.6, 1.1 Hz, 1H), 5.18 (dd, *J* = 10.8, 1.1 Hz, 1H), 4.57 (d, *J* = 12.2 Hz, 1H), 4.52 (d, *J* = 12.2 Hz, 1H), 3.72 (s, 3H), 3.40 (d, *J* = 8.8 Hz, 1H), 3.29 (d, *J* = 8.8 Hz, 1H), 1.34 (s, 3H).

^{13}C NMR ($CDCl_3$, 100 MHz): δ = 153.5, 143.2, 138.3, 128.6, 127.9, 127.8, 120.0, 115.3, 114.3, 76.9, 73.5, 58.8, 55.8, 21.3.

IR (film, cm^{-1}): ν = 3382, 2974, 2831, 2832, 1508, 1462, 1366, 1235, 1177, 1093, 1038, 922, 823, 737, 698.

HRMS (TOF ES+): calc. for $C_{19}H_{24}NO_2$ $(M+H)^+$: 298.1814; found: 298.1807.

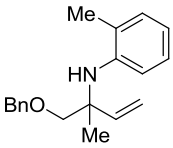

255d

Compound **255d**:

^{1}H NMR ($CDCl_3$, 400 MHz): δ = 7.38-7.30 (m, 5H), 7.05-6.98 (m, 2H), 6.84 (dd, *J* = 8.1, 1.0 Hz, 1H), 6.64 (td, *J* = 7.3, 1.1 Hz, 1H), 6.03 (dd, *J* = 17.6, 10.8 Hz, 1H), 5.27 (dd, *J* = 17.5, 1.0 Hz, 1H), 5.24 (dd, *J* = 10.7, 1.1 Hz, 1H), 4.59 (s, 2H), 4.39 (bs, NH), 3.48 (d, *J* = 8.7 Hz, 1H), 3.36 (d, *J* = 8.7 Hz, 1H), 2.15 (s, 3H), 1.48 (s, 3H).

^{13}C NMR ($CDCl_3$, 100 MHz): δ = 144.8, 143.2, 138.3, 130.4, 128.6, 127.9, 127.6, 126.4, 123.6, 117.2, 115.6, 114.1, 77.9, 73.5, 58.0, 28.8, 18.0.

IR (film, cm^{-1}): ν = 3408, 2976, 2857, 1605, 1586, 1509, 1442, 1316, 1089, 1076, 921, 837, 745, 696.

HRMS (TOF ES+): calc. for $C_{19}H_{24}NO$ $(M+H)^+$: 282.1848; found: 282.1858.

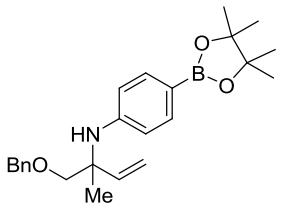

255h

Compound **255h**:

^{1}H NMR ($CDCl_3$, 400 MHz): δ = 7.56-7.53 (m, 2H), 7.34-7.29 (m, 5H), 6.67-6.64 (m, 2H), 5.94 (dd, *J* = 17.6, 10.7 Hz, 1H), 5.22 (dd, *J* = 17.6, 1.0 Hz,1H), 5.20 (dd, *J* = 10.7, 1.0 Hz, 1H), 4.57 (d, *J* = 12.1 Hz, 1H), 4.52 (d, *J* = 12.2 Hz, 1H), 3.40 (d, *J* = 8.9 Hz, 1H), 3.29 (d, *J* = 8.9 Hz, 1H), 1.43 (s, 3H), 1.29 (s, 12H).

^{13}C NMR ($CDCl_3$, 100 MHz): δ = 149.5, 142.2, 138.2, 136.0, 128.7, 128.0, 127.8, 115.9, 115.0, 83.3, 77.4, 73.6, 58.0, 25.1, 25.0, 21.0, 27.1.

IR (film, cm^{-1}): ν = 3392, 2977, 1708, 1499, 1396, 1358, 1315, 1176, 1143, 1089, 963, 861, 837, 828, 796.

HRMS (TOF ES+): calc. for $C_{24}H_{33}BNO_3$ $(M+H)^+$: 394.2560; found: 394.2553.

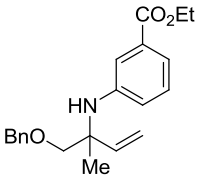

255j

Compound **255j**:

^{1}H NMR ($CDCl_3$, 400 MHz): δ = 7.39-7.30 (m, 7H), 7.13 (t, *J* = 8.0 Hz, 1H), 6.88 (ddd, *J* = 8.1, 2.5, 1.0 Hz, 1H), 5.97 (dd, *J* = 17.6, 10.7 Hz, 1H), 5.26 (dd, *J* = 17.6, 1.0 Hz, 1H), 5.24 (dd, *J* = 10.7, 1.0 Hz, 1H), 4.57 (d, *J* = 12.2 Hz, 1H), 4.53 (d, *J* = 12.2 Hz, 1H), 4.46 (bs, NH), 4.31 (q, *J* = 7.1 Hz, 2H), 4.54 (d, *J* = 12.2 Hz, 1H), 4.53 (d, *J* = 12.2 Hz, 1H), 1.43 (s, 3H), 1.35 (t, *J* = 7.1 Hz, 1H).

^{13}C NMR ($CDCl_3$, 100 MHz): δ = 167.2, 146.8, 142.4, 138.1, 131.1, 128.8, 128.6, 128.0, 127.8, 120.4, 119.0, 117.2, 116.0, 77.2, 73.6, 60.9, 58.2, 20.9, 14.5.

IR (film, cm^{-1}): ν = 3394, 2979, 2953, 2861, 1714, 1604, 1486, 1366, 1279, 1236, 1104, 1080, 1026, 998, 923, 752, 698.

HRMS (TOF ES+): calc. for $C_{21}H_{26}NO_3$ $(M+H)^+$: 340.1913; found: 340.1925.

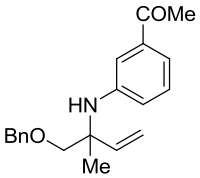

255k

Compound **255k**:

^{1}H NMR ($CDCl_3$, 400 MHz): δ = 7.35-7.29 (m, 7H), 7.16 (t, *J* = 7.9 Hz, 1H), 6.90 (ddd, *J* = 8.0, 2.5, 1.0 Hz, 1H), 5.97 (dd, *J* = 17.6, 10.7 Hz, 1H), 5.27 (dd, *J* = 17.6, 1.1 Hz, 1H), 5.25 (dd, *J* = 10.7, 1.0 Hz, 1H), 4.57 (d, *J* = 12.1 Hz, 1H), 4.53 (d, *J* = 12.1 Hz, 1H), 3.42 (d, *J* = 8.9 Hz, 1H), 3.31 (d, *J* = 8.9 Hz, 1H), 2.50 (s, 3H), 1.43 (s, 3H).

^{13}C NMR ($CDCl_3$, 100 MHz): δ = 198.8, 147.0, 142.3, 138.1, 137.9, 129.0, 128.6, 128.0, 127.8, 120.7, 118.0, 116.0, 115.6, 77.1, 73.6, 58.2, 26.8, 20.8.

IR (film, cm^{-1}): ν = 3485, 3029, 2977, 2859, 1679, 1600, 1484, 1425, 1356, 1275, 1233, 1092, 999, 924, 782, 737, 696.

HRMS (TOF ES+): calc. for $C_{20}H_{24}NO_2$ $(M+H)^+$: 310.1807; found: 310.1824.

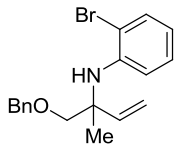

255m

Compound **255m**:

^{1}H NMR ($CDCl_3$, 400 MHz): δ = 7.40 (dd, *J* = 7.9, 1.5 Hz, 1H), 7.35-7.33 (m, 5H), 7.15-7.00 (m, 1H), 6.86 (dd, *J* = 8.2, 1.5 Hz, 1H), 6.53-6.51 (m, 1H), 5.97 (dd, *J* = 17.6, 10.7 Hz, 1H), 5.26 (dd, *J* = 17.6, 1.0 Hz, 1H), 5.24 (dd, *J* = 10.7, 0.9 Hz, 1H), 5.17 (bs, NH), 4.61 (d, *J* = 12.2 Hz, 1H), 4.57 (d, *J* = 12.2 Hz, 1H), 3.46 (d, *J* =8.9 Hz, 1H), 3.34 (d, *J* = 8.9 Hz, 1H), 1.46 (s, 3H).

^{13}C NMR ($CDCl_3$, 100 MHz): δ = 143.8, 142.3, 138.2, 132.7, 128.6, 127.9, 127.7, 127.7, 118.0, 116.1, 115.2, 111.6, 73.5, 58.3, 20.7.

IR (film, cm^{-1}): ν = 3372, 2978, 2857, 1593, 1505, 1462, 1322, 1209, 1172, 1093, 1018, 925, 738, 696.

HRMS (TOF ES+): calc. for $C_{18}H_{21}NOBr$ $(M+H)^+$: 346.0807; found: 346.0823.

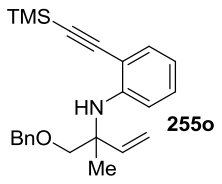

255o

Compound **255o**:

^{1}H NMR (CDCl$_3$, 400 MHz): δ = 7.32-7.27 (m, 6H), 7.05-7.01 (m, 1H), 6.78 (d, *J* = 9.0 Hz, 1H), 6.55 (td, *J* = 7.4, 1.0 Hz, 1H), 5.98 (dd, *J* = 17.6, 10.8 Hz, 1H), 5.45 (bs, NH), 5.25 (dd, *J* = 17.5, 1.0 Hz, 1H), 5.22 (dd, *J* = 10.7, 1.0 Hz, 1H), 4.62 (d, *J* = 12.4 Hz, 1H), 4.54 (d, *J* = 12.4 Hz 1H), 3.48 (d, *J* = 9.0 Hz, 1H), 3.34 (d, *J* = 9.0 Hz, 1H), 1.47 (s, 3H), 0.19 (s, 9H).

^{13}C NMR (CDCl$_3$, 100 MHz): δ = 148.2, 142.4, 138.3, 132.6, 129.3, 128.5, 127.7, 127.5, 116.3, 115.8, 113.4, 109.0, 102.5, 100.3, 77.2, 73.6, 58.1, 21.3, 0.3.

IR (film, cm^{-1}): ν = 3374, 2958, 2897, 2856, 2144, 1600, 1574, 1508, 1456, 1324, 1284, 1249, 1097, 914, 867, 842, 745, 698.

HRMS (TOF ES+): calc. for $C_{23}H_{30}NOSi$ $(M+H)^+$: 364.2097; found: 364.2088.

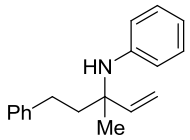

256a

Compound **256a**:

^{1}H NMR (CDCl$_3$, 400 MHz): δ = 7.29-7.20 (m, 2H), 7.18-7.11 (m, 5H), 6.73-6.70 (m, 3H), 6.02 (dd, *J* = 17.5, 10.7 Hz, 1H), 5.27 (dd, *J* = 17.5, 1.1 Hz, 1H), 5.22 (dd, *J* = 10.7, 1.1 Hz, 1H), 3.72 (bs, NH), 2.69-2.63 (m, 2H), 2.10-2.05 (m, 1H), 1.95-1.87 (m, 1H), 1.44 (s, 3H).

^{13}C NMR (CDCl$_3$, 100 MHz): δ = 146.6, 145.2, 142.4, 129.0, 128.6, 128.5, 126.0, 117.7, 115.9, 114.0, 57.4, 43.0, 30.3, 25.3.

IR (film, cm^{-1}): ν = 3412, 3053, 2977, 2931, 2861, 1711, 1600, 1496, 1454, 1317, 1256, 1180, 996, 919, 747, 695.

HRMS (TOF ES+): calc. for $C_{18}H_{22}N$ $(M+H)^+$: 252.1752; found: 252.1740.

Compound **256b**:

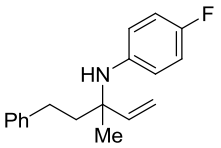

256b

^{1}H NMR (CDCl$_3$, 400 MHz): δ = 7.29-7.24 (m, 2H), 7.20-7.17 (m, 1H), 7.13-7.11 (m, 2H), 6.86-6.82 (m, 2H), 6.68-6.65 (m, 2H), 5.99 (dd, *J* = 17.8, 10.4 Hz, 1H), 5.22 (dd, *J* = 10.5, 1.1 Hz, 1H), 5.21 (dd, *J* = 17.5, 1.1 Hz, 1H), 3.56 (bs, NH), 2.67-2.60 (m, 2H), 2.04-2.00 (m, 1H), 1.91-1.88 (m, 1H), 1.40 (s, 3H).

^{13}C NMR (CDCl$_3$, 100 MHz): δ = 157.5, 155.2, 145.3, 142.8, 142.4, 128.6, 128.5, 126.0, 117.5, 117.4, 115.5, 115.3, 114.1, 57.7, 42.8, 30.3, 25.2.

IR (film, cm^{-1}): ν = 3413, 3026, 2977, 2930, 1710, 1637, 1507, 1315, 1214, 920, 822, 747, 700.

HRMS (TOF ES+): calc. for $C_{18}H_{21}NF$ $(M+H)^+$: 270.1658; found: 270.1649.

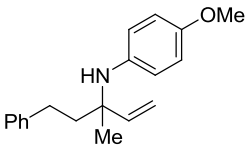

256c

Compound **256c**:

^{1}H NMR ($CDCl_3$, 400 MHz): δ = 7.28-7.24 (m, 2H), 7.19-7.11 (m, 3H), 6.72 (m, 4H), 6.00 (dd, *J* = 17.8, 10.6 Hz, 1H), 5.18 (dd, *J* = 17.7, 1.1 Hz, 1H), 5.18 (dd, *J* = 10.5, 1.1 Hz, 1H), 3.74 (s, 3H), 2.67-2.61 (m, 2H), 2.00-1.96 (m, 1H), 1.90-1.84 (m, 1H), 1.36 (s, 3H).

^{13}C NMR ($CDCl_3$, 100 MHz): δ = 153.0, 145.7, 142.6, 140.2, 128.6, 128.5, 126.0, 118.9, 114.5, 113.8, 57.9, 55.8, 43.0, 30.4, 25.1.

IR (film, cm^{-1}): ν = 3397, 3025, 2930, 2830, 1711, 1603, 1507, 1454, 1234, 1178, 1038, 917, 820, 746, 699.

HRMS (TOF ES+): calc. for $C_{19}H_{24}NO$ $(M+H)^+$: 282.1858; found: 282.1843.

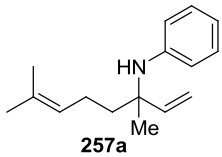

257a

Compound **257a**:

^{1}H NMR ($CDCl_3$, 400 MHz): δ = 7.11-7.07 (m, 2H), 6.69-6.66 (m, 3H), 5.95 (dd, *J* = 17.5, 10.8 Hz, 1H), 5.17 (dd, *J* = 17.6, 1.1 Hz, 1H), 5.16 (dd, *J* = 10.7, 1.1 Hz, 1H), 5.13-5.06 (m, 1H), 3.72 (bs, NH), 2.03-1.99 (m, 2H), 1.77-1.70 (m, 1H), 1.67 (s, 3H), 1.60-1.53 (m, 1H), 1.54 (s, 3H), 1.36 (s, 3H).

^{13}C NMR ($CDCl_3$, 100 MHz): δ = 146.8, 145.4, 132.1, 128.9, 124.3, 117.5, 115.8, 113.7, 57.4, 41.3, 25.9, 24.8, 22.5, 17.7.

IR (film, cm^{-1}): ν = 3405, 2967, 2826, 2855, 1712, 1600, 1498, 1450, 1373, 1256, 1181, 995, 916, 821, 746, 693.

HRMS (TOF ES+): calc. for $C_{16}H_{24}N$ $(M+H)^+$: 230.1909; found: 230.1901.

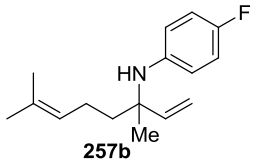

257b

Compound **257b**:

^{1}H NMR ($CDCl_3$, 400 MHz): δ = 6.82-6.78 (m, 2H), 6.64-6.61 (m, 2H), 5.92 (dd, *J* = 18.0, 10.4 Hz, 1H), 5.15 (dd, *J* = 10.5, 1.1 Hz, 1H), 5.14 (dd, *J* = 17.5, 1.1 Hz, 1H), 5.12-5.05 (m, 1H), 3.56 (bs, NH), 2.02-1.98 (m, 2H), 1.70-1.67 (m, 1H), 1.66 (s, 3H), 1.60-1.55 (m, 1H), 1.53 (s, 3H), 1.31 (s, 3H).

^{13}C NMR ($CDCl_3$, 100 MHz): δ = 157.4, 155.1, 145.5, 143.0, 143.0, 132.1, 124.2, 117.3, 117.3, 115.4, 115.2, 113.8, 57.7, 41.0, 25.9, 24.7, 22.5, 17.7.

IR (film, cm^{-1}): ν = 3389, 2967, 2928, 2852, 2831, 1713, 1440, 1373, 1234, 1178, 1114, 1039, 916, 819, 764, 751, 680.

HRMS (TOF ES+): calc. for $C_{16}H_{23}NF$ $(M+H)^+$: 248.1815; found: 248.1800.

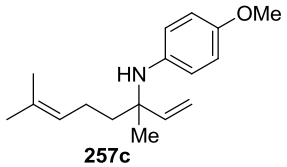

257c

Compound **257c**:

^{1}H NMR ($CDCl_3$, 400 MHz): δ = 6.68 (m, 4H), 5.93 (dd, *J* = 17.8, 10.4 Hz, 1H), 5.12 (dd, *J* = 10.5, 1.2 Hz, 1H), 5.12 (dd, *J* = 17.8, 1.2 Hz, 1H), 5.10-5.07 (m, 1H), 3.71 (s, 3H), 2.01-1.97 (m, 2H), 1.70-1.65 (m, 1H), 1.66 (s, 3H), 1.56-1.52 (m, 1H), 1.54 (s, 3H), 1.28 (s, 3H).

^{13}C NMR (CDCl$_3$, 100 MHz): δ = 152.8, 145.9, 140.5, 132.0, 124.4, 118.7, 114.4, 113.5, 57.9, 55.8, 41.2, 25.9, 24.7, 22.7, 17.8.

IR (film, cm^{-1}): ν = 3400, 2967, 2911, 2852, 1713, 1508, 1440, 1234, 1178, 1114, 1039, 819, 763, 751, 680.

HRMS (TOF ES+): calc. for $C_{17}H_{26}NO$ $(M+H)^+$: 260.2014; found: 260.1998.

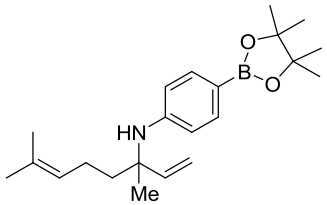

257h

Compound **257h**:

^{1}H NMR (CDCl$_3$, 400 MHz): δ = 7.56-7.53 (m, 2H), 6.63-6.61 (m, 2H), 5.90 (dd, *J* = 17.7, 10.6 Hz, 1H), 5.15 (dd, *J* = 17.6, 1.0 Hz, 1H), 5.15 (dd, *J* = 10.6, 1.0 Hz, 1H), 5.09-5.06 (m, 1H), 2.06-1.94 (m, 2H), 1.78-1.70 (m, 1H), 1.66 (s, 3H), 1.61-1.54 (m, 1H), 1.54 (s, 3H), 1.37 (s, 3H), 1.29 (s, 12H).

^{13}C NMR (CDCl$_3$, 100 MHz): δ = 149.4, 144.6, 136.0, 132.2, 124.2, 114.4, 114.0, 83.3, 57.4, 41.3, 25.9, 25.0, 24.9, 22.5, 17.8.

IR (film, cm^{-1}): ν = 3393, 2975, 2927, 2872, 1713, 1603, 1451, 1396, 1357, 1315, 1281, 1186, 1141, 1089, 962, 918, 861, 822, 736, 762.

HRMS (TOF ES+): calc. for $C_{22}H_{35}BNO_2$ $(M+H)^+$: 356.2761; found: 356.2760.

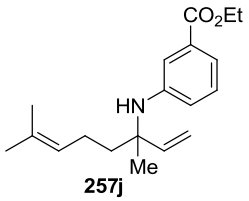

257j

Compound **257j**:

^{1}H NMR ($CDCl_3$, 400 MHz): δ = 7.34-7.30 (m, 2H), 7.12 (t, *J* = 7.9 Hz, 1H), 6.84 (ddd, *J* = 8.1, 2.5, 0.84 Hz, 1H), 5.92 (dd, *J* = 18.0, 10.3 Hz, 1H), 5.17 (dd, *J* = 17.8, 1.0 Hz, 1H), 5.17 (dd, *J* = 10.6, 1.0 Hz, 1H), 5.10-5.05 (m, 1H), 4.30 (q, *J* = 7.1 Hz, 2H), 3.89 (bs, NH), 2.05-1.93 (m, 2H), 1.78-1.69 (m, 1H), 1.66 (s, 3H), 1.61-1.54 (m, 1H), 1.52 (s, 3H), 1.36 (s, 3H), 1.34 (t, *J* = 7.1 Hz, 3H).

^{13}C NMR ($CDCl_3$, 100 MHz): δ = 167.2, 146.8, 144.9, 132.3, 131.1, 128.8, 124.1, 119.6, 118.4, 116.6, 114.1, 60.9, 57.5, 41.1, 25.9, 24.8, 22.5, 17.8, 14.5.

IR (film, cm^{-1}): ν = 3396, 2976, 2928, 2856, 1704, 1604, 1587, 1513, 1486, 1328, 1277, 1234, 1105, 1026, 918, 822, 752, 686.

HRMS (TOF ES+): calc. for $C_{19}H_{27}NO_2$ $(M+Na)^+$: 324.1939; found: 324.1930.

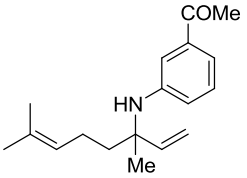

257k

Compound **257k**:

^{1}H NMR ($CDCl_3$, 400 MHz): δ = 7.25-7.24 (m, 1H), 7.21-7.19 (m, 1H), (t, *J* = 7.7 Hz, 1H), 6.85 (ddd, *J* = 8.0, 2.5, 1.0 Hz, 1H), 5.92 (dd, *J* = 17.1, 11.1 Hz, 1H), 5.18 (dd, *J* = 11.0, 1.0 Hz, 1H), 5.17 (dd, *J* = 17.3, 1.0 Hz, 1H), 5.09-5.05 (m, 1H), 3.93 (bs, NH), 2.50 (s, 3H), 2.04-1.93 (m, 2H), 1.78-1.69 (m, 1H), 1.65 (s, 3H), 1.62-1.54 (m, 1H), 1.52 (s, 3H), 1.36 (s, 3H).

^{13}C NMR ($CDCl_3$, 100 MHz): δ = 198.8, 147.0, 144.8, 137.9, 132.3, 129.0, 124.0, 119.9, 117.5, 114.9, 114.1, 57.5, 41.1, 26.8, 25.8, 24.7, 22.4, 17.7.

IR (film, cm^{-1}): ν = 3382, 2969, 2926, 2854, 1675, 1599, 1585, 1523, 1484, 1426, 1355, 1331, 1275, 1231, 1138, 996, 917, 778, 688.

HRMS (TOF ES+): calc. for $C_{18}H_{25}NO$ $(M+Na)^+$: 294.1834 ; found: 294.1824.

5.7 General Procedure for Preparation of Reverse Prenylated Indoles

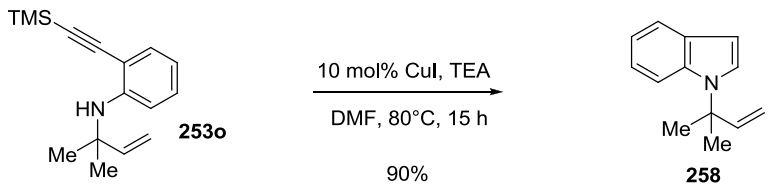

A 10 mL Schlenk flask was charged with allylic aryl amine **253o** (20 mg, 0.08 mmol) and dissolved in 0.5 mL of DMF under argon. Triethylamine (16 uL, 0.12 mmol, 1.5 equiv.) was added to the flask followed by CuI (1.5 mg, 8 umol, 10 mol%). The flask was sealed and heated at 80ºC on an oil bath. The reaction progress was monitored by GC. After15 hours, the reaction was allowed to cool and was purified by adsorbing directly onto a Teledyne Isco 5g silica load cartridge followed by elution onto a 4g Teledyne Isco column (0 → 20% EA/Hex) yielding compound **258** as a yellow oil (13 mg, 90% yield).

Compound **258**:

^{1}H NMR ($CDCl_3$, 400 MHz): δ = 7.63-7.61 (m, 1H), 7.54-7.51 (m, 1H), 7.30 (d, *J* = 3.3 Hz, 1H), 7.13-7.05 (m, 2H), 6.48 (dd, *J* = 3.3, 0.8 Hz, 1H), 6.15 (dd, *J* = 17.4, 10.7 Hz, 1H), 5.22 (dd, *J* = 10.6, 0.6 Hz, 1H), 5.16 (dd, *J* = 17.5, 0.6 Hz, 1H), 1.76 (s, 6H).

^{13}C NMR ($CDCl_3$, 100 MHz): δ = 144.4, 135.5, 130.2, 125.2, 121.1, 120.8, 119.3, 114.0, 113.6, 100.8, 59.2, 28.1.

IR (film, cm^{-1}): ν = 3047, 2980, 2937, 1512, 1455, 1315, 1291, 1228, 1209, 1017, 991, 920, 764, 738, 711.

HRMS (TOF ES+): calc. for $C_{13}H_{16}N$ $(M+H)^+$: 186.1283; found: 186.1292.

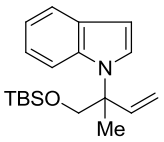

259

Compound **259**:

^{1}H NMR ($CDCl_3$, 400 MHz): δ = 7.60-7.58 (m, 1H), 7.45-7.44 (m, 1H), 7.38 (d, *J* = 3.3 Hz, 1H), 7.09-7.02 (m, 2H), 6.45 (dd, *J* = 3.3, 0.8 Hz, 1H), 6.18 (dd, *J* = 17.6, 10.9 Hz, 1H), 5.27 (dd, *J* = 10.8, 0.7 Hz, 1H), 5.09 (dd, *J* = 17.6, 0.7 Hz, 1H), 4.00 (d, *J* = 10.3 Hz, 1H), 3.97 (d, *J* = 10.3 Hz, 1H), 1.73 (s, 3H), 0.83 (s, 9H), -0.05 (s, 3H), -0.14 (s, 3H).

^{13}C NMR ($CDCl_3$, 100 MHz): δ = 140.7, 135.4, 130.5, 126.9, 121.0, 120.5, 119.2, 115.8, 114.0, 100.7, 68.4, 63.4, 25.9, 23.5, 18.3, -5.4, -5.5.

IR (film, cm^{-1}): ν = 2953, 2928, 2856, 1513, 1456, 1410, 1316, 1253, 1230, 1105, 1007, 923, 835, 777, 738, 710, 670.

HRMS (TOF ES+): calc. for $C_{19}H_{30}NOSi$ $(M+H)^+$: 316.2097; found: 316.2105.

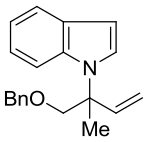

260

Compound **260**:

^{1}H NMR ($CDCl_3$, 400 MHz): δ = 7.63-7.60 (m, 1H), 7.45-7.43 (m, 1H), 7.37 (d, *J* = 3.3 Hz, 1H), 7.28-7.24 (m, 3H), 7.19 (m, 2H), 7.09-7.04 (m, 2H), 6.49 (dd, *J* = 3.3, 0.84 Hz, 1H), 6.21 (dd, *J* = 17.6, 10.9 Hz, 1H), 5.29 (dd, *J* = 10.9, 0.6 Hz, 1H), 5.12 (dd, *J* = 17.6, 0.6 Hz, 1H), 4.40 (s, 2H), 3.90 (d, *J* = 10.0 Hz, 1H), 3.87 (d, *J* = 9.9 Hz, 1H) 1.80 (s, 3H).

^{13}C NMR ($CDCl_3$, 100 MHz): δ = 140.8, 138.0, 135.4, 130.2, 128.5, 127.8, 127.7, 126.7, 122.9, 121.1, 120.7, 119.3, 115.8, 114.0, 101.0, 75.0, 73.5, 62.5, 24.0.

IR (film, cm^{-1}): ν = 3086, 3027, 2959, 1513, 1455, 1361, 1314, 1294, 1230, 1207, 1098, 1018, 925, 738, 698.

HRMS (TOF ES+): calc. for $C_{20}H_{22}NO$ $(M+H)^+$: 292.1701; found: 292.1712.

5.8 Procedure for the Preparation of (1*S*,4*S*)-2,5-Diarylbicyclo[2.2.2]octa-2,5-dienes

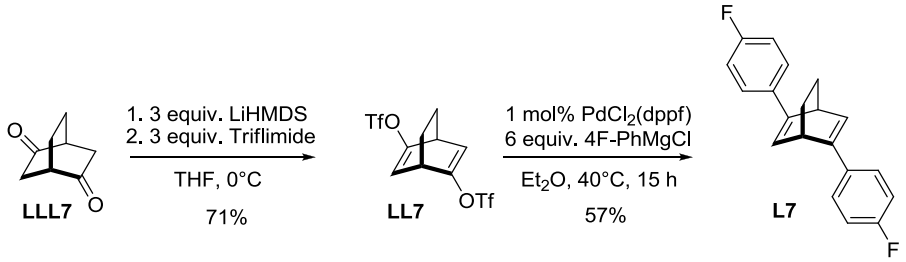

The following is a modification of the literature procedure).[130] A 50 mL Schlenk flask was charged with LiHMDS (3.3 mL, 1.0M in THF, 3.3 mmol, 3.0 equiv) and THF (15 mL), and the resulting solution was cooled at 0°C. A solution of (1*S*,4*S*)-bicyclo[2.2.2]octane-2,5-dione **LLL7** (150 mg, 1.1 mmol, 1.0 equiv) in THF (3 mL) was then added dropwise via cannula to the reaction flask and allowed to stir for 1 h at 0°C. A solution of 2-[*N*,*N*-bis(trifluoromethyl(sulfonyl)amino]pyridine (1.2 g, 3.3 mmol, 3 equiv) in THF (3 mL) was added slowly to the Schlenk flask and the resulting mixture was stirred at 0°C for 2 h. After monitoring progress by TLC, the reaction was quenched by addition of ice water (30 mL) and concentrated to remove the organics. The aqueous layer was extracted with diethyl ether (3 x 30 mL), and the combined organic extracts were dried over magnesium sulfate and concentrated to a yellow oil. The oil was purified by loading onto a 5g RediSep load cartridge followed by elution onto a pre-equilibrated 24g RediSep column, 10% diethyl ether/hexane resulting in bis-vinyl triflate **LL7** (311 mg, 71%) a colorless oil.

<u>(1*S*,4*S*)-2,5-Bis(trifluoromethanesulfonyloxy)bicyclo[2.2.2]octa-2,5-diene:</u>

^{1}H NMR ($CDCl_3$, 400MHz): 6.14 (dd, *J* = 7.1, 2.9 Hz, 2H), 3.71-3.68 (m, 2H), 1.88-1.80 (m, 2H), 1.61-1.51 (m, 2H). ^{1}H NMR matches with the literature report.[130]

To a 10 mL oven-dried Schlenk flask was charged with (1*S*,4*S*)-2,5-bis(trifluoromethanesulfonyloxy)bicyclo[2.2.2]octa-2,5-diene **LL7** (513 mg, 1.28 mmol, 1.0 equiv), Et_2O (3 mL), [1,1'-bis(diphenylphosphino)-ferrocene]palladium(II)dichloride (9.3 mg, 13 μmol, 1 mol%), and 4-fluorophenyl magnesium bromide (7.7 mL, 1 M in THF, 7.7 mmol, 6.0 equiv). The reaction mixture was stirred for 15 h at 40ºC. After monitoring progress by TLC, the reaction was cooled to room temperature, diluted with water, and extracted with diethyl ether. The combined ether layers dried over magnesium sulfate, filtered and concentrated. The crude product was loaded in dichloromethane onto a 25g RediSep load cartridge and eluted onto a pre-equilibrated 40g RediSep column (0 - 10% ethyl acetate/hexane) resulting in a light yellow solid which was recystallized in three crops from hexanes yielding the corresponding (1*S*,4*S*)-2,5-bis(4-fluorophenyl))bicyclo[2.2.2]octa-2,5-diene **L7** as white, powdery crystals (213 mg, 57%).

(1*S*,4*S*)-2,5-Bis(4-fluorophenyl))bicyclo[2.2.2]octa-2,5-diene (**L7**):

^{1}H NMR ($CDCl_3$, 400 MHz): δ = 7.39-7.34 (m, 4H), 7.02-6.96 (m, 4H), 6.54 (dd, *J* = 6.4, 2.0 Hz, 2H), 4.14 (d, J = 6.4 Hz, 2H), 1.52 (s, 4H).

^{19}F NMR ($CDCl_3$, 376 MHz): δ = -116.0.

^{13}C NMR ($CDCl_3$, 100 MHz): δ = 163.4, 160.9, 146.1, 134.4, 128.8, 126.5, 126.4, 115.6, 115.3, 40.3, 25.8.

IR (film, cm^{-1}): ν = 3058, 2991, 2959, 2946, 2936, 2908, 2871, 1891, 1645, 1631, 1600, 1505, 1410, 1326, 1303, 1222, 1163, 1149, 1098, 1010, 839, 812, 796.

HRMS (TOF EI+): calc. for $C_{20}H_{16}F_2$ $(M)^{+\cdot}$: 294.1220; found: 294.1226.

$[\alpha]^{20}_D$: +12.6, c = 1, $CHCl_3$

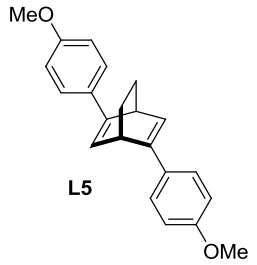

(1*S*,4*S*)-2,5-Bis(4-methoxyphenyl))bicyclo[2.2.2]octa-2,5-diene (**L5**):

^{1}H NMR ($CDCl_3$, 400 MHz): δ = 7.36 (d, *J* = 8.9 Hz, 4H), 6.85 (d, *J* = 8.9 Hz, 4H), 6.50 (dd, *J* = 6.4, 2.1 Hz, 2H), 4.13 (d, *J* = 6.1Hz, 2H), 3.79 (s, 6H).

^{13}C NMR ($CDCl_3$, 100 MHz): δ = 158.9, 146.6, 131.1, 127.3, 126.0, 113.9, 55.6, 40.2, 26.0.

IR (film, cm^{-1}): ν = 3062, 3032, 2994, 2954, 2942, 2905, 2867, 2833, 2059, 1885, 1857, 1735, 1644, 1601, 1508, 1464, 1453, 1313, 1293, 1252, 1235, 1186, 1148, 1112, 1036, 913, 835, 794.

HRMS (TOF EI+): calc. for $C_{22}H_{22}O_2$ $(M)^{+\cdot}$: 318.1620; found: 318.1634.

$[\alpha]^{20}_D$: +0.63, c = 2, $CHCl_3$

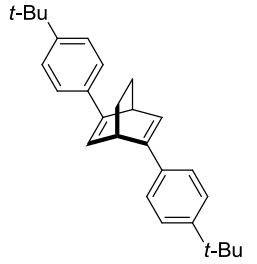

(1*S*,4*S*)-2,5-Bis(4-*tert*-butylphenyl))bicyclo[2.2.2]octa-2,5-diene (**L6**):

^{1}H NMR ($CDCl_3$, 400 MHz): δ = 7.38-7.32 (m, 8H), 5.57 (dd, *J* = 6.4, 2.2 Hz, 2H), 4.18 (d, *J* = 6.2, 2H), 1.52 (bs, 4H), 1.30 (s, 18H).

^{13}C NMR ($CDCl_3$, 100 MHz): δ = 150.0, 146.7, 135.6, 128.8, 125.6, 124.6, 40.2, 34.7, 31.5, 26.0.

IR (film, cm^{-1}): ν = 3048, 2959, 2902, 2865, 1903, 1604, 1513, 1475, 1461, 1409, 1362, 1268, 1242, 1202, 1150, 1112, 1024, 1008, 839, 829, 814, 802.

HRMS (TOF EI+): calc. for $C_{28}H_{34}$ $(M)^{+\cdot}$: 370.2661; found: 370.2679.

$[\alpha]^{20}_D$: +21.5, c = 1, $CHCl_3$

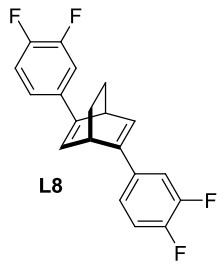

(1*S*,4*S*)-2,5-Bis(3,4-difluorophenyl))bicyclo[2.2.2]octa-2,5-diene (**L8**):

^{1}H NMR ($CDCl_3$, 400 MHz): δ = 7.21-7.16 (m, 2H), 7.13-7.05 (m, 4H), 6.56 (dd, *J* = 6.4, 2.2 Hz, 2H), 4.10 (dd, *J* = 6.4, 2.0 Hz, 2H), 1.53-1.50 (m, 4H).

^{19}F NMR ($CDCl_3$, 376 MHz): δ = -138.0 (d, *J* = 21 Hz), -140.4 (d, *J* = 21 Hz).

^{13}C NMR ($CDCl_3$, 100 MHz): δ = 145.4, 142.6, 135.2, 129.9, 127.6, 120.9, 120.9, 120.8, 120.8, 117.5, 117.3, 113.9, 113.7, 40.2, 25.7.

IR (film, cm^{-1}): ν = 3058, 2947, 2909, 2870, 1875, 1729, 1684, 1643, 1608, 1597, 1429, 1300, 1284, 1268, 1233, 1168, 1116, 893, 875, 845, 822, 803.

HRMS (TOF EI+): calc. for $C_{20}H_{14}F_4$ $(M)^{+\cdot}$: 330.1032; found: 330.1047.

$[\alpha]^{20}_D$: +2.6, c = 2, $CHCl_3$

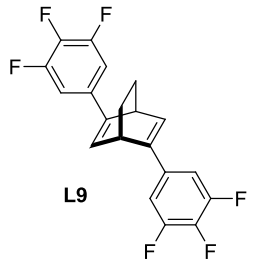

(1*S*,4*S*)-2,5-Bis(3,4,5-trifluorophenyl))bicyclo[2.2.2]octa-2,5-diene (**L9**):

^{1}H NMR ($CDCl_3$, 400 MHz): δ = 7.02-6.94 (m, 4H), 6.58 (dd, *J* = 6.4, 1.9 Hz, 2H), 4.08 (dd, *J* = 6.4, 1.9 Hz, 2H), 1.57-1.46 (m, 4H).

^{19}F NMR ($CDCl_3$, 376 MHz): -134.6 (d, *J* = 21 Hz), -162.6 (t, *J* = 21Hz).

^{13}C NMR ($CDCl_3$, 100 MHz): δ = 152.8, 152.8, 152.7, 150.3, 150.3, 150.2, 144.6, 144.6, 140.3, 140.2, 140.0, 137.8, 137.7, 137.5, 134.2, 134.2, 134.1, 134.1. 134.1, 134.0, 134.0, 130.9, 109.0, 109.0, 108.8, 108.8, 40.1, 25.5.

IR (film, cm^{-1}): ν = 3058, 2965, 2941, 2911, 2872, 1722, 1694, 1615, 1586, 1527, 1433, 1359, 1317, 1289, 1246, 1150, 1040, 873, 862, 845, 834, 810.

HRMS (TOF EI+): calc. for $C_{20}H_{12}F_6$ $(M)^{+\cdot}$: 366.0843; found: 366.0854.

$[\alpha]^{20}_{D}$: +11.6, c = 1, $CHCl_3$

5.9 General Procedure for the Preparation of Mono-protected Allylic Diols

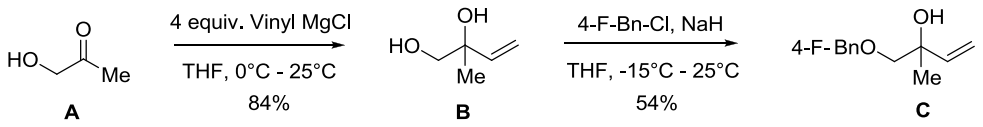

A 100 mL Schlenk flask was charged with vinylmagnesium chloride (60 mL, 96 mmol, 4.0 equiv) and cooled to 0ºC. Acetol **A** (1.6 mL, 23 mmol, 1.0 equiv) was then added dropwise to the reaction and allowed to equilibrate to ambient temperature with overnight stirring. After monitoring progress by TLC, the reaction was cooled to 0ºC, quenched with slow addition of methanol, and concentrated. The crude material was filtered through a short silica pad with 10% methanol in dichloromethane and concentrated. The brown dry solid was suspended in ethyl acetate and 1N HCl was added while magnetically stirring until complete dissolution of the solids resulting in a yellow organic layer and cloudy aqueous layer. The two layers were separated, the aqueous layer was

further extracted with ethyl acetate (2X). The combined organic extracts were concentrated *in vacuo* yielding 2-methyl-but-3-ene-1,2-diol **B** (2 g, 84%) as a yellow oil .

2-Methyl-but-3-ene-1,2-diol (**B**):

^{1}H NMR ($CDCl_3$, 400 MHz): δ = 5.87 (dd, *J* = 17.4, 10.8Hz, 1H), 5.32 (dd, *J* = 17.4, 1.1 Hz, 1H), 5.17 (dd, *J* = 10.8, 1.1 Hz, 1H), 3.49 (d, *J* = 11.0 Hz, 1H), 3.43 (d, *J* = 11.0 Hz, 1H), 1.25 (s, 3H).

^{13}C NMR ($CDCl_3$, 100 MHz): δ = 142.1, 114.6, 73.8, 69.8, 24.1.

IR (film, cm^{-1}): ν = 3397, 3090, 2985, 2976, 2931, 2880, 1724, 1642, 1512, 1461, 1414, 1377, 1253, 1155, 1101, 1040, 1027, 924, 892, 817.

A 10 mL Schlenk flask was charged with 2-methyl-but-3-ene-1,2-diol **B** (0.17 g, 1.7 mmol, 1.0 equiv) and THF (2 mL), and the solution was cooled to -15ºC. NaH (0.17g, 60% dispersion, 4.2 mmol, 2.5 equiv) that had been washed with hexanes (5X) was then added dropwise. The suspension was stirred 30 min, and 4-fluorobenzylbromide (0.23 mL, 1.8 mmol, 1.1 equiv) in THF (2 mL) was then added slowly via cannula. The mixture was allowed to warm slowly to ambient temperature overnight. After monitoring progress by TLC, the reaction was quenched by addition of methanol, brine, and extracted with ethyl acetate (3X). The combined organic extracts were dried over magnesium sulfate and concentrated *in vacuo*. The crude product was loaded in dichloromethane onto a 5g RediSep load cartridge and eluted onto a pre-equilibrated 40g RediSep column (0-20% ethyl acetate/hexane) yielding 1-(4-fluorobenzyloxy)-2-methyl-but-3-ene-2-ol **C** (190 mg, 54%) as a viscous oil.

1-(4-Fluorobenzyloxy)-2-methyl-but-3-ene-2-ol (**C**):

^{1}H NMR ($CDCl_3$, 400 MHz): δ = 7.28-7.25 (m, 2H), 7.01 (t, *J* = 8.7 Hz, 2H), 5.90 (dd, *J* = 17.3, 10.8 Hz, 1H), 5.29 (dd, *J* = 17.3, 1.3 Hz, 1H), 5.11 (dd, *J* = 10.8, 1.3 Hz, 1H), 4.51 (s, 2H), 3.36 (d, *J* = 9.0 Hz, 1H), 3.31 (d, *J* = 9.0 Hz, 1H), 2.40 (bs, OH), 1.25 (s, 3H).

^{13}C NMR ($CDCl_3$, 100 MHz): δ = 163.8, 142.5, 134.0, 133.9, 129.6, 129.5, 115.6, 115.4, 113.6, 77.4, 73.0, 24.6.

IR (film, cm^{-1}): ν = 3448, 3083, 2978, 2931, 2861, 1603, 1509, 1415, 1366, 1221, 1156, 1089, 924, 824.

HRMS (TOF ES+): calc. for $C_{12}H_{15}O_2FNa$ $(M + Na)^+$: 233.0954; found 233.0964.

Procedure for the Preparation of Tertiary Allylic Trichloroacetimidates

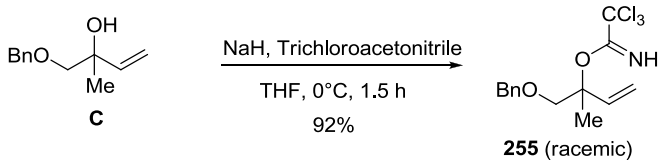

A 10 mL oven-dried Schlenk flask was charged with NaH (60% dispersion, washed 5x with hexanes, 83 mg, 2.0 mmol, 0.4 equiv) and THF (0.9 mL). The suspension was cooled to 0°C, and 1-(benzyloxy)2-methyl-but-3-en-2-ol **C**(1.0 g, 5.2 mmol, 1.0 equiv) was added dropwise. The resulting mixture was allowed to stir for 30 min. Trichloroacetonitrile (1.6 mL, 15.6 mmol, 3.0 equiv) and THF (0.9 mL) were added to a separate oven-dried Schlenk flask and cooled to 0 ^{o}C. The alcohol/sodium alkoxide solution was then transferred slowly to the trichloroacetonitrile solution via cannula. The reaction mixture was stirred at 0 ^{o}C for 1.5 h, quenched with methanol, and loaded directly onto a RediSep load cartridge containing pre-equilibrated and dried silica. The crude product was then purified by silica gel flash column chromatography (20% ethyl acetate/hexane + 1% triethylamine) to provide tertiary allylic trichloroacetimidate **255** (1.7 g, 92%) as a brown oil.

<u>Compound **255**:</u>

^{1}H NMR ($CDCl_3$, 400 MHz): δ = 8.30 (bs, NH), 7.34-7.27 (m, 5H), 6.10 (dd, *J* = 17.6, 11.0 Hz, 1H), 5.33 (dd, *J* = 17.6, 0.7 Hz, 1H), 5.24 (dd, *J* = 11.0, 0.8 Hz, 1H), 4.64 (d, *J* = 12.3 Hz, 1H), 4.61 (d, *J* = 12.3 Hz, 1H), 3.78 (d, *J* = 10.4 Hz, 1H), 3.71 (d, *J* = 10.4 Hz, 1H), 1.70 (s, 3H).

^{13}C NMR ($CDCl_3$, 100 MHz): δ = 160.1, 138.8, 138.6, 128.5, 127.7, 1276, 115.5, 85.9, 75.2, 73.7, 20.4.

IR (film, cm^{-1}): ν = 3334, 2860, 1663, 1453, 1317, 1078, 793, 734, 696.

HRMS (TOF ES+): calc. for $C_{14}H_{16}Cl_3NO_2Na$ $(M+Na)^+$: 358.0144; found: 358.0143.

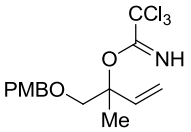

299

Compound **299**:

^{1}H NMR ($CDCl_3$, 400 MHz): δ = 8.32 (bs, NH), 7.28 (d, *J* = 8.7, 2H), 6.88 (d, *J* = 8.7 Hz, 2H), 6.08 (dd, *J* = 17.6, 11.0 Hz, 1H), 5.34 (dd, *J* = 17.6, 0.7 Hz, 1H), 5.26 (dd, *J* = 11.0, 0.7 Hz, 1H), 4.60 (d, *J* = 11.8 Hz, 1H), 4.56 (d, *J* = 11.9 Hz, 1H), 3.81 (s, 2H), 3.77 (d, *J* = 10.4 Hz, 1H), 3.71 (d, *J* = 10.4 Hz, 1H), 1.72 (s, 3H).

^{13}C NMR ($CDCl_3$, 100 MHz): δ = 160.1, 159.3, 138.8, 130.6, 129.3, 115.5, 113.9, 86.0, 74.8, 73.4, 55.5, 20.4.

IR (film, cm^{-1}): ν = 3333, 3089, 2997, 2936, 2908, 2860, 2837, 1663, 1612, 1513, 1464, 1317, 1302, 1246, 1173, 1082, 1036, 972, 926, 871, 822, 794.

HRMS (TOF ES+): calc. for $C_{15}H_{18}Cl_3NO_3Na$ $(M+Na)^+$: 388.0250; found: 388.0249.

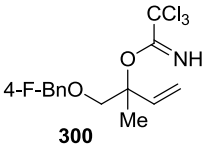

300

Compound **300**:

^{1}H NMR ($CDCl_3$, 400 MHz): δ = 8.30 (s, NH), 7.31-7.27 (m, 2H), 7.04-6.97 (m, 2H), 6.09 (dd, *J* = 17.6, 11.0 Hz, 1H), 5.32 (dd, *J* = 17.6, 0.7 Hz, 1H), 5.24 (dd, *J* = 11.0, 0.7 Hz, 1H), 4.60 (d, *J* = 12.1 Hz, 1H), 4.55 (d, *J* = 12.1 Hz, 1H), 3.76 (d, *J* = 10.4 Hz, 1H), 3.70 (d, *J* = 10.4 Hz, 1H), 1.69 (s, 3H).

^{13}C NMR ($CDCl_3$, 100 MHz): δ = 163.7, 161.2, 160.1, 158.9, 138.7, 137.2, 134.3, 134.2, 133.5, 129.4, 129.4, 125.0, 118.4, 115.6, 115.5, 115.3, 92.5, 85.9, 75.1, 73.0, 20.3.

IR (film, cm^{-1}): ν = 3335, 3091, 2987, 2937, 2863, 1664, 1604, 1509, 1414, 1370, 1318, 1221, 1082, 972, 927, 871, 823, 794.

HRMS (TOF ES+): calc. for $C_{14}H_{15}Cl_3NO_2FNa$ $(M+Na)^+$: 376.0050; found: 376.0060.

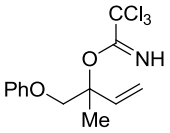

301

Compound **301**:

^{1}H NMR ($CDCl_3$, 400 MHz): δ = 8.33 (bs, NH), 7.28-7.23 (m, 2H), 6.92-6.89 (m, 3H), 6.20 (dd, *J* = 17.6, 11.1 Hz, 1H), 5.42 (dd, *J* = 17.6, 0.6 Hz, 1H), 5.30 (dd, *J* = 11.0, 0.6 Hz, 1H), 4.34 (d, *J* = 9.6 Hz, 1H), 4.23 (d, *J* = 9.6 Hz, 1H), 1.79 (s, 3H).

^{13}C NMR ($CDCl_3$, 100 MHz): δ = 160.1, 159.0, 138.4, 129.6, 121.3, 116.0, 115.1, 84.7, 72.0, 21.0.

IR (film, cm^{-1}): ν = 3335, 3091, 3066, 3041, 2991, 2939, 2878, 1744, 1664, 1599, 1588, 1496, 1462, 1413, 1369, 1318, 1302, 1246, 1171, 1080, 1052, 976, 929, 875, 839, 795.

HRMS (TOF ES+): calc. for $C_{13}H_{14}Cl_3NO_2Na$ $(M+Na)^+$: 343.9988; found: 343.9987.

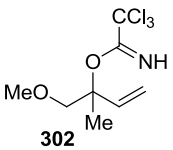

302

Compound **302**:

^{1}H NMR ($CDCl_3$, 400 MHz): δ = 8.30 (bs, NH), 6.07 (dd, *J* = 17.6, 11.0 Hz, 1H), 5.32 (dd, *J* = 17.6, 0.8 Hz, 1H), 5.24 (dd, *J* = 11.1, 0.8 Hz, 1H), 3.67 (s, 2H), 3.42 (s, 3H), 1.66 (s, 1H).

^{13}C NMR ($CDCl_3$, 100 MHz): δ = 160.2, 138.8, 115.5, 92.6, 85.8, 77.7, 60.1, 20.3.

IR (film, cm^{-1}): ν = 3337, 3093, 2988, 2929, 2892, 2829, 1784, 1735, 1664, 1545, 1452, 1413, 1367, 1318, 1197, 1113, 1083, 972, 926, 871, 831, 795.

HRMS (TOF ES+): calc. for $C_8H_{12}Cl_3NO_2Na$ $(M+Na)^+$: 281.9831; found: 281.9845.

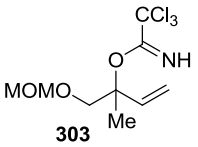

303

Compound **303**:

^{1}H NMR ($CDCl_3$, 400 MHz): δ = 8.31 (bs, NH), 6.08 (dd, *J* = 17.6, 11.0 Hz, 1H), 5.33 (d, *J* = 17.6 Hz, 1H), 5.25 (d, *J* = 11.0 Hz, 1H), 4.67 (s, 1H), 4.66 (s, 1H), 3.83 (d, *J* = 10.6 Hz, 1H), 3.77 (d, *J* = 10.6 Hz, 1H), 3.35 (s, 3H), 1.69 (s, 3H).

^{13}C NMR ($CDCl_3$, 100 MHz): δ = 160.1, 138.7, 115.7, 97.0, 92.5, 85.4, 72.6, 55.5, 20.2.

IR (film, cm^{-1}): ν = 3333, 3091, 2940, 2889, 2824, 1666, 1464, 1449, 1413, 1382, 1319, 1150, 1113, 1086, 1047, 976, 921, 872, 832, 797.

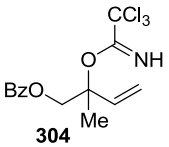

304

Compound **304**:

^{1}H NMR (CDCl$_3$, 400 MHz): δ = 8.39 (bs, NH), 8.05-8.00 (m, 2H), 7.56-7.53 (m, 1H), 7.52-7.37 (m, 2H), 6.13 (dd, *J* = 17.6, 11.0 Hz, 1H), 5.43 (d, *J* = 17.7 Hz, 1H), 5.31 (d, *J* = 11.1 Hz, 1H), 4.68 (d, *J* = 11.5 Hz, 1H), 4.64 (d, *J* = 11.6 Hz, 1H), 1.77 (s, 3H).

^{13}C NMR (CDCl$_3$, 100 MHz): δ = 166.3, 159.9, 137.8, 133.3, 129.8, 128.6, 116.5, 92.3, 84.1, 68.0, 20.6.

IR (film, cm^{-1}): ν = 3336, 3090, 3069, 2990, 2943, 2899, 1720, 1666, 1545, 1451, 1383, 1314, 1268, 1176, 1110, 1082, 1069, 1026, 931, 829, 794.

HRMS (TOF ES+): calc. for $C_{14}H_{14}Cl_3NO_3Na$ $(M+Na)^+$: 371.9937; found: 371.9944.

5.10 General Procedure for Regio- and Enantioselective Amination of Racemic Tertiary Allylic Trichloroacetimidates with [RhCl(ethylene)]$_2$/ **L7**

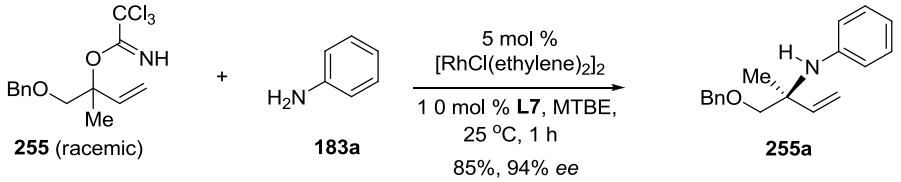

A 10 mL oven-dried Schlenk flask was charged with [RhCl(ethylene)$_2$]$_2$ (2.7 mg, 7.0 μmol, 5 mol%) and (1*S*,4*S*)-2,5-bis(4-fluorophenyl))bicyclo[2.2.2]octa-2,5-diene (**L7**) (4.1 mg, 14 μmol, 10 mol%) in a glove box. The flask was sealed, removed from the glove box, and MTBE (0.35 mL) was added to the Schlenk and stirred for 15 min resulting in a bright-red solution. A separate 10 mL Schlenk flask was charged with allylic imidate **255** (47 mg, 0.14 mmol, 1.0 equiv), MTBE (0.35 mL) and aniline **183a** (18 μL, 0.21 mmol, 1.5 equiv). The rhodium catalyst solution was then added to the flask containing the solution of **255** and **183a**. The mixture was stirred at room temperature under argon. Reaction progress was monitored by GC at 1 h. The crude reaction was purified by adsorbing directly onto a dry 5g Teledyne Isco silica cartridge using vacuum followed by elution onto a pre-equilibrated 24g silica flash column (0 → 10% ethyl

acetate/hexane + 1 % triethylamine) providing allylic aminde **255a** (32 mg, 85%, branched/linear > 99:1) as pale yellow oil.

Compound **255a**:

^{1}H NMR ($CDCl_3$, 400 MHz): δ = 7.37-7.27 (m, 5H), 7.12-7.07 (m, 2H), 6.70-6.67 (m, 3H), 5.99 (dd, *J* = 17.6, 10.7 Hz, 1H), 5.25 (dd, *J* = 17.6, 1.1 Hz, 1H), 5.21 (dd, *J* = 10.7, 1.1 Hz, 1H), 4.59 (d, *J* = 12.3 Hz, 1H), 4.55 (d, *J* = 12.3 Hz, 1H), 4.33 (bs, NH), 3.40 (d, *J* = 8.9 Hz, 1H), 3.31 (d, *J* = 8.9 Hz, 1H), 1.42 (s, 3H).

^{13}C NMR ($CDCl_3$, 100 MHz): δ = 146.8, 142.9, 138.3, 128.9, 128.6, 127.9, 127.7, 118.0, 116.5, 115.6, 73.5, 58.1, 21.0.

IR (film, cm^{-1}): ν = 3394, 2904, 2857, 1601, 1498, 1316, 1092, 1078, 1028, 997, 922, 747, 695.

HRMS (TOF ES+): calc. for $C_{18}H_{22}NO$ $(M+H)^+$: 268.1698; found: 268.1701.

$[\alpha]^{20}_D$: -11.4, c = 2, $CHCl_3$

HPLC: 2.5mg/mL in 50/50 IPA/Hex, 2 μL injection, 4.6 x 250mm Chiralcel OD-H, 0.6 mL/min., 2.5% IPA in hexanes, 254 nm, major 8.65 min., minor 8.97 min., 94% *ee*

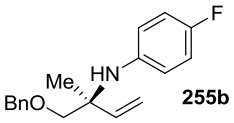

255b

Compound **255b**:

^{1}H NMR ($CDCl_3$, 400 MHz): δ = 7.37-7.27 (m, 5H), 7.12-7.07 (m, 2H), 6.70-6.67 (m, 3H), 5.99 (dd, *J* = 17.6, 10.7 Hz, 1H), 5.25 (dd, *J* = 17.6, 1.1 Hz, 1H), 5.21 (dd, *J* = 10.7, 1.1 Hz, 1H), 4.56 (d, *J* = 12.2 Hz, 1H), 4.53 (d, *J* = 12.2 Hz, 1H), 4.16 (bs, NH), 3.40 (d, *J* = 8.9 Hz, 1H), 3.29 (d, *J* = 8.8 Hz, 1H), 1.42 (s, 3H).

^{13}C NMR ($CDCl_3$, 100 MHz): δ = 157.8, 155.5, 142.9, 138.2, 128.6, 127.9, 127.8, 118.4, 118.3, 115.7, 115.4, 115.2, 100.2, 76.9, 73.6, 58.5, 21.1.

IR (film, cm^{-1}): ν = 3387, 3086, 3063, 3031, 3005, 2858, 1740, 1638, 1611, 1506, 1454, 1367, 1212, 1092, 1077, 1028, 1001, 924, 822, 791, 735, 697.

HRMS (TOF ES+): calc. for $C_{18}H_{21}FNO$ $(M+H)^+$: 286.1626; found: 286.1607.

$[\alpha]^{20}_D$: -10.0, c = 2, $CHCl_3$

HPLC: 2.5mg/mL in 50/50 IPA/Hex, 2 μL injection, 4.6 x 250mm Chiralcel OD-H, 0.6 mL/min., 2.5% IPA in hexanes, 254 nm, major 8.64 min., minor 8.26 min., 96% *ee*

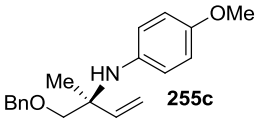

255c

Compound **255c**:

^{1}H NMR ($CDCl_3$, 400 MHz): δ = 7.35-7.28 (m, 5H), 6.76-6.67 (m, 4H), 6.00 (dd, *J* = 17.6, 10.9 Hz, 1H), 5.20 (dd, *J* = 17.6, 1.1 Hz, 1H), 5.18 (dd, *J* = 10.8, 1.1 Hz, 1H), 4.57 (d, *J* = 12.2 Hz, 1H), 4.52 (d, *J* = 12.2 Hz, 1H), 3.72 (s, 3H), 3.40, (d, *J* = 8.8 Hz, 1H), 3.29 (d, *J* = 8.8 Hz, 1H) (s, 3H).

^{13}C NMR ($CDCl_3$, 100 MHz): δ = 153.5, 143.2, 138.3, 128.6, 127.9, 127.8, 120.0, 115.3, 114.3, 76.9, 73.5, 58.8, 55.8, 21.3.

IR (film, cm^{-1}): ν = 3379, 2833, 1508, 1454, 1236, 1095, 1077, 1038, 923, 823, 737, 698.

HRMS (TOF ES+): calc. for $C_{19}H_{24}NO_2$ $(M+H)^+$: 298.1814; found: 298.1807.

$[\alpha]^{20}_D$: -8.4, c = 2, $CHCl_3$

HPLC: 2.5mg/mL in 50/50 IPA/Hex, 2 μL injection, 4.6 x 250mm Chiralcel OD-H, 0.6 mL/min., 1% IPA in hexanes, 254 nm, major 21.45 min., minor 20.47 min., 90% *ee*

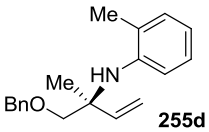

255d

Compound **255d**:

^{1}H NMR ($CDCl_3$, 400 MHz): δ = 7.38-7.30 (m, 5H), 7.05-7.00 (m, 2H), 6.84 (dd, *J* = 8.1, 1.0 Hz, 1H), 6.60 (td, *J* = 7.3, 1.0 Hz, 1H), 6.03 (dd, *J* = 17.6, 10.8 Hz, 1H), 5.27 (dd, *J* = 17.5, 1.0 Hz, 1H), 5.24 (dd, *J* = 10.7, 1.1 Hz, 1H), 4.59 (s, 2H), 4.39 (bs, NH), 3.48 (d, *J* = 8.7 Hz, 1H), 3.36 (d, *J* = 8.7 Hz, 1H), 2.15 (s, 3H), 1.48 (3H).

^{13}C NMR ($CDCl_3$, 100 MHz): δ = 144.8, 143.2, 138.3, 130.4, 128.6, 127.9, 127.6, 126.4, 123.6, 117.2, 115.6, 114.1, 76.9, 73.5, 58.0, 20.8, 18.0.

IR (film, cm^{-1}): ν = 3409, 2857, 1605, 1586, 1509, 1481, 1453, 1090, 1076, 921, 744, 697.

HRMS (TOF ES+): calc. for $C_{19}H_{24}NO$ $(M+H)^+$: 282.1848; found: 282.1858.

[α]^{20}D: -15.2, c = 1, $CHCl_3$

HPLC: 2.5mg/mL in ethanol, 2 μL injection, 4.6 x 150mm Chiralcel OJ-3, 0.5 mL/min., 0.5 ethanol: 100 hexanes, 254 nm, major 23.56 min., minor 13.25 min., 89% *ee*

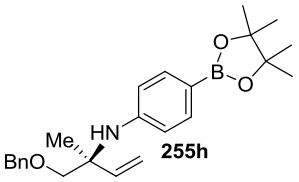

255h

Compound **255h**:

^{1}H NMR ($CDCl_3$, 400 MHz): δ = 7.55-7.53 (m, 2H), 7.34-7.29 (m, 5H), 6.67-6.64 (m, 2H), 5.94 (dd, *J* = 17.6, 10.7 Hz, 1H), 5.21 (dd, *J* = 17.6, 1.0 Hz, 1H), 5.20 (dd, *J* = 10.7, 1.0 Hz, 1H), 4.55 (s, 1H), 4.53 (s, 1H), 3.39 (d, *J* = 8.9 Hz, 1H), 3.29 (d, *J* = 8.9 Hz, 1H), 1.43 (s, 3H), 1.29 (s, 12H).

^{13}C NMR ($CDCl_3$, 100 MHz): δ = 149.5, 142.2, 138.2, 136.0, 128.7, 128.0, 127.8, 116.9, 116.7, 115.9, 115.0, 83.3, 76.9, 73.6, 58.0, 25.0, 21.0.

IR (film, cm^{-1}): ν = 3392, 2977, 1708, 1499, 1396, 1358, 1315, 1176, 1143, 1089, 963, 861, 837, 828, 796, 736.

HRMS (TOF ES+): calc. for $C_{24}H_{33}BNO_3$ $(M+H)^+$: 394.2560; found: 394.2553.

$[\alpha]^{20}_D$: -12.1, c = 2, $CHCl_3$

HPLC: 2.5mg/mL in 50/50 IPA/Hex, 2 μL injection, 4.6 x 250mm Chiralcel OD-H, 0.6 mL/min., 2.5% IPA in hexanes, 254 nm, major 6.80 min., minor 7.57 min., 91% *ee*

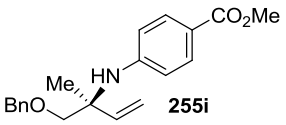

255i

Compound **255i**:

^{1}H NMR ($CDCl_3$, 400 MHz): δ = 7.75 (d, *J* = 5.0 Hz, 2H), 7.37-7.29 (m, 5H), 6.62 (d, *J* = 5.0 Hz, 2H), 5.93 (dd, *J* = 17.7, 10.6 Hz, 1H), 5.25 (d, *J* = 17.5 Hz, 1H), 5.24 (d, *J* = 10.7 Hz, 1H), 4.80 (bs, NH), 4.56 (d, *J* = 15.2 Hz, 1H), 4.54 (d, *J* = 15.2 Hz, 1H), 3.82 (s, 3H), 3.41 (d, *J* = 9.0 Hz, 1H), 3.70 (d, *J* = 9.0 Hz, 1H), 1.46 (s, 3H).

^{13}C NMR ($CDCl_3$, 100 MHz): δ = 167.5, 150.9, 141.6, 138.0, 131.1, 128.7, 128.1, 127.8, 118.5, 116.3, 114.4, 76.9, 73.6, 58.1, 51.7, 20.9.

IR (film, cm^{-1}): ν = 3385, 3086, 3063, 3028, 2982, 2946, 2902, 2860, 1704, 1601, 1519, 1495, 1454, 1433, 1338, 1312, 1272, 1173, 1104, 1077, 1028, 999, 925, 841, 818.

HRMS (TOF ES+): calc. for calc. for $C_{20}H_{24}NO_3$ $(M+H)^+$: 326.1756; found: 326.1767.

$[\alpha]^{20}_D$: -19.5, c = 1, $CHCl_3$

HPLC: 2.5mg/mL in 50/50 IPA/Hex, 2 μL injection, 4.6 x 150mm Chiralcel OJ-3, 1 mL/min., 2.5% IPA in hexanes for 10 minutes, gradient to 5% IPA in hexanes over 50 minutes, 254 nm, major 31.70 min., minor 35.56 min., 85% *ee*

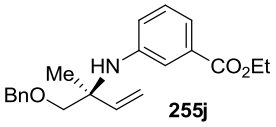

255j

Compound **255j**:

^{1}H NMR ($CDCl_3$, 400 MHz): δ = 7.39-7.30 (m, 7H), 7.13 (t, *J* = 8.0 Hz, 1H), 6.86 (ddd, *J* = 8.1, 2.5, 1.0 Hz, 1H), 5.97 (dd, *J* = 17.6, 10.7 Hz, 1H), 5.26 (dd, *J* = 17.6, 1.0 Hz, 1H), 5.24 (dd, *J* = 10.7, 1.0 Hz, 1H), 4.54 (d, *J* = 12.2 Hz, 1H), 4.53 (d, *J* = 12.2 Hz, 1H), 4.46 (bs, NH), 4.32 (q, *J* = 7.1 Hz, 2H), 3.42 (d, *J* = 8.9 Hz, 1H), 3.30 (d, *J* = 8.9 Hz, 1H), 1.42 (s, 3H), 1.35 (t, *J* = 7.1 Hz, 3H).

^{13}C NMR ($CDCl_3$, 100 MHz): δ = 167.2, 146.8, 142.4, 138.1, 131.1, 128.8, 128.7, 128.0, 127.8, 120.4, 119.0, 117.2, 116.0, 76.9, 73.6, 60.9, 58.1, 20.9, 14.5.

IR (film, cm^{-1}): ν = 3394, 3086, 3063, 3029, 2979, 2933, 2903, 2860, 1714, 1604, 1586, 1509, 1486, 1392, 1279, 1236, 1172, 1104, 1080, 1027, 999, 924, 752, 698.

HRMS (TOF ES+): calc. for $C_{21}H_{26}NO_3$ $(M+H)^+$: 340.1913; found: 340.1925.

$[\alpha]^{20}_D$: -13.7, c = 2, $CHCl_3$

HPLC: 2.5mg/mL in 50/50 IPA/Hex, 2 μL injection, 4.6 x 250mm Chiralcel OD-H, 1 mL/min., 1% IPA in hexanes, 254 nm, major 23.10 min., minor 21.64 min., 94% *ee*

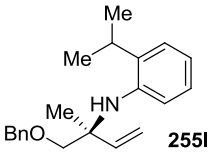

255l

Compound **255l**:

^{1}H NMR ($CDCl_3$, 400 MHz): δ = 7.35-7.29 (m, 5H), 7.11 (dd, *J* = 7.6, 1.2 Hz, 1H), 6.96 (td, *J* = 8.5, 0.9 Hz, 1H), 6.85 (dd, *J* = 8.1, 0.9 Hz, 1H), 6.70 (t, *J* = 6.7 Hz, 1H), 6.02 (dd, *J* = 17.6, 10.7 Hz, 1H), 5.25 (dd, *J* = 17.6, 0.9 Hz, 1H), 5.22 (dd, *J* = 10.7, 0.9 Hz, 1H),

4.62 (bs, NH), 4.58 (s, 2H), 3.47 (d, *J* = 8.7 Hz, 1H), 3.34 (d, *J* = 8.7 Hz, 1H), (h, *J* = 6.7 Hz, 1H), 1.45 (s, 3H), 1.22 (d, *J* = 6.8 Hz, 3H), 1.20 (d, *J* = 6.8 Hz, 3H).

^{13}C NMR ($CDCl_3$, 100 MHz): δ = 143.6, 143.5, 138.3, 133.9, 128.6, 127.9, 127.7, 125.9, 125.1, 117.7, 115.5, 115.1, 78.1, 73.6, 27.5, 22.8, 22.4, 20.5.

IR (film, cm^{-1}): ν = 3418, 3086, 3063, 3031, 2961, 2933, 2901, 2864, 1710, 1603, 1584, 1509, 1452, 1412, 1365, 1297, 1277, 1208, 1175, 1089, 1076, 1039, 1028, 1000, 922, 844.

HRMS (TOF ES+): calc. for $C_{21}H_{28}NO$ $(M+H)^+$: 310.2171; found: 310.2183.

$[\alpha]^{20}_D$: -13.5, c = 1, $CHCl_3$

HPLC: 2 mg/mL in ethanol, 1 μL injection, 4.6 x 150mm Chiralcel OJ-3, 0.3 mL/min., 0.5 ethanol: 100 hexanes, 254 nm, major 10.55 min., minor 9.92 min., 94% *ee*

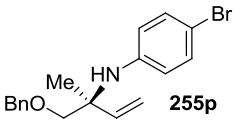

255p

Compound **255p**:

^{1}H NMR ($CDCl_3$, 400 MHz): δ = 7.36-7.26 (m, 5H), 7.17-7.14 (m, 2H), 6.59-6.56 (m, 2H), 5.92 (dd, *J* = 17.7, 10.9 Hz, 1H), 5.22 (dd, *J* = 17.4, 0.8 Hz, 1H), 5.21 (dd, *J* = 11.0, 0.8 Hz, 1H), 4.56 (d, *J* = 12.2 Hz, 1H), 4.52 (d, *J* = 12.2 Hz, 1H), 3.38 (d, *J* = 8.9 Hz, 1H), 3.26 (d, *J* = 8.9 Hz, 1H), 1.39 (s, 3H).

^{13}C NMR ($CDCl_3$, 100 MHz): δ = 145.8, 142.3, 138.0, 131.6, 128.7, 128.0, 127.8, 117.9, 116.0, 109.7, 76.9, 73.5, 58.1, 20.8.

IR (film, cm^{-1}): ν = 3059, 2992, 2959, 2871, 2042, 1970, 1909, 1766, 1598, 1504, 1410, 1326, 1302, 1238, 1219, 1208, 1161, 1148, 1098, 1010, 837, 810, 795.

HRMS (TOF ES+): calc. for $C_{18}H_{21}NOBr$ $(M+H)^+$: 346.0807; found: 346.0818.

$[\alpha]^{20}_D$: -12.9, c = 2, $CHCl_3$

HPLC: 2.5mg/mL in 50/50 IPA/Hex, 2 μL injection, 4.6 x 250mm Chiralcel OD-H, 0.6 mL/min., 1% IPA in hexanes, 254 nm, major 14.70 min., minor 12.18 min., 91% *ee*

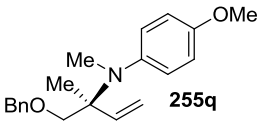

255q

Compound **255q**:

^{1}H NMR (CDCl$_3$, 400 MHz): δ = 7.32-7.31 (m, 4H), 7.28-7.25 (m, 1H), 7.10 (d, *J* = 8.9 Hz, 2H), 6.74 (d, *J* = 8.9 Hz, 2H), 5.98 (dd, *J* = 17.7, 10.9 Hz, 1H), 5.17 (dd, *J* = 11.0, 1.1 Hz, 1H), 5.07 (dd, *J* = 17.7, 1.1 Hz, 1H), 4.52 (d, *J* = 12.4 Hz, 1H), 4.48 (d, *J* = 12.4 Hz, 1H), 3.76 (s, 3H), 3.27 (s, 2H), 2.69 (s, 3H), 1.18 (s, 3H).

^{13}C NMR (CDCl$_3$, 100 MHz): δ = 156.6, 143.1, 141.3, 138.6, 128.9, 128.5, 127.9, 127.7, 114.8, 113.3, 76.1, 73.5, 62.2, 55.5, 38.0, 18.6.

IR (film, cm^{-1}): ν = 3084, 3062, 3032, 2979, 2946, 2902, 2796, 1744, 1606, 1506, 1454, 1412, 1365, 1285, 1241, 1179, 1100, 1077, 1035, 1007, 917, 884, 837, 810.

HRMS (TOF ES+): calc. for $C_{20}H_{26}NO_2$ $(M+H)^+$: 312.1964; found: 312.1964.

$[\alpha]^{20}_D$: +2.7, c = 2, $CHCl_3$

HPLC: 2 mg/mL in ethanol, 2 μL injection, 4.6 x 150mm Chiralcel OJ-3, 0.5 mL/min., 0.5 ethanol: 100 hexanes, 254 nm, major 26.29 min., minor 18.97 min., 93% *ee*

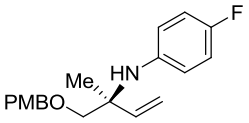

299b

Compound **299b**:

^{1}H NMR ($CDCl_3$, 400 MHz): δ = 7.23 (dd, *J* = 6.7, 1.9 Hz, 2H), 6.88 (dd, *J* = 6.6, 2.0 Hz, 2H), 6.80 (t, *J* = 6.8 Hz, 2H), 6.68 (m, 2H), 5.96 (dd, *J* = 17.5, 10.9 Hz, 1H), 5.21 (dd, *J* = 17.3, 0.8 Hz, 1H), 5.20 (dd, *J* = 11.1, 0.9 Hz, 1H), 4.48 (d, *J* = 11.8 Hz, 1H), 4.45 (d, *J* = 11.8 Hz, 1H), 4.16 (bs, NH), 3.81 (s, 3H), 3.35 (d, *J* = 8.9 Hz, 1H), 3.24 (d, *J* = 8.8 Hz, 1H), 1.35 (s, 3H).

^{13}C NMR ($CDCl_3$, 100 MHz): δ = 159.4, 157.7, 155.4, 143.0, 130.2, 129.4, 118.3, 188.2, 115.6, 115.4, 115.1, 114.0, 76.6, 73.2, 58.4, 55.4, 20.9.

IR (film, cm^{-1}): ν = 3389, 3084, 2977, 2934, 2904, 2858, 1612, 1507, 1463, 1366, 1302, 1247, 1213, 1172, 1085, 1034, 1004, 925, 822, 794.

HRMS (TOF ES+): calc. for $C_{19}H_{23}NO_2F$ $(M+H)^+$: 316.1713; found: 316.1716.

$[\alpha]^{20}_D$: -9.6, c = 1, $CHCl_3$

HPLC: 2.5mg/mL in 50/50 IPA/Hex, 2 μL injection, 4.6 x 150mm Chiralcel OJ-3, 1 mL/min., 1% IPA in hexanes, 254 nm, major 39.24 min., minor 32.98 min., 93% *ee*

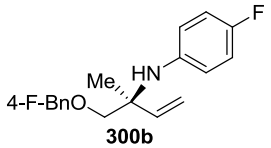

300b

Compound **300b**:

^{1}H NMR ($CDCl_3$, 400 MHz): δ = 7.27-7.25 (m, 2H), 7.02 (t, *J* = 8.6 Hz, 2H), 6.80 (t, *J* = 8.6 Hz, 2H), 6.68-6.65 (m, 2H), 5.95 (dd, *J* = 17.7, 10.6 Hz, 1H), 5.21 (d, *J* = 16.9 Hz, 1H), 5.20 (d, *J* = 11.4 Hz, 1H), 4.50 (d, *J* = 12.7 Hz, 1H), 4.47 (d, *J* = 12.7 Hz, 1H), 4.12 (bs, NH), 3.37 (d, *J* = 8.8 Hz, 1H), 3.25 (*J* = 8.8 Hz, 1H), 1.35 (s, 3H).

^{13}C NMR ($CDCl_3$, 100 MHz): δ = 163.7, 161.3, 157.8, 155.4, 142.8, 133.9, 129.6, 129.5, 118.3, 188.3, 115.7, 115.6, 115.4, 115.2, 76.8, 72.8, 58.4, 21.1.

IR (film, cm^{-1}): ν = 3385, 3086, 2981, 2932, 2861, 1604, 1507, 1401, 1367, 1220, 1156, 1088, 1014, 1004, 925, 822, 794.

HRMS (TOF ES+): calc. for $C_{18}H_{20}NOF_2$ $(M+H)^+$: 304.1513; found: 304.1521.

$[\alpha]^{20}_D$: -10.7, c = 1, $CHCl_3$

HPLC: 2.5mg/mL in 50/50 IPA/Hex, 2 μL injection, 4.6 x 150mm Chiralcel OJ-3, 1 mL/min., 1% IPA in hexanes, 254 nm, major 17.42 min., minor 14.77 min., 92% *ee*

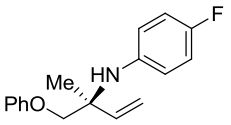

301b

Compound **301b**:

^{1}H NMR ($CDCl_3$, 400 MHz): δ = 7.30 (m, 2H), 6.92-6.80 (m, 3H), 6.80-6.76 (m, 2H), 6.75-6.68 (m, 2H), 6.09 (dd, *J* = 17.6, 10.7 Hz, 1H), 5.32 (d, *J* = 17.6 Hz, 1H), 5.30 (d, *J* = 10.8 Hz, 1H), 4.16 (bs, NH), 3.88 (d, *J* = 8.7 Hz, 1H), 3.76 (d, *J* = 8.8 Hz, 1H), 1.47 (s, 3H).

^{13}C NMR ($CDCl_3$, 100 MHz): δ = 158.7, 142.5, 142.3, 129.7, 121.4, 118.8, 118.7, 116.3, 115.5, 115.2, 114.8, 103.7, 74.1, 58.1, 21.1.

IR (film, cm^{-1}): ν = 3392, 3085, 3062, 3039, 2980, 2932, 2872, 1855, 1599, 1588, 1506, 1495, 1457, 1302, 1239, 1211, 1170, 1039, 926, 821, 787.

HRMS (TOF ES+): calc. for $C_{17}H_{19}NOF$ $(M+H)^+$: 272.1451; found: 272.1455.

$[\alpha]^{20}_D$: -0.99, c = 1, $CHCl_3$

HPLC: 2.5mg/mL in 50/50 IPA/Hex, 1 μL injection, 4.6 x 150mm Chiralcel OJ-3, 0.3 mL/min., 0.5 ethanol: 100 hexanes, 254 nm, major 56.87 min., minor 55.59 min., 80% *ee*

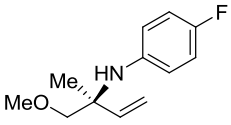

302b

Compound **302b**:

^{1}H NMR ($CDCl_3$, 400 MHz): δ = 6.83-6.78 (m, 2H), 6.70-6.66 (m, 2H), 5.95 (dd, *J* = 17.8, 10.9 Hz, 1H), 5.22 (d, *J* = 17.4 Hz, 1H), 5.21 (d, *J* = 11.0 Hz, 1 H), 4.12 (bs, NH), 3.37 (s, 3H), 3.27 (d, *J* = 8.9 Hz, 1H), 3.18 (d, *J* = 8.9 Hz, 1H), 1.33 (s, 3H).

^{13}C NMR ($CDCl_3$, 100 MHz): δ = 157.7, 155.4, 142.9, 118.4, 118.3, 115.7, 115.4, 115.2, 79.8, 59.4, 58.3, 20.6.

IR (film, cm^{-1}): ν = 3391, 2982, 2931, 2890, 2827, 1857, 1741, 1684, 1612, 1506, 1457, 1314, 1214, 1102, 1041, 1002, 974, 923, 822, 793.

HRMS (TOF ES+): calc. for $C_{12}H_{17}NOF$ $(M+H)^+$: 210.1294; found: 210.1300.

$[\alpha]^{20}_D$: -10.2, c = 1, $CHCl_3$

HPLC: 2.5mg/mL in 50/50 IPA/Hex, 1 μL injection, 4.6 x 150mm Chiralcel OJ-3, 0.5 mL/min., 0.5 ethanol: 100 hexanes, 254 nm, major 8.14 min., minor 7.52 min., 86% *ee*

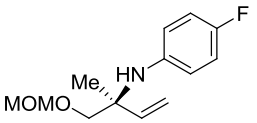

303b

Compound **303b**:

^{1}H NMR ($CDCl_3$, 400 MHz): δ = 6.82-6.77 (m, 2H), 6.70-6.65 (m, 2H), 5.95 (dd, *J* = 17.6, 10.8 Hz, 1H), 5.23 (dd, *J* = 17.9, 1.0 Hz, 1H), 5.22 (dd, *J* = 10.7, 1.0 Hz, 1H), 4.64 (d, *J* = 9.4 Hz, 1H), 4.61 (d, *J* = 9.4 Hz, 1H), 4.11 (bs, NH), 3.47 (d, *J* = 9.4 Hz, 1H), 3.37 (d, *J* = 9.4 Hz, 1H), 3.33 (s, 3H).

^{13}C NMR ($CDCl_3$, 100 MHz): δ = 157.7, 155.4, 142.8, 142.7, 142.6, 118.2, 118.1, 115.8, 115.6, 115.4, 115.3, 115.2, 96.9, 74.7, 58.0, 55.5, 21.1.

IR (film, cm^{-1}): ν = 3385, 3085, 3034, 2977, 2932, 2887, 2824, 1735, 1666, 1612, 1508, 1454, 1402, 1380, 1315, 1214, 1148, 1107, 1040, 921, 824, 794.

HRMS (TOF ES+): calc. for $C_{13}H_{19}NO_2F$ $(M+H)^+$: 240.1400; found: 240.1397.

$[\alpha]^{20}_D$: -13.8, c = 1, $CHCl_3$

HPLC: 2 mg/mL in 50/50 IPA/Hex, 1 μL injection, 4.6 x 150mm Chiralcel OJ-3, 0.5 mL/min., 0.5 ethanol: 100 hexanes, 254 nm, major 10.73 min., minor 10.41 min., 89% *ee*

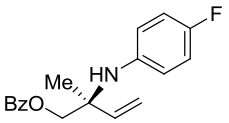

304b

Compound **304b**:

^{1}H NMR ($CDCl_3$, 400 MHz): δ = 8.04-8.01 (m, 2H), 7.57 (tt, J = 7.4, 1.3 Hz, 1H), 7.45 (t, J = 7.4 Hz, 2H), 6.85-6.79 (m, 2H), 6.72-6.69 (m, 2H), 6.02 (dd, J = 17.6, 10.7 Hz, 1H), 5.33 (dd, 17.5, 0.8 Hz, 1H), 5.30 (dd, J = 10.7, 0.8 Hz, 1H), 4.33 (d, J = 11.0 Hz, 1H), 4.28 (d, J = 11.1 Hz, 1H), 1.44 (s, 3H).

^{13}C NMR ($CDCl_3$, 100 MHz): δ = 166.5, 158.1, 155.8, 142.1, 142.0, 141.5, 133.5, 130.1, 129.8, 128.7, 118.8, 118.7, 116.5, 115.6, 115.4, 70.1, 58.1, 22.6.

IR (film, cm^{-1}): ν = 3402, 3087, 3063, 2981, 2938, 2890, 1718, 1602, 1507, 1451, 1381, 1364, 1314, 1268, 1215, 1176, 1110, 1070, 1027, 990, 928, 824, 786.

HRMS (TOF ES+): calc. for $C_{18}H_{19}NO_2F$ $(M+H)^+$: 300.1400; found: 30.1408.

$[\alpha]^{20}_D$: +5.1, c = 1, $CHCl_3$

HPLC: 2 mg/mL in 50/50 IPA/Hex, 2 μL injection, 4.6 x 150mm Chiralcel OJ-3, 0.5 mL/min., 0.5 ethanol: 100 hexanes, 254 nm, major 33.23 min., minor 34.81 min., 59% *ee*

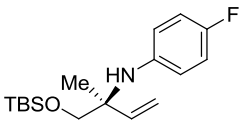

254b

Compound **254b**:

^{1}H NMR ($CDCl_3$, 400 MHz): δ = 6.82-6.77 (m, 2H), 6.68-6.64 (m, 2H), 5.93 (dd, *J* = 17.5, 10.9 Hz, 1H), 5.22 (dd, *J* = 7.3, 1.1 Hz, 1H), 5.19 (s, 1H), 4.20 (bs, 1H), 3.47 (d, *J* = 9.4 Hz, 1H), 3.33 (d, *J* = 9.4 Hz, 1H), 1.29 (s, 3H), 0.91 (s, 9H), 0.05 (s, 6H).

^{13}C NMR ($CDCl_3$, 100 MHz): δ = 157.7, 155.4, 143.2, 143.0, 118.1, 118.0, 115.8, 115.4, 115.2, 70.2, 59.1, 26.1, 19.9, 18.5, -5.3.

IR (film, cm^{-1}): ν = 3384, 2953, 2929, 2857, 1508, 1252, 1221, 1215, 1172, 835, 795, 776.

HRMS (TOF ES+): calc. for $C_{17}H_{29}FNOSi$ $(M+H)^+$: 310.1985; found: 310.2002.

$[\alpha]^{20}_D$: -4.2, c = 2, $CHCl_3$

HPLC: 2 mg/mL in ethanol, 1 μL injection, 4.6 x 150mm Chiralcel OJ-3, 0.3 mL/min., 0.5 ethanol: 100 hexanes, 254 nm, major 6.89 min., minor 6.76 min., 76% *ee*

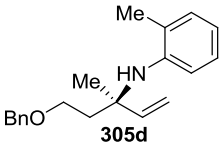

305d

Compound **305d**:

^{1}H NMR ($CDCl_3$, 400 MHz): δ = 7.38-7.30 (m, 5H), 7.00-6.97 (m, 2H), 6.77-6.75 (m, 1H), 6.57 (t, *J*= 7.3 Hz, 1H), *5*.97 (dd, *J* = 17.7, 10.4 Hz, 1H), 5.18 (dd, *J* = 17.7, 1.1 Hz, 1H), 5.18 (dd, *J* = 10.5, 1.1 Hz, 1H), 4.72 (s, NH), 4.51 (s, 2H), 3.67-3.64 (m, 2H), 2.09-2.01 (m, 1H), 1.97 (s, 3H), 1.95-1.90 (m, 1H), 1.48 (s, 3H).

^{13}C NMR ($CDCl_3$, 100 MHz): δ =145.2, 144.8, 138.1, 130.2, 128.6, 128.1, 127.9, 126.2, 122.9, 116.2, 114.0, 113.4, 73.6, 67.1, 57.0, 42.4, 24.2, 18.1.

IR (film, cm^{-1}): ν =3408, 3083, 3060, 3029, 2971, 2915, 2858, 1708, 1604, 1587, 1522, 1482, 1453, 1363, 1308, 1262, 1157, 1094, 1052, 1028, 1000, 917, 846.

HRMS (TOF ES+): calc. for $C_{20}H_{26}NO$ $(M+H)^+$: Calc. 296.2014; found: 296.1996.

HPLC: 2.5 mg/mL in 50/50 IPA/Hexanes, 2 μL injection, 4.6 x 250mm Chiralcel OD-H, 0.6 mL/min., 1% IPA in hexanes, 254 nm, major 10.97 min., minor 10.34 min., 56% *ee*

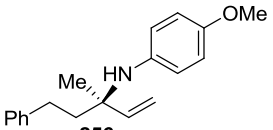

256c

Compound **256c**:

^{1}H NMR ($CDCl_3$, 400 MHz): δ = 7.28-7.24 (m, 2H), 7.19-7.11 (m, 3H), 6.72 (m, 4H), 6.00 (dd, *J* = 17.8, 10.6 Hz, 1H), 5.18 (dd, *J* = 17.7, 1.1 Hz, 1H), 5.18 (dd, *J* = 10.5, 1.1 Hz, 1H), 3.74 (s, 3H), 2.67-2.61 (m, 2H), 2.00-1.96 (m, 1H), 1.90-1.84 (m, 1H), 1.36 (s, 3H).

^{13}C NMR ($CDCl_3$, 100 MHz): δ = 153.0, 145.7, 142.6, 140.2, 128.6, 128.5, 126.0, 118.9, 114.5, 113.8, 57.9, 55.8, 43.0, 30.4, 25.1.

IR (film, cm^{-1}): ν = 3397, 3025, 2930, 2830, 1711, 1603, 1507, 1454, 1234, 1178, 1038, 917, 820, 746, 699.

HRMS (TOF ES+): calc. for $C_{19}H_{24}NO$ $(M+H)^+$: 282.1858; found: 282.1843.

HPLC: 2.5 mg/mL in 50/50 IPA/Hexanes, 2 μL injection, 4.6 x 150mm Chiralcel OJ-3, 1 mL/min., 1% IPA in hexanes, 254 nm, major 13.13 min., minor 26.00 min., 52% *ee*

See Procedure for Preparation of Secondary Allylic Trichloroacetimidates Pg. 125

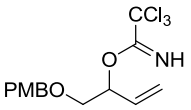

308

Compound **308**:

^{1}H NMR ($CDCl_3$, 400 MHz): δ = 8.35 (bs, NH), 7.24 (d, *J* = 8.7 Hz, 2H), 6.85 (d, *J* = 8.7 Hz, 2H), 5.93-5.85 (m, 1H), 5.62-5.58 (m, 1H), 5.43 (dt, *J* = 17.3, 1.4 Hz, 1H), 5.27 (dt, *J* = 10.7, 1.3 Hz, 1H), 4.52 (s, 2H), 3.78 (s, 3H), 3.70-3.62 (m, 2H).

^{13}C NMR ($CDCl_3$, 100 MHz): δ = 162.1, 159.4, 132.8, 130.3, 129.4, 118.2, 114.0, 91.9, 78.4, 73.2, 71.0, 55.5.

IR (film, cm^{-1}): ν = 3342, 3001, 2933, 2907, 2862, 2837, 1733, 1665, 1613, 1586, 1514, 1464, 1362, 1301, 1248, 1173, 1081, 1036, 989, 931, 849, 822.

HRMS (TOF ES+): calc. for $C_{14}H_{16}Cl_3NO_3$ $(M+Na)^+$: 374.0093; found: 374.0095.

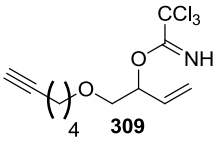

309

Compound **309**:

^{1}H NMR ($CDCl_3$, 400 MHz): δ = 8.30 (s, NH), 5.89-5.82 (m, 1H), 5.54-5.51 (m, 1H), 5.40 (dt, *J* = 13.8, 1.0 HZ, 1H), 5.23 (dt, *J* = 8.6, 1.0 Hz, 1H), 3.64-3.57 (m, 2H), 3.56-3.49 (m, 2H), 2.17-2.12 (m, 2H), 1.73-1.66 (m, 5H).

IR (film, cm^{-1}): ν = 3343, 2950, 2920, 2862, 1664, 1647, 1434, 1345, 1286, 1123, 1074, 987, 973, 930, 872, 813, 793, 743.

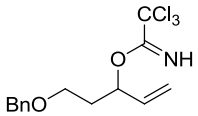

310

Compound **310**:

^{1}H NMR ($CDCl_3$, 400 MHz): δ = 8.30 (bs, NH), 7.32-7.25 (m, 5H), 5.91-5.83 (m, 1H), 5.59-5.55 (m, 1H), 5.35 (dt, *J* = 17.3, 1.3 Hz, 1H), 5.21 (dt, *J* = 10.6, 1.2 Hz, 1H), 4.48 (s, 2H), 3.60-3.56 (m, 2H), 2.08-2.01 (m, 2H).

^{13}C NMR ($CDCl_3$, 100 MHz): δ = 161.9, 138.4, 135.6, 128.6, 127.9, 127.8, 117.0, 91.9, 76.7, 73.3, 66.0, 34.8.

IR (film, cm^{-1}): ν = 3343, 3087, 3064, 3030, 2953, 2924, 2860, 2796, 1952, 1872, 1735, 1662, 1495, 1454, 1422, 1413, 1360, 1299, 1285, 1204, 1074, 1028, 977, 925, 805.

HRMS (TOF ES+): calc. for $C_{14}H_{16}Cl_3NO_2$ $(M+Na)^+$: 358.0144; found: 358.0149.

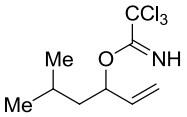

311

Compound **311**:

^{1}H NMR ($CDCl_3$, 400 MHz): δ = 8.26 (bs, NH), 5.89-5.80 (m, 1H), 5.46-5.41 (m, 1H), 5.33 (dt, *J* = 17.3, 1.3, 1H), 5.18 (dt, *J* = 10.6, 1.2 Hz, 1H), 1.82-1.73 (m, 2H), 1.49-1.42 (m, 1H), 0.93 (d, *J* = 3.6 Hz, 3H), 0.92 (d, *J* = 3.7 Hz, 3H).

^{13}C NMR ($CDCl_3$, 100 MHz): δ = 162.2, 136.2, 116.7, 92.1, 78.2, 43.6, 24.7, 23.2, 22.4.

IR (film, cm^{-1}): ν = 3348, 3087, 2958, 2934, 2871, 1766, 1722, 1661, 1469, 1424, 1387, 1368, 1336, 1299, 1285, 1172, 1129, 1074, 978, 924, 853, 827.

HRMS (TOF ES+): calc. for $C_9H_{15}Cl_3NO$ $(M+H)^+$: 258.0219; found: 258.0221.

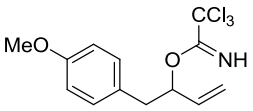

312

Compound **312**:

^{1}H NMR ($CDCl_3$, 400 MHz): δ = 8.26 (bs, NH), 7.16 (d, *J* = 8.6 Hz, 2H), 6.80 (d, *J* = 8.6 Hz, 2H), 5.89-5.81 (m, 1H), 5.55-5.50 (m, 1H), 5.31 (dt, *J* = 17.3, 1.3 Hz, 1H), 5.19 (dt, *J* = 10.6, 1.2 Hz, 1H), 3.76 (s, 3H), 3.04 (dd, *J* = 14.0, 7.2 Hz, 1H), 2.92 (dd, *J* = 14.0, 5.9 Hz, 1H).

^{13}C NMR ($CDCl_3$, 100 MHz): δ = 161.9, 158.5, 135.2, 130.9, 128.9, 117.3, 113.8, 91.9, 80.2, 55.4, 40.0.

IR (film, cm^{-1}): ν = 3341, 2998, 2851, 2836, 1743, 1662, 1646, 1613, 1585, 1514, 1465, 1442, 1344, 1302, 1248, 1178, 1080, 1037, 988, 928, 823.

HRMS (TOF ES+): calc. for $C_{13}H_{14}Cl_3NO_2$ $(M+Na)^+$ calc.: 343.9988; found: 343.9990.

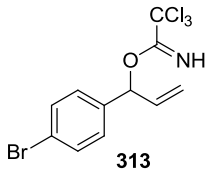

Compound **313**:

^{1}H NMR ($CDCl_3$, 400 MHz): δ = 8.37 (s, NH), 7.50-7.45 (m, 2H), 7.30-7.27 (m, 2H), 6.29 (d, *J* = 5.6 Hz, 1H), 6.05-5.97 (m, 1H), 5.39 (dt, *J* = 17.1, 1.3 Hz, 1H), 5.29 (dt, *J* = 10.4, 1.2 Hz, 1H).

^{13}C NMR ($CDCl_3$, 100 MHz): δ = 161.4, 137.6, 135.4, 131.9, 128.9, 122.4, 117.9, 91.6, 80.0.

IR (film, cm^{-1}): ν = 3341, 3088, 3021, 2989, 2932, 1741, 1664, 1594, 1488, 1410, 1338, 1317, 1281, 1232, 1197, 1070, 1011, 984, 931, 833.

HRMS (TOF ES+): calc. for $C_{11}H_9BrCl_3NO$ $(M+Na)^+$ calc.: 377.8831; found: 377.8834

5.11 General Procedure for Regio- and Enantioselective Amination of Racemic Secondary Allylic Trichloroacetimidates with [RhCl(ethylene)]$_2$/ **L1**

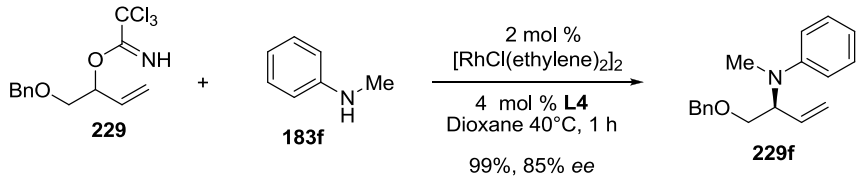

Procedure A for Small Scale: A 10 mL oven-dried Schlenk flask was charged with [RhCl(ethylene)$_2$]$_2$ (1.1 mg, 2.8 μmol, 2 mol%) and (1*S*,4*S*)-2,5-diphenylbicyclo[2.2.2]octa-2,5-diene (**L4**) (1.5 mg, 5.6 μmol, 4 mol%) in a glove box. The flask was sealed, removed from the glove box, and dioxane (0.35 mL) was added to the Schlenk and stirred for 15 min resulting in a bright-red solution. A separate 10 mL Schlenk flask was charged with allylic imidate **229** (45 mg, 0.14 mmol, 1.0 equiv), dioxane (0.35 mL) and aniline **183f** (23 μL, 0.21 mmol, 1.5 equiv). The rhodium catalyst solution was then added to the flask containing the solution of **229** and **183f**. The mixture was immediately placed in an oil bath at 40°C and stirred under argon. The progress of the reaction was monitored by GC at 1 h. The crude reaction was purified by adsorbing directly onto a dry 5g Teledyne Isco silica cartridge using vacuum followed by elution onto a pre-equilibrated 24g silica flash column (0 → 10% ethyl acetate/hexane) providing allylic amine **229f** (37 mg, 99%, branched/linear > 84:1) as pale yellow oil.

<u>Compound **229f**</u>:

^{1}H NMR (CDCl$_3$, 400 MHz): δ = 7.33-7.22 (m, 7H), 6.82 (d, *J* = 8.7 Hz, 2H), 6.75 (t, *J* = 7.2 Hz, 1H), 5.94-5.86 (m, 1H), 5.26 (d, *J* = 1.8 Hz, 1H), 5.23 (d, *J* = 7.5, 1.6 Hz, 1H), 4.62-4.57 (m, 1H), 4.55 (d, *J* = 12.3 Hz, 1H), 4.51 (d, *J* = 12.3 Hz, 1H), 3.74-3.66 (m, 2H), 3.50 (s, 1H), 2.83 (s, 9H).

IR (film, cm^{-1}): ν =2858, 2815, 1596, 1503, 1453, 1359, 1312, 1289, 1209, 1094, 1028, 990, 921, 745, 712, 691.

$[\alpha]^{20}_{D}$: +17.43, c =, $CHCl_3$

HPLC: 2.5mg/mL in 50/50 IPA/Hex, 2 μL injection, 4.6 x 250mm Chiralcel OD-H, 0.6 mL/min., 1% IPA in hexanes, 254 nm, major 21.03 min., minor 13.15 min., 85% *ee.*

*Note: When reactions were scaled and required concentration with catalyst prior to purification, significant isomerization from the branched amine **229f** to the linear amine product was observed during isolation. To avoid isomerization, the following procedure was used on a 0.5 g scale to prepare **229f**:*

Procedure B for Larger Scale: The progress of the reaction was monitored by GC at 1 h. The crude reaction was allowed to equilibrate to RT, filtered through a silica pad with 20% ethyl acetate in hexanes and concentrated. The crude oil was purified by adsorbing in dichloromethane onto a dry 25g Teledyne Isco silica cartridge using vacuum followed by elution onto a pre-equilibrated 40g silica flash column (0 → 20% ethyl acetate/hexane) providing allylic amine **6a** (410 mg, 99%, branched/linear > 23:1) as pale yellow oil.

$[\alpha]^{20}_{D}$ +15.91:, c = 1, $CHCl_3$

HPLC: 2.5mg/mL in 50/50 IPA/Hex, 2 μL injection, 4.6 x 250mm Chiralcel OD-H, 0.6 mL/min., 1% IPA in hexanes, 254 nm, major 20.05 min., minor 12.93 min., 87% *ee.*

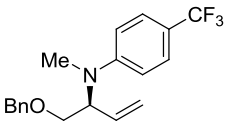

229r

Compound **229r**:

^{1}H NMR ($CDCl_3$, 400 MHz): δ = 7.43 (d, J = 8.5 Hz, 2H), 7.31-7.22 (m, 5H), 6.77 (d, *J* = 8.8 Hz, 2H), 5.87-5.79 (m, 1H), 5.25 (dt, *J* = 10.7, 1.6 Hz, 1H), 5.18 (dt, *J* = 17.4, 1.6 Hz, 1H), 4.64-4.60 (m, 1H), 4.52 (d, *J* = 12.0 Hz, 1H), 4.49 (d, *J* = 12.0 Hz, 1H), 3.69-3.67 (m, 2H), 2.84 (s, 3H).

^{13}C NMR ($CDCl_3$, 100 MHz): δ = 152.7, 138.1, 134.1, 128.6, 127.9, 127.8, 126.6, 126.6, 126.5, 126.5, 117.5, 112.1, 73.4, 70.1, 60.0, 32.6.

IR (film, cm^{-1}): ν = 3088, 3066, 3029, 2946, 2890, 2860, 2838, 1615, 1529, 1455, 1385, 1329, 1201, 1164, 1108, 1071, 987, 928, 818.

HRMS (TOF ES+): calc. for $C_{19}H_{21}F_3NO$ $(M+H)^+$: 336.1575; found: 336.1581.

$[\alpha]^{20}_D$ = +14.24**:**, c = 1, $CHCl_3$

HPLC: 2.5mg/mL in 50/50 IPA/Hex, 2 μL injection, 4.6 x 150mm Chiralcel OJ-3, 1 mL/min., 2.5% IPA in hexanes, 254 nm, major 10.28 min., minor 8.21 min., 93% *ee.*

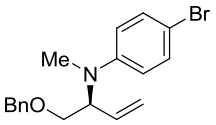

229s

Compound **229s**:

^{1}H NMR ($CDCl_3$, 400 MHz): δ = 7.33-7.22 (m, 7H), 6.64 (d, *J* = 9.1 Hz, 2H), 5.84-5.76 (m, 1H), 5.21 (dt, *J* = 10.7, 1.5 Hz, 1H), 5.16 (dt, *J* = 17.4, 1.4 Hz, 1H), 4.51 (d, *J* = 12.1 Hz, 1H), 4.48 (d, *J* = 12.0 Hz, 1H), 3.67-3.60 (m, 2H), 2.75 (s, 3H).

^{13}C NMR ($CDCl_3$, 100 MHz): δ = 156.6, 138.1, 134.4, 131.9, 128.6, 127.9, 127.8, 117.4, 115.0, 73.3, 70.1, 60.4, 32.6.

IR (film, cm^{-1}): ν = 3085, 3064, 3030, 2861, 1865, 1736, 1673, 1639, 1591, 1495, 1454, 1380, 1361, 1309, 1272, 1251, 1208, 1110, 1028, 993, 924, 807.

HRMS (TOF ES+): calc. for $C_{18}H_{21}BrNO$ $(M+H)^+$: 346.0807; found: 346.0814.

$[\alpha]^{20}_D$: +9.70, c = 1, $CHCl_3$

HPLC: 2 mg/mL in 50/50 IPA/Hex, 2 μL injection, 4.6 x 250mm Chiralcel OD-H, 0.6 mL/min., 1% IPA in hexanes, 254 nm, major 12.5 min., minor 11.4 min., 83% *ee.*

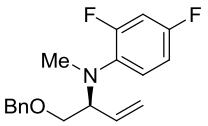

229t

Compound **229t**:

^{1}H NMR ($CDCl_3$, 400 MHz): δ = 7.33-7.23 (m, 5H), 6.95-6.89 (m, 1H), 6.79-6.71 (m, 2H), 5.90-5.81 (m, 1H), 5.21 (dt, *J* = 10.7, 1.4 Hz, 1H), 5.20 (dt, *J* = 17.2, 1.6 Hz, 1H), 4.48 (s, 2H), 4.12-4.07 (m, 1H), 3.69 (ddd, *J* = 10.0, 7.3, 1.1 Hz, 1H), 3.57 (dd, *J* = 10.0, 5.8 Hz, 1H), 2.71 (s, 3H).

^{13}C NMR ($CDCl_3$, 100 MHz): δ = 157.5 (dd, $J_{C\text{-}F}$ = 241, 11.4 Hz), 155.8 (dd, $J_{C\text{-}F}$ = 246, 11.7 Hz), 138.4, 136.9 (dd, $J_{C\text{-}F}$ = 9.0, 3.5 Hz), 135.0, 128.5, 127.8, 122.0 (dd, $J_{C\text{-}F}$ = 9.1, 4.4 Hz), 117.8, 110.6 (dd, $J_{C\text{-}F}$ = 21.3, 3.5 Hz), 104.6 (t, $J_{C\text{-}F}$ = 26 Hz), 73.2, 70.5, 63.7, 63.6, 34.6.

IR (film, cm^{-1}): ν = 3083, 3031, 2947, 2859, 2805, 1592, 1505, 1454, 1361, 1268, 1141, 1114, 1095, 994, 964, 927, 848.

HRMS (TOF ES+): calc. for $C_{18}H_{20}F_2NO$ $(M+H)^+$: 304.1513; found: 304.1514.

$[\alpha]^{20}_D$: +19.57, c = 1, $CHCl_3$

HPLC: 2.5mg/mL in 50/50 IPA/Hex, 2 μL injection, 4.6 x 150mm Chiralcel OJ-3, 1 mL/min., 1% IPA in hexanes, 254 nm, major 7.60 min., minor 9.08 min., 91% *ee.*

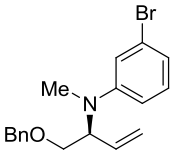

229u

Compound **229u**:

^{1}H NMR ($CDCl_3$, 400 MHz): δ = 7.32-7.22 (m, 9H), 6.64 (d, *J* = 9.0 Hz, 2H), 5.84-5.76 (m, 1H), 5.21 (dt, *J* = 10.7, 1.4 Hz, 1H), 5.16 (dt, *J* = 17.4, 1.3 Hz, 1H), 4.51 (d, *J* = 12.0 Hz, 1H), 4.47 (d, *J* = 12.0 Hz, 1H), 4.50-4.46 (m, 1H), 3.67-3.60 (m, 2H), 2.75 (s, 3H).

^{13}C NMR ($CDCl_3$, 100 MHz): δ = 151.8, 134.3, 130.6, 130.4, 128.6, 127.9, 127.8, 119.6, 117.4, 116.0, 114.9, 111.8, 73.3, 70.2, 60.2, 32.6.

IR (film, cm^{-1}): ν = 3086, 3065, 3029, 2882, 2861, 2816, 1639, 1591, 1554, 1489, 1453, 1430, 1361, 1325, 1265, 1210, 1095, 1077, 1028, 983, 927, 914, 833.

HRMS (TOF ES+): calc. for $C_{18}H_{21}BrNO$ $(M+H)^+$: 346.0807; found: 346.0833.

$[\alpha]^{20}_D$: +14.90, c = 1, $CHCl_3$

HPLC: 2 mg/mL in 50/50 IPA/Hex, 2 μL injection, 4.6 x 250mm Chiralcel OD-H, 0.6 mL/min., 1% IPA in hexanes, 254 nm, major 31.3 min., minor 13.2 min., 89% *ee.*

Compound **229v**:

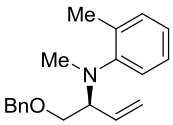

229v

^{1}H NMR ($CDCl_3$, 400 MHz): δ = 7.30-7.24 (m, 5H), 7.16-7.07 (m, 3H), 6.94 (td, *J* = 7.2, 1.5 Hz, 1H), 5.95-5.87 (m, 1H), 5.26-5.21 (m, 2H), 4.46 (d, *J* = 12.0 Hz, 1H), 4.44

(d, J = 12.1 Hz, 1H), 3.80-3.76 (m, 1H), 3.70-3.66 (m, 1H), 3.60-3.55 (m, 1H), 2.66 (s, 3H), 2.29 (s, 3H).

^{13}C NMR ($CDCl_3$, 100 MHz): δ = 151.7, 138.5, 136.0, 133.3, 131.3, 128.5, 127.8, 127.7, 126.2, 123.0, 122.0, 117.5, 73.3, 70.7, 64.0, 36.0, 18.7.

IR (film, cm^{-1}): ν = 3064, 3027, 2945, 2855, 2798, 1598, 1491, 1453, 1361, 1254, 1204, 1101, 1051, 1028, 993, 923, 848.

HRMS (TOF ES+): calc. for $C_{19}H_{24}NO$ $(M+H)^+$: 282.1858; found: 282.1864.

$[\alpha]^{20}_D$:+5.70, c = 1, $CHCl_3$

HPLC: 2.5mg/mL in 50/50 IPA/Hex, 2 μL injection, 4.6 x 150mm Chiralcel OJ-3, 1 mL/min., 1% IPA in hexanes, 254 nm, major 7.44 min., minor 6.30 min., 89% *ee.*

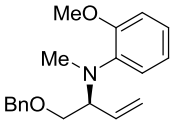

229w

Compound **229w**:

^{1}H NMR ($CDCl_3$, 400 MHz): δ = 7.31-7.24 (m, 5H), 6.96-6.82 (m, 4H), 5.99-5.90 (m, 1H), 5.20 (d, J = 10.7 Hz, 1H), 5.16 (d, J = 17.5 Hz, 1H), 4.47 (s, 2H), 4.29-4.24 (m, 1H), 3.82, (s, 3H), 3.74 (dd, J = 9.7, 6.2 Hz, 1H), 3.63 (dd, J = 9.7, 7.0 Hz, 1H), 2.71 (s, 3H).

^{13}C NMR ($CDCl_3$, 100 MHz): δ = 152.7, 141.6, 138.6, 136.0, 128.5, 127.8, 127.7, 122.4, 120.9, 120.7, 117.5, 111.5, 73.1, 70.6, 62.2, 55.6, 34.6.

IR (film, cm^{-1}): ν = 3063, 3030, 2943, 2855, 2800, 1638, 1593, 1499, 1454, 1360, 1234, 1182, 1098, 1054, 1028, 996, 918.

HRMS (TOF ES+): calc. for $C_{19}H_{24}NO_2$ $(M+H)^+$: 298.1807; found: 298.1803.

$[\alpha]^{20}_D$: +19.18, c = 1, $CHCl_3$

HPLC: 2.5mg/mL in 50/50 IPA/Hex, 2 μL injection, 4.6 x 150mm Chiralcel OJ-3, 1 mL/min., 2.5% IPA in hexanes, 254 nm, major 6.94 min., minor 8.59 min., 85% *ee.*

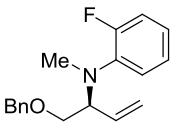

229x

Compound **229x**:

^{1}H NMR ($CDCl_3$, 400 MHz): δ = 7.32-7.23 (m, 5H), 7.01- 6.93 (m, 3H), 6.86-6.83 (m, 1H), 5.94-5.85 (m, 1H), 5.24-5.20 (m, 2H), 4.48 (s, 2H), 4.30-4.28 (m, 1H), 3.75-3.71 (m, 1H), 3.64-3.60 (m, 1H), 2.76 (s, 3H).

^{13}C NMR ($CDCl_3$, 100 MHz): δ = 154.3, 138.4, 135.1, 128.5, 127.8, 127.7, 124.3, 121.2, 120.7, 117.6, 116.4, 116.2, 73.2, 70.5, 63.0, 62.9, 33.9.

IR (film, cm^{-1}): ν = 3084, 3065, 3030, 2948, 2858, 2806, 1610, 1501, 1454, 1360, 1311, 1256, 1210, 1098, 1039, 1028, 993, 924.

HRMS (TOF ES+): calc. for $C_{18}H_{21}FNO$ $(M+H)^+$: 286.1607; found: 286.1606.

$[\alpha]^{20}_D$: +28.79, c = 1, $CHCl_3$

HPLC: 2.5 mg/mL in 50/50 IPA/Hex, 2 μL injection, 4.6 x 150mm Chiralcel OJ-3, 1 mL/min., 1% IPA in hexanes, 254 nm, major 8.45 min., minor 11.18 min., 91% *ee.*

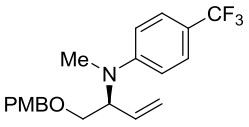

308r

Compound **308r**:

^{1}H NMR ($CDCl_3$, 400 MHz): δ = 7.42 (d, *J* = 8.7 Hz, 2H), 7.14 (d, *J* = 8.7 Hz, 2H), 6.83 (d, *J* = 8.6 Hz, 2H), 6.75 (d, *J* = 8.8 Hz, 2H), 5.85-5.77 (m, 1H), 5.22 (dt, *J* = 10.7, 1.5 Hz, 1H), 5.16 (dt, 17.4, 1.6 Hz, 1H), 4.61-4.57 (m, 1H), 4.43 (d, *J* = 11.7 Hz, 1H), 4.42 (d, *J* = 11.7 Hz, 1H), 3.78 (s, 3H), 3.67-3.60 (m, 2H), 2.82 (s, 3H).

^{13}C NMR ($CDCl_3$, 100 MHz): δ = 159.5, 152.7, 134.1, 130.1, 129.5, 126.6, 126.5, 117.4, 114.0, 112.1, 73.0, 69.7, 59.9, 55.5, 32.6.

IR (film, cm^{-1}): ν = 3093, 3063, 3034, 3005, 2953, 2906, 2856, 2837, 1889, 1764, 1715, 1664, 1614, 1528, 1514, 1466, 1385, 1361, 1327, 1248, 1200, 1163, 1104, 1069, 1035, 985, 927, 818.

HRMS (TOF ES+): calc. for $C_{20}H_{23}F_3NO_2$ $(M+H)^+$: 366.1681; found: 366.1672.

[α]^{20}D: +14.07, c = 1, $CHCl_3$

HPLC: 2 mg/mL in 50/50 IPA/Hex, 2 μL injection, 4.6 x 250mm Chiralcel OD-H, 0.6 mL/min., 1% IPA in hexanes, 254 nm, major 19.78 min., minor 15.14 min., 94% *ee.*

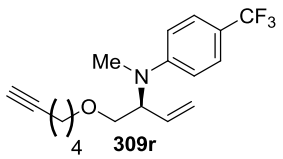

309r

Compound **309r**:

^{1}H NMR ($CDCl_3$, 400 MHz): δ = 7.41 (d, *J* = 8.6 Hz, 2H), 6.76 (d, *J* = 8.8 Hz, 2H), 5.86-5.78 (m, 1H), 5.23 (dt, *J* = 10.6, 1.5 Hz, 1H), 5.17 (dt, *J* = 17.3, 1.8 Hz, 1H), 4.57-4.52 (m, 1H), 3.65-3.60 (m, 2H), 3.50-3.45 (m, 2H), 2.85 (s, 3H), 2.14-2.10 (m, 2H), 1.76-1.72 (m, 3H), 1.69-1.62 (m, 2H).

^{13}C NMR ($CDCl_3$, 100 MHz): δ = 152.7, 134.2, 126.6, 126.5, 117.3, 112.0, 78.6, 77.4, 76.0, 69.9, 59.9, 32.6, 29.2, 16.0, 3.6.

IR (film, cm^{-1}): ν = 3091, 2922, 2865, 1769, 1723, 1615, 1572, 1529, 1478, 1434, 1386, 1329, 1247, 1200, 1164, 1113, 1071, 989, 930, 820.

HRMS (TOF ES+): calc. for $C_{18}H_{23}NOF_3$ $(M+H)^+$: 326.1732; found: 326.1726.

[α]^{20}D: +17.05, c = 1, $CHCl_3$

HPLC: 2.5mg/mL in 50/50 IPA/Hex, 2 μL injection, 4.6 x 150mm Chiralcel OJ-3, 1 mL/min., 1% IPA in hexanes, 254 nm, major 10.02 min., minor 6.61 min., 89% *ee.*

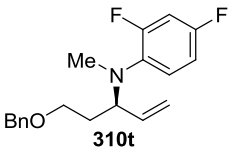

310t

Compound **310t**:

^{1}H NMR ($CDCl_3$, 400 MHz): δ = 7.29-7.24 (m, 5H), 6.90-6.88 (m, 1H), 6.78-6.71 (m, 2H), 5.84-5.76 (m, 1H), 5.13 (dt, *J* = 10.4, 1.3 Hz, 1H), 5.04 (dt, *J* = 17.3, 1.4 Hz, 1H), 4.40 (s, 2H), 3.98-3.93 (m, 1H), 3.51 (t, = 6.6 Hz, 2H), 2.64 (s, 3H), 2.04-1.95 (m, 1H), 1.88-1.79 (m, 1H).

^{13}C NMR ($CDCl_3$, 100 MHz): δ = 157.8 (dd, J_{C-F} = 252, 11.4 Hz), 155.8 (dd, J_{C-F} = 245, 11.5 Hz), 138.6, 137.0, 136.7 (dd, J_{C-F} = 8.9, 3.4 Hz), 128.5, 127.9, 127.7, 121.7 (dd, J_{C-F} = 9.1, 4.5 Hz), 117.0, 110.6 (dd, J_{C-F} = 21.1, 3.7 Hz), 104.6 (t, J_{C-F} = 25.1 Hz), 73.2, 67.7, 61.4, 61.4, 33.9, 31.6.

IR (film, cm^{-1}): ν = 3079, 3066, 3031, 2948, 2861, 2803, 1592, 1506, 1454, 1421, 1364, 1269, 1245, 1215, 1141, 1113, 1097, 1028, 996, 968, 925, 848, 804.

HRMS (TOF ES+): calc. for $C_{19}H_{22}F_2NO$ $(M+H)^+$: 318.1669; found: 318.1668.

[α]^{20}D: +26.96, c = 1, $CHCl_3$

HPLC: 2.5mg/mL in 50/50 IPA/Hex, 2 μL injection, 4.6 x 150mm Chiralcel OJ-3, 0.6 mL/min., 2.5% IPA in hexanes, 254 nm, major 7.14 min., minor 8.22 min., 88% *ee.*

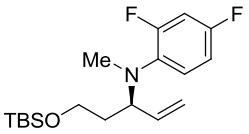

223t

Compound **223t**:

^{1}H NMR (CDCl$_3$, 400 MHz): 4:1 mixture of rotamers δ = 6.90-6.71 (m, 3H), 5.86-5.74 (m, 1H), 5.37-5.32 (m, 0.2H), 5.26-5.04 (m, 2H), 3.96-3.92 (m, 0.8H), 3.64-3.60 (m, 2H), 2.64 (s, 2.4H), 2.04 (s, 0.6H), 1.93-1.84 (m, 1H), 1.78-1.67 (m, 1H), 0.86 (s, 3H), 0.83 (s, 6H), 0.02 (s, 2H), -0.02 (s, 2H), -0.05 (s, 2H).

^{13}C NMR (CDCl$_3$, 100 MHz): δ = 170.4, 157.4 (dd, $J_{C\text{-}F}$ = 241, 12.5 Hz), 153.4 (dd, $J_{C\text{-}F}$ = 240, 11.7 Hz), 137.1, 136.8, 136.7, 136.6, 121.7 (dd, $J_{C\text{-}F}$ = 9.1, 4.5 Hz), 116.9, 116.7, 110.5 (dd, $J_{C\text{-}F}$ = 21.1, 3.6 Hz), 104.7 (t, $J_{C\text{-}F}$ = 26 Hz), 103.8, 77.4, 72.2, 61.0, 60.3, 59.2, 37.4, 34.4, 34.1, 26.1, 21.4, 18.4, -5.3.

IR (film, cm^{-1}): ν = 3080, 2953, 2930, 2856, 2801, 1741, 1592, 1508, 1471, 1370, 1269, 1245, 1180, 1141, 1095, 1040, 1010, 993, 969, 926, 836, 814.

HRMS (TOF ES+): calc. for $C_{18}H_{30}F_2NOSi$ $(M+H)^+$: 342.2065; found: 342.2062.

[α]^{20}D: +22.27, c = 1, $CHCl_3$

HPLC: 2.5mg/mL in 50/50 IPA/Hex, 2 μL injection, 4.6 x 150mm Chiralcel OJ-3, 0.3 mL/min., 1% IPA in hexanes, 254 nm, major 6.28 min., minor 6.53 min., 87% *ee.*

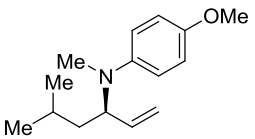

311q

Compound **311q**:

^{1}H NMR ($CDCl_3$, 400 MHz): δ = 6.80 (dt, *J* = 9.3, 2.6 Hz, 2H), 6.75 (dt, *J* = 9.3, 2.5 Hz, 2H), 5.80-5.72 (m, 1H), 5.08 (dt, *J* = 10.5, 1.5 Hz, 1H), 5.05 (dt, *J* = 17.2, 1.6 Hz, 1H), 4.18-4.13 (m, 1H), 3.74 (s, 3H), 2.67 (s, 3H), 1.63-1.55 (m, 2H), 1.41-1.34 (m, 1H), 0.90 (d, *J* = 6.4 Hz, 3H), 0.86 (d, *J* = 6.4 Hz, 3H).

^{13}C NMR ($CDCl_3$, 100 MHz): δ = 151.9, 145.5, 137.9, 115.7, 115.6, 114.8, 59.8, 55.9, 41.2, 32.4, 25.0, 23.2, 22.7.

IR (film, cm^{-1}): ν = 3072, 2954, 2934, 2909, 2869, 2832, 2800, 1638, 1510, 1467, 1384, 1366, 1286, 1244, 1181, 1132, 1101, 1040, 991, 951, 920, 815.

HRMS (TOF ES+): calc. for $C_{15}H_{24}NO$ $(M+H)^+$: 234.1858; found: 234.1858.

$[\alpha]^{20}_D$: +56.97, c = 1, $CHCl_3$

HPLC: 2 mg/mL in 50/50 IPA/Hex, 2 μL injection, 4.6 x 250mm Chiralcel OD-H, 0.3 mL/min., 100% hexanes, 254 nm, major 61.6 min., minor 70.6 min., 91% *ee.*

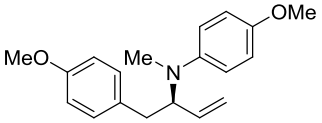

312q

Compound **312q**:

^{1}H NMR ($CDCl_3$, 400 MHz): 7.07 (d, *J* = 8.6 Hz, 2H), 6.77 (d, *J* = 8.9 Hz, 4H), 6.70 (d, *J* = 9.2 Hz, 2H), 5.87-5.79 (m, 1H), 5.11 (dt, *J* = 10.6, 1.5 Hz, 1H), 5.05 (dt, *J* = 17.3, 1.6 Hz, 1H), 4.32-4.29 (m, 1H), 3.75 (s, 3H), 3.73 (s, 3H), 2.94-2.87 (m, 1H), 2.83-2.78 (m, 1H), 2.74 (s, 3H).

^{13}C NMR ($CDCl_3$, 100 MHz): δ = 158.1, 152.2, 145.1, 136.8, 131.4, 130.2, 116.5, 116.3, 114.6, 113.9, 111.2, 64.6, 55.9, 55.4, 37.2, 33.1.

IR (film, cm^{-1}): ν = 3064, 3033, 2997, 2933, 2908, 2834, 1735, 1661, 1611, 1583, 1510, 1464, 1441, 1420, 1300, 1245, 1178, 1107, 1037, 990, 975, 922, 817.

HRMS (TOF ES+): calc. for $C_{19}H_{24}NO_2$ $(M+H)^+$: 298.1807; found: 298.1830.

$[\alpha]^{20}_D$: +18.50, c = 1, $CHCl_3$

HPLC: 2.5mg/mL in 50/50 IPA/Hex, 2 μL injection, 4.6 x 150mm Chiralcel OJ-3, 0.75 mL/min., 2.5% IPA in hexanes, 254 nm, major 25.3 min., minor 28.4 min., 87% *ee.*

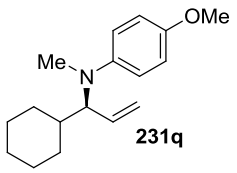

231q

Compound **231q**:

^{1}H NMR ($CDCl_3$, 400 MHz): δ = 6.78 (d, *J* = 9.2 Hz, 2H), 6.71 (d, *J* = 9.2 Hz, 2H), 5.80-5.71 (m, 1H), 5.07 (ddd, *J* = 10.3, 1.8, 0.8 Hz, 1H), 4.97 (ddd, *J* = 17.2, 1.8, 0.8 Hz, 1H), 3.73 (s, 3H), 3.67-3.63 (m, 1H), 2.68 (s, 3H), 1.84-1.53 (m, 7H), 1.26-1.10 (m, 3H), 0.93-0.84 (m, 2H).

^{13}C NMR ($CDCl_3$, 100 MHz): δ = 151.6, 145.8, 135.5, 117.0, 115.4, 114.7, 68.7, 55.9, 39.5, 32.6, 31.2, 30.8, 26.8, 26.4.

IR (film, cm^{-1}): ν = 3069, 3038, 2924, 2851, 1745, 1662, 1636, 1578, 1510, 1464, 1450, 1365, 1313, 1278, 1244, 1180, 1090, 1040, 992, 975, 920, 813.

HRMS (TOF ES+): calc. for $C_{17}H_{26}NO$ $(M+H)^+$: 260.2014; found: 260.2007.

$[\alpha]^{20}_D$: +24.94, c = 1, $CHCl_3$

HPLC: 2 mg/mL in ethanol, 12 μL injection, 4.6 x 150mm Chiralcel OJ-3, 1 mL/min., 2.5% IPA in hexanes, 254 nm, major 4.5 min., minor 3.8 min., 96% *ee.*

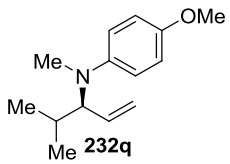

232q

Compound **232q**:

^{1}H NMR ($CDCl_3$, 400 MHz): δ = 6.80-6.77 (m, 2H), 6.74-6.71 (m, 2H), 5.81-5.72 (m, 1H), 5.10-5.07 (m, 1H), 5.02-4.97 (m, 1H), 3.74 (s, 3H), 3.57-3.52 (m, 1H), 2.68 (s, 3H), 1.90-1.53 (m, 1H), 0.93 (d, *J* = 2.1 Hz, 3H), 0.91 (d, *J* = 2.0 Hz, 3H).

^{13}C NMR ($CDCl_3$, 100 MHz): δ = 151.7, 145.8, 135.7, 128.7, 124.9, 116.9, 115.6, 114.7, 70.0, 55.9, 32.7, 30.2, 20.6, 20.5.

IR (film, cm^{-1}): ν = 3077, 2956, 2905, 2870, 2832, 2805, 1636, 1607, 1577, 1511, 1466, 1385, 1366, 1277, 1244, 1181, 1086, 1040, 975, 918, 814.

HRMS (TOF ES+): calc. for $C_{14}H_{22}NO$ $(M+H)^+$: 220.1701; found: 220.1703.

$[\alpha]^{20}_D$: +40.40, c = 1, $CHCl_3$

HPLC: 2.5mg/mL in 50/50 IPA/Hex, 2 μL injection, 4.6 x 150mm Chiralcel OJ-3, 0.6 mL/min., 1% IPA in hexanes, 254 nm, major 5.43 min., minor 4.98 min., 95% *ee.*

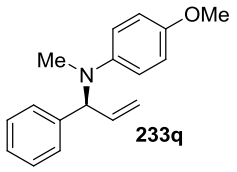

233q

Compound **233q**:

^{1}H NMR ($CDCl_3$, 400 MHz): δ = 7.34-7.29 (m, 5H), 6.80 (d, *J* = 9.3 Hz, 2H), 6.77 (d, *J* = 9.3 Hz, 2H), 6.14-6.06 (m, 1H), 5.28 (d, *J* = 10.2 Hz, 1H), 5.24 (d, *J* = 6.4 Hz, 1H), 5.18 (d, *J* = 17.2 Hz, 1H), 3.74 (s, 3H), 2.66 (s, 3H).

^{13}C NMR ($CDCl_3$, 100 MHz): δ = 151.7, 145.8, 135.7, 128.7, 124.9, 116.9, 115.6, 114.7, 70.0, 55.9, 32.7, 30.2, 20.6, 20.5.

IR (film, cm^{-1}): ν = 3065, 2955, 2906, 2870, 2832, 2805, 1510, 1466, 1385, 1366, 1278, 1244, 1181, 1085, 1040, 994, 974, 920, 814.

HRMS (TOF ES+): calc. for $C_{17}H_{20}NO$ $(M+H)^+$: 254.1545; found: 254.1552.

$[\alpha]^{20}_{D}$: +45.50, c = 1, $CHCl_3$

HPLC: 2.5mg/mL in 50/50 IPA/Hex, 2 μL injection, 4.6 x 150mm Chiralcel OJ-3, 1 mL/min., 5% IPA in hexanes, 254 nm, major 9.58 min., minor 11.6 min., 93% *ee.*

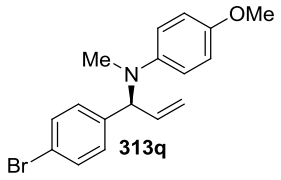

313q

Compound **313q**:

^{1}H NMR ($CDCl_3$, 400 MHz): δ = 7.45 (d, *J* = 8.5 Hz, 2H), 7.19 (d, *J* = 8.6 Hz, 2H), 6.83 (d, *J* = 9.5 Hz, 2H), 6.79 (d, *J* = 9.4 Hz, 2H), 6.12-6.03 (m, 1H), 5.32 (dt, *J* = 10.3, 1.4 Hz, 1H), 5.21 (dt, *J* = 17.0, 1.4 Hz, 1H), 5.18 (s, 1H), 3.78 (s, 3H), 2.68 (s, 3H).

^{13}C NMR ($CDCl_3$, 100 MHz): δ = 152.6, 144.8, 140.0, 135.8, 131.6, 129.8, 121.2, 118.4, 116.7, 114.7, 67.0, 55.9, 35.2.

IR (film, cm^{-1}): ν = 3043, 2990, 2949, 2903, 2831, 2805, 1741, 1588, 1508, 1485, 1402, 1368, 1276, 1241, 1179, 1119, 1071, 1037, 1009, 927, 862, 814.

HRMS (TOF ES+): calc. for $C_{17}H_{19}BrNO$ $(M+H)^+$: 332.0650; found: 332.0643.

$[\alpha]^{20}_{D}$: -41.59, c = 1 $CHCl_3$

HPLC: 2.5 mg/mL in 50/50 IPA/Hex, 2 μL injection, 4.6 x 250mm Chiralcel OD-H, 0.6 mL/min., 5% IPA in hexanes, 254 nm, major 8.80 min., minor 8.13 min., 86% *ee.*

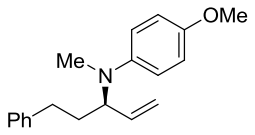

227q

Compound **227q**:

^{1}H NMR ($CDCl_3$, 400 MHz): δ = 7.27-7.23 (m, 2H), 7.19-7.12 (m, 3H), 6.81-6.79 (m, 2H), 6.73-6.71 (m, 2H), 5.48-5.75 (m, 1H), 5.15-5.06 (m, 2H), 4.10-4.05 (m, 1H), 3.75 (s, 3H), 2.73 (s, 3H), 2.68-2.56 (m, 2H), 2.05-1.93 (m, 1H), 1.92-1.85 (m, 1H).

^{13}C NMR ($CDCl_3$, 100 MHz): δ = 152.1, 145.4, 142.2, 137.4, 128.7, 128.5, 126.0, 116.1, 116.0, 114.8, 61.4, 56.0, 33.8, 33.0, 32.5.

IR (film, cm^{-1}): ν = 3062, 3026, 2999, 2944, 2860, 2831, 2803, 1638, 1603, 1509, 1454, 1379, 1243, 1180, 1117, 1038, 921, 815.

HRMS (TOF ES+): calc. for $C_{19}H_{24}NO$ $(M+H)^+$: 282.1858; found: 282.1854.

$[\alpha]^{20}_D$ +33.95:, c = 1, $CHCl_3$

HPLC: 2 mg/mL in 50/50 IPA/Hex, 2 μL injection, 4.6 x 250mm Chiralcel OD-H, 0.6 mL/min., 1% IPA in hexanes, 254 nm, major 12.69 min., minor 14.31 min., 84% *ee.*

5.12 General Procedure for Preparation of *N*-methyl Homophenylalanine Derivatives

Secondary amine **314** was prepared using a modified literature procedure.[159] A round bottom flask was charged with 387 mg (1.37 mmol) of **227q** and 16 mL of acetonitrile. The flask was cooled to 0°C and ammonium cerium (IV) nitrate (3 equiv., 2.26 g, 4.12 mmol) in 8 mL of distilled water was added slowly to the flask which immediately became a deep purple solution and returned to a yellow solution at the end of the addition. At 1 hr, saturated aqueous sodium bicarbonate solution was added to attain a pH of 5-6, followed by addition of anhydrous sodium sulfite until a brown solution with insoluble light brown sludge was visible. The brown solution was collected and the brown solids were washed 4x with 25 mL of ethyl acetate and the combined organics were dried over sodium sulfate, filtered and concentrated. Purification by loading onto a 5 g Isco load cartridge and elution (5-20% MeOH/dichloromethane/1% TEA) onto a 24 g column yielded **314** as a light yellow oil (206 mg, 85%).

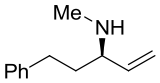

314

Compound **314**:

^{1}H NMR ($CDCl_3$, 400 MHz): δ = 7.26-7.22 (m. 2H), 7.17-7.12 (m, 3H), 5.74-5.65 (m, 1H), 5.32 (dd, *J* = 10.2, 1.3 Hz, 1H), 5.24 (dd, *J* = 17.1, 0.72 Hz, 1H), 3.17-3.12 (m, 1H), 2.69-2.61 (m, 1H), 2.59-2.51 (m, 1H), 2.45 (s, 3H), 2.05-1.96 (m, 1H), 1.88-1.78 (m, 1H).

^{13}C NMR ($CDCl_3$, 100 MHz): δ = 141.3, 136.6, 128.7, 128.6, 126.2, 120.5, 63.5, 35.4, 32.8, 32.0.

IR (film, cm^{-1}): ν = 3316, 3062, 3026, 2935, 2852, 2789, 1945, 1865, 1804, 1742, 1639, 1603, 1495, 1475, 1453, 1414, 1314, 1136, 1114, 1030, 994, 917.

HRMS (TOF ES+): calc. for $C_{12}H_{18}N$ $(M+H)^+$: 176.1439; found: 176.1446.

$[\alpha]^{20}_D$:+3.32, c = 1, MeOH

A flask was charged with 57 mg (0.33 mmol) of **314** and 1.5 mL of anhydrous pyridine. Acetic anhydride (2 equiv., 0.061 mL, 0.65 mmol) and 4-dimethylaminopyridine (5 mol%, 2 mg, 0.016 mmol) was added to the flask. After stirring for 15 hours, the reaction was diluted with saturated sodium bicarbonate and extracted with dichloromethane. The organics were washed with saturated aqueous sodium chloride, dried over magnesium sulfate and concentrated. The crude material was adsorbed onto an Isco 5g load cartridge and purified on a 24 g column (0-100% ethyl acetate/hexanes) yielding acetylated **314** as a clear oil (67 mg, 95%).

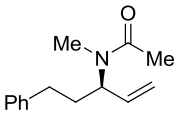

Acetylated **314**

Compound Acetylated **314**:

^{1}H NMR ($CDCl_3$, 400 MHz): 1:1 mixture of rotamers δ = 7.29-7.23 (m, 2H), 7.20-7.13 (m, 3H), 5.76-5.68 (m, 1H), 5.30-5.23 (m, 0.5H), 5.19-5.05 (m, 2H), 4.15-4.08 (m, 0.5H), 2.78 (s, 1.5H), 2.73 (s, 1.5H), 2.65-2.50 (m, 2H), 2.07 (s, 1.5H), 2.03-1.94 (m, 1H), 1.89 (s, 1.5H), 1.89-1.80 (m, 1H).

^{13}C NMR ($CDCl_3$, 100 MHz): δ = 171.3, 171.1, 141.9, 140.7, 136.7, 136.1, 128.8, 128.5, 128.5, 128.4, 126.5, 126.1, 116.8, 116.5, 58.7, 54.2, 33.3, 32.8, 32.4, 32.3, 30.4, 27.3, 22.4, 21.6.

IR (film, cm^{-1}): ν = 3084, 3062, 3026, 2978, 2941, 2862, 1951, 1874, 1739, 1636, 1495, 1454, 1428, 1398, 1360, 1327, 1252, 1125, 1076, 1006, 924.

HRMS (TOF ES+): calc. for $C_{14}H_{20}NO$ $(M+H)^+$: 218.1545; found: 218.1553.

$[\alpha]^{20}_D$:+16.60, c = 1, $CHCl_3$

A flask was charged with 172 mg (0.98 mmol) of **314**, 2.5 mL of THF and 2.5 mL of distilled water. Potassium carbonate (2 equiv., 271 mg, 1.96 mmol) was added to the flask followed by 236 mg (1.1 equiv., 1.08 mmol) of di-*tert*-butyl dicarbonate. After stirring for 15 hours, the reaction was diluted with saturated sodium bicarbonate and extracted with dichloromethane. The organics were washed with brine, dried over sodium sulfate and concentrated. The crude material was adsorbed onto an Isco 5g load cartridge and purified on a 12 g column (0-50% ethyl acetate/hexanes) yielding Boc-protected **314** as a clear oil (232 mg, 86%).

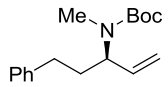

Boc-protected **314**

Compound Boc-protected **314**:

^{1}H NMR ($CDCl_3$, 400 MHz): δ = 7.28-7.24 (m, 2H), 7.18-7.15 (m, 3H), 5.79-5.71 (m, 1H), 5.14-5.06 (m, 2H), 2.69 (bs, 3H), 2.57 (bs, 1H), 1.88-1.82 (m, 2H), 1.44 (bs, 9H).

^{13}C NMR ($CDCl_3$, 100 MHz): δ = 156.3, 137.3, 128.6, 126.1, 116.2, 85.4, 79.7, 33.2, 32.7, 28.7, 27.6.

IR (film, cm^{-1}): ν =3085, 3026, 3004, 2976, 2931, 2865, 1810, 1758, 1687, 1584, 1496, 1478, 1454, 1389, 1365, 1328, 1255, 1166, 1134, 1072, 976, 921, 875.

HRMS (TOF ES+): calc. for $C_{17}H_{25}NO_2$ $(M+Na)^+$: 298.1783; found: 298.1779.

$[\alpha]^{20}_D$: +11.77, c = 1, MeOH

315 was prepared following a literature procedure.[44] A flask was charged with 50 mg (0.18 mmol) of Boc-protected **314**, 0.6 mL of carbon tetrachloride, 0.6 mL of acetonitrile and 0.8 mL of distilled water. The biphasic mixture was stirred vigorously and 155 mg (4 equiv., 0.73 mmol) of sodium periodate was added and allowed to dissolve. $RuCl_3$ hydrate (1.5mg, 4 mol%, 7μmol) was added and stirring was continued for 15 hour. The reaction was diluted with distilled water and extracted with dichloromethane. The organics were dried over sodium sulfate, filtered and concentrated yielding **315** as brown oil (49 mg, 92%).

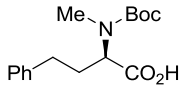

315

<u>Compound **315**:</u>

^{1}H NMR ($CDCl_3$, 400 MHz): δ = 1:1 mixture of rotamers 9.57 (s, 0.65H), 7.27-7.24 (m, 2H), 7.18-7.16 (m, 3H), 4.38-4.31 (m, 0.5H), 3.92-3.87 (m, 0.5H), 2.90 (s, 1.5H), 2.81 (s, 1.5H), 2.68-2.64 (m, 2H), 2.36-2.20 (m, 1H), 2.00-1.86 (m, 1H), 1.51-1.40 (m, 9H).

^{13}C NMR ($CDCl_3$, 100 MHz): δ = 200.3, 200.0, 141.1, 128.5, 126.4, 66.2, 65.2, 53.6, 32.7, 32.4, 32.2, 31.3, 30.8, 28.9, 28.6, 28.5, 28.1, 8.6.

IR (film, cm^{-1}): ν = 3596-2716 br, 3085, 3061, 2975, 2929, 2868, 2716, 1948, 1736, 1688, 1603, 1495, 1479, 1454, 1391, 1366, 1325, 1252, 1153, 1085, 1030, 983, 866.

HRMS (TOF ES-): calc. for $C_{16}H_{22}NO_4$ $(M-H)^-$: 292.1549; found: 292.1553.

$[\alpha]^{20}_D$: +9.79, c = 1 MeOH

316 was prepared following a literature procedure.[44] A flask was charged with 32 mg (0.15 mmol) of acetylated **314**, 0.5 mL of carbon tetrachloride, 0.5 mL of acetonitrile and 0.7 mL of distilled water. The biphasic mixture was stirred vigorously and 126 mg (4 equiv., 0.59 mmol) of sodium periodate was added and allowed to dissolve. $RuCl_3$ hydrate (1.2mg, 4 mol%, 6μmol) was added and stirring was continued for 1 hour. The reaction was diluted with distilled water and extracted with dichloromethane. The organics were dried over sodium sulfate, filtered and concentrated yielding **316** as brown oil (34 mg, 98%).

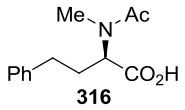

316

<u>Compound **316**:</u>

^{1}H NMR ($CDCl_3$, 400 MHz): δ = 1:1 mixture of rotamers δ = 9.45 (s, 0.5H), 7.30-7.25 (m, 2H), 7.21-7.14 (m, 3H), 5.15-5.11 (m, 0.5H), 4.67-4.63 (m, 0.5H), 2.88 (s, 3H), 2.74-2.61 (m, 1H), 2.59-2.51 (m, 1H), 2.38-2.30 (m, 1H), 2.13 (s, 1.5H), 2.10 (s, 1.5H), 2.04-1.90 (m, 1H).

^{13}C NMR ($CDCl_3$, 100 MHz): δ = 174.4, 172.8, 172.4, 140.9, 140.8, 140.0, 129.0, 128.9, 128.8, 128.6, 128.5, 126.7, 126.5, 126.3, 64.8, 59.5, 56.8, 34.5, 33.0, 32.8, 32.6, 32.0, 31.6, 30.4, 30.2, 28.9, 27.7, 22.0, 21.7, 21.5.

δ = **IR (film, cm^{-1}):** ν = 3677-2259 br, 3084, 3060, 3027, 3001, 2930, 2861, 1728, 1644, 1601, 1495, 1454, 1404, 1322, 1241, 1212, 1173, 1127, 1086, 1029, 1018, 912.

HRMS (TOF ES-): calc. for $C_{13}H_{16}NO_3$ $(M-H)^-$: 234.1130; found: 234.1131.

$[\alpha]^{20}_D$: +8.14, c = 1 MeOH

Compound **317** was prepared following a modified literature procedure.[125] A round bottom flask was charged with 40 mg (0.18 mmol) of acetylated **314**, 1.5 mL of dichloromethane, and 0.37 mL of 2.5 M methanolic NaOH (5 equiv., 0.92 mmol). The flask was cooled to -78°C and subjected to ozonolysis for 30 minutes. The crude reaction was adsorbed onto a 5g Isco load cartridge followed by elution onto a 12g silica column (0-100% EA/Hexanes) resulting in 31 mg (68%) of **317** as a clear oil.

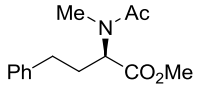

317

Compound **317**:

^{1}H NMR ($CDCl_3$, 400 MHz): 3:1 mixture of rotamers δ = 7.30-7.15 (m, 5H), 5.26-5.22 (m, 0.75H), 4.22-4.19 (m, 0.25H), 3.71 (s, 0.75H), 3.67 (s, 2.25H), 2.87 (s, 2.25H), 2.84 (s, 0.75H), 2.66-2.56 (m, 1H), 2.55-2.51 (m, 1H), 2.33-2.26 (m, 1H), 2.10 (s, 2.25H), 2.01-1.97 (m, 1H), 1.84 (s, 0.75H).

^{13}C NMR ($CDCl_3$, 100 MHz): δ = 172.0, 171.9, 171.7, 171.4, 141.0, 139.9, 128.9, 128.6, 128.5, 126.8, 126.3, 59.3, 56.0, 52.7, 52.4, 32.8, 32.5, 31.8, 30.4, 28.6, 22.1, 21.6.

IR (film, cm^{-1}): ν = 3027, 2952, 2932, 1737, 1650, 1495, 1454, 1434, 1399, 1364, 1327, 1247, 1211, 1169, 1126, 1089, 1013, 912.

HRMS (TOF ES+): calc. for $C_{14}H_{19}NO_3$ $(M+Na)^+$: 272.1263; found: 272.1261.

$[\alpha]^{20}_D$: +11.19, c = 1 MeOH

HPLC: 2.5 mg/mL in 50/50 IPA/Hex, 2 μL injection, 4.6 x 150mm Chiralcel OJ-3, 0.3 mL/min., 8% IPA in hexanes, 210 nm, minor rotamer: major 20.17 min., minor 21.21 min., 83% ee, major rotamer: major 43.69 min., minor 45.07 min., 84% *ee.*

5.13 Additional DYKAT Amination Products of Secondary Racemic Trichloroacetimidates

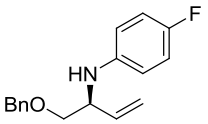

229b

Compound **229b**:

^{1}H NMR (CDCl$_3$, 400 MHz): δ = 7.37-7.27 (m, 5H), 6.84 (t, *J* = 6.7 Hz, 2H), 6.57-6.52 (m, 2H), 5.84-5.76 (m, 1H), 5.30 (dt, *J* = 17.3, 1.3 Hz, 1H), 5.19 (dt, *J* = 10.3, 1.2 Hz, 1H), 4.55 (d, *J* = 12.1 Hz, 1H), 4.54 (d, *J* = 12.1 Hz, 1H), 4.07 (s, NH), 3.97-3.93 (m, 1H), 3.61 (dd, *J* = 9.6, 4.3 Hz, 1H), 3.51 (dd, *J* = 9.6, 6.5 Hz, 1H).

^{13}C NMR (CDCl$_3$, 100 MHz):. δ = 156.1, (d, J_{CF} = 234 Hz), 144.1, 138.0, 137.4, 128.7, 128.1, 128.0, 117.1, 115.8, 115.6, 115.0, 114.9, 73.4, 72.7.

IR (film, cm^{-1}): ν = 3398, 2898, 2858, 1602, 1508, 1453, 1360, 1313, 1215, 1095, 1076, 1027, 992, 922, 819736, 696.

[α]D^{25}: -7.0, *c* = 2, CHCl$_3$

HPLC: 2 mg/mL in 50/50 IPA/Hex, 2 μL injection, 4.6 x 150mm Chiralcel OJ-3, 1 mL/min., 2.5% IPA in hexanes, 254 nm, major 16.2 min., minor 14.4 min., 87% *ee*.

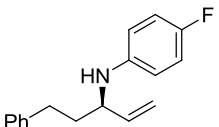

227b

Compound **227b**:

^{1}H NMR (CDCl$_3$, 400 MHz): δ = 7.29-7.24 (m, 2H), 7.21-7.16 (m, 3H), 6.83 (t, *J* = 8.8 Hz, 2H), 6.46 (dd, *J* = 9.0, 4.4 Hz, 2H), 5.78-5.69 (m, 1H), 5.18 (dt, *J* = 17.2, 1.3 Hz, 1H), 5.14 (dt, *J* = 10.3, 1.2 Hz, 1H), 3.74 (q, *J* = 6.1 Hz, 1H), 3.50 (s, NH), 2.73 (t, *J* = 6.9 Hz, 2H), 1.92-1.87 (m, 2H).

^{13}C NMR (CDCl$_3$, 100 MHz): δ = 155.9,(d, J_{CF} = 233Hz), 143.9, 141.8, 139.9, 128.7, 126.2, 115.8, 115.6, 114.5, 114.4, 56.2, 37.4, 32.4.

IR (film, cm^{-1}): ν = 3412, 3083, 3061, 3026, 3003, 2977, 2922, 2857, 1507, 1454, 1313, 1218, 992, 920, 817, 778, 749, 699.

[α]$_D^{25}$ +0.33, *c* = 2, CHCl$_3$

HPLC: 2 mg/mL in 50/50 IPA/Hex, 2 μL injection, 4.6 x 250mm Chiralcel OD-H, 1 mL/min., 2.5% IPA in hexanes, 254 nm, major 16.1 min., minor 11.2 min., 93% *ee*.

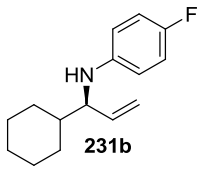

231b

Compound **231b**:

^{1}H NMR (CDCl$_3$, 400 MHz): δ = 6.82 (t, *J* = 8.8 Hz, 1H), 6.49 (dd, *J* = 9.1, 4.4 Hz, 1H), 5.75-5.62 (m, 1H), 5.14 (d, *J* = 2.0 Hz, 1H), 5.11 (dd, *J* = 3.8, 1.5 Hz, 1H), 3.53 (bs, 2H), 1.84-1.62 (m, 5H), 1.48-1.44 (m, 1H), 1.25-1.03 (m, 5H).

^{13}C NMR (CDCl$_3$, 100 MHz): δ = 155.7, (d, J_{CF} = 234 Hz), 144.5, 138.5, 116.1, 115.8, 115.5, 114.3, 114.2, 62.0, 42.9, 29.7, 29.5, 26.7, 26.5, 26.4.

IR (film, cm^{-1}): ν = 3422, 2923, 2851, 1507, 1449, 1315, 1289, 993, 917, 816.

[α]$_D^{25}$ -3.3, *c* = 2, CHCl$_3$

HPLC: 2 mg/mL in 50/50 IPA/Hex, 2 μL injection, 4.6 x 150mm Chiralcel OJ-3, 1 mL/min., 2.5% IPA in hexanes, 254 nm, major 4.2 min., minor 4.5 min., 90% *ee*.

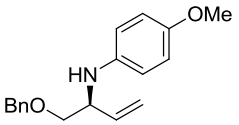

229c

Compound **229c**:

^{1}H NMR ($CDCl_3$, 400 MHz): δ = 7.36-7.27 (m, 5H), 6.74 (d, *J* = 9.0 Hz, 2H), 6.60 (d, *J* = 9.0 Hz, 2H), 5.87-5.79 (m, 1H), 5.31 (dt, *J* = 17.3, 1.3 Hz, 1H), 5.18 (dt, *J* = 10.3, 1.2 Hz, 1H), 4.56 (d, *J* = 12.0 Hz, 1H), 4.52 (d, *J* = 12.0 Hz, 1H), 3.98-3.94 (m, 1H), 3.72 (s, 3H), 3.60 (dd, *J* = 9.5, 4.5 Hz, 1H), 3.53 (dd, *J* = 9.5, 6.4 Hz, 1H).

^{13}C NMR ($CDCl_3$, 100 MHz): δ = 152.7, 141.8, 138.2, 137.9, 128.6, 128.0, 127.9, 116.9, 115.7, 115.0, 73.4, 72.8, 57.2, 56.0.

IR (film, cm^{-1}): ν = 3387, 2931, 2902, 2857, 2832, 1601, 1509, 1463, 1453, 1233, 1178, 1097, 1036, 992, 818, 736, 697.

$[\alpha]_D^{25}$ -11.2, *c* = 2, $CHCl_3$

HPLC: 2 mg/mL in 50/50 IPA/Hex, 2 μL injection, 4.6 x 250mm Chiralcel OD-H, 1 mL/min., 5% IPA in hexanes, 254 nm, major 9.3 min., minor 9.8 min., 80% *ee*.

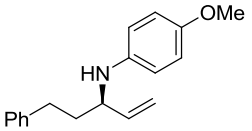

227c

Compound **227c**:

^{1}H NMR ($CDCl_3$, 400 MHz): δ = 7.29-7.25 (m, 2H), 7.20-7.16 (m, 3H), 6.73 (d, *J* = 8.8 Hz, 2H), 6.51 (d, *J* = 8.8 Hz, 2H), 5.78-5.69 (m, 1H), 5.20 (d, *J* = 17.2 Hz, 1H), 5.13 (d, *J* = 10.3 Hz, 1H), 3.75 (q, *J* = 6.7 Hz, 1H), 3.73 (s, 3H), 3.36 (bs, NH), 2.73 (t, *J* = 7.7 Hz, 2H), 1.91-1.85 (m, 2H).

^{13}C NMR ($CDCl_3$, 100 MHz): δ = 152.2, 142.0, 141.7, 140.3, 128.7, 128.6, 126.1, 115.7, 115.0, 114.9, 56.5, 55.9, 37.5, 32.3.

IR (film, cm^{-1}): ν = 3395, 3081, 3061, 3025, 2998, 2932, 2856, 2830, 1602, 1508, 1463, 1453, 1441, 1231, 1178, 1036, 992, 817, 816, 747, 699.

[α]$_D^{25}$ +1.5, *c* = 2, $CHCl_3$

HPLC: 2 mg/mL in 50/50 IPA/Hex, 2 μL injection, 4.6 x 250mm Chiralcel OD-H, 0.6 mL/min., 2.5% IPA in hexanes, 254 nm, major 28.0 min., minor 27.2 min., 89% *ee*.

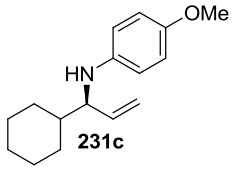

231c

Compound **231c**:

^{1}H NMR ($CDCl_3$, 400 MHz): δ = 6.73 (d, *J* = 8.8 Hz, 2H), 6.53 (d, *J* = 8.8 Hz, 2H), 5.72-5.63, (m, 1H), 5.13 (dt, *J* = 9.4, 1.2 Hz, 1H), 5.11 (dt, *J* = 18.3, 0.96 Hz, 1H), 3.71 (s, 3H), 3.53 (t, *J* = 6.5 Hz, 1H), 3.41 (s, NH), 1.85-1.64 (m, 5H), 1.51-1.44 (m, 1H), 1.28-1.00 (m, 5H).

^{13}C NMR ($CDCl_3$, 100 MHz): δ = 151.9, 142.4, 138.9, 115.9, 115.0, 114.8, 62.3, 56.0, 42.9, 29.7, 29.5, 26.8, 26.6, 26.5.

IR (film, cm^{-1}): ν = 3405, 2922, 2850, 2831, 1509, 1481, 1463, 1448, 1232, 1178, 1038, 994, 915, 815.

[α]$_D^{25}$ -10.7, *c* = 2, $CHCl_3$

HPLC: 2 mg/mL in 50/50 IPA/Hex, 2 μL injection, 4.6 x 150mm Chiralcel OJ-3, 1 mL/min., 2.5% IPA in hexanes, 254 nm, major 9.3 min., minor 8.7 min., 95% *ee*.

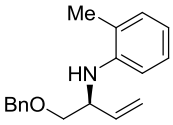

229d

Compound **229d**:

^{1}H NMR (CDCl$_3$, 400 MHz): δ = 7.34-7.30 (m, 5H), 7.05-7.03 (m, 2H), 6.66-6.59 (m, 2H), 5.89-5.81 (m, 1H), 5.32 (d, *J* = 17.3 Hz, 1H), 5.21 (d, *J* = 10.4 Hz, 1H), 4.56 (d, *J* = 12.0 Hz, 1H), 4.55 (d, *J* = 12.0 Hz, 1H), 4.11-4.08 (m, 1H + NH), 3.66-3.57 (m, 2H), 2.15 (s, 3H).

^{13}C NMR (CDCl$_3$, 100 MHz): δ = 145.7, 138.2, 137.7, 130.2, 128.7, 128.0, 127.8, 127.1, 122.6, 117.4, 116.8, 111.3, 73.2, 72.7, 55.9, 17.7.

IR (film, cm^{-1}): ν = 3405, 2895, 2857, 1605, 1586, 1508, 1477, 1448, 1359, 1313, 1262, 1102, 1050, 1026, 989, 920, 744, 715, 697.

[α]$_D^{25}$ -11.3, *c* = 2, CHCl$_3$

HPLC: 2 mg/mL in 50/50 IPA/Hex, 2 μL injection, 4.6 x 150mm Chiralcel OJ-3, 0.6 mL/min., 1% IPA in hexanes, 254 nm, major 22.5 min., minor 24.4 min., 90% *ee*.

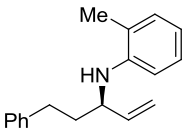

227d

Compound **227d**:

^{1}H NMR ($CDCl_3$, 400 MHz): δ = 7.30-7.26 (m, 2H), 7.21-7.17 (m, 3H), 7.08-7.03 (m, 2H), 6.62 (t, *J* = 7.4 Hz, 1H), 6.51 (d, *J* = 7.9 Hz, 1H), 5.83-5.75 (m, 1H), 5.21 (dt, *J* = 17.2, 1.4 Hz, 1H), 5.13 (dt, *J* = 10.3, 1.2 Hz, 1H), 3.90 (q, *J* = 6.5 Hz, 1H), 3.47 (s, NH), 2.73 (t, *J* = 7.5 Hz, 2H), 2.1 (s, 3H), 1.98-1.94 (m, 2H).

^{13}C NMR ($CDCl_3$, 100 MHz): δ = 145.4, 141.9, 140.0, 130.3, 128.7, 127.1, 126.1, 121.8, 116.9, 115.5, 110.9, 55.4, 37.6, 32.5, 17.7.

IR (film, cm^{-1}): ν = 3434, 3025, 2920, 2854, 1605, 1586, 1509, 1497, 1478, 1447, 1314, 1257, 990, 916, 744, 698, 682.

[α]$_D^{25}$ -8.1, *c* = 2, $CHCl_3$

HPLC: 2 mg/mL in 50/50 IPA/Hex, 2 μL injection, 4.6 x 250mm Chiralcel OD-H, 1 mL/min., 2.5% IPA in hexanes, 254 nm, major 7.9 min., minor 6.4 min., 96% *ee*.

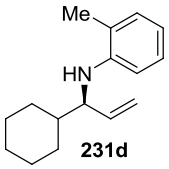

231d

Compound **231d**:

^{1}H NMR ($CDCl_3$, 400 MHz): δ = 7.08-7.01 (m, 2H), 6.61-6.54 (m, 2H), 5.77-5.68 (m, 1H), 5.16 (dt, *J* = 9.2, 1.4 Hz, 1H), 5.14 (dt, *J* = 18.4, 1.2 Hz, 1H), 3.70-3.69 (m, 1H), 3.56 (bs, NH) 2.15 (s, 3H), 1.88-1.74 (m, 5H), 1.69-1.55 (m, 1H), 1.27-1.05 (m, 5H).

^{13}C NMR ($CDCl_3$, 100 MHz): Matches literature compound.[7a]

IR (film, cm^{-1}): ν = 3442, 2922, 1605, 1586, 1509, 1477, 1447, 1315, 1302, 1288, 1254, 1051, 984, 916, 794, 743, 713.

[α]$_D^{25}$ +1.2, *c* = 2, $CHCl_3$

HPLC: 2 mg/mL in 50/50 IPA/Hex, 1 μL injection, 4.6 x 250mm Chiralcel OD-H, 0.6 mL/min., 1% IPA in hexanes, 254 nm, major 8.1 min., minor 7.8 min., 82% *ee*.

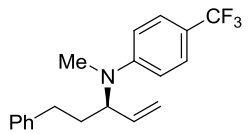

227r

Compound **227r**:

^{1}H NMR ($CDCl_3$, 400 MHz): δ = (2:1 mixture of b/l) Branched : 7.41 (d, *J* = 8.8 Hz, 2H), 7.25-7.22 (m, 2H), 7.19-7.15 (m, 1H), 7.11-7.07 (m, 2H), 6.68 (d, *J* = 8.9 Hz, 2H), 5.82-5.74 (m, 1H), 5.16 (dt, *J* = 10.6, 1.5 Hz, 1H), 5.09 (dt, *J* = 17.3, 1.4 Hz, 1H), 4.33-4.28 (m, 1H), 2.82 (s, 3H), 2.58-2.51 (m, 1H), 2.33 (q, *J* = 7.7 Hz, 1H), 2.04-1.97 (m, 2H).

^{13}C NMR ($CDCl_3$, 100 MHz): δ = 152.7, 141.4, 136.6, 128.7, 128.6, 126.6, 126.5, 126.3, 116.3, 111.9, 111.4, 59.0, 33.9, 32.9, 31.7.

IR (film, cm^{-1}): ν = 3085, 3063, 3027, 2943, 2858, 1616, 1529, 1496, 1478, 1454, 1385, 1329, 1200, 1164, 1111, 1071, 989, 925, 818, 748, 700.

[α]D^{25} +9.0, *c* = 2, $CHCl_3$

HRMS (ESI): calc. for $C_{19}H_{21}NF_3$ $(M+H)^+$: 320.1626; found: 320.1609.

HPLC: 2 mg/mL in 50/50 IPA/Hex, 2 μL injection, 4.6 x 250mm Chiralcel OD-H, 0.6 mL/min., 1% IPA in hexanes, 254 nm, major 10.2 min., minor 10.7 min., 57% *ee*.

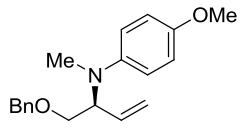

229q

Compound **229q**:

^{1}H NMR ($CDCl_3$, 400 MHz): δ = 7.33-7.25 (m, 5H), 6.81 (d, *J* = 9.0 Hz, 2H), 6.79 (d, *J* = 9.2 Hz, 2H), 5.88-5.80 (m, 1H), 5.20 (dt, *J* = 9.8, 1.4 Hz, 1H), 5.19 (dt, *J* = 18.7, 1.6

Hz, 1H), 4.50 (s, 2H), 4.39-4.35 (m, 1H), 3.75 (s, 3H), 3.67 (dd, J = 9.8, 6.9 Hz, 1H), 3.61 (dd, J = 9.8, 6.4 Hz, 1H), 2.74, (s, 3H).

^{13}C NMR ($CDCl_3$, 100 MHz): δ = 152.3, 145.1, 138.4, 135.2, 128.5, 127.9, 127.8, 117.2, 116.2, 114.7, 73.3, 70.4, 62.0, 56.0, 33.6.

IR (film, cm^{-1}): ν = 3083, 3062, 3030, 2989, 2896, 2861, 2833, 1716, 1640, 1510, 1464, 1454, 1244, 1181, 1105, 1038, 993, 925, 816, 737, 699.

HRMS (ESI): calc. for $C_{19}H_{24}NO_2$ $(M+H)^+$: 298.1807; found: 298.1791.

[α]$_D^{25}$ +2.4, c = 2, $CHCl_3$

HPLC: 2.5 mg/mL in 50/50 IPA/Hex, 2 μL injection, 4.6 x 250mm Chiralcel OD-H, 0.6 mL/min., 1% IPA in hexanes, 254 nm, major 19.9 min., minor 18.7 min., 56% *ee*

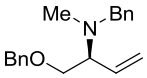

229y

Compound **229y**:

^{1}H NMR ($CDCl_3$, 400 MHz): δ = 7.32-7.21 (m, 10H), 5.90-5.80 (m, 1H), 5.26 (d, J = 10.4 Hz, 1H), 5.20 (d, J = 17.3 Hz, 1H), 4.53 (s, 2H), 3.71-3.65 (m, 2H), 3.57-3.48 (m, 2H), 3.34-3.29 (q, J = 7.3 Hz, 1H), 2.21 (s, 3H).

^{13}C NMR ($CDCl_3$, 100 MHz): δ = 135.3, 129.0, 128.5, 128.4, 127.9, 127.7, 127.0, 118.5, 73.3, 71.4, 65.2, 58.7, 38.5.

IR (film, cm^{-1}): ν = 3085, 3063, 3028, 2975, 2944, 2850, 2791, 1954, 1870, 1811, 1663, 1639, 1605, 1586, 1510, 1494, 1453, 1419, 1363, 1314, 1259, 1207, 1103, 1076, 1038, 1027, 994, 923.

HRMS (ESI): calc. for $C_{19}H_{24}NO$ $(M+H)^+$: 282.1858; found: 282.1846.

[α]$_D^{25}$ -4.4, c = 2, $CHCl_3$

HPLC: 2 mg/mL in 50/50 IPA/Hex, 1 μL injection, 4.6 x 250mm Chiralcel OD-H, 0.15 mL/min., 1% IPA in hexanes, 254 nm, major 41.9 min., minor 40.5 min., 34% *ee*.

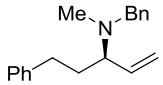

227y

Compound **227y**:

^{1}H NMR ($CDCl_3$, 400 MHz): δ = 7.33-7.13 (m, 10H), 5.86-5.77 (m, 1H), 5.24 (dd, *J* = 10.3, 1.8 Hz, 1H), 5.08 (dd, *J* = 17.2, 1.3 Hz, 1H), 3.64 (d, *J* = 13.3 Hz, 1H), 3.39 (d, *J* = 13.2 Hz, 1H), 2.99 (q, *J* = 7.6 Hz, 1H), 2.69-2.64 (m, 1H), 2.15 (s, 3H), 2.03-1.94 (m, 1H), 1.81-1.72 (m, 1H).

^{13}C NMR ($CDCl_3$, 100 MHz): δ = 142.8, 140.2, 136.7, 129.0, 128.7, 128.5, 128.4, 126.9, 125.9, 117.9, 65.8, 58.2, 37.6, 34.4, 32.9.

IR (film, cm^{-1}): ν = 3083, 3062, 3026, 2939, 2851, 2790, 1945, 1869, 1803, 1718, 1636, 1603, 1495, 1454, 1418, 1367, 1316, 1259, 1214, 1155, 1125, 1076, 1028, 998, 921, 740, 698.

HRMS (ESI): calc. for $C_{19}H_{24}N$ $(M+H)^+$: 266.1909; found: 266.1885.

[α]D^{25} -3.2, *c* = 2, $CHCl_3$

HPLC: 2 mg/mL in 50/50 IPA/Hex, 1 μL injection, 4.6 x 150mm Chiralcel OJ-3, 0.6 mL/min., 1% IPA in hexanes, 254 nm, major 8.6 min., minor 7.5 min., 53% *ee*.

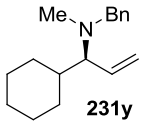

231y

Compound **231y**:

^{1}H NMR ($CDCl_3$, 400 MHz): δ = 7.32-7.18 (m, 5H), 5.64 (dt, *J* = 17.1, 9.9 Hz, 1H), 5.23 (dd, *J* = 9.8, 2.0 Hz, 1H), 4.96 (dd, *J* = 17.2, 2.0 Hz, 1H), 3.60 (d, *J* = 13.5 Hz, 1H), 3.33 (d, *J* = 13.5 Hz, 1H), 2.51 (t, *J* = 9.6 Hz, 1H), 2.16 (d, *J* = 13.2 Hz, 1H), 2.09 (s, 3H), 1.75-1.64 (m, 4H), 1.52-1.44 (m, 1H), 1.23-1.12 (m, 3H), 0.94-0.87 (m, 1H), 0.85-0.74 (m, 1H).

^{13}C NMR ($CDCl_3$, 100 MHz): δ = 140.7, 135.5, 128.9, 128.3, 126.7, 118.4, 72.1, 58.4, 38.8, 37.5, 30.9, 30.7, 27.1, 26.6.

IR (film, cm^{-1}): ν = 3083, 3064, 3027, 2973, 2922, 2849, 2791, 1723, 1494, 1450, 1417, 1366, 1261, 1230, 1125, 1021, 977, 919, 833, 740, 699.

HRMS (ESI): calc. for $C_{17}H_{26}N$ $(M+H)^+$: 244.2065; found: 244.2048.

[α]D^{25} -35.8, *c* =2, $CHCl_3$

HPLC: 2 mg/mL in 50/50 IPA/Hex, 1 μL injection, 4.6 x 150mm Chiralcel OJ-3, 0.6 mL/min., 1% IPA in hexanes, 254 nm, major 8.6 min., minor 7.5 min., 53% *ee*.

5.14 Preparation of Allylic Trichloroacetimidate **377**

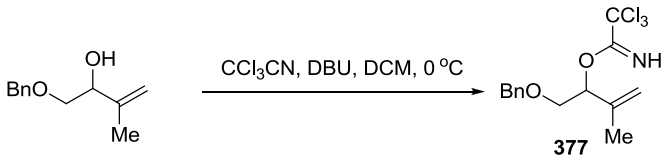

A 100 mL oven-dried Schlenk flask was charged with alcohol (0.850 g, 4.42 mmol, 1 equiv) and dry dichoromethane (25 mL). Trichloroacetonitrile (1.30 mL, 13.3 mmol, 3 equiv) was added. The resulting solution was cooled to 0 ^{O}C, and DBU was added (0.17 mL, 1.11 mmol, 0.25 equiv). The reaction mixture was allowed to warm to room temperature and stir overnight. The mixture was concentrated *in vacuo*, and the resulting

residue was purified by silica gel flash chromatography (4/1 hexane/ethyl acetate + 1% triethylamine) to provide **377** (1.36 g, 91%) as a brown oil.

^{1}H NMR ($CDCl_3$, 500 MHz): δ = 8.34 (s, NH), 7.33 – 7.25 (m, 5H), 5.49 (dd, *J* = 6.8, 3.9 Hz, 1H), 5.14 (s, 1H), 5.03 – 4.97 (m, 1H), 4.61 (s, 2H), 3.83 – 3.59 (m, 2H), 1.80 (s, 3H).

^{13}C NMR ($CDCl_3$, 126 MHz): δ = 162.0, 140.6, 138.3, 128.6, 127.8, 127.8, 113.9, 81.0, 73.5, 70.8, 19.4

IR (film, cm^{-1}): ν = 3344, 3078, 3064, 3031, 2920, 1702, 1665, 1496, 1453, 1319, 1285, 1076, 907, 794

HRMS (TOF ESI+): calc. for $C_{14}H_{16}Cl_3NO_2Na$ (M+Na): 358.0144; found: 358.0148.

5.15 General Procedure for Asymmetric Amination of Branched Allylic Trichloroacetimidates with 2-Aminobenzaldehyde **183z**

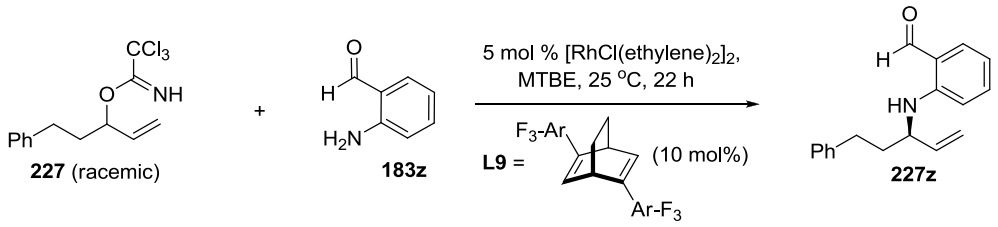

A 10 mL oven-dried Schlenk flask was charged with $[RhCl(ethylene)_2]_2$ (3.9 mg, 10 μmol, 5 mol%) and (1*S*,4*S*)-2,5-bis(3,4,5-trifluorophenyl))bicyclo[2.2.2]octa-2,5-diene (**L9**) (7.3 mg, 20 μmol, 10 mol%) in a glove box. The flask was sealed, removed from the glove box, MTBE (0.5 mL) added and stirred under nitrogen for 15 min resulting in a dark red solution. A separate 10 mL Schlenk flask was charged with allylic imidate **227** (61 mg, 0.20 mmol, 1.0 equiv), MTBE (0.5 mL) and 2-aminobenzaldehyde **183z** (36 mg, 0.3 mmol, 1.5 equiv). The rhodium catalyst solution was transferred to the flask

containing the solution of **227** and **183z** using a glass pipette. The mixture was stirred at room temperature under nitrogen. Reaction progress was monitored by TLC at 22 h. The crude reaction was purified by adsorbing directly onto a dry 5g Teledyne Isco silica cartridge using vacuum followed by elution onto a pre-equilibrated 24g silica flash column (0 → 20% diethyl ether/hexane) providing allylic amine **227z** (34 mg, 64%, 84% *ee*, branched/linear > 99:1) as bright yellow oil.

Compound **227z:**

^{1}H NMR ($CDCl_3$, 400 MHz): δ = 9.91 (s, 1H), 8.55 (d, *J* = 6.2 Hz, NH), 7.53 (d, *J* = 7.5 Hz, 1H), 7.43 – 7.28 (m, 3H), 7.26-7.22 (m, 3H), 6.74 (t, *J* = 7.4 Hz, 1H), 6.64 (d, *J* = 8.6 Hz, 1H), 5.85 (ddd, *J* = 16.5, 10.3, 5.9 Hz, 1H), 5.27 (d, *J* = 17.2 Hz, 1H), 5.22 (d, *J* = 10.3 Hz, 1H), 4.01 (p, *J* = 6.6 Hz, 1H), 2.97 – 2.69 (m, 2H), 2.06 (dd, *J* = 14.8, 7.4 Hz, 2H).

^{13}C NMR ($CDCl_3$, 100 MHz): δ = 194.3, 150.5, 141.5, 138.8, 136.9, 135.9, 128.7, 128.7, 126.2, 118.7, 115.8, 115.2, 112.1, 54.4, 37.3, 32.3.

IR (film, cm^{-1}): ν = 3316, 3083, 3061, 3026, 2944, 2921, 2861, 2830, 2746, 1704, 1652, 1608, 1579, 1518, 1461, 1429, 1399, 1333, 1201, 1158, 1041, 992, 921, 879, 799, 751, 701.

HRMS (ESI): calc. for $C_{18}H_{20}NO$ (M+H): 266.1545; found: 266.1516.

HPLC: 2.5mg/mL in 50/50 IPA/Hex, 2 μL injection, 4.6 x 250mm Chiralcel OD-H, 1 mL/min., 5% IPA in hexanes, 254 nm, major 5.55 min., minor 5.96 min., 84% *ee*.

$[\alpha]^{20}_D$: +1.8, c = 2.0, $CHCl_3$.

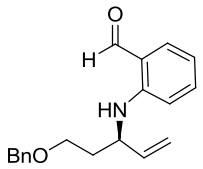

310z

Compound **310z:**

^{1}H NMR ($CDCl_3$, 400 MHz): δ = 9.80 (s, 1H), 8.41 (d, *J* = 7.1 Hz, NH), 7.50 – 7.39 (m, 1H), 7.36 – 7.30 (m, 1H), 7.29 – 7.24 (m, 2H), 6.72 – 6.64 (m, 1H), 5.77 (ddd, *J* = 17.1, 10.3, 5.8 Hz, 1H), 4.49 (d, *J* = 12.0 Hz, 1H), 4.45 (d, *J* = 12.0 Hz, 1H), 4.30 – 4.15 (m, 1H), 3.69 – 3.45 (m, 1H), 2.12 – 1.74 (m, 1H).

^{13}C NMR ($CDCl_3$, 100 MHz): δ = 194.3, 150.6, 138.7, 138.5, 136.9, 135.9, 128.6, 127.9, 127.8, 118.7, 115.6, 115.2, 112.1, 73.3, 66.6, 52.1, 35.9.

IR (film, cm^{-1}): ν = 3314, 3084, 3063, 3030, 3007, 2943,2918, 2860, 2745, 1651, 1608, 1579, 1518, 1461, 1432, 1399, 1332, 1200, 1160, 1103, 1041, 1028, 992, 923, 880, 806.

HRMS (ESI): calc. for $C_{19}H_{21}NO_2Na$ (M+Na): 318.1470; found: 318.1460.

HPLC: 2.5mg/mL in 50/50 IPA/Hex, 2 μL injection, 4.6 x 250mm Chiralcel OJ-3, 1 mL/min., 2.5% IPA in hexanes, 254 nm, major 9.64 min., minor 11.53 min., 87% *ee*.

$[\alpha]^{20}_D$: -2.1, c = 2.0, $CHCl_3$.

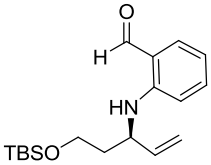

223z

Compound **223z:**

^{1}H NMR ($CDCl_3$, 400 MHz): δ = 9.81 – 9.80 (m, 1H), 8.36 (d, *J* = 7.0 Hz, NH), 7.43 (dd, *J* = 7.7, 1.6 Hz, 1H), 7.32 (ddd, *J* = 8.3, 7.1, 1.3 Hz, 1H), 6.70 (d, *J* = 8.6 Hz, 1H), 6.68 – 6.62 (m, 1H), 5.79 (ddd, *J* = 17.2, 10.3, 5.8 Hz, 1H), 5.20 (dt, *J* = 17.2, 1.3 Hz, 1H), 5.12 (dt, *J* = 10.3, 1.3 Hz, 1H), 4.28 – 4.17 (m, 1H), 3.78 – 3.72 (m, 1H), 3.72 – 3.67 (m, 1H), 1.87 (dd, *J* = 7.2, 1.8 Hz, 1H), 1.83 (dd, *J* = 5.8, 1.8 Hz, 1H), 0.85 (s, 9H), -0.02 (d, *J* = 11.8 Hz, 6H).

^{13}C NMR ($CDCl_3$, 100 MHz): δ = 194.3, 150.6, 138.9, 136.8, 135.9, 118.6, 115.5, 115.1, 112.2, 59.5, 51.6, 38.7, 26.1, 18.5, -5.2, -5.3.

IR (film, cm^{-1}): ν = 3314, 3082, 2953, 2929, 2857, 2823, 2741, 1741, 1654, 1610, 1580, 1519, 1462, 1434, 1397, 1332, 1255, 1199, 1160, 1102, 1007, 990, 938, 923, 880, 836, 796.

HRMS (ESI): calc. for $C_{18}H_{30}NO_2Si$ (M+H): 320.2046; found: 320.2027.

HPLC: Could not separate enantiomers (*ee* was based on the hydroacylation step).

$[\alpha]^{20}_D$: -17.9, c = 2.0, $CHCl_3$.

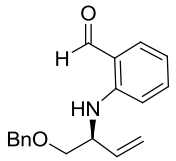

229z

Compound **229z:**

^{1}H NMR ($CDCl_3$, 400 MHz): δ 9.87 – 9.81 (m, 1H), 8.65 (s, NH), 7.46 (dd, *J* = 7.7, 1.6 Hz, 1H), 7.40 – 7.25 (m, 6H), 6.71 – 6.63 (m, 2H), 5.87 (ddd, *J* = 17.3, 10.4, 5.5 Hz, 1H), 5.30 (dt, *J* = 17.3, 1.3 Hz, 1H), 5.21 (dt, *J* = 10.4, 1.3 Hz, 1H), 4.60 (s, 2H), 4.27 – 4.16 (m, 1H), 3.66 – 3.57 (m, 2H).

^{13}C NMR ($CDCl_3$, 100 MHz): δ 194.2, 150.3, 138.1, 136.9, 136.2, 135.8, 128.7, 127.9, 119.0, 117.0, 115.4, 112.1, 73.7, 72.6, 55.2.

IR (film, cm^{-1}): 3316, 3055, 3064, 3030, 2982, 2859, 2744, 1730, 1654, 1608, 1576, 1518, 1461, 1432, 1399, 1361, 1330, 1264, 1200, 1160, 1106, 1042, 1028, 992, 925, 877, 856, 797.

HRMS (ESI): calc. for $C_{18}H_{20}NO_2$ (M+H): 282.1494; found: 282.1489.

HPLC: 2.5 mg/mL in 50/50 IPA/Hex, 2 μL injection, 4.6 x 250mm Chiralcel OD-H, 1 mL/min., 2.5% IPA in hexanes, 254 nm, major 9.68 min., minor 8.71 min., 86% *ee*.
$[\alpha]^{20}_{D}$: -54.9, c = 2.0, $CHCl_3$.

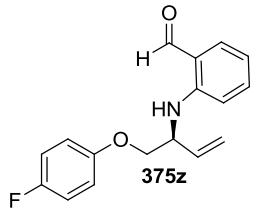

375z

Compound **375z:**

^{1}H NMR ($CDCl_3$, 400 MHz): δ = 9.84 (d, *J* = 0.5 Hz, 1H), 8.71 (d, *J* = 6.7 Hz, NH), 7.48 (dd, *J* = 7.9, 1.7 Hz, 1H), 7.41 – 7.32 (m, 1H), 6.99 – 6.92 (m, 2H), 6.90 – 6.84 (m, 2H), 6.75 – 6.69 (m, 2H), 5.96 (ddd, *J* = 17.2, 10.4, 5.5 Hz, 1H), 5.35 (dt, *J* = 17.5, 1.2Hz, 1H), 5.32 (dt, *J* = 4.08 (s, 1H), 4.06 (s, 1H).

^{13}C NMR ($CDCl_3$, 100 MHz): δ = 194.4, 157.8 (d, J_{CF} = 235 Hz), 154.9, 150.2, 136.9, 135.9, 135.5, 119.1, 117.6, 116.3, 116.2, 116.0, 115.7, 112.0, 71.2, 54.5.

IR (film, cm^{-1}): ν = 3311, 3082, 2927, 2867, 2828, 2747, 1652, 1608, 1578, 1519, 1504, 1461, 1433, 1399, 1330, 1293, 1246, 1201, 1160, 1097, 1042, 990, 928, 871, 827, 798.

HRMS (ESI): calc. for $C_{17}H_{17}NO_2F$ (M+H): 286.1243; found: 286.1238.

HPLC: 2 mg/mL in 50/50 IPA/Hex, 2 μL injection, 4.6 x 250mm Chiralcel OD-H, 1 mL/min., 2.5% IPA in hexanes, 254 nm, major 10.65 min., minor 8.60 min., 80% *ee*.

$[\alpha]^{20}_{D}$: -40.7, c = 2.0, $CHCl_3$.

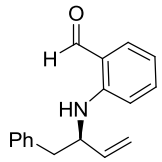

230z

Compound **230z**:

^{1}H NMR ($CDCl_3$, 400 MHz): δ = 9.79 (d, *J* = 0.5 Hz, 1H), 8.52 (d, *J* = 6.5 Hz, NH), 7.42 (dd, *J* = 7.7, 1.6 Hz, 1H), 7.33 – 7.24 (m, 5H), 7.23 – 7.18 (m, 1H), 6.68 – 6.63 (m, 1H), 6.62 (d, *J* = 9.2 Hz, 1H), 5.82 (ddd, *J* = 17.2, 10.3, 5.6 Hz, 1H), 5.15(dt, *J* =17.2, 1.3 Hz, 1H), 5.13 (dt, *J* = 10.4, 1.2 Hz, 1H), 4.28 – 4.16 (m, 1H), 2.99 (dd, *J* = 11.3, 4.7 Hz, 1H), 2.95 (dd, *J* = 11.3, 4.3 Hz, 1H).

^{13}C NMR ($CDCl_3$, 100 MHz): δ = 194.2, 150.2, 138.2, 137.7, 136.8, 135.8, 129.8, 128.6, 126.8, 118.7, 115.9, 115.2, 112.1, 56.6, 42.3.

IR (film, cm^{-1}): ν = 3316, 3084, 3062, 3028, 2924, 2855, 2827, 2744, 1654, 1608, 1578, 1518, 1460, 1429, 1398, 1331, 1250, 1199, 1183, 1158, 1110, 1042, 992, 923, 884, 839, 784.

HRMS (ESI): calc. for $C_{17}H_{18}NO$ (M+H): 252.1388; found: 252.1394.

HPLC: 2 mg/mL in 50/50 IPA/Hex, 2 μL injection, 4.6 x 250mm Chiralcel OD-H, 1 mL/min., 2.5% IPA in hexanes, 254 nm, major 8.71 min., minor 6.56 min., 92% *ee*.

$[\alpha]^{20}_D$: +73.0, c = 2.0, $CHCl_3$.

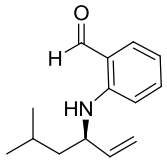

311z

Compound **311z:**

^{1}H NMR ($CDCl_3$, 400 MHz) δ = 9.81 (s, 1H), 8.34 (s, NH), 7.44 (dd, *J* = 8.0, 1.6 Hz, 1H), 7.33 (dd, *J* = 8.3, 7.3 Hz, 1H), 6.71 – 6.58 (m, 2H), 5.17 (dd, *J* = 17.2, 1.2 Hz, 1H), 5.10 (dd, *J* = 10.3, 1.1 Hz, 1H), 4.04 – 3.93 (m, 1H), 1.80 (td, *J* = 13.3, 6.7 Hz, 1H), 1.64

– 1.55 (m, 1H), 1.48 (dt, *J* = 13.8, 7.0 Hz, 1H), 0.96 (d, *J* = 6.6 Hz, 3H), 0.89 (d, *J* = 6.6 Hz, 3H).

^{13}C NMR ($CDCl_3$, 100 MHz) δ = 194.3, 150.6, 139.4, 136.9, 135.9, 118.6, 115.2, 115.0, 112.0, 53.5, 45.1, 24.9, 23.0, 22.6.

IR (film, cm^{-1}): 3319, 3083, 2957, 2926, 2869, 2822, 2743, 1734, 1655, 1580, 1519, 1462, 1428, 1333, 1265, 1200, 1159, 1114, 1042, 991, 921, 845, 789, 751, 711, 663.

HRMS (ESI): calc. for $C_{14}H_{20}NO$ (M+H): 218.1545; found: 218.1557.

HPLC: 2.5mg/mL in 50/50 IPA/Hex, 2 μL injection, 4.6 x 250mm Chiralcel OD-H, 1 mL/min., 1% IPA in hexanes, 254 nm, major 5.90 min., minor 4.81 min., 80% *ee*.

$[\alpha]^{20}_{D}$: -62.6, c = 2.0, $CHCl_3$.

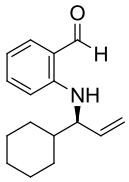

231z

Compound **231z:**

^{1}H NMR ($CDCl_3$, 400 MHz): δ = 9.81 (s, 1H), 8.56 (d, *J* = 6.2 Hz, NH), 7.43 (dd, *J* = 7.9, 1.6 Hz, 1H), 7.36 – 7.26 (m, 1H), 6.63 (dd, *J* = 8.4, 5.6 Hz, 1H), 5.73 (ddd, *J* = 10.9, 9.9, 6.2 Hz, 1H), 5.18 – 5.09 (m, 1H), 3.79 (dd, *J* = 12.7, 6.4 Hz, 1H), 1.92 – 1.62 (m, 3H), 1.62 – 1.53 (m, 1H), 1.32 – 1.03 (m, 3H).

^{13}C NMR ($CDCl_3$, 100 MHz): δ = 194.3, 137.4, 136.9, 135.8, 116.2, 114.8, 112.0, 60.4, 42.7, 29.7, 29.2, 26.6, 26.5, 26.5.

IR (film, cm^{-1}): ν = 3316, 3080, 2927, 2853, 2740, 1655, 1609, 1579, 1519, 1461, 1431, 1398, 1334, 1201, 1158, 1041, 994, 921, 876, 812, 750, 707, 663.

HRMS (ESI): calc. for $C_{16}H_{21}NO$ (M+H): 244.1701; found 244.1705.

HPLC: 2.5 mg/mL in 50/50 IPA/Hex, 2 μL injection, 4.6 x 150mm Chiralcel OJ-3, 1 mL/min., 2.5% IPA in hexanes, 254 nm, major 2.74 min., minor 3.02 min., 80% *ee*.

$[\alpha]^{20}_{D}$: -32.9, c = 2.0, $CHCl_3$.

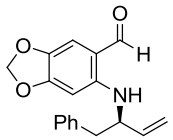

230za

Compound **230za:**

^{1}H NMR ($CDCl_3$, 500 MHz): δ = 9.51 (s, 1H), 8.99 (d, *J* = 6.5 Hz, NH), 7.31 – 7.25 (m, 3H), 7.22 – 7.16 (m, 1H), 6.77 (s, 1H), 6.13 (s, 1H), 5.87 (s, 2H), 5.83 – 5.73 (m, 1H), 5.17 – 5.09 (m, 2H), 4.10 (p, *J* = 6.8 Hz, 1H), 3.00 – 2.88 (m, 2H).

^{13}C NMR ($CDCl_3$, 126 MHz): δ = 190.7, 154.7, 150.0, 138.4, 138.2, 137.7, 129.8, 128.6, 126.9, 116.0, 112.7, 111.7, 101.6, 92.6, 57.3, 42.3.

IR (film, cm^{-1}): ν = 3282, 3087, 3064, 3027, 2919, 2850, 2741, 1650, 1599, 1516, 1474, 1451, 1396, 1372, 1279, 1231, 1175, 1084, 1040, 992, 937, 860, 816, 794.

HRMS (ESI): calc. for $C_{18}H_{18}NO_3$ (M+H): 296.1287; found: 296.1275.

HPLC: 2.5mg/mL in 50/50 IPA/Hex, 2 μL injection, 4.6 x 150mm Chiralcel OJ-3, 1 mL/min., 10% IPA in hexanes, 254 nm, major 30.69 min., minor 27.93 min., 94 % *ee*.

$[\alpha]^{20}_{D}$: +28.1, c = 2.0, $CHCl_3$.

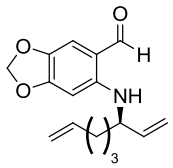

376za

Compound **376za:**

^{1}H NMR ($CDCl_3$, 400 MHz): δ = 9.52 (s, 1H), 8.88 (d, *J* = 6.5 Hz, NH), 6.79 (d, *J* = 3.4 Hz, 1H), 6.17 (s, 1H), 5.89 (dd, *J* = 3.6, 1.2 Hz, 2H), 5.84 – 5.66 (m, 2H), 5.16(dt, J = 17.2, 1.2 Hz, 1H), 5.12 (dt, J = 11.5, 1.2 Hz, 1H), 5.00 (ddd, *J* = 17.1, 3.5, 1.6 Hz, 1H), 4.94 (ddt, *J* = 10.2, 2.1, 1.2 Hz, 1H), 3.82 (p, *J* = 6.6 Hz, 1H), 2.22 – 1.93 (m, 2H), 1.73 – 1.63 (m, 2H), 1.57 – 1.45 (m, 2H).

^{13}C NMR ($CDCl_3$, 100 MHz): δ = 190.7, 154.8, 150.4, 139.0, 138.5, 138.3, 115.7, 115.1, 112.7, 111.5, 101.6, 92.5, 55.8, 35.1, 33.7, 25.2.

IR (film, cm^{-1}): ν = 3277, 3077, 3002, 2977, 2934, 2859, 2739, 1642, 1598, 1515, 1473, 1450, 1397, 1371, 1277, 1228, 1170, 1081, 1040, 993, 938, 920, 861, 817, 795.

HRMS (ESI): calc. for $C_{16}H_{20}NO_3$ (M+H): 274.1443; found: 274.1438.

HPLC: 2.5mg/mL in 50/50 IPA/Hex, 2 μL injection, 4.6 x 250mm Chiralcel OD-H, 1 mL/min., 1% IPA in hexanes, 254 nm, major 8.90 min., minor 8.40 min., 84% *ee*.

$[\alpha]^{20}_D$: -65.2, c = 2.0, $CHCl_3$.

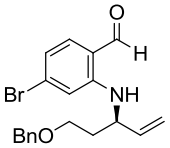

310zb

Compound **310zb:**

^{1}H NMR ($CDCl_3$, 400 MHz): δ = 9.74 (s, 1H), 8.49 (d, *J* = 6.4 Hz, NH), 7.33 – 7.24 (m, 3H), 6.87 (s, 1H), 6.79 (d, *J* = 8.3 Hz, 1H), 5.84 – 5.64 (m, 1H), 5.18 (d, *J* = 18.9 Hz, 1H), 5.14 (d, *J* = 11.0 Hz, 1H), 4.56 – 4.42 (m, 1H), 4.29 – 4.12 (m, 1H), 3.56 (t, *J* = 5.4 Hz, 1H), 2.10 – 1.79 (m, 1H).

^{13}C NMR ($CDCl_3$, 100 MHz): δ = 193.4, 138.4, 138.0, 131.7, 128.6, 128.0, 127.8, 126.9, 118.6, 117.5, 116.0, 115.1, 73.3, 66.4, 52.3, 35.8.

IR (film, cm^{-1}): ν = 3313, 3063, 2936, 2866, 1726, 1657, 1599, 1570, 1505, 1451, 1434, 1314, 1262, 1177, 1104, 1095, 1069, 1027, 905, 815, 804, 788, 734, 709.

HRMS (ESI): calc. for $C_{19}H_{21}BrNO_2$ (M+H): 374.0756; found: 374.0768.

HPLC: 2.5mg/mL in 50/50 IPA/Hex, 2 μL injection, 4.6 x 250mm Chiralcel OD-H, 1 mL/min., 2.5% IPA in hexanes, 254 nm, major 7.68 min., minor 6.86 min., 93% *ee.*

[α]^{20}D: -2.0, c = 2.0, $CHCl_3$.

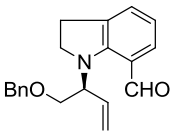

229zc

Compound **229zc:**

^{1}H NMR ($CDCl_3$, 500 MHz): δ = 9.89 (s, 1H), 7.41 (d, *J* = 7.9 Hz, 1H), 7.33 – 7.27 (m, 2H), 7.25 (dt, *J* = 6.2, 2.4 Hz, 4H), 7.14 (td, *J* = 7.1, 1.3 Hz, 1H), 6.69 – 6.62 (m, 1H), 5.77 (ddd, *J* = 17.4, 10.6, 5.3 Hz, 1H), 5.22 – 5.13 (m, 3H), 4.59 – 4.52 (m, 1H), 4.51 (d, *J* = 12.1 Hz, 1H), 3.79 – 3.70 (m, 1H), 3.70 – 3.59 (m, 3H), 3.01 (t, *J* = 8.9 Hz, 2H).

^{13}C NMR ($CDCl_3$, 126 MHz): δ = 190.6, 153.4, 138.2, 133.7, 133.3, 132.1, 129.3, 128.6, 127.9, 127.8, 118.9, 118.2, 117.2, 73.1, 70.5, 60.4, 47.6, 28.0.

IR (film, cm^{-1}): ν = 3064, 3029, 2857, 1675, 1612, 1561, 1487, 1454, 1417, 1361, 1278, 1200, 1101, 994, 946, 925.

HRMS (ESI): calc. for $C_{20}H_{22}NO_2$ (M+H): 308.1651; found: 308.1633.

HPLC: 2.5mg/mL in 50/50 IPA/Hex, 2 μL injection, 4.6 x 250mm Chiralcel OD-H, 1 mL/min., 2.5% IPA in hexanes, 254 nm, major 13.34 min., minor 14.278 min., 88 % *ee*.

[α]^{20}D: +79.8, c = 2.0, $CHCl_3$.

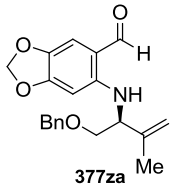

377za

Compound **377za:**

^{1}H NMR ($CDCl_3$, 500 MHz): 9.57 (s, 1H), 9.19 (s, NH), 7.35 (m, 4H), 7.27 (m, 1H), 6.81 (s, 1H), 6.12 (s, 1H), 5.89 (dd, *J* = 4.5, 1.1 Hz, 2H), 5.02 (s, 1H), 4.97 (s, 1H), 4.60 (s, 2H), 4.01 (q, *J* = 6.0 Hz, 1H), 3.68 – 3.55 (m, 2H), 1.71 (s, 3H).

^{13}C NMR ($CDCl_3$, 126 MHz): δ = 190.7, 154.7, 150.2, 142.9, 138.5, 138.1, 128.6, 128.0, 127.9, 113.9, 112.8, 111.9, 101.6, 92.7, 73.7, 72.0, 59.3, 19.3.

IR (film, cm^{-1}): ν = 3295, 2978, 2908, 2867, 2366, 2357, 2338, 1650, 1598, 1516, 1475, 1373, 1278, 1232, 1110, 1040, 938, 911, 808, 776, 743.

HRMS (TOF ESI+): calc. for $C_{20}H_{21}NO_4Na$ (M+Na): 362.1368; found: 362.1370.

HPLC: 2.5mg/mL in 50/50 IPA/Hex, 2 μL injection, 4.6 x 150mm Chiralcel OD-H, 1 mL/min., 5% IPA in hexanes, 254 nm, major 11.03 min., minor 11.97 min., 13 % *ee.*

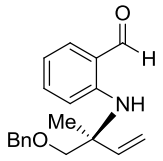

390

Compound **390:**

^{1}H NMR ($CDCl_3$, 400 MHz): δ = 9.82 (d, *J* = 0.5 Hz, 1H), 8.98 (s, NH), 7.44 (dd, *J* = 7.7, 1.7 Hz, 1H), 7.42 – 7.37 (m, 2H), 7.36 – 7.30 (m, 2H), 7.30 – 7.19 (m, 2H), 6.83 (d, *J* = 8.6 Hz, 1H), 6.64 (ddd, *J* = 7.9, 7.1, 0.9 Hz, 1H), 6.03 – 5.92 (m, 1H), 5.26 (dd, *J* = 3.7,

0.8 Hz, 1H), 5.22 (dd, *J* = 3.3, 0.8 Hz, 1H), 4.67 (d, *J* = 12.2 Hz, 1H), 4.61 (d, *J* = 12.2 Hz, 1H), 3.49 (d, *J* = 9.1 Hz, 1H), 3.41 (d, *J* = 9.0 Hz, 1H), 1.52 (s, 3H).

^{13}C NMR ($CDCl_3$, 100 MHz): δ = 194.2, 149.7, 141.7, 138.3, 137.3, 134.8, 128.6, 127.9, 127.8, 119.6, 116.1, 114.9, 114.6, 77.4, 73.8, 58.0, 21.4.

IR (film, cm^{-1}): ν = 3300, 3086, 3061, 3029, 3005, 2982, 2937, 2858, 2743, 1655, 1608, 1579, 1520, 1460, 1433, 1401, 1333, 1272, 1248, 1199, 1162, 1114, 1097, 1044, 999, 926, 874, 810, 750, 698, 659.

HRMS (ESI): calc. for $C_{19}H_{21}NO_2Na$ (M+Na): 318.1470; found: 318.1462.

HPLC: 2.5mg/mL in 50/50 IPA/Hex, 2 μL injection, 4.6 x 150mm Chiralcel OJ-3, 1 mL/min., 5% IPA in hexanes, 254 nm, major 9.35 min., minor 12.08 min., 96% *ee*.

$[\alpha]^{20}_D$: -45.7, c = 2.0, $CHCl_3$.

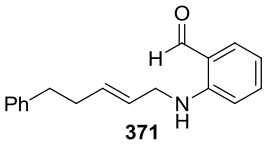

371

Compound **371:**

^{1}H NMR ($CDCl_3$, 400 MHz): δ = 9.82 – 9.80 (m, 1H), 8.36 (s, NH), 7.45 (dd, *J* = 7.7, 1.6 Hz, 1H), 7.36 (ddd, *J* = 7.2, 4.4, 1.2 Hz, 1H), 7.29 – 7.22 (m, 2H), 7.20 – 7.12 (m,3H), 6.74 – 6.58 (m, 2H), 5.80 – 5.64 (m, 1H), 5.55 (dtt, *J* = 15.4, 5.5, 1.3 Hz, 1H), 3.80 (tt, *J* = 21.7, 10.9 Hz, 1H), 2.75 – 2.59 (m, 1H), 2.36 (td, *J* = 7.7, 1.0 Hz, 1H).

^{13}C NMR ($CDCl_3$, 100 MHz): δ = 194.2, 150.8, 141.9, 136.9, 135.9, 132.5, 128.7, 128.5, 126.4, 126.04, 118.7, 115.1, 111.4, 44.5, 35.8, 34.3.

IR (film, cm^{-1}): ν = 3334, 3083, 3061, 3026, 2918, 2847, 2743, 1655, 1609, 1577, 1519, 1457, 1429, 1398, 1332, 1199, 1160, 1042, 970, 870.

HRMS (ESI): calc. for $C_{18}H_{19}NONa$ (M+Na): 288.1364; found: 288.1368.

5.16 General Procedure for Intramolecular Hydroacylation of Allylic Arylamines Containing *ortho*-Aldehyde Functionality

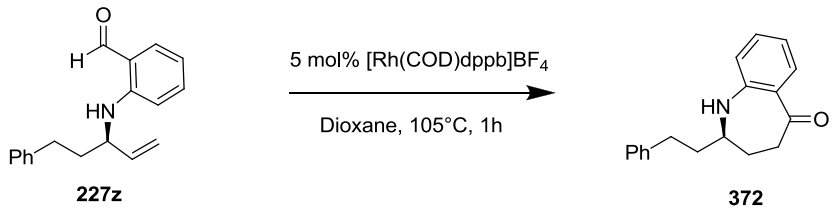

A 10 mL oven-dried Schlenk flask was charged with **227z** (9.1 mg, 0.034 mmol) and transferred into a glove box where [Rh(COD)dppb]BF_4 (1.2 mg, .0017 mmol, 5 mol%) was added. The flask was removed from the glove box, charged with 0.5 mL of dioxane, sealed under nitrogen and heated to 105°C on an oil bath. The mixture was stirred at elevated temperature for 1 hour. Reaction progress was monitored by TLC. The crude reaction was purified by adsorbing directly onto a dry 5g Teledyne Isco silica cartridge using vacuum followed by elution onto a pre-equilibrated 24g silica flash column (0 → 20% ethyl acetate /hexane) providing dihydro-benzazapinone **372** (9.0 mg, 99%), as a semi-solid.

Compound **372:**

^{1}H NMR ($CDCl_3$, 400 MHz): δ = 7.69 (dd, *J* = 7.9, 1.6 Hz, 1H), 7.31 – 7.23 (m, 2H), 7.22 – 7.15 (m, 2H), 7.14 – 7.08 (m, 2H), 6.79 (ddd, *J* = 8.0, 7.2, 1.0 Hz, 1H), 6.51 (dd, *J* = 8.1, 0.6 Hz, 1H), 4.05 (s,NH), 3.08 (dt, *J* = 11.8, 5.9 Hz, 1H), 3.02 – 2.93 (m, 1H), 2.80 – 2.66 (m, 1H), 2.66 – 2.55 (m, 1H), 2.25 – 2.12 (m, 1H), 2.03 – 1.88 (m, 3H).

^{13}C NMR ($CDCl_3$, 100 MHz): δ = 194.3, 150.8, 137.1, 136.9, 135.8, 118.6, 116.4, 114.9, 112.0, 60.7, 32.6, 19.1, 18.6.

IR (film, cm^{-1}): ν = 3360, 3084, 3060, 3026, 2925, 2855, 1749, 1658, 1604, 1508, 1496, 1477, 1453, 1433, 1367, 1330, 1290, 1232, 1177, 1158, 1110, 1075, 1033, 912, 857, 838, 755, 701.

HRMS (ESI): calc. for $C_{18}H_{20}NO$ (M+H): 266.1545; found: 266.1542.

HPLC: 2.5mg/mL in 50/50 IPA/Hex, 2 μL injection, 4.6 x 250mm Chiralcel OJ-3, 1 mL/min., 5% IPA in hexanes, 254 nm, major 35.27 min., minor 32.64 min., 84% *ee*.

$[\alpha]^{20}_{D}$: -30.9, c = 2.0, $CHCl_3$.

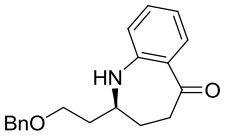

378

Compound **378:**

^{1}H NMR ($CDCl_3$, 400 MHz): δ = 7.69 (dd, *J* = 7.9, 1.6 Hz, 1H), 7.40 – 7.25 (m, 5H), 7.15 (ddd, *J* = 8.2, 7.1, 1.7 Hz, 1H), 6.77 (ddd, *J* = 8.0, 7.1, 1.0 Hz, 1H), 6.50 (dd, *J* = 8.2, 0.7 Hz, 1H), 5.35 (bs, NH), 4.57 – 4.42 (m, 2H), 3.69 (ddd, *J* = 9.0, 5.3, 3.5 Hz, 1H), 3.55 (td, *J* = 9.5, 2.9 Hz, 1H), 3.17 (ddt, *J* = 13.0, 8.8, 4.2 Hz, 1H), 2.99 (td, *J* = 11.5, 8.3 Hz, 1H), 2.56 (ddd, *J* = 11.3, 6.4, 2.1 Hz, 1H), 2.22 – 2.04 (m, 1H), 1.96 (dddd, *J* = 14.8, 12.7, 6.3, 3.0 Hz, 2H), 1.86 – 1.73 (m, 1H).

^{13}C NMR ($CDCl_3$, 100 MHz): δ = 203.0, 153.4, 138.0, 132.6, 129.3, 128.7, 128.1, 128.0, 125.4, 118.72, 118.3, 73.7, 69.6, 60.2, 41.0, 38.2, 35.3.

IR (film, cm^{-1}): ν = 3354, 2919, 2860, 1667, 1603, 1508, 1477, 1452, 1434, 1363, 1332, 1290, 1245, 1159, 1114, 1075, 1050, 1027, 781, 755, 740, 699.

HRMS (ESI): calc. for $C_{19}H_{21}NO_2Na$ (M+Na): 318.1470; found: 318.1465.

HPLC: 2.5mg/mL in 50/50 IPA/Hex, 2 μL injection, 4.6 x 250mm Chiralcel OD-H, 1 mL/min., 2.5% IPA in hexanes, 254 nm, major 40.60 min., minor 47.15 min., 89% *ee*.

$[\alpha]^{20}_{D}$: -68.6, c = 2.0, $CHCl_3$.

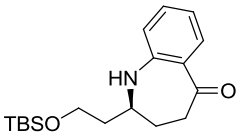

379

Compound **379:**

^{1}H NMR ($CDCl_3$, 400 MHz): δ = 7.68 (dd, *J* = 7.9, 1.6 Hz, 1H), 7.20 (ddd, *J* = 8.2, 7.1, 1.7 Hz, 1H), 6.77 (ddd, *J* = 8.0, 7.1, 1.0 Hz, 1H), 6.70 (dd, *J* = 8.2, 0.7 Hz, 1H), 5.51 (s, NH), 3.85 (ddd, *J* = 10.6, 5.3, 3.7 Hz, 1H), 3.70 (ddd, *J* = 10.7, 8.5, 3.4 Hz, 1H), 3.17 (qd, *J* = 8.7, 4.5 Hz, 1H), 3.00 (td, *J* = 11.5, 8.4 Hz, 1H), 2.56 (ddd, *J* = 11.3, 6.4, 2.1 Hz, 1H), 2.10 (ddd, *J* = 18.0, 11.9, 6.2 Hz, 1H), 1.98 (tdd, *J* = 12.6, 8.4, 2.1 Hz, 1H), 1.89 – 1.71 (m, 2H), 0.98 – 0.88 (m, 10H).

^{13}C NMR ($CDCl_3$, 126 MHz): δ = 203.2, 153.4, 132.6, 129.4, 125.4, 118.7, 118.2, 62.5, 60.3, 41.0, 38.4, 37.8, 26.2, 18.5, -5.1, -5.3.

IR (film, cm^{-1}): ν = 3356, 2952, 2928, 2883, 2856, 1670, 1603, 1506, 1476, 1450, 1432, 1388, 1361, 1331,1321, 1288, 1253, 1195, 1158, 1101, 1075, 1045, 1029, 996, 950, 910, 836, 810, 778, 755, 729, 683.

HRMS (ESI): calc. for $C_{17}H_{30}NOSi$ (M+H): 320.2046; found: 320.2056

HPLC: 2.5mg/mL in 50/50 IPA/Hex, 2 μL injection, 4.6 x 150mm Chiralcel OJ-3, 1 mL/min., 2.5% IPA in hexanes, 254 nm, major 3.47 min., minor 3.25 min., 83% *ee.*

$[\alpha]^{20}_D$: -49.9, c = 2.0, $CHCl_3$.

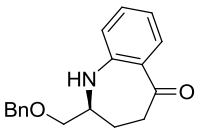

380

Compound **380:**

^{1}H NMR ($CDCl_3$, 400 MHz): δ = 7.73 (dd, *J* = 7.9, 1.6 Hz, 1H), 7.40 – 7.28 (m, 5H), 7.28 – 7.22 (m, 2H), 6.83 (ddd, *J* = 8.0, 7.2, 1.0 Hz, 1H), 6.77 (dd, *J* = 8.1, 0.7 Hz, 1H), 4.67 (s, NH), 4.53 (d, *J* = 12.0 Hz, 1H), 4.49 (d, *J* = 12.0 Hz, 1H), 3.56 (dd, *J* = 10.0, 3.7 Hz, 1H), 3.51 – 3.42 (m, 1H), 3.42 – 3.30 (m, 1H), 2.99 (td, *J* = 11.7, 7.6 Hz, 1H), 2.63 (ddd, *J* = 11.7, 5.9, 3.1 Hz, 1H), 2.01 (ddd, *J* = 17.5, 11.6, 5.6 Hz, 1H), 1.88 – 1.76 (m, 1H).

^{13}C NMR ($CDCl_3$, 100 MHz): δ = 202.4, 152.4, 137.8, 133.0, 129.6, 128.8, 128.2, 128.0, 125.8, 119.5, 119.0, 73.2, 72.1, 58.1, 40.6, 32.4.

IR (film, cm^{-1}): 3359, 3086, 3061, 3028, 2920, 2858, 1663, 1602, 1496, 1473, 1452, 1432, 1362, 1320, 1287, 1248, 1227, 1201, 1174, 1159, 1107, 1092, 1075, 1028, 989, 938, 902, 855, 806, 753, 738, 697.

HRMS (ESI): calc. for $C_{18}H_{20}NO_2$ (M+H): 282.1494; found: 282.1488.

HPLC: 2.5mg/mL in 50/50 IPA/Hex, 2 μL injection, 4.6 x 250mm Chiralcel OD-H, 1 mL/min., 10% IPA in hexanes, 254 nm, major 12.27 min., minor 13.45 min., 86% *ee*

$[\alpha]^{20}_D$: -35.6, c = 2.0, $CHCl_3$.

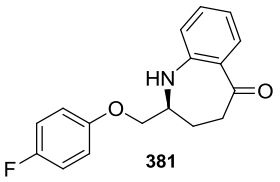

381

Compound **381:**

^{1}H NMR ($CDCl_3$, 400 MHz): δ = 7.76 (dd, *J* = 7.9, 1.6 Hz, 1H), 7.28 (ddd, *J* = 8.6, 7.2, 1.6 Hz, 1H), 7.01 – 6.92 (m, 1H), 6.90 – 6.77 (m, 1H), 4.66 (s, NH), 4.01 (dd, *J* = 9.8, 3.6 Hz, 1H), 3.95 – 3.86 (m, 1H), 3.59 – 3.45 (m, 1H), 3.05 (td, *J* = 11.7, 7.3 Hz, 1H), 2.70

(ddd, J = 11.9, 5.7, 3.5 Hz, 1H), 2.13 (dtd, J = 17.1, 11.4, 5.6 Hz, 1H), 1.96 (tdd, J = 12.8, 7.3, 3.5 Hz, 1H).

^{13}C NMR ($CDCl_3$, 100 MHz): δ = 202.1, 157.9 (d, J = 239.5 Hz), 154.4 (d, J = 2.2 Hz), 151.8, 133.2, 129.7, 126.1, 120.0, 119.2, 116.4, 116.2, 116.0, 115.9, 70.7, 58.0, 40.5, 32.0.

IR (film, cm^{-1}): ν = 3346, 3059, 2926, 2857, 1661, 1604, 1506, 1477, 1462, 1393, 1365, 1321, 1294, 1244, 1201, 1160, 1114, 1097, 1054, 994, 946, 918, 828, 759, 730, 687, 669.

HRMS (ESI): calc. for $C_{17}H_{17}NO_2F$ (M+H): 286.1243; found: 286.1254.

HPLC: 2.5mg/mL in 50/50 IPA/Hex, 2 μL injection, 4.6 x 250mm Chiralcel OD-H, 1 mL/min., 10% IPA in hexanes, 254 nm, major 14.18 min., minor 15.42 min., 80% *ee.*

$[\alpha]^{20}_D$: -19.8, c = 2.0, $CHCl_3$.

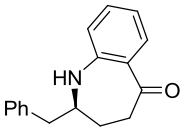

382

Compound **382**:

^{1}H NMR ($CDCl_3$, 400 MHz:) δ = 7.91 – 7.87 (m, 1H), 7.59 – 7.39 (m, 3H), 7.38 – 7.23 (m, 3H), 6.98 (t, J = 7.5 Hz, 1H), 6.68 (d, J = 8.1 Hz, 1H), 4.35 (s, NH), 3.60 – 3.43 (m, 1H), 3.31 – 3.08 (m, 2H), 3.00 (dd, J = 14.1, 9.0 Hz, 1H), 2.82 (ddd, J = 11.5, 6.2, 2.5 Hz, 1H), 2.46 – 2.25 (m, 1H), 2.26 – 2.07 (m, 1H).

^{13}C NMR ($CDCl_3$, 100 MHz): 202.8, 152.3, 137.7, 132.9, 129.5, 129.0, 129.0, 127.2, 125.8, 119.4, 118.4, 60.0, 42.4, 41.0, 37.0.

IR (film, cm^{-1}): ν = 3353, 3060, 3027, 2921, 2854, 1731, 1661, 1602, 1495, 1474, 1452, 1431, 1364, 1331, 1284, 1243, 1179, 1159, 1109, 1073, 1030, 992, 755, 727, 701.

HRMS (ESI): calc. for $C_{17}H_{18}NO$ (M+H): 252.1388; found: 252.1391.

HPLC: 2.5mg/mL in 50/50 IPA/Hex, 2 μL injection, 4.6 x 250mm Chiralcel OD-H, 1 mL/min., 10% IPA in hexanes, 254 nm, major 11.96., minor 11.41 min., 92% *ee*.

$[\alpha]^{20}_{D}$: -71.1, c = 2.0, $CHCl_3$.

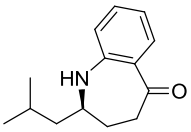

383

Compound **383:**

^{1}H NMR ($CDCl_3$, 400 MHz): δ = 7.70 (dd, *J* = 7.9, 1.6 Hz, 1H), 7.24 – 7.17 (m, 1H), 6.79 (ddd, *J* = 8.0, 7.2, 1.0 Hz, 1H), 6.71 (dd, *J* = 8.1, 0.6 Hz, 1H), 4.08 (s, NH), 3.12 – 2.91 (m, 2H), 2.58 (ddd, *J* = 11.2, 6.5, 1.9 Hz, 1H), 2.20 – 2.05 (m, 1H), 1.88 (tdd, *J* = 12.6, 8.3, 2.0 Hz, 1H), 1.66 (ddd, *J* = 20.3, 13.5, 6.8 Hz, 1H), 1.56 – 1.34 (m, 2H), 0.89 (d, *J* = 6.6 Hz, 3H), 0.84 (d, *J* = 6.5 Hz, 3H).

^{13}C NMR ($CDCl_3$, 100 MHz): δ = 203.2, 152.9, 132.7, 129.4, 125.6, 119.0, 117.9, 57.9, 45.6, 41.2, 38.1, 25.5, 22.8.

IR (film, cm^{-1}): 3355, 2956, 2926, 2868, 1655, 1604, 1578, 1503, 1475, 1449, 1431, 1369, 1334, 1322, 1290, 1249, 1225, 1196, 1157, 1030, 988, 917, 784, 754, 732, 684.

HRMS (ESI): calc. for $C_{14}H_{20}NO$ (M+H): 218.1545; found: 218.1558.

HPLC: 2.5mg/mL in 50/50 IPA/Hex, 2 μL injection, 4.6 x 250mm Chiralcel OD-H, 1 mL/min., 2.5% IPA in hexanes, 254 nm, major 7.90., minor 9.32 min., 78% *ee*.

$[\alpha]^{20}_{D}$: -9.10, c = 2.0, $CHCl_3$.

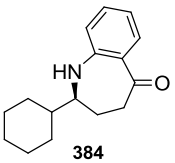

384

Compound **384:**

^{1}H NMR ($CDCl_3$, 400 MHz): δ = 7.75 – 7.64 (m, 1H), 7.28 – 7.17 (m, 1H), 7.28 – 7.16 (m, 1H), 6.85 – 6.68 (m, 1H), 4.18 (s, NH), 2.97 (qd, *J* = 11.3, 2.8 Hz, 1H), 2.85 – 2.71 (m, 1H), 2.64 – 2.50 (m, 1H), 2.18 – 1.92 (m, 1H), 1.89 – 1.61 (m, 3H), 1.45 (dt, *J* = 33.7, 14.2 Hz, 1H), 1.33 – 0.91 (m, 3H).

^{13}C NMR ($CDCl_3$, 100 MHz): δ = 203.2, 153.3, 132.7, 129.4, 125.6, 118.9, 117.9, 64.8, 43.1, 41.1, 34.7, 30.3, 29.4, 26.5, 26.3.

IR (film, cm^{-1}): ν = 3373, 2925, 2852, 1733, 1658, 1603, 1476, 1450, 1324, 1269, 1170, 1158, 1111, 1095, 1070, 1027, 756, 733, 711.

HRMS (ESI): calc. for $C_{16}H_{22}NO$ (M+H): 244.1701; found: 244.1720.

HPLC: 2.5mg/mL in 50/50 IPA/Hex, 2 μL injection, 4.6 x 250mm Chiralcel OD-H, 1 mL/min., 2.5% IPA in hexanes, 254 nm, major 9.92 min., minor 11.6 min., 80% *ee*

$[\alpha]^{20}_D$: -10.2, c=2.0, $CHCl_3$.

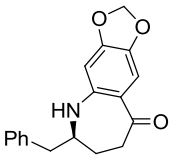

385

Compound **385:**

^{1}H NMR ($CDCl_3$, 400 MHz): δ = 7.30 (t, *J* = 7.3 Hz, 1H), 7.23 (dd, *J* = 8.5, 5.9 Hz, 1H), 7.14 (d, *J* = 7.2 Hz, 1H), 5.93 (s, 1H), 5.88 (s, 1H), 5.84 (s, 1H), 3.98 (s, N H), 3.40 – 3.20 (m, 1H), 2.97 (dt, *J* = 10.3, 8.5 Hz, 1H), 2.75 (dd, *J* = 14.1, 9.4 Hz, 1H), 2.61 (ddd, *J* = 11.6, 5.4, 2.9 Hz, 1H), 2.14 (ddd, *J* = 17.6, 11.8, 5.6 Hz, 1H), 2.01 – 1.86 (m, 1H).

^{13}C NMR ($CDCl_3$, 100 MHz): δ = 200.6, 152.1, 150.6, 142.1, 137.8, 129.1, 129.0, 127.2, 119.4, 107.43, 101.7, 99.0, 60.8, 42.3, 41.0, 36.6.

IR (film, cm^{-1}): ν = 3351, 3061, 3027, 2922, 2854, 1652, 1627, 1616, 1500, 1474, 1453, 1363, 1238, 1201, 1129, 1040, 938, 879, 831, 756, 729, 702.

HRMS (ESI): calc. for $C_{18}H_{18}NO_3$ (M+H): 296.1287; found: 296.1299.

HPLC: 2.5mg/mL in 50/50 IPA/Hex, 2 μL injection, 4.6 x 250mm Chiralcel OJ-3, 1 mL/min., 10% IPA in hexanes, 254 nm, major 30.69 min., minor 27.93 min., 95% *ee*.

$[\alpha]^{20}_D$: +21.6, c = 2.0, $CHCl_3$.

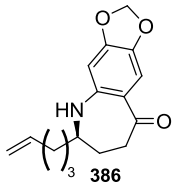

Compound **386:**

^{1}H NMR ($CDCl_3$, 400 MHz): 1:1 Mixture of (*E*) Isomerized and Desired Hydroacylation products δ = 7.20 (s, 1H), 6.22 – 6.19 (m, 1H), 5.90 (s, 1H), 5.87 (s, 1H), 5.78 – 5.70 (m, 0.4H), 5.47-5.32 (m, 1H), 5.13 – 4.58 (m, 0.8H), 4.03 (bs, NH), 2.98 – 2.90 (m, 2H), 2.59-2.55 (m, 1H), 2.13-2.01 (m, 3H), 1.86 – 1.78 (m, 1H), 1.63-1.53(m, 4H), 1.46-1.41 (m, 1H).

^{13}C NMR ($CDCl_3$, 100 MHz): 200.9, 167.8, 152.0, 152.0,151.10, 141.9, 138.2, 130.0, 129.1, 126.6, 125.6, 119.1, 119.1,115.4, 111.9, 107.4, 101.6, 98.6, 98.6, 60.5, 60.4, 60.3, 41.1, 37.4, 37.3, 35.9, 35.8, 33.6, 29.9, 29.9, 25.9, 24.2, 23.0, 18.1, 13.0

IR (film, cm^{-1}): 3355, 3316, 2968, 2926, 2856, 1730, 1653, 1626, 1616, 1504, 1475, 1239, 1203, 1040, 886, 820, 802, 773.

HRMS (ESI): calc. for $C_{16}H_{20}NO_3$ (M+H): 274.1443; found: 274.1441.

HPLC: The two olefin products (i.e. desired terminal and isomerized internal olefins) were not resolved. 2.5mg/mL in 50/50 IPA/Hex, 2 μL injection, 4.6 x 250mm Chiralcel

OJ-3, 1 mL/min., 1% IPA in hexanes, 230 nm, major 50.29 min., minor 74.71 min., 86% *ee*.

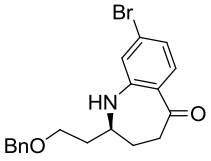

387

Compound **387:**

^{1}H NMR ($CDCl_3$, 400 MHz): δ 7.52 = (d, *J* = 8.4 Hz, 1H), 7.44 – 7.35 (m, 2H), 7.33 (dd, *J* = 9.5, 4.5 Hz, 3H), 6.88 (dd, *J* = 8.4, 1.8 Hz, 1H), 6.67 (d, *J* = 1.8 Hz, 1H), 5.46 (s, NH), 4.50 (d, *J* = 11.3 Hz, 1H), 4.46 (d, *J* = 11.3 Hz, 1H), 3.78 – 3.64 (m, 1H), 3.56 (td, *J* = 9.6, 2.5 Hz, 1H), 3.15 (ddd, *J* = 13.2, 8.7, 4.0 Hz, 1H), 2.93 (td, *J* = 11.6, 8.4 Hz, 1H), 2.54 (ddd, *J* = 11.4, 6.5, 2.1 Hz, 1H), 2.08 (ddd, *J* = 11.6, 9.1, 5.7 Hz, 1H), 1.94 (m, 2H), 1.79 (dtd, *J* = 8.5, 5.8, 2.7 Hz, 1H).

^{13}C NMR ($CDCl_3$, 100 MHz): 202.1,154.1, 137.7, 130.9, 128.9, 128.4, 128.3, 127.3, 124.2, 122.0, 120.8, 74.0, 69.8, 60.4, 40.9, 38.1, 35.2

IR (film, cm^{-1}): ν = 3355, 3061, 3029, 2923, 2858, 1729, 1670, 1591, 1503, 1468, 1450, 1398, 1362, 1312, 1278, 1240, 1217, 1196, 1118, 1093, 1067, 1043, 1027, 993, 887, 858, 811, 767, 748, 699.

HRMS (ESI): calc. for $C_{19}H_{21}BrNO_2$ (M+H): 374.0756; found: 374.0765.

HPLC: 2.5mg/mL in 50/50 IPA/Hex, 2 μL injection, 4.6 x 250mm Chiralcel OD-H, 1 mL/min., 2.5% IPA in hexanes, 254 nm, major 21.84 min., minor 23.67 min., 94% *ee*.

$[\alpha]^{20}_D$: -37.2 , c = 2.0, $CHCl_3$.

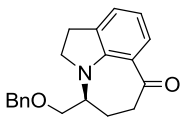

388

Compound **388:**

^{1}H NMR ($CDCl_3$, 500 MHz): δ = 7.63 (d, *J* = 8.1 Hz, 1H), 7.37 – 7.30 (m, 2H), 7.27 (q, *J* = 5.9 Hz, 3H), 7.14 – 7.08 (m, 1H), 6.63 – 6.54 (m, 1H), 5.28 (s, 1H), 4.50 (d, *J* = 12.1 Hz, 1H), 4.47 (d, *J* = 12.0 Hz, 1H), 3.87 (td, *J* = 10.0, 6.3 Hz, 1H), 3.64 (dt, *J* = 18.3, 9.1 Hz, 1H), 3.61 – 3.47 (m, 3H), 3.05 (ddd, *J* = 16.3, 10.2, 6.3 Hz, 1H), 3.00 – 2.90 (m, 1H), 2.83 – 2.68 (m, 2H), 2.28 – 2.10 (m, 2H).

^{13}C NMR ($CDCl_3$, 100 MHz): 200.2, 151.7, 138.0, 133.0, 128.9, 128.7, 128.4, 128.0, 127.8, 118.7, 117.3, 73.7, 70.0, 59.6, 54.2, 39.3, 28.1, 25.1.

IR (film, cm^{-1}): ν = 3064, 3029, 2923, 2855, 1723, 1658, 1611, 1572, 1494, 1454, 1437, 1395, 1359, 1336, 1302, 1261, 1236, 1103, 1090, 1043, 1029, 917, 800, 736, 699.

HRMS (ESI): calc. for $C_{20}H_{22}NO_2$ (M+H): 308.1651; found: 308.1650.

HPLC: 2.5mg/mL in 50/50 IPA/Hex, 2 μL injection, 4.6 x 250mm Chiralcel OD-H, 1 mL/min., 5% IPA in hexanes, 254 nm, major 22.02 min., minor 19.35 min., 84% *ee*.

$[\alpha]^{20}_D$: +34.8, c = 2.0, $CHCl_3$.

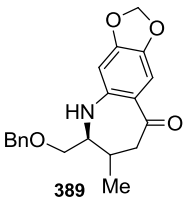

389

Compound **389:**

^{1}H NMR ($CDCl_3$, 500 MHz): δ = 7.37 – 7.25 (m, 5H), 7.16 (s, 1H), 6.25 (s, 1H), 5.91 (d, *J* = 1.2 Hz, 1H), 5.87 (d, *J* = 1.2 Hz, 1H), 4.48 (d, *J* = 12.0 Hz, 1H), 4.47 (d, *J* = 12.1 Hz, 1H), 4.26 (s, NH), 3.55 – 3.48 (m, 2H), 3.26 – 3.20 (m, 1H), 2.59 – 2.55 (m, 2H), 2.39 (m, *J* = 14.5, 7.5, 3.5 Hz, 1H), 0.89 (d, *J* = 6.5 Hz, 3H).

^{13}C NMR ($CDCl_3$, 126 MHz): δ = 199.8, 152.0, 141.8, 137.8, 128.8, 128.2, 127.9, 119.2, 107.2, 101.6, 98.4, 73.2, 70.3, 62.9, 50.4, 39.2, 29.9, 18.3, 14.7.

IR (film, cm^{-1}): ν = 3383, 3353, 3317, 2960, 2924, 2872, 1651, 1630, 1502, 1475, 1381, 1361, 1240, 1205, 1039, 937, 740, 700.

HRMS (TOF ESI+): calc. for $C_{20}H_{21}NO_4Na$ (M+Na): 362.1368; found: 362.1364.

HPLC: 2.5mg/mL in 50/50 IPA/Hex, 2 μL injection, 4.6 x 250mm Chiralcel OJ-3, 1 mL/min., 10% IPA in hexanes, 254 nm, major 33.30 min., minor 28.79 min., 11% *ee*, major 35.41 min., minor 42.46 min., 15% *ee.*

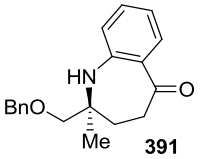

391

Compound **391:**

^{1}H NMR ($CDCl_3$, 400 MHz): δ = 7.87 (dd, *J* = 7.9, 1.6 Hz, 1H), 7.40 – 7.25 (m, 6H), 6.99 – 6.89 (m, 1H), 6.72 (dd, *J* = 8.0, 0.8 Hz, 1H), 4.53 (d, *J* = 12.1 Hz, 1H), 4.49 (d, *J* = 12.1 Hz, 1H), 4.18 (s, NH), 3.31 (d, *J* = 8.8 Hz, 1H), 3.23 (d, *J* = 8.8 Hz, 1H), 2.88 – 2.65 (m, 2H), 1.85 – 1.63 (m, 2H), 1.25 (s, *J* = 5.9 Hz, 3H).

^{13}C NMR ($CDCl_3$, 100 MHz): δ = 201.8, 148.5, 138.3, 134.1, 130.3, 128.7, 128.0, 127.8, 122.9, 121.3, 76.8, 73.6, 58.4, 39.0, 33.0, 25.2.

IR (film, cm^{-1}): ν = 3085, 3086, 3061, 3030, 2968, 2925, 2863, 1730, 1666, 1601, 1472, 1455, 1371, 1354, 1329, 1302, 1245, 1208, 1179, 1158, 1104, 1026, 966, 912, 860, 771, 753, 699.

HRMS (ESI): calc. for $C_{19}H_{22}NO_2$ (M+H): 296.1651; found: 296.1654.

HPLC: 2.5mg/mL in 50/50 IPA/Hex, 2 μL injection, 4.6 x 250mm Chiralcel OD-H, 1 mL/min., 10% IPA in hexanes, 254 nm, major 11.56 min., minor 13.20 min., 94% *ee*.

$[\alpha]^{20}_{D}$: +66.4, c = 2.0, $CHCl_3$.

5.17 Hydroacylations for 6-membered rings performed with 5 mol% $[Rh(COD)_2]OTf$

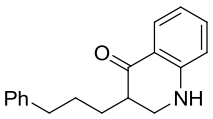

373

Compound **373:**

^{1}H NMR ($CDCl_3$, 400 MHz): δ = 7.83 (dd, *J* = 8.0, 1.5 Hz, 1H), 7.30 – 7.23 (m, 3H), 7.18 – 7.14 (m, 3H), 6.76 – 6.68 (m, 1H), 6.62 (d, *J* = 8.2 Hz, 1H), 4.32 (s, NH), 3.57 (ddd, *J* = 11.9, 4.8, 2.3 Hz, 1H), 3.34 – 3.26 (m, 1H), 2.75 – 2.57 (m, 2H), 2.53 (ddd, *J* = 13.9, 9.1, 5.2 Hz, 1H), 1.99 – 1.85 (m, 1H), 1.80 – 1.59 (m, 2H), 1.58 – 1.43 (m, 2H).

^{13}C NMR ($CDCl_3$, 100 MHz): δ = 195.1, 151.5, 142.4, 135.0, 128.6, 128.5, 128.2, 126.0, 118.2, 115.7, 46.6, 46.4, 36.2, 29.2, 27.0.

IR (film, cm^{-1}): ν = 3356, 3059, 3026, 2927, 2855, 1660, 1611, 1509, 1454, 1438, 1362, 1342, 1238, 1154, 1127, 1067, 941.

HRMS (ESI): calc. for $C_{18}H_{20}NO$ (M+H): 266.1545; found: 266.1544.

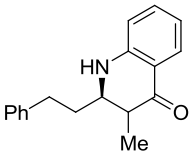

374

Compound **374** (2:1 mixture of diastereomers)**:**

^{1}H NMR ($CDCl_3$, 400 MHz): δ = 7.80 (d, *J* = 7.9 Hz, 1H), 7.33 – 7.24 (m, 3H), 7.23 – 7.13 (m, 3H), 6.70 (t, *J* = 7.5 Hz, 1H), 6.59 – 6.43 (m, 1H), 4.27 (s, 0.65 NH), 4.11 (s,

0.35 NH), 3.59 (dd, *J* = 10.3, 6.6 Hz, 0.39H), 3.33 (dd, *J* = 10.9, 7.8 Hz, 0.72H), 2.84 – 2.56 (m, 2H), 2.49 (dq, *J* = 14.1, 7.0 Hz, 1H), 2.06 – 1.80 (m, 2H), 1.22 (d, *J* = 6.9 Hz, 2H), 1.10 (d, *J* = 7.2 Hz, 1H).

^{13}C NMR ($CDCl_3$, 100 MHz): δ = 196.5, 170.8, 150.6, 150.1, 141.0, 138.4, 135.3, 128.9, 128.5, 128.0, 126.5, 118.1, 118.0, 115.8, 115.7, 58.3, 56.2, 45.7, 45.0, 34.7, 32.6, 31.9, 31.8, 12.8, 9.5.

IR (film, cm^{-1}): ν = 3345, 3027, 2973, 2927, 2852, 1655, 1612, 1580, 1508, 1497, 1483, 1454, 1440, 1374, 1348, 1308, 1257, 1208, 1155, 970, 953, 912, 754, 717.

HRMS (ESI): calc. for $C_{18}H_{20}NO$ (M+H): 266.1545; found: 266.1544.

APPENDIX A:
NMR SPECTRAL DATA

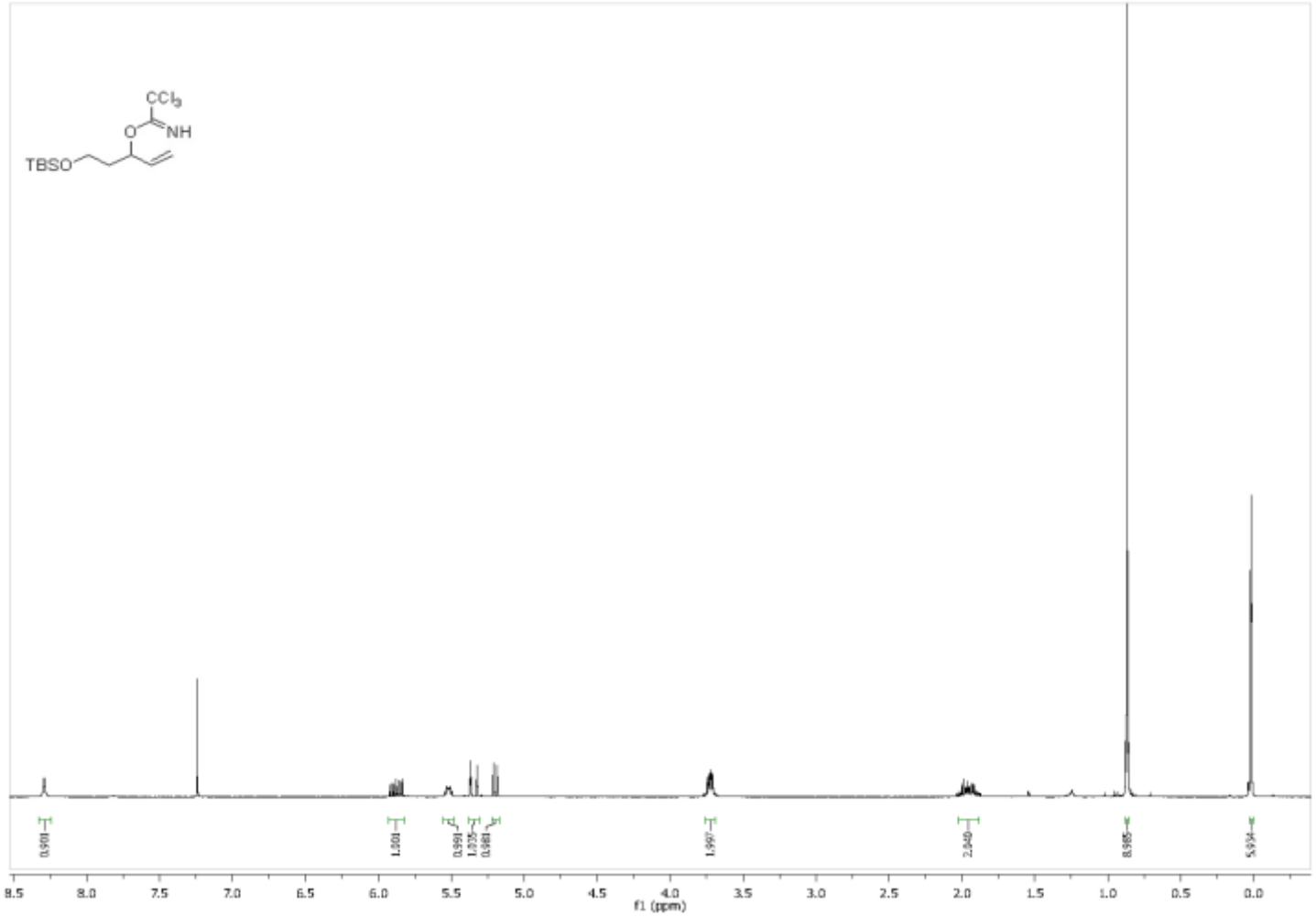

Figure A1 400 MHz 1H NMR ($CDCl_3$) Spectra of Compound **223**

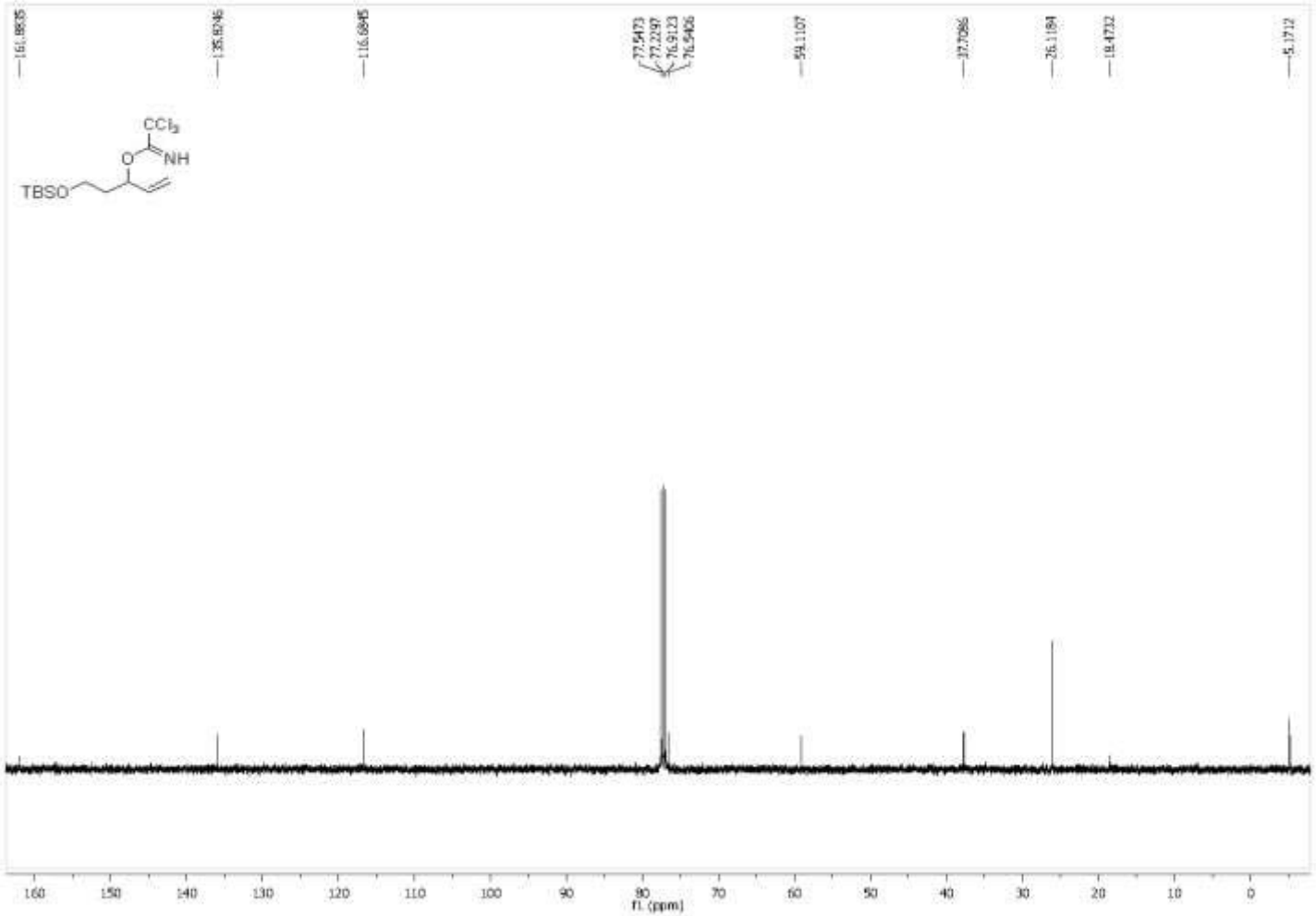

Figure A2 100 MHz 13C NMR ($CDCl_3$) Spectra of Compound **223**

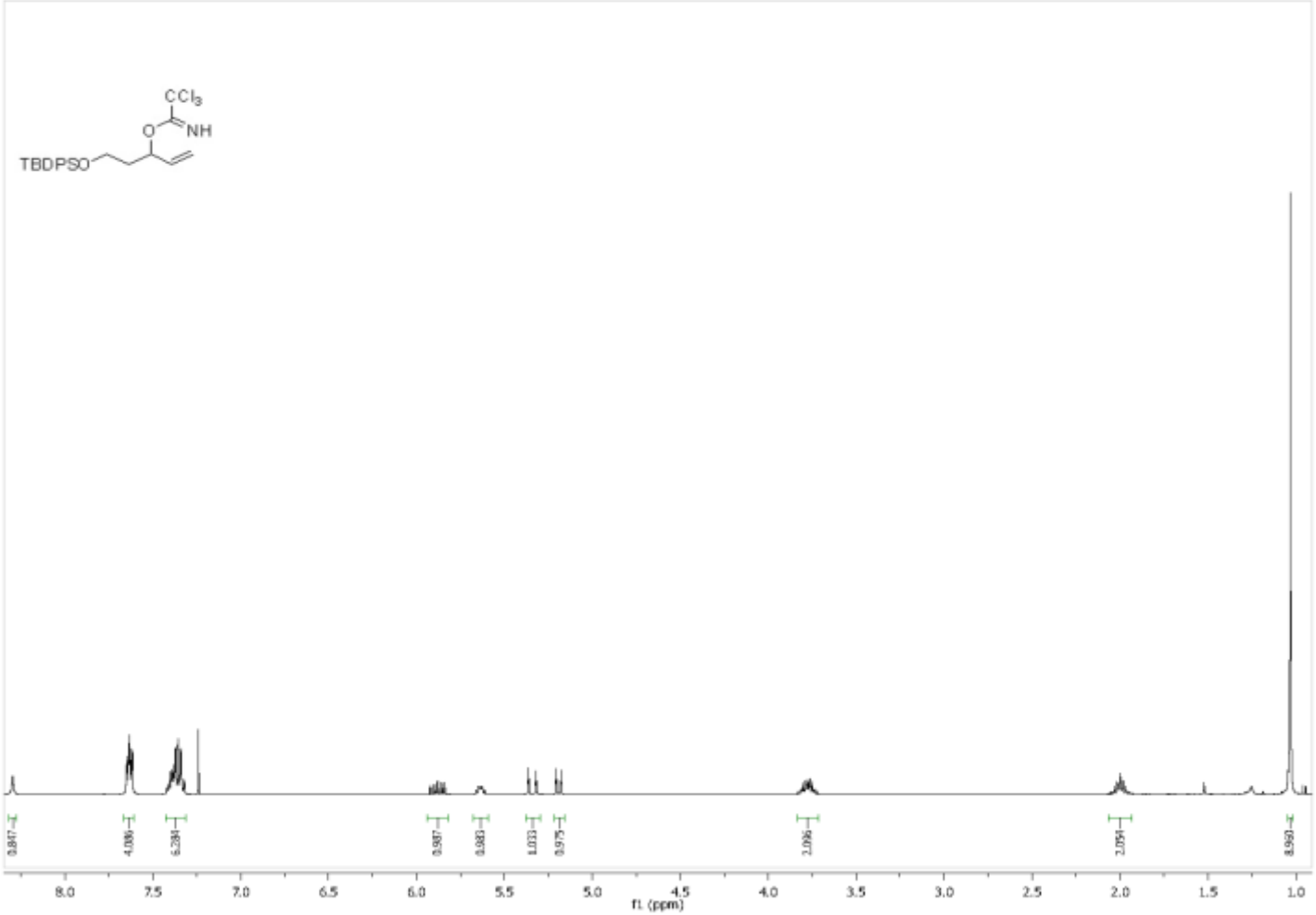

Figure A3 400 MHz 1H NMR ($CDCl_3$) Spectra of Compound **226**

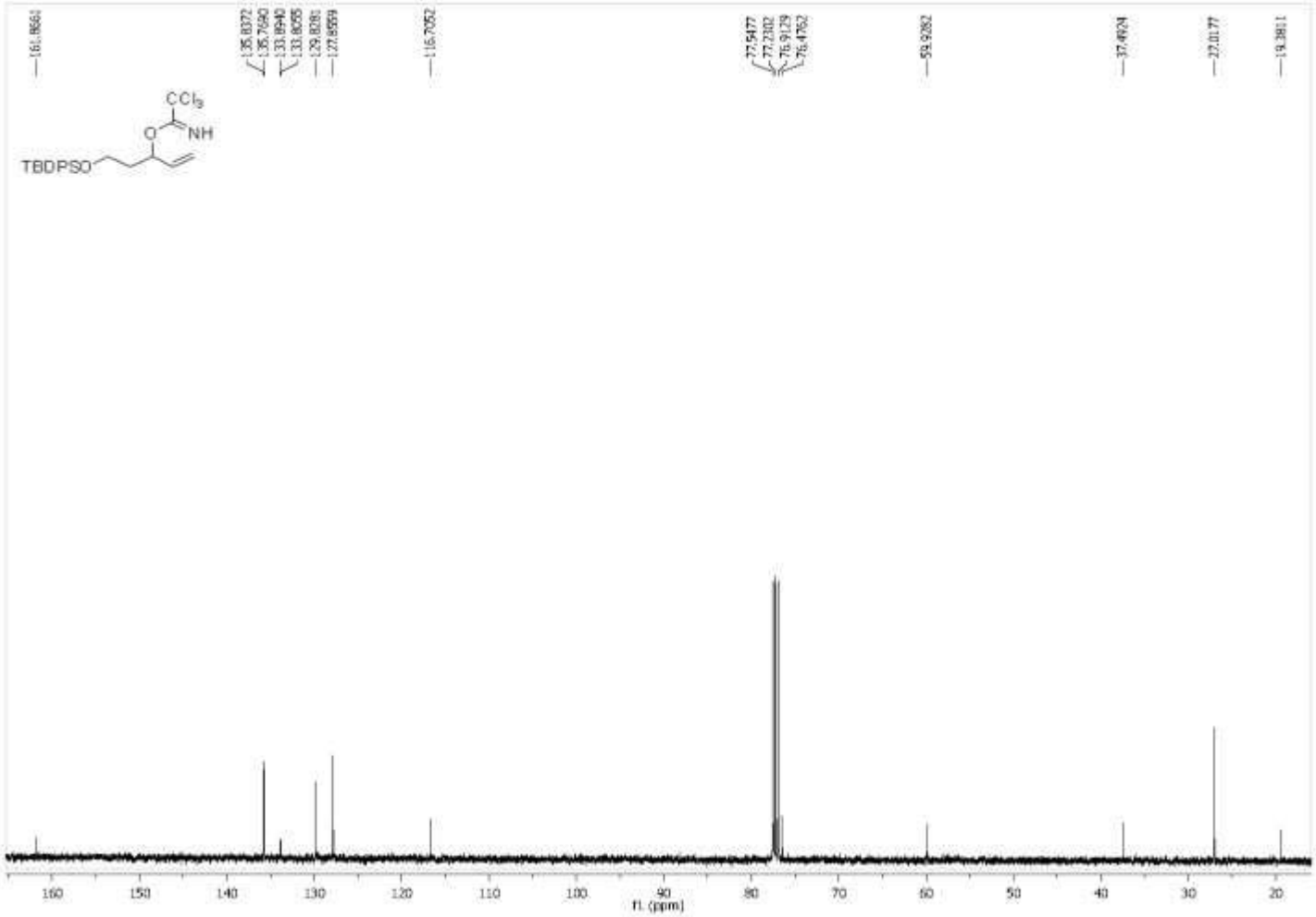

Figure A4 100 MHz 13C NMR ($CDCl_3$) Spectra of Compound **226**

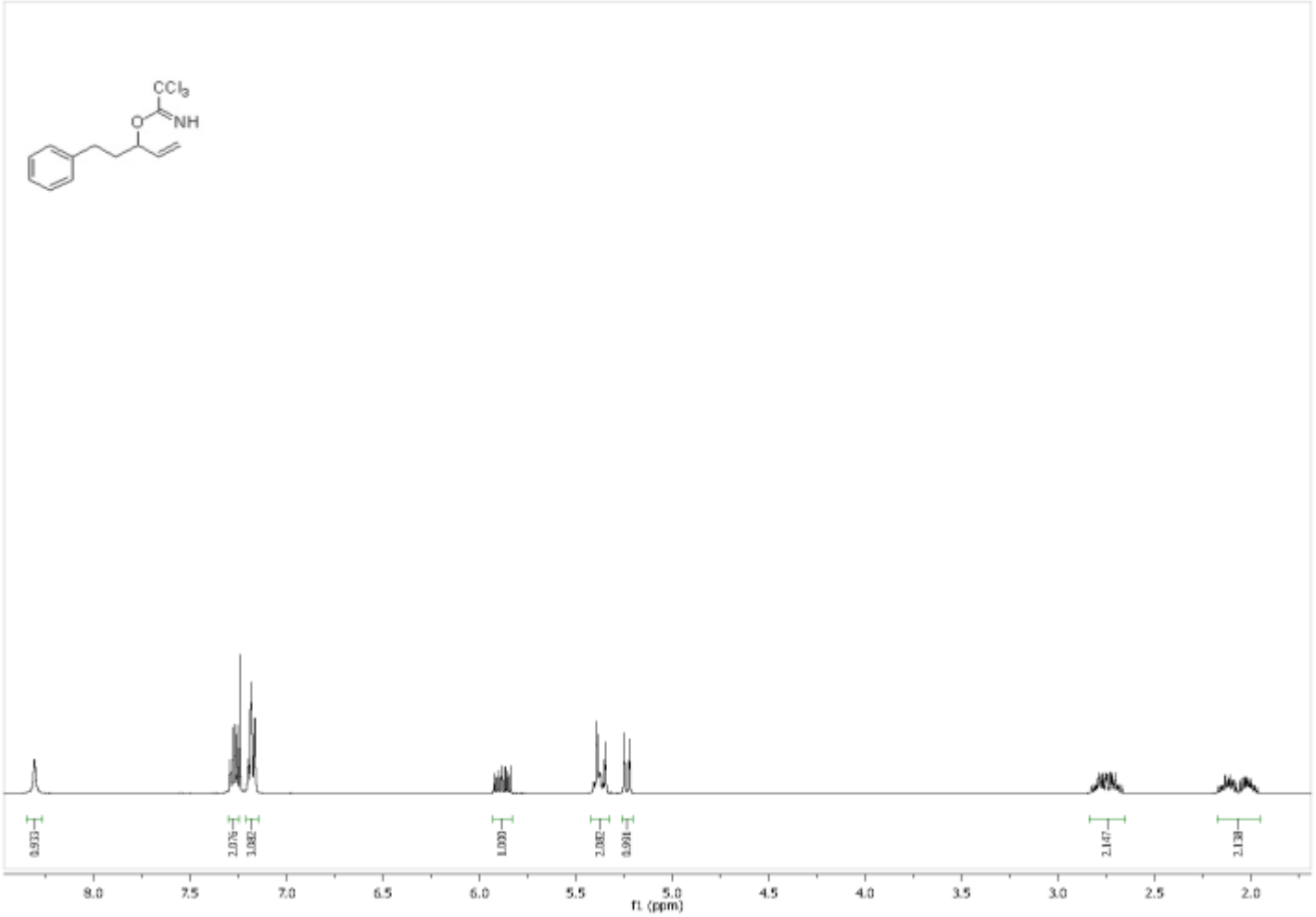

Figure A5 400 MHz 1H NMR ($CDCl_3$) Spectra of Compound **227**

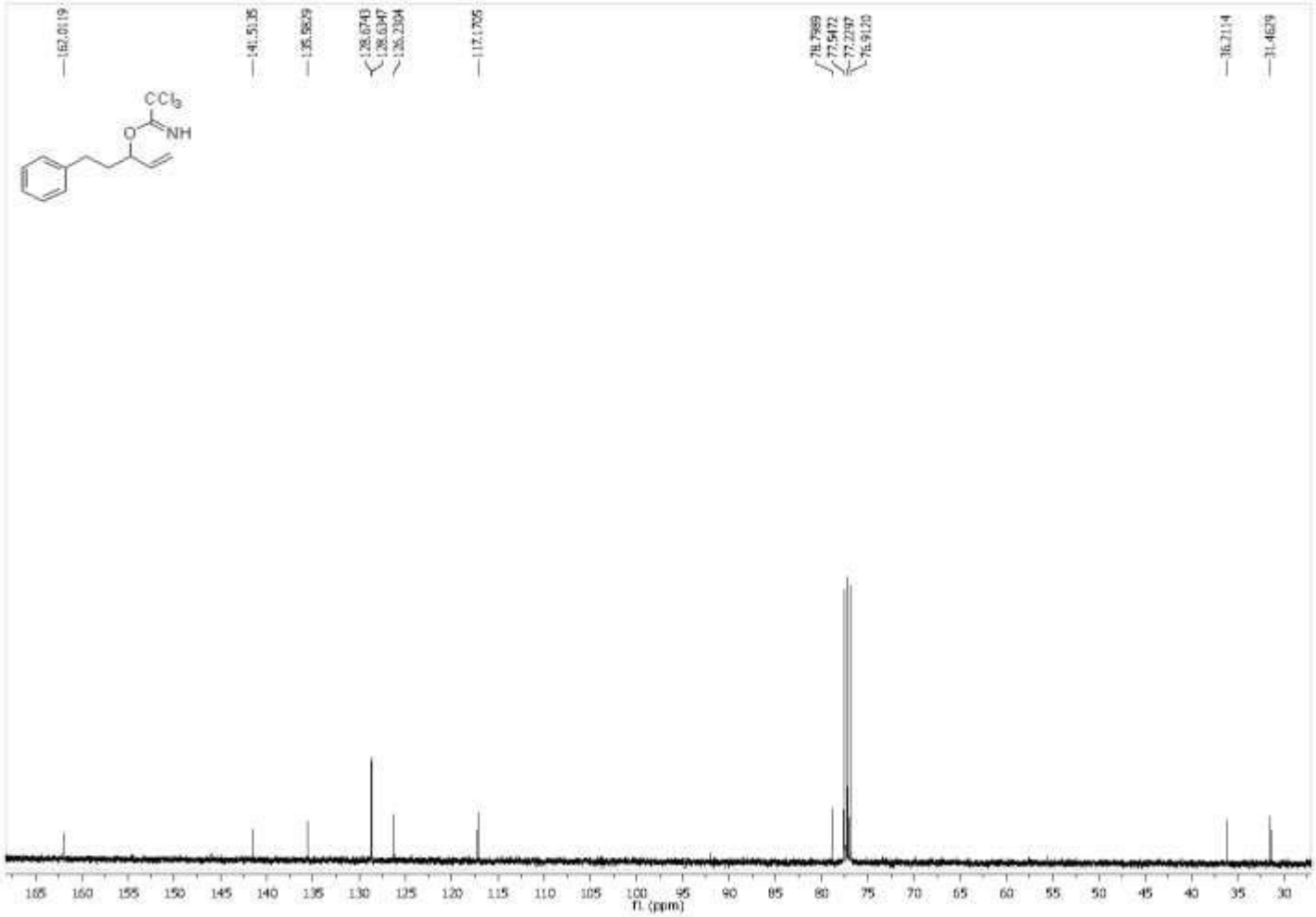

Figure A6 100 MHz 13C NMR ($CDCl_3$) Spectra of Compound **227**

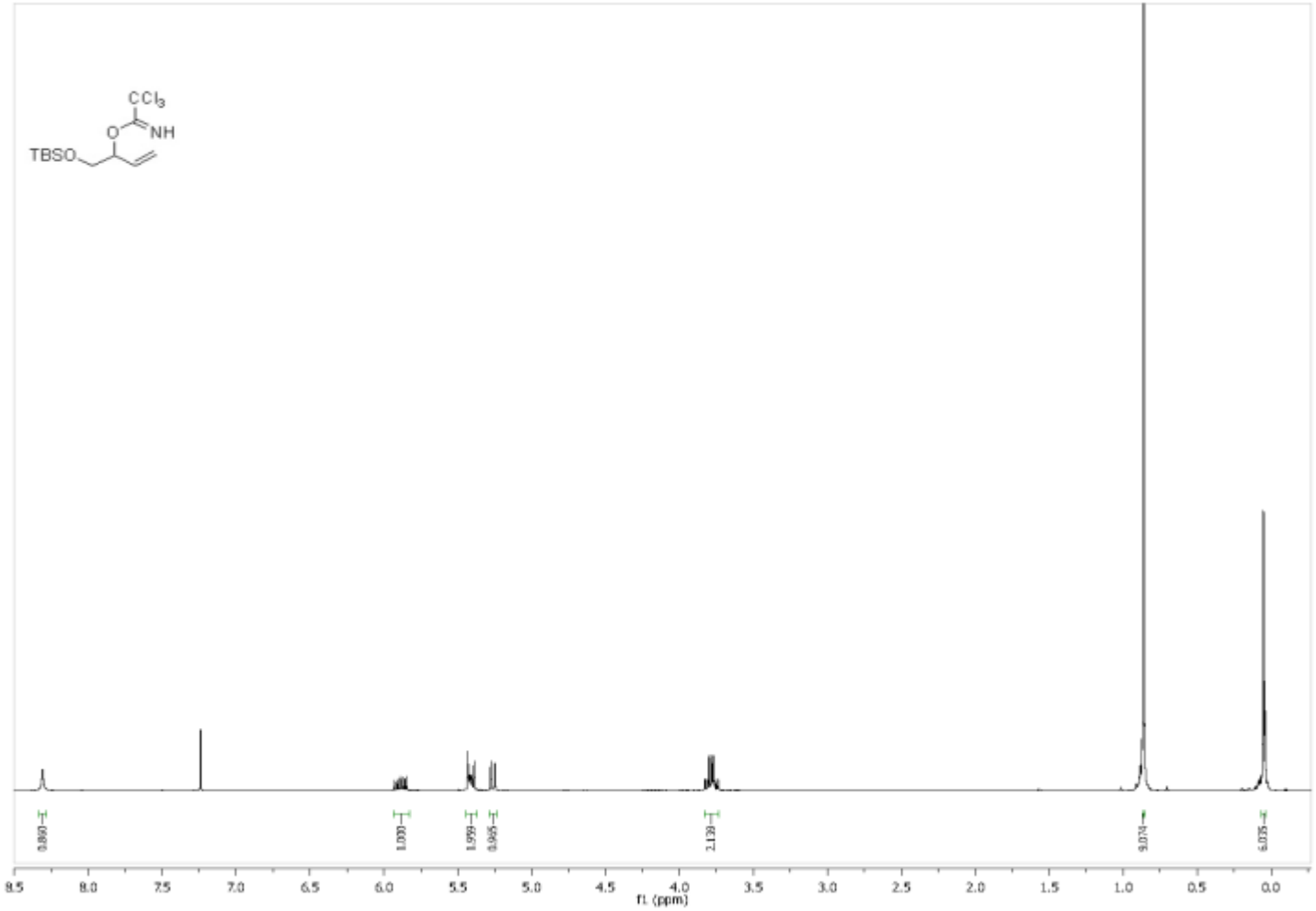

Figure A7 400 MHz 1H NMR ($CDCl_3$) Spectra of Compound **228**

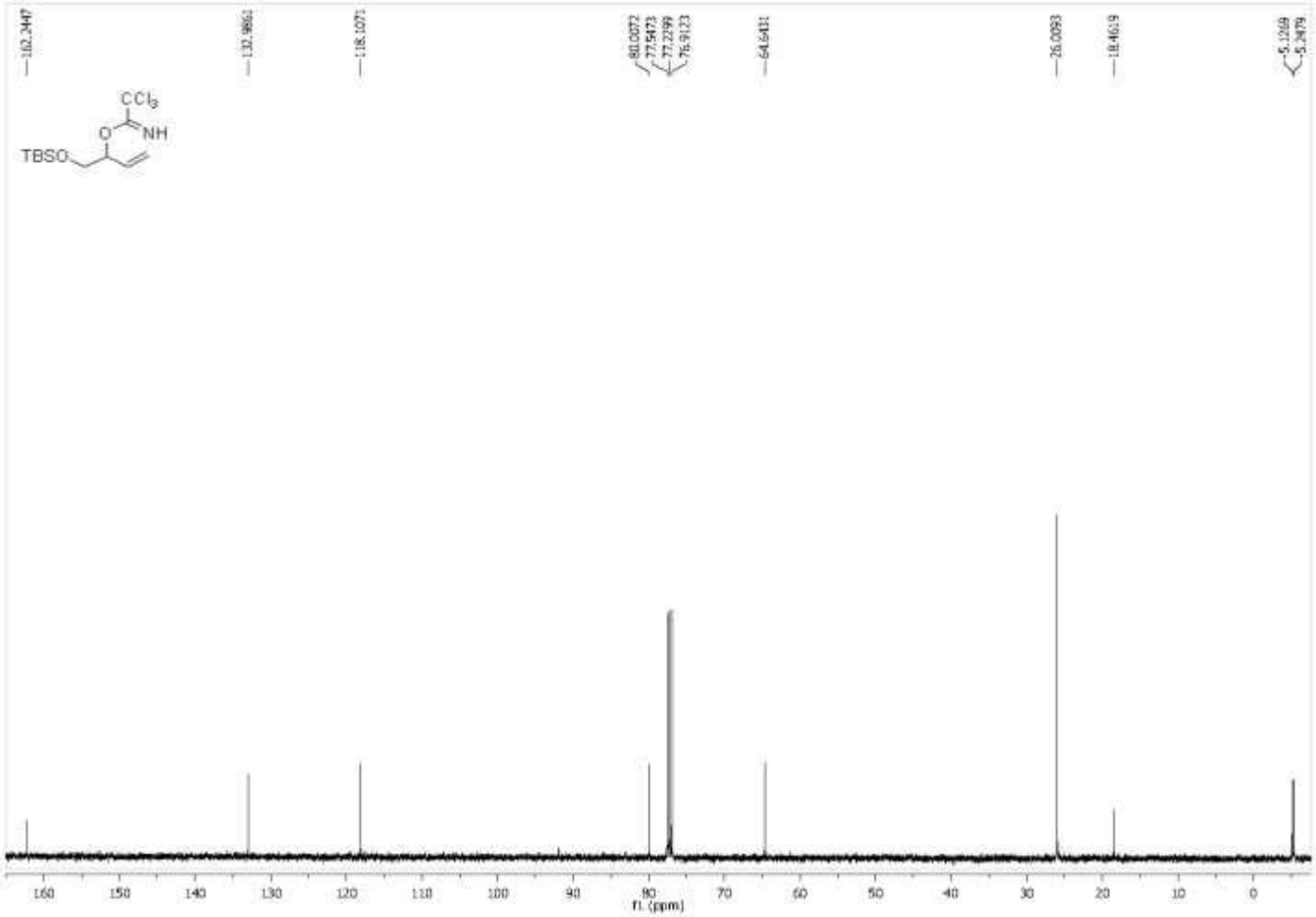

Figure A8 100 MHz 13C NMR ($CDCl_3$) Spectra of Compound **228**

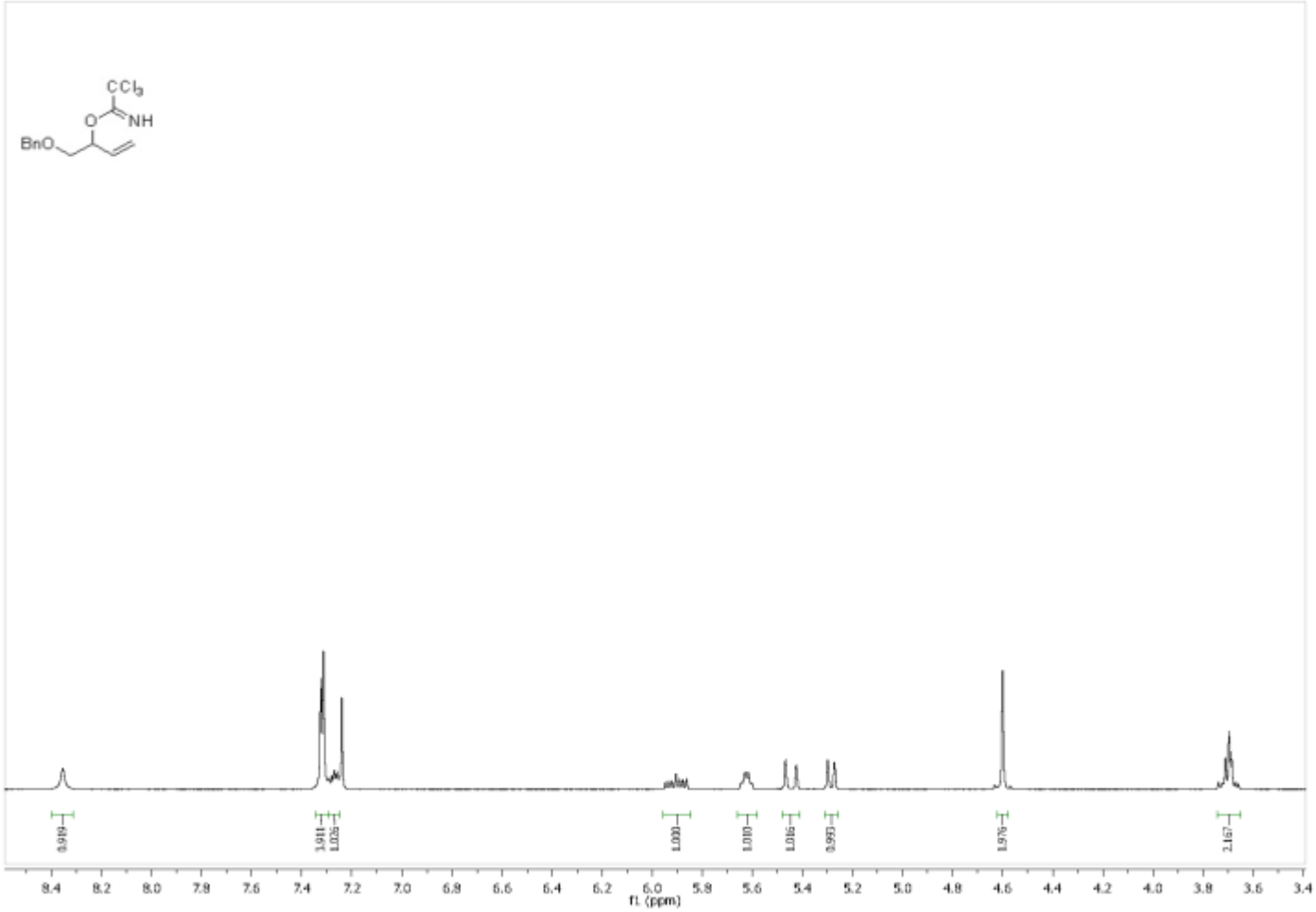

Figure A9 400 MHz 1H NMR ($CDCl_3$) Spectra of Compound **229**

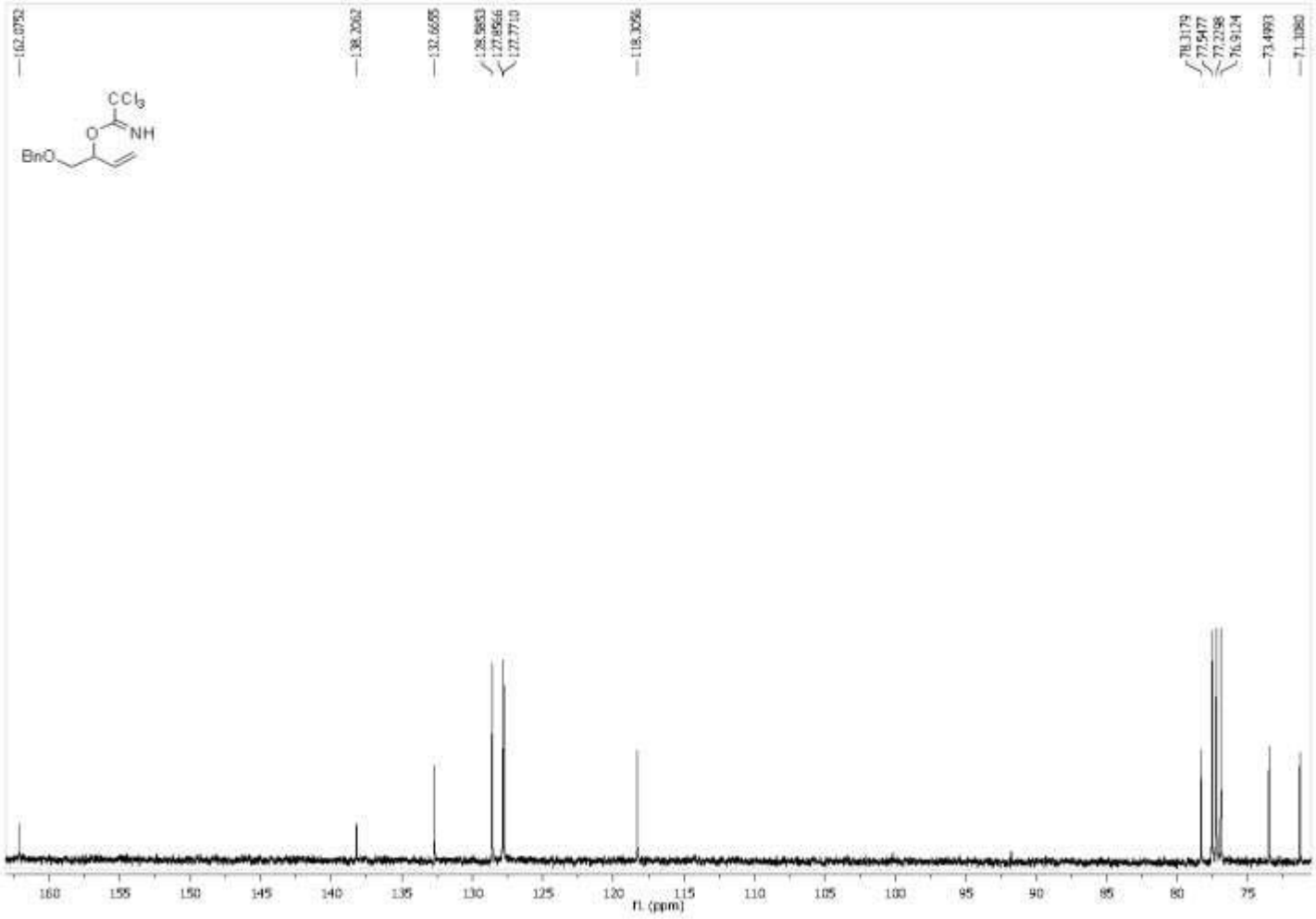

Figure A10 100 MHz 13C NMR ($CDCl_3$) Spectra of Compound **229**

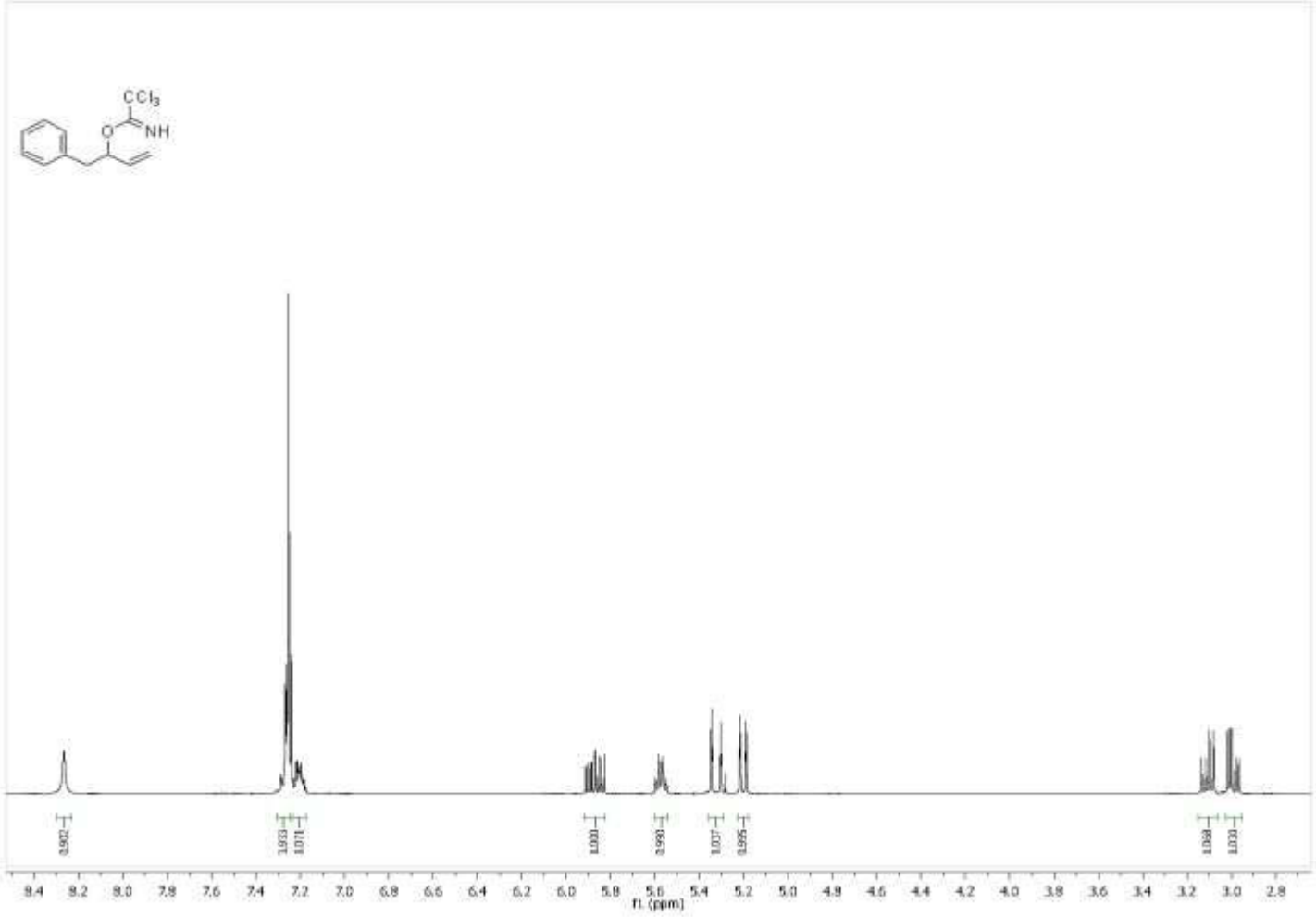

Figure A11 400 MHz 1H NMR ($CDCl_3$) Spectra of Compound **230**

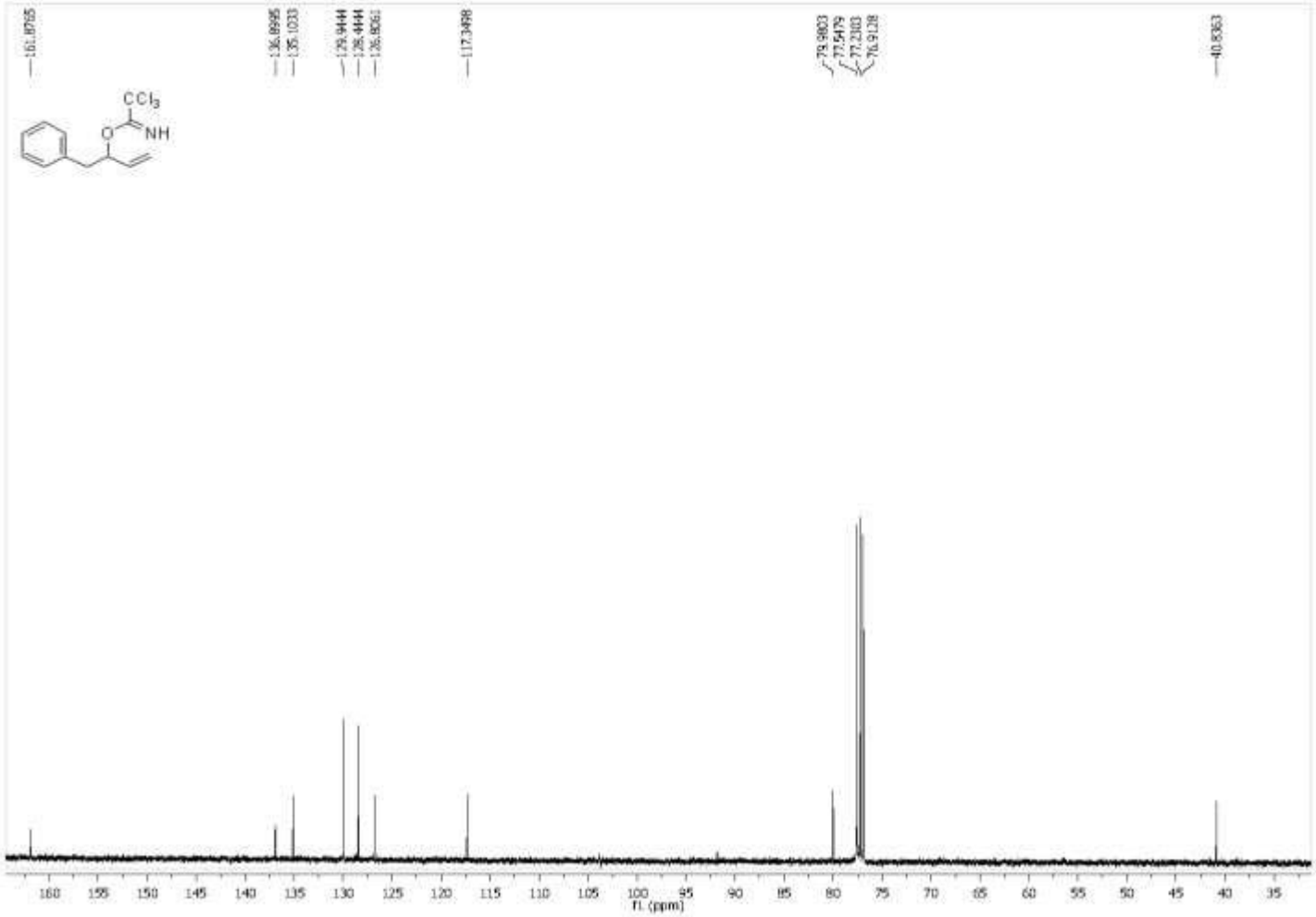

Figure A12 100 MHz 13C NMR ($CDCl_3$) Spectra of Compound **230**

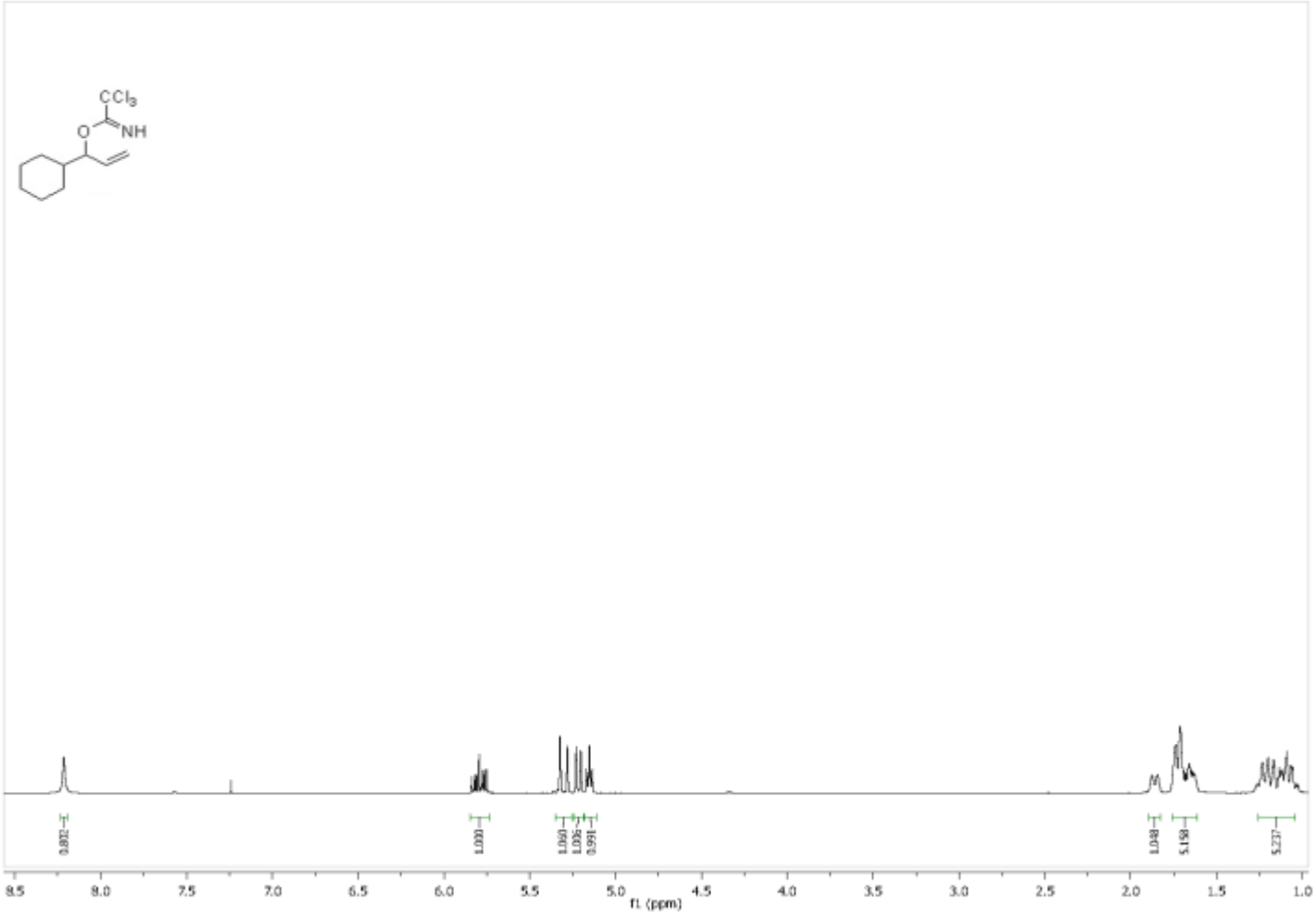

Figure A13 400 MHz 1H NMR ($CDCl_3$) Spectra of Compound **231**

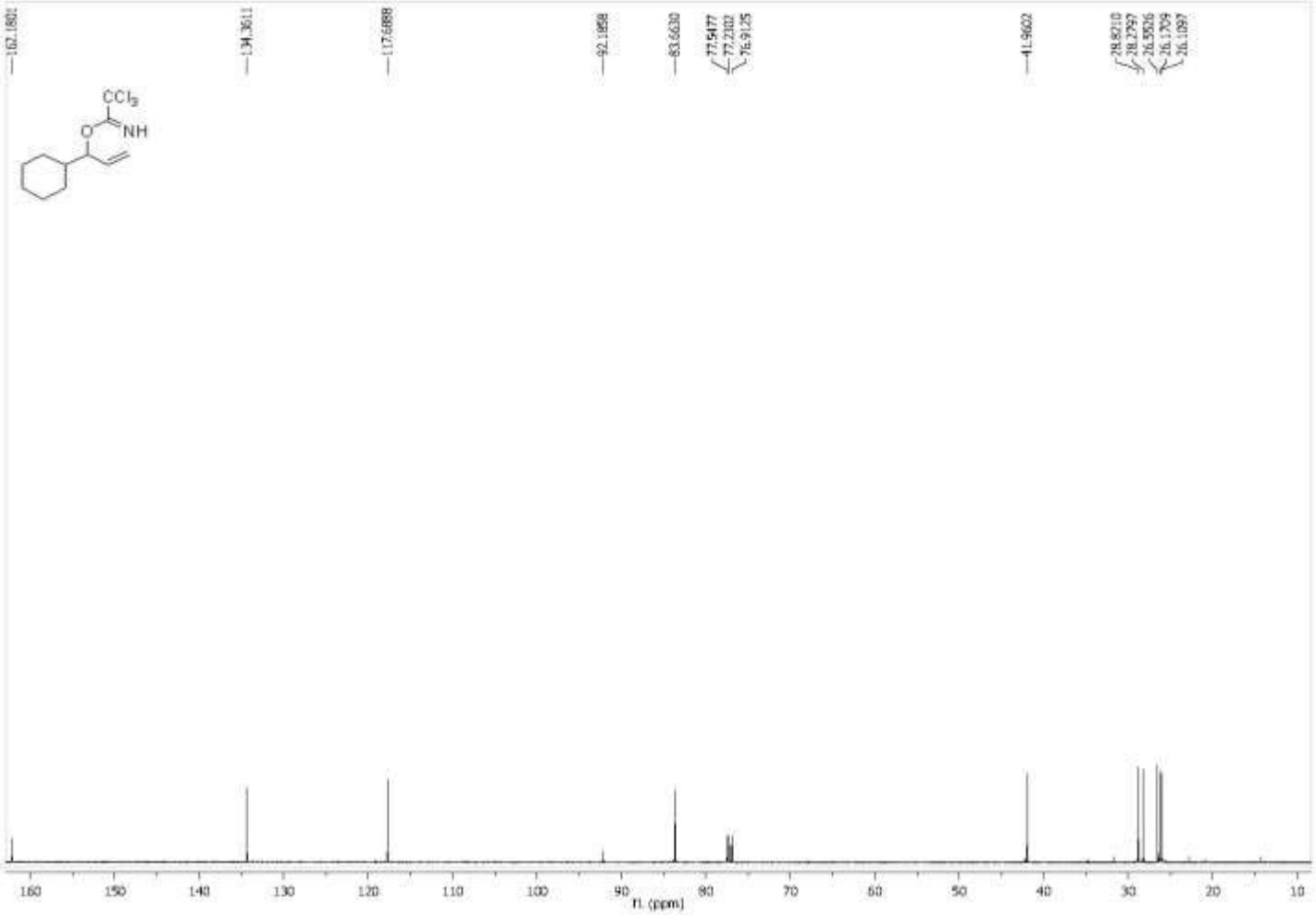

Figure A14 100 MHz 13C NMR ($CDCl_3$) Spectra of Compound **231**

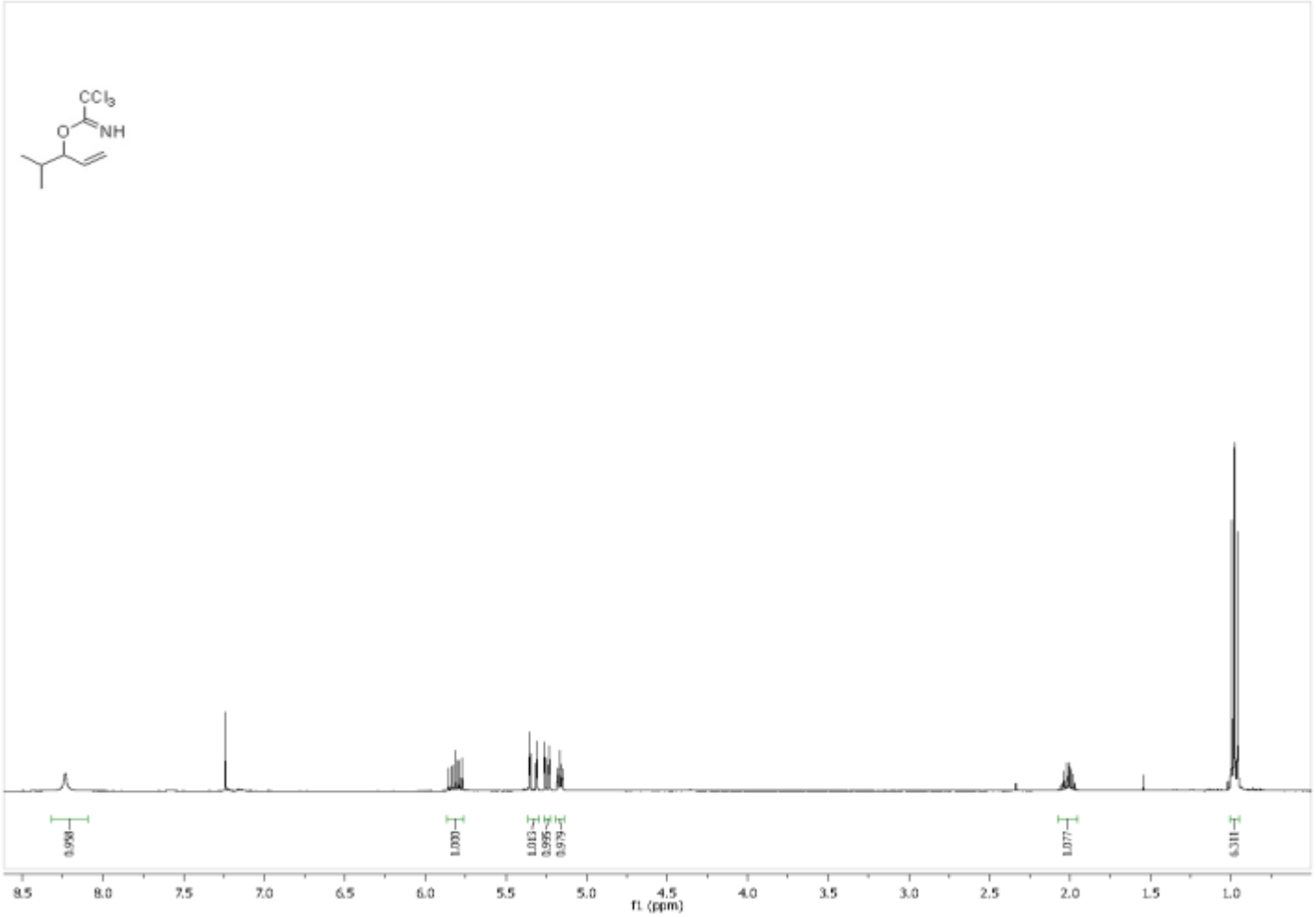

Figure A15 400 MHz 1H NMR ($CDCl_3$) Spectra of Compound **232**

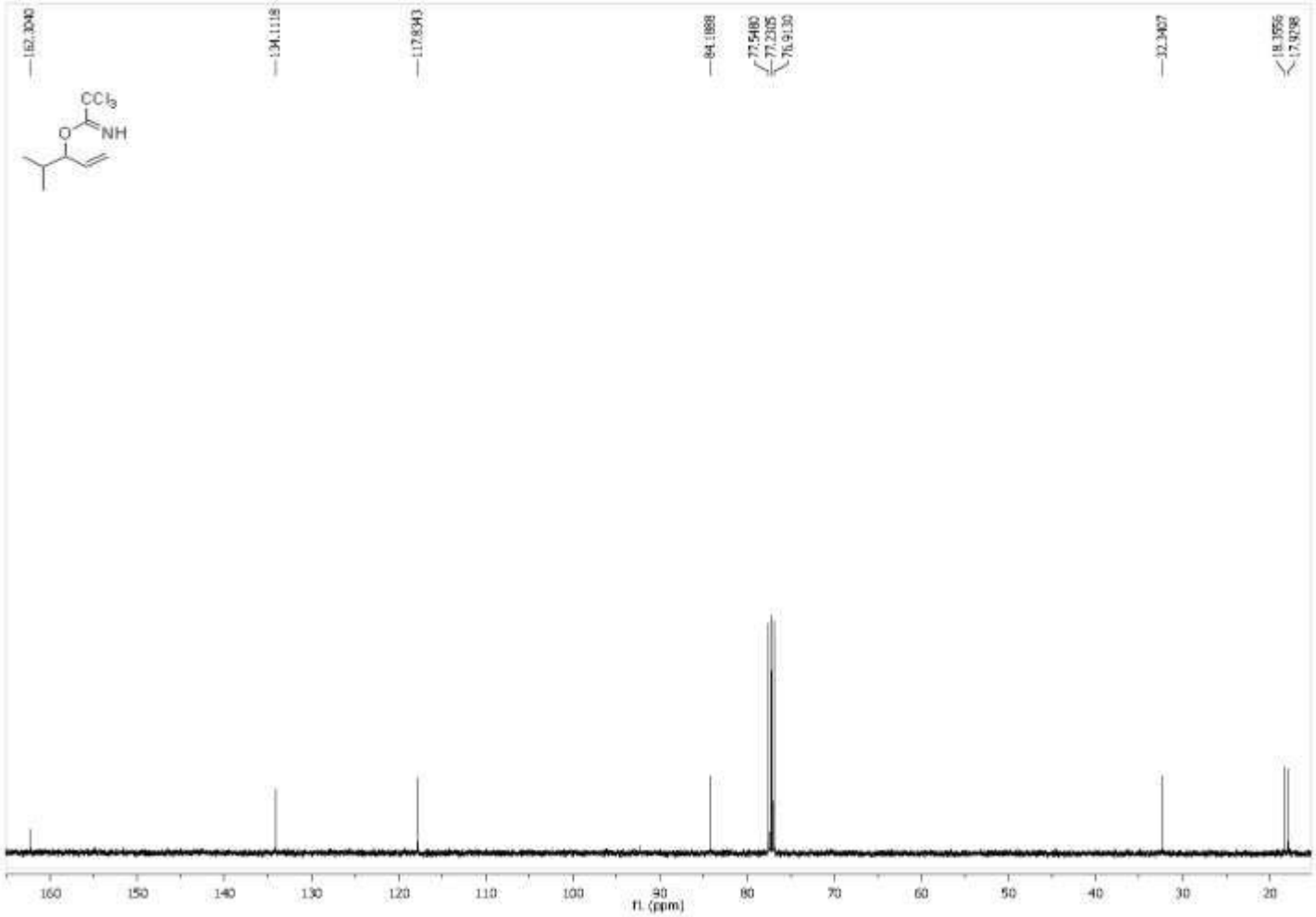

Figure A16 100 MHz 13C NMR ($CDCl_3$) Spectra of Compound **232**

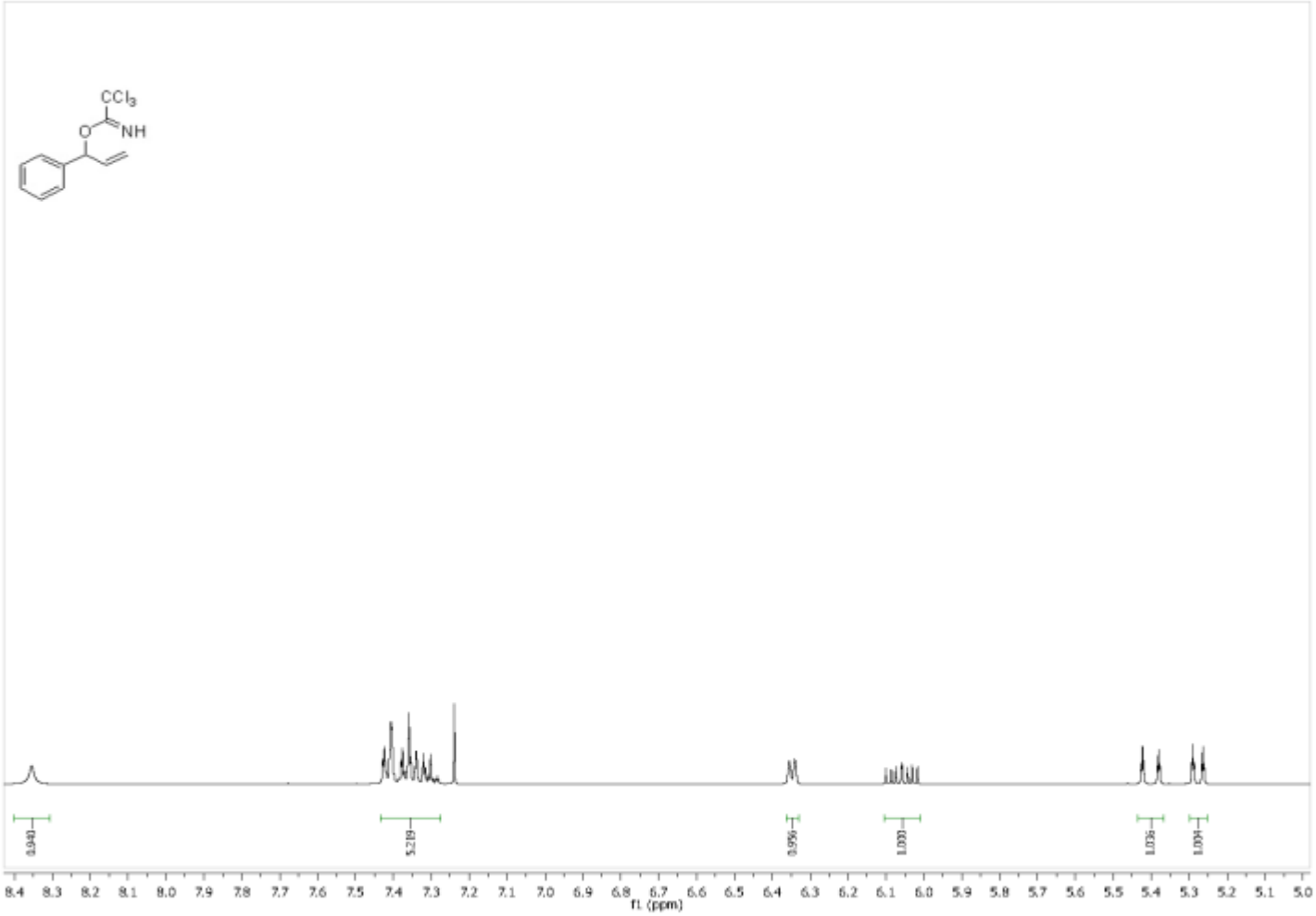

Figure A17 400 MHz 1H NMR ($CDCl_3$) Spectra of Compound **233**

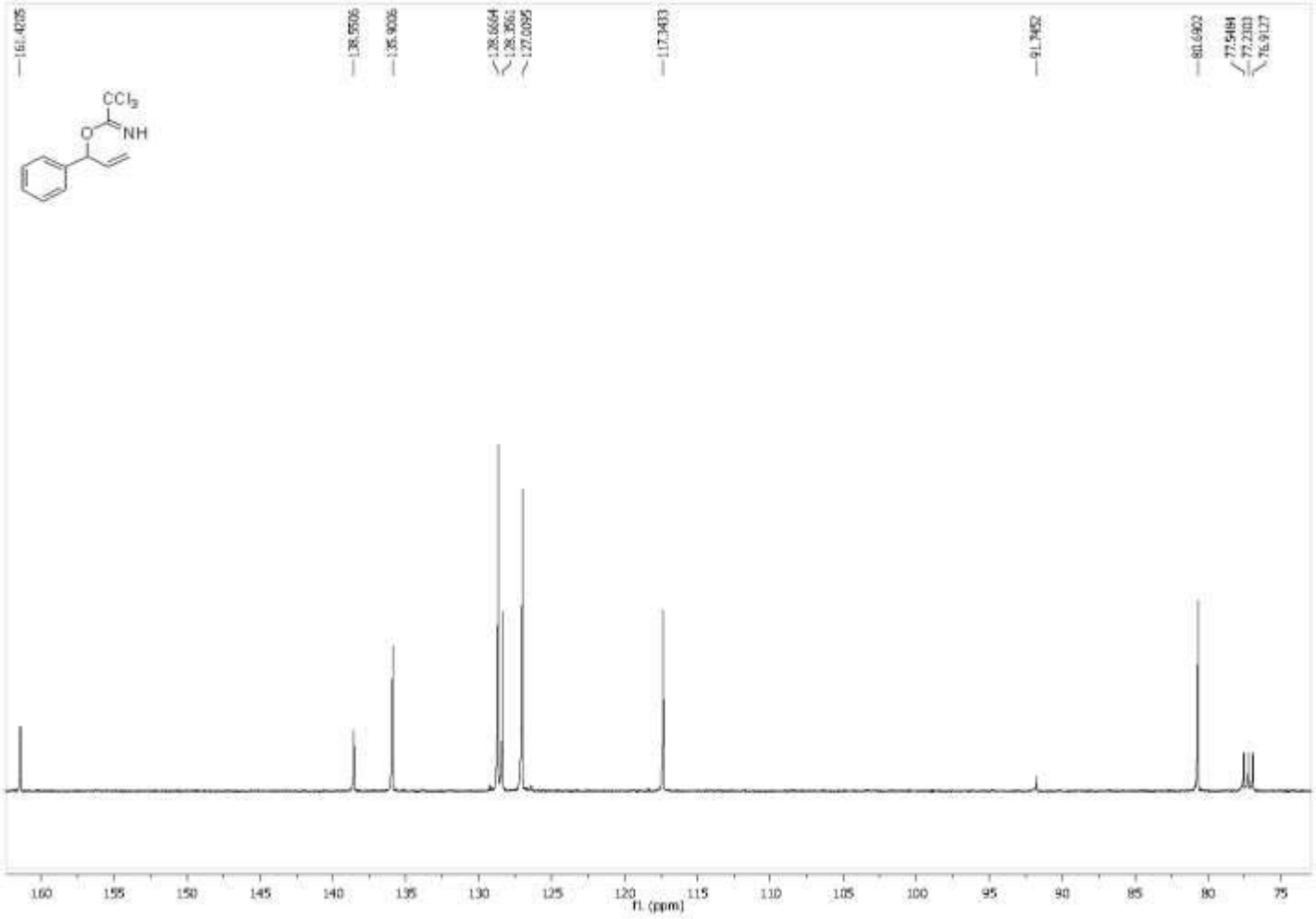

Figure A18 100 MHz 13C NMR ($CDCl_3$) Spectra of Compound **233**

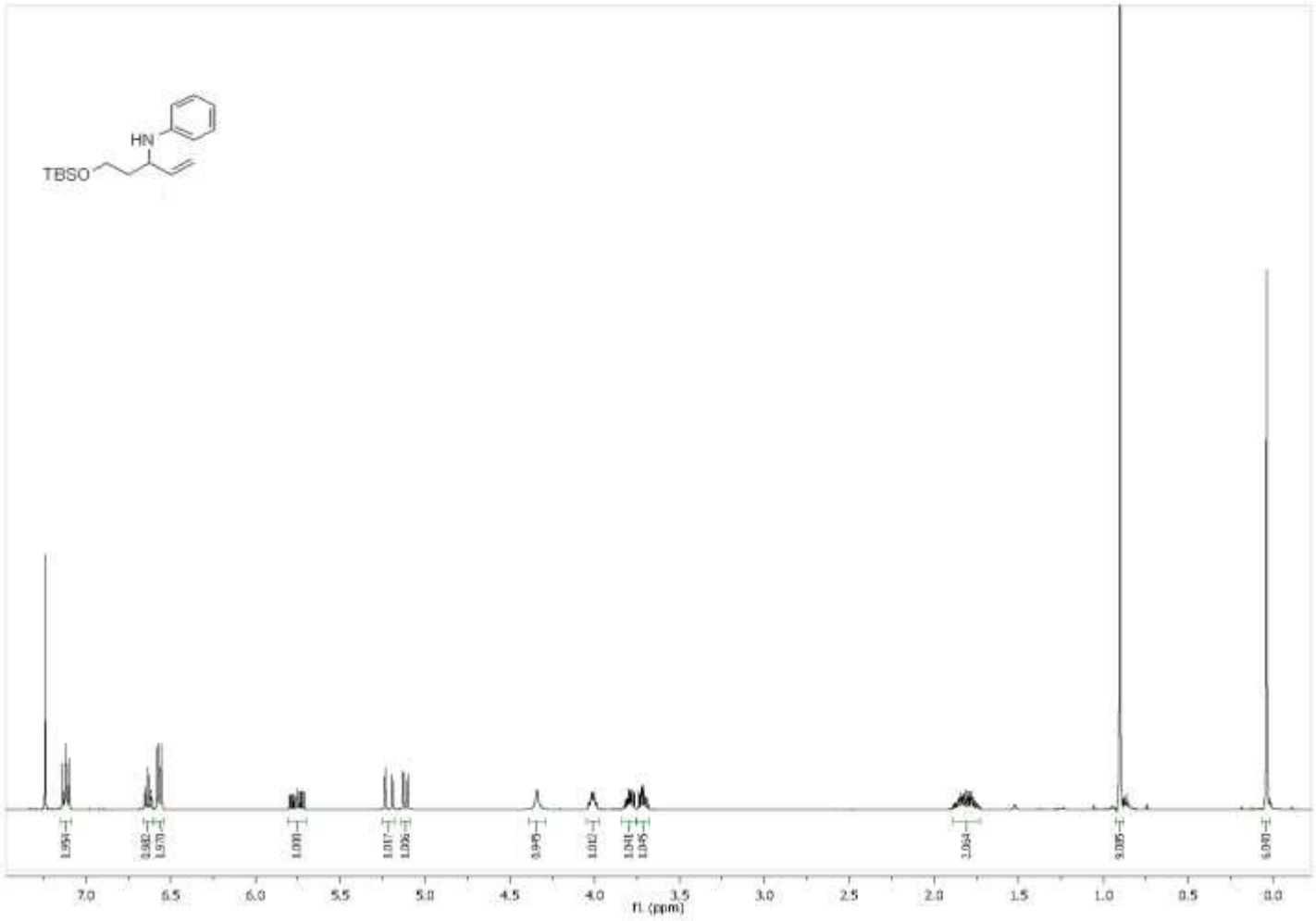

Figure A19 400 MHz 1H NMR ($CDCl_3$) Spectra of Compound **224**

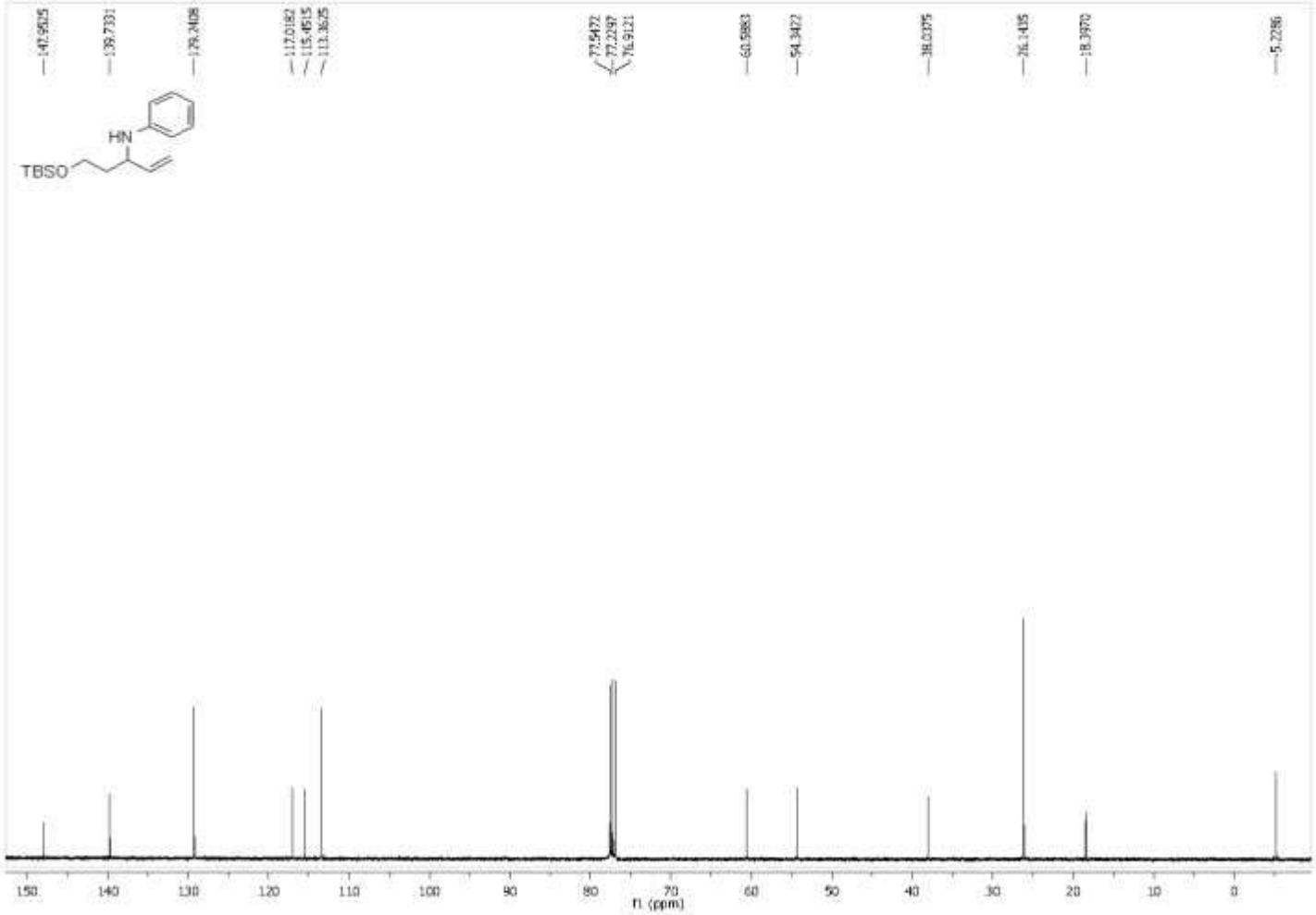

Figure A20 100 MHz 13C NMR ($CDCl_3$) Spectra of Compound **224**

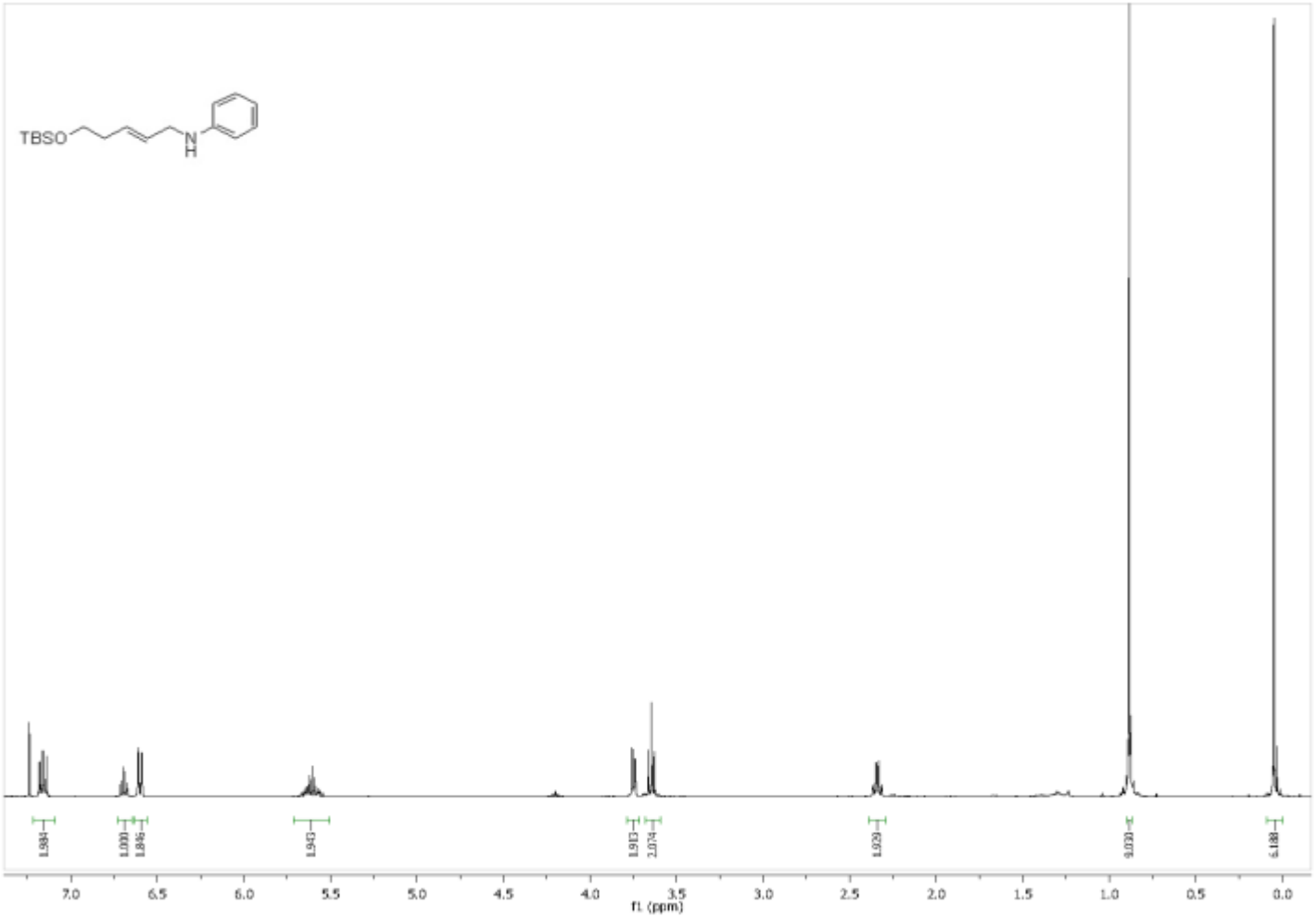

Figure A21 400 MHz 1H NMR ($CDCl_3$) Spectra of Compound **225**

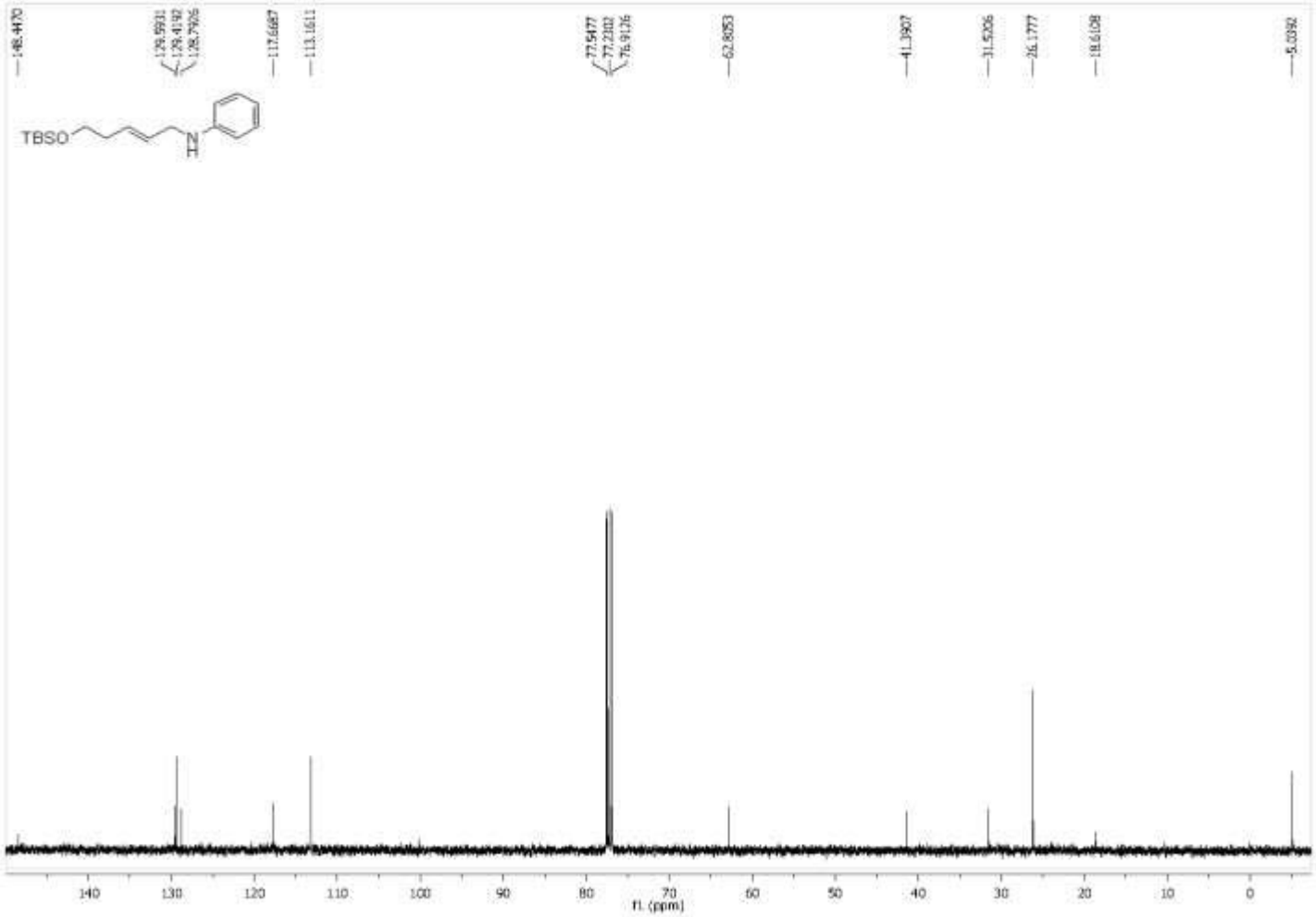

Figure A22 100 MHz 13C NMR ($CDCl_3$) Spectra of Compound **225**

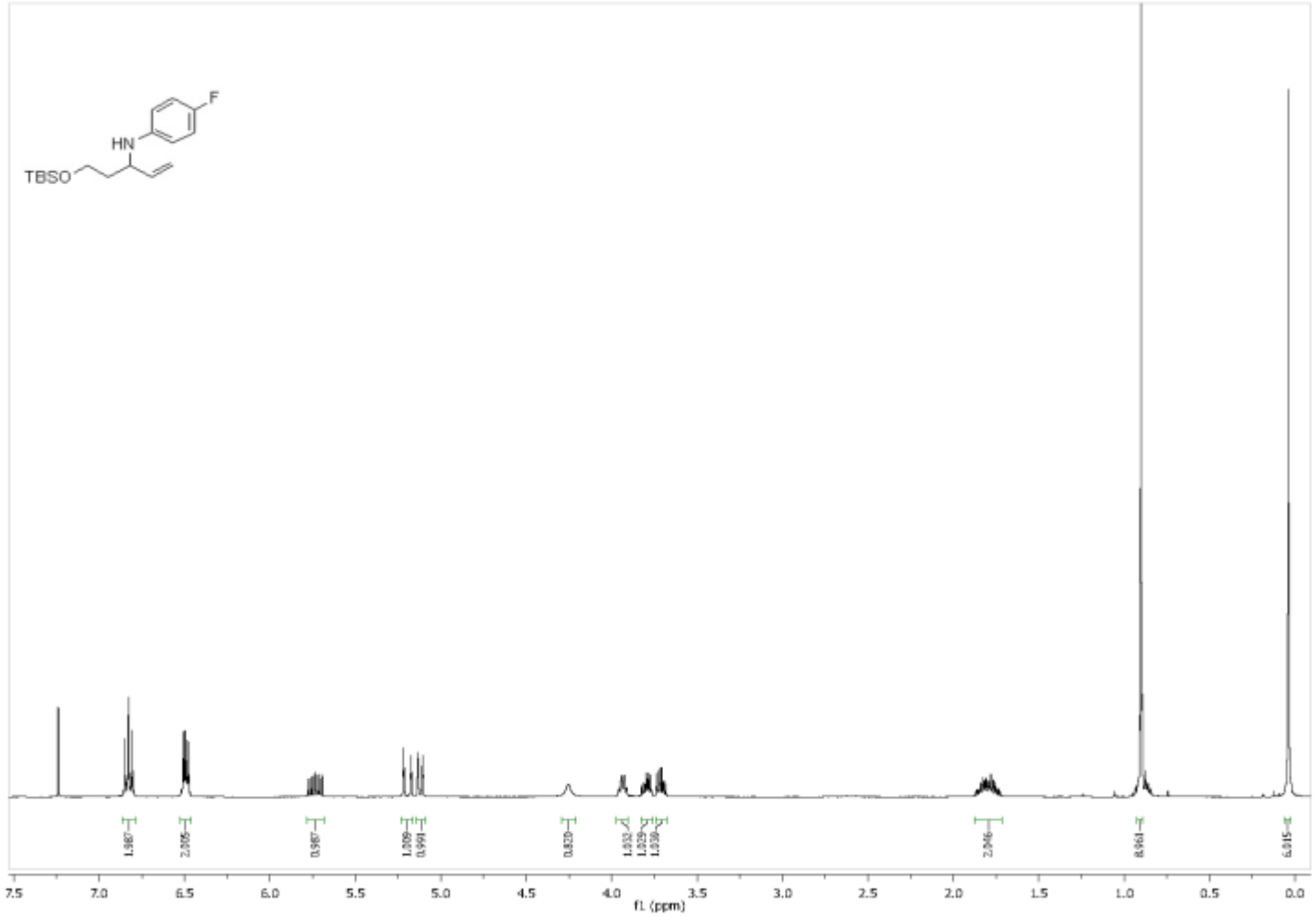

Figure A23 400 MHz 1H NMR ($CDCl_3$) Spectra of Compound **223b**

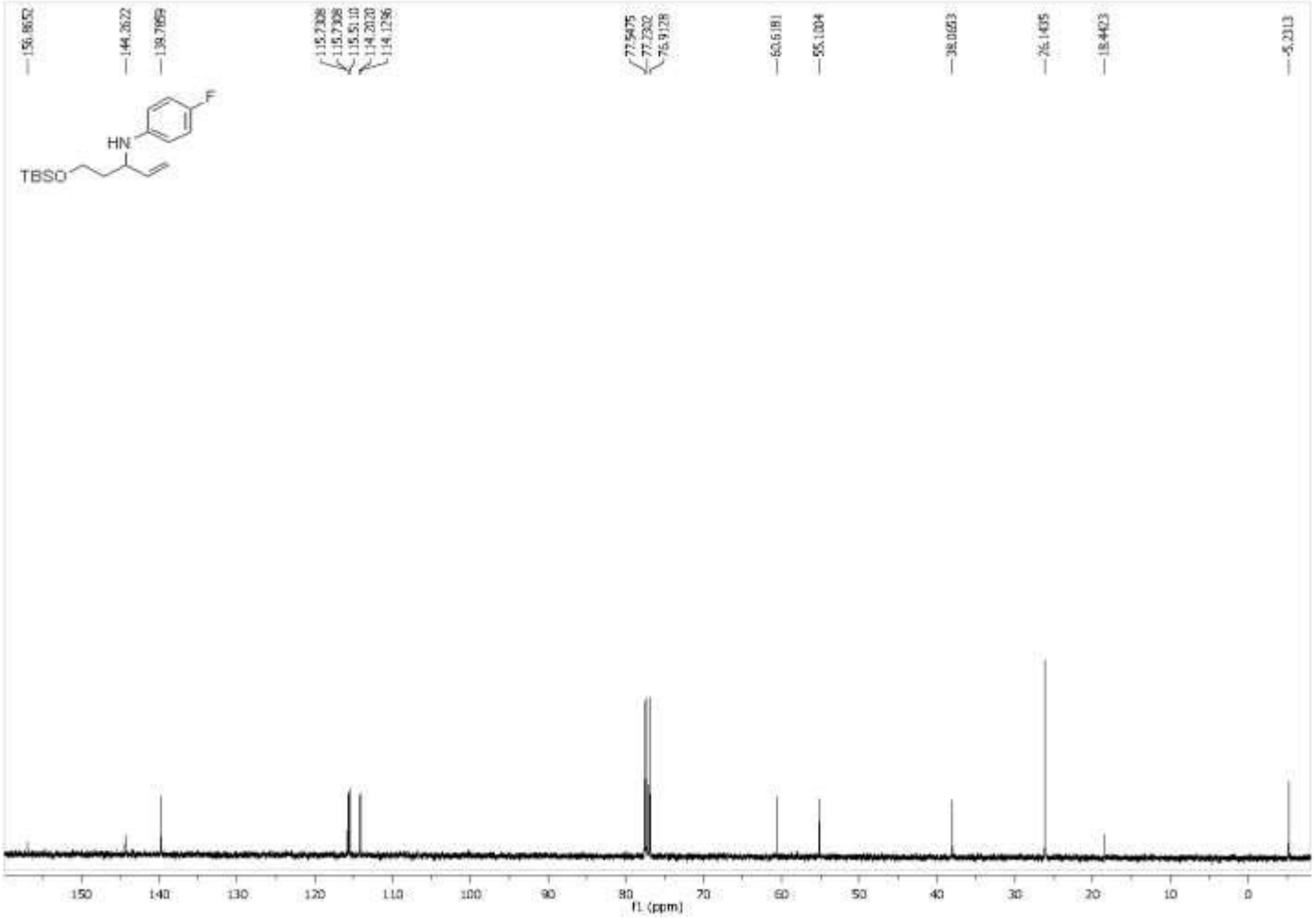

Figure A24 100 MHz 13C NMR ($CDCl_3$) Spectra of Compound **223b**

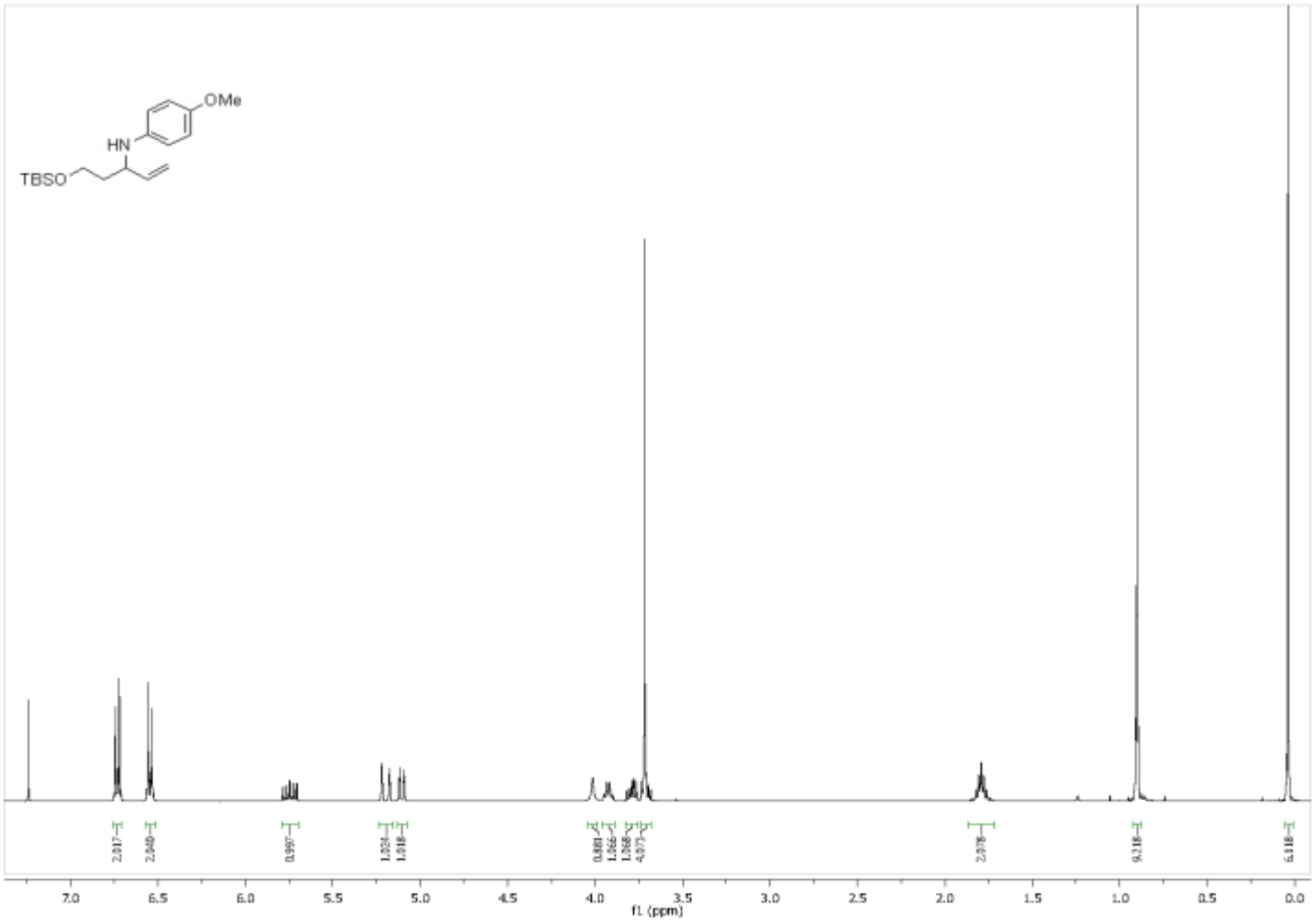

Figure A25 400 MHz 1H NMR ($CDCl_3$) Spectra of Compound **223c**

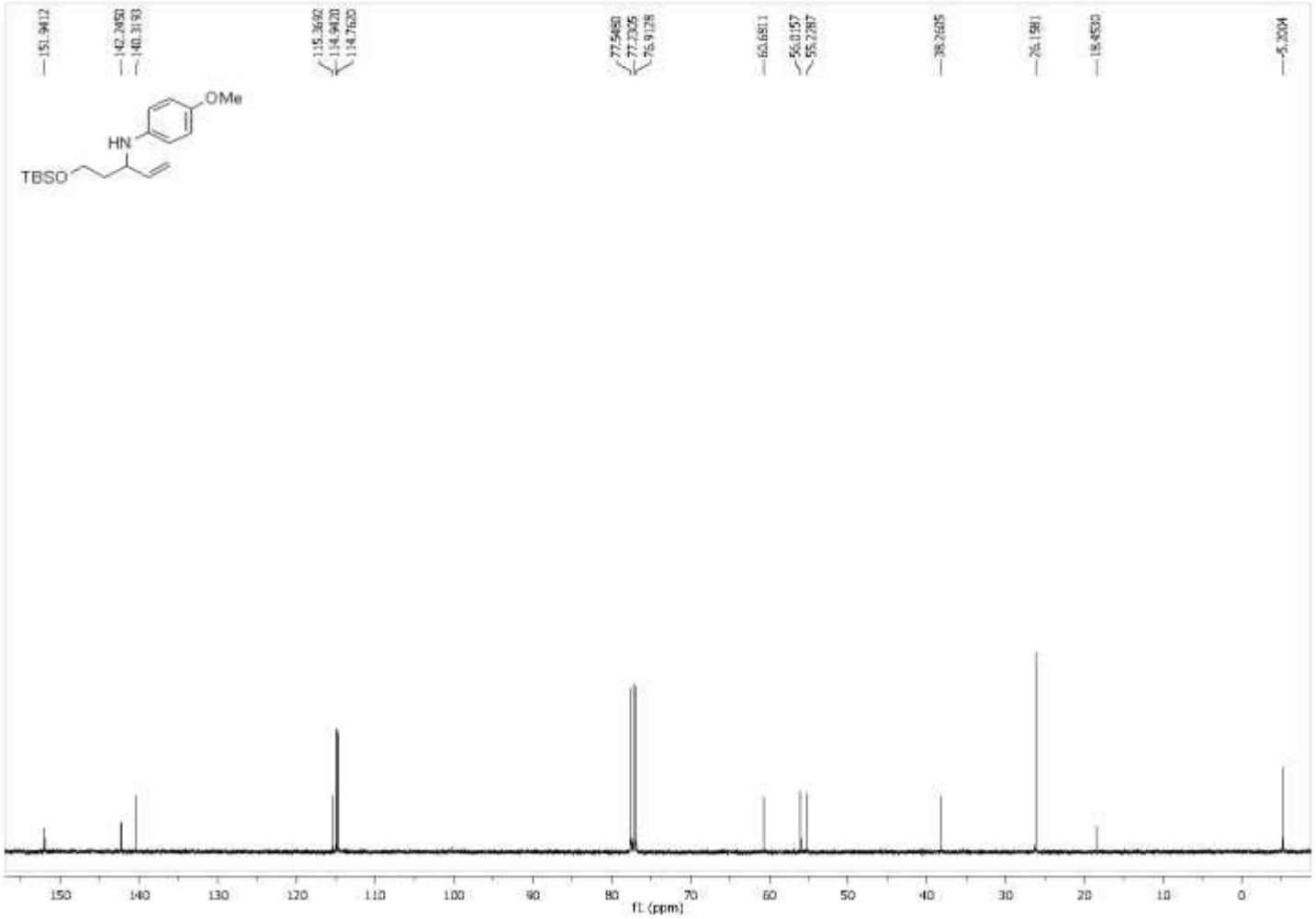

Figure A26 100 MHz 13C NMR ($CDCl_3$) Spectra of Compound **223c**

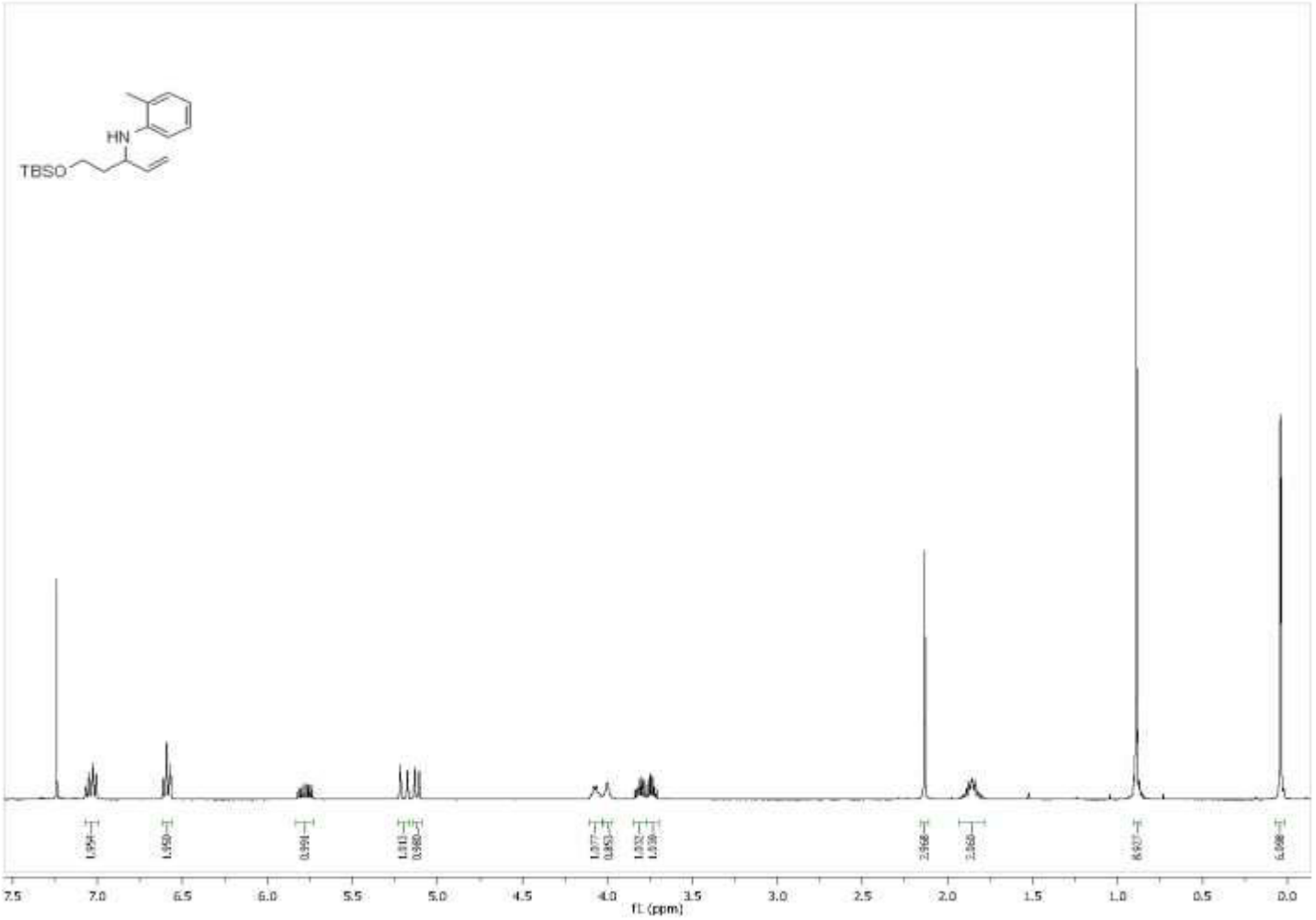

Figure A27 400 MHz 1H NMR ($CDCl_3$) Spectra of Compound **223d**

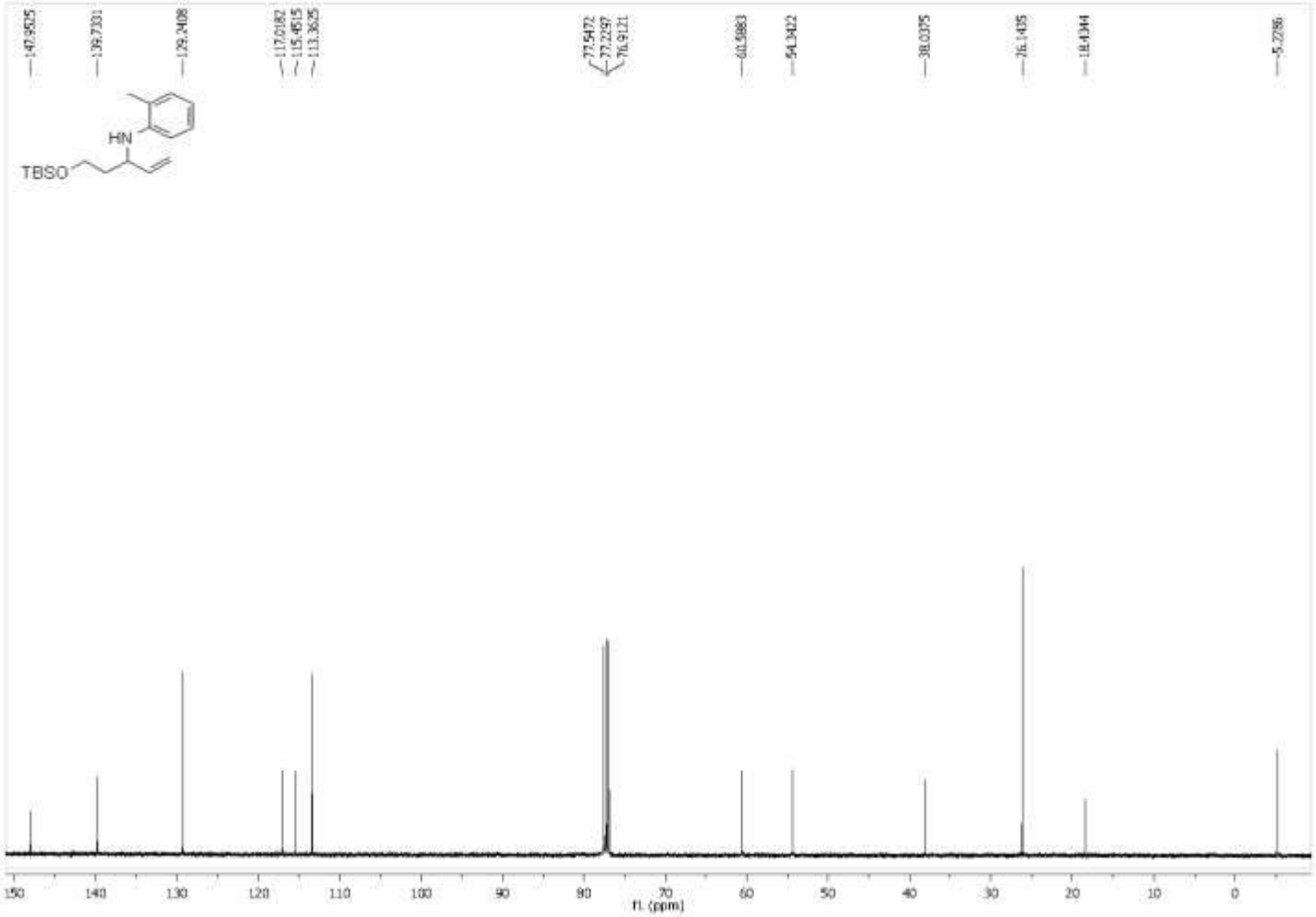

Figure A28 100 MHz 13C NMR ($CDCl_3$) Spectra of Compound **223d**

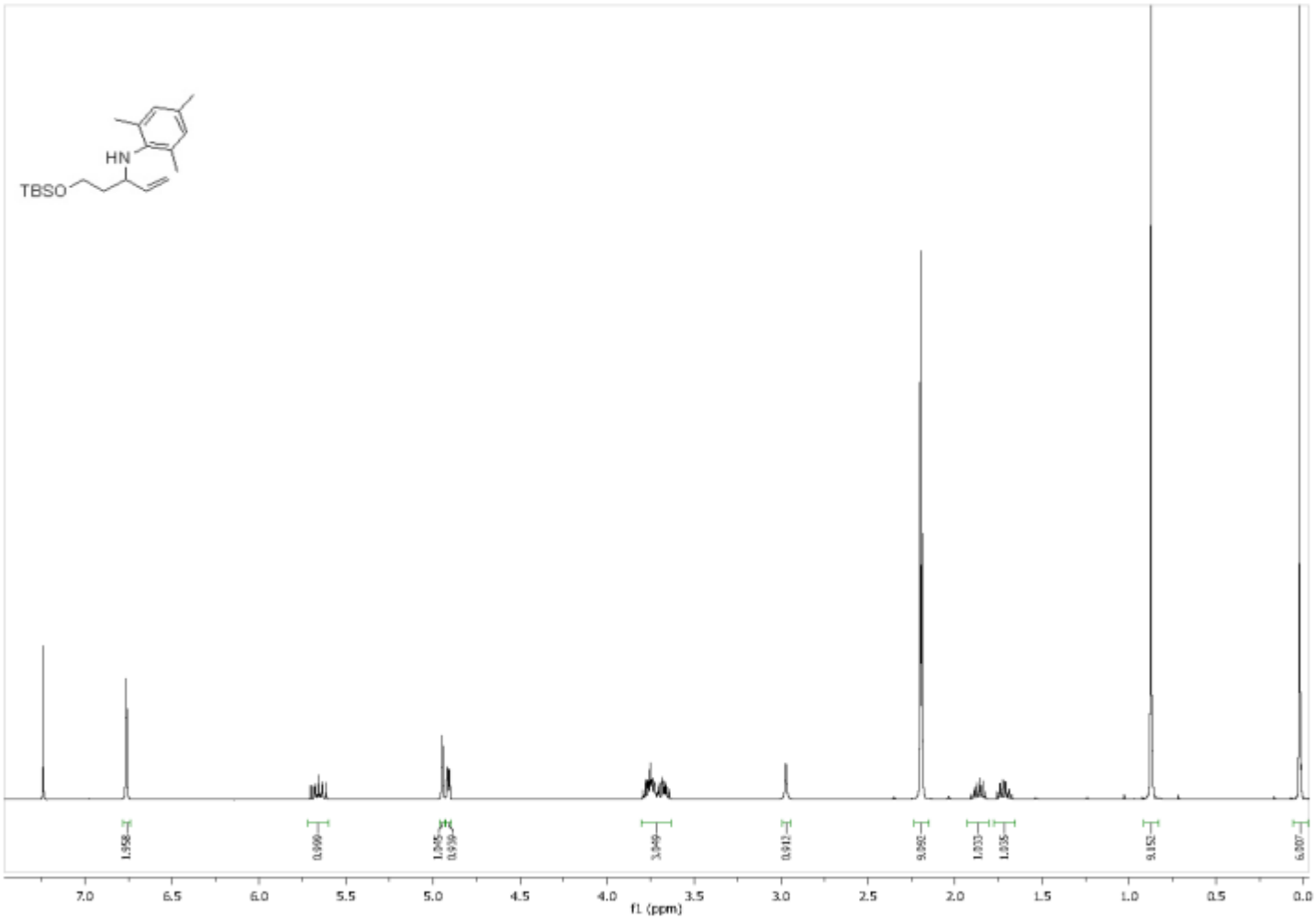

Figure A29 400 MHz 1H NMR ($CDCl_3$) Spectra of Compound **223e**

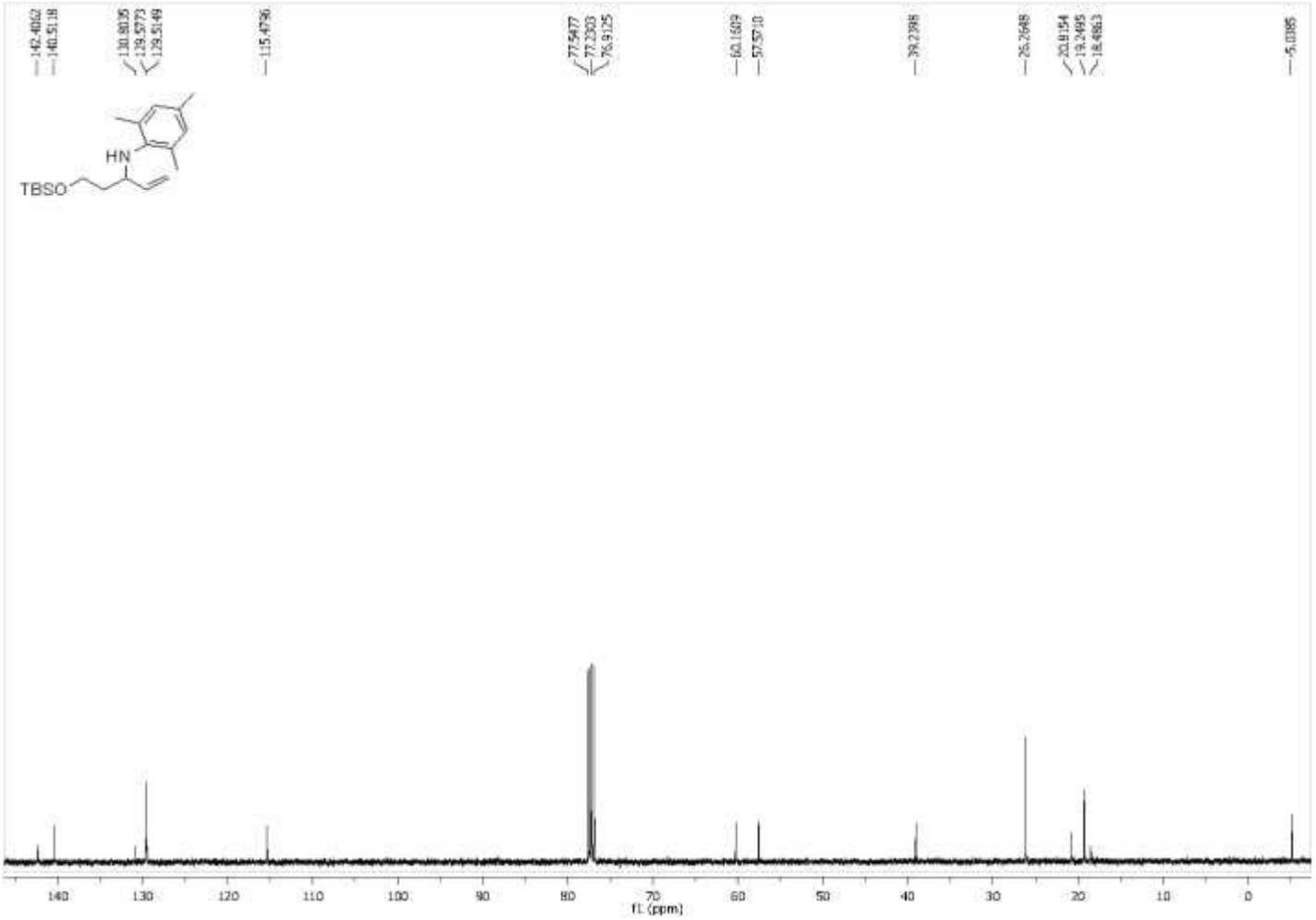

Figure A30 100 MHz 13C NMR ($CDCl_3$) Spectra of Compound **223e**

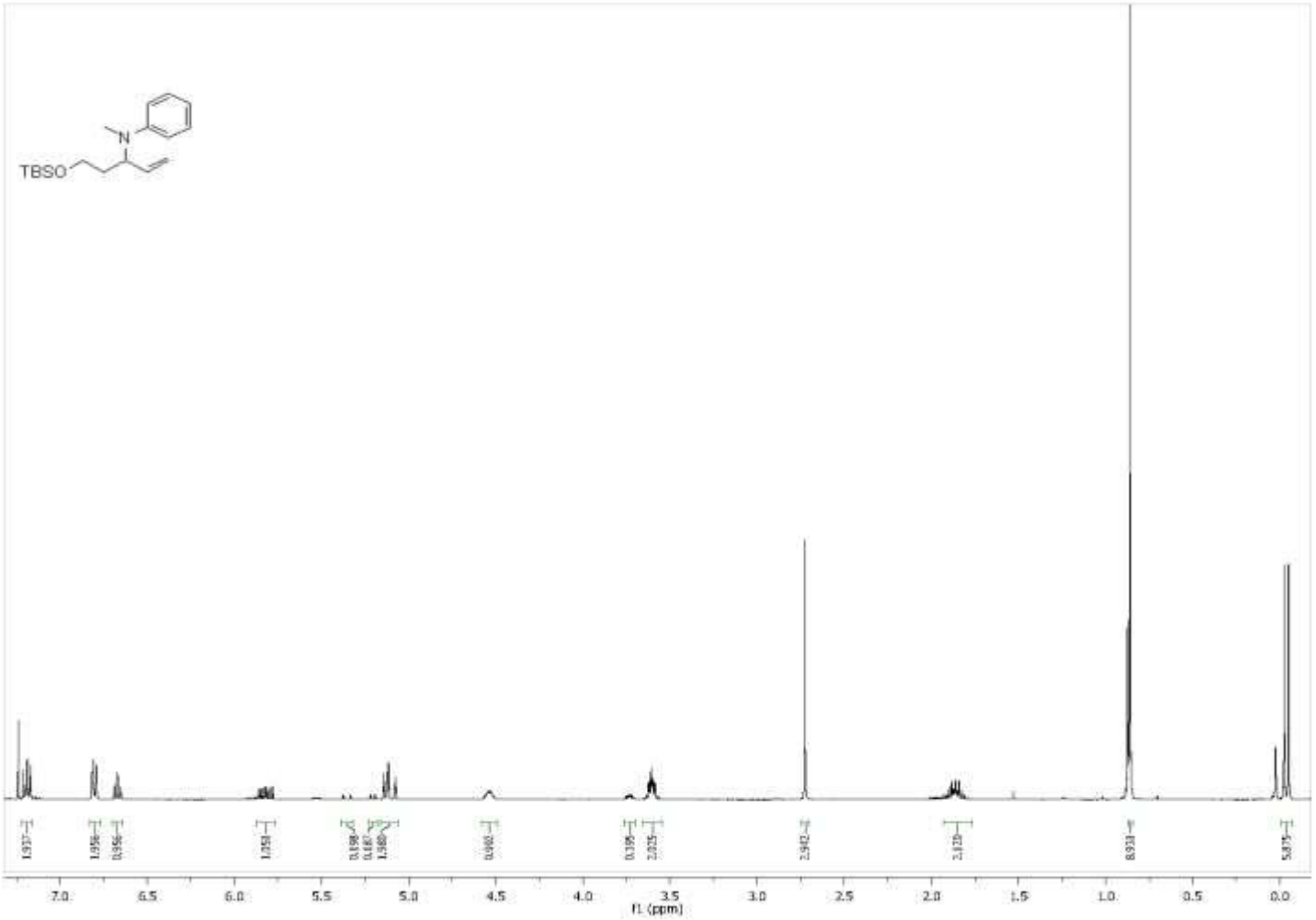

Figure A31 400 MHz 1H NMR ($CDCl_3$) Spectra of Compound **223f**

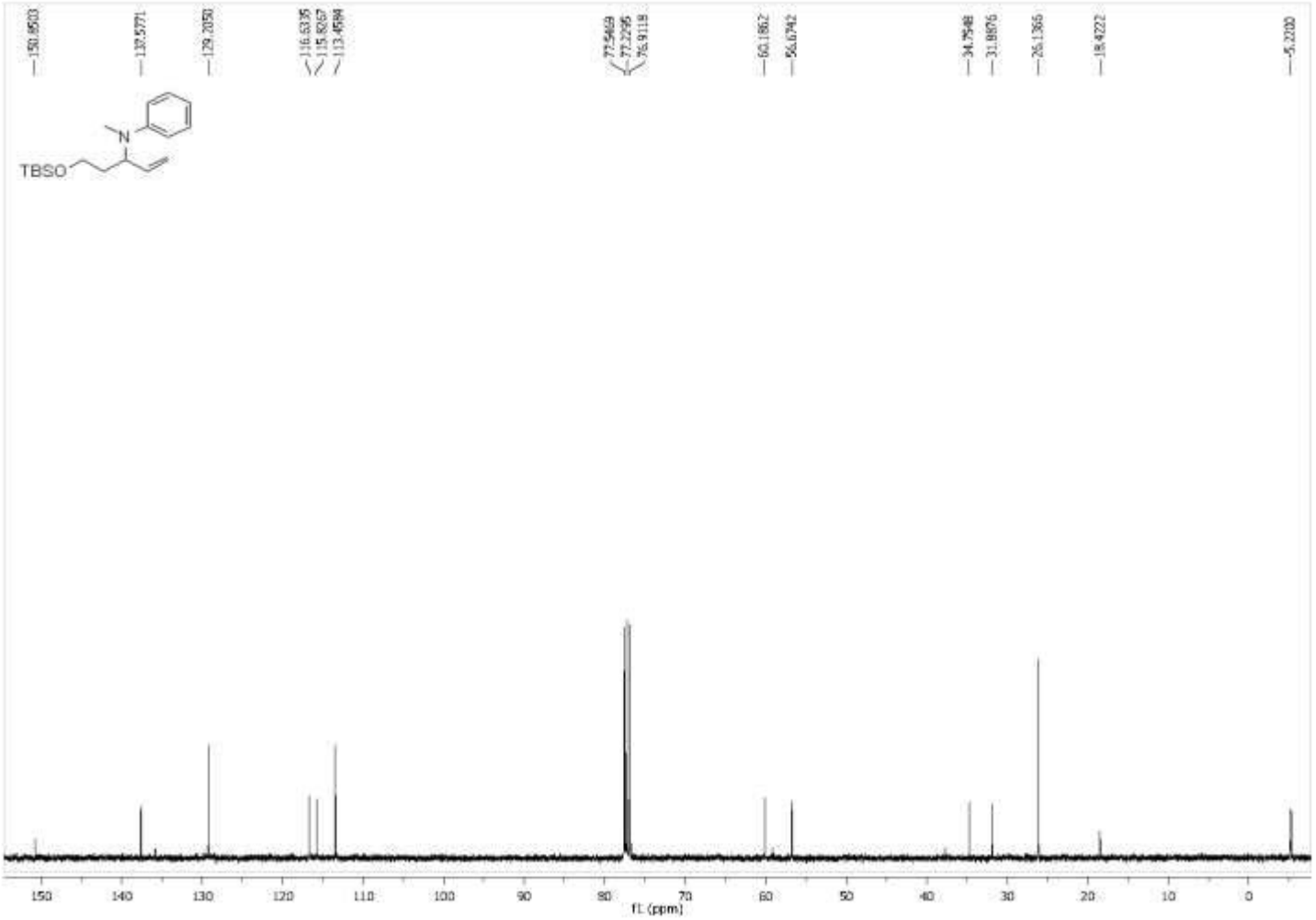

Figure A32 100 MHz 13C NMR ($CDCl_3$) Spectra of Compound **223f**

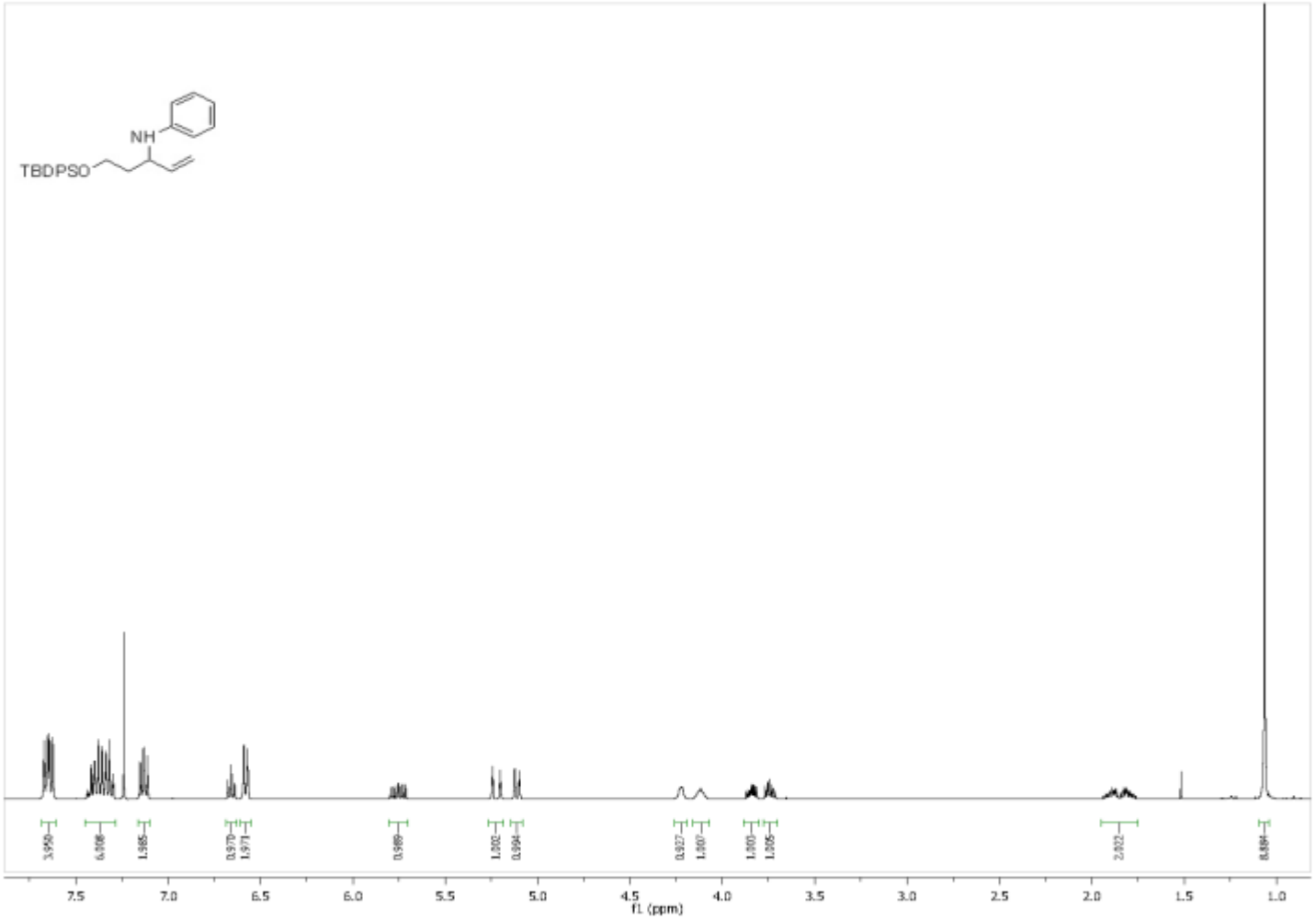

Figure A33 400 MHz 1H NMR ($CDCl_3$) Spectra of Compound **226a**

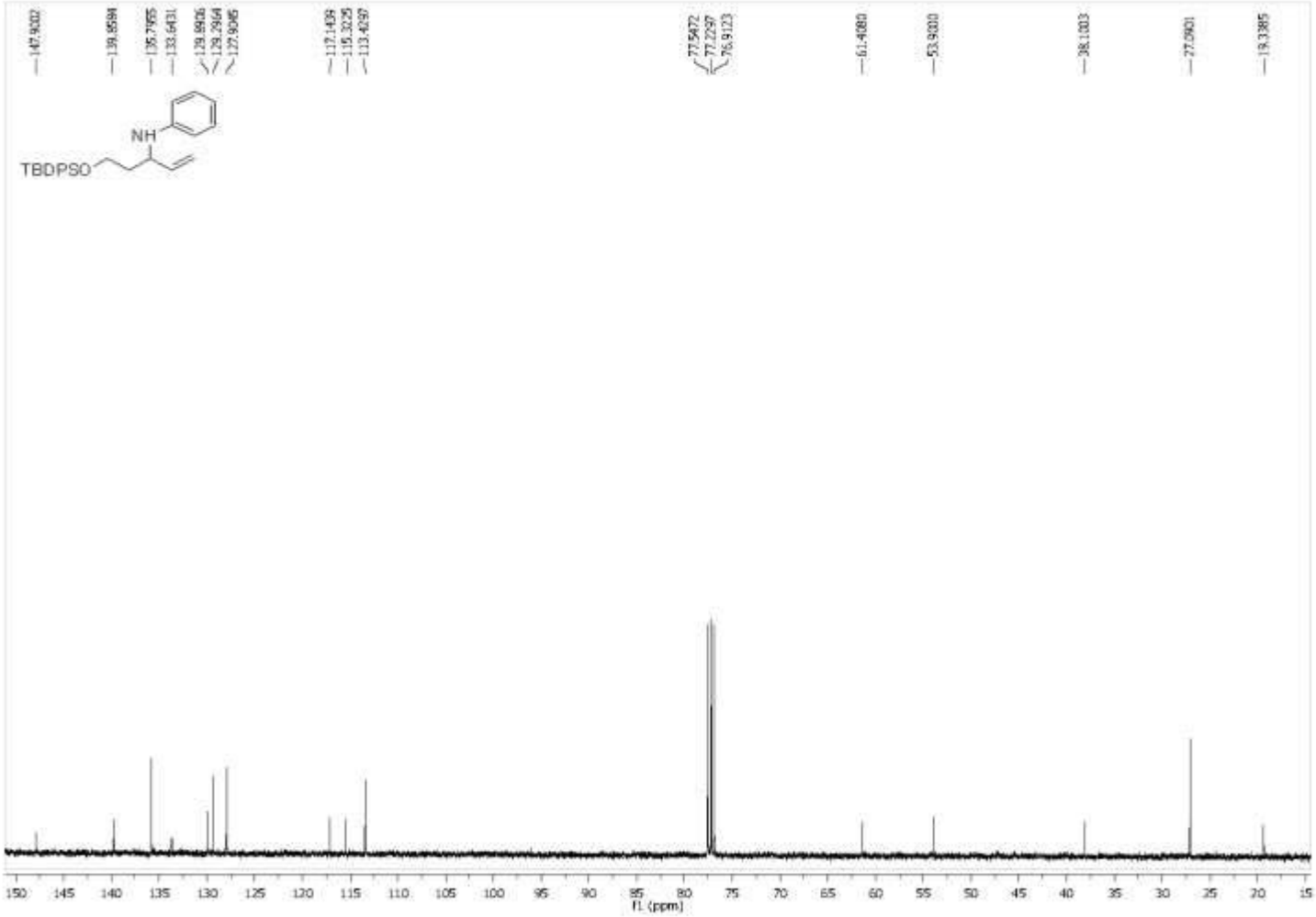

Figure A34 100 MHz 13C NMR ($CDCl_3$) Spectra of Compound **226a**

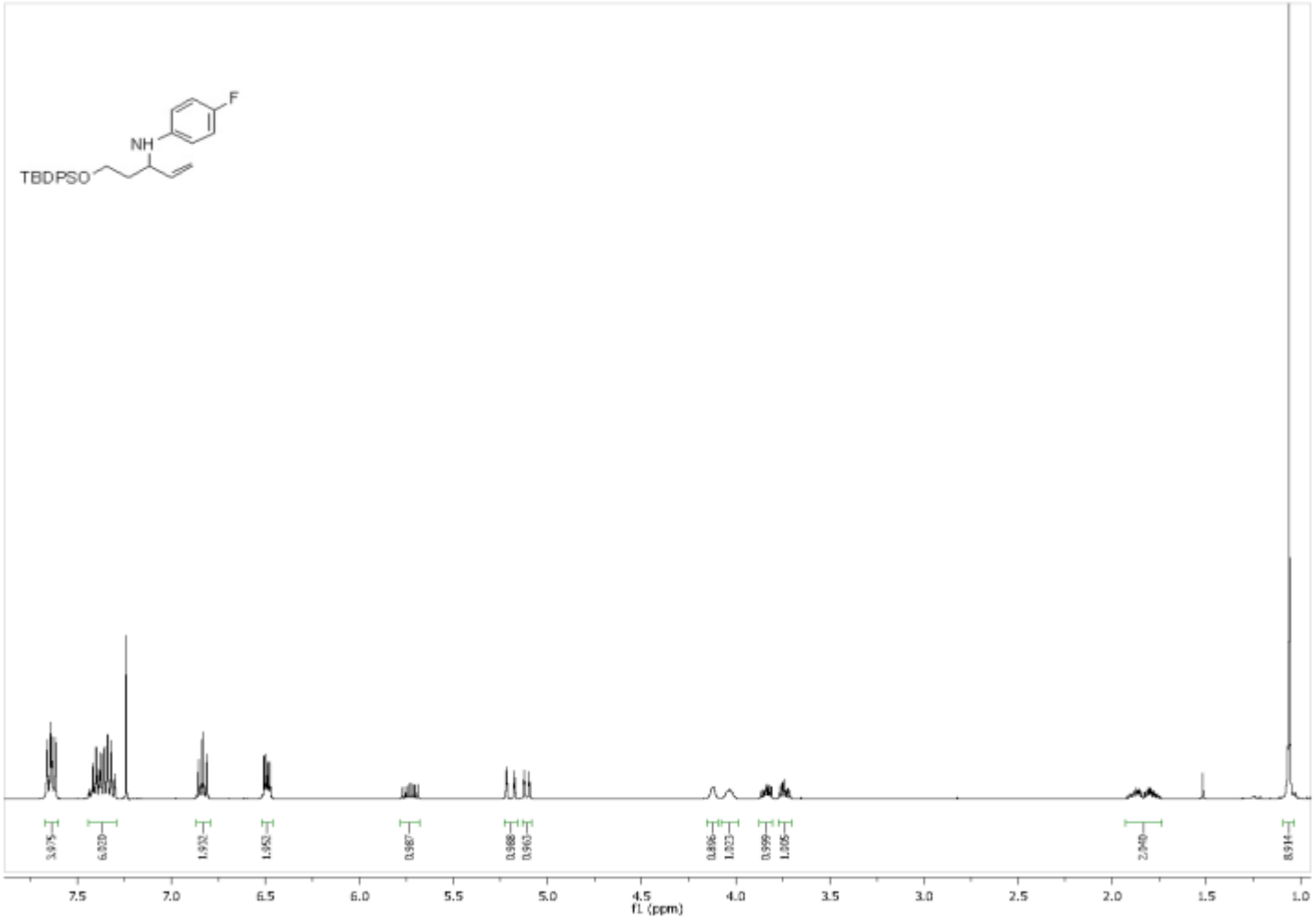

Figure A35 400 MHz 1H NMR ($CDCl_3$) Spectra of Compound **226b**

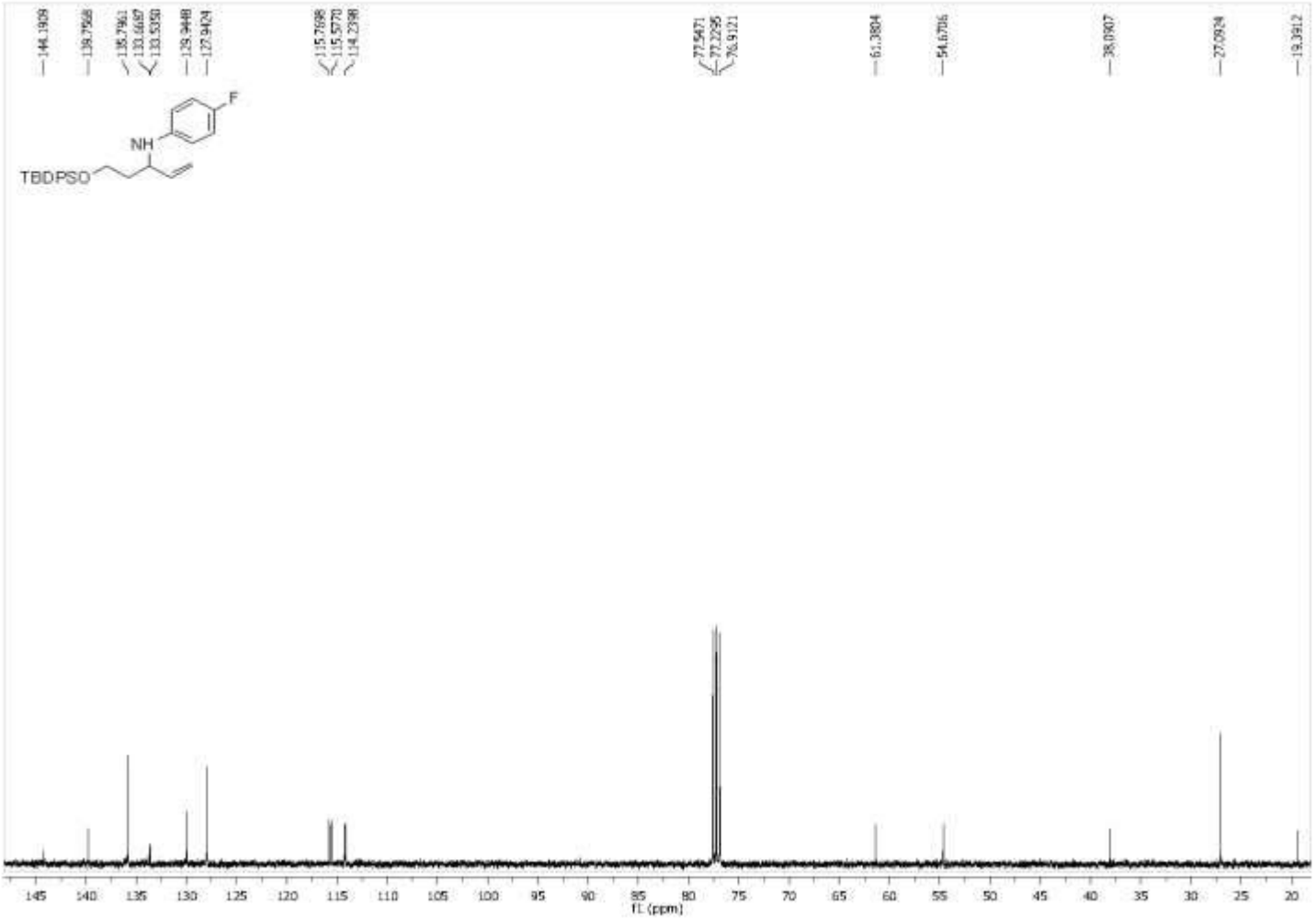

Figure A36 100 MHz 13C NMR ($CDCl_3$) Spectra of Compound **226b**

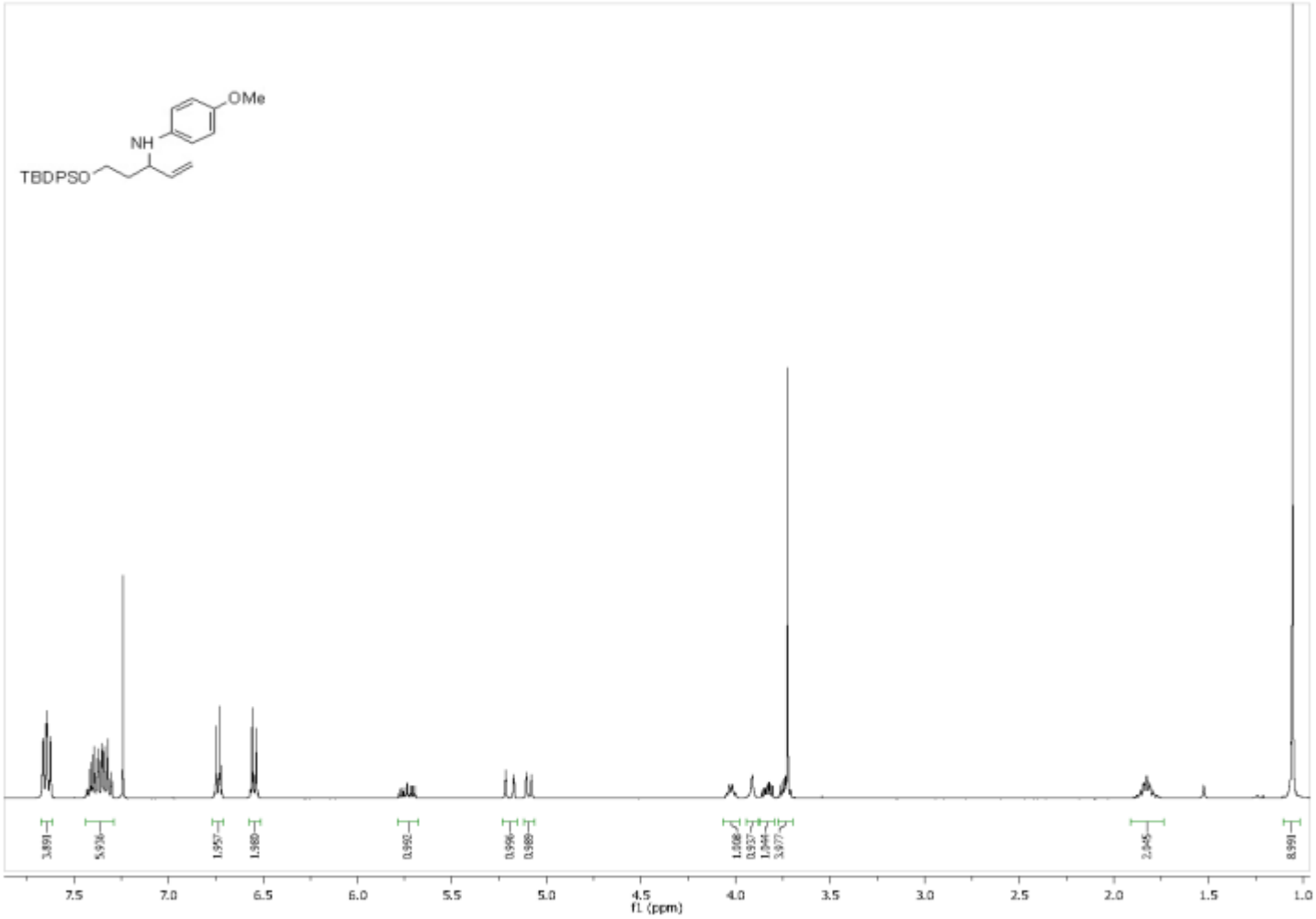

Figure A37 400 MHz 1H NMR ($CDCl_3$) Spectra of Compound **226c**

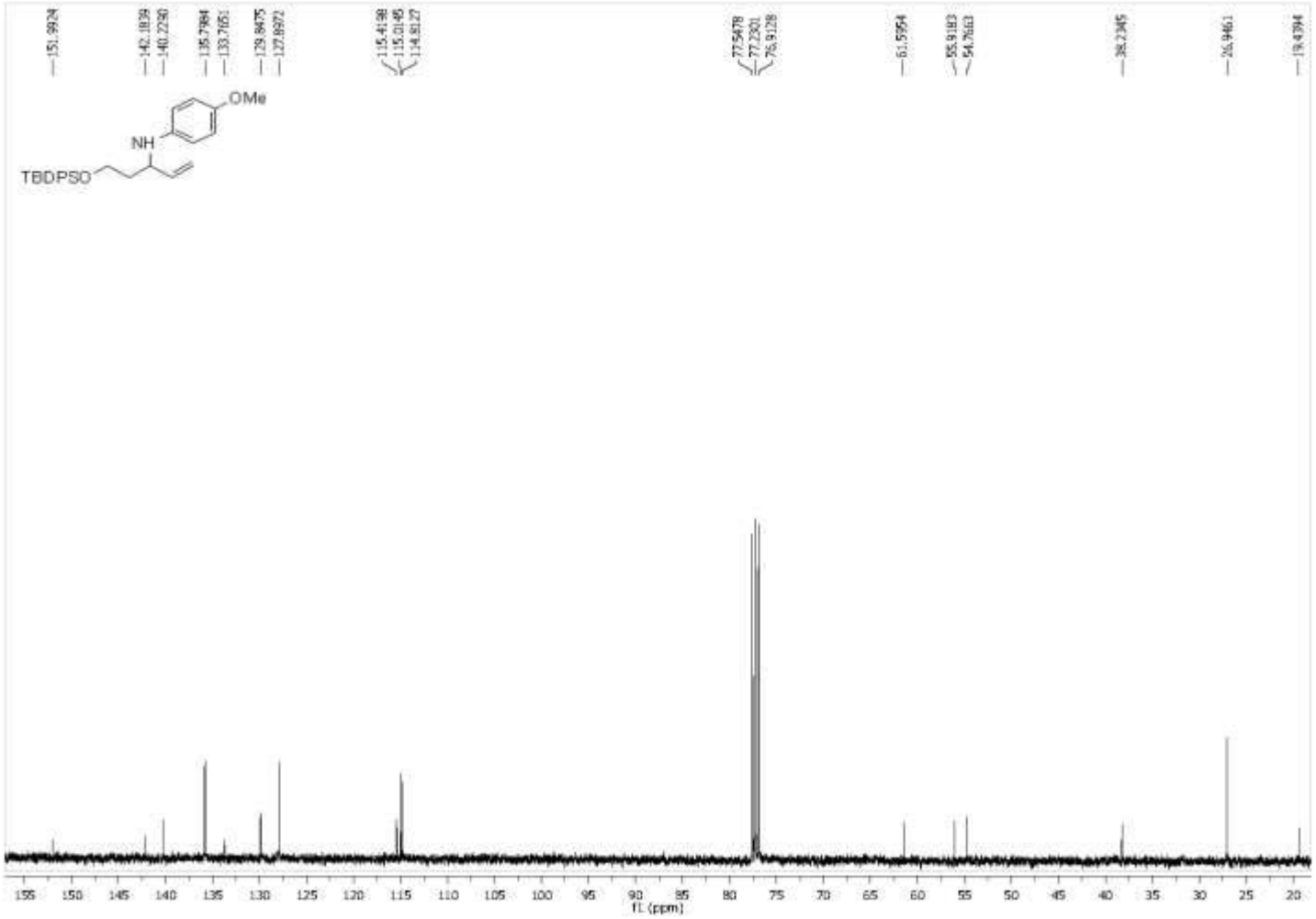

Figure A38 100 MHz 13C NMR ($CDCl_3$) Spectra of Compound **226c**

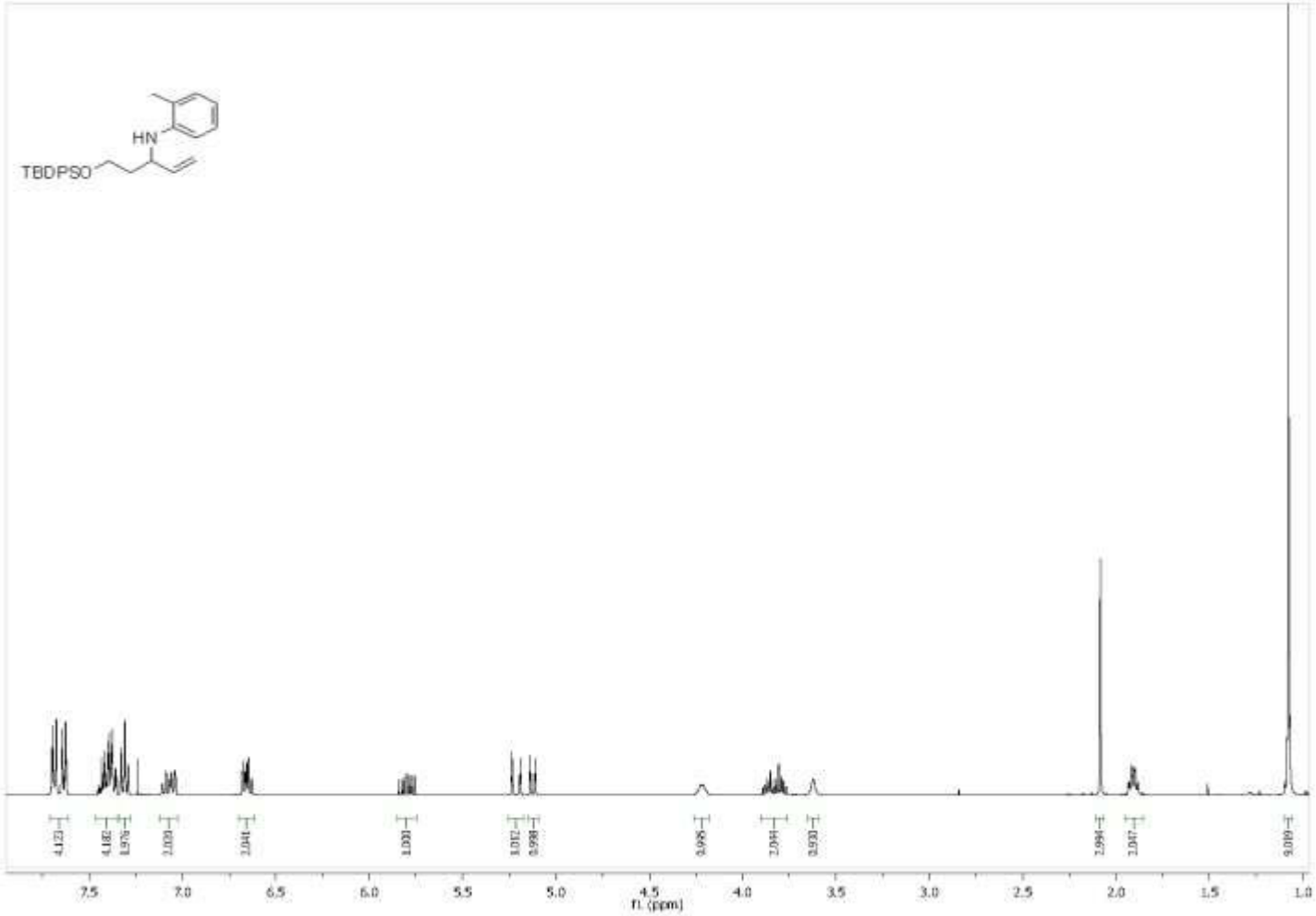

Figure A39 400 MHz 1H NMR ($CDCl_3$) Spectra of Compound **226d**

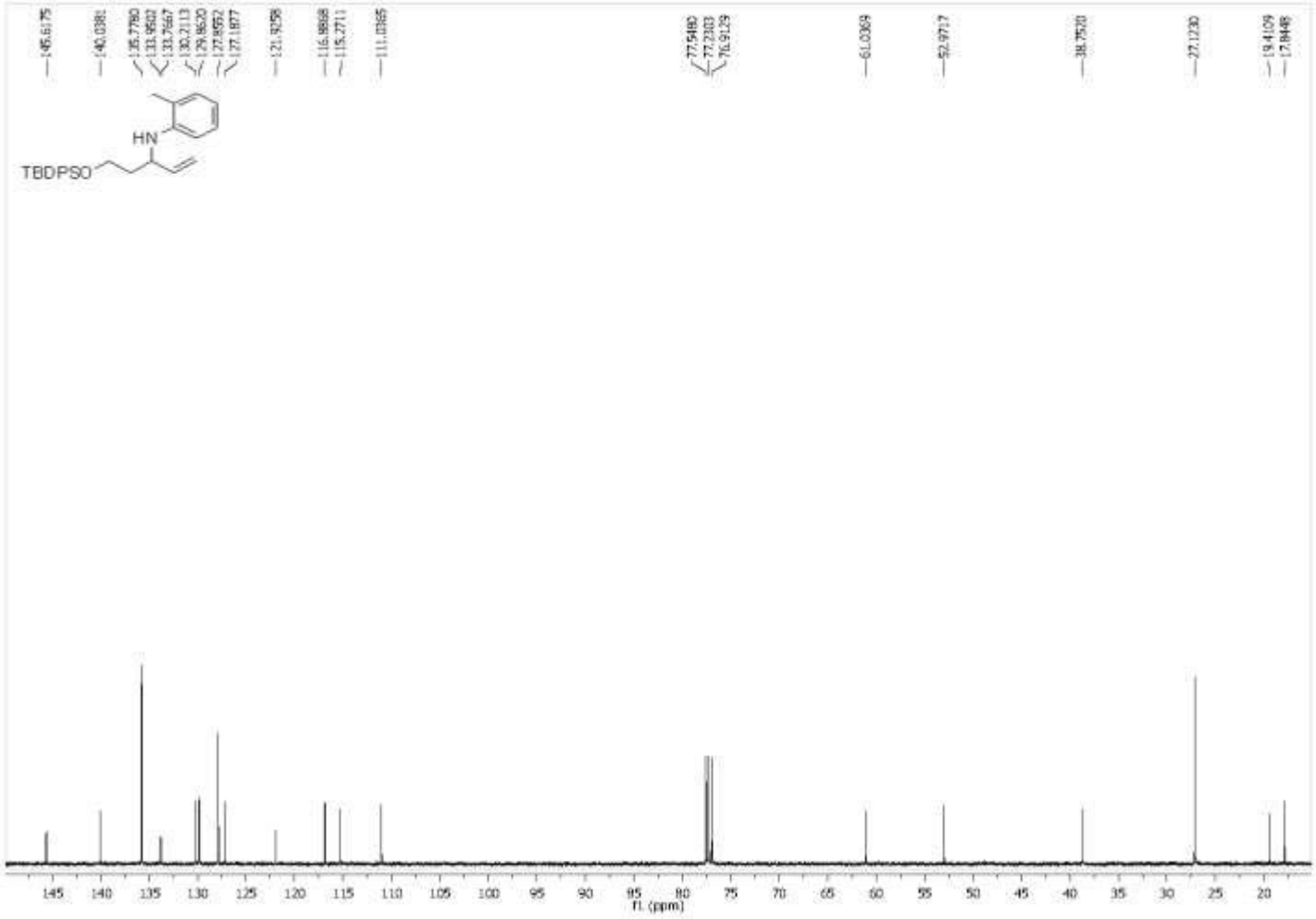

Figure A40 100 MHz 13C NMR ($CDCl_3$) Spectra of Compound **226d**

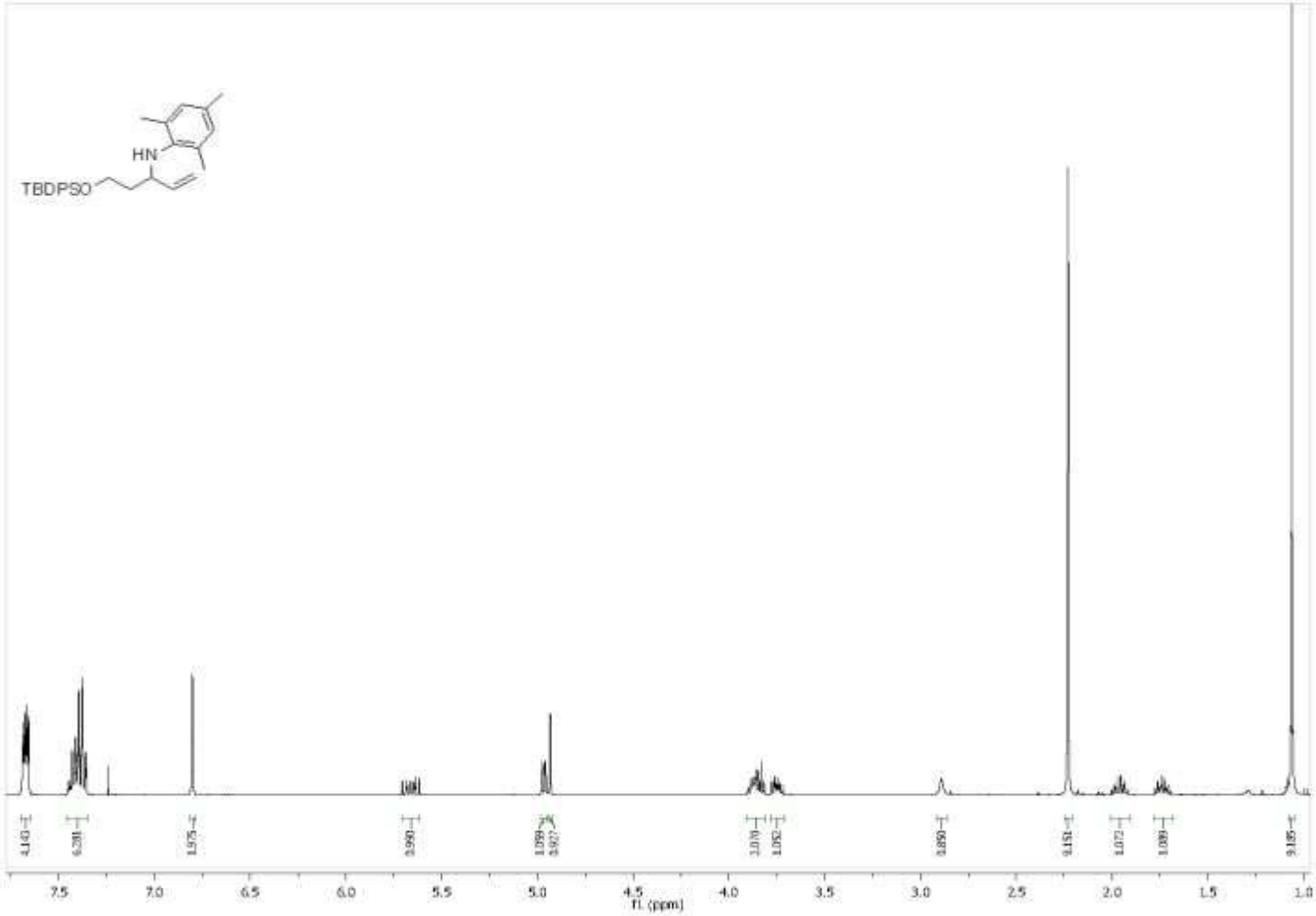

Figure A41 400 MHz 1H NMR ($CDCl_3$) Spectra of Compound **226e**

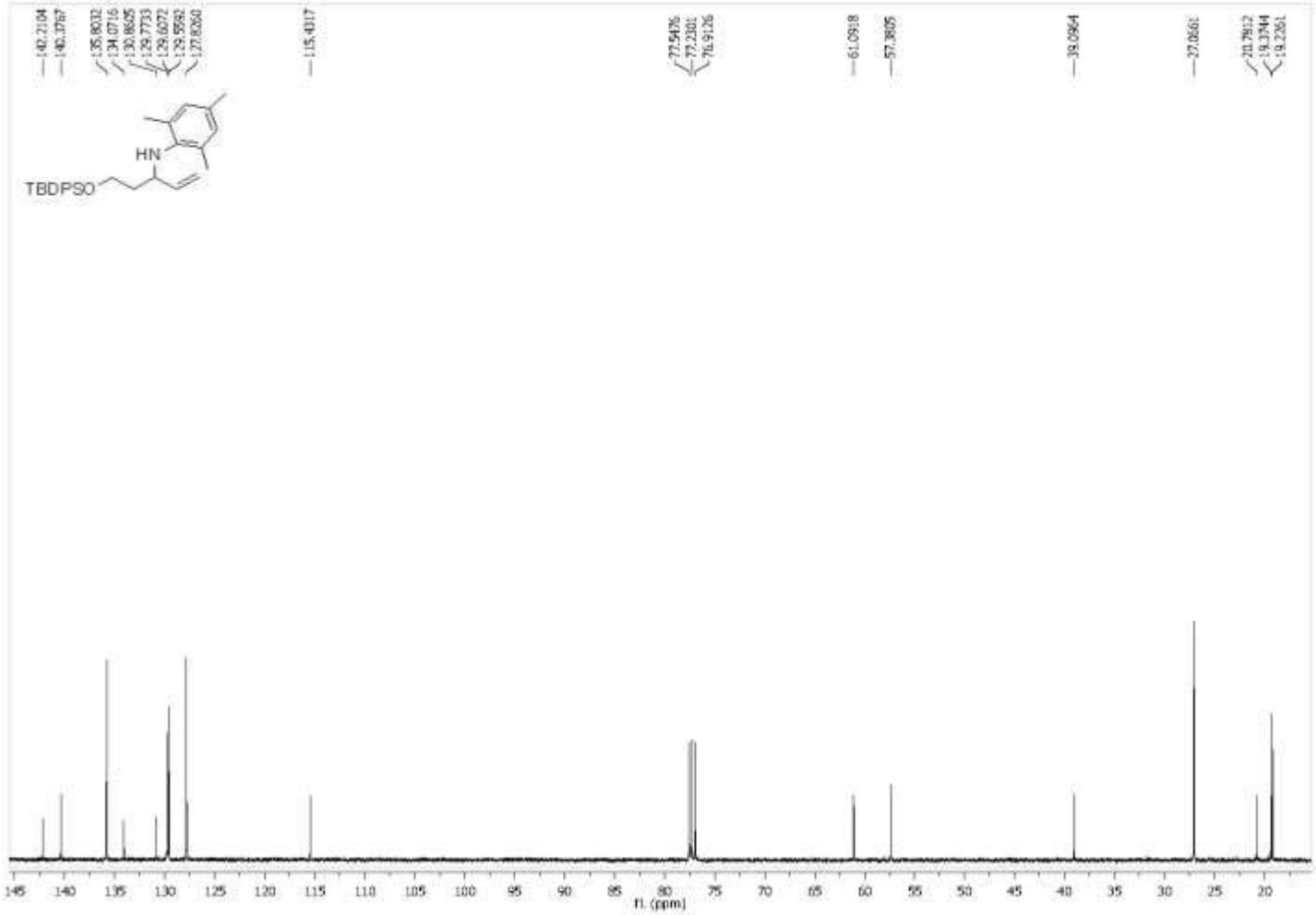

Figure A42 100 MHz 13C NMR ($CDCl_3$) Spectra of Compound **226e**

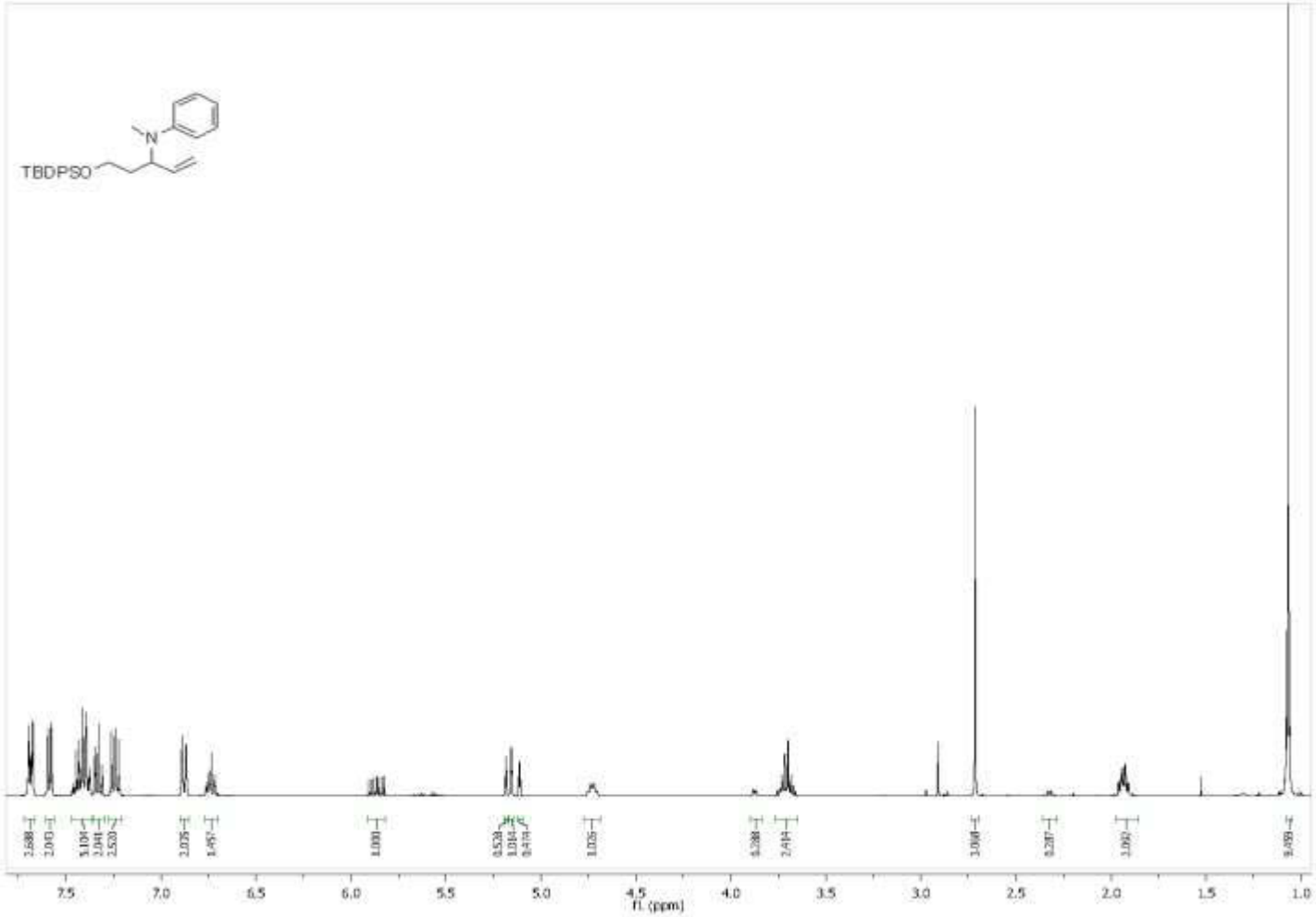

Figure A43 400 MHz 1H NMR ($CDCl_3$) Spectra of Compound **226f**

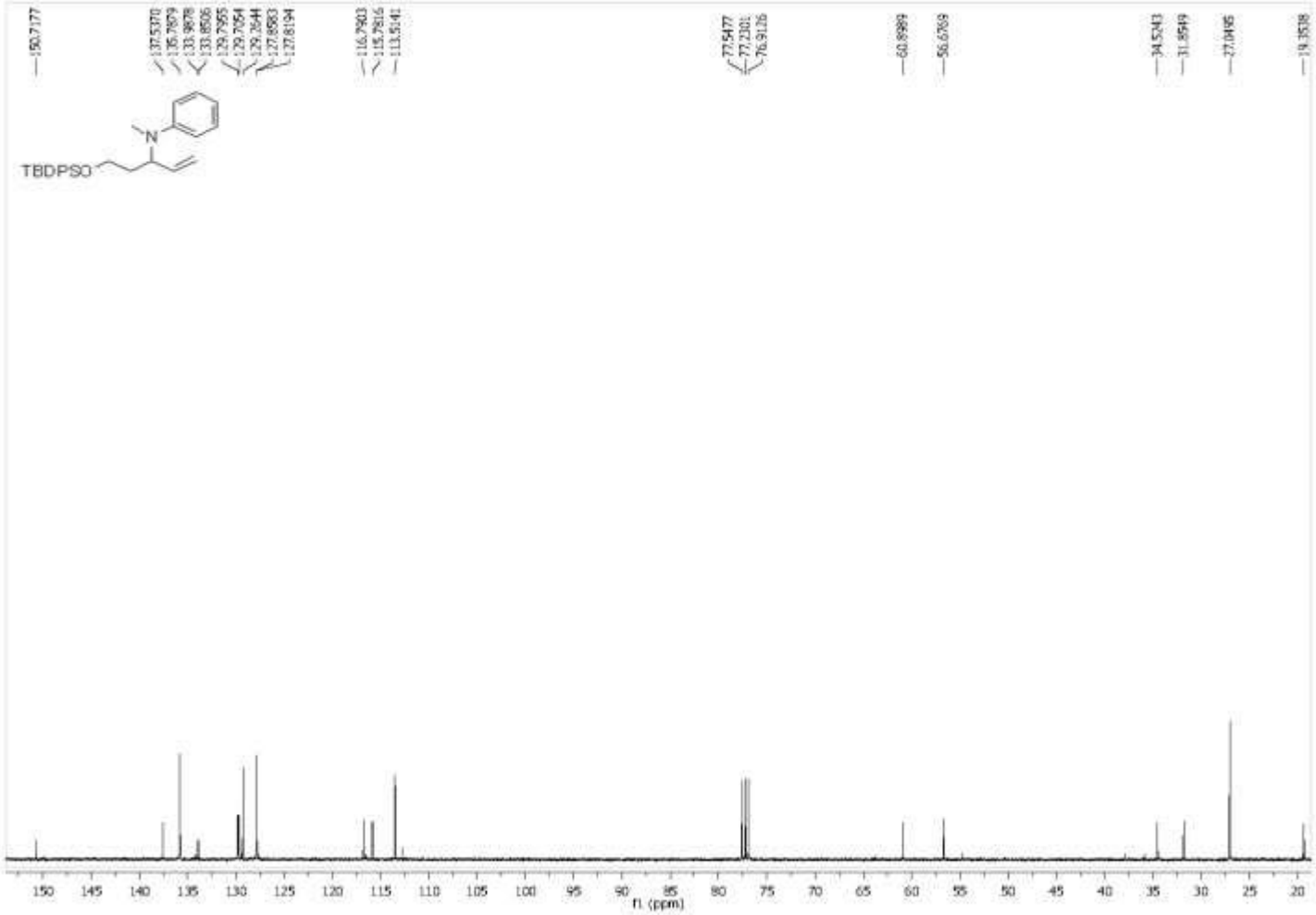

Figure A44 100 MHz 13C NMR ($CDCl_3$) Spectra of Compound **226f**

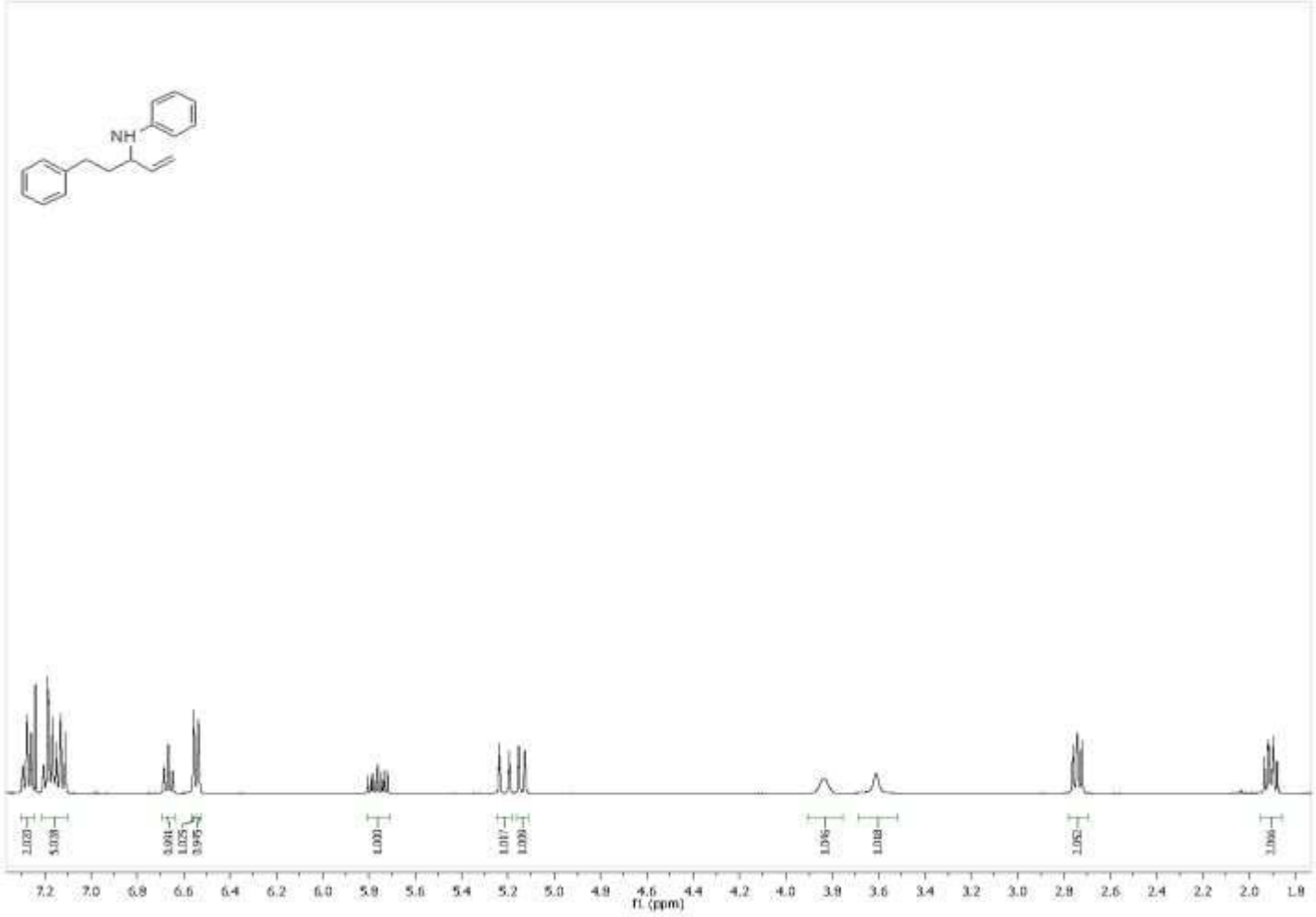

Figure A45 400 MHz 1H NMR ($CDCl_3$) Spectra of Compound **227a**

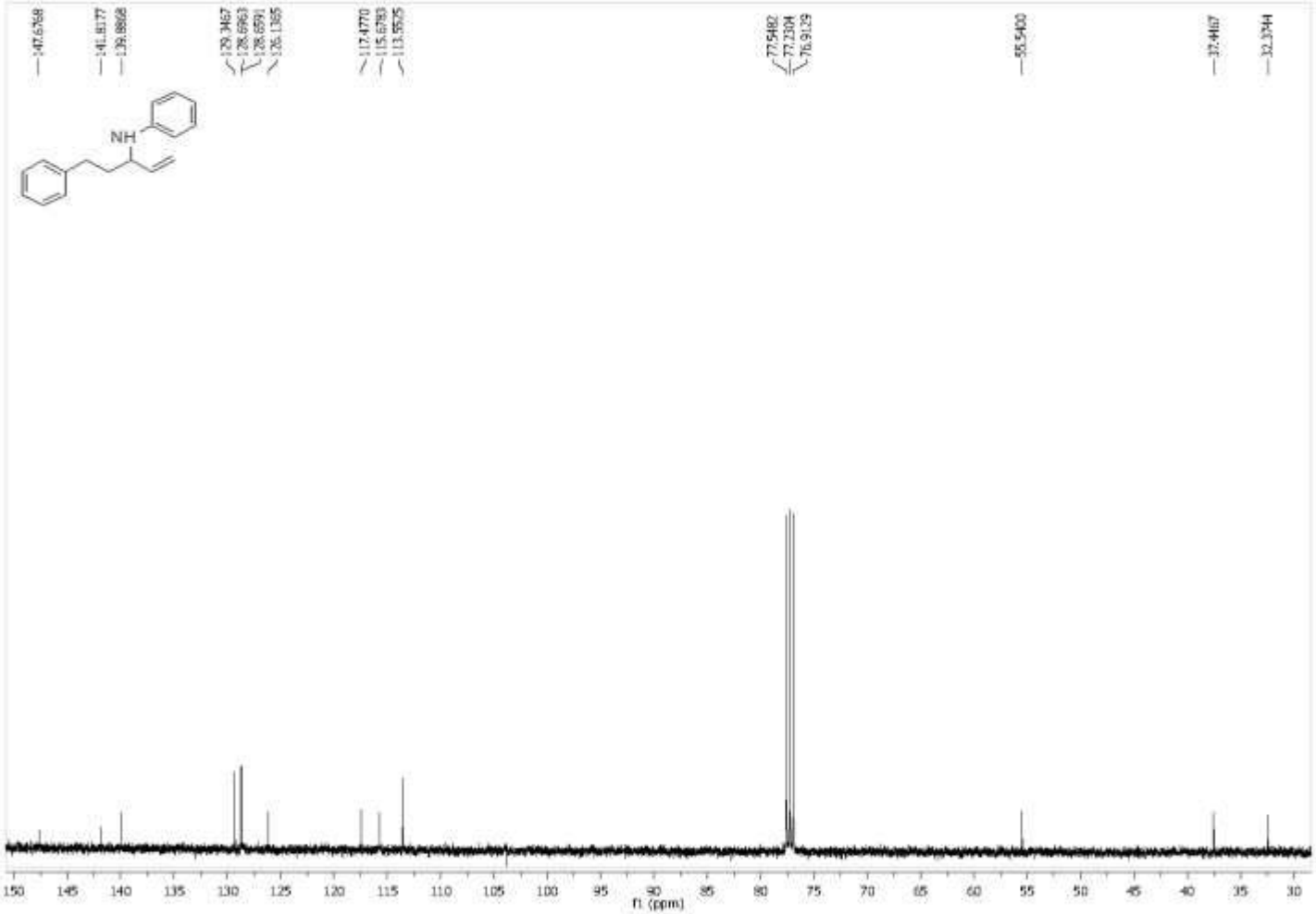

Figure A45 400 MHz 1H NMR ($CDCl_3$) Spectra of Compound **227a**

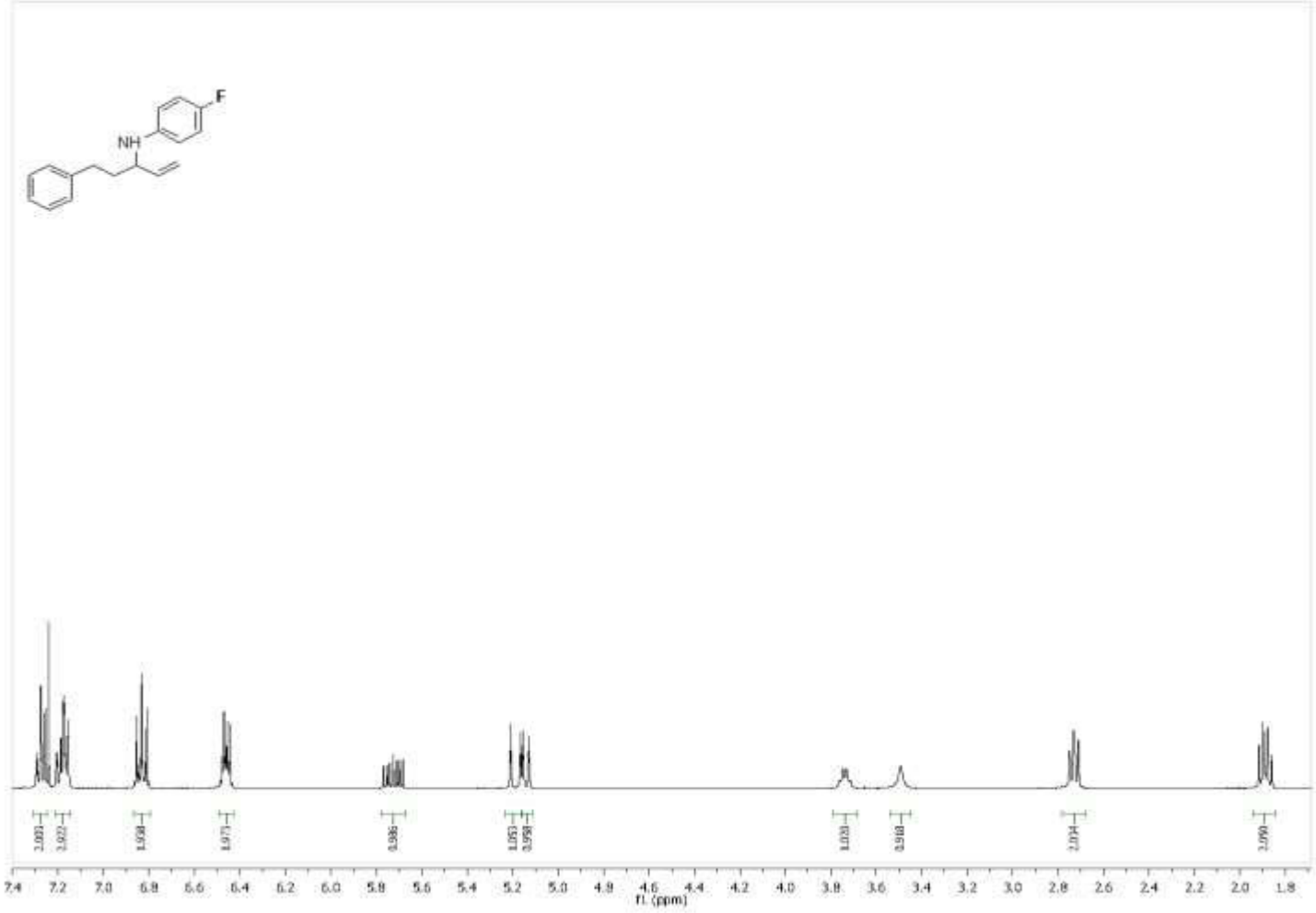

Figure A47 400 MHz 1H NMR ($CDCl_3$) Spectra of Compound **227b**

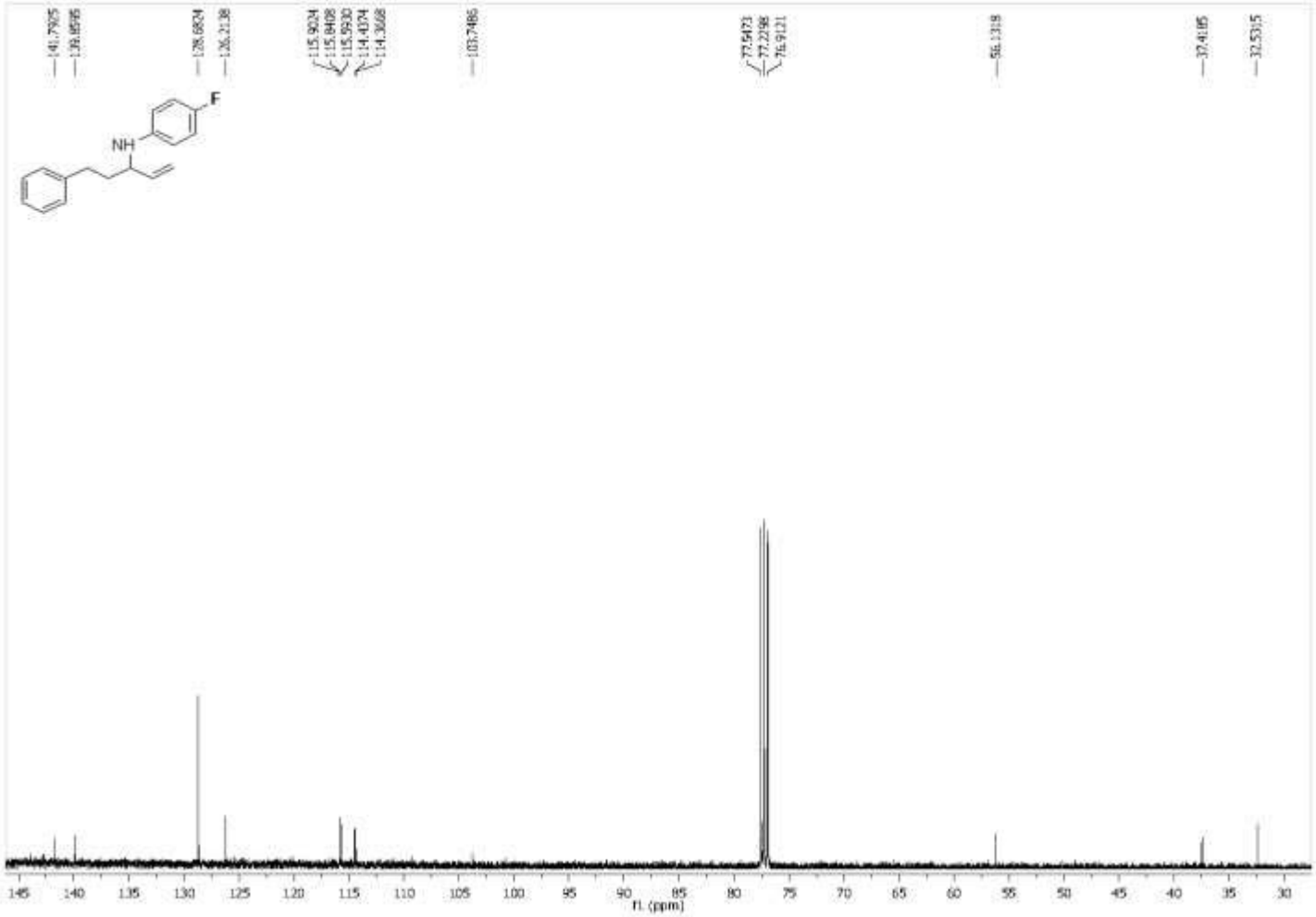

Figure A48 100 MHz 13C NMR ($CDCl_3$) Spectra of Compound **227b**

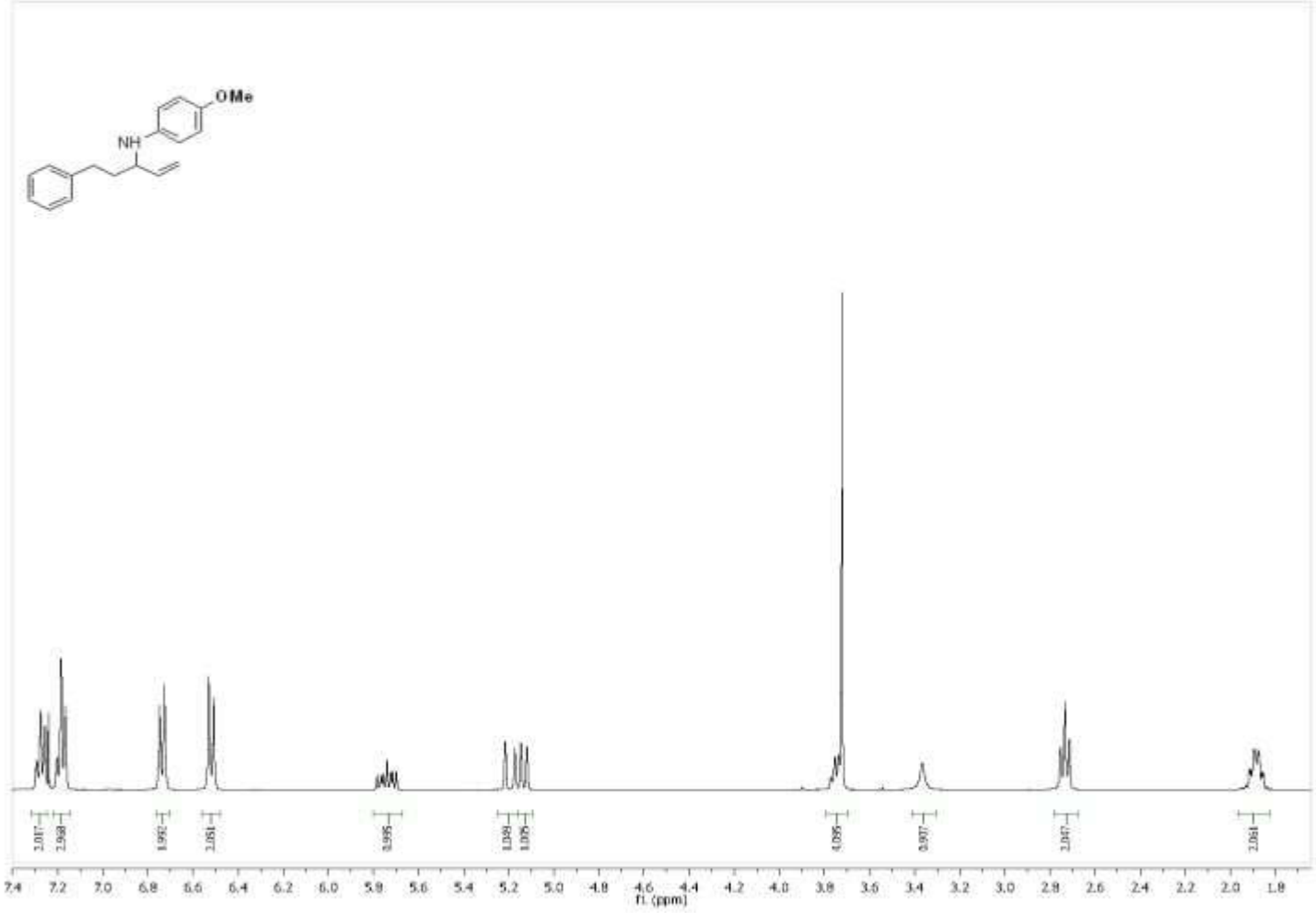

Figure A49 400 MHz 1H NMR ($CDCl_3$) Spectra of Compound **227c**

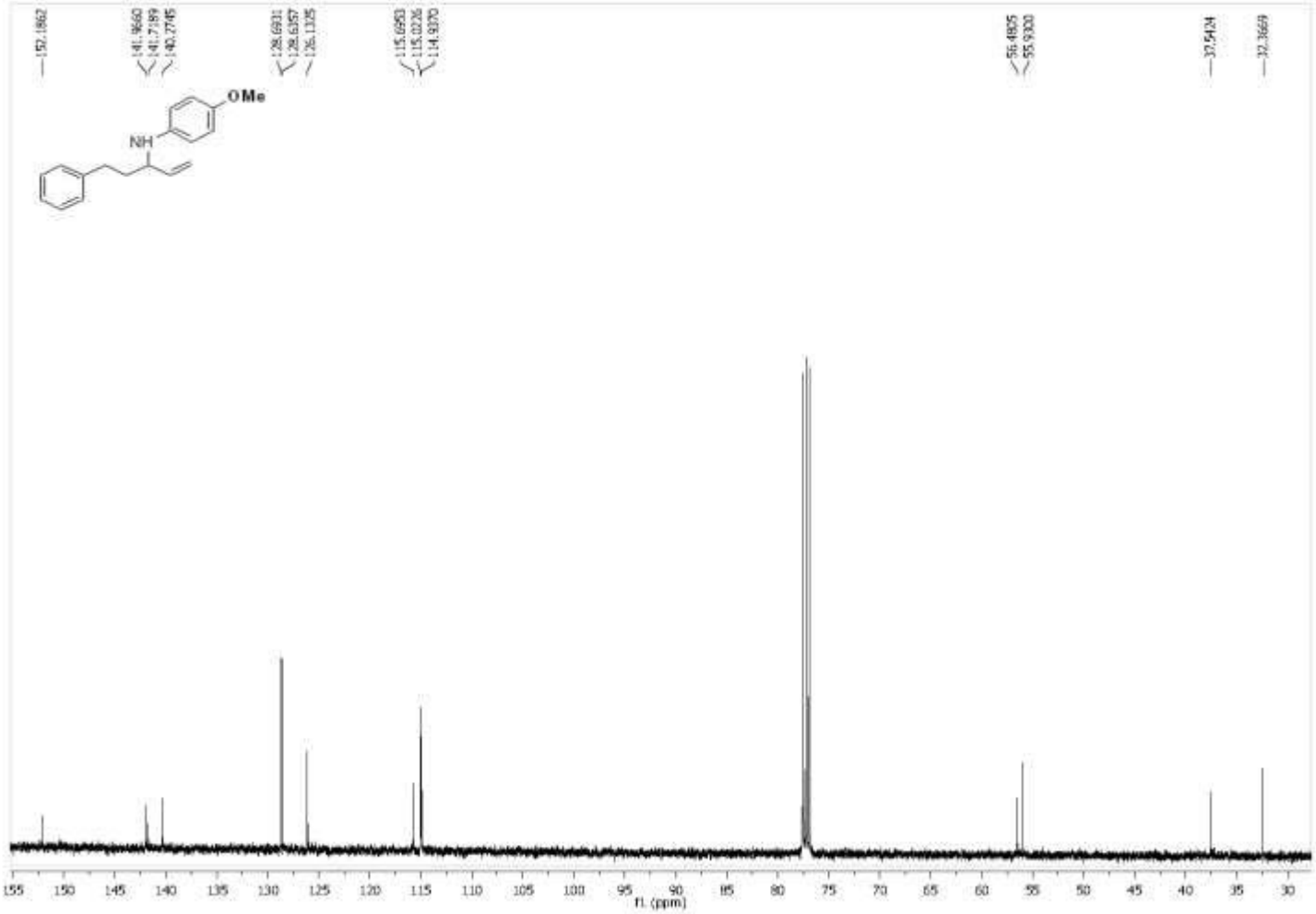

Figure A50 100 MHz 13C NMR ($CDCl_3$) Spectra of Compound **227c**

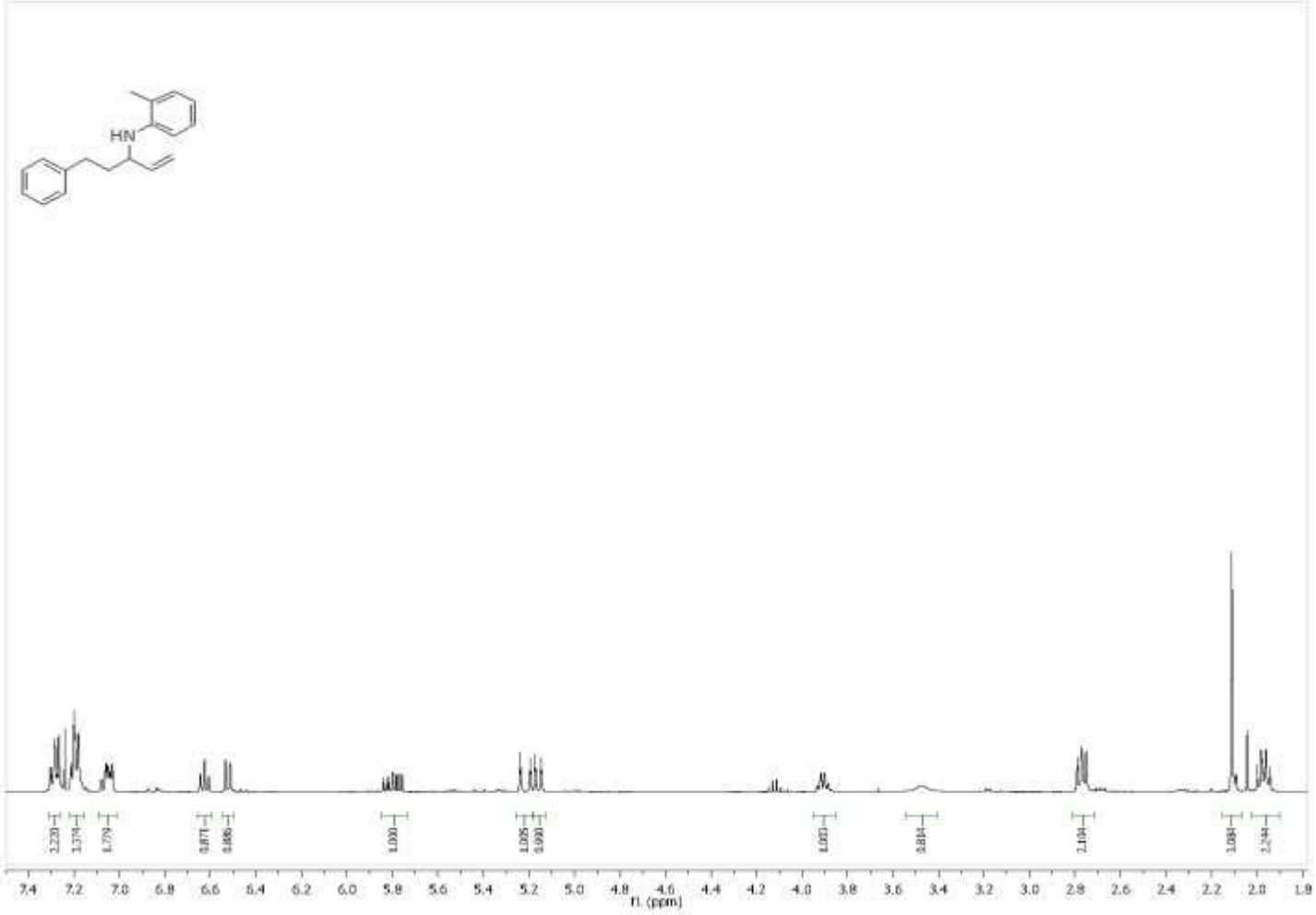

Figure A51 400 MHz 1H NMR ($CDCl_3$) Spectra of Compound **227d**

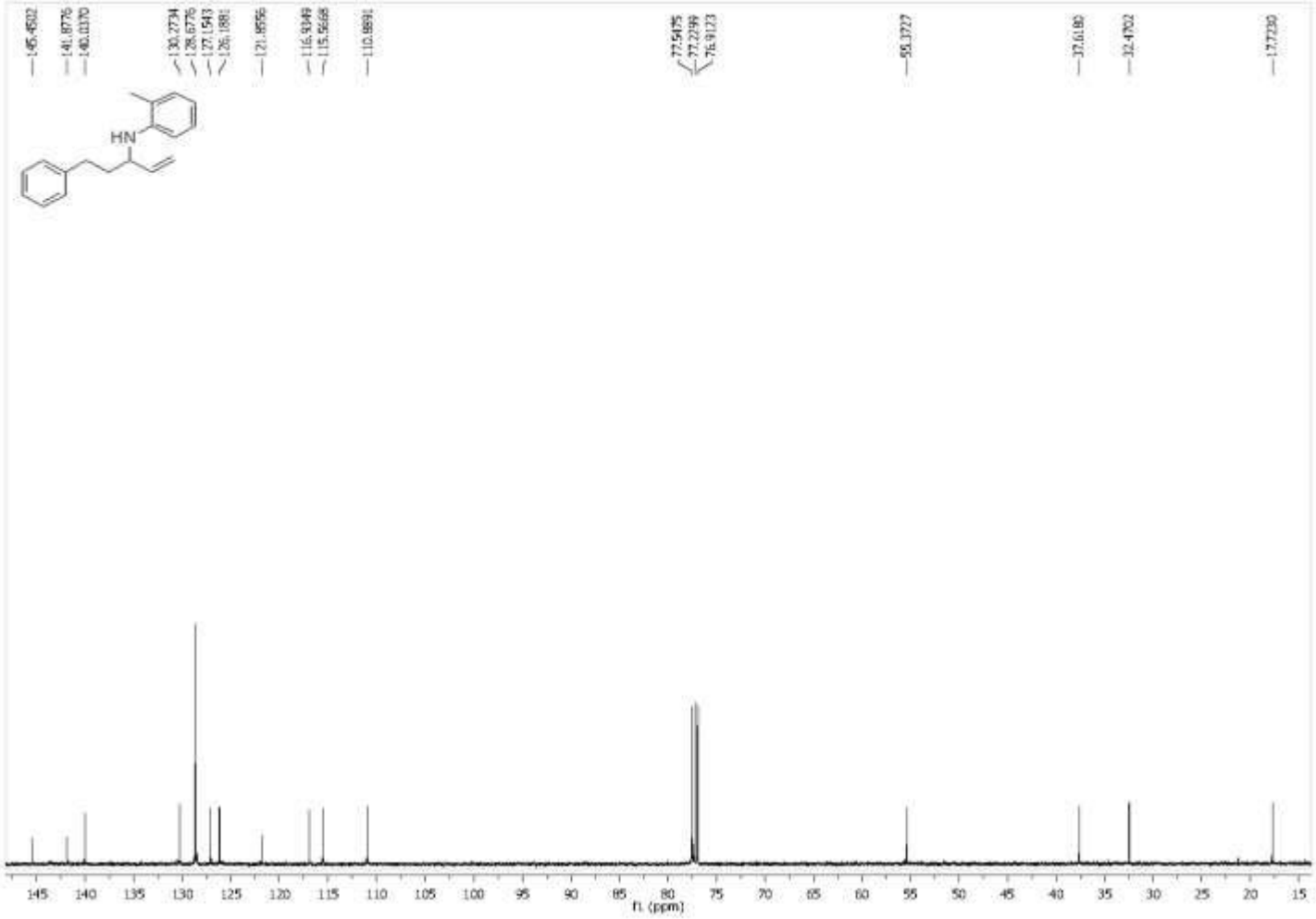

Figure A52 100 MHz 13C NMR ($CDCl_3$) Spectra of Compound **227d**

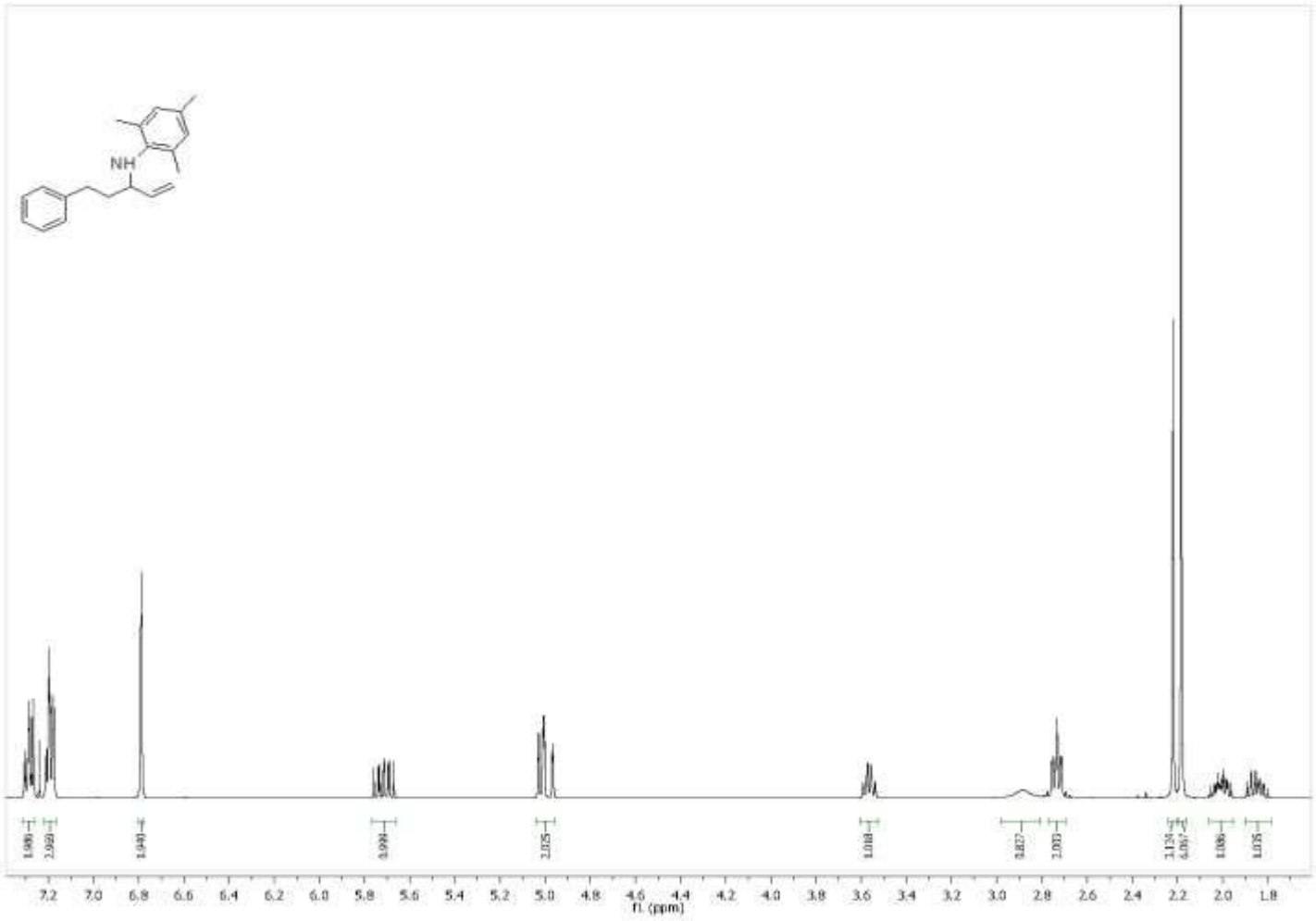

Figure A53 400 MHz 1H NMR ($CDCl_3$) Spectra of Compound **227e**

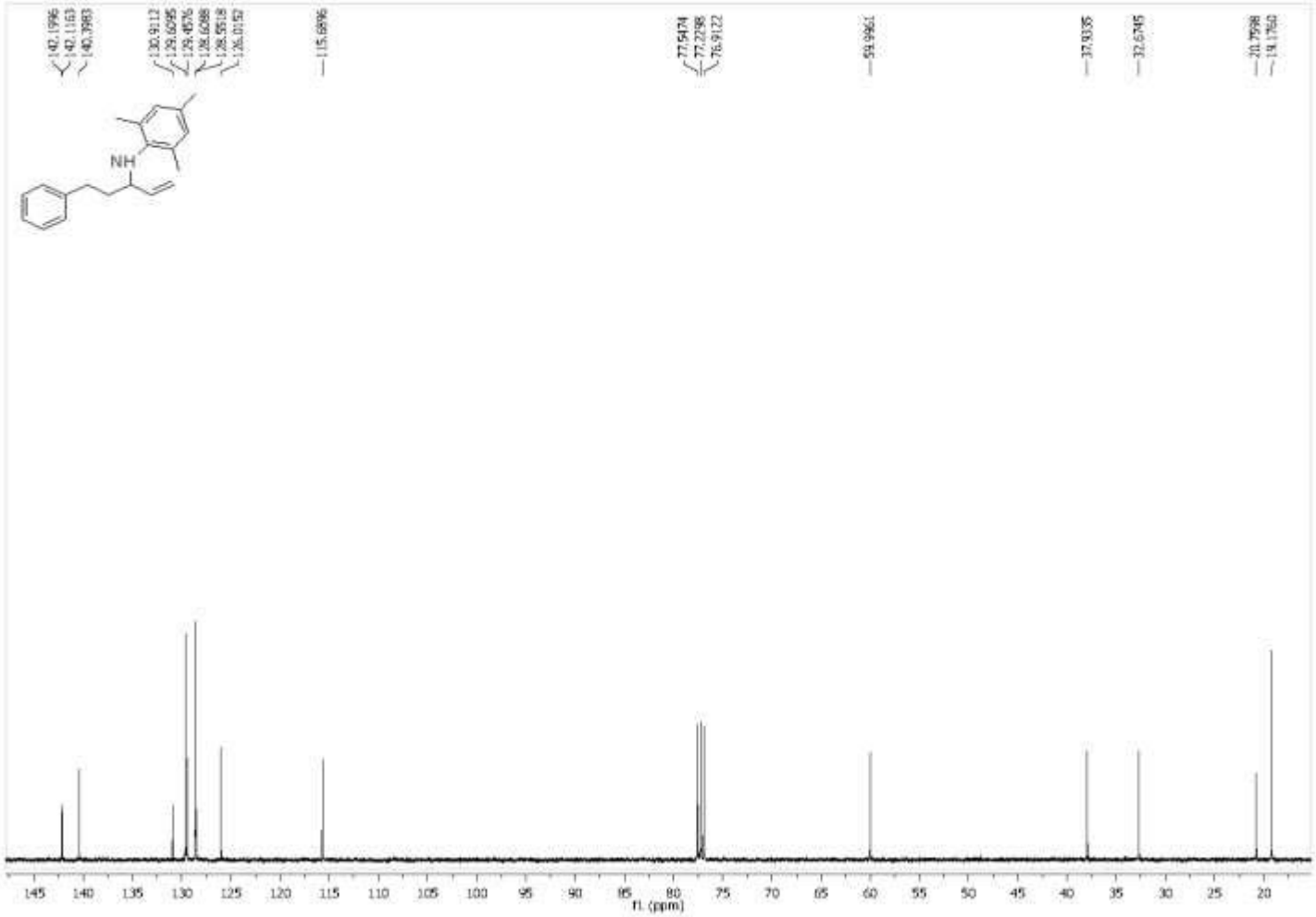

Figure A54 100 MHz 13C NMR ($CDCl_3$) Spectra of Compound **227e**

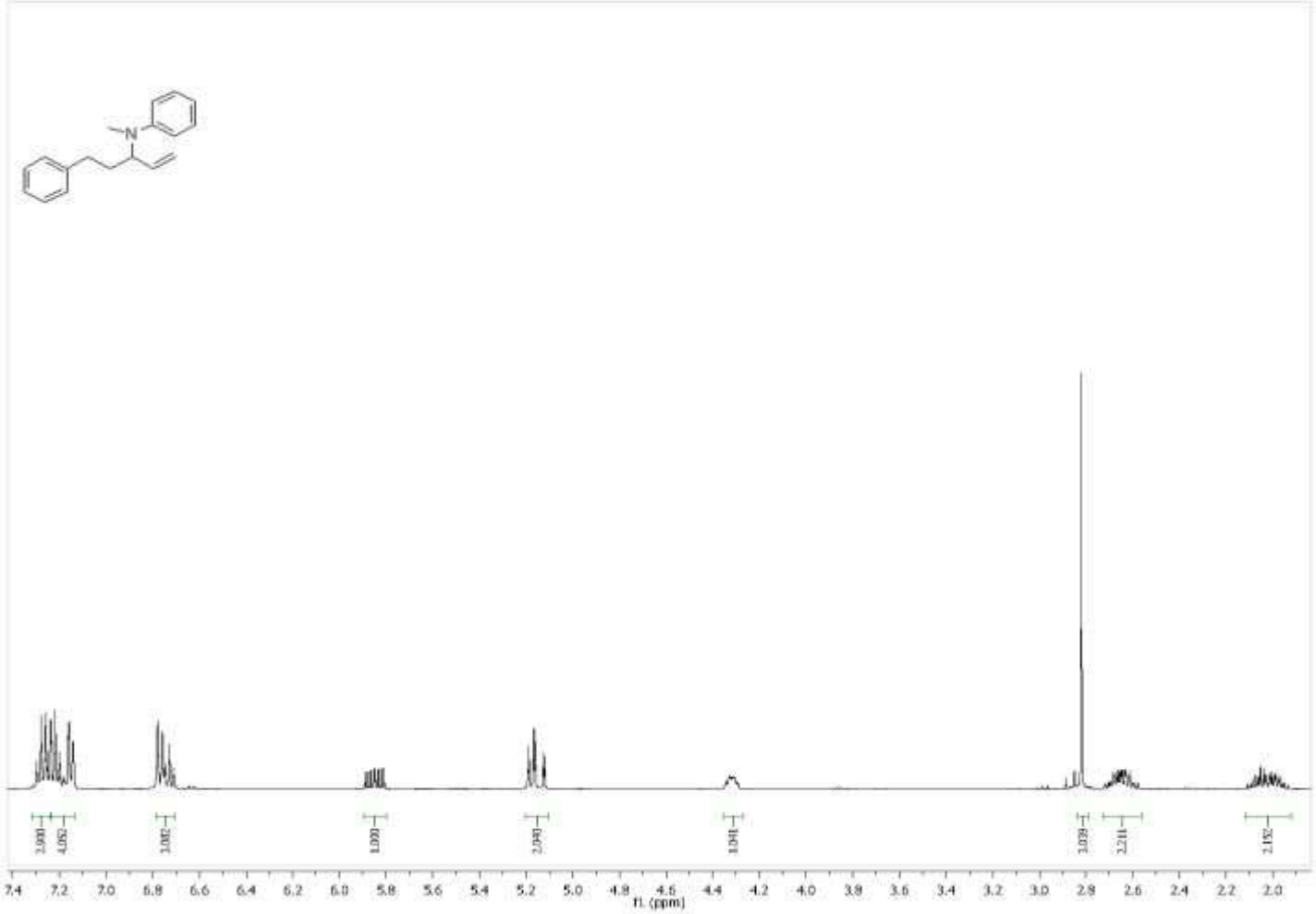

Figure A55 400 MHz 1H NMR ($CDCl_3$) Spectra of Compound **227f**

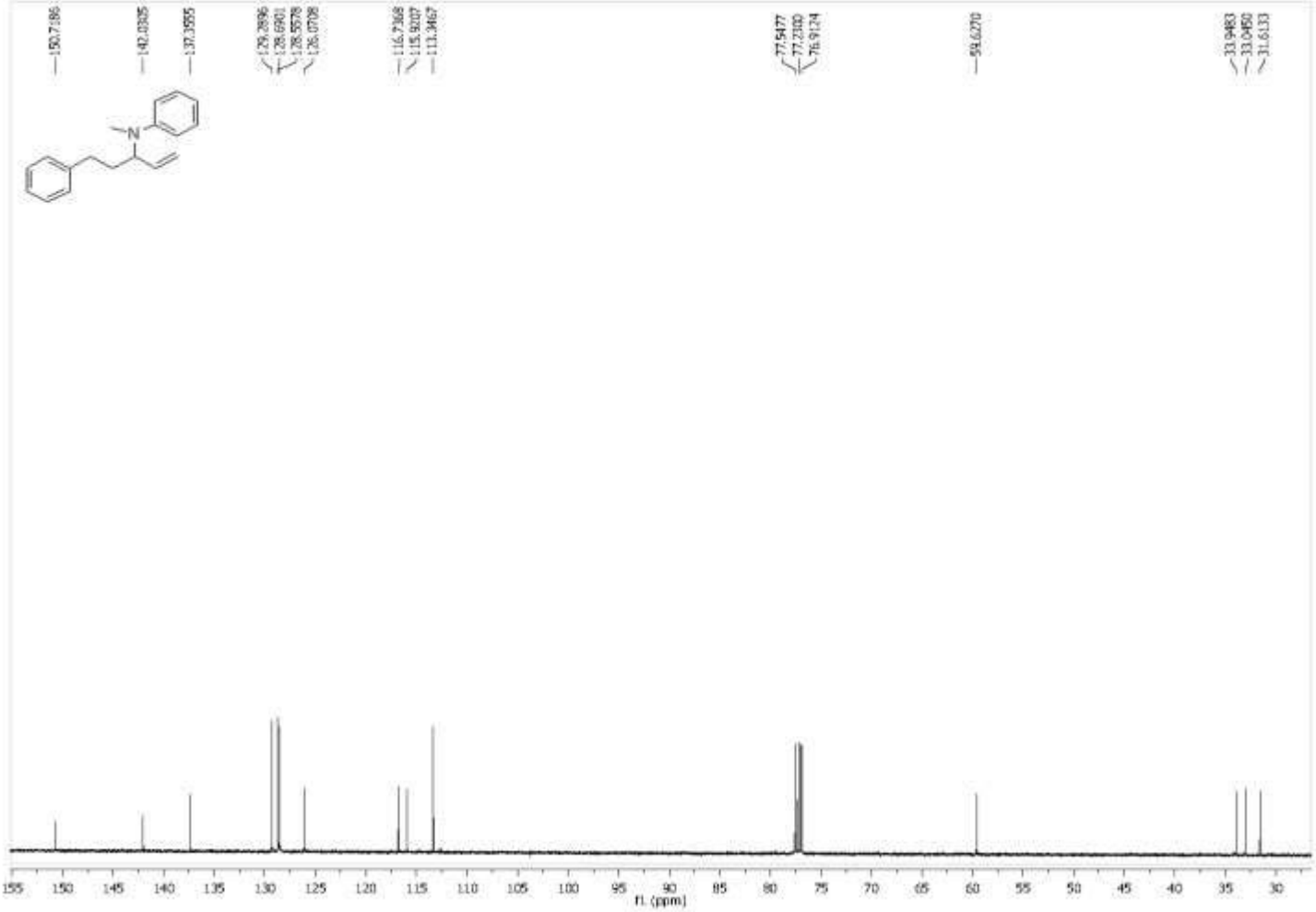

Figure A56 100 MHz 13C NMR ($CDCl_3$) Spectra of Compound **227f**

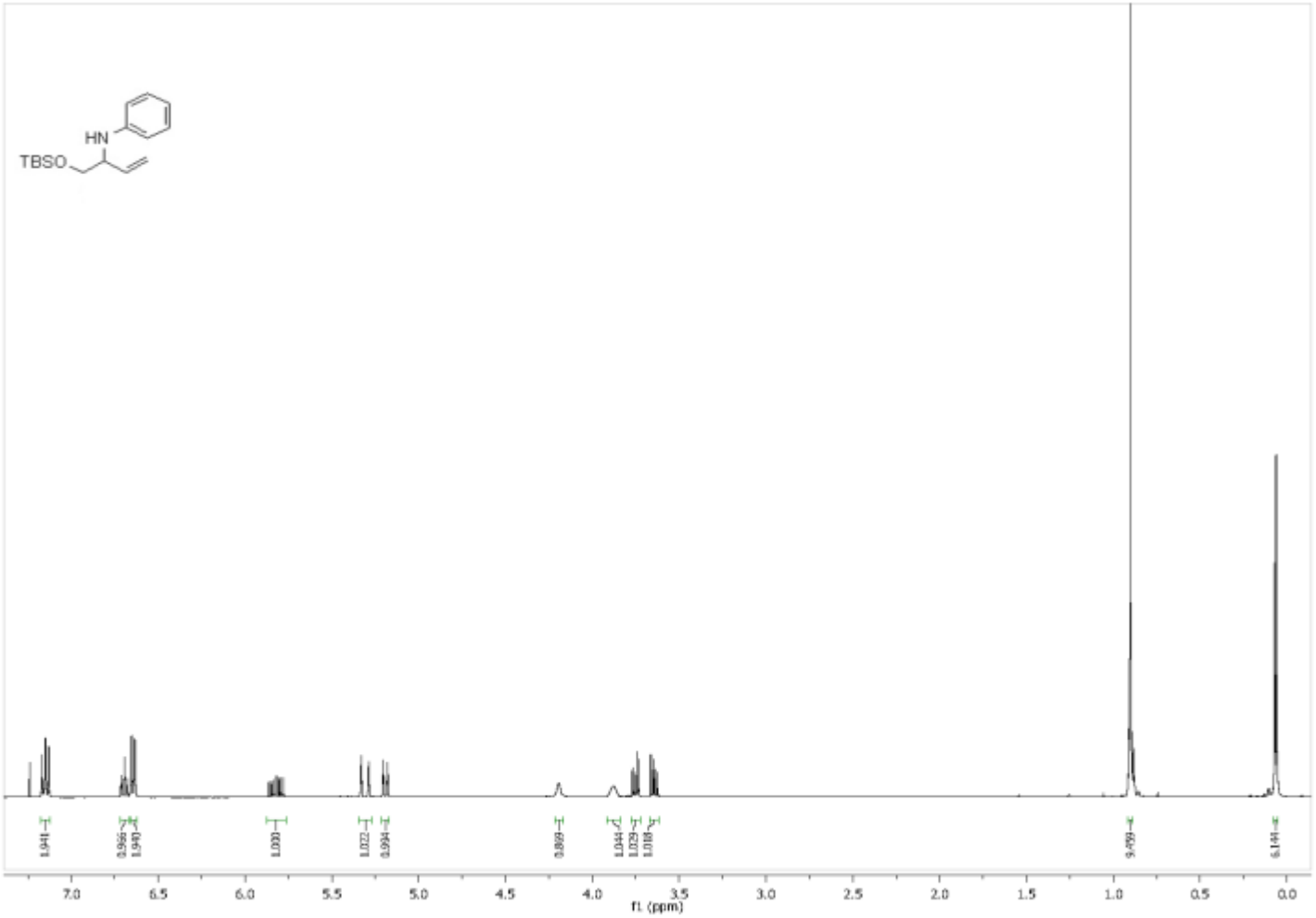

Figure A57 400 MHz 1H NMR ($CDCl_3$) Spectra of Compound **228a**

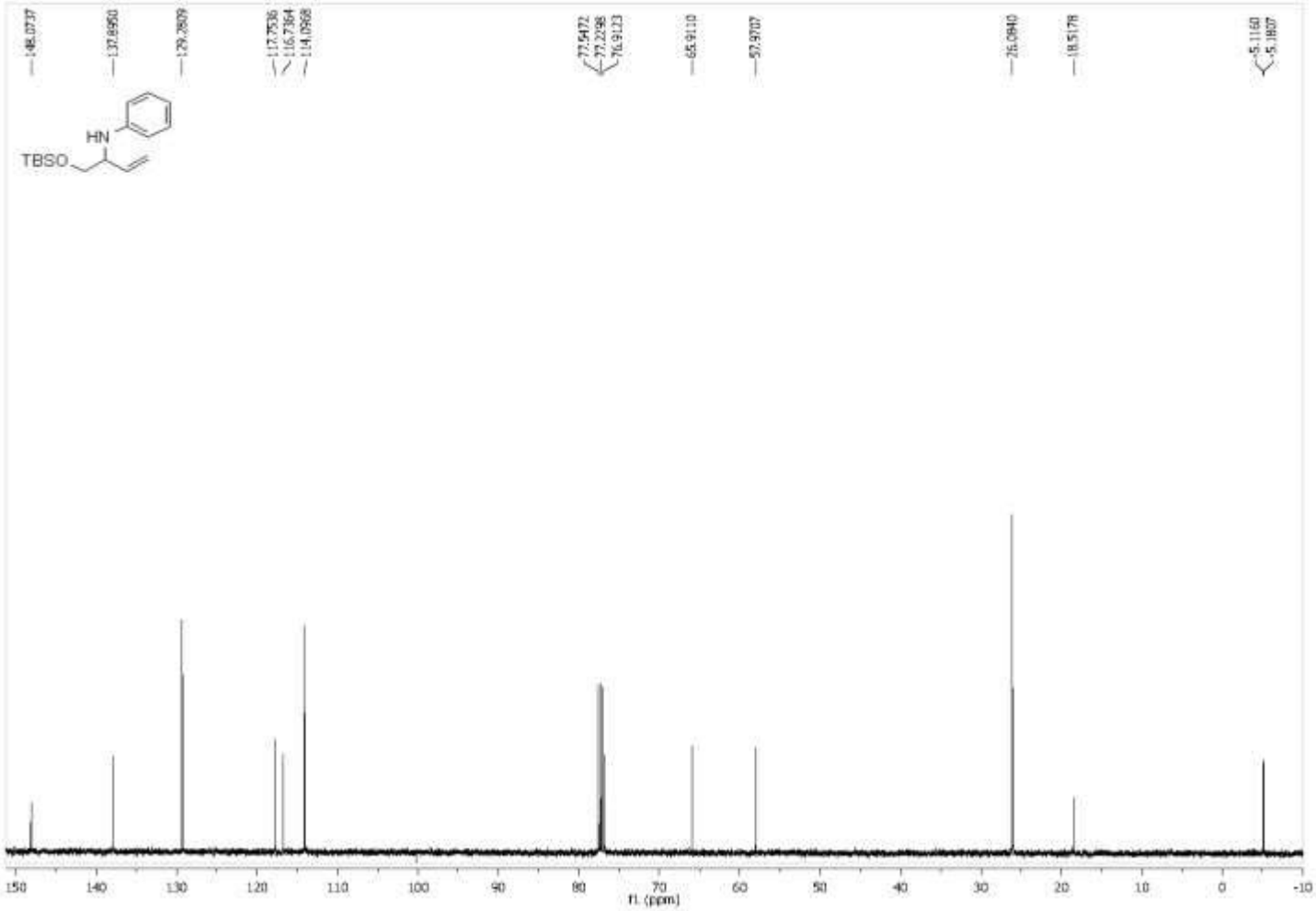

Figure A58 100 MHz 13C NMR ($CDCl_3$) Spectra of Compound **228a**

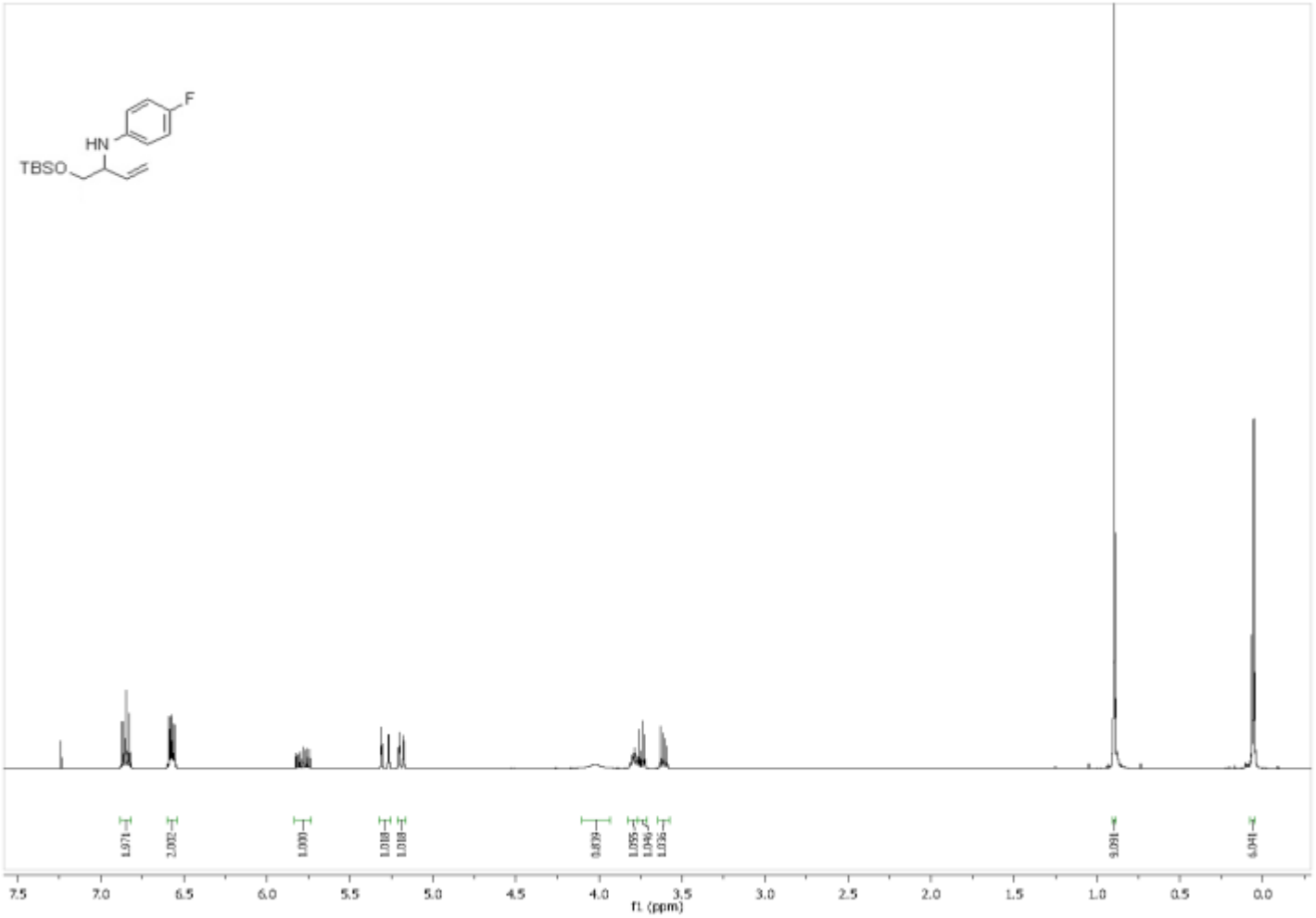

Figure A59 400 MHz 1H NMR ($CDCl_3$) Spectra of Compound **228b**

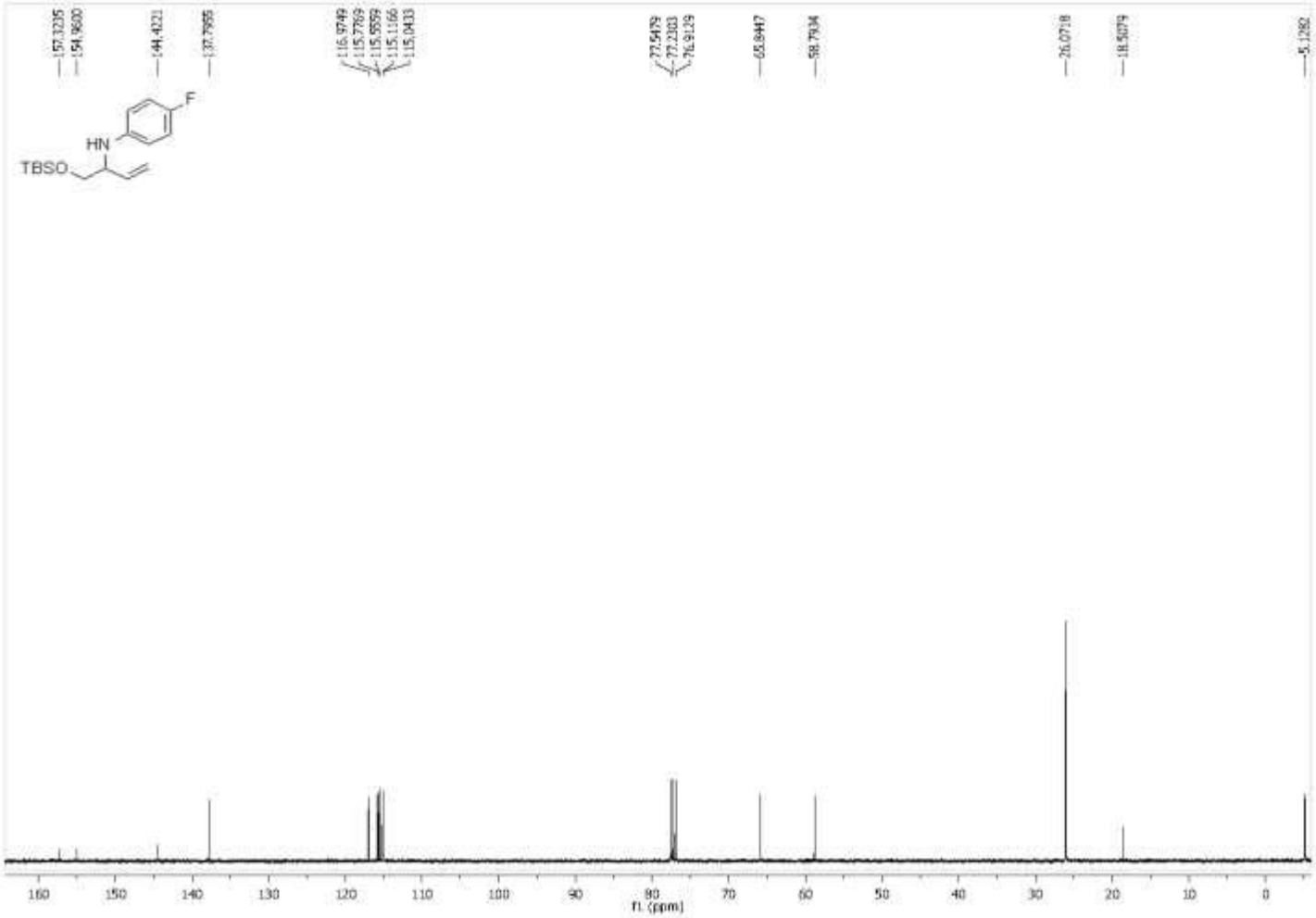

Figure A60 100 MHz 13C NMR ($CDCl_3$) Spectra of Compound **228b**

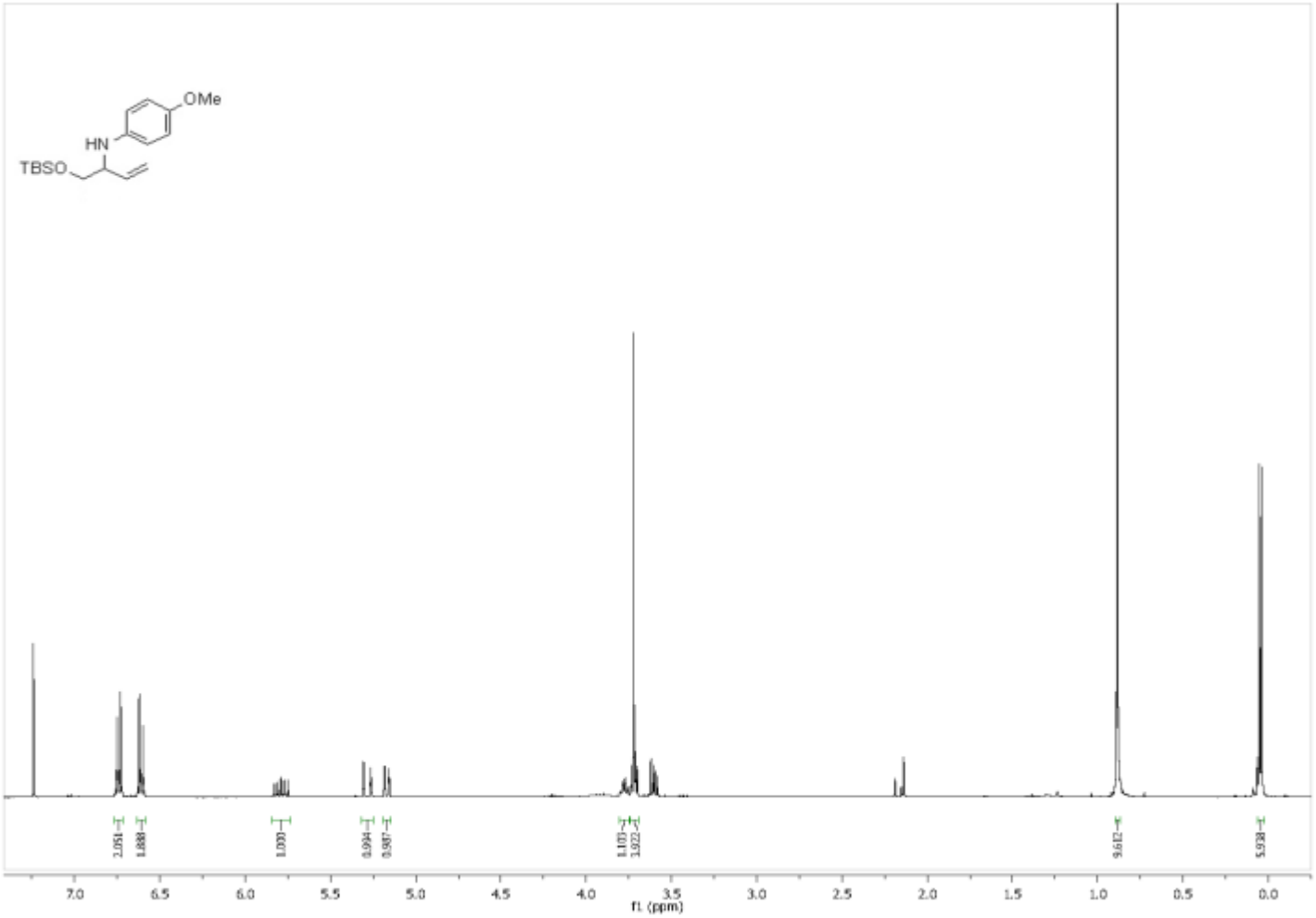

Figure A61 400 MHz 1H NMR ($CDCl_3$) Spectra of Compound **228c**

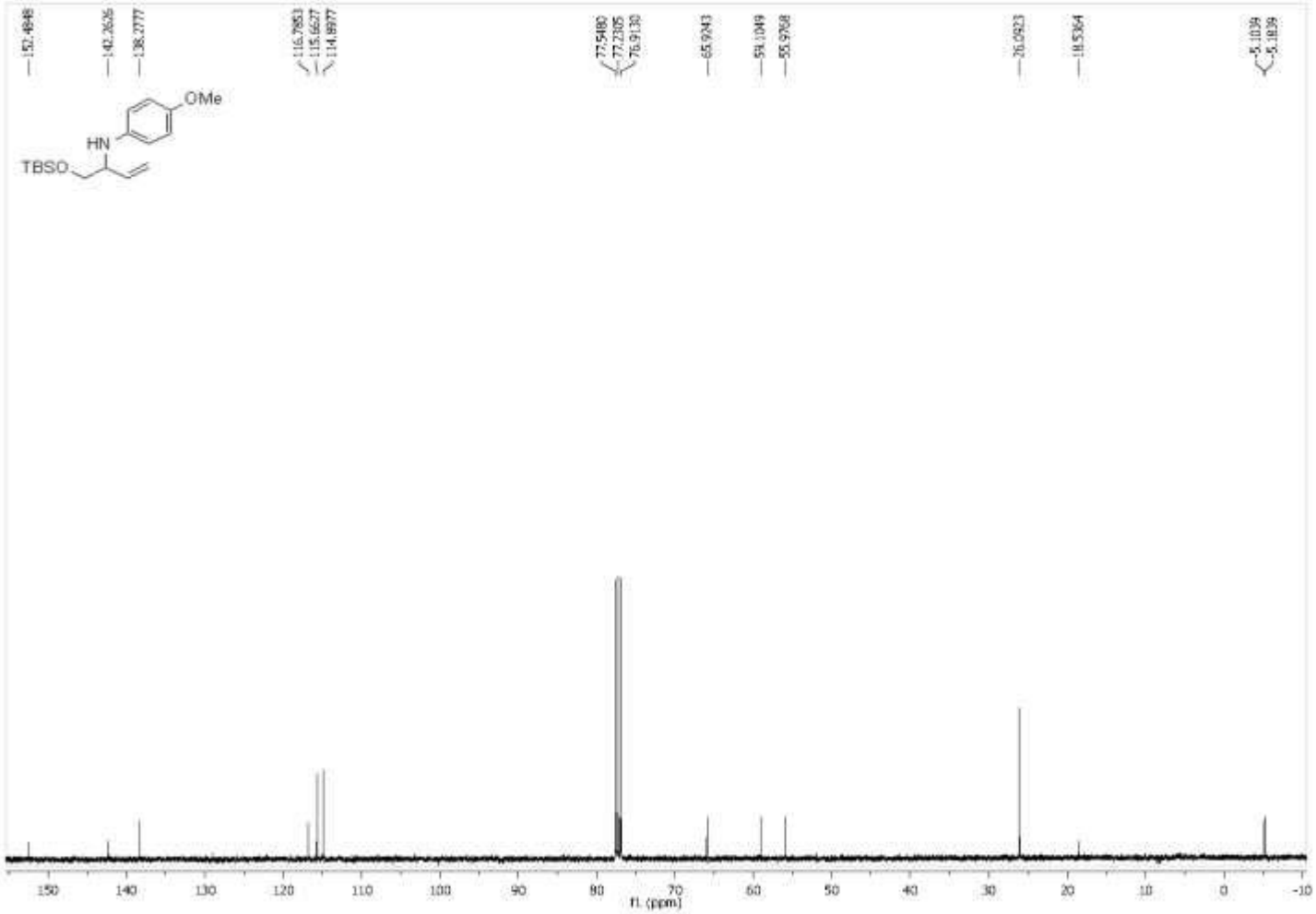

Figure A62 100 MHz 13C NMR ($CDCl_3$) Spectra of Compound **228c**

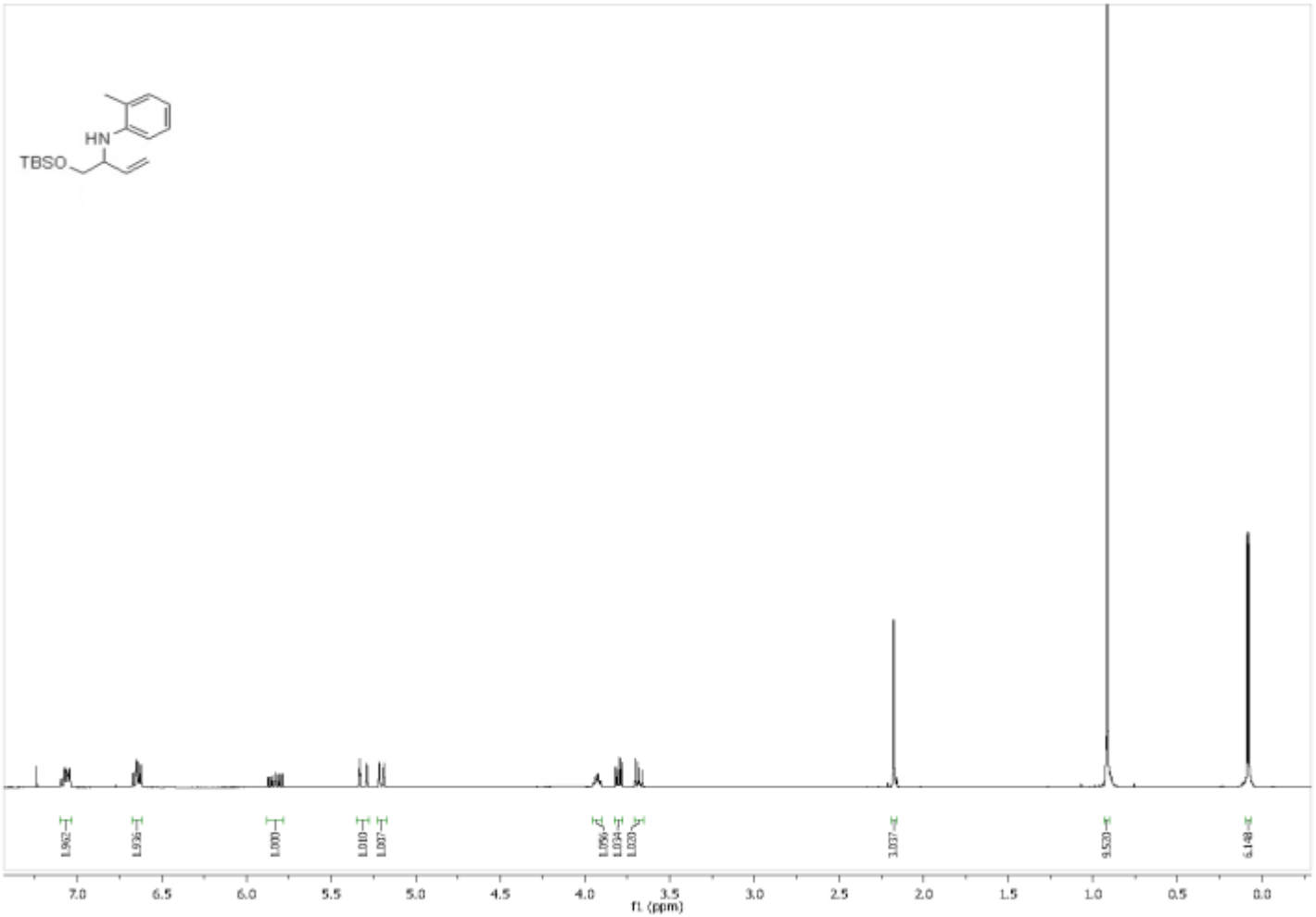

Figure A63 400 MHz 1H NMR ($CDCl_3$) Spectra of Compound **228d**

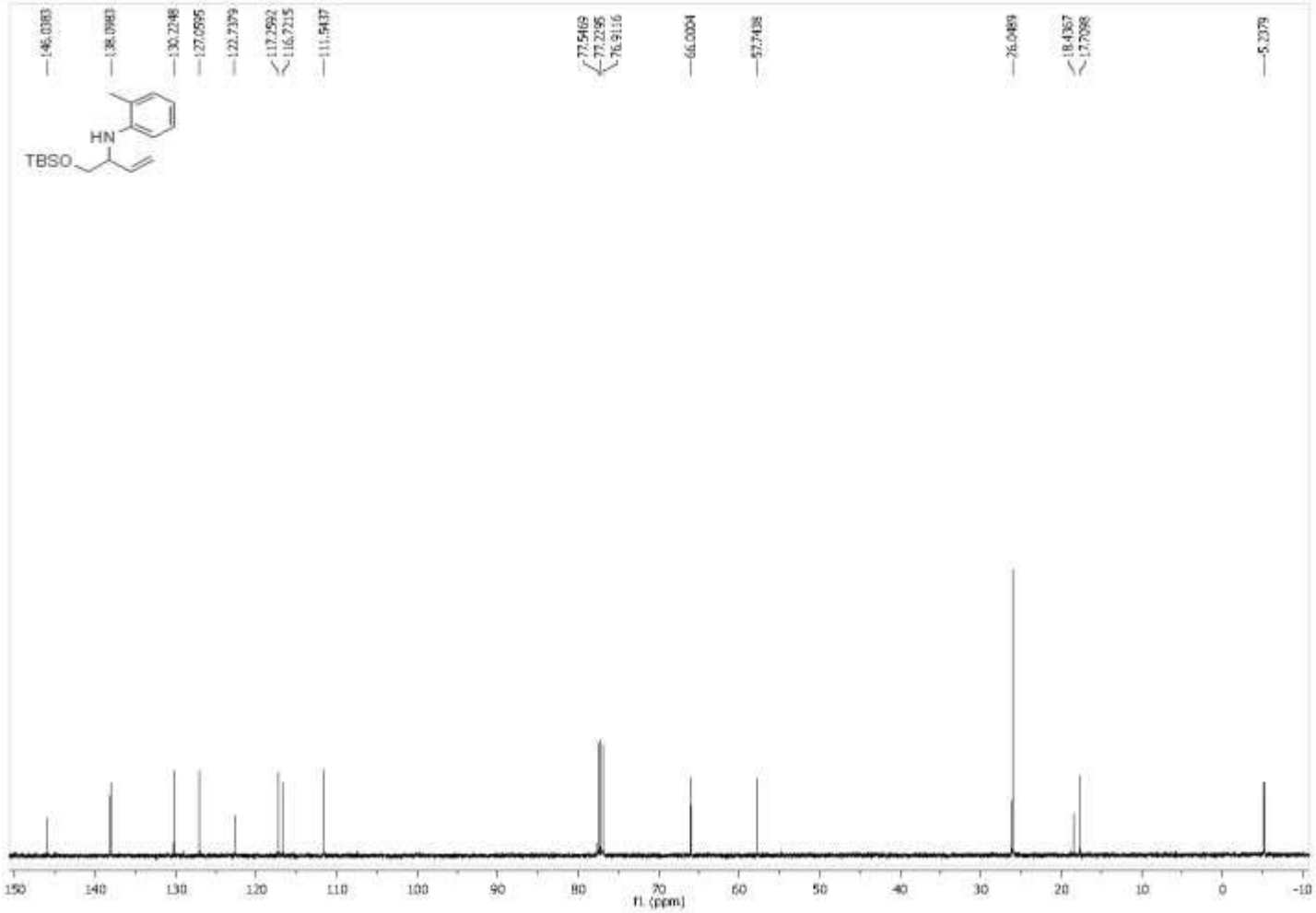

Figure A64 100 MHz 13C NMR ($CDCl_3$) Spectra of Compound **228d**

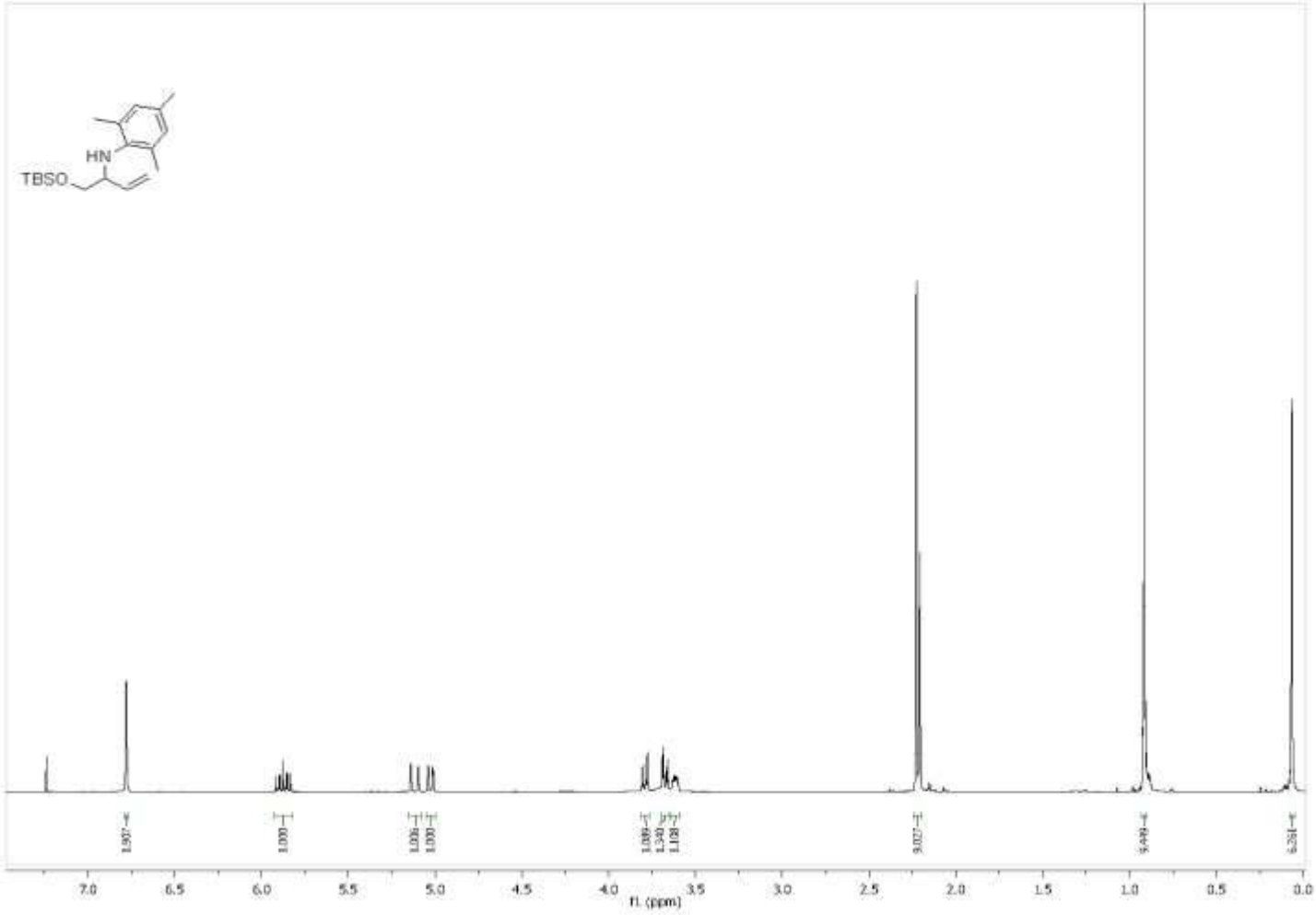

Figure A65 400 MHz 1H NMR ($CDCl_3$) Spectra of Compound **228e**

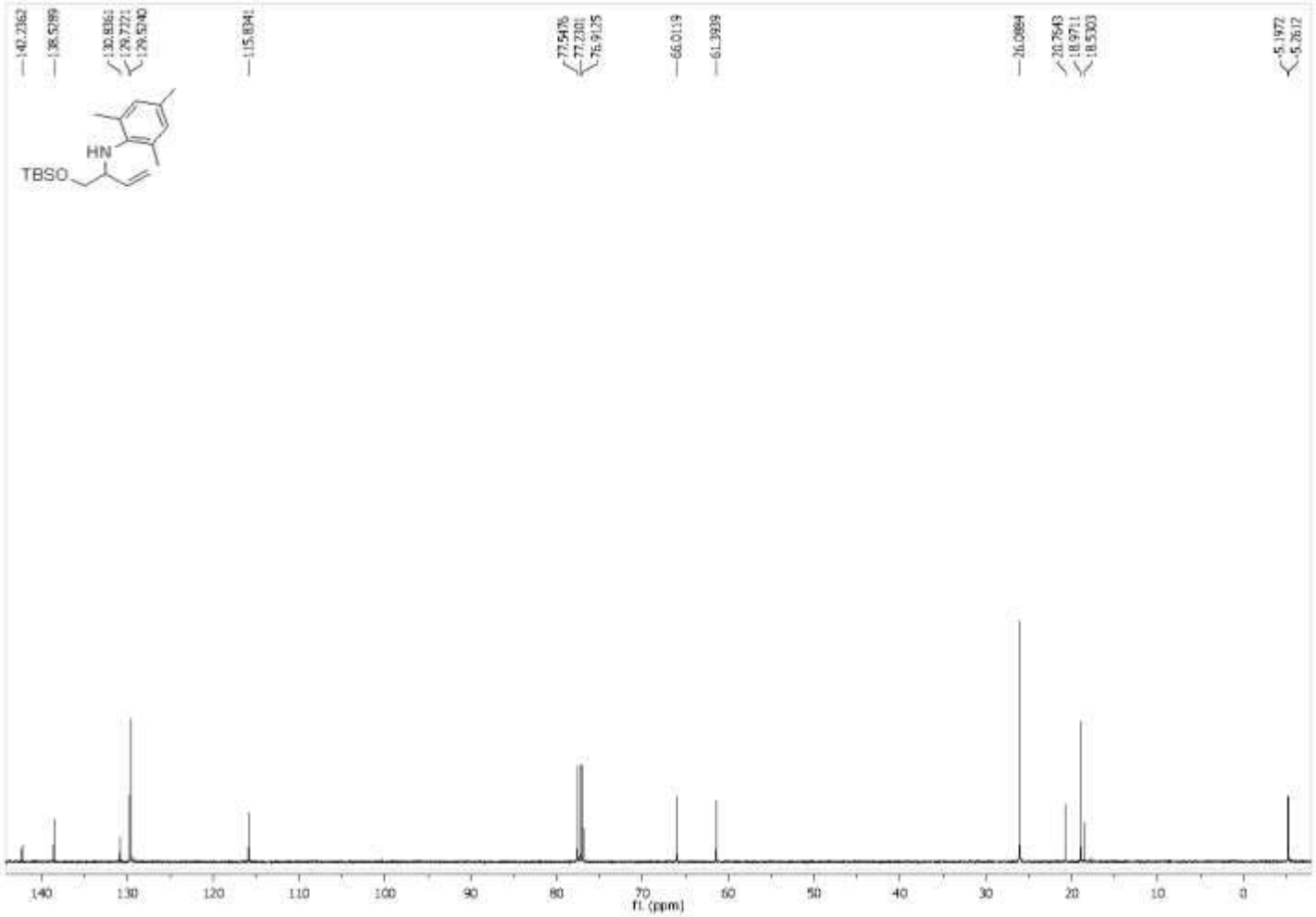

Figure A66 100 MHz 13C NMR ($CDCl_3$) Spectra of Compound **228e**

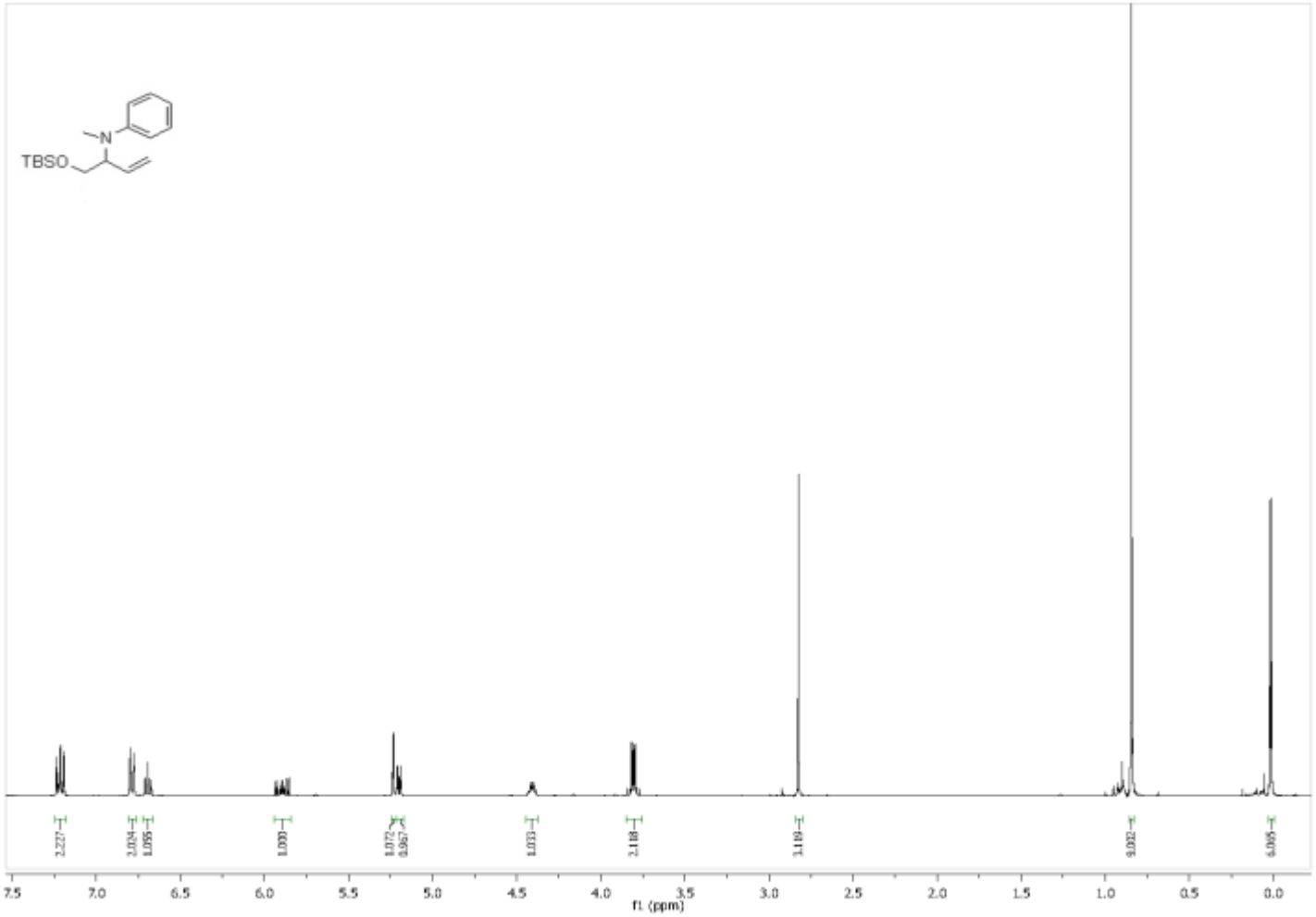

Figure A67 400 MHz 1H NMR ($CDCl_3$) Spectra of Compound **228f**

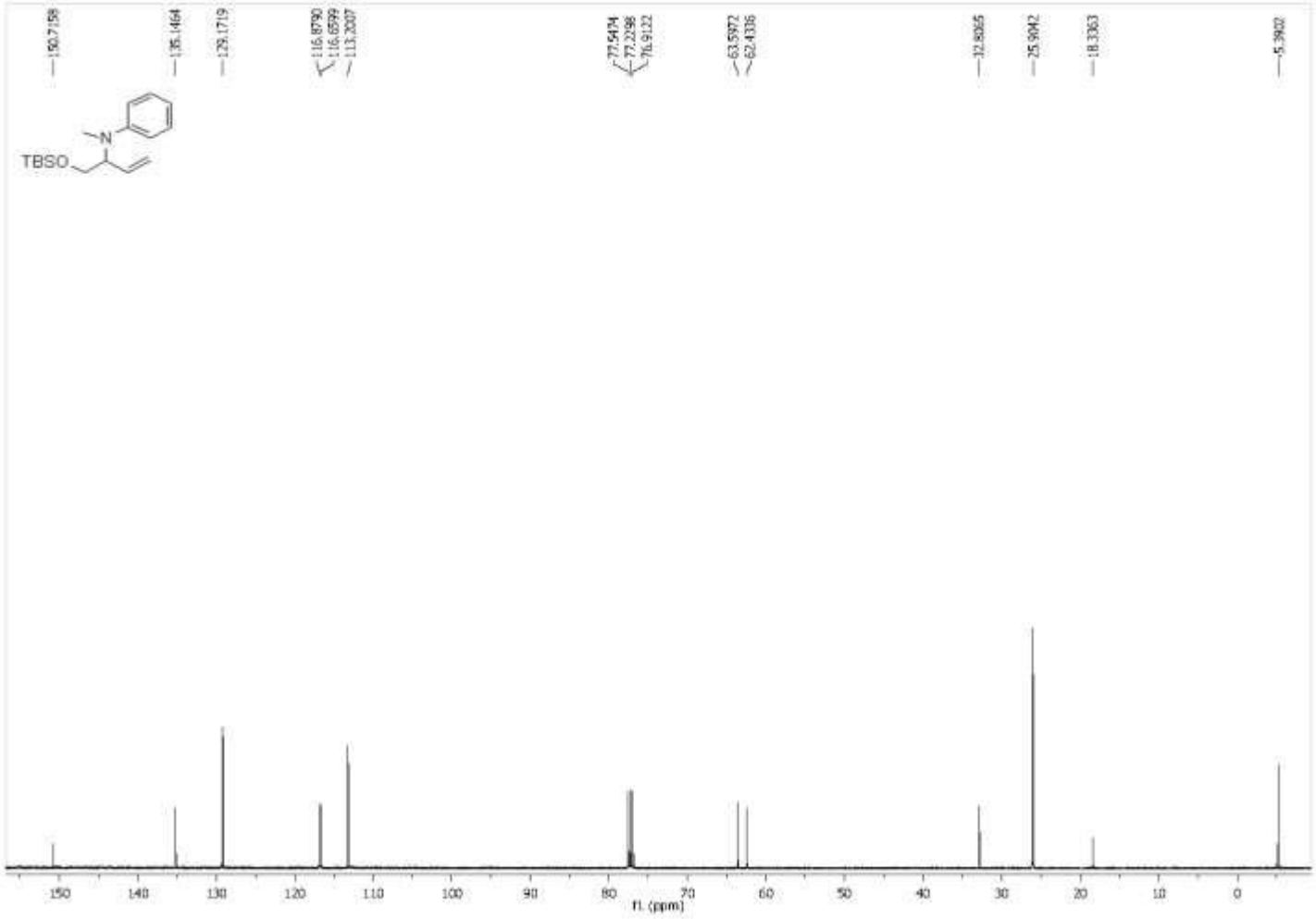

Figure A68 100 MHz 13C NMR ($CDCl_3$) Spectra of Compound **228f**

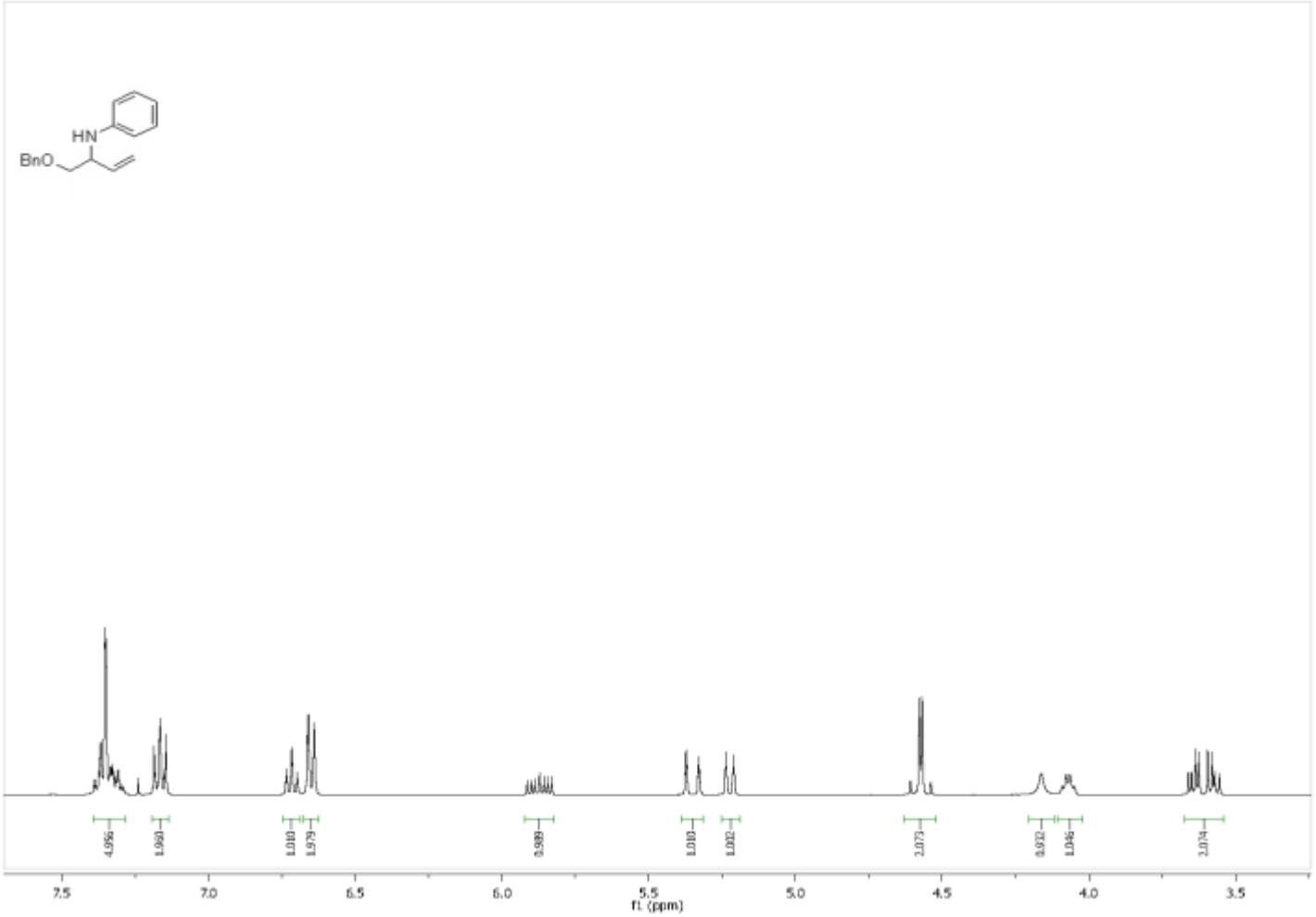

Figure A69 400 MHz 1H NMR ($CDCl_3$) Spectra of Compound **229a**

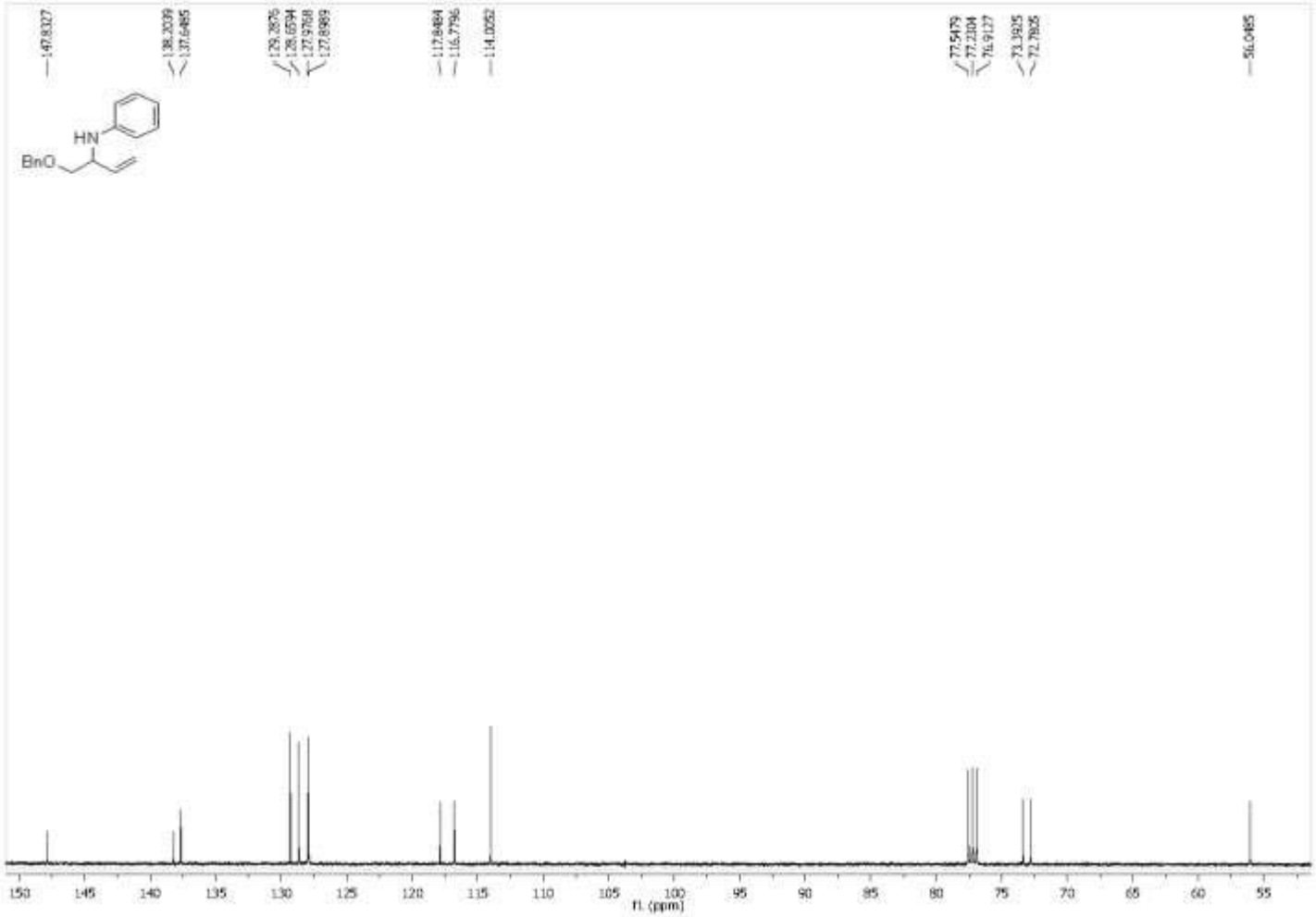

Figure A70 100 MHz 13C NMR ($CDCl_3$) Spectra of Compound **229a**

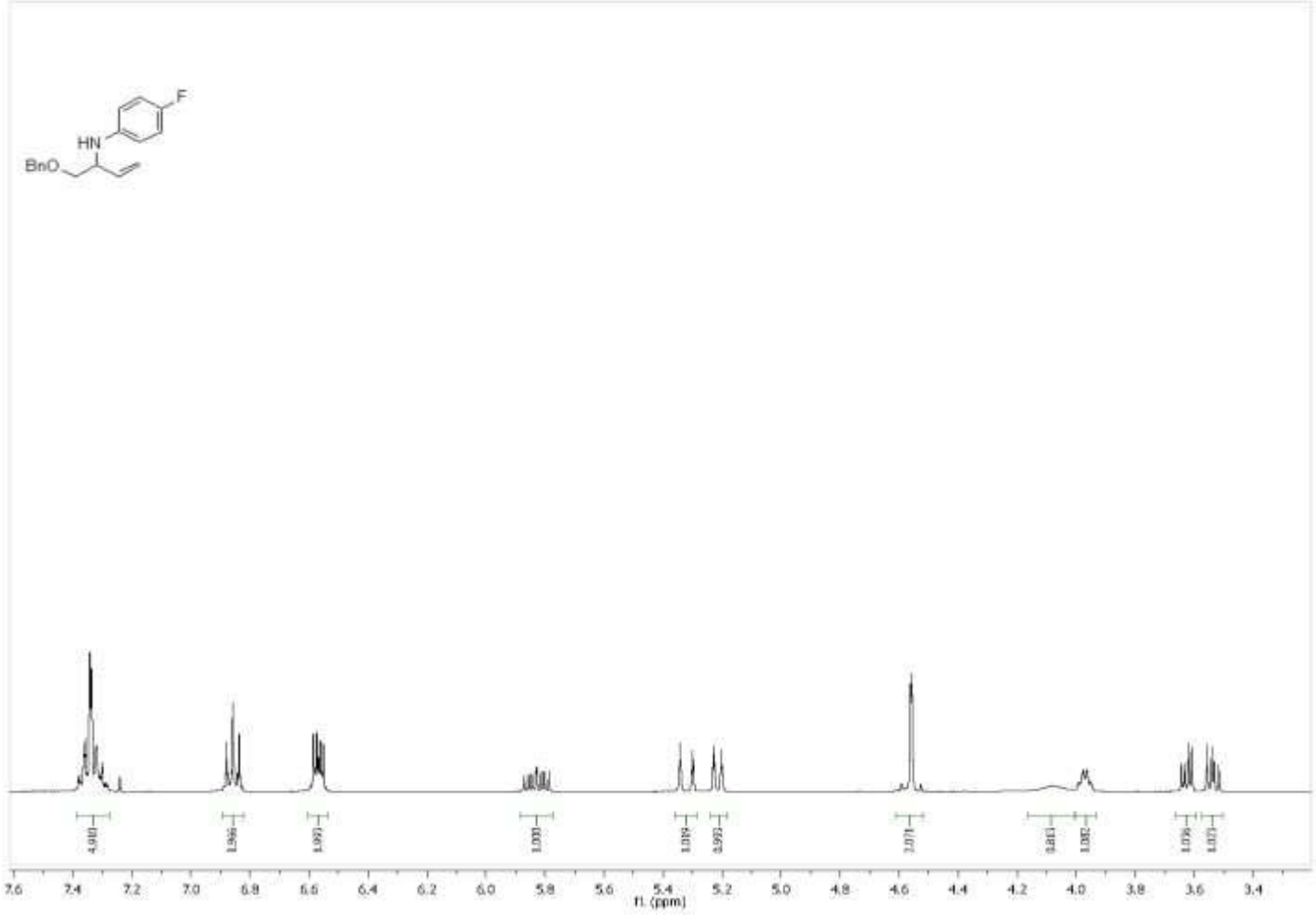

Figure A71 400 MHz 1H NMR ($CDCl_3$) Spectra of Compound **229b**

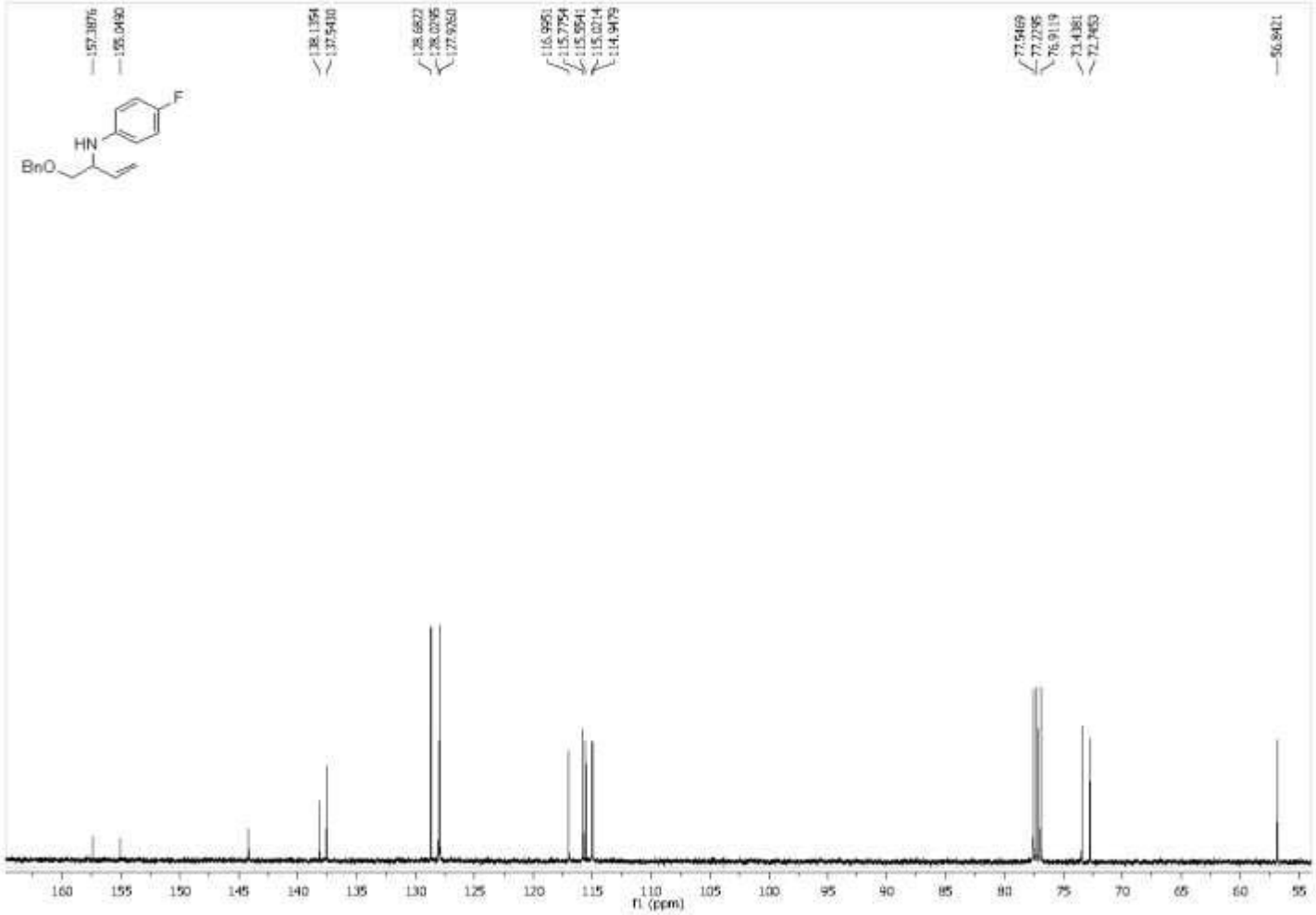

Figure A72 100 MHz 13C NMR ($CDCl_3$) Spectra of Compound **229b**

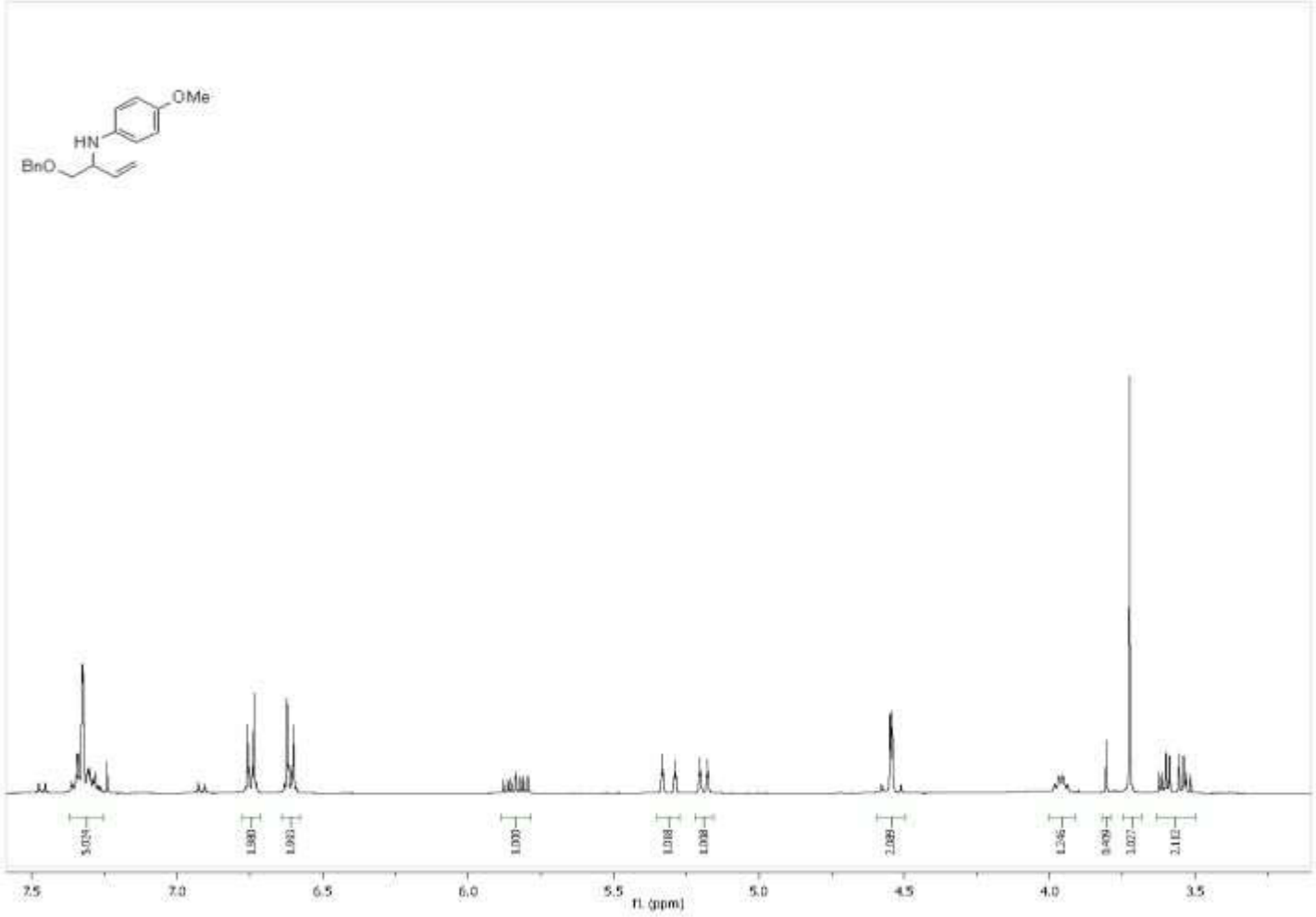

Figure A73 400 MHz 1H NMR ($CDCl_3$) Spectra of Compound **229c**

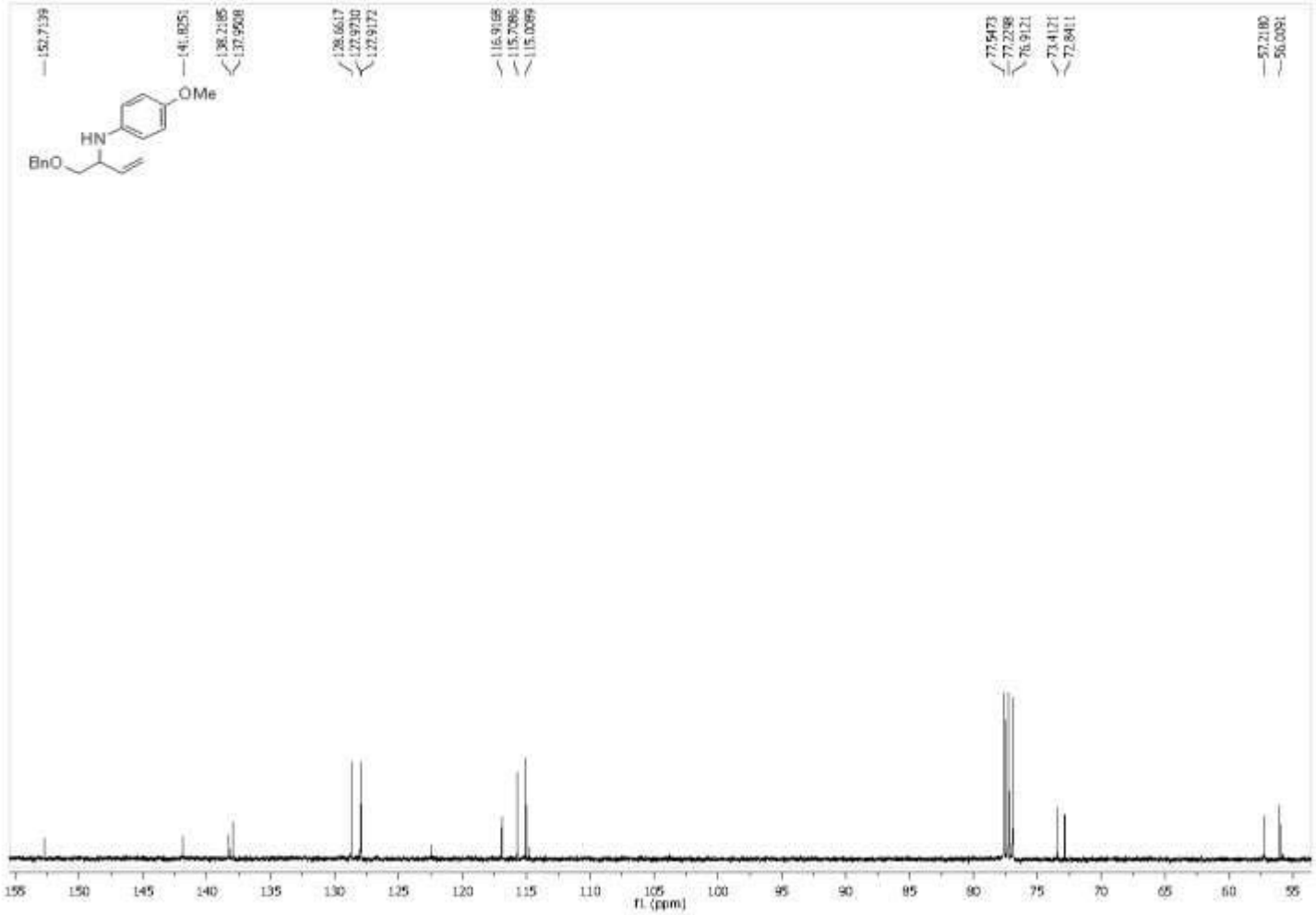

Figure A74 100 MHz 13C NMR ($CDCl_3$) Spectra of Compound **229c**

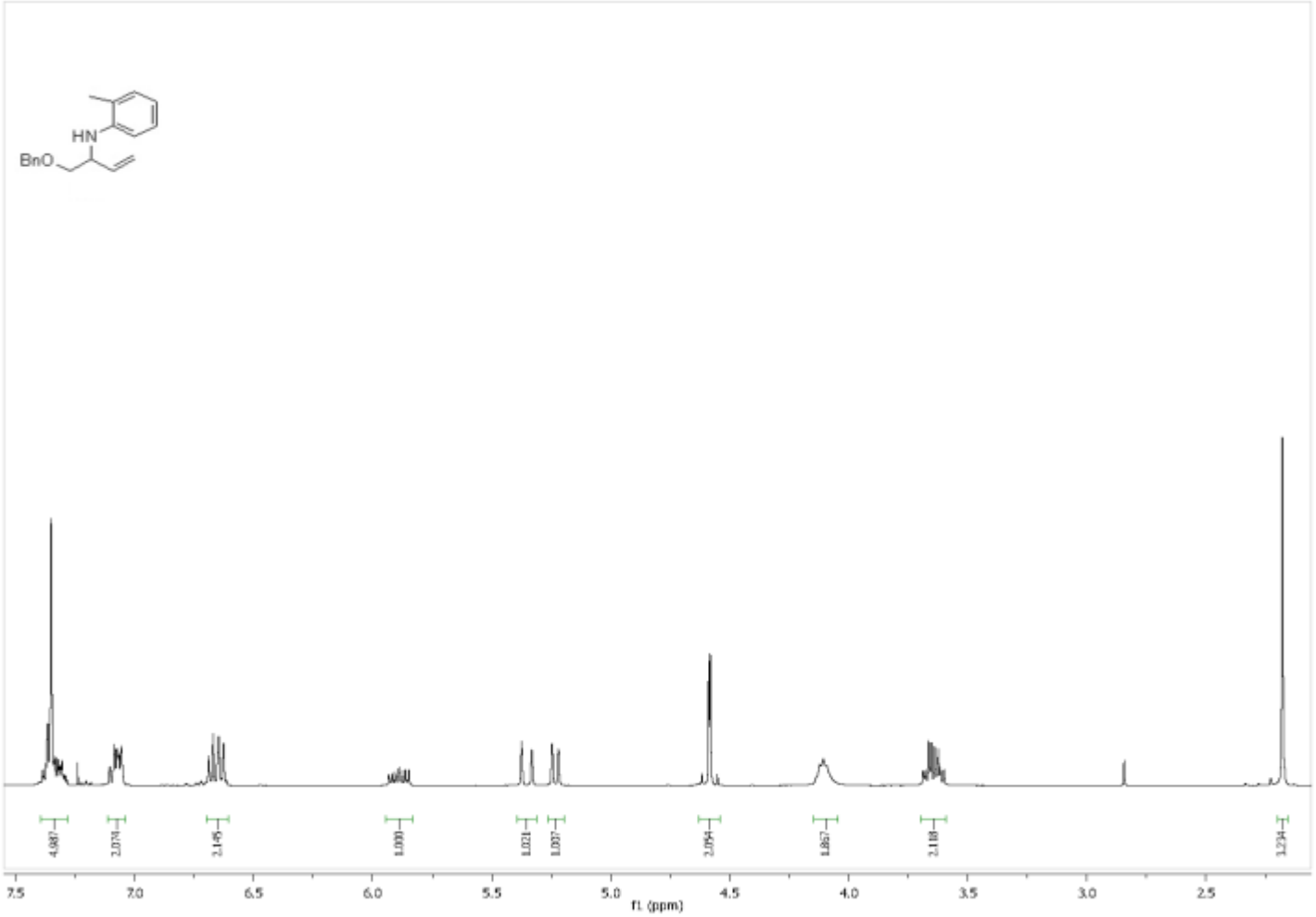

Figure A75 400 MHz 1H NMR ($CDCl_3$) Spectra of Compound **229d**

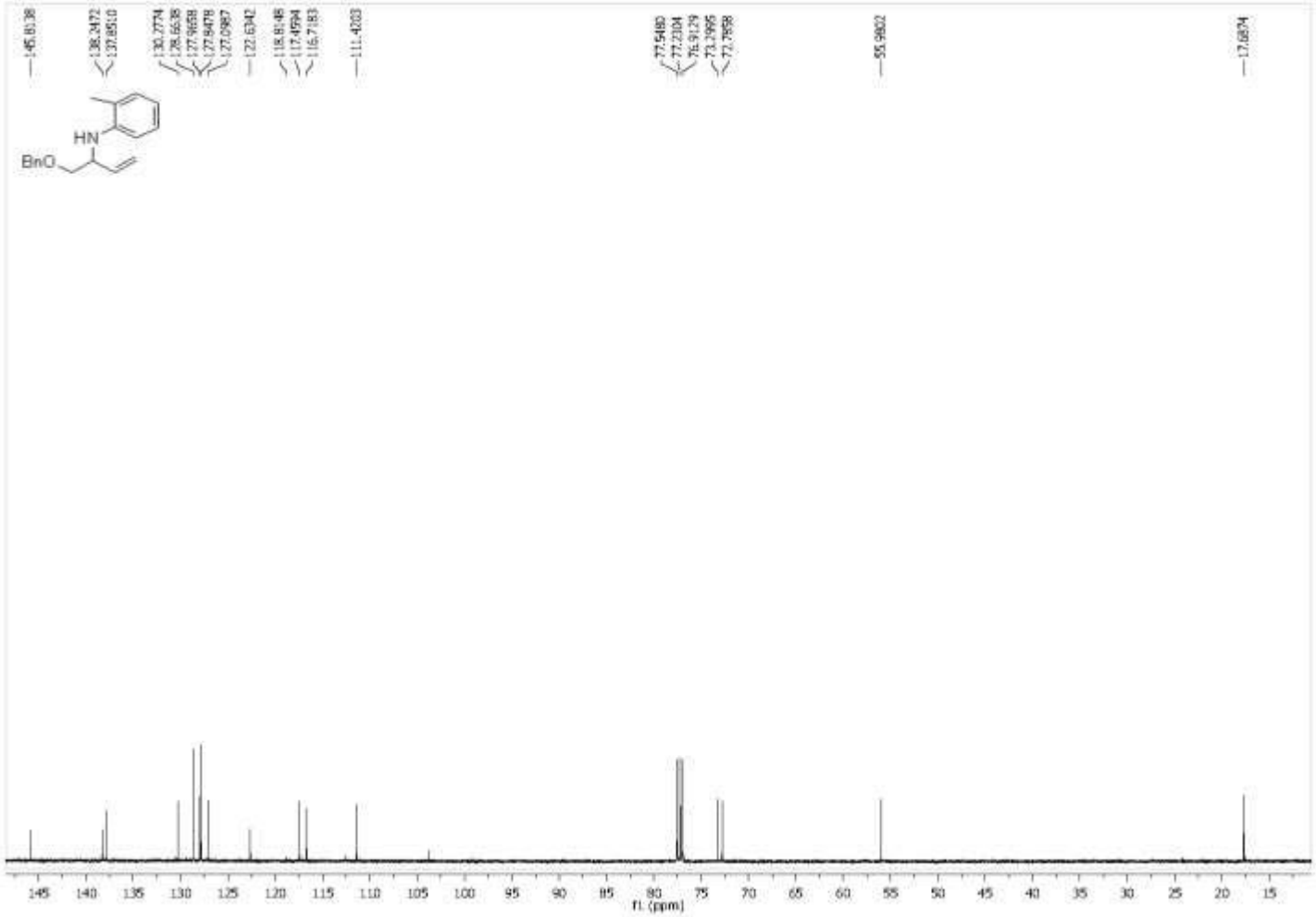

Figure A76 100 MHz 13C NMR ($CDCl_3$) Spectra of Compound **229d**

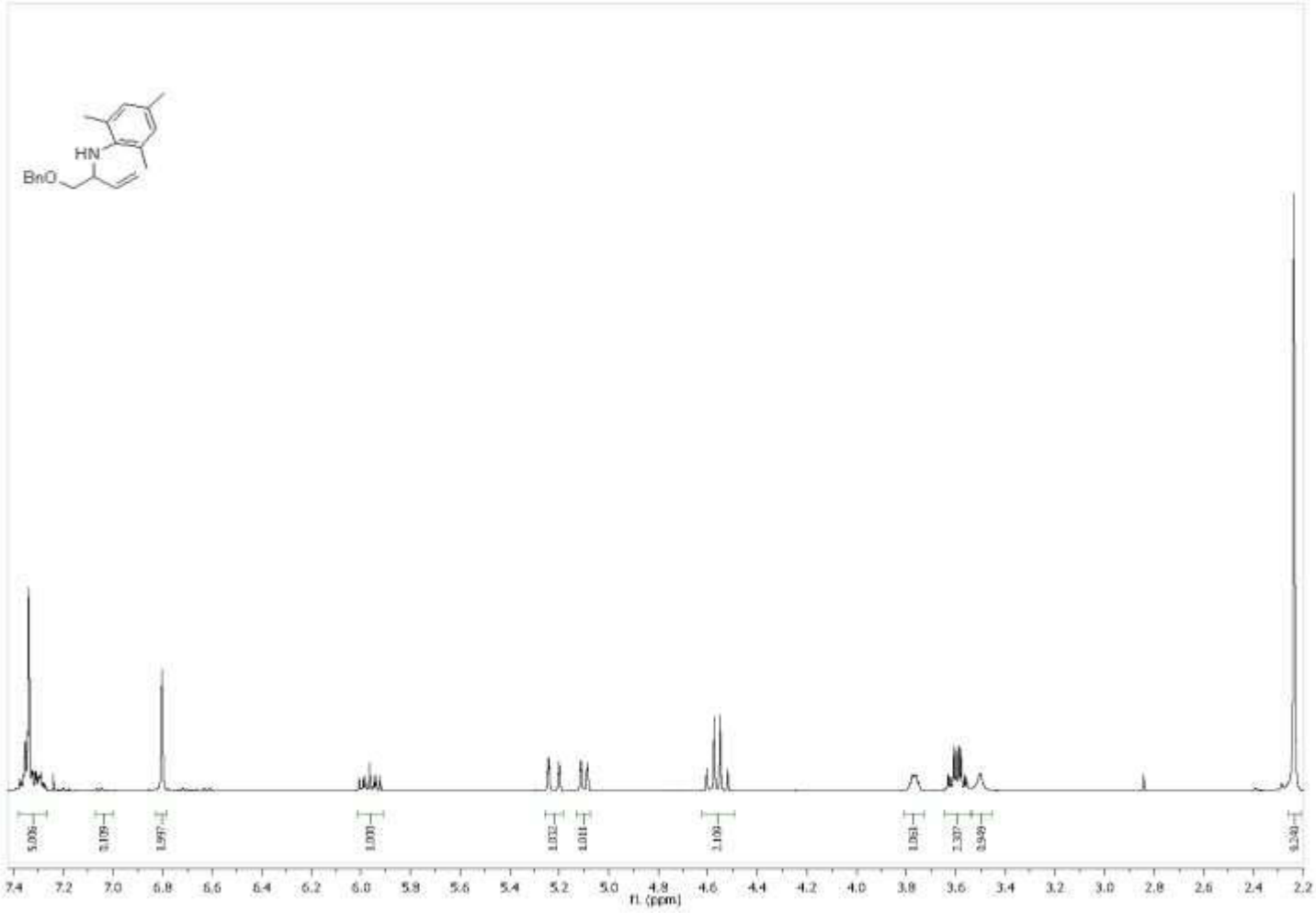

Figure A77 400 MHz 1H NMR ($CDCl_3$) Spectra of Compound **229e**

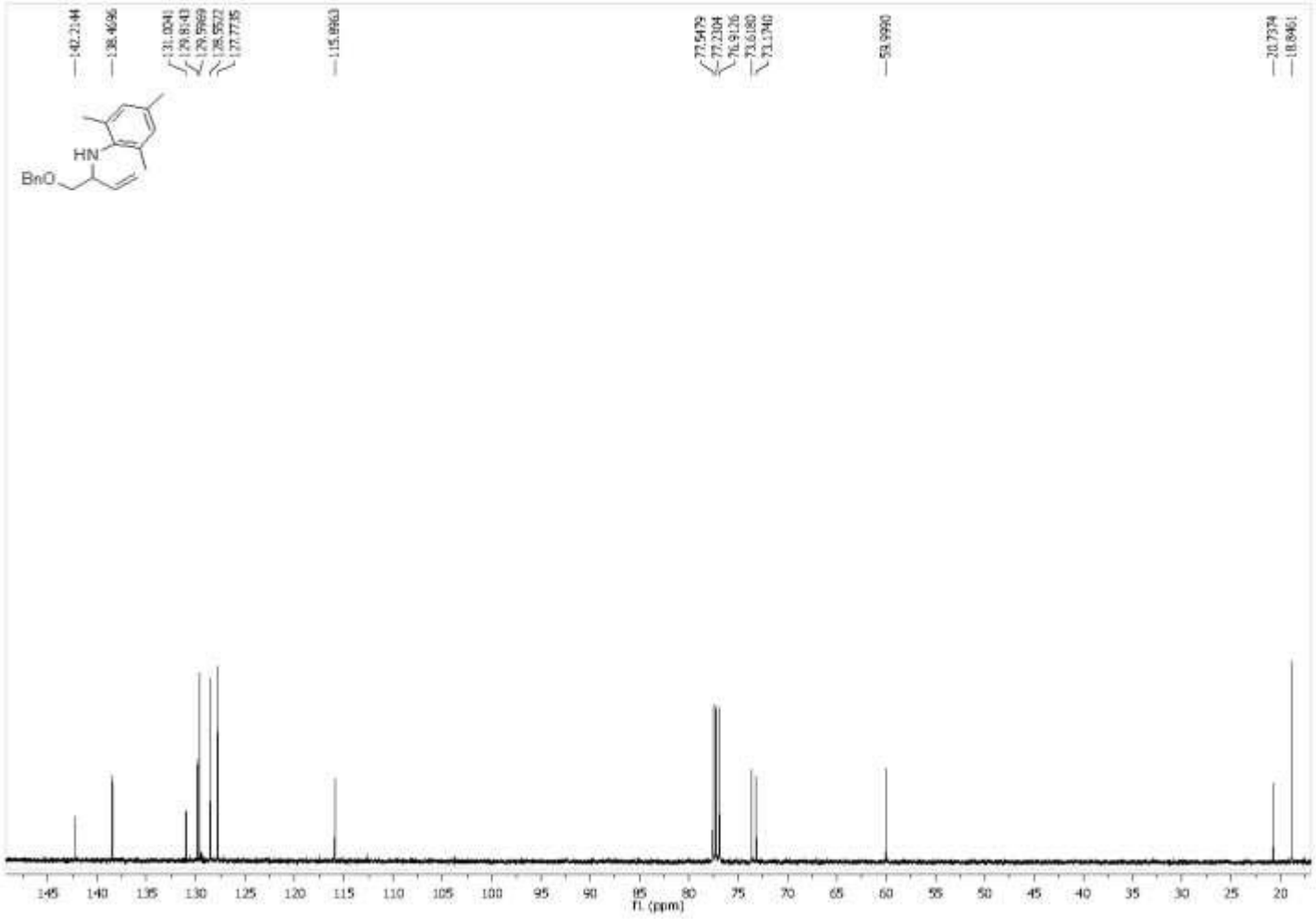

Figure A78 100 MHz 13C NMR ($CDCl_3$) Spectra of Compound **229e**

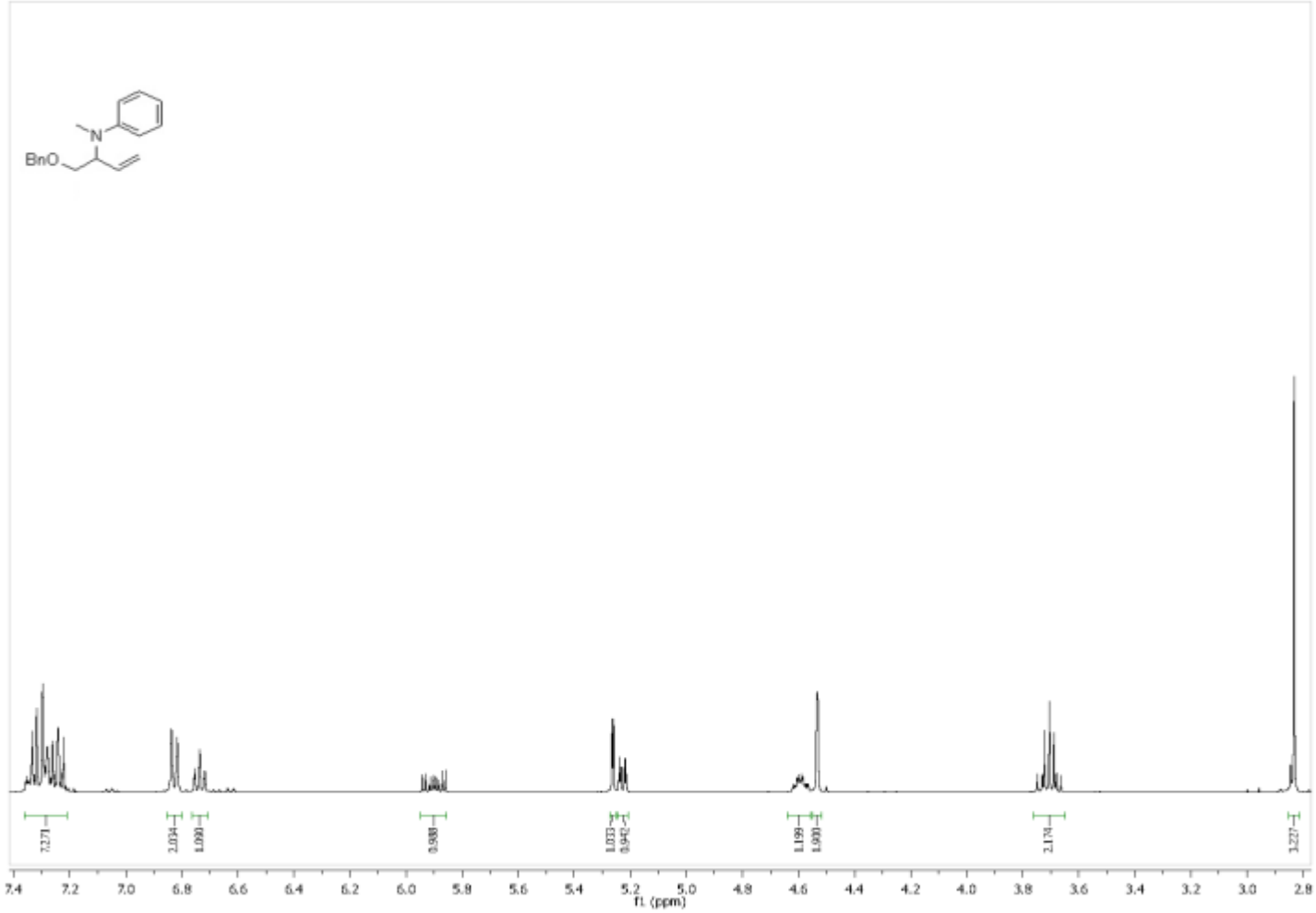

Figure A79 400 MHz 1H NMR ($CDCl_3$) Spectra of Compound **229f**

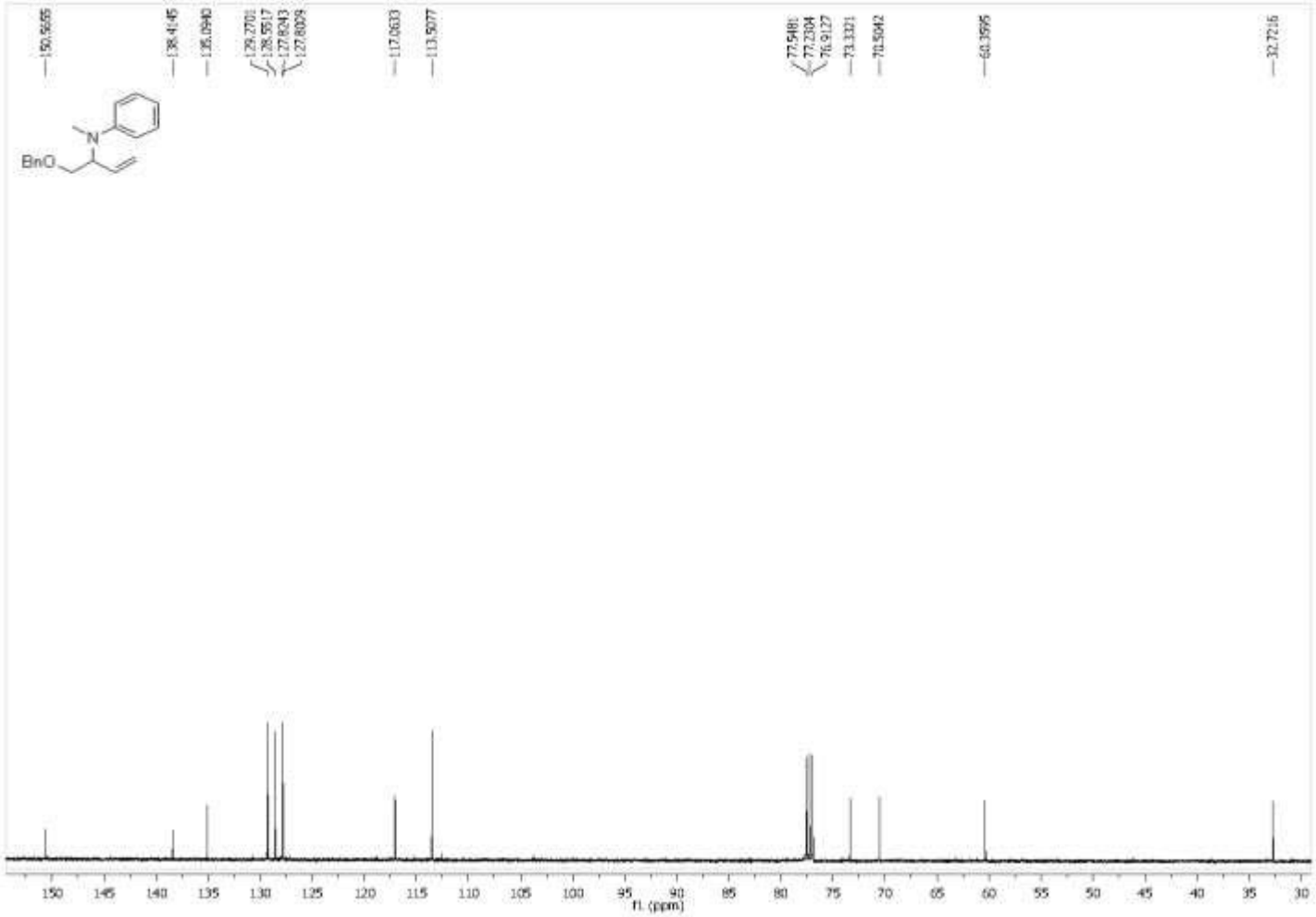

Figure A80 100 MHz 13C NMR ($CDCl_3$) Spectra of Compound **229f**

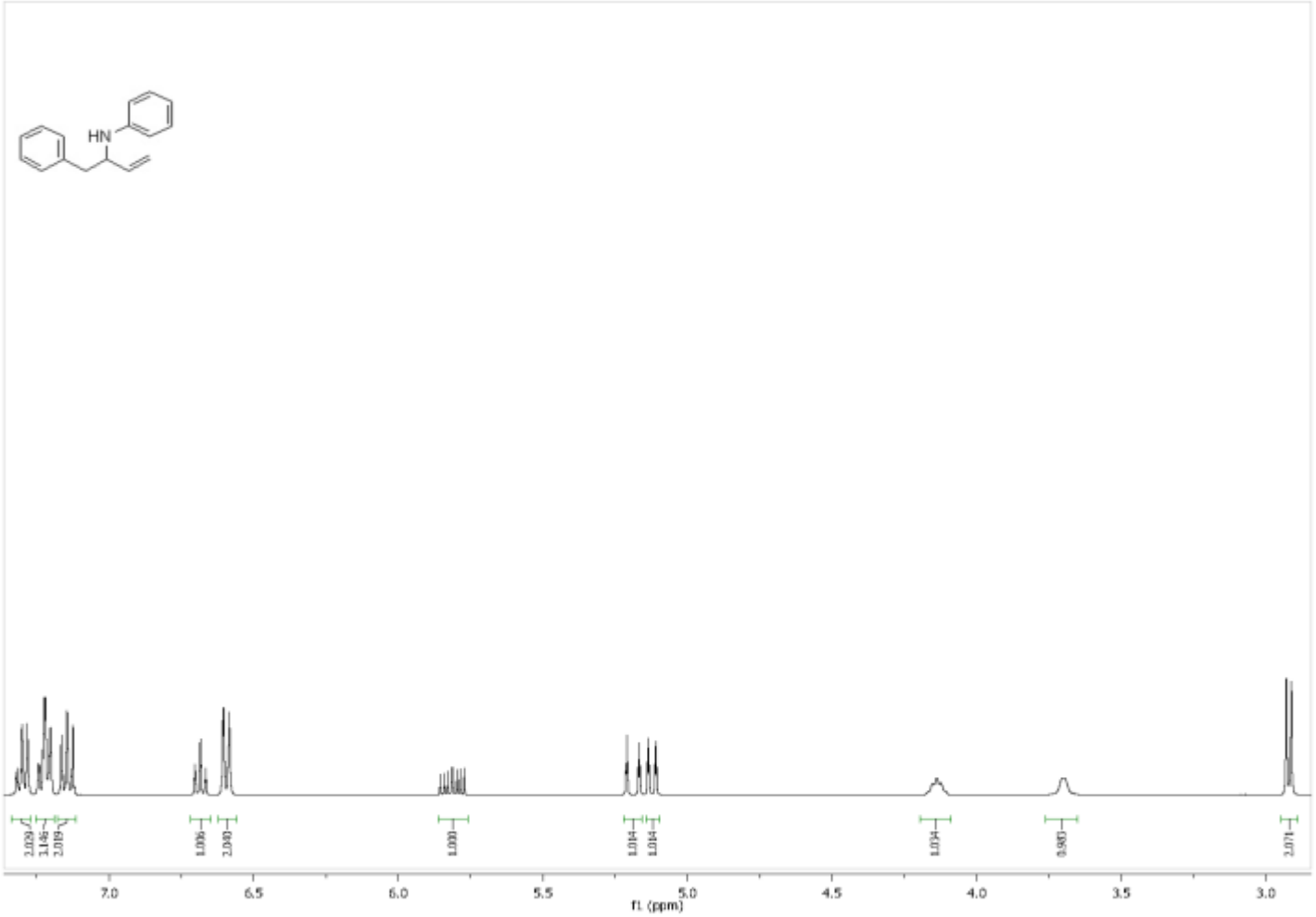

Figure A81 400 MHz 1H NMR ($CDCl_3$) Spectra of Compound **230a**

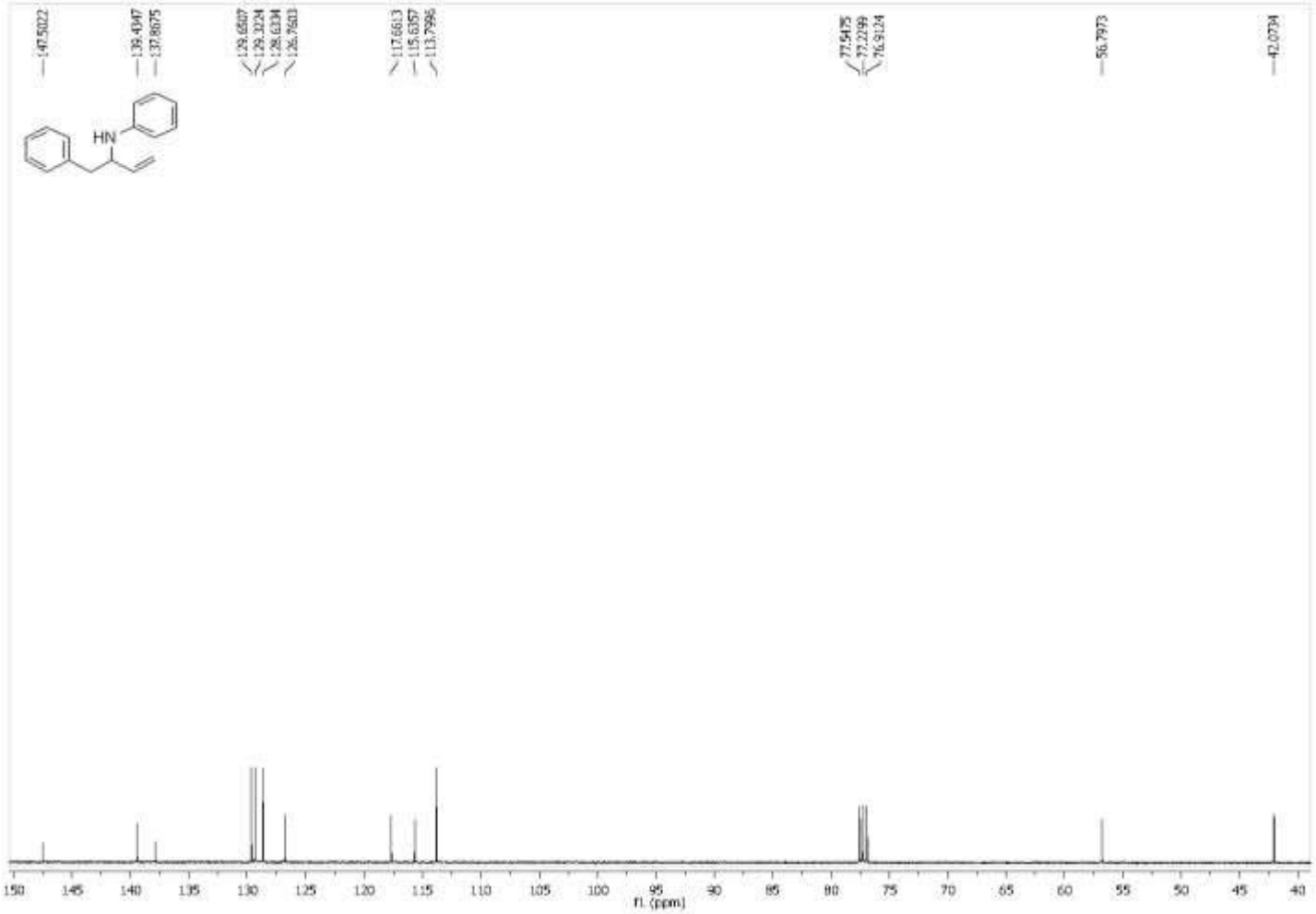

Figure A82 100 MHz 13C NMR ($CDCl_3$) Spectra of Compound **230a**

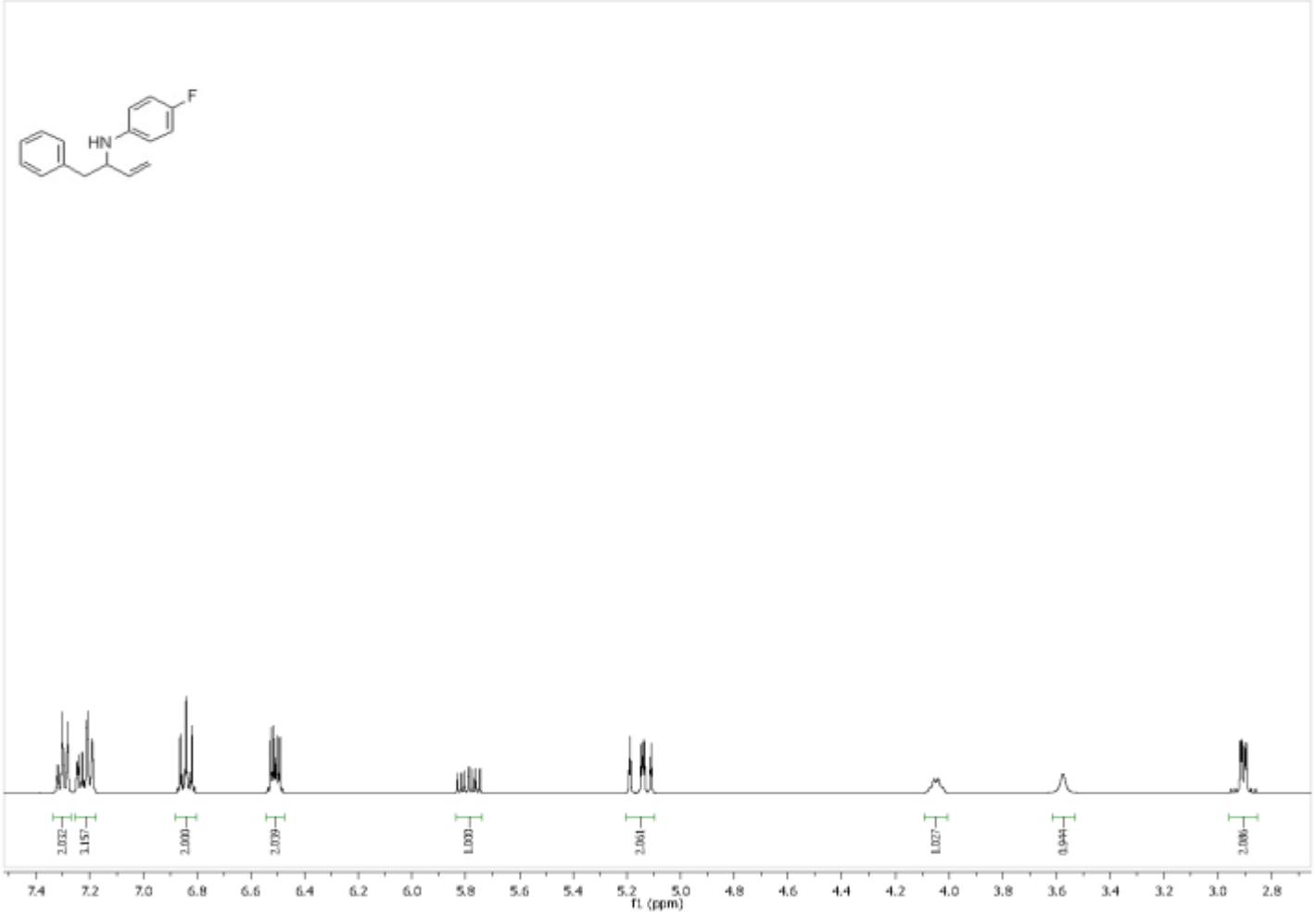

Figure A83 400 MHz 1H NMR ($CDCl_3$) Spectra of Compound **230b**

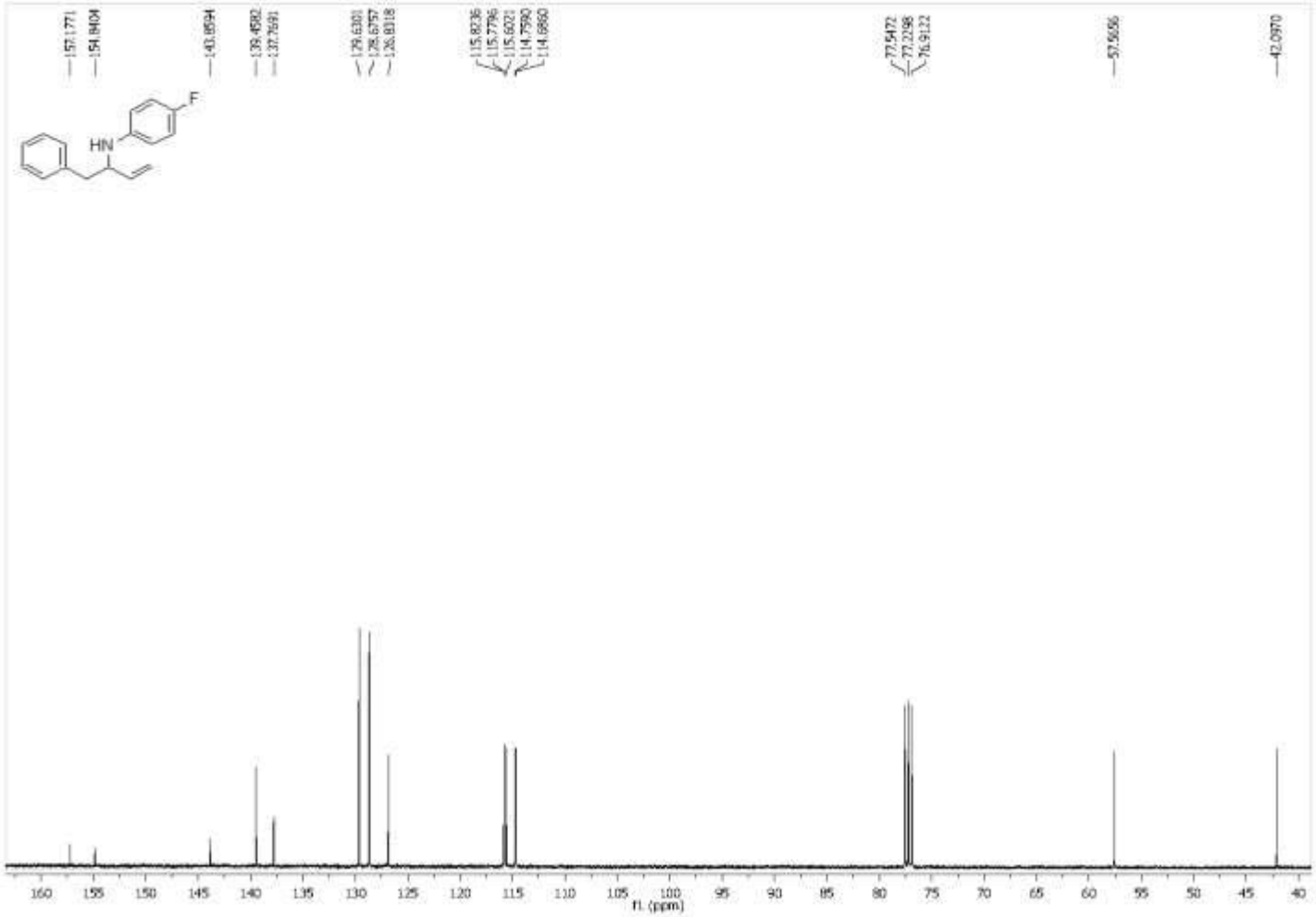

Figure A84 100 MHz 13C NMR ($CDCl_3$) Spectra of Compound **230b**

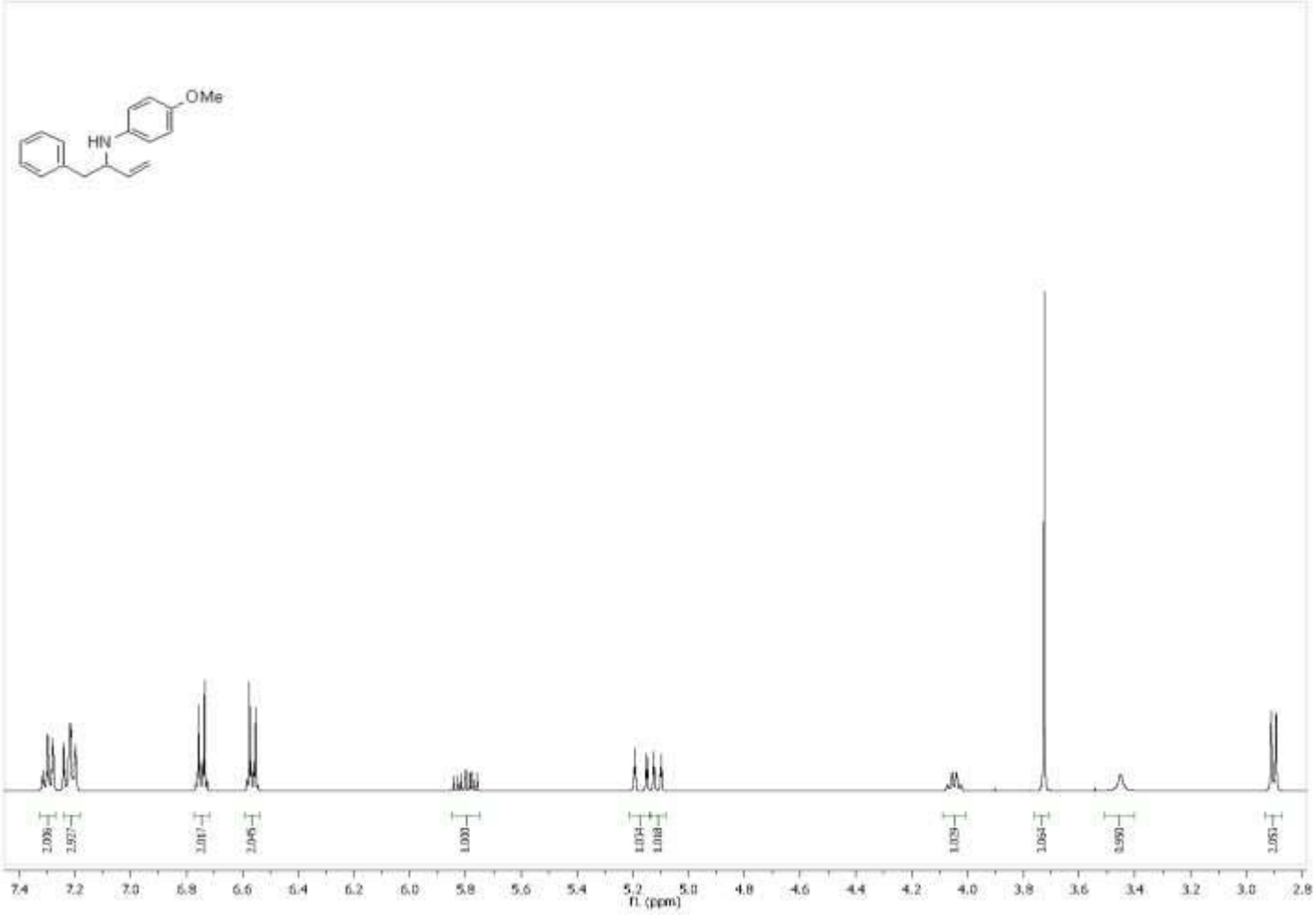

Figure A85 400 MHz 1H NMR ($CDCl_3$) Spectra of Compound **230c**

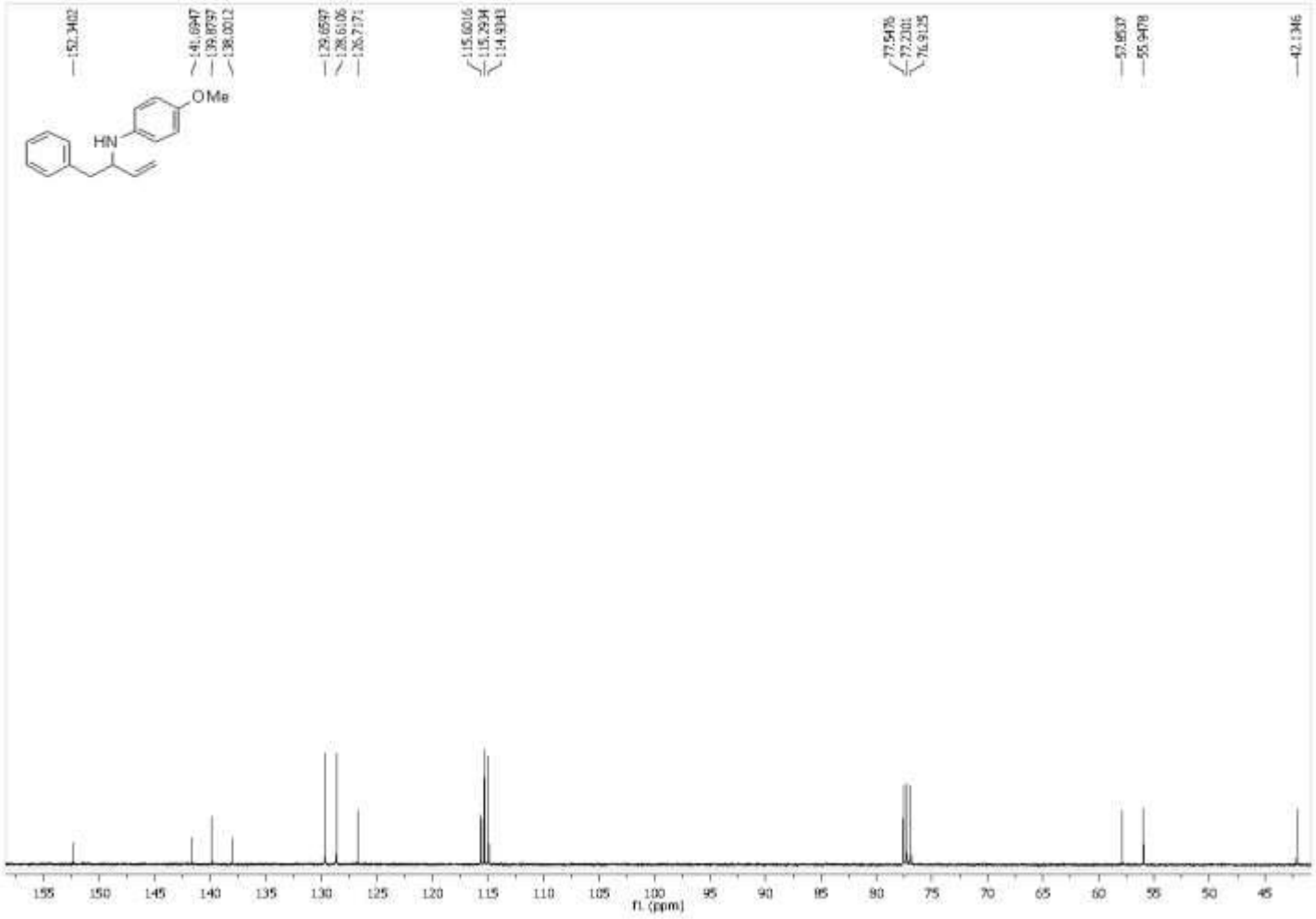

Figure A86 100 MHz 13C NMR ($CDCl_3$) Spectra of Compound **230c**

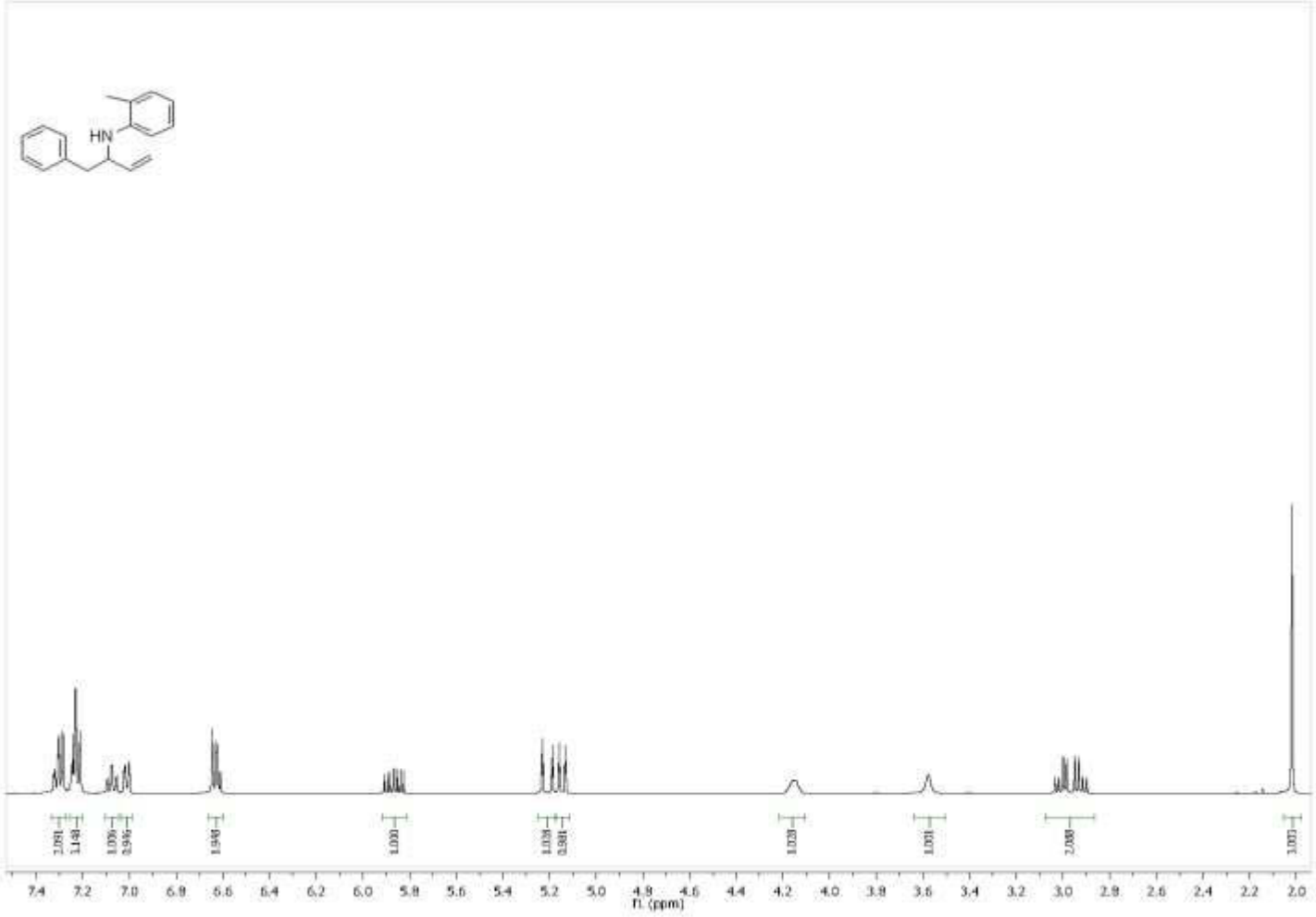

Figure A87 400 MHz 1H NMR ($CDCl_3$) Spectra of Compound **230d**

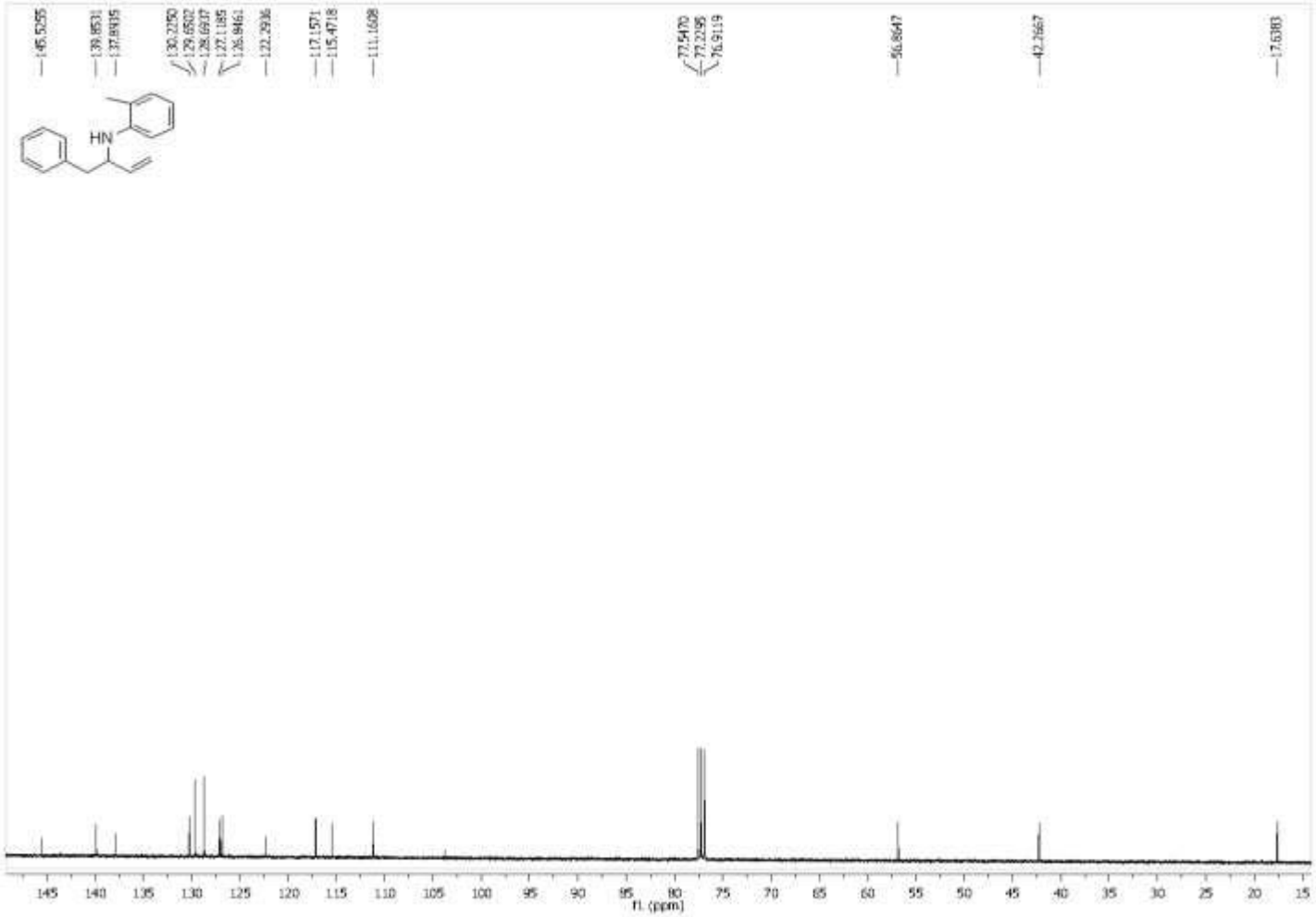

Figure A88 100 MHz 13C NMR ($CDCl_3$) Spectra of Compound **230d**

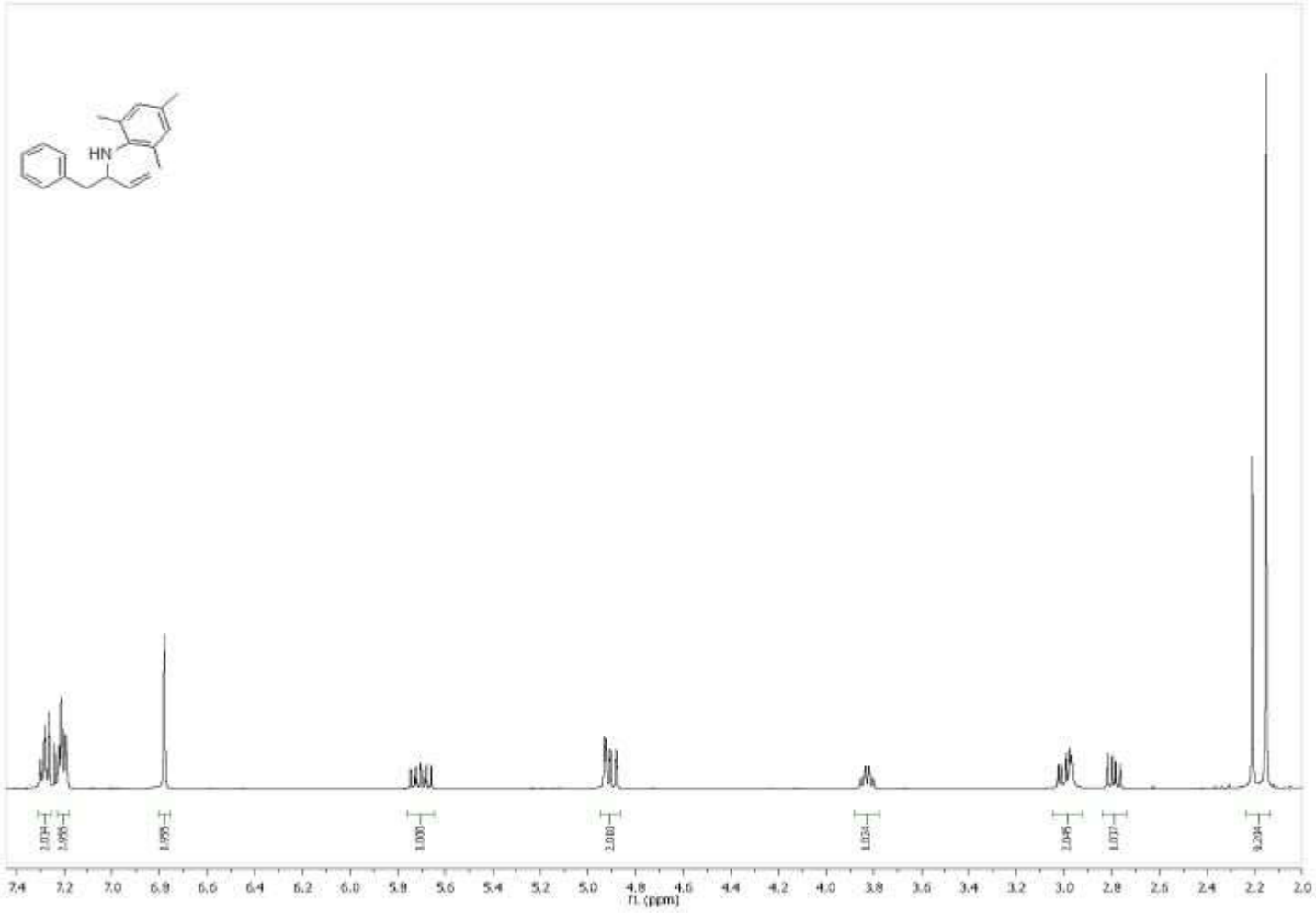

Figure A89 400 MHz 1H NMR ($CDCl_3$) Spectra of Compound **230e**

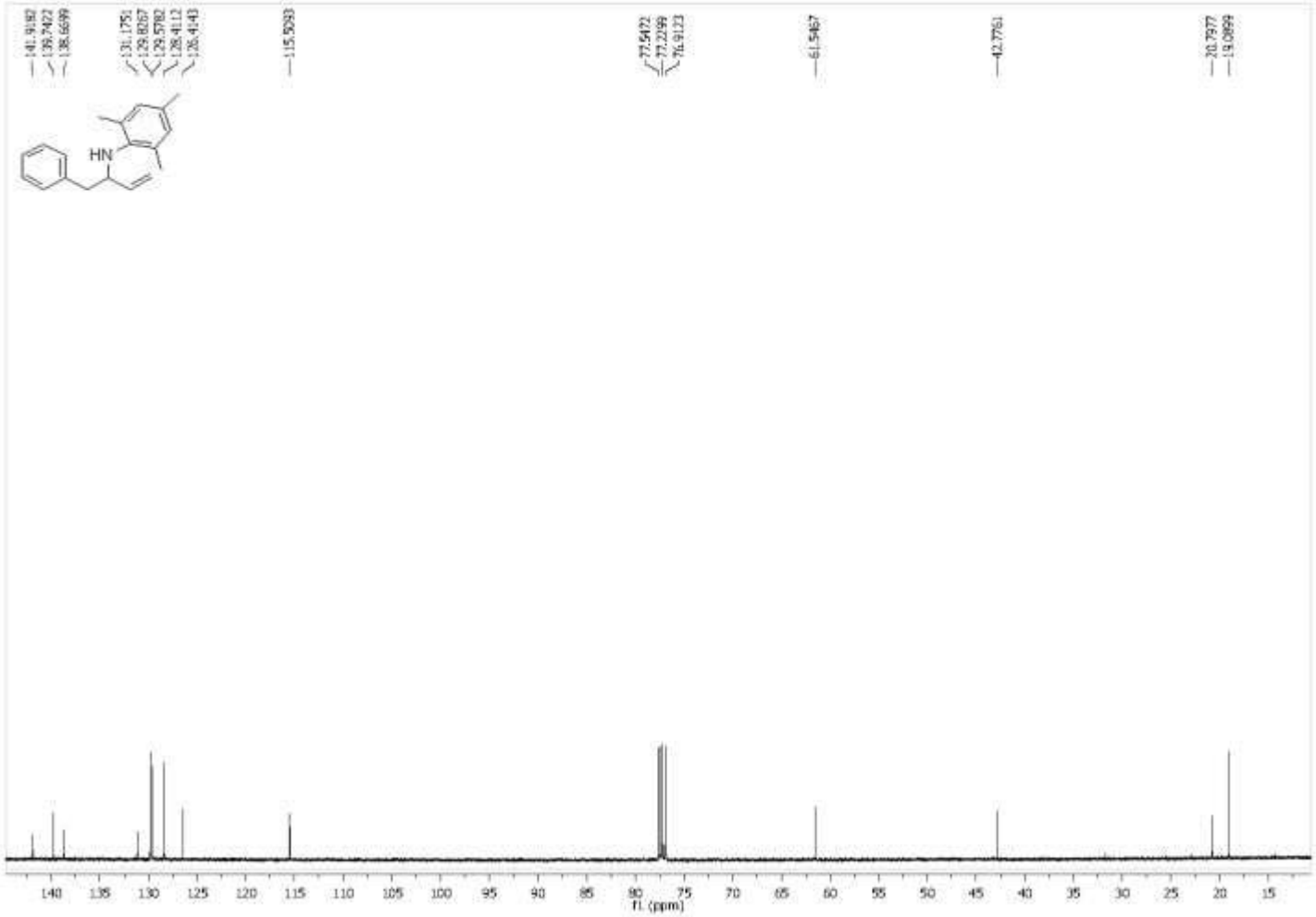

Figure A90 100 MHz 13C NMR ($CDCl_3$) Spectra of Compound **230e**

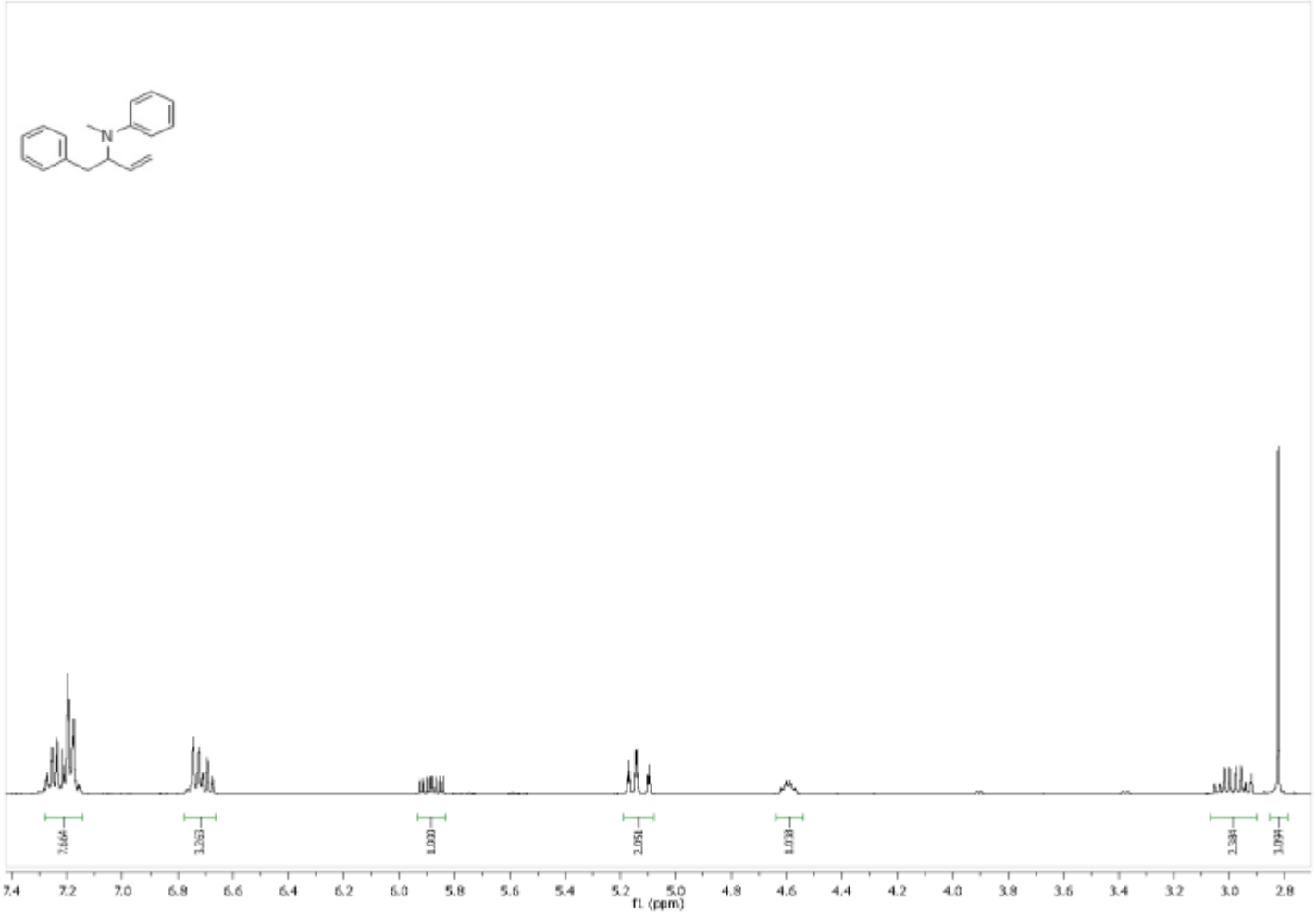

Figure A91 400 MHz 1H NMR ($CDCl_3$) Spectra of Compound **230f**

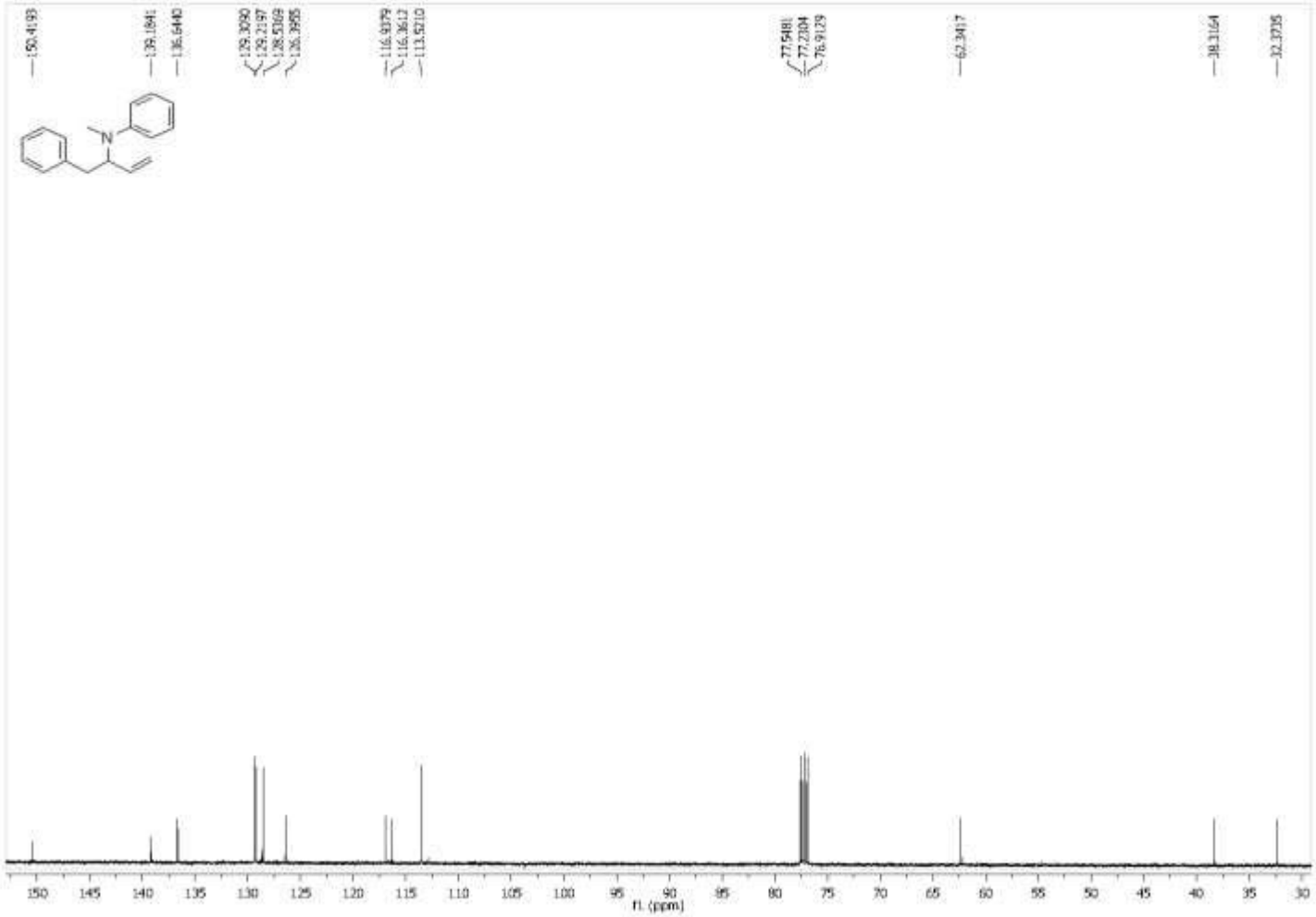

Figure A92 100 MHz 13C NMR ($CDCl_3$) Spectra of Compound **230f**

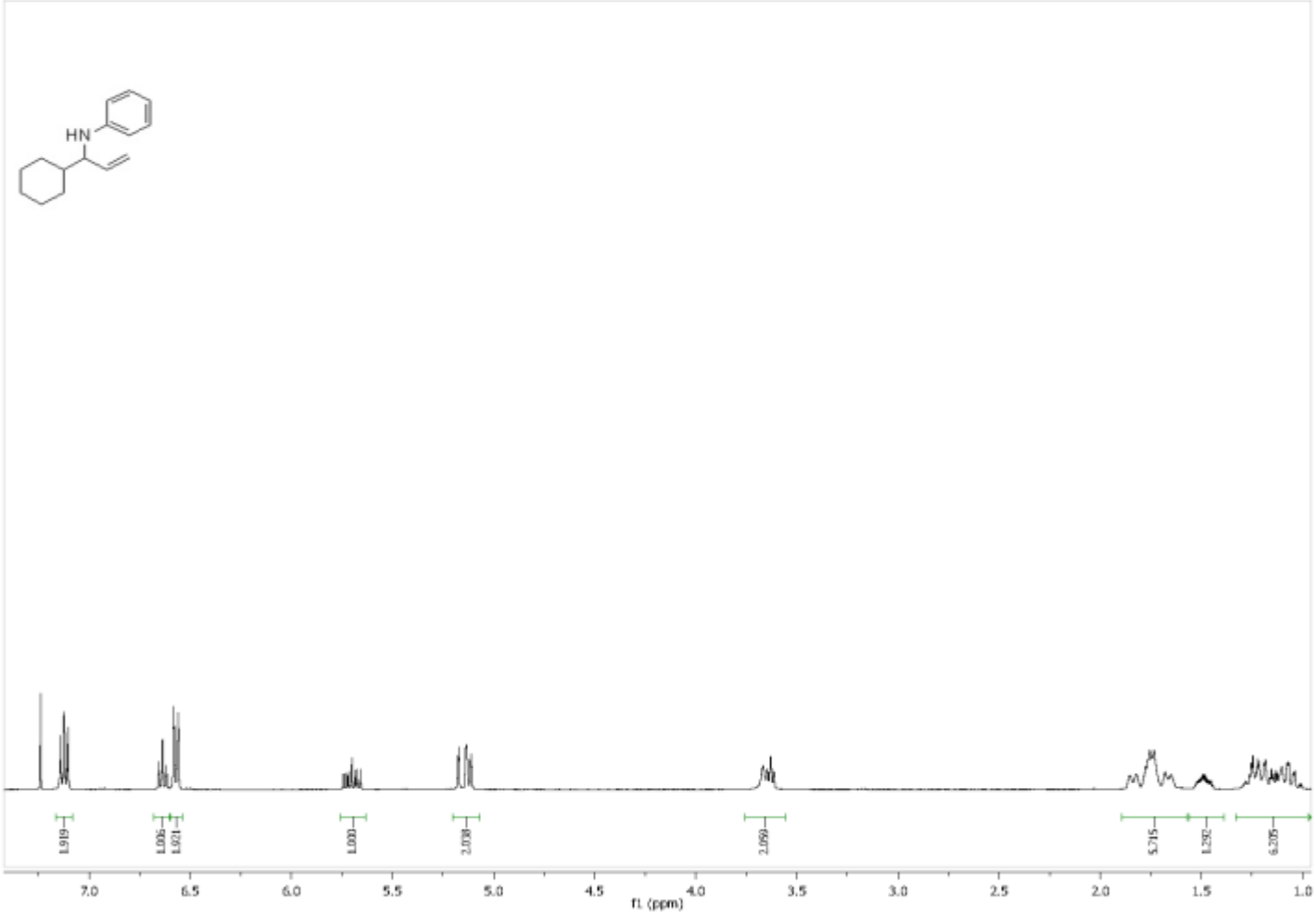

Figure A93 400 MHz 1H NMR ($CDCl_3$) Spectra of Compound **231a**

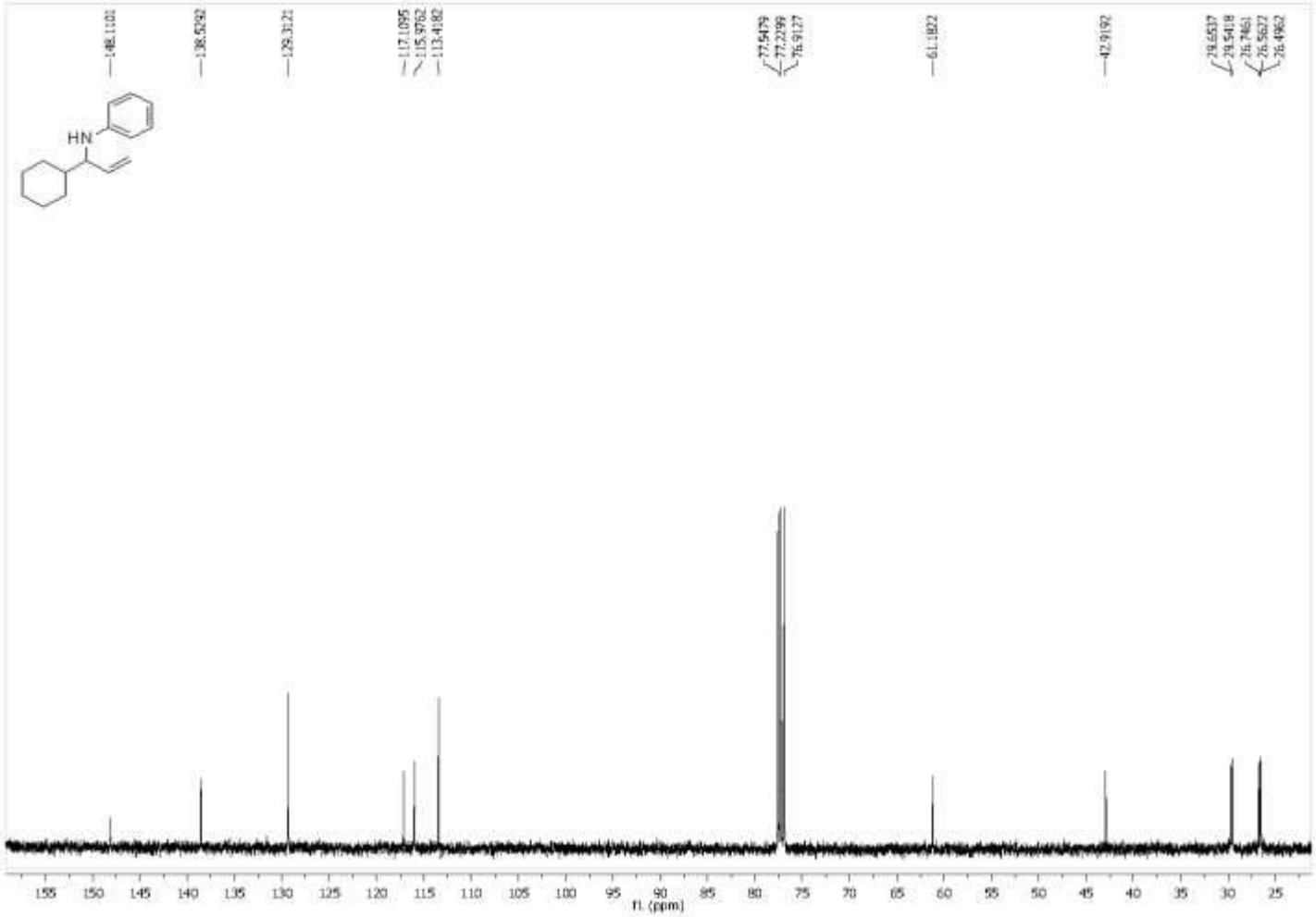

Figure A94 100 MHz 13C NMR ($CDCl_3$) Spectra of Compound **231a**

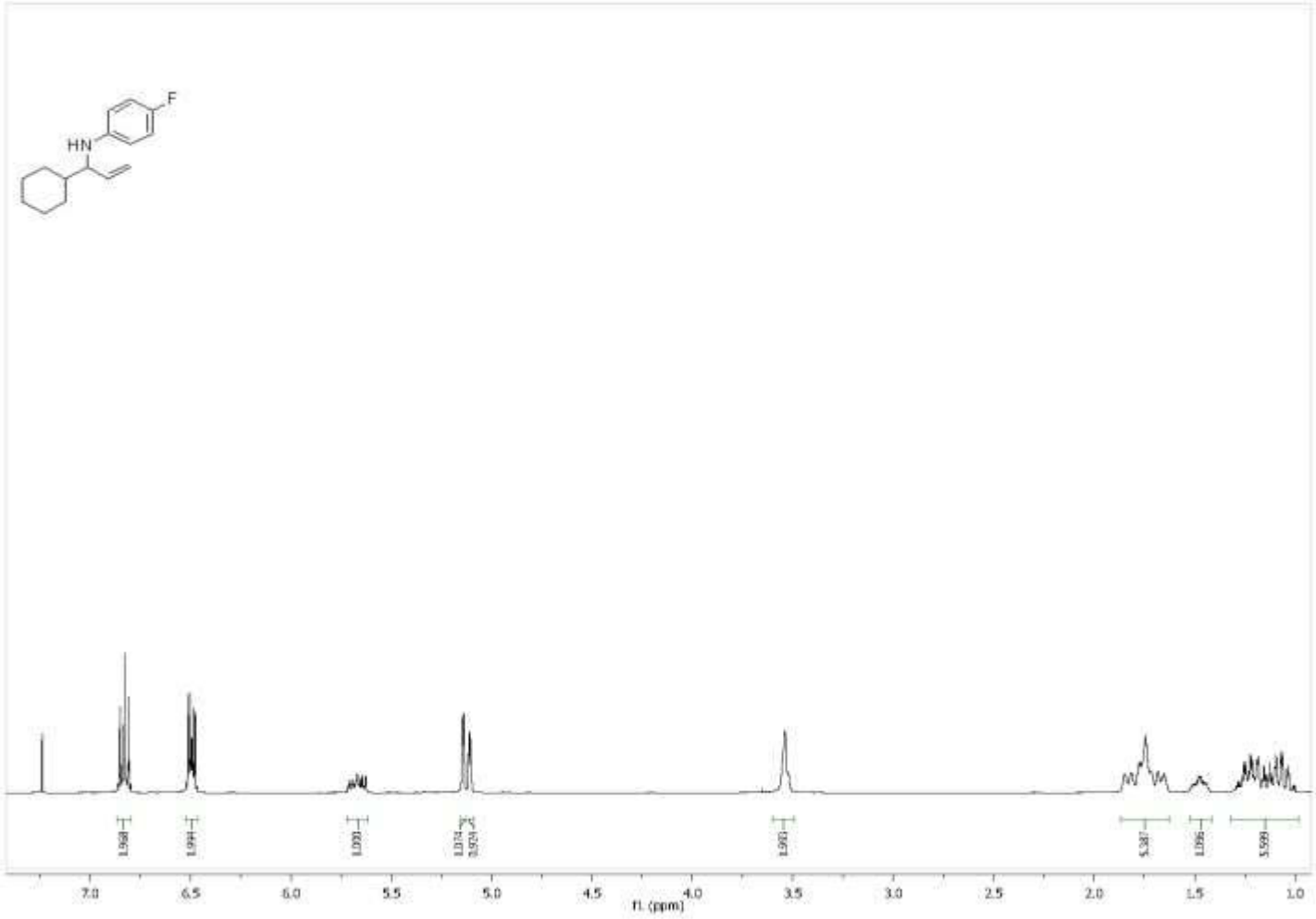

Figure A95 400 MHz 1H NMR ($CDCl_3$) Spectra of Compound **231b**

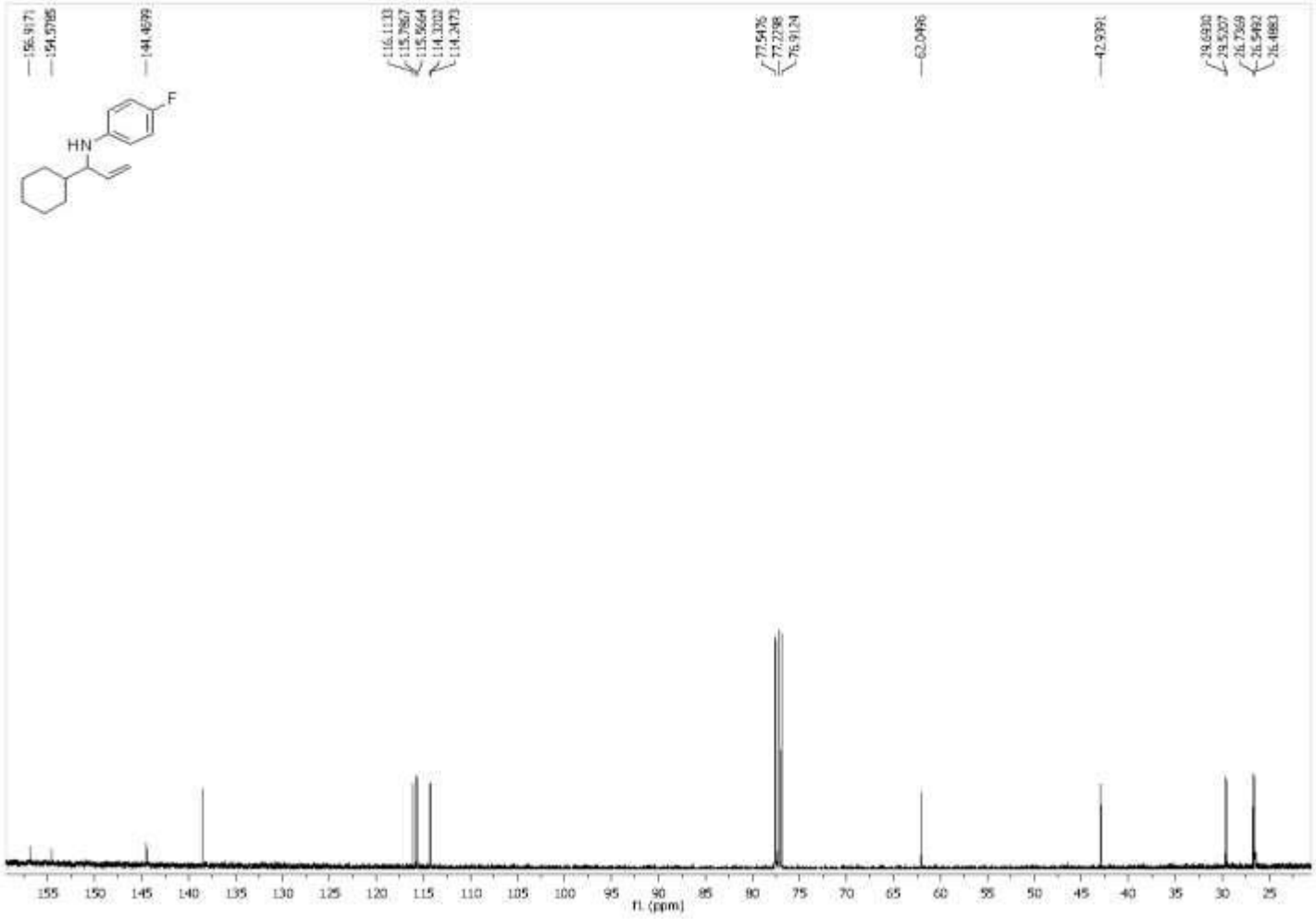

Figure A96 100 MHz 13C NMR ($CDCl_3$) Spectra of Compound **231b**

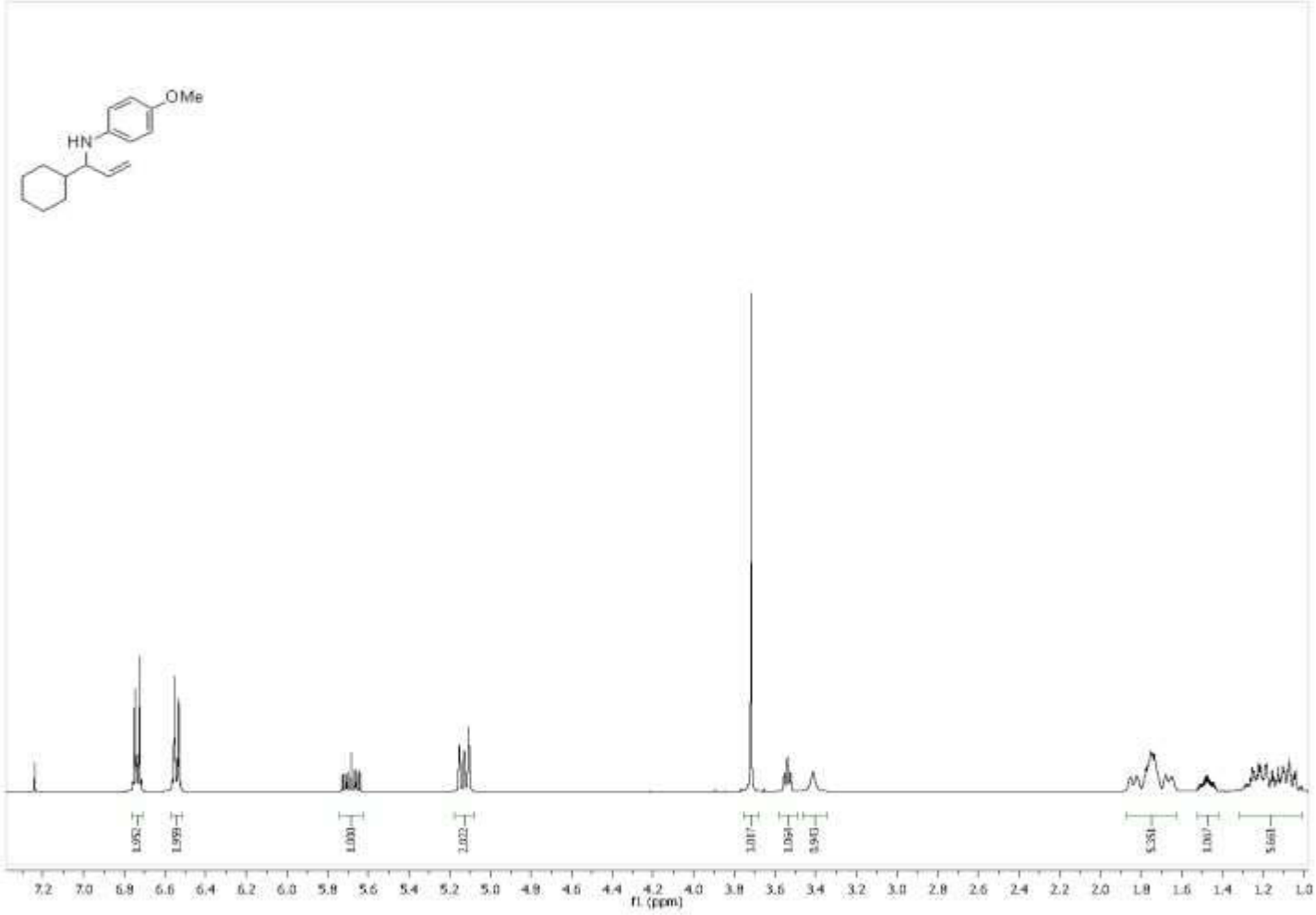

Figure A97 400 MHz 1H NMR ($CDCl_3$) Spectra of Compound **231c**

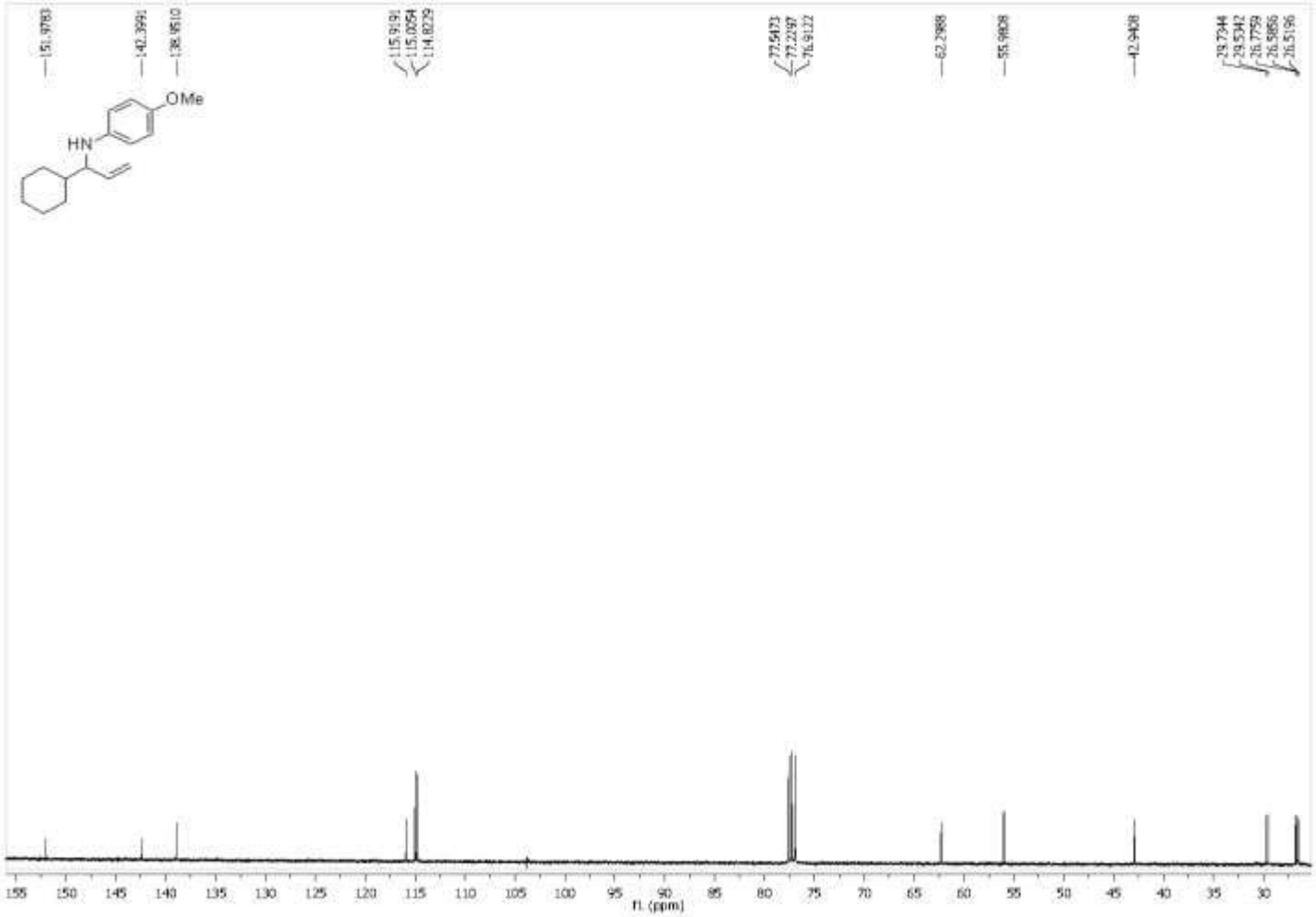

Figure A98 100 MHz 13C NMR ($CDCl_3$) Spectra of Compound **231c**

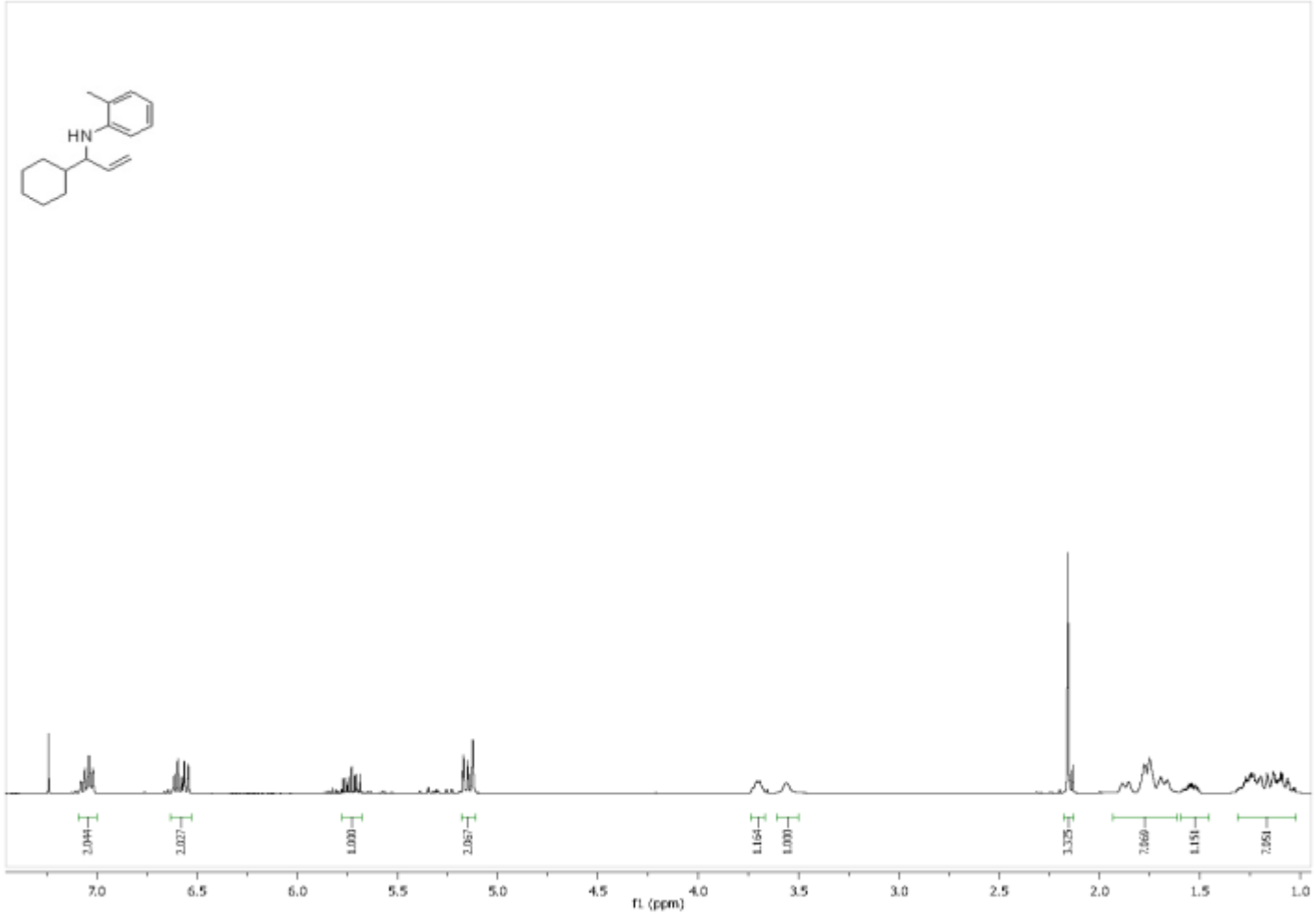

Figure A99 400 MHz 1H NMR ($CDCl_3$) Spectra of Compound **231d**

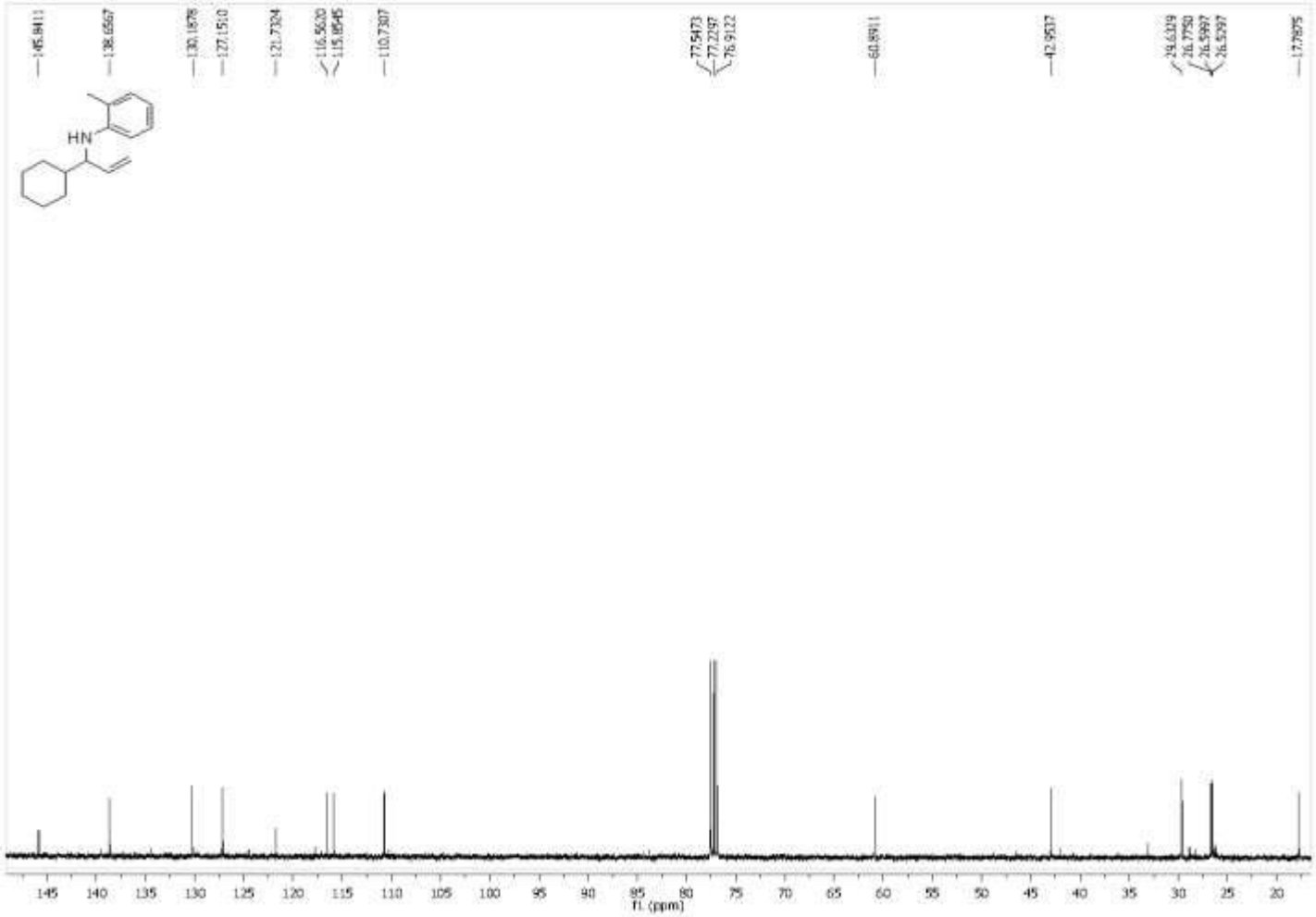

Figure A100 100 MHz 13C NMR ($CDCl_3$) Spectra of Compound **231d**

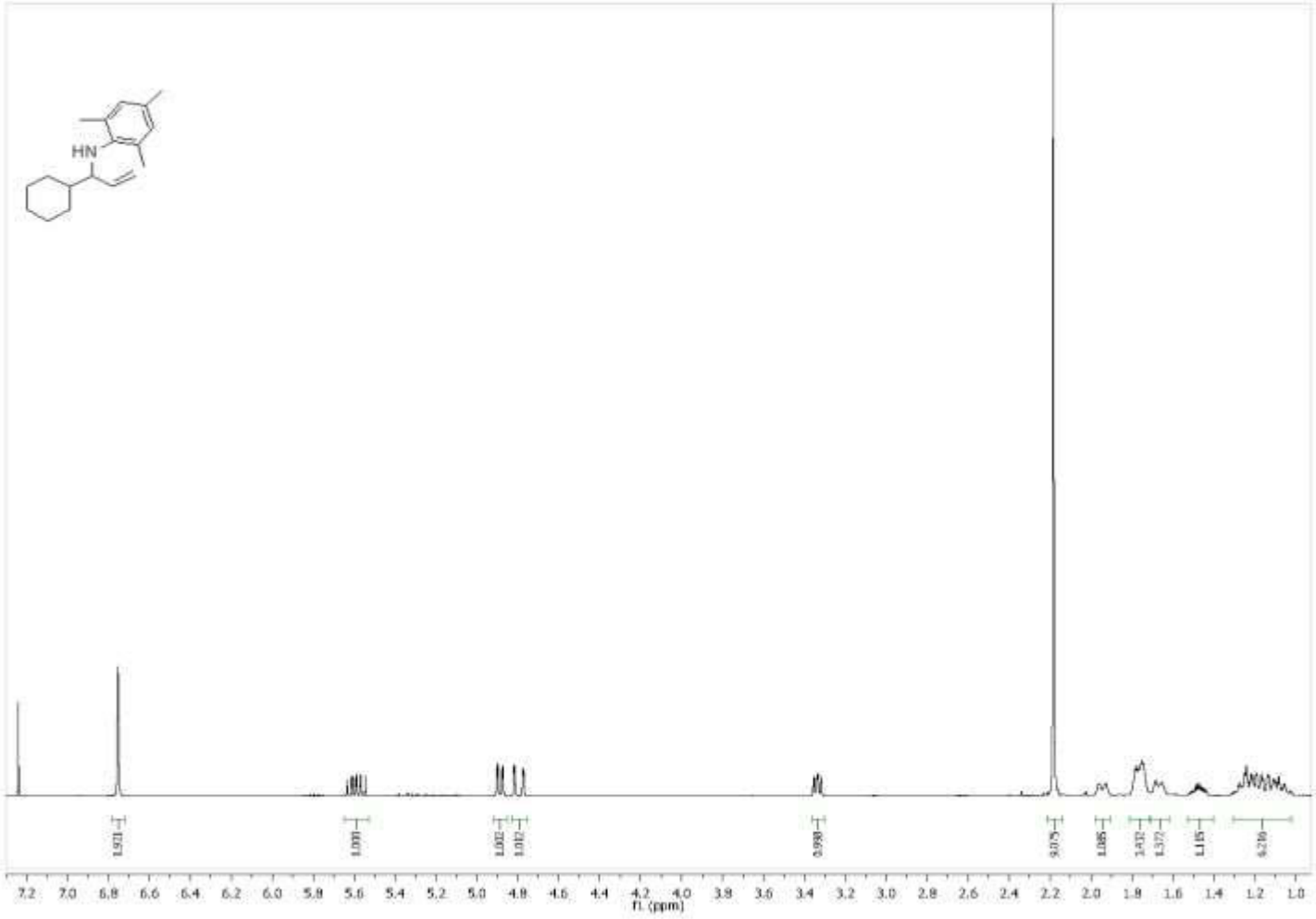

Figure A101 400 MHz 1H NMR ($CDCl_3$) Spectra of Compound **231e**

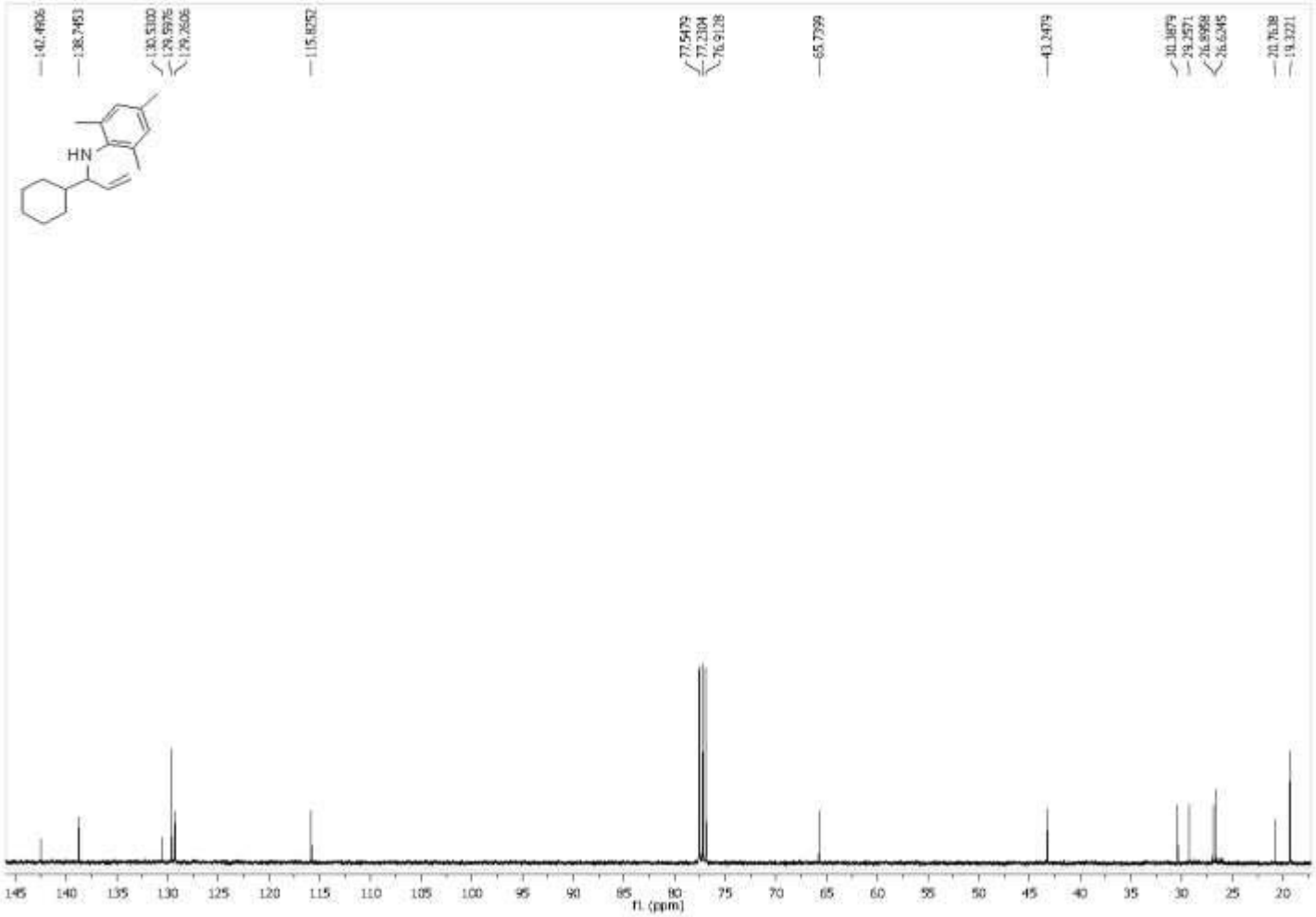

Figure A102 100 MHz 13C NMR ($CDCl_3$) Spectra of Compound **231e**

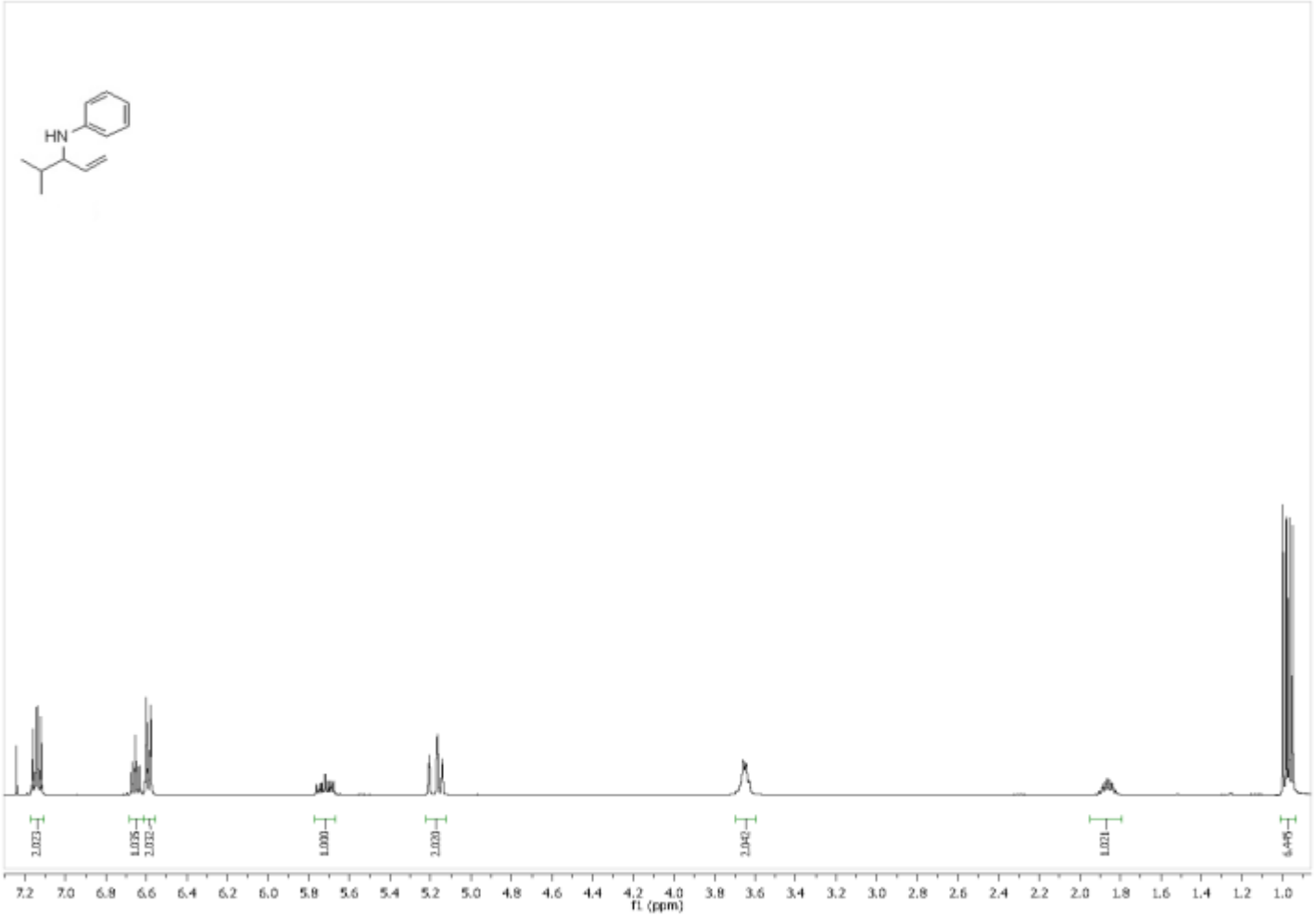

Figure A103 400 MHz 1H NMR ($CDCl_3$) Spectra of Compound **232a**

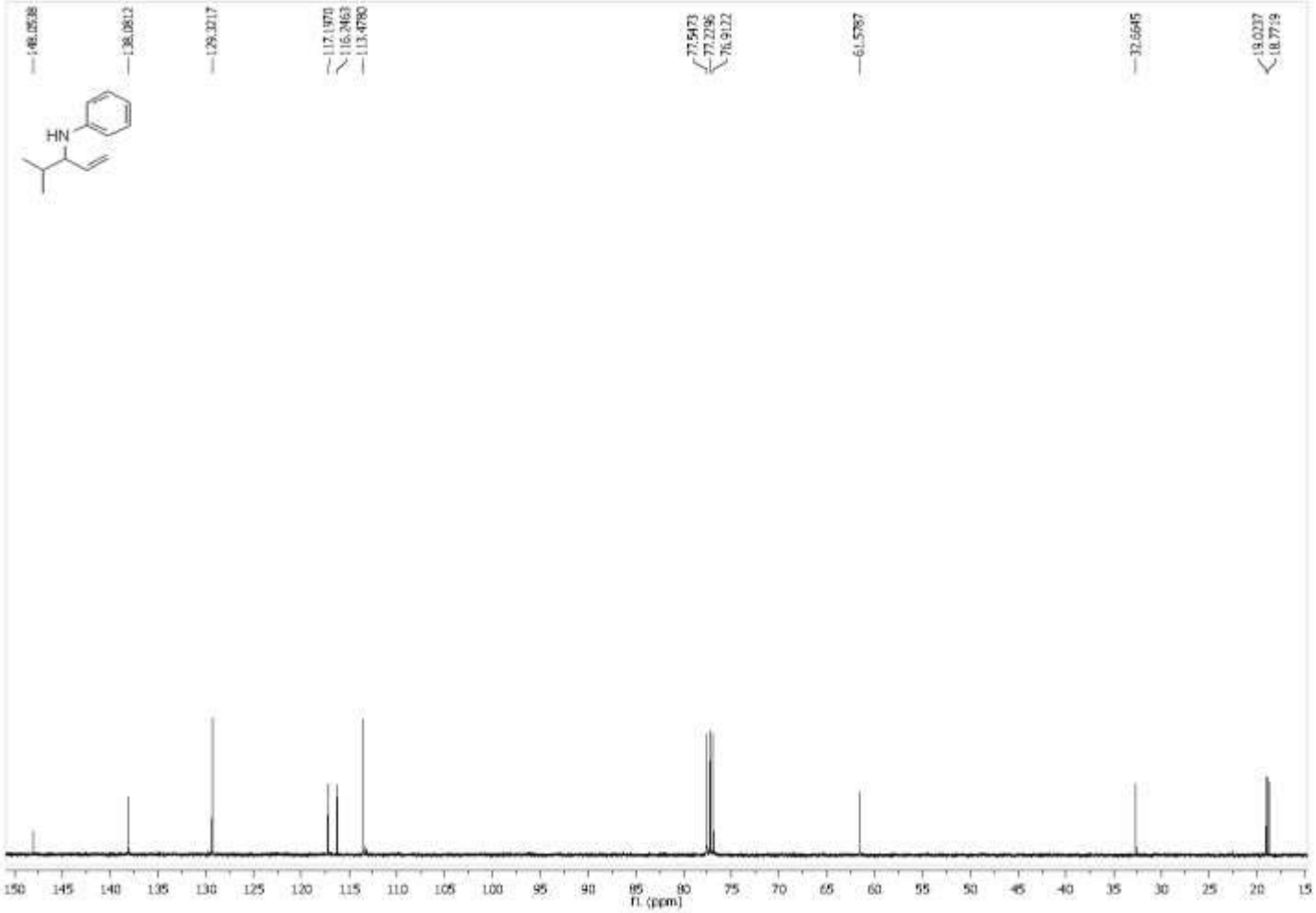

Figure A104 100 MHz 13C NMR ($CDCl_3$) Spectra of Compound **232a**

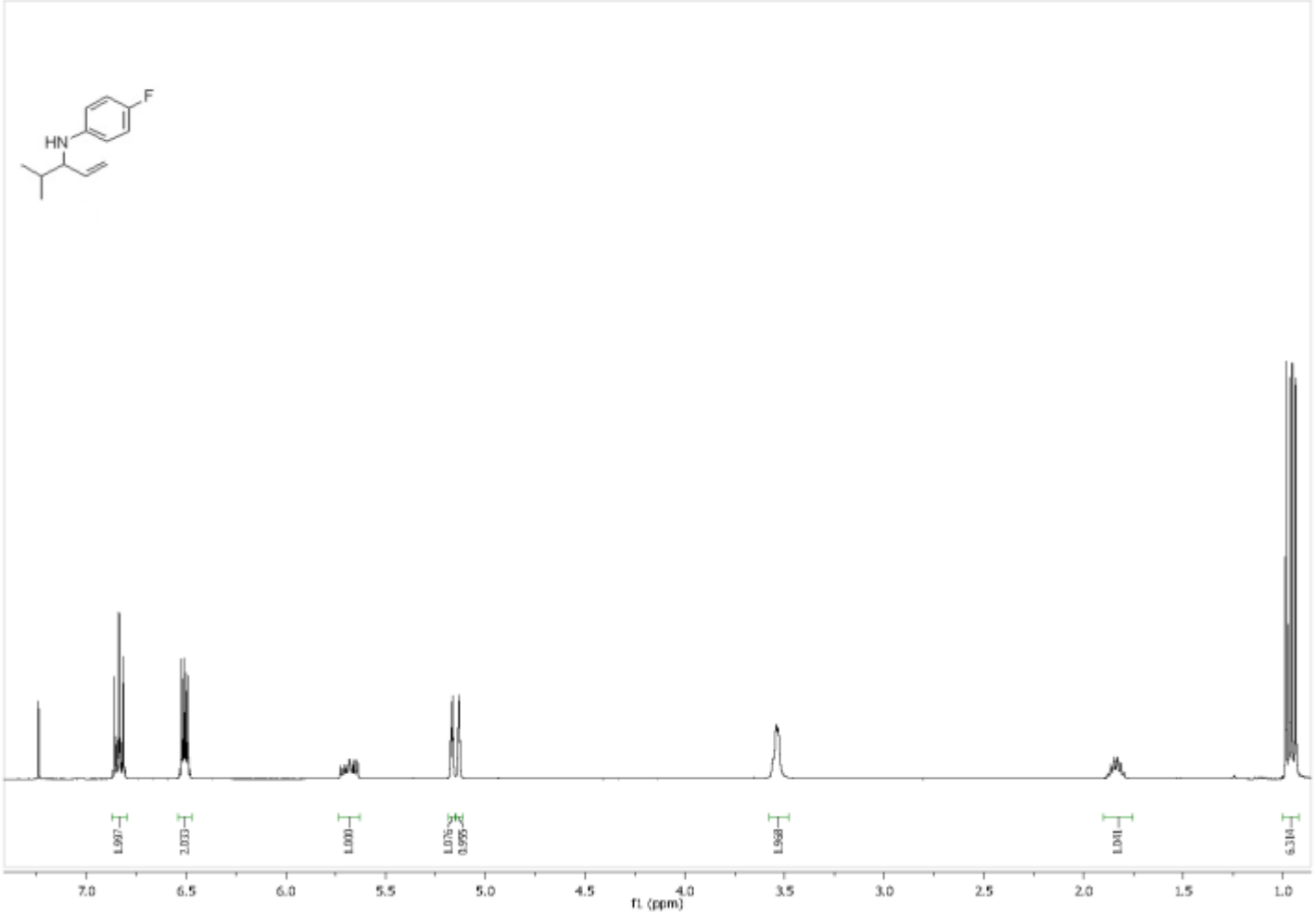

Figure A105 400 MHz 1H NMR ($CDCl_3$) Spectra of Compound **232b**

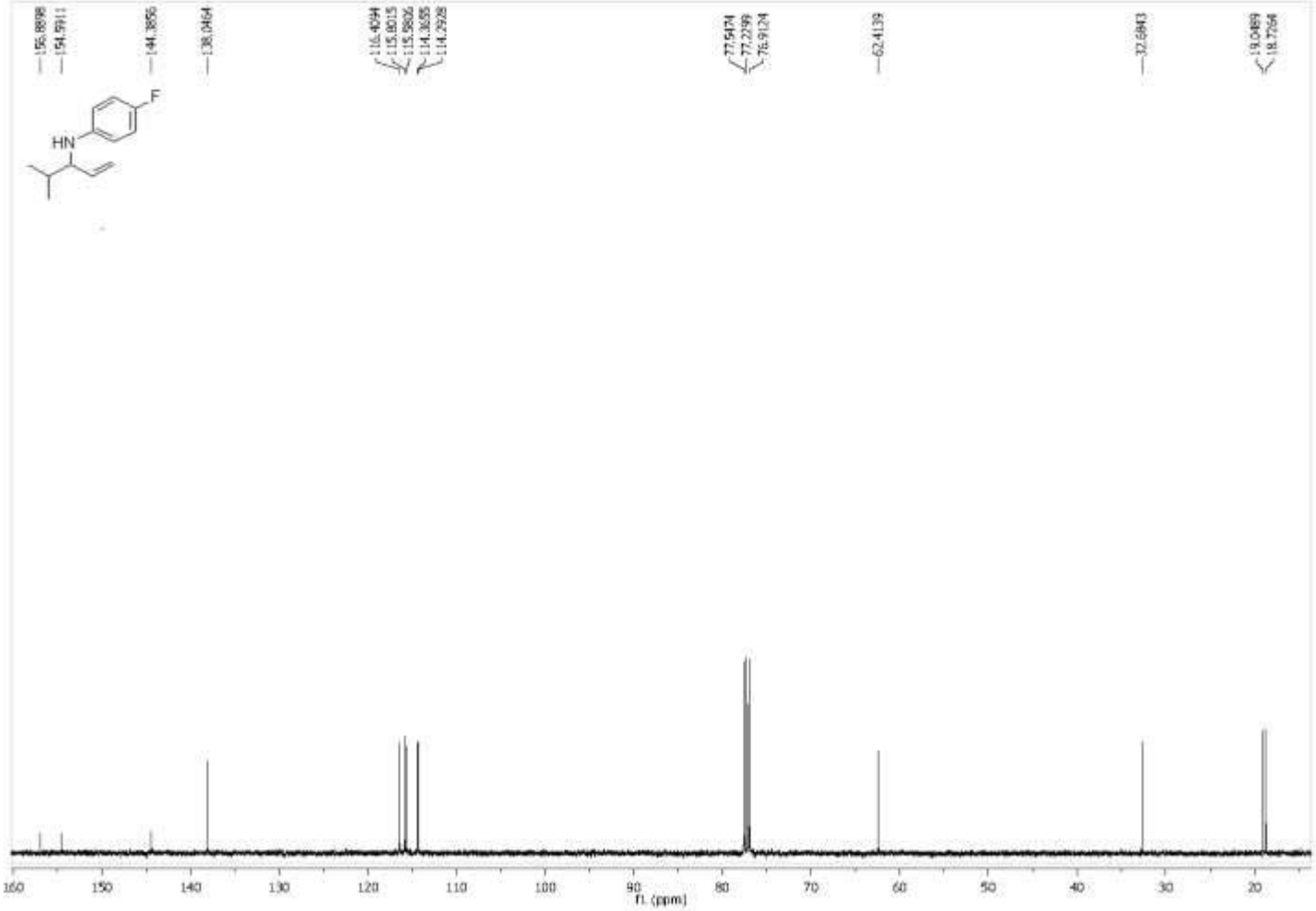

Figure A106 100 MHz 13C NMR ($CDCl_3$) Spectra of Compound **232b**

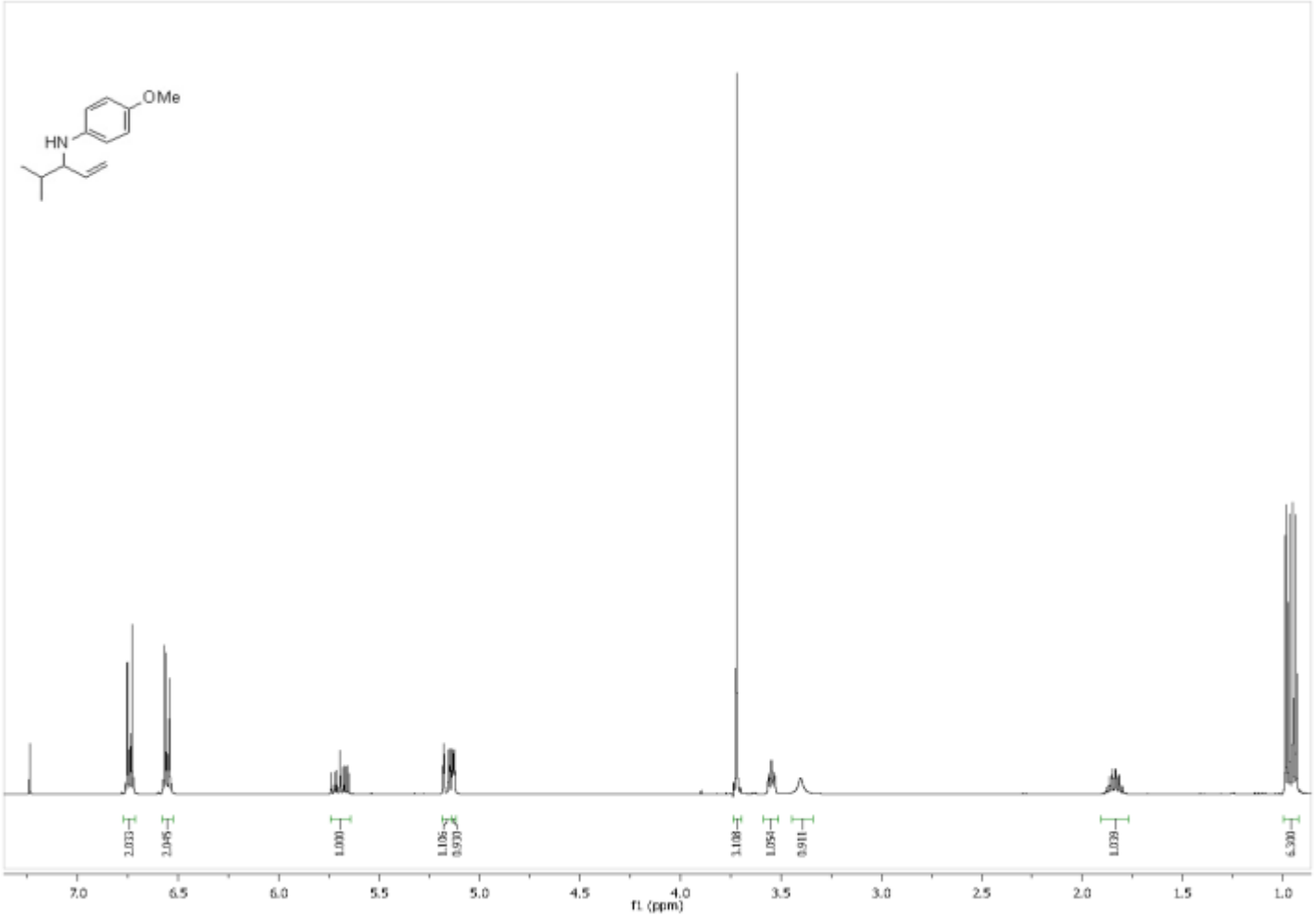

Figure A107 400 MHz 1H NMR ($CDCl_3$) Spectra of Compound **232c**

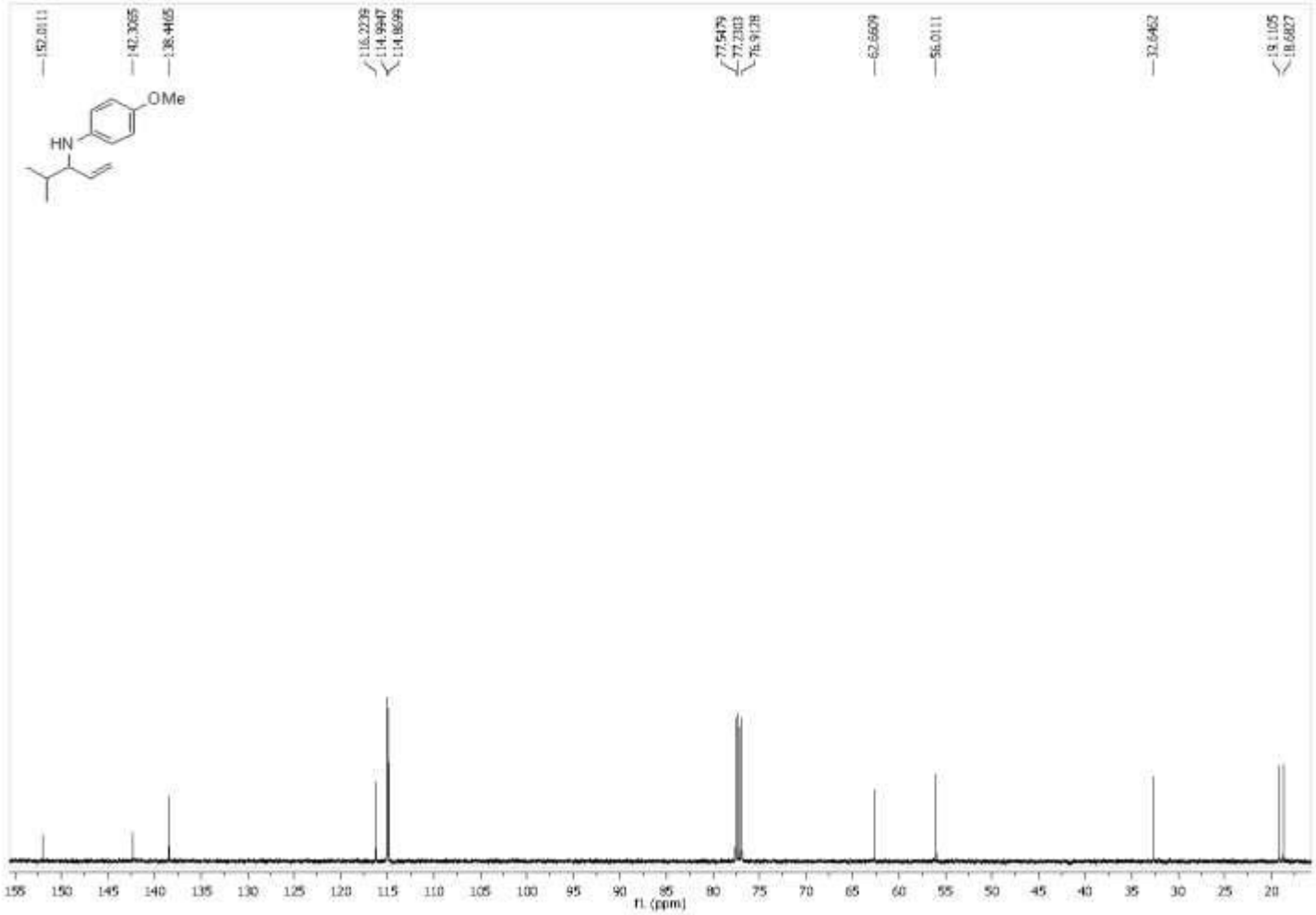

Figure A108 100 MHz 13C NMR ($CDCl_3$) Spectra of Compound **232c**

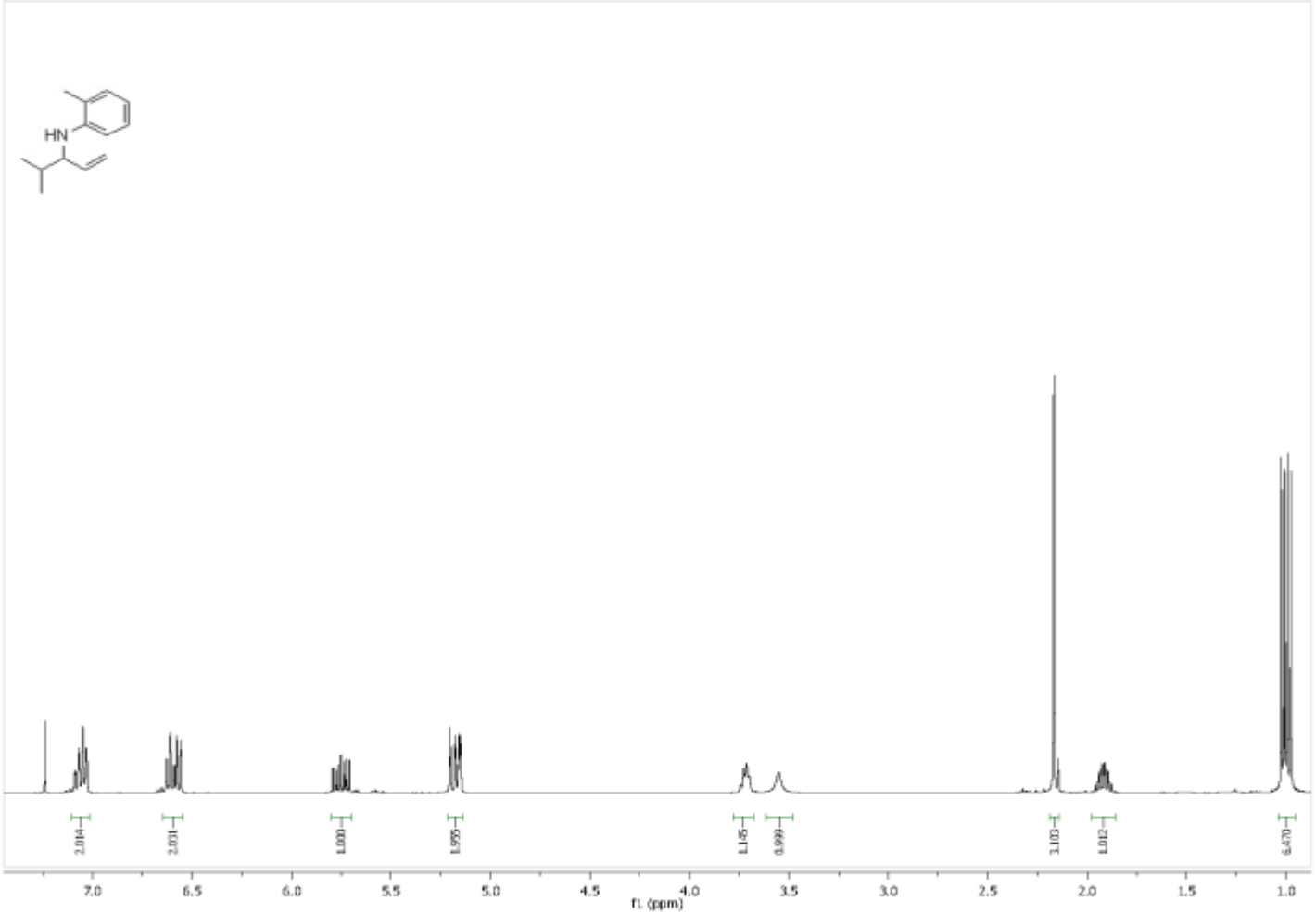

Figure A109 400 MHz 1H NMR ($CDCl_3$) Spectra of Compound **232d**

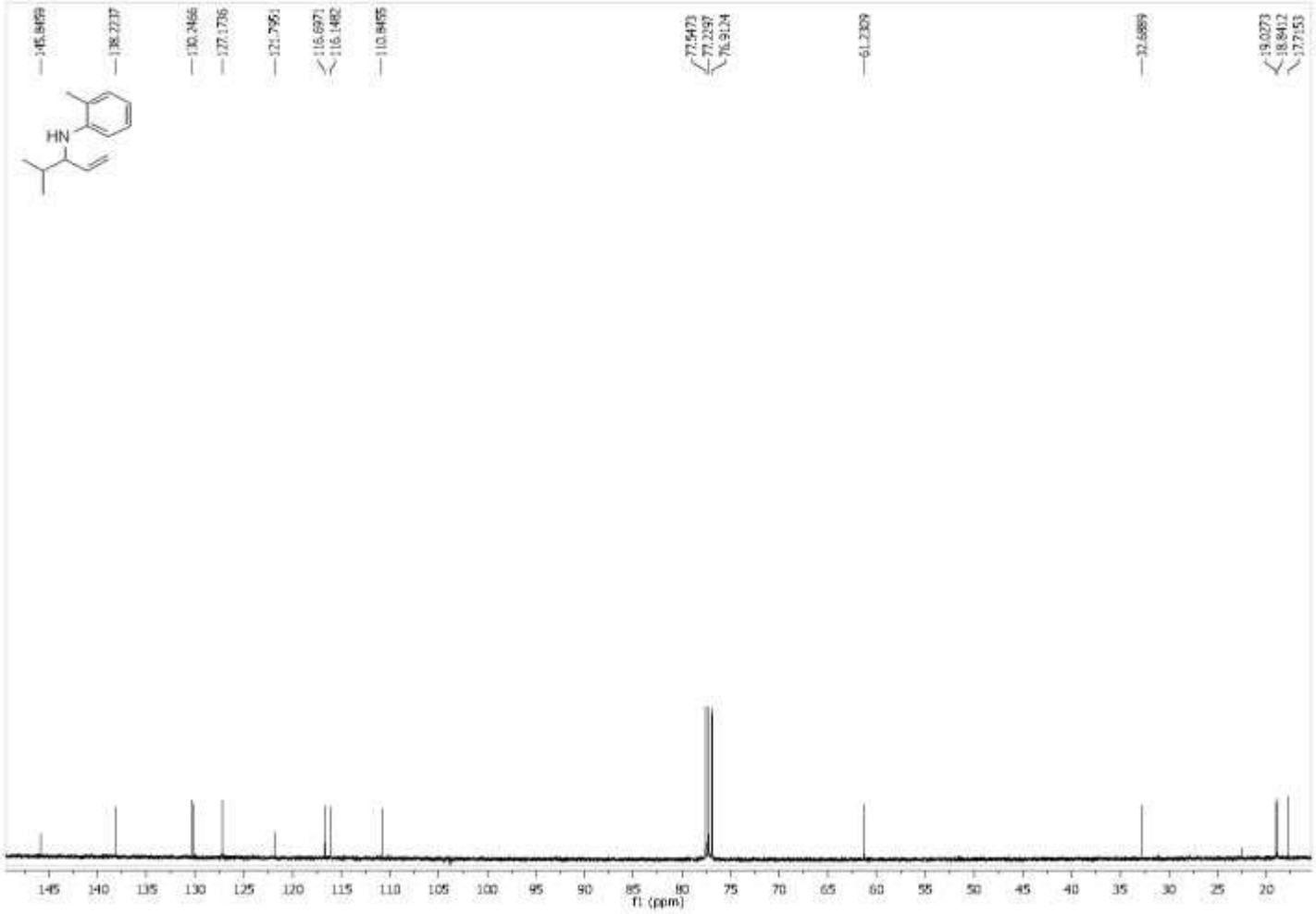

Figure A110 100 MHz 13C NMR ($CDCl_3$) Spectra of Compound **232d**

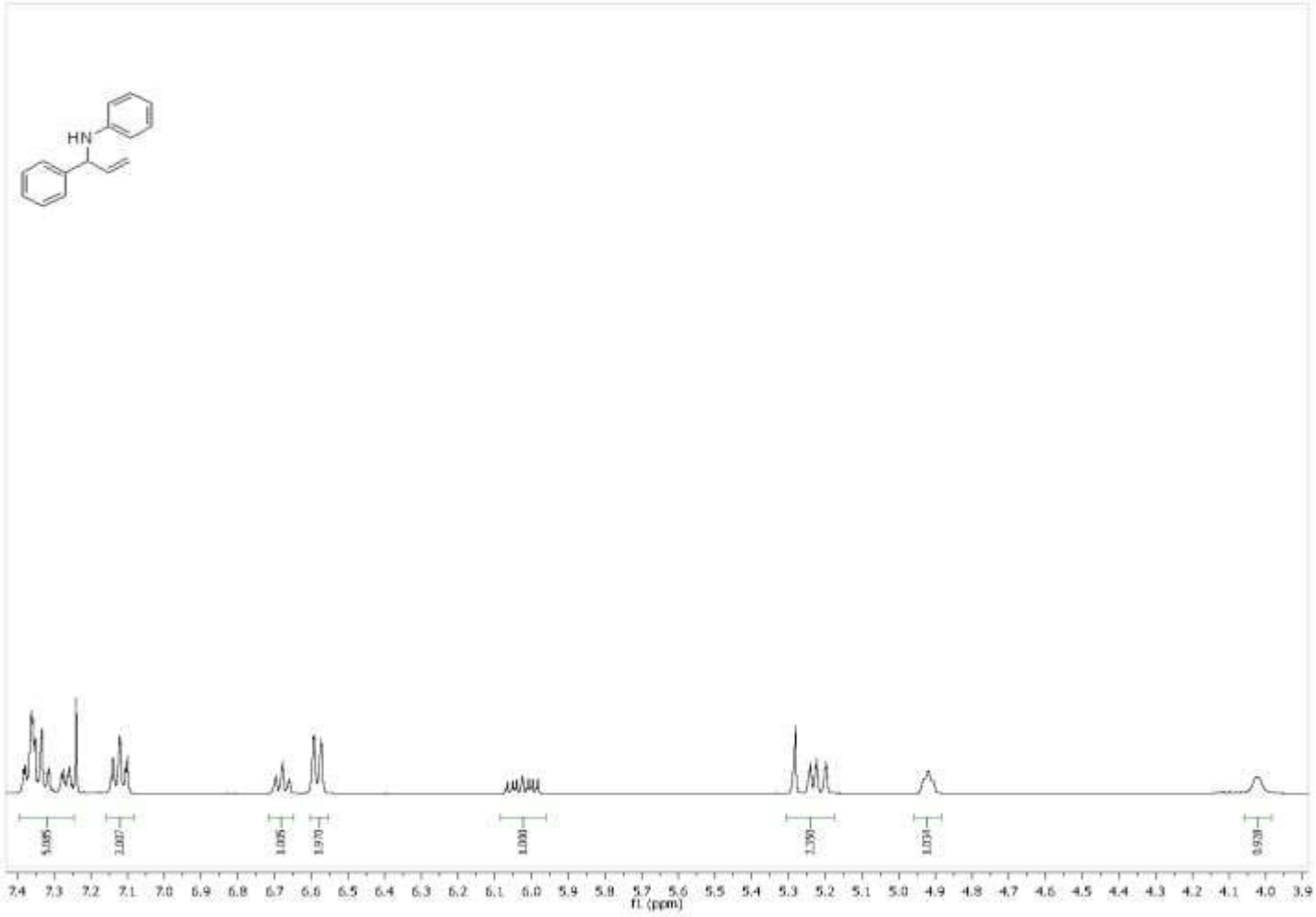

Figure A111 400 MHz 1H NMR ($CDCl_3$) Spectra of Compound **233a**

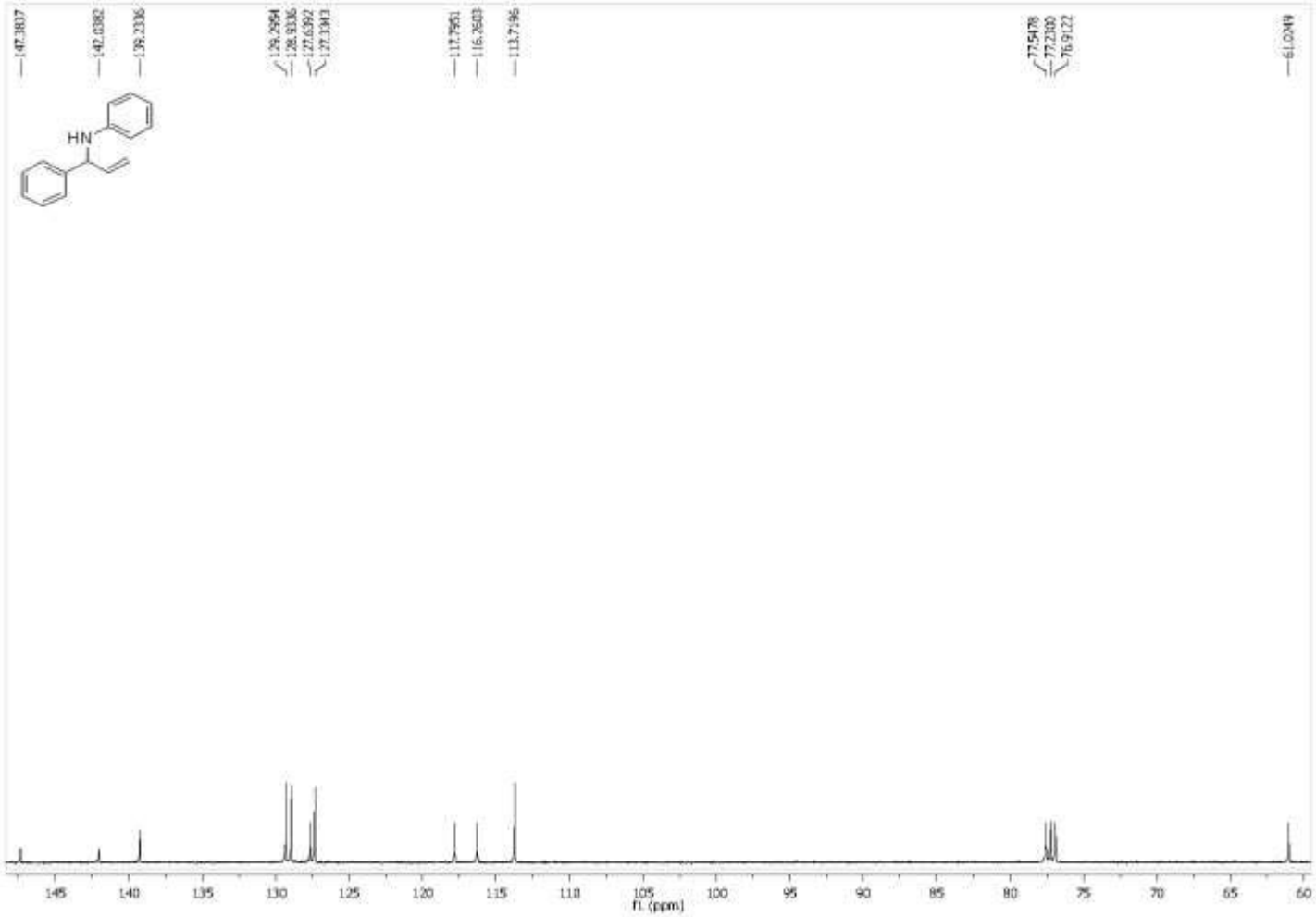

Figure A112 100 MHz 13C NMR ($CDCl_3$) Spectra of Compound **233a**

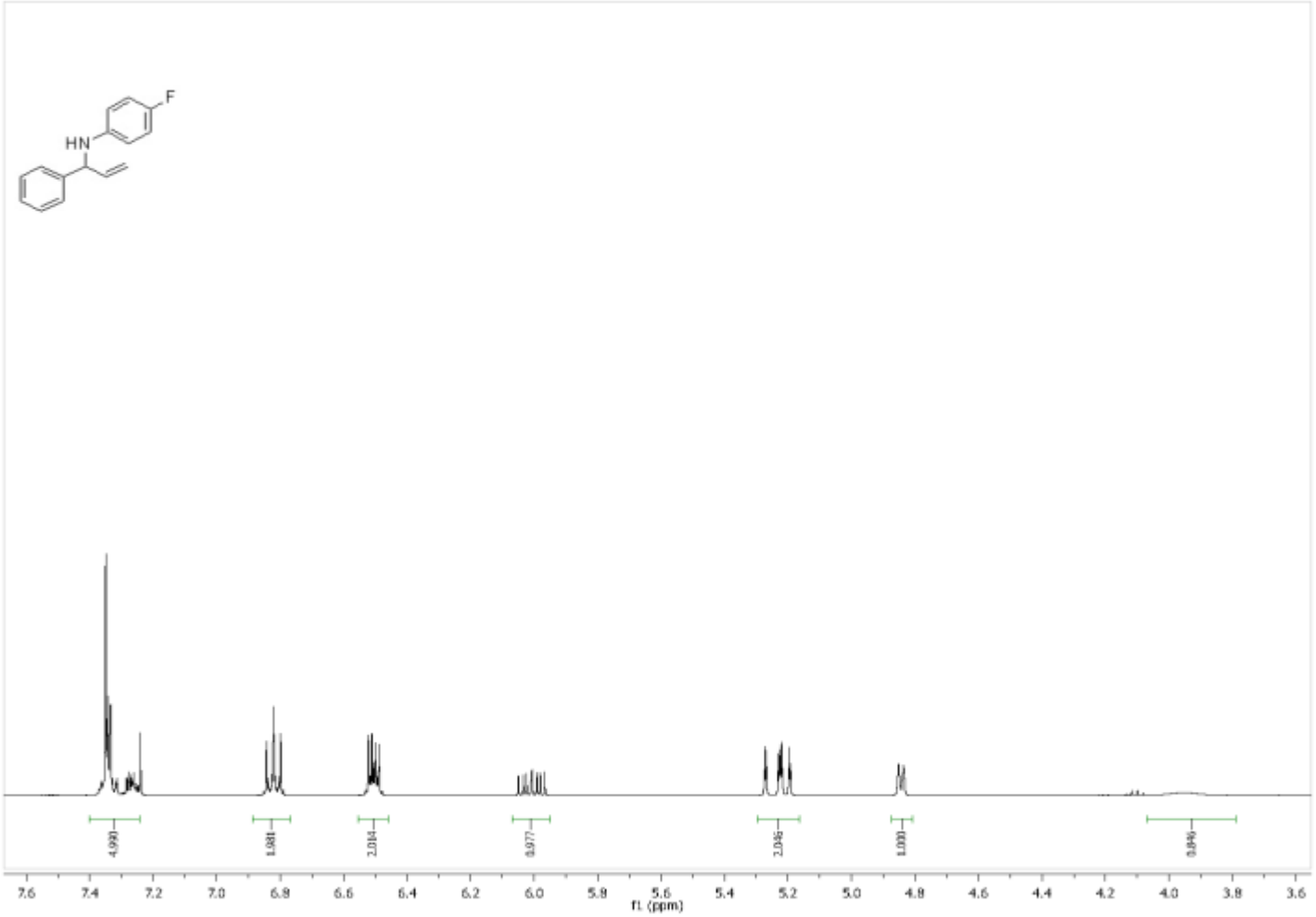

Figure A113 400 MHz 1H NMR ($CDCl_3$) Spectra of Compound **233b**

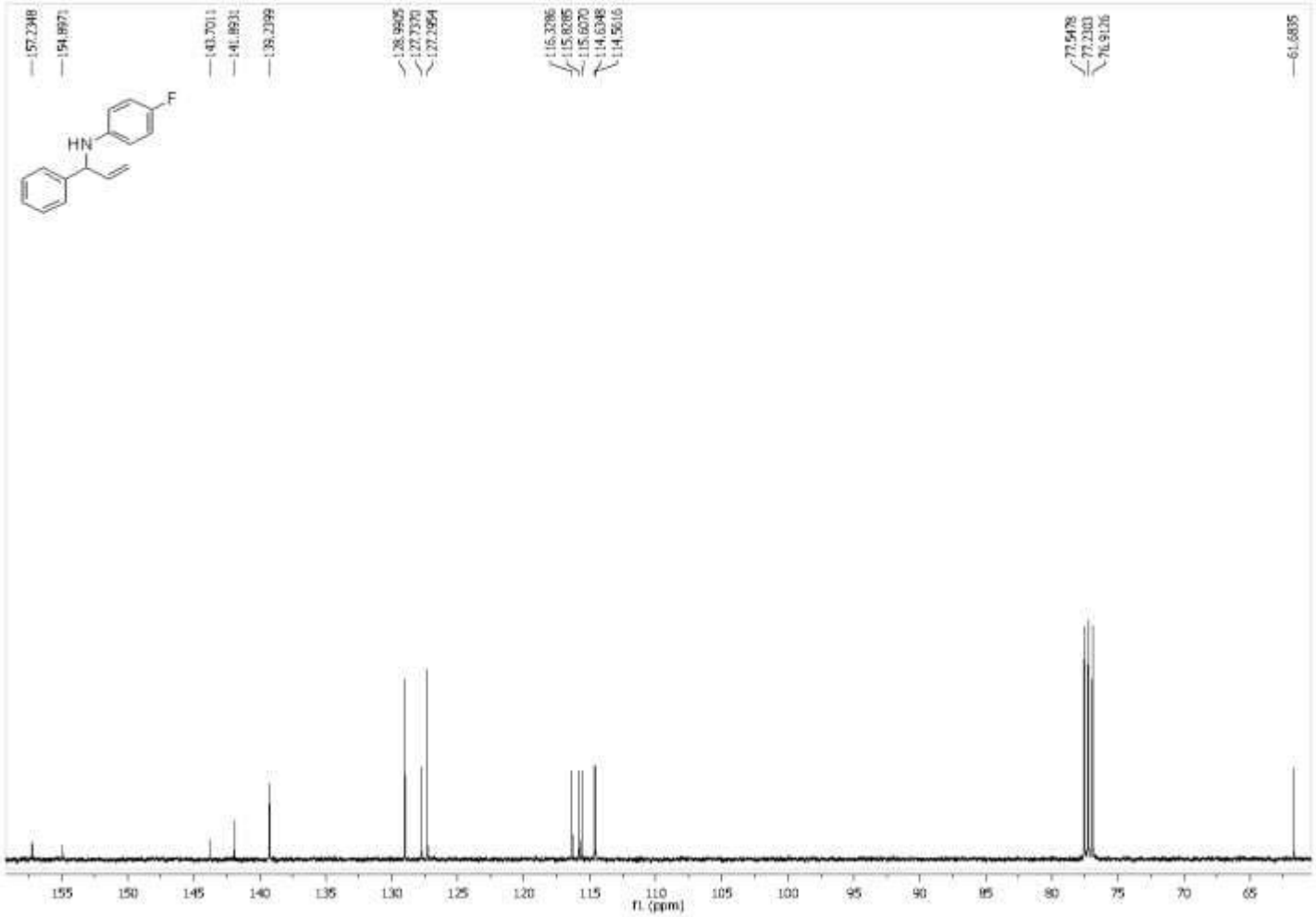

Figure A114 100 MHz 13C NMR ($CDCl_3$) Spectra of Compound **233b**

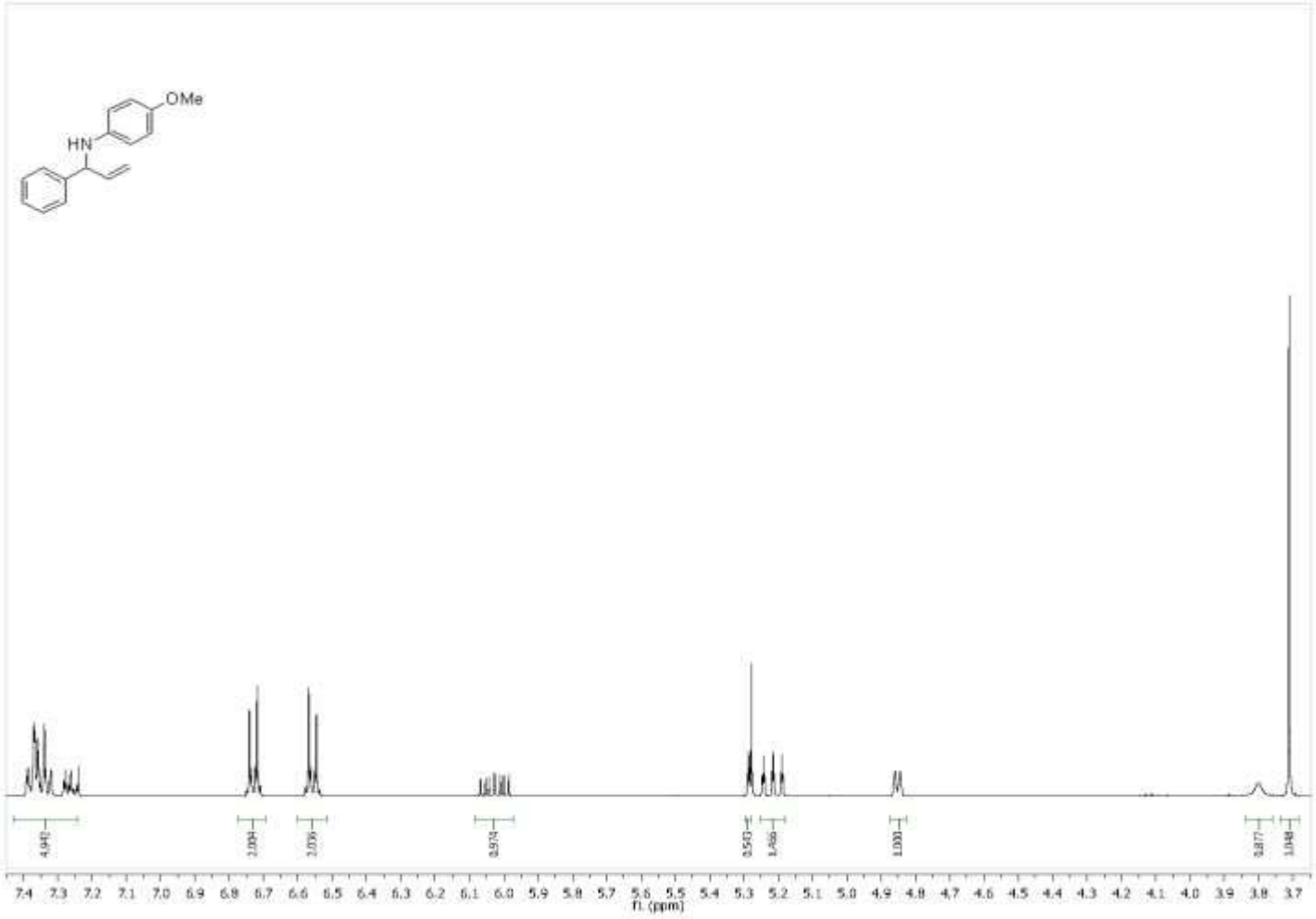

Figure A115 400 MHz 1H NMR ($CDCl_3$) Spectra of Compound **233c**

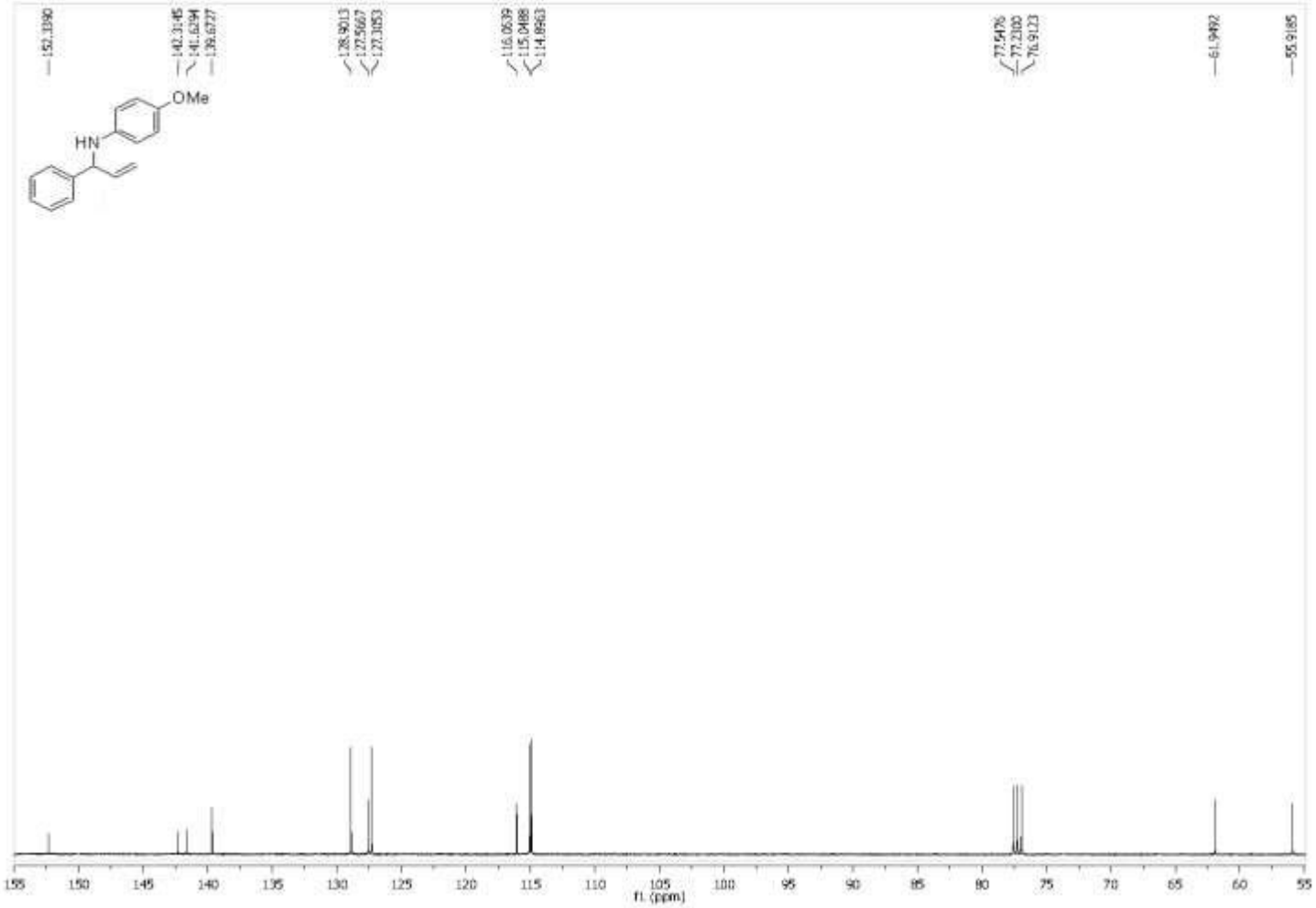

Figure A116 100 MHz 13C NMR ($CDCl_3$) Spectra of Compound **233c**

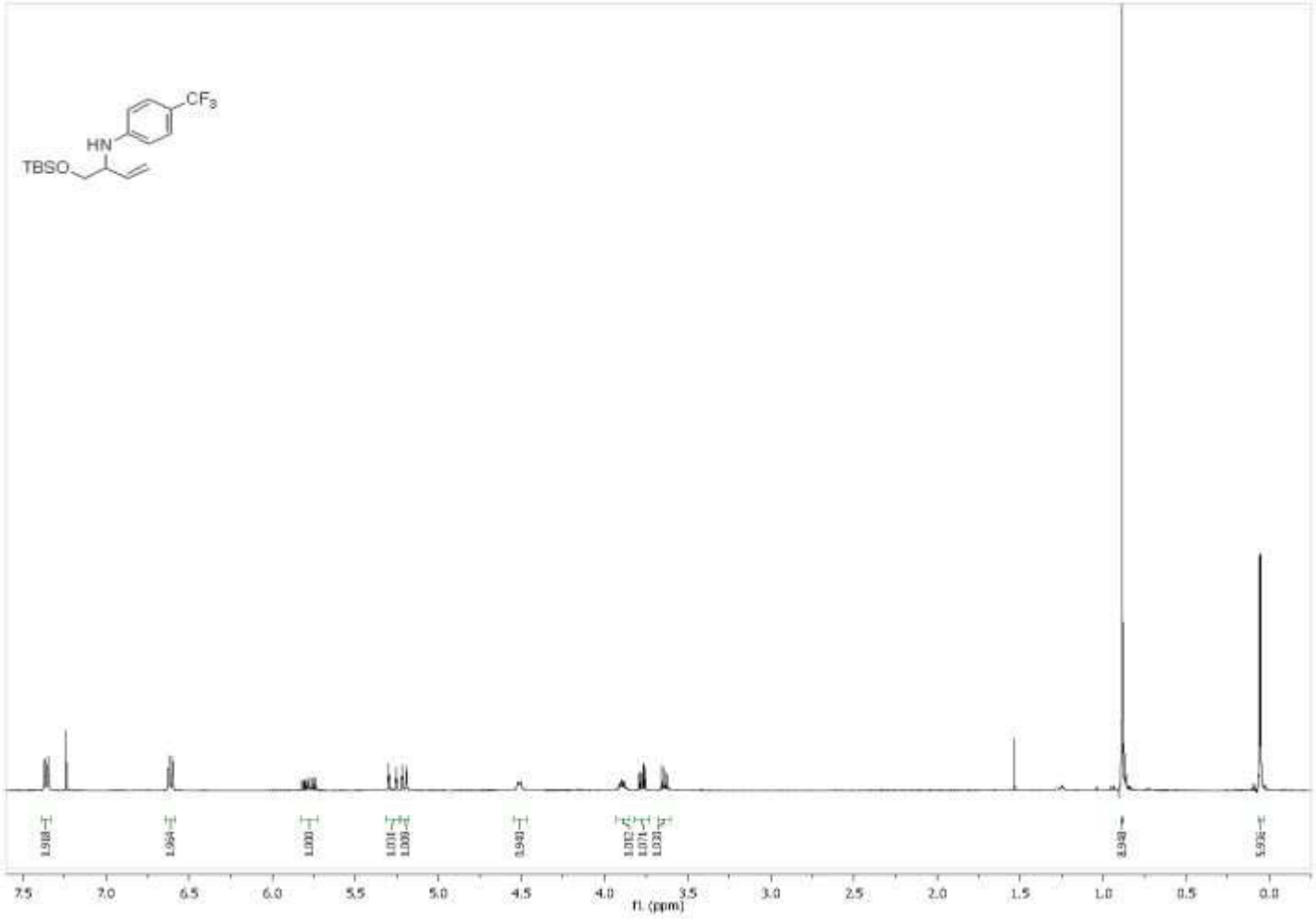

Figure A117 400 MHz 1H NMR ($CDCl_3$) Spectra of Compound **242**

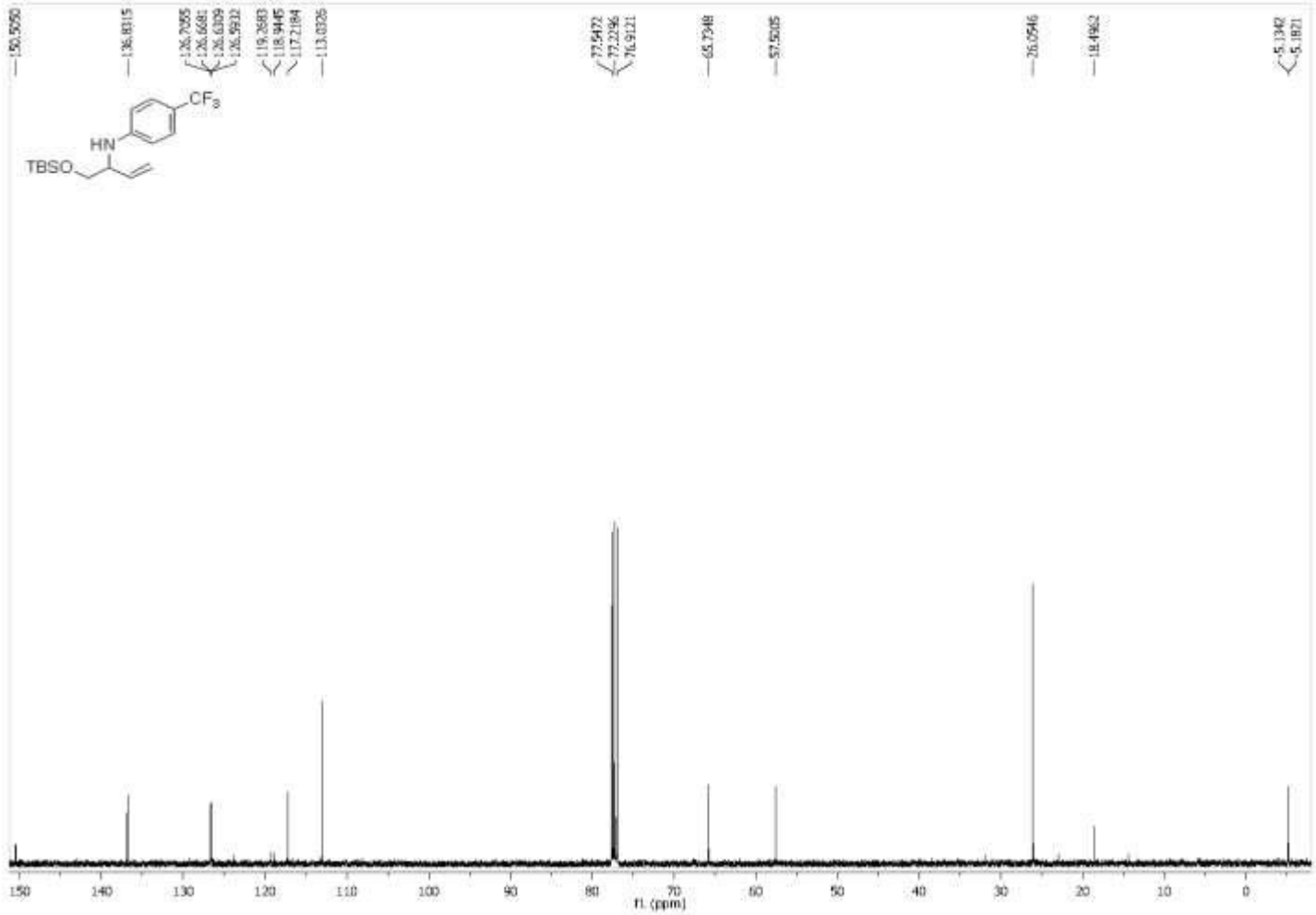

Figure A118 100 MHz 13C NMR ($CDCl_3$) Spectra of Compound **242**

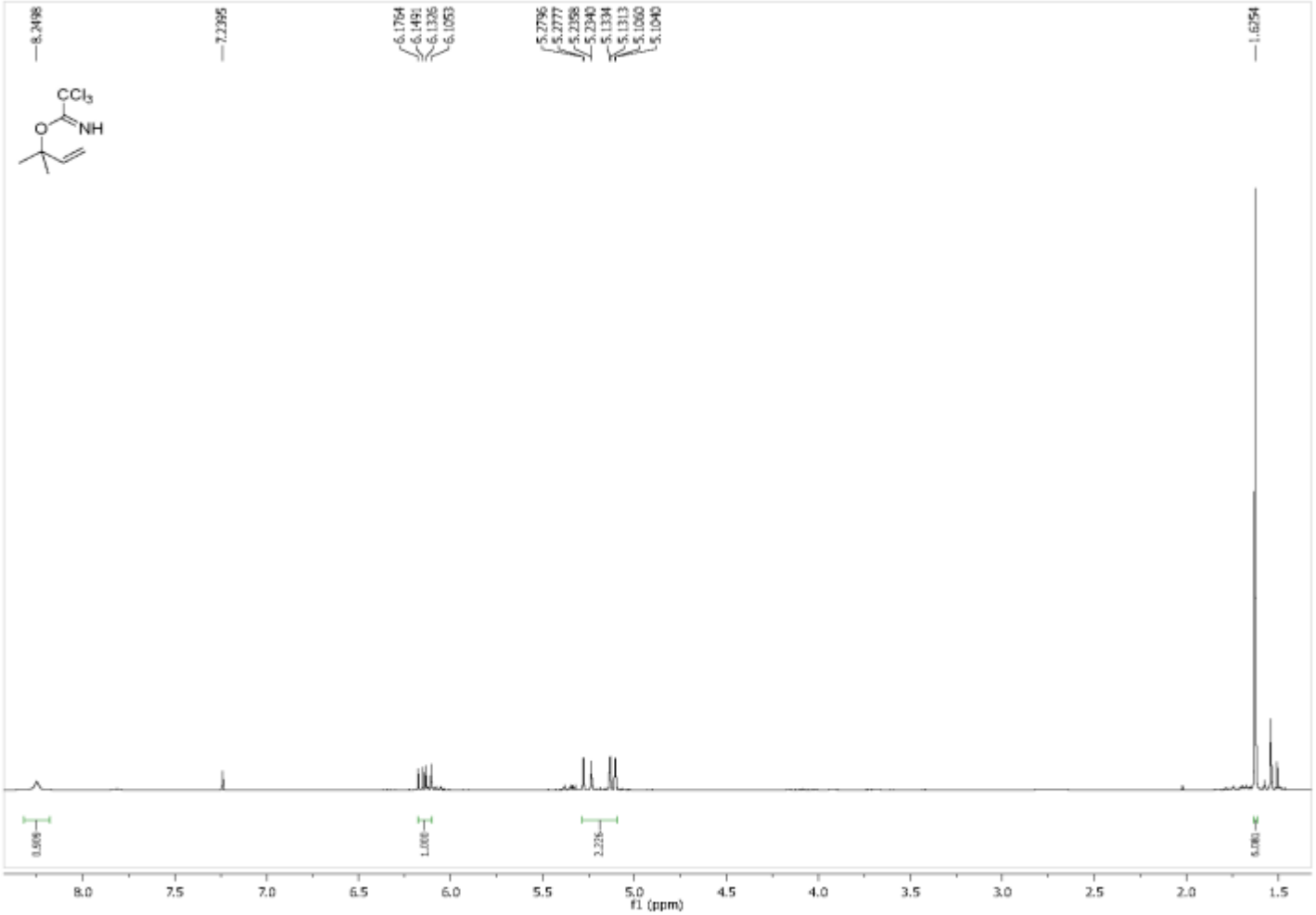

Figure A119 400 MHz 1H NMR ($CDCl_3$) Spectra of Compound **253**

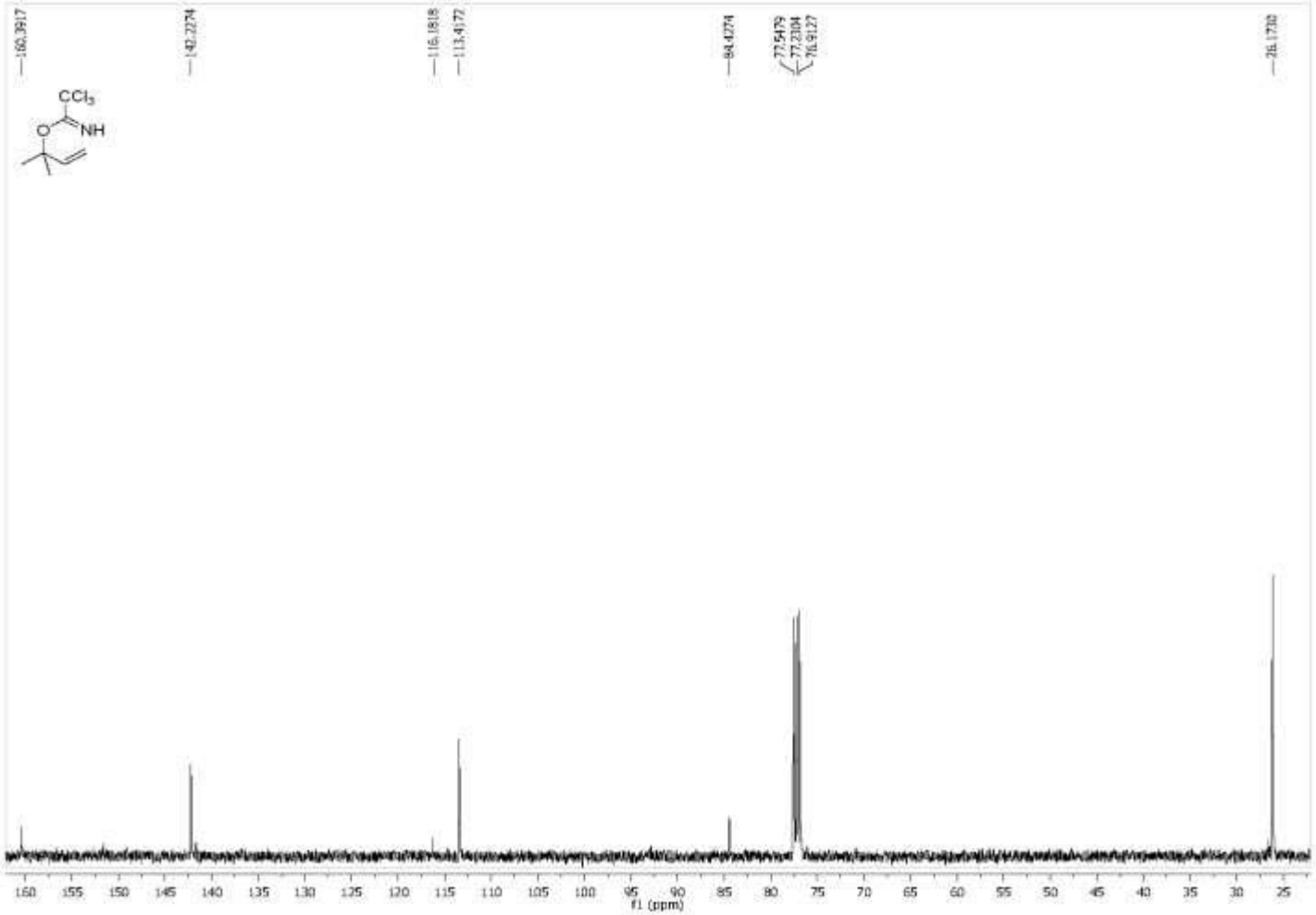

Figure A120 100 MHz 13C NMR ($CDCl_3$) Spectra of Compound **253**

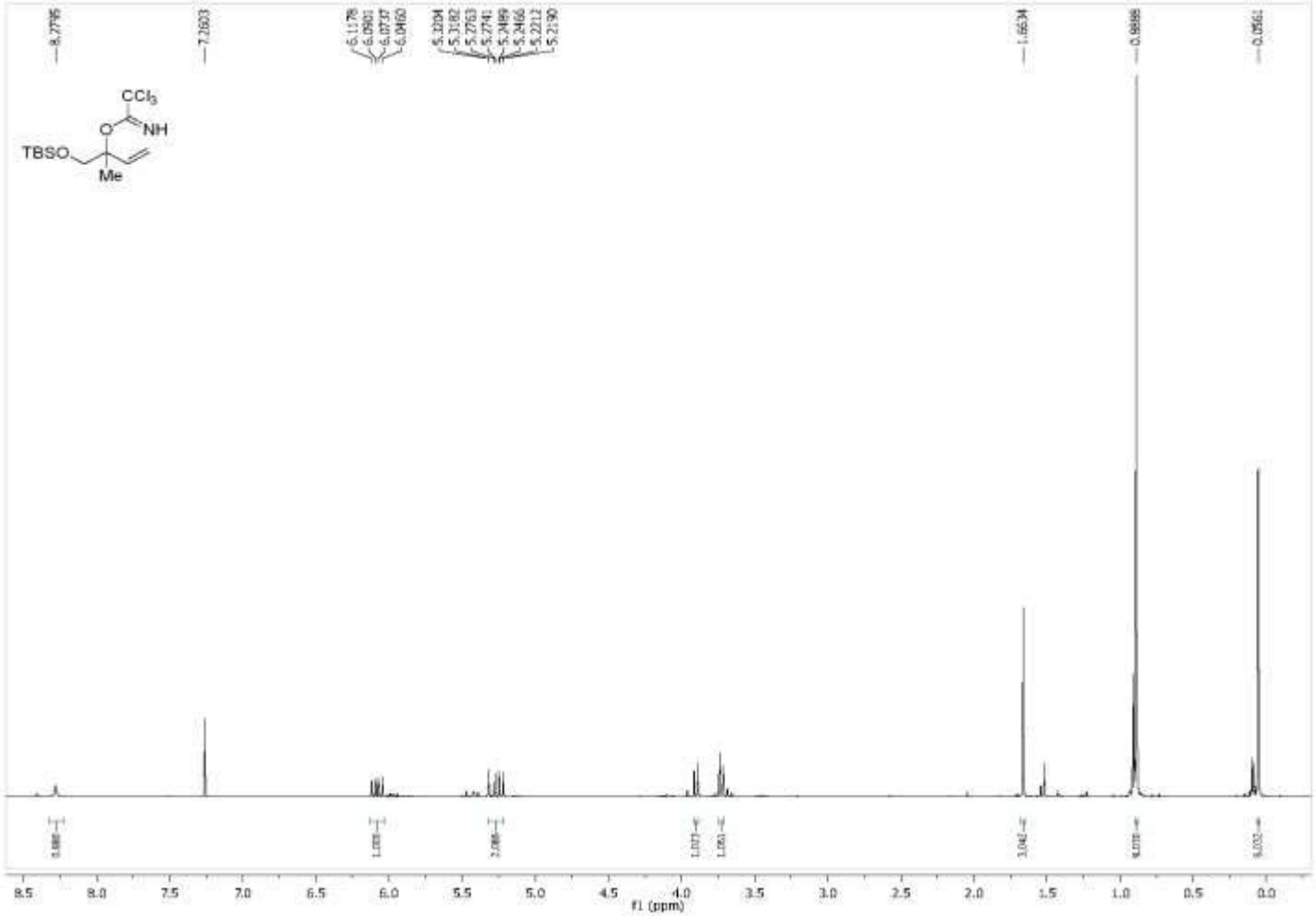

Figure A121 400 MHz 1H NMR ($CDCl_3$) Spectra of Compound **254**

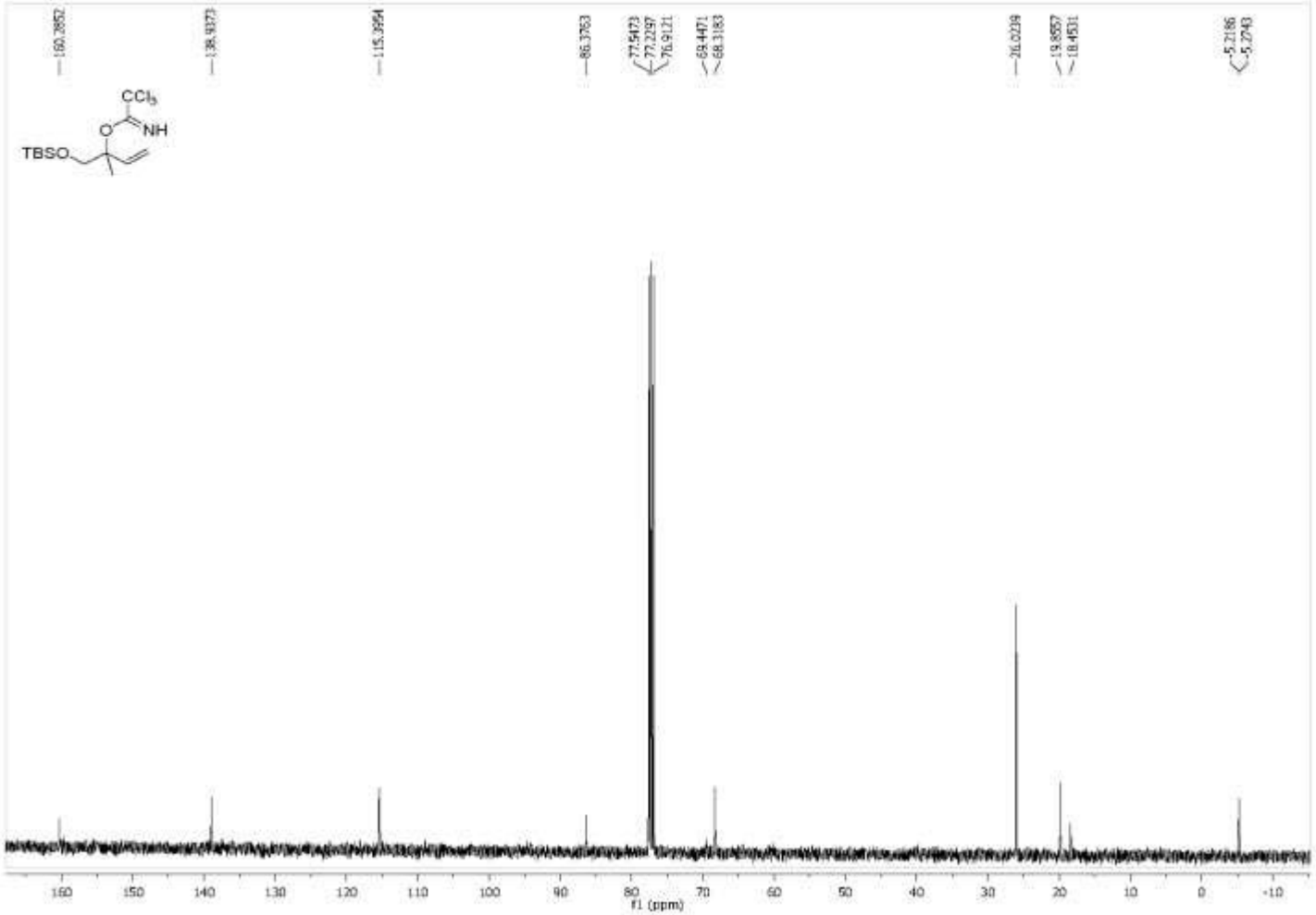

Figure A122 100 MHz 13C NMR ($CDCl_3$) Spectra of Compound **254**

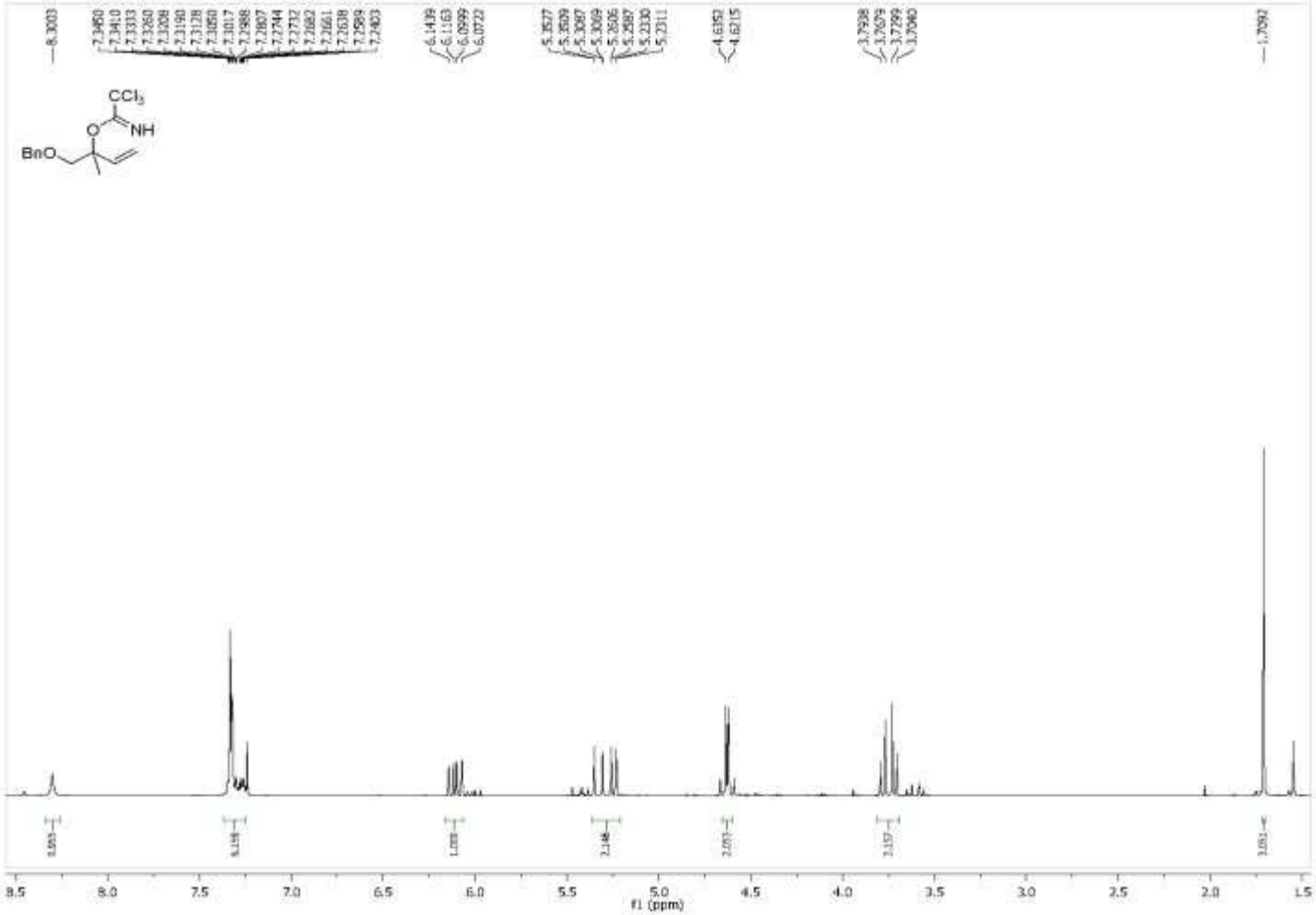

Figure A123 400 MHz 1H NMR ($CDCl_3$) Spectra of Compound **255**

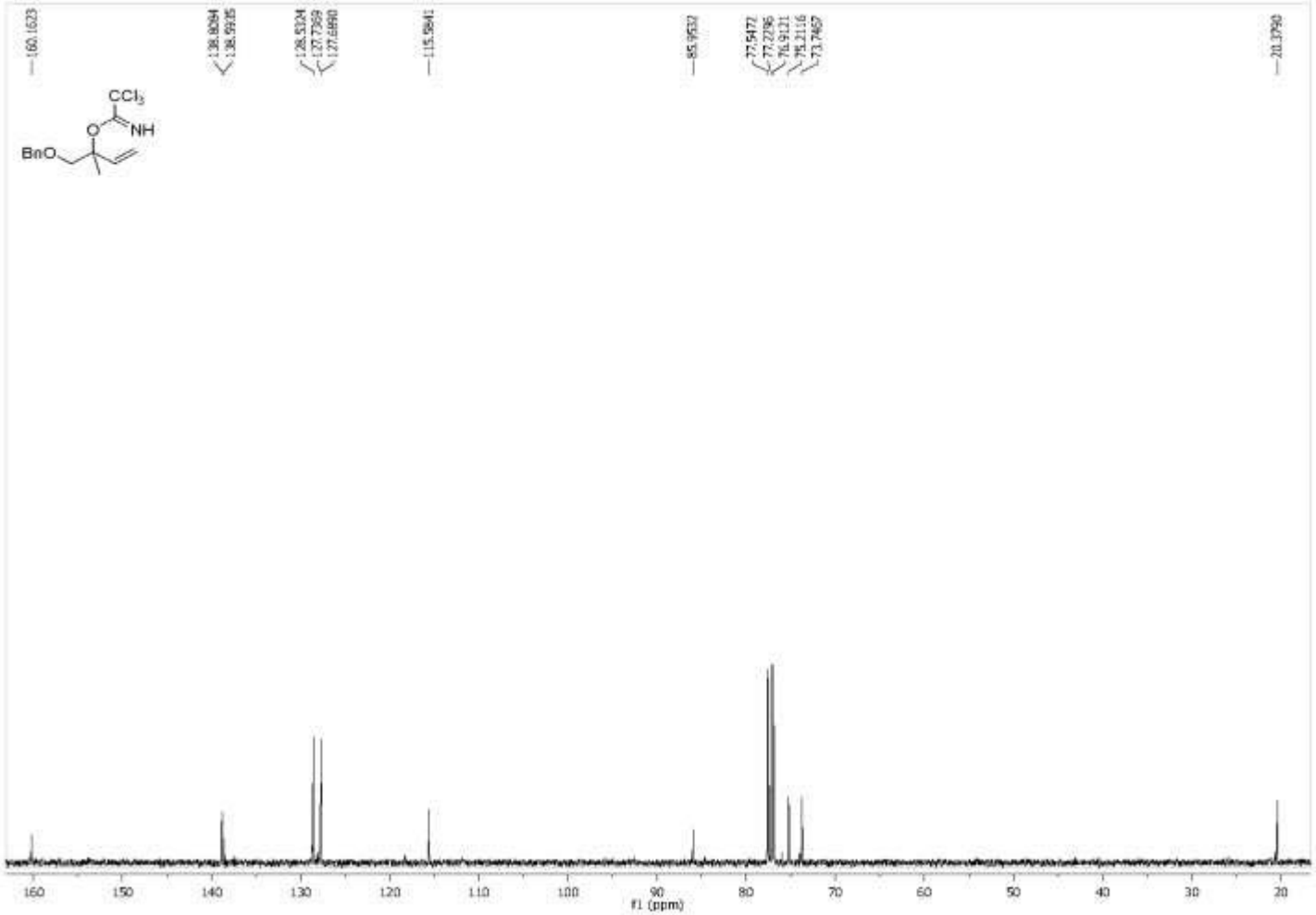

Figure A124 100 MHz 13C NMR ($CDCl_3$) Spectra of Compound **255**

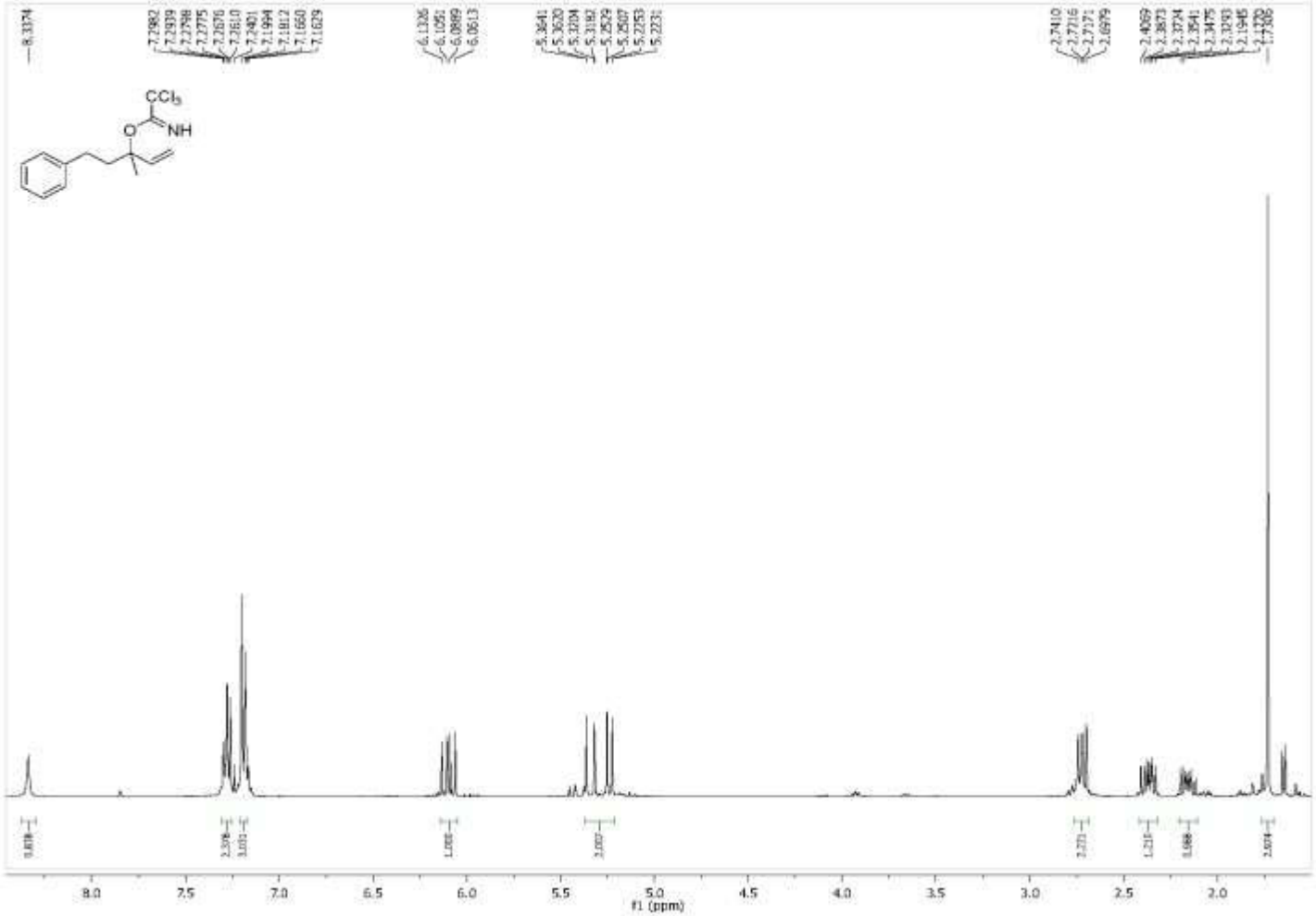

Figure A125 400 MHz 1H NMR ($CDCl_3$) Spectra of Compound **256**

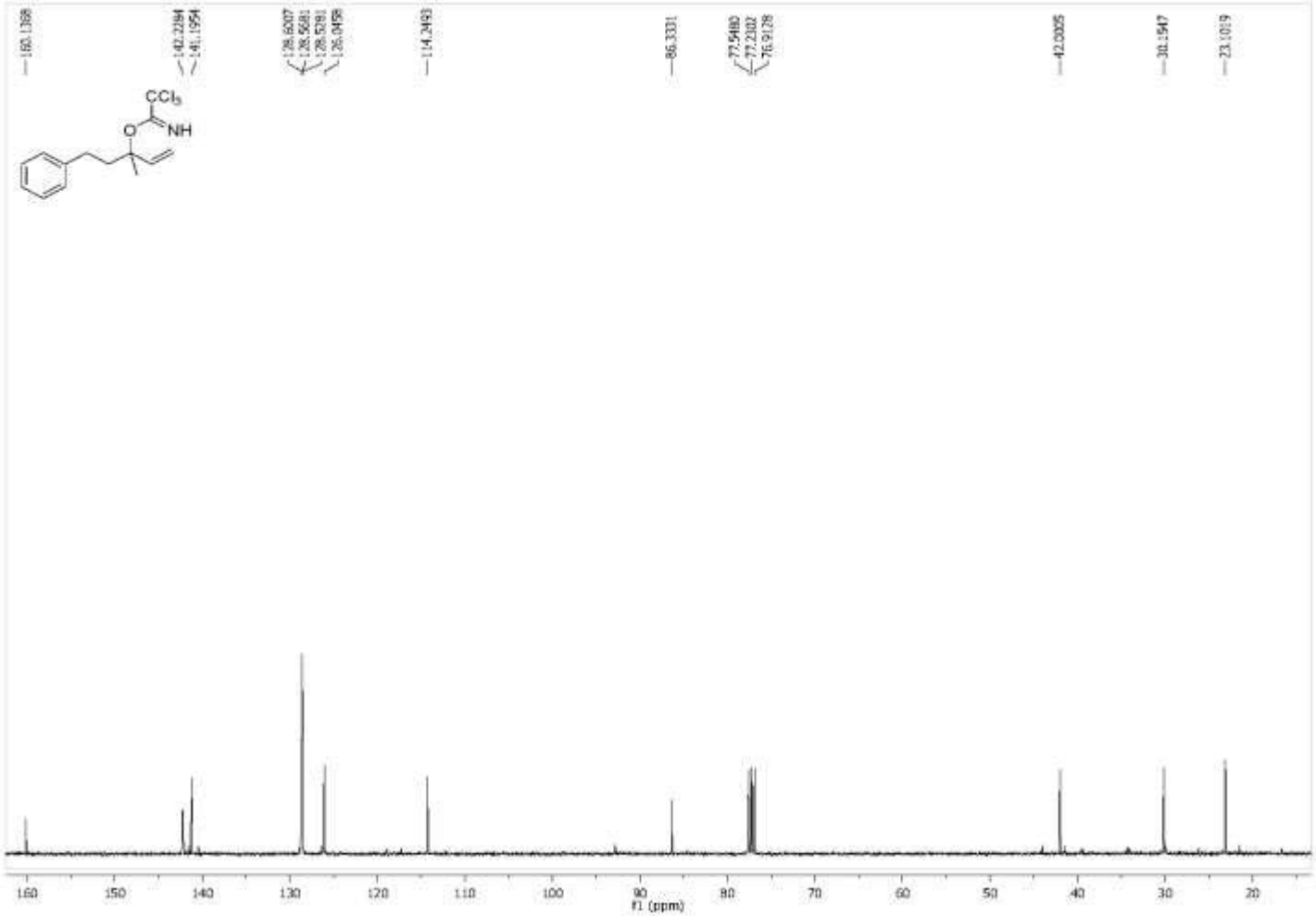

Figure A126 100 MHz 13C NMR ($CDCl_3$) Spectra of Compound **256**

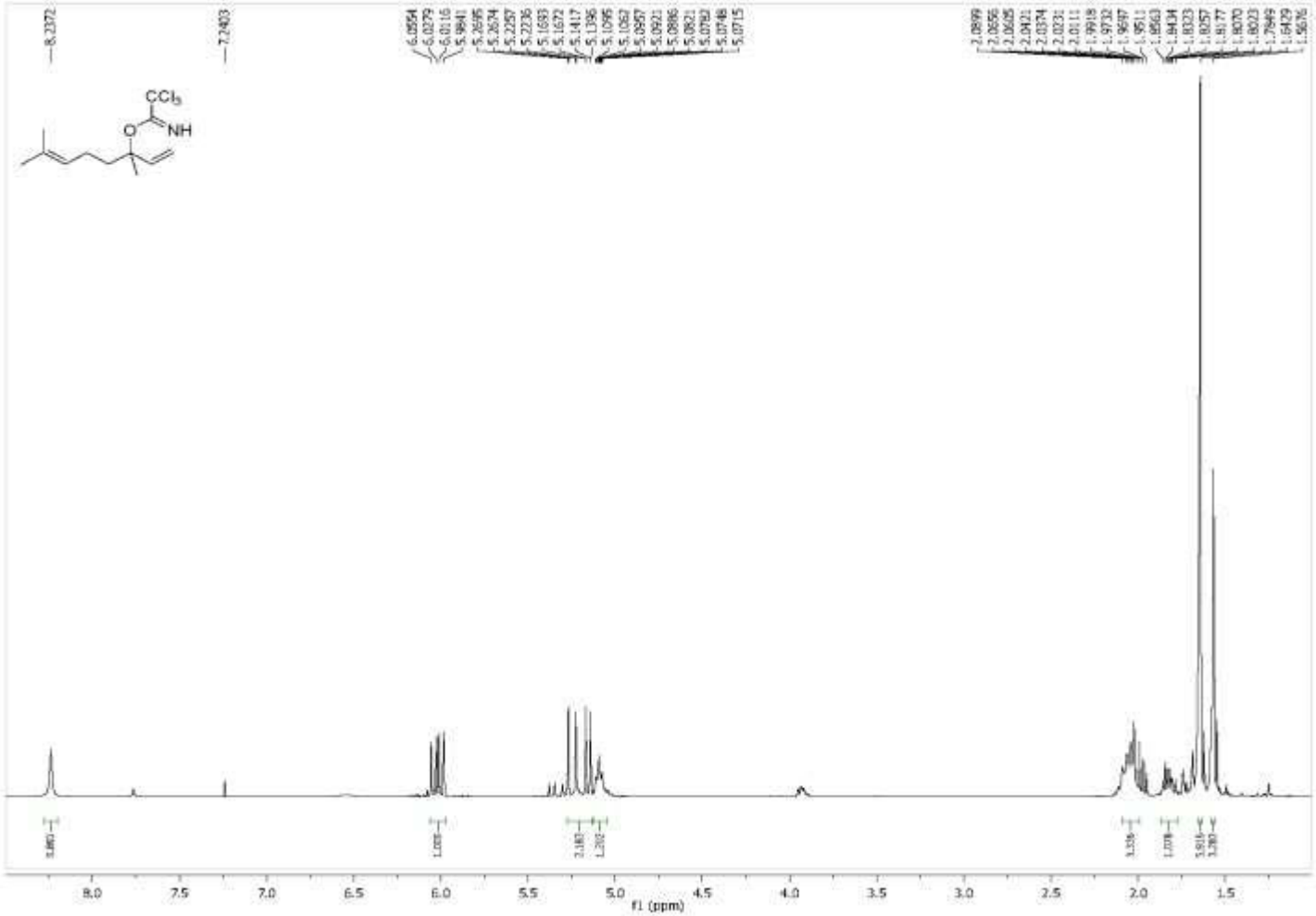

Figure A127 400 MHz 1H NMR ($CDCl_3$) Spectra of Compound **257**

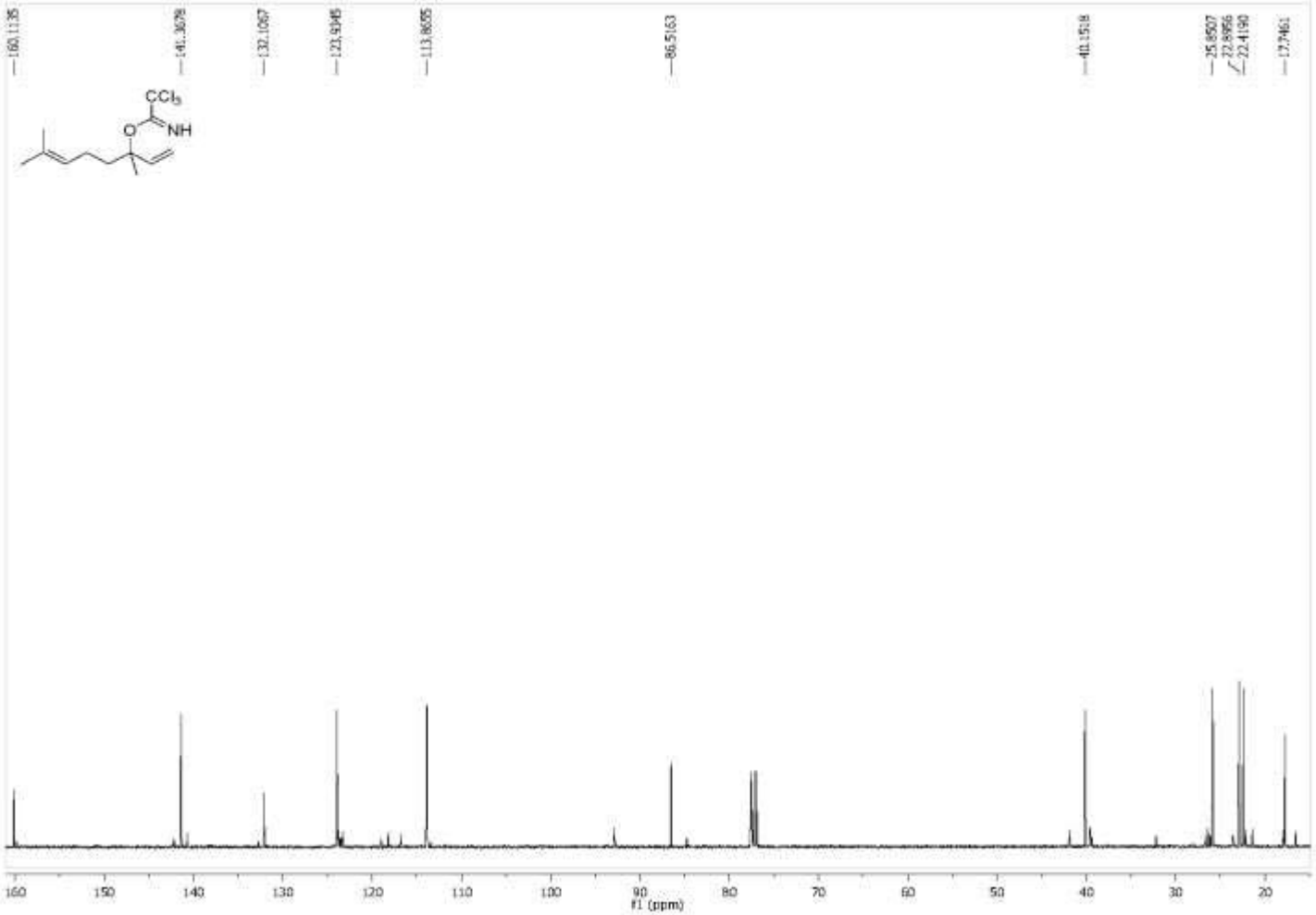

Figure A128 100 MHz 13C NMR ($CDCl_3$) Spectra of Compound **257**

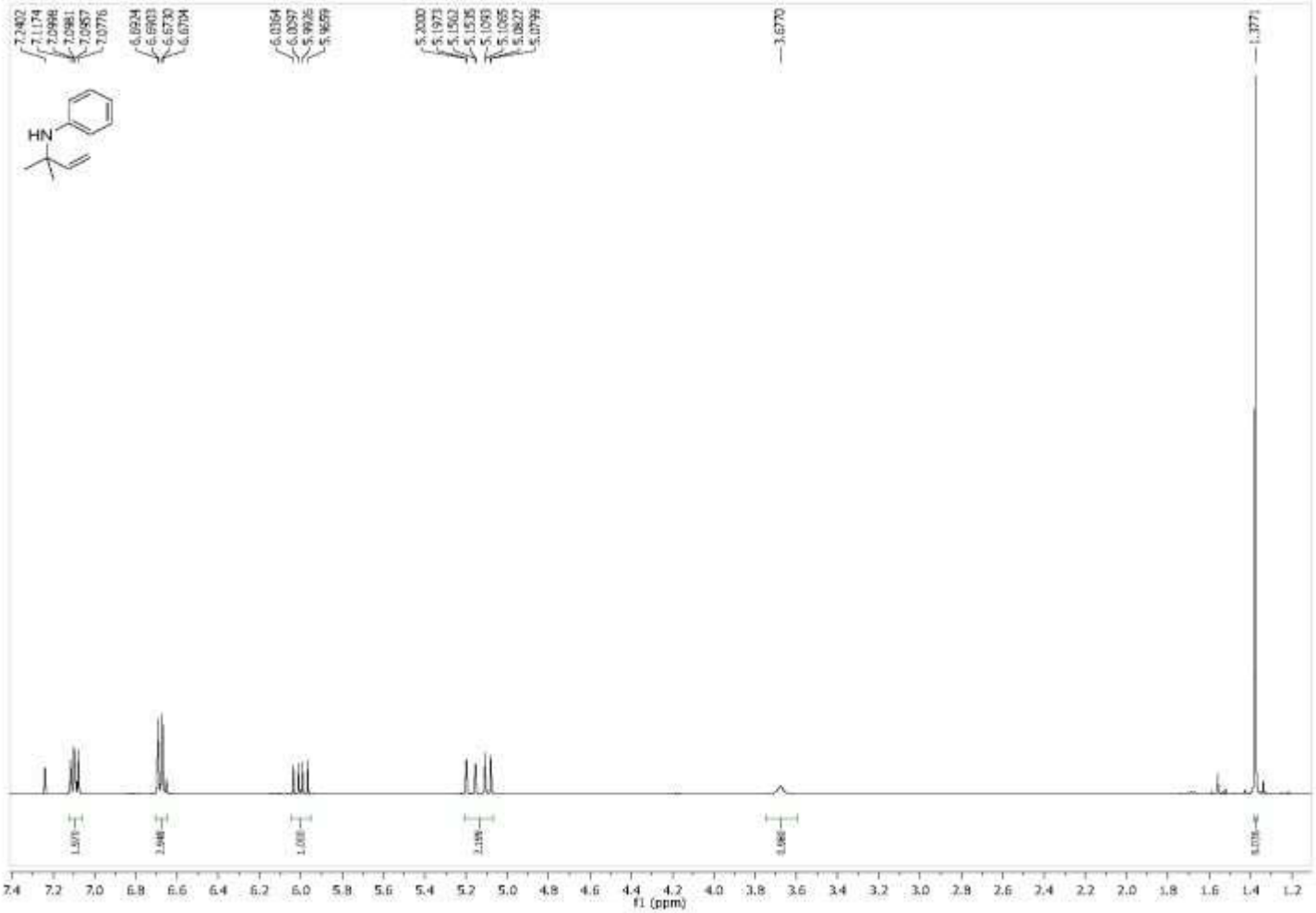

Figure A129 400 MHz 1H NMR ($CDCl_3$) Spectra of Compound **175**

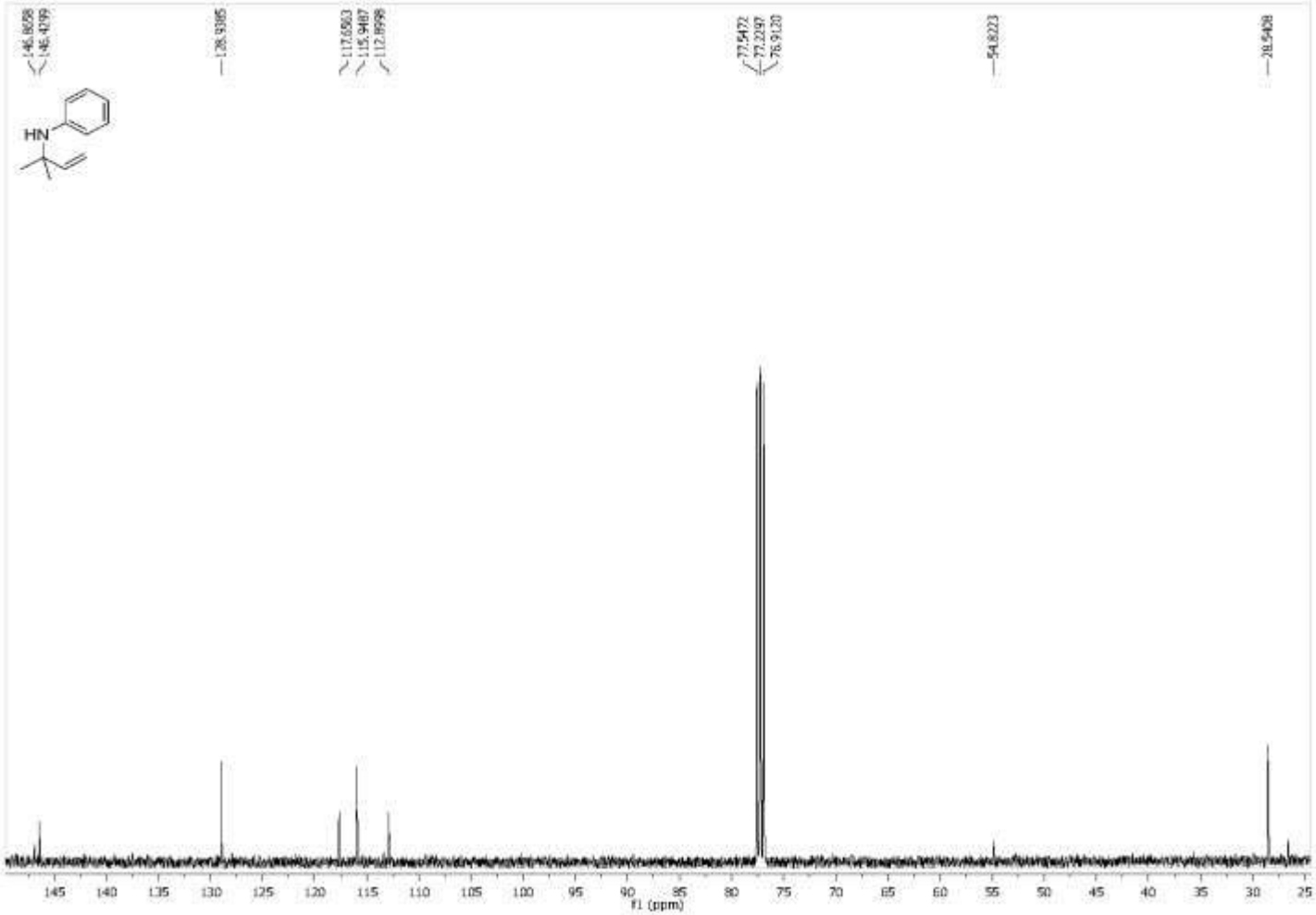

Figure A130 100 MHz 13C NMR ($CDCl_3$) Spectra of Compound **175**

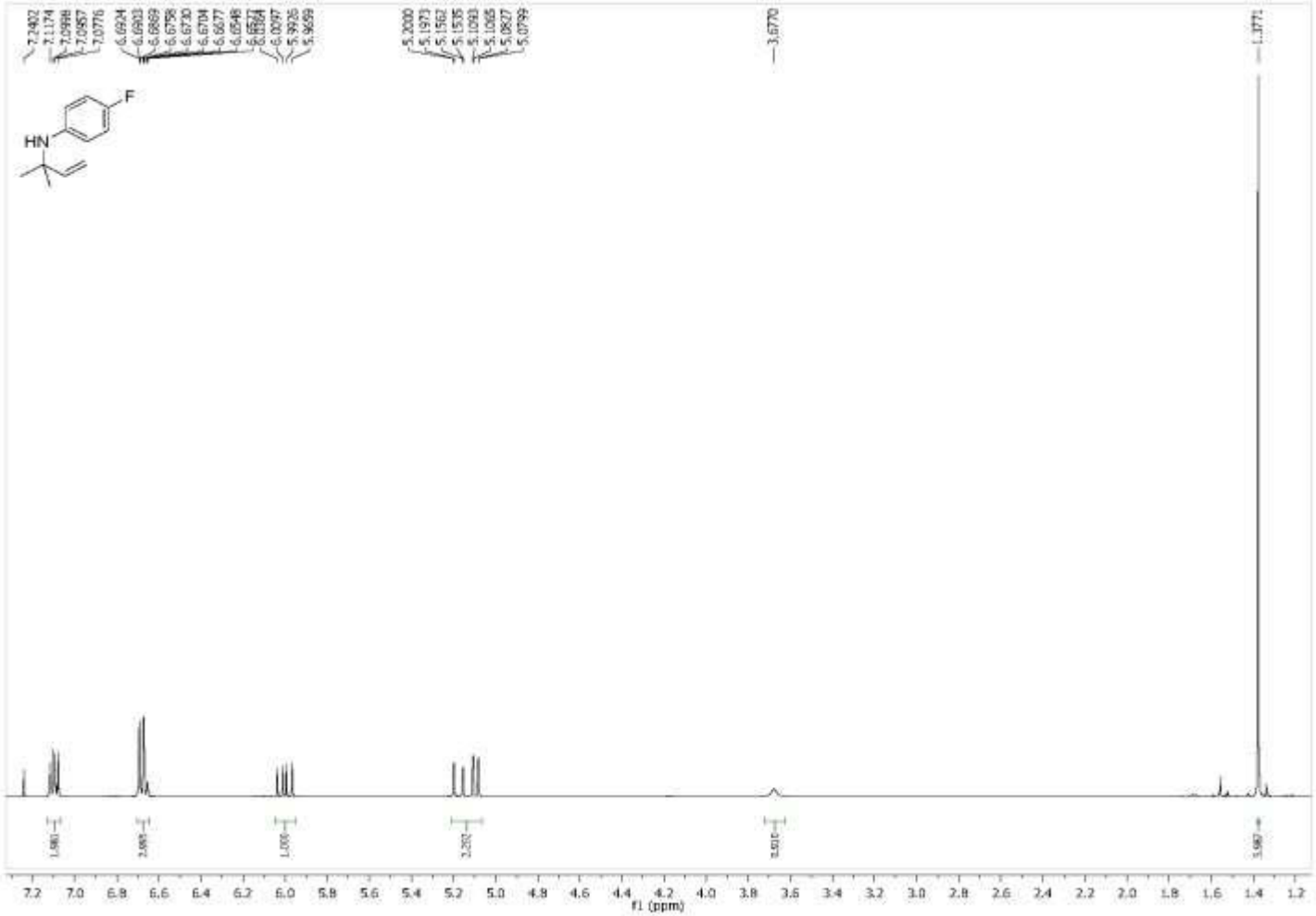

Figure A131 400 MHz 1H NMR ($CDCl_3$) Spectra of Compound **253b**

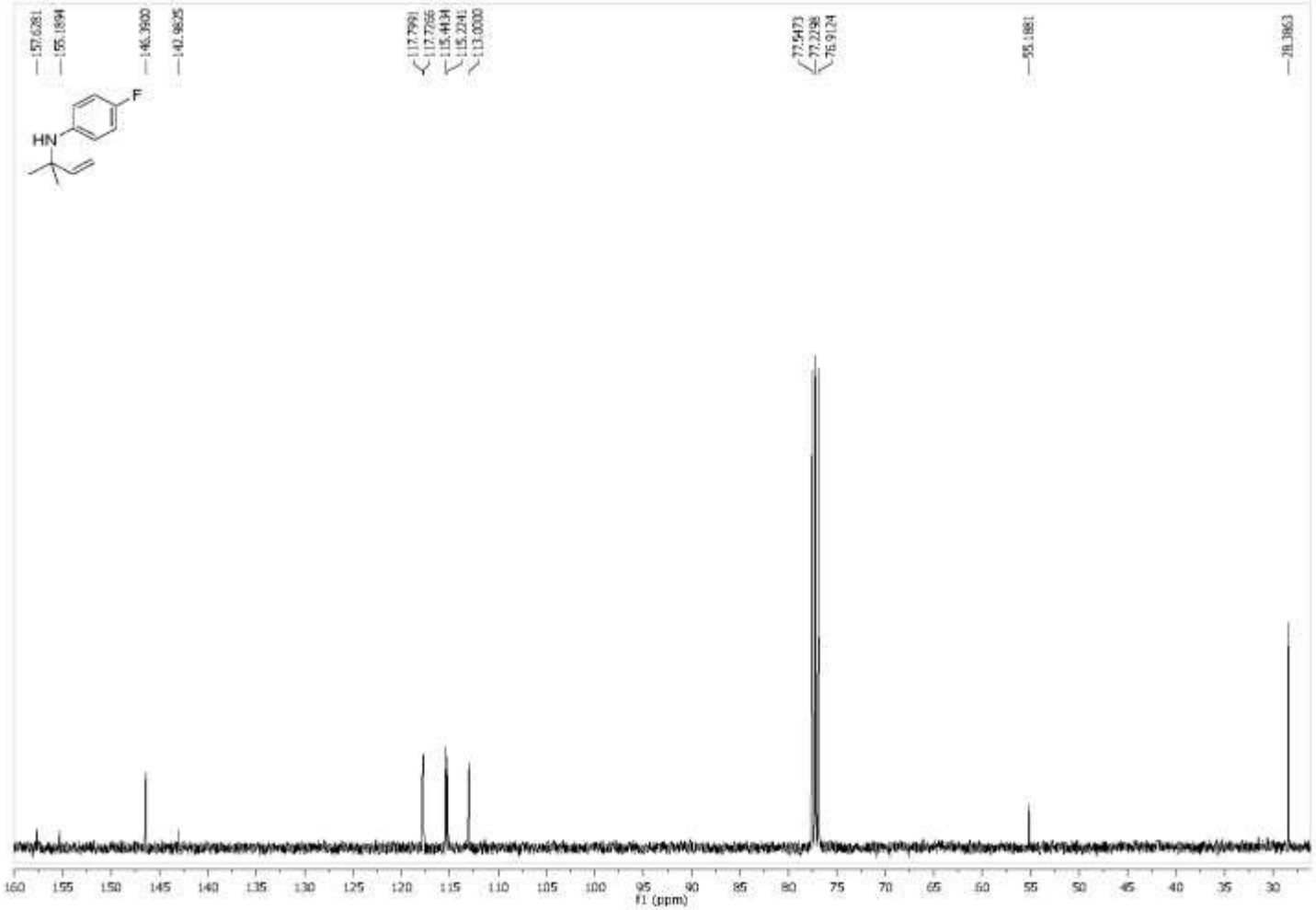

Figure A132 100 MHz 13C NMR ($CDCl_3$) Spectra of Compound **253b**

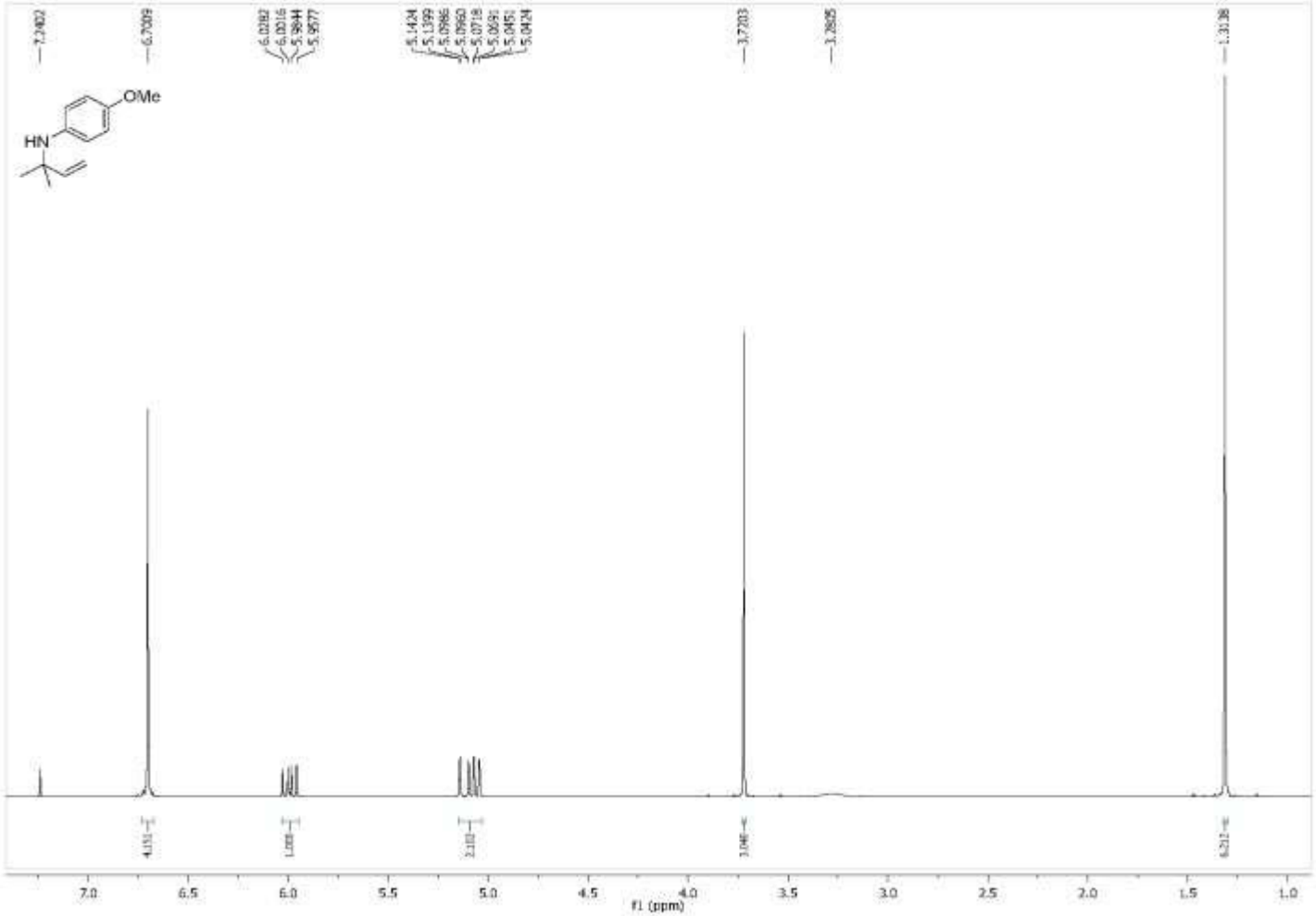

Figure A133 400 MHz 1H NMR ($CDCl_3$) Spectra of Compound **253c**

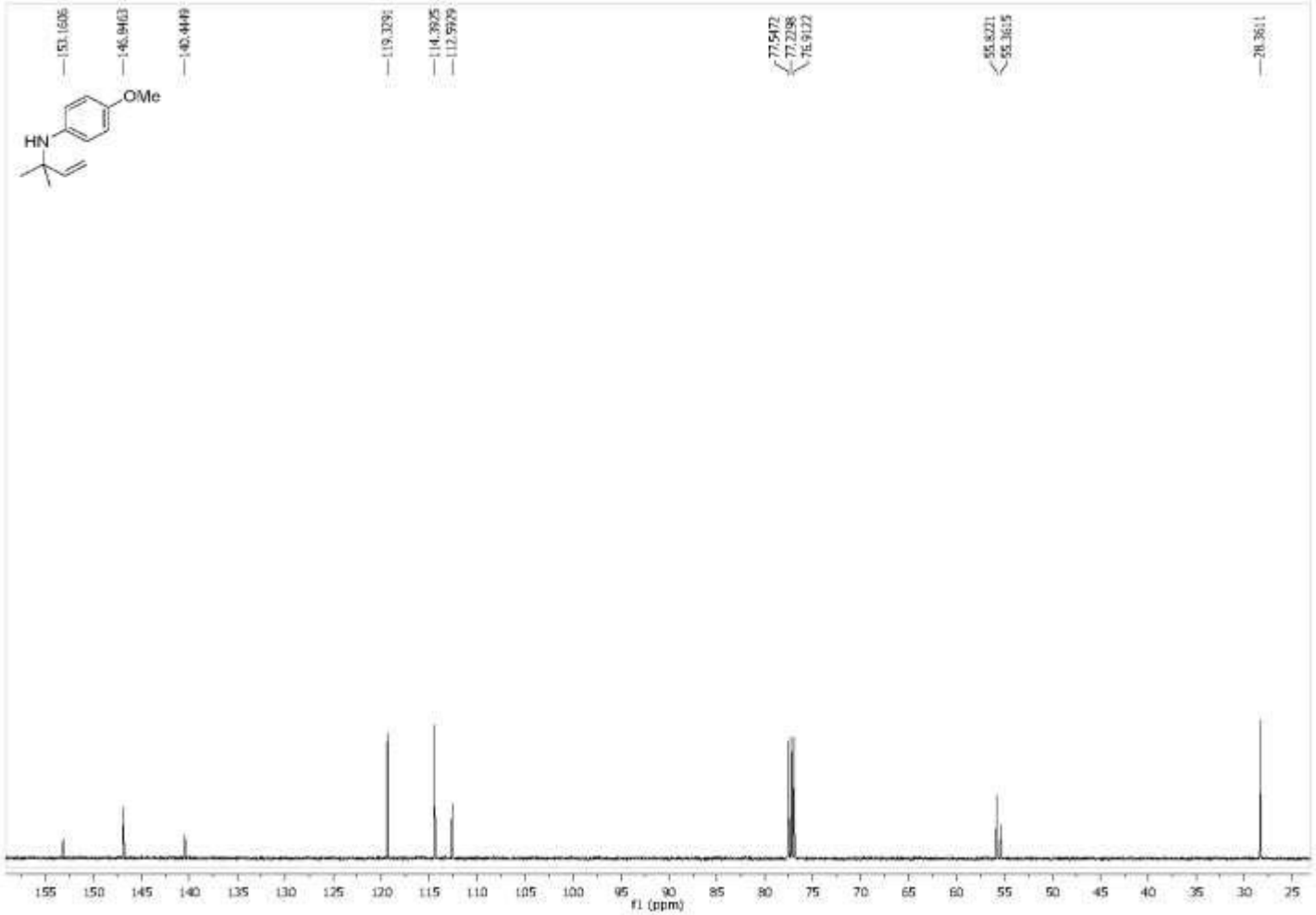

Figure A134 100 MHz 13C NMR ($CDCl_3$) Spectra of Compound **253c**

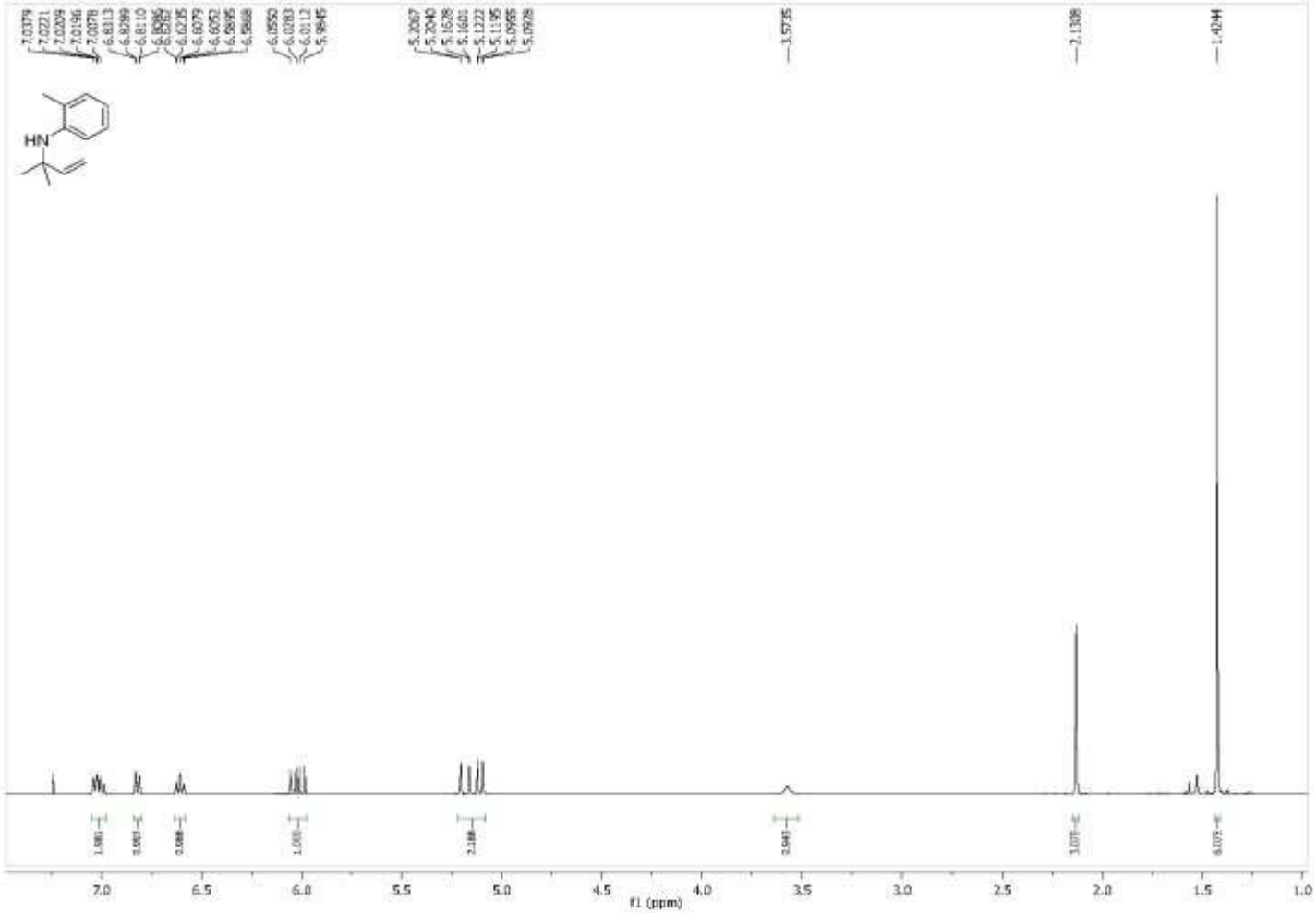

Figure A135 400 MHz 1H NMR ($CDCl_3$) Spectra of Compound **253d**

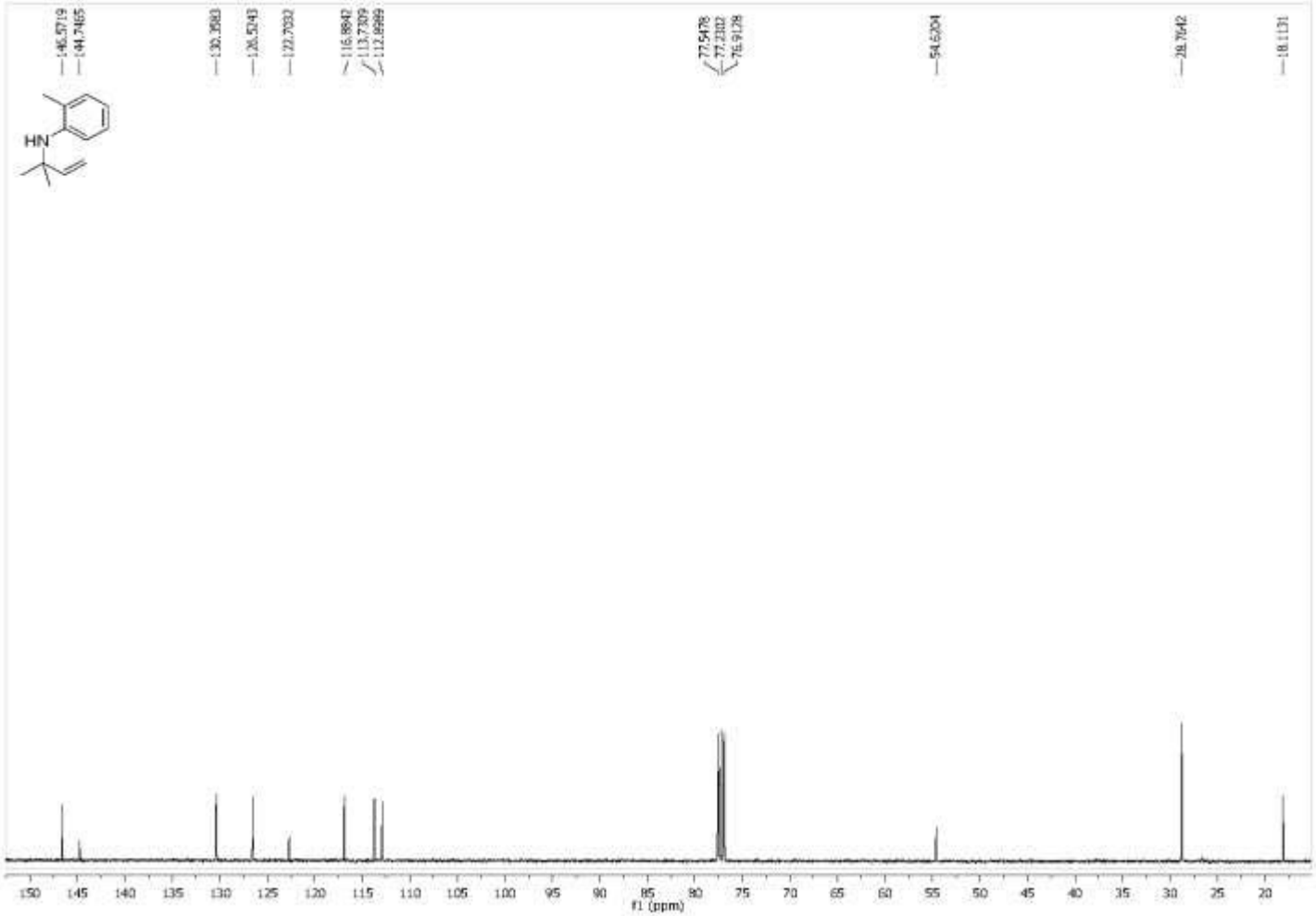

Figure A136 100 MHz 13C NMR ($CDCl_3$) Spectra of Compound **253d**

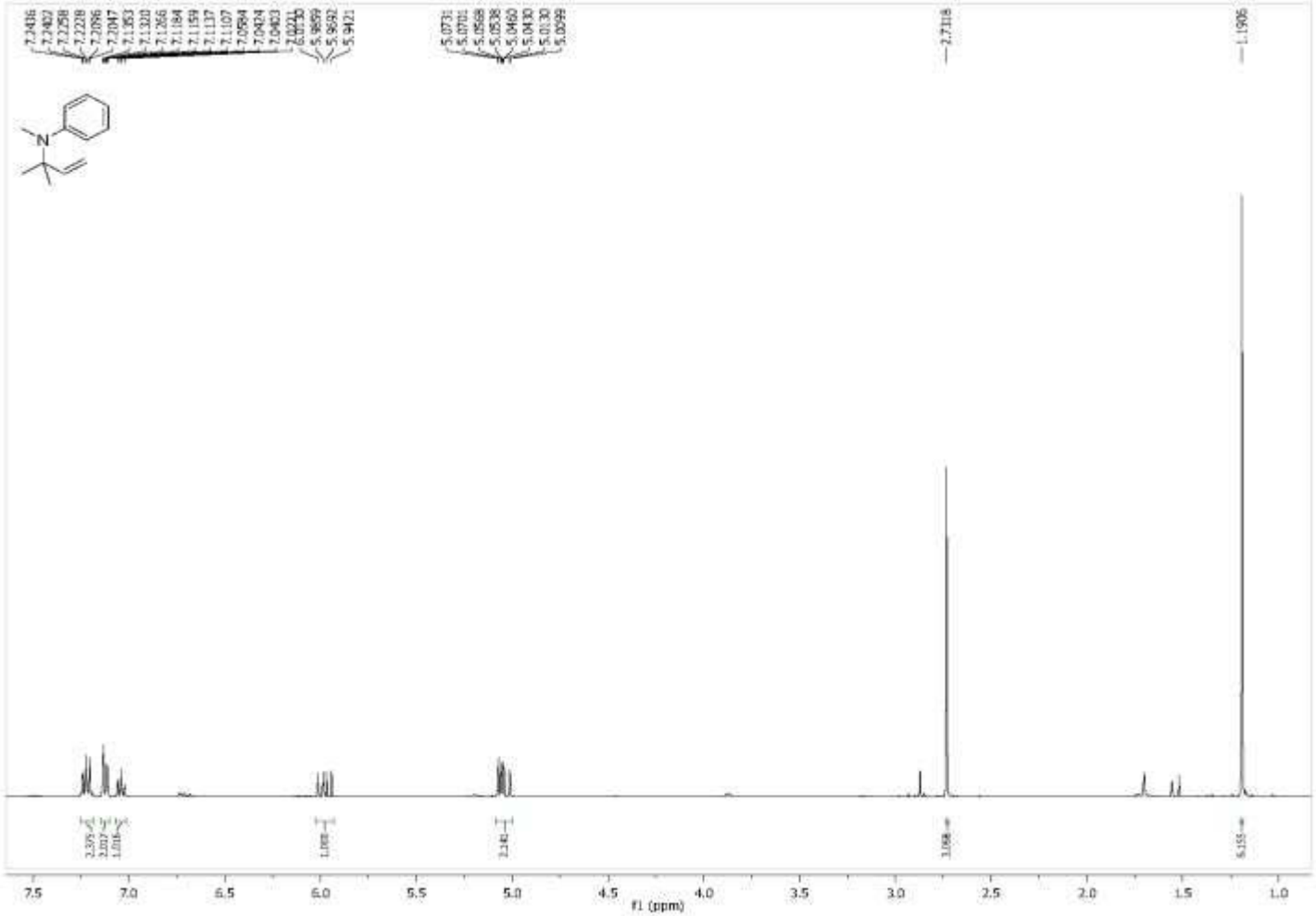

Figure A137 400 MHz 1H NMR ($CDCl_3$) Spectra of Compound **253f**

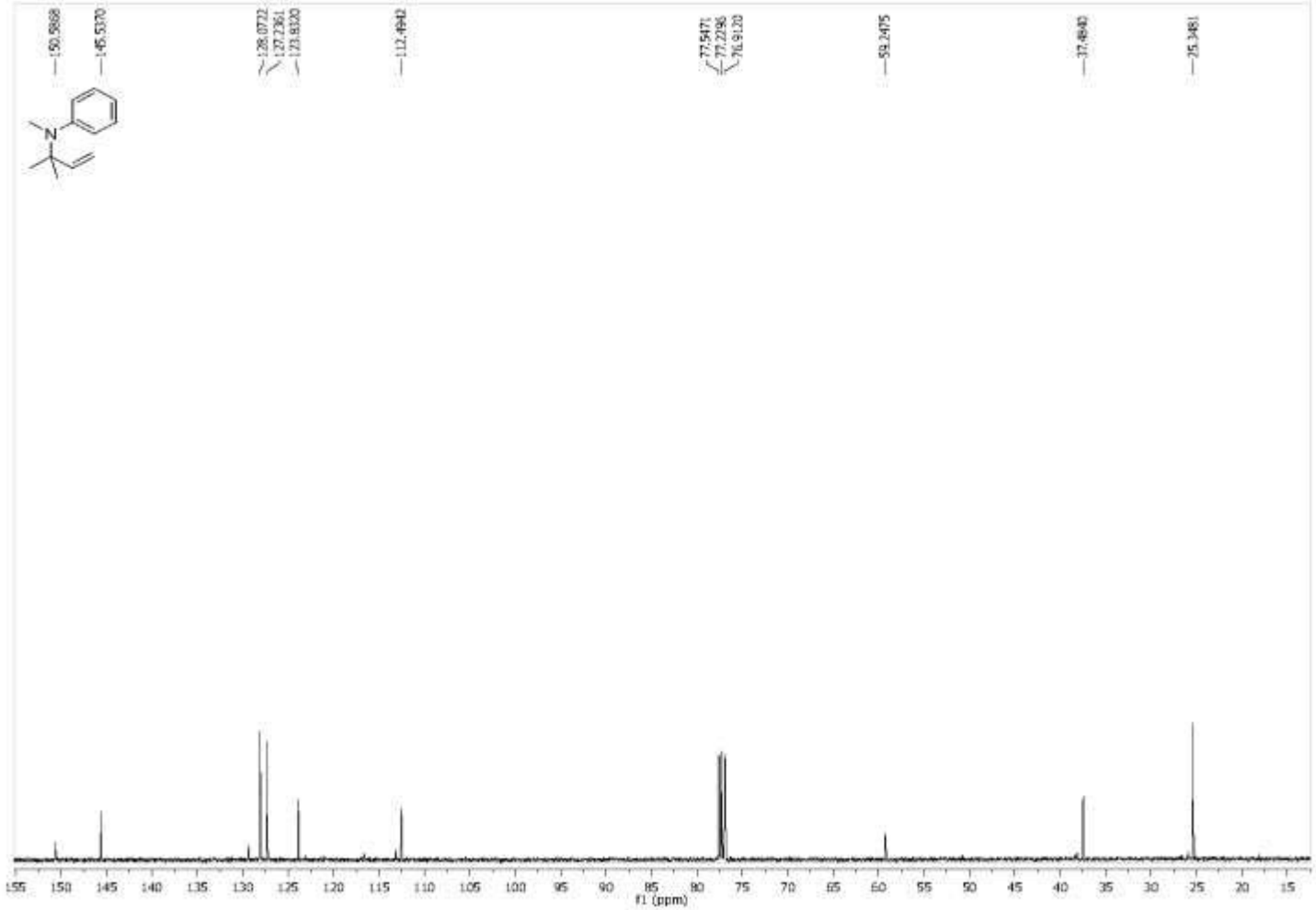

Figure A138 100 MHz 13C NMR ($CDCl_3$) Spectra of Compound **253f**

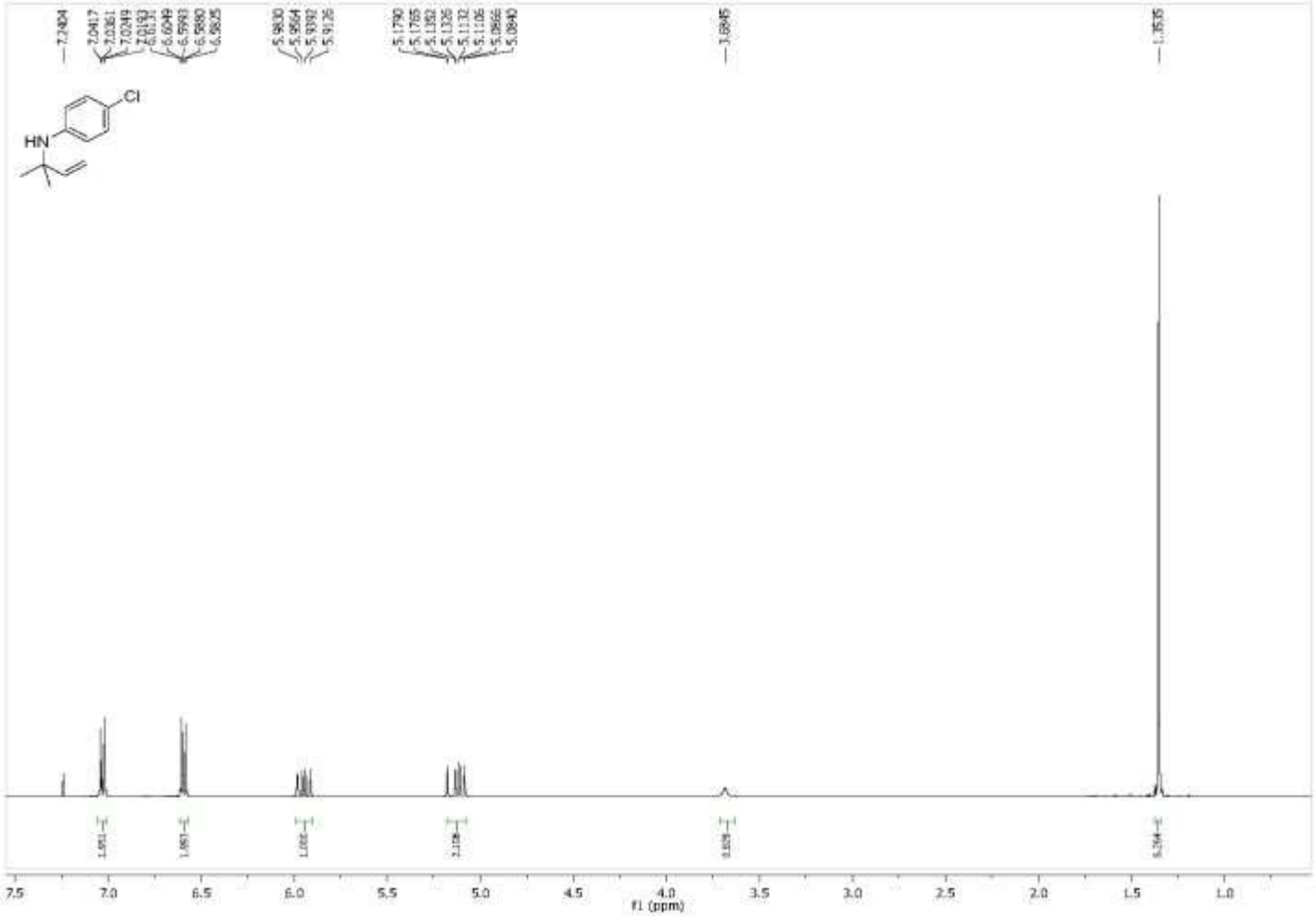

Figure A139 400 MHz 1H NMR ($CDCl_3$) Spectra of Compound **253g**

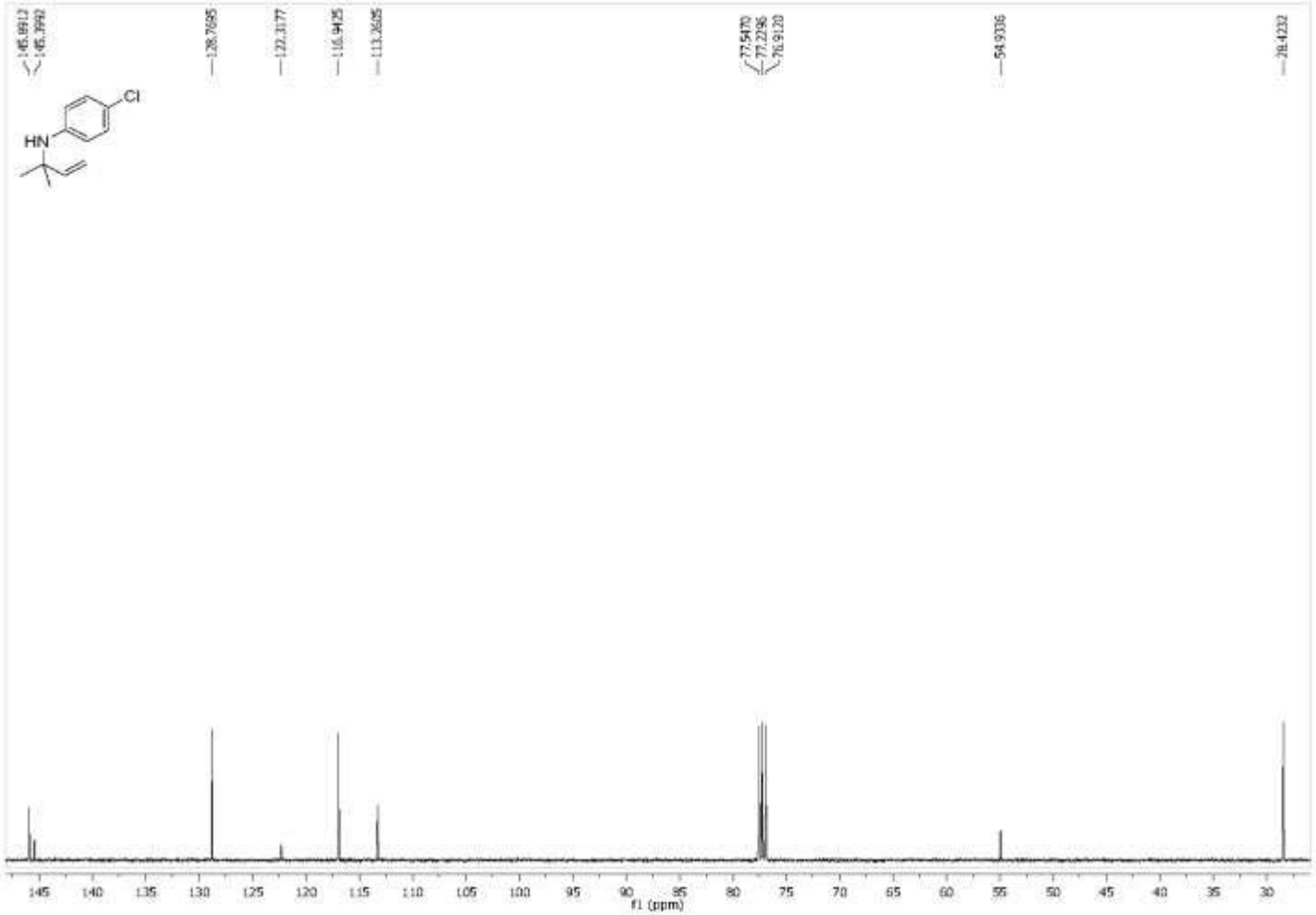

Figure A140 100 MHz 13C NMR ($CDCl_3$) Spectra of Compound **253g**

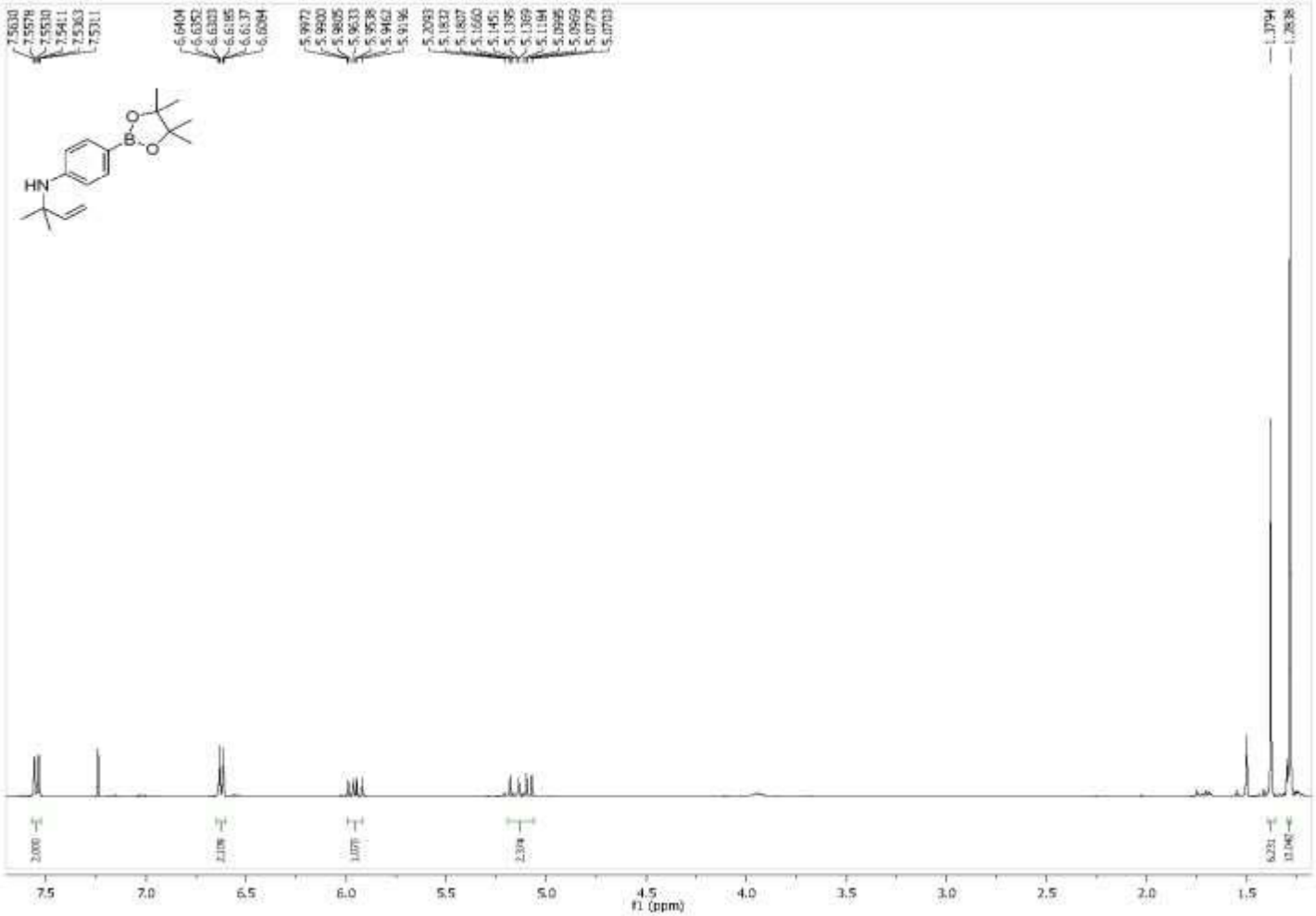

Figure A141 400 MHz 1H NMR ($CDCl_3$) Spectra of Compound **253h**

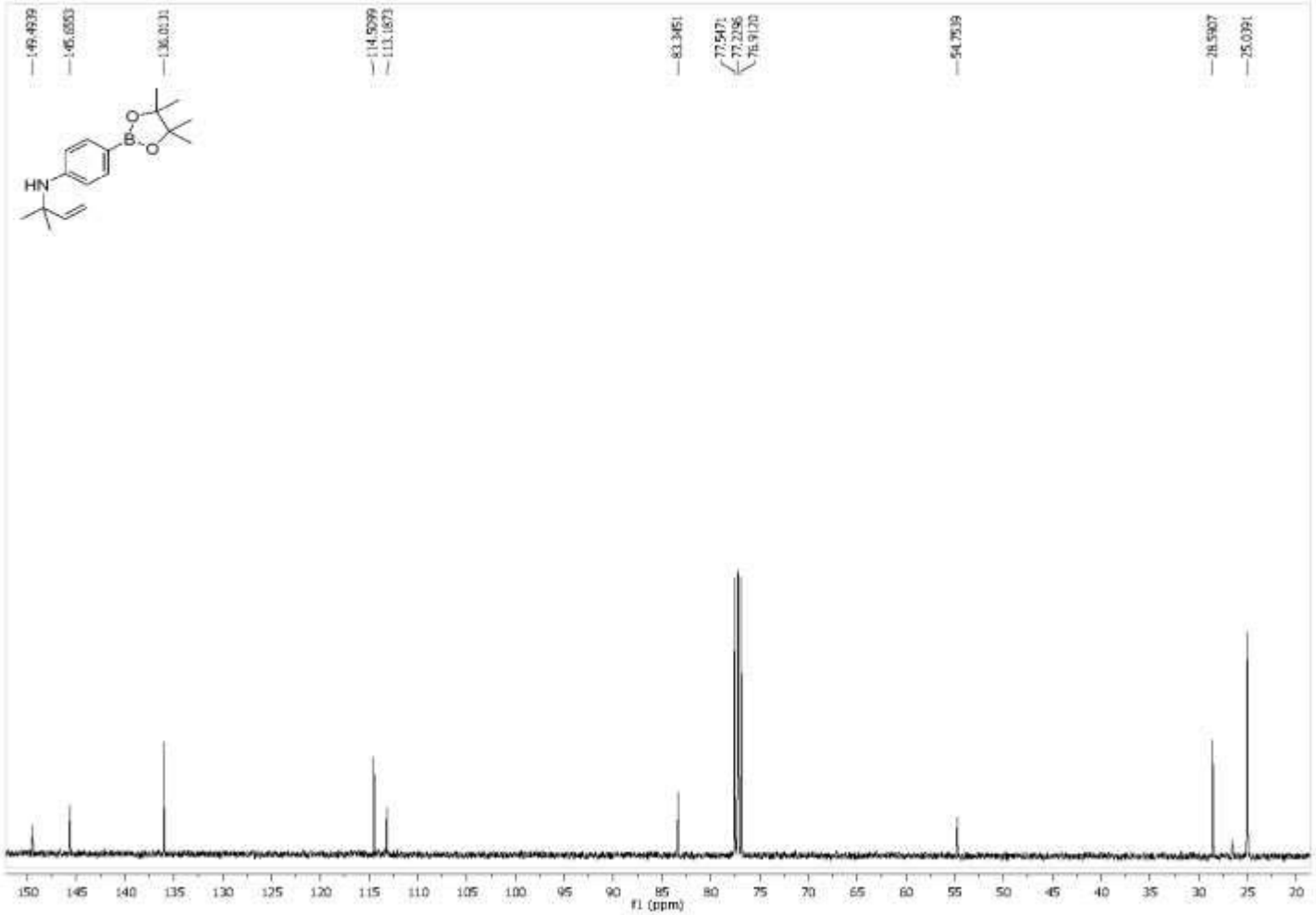

Figure A142 100 MHz 13C NMR ($CDCl_3$) Spectra of Compound **253h**

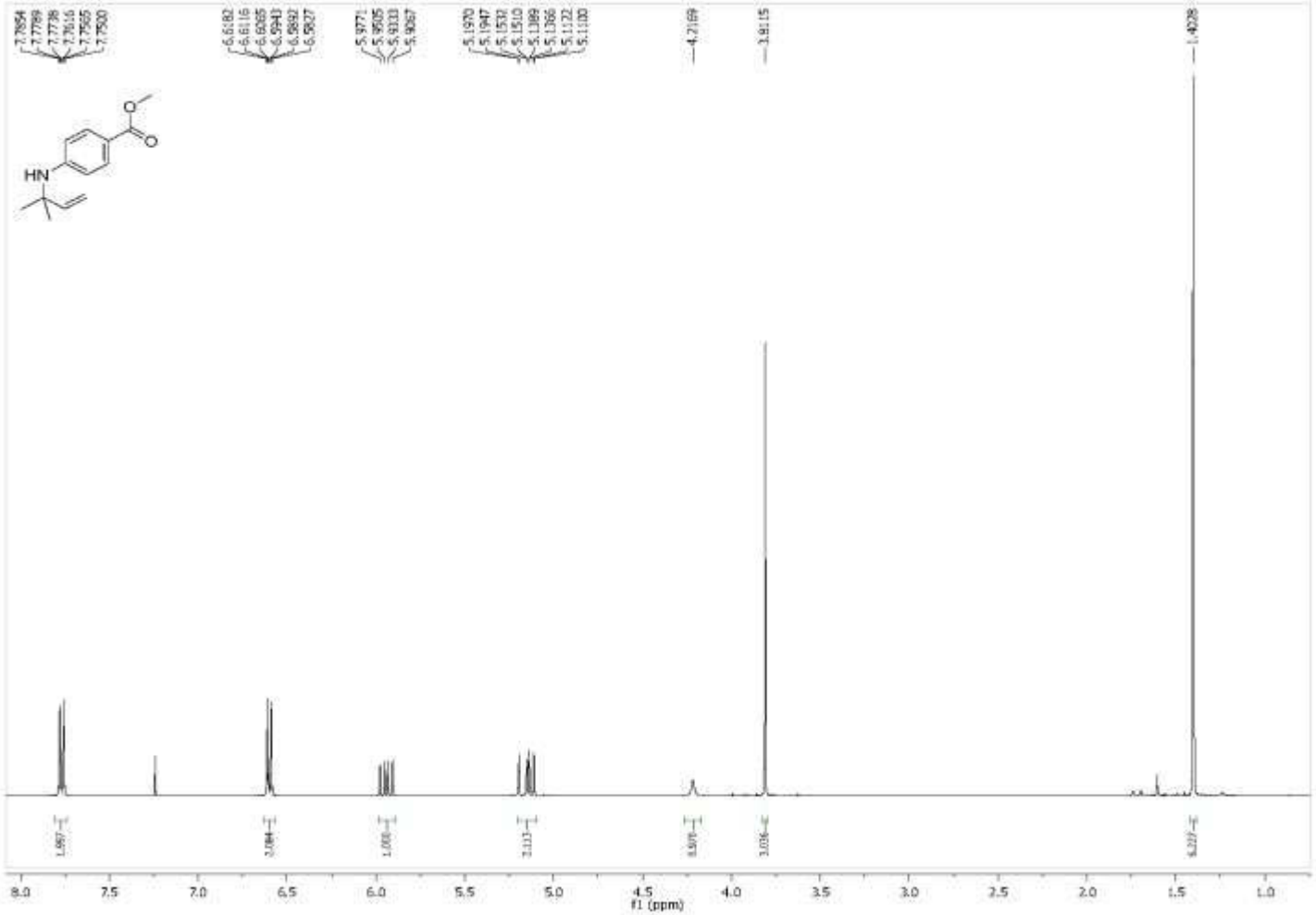

Figure A143 400 MHz 1H NMR ($CDCl_3$) Spectra of Compound **253i**

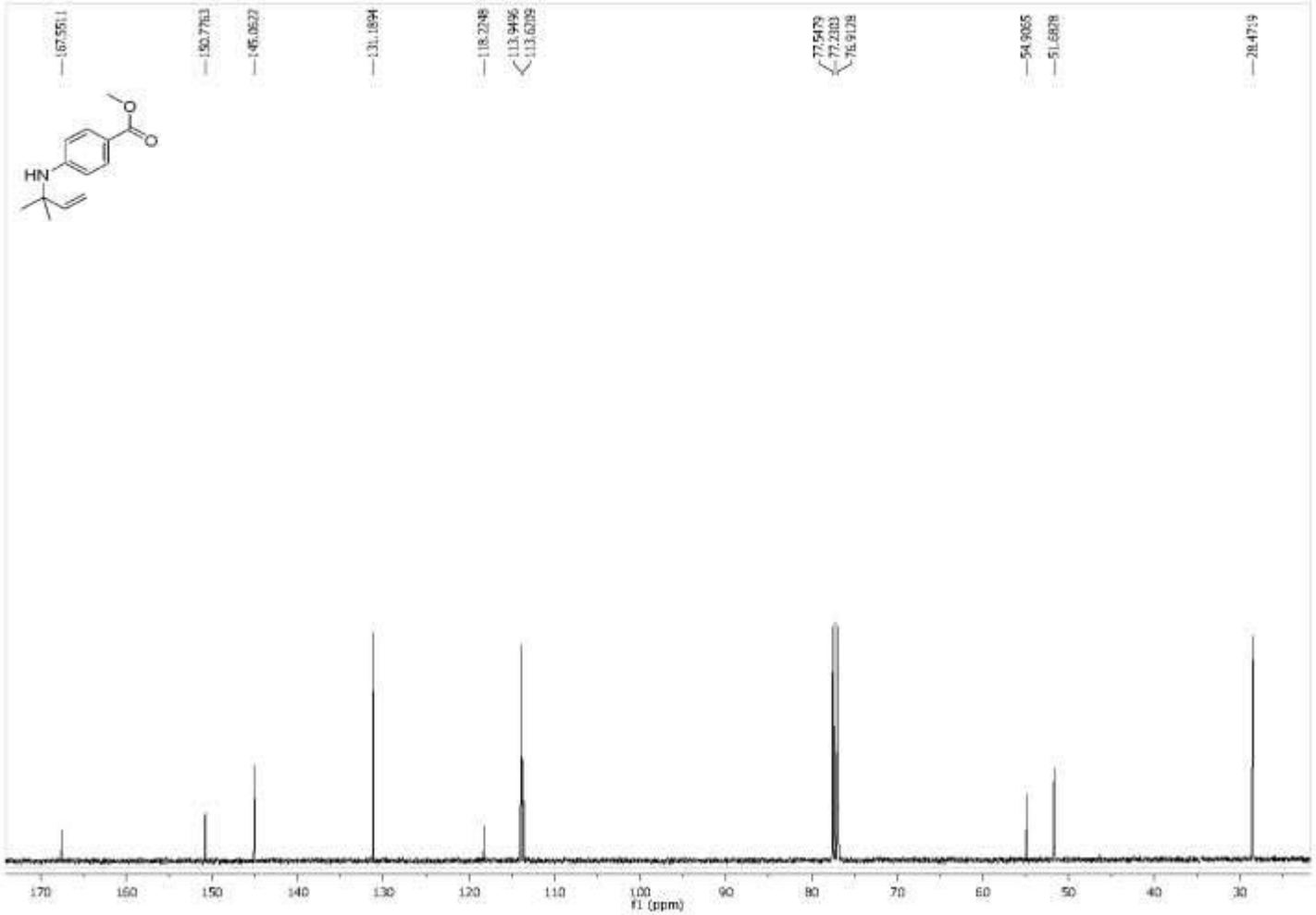

Figure A144 100 MHz 13C NMR ($CDCl_3$) Spectra of Compound **253i**

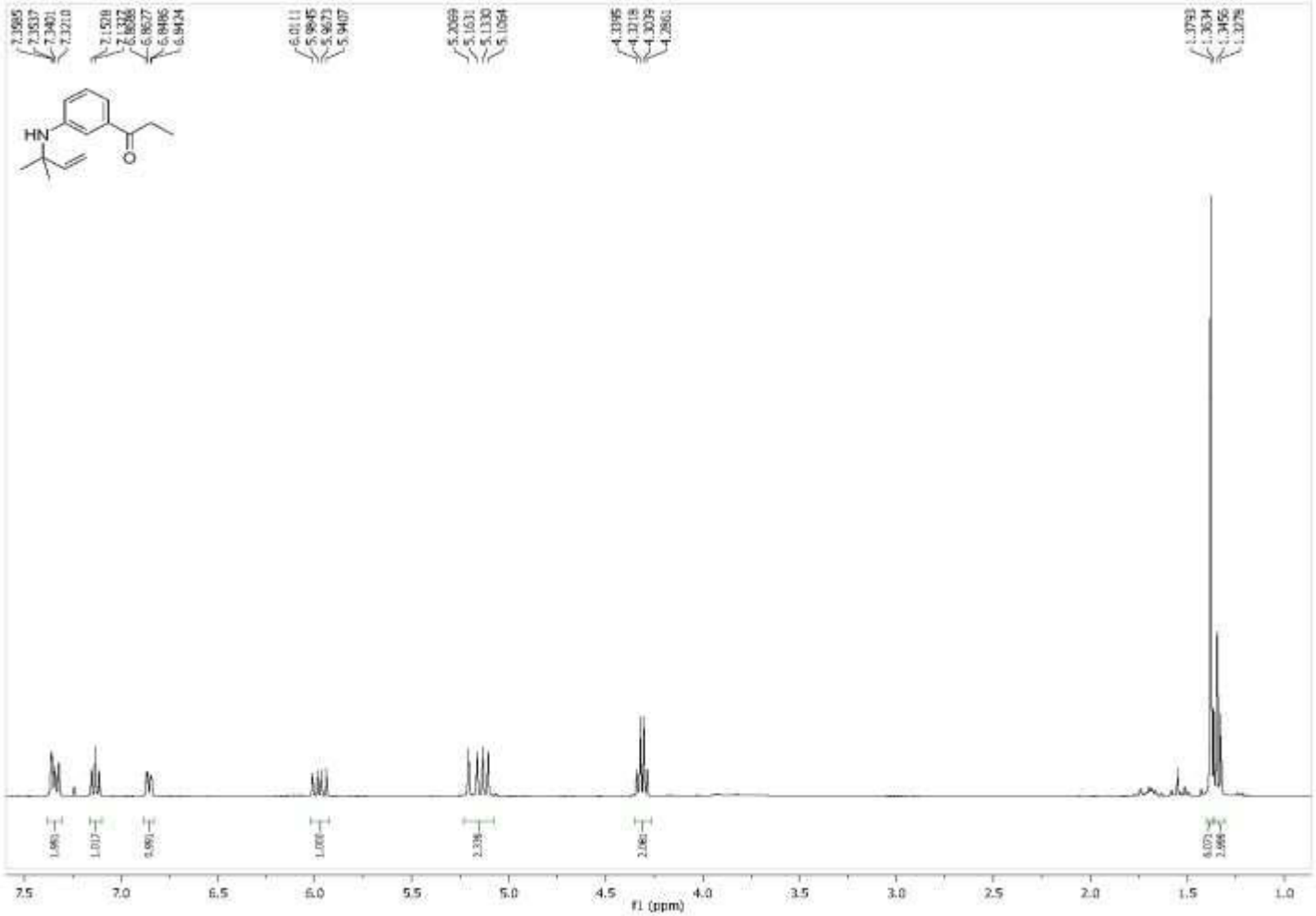

Figure A145 400 MHz 1H NMR ($CDCl_3$) Spectra of Compound **253j**

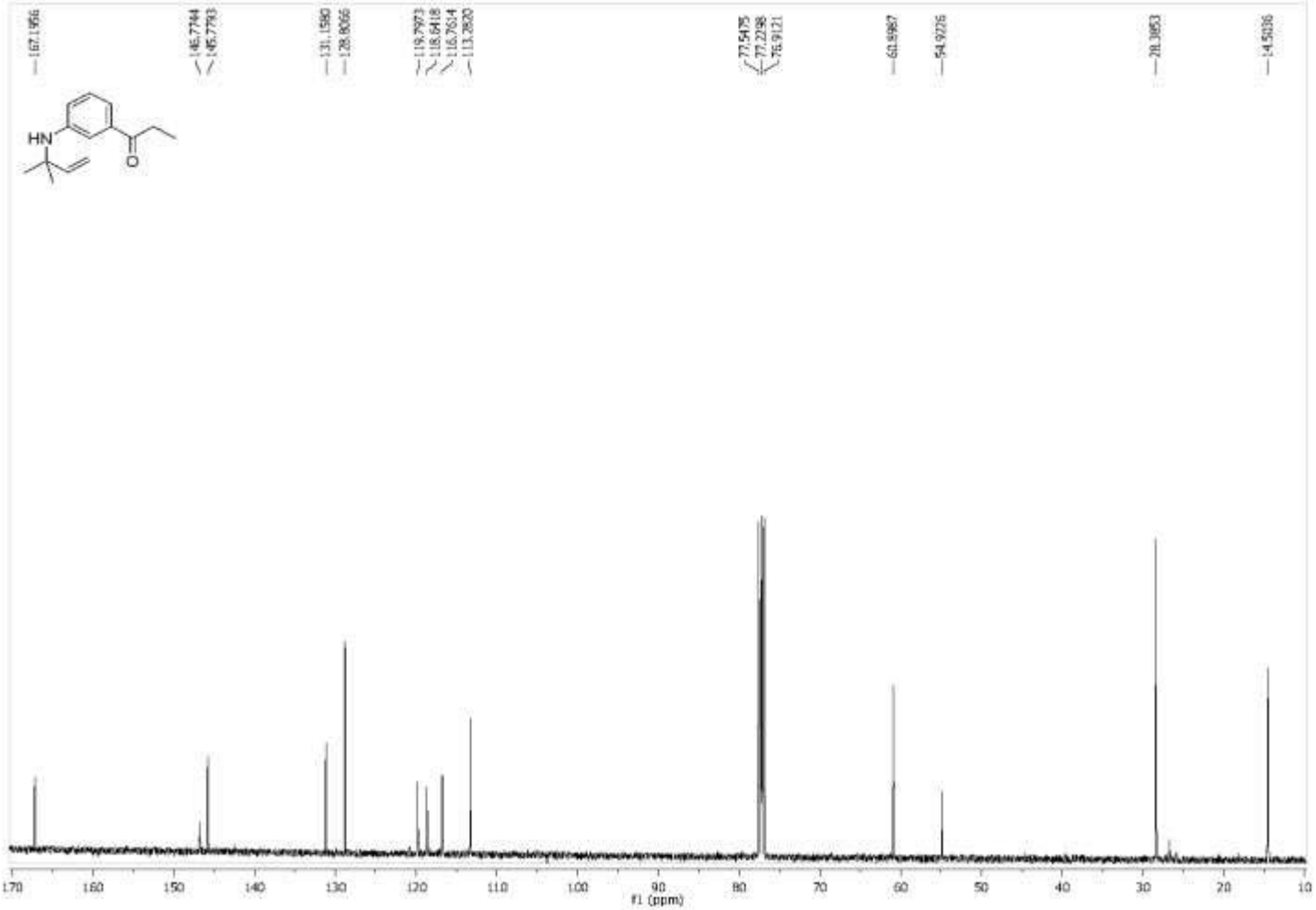

Figure A146 100 MHz 13C NMR ($CDCl_3$) Spectra of Compound **253j**

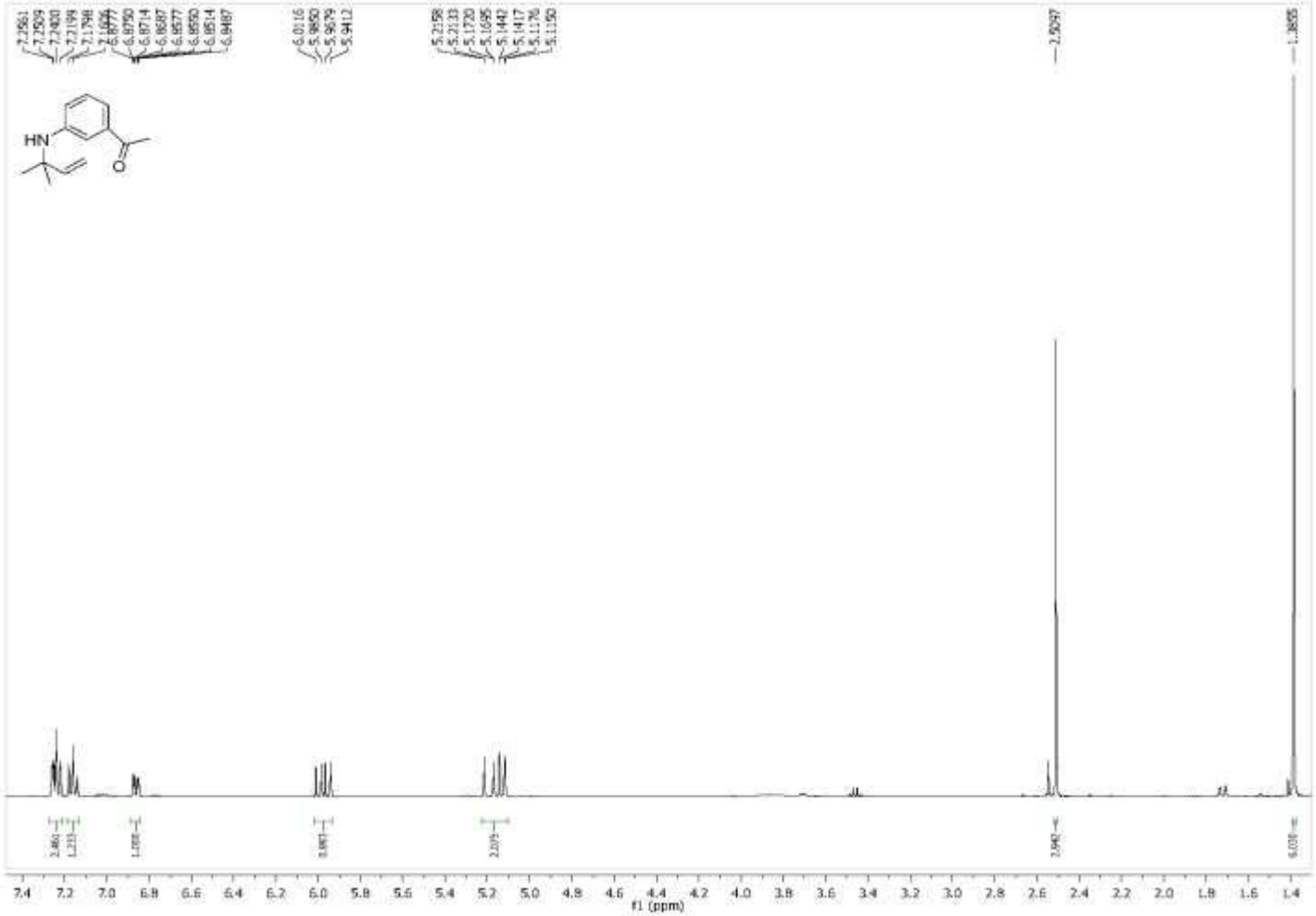

Figure A147 400 MHz 1H NMR ($CDCl_3$) Spectra of Compound **253k**

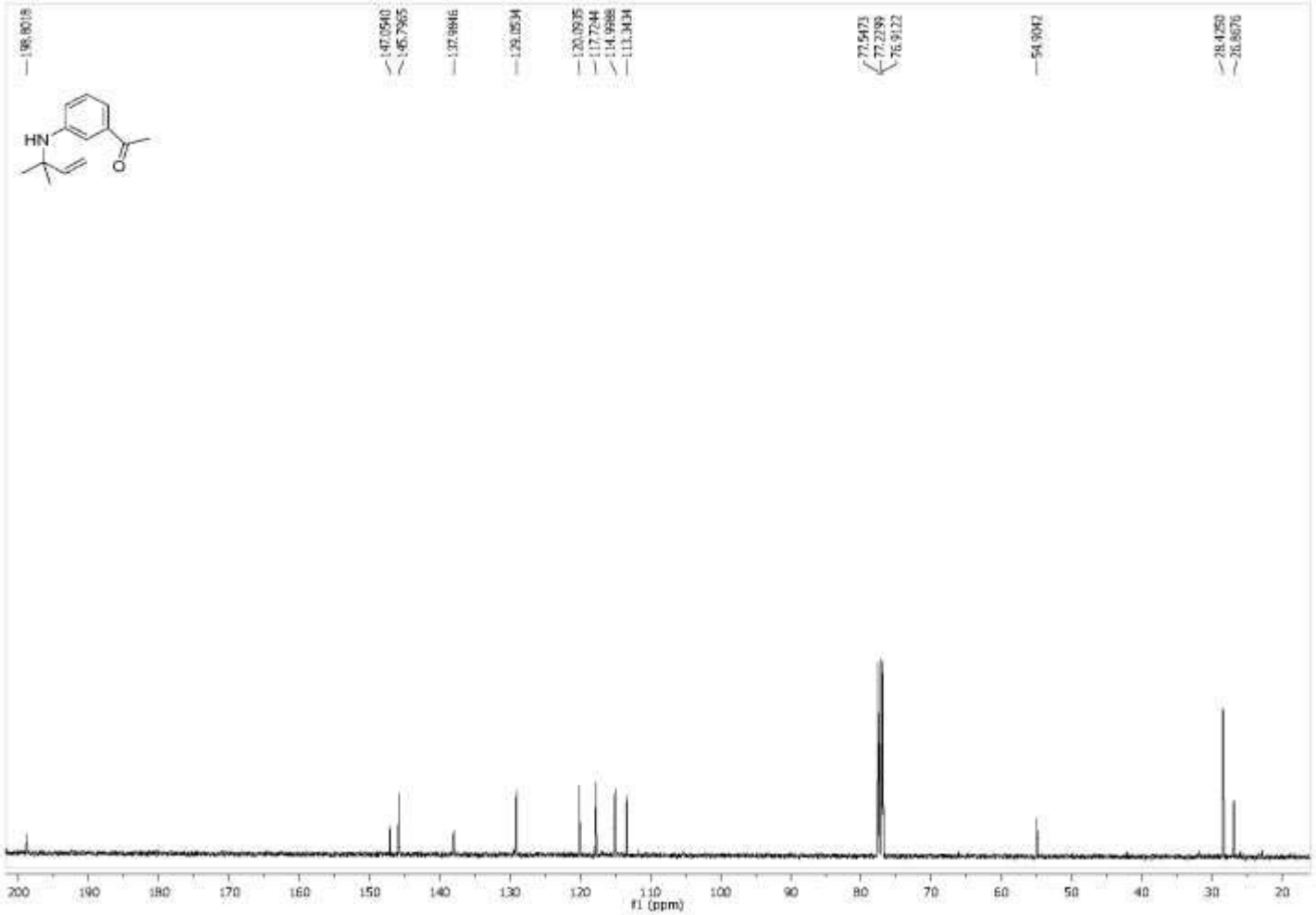

Figure A148 100 MHz 13C NMR ($CDCl_3$) Spectra of Compound **253k**

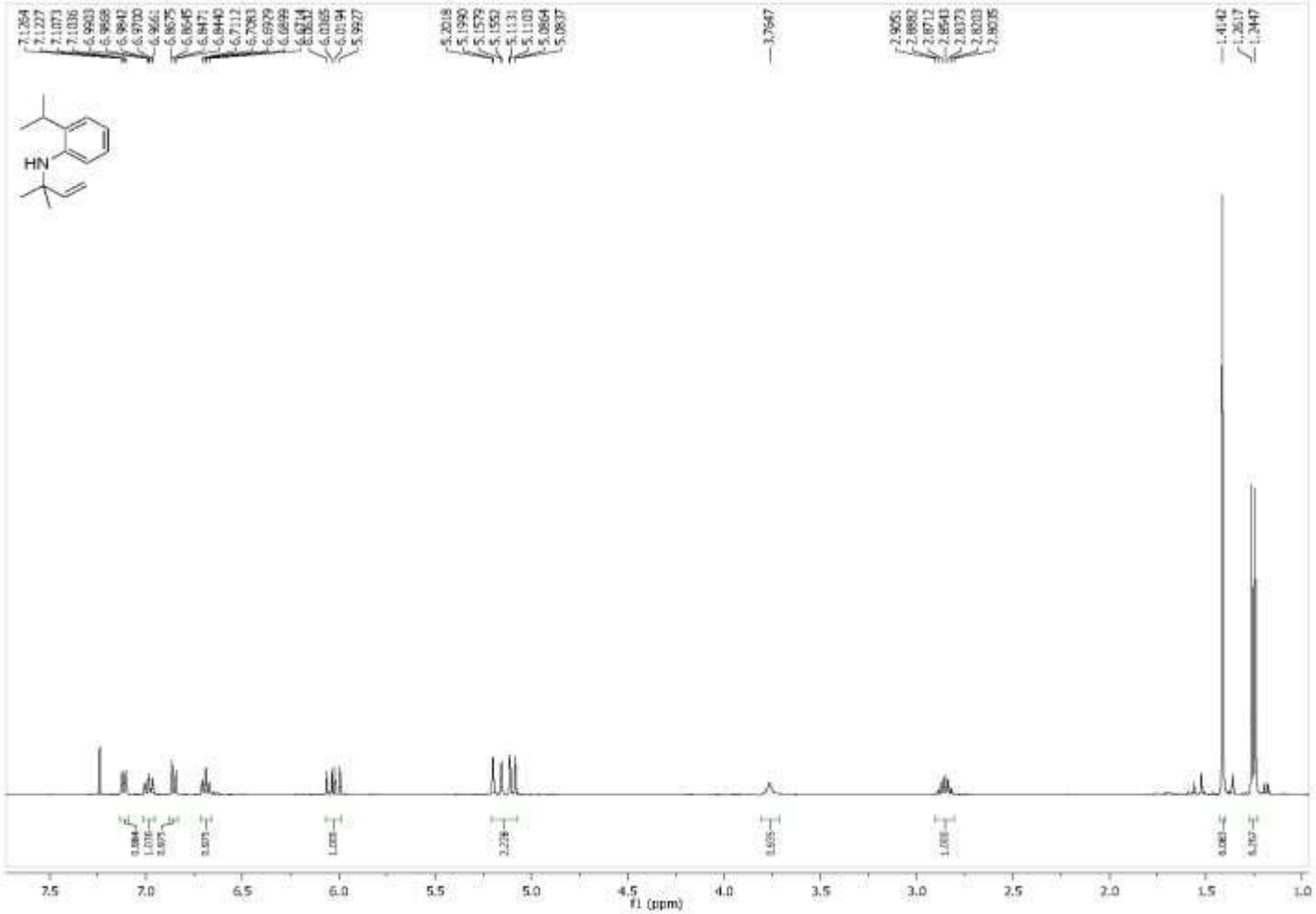

Figure A149 400 MHz 1H NMR ($CDCl_3$) Spectra of Compound **253l**

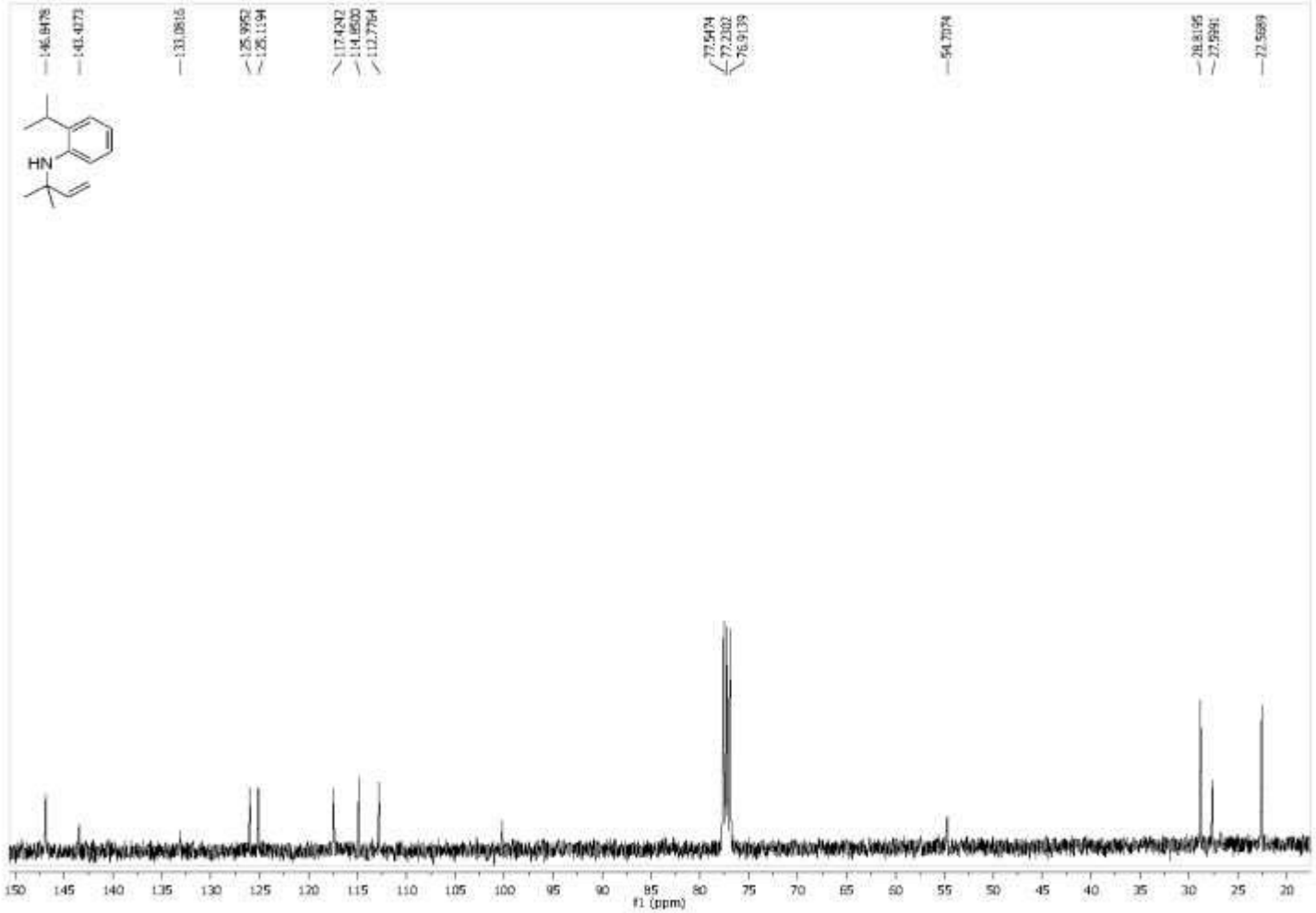

Figure A150 100 MHz 13C NMR ($CDCl_3$) Spectra of Compound **253l**

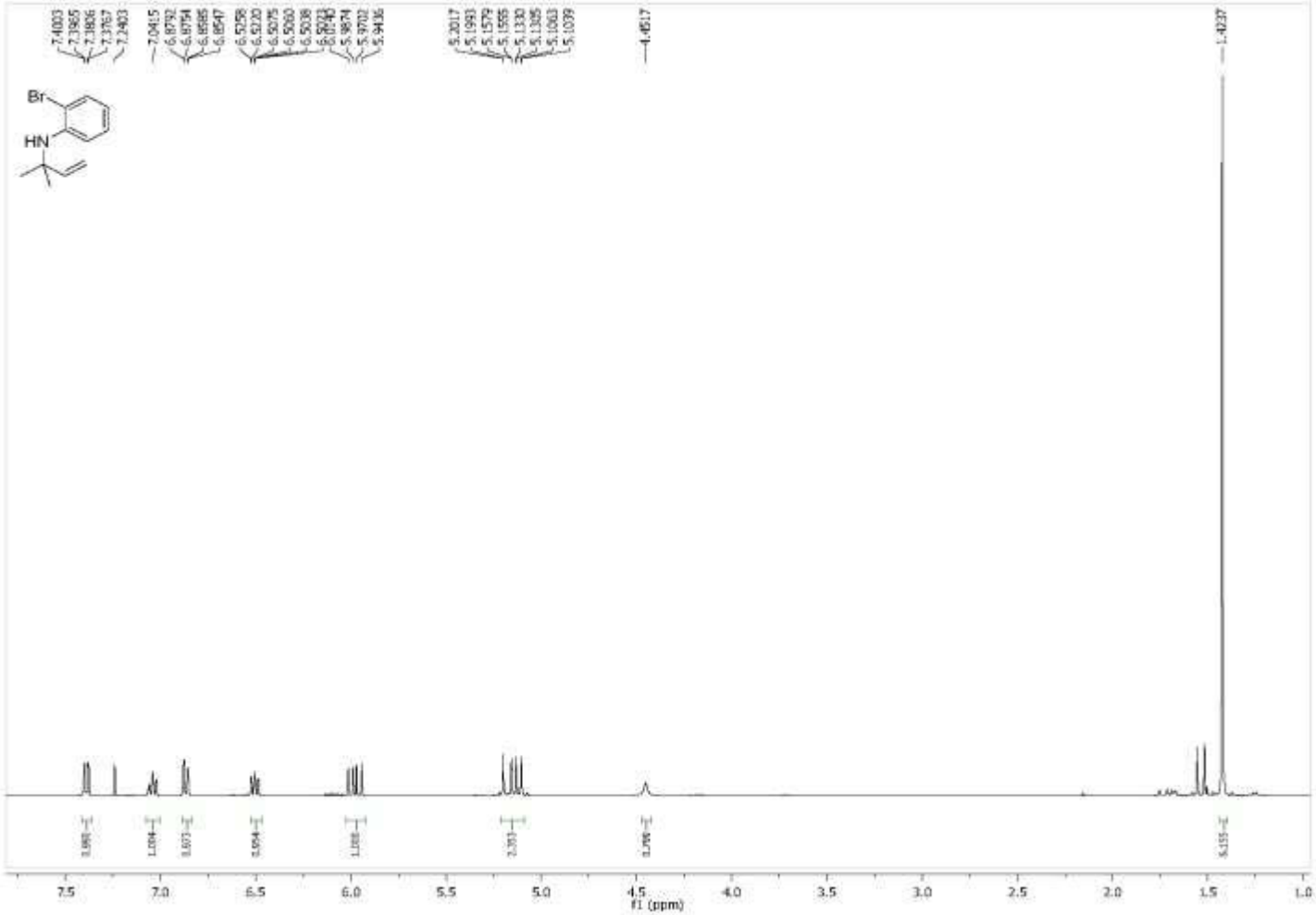

Figure A151 400 MHz 1H NMR ($CDCl_3$) Spectra of Compound **253m**

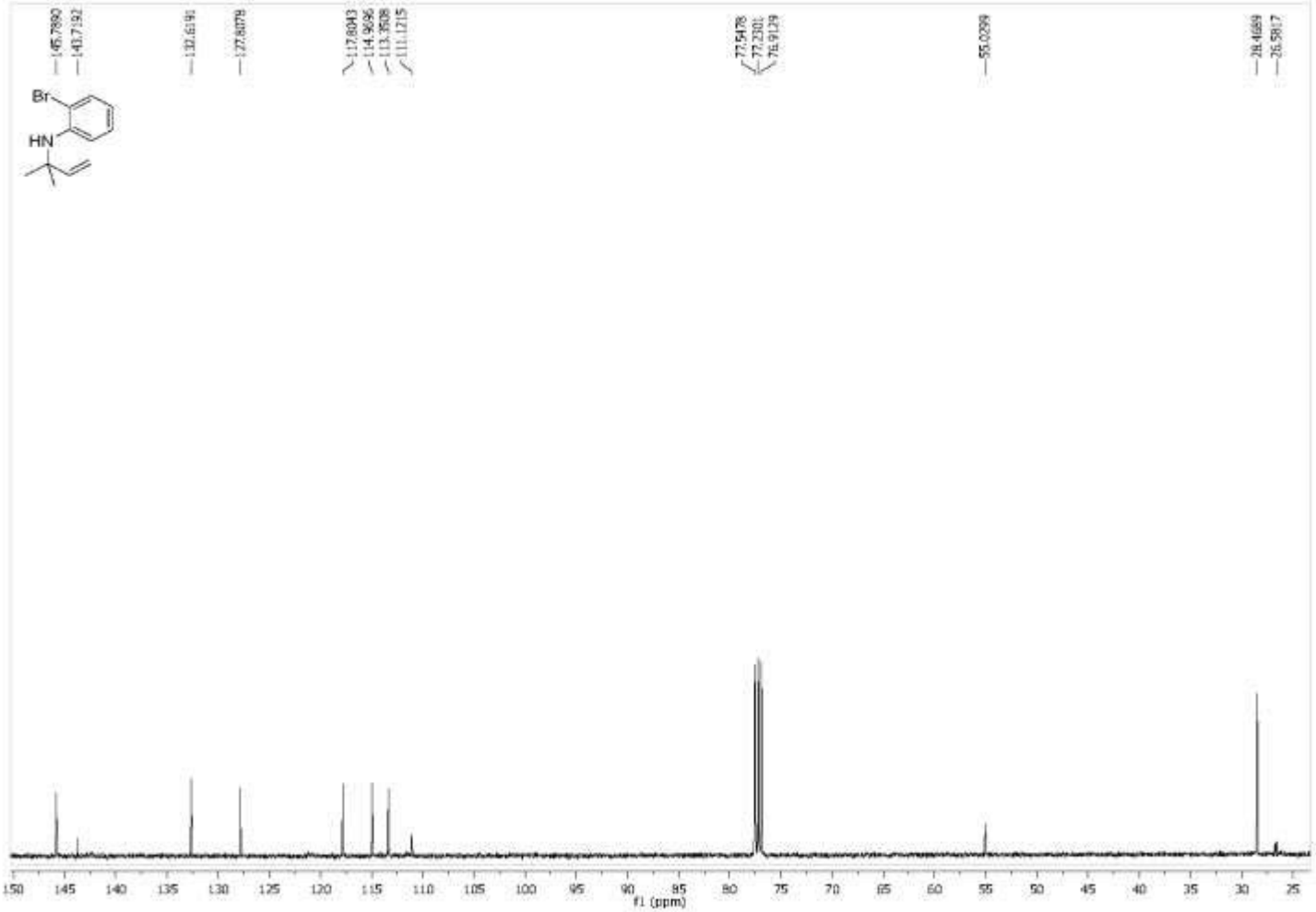

Figure A152 100 MHz 13C NMR ($CDCl_3$) Spectra of Compound **253m**

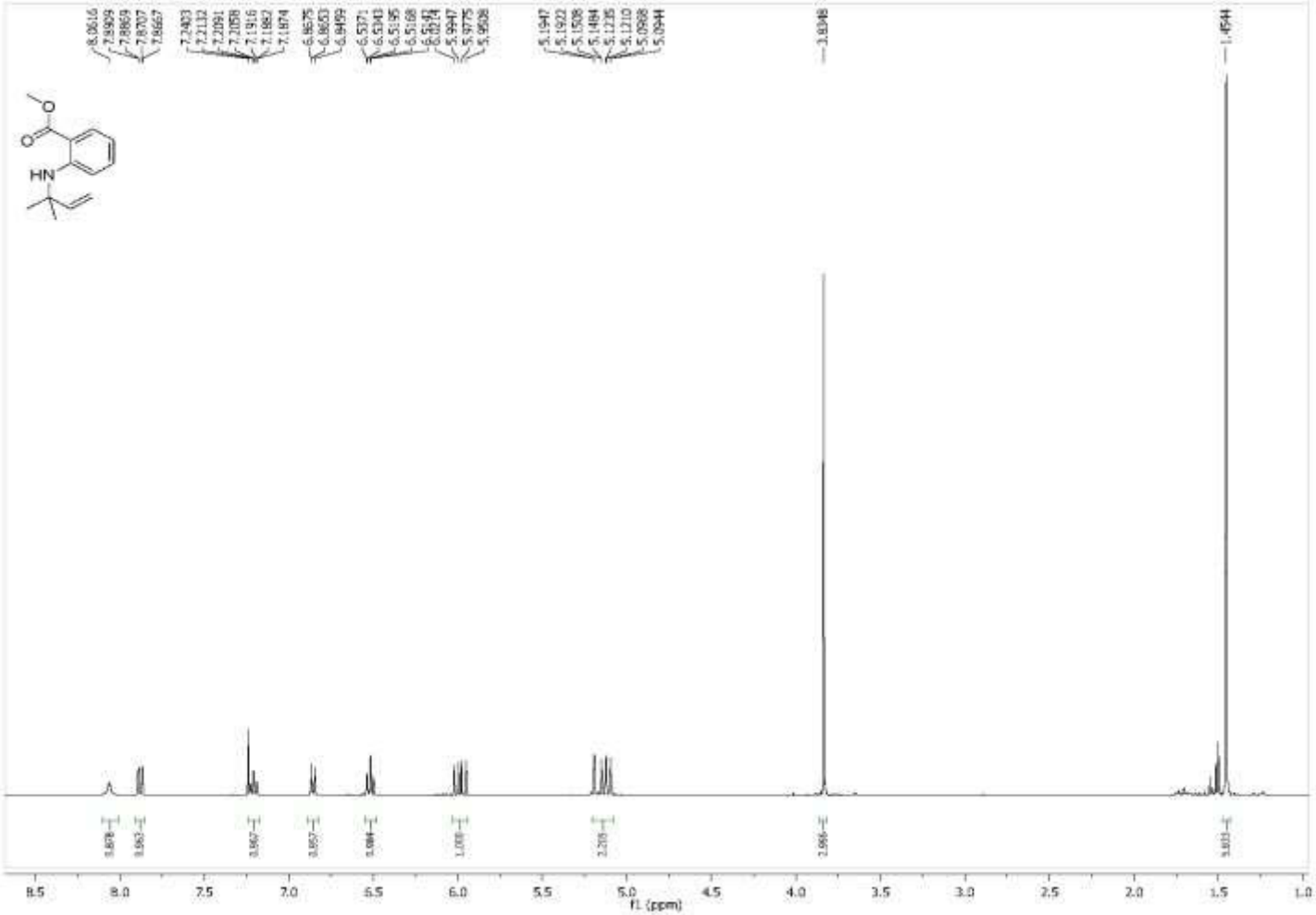

Figure A153 400 MHz 1H NMR ($CDCl_3$) Spectra of Compound **253n**

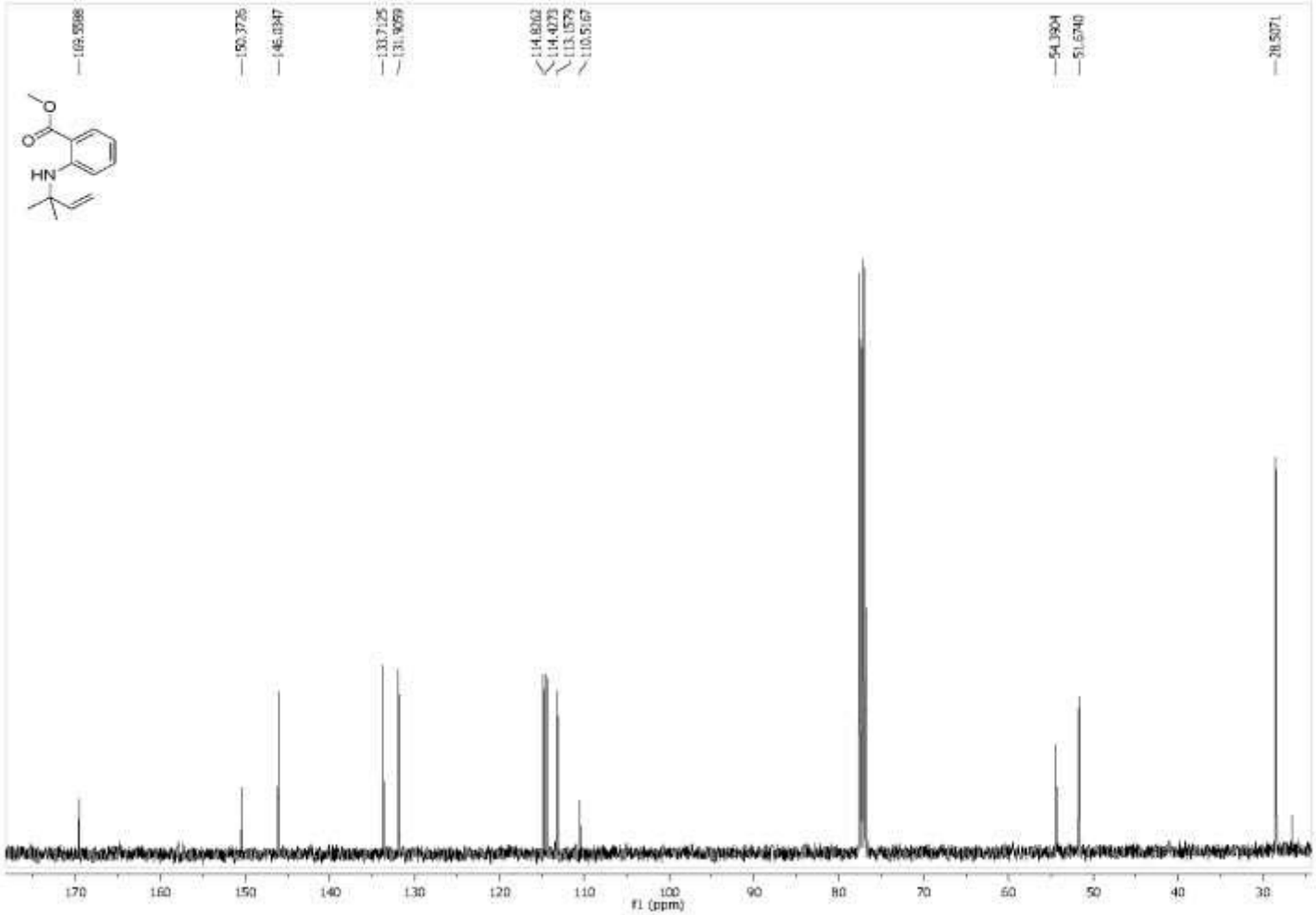

Figure A154 100 MHz 13C NMR ($CDCl_3$) Spectra of Compound **253n**

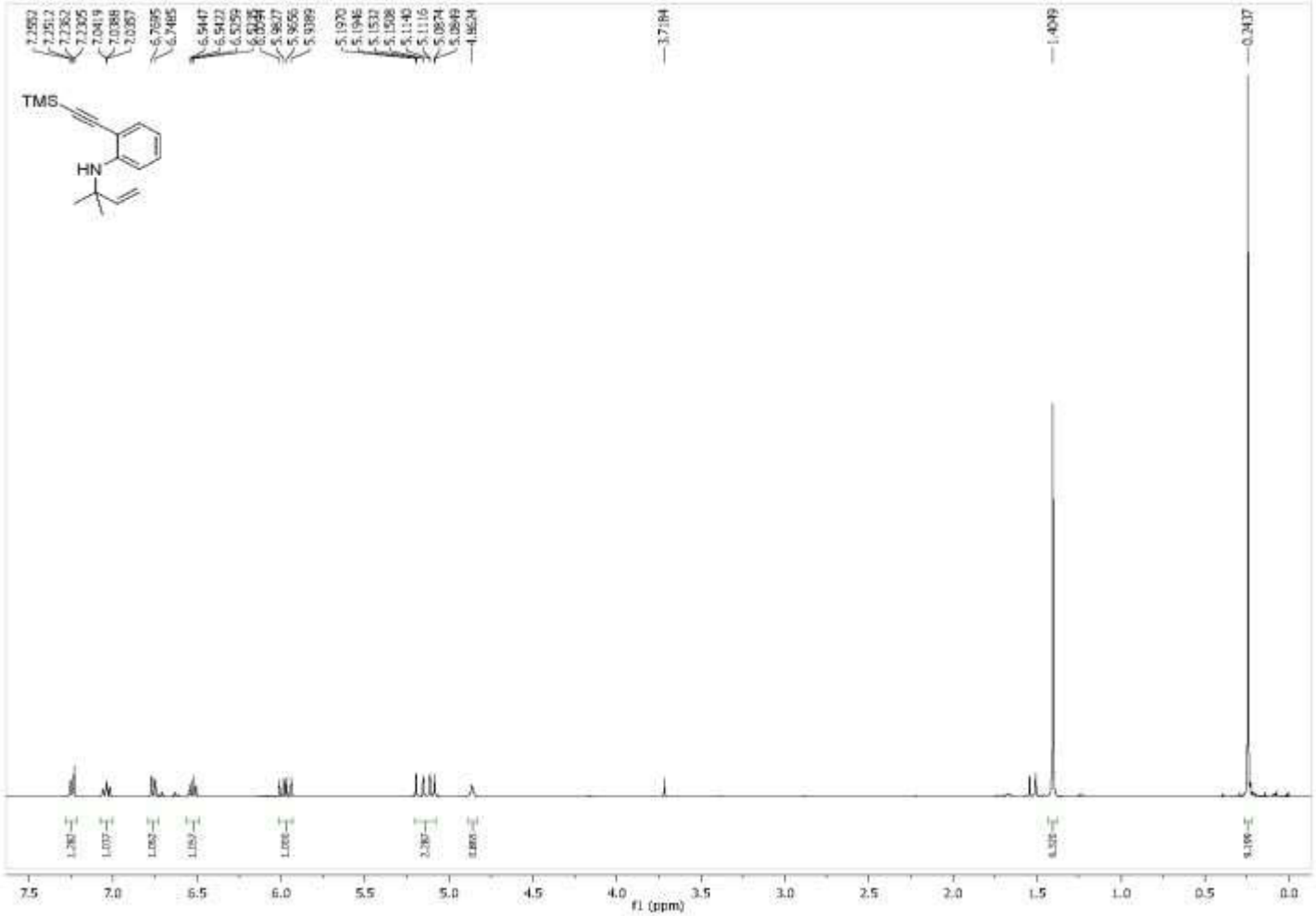

Figure A155 400 MHz 1H NMR ($CDCl_3$) Spectra of Compound **253o**

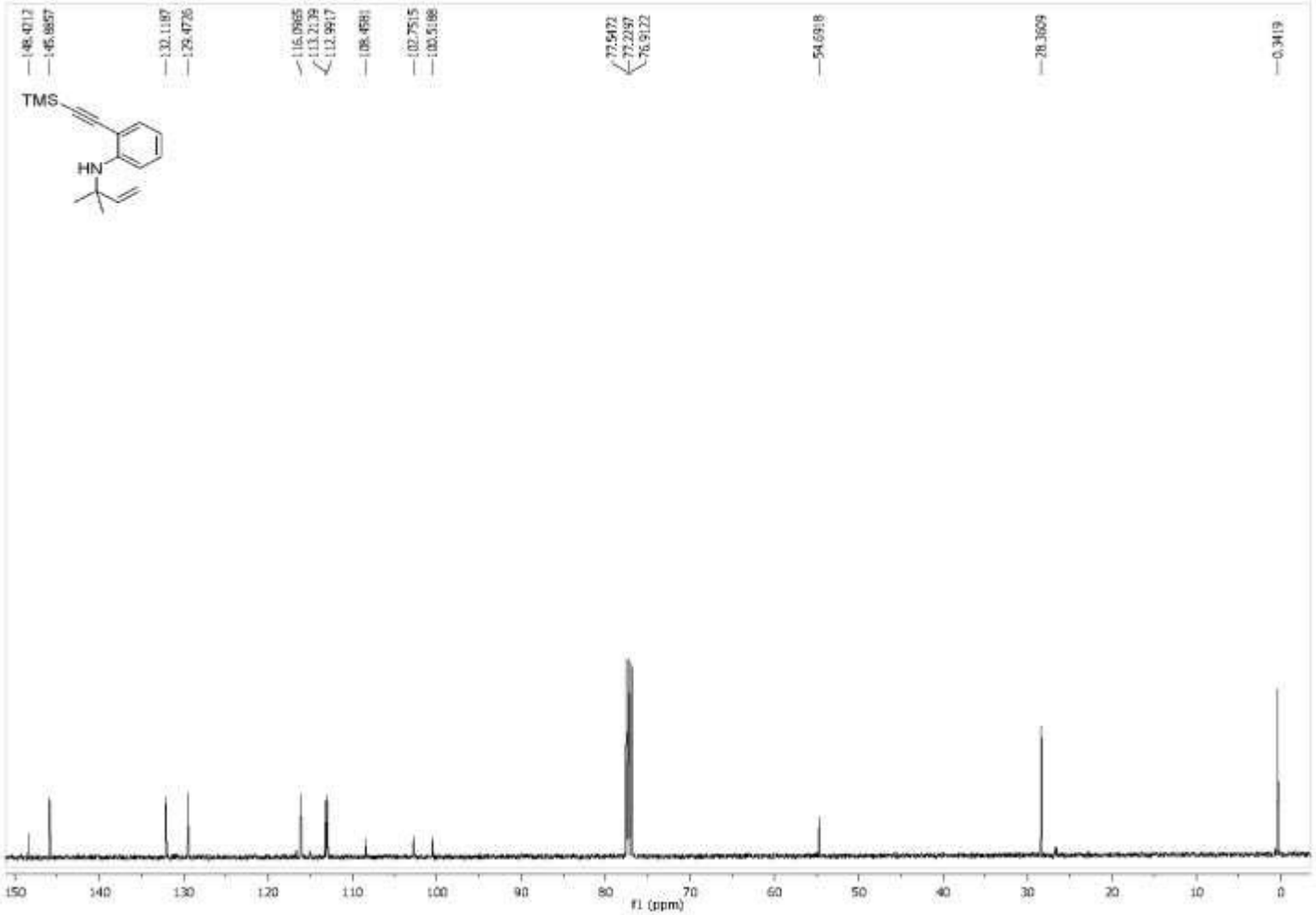

Figure A156 100 MHz 13C NMR ($CDCl_3$) Spectra of Compound **253o**

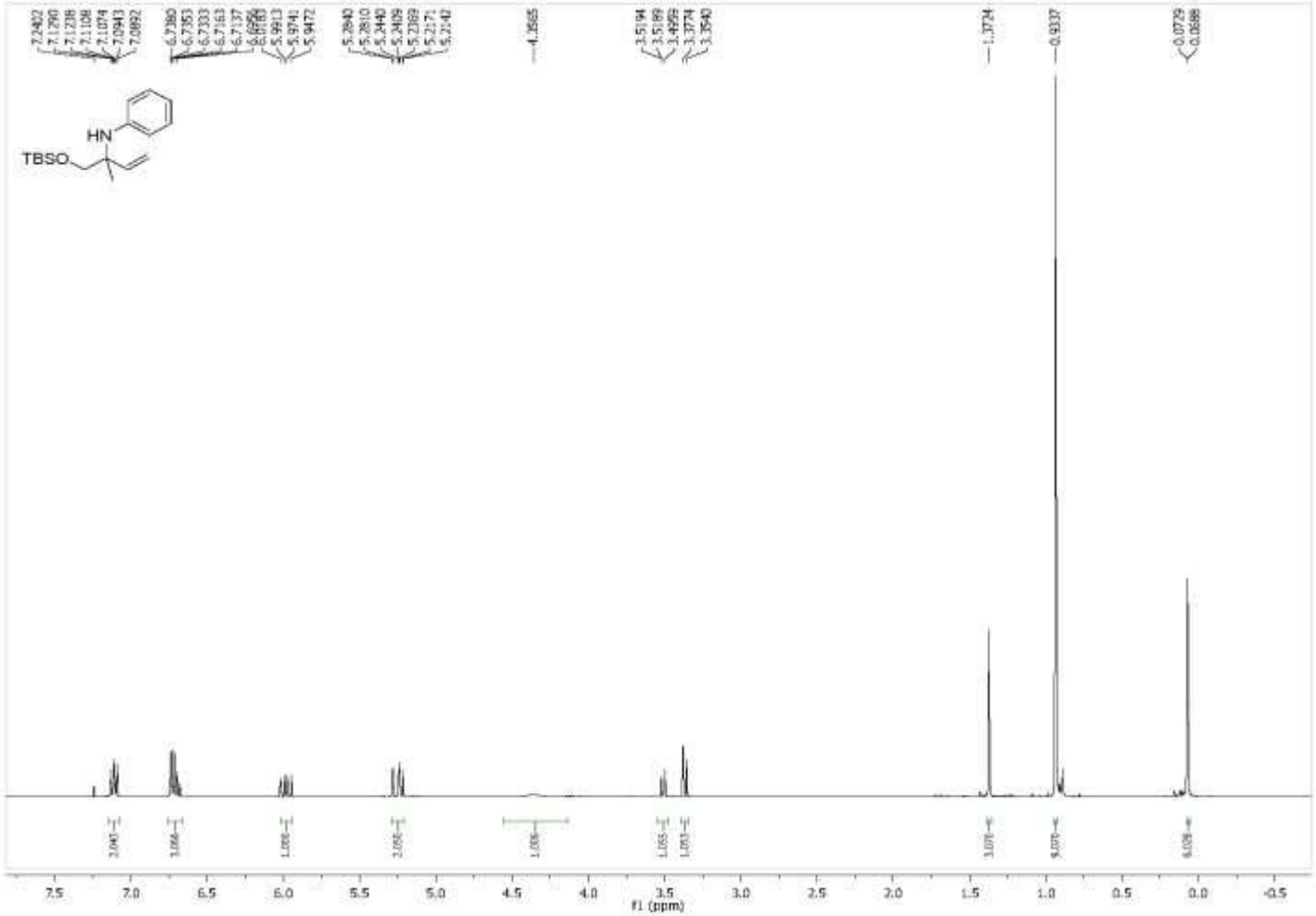

Figure A157 400 MHz 1H NMR ($CDCl_3$) Spectra of Compound **254a**

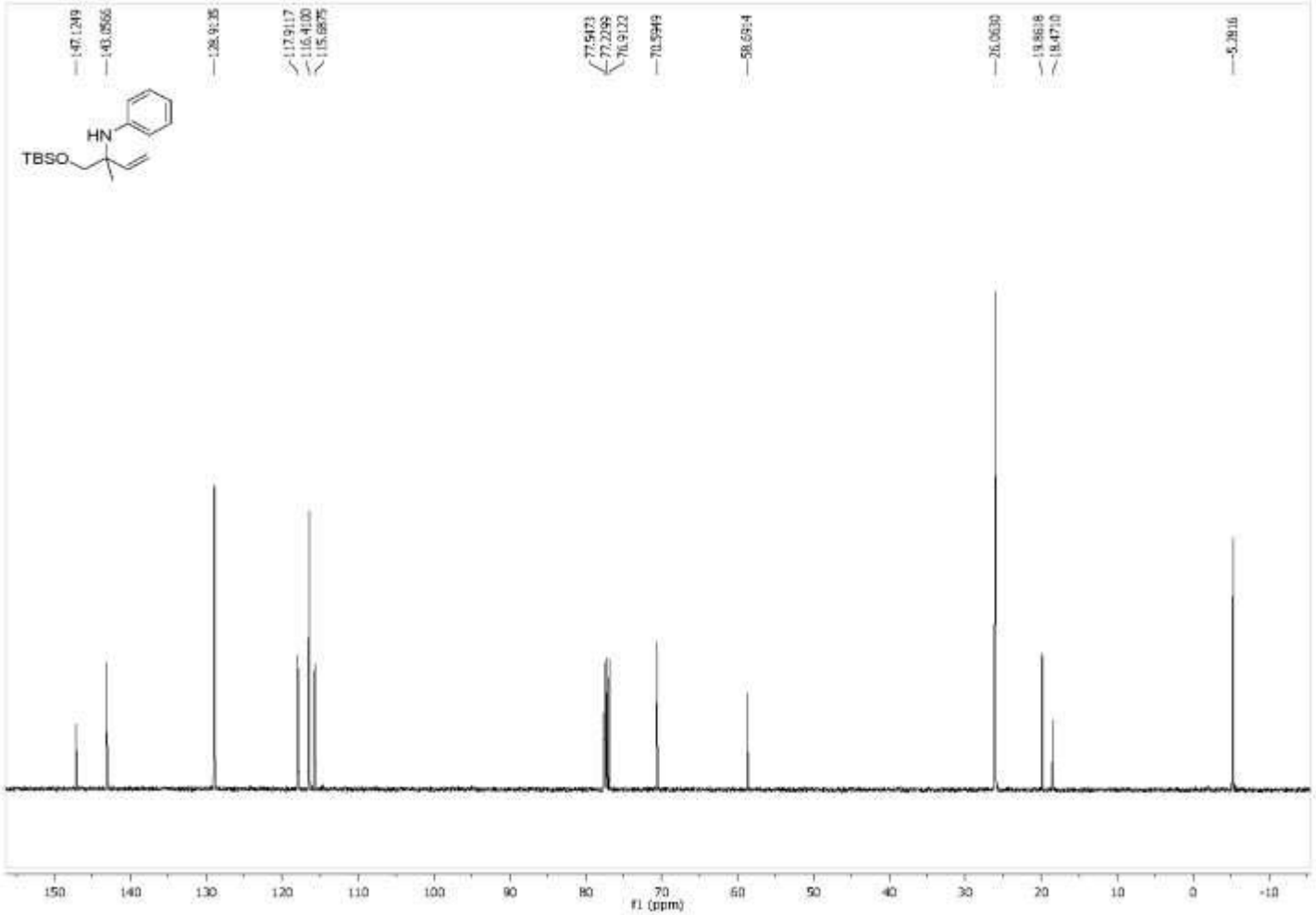

Figure A158 100 MHz 13C NMR ($CDCl_3$) Spectra of Compound **254a**

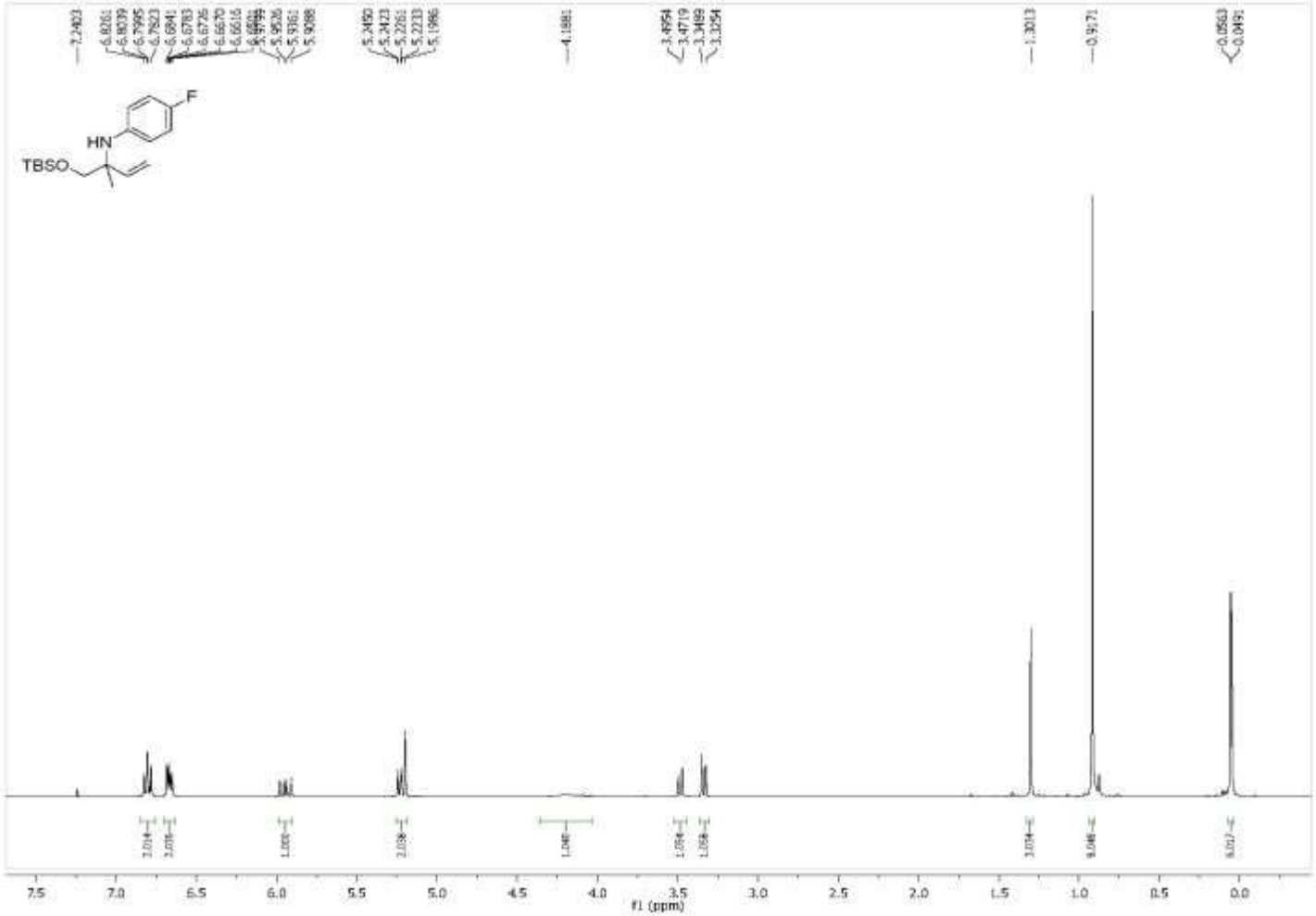

Figure A159 400 MHz 1H NMR ($CDCl_3$) Spectra of Compound **254b**

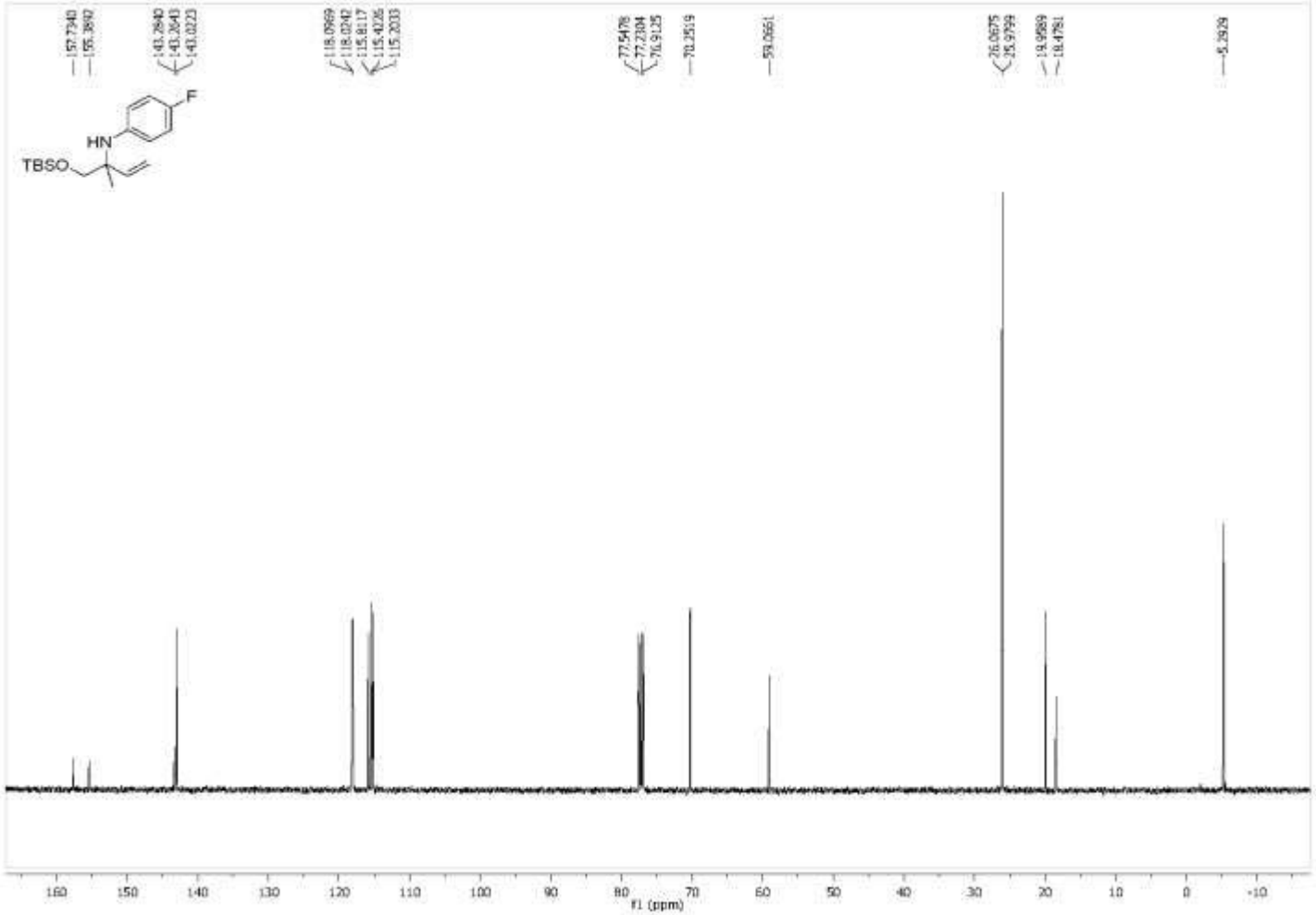

Figure A160 100 MHz 13C NMR ($CDCl_3$) Spectra of Compound **254b**

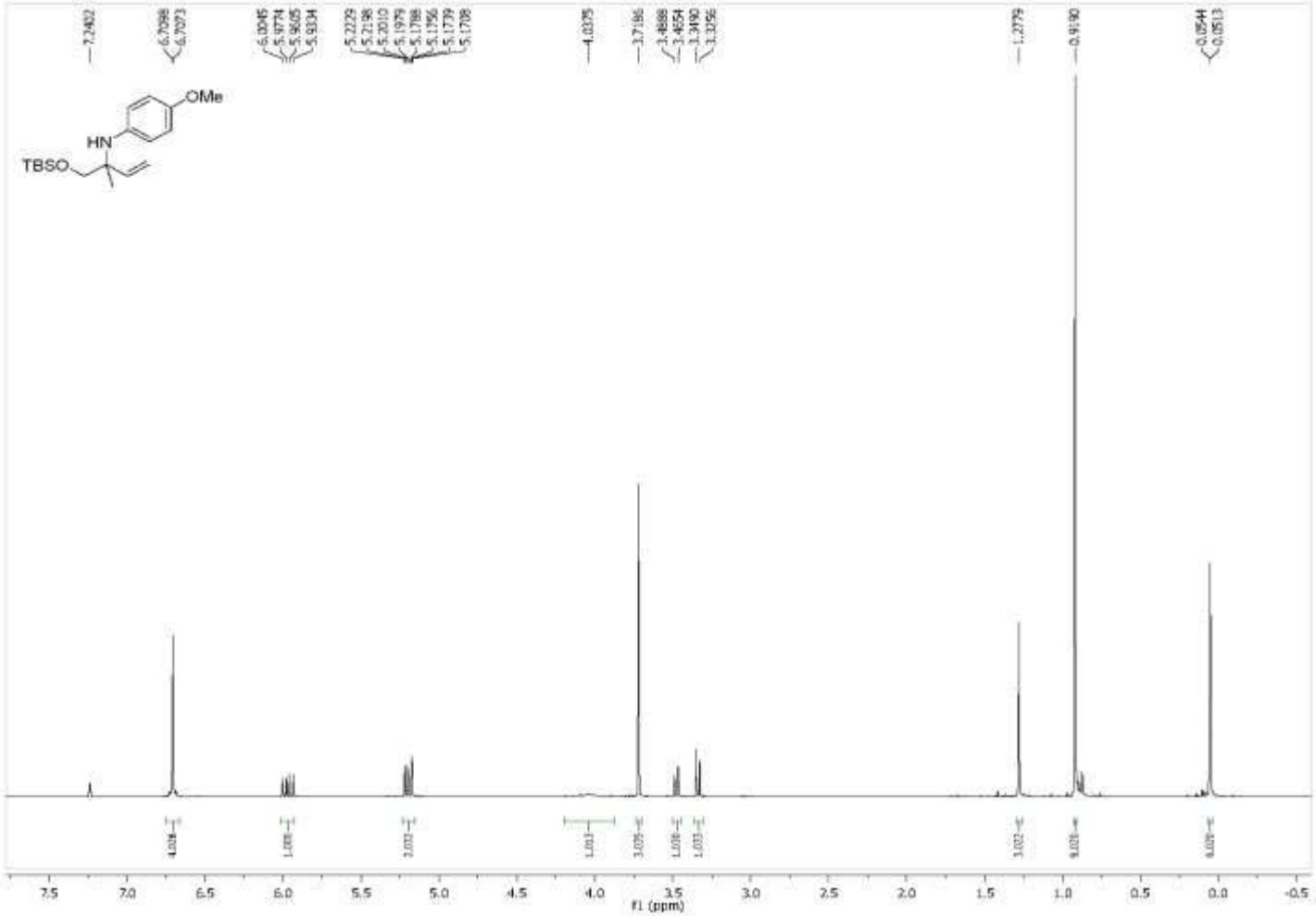

Figure A161 400 MHz 1H NMR ($CDCl_3$) Spectra of Compound **254c**

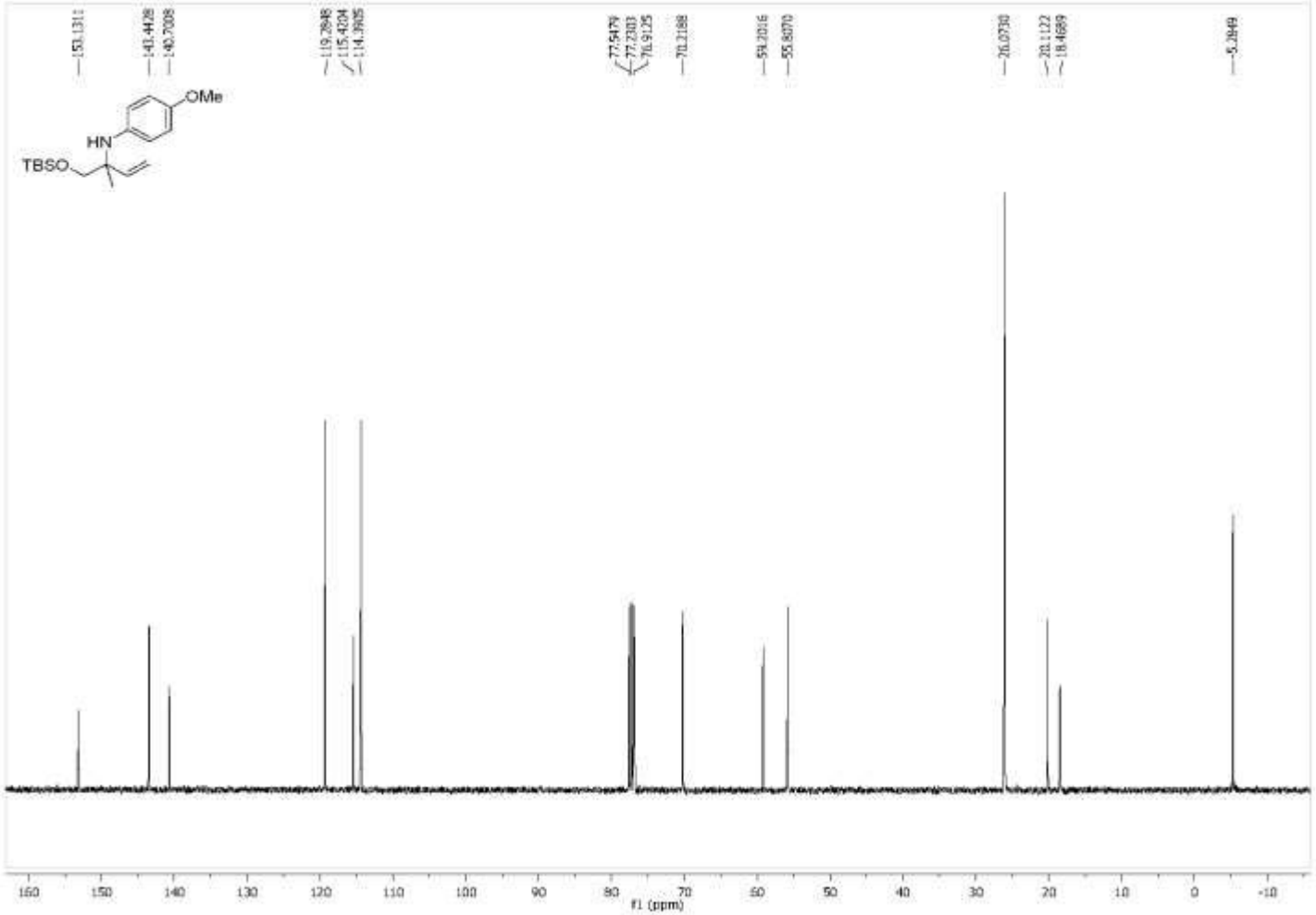

Figure A162 100 MHz 13C NMR ($CDCl_3$) Spectra of Compound **254c**

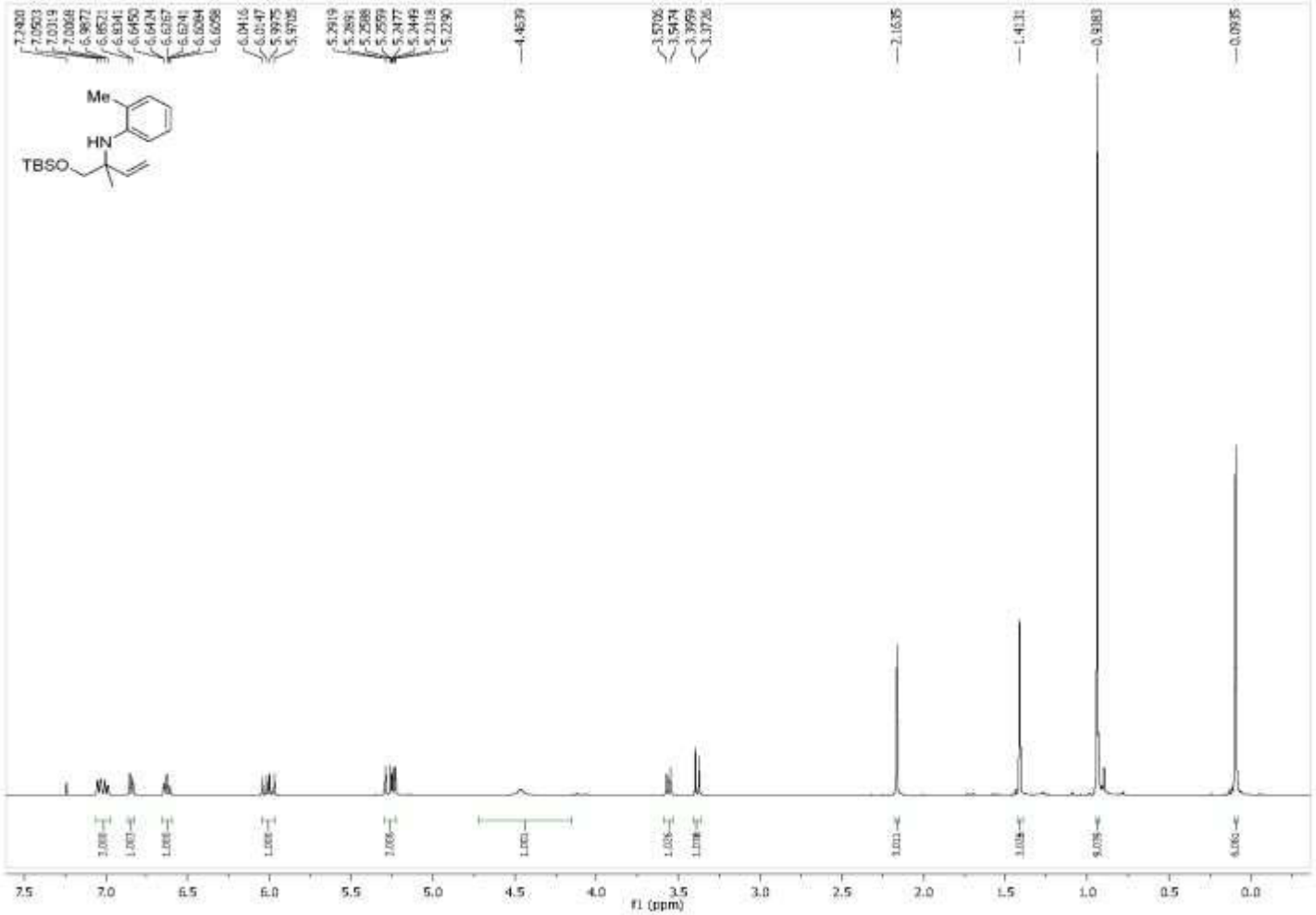

Figure A163 400 MHz 1H NMR ($CDCl_3$) Spectra of Compound **254d**

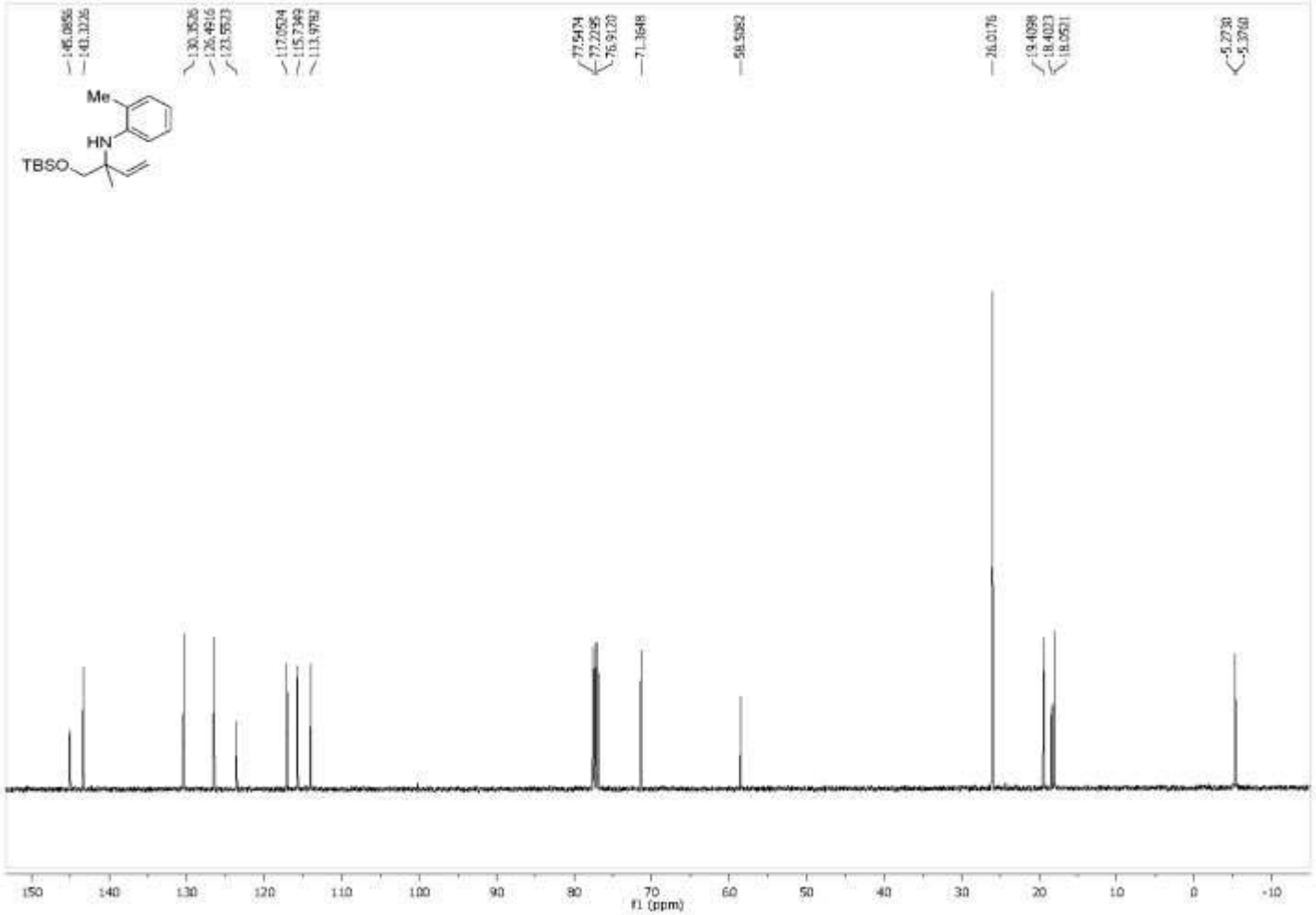

Figure A164 100 MHz 13C NMR ($CDCl_3$) Spectra of Compound **254d**

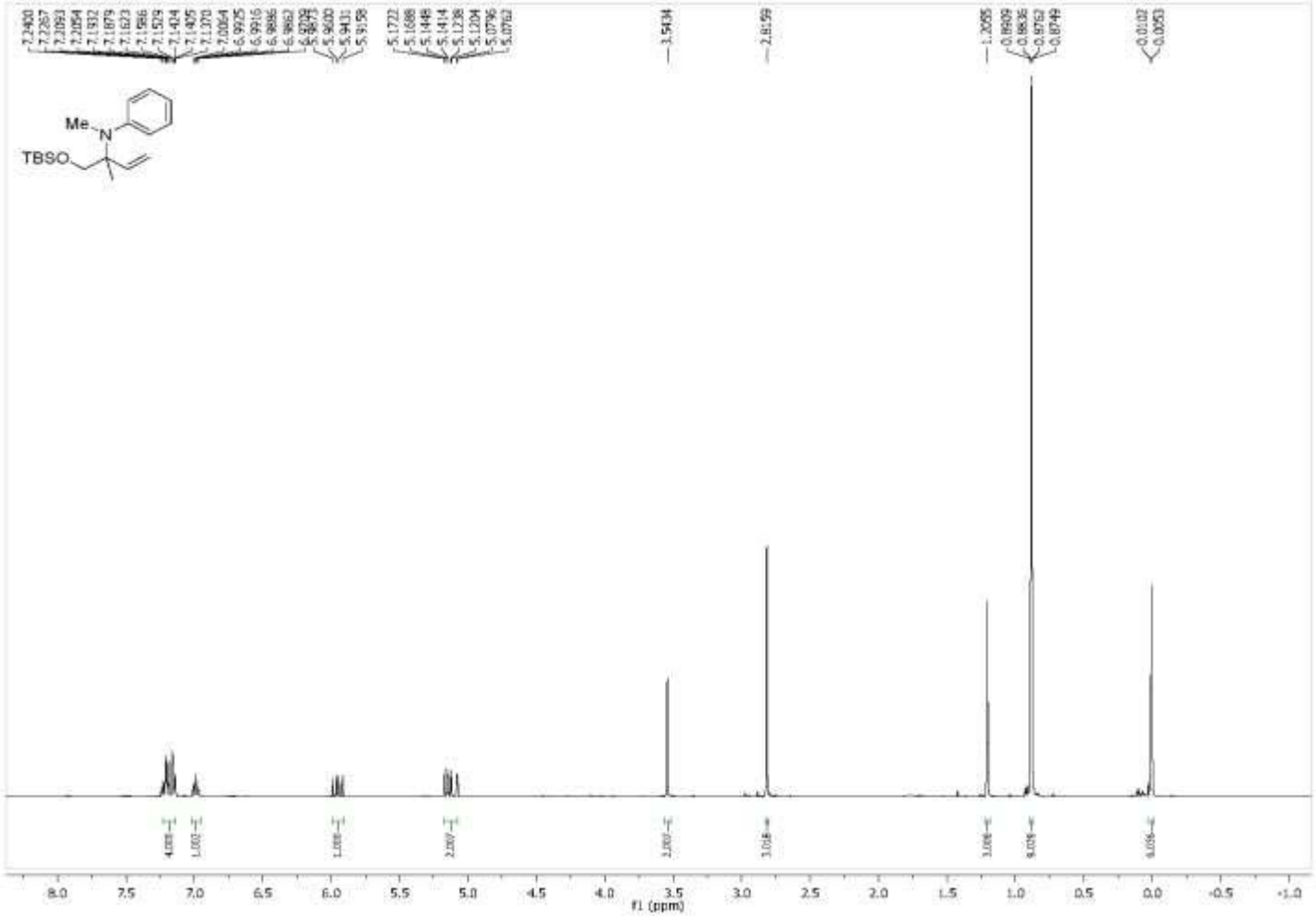

Figure A165 400 MHz 1H NMR ($CDCl_3$) Spectra of Compound **254f**

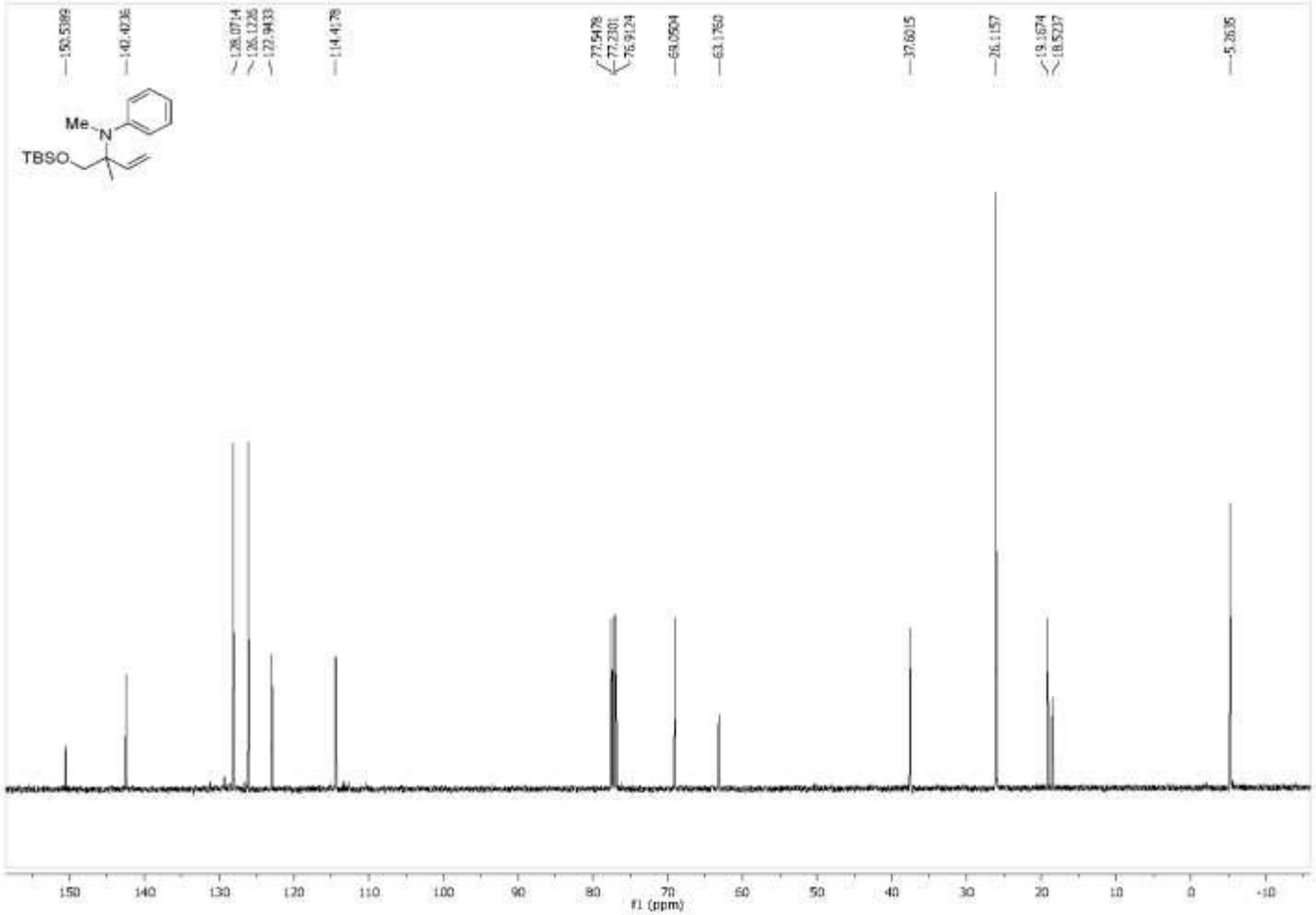

Figure A166 100 MHz 13C NMR ($CDCl_3$) Spectra of Compound **254f**

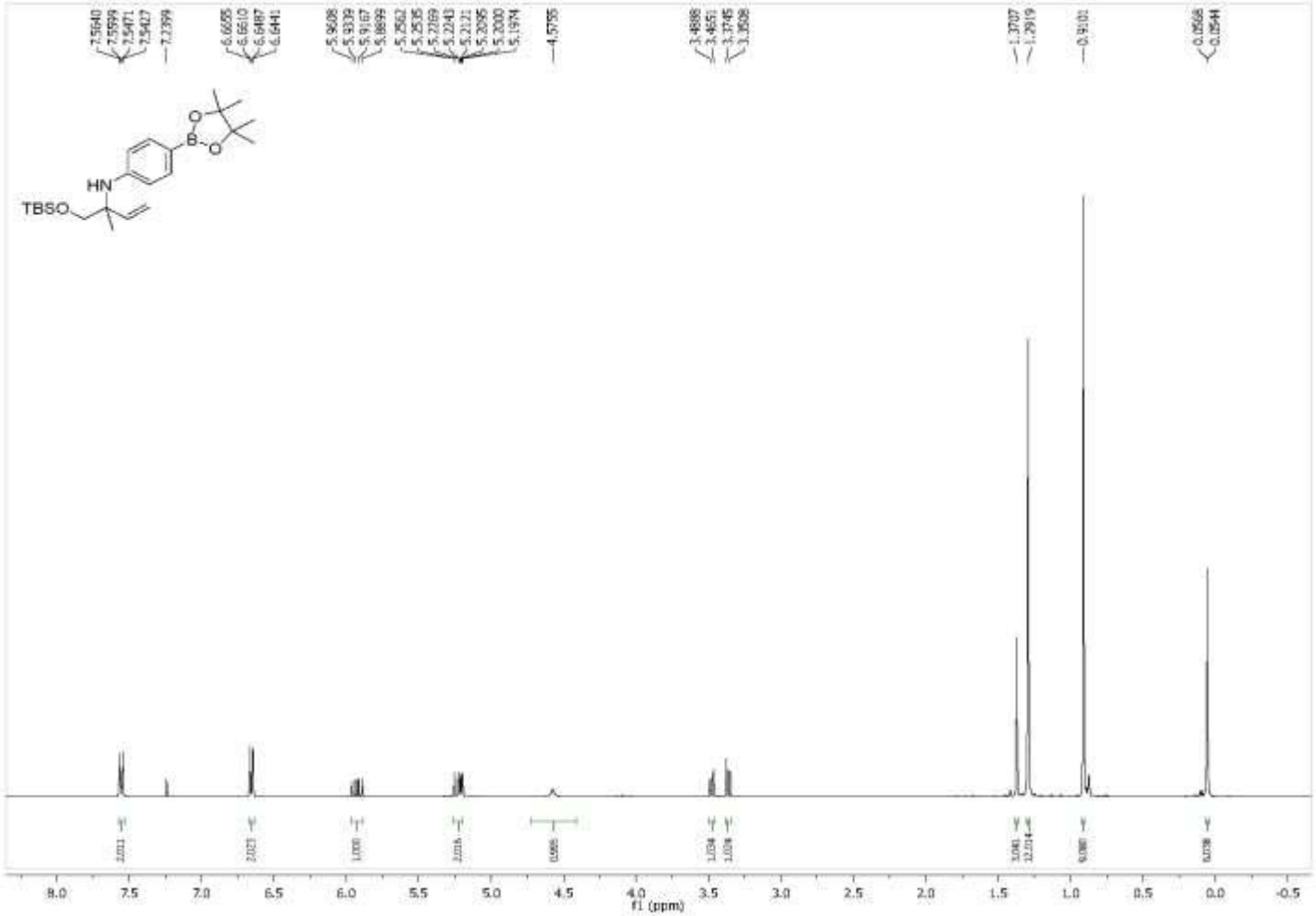

Figure A167 400 MHz 1H NMR ($CDCl_3$) Spectra of Compound **254h**

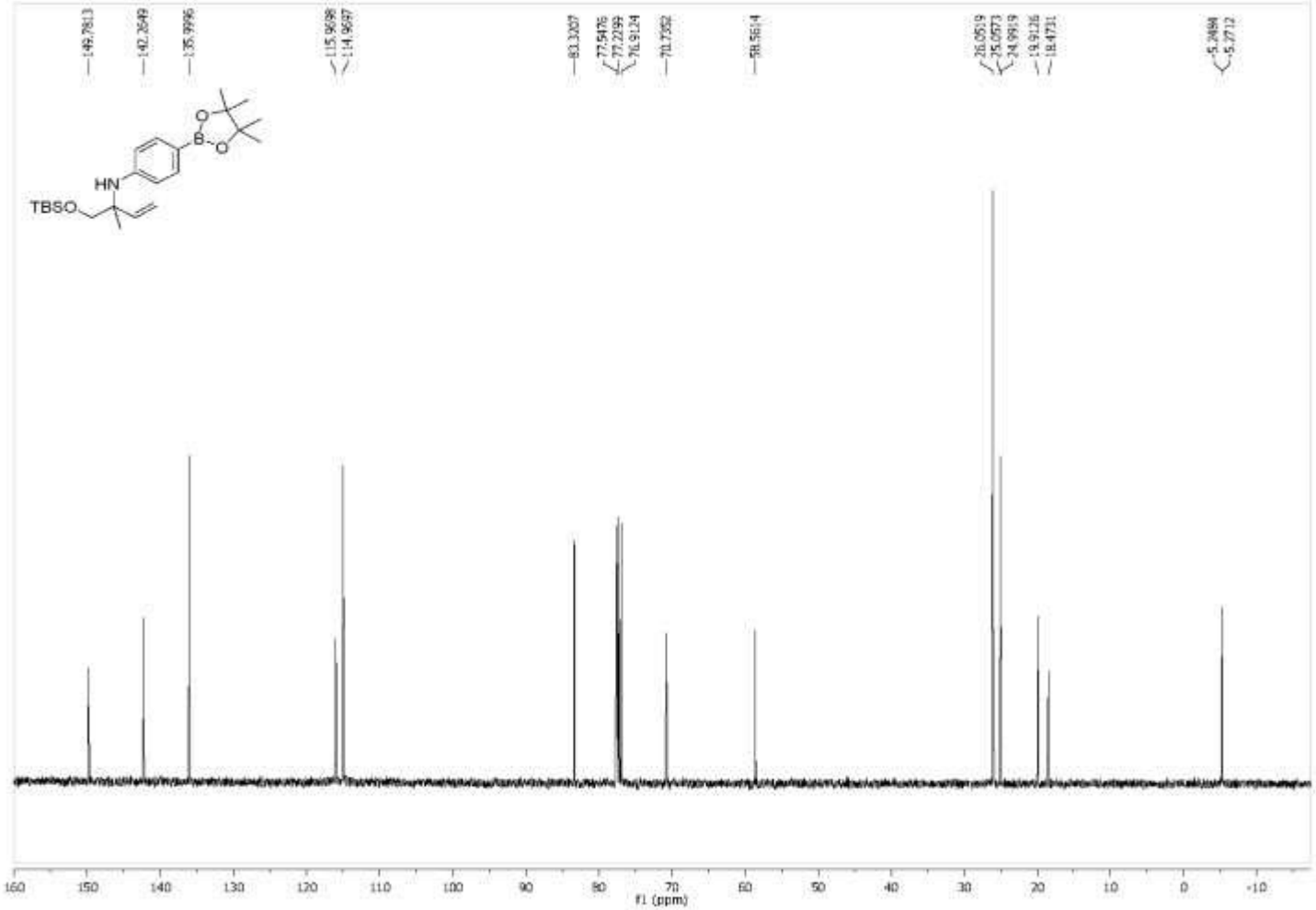

Figure A168 100 MHz 13C NMR ($CDCl_3$) Spectra of Compound **254h**

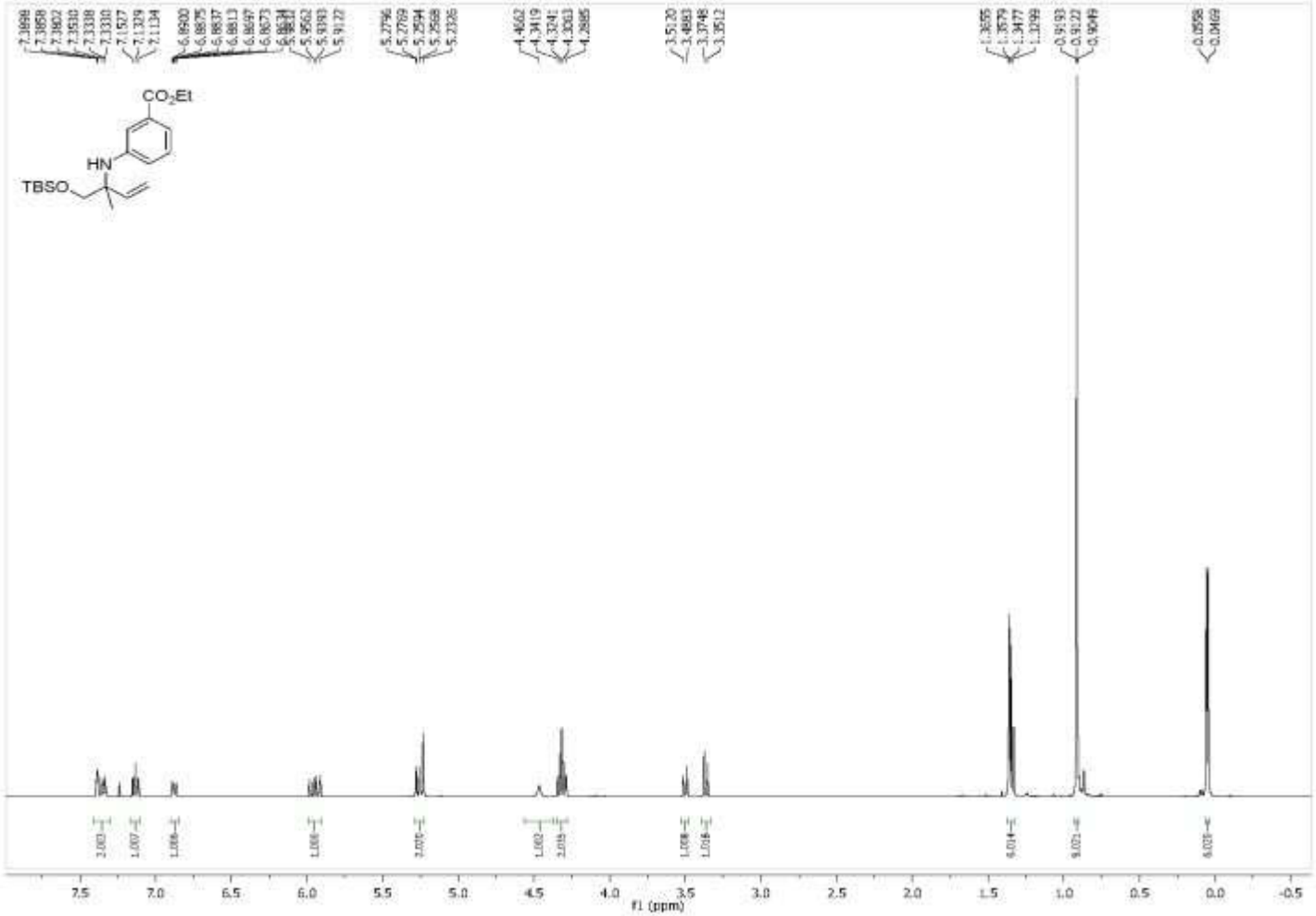

Figure A169 400 MHz 1H NMR ($CDCl_3$) Spectra of Compound **254j**

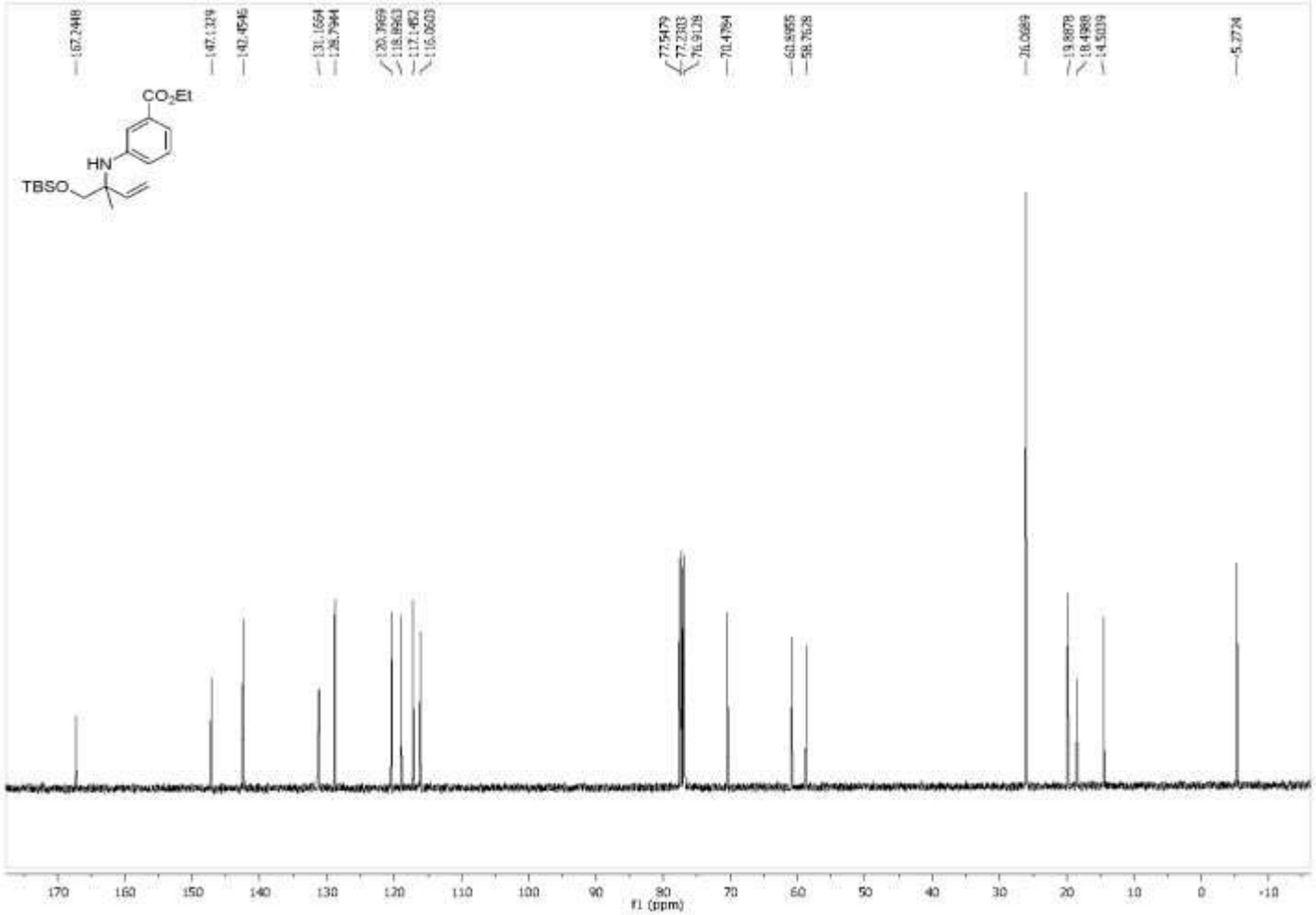

Figure A170 100 MHz 13C NMR ($CDCl_3$) Spectra of Compound **254j**

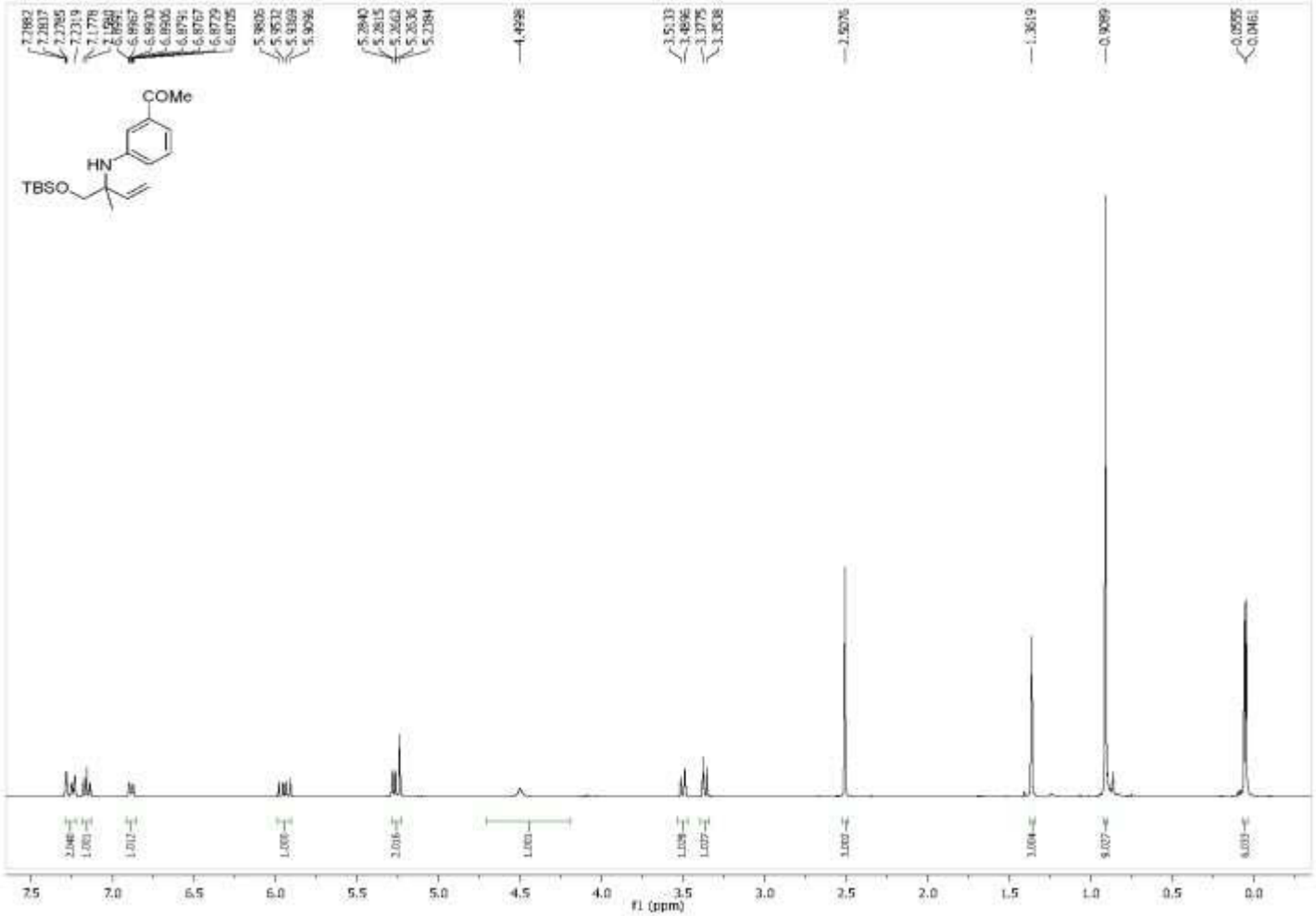

Figure A171 400 MHz 1H NMR ($CDCl_3$) Spectra of Compound **254k**

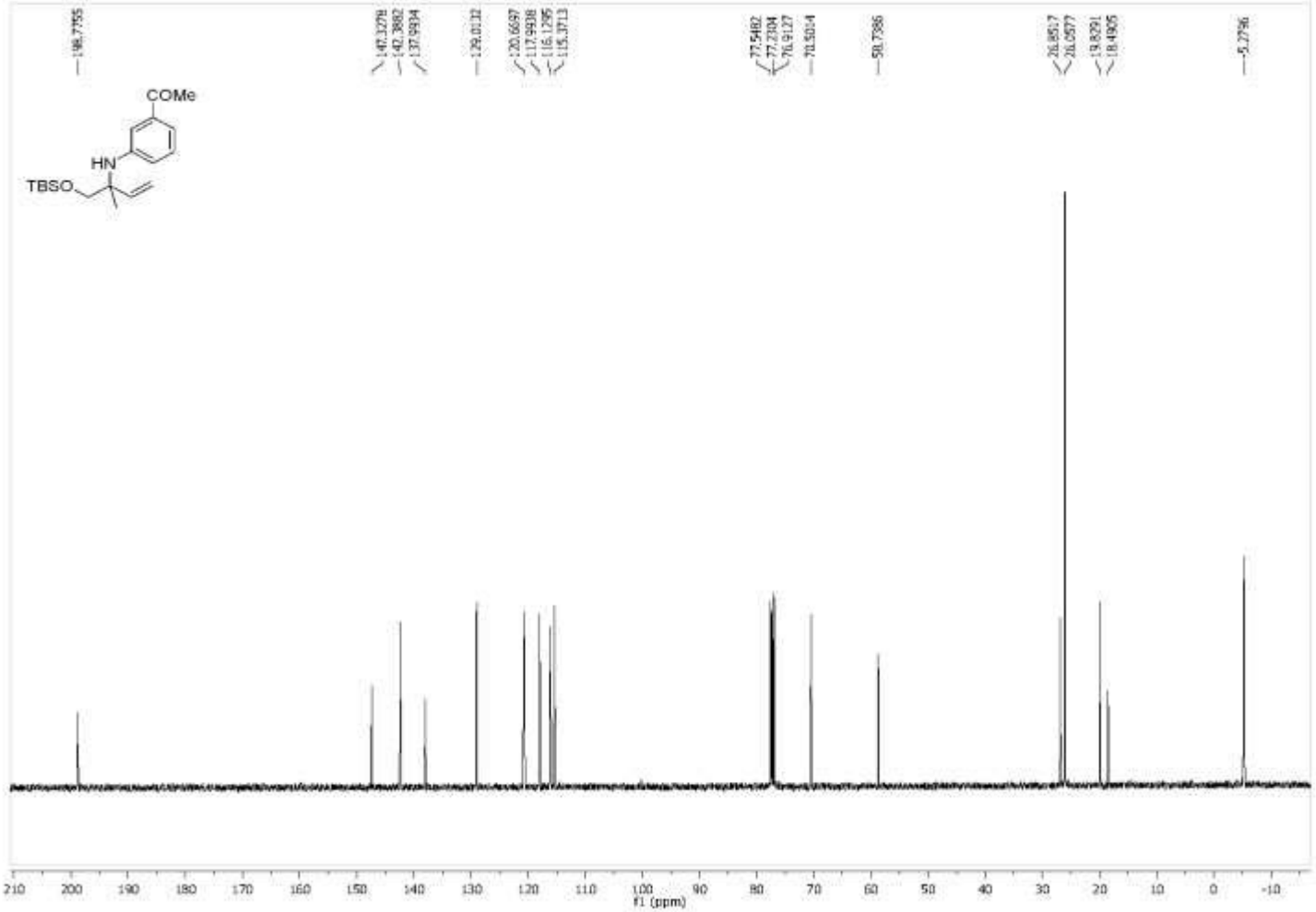

Figure A172 100 MHz 13C NMR ($CDCl_3$) Spectra of Compound **254k**

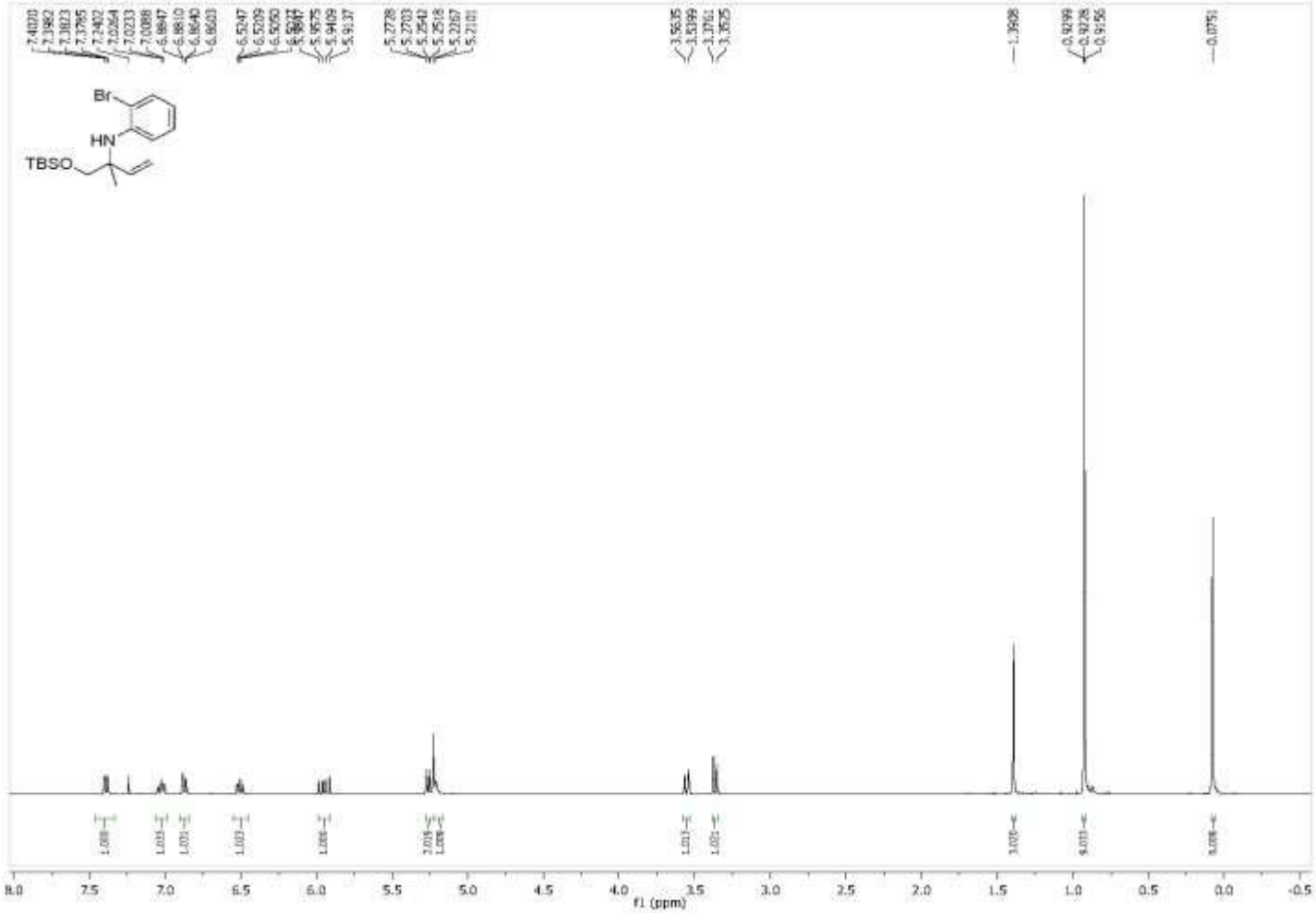

Figure A173 400 MHz 1H NMR ($CDCl_3$) Spectra of Compound **254m**

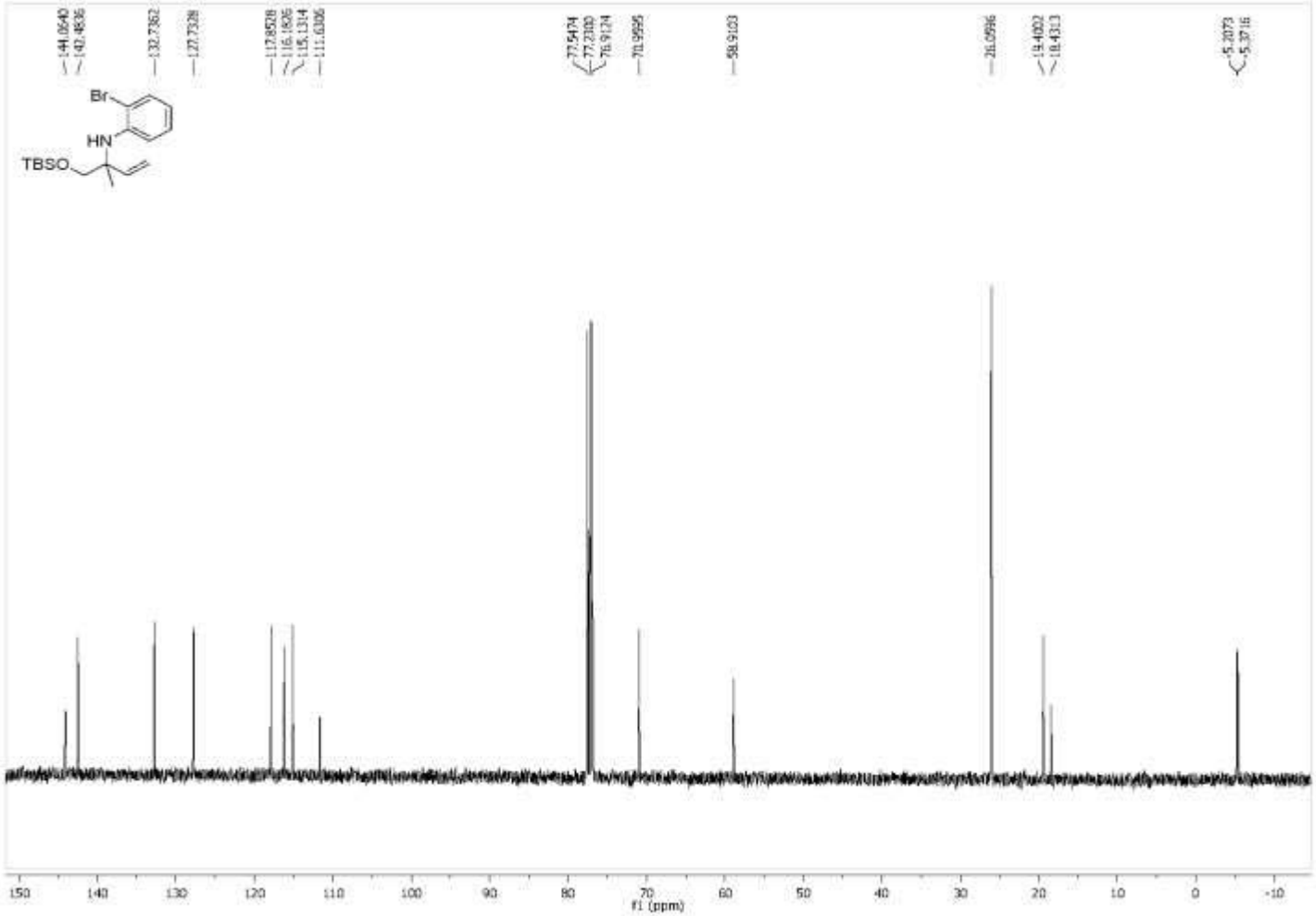

Figure A174 100 MHz 13C NMR ($CDCl_3$) Spectra of Compound **254m**

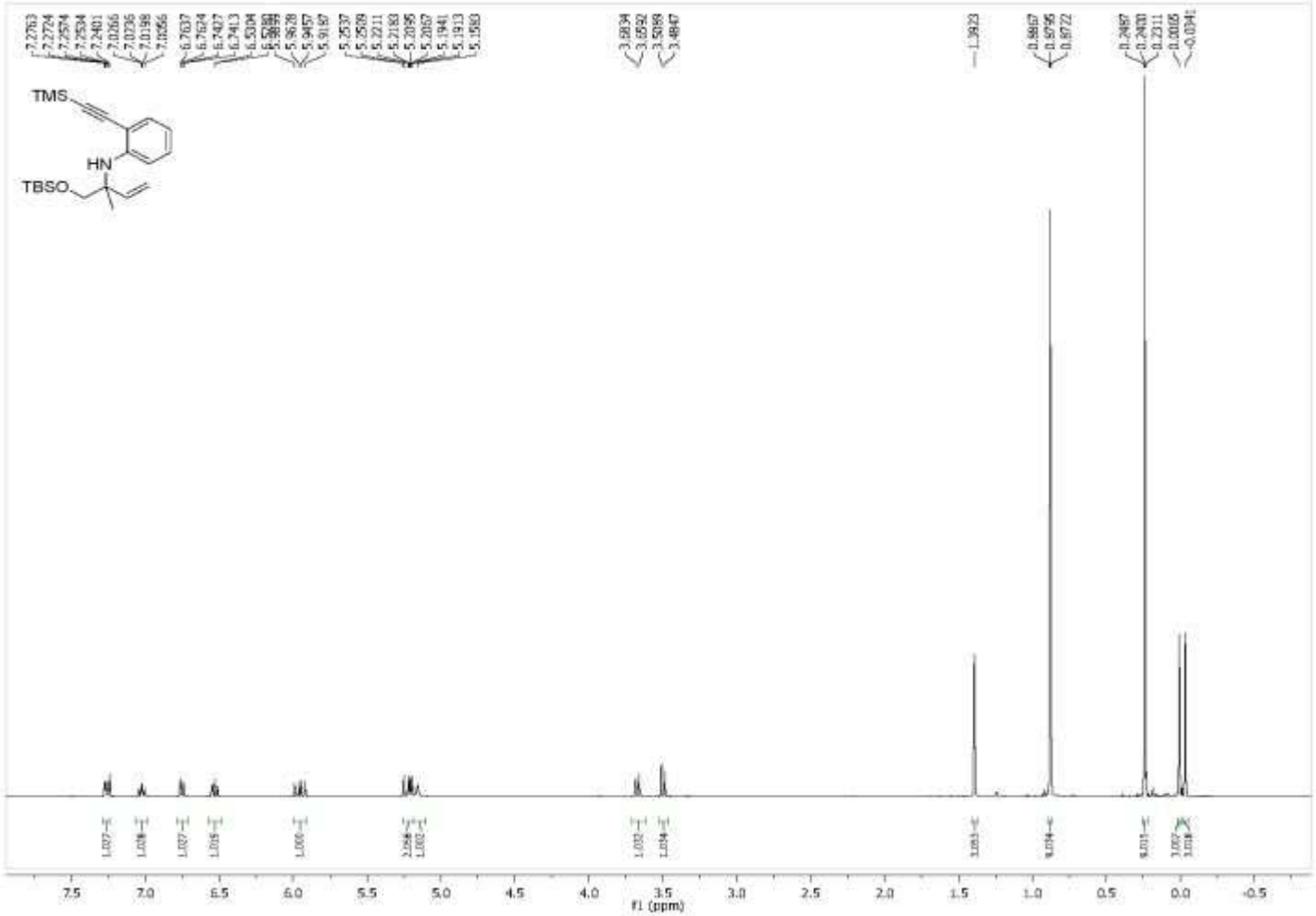

Figure A175 400 MHz 1H NMR ($CDCl_3$) Spectra of Compound **254o**

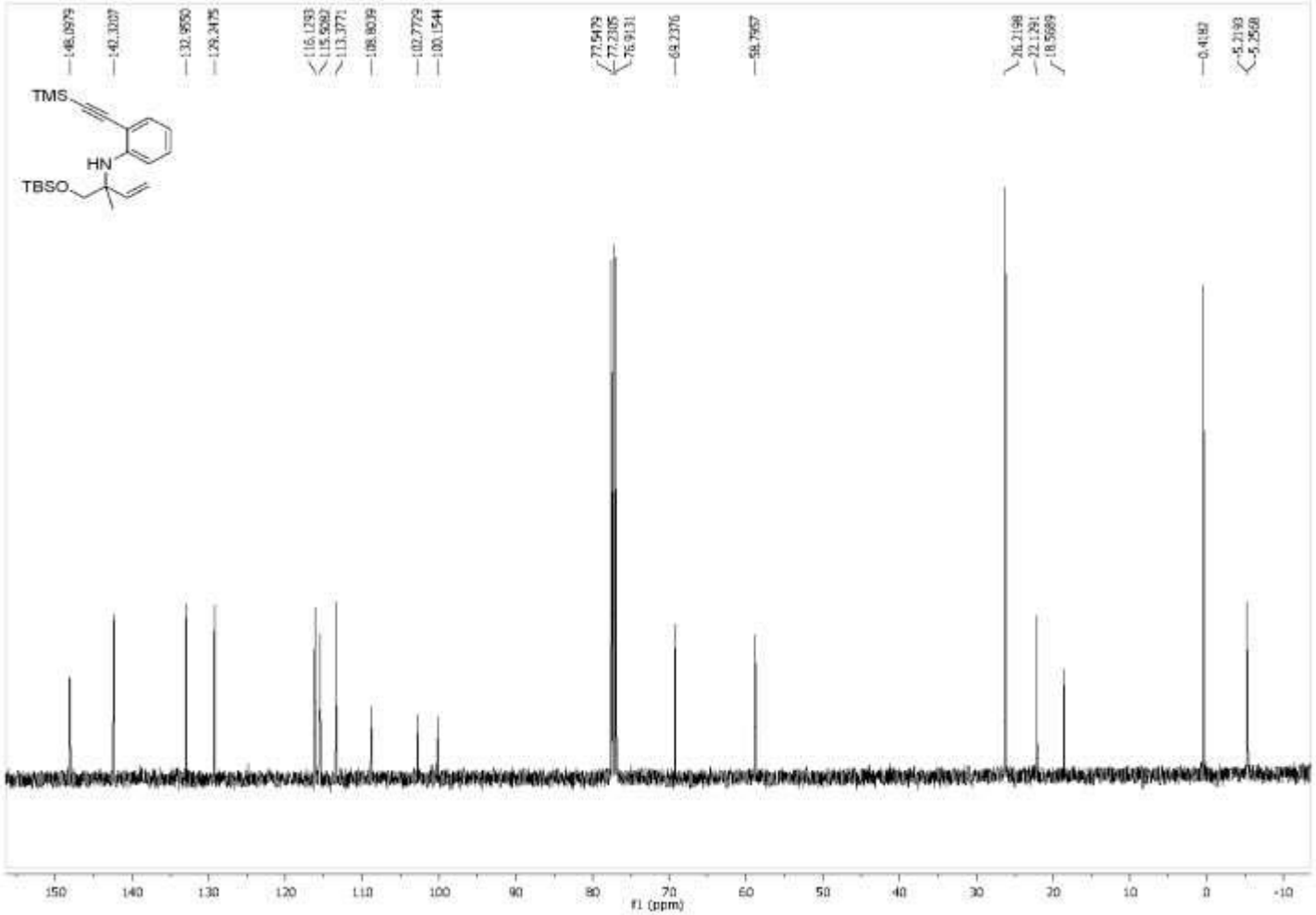

Figure A176 100 MHz 13C NMR ($CDCl_3$) Spectra of Compound **254o**

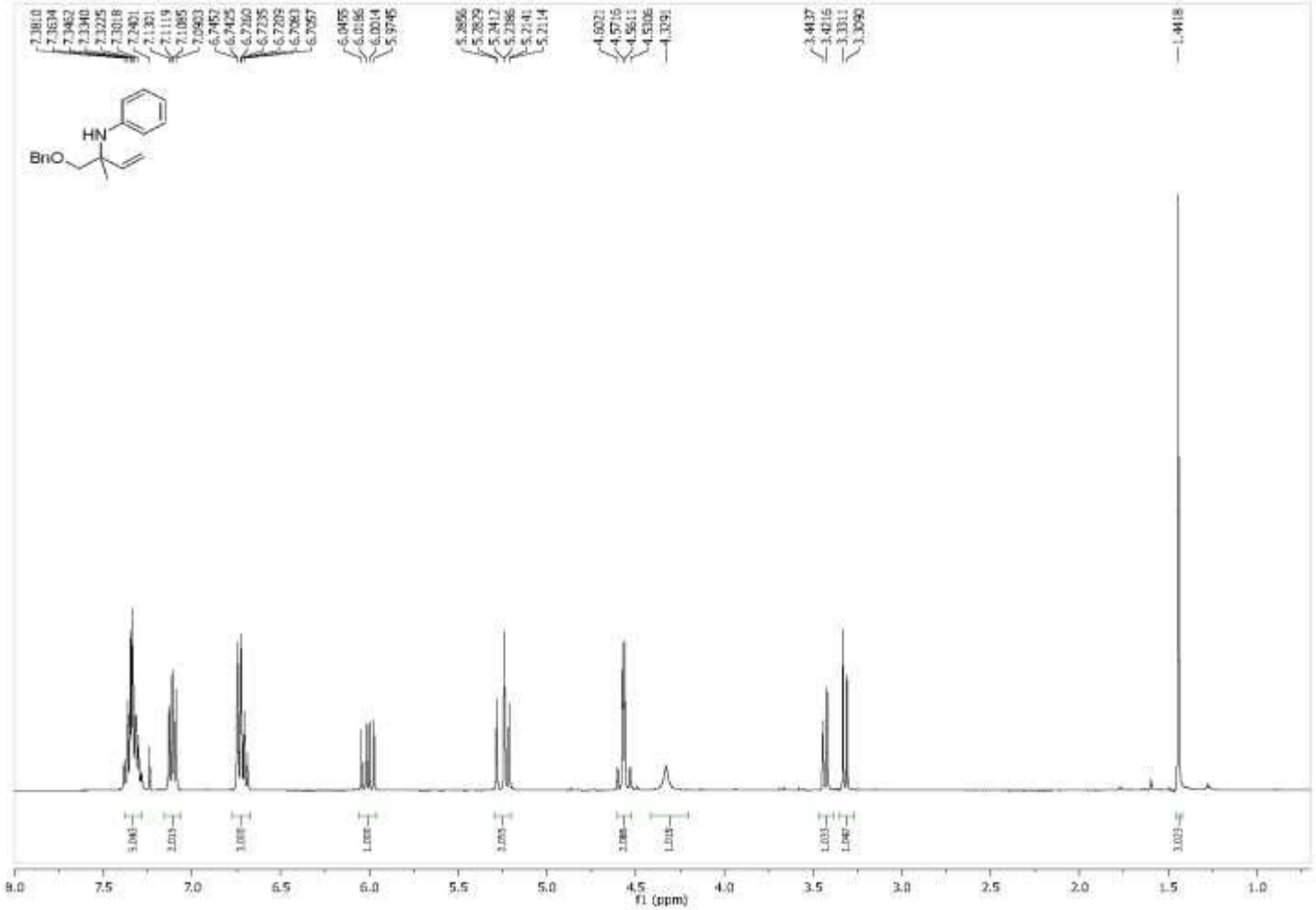

Figure A177 400 MHz 1H NMR ($CDCl_3$) Spectra of Compound **255a**

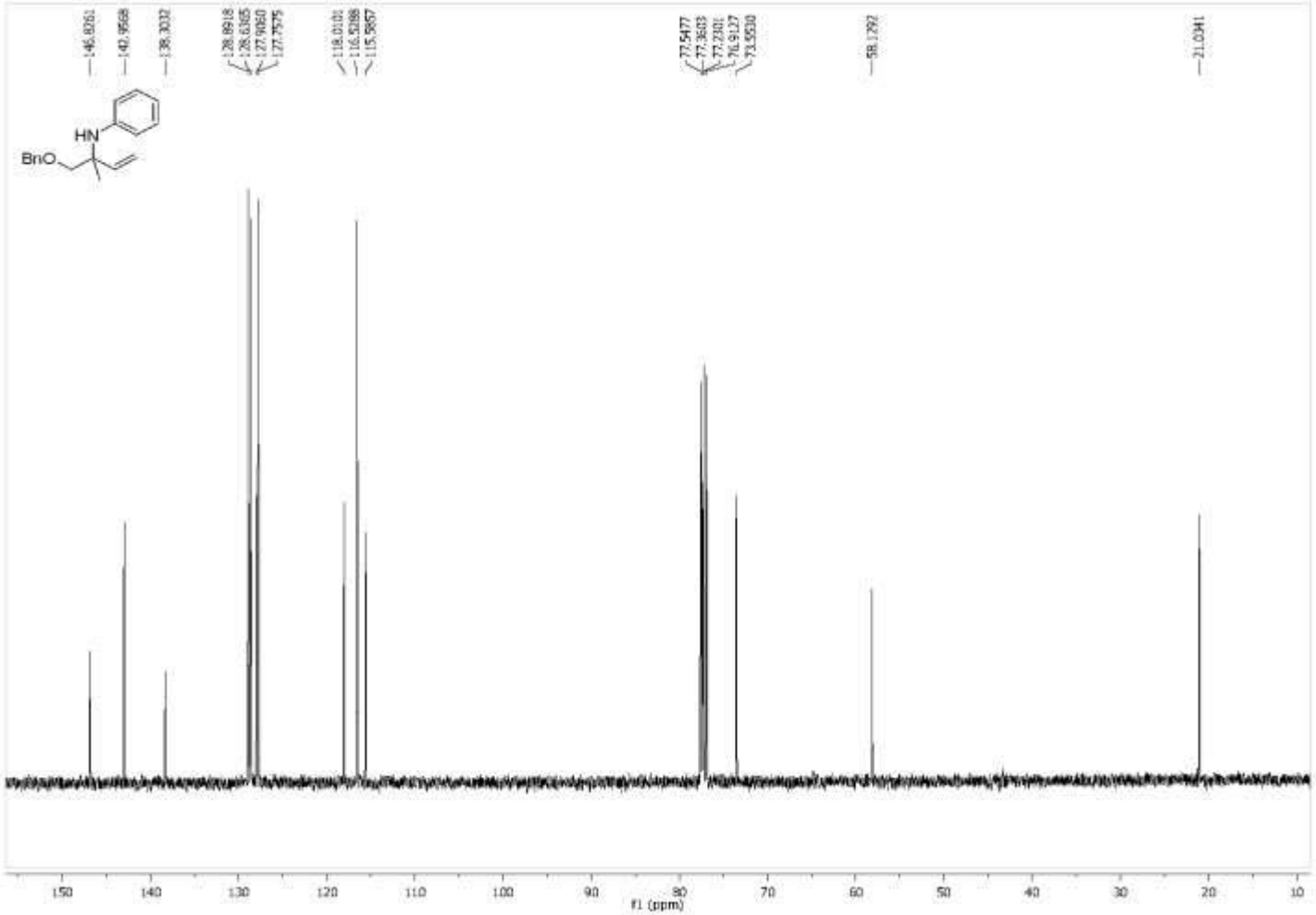

Figure A178 100 MHz 13C NMR ($CDCl_3$) Spectra of Compound **255a**

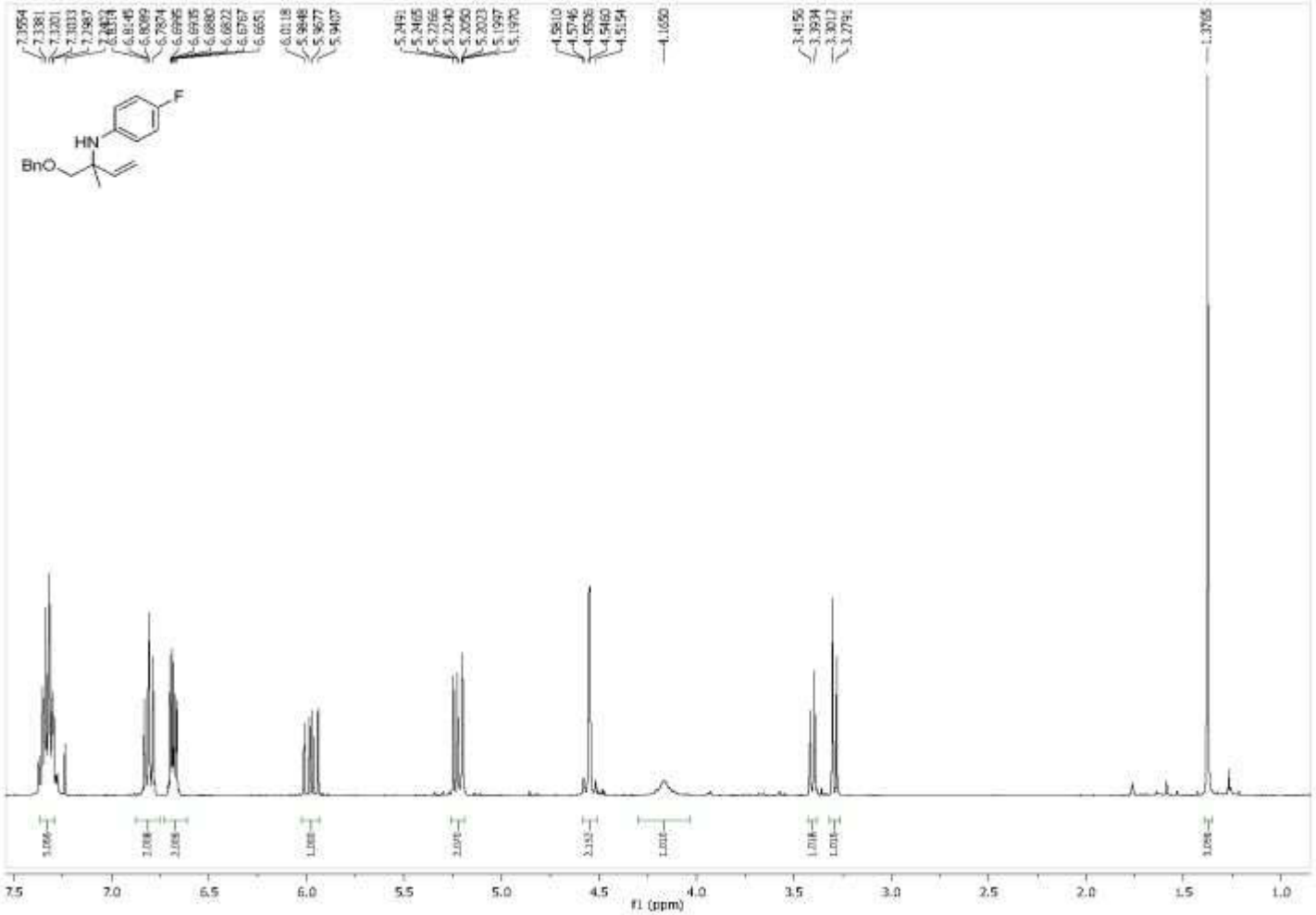

Figure A179 400 MHz 1H NMR ($CDCl_3$) Spectra of Compound **255b**

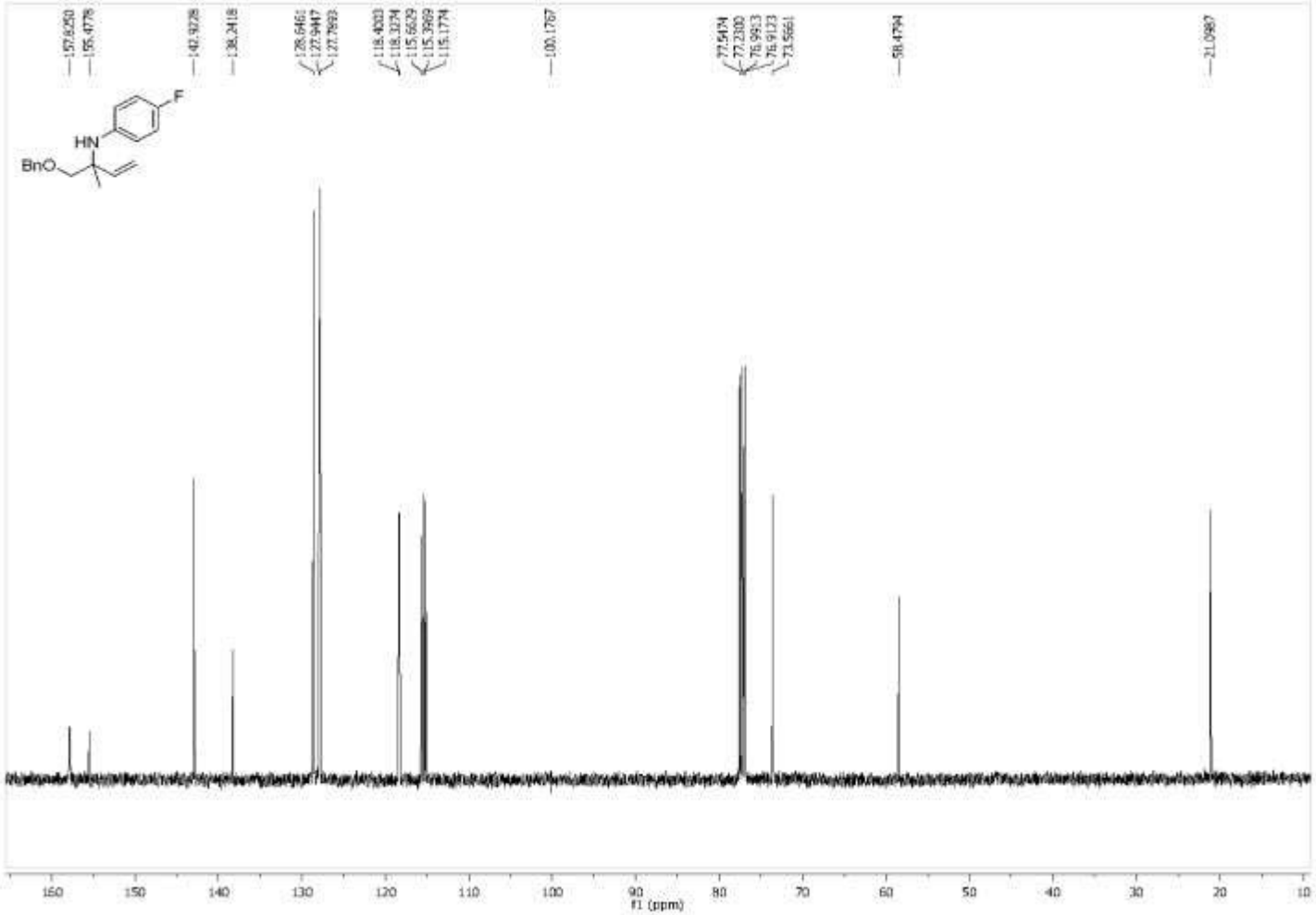

Figure A180 100 MHz 13C NMR ($CDCl_3$) Spectra of Compound **255b**

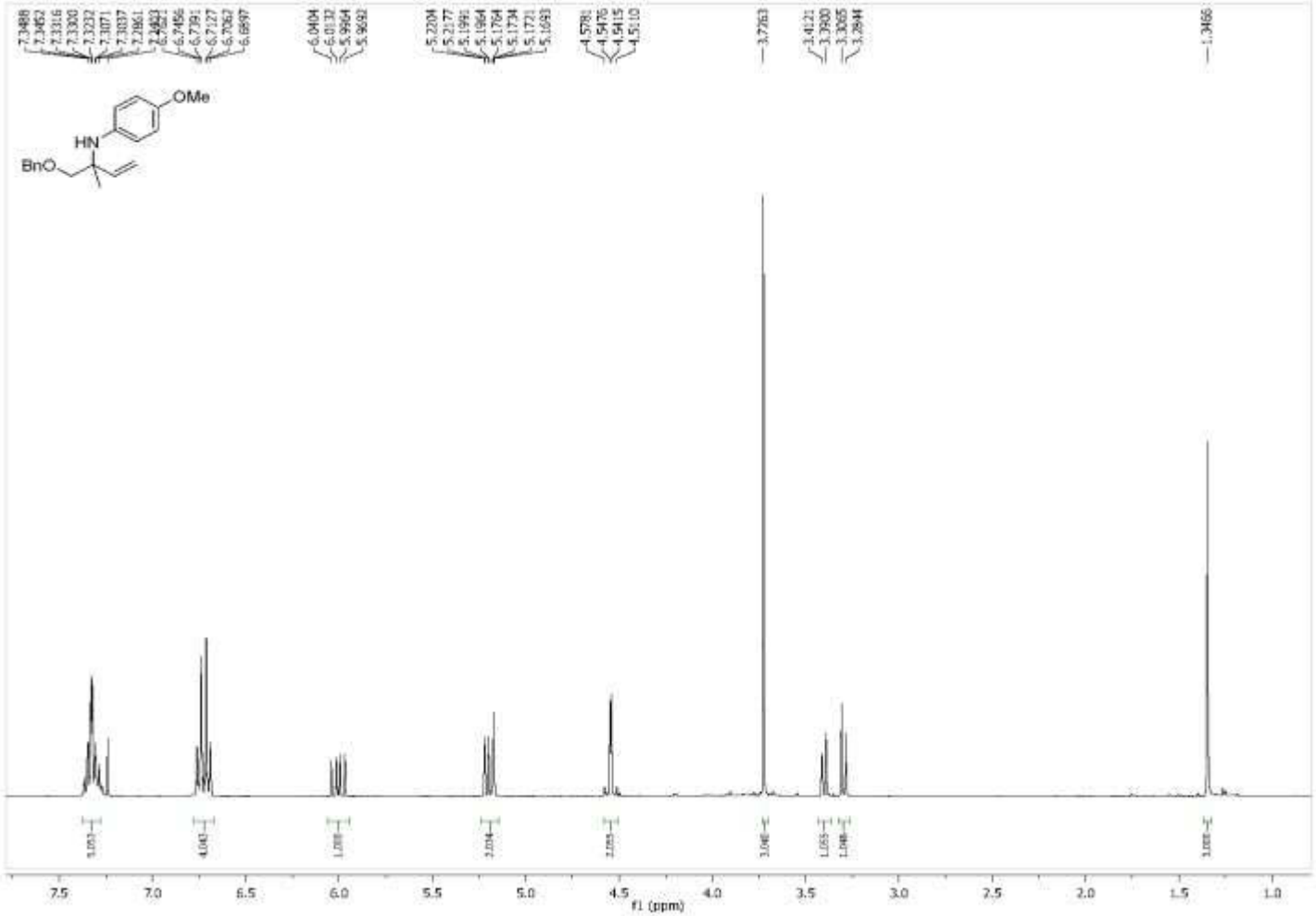

Figure A181 400 MHz 1H NMR ($CDCl_3$) Spectra of Compound **255c**

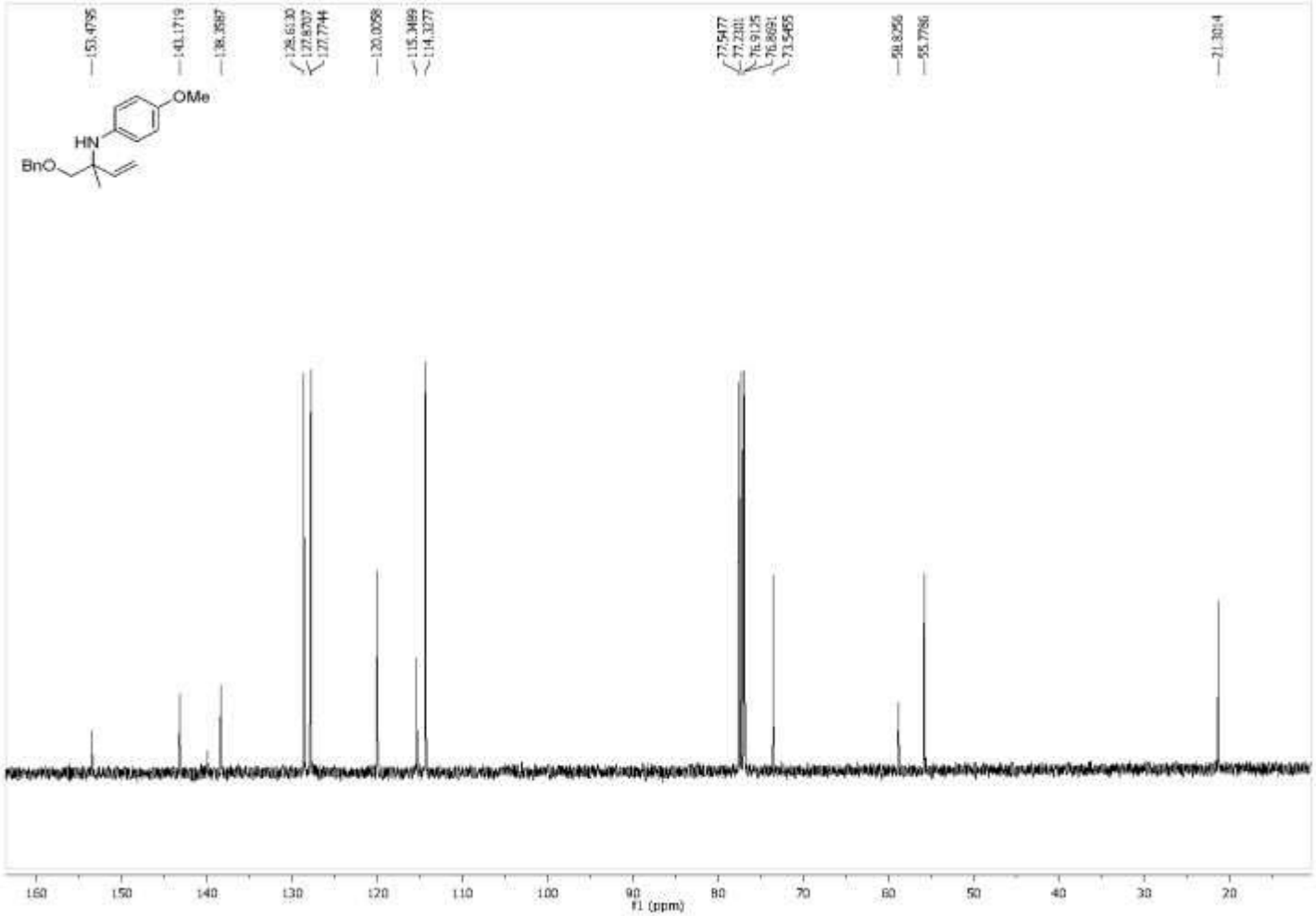

Figure A182 100 MHz 13C NMR ($CDCl_3$) Spectra of Compound **255c**

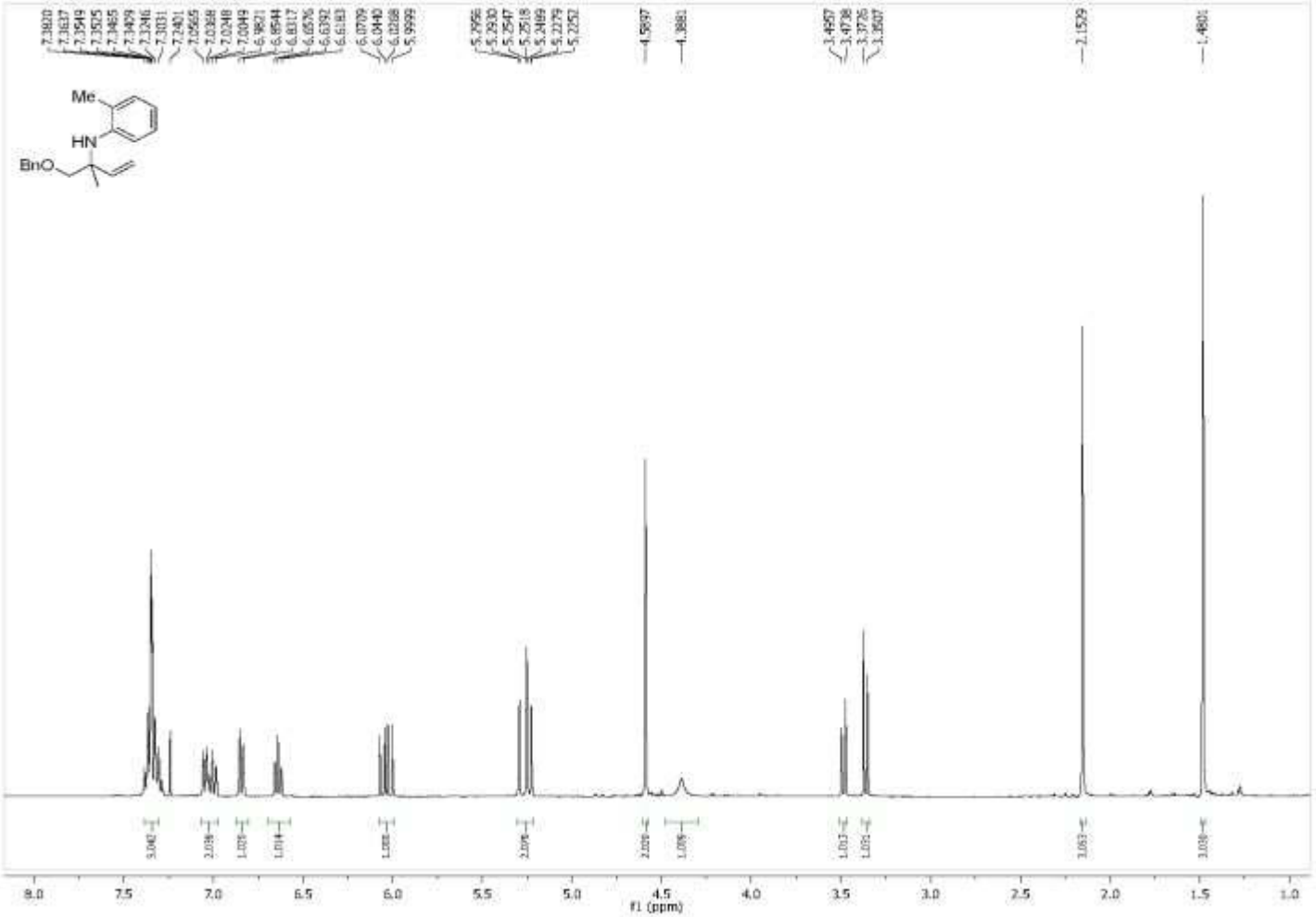

Figure A183 400 MHz 1H NMR ($CDCl_3$) Spectra of Compound **255d**

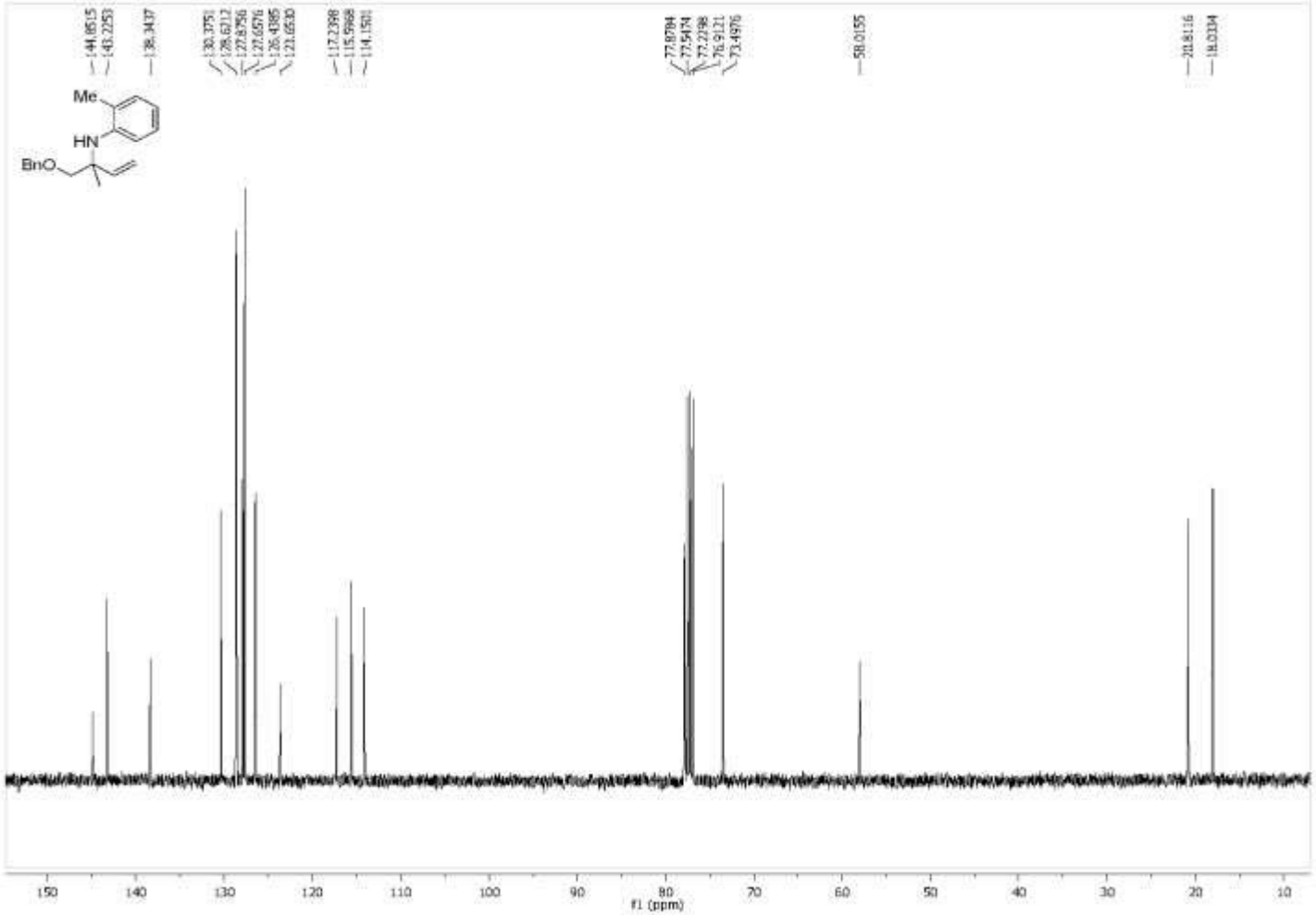

Figure A184 100 MHz 13C NMR ($CDCl_3$) Spectra of Compound **255d**

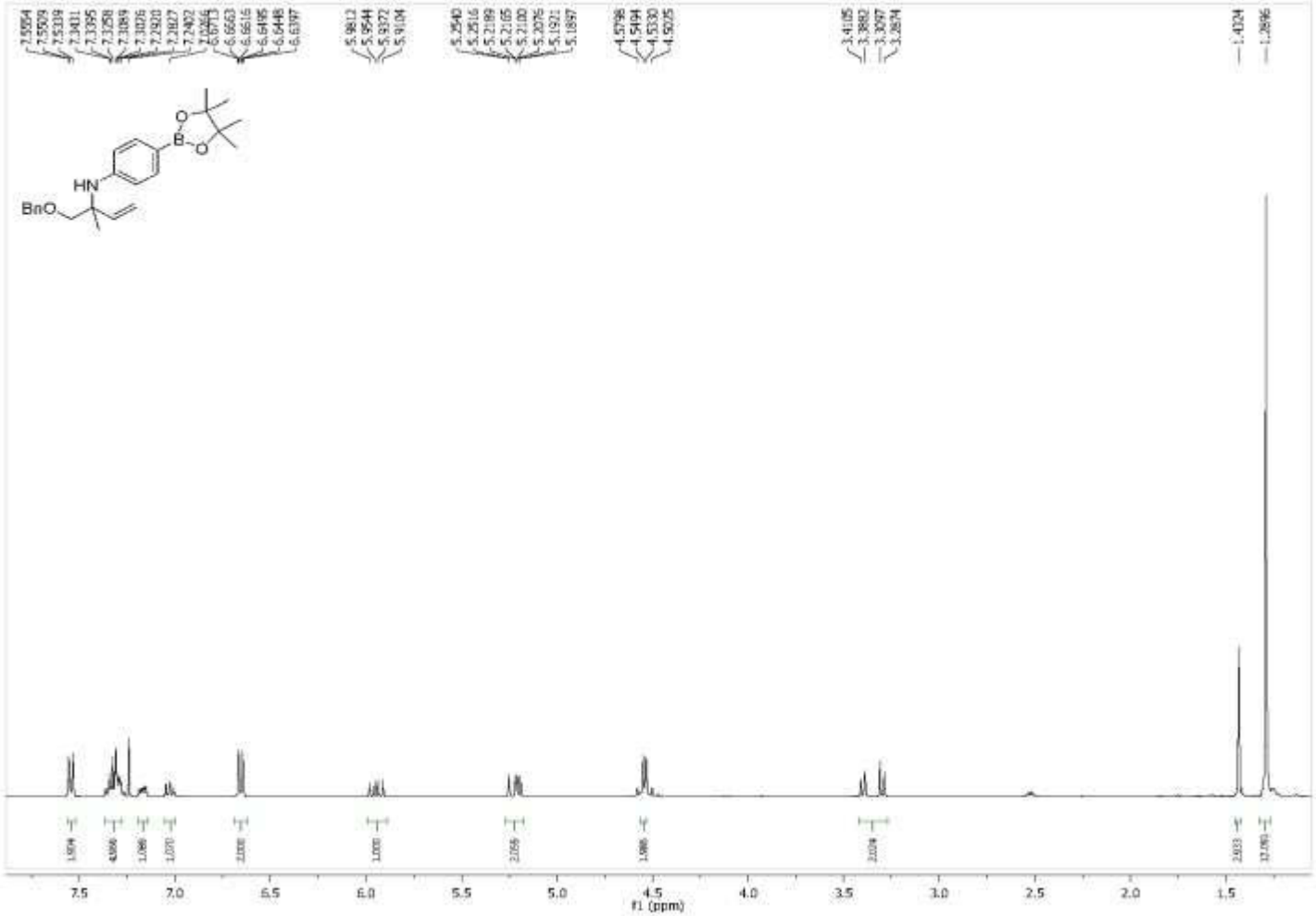

Figure A185 400 MHz 1H NMR ($CDCl_3$) Spectra of Compound **255h**

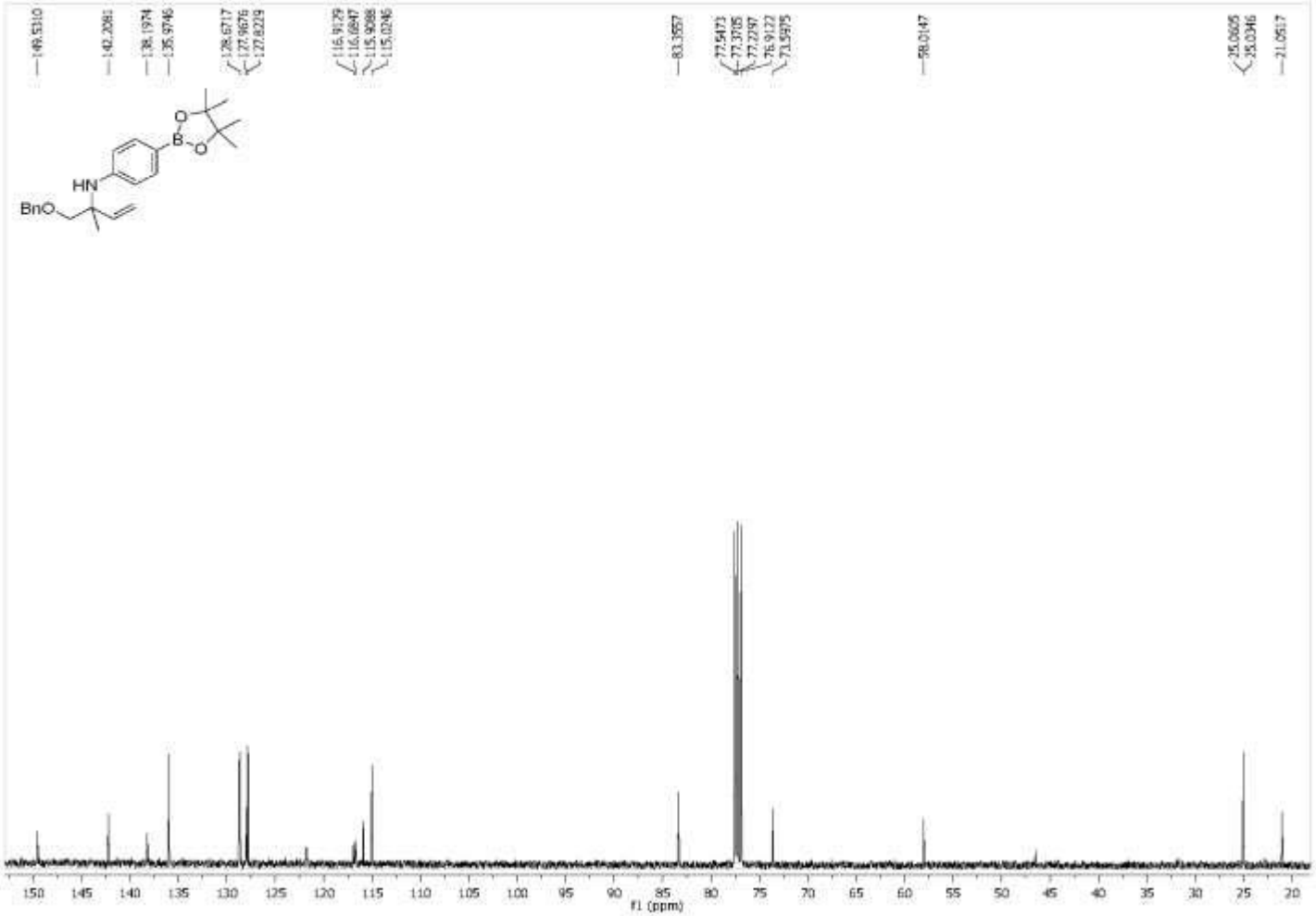

Figure A186 100 MHz 13C NMR ($CDCl_3$) Spectra of Compound **255h**

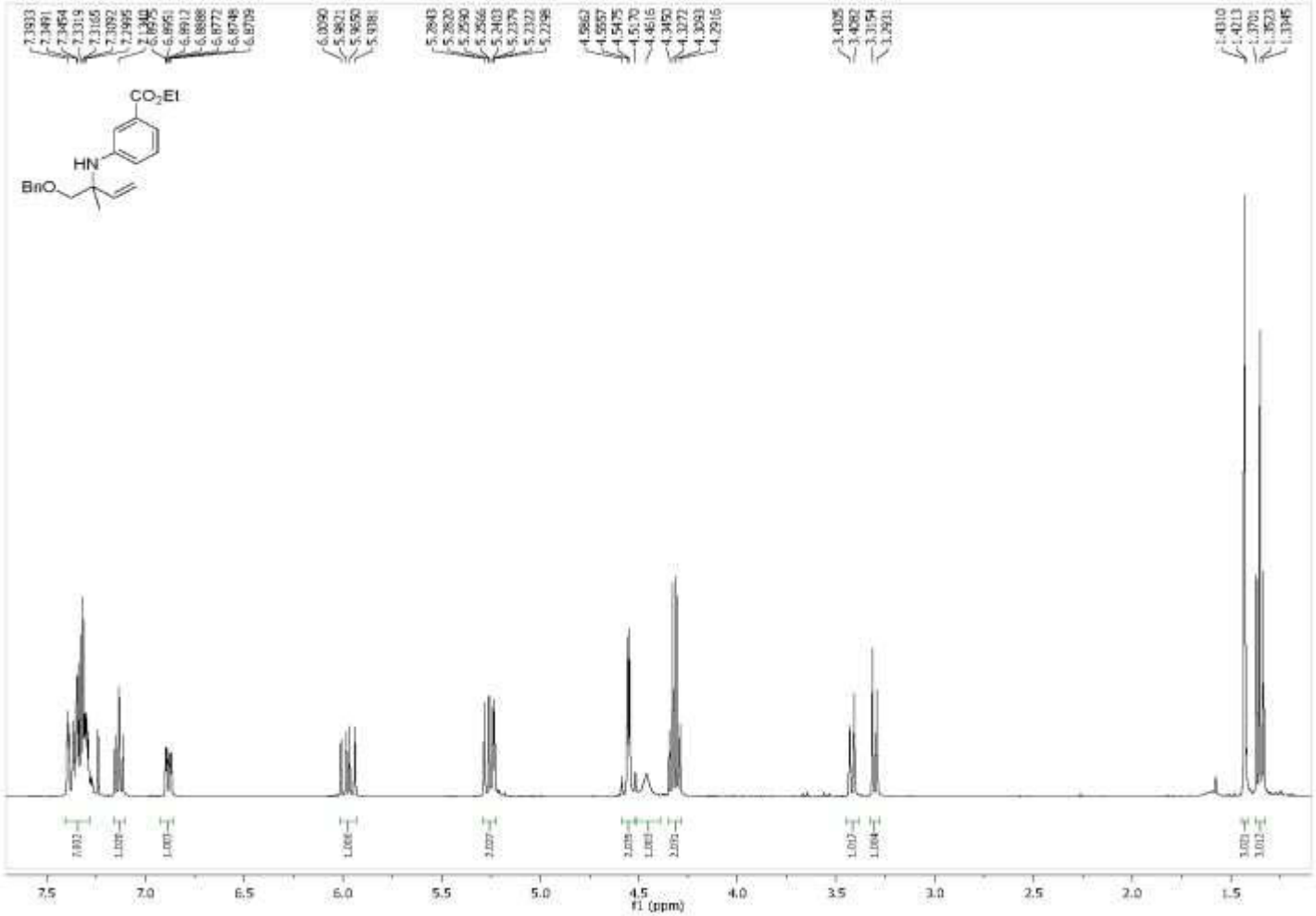

Figure A187 400 MHz 1H NMR ($CDCl_3$) Spectra of Compound **255j**

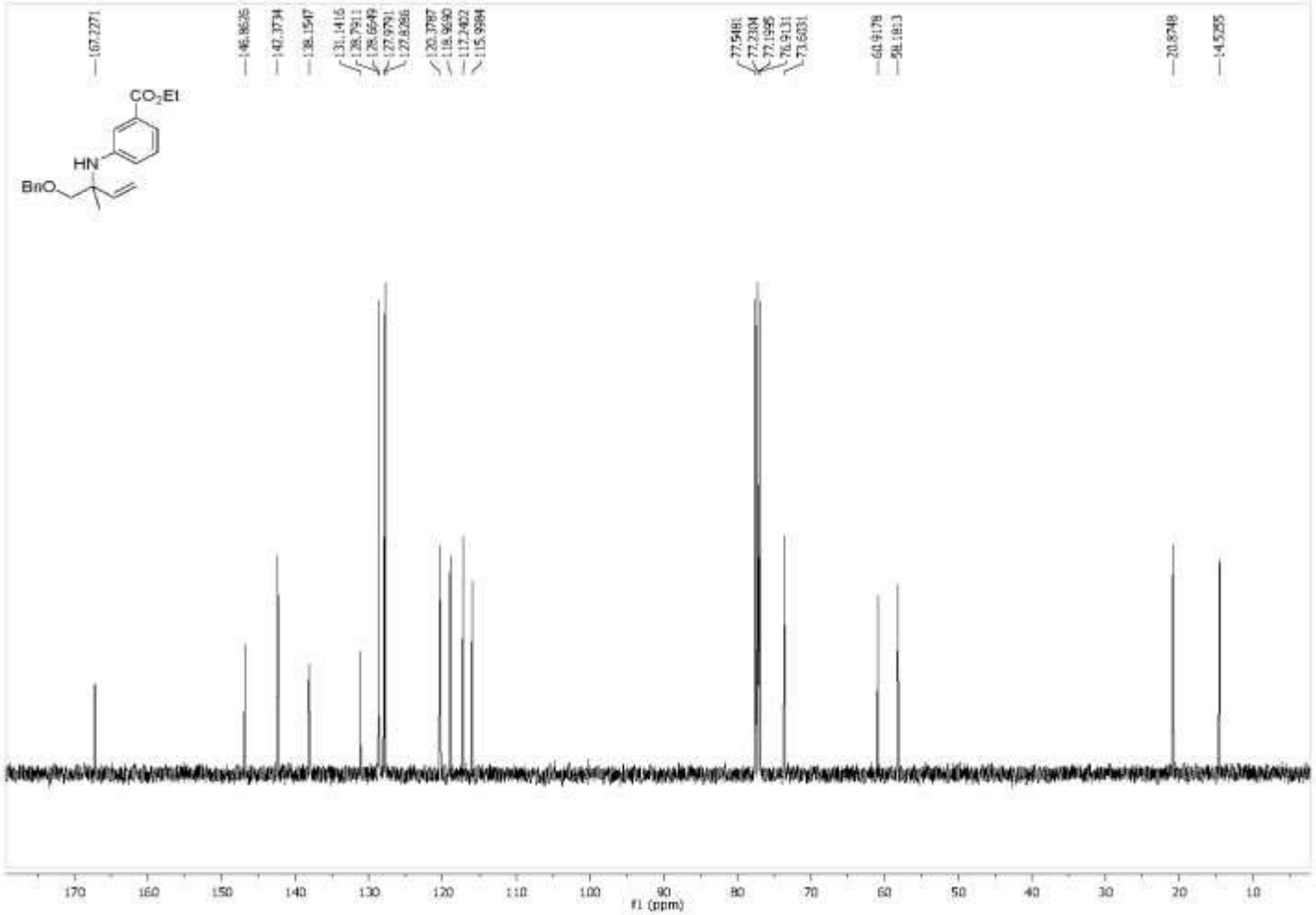

Figure A188 100 MHz 13C NMR ($CDCl_3$) Spectra of Compound **255j**

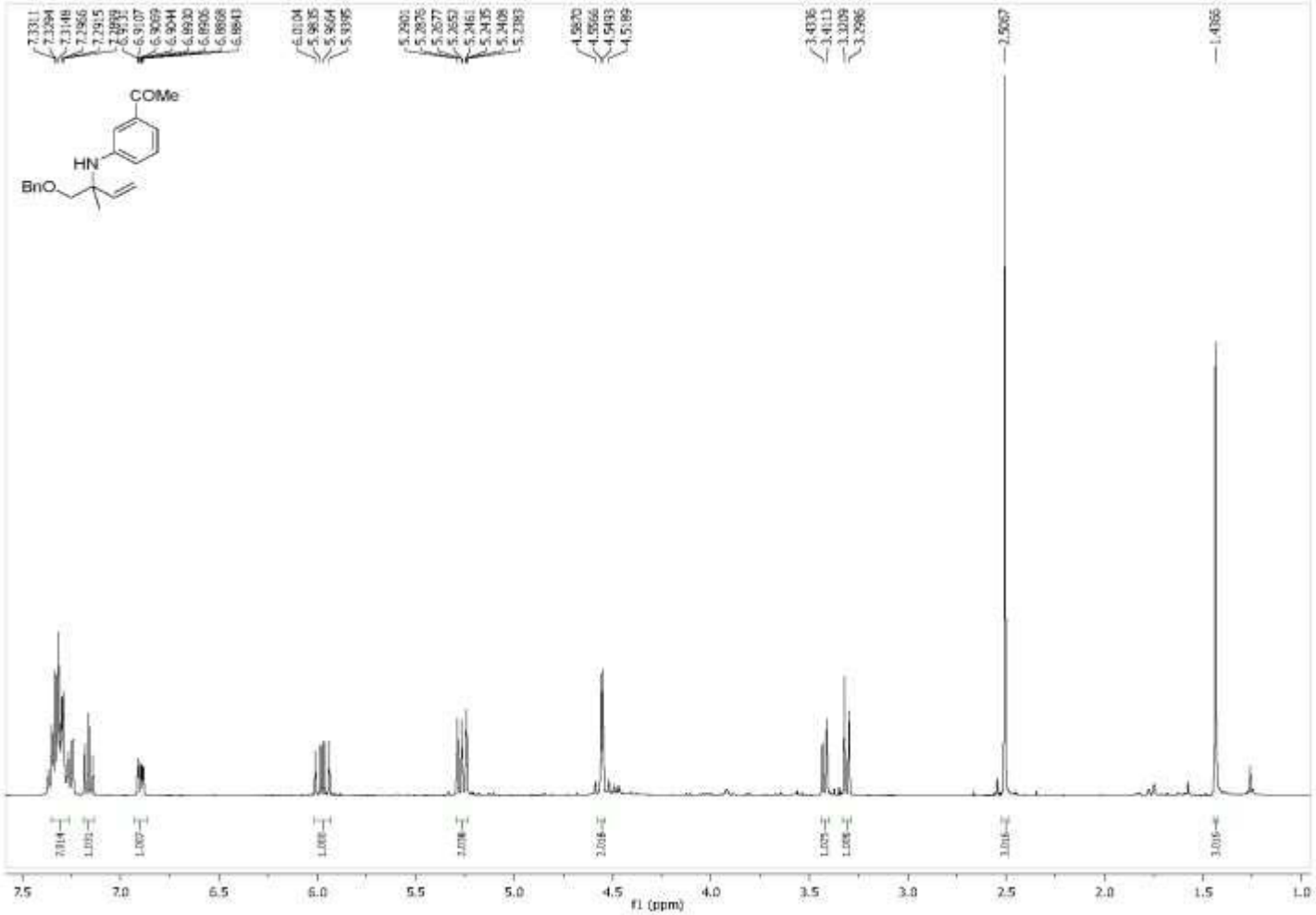

Figure A189 400 MHz 1H NMR ($CDCl_3$) Spectra of Compound **255k**

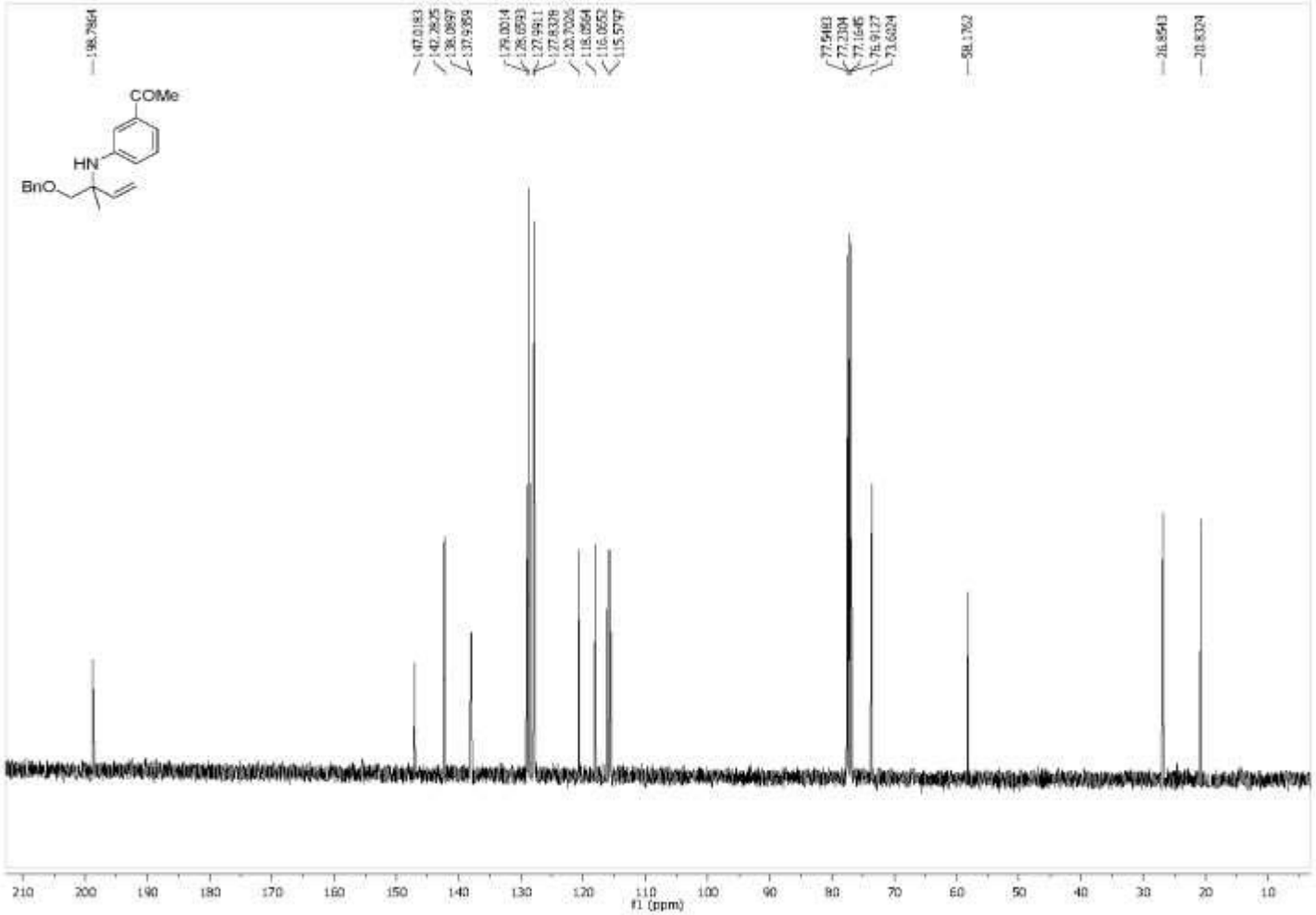

Figure A190 100 MHz 13C NMR ($CDCl_3$) Spectra of Compound **255k**

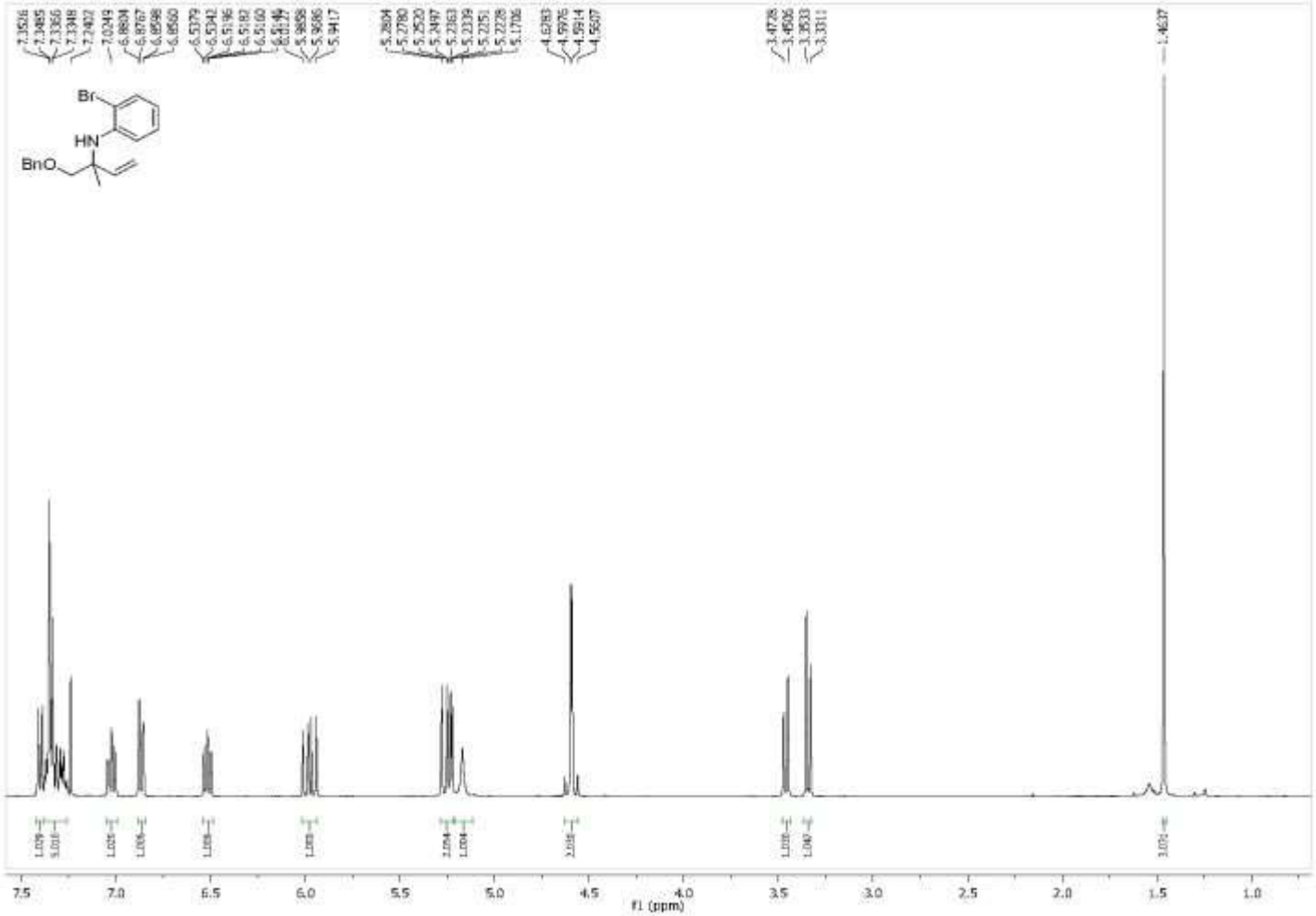

Figure A191 400 MHz 1H NMR ($CDCl_3$) Spectra of Compound **255m**

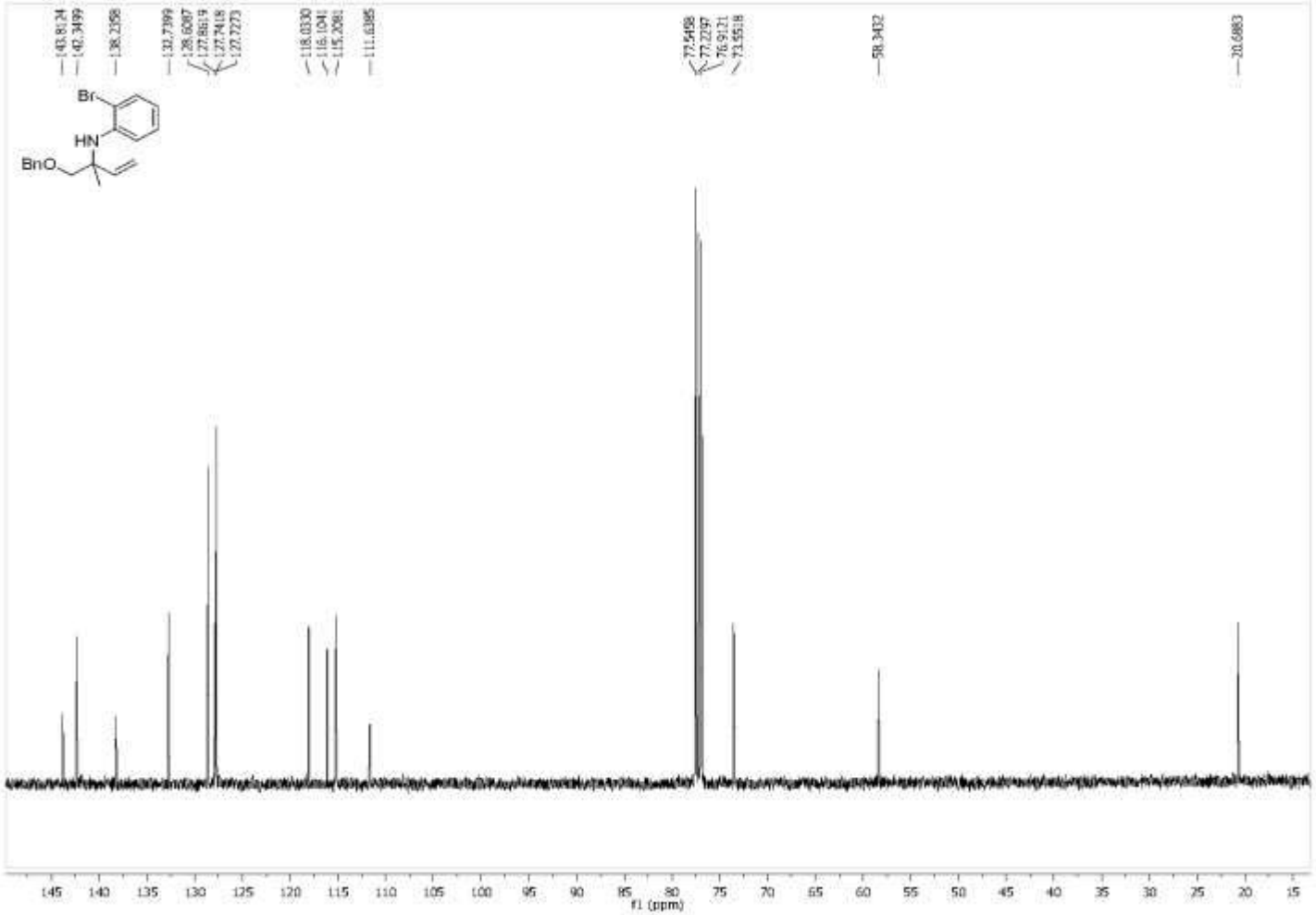

Figure A192 100 MHz 13C NMR ($CDCl_3$) Spectra of Compound **255m**

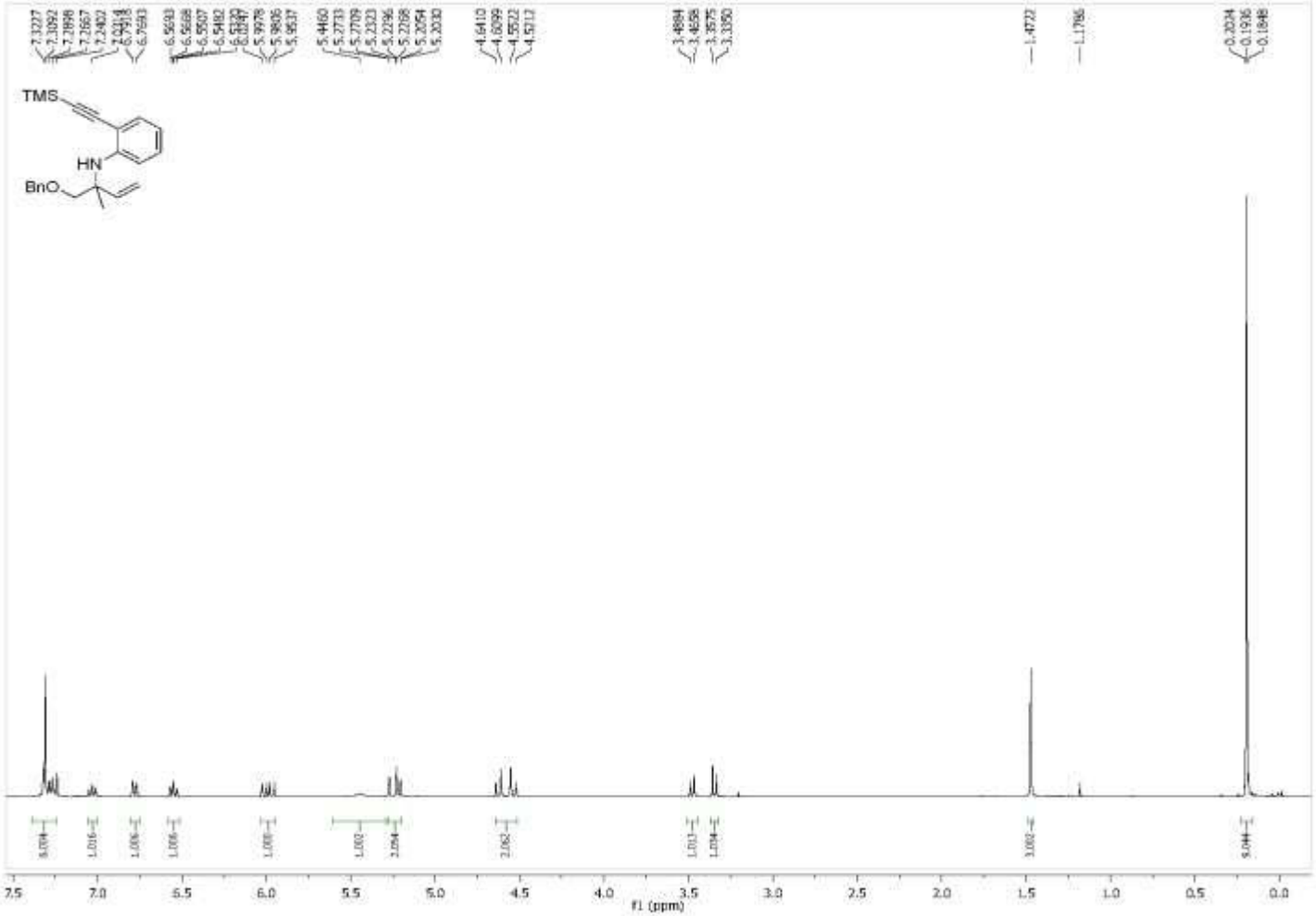

Figure A193 400 MHz 1H NMR ($CDCl_3$) Spectra of Compound **255o**

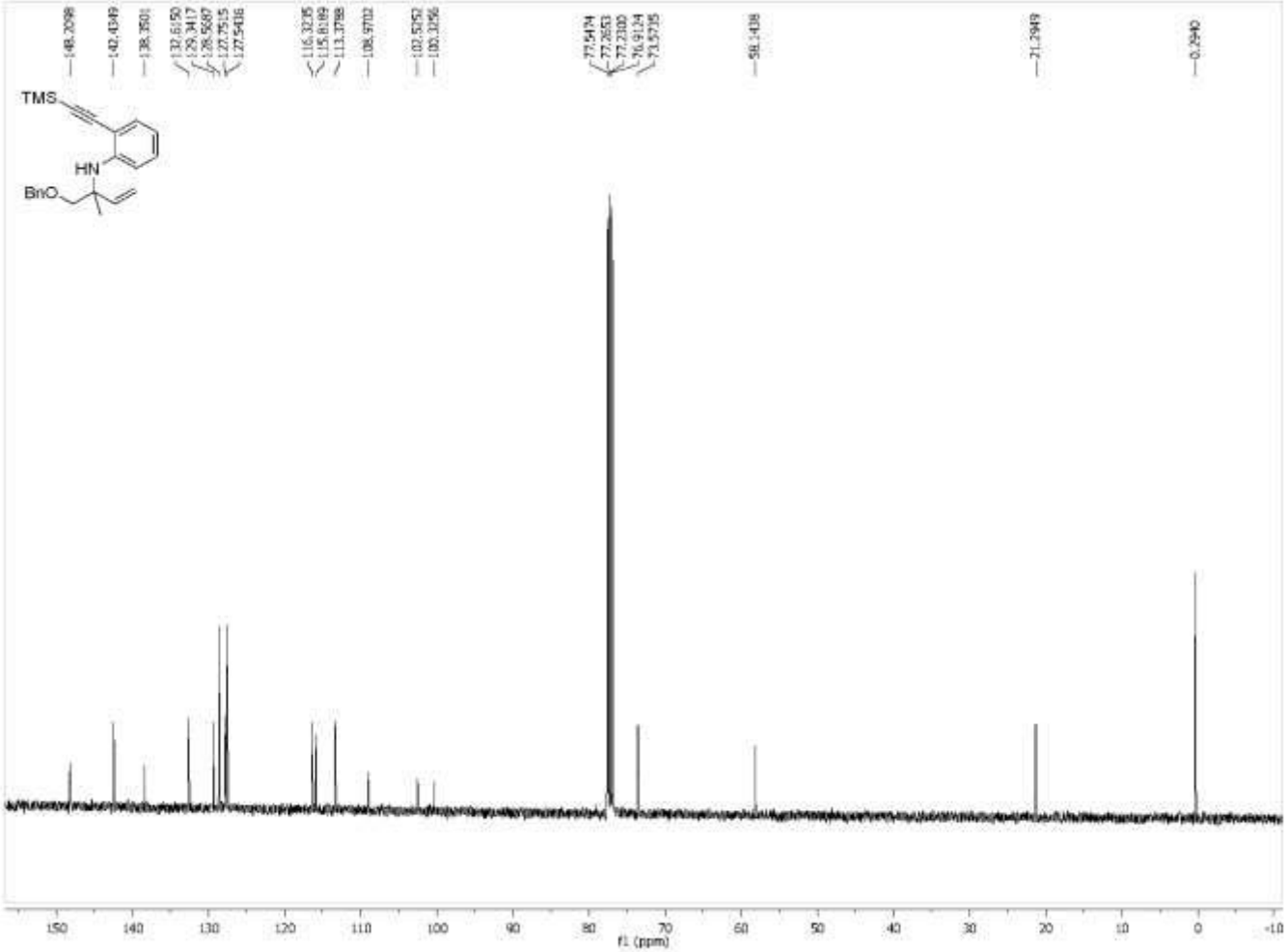

Figure A194 100 MHz 13C NMR ($CDCl_3$) Spectra of Compound **255o**

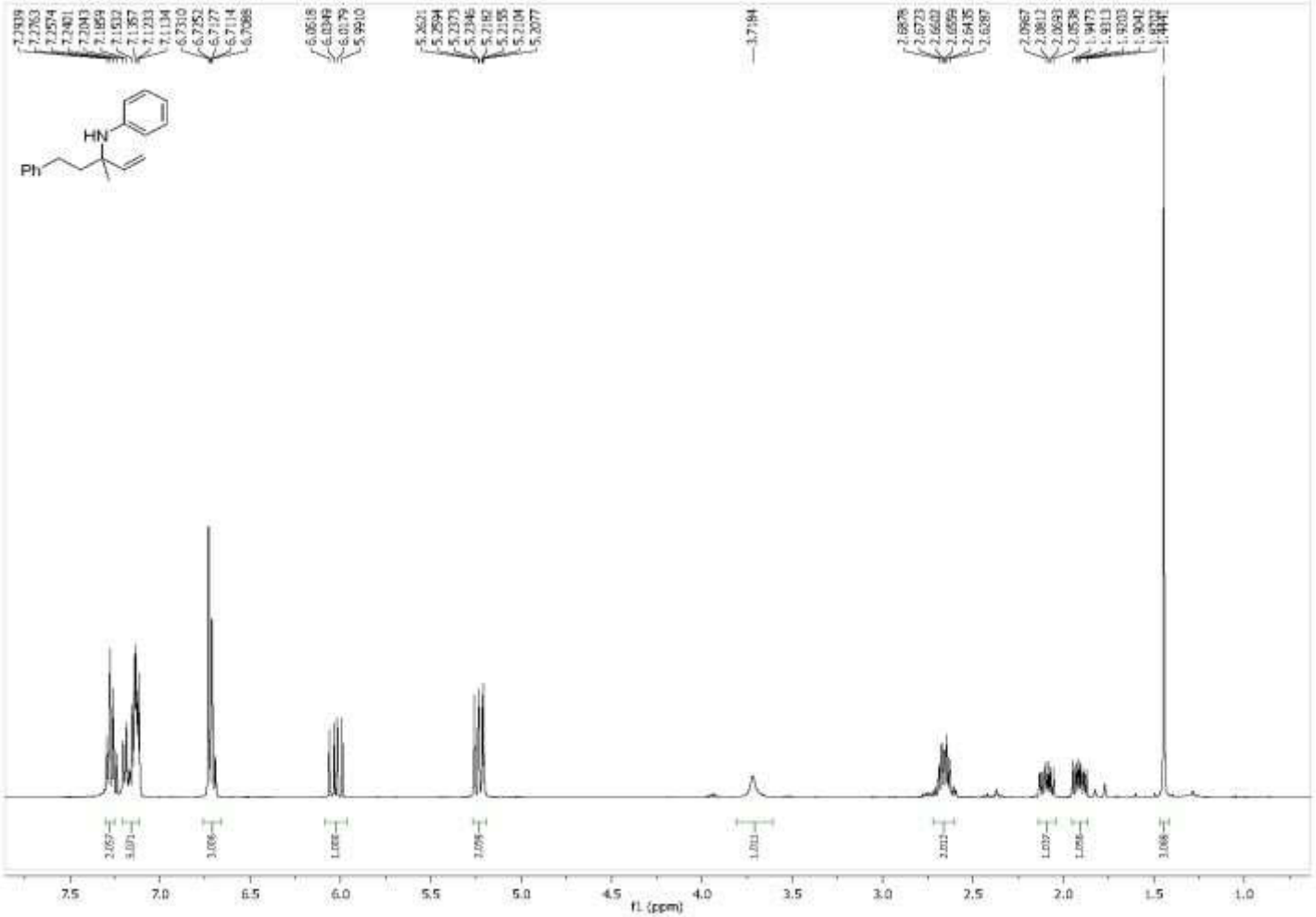

Figure A195 400 MHz 1H NMR ($CDCl_3$) Spectra of Compound **256a**

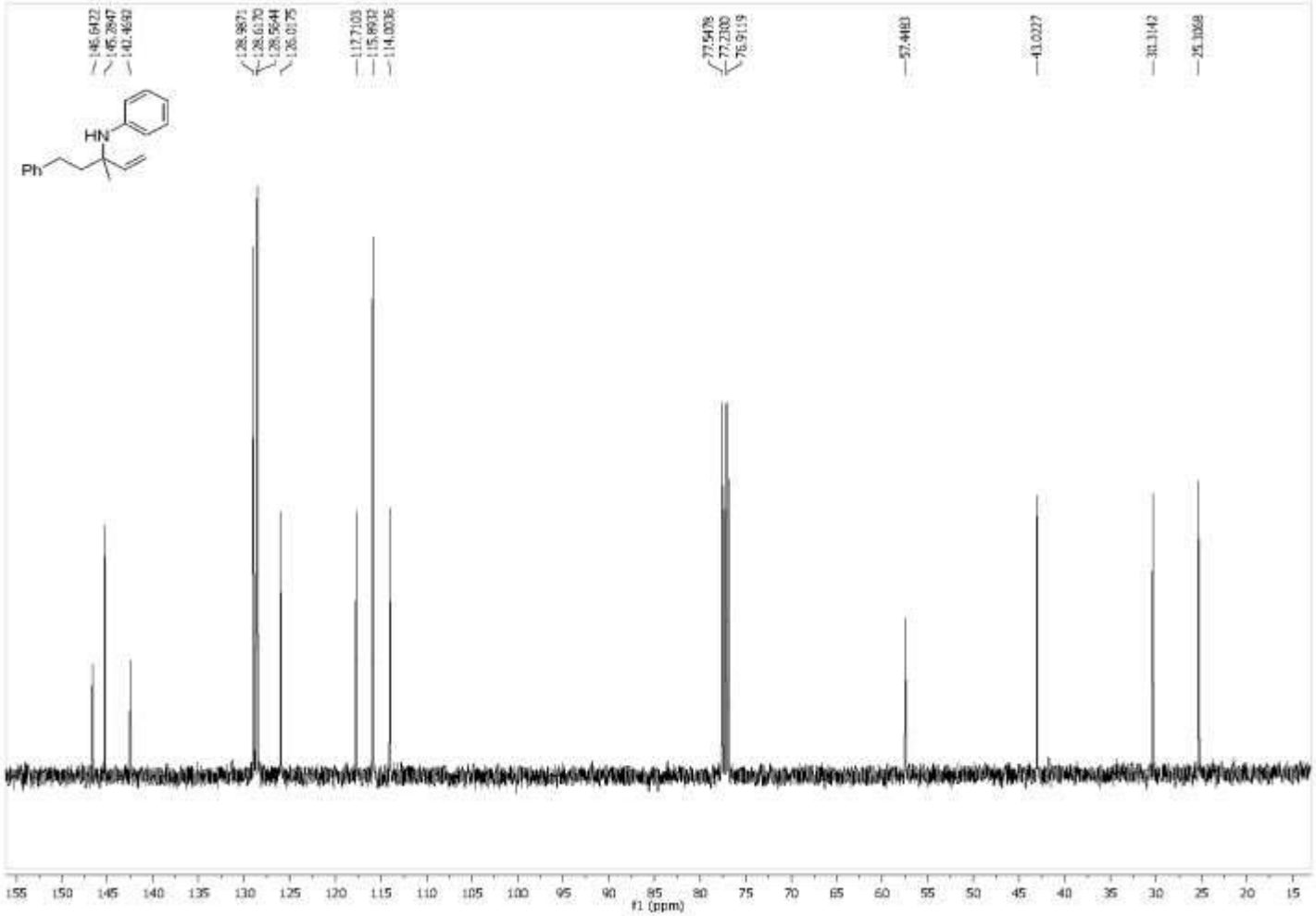

Figure A196 100 MHz 13C NMR ($CDCl_3$) Spectra of Compound **256a**

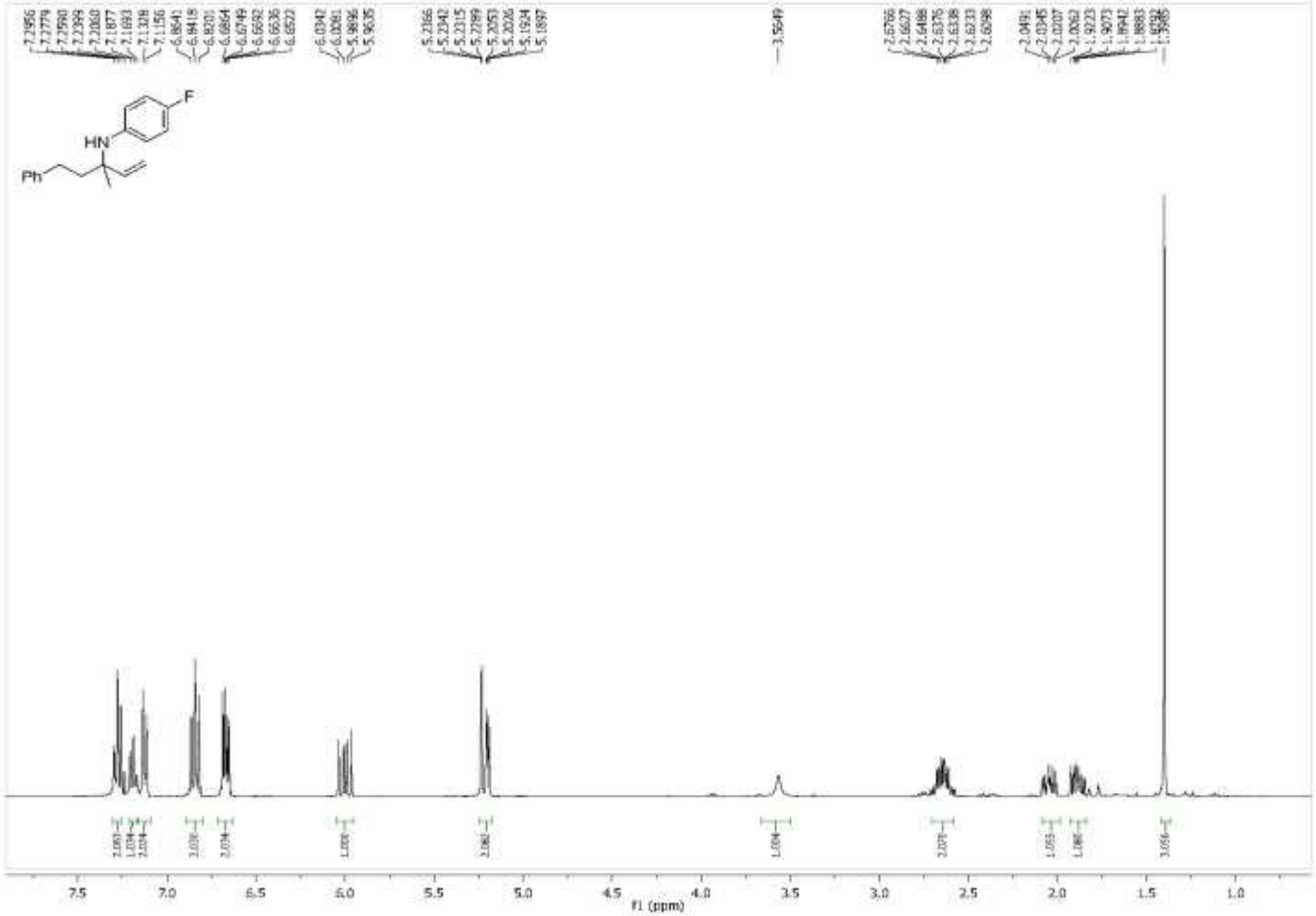

Figure A197 400 MHz 1H NMR ($CDCl_3$) Spectra of Compound **256b**

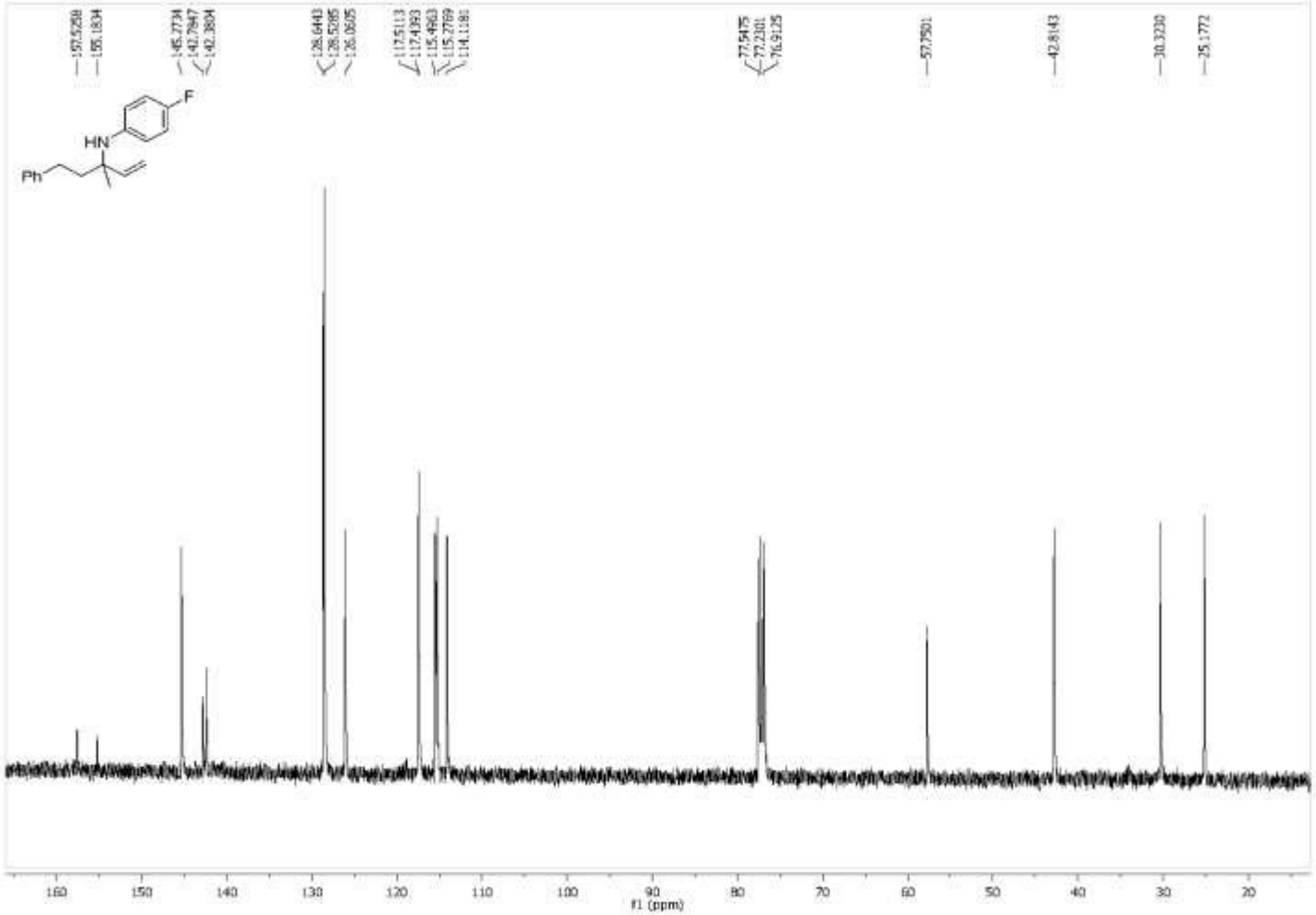

Figure A198 100 MHz 13C NMR ($CDCl_3$) Spectra of Compound **256b**

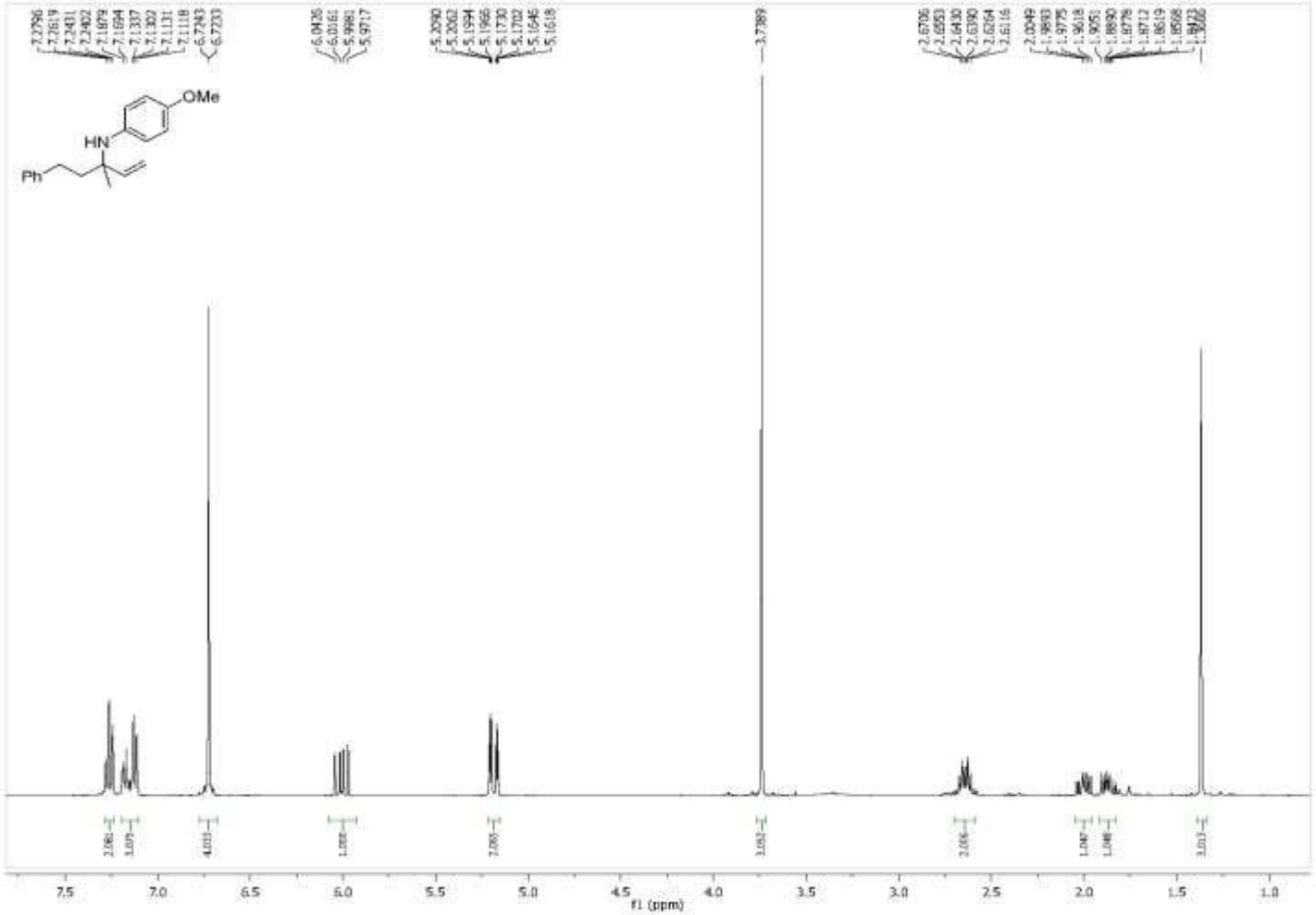

Figure A199 400 MHz 1H NMR ($CDCl_3$) Spectra of Compound **256c**

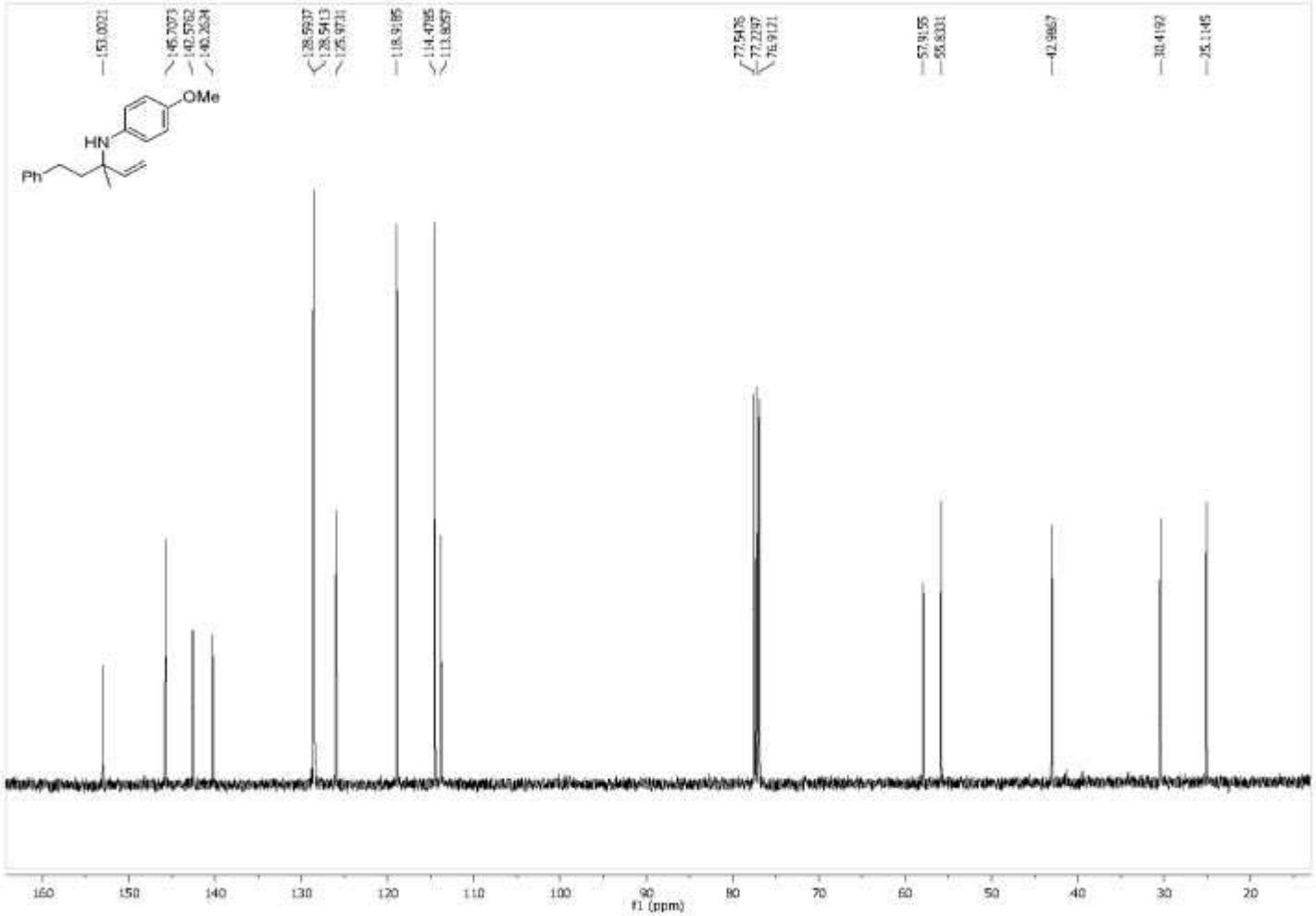

Figure A200 100 MHz 13C NMR ($CDCl_3$) Spectra of Compound **256c**

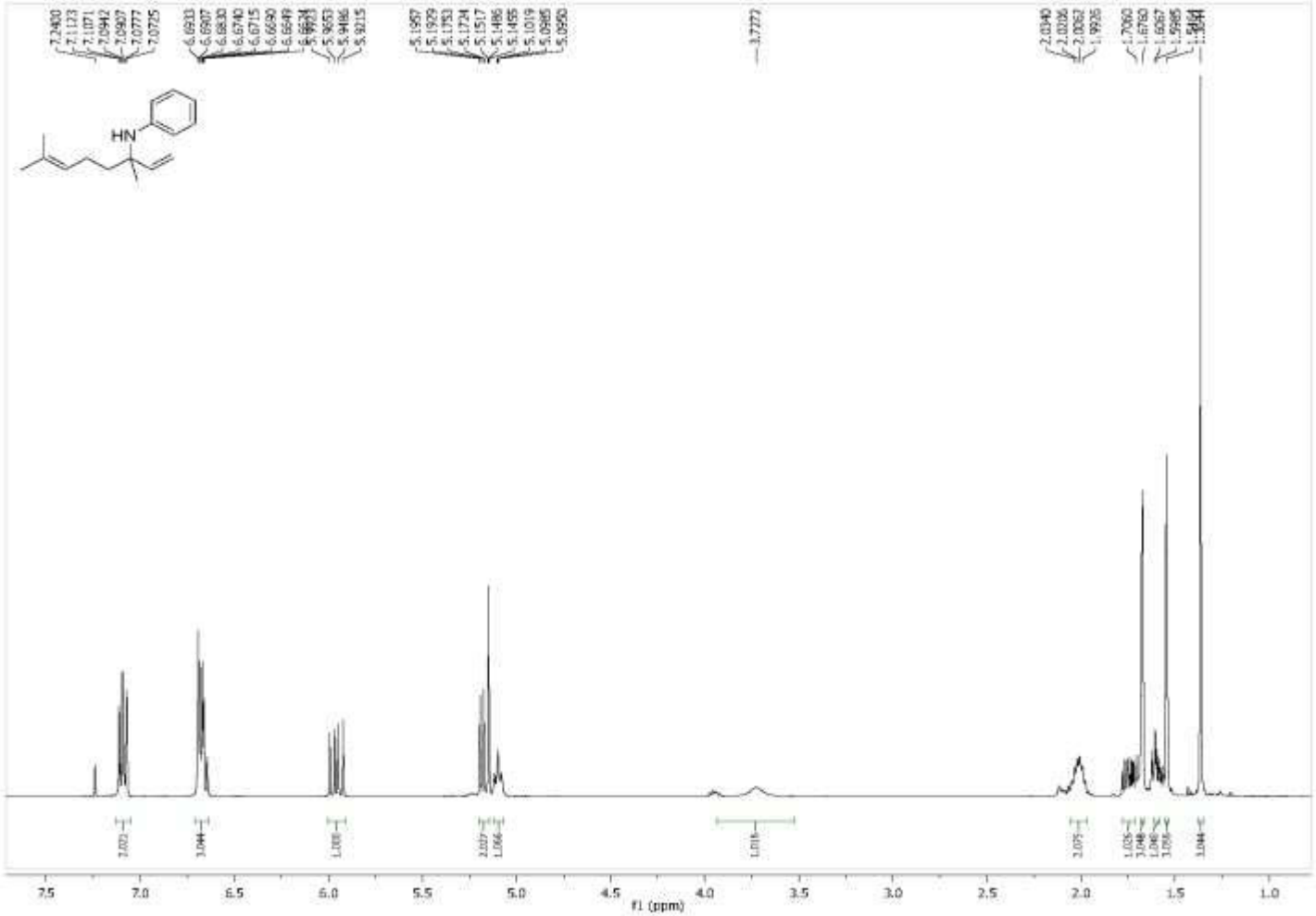

Figure A201 400 MHz 1H NMR ($CDCl_3$) Spectra of Compound **257a**

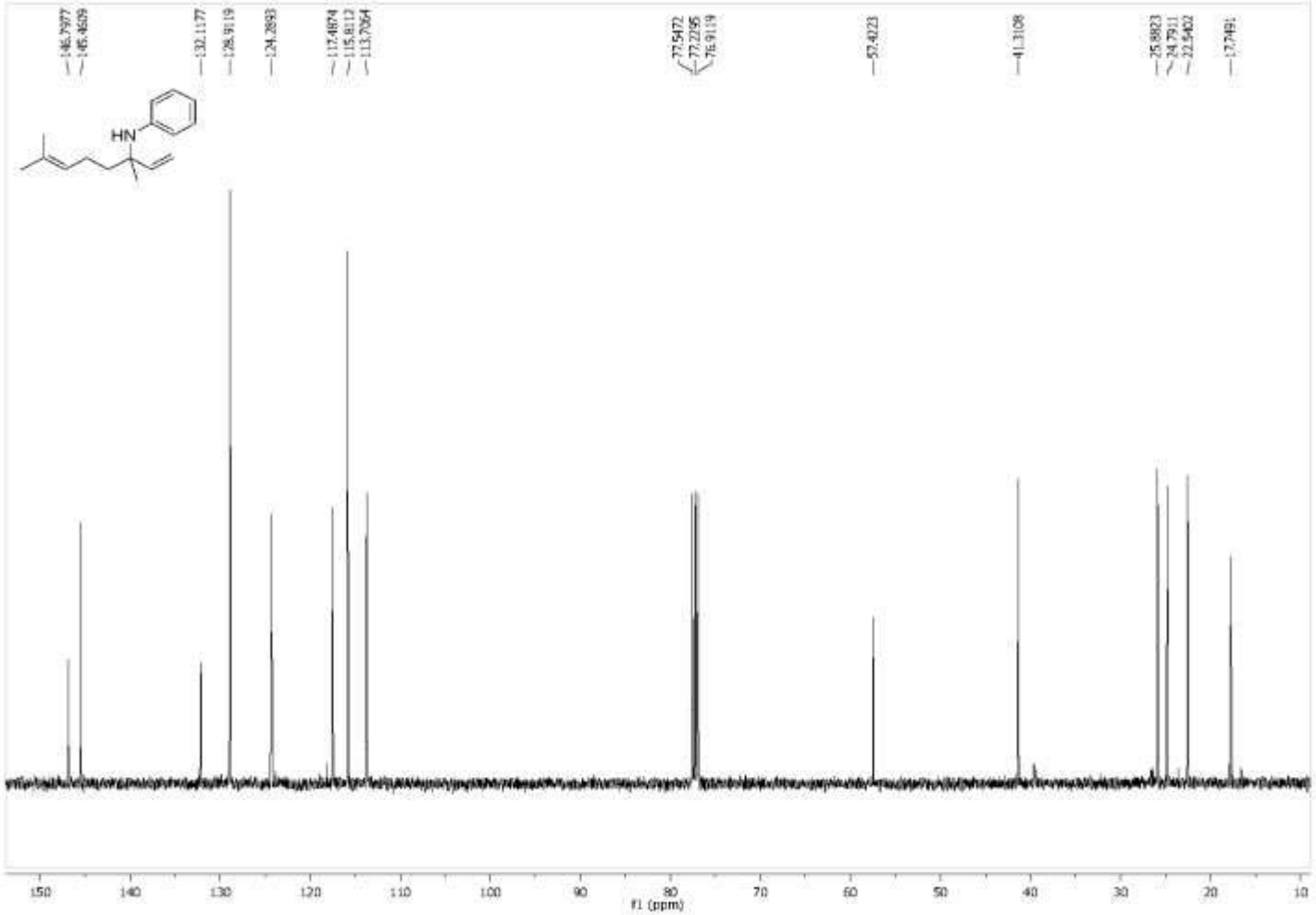

Figure A202 100 MHz 13C NMR ($CDCl_3$) Spectra of Compound **257a**

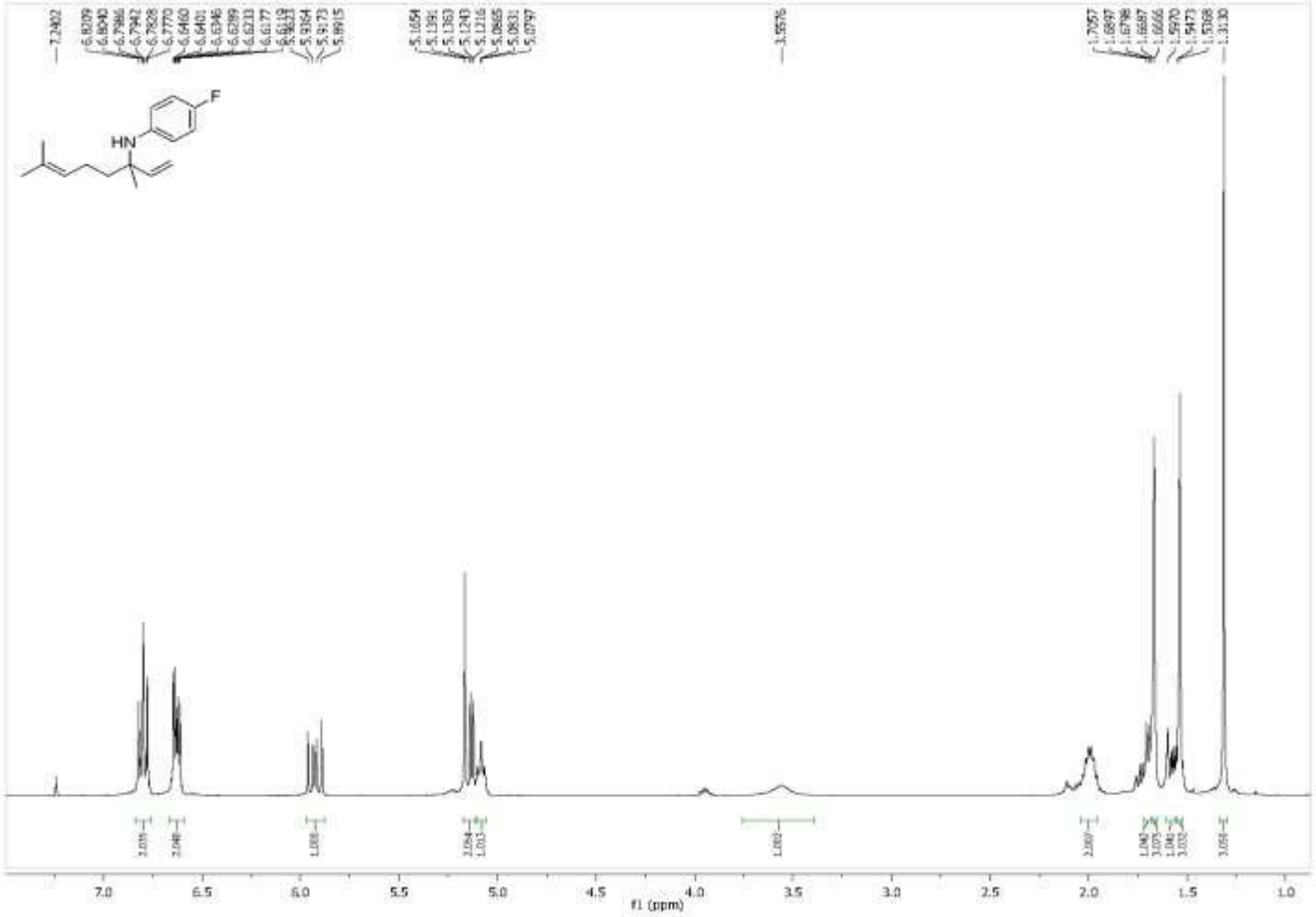

Figure A203 400 MHz 1H NMR ($CDCl_3$) Spectra of Compound **257b**

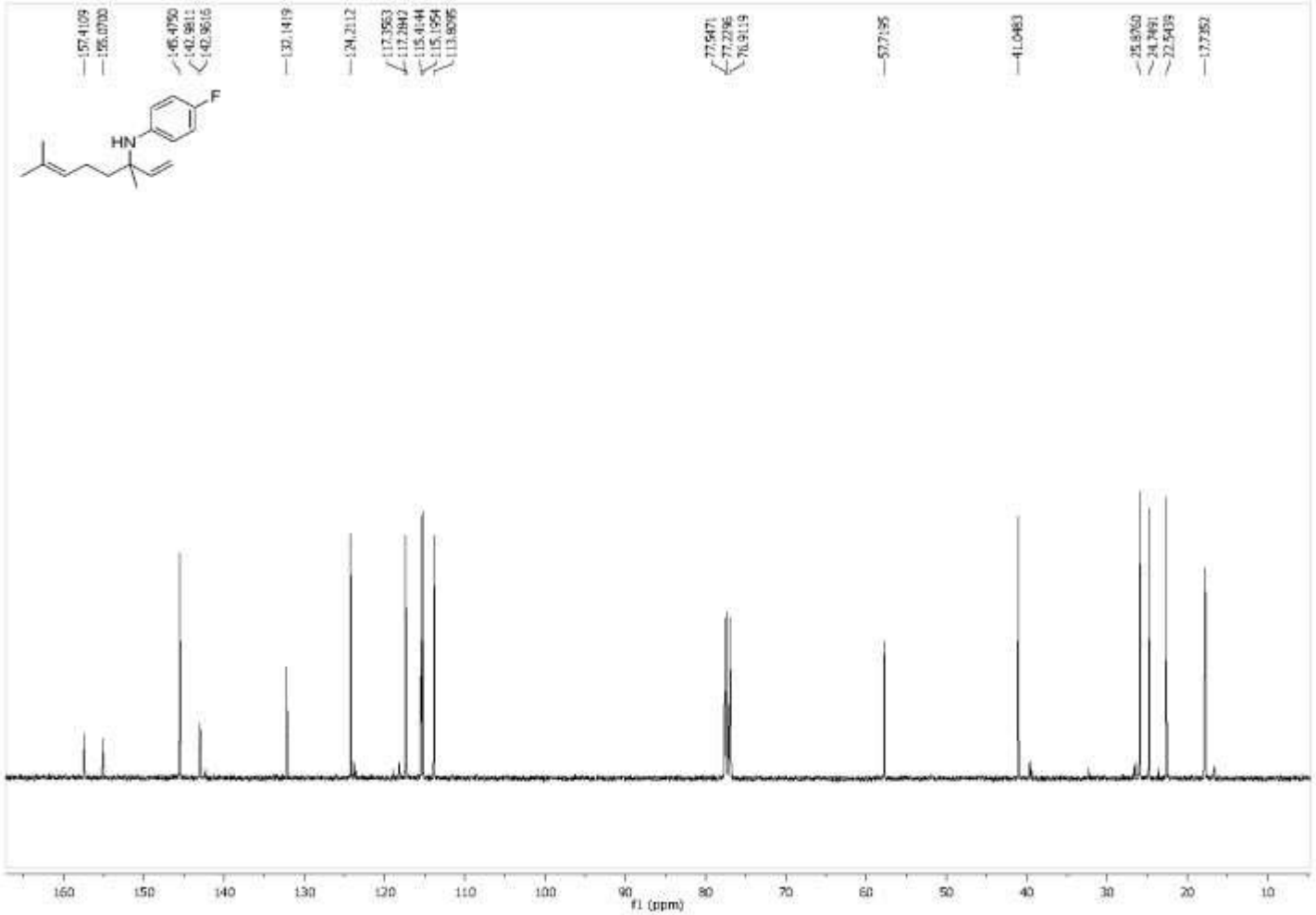

Figure A204 100 MHz 13C NMR ($CDCl_3$) Spectra of Compound **257b**

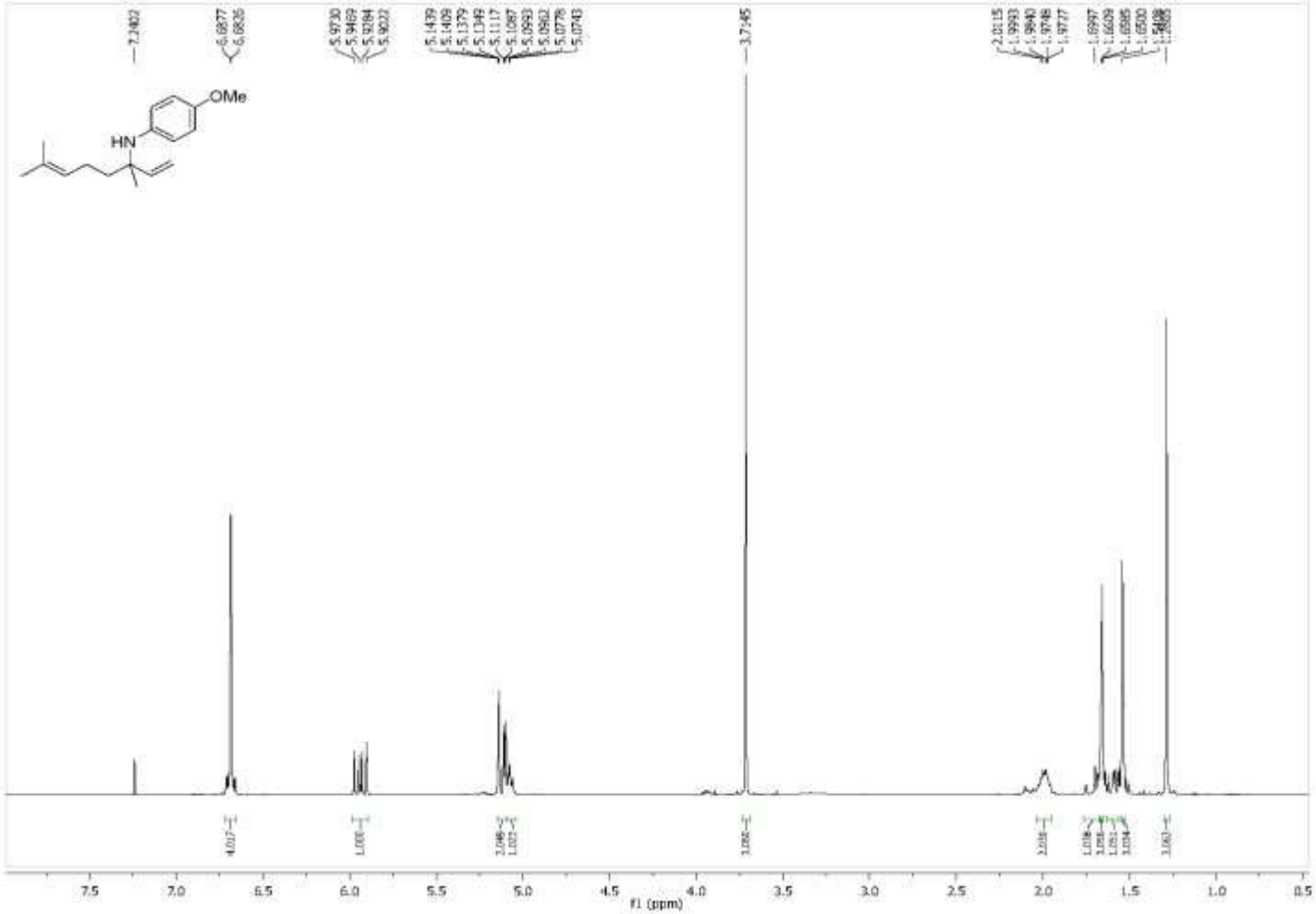

Figure A205 400 MHz 1H NMR ($CDCl_3$) Spectra of Compound **257c**

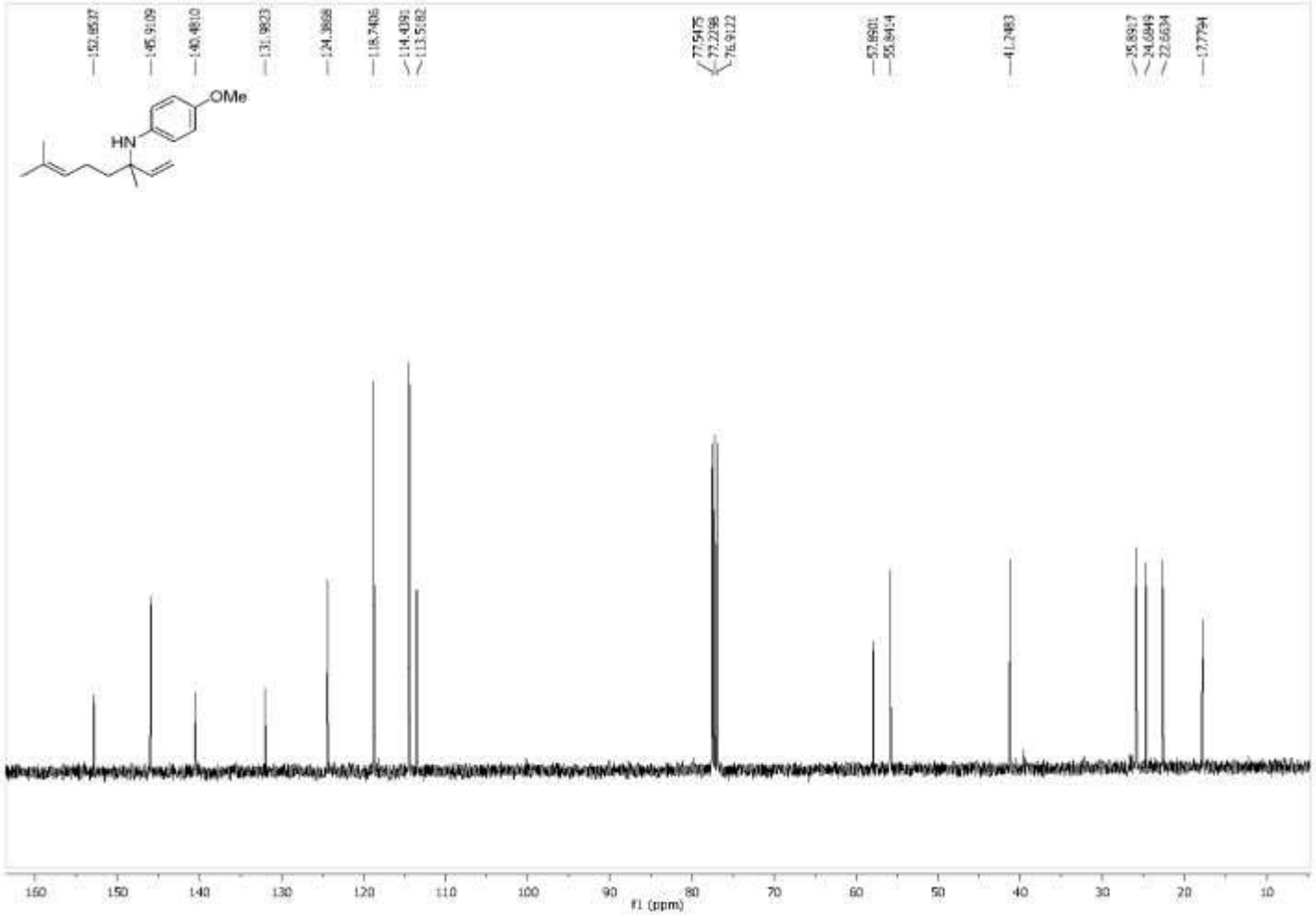

Figure A206 100 MHz 13C NMR ($CDCl_3$) Spectra of Compound **257c**

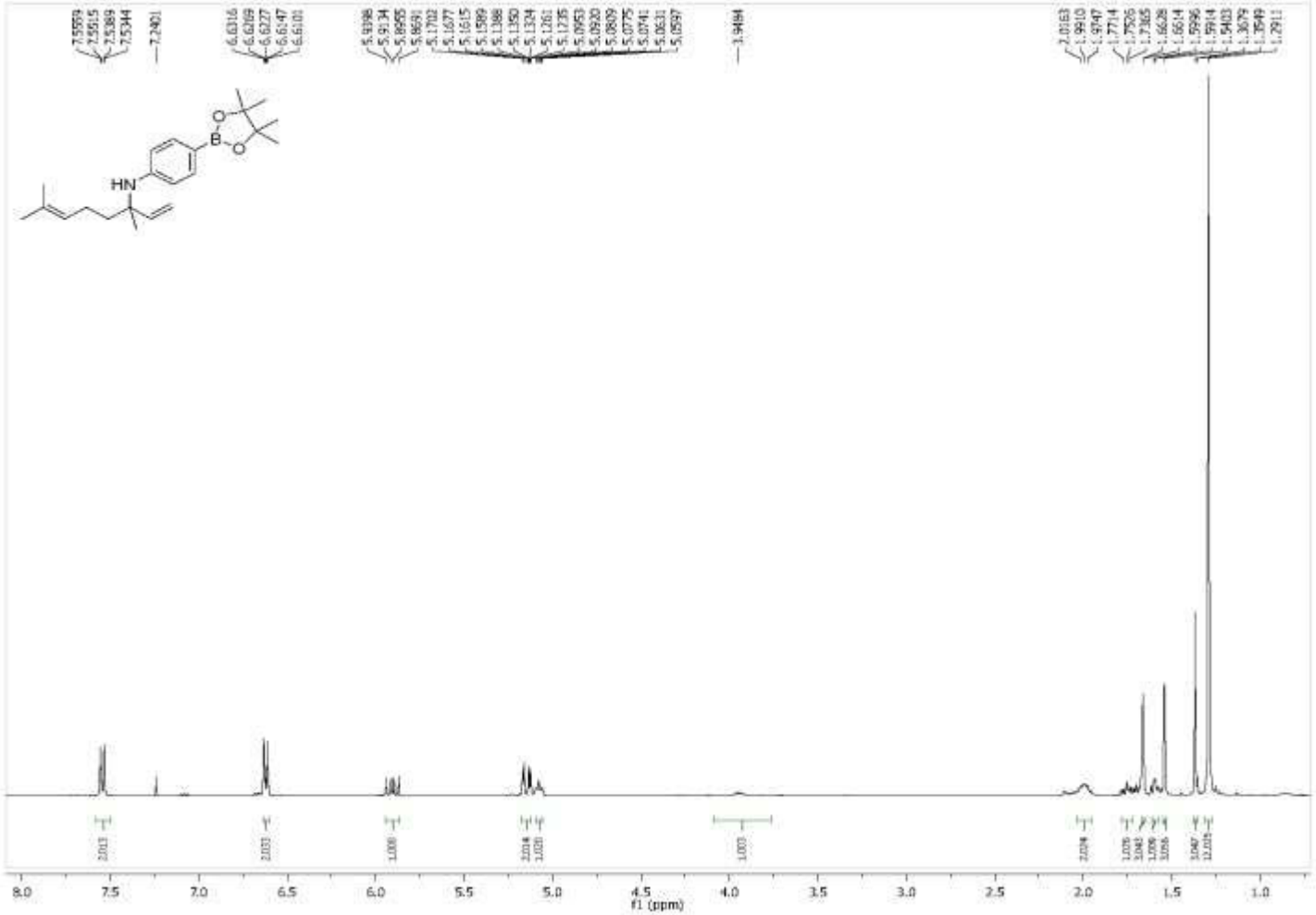

Figure A207 400 MHz 1H NMR ($CDCl_3$) Spectra of Compound **257h**

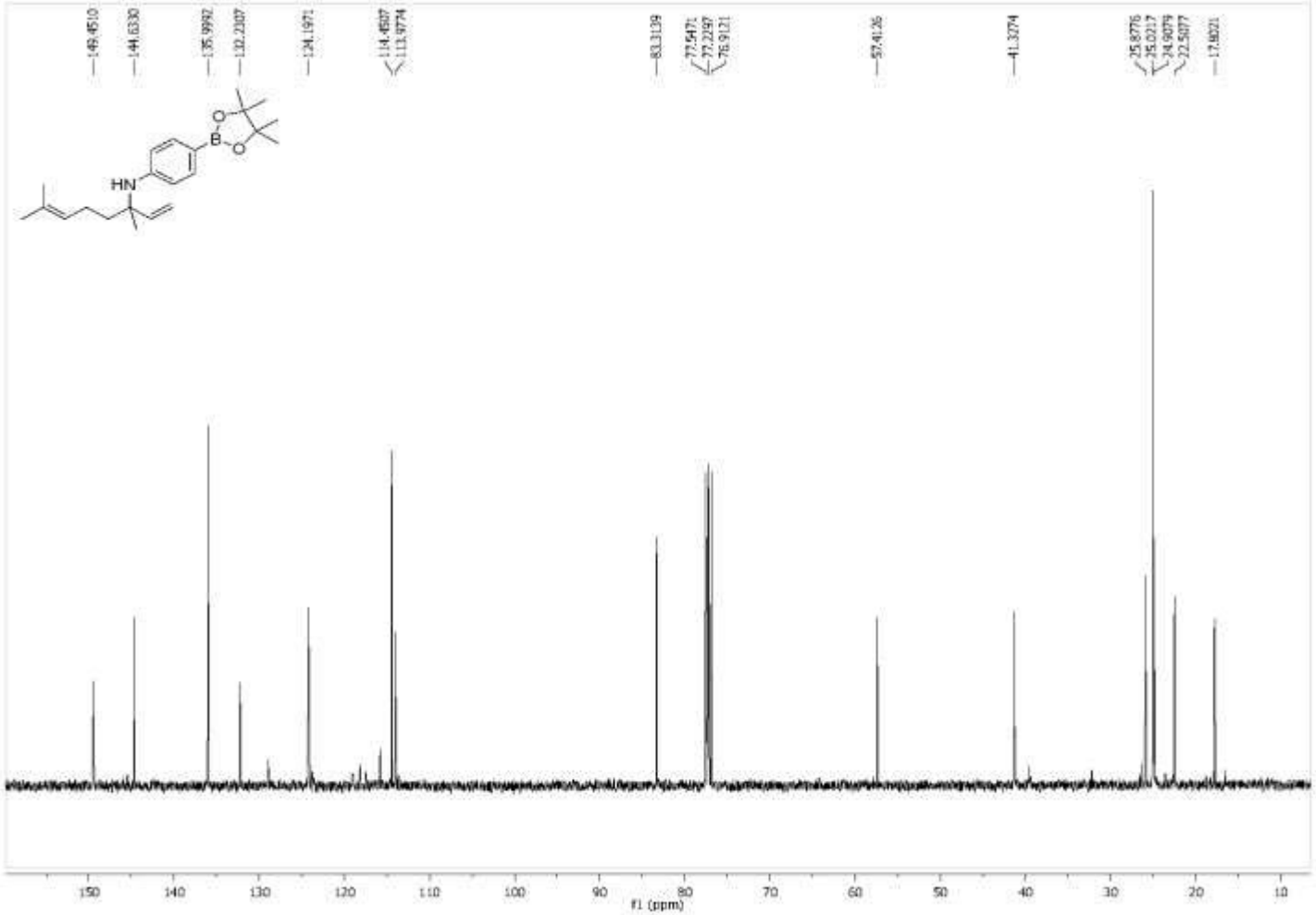

Figure A208 100 MHz 13C NMR ($CDCl_3$) Spectra of Compound **257h**

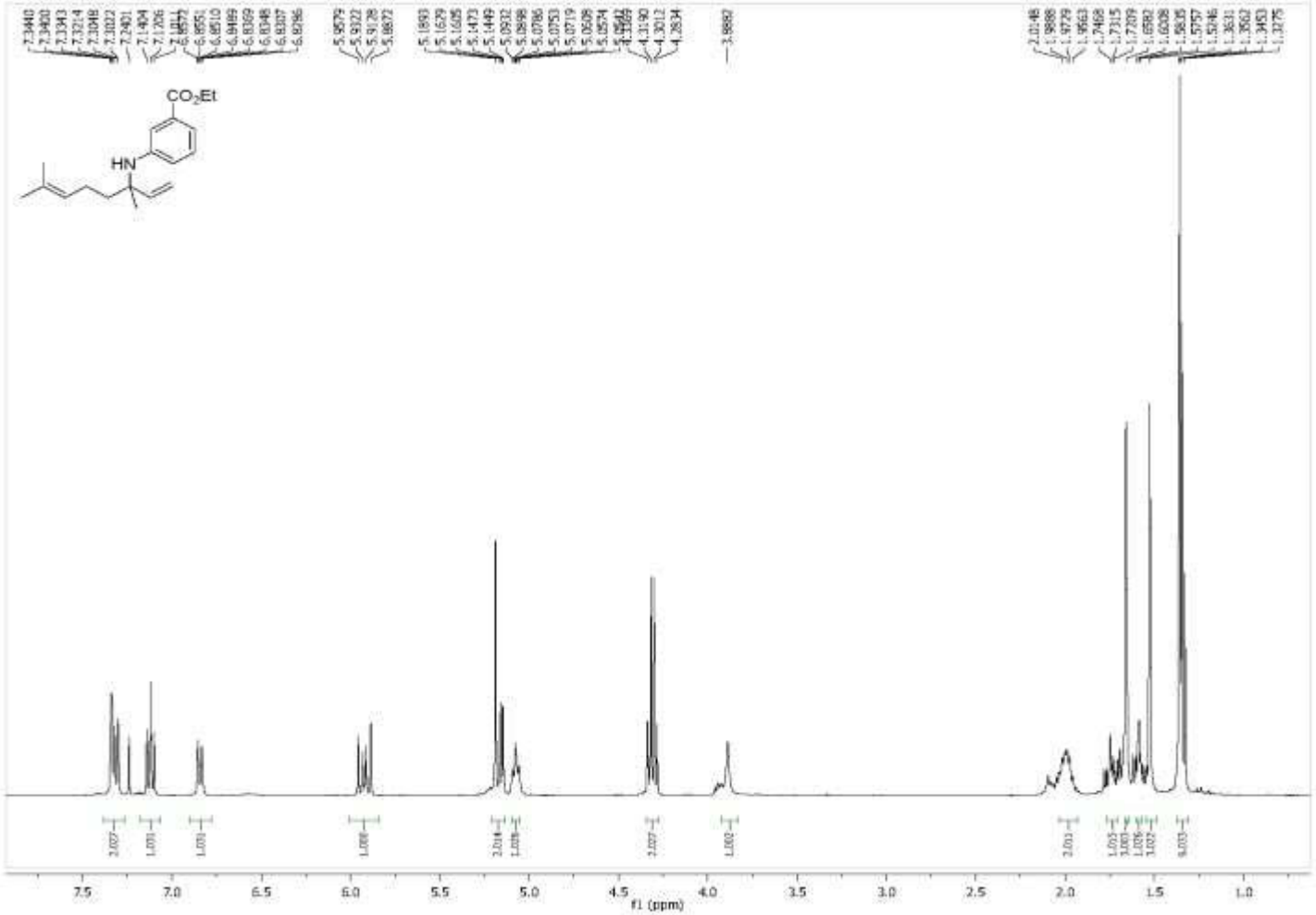

Figure A209 400 MHz 1H NMR ($CDCl_3$) Spectra of Compound **257j**

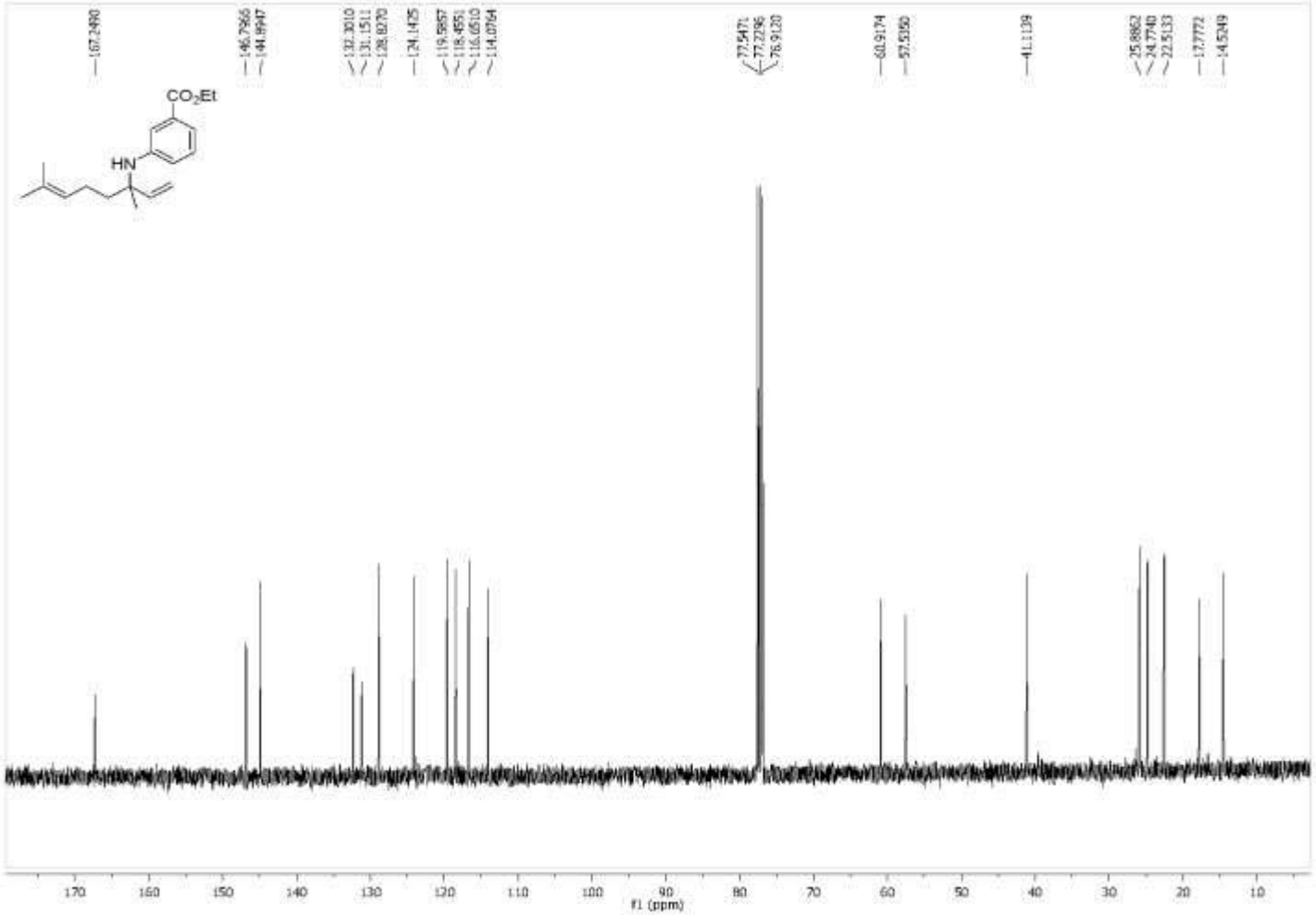

Figure A210 100 MHz 13C NMR ($CDCl_3$) Spectra of Compound **257j**

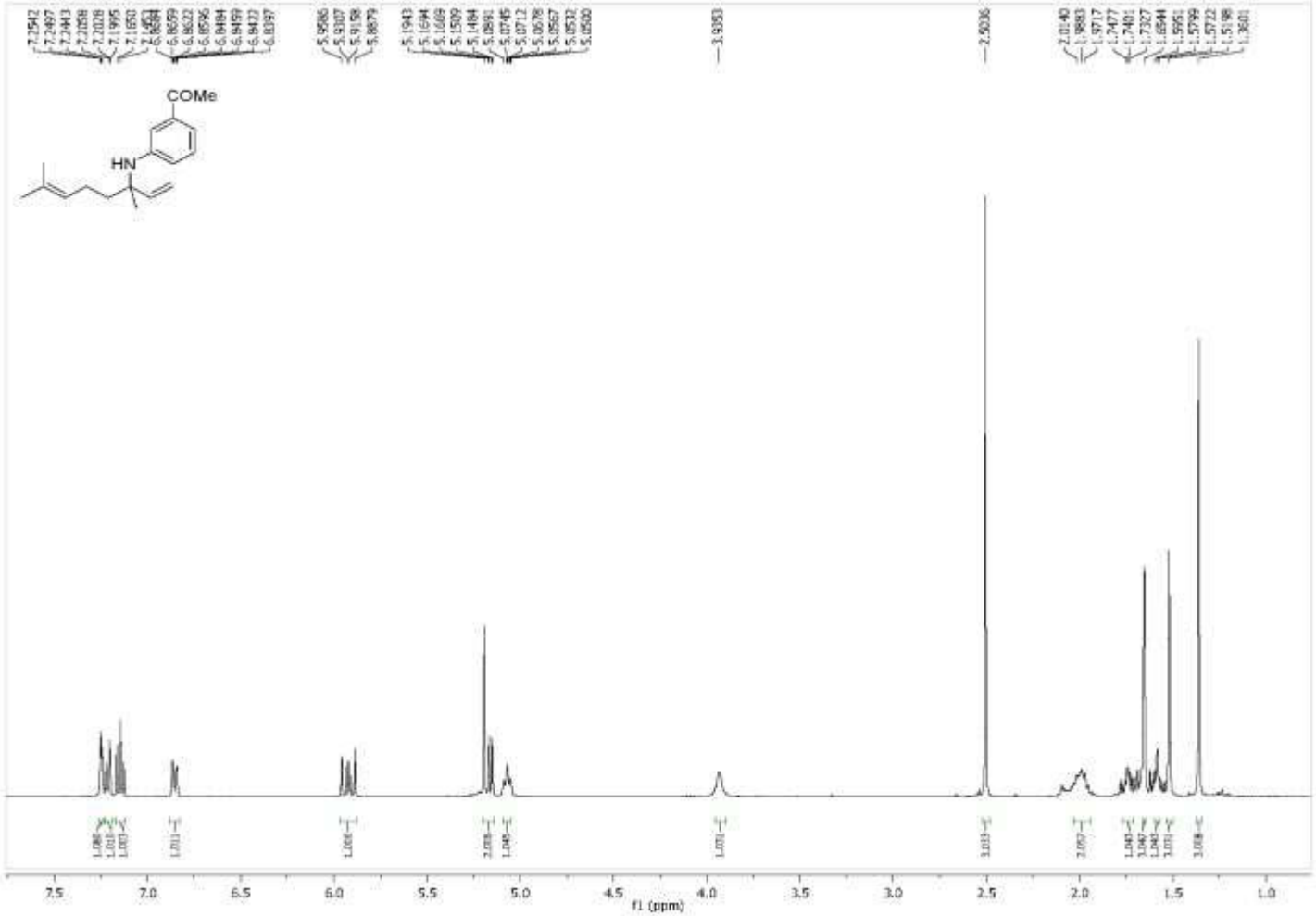

Figure A211 400 MHz 1H NMR ($CDCl_3$) Spectra of Compound **257k**

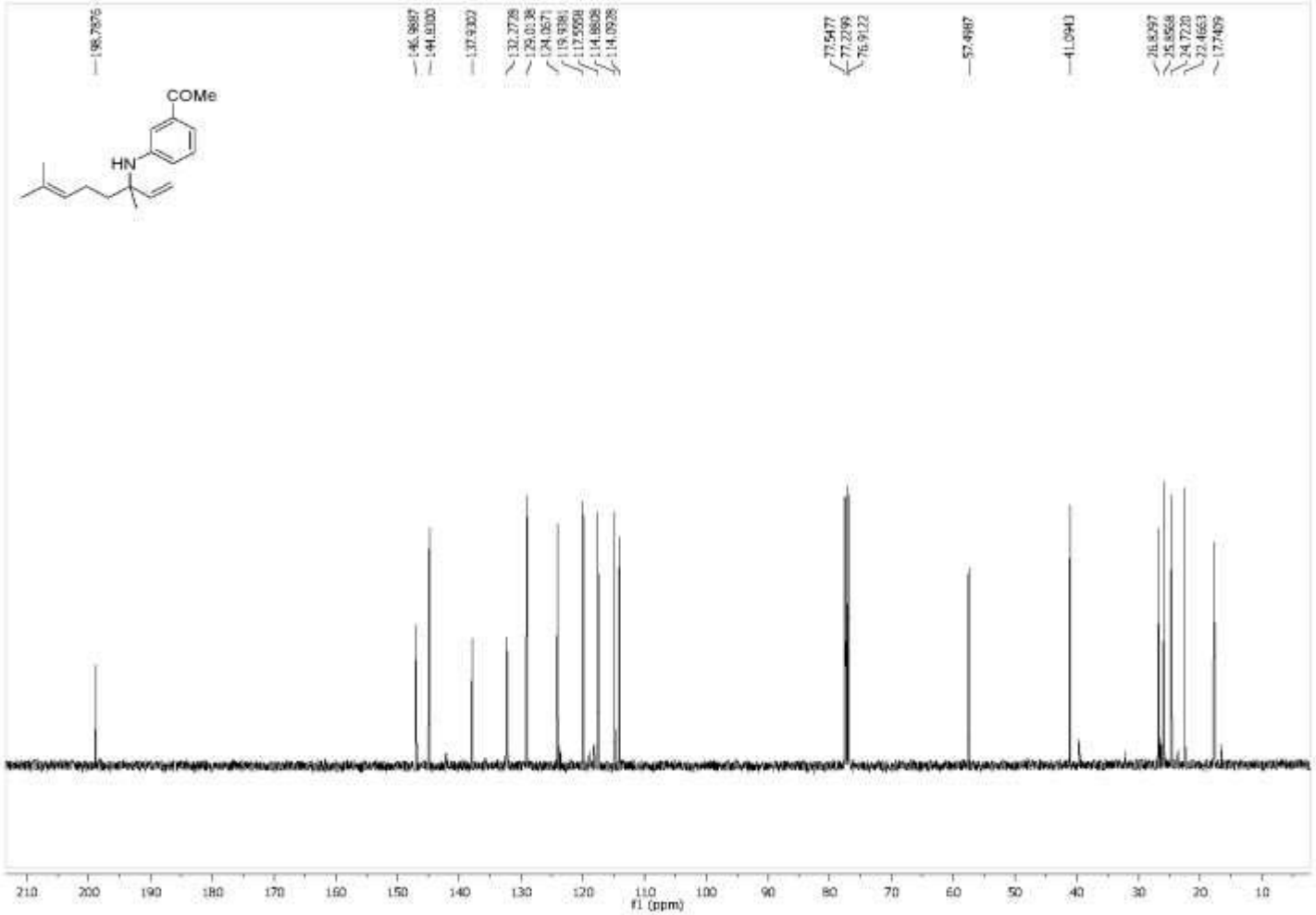

Figure A212 100 MHz 13C NMR ($CDCl_3$) Spectra of Compound **257k**

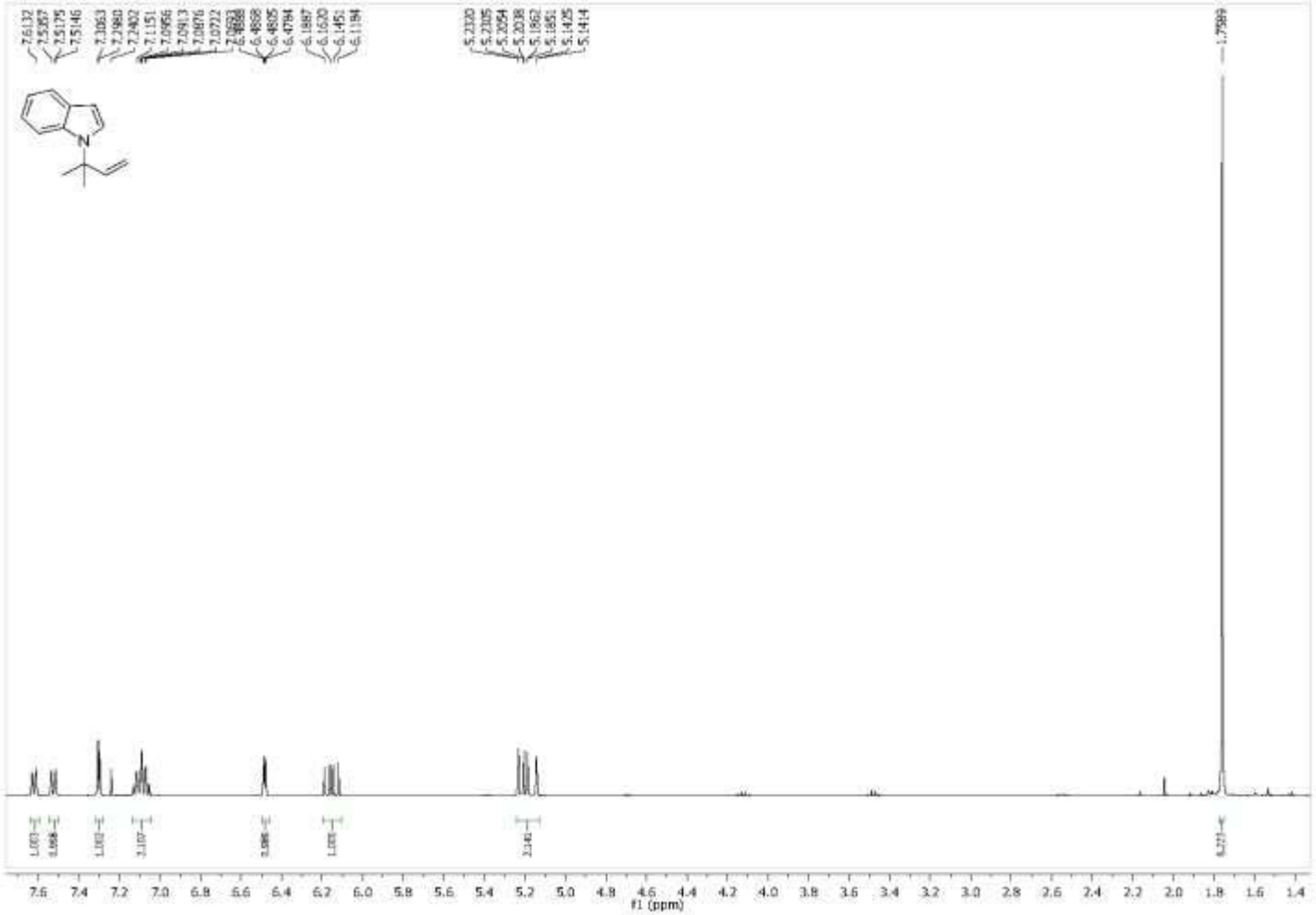

Figure A213 400 MHz 1H NMR ($CDCl_3$) Spectra of Compound **258**

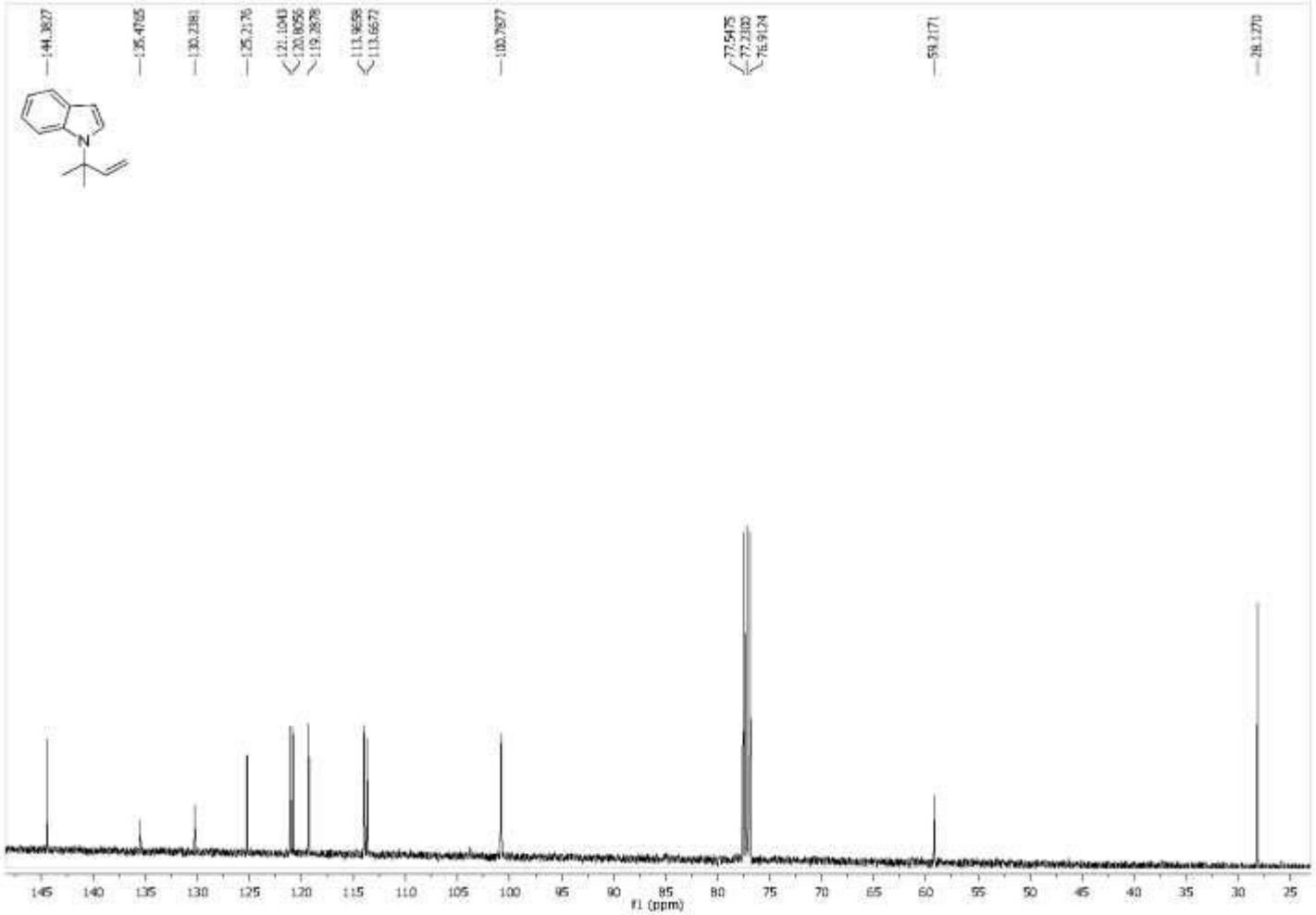

Figure A214 100 MHz 13C NMR ($CDCl_3$) Spectra of Compound **258**

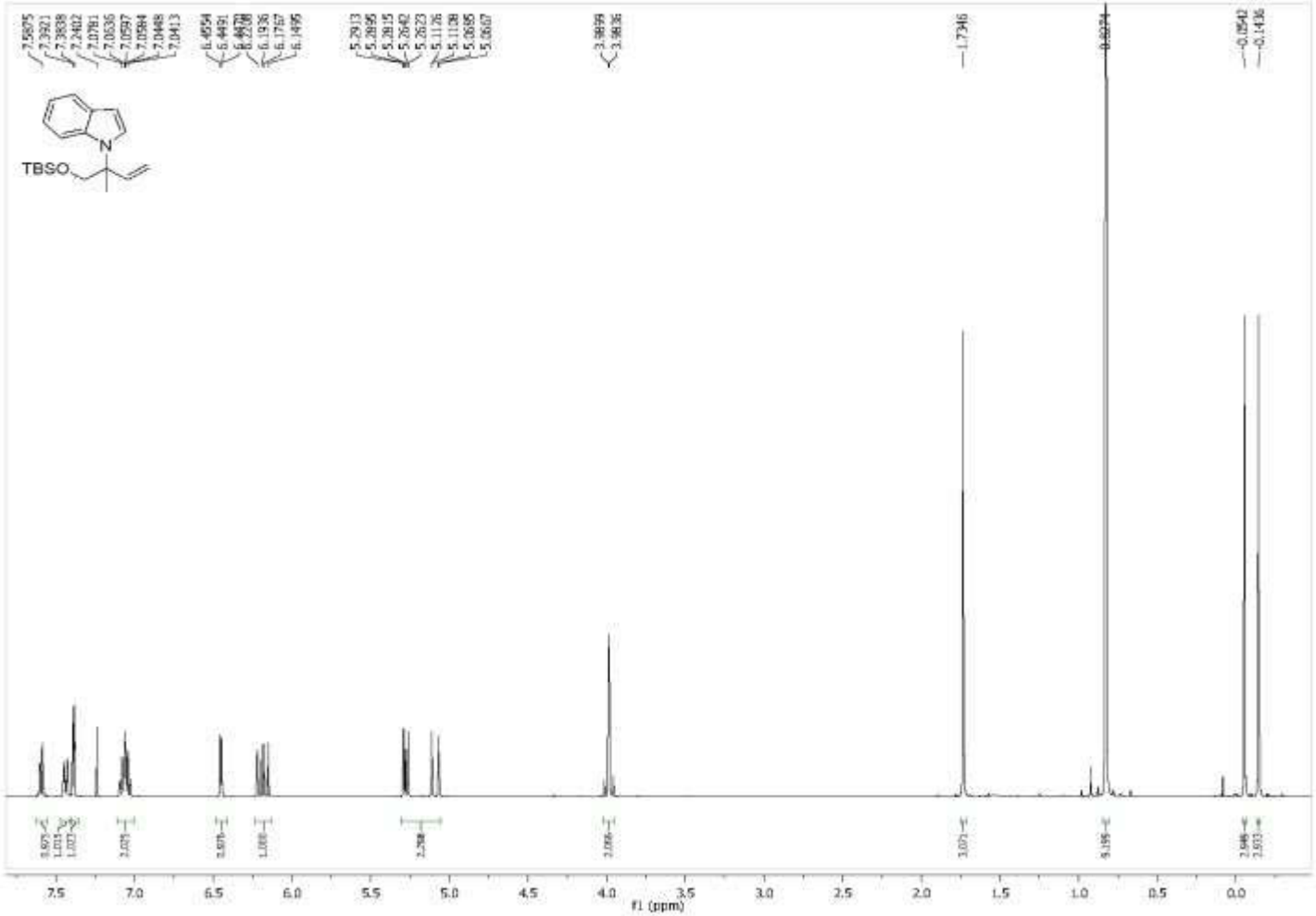

Figure A215 400 MHz 1H NMR ($CDCl_3$) Spectra of Compound **259**

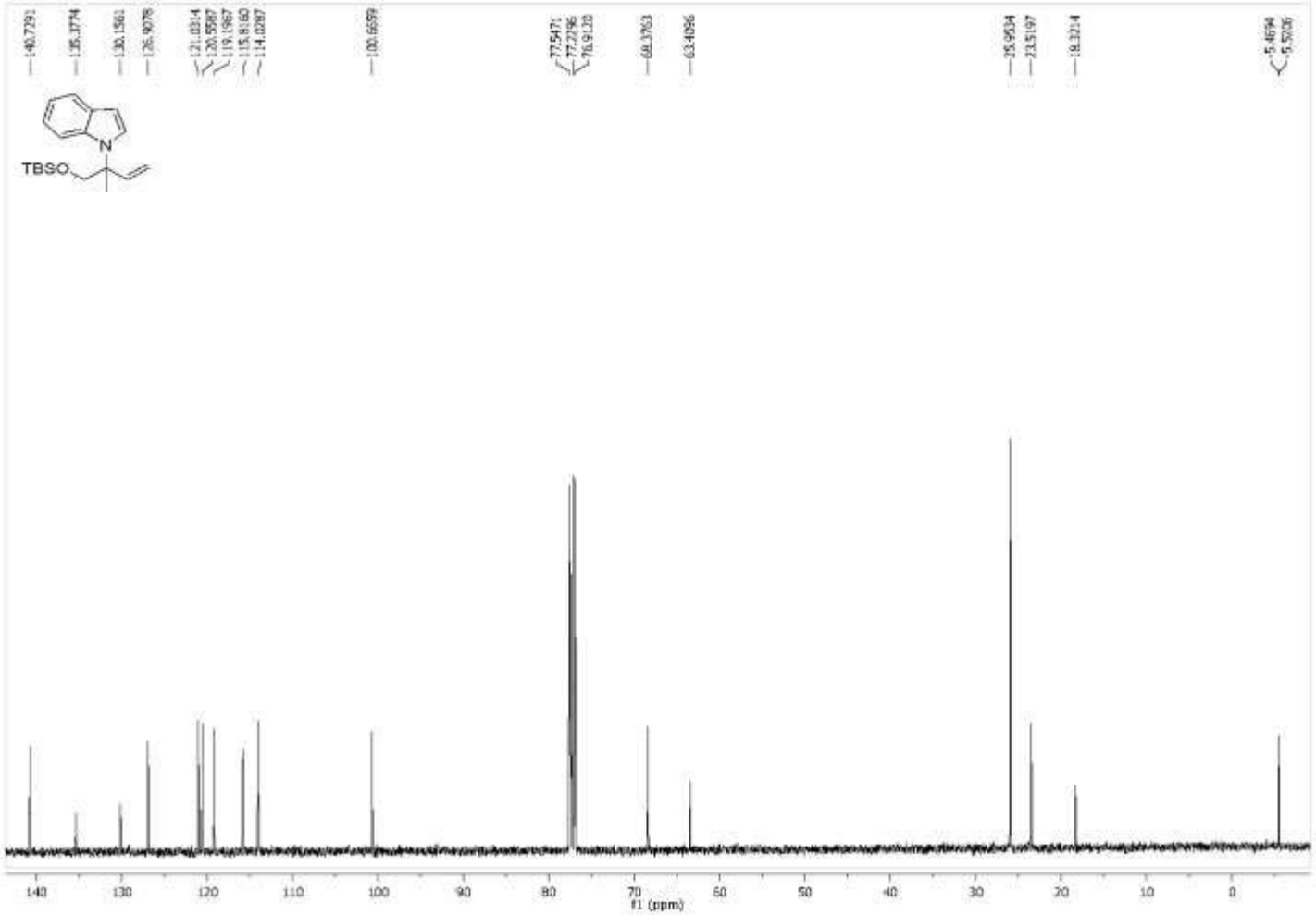

Figure A216 100 MHz 13C NMR ($CDCl_3$) Spectra of Compound **259**

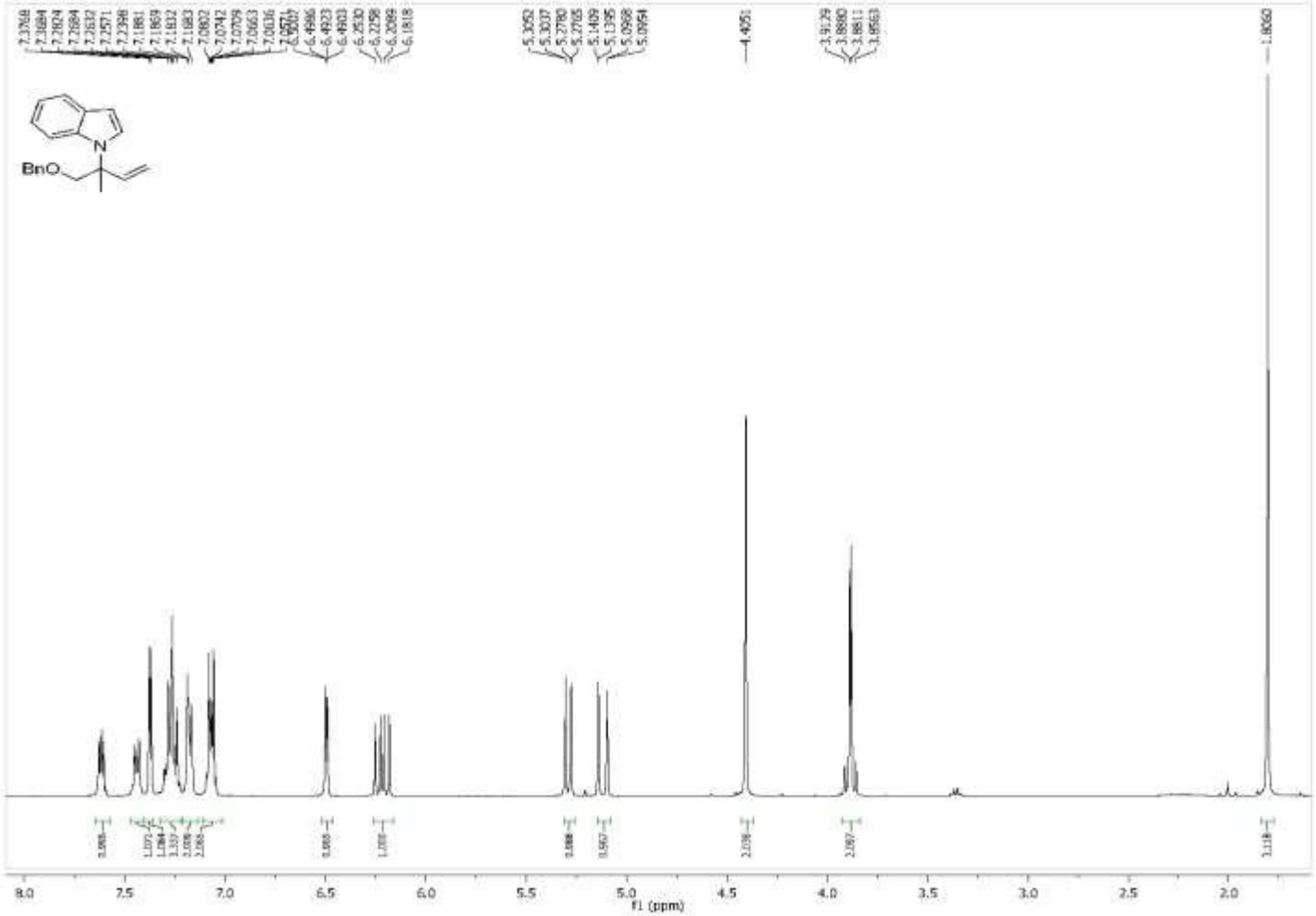

Figure A217 400 MHz 1H NMR ($CDCl_3$) Spectra of Compound **260**

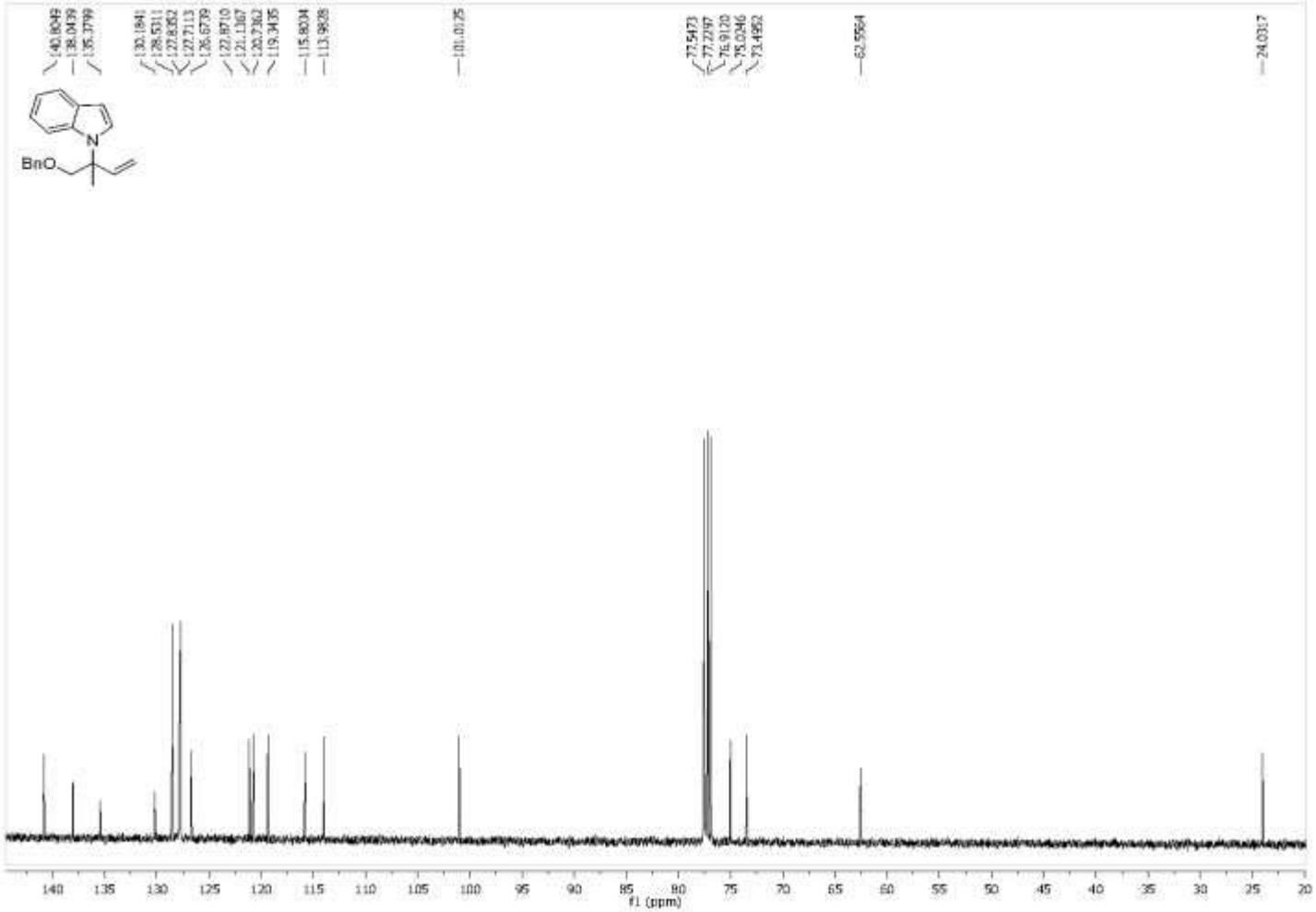

Figure A218 100 MHz 13C NMR ($CDCl_3$) Spectra of Compound **260**

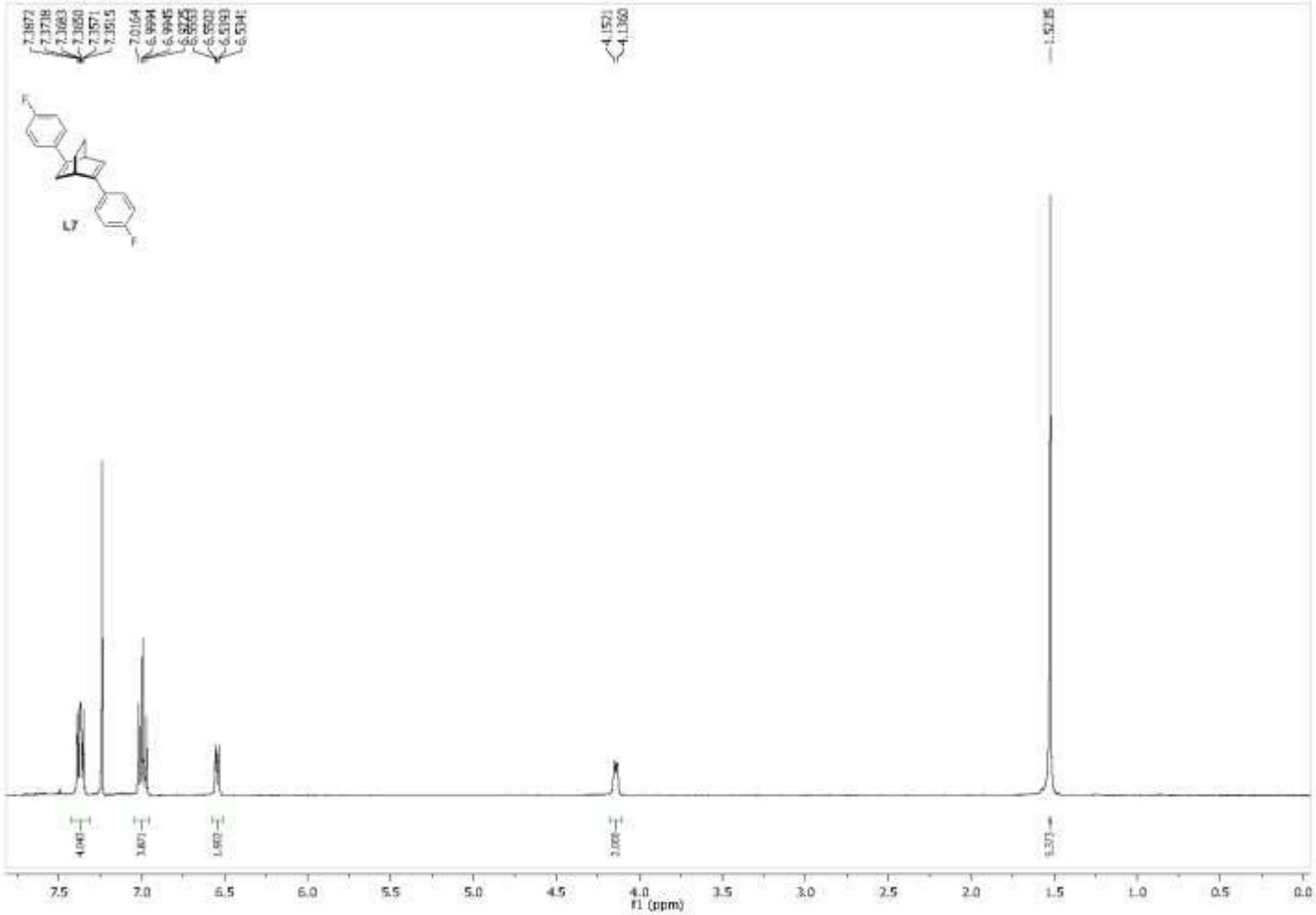

Figure A219 400 MHz 1H NMR ($CDCl_3$) Spectra of Compound **L7**

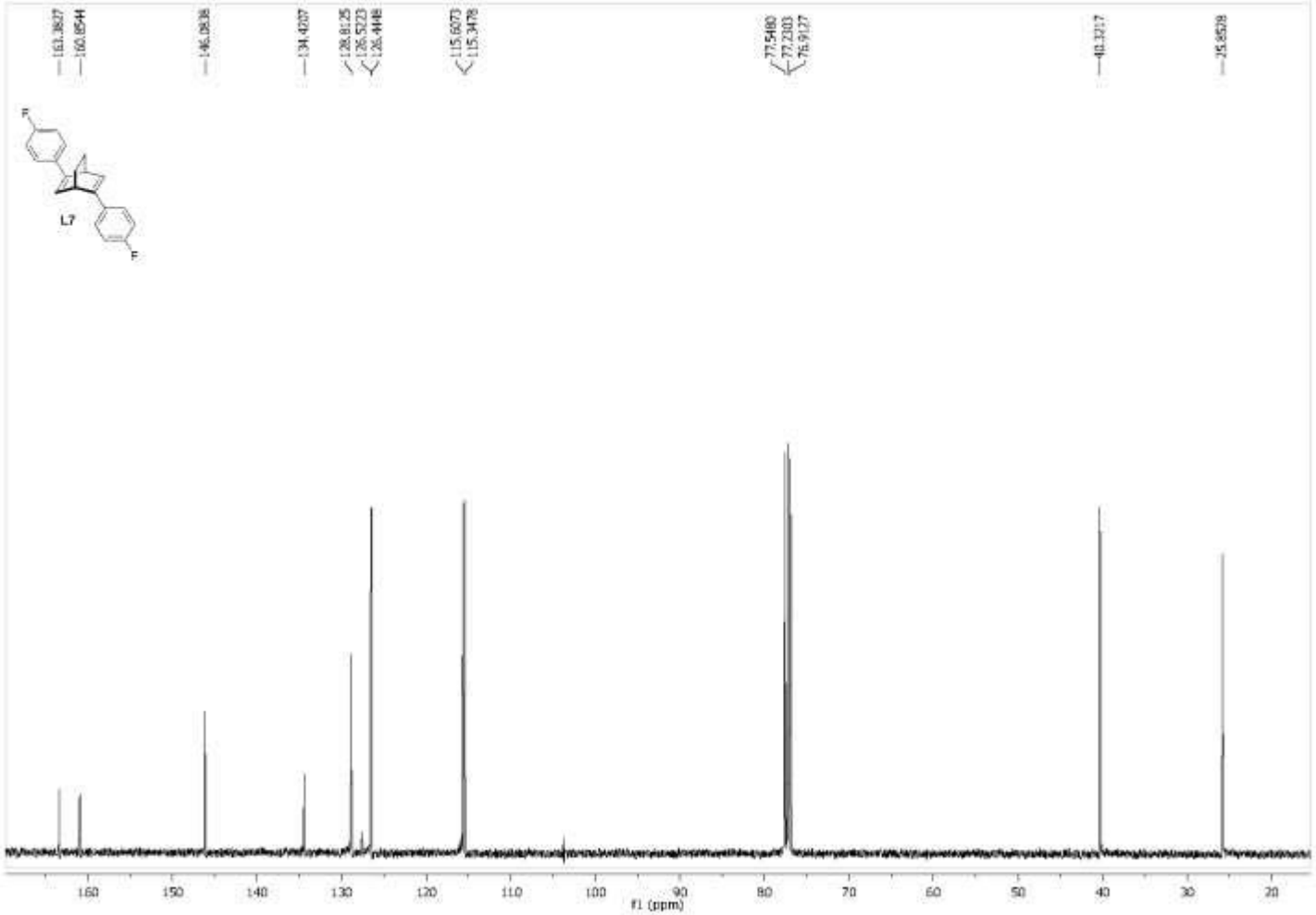

Figure A220 100 MHz 13C NMR ($CDCl_3$) Spectra of Compound **L7**

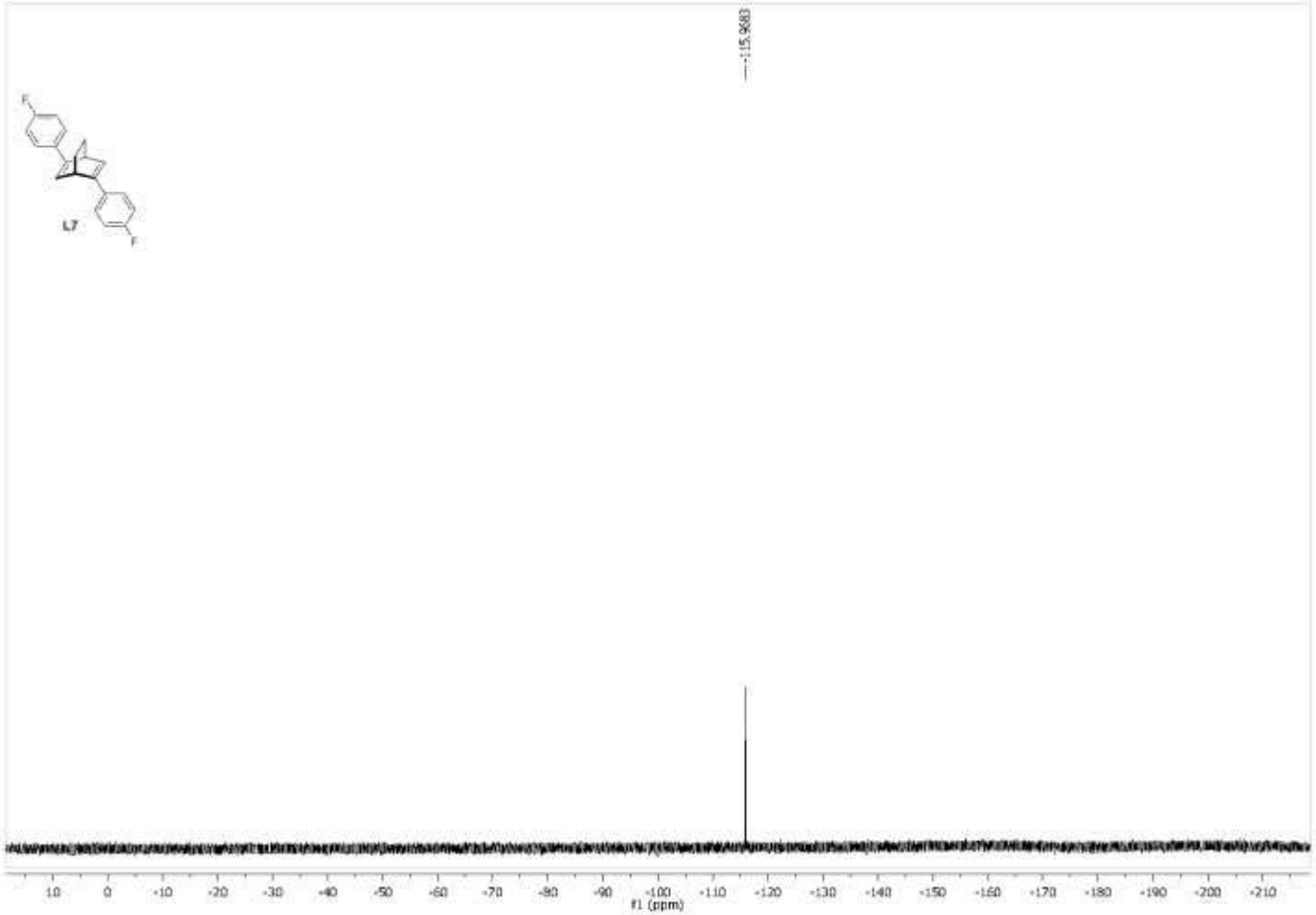

Figure A221 376 MHz 19F ($CDCl_3$) Spectra of Compound **L7**

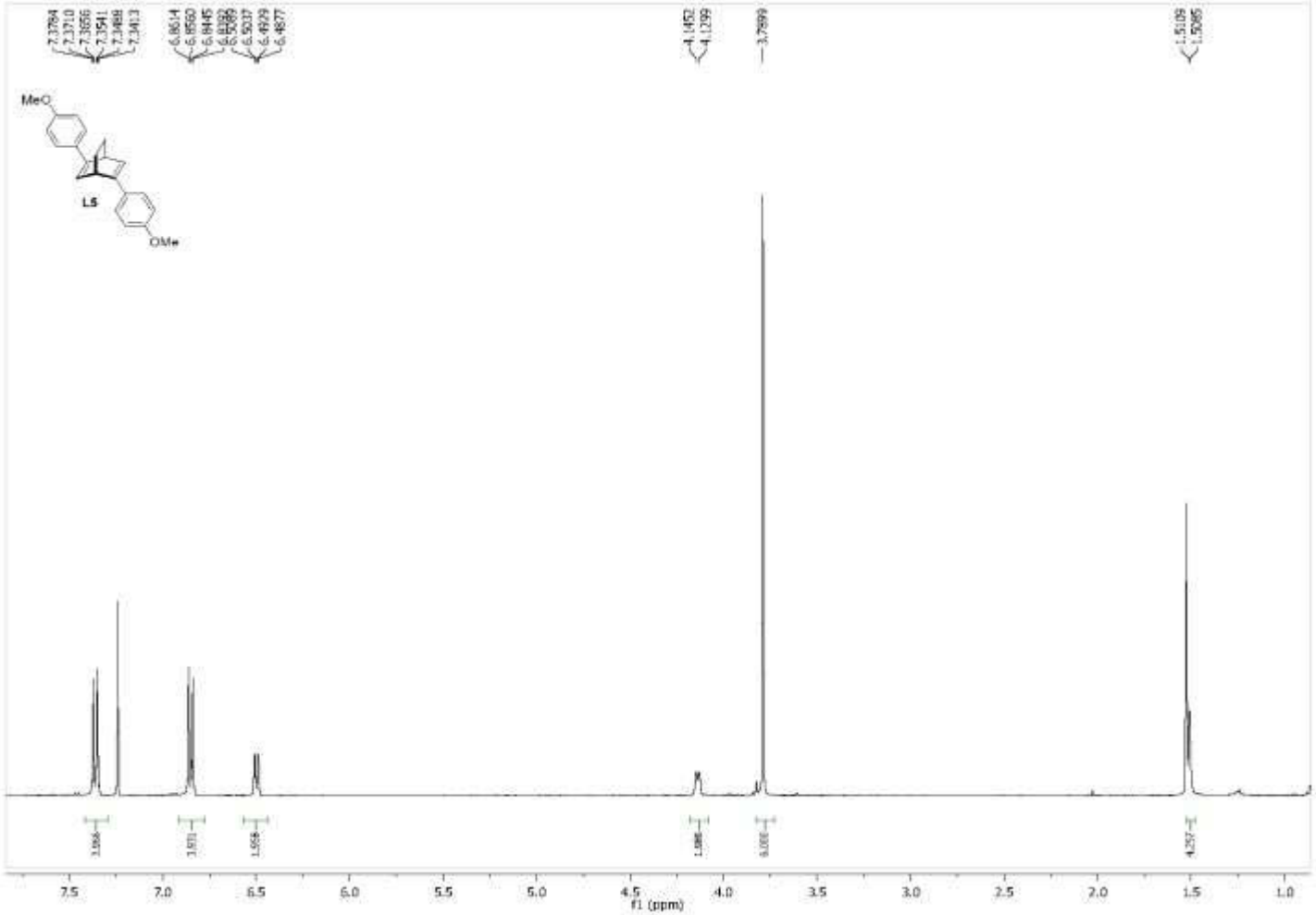

Figure A222 400 MHz 1H NMR ($CDCl_3$) Spectra of Compound **L5**

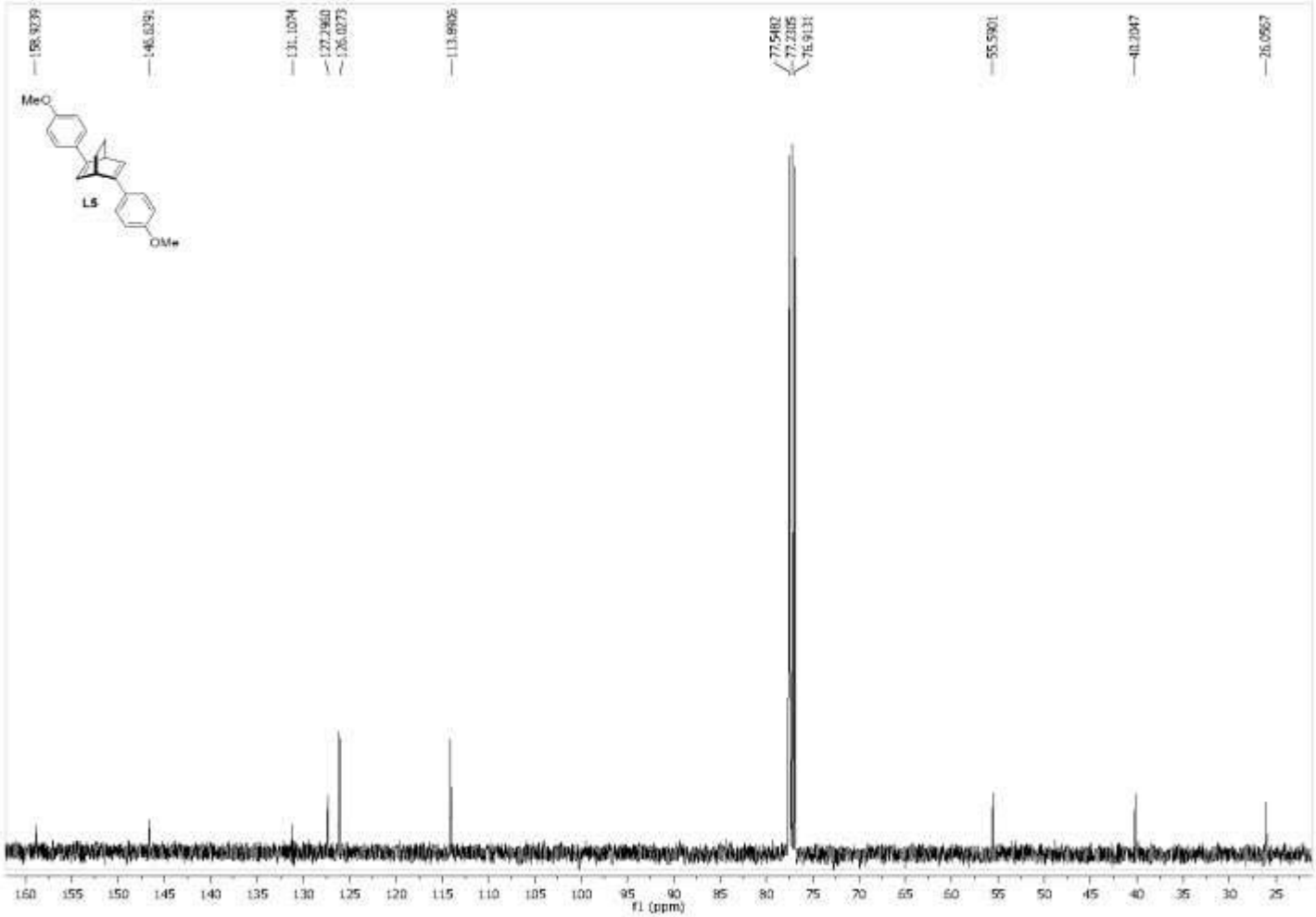

Figure A223 100 MHz 13C NMR ($CDCl_3$) Spectra of Compound **L5**

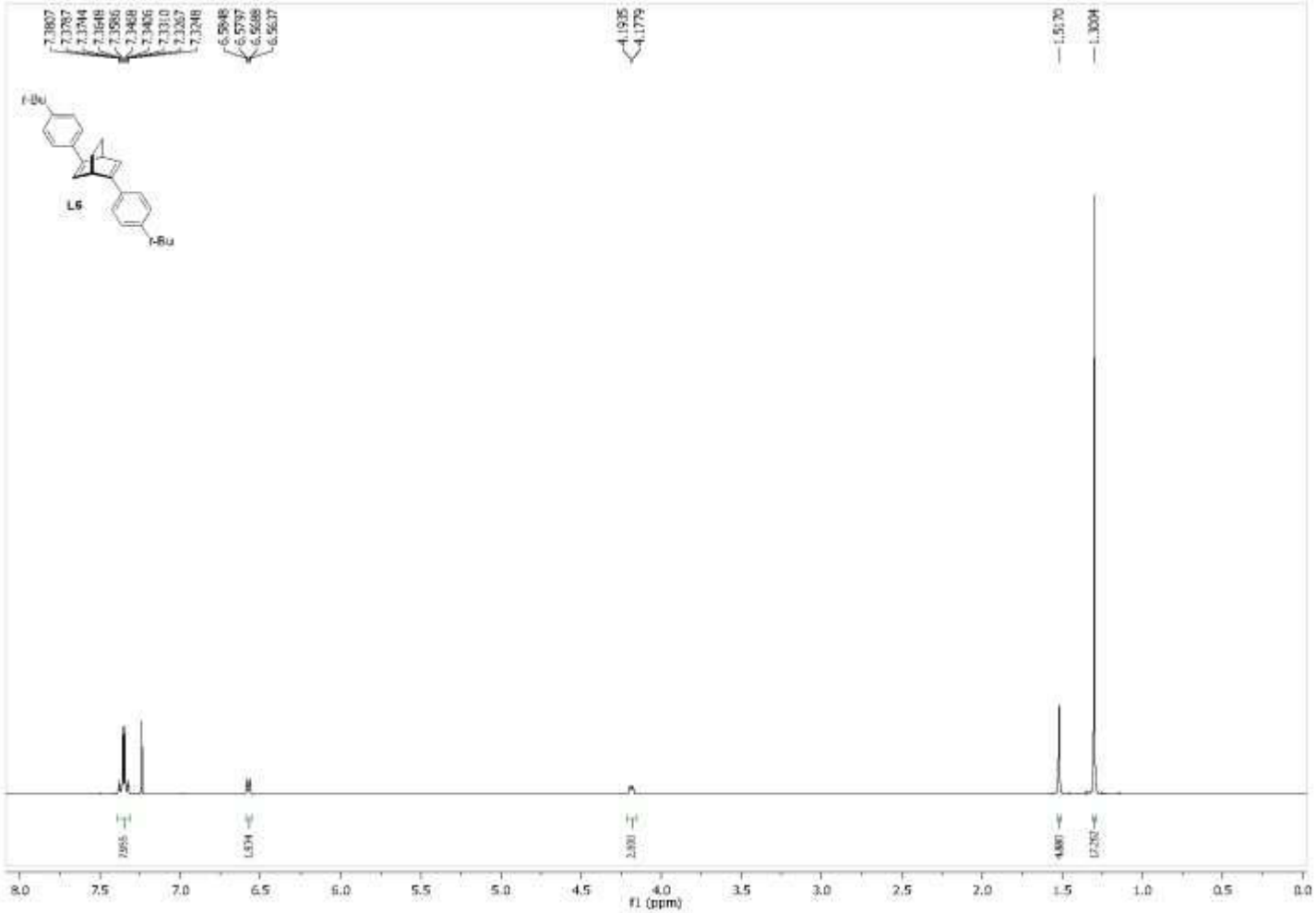

Figure A224 400 MHz 1H NMR ($CDCl_3$) Spectra of Compound **L6**

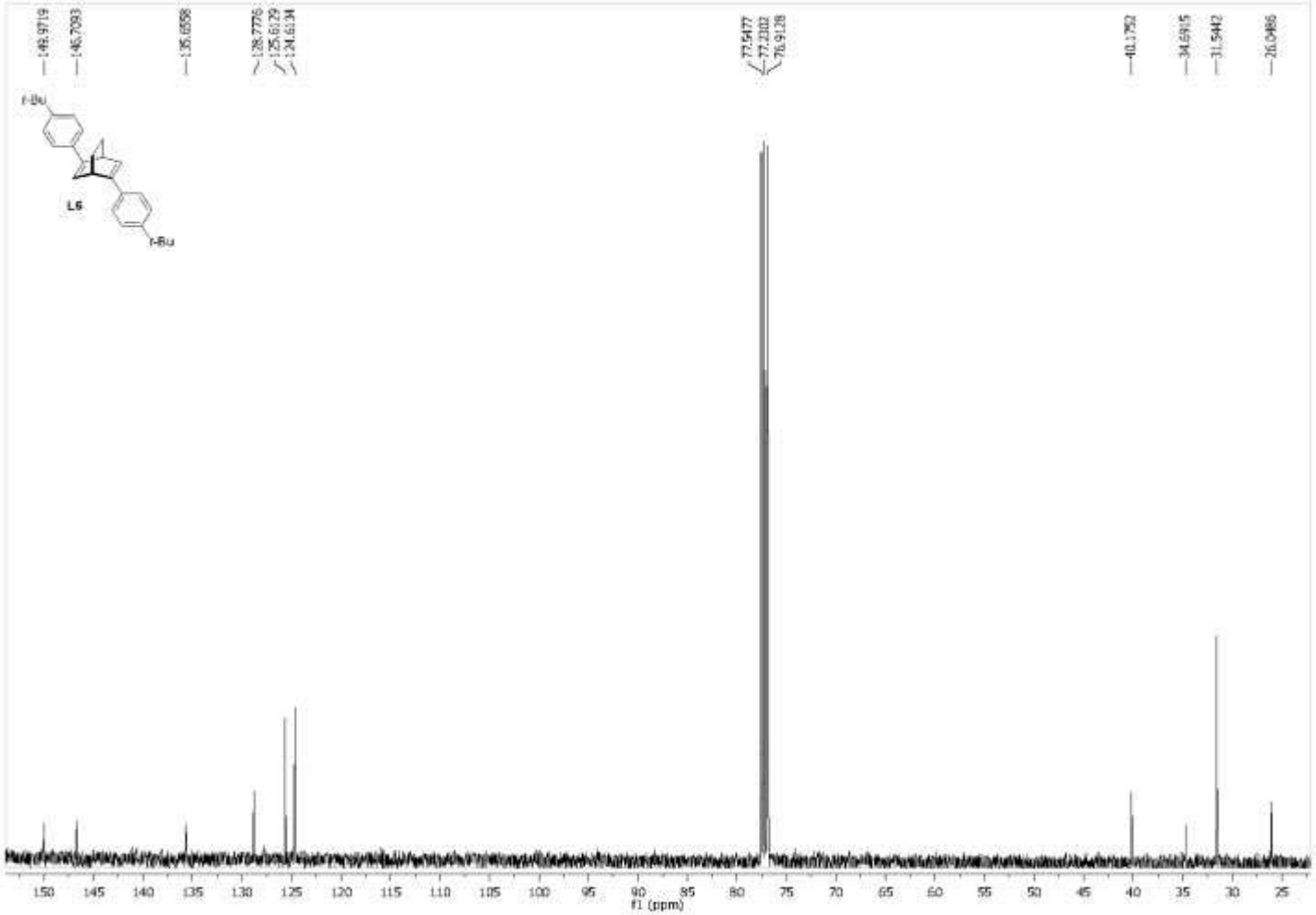

Figure A225 100 MHz 13C NMR ($CDCl_3$) Spectra of Compound **L6**

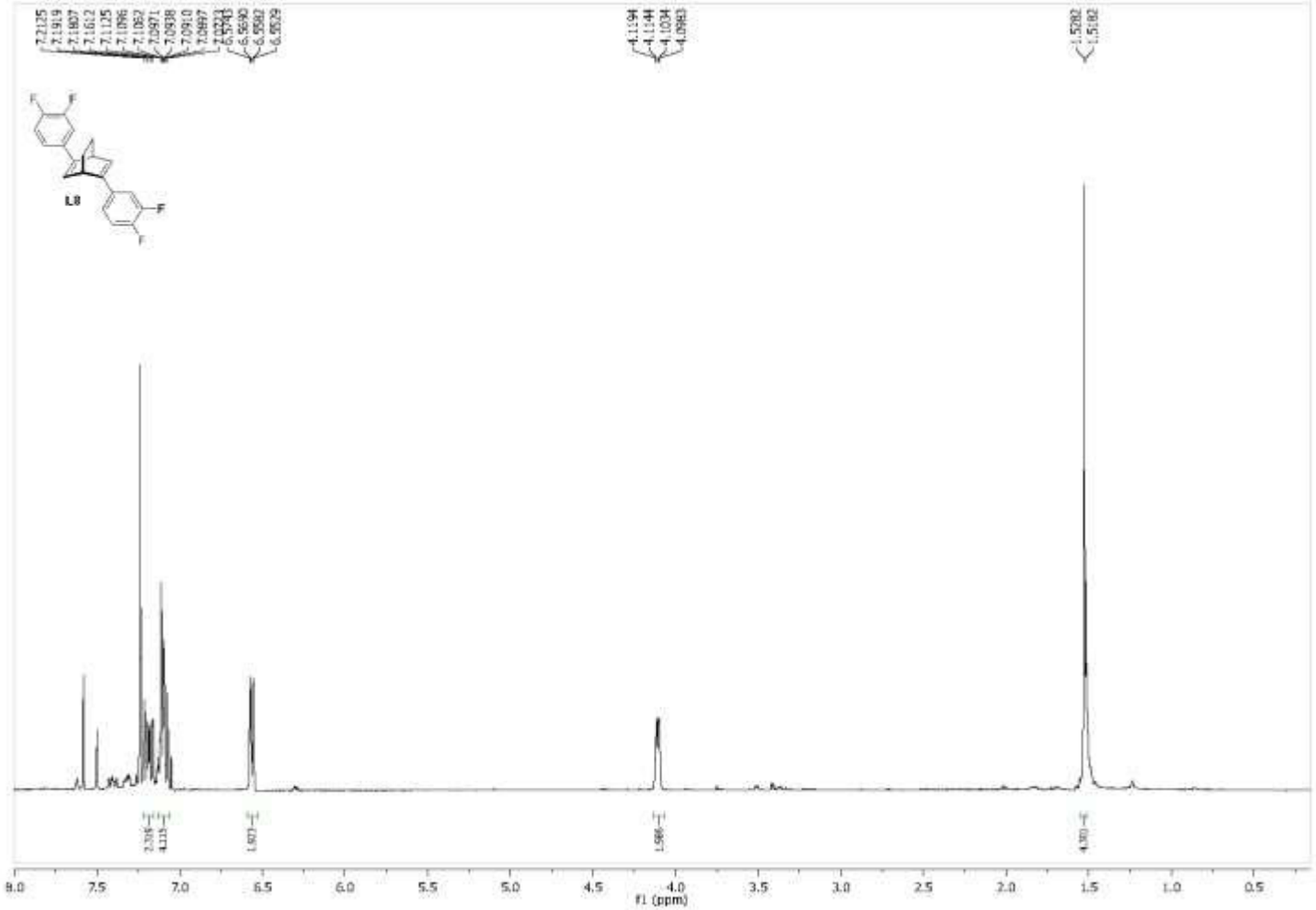

Figure A226 400 MHz 1H NMR ($CDCl_3$) Spectra of Compound **L8**

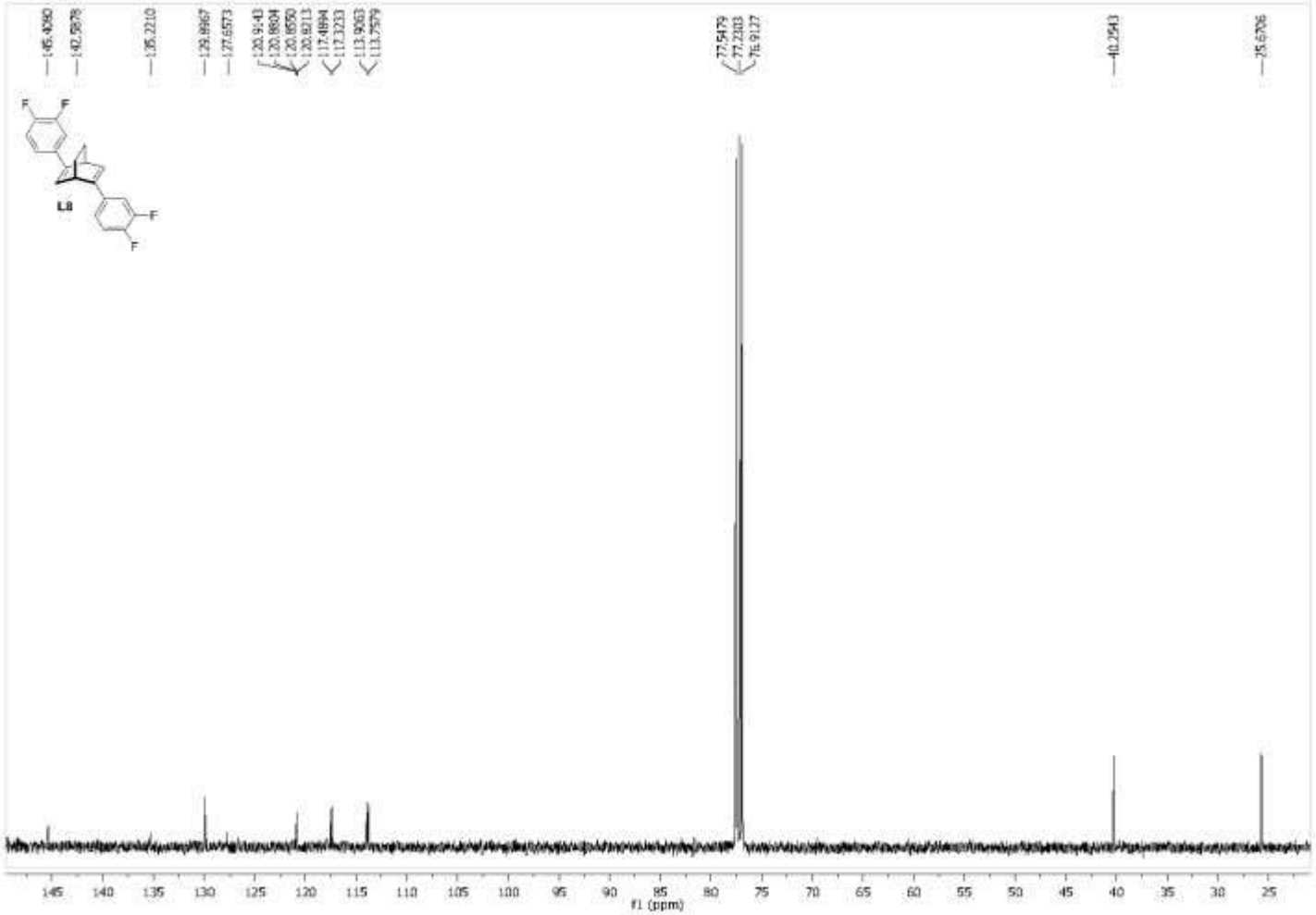

Figure A227 100 MHz 13C NMR ($CDCl_3$) Spectra of Compound **L8**

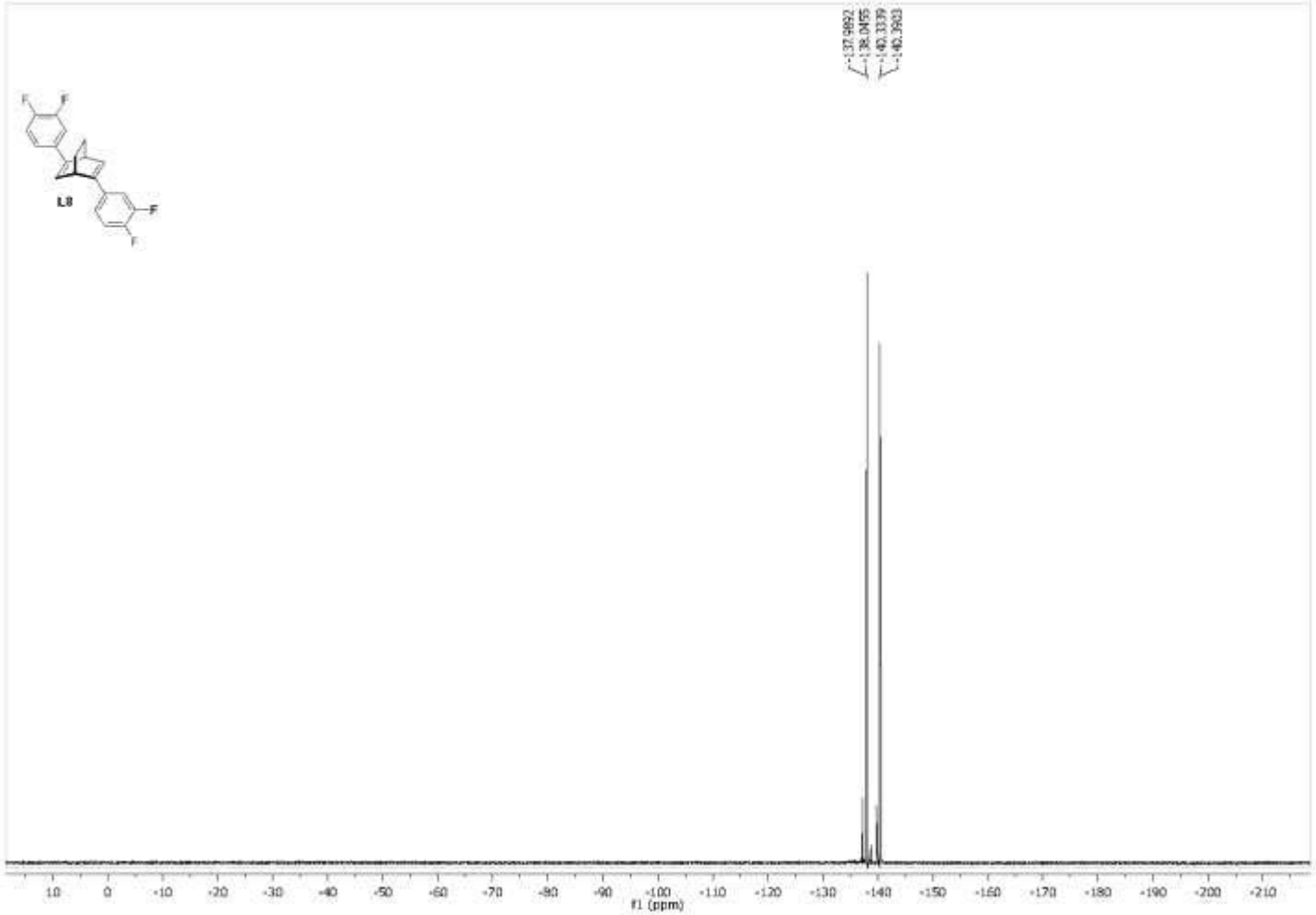

Figure A228 376 MHz 19F ($CDCl_3$) Spectra of Compound **L8**

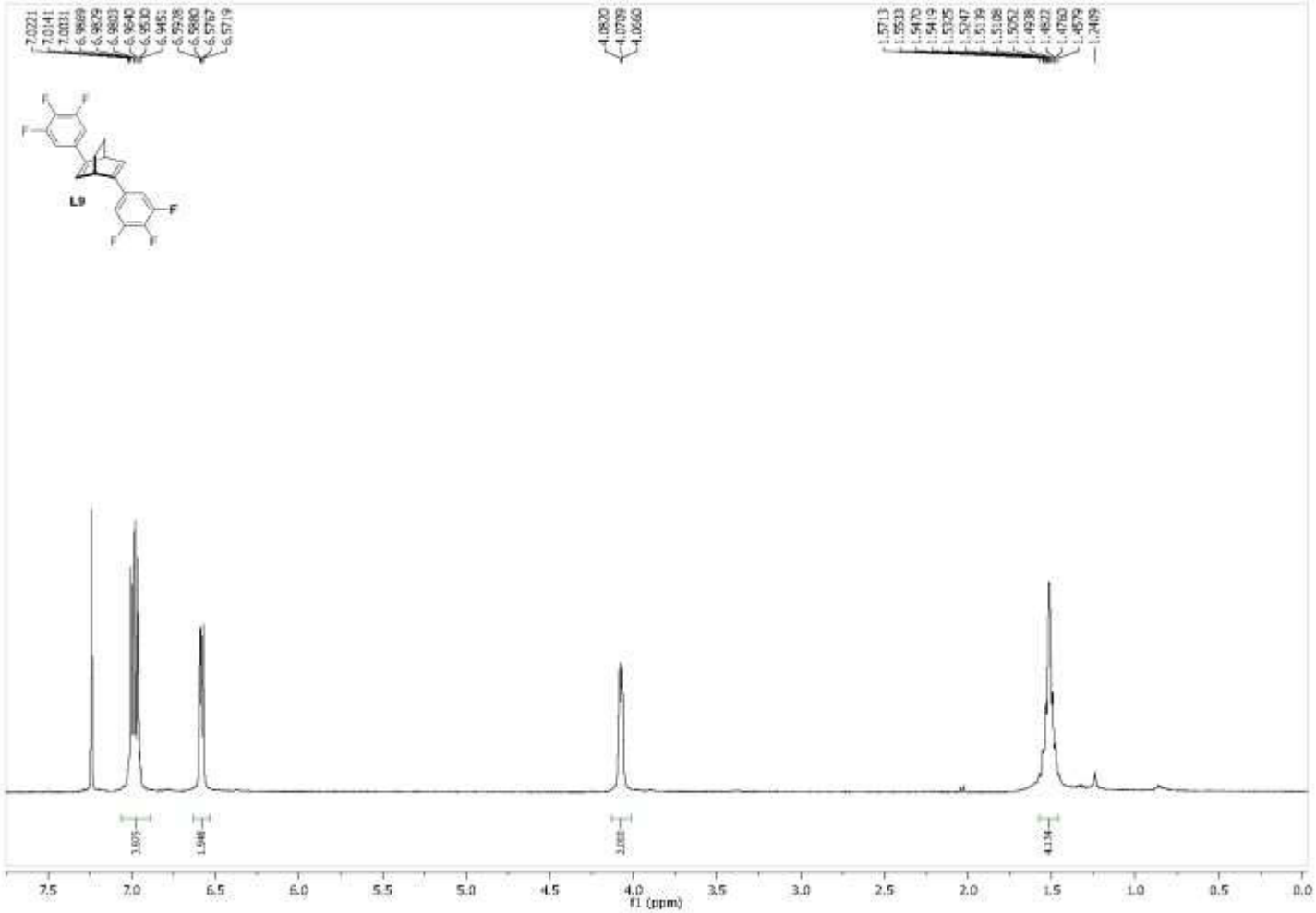

Figure A229 400 MHz 1H NMR ($CDCl_3$) Spectra of Compound **L9**

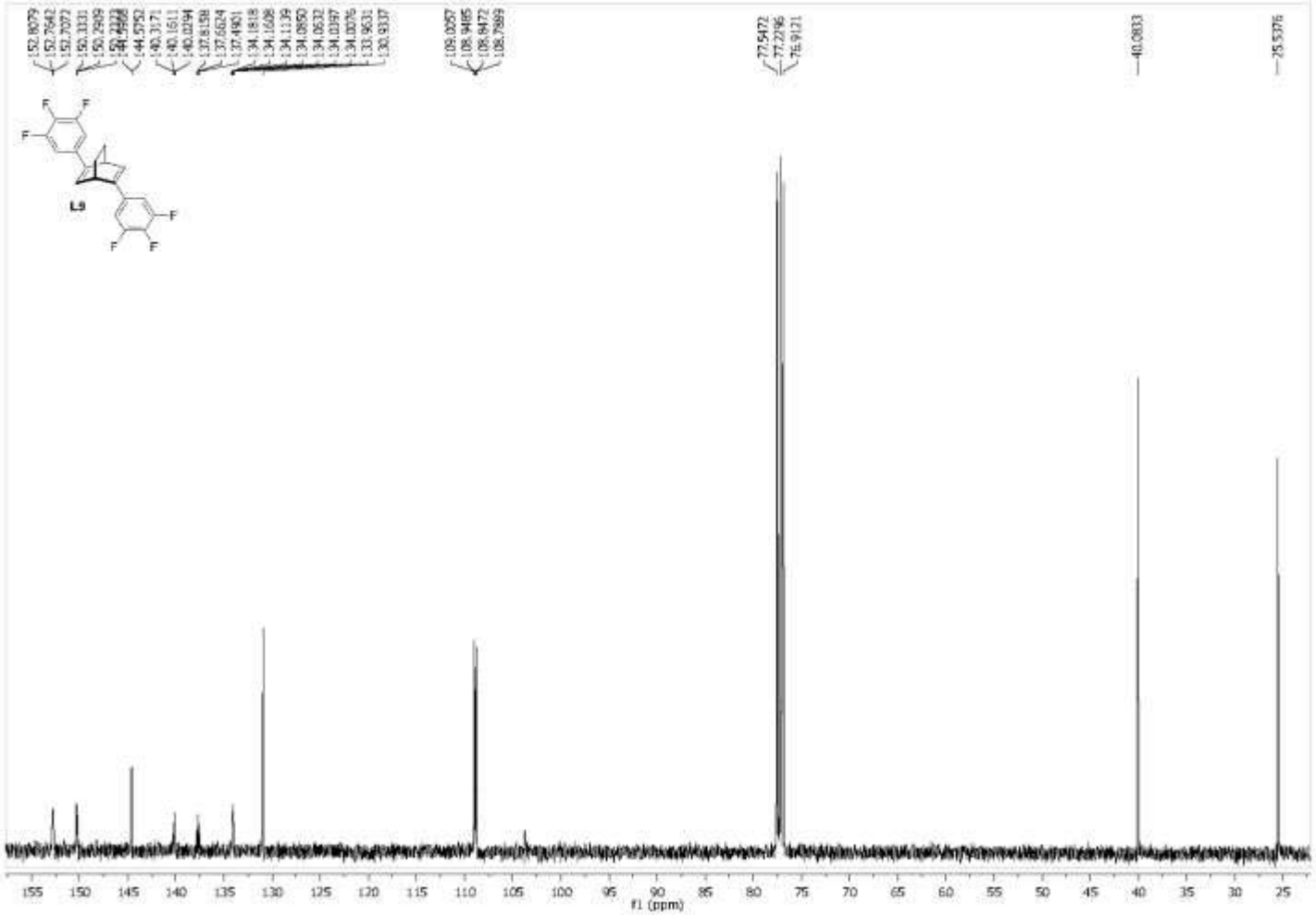

Figure A230 100 MHz 13C NMR ($CDCl_3$) Spectra of Compound **L9**

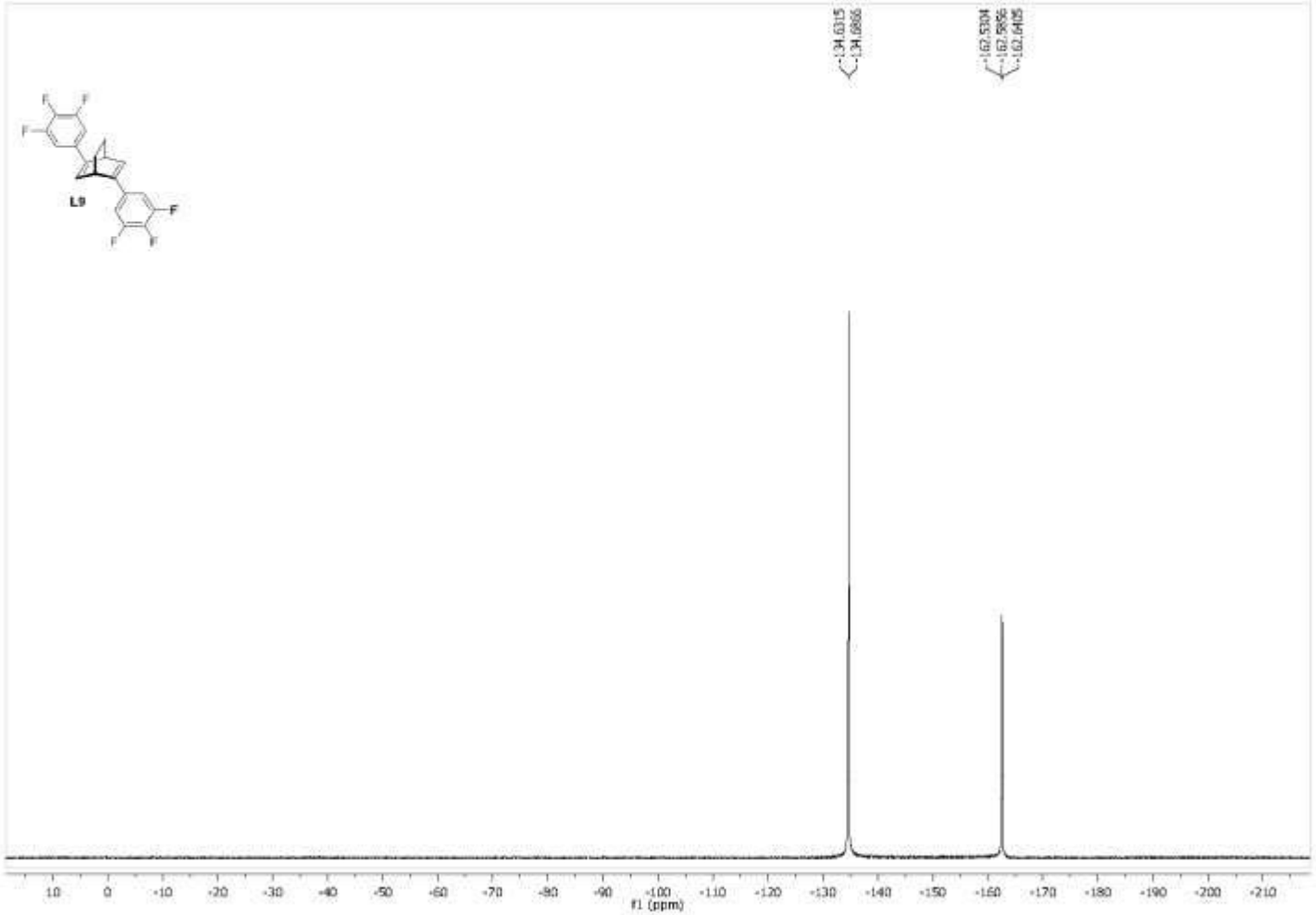

Figure A231 376 MHz 19F ($CDCl_3$) Spectra of Compound **L9**

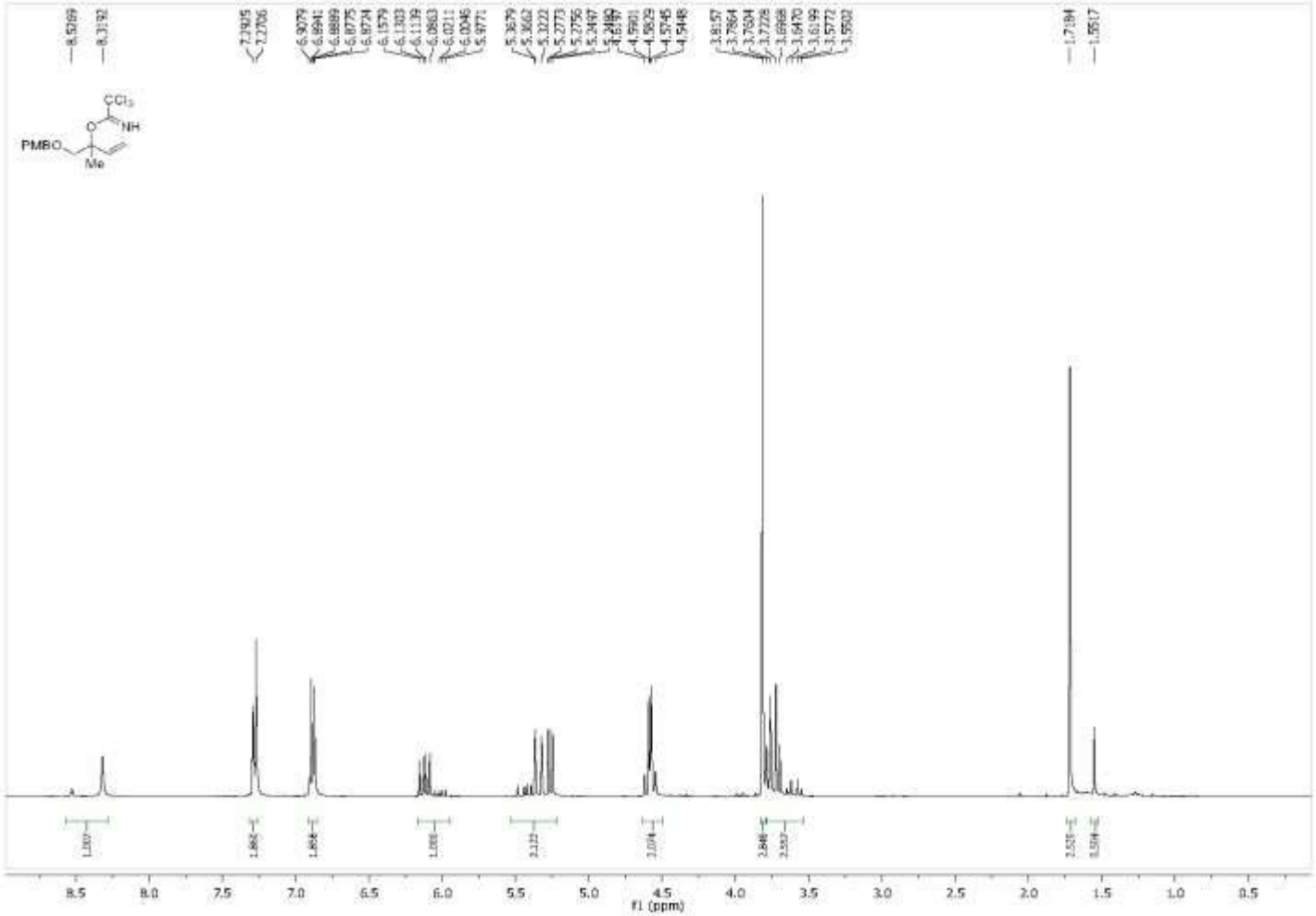

Figure A232 400 MHz 1H NMR ($CDCl_3$) Spectra of Compound **299**

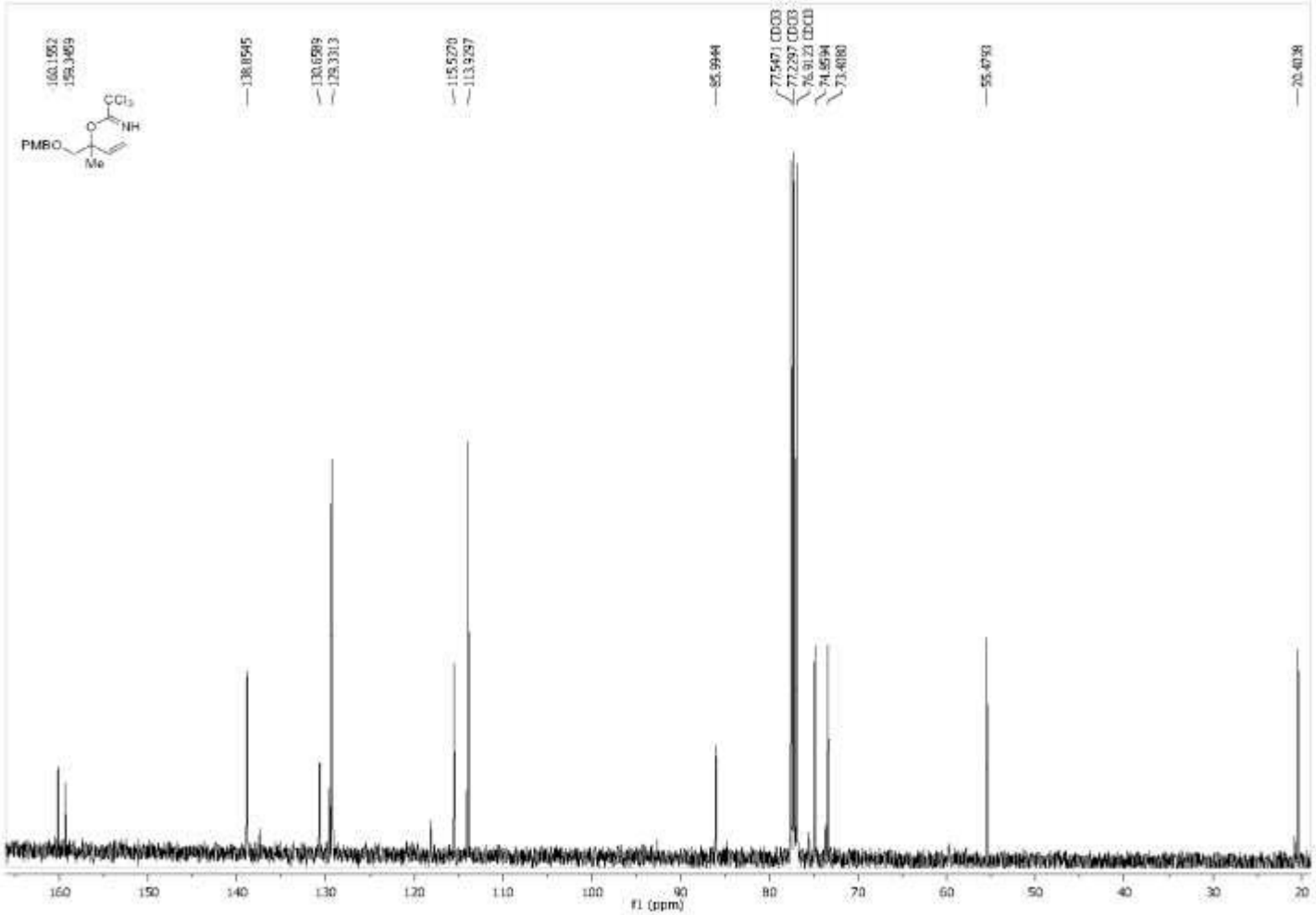

Figure A233 100 MHz 13C NMR ($CDCl_3$) Spectra of Compound **299**

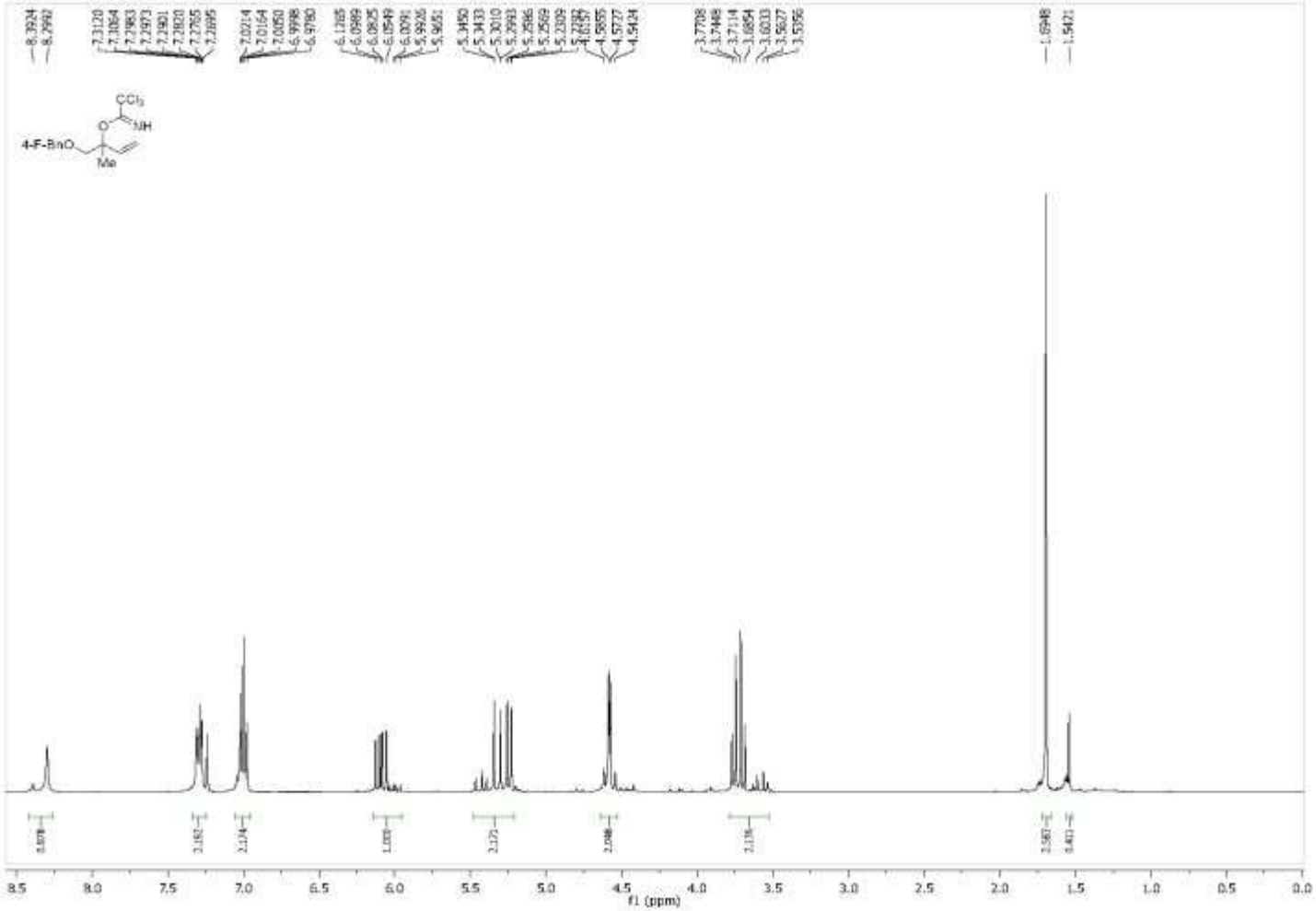

Figure A234 400 MHz 1H NMR ($CDCl_3$) Spectra of Compound **300**

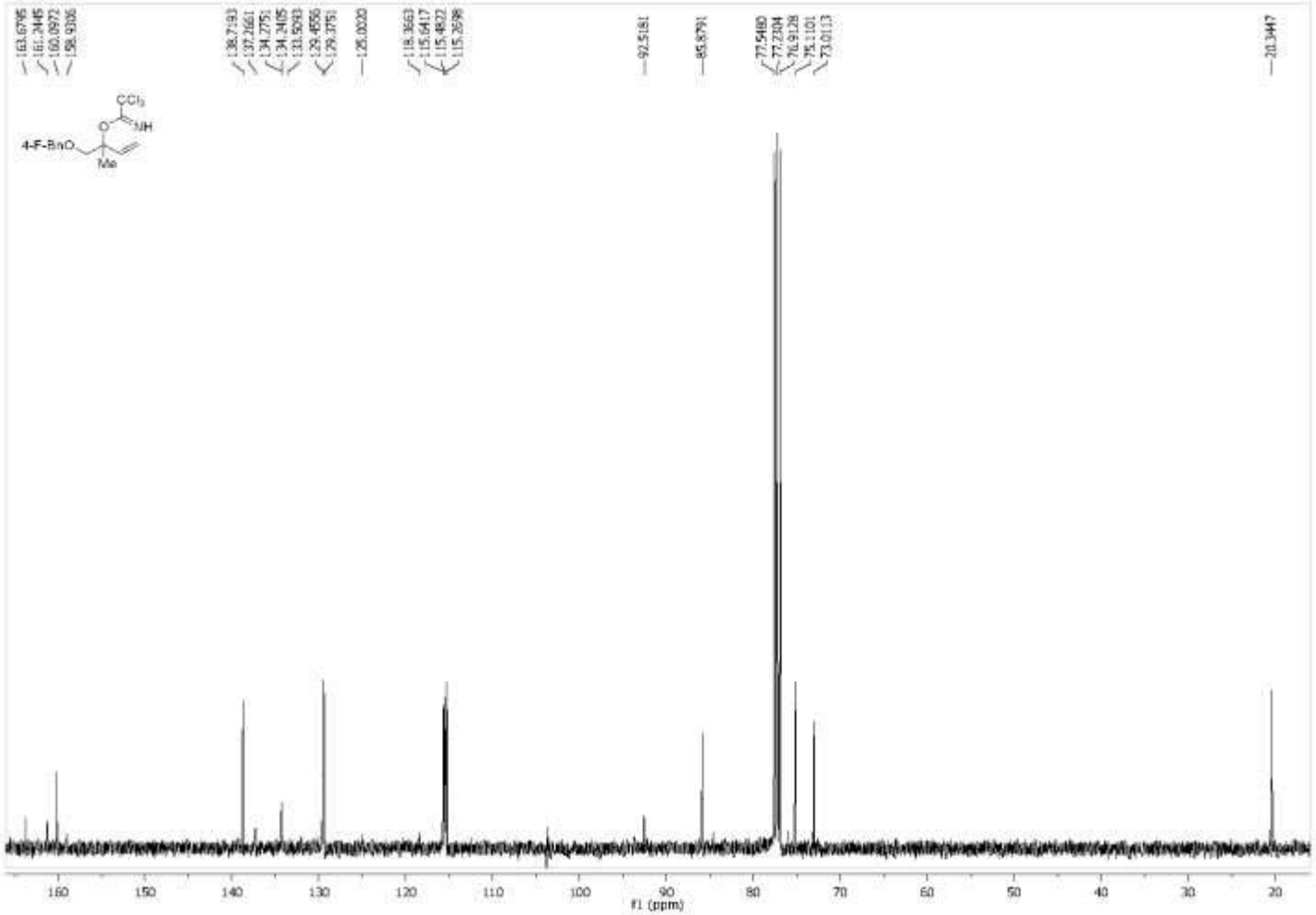

Figure A235 100 MHz 13C NMR ($CDCl_3$) Spectra of Compound **300**

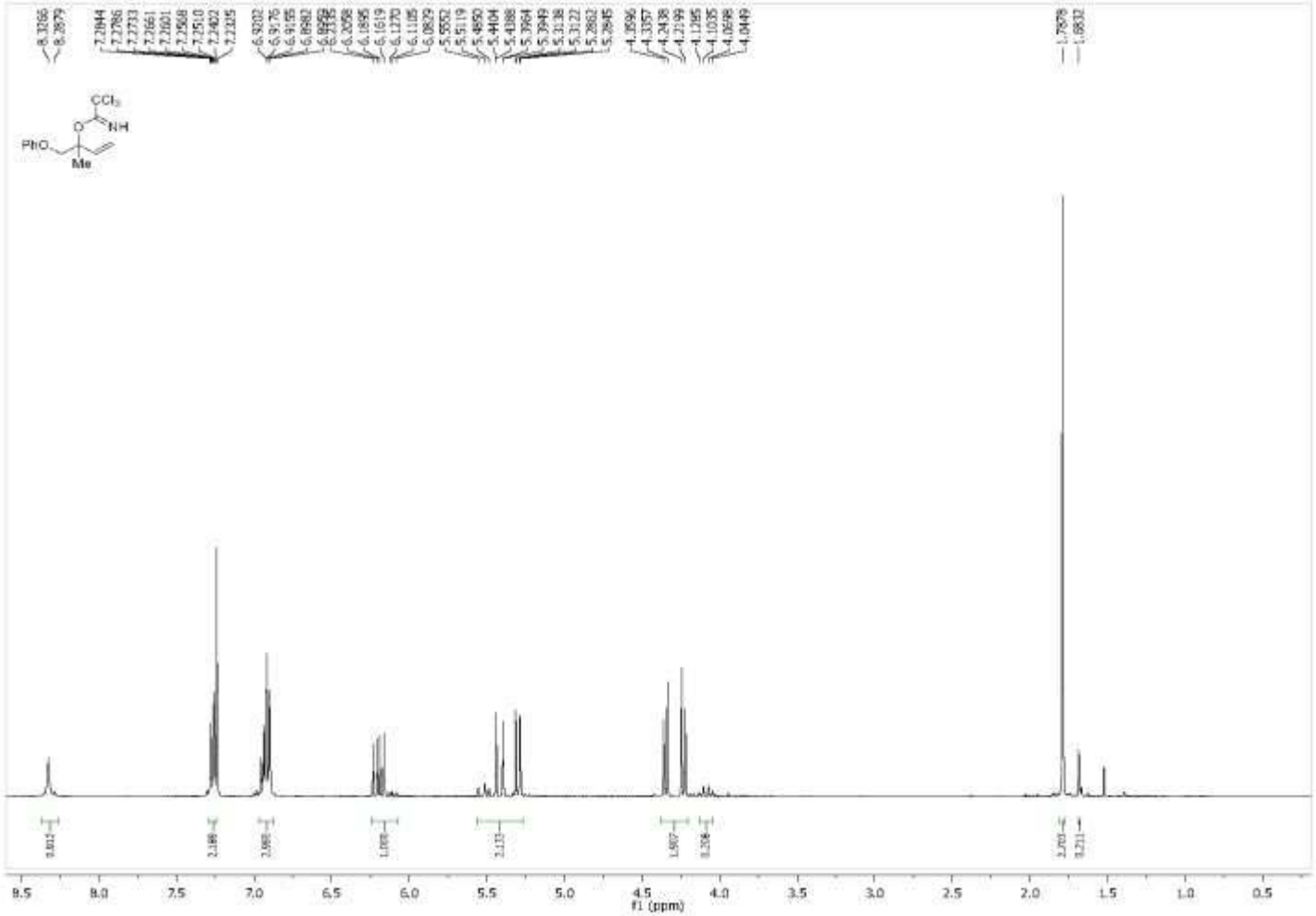

Figure A236 400 MHz 1H NMR ($CDCl_3$) Spectra of Compound **301**

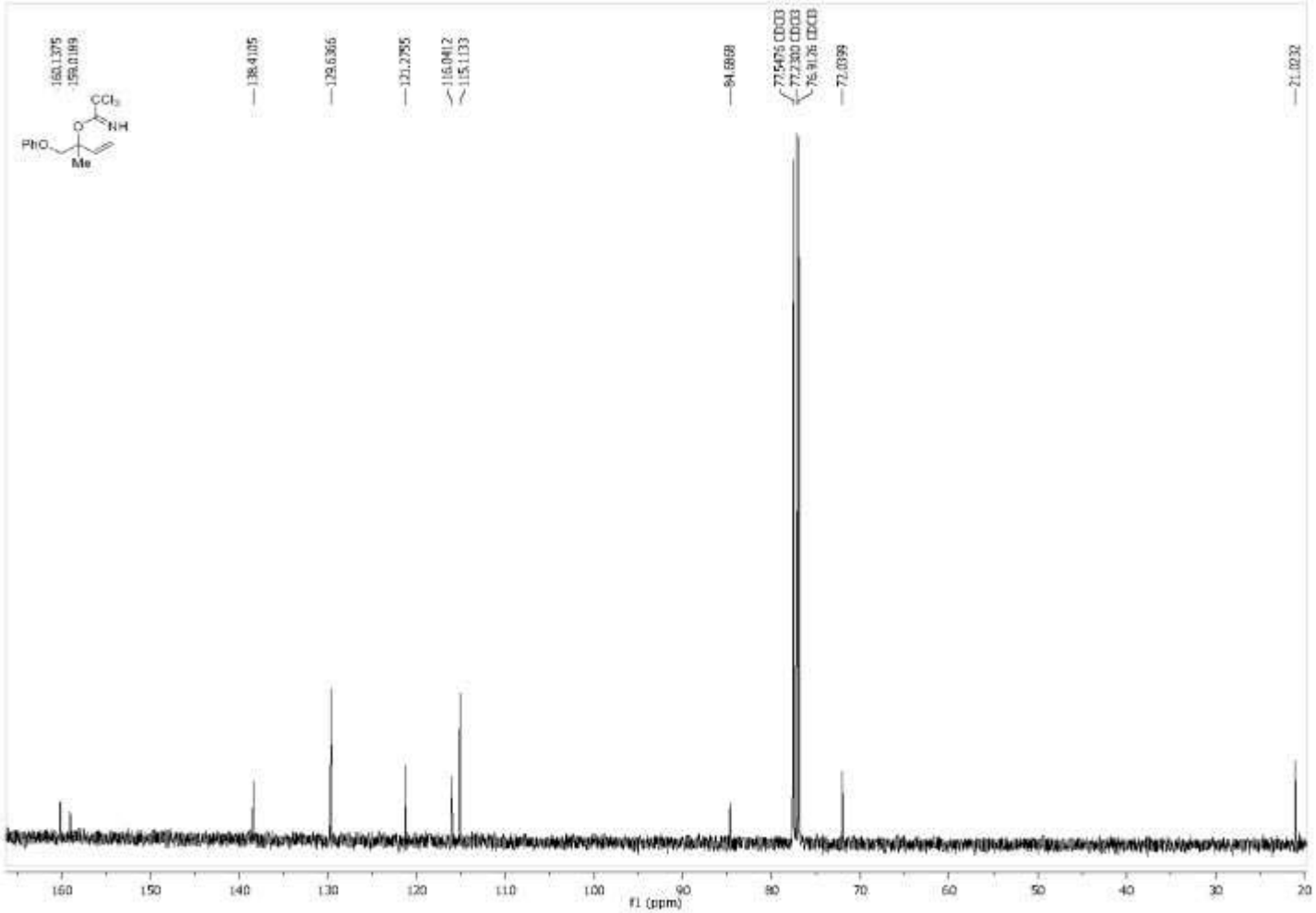

Figure A237 100 MHz 13C NMR ($CDCl_3$) Spectra of Compound **301**

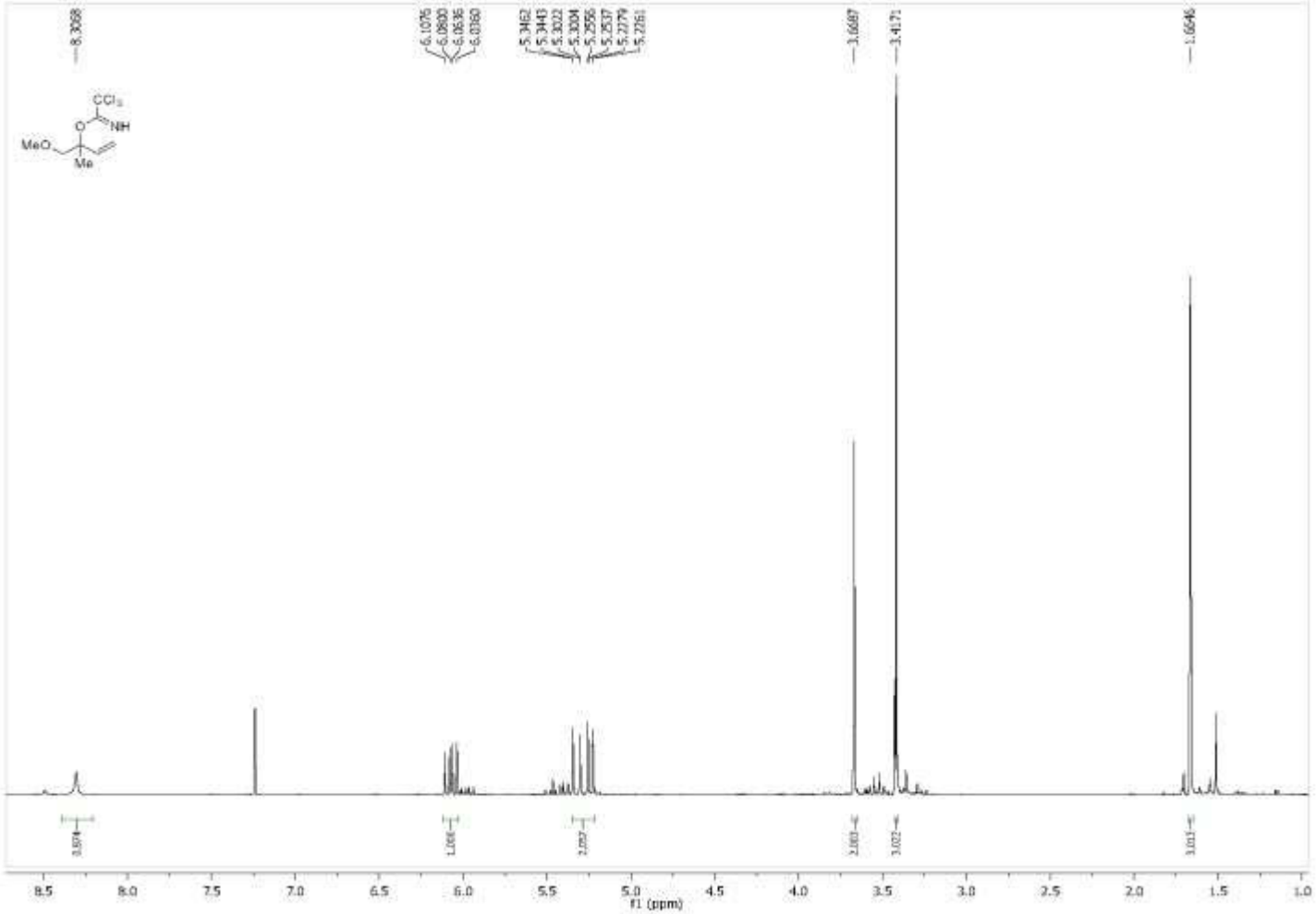

Figure A238 400 MHz 1H NMR ($CDCl_3$) Spectra of Compound **302**

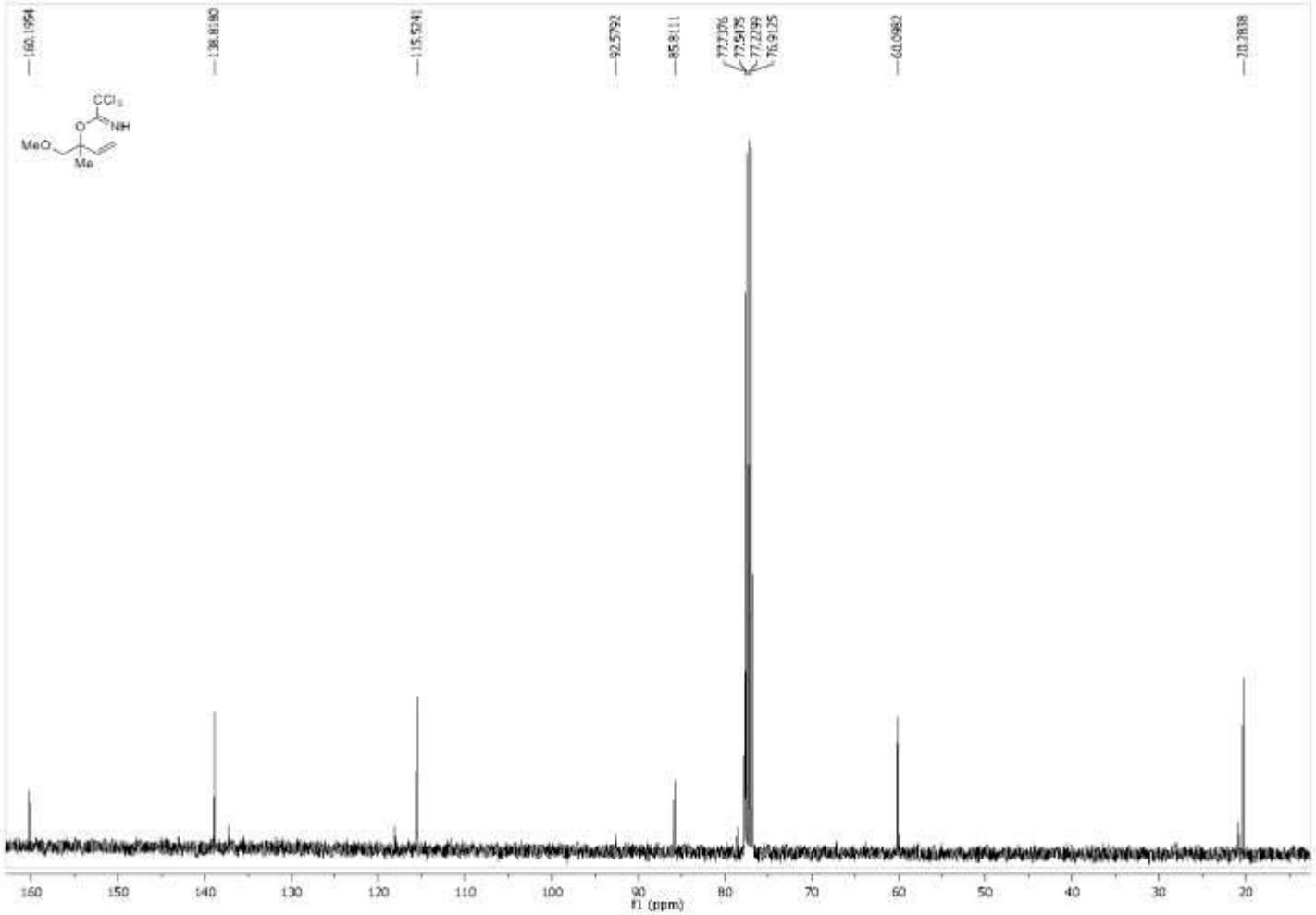

Figure A239 100 MHz 13C NMR ($CDCl_3$) Spectra of Compound **302**

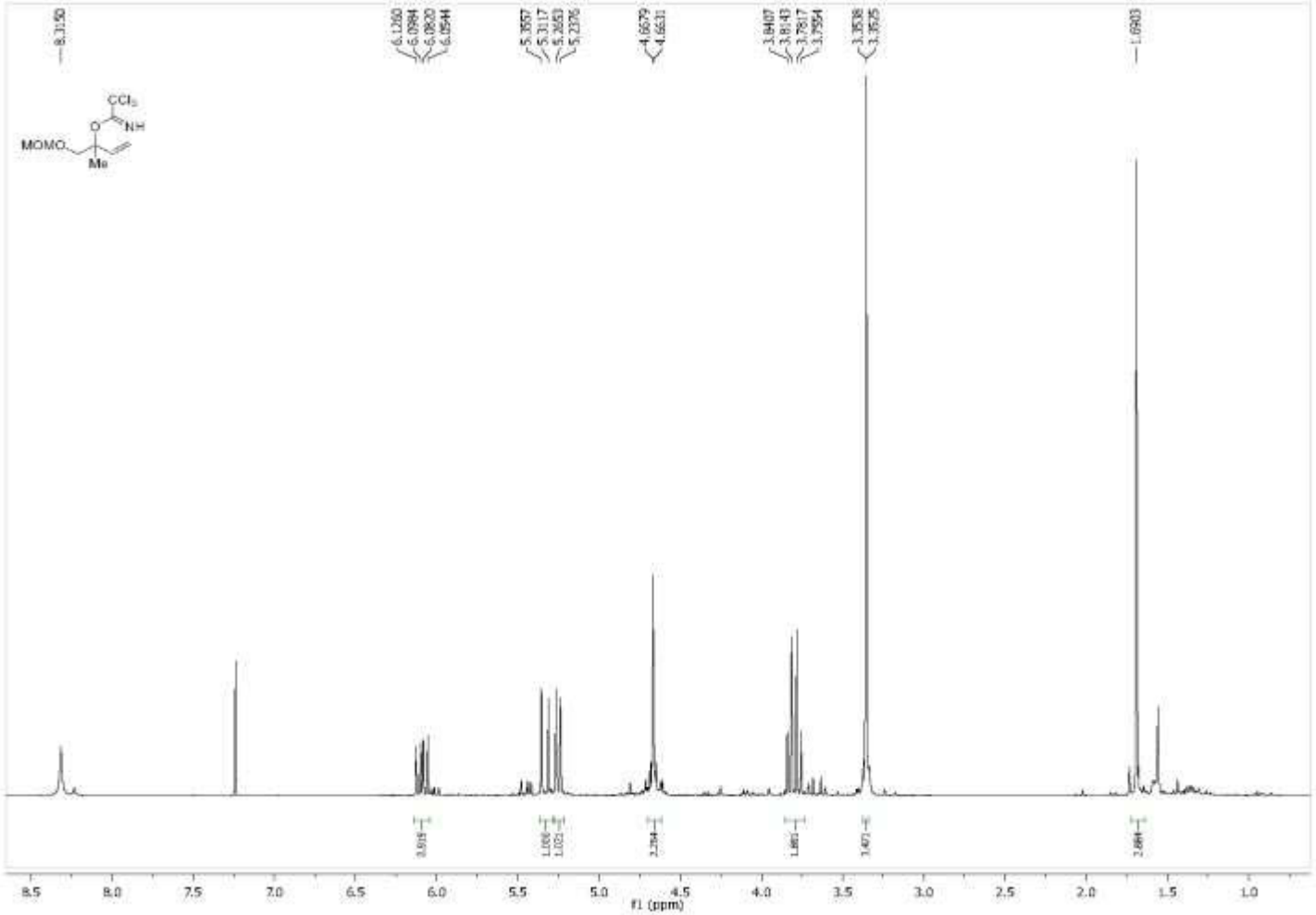

Figure A240 400 MHz 1H NMR ($CDCl_3$) Spectra of Compound **303**

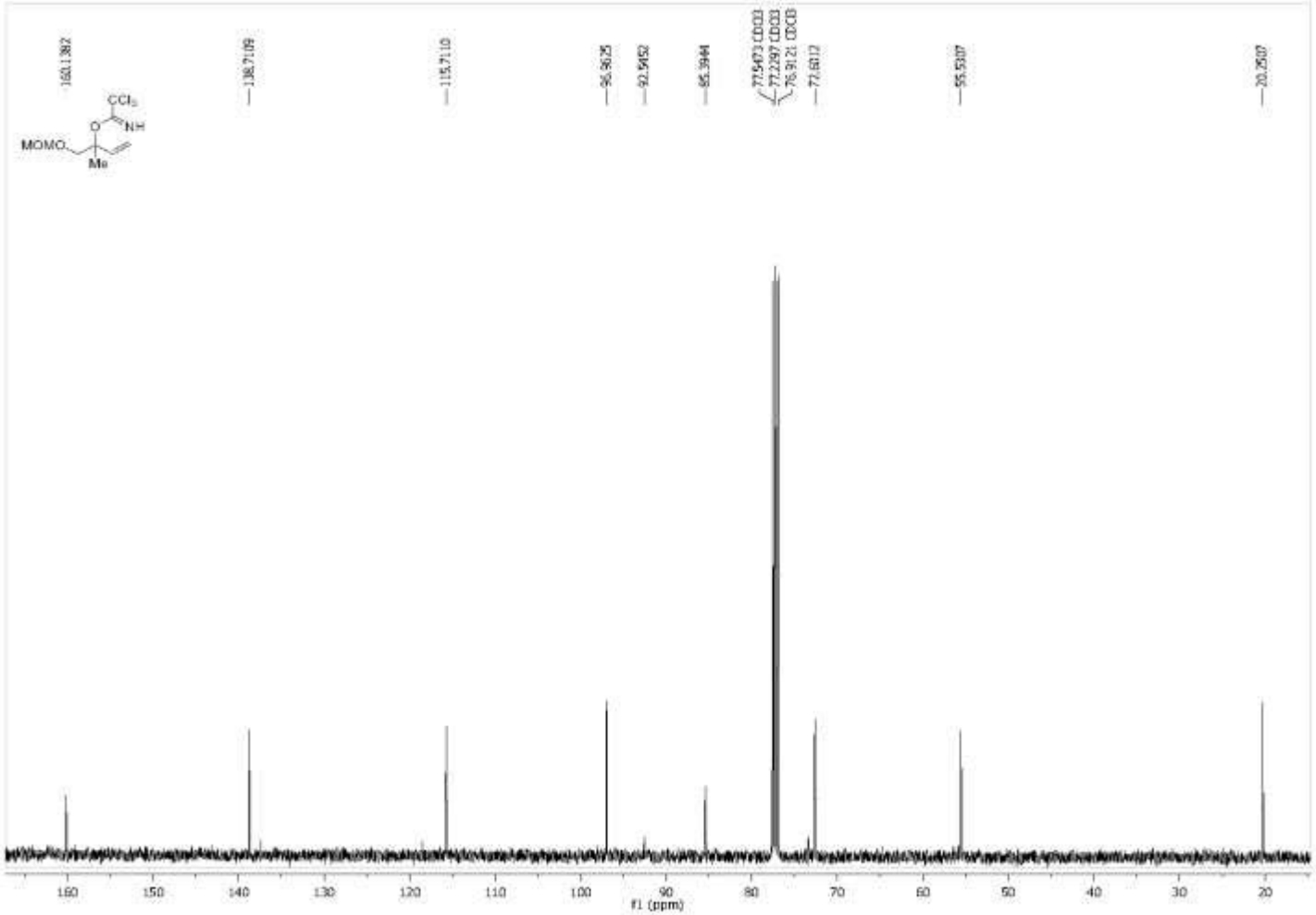

Figure A241 100 MHz 13C NMR ($CDCl_3$) Spectra of Compound **303**

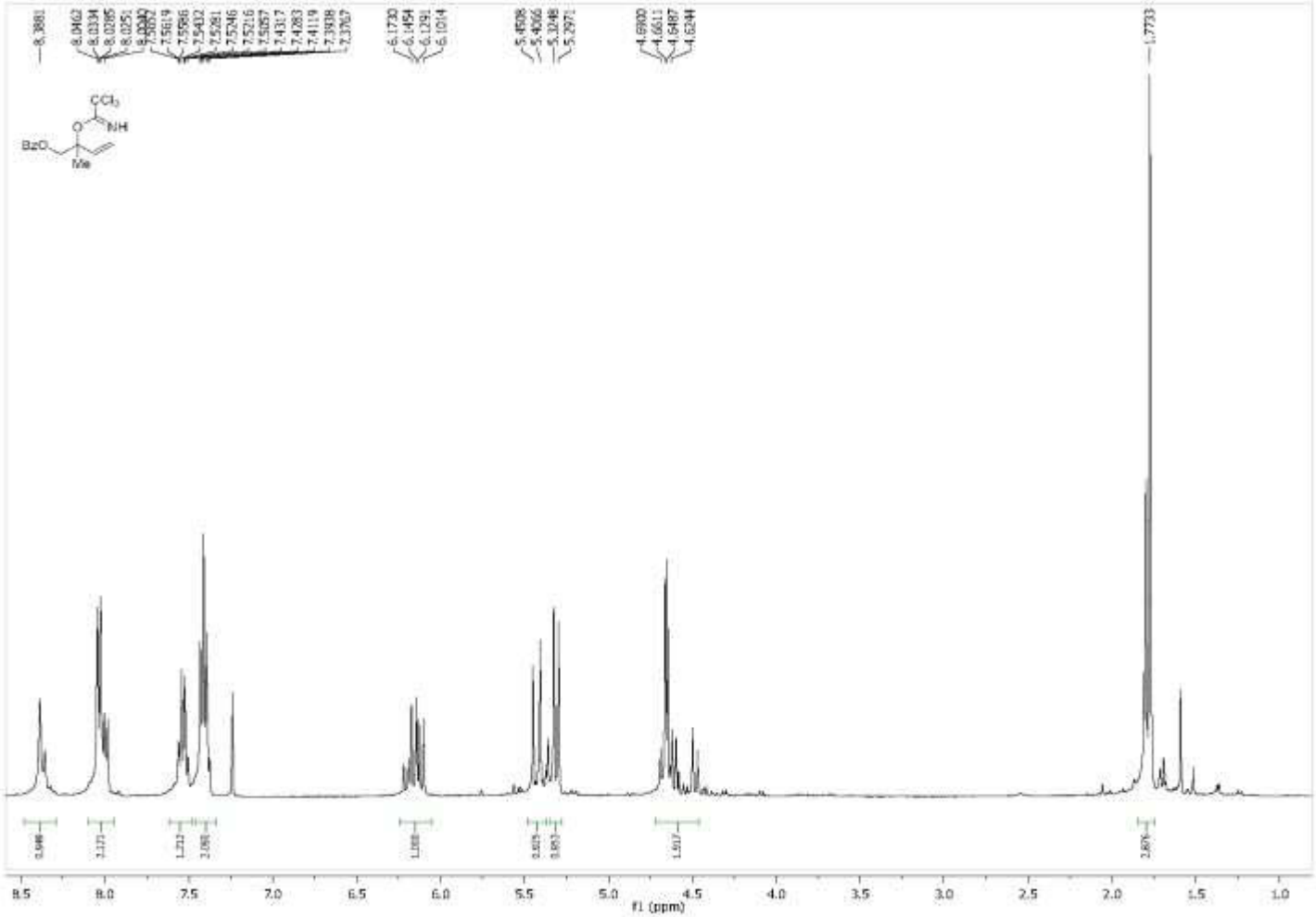

Figure A242 400 MHz 1H NMR ($CDCl_3$) Spectra of Compound **304**

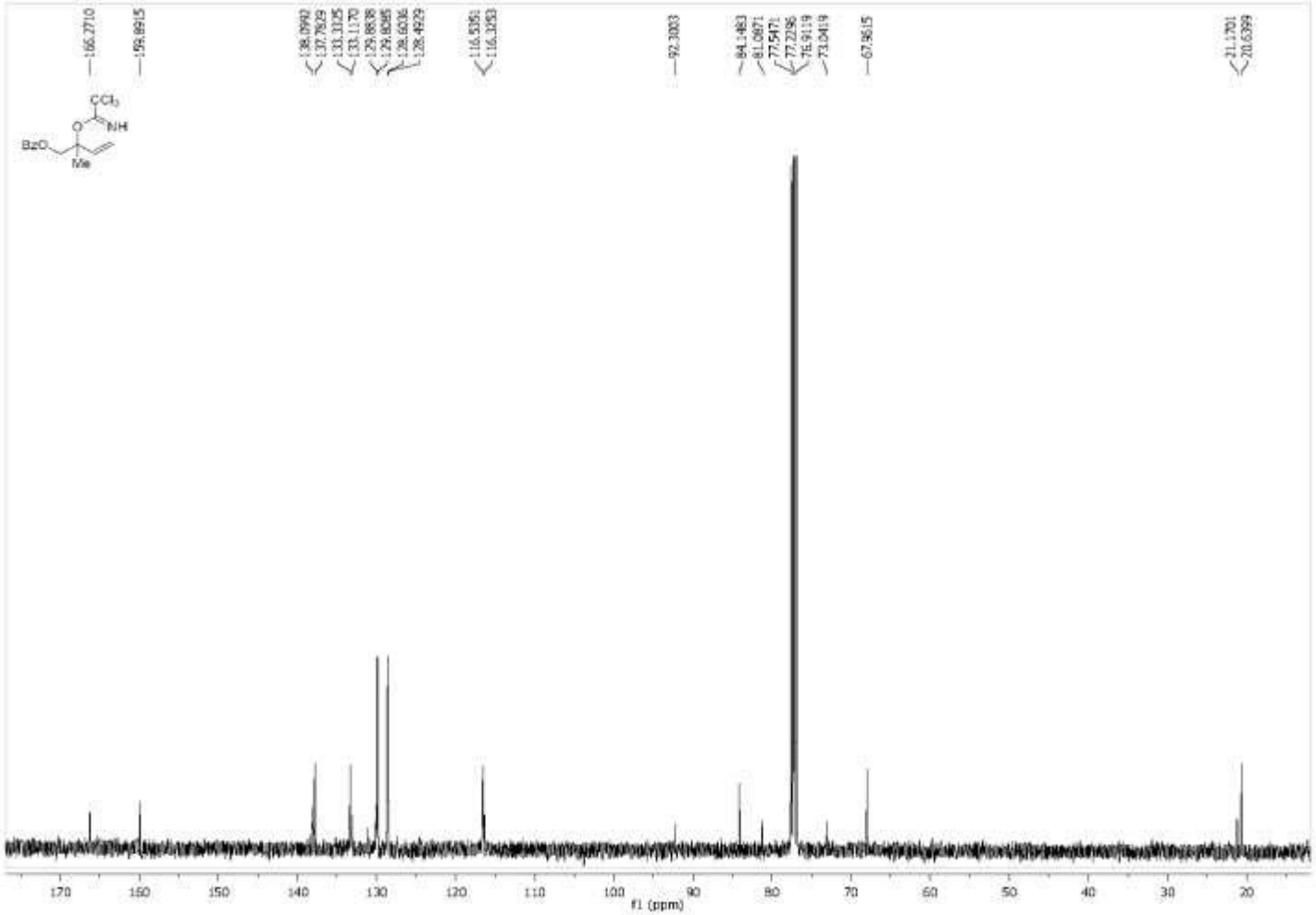

Figure A243 100 MHz 13C NMR ($CDCl_3$) Spectra of Compound **304**

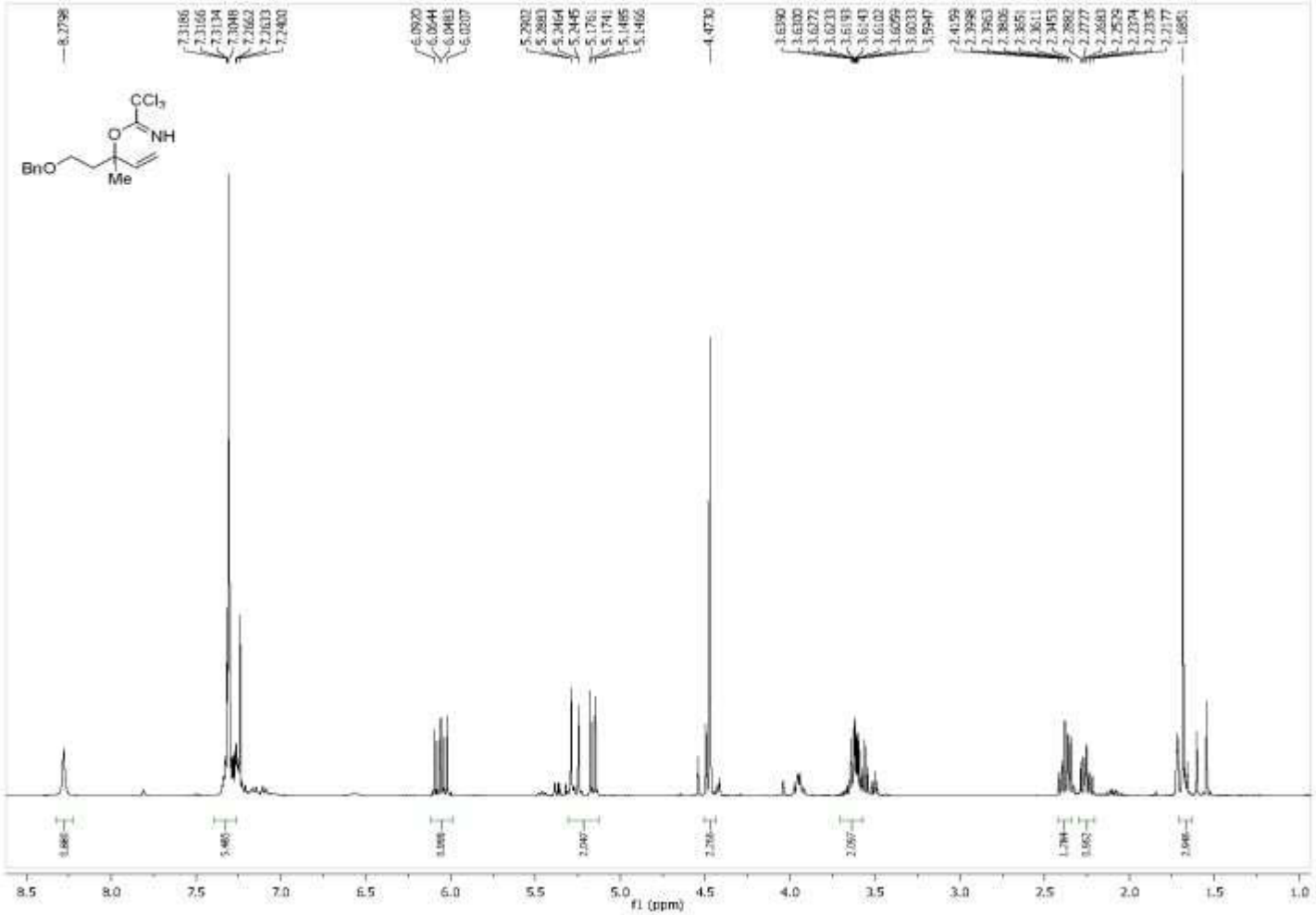

Figure A244 400 MHz 1H NMR ($CDCl_3$) Spectra of Compound **305**

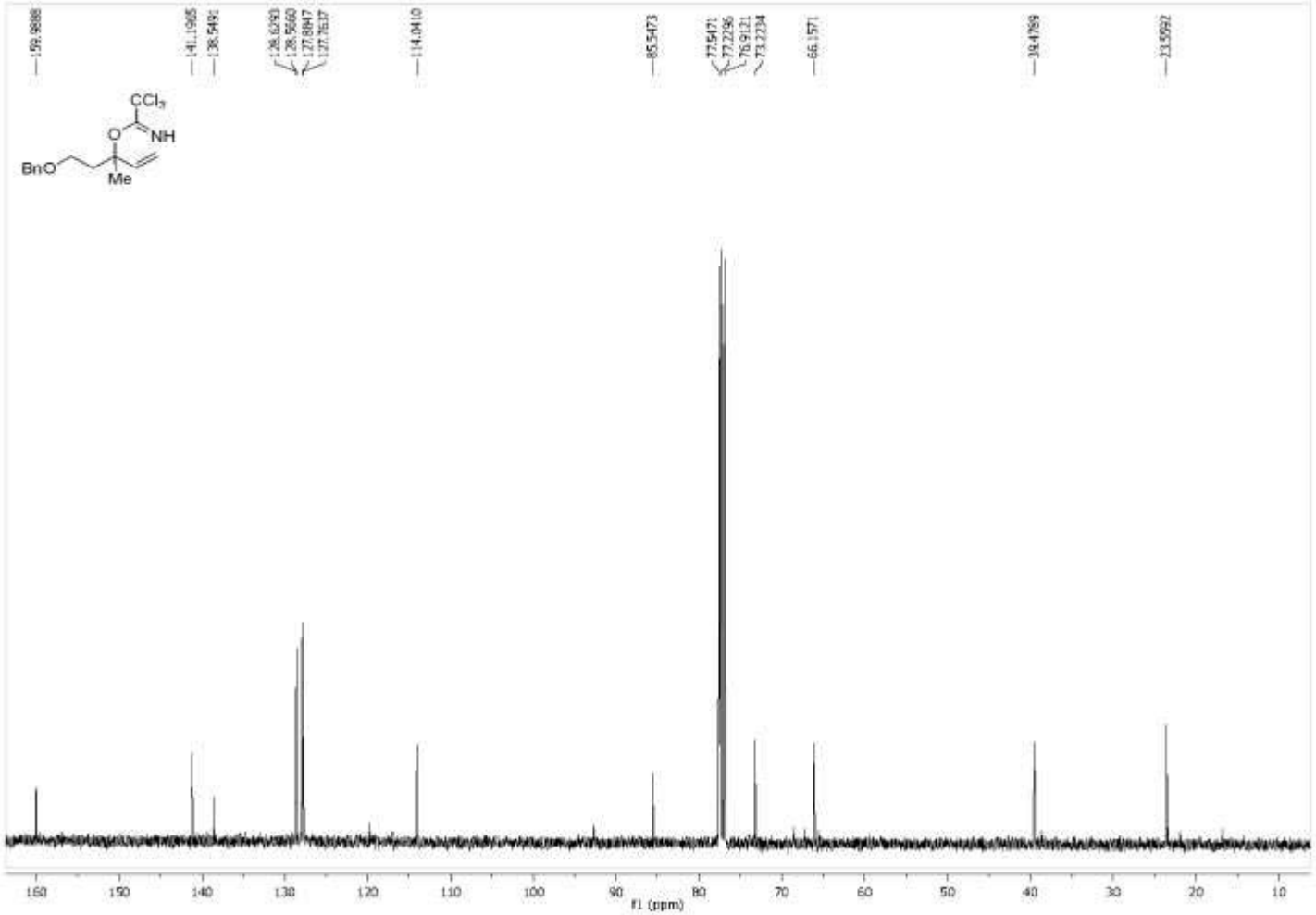

Figure A245 100 MHz 13C NMR ($CDCl_3$) Spectra of Compound **305**

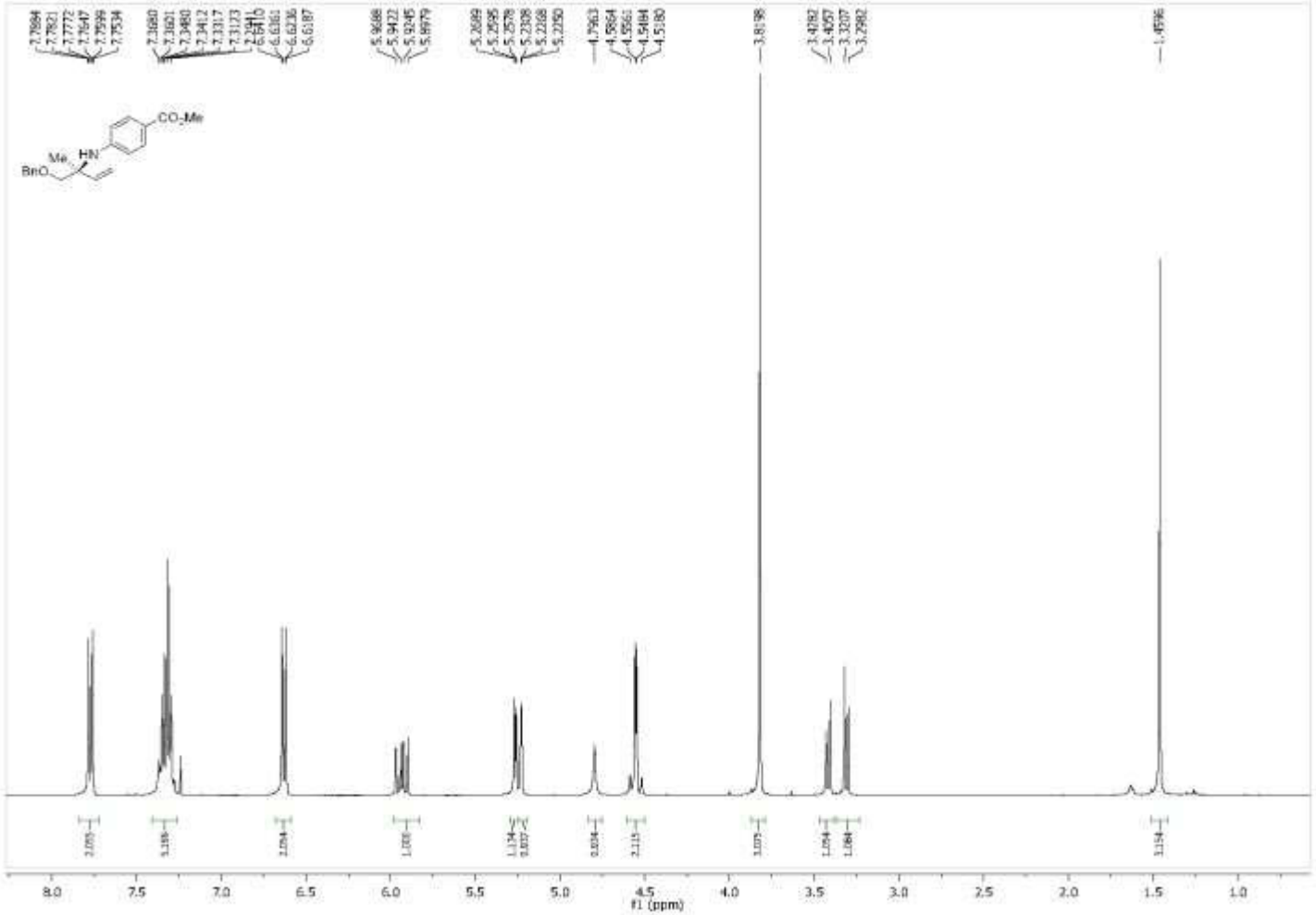

Figure A246 400 MHz 1H NMR ($CDCl_3$) Spectra of Compound **255i**

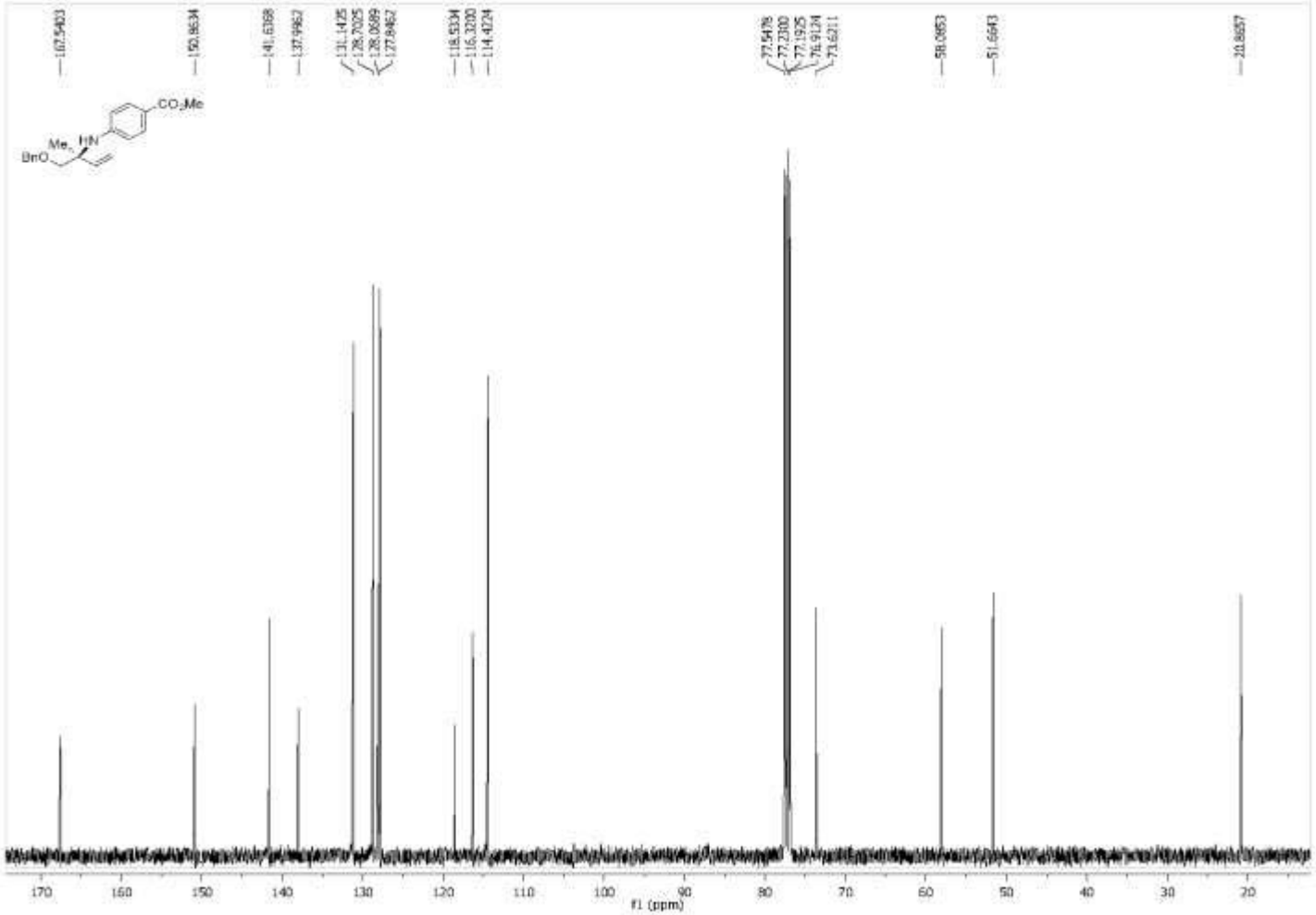

Figure A247 100 MHz 13C NMR ($CDCl_3$) Spectra of Compound **255i**

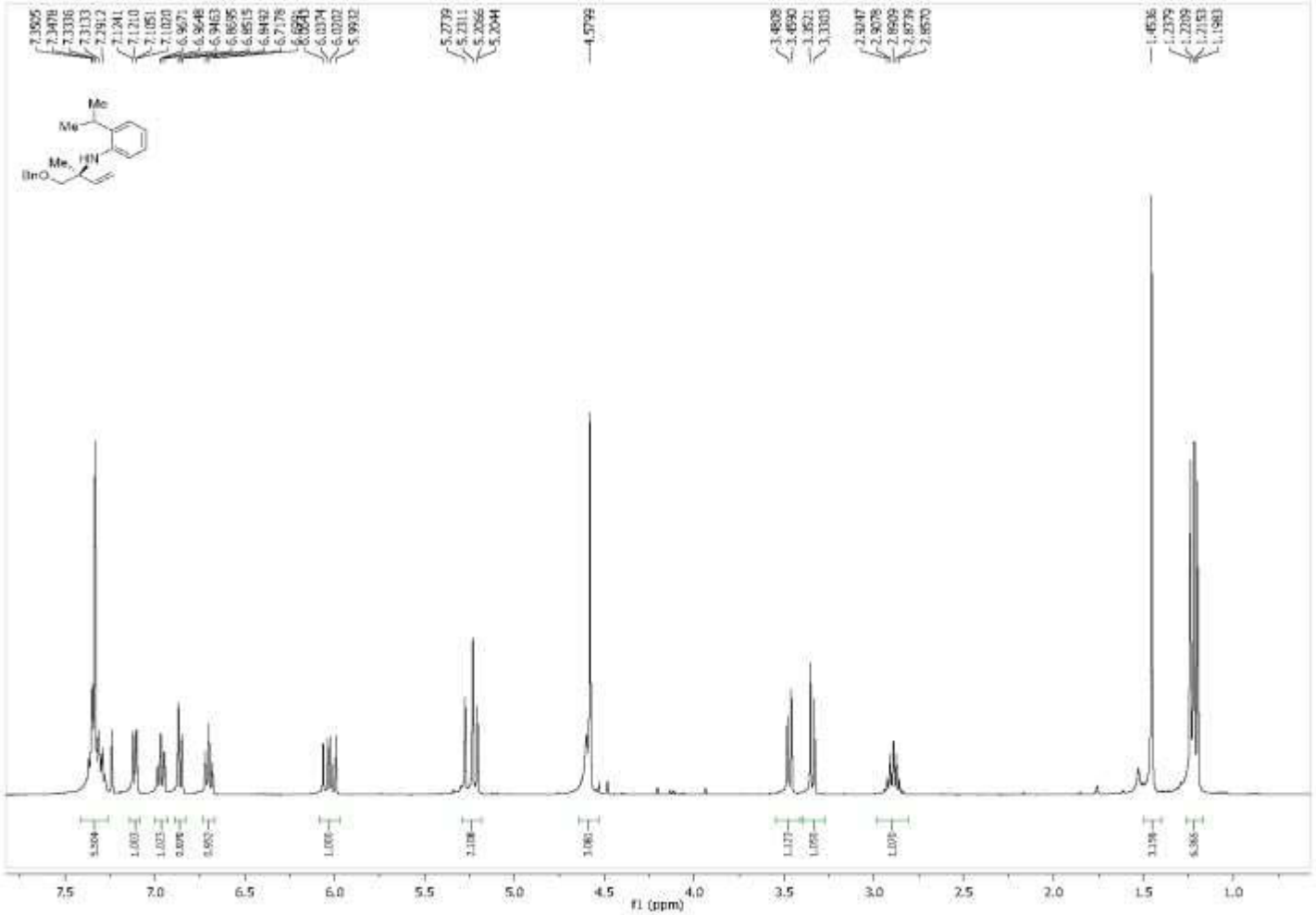

Figure A248 400 MHz 1H NMR ($CDCl_3$) Spectra of Compound **255l**

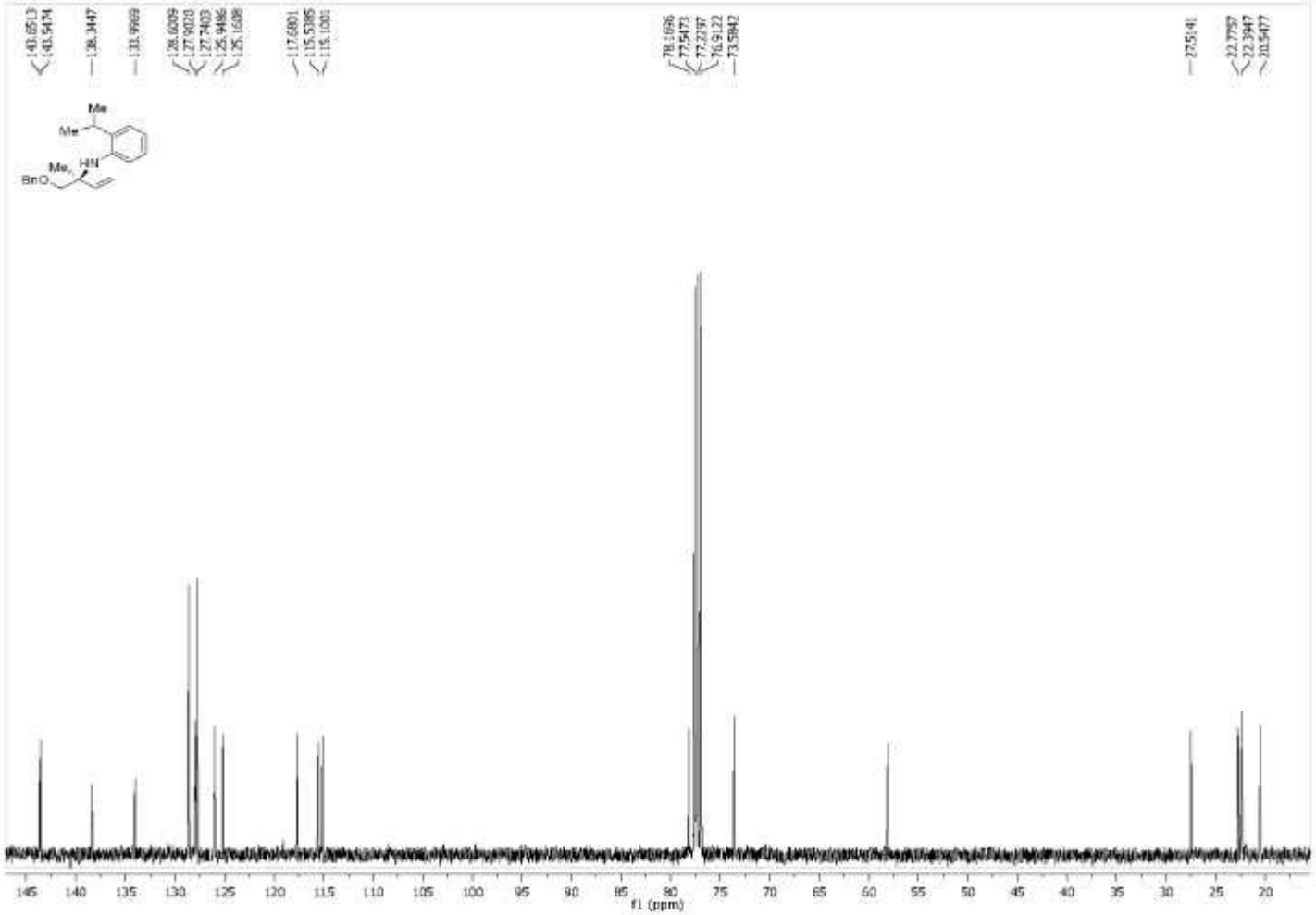

Figure A249 100 MHz 13C NMR ($CDCl_3$) Spectra of Compound **255l**

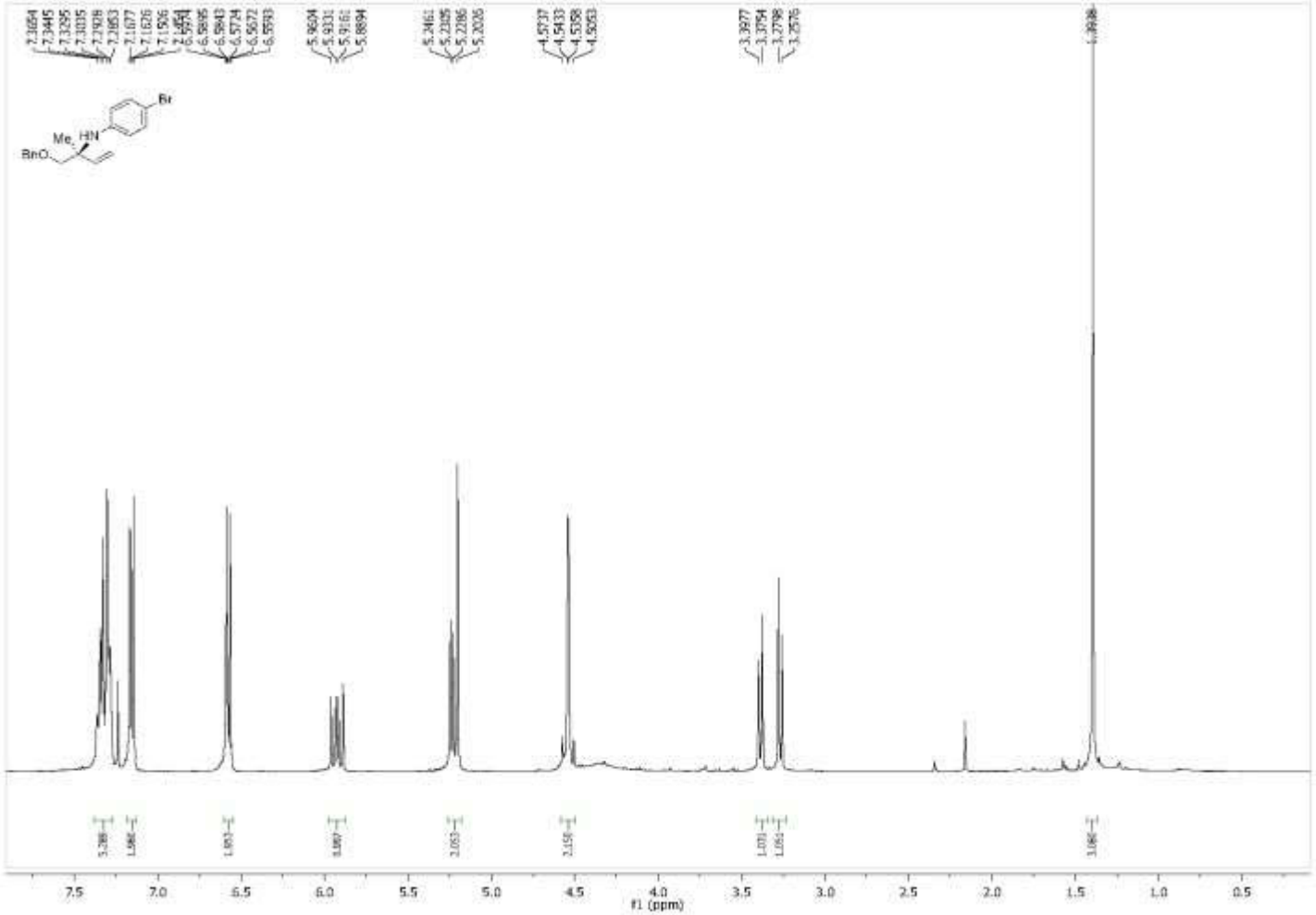

Figure A250 400 MHz 1H NMR ($CDCl_3$) Spectra of Compound **255p**

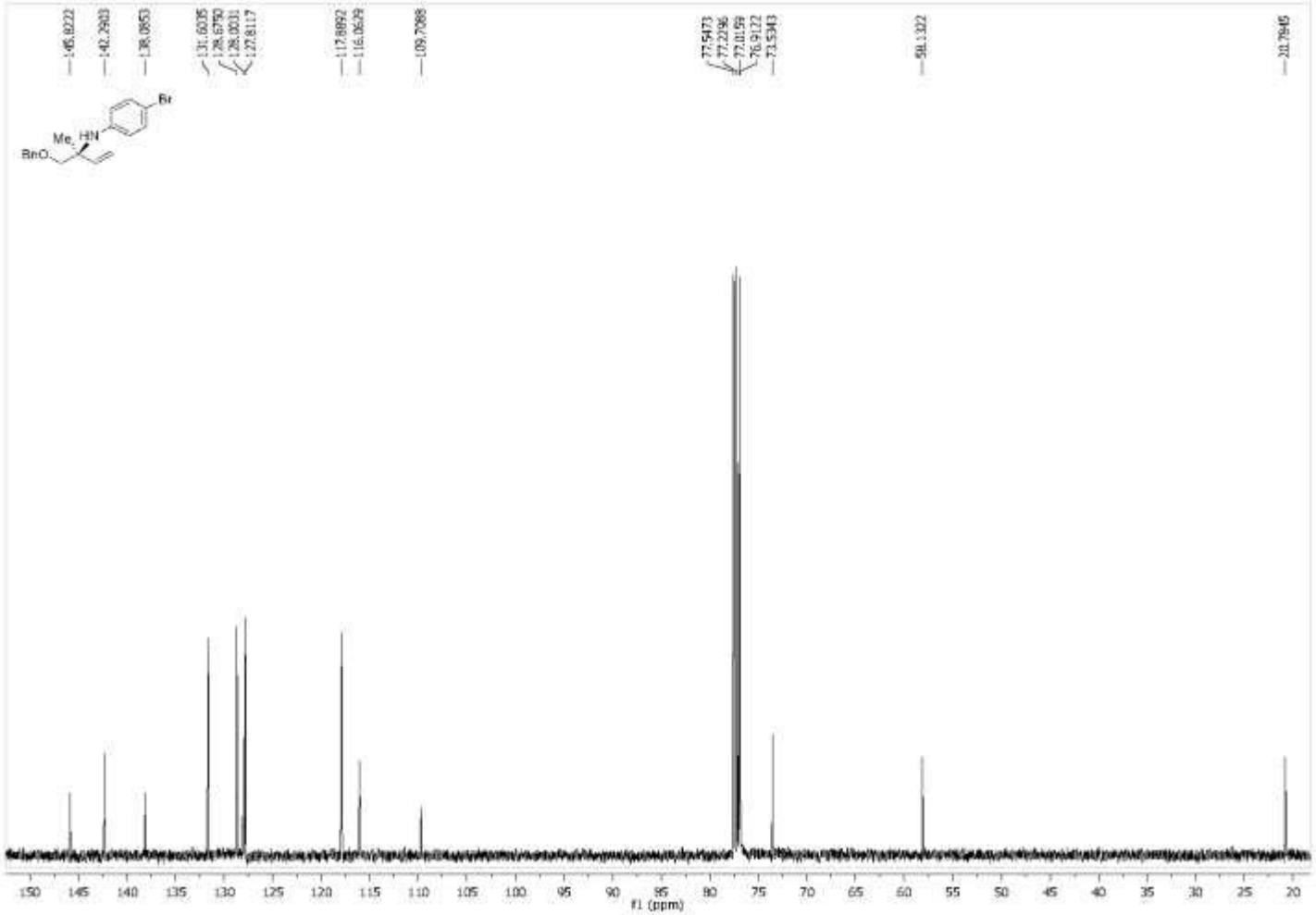

Figure A251 100 MHz 13C NMR ($CDCl_3$) Spectra of Compound **255p**

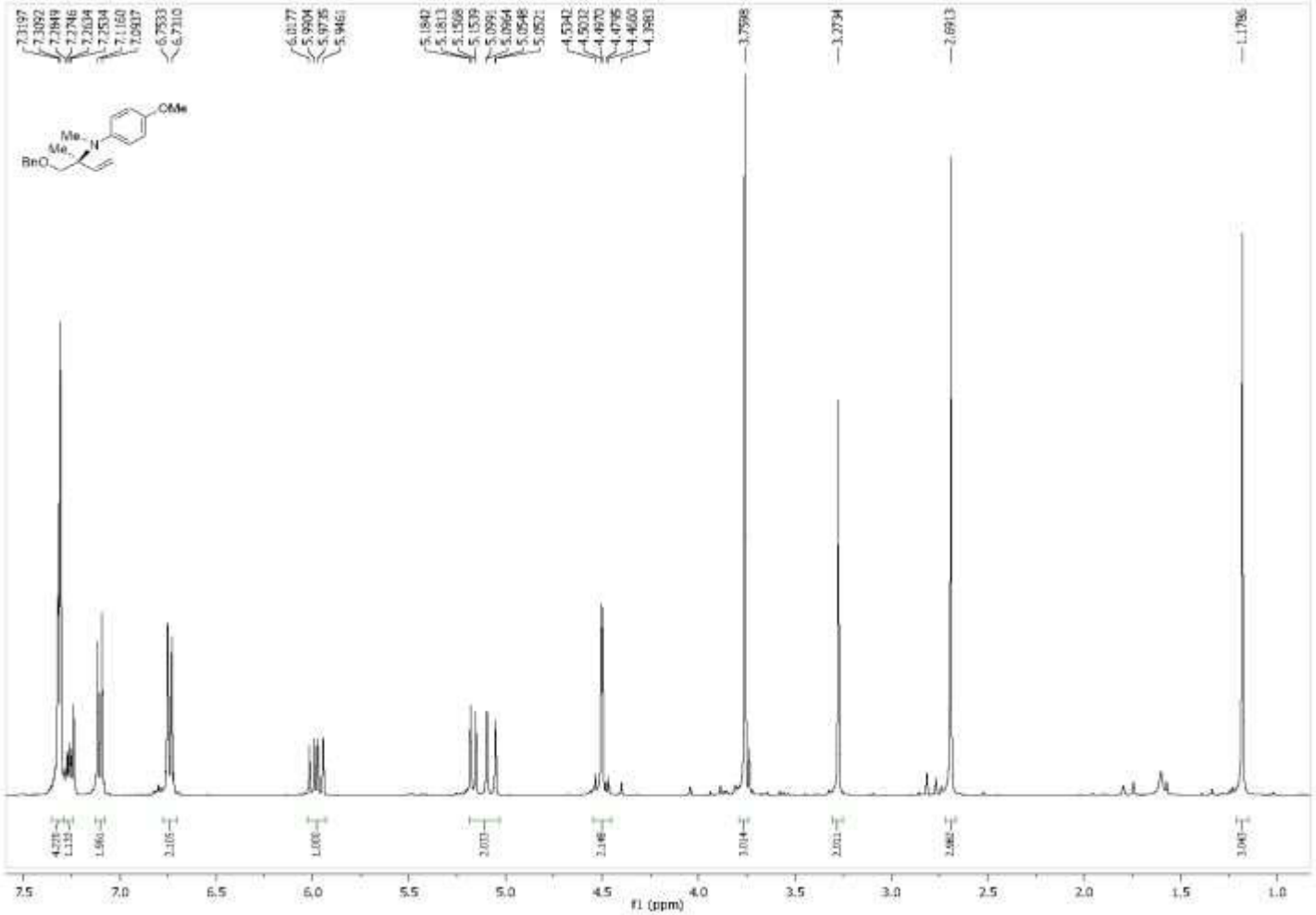

Figure A252 400 MHz 1H NMR ($CDCl_3$) Spectra of Compound **255q**

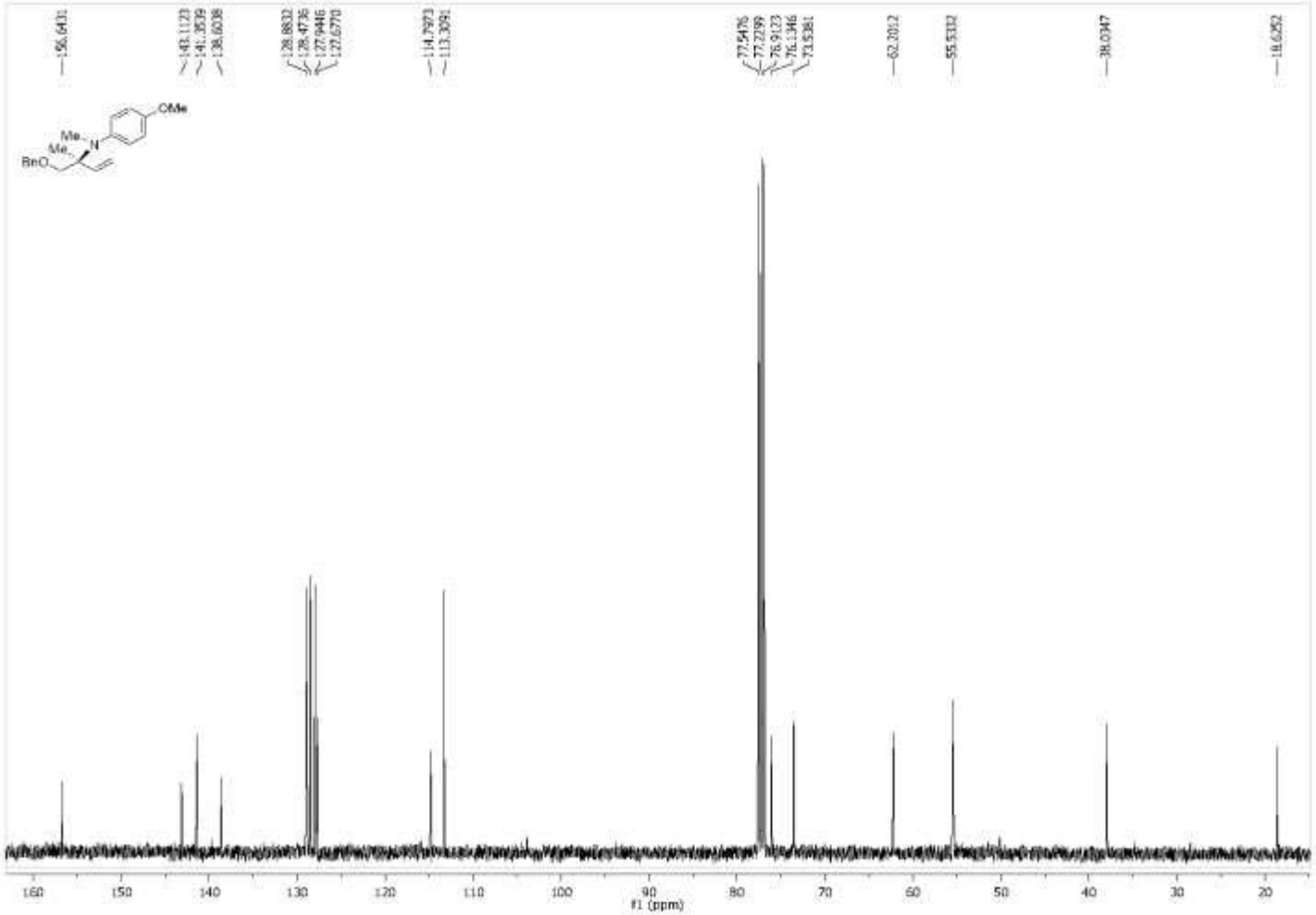

Figure A253 100 MHz 13C NMR ($CDCl_3$) Spectra of Compound **255q**

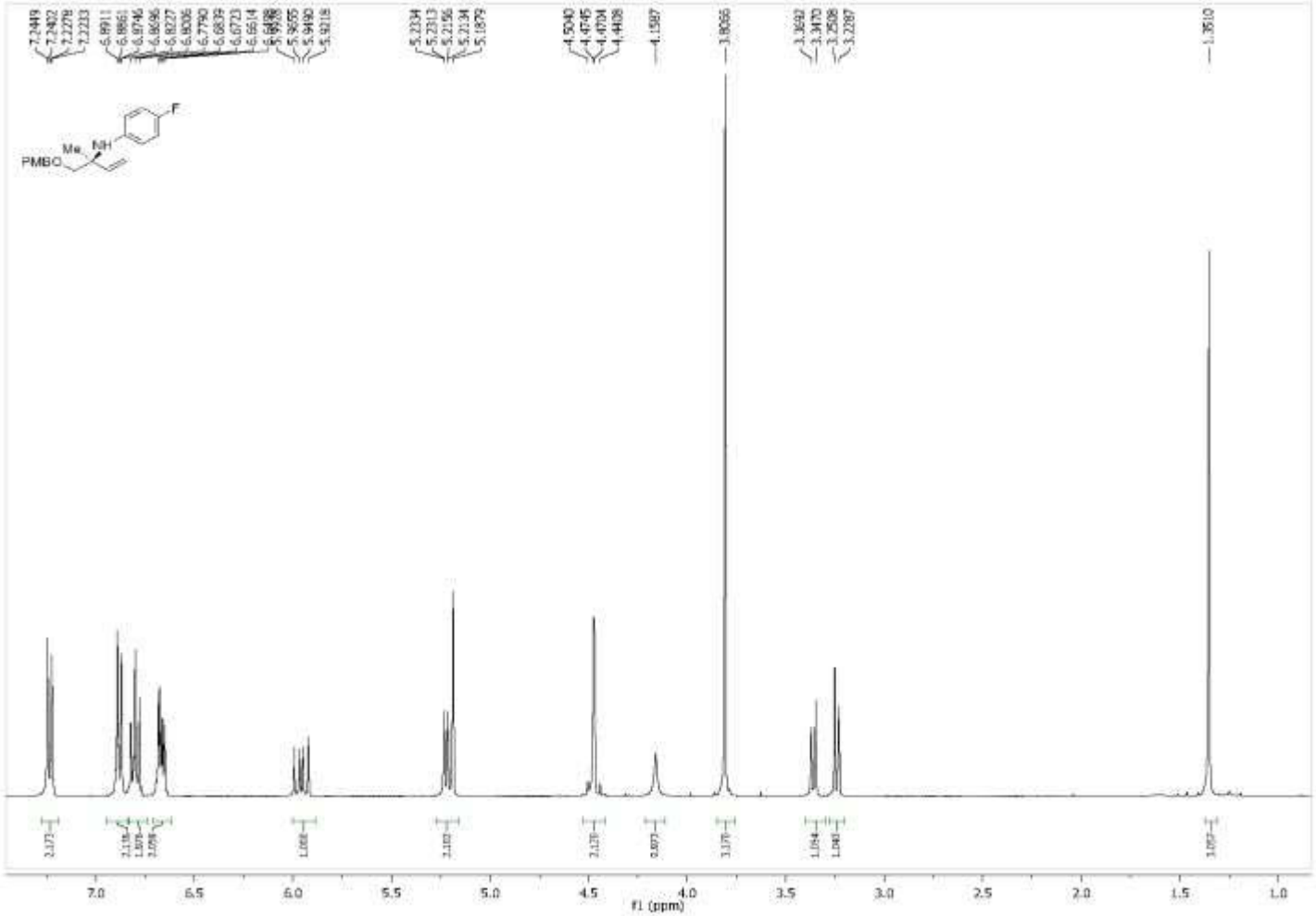

Figure A254 400 MHz 1H NMR ($CDCl_3$) Spectra of Compound **299b**

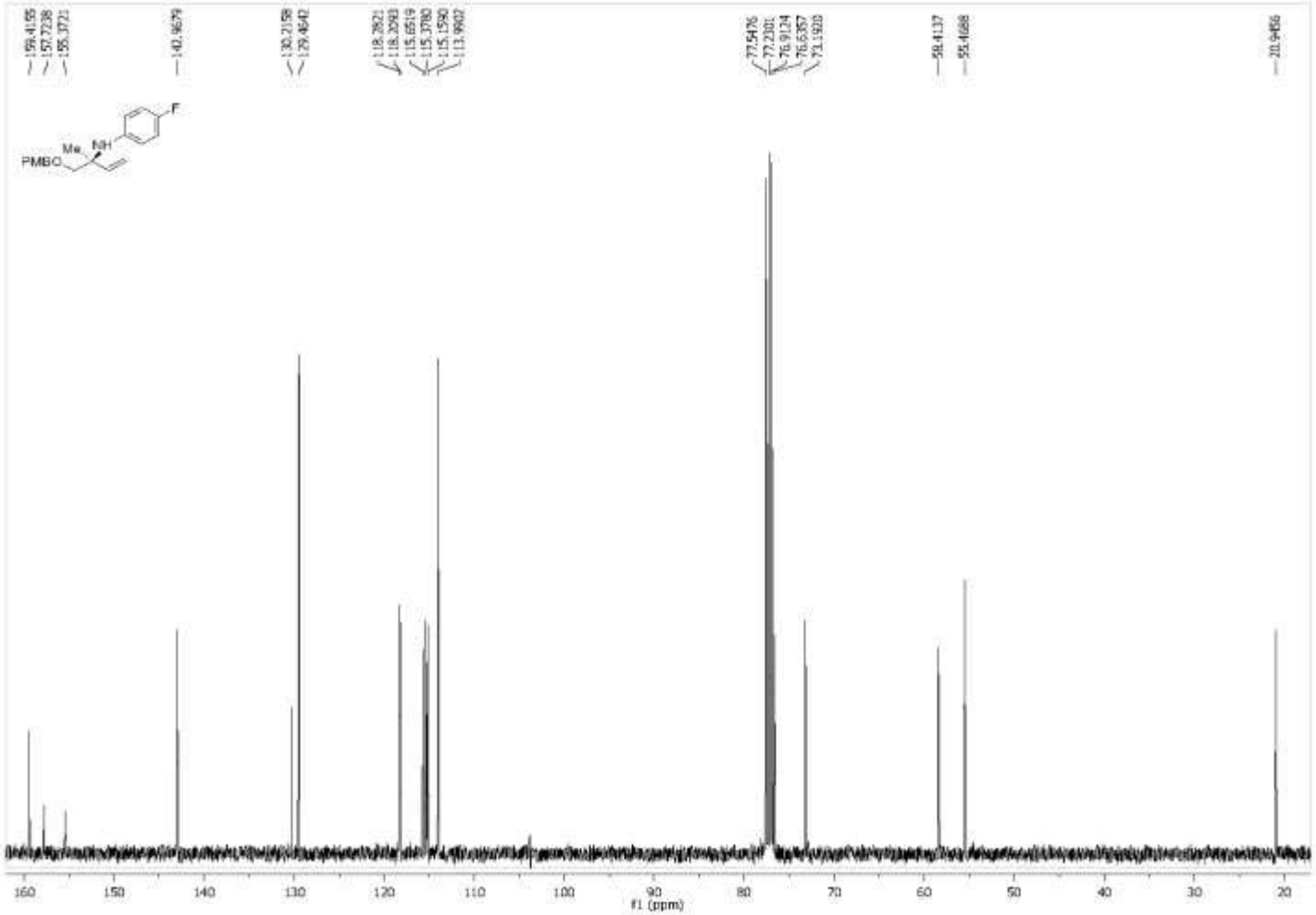

Figure A255 100 MHz 13C NMR ($CDCl_3$) Spectra of Compound **299b**

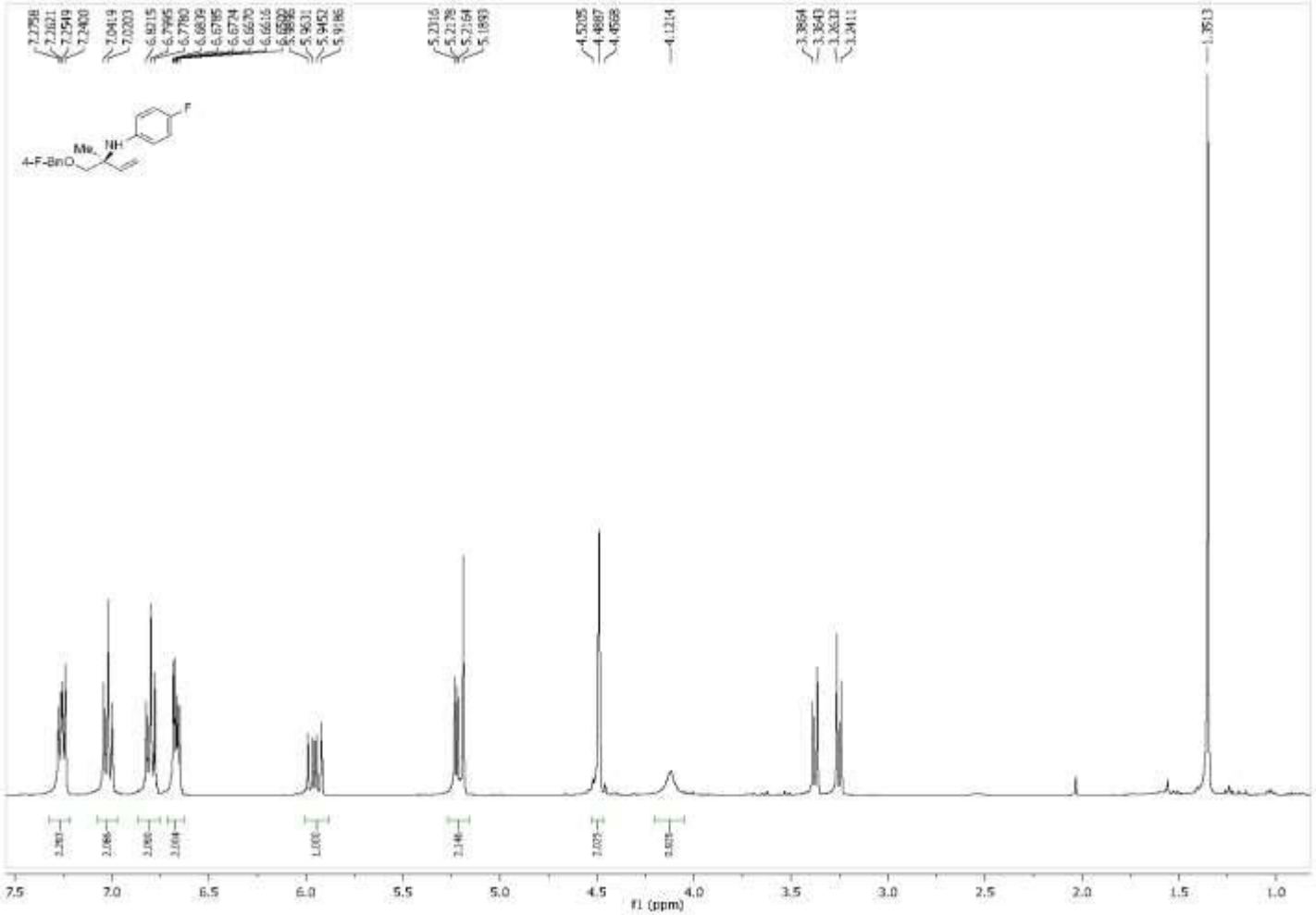

Figure A256 400 MHz 1H NMR ($CDCl_3$) Spectra of Compound **300b**

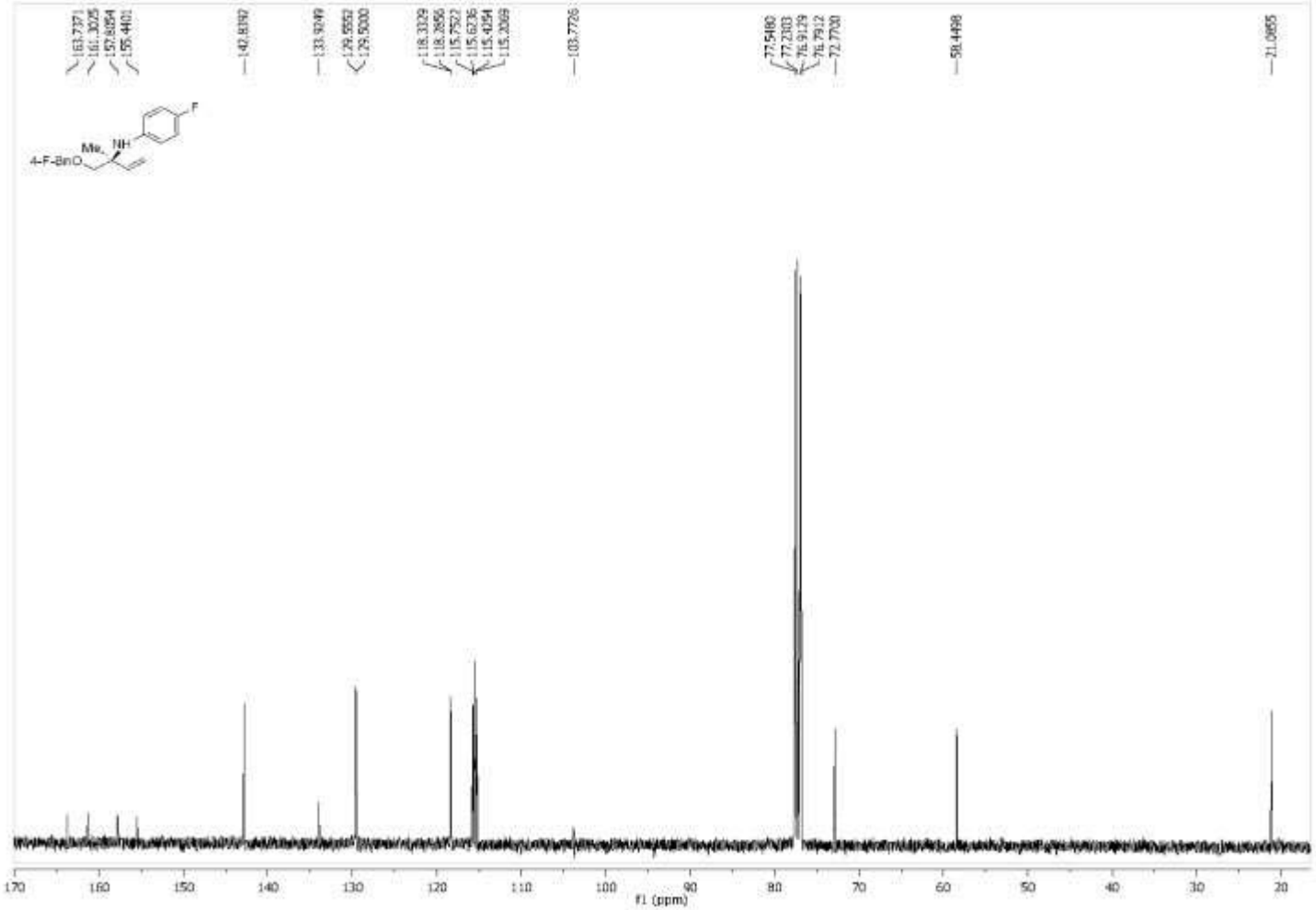

Figure A257 100 MHz 13C NMR ($CDCl_3$) Spectra of Compound **300b**

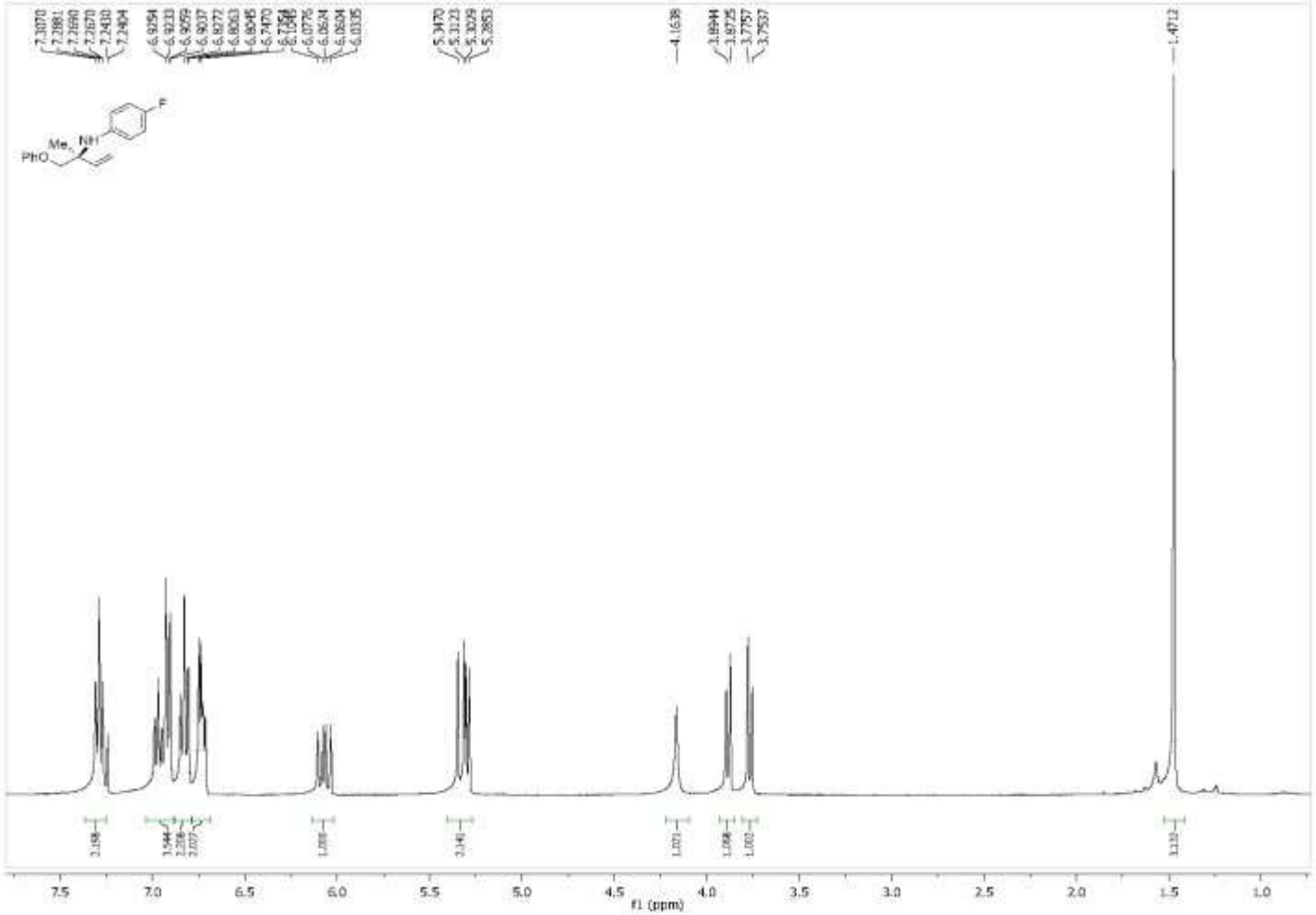

Figure A258 400 MHz 1H NMR ($CDCl_3$) Spectra of Compound **301b**

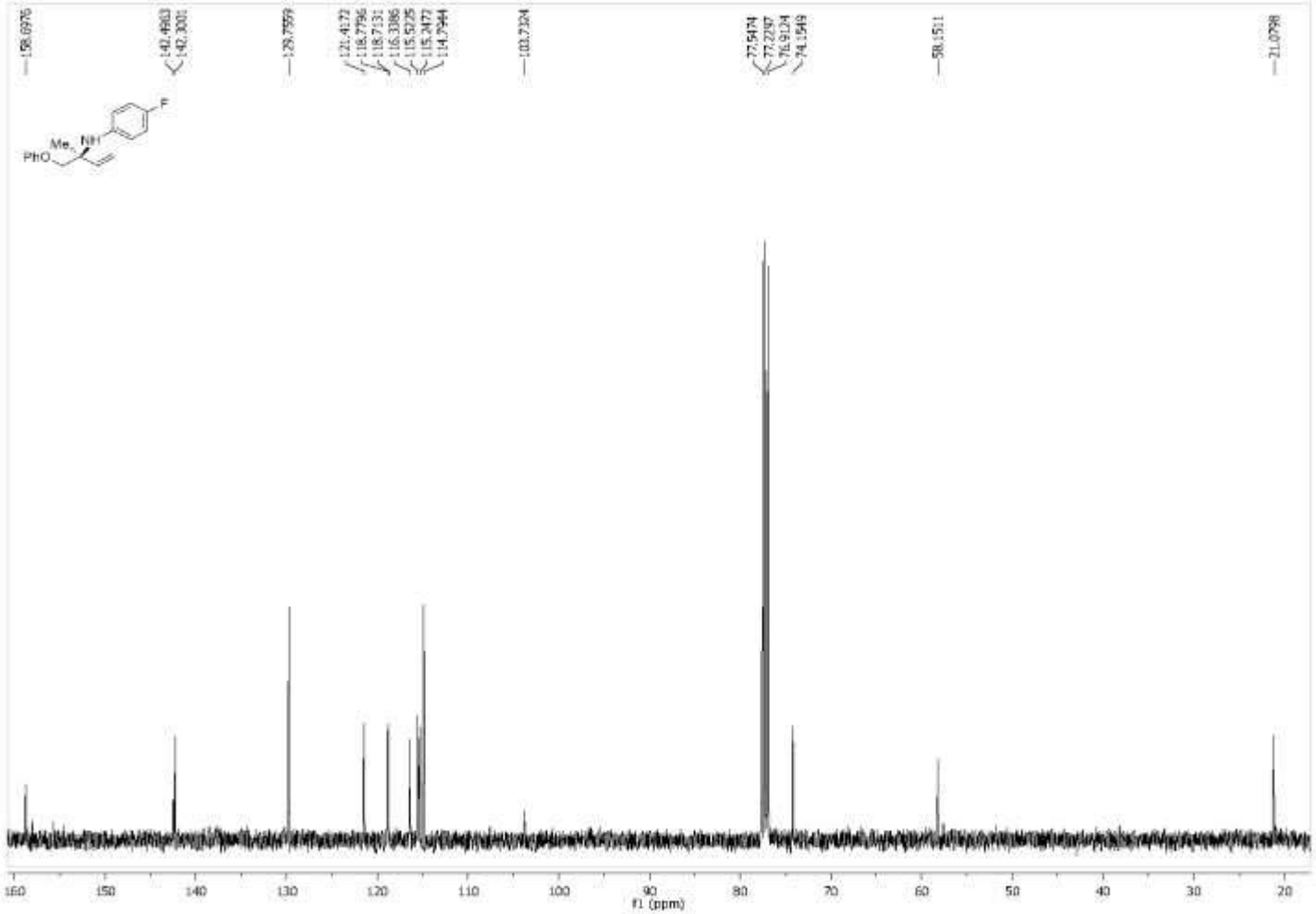

Figure A259 100 MHz 13C NMR ($CDCl_3$) Spectra of Compound **301b**

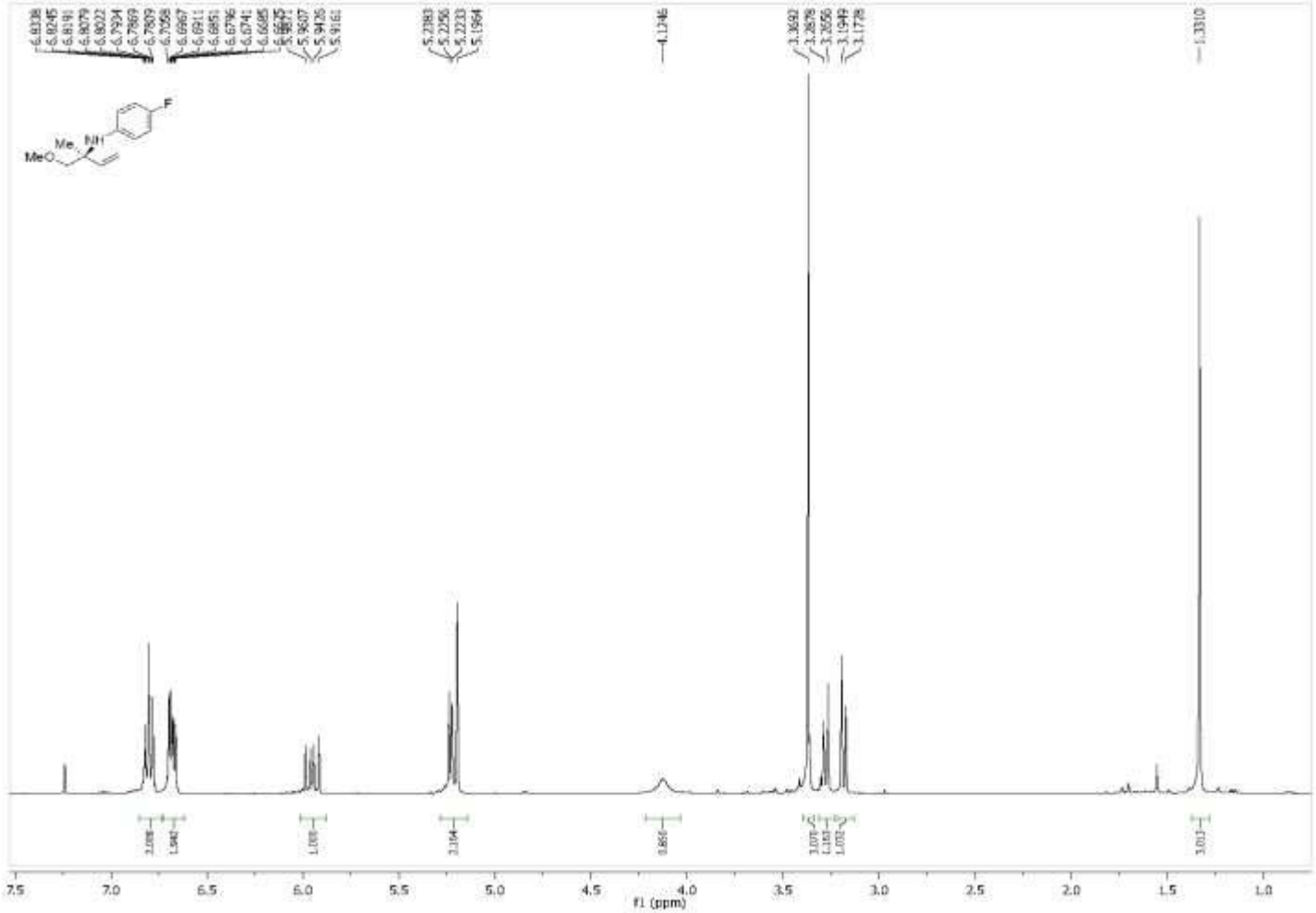

Figure A260 400 MHz 1H NMR ($CDCl_3$) Spectra of Compound **302b**

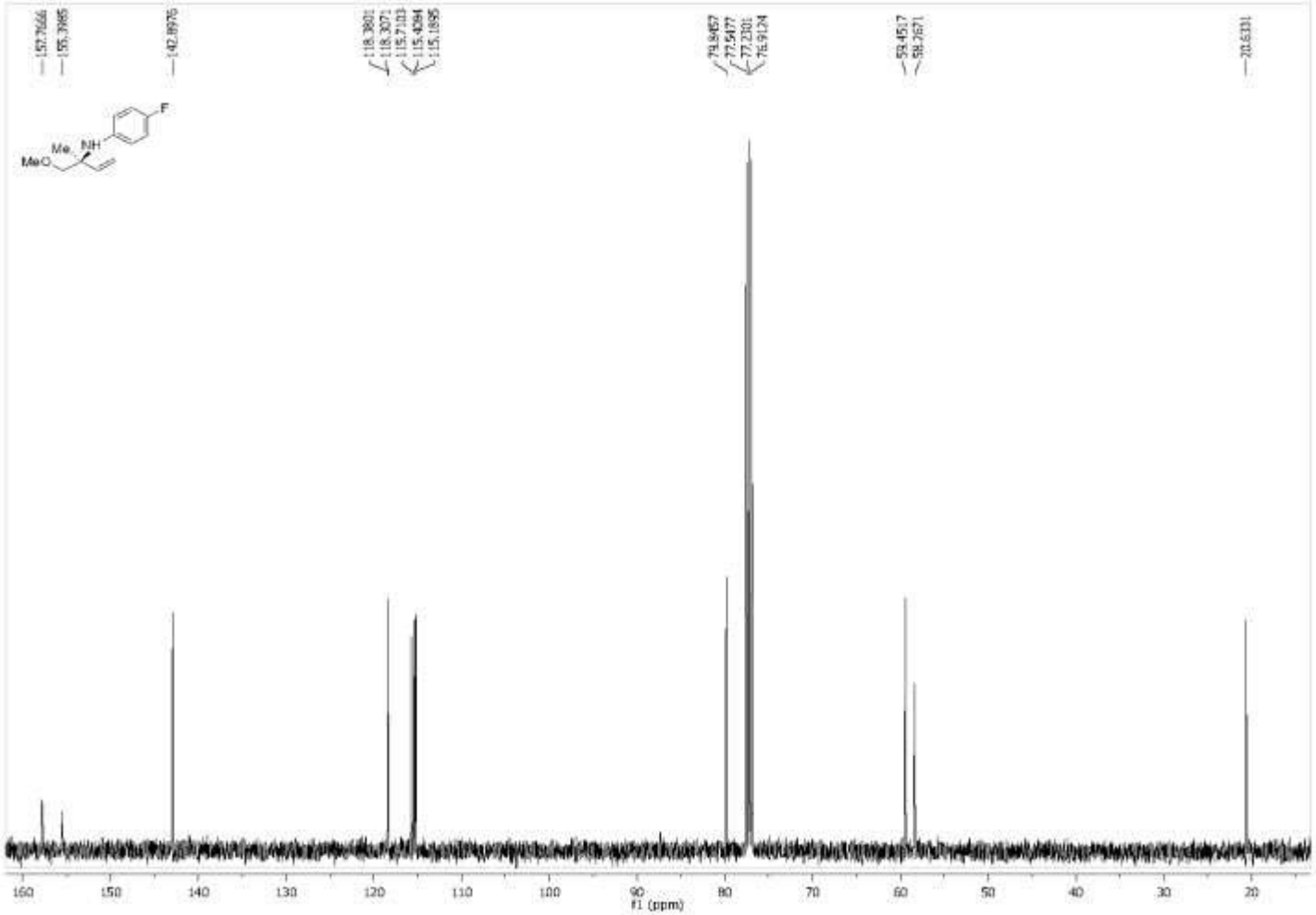

Figure A261 100 MHz 13C NMR ($CDCl_3$) Spectra of Compound **302b**

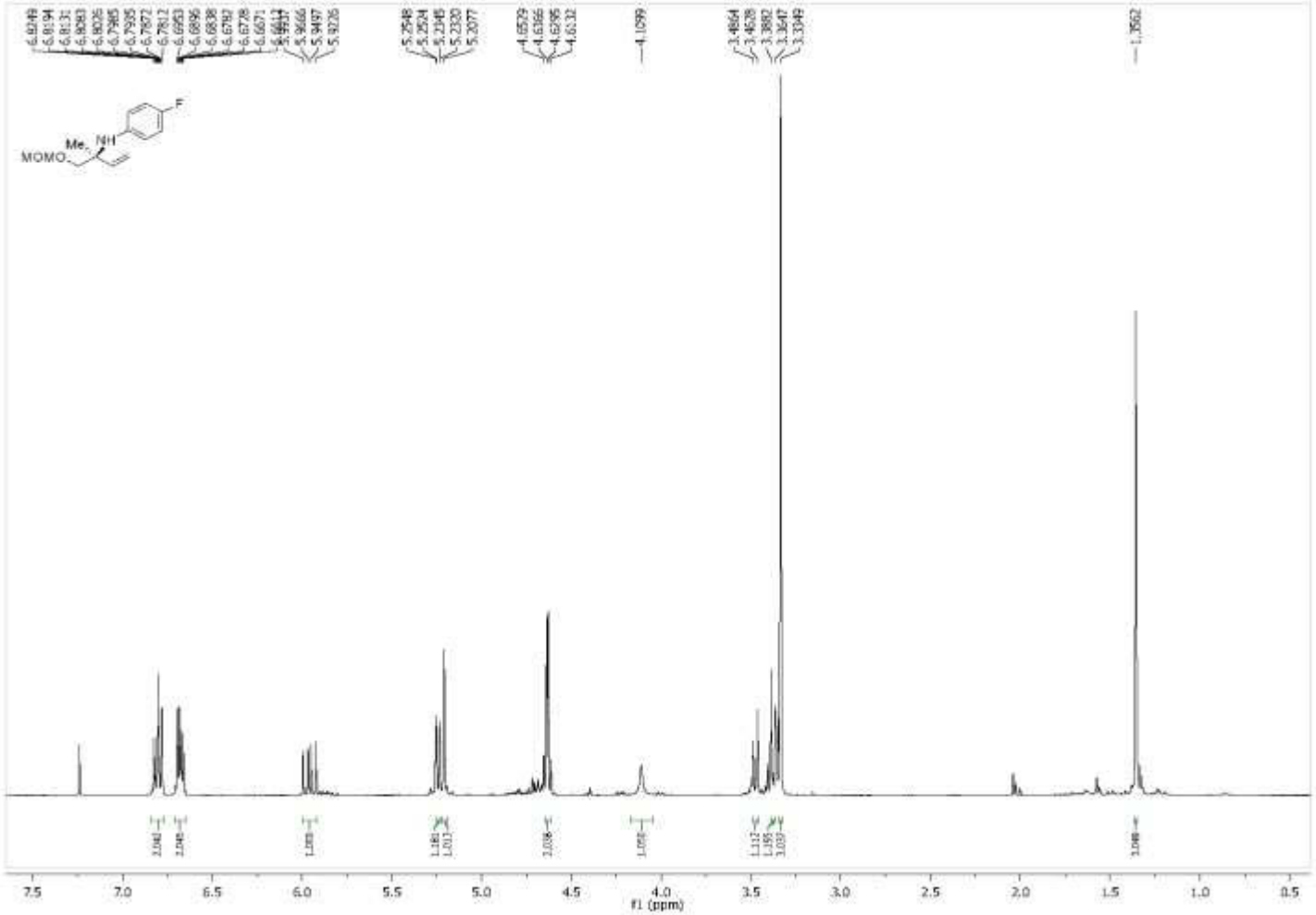

Figure A262 400 MHz 1H NMR ($CDCl_3$) Spectra of Compound **303b**

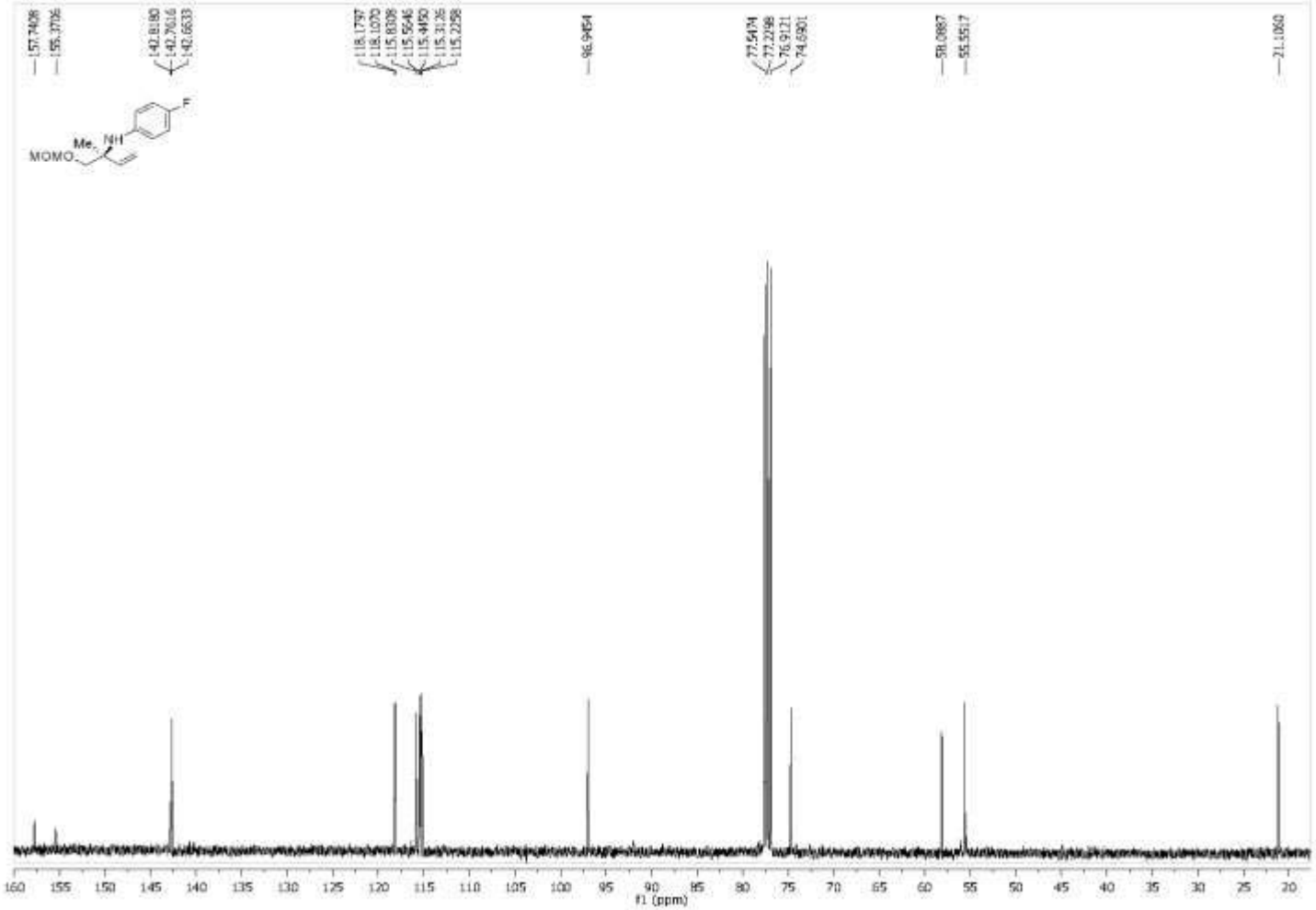

Figure A263 100 MHz 13C NMR ($CDCl_3$) Spectra of Compound **303b**

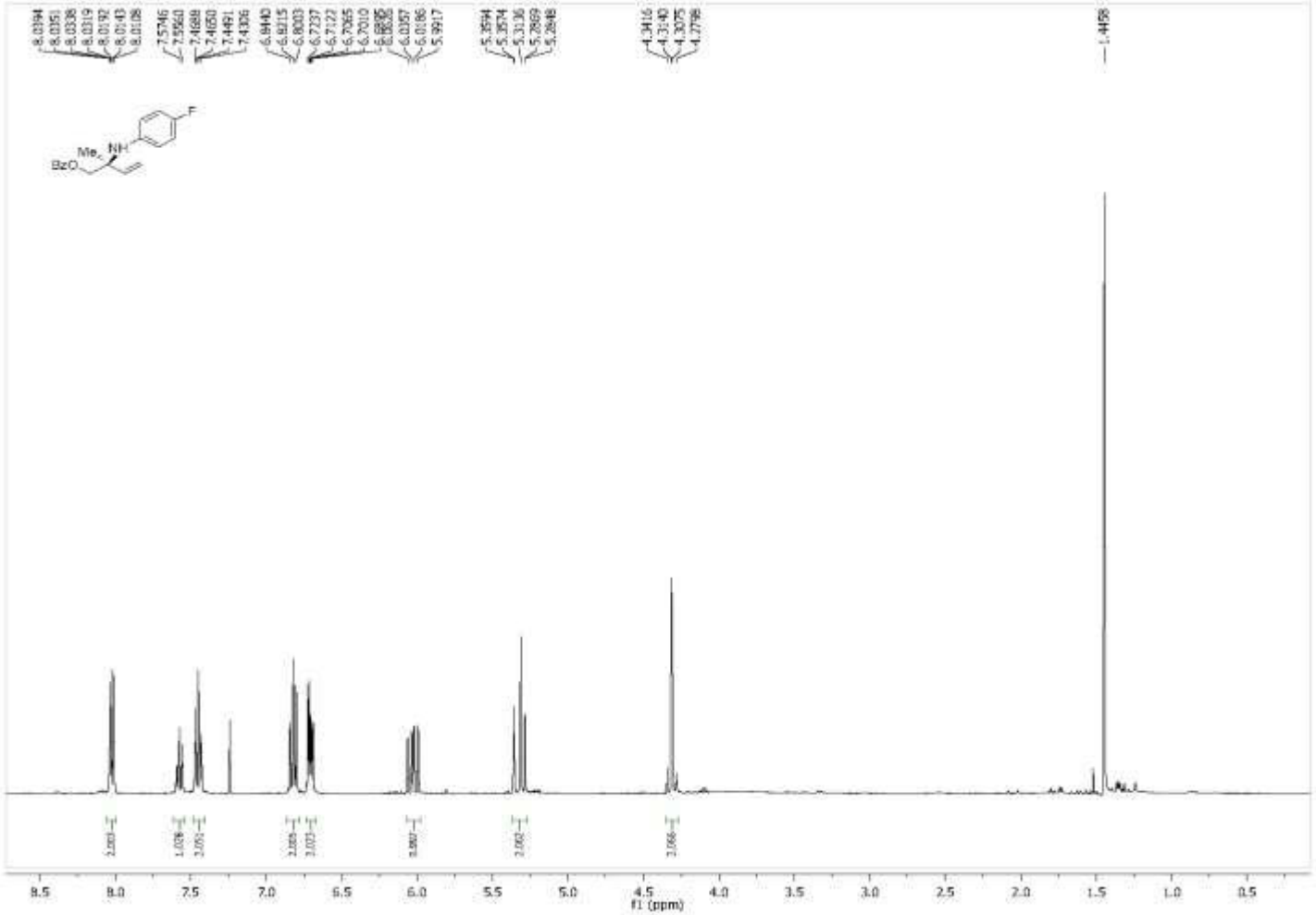

Figure A264 400 MHz 1H NMR ($CDCl_3$) Spectra of Compound **304b**

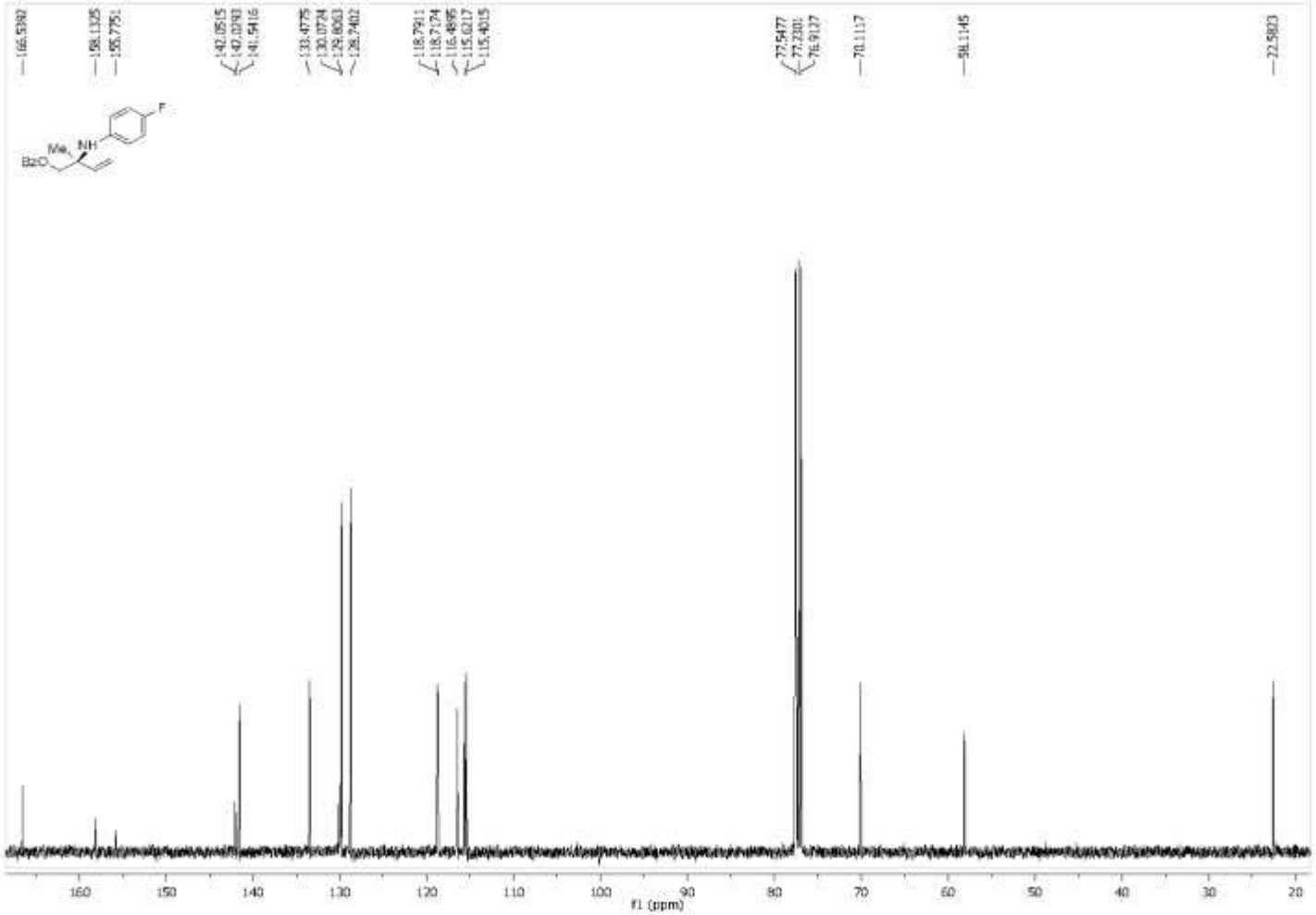

Figure A265 100 MHz 13C NMR ($CDCl_3$) Spectra of Compound **304b**

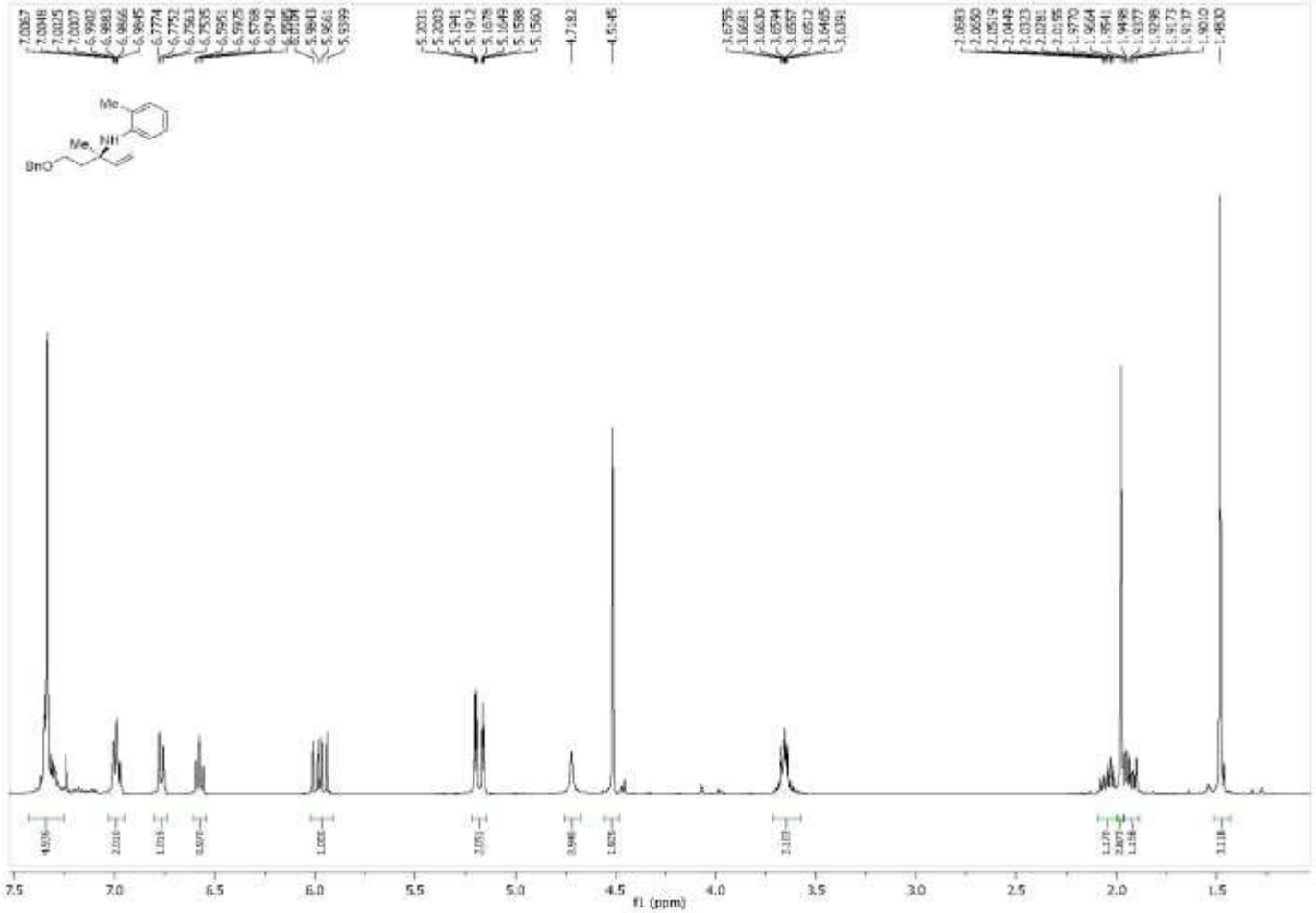

Figure A266 400 MHz 1H NMR ($CDCl_3$) Spectra of Compound **305d**

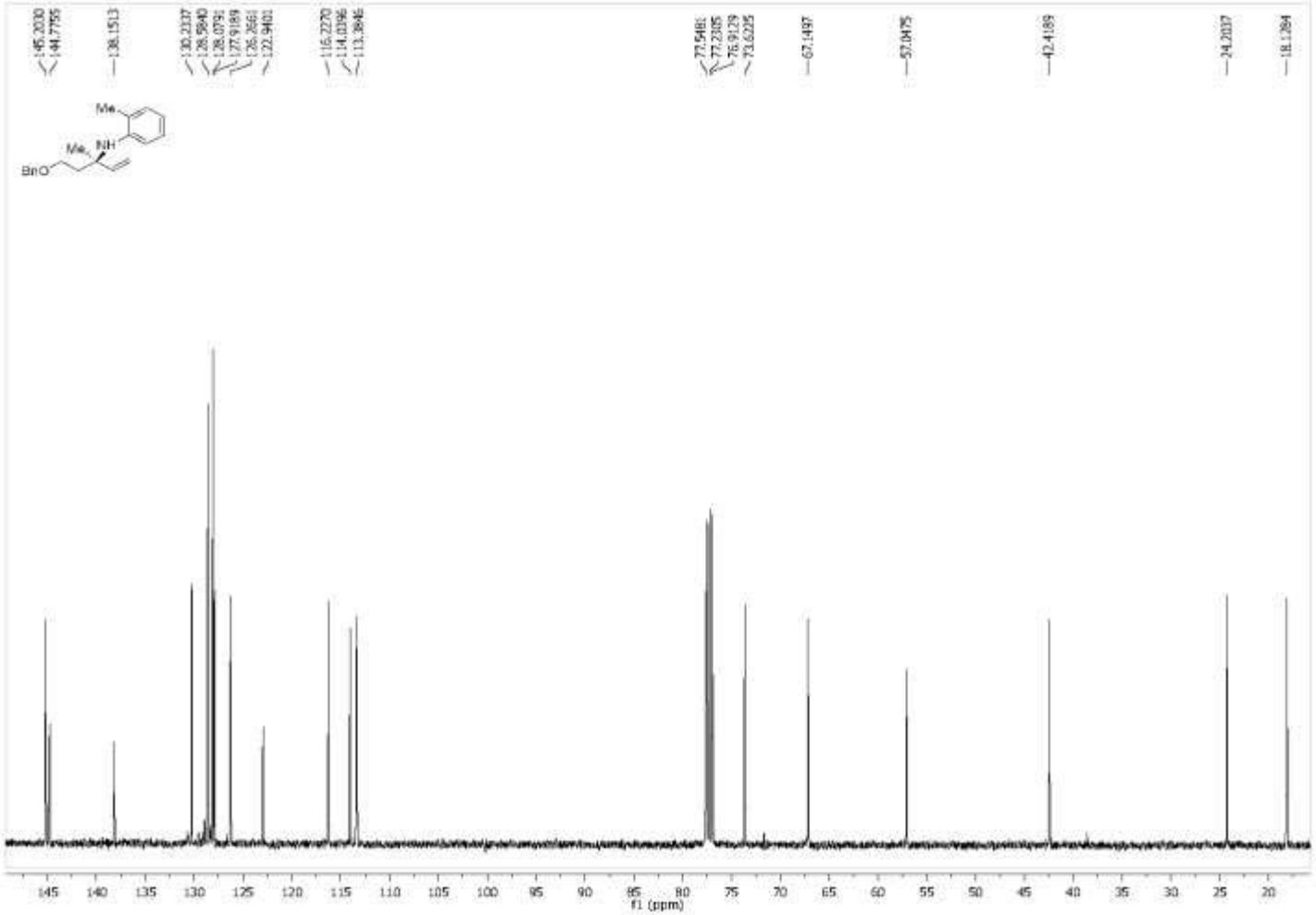

Figure A267 100 MHz 13C NMR ($CDCl_3$) Spectra of Compound **305d**

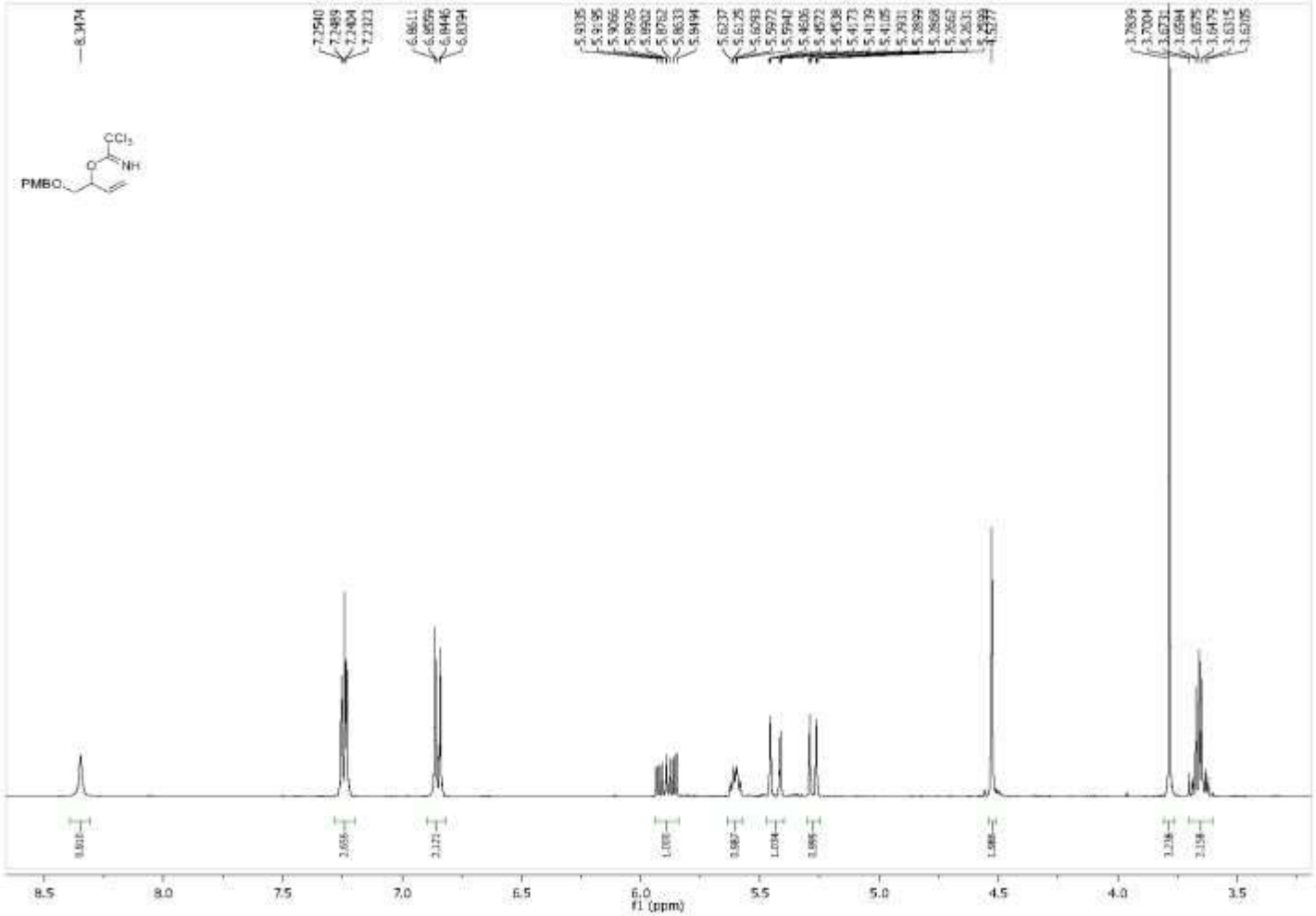

Figure A268 400 MHz 1H NMR ($CDCl_3$) Spectra of Compound **308**

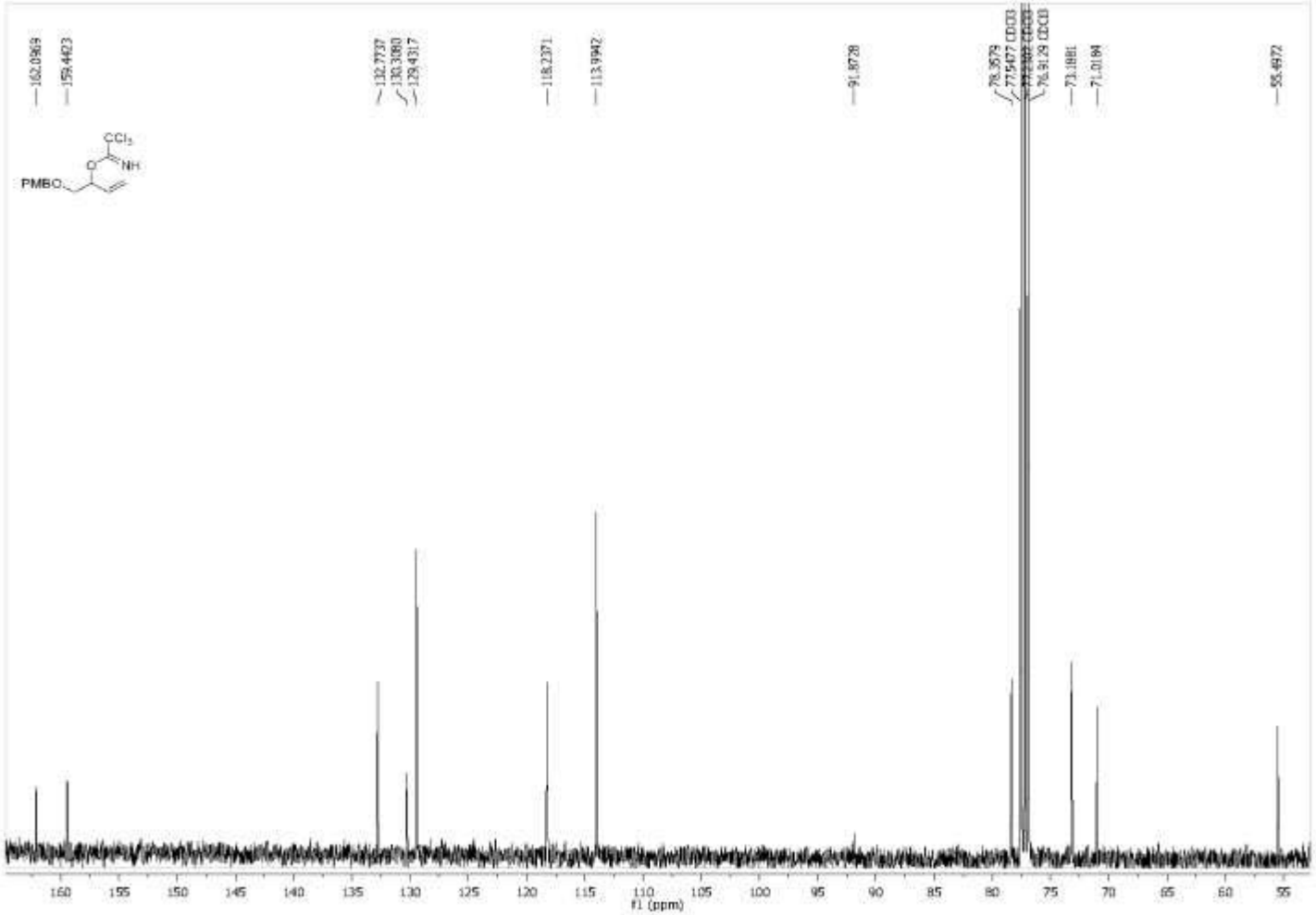

Figure A269 100 MHz 13C NMR ($CDCl_3$) Spectra of Compound **308**

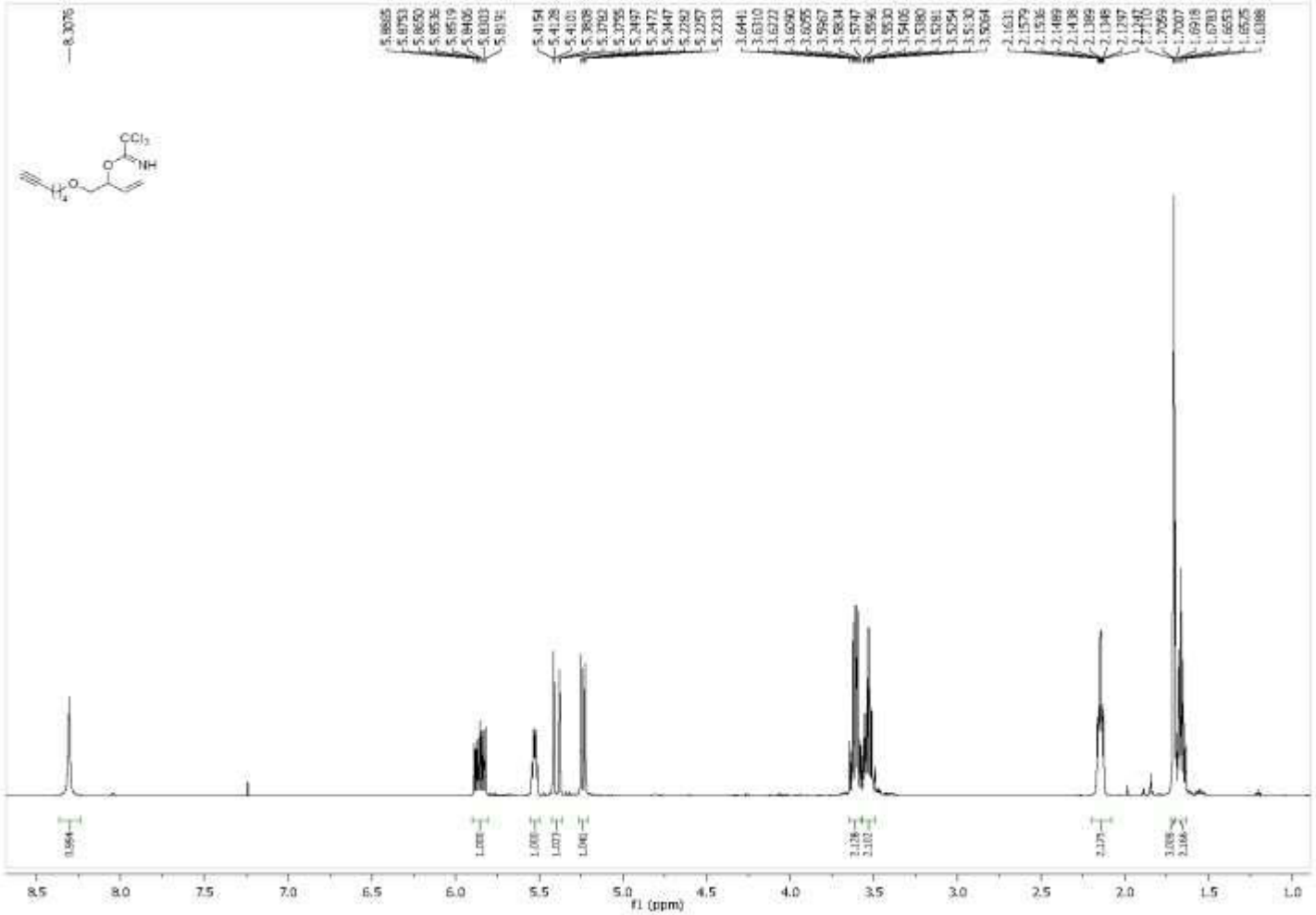

Figure A270 400 MHz 1H NMR ($CDCl_3$) Spectra of Compound **309**

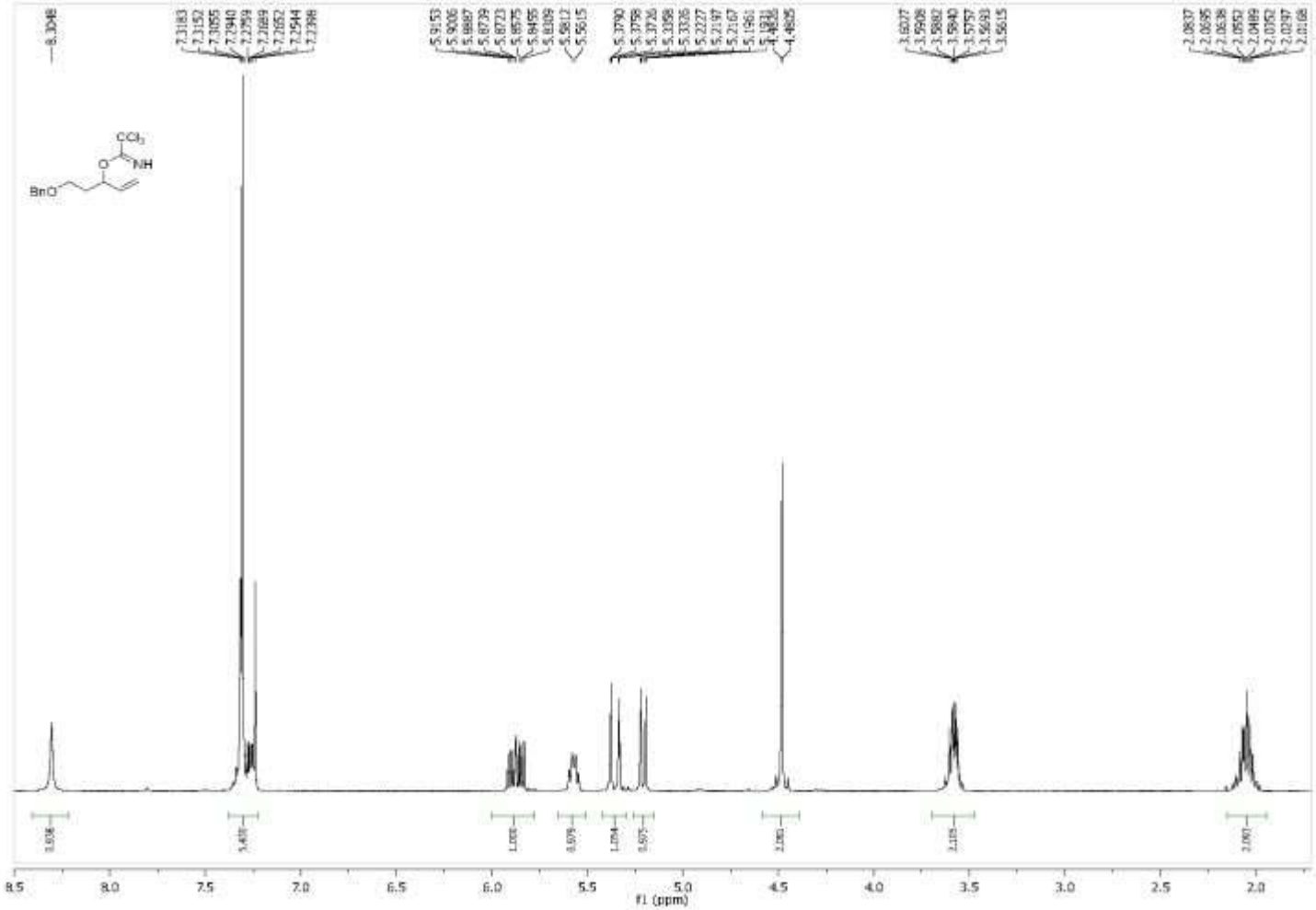

Figure A271 400 MHz 1H NMR ($CDCl_3$) Spectra of Compound **310**

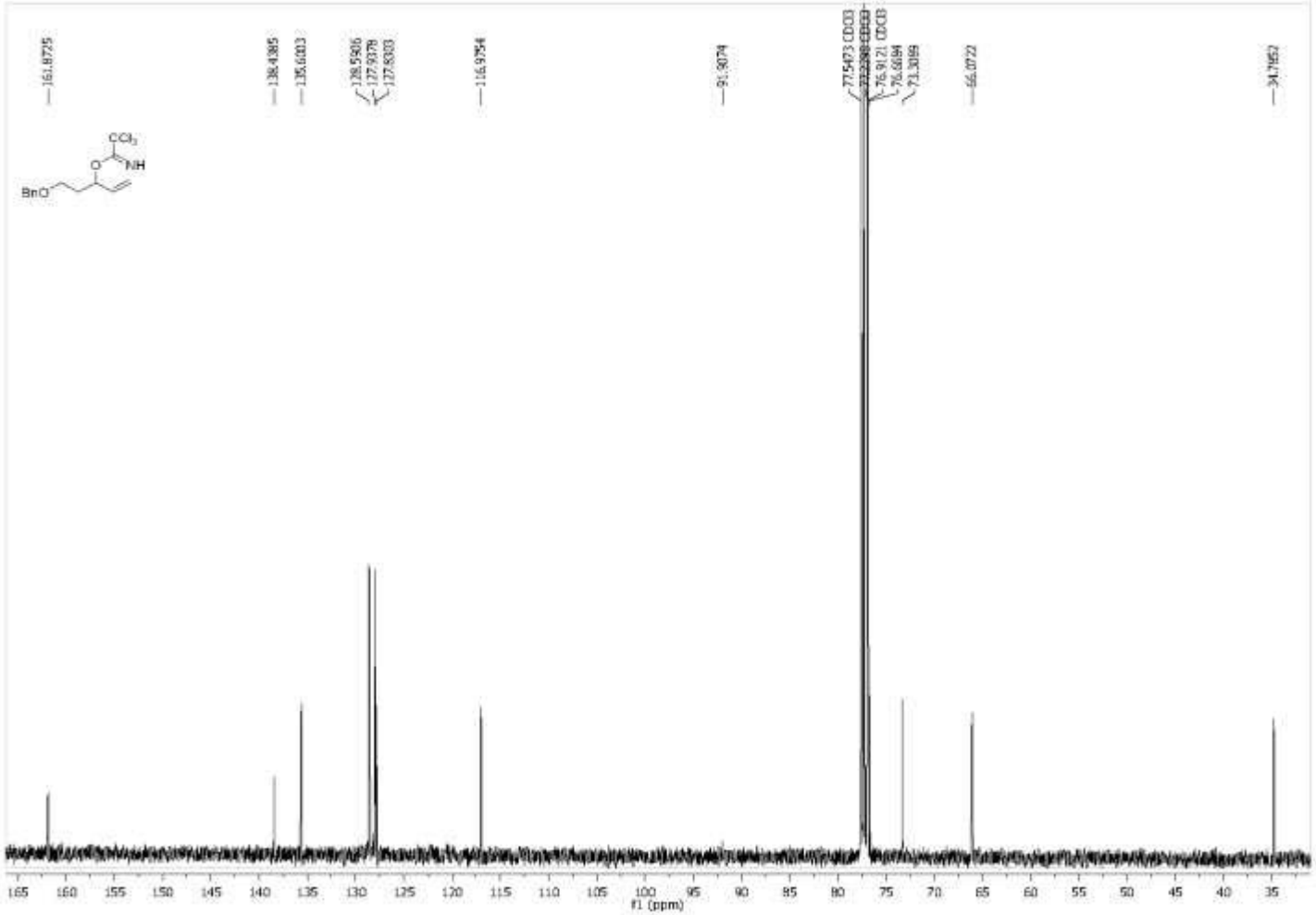

Figure A272 100 MHz 13C NMR ($CDCl_3$) Spectra of Compound **310**

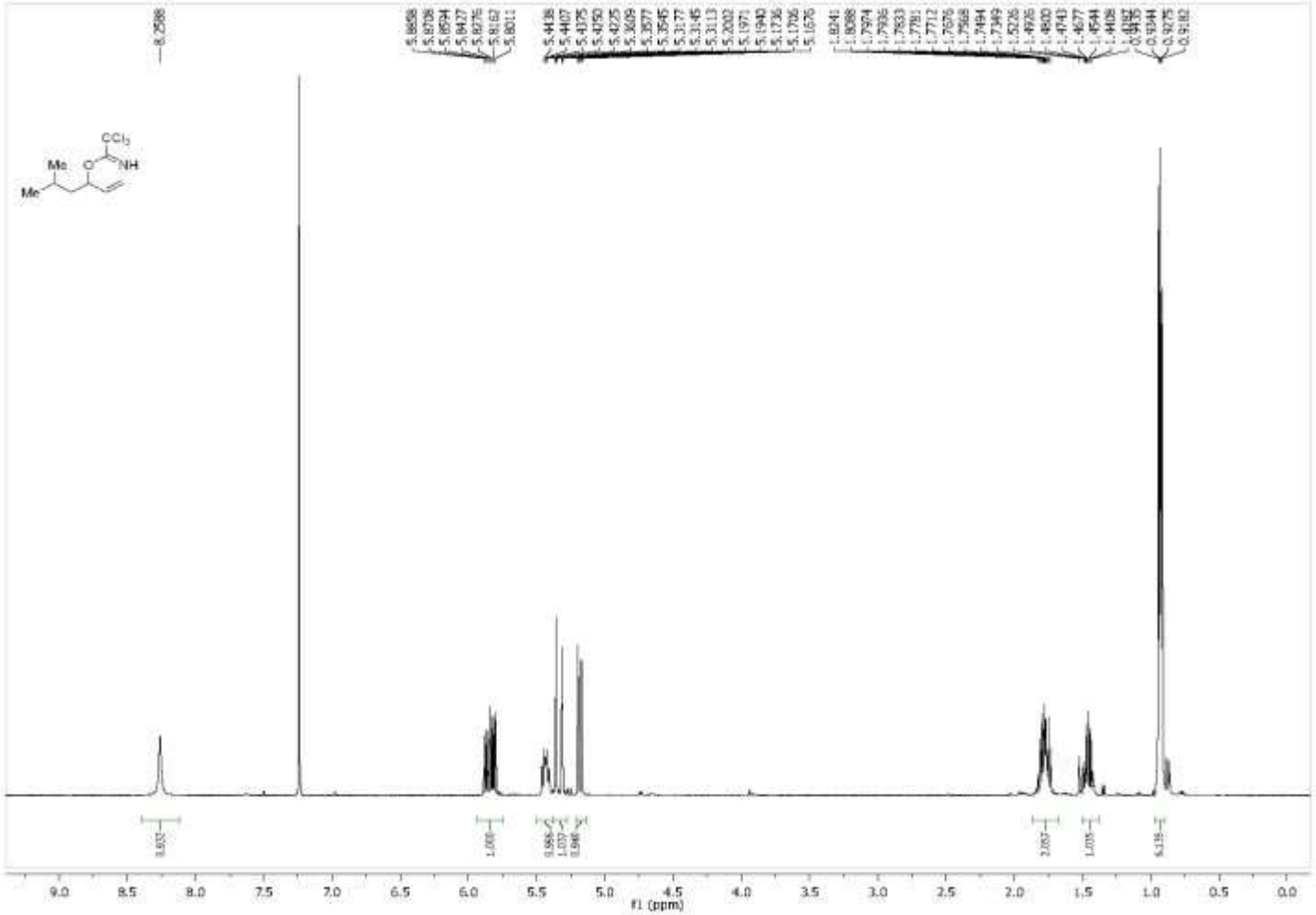

Figure A273 400 MHz 1H NMR ($CDCl_3$) Spectra of Compound **311**

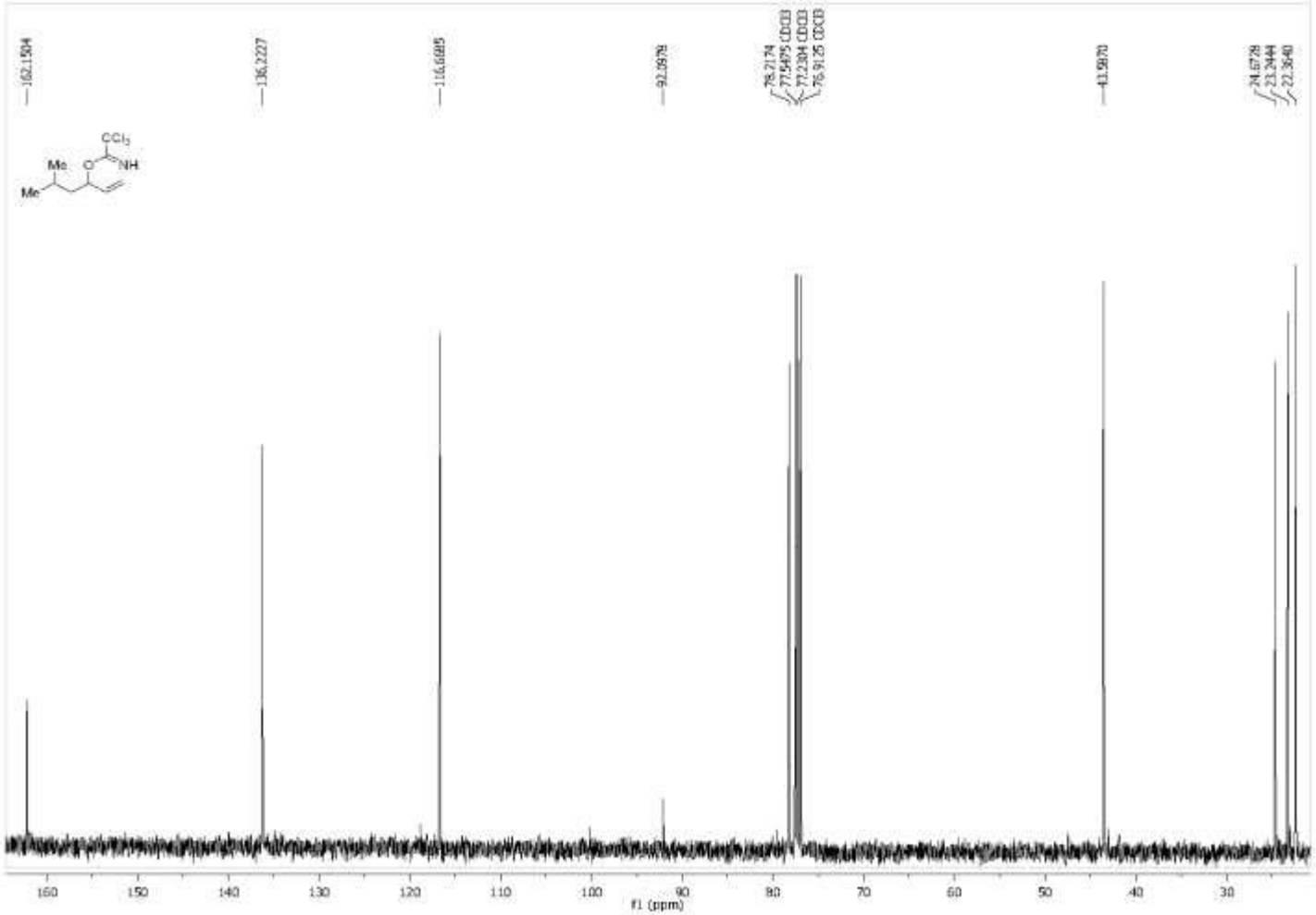

Figure A274 100 MHz 13C NMR ($CDCl_3$) Spectra of Compound **311**

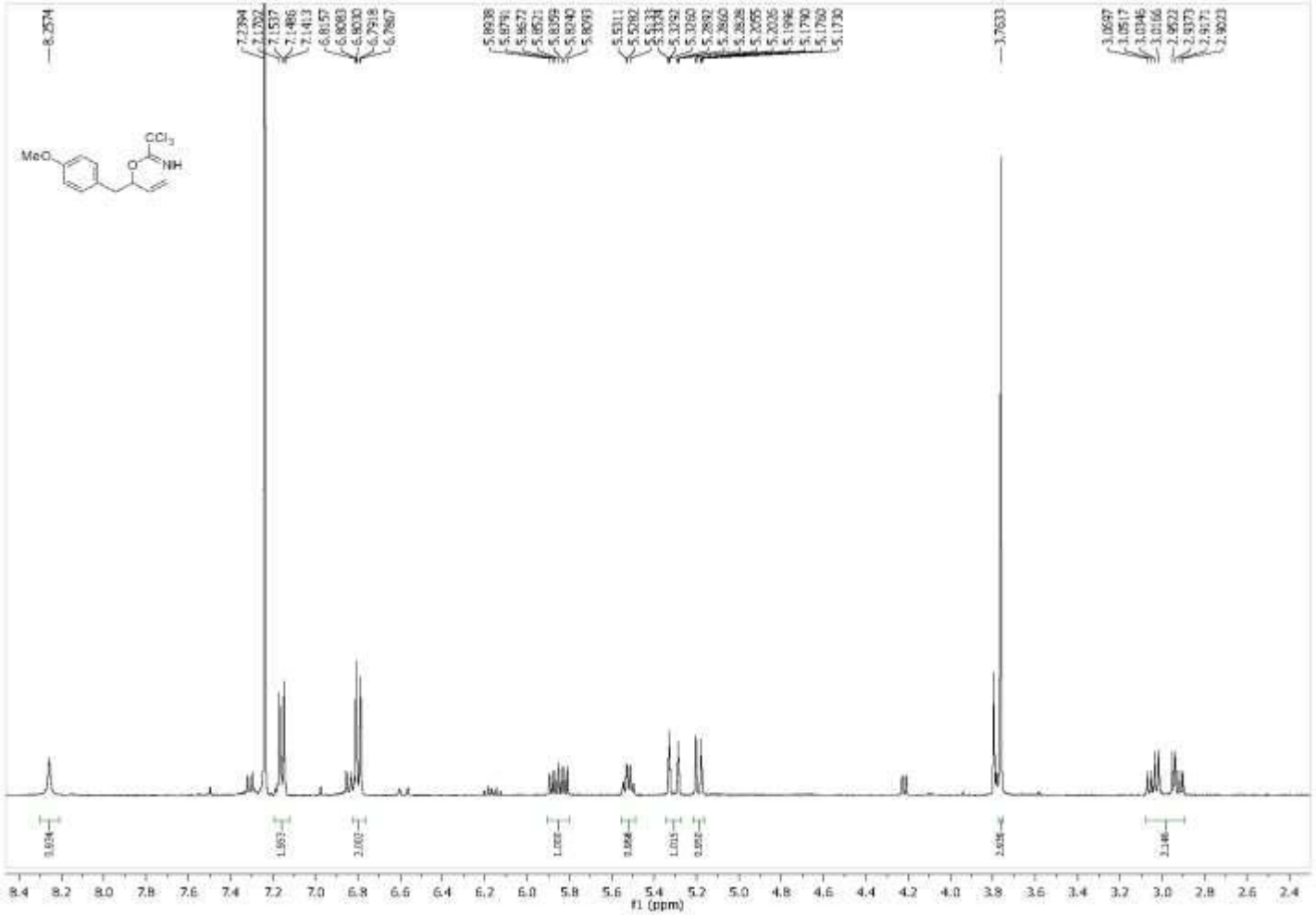

Figure A275 400 MHz 1H NMR ($CDCl_3$) Spectra of Compound **312**

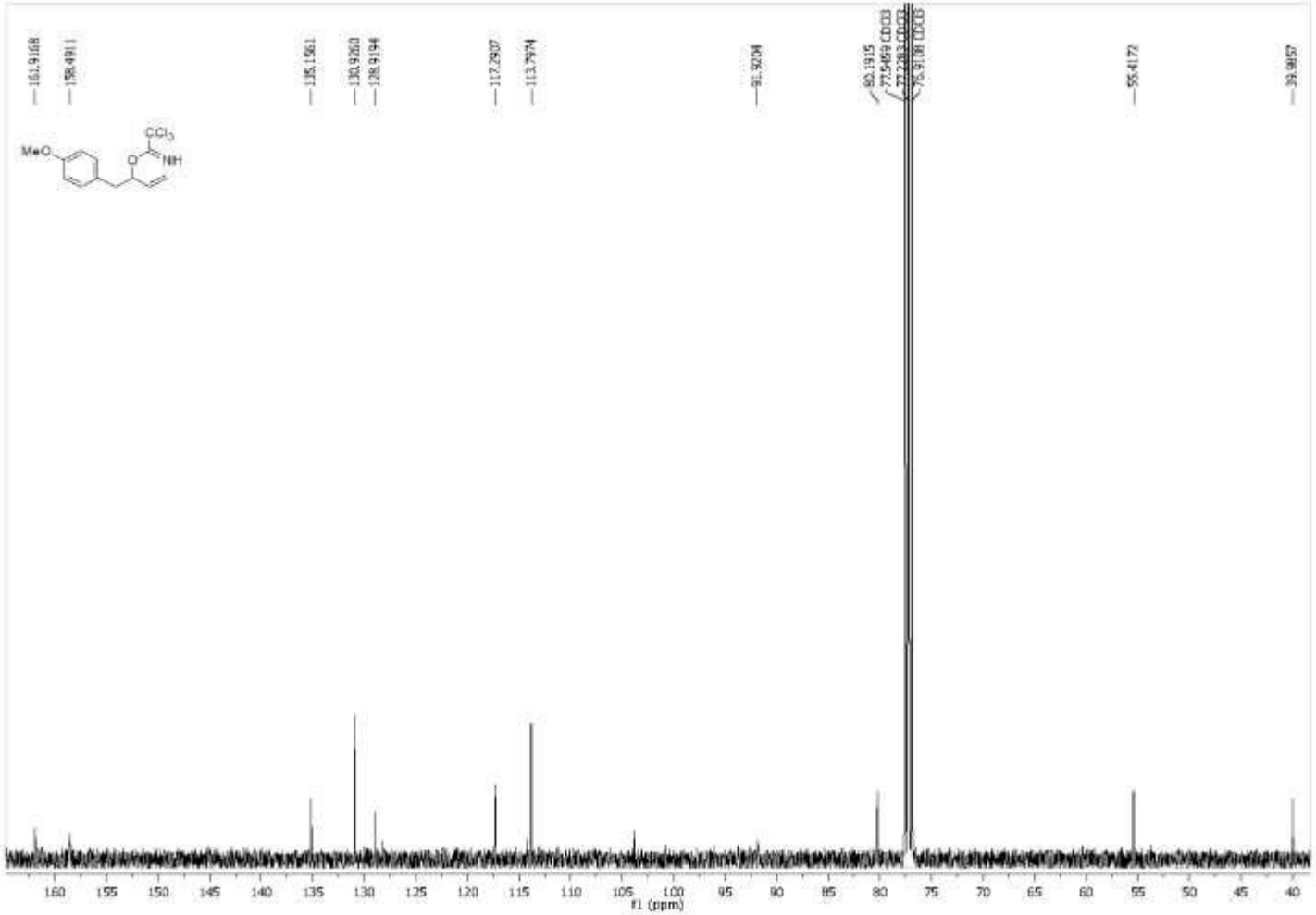

Figure A276 100 MHz 13C NMR ($CDCl_3$) Spectra of Compound **312**

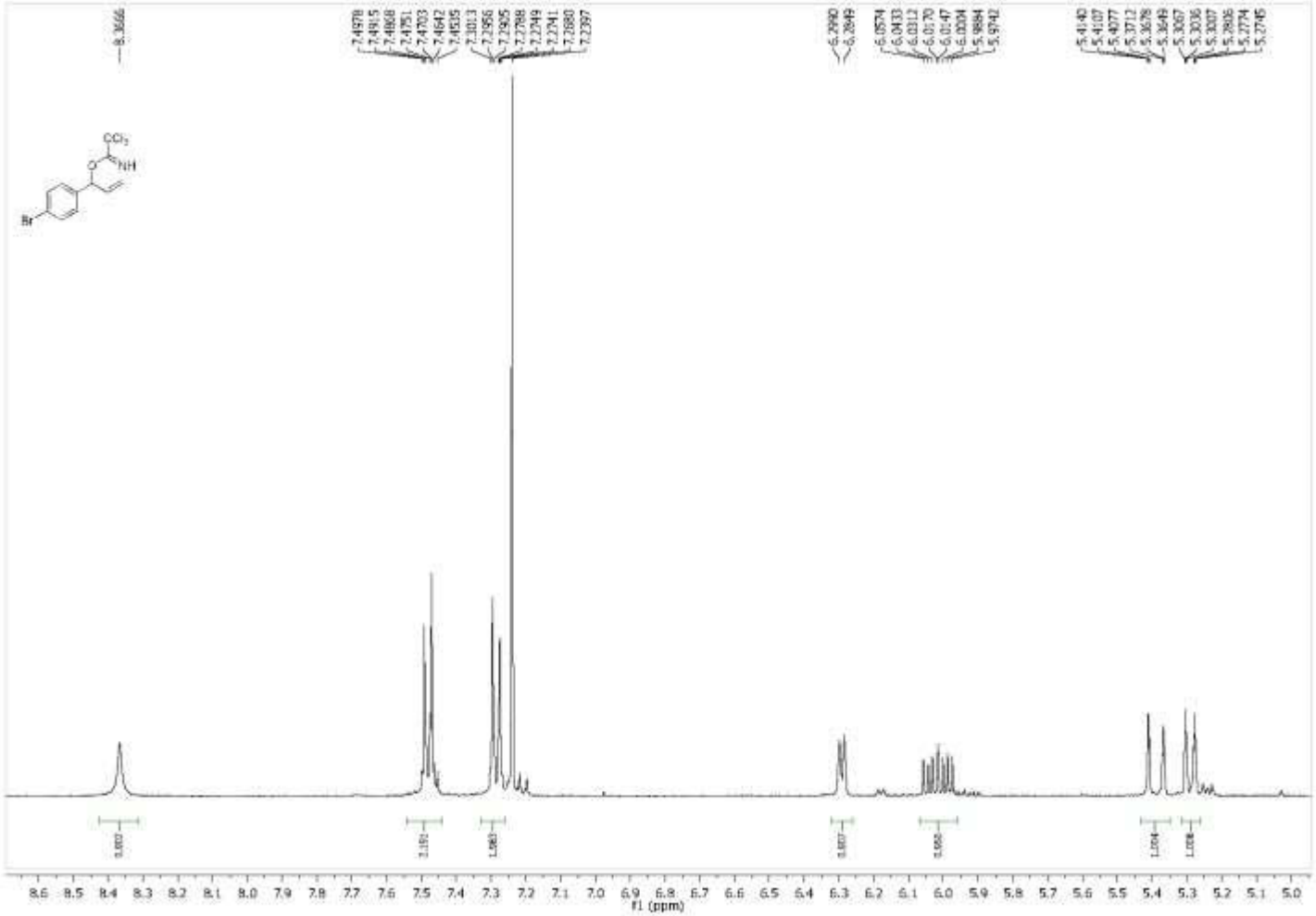

Figure A277 400 MHz 1H NMR ($CDCl_3$) Spectra of Compound **313**

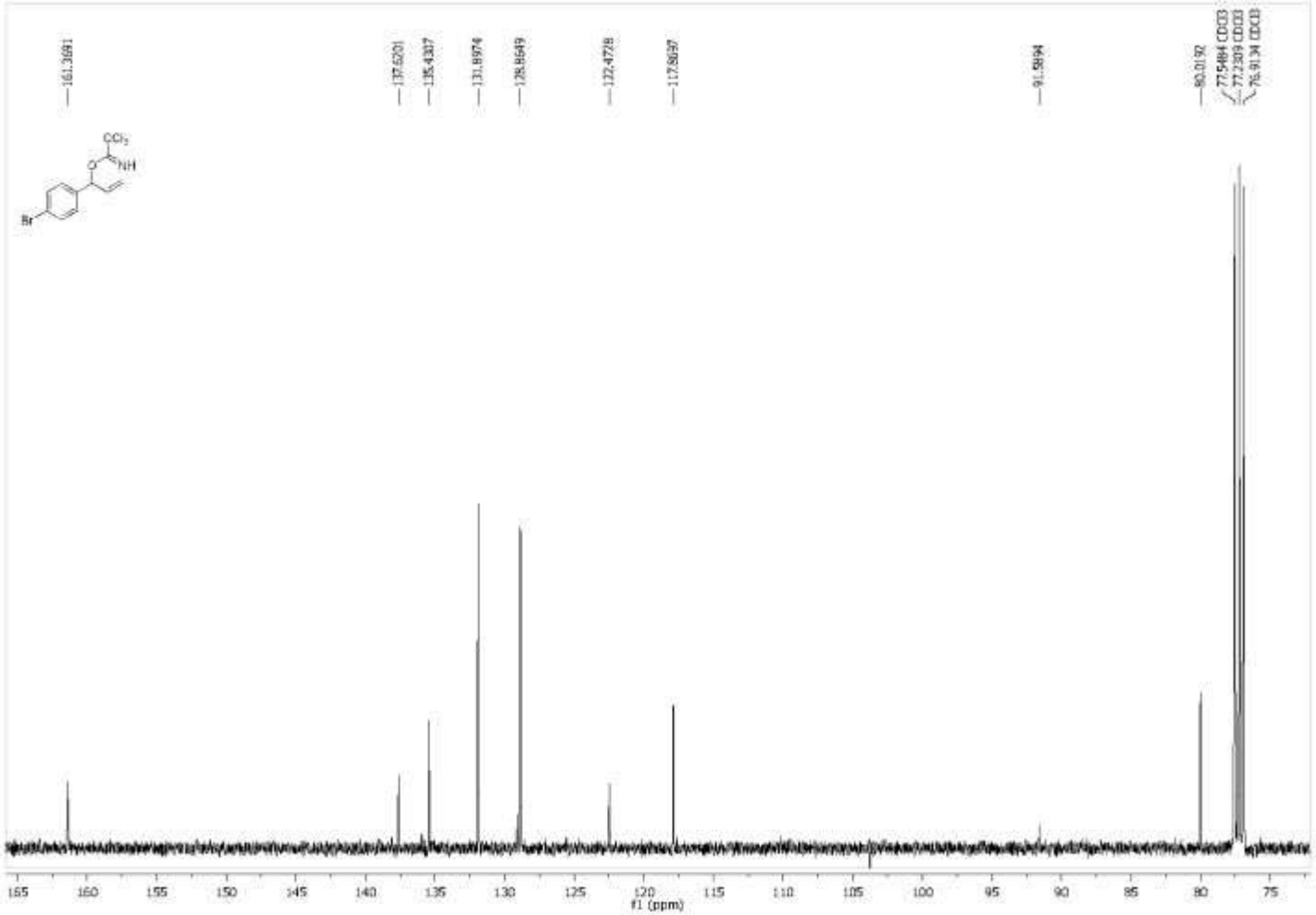

Figure A278 100 MHz 13C NMR ($CDCl_3$) Spectra of Compound **313**

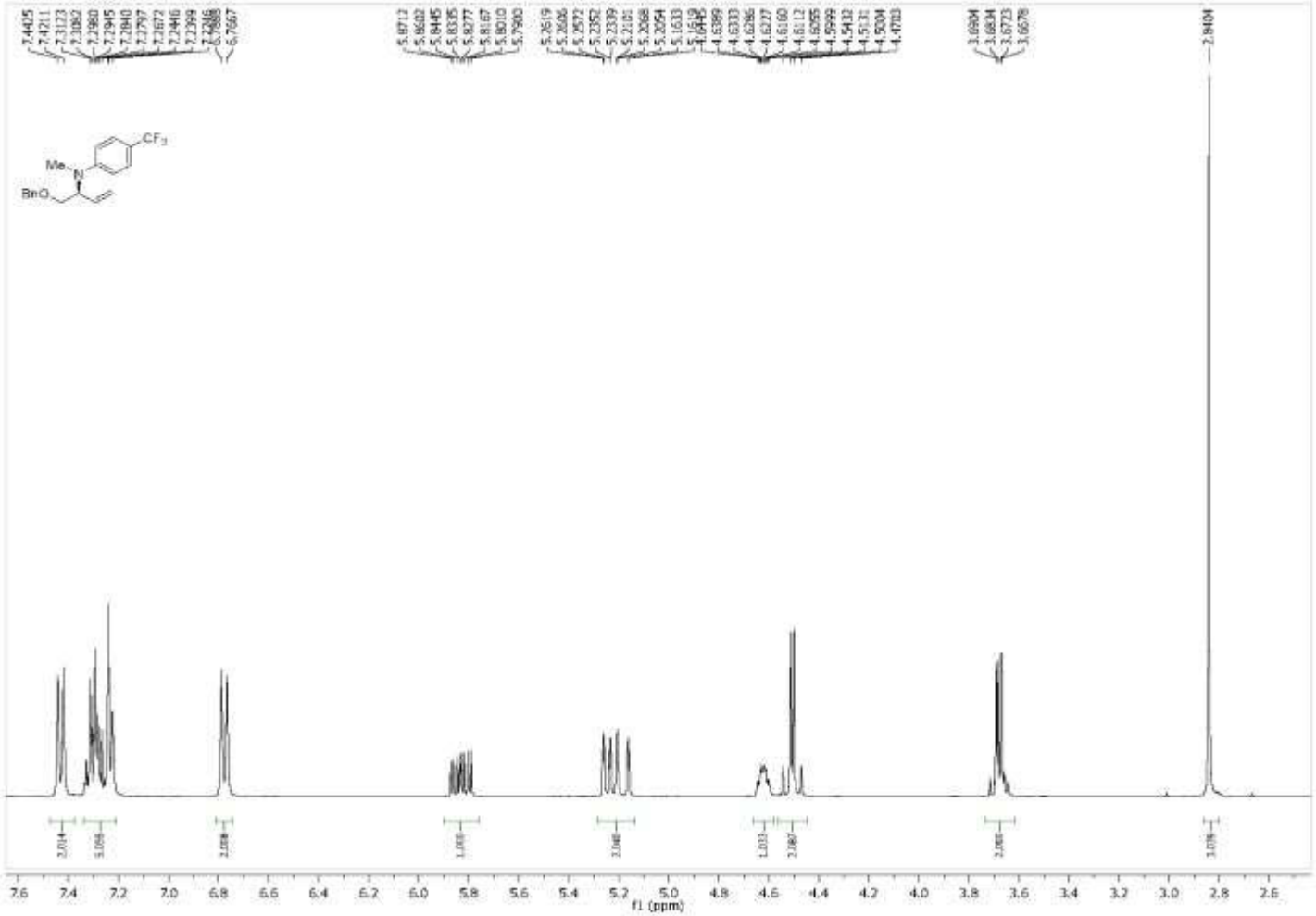

Figure A279 400 MHz 1H NMR ($CDCl_3$) Spectra of Compound **229r**

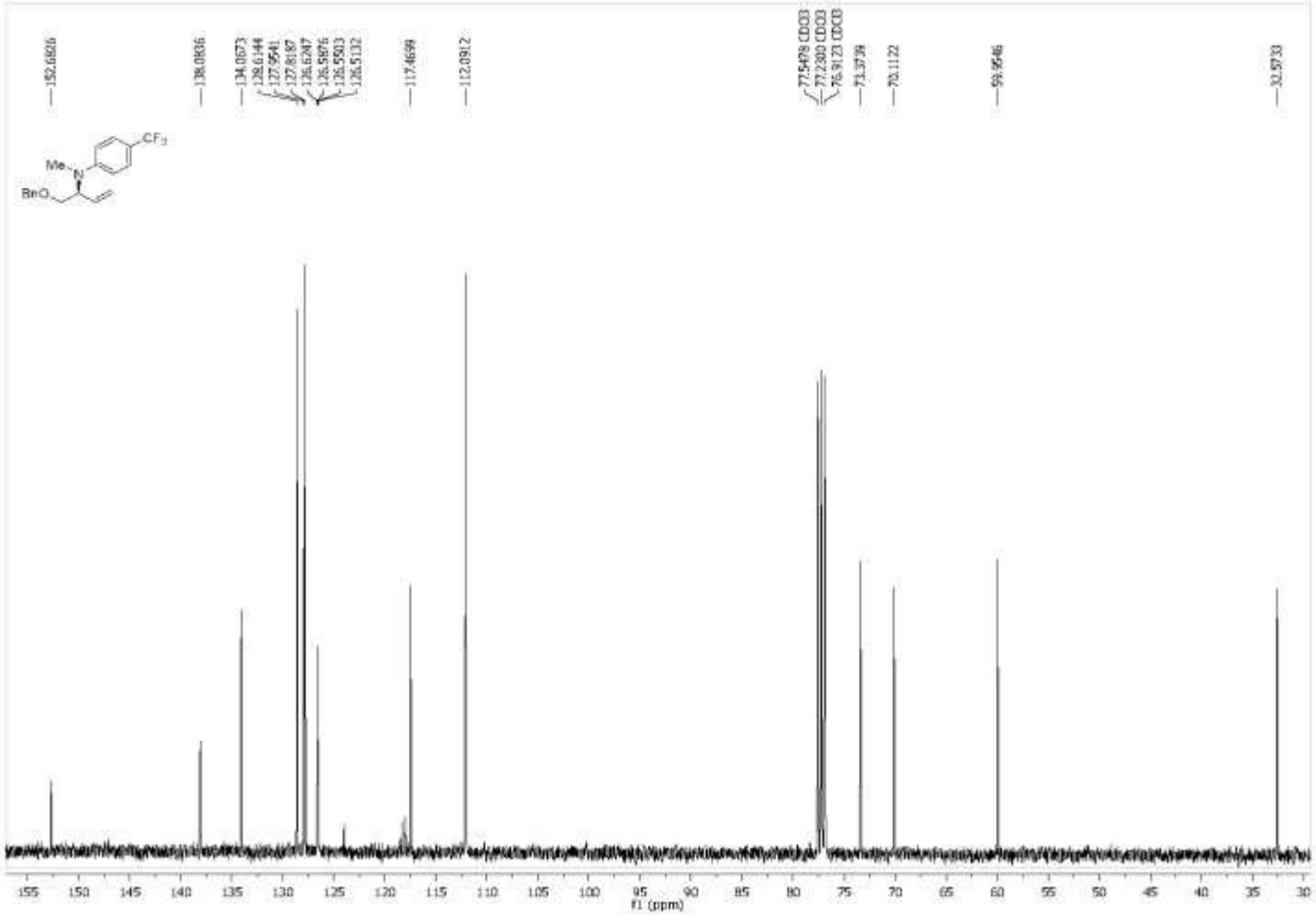

Figure A280 100 MHz 13C NMR ($CDCl_3$) Spectra of Compound **229r**

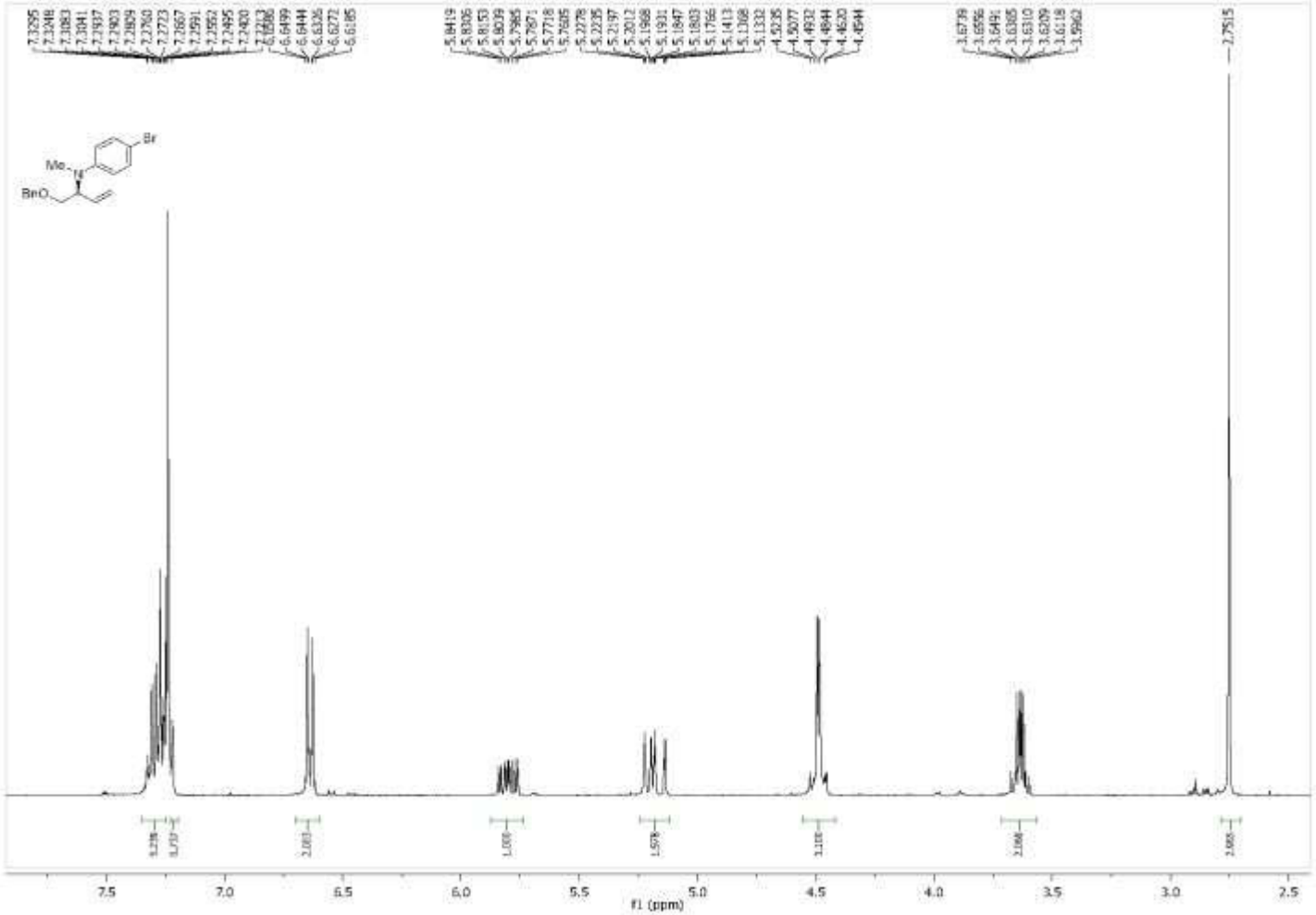

Figure A281 400 MHz 1H NMR ($CDCl_3$) Spectra of Compound **229s**

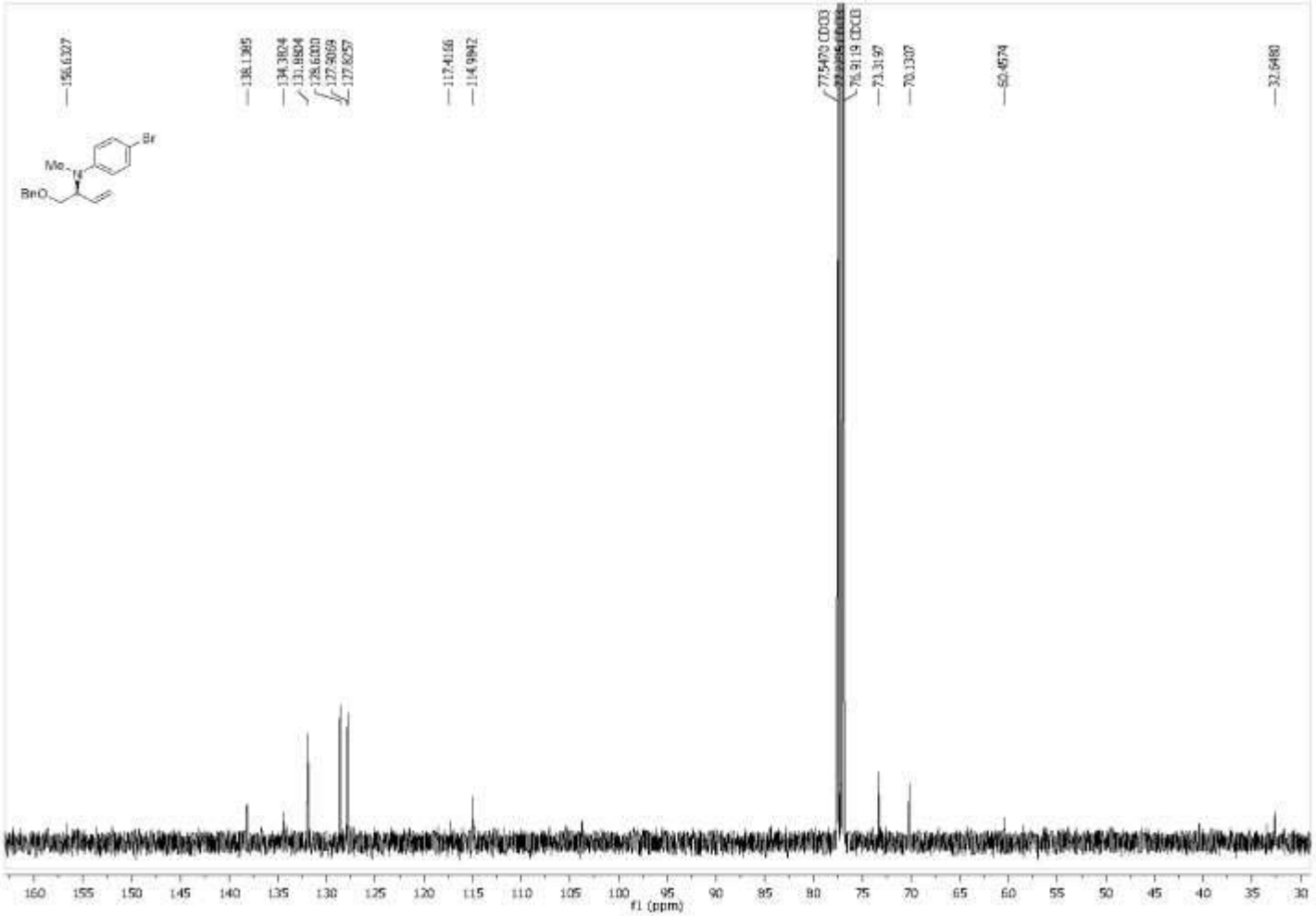

Figure A282 100 MHz 13C NMR ($CDCl_3$) Spectra of Compound **229s**

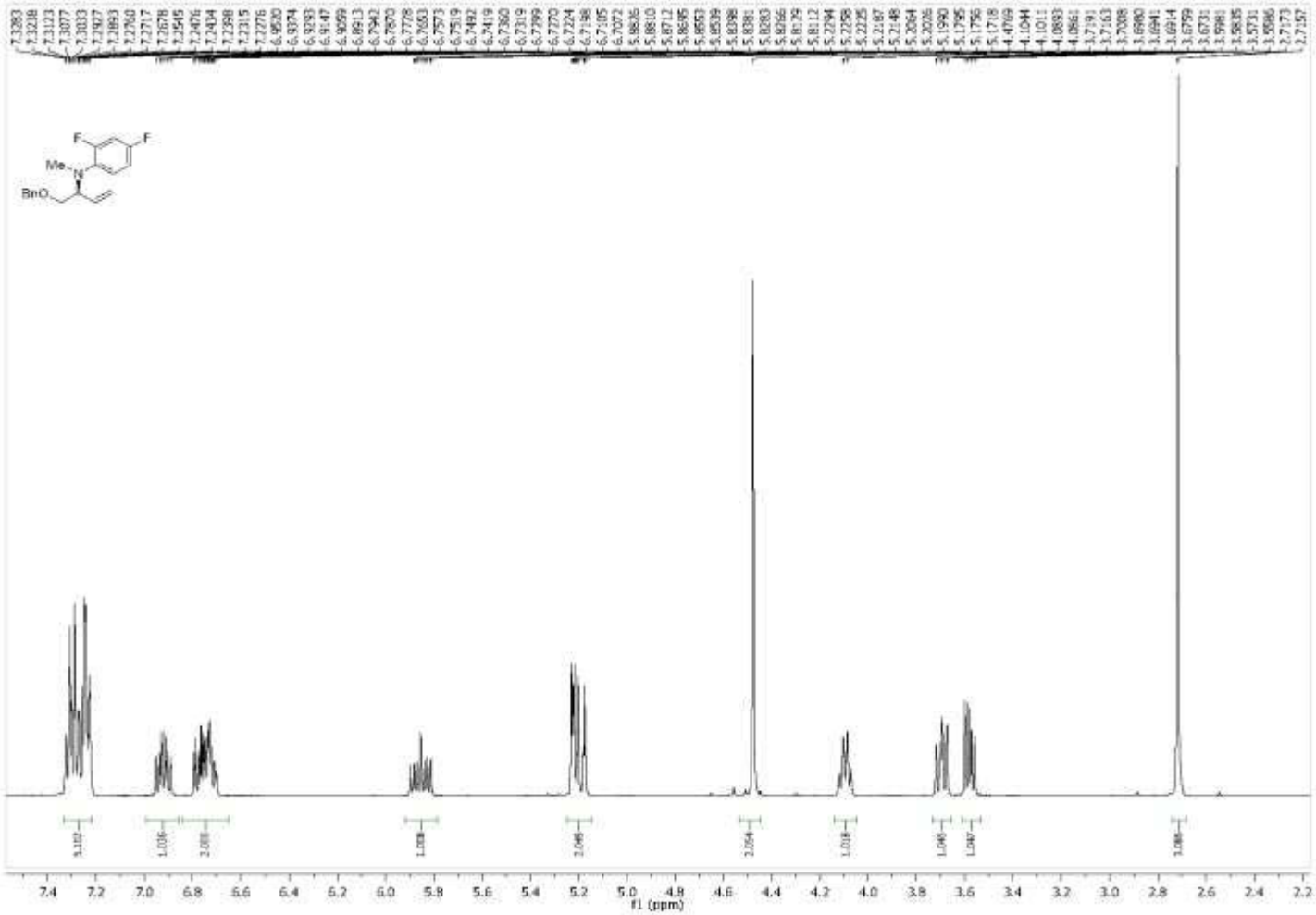

Figure A283 400 MHz 1H NMR ($CDCl_3$) Spectra of Compound **229t**

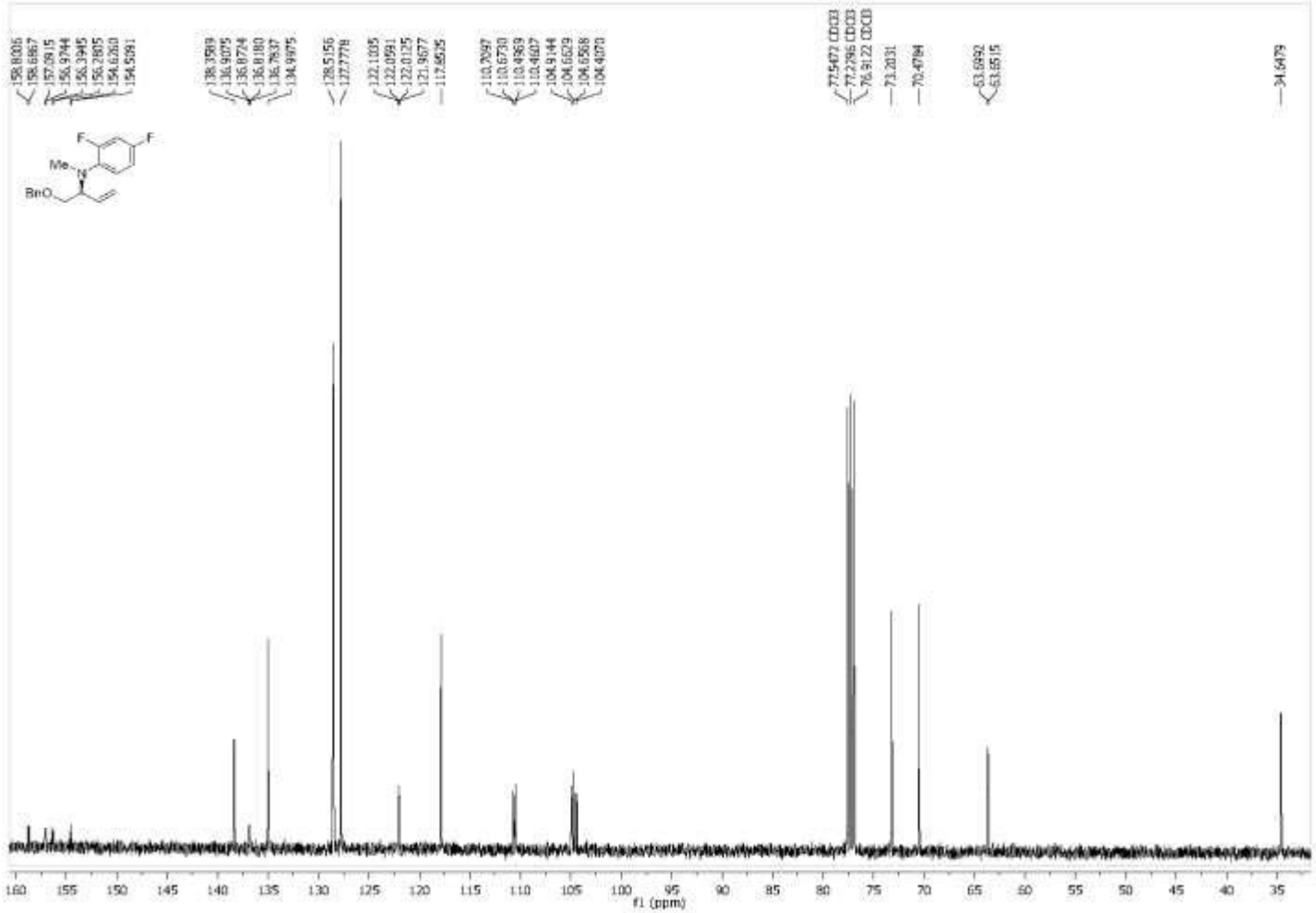

Figure A284 100 MHz 13C NMR ($CDCl_3$) Spectra of Compound **229t**

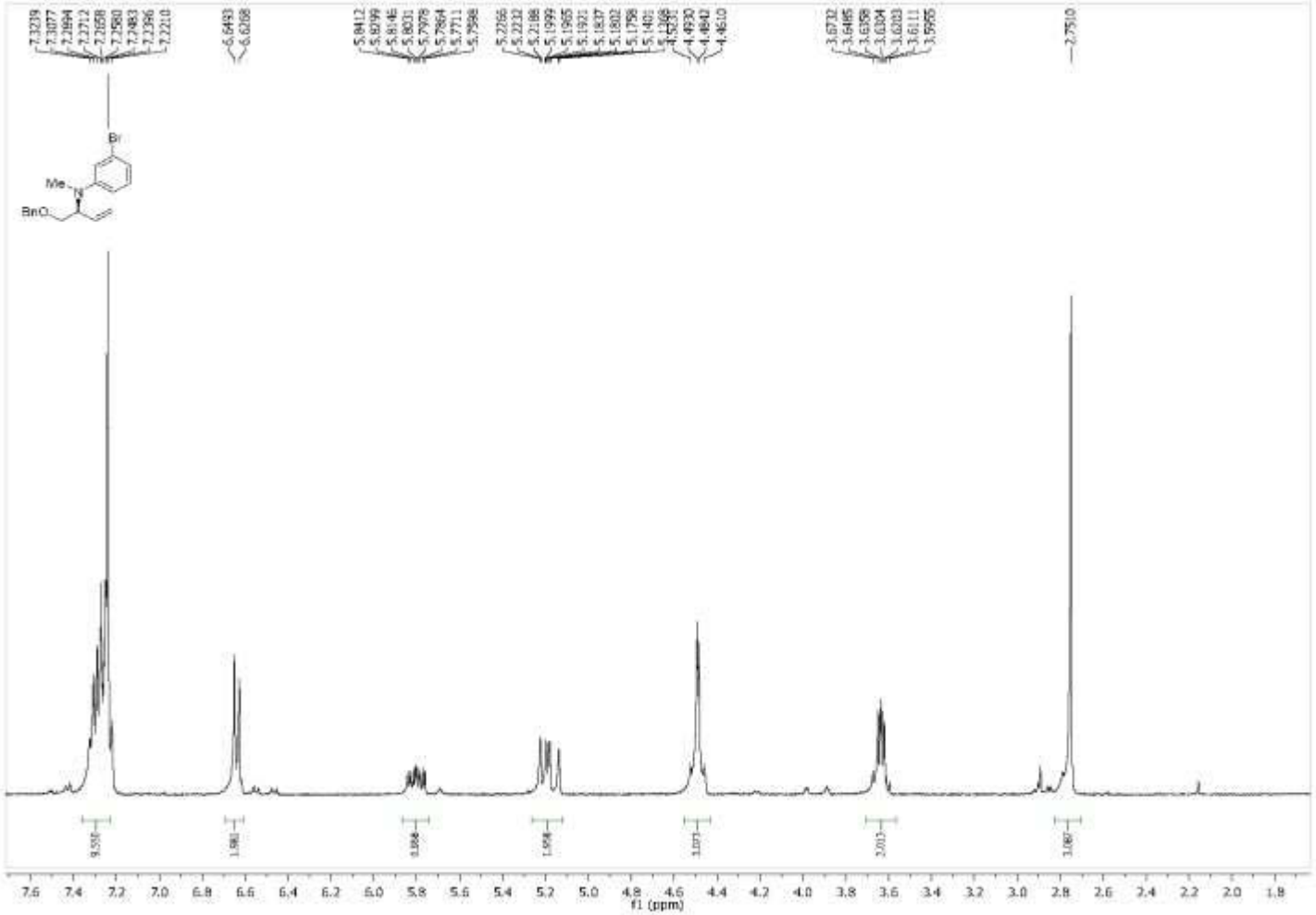

Figure A285 400 MHz 1H NMR ($CDCl_3$) Spectra of Compound **229u**

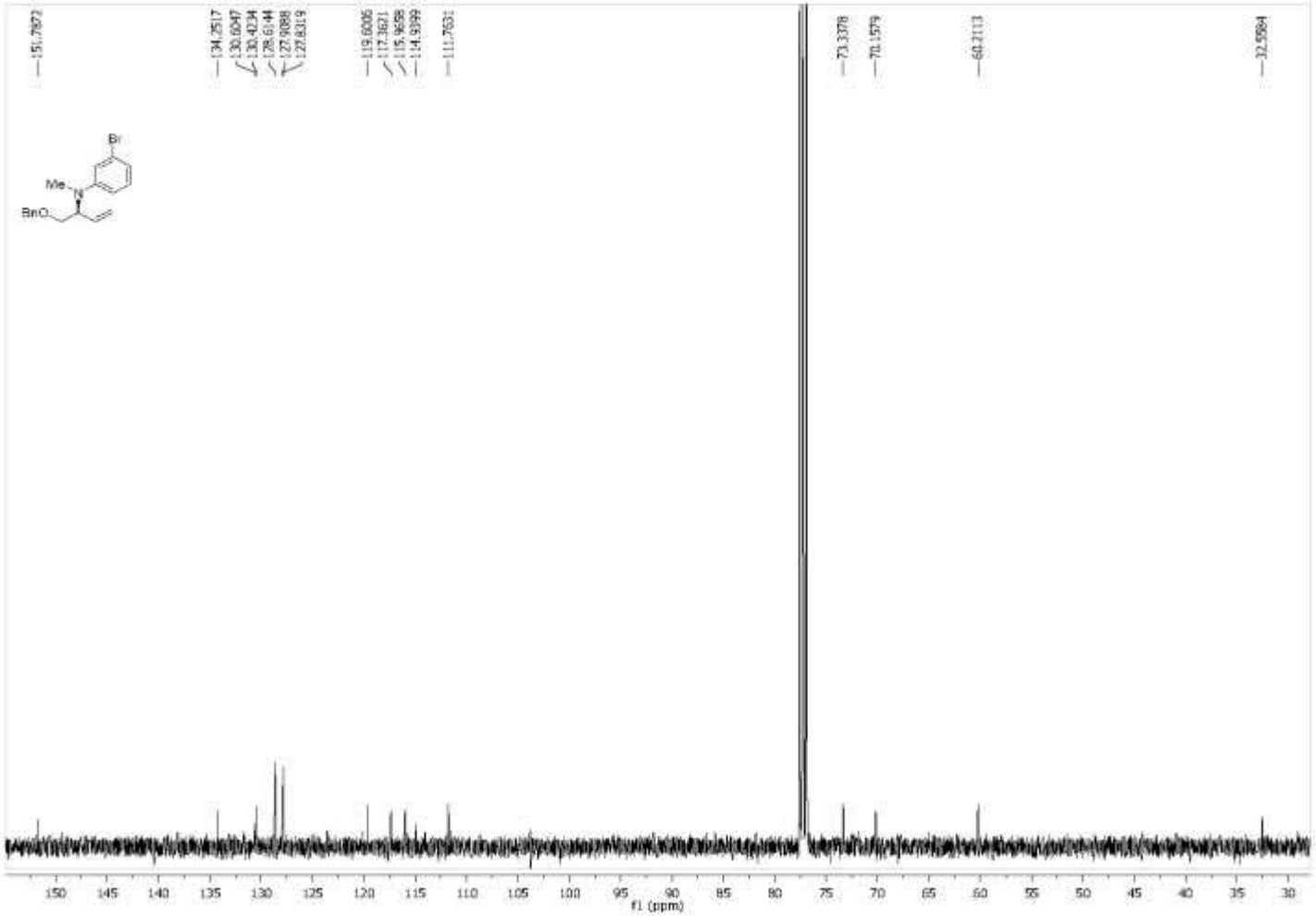

Figure A286 100 MHz 13C NMR ($CDCl_3$) Spectra of Compound **229u**

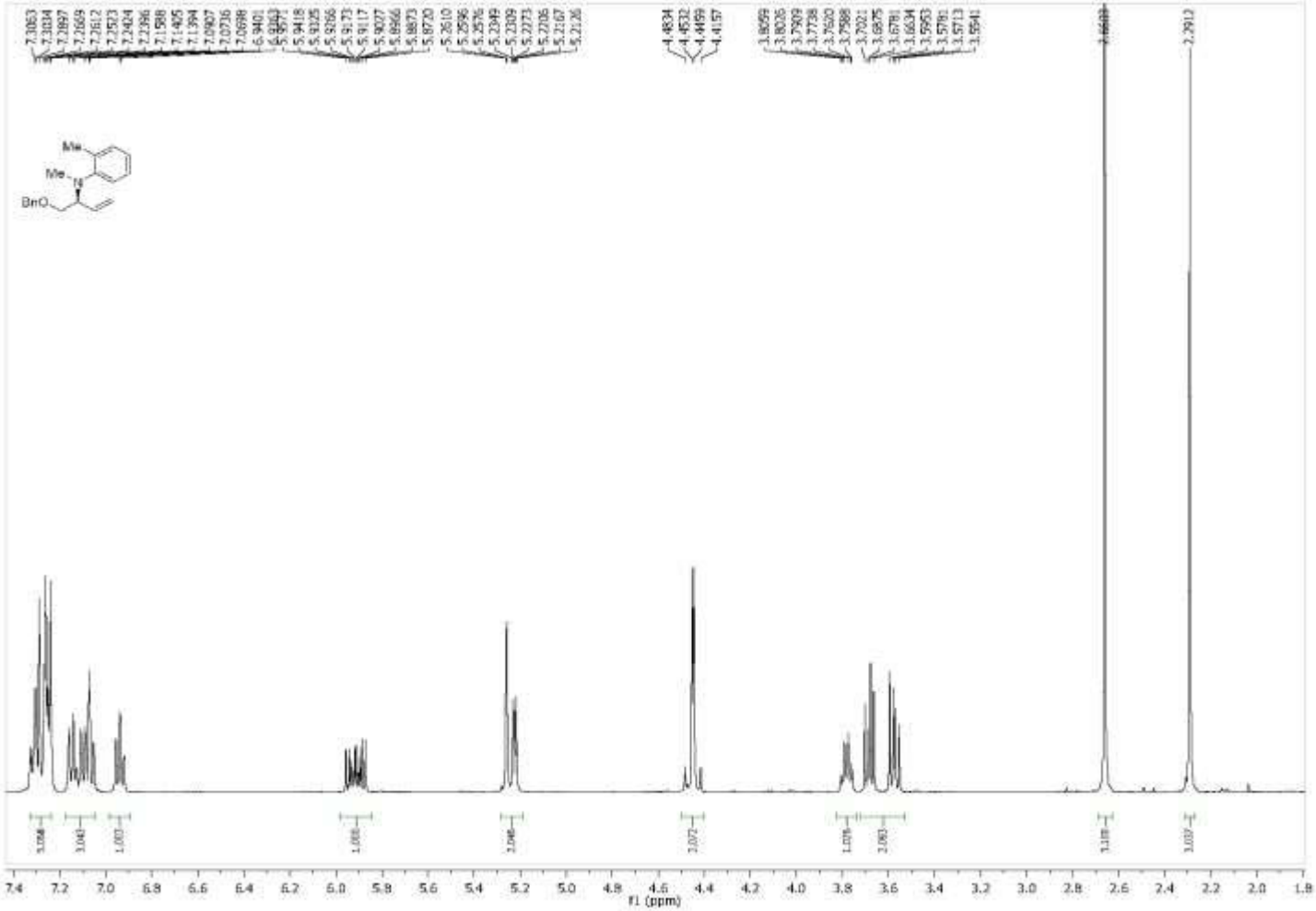

Figure A287 400 MHz 1H NMR ($CDCl_3$) Spectra of Compound **229v**

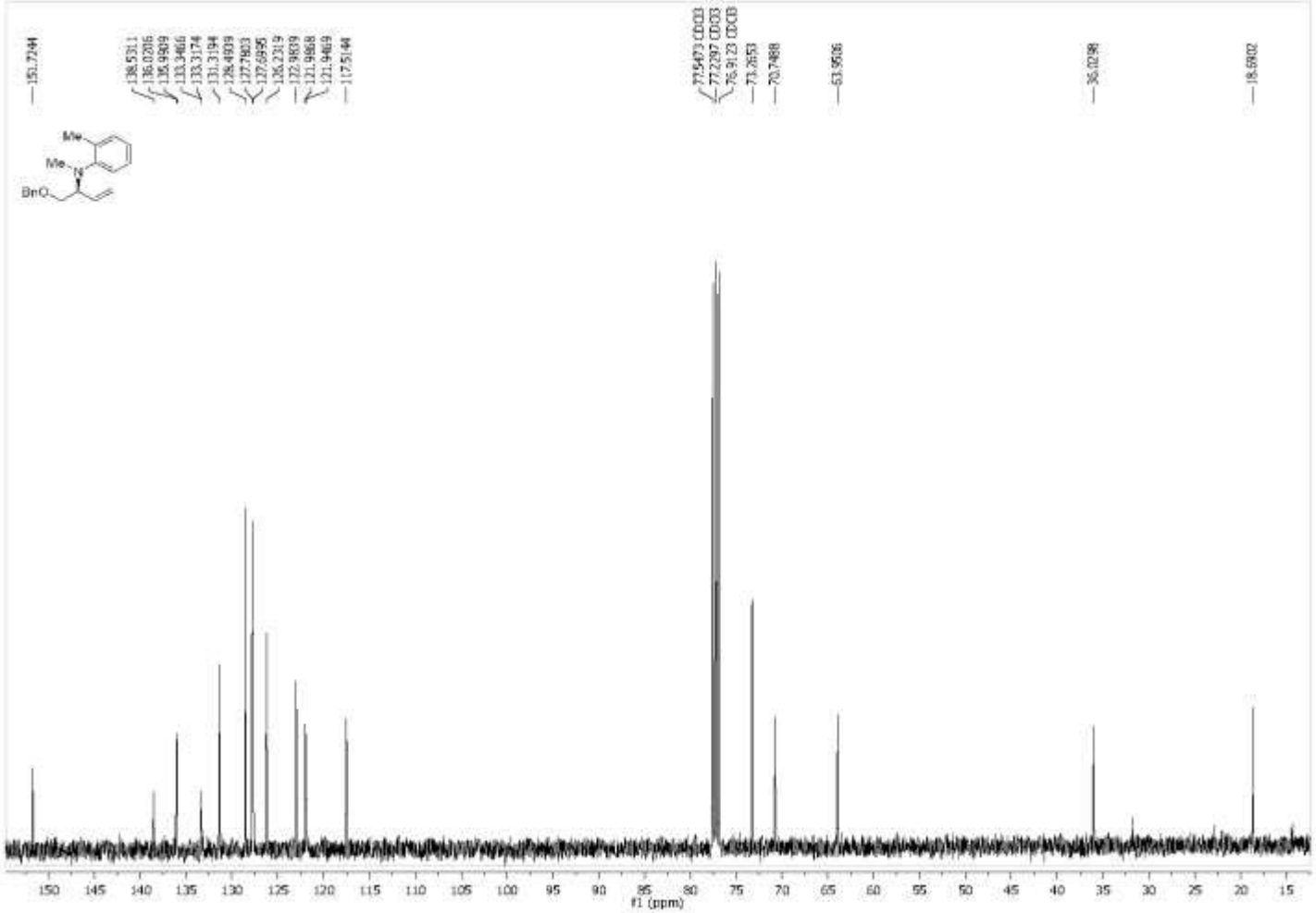

Figure A288 100 MHz 13C NMR ($CDCl_3$) Spectra of Compound **229v**

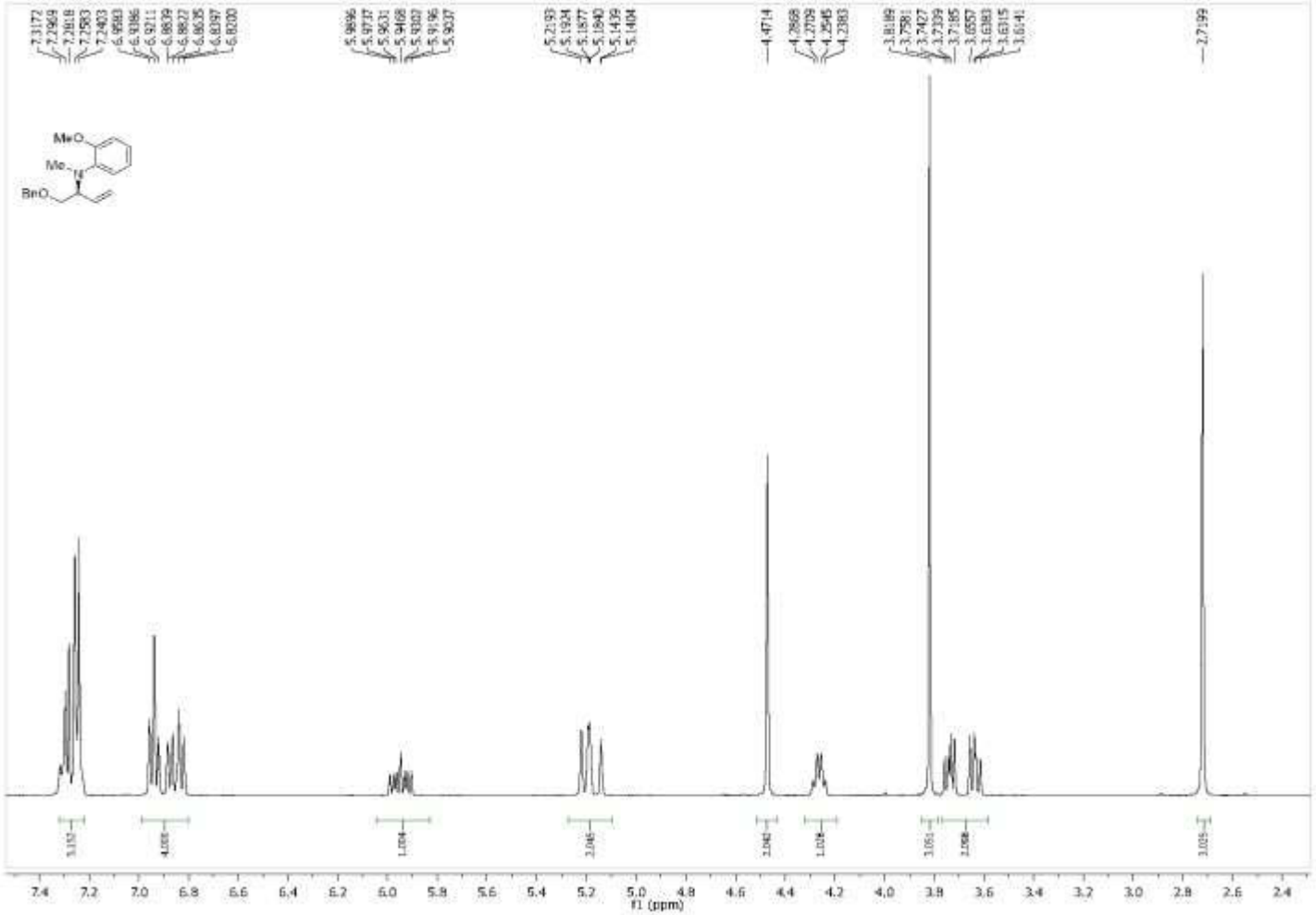

Figure A289 400 MHz 1H NMR ($CDCl_3$) Spectra of Compound **229w**

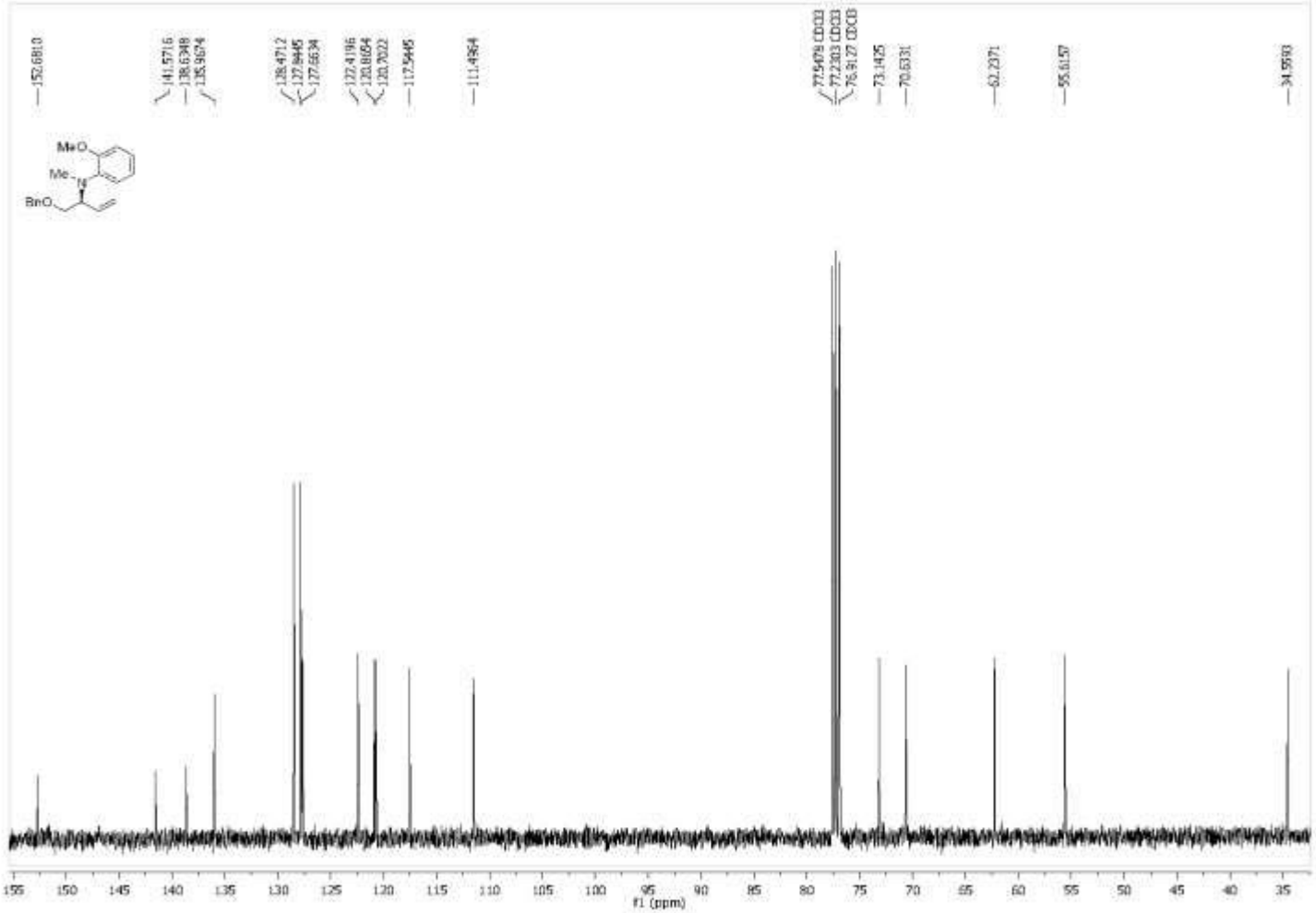

Figure A290 100 MHz 13C NMR ($CDCl_3$) Spectra of Compound **229w**

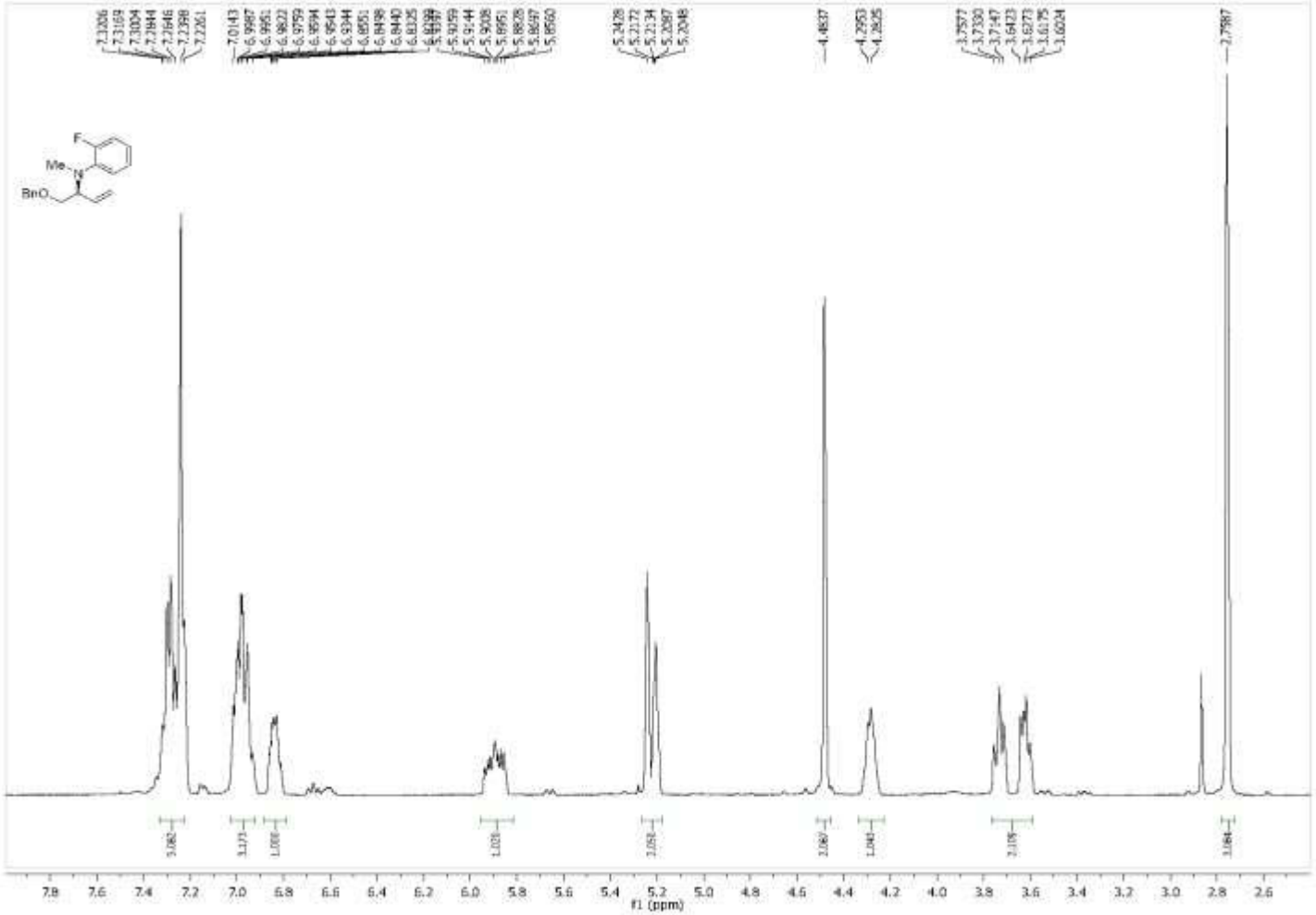

Figure A291 400 MHz 1H NMR ($CDCl_3$) Spectra of Compound **229x**

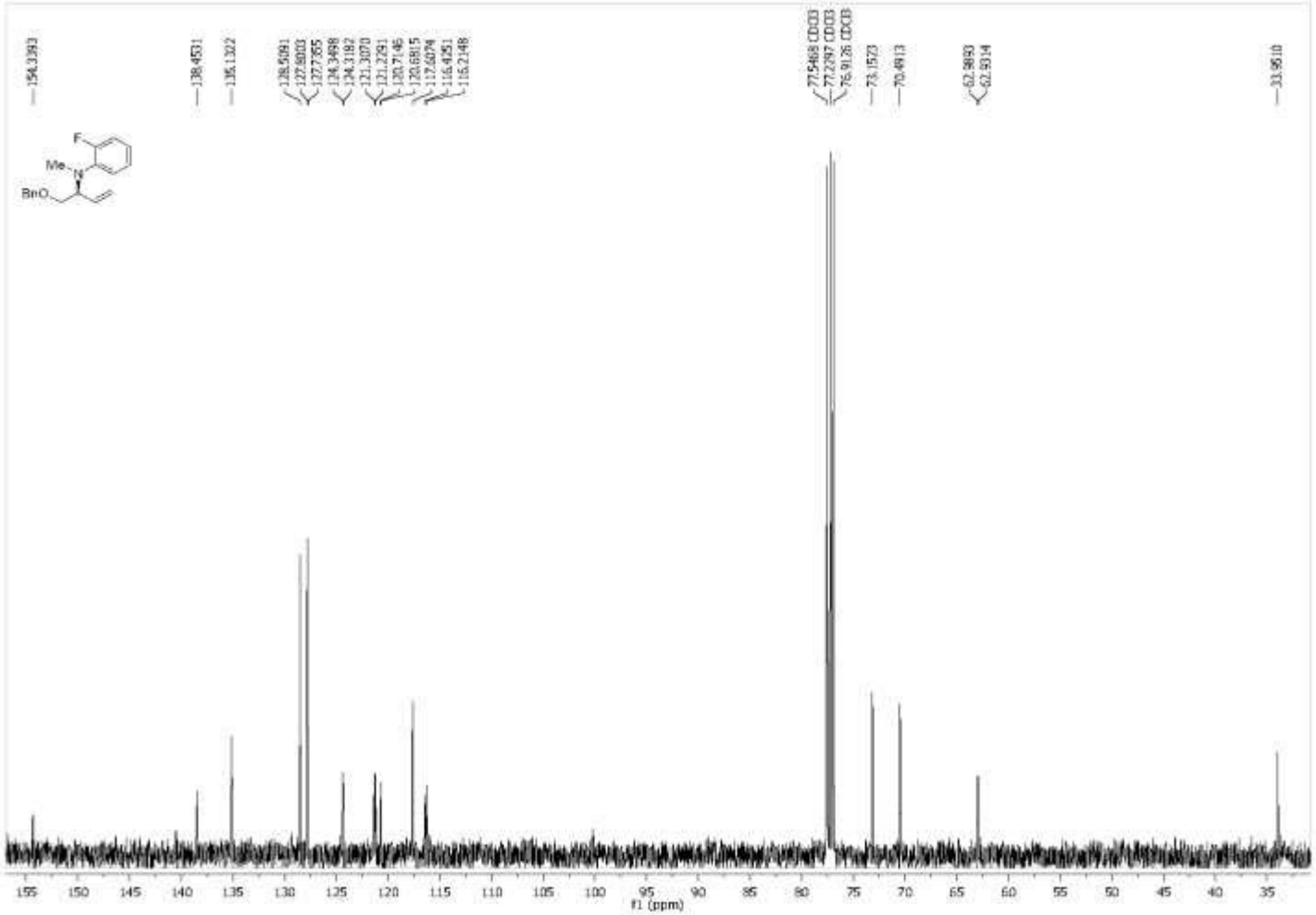

Figure A292 100 MHz 13C NMR ($CDCl_3$) Spectra of Compound **229x**

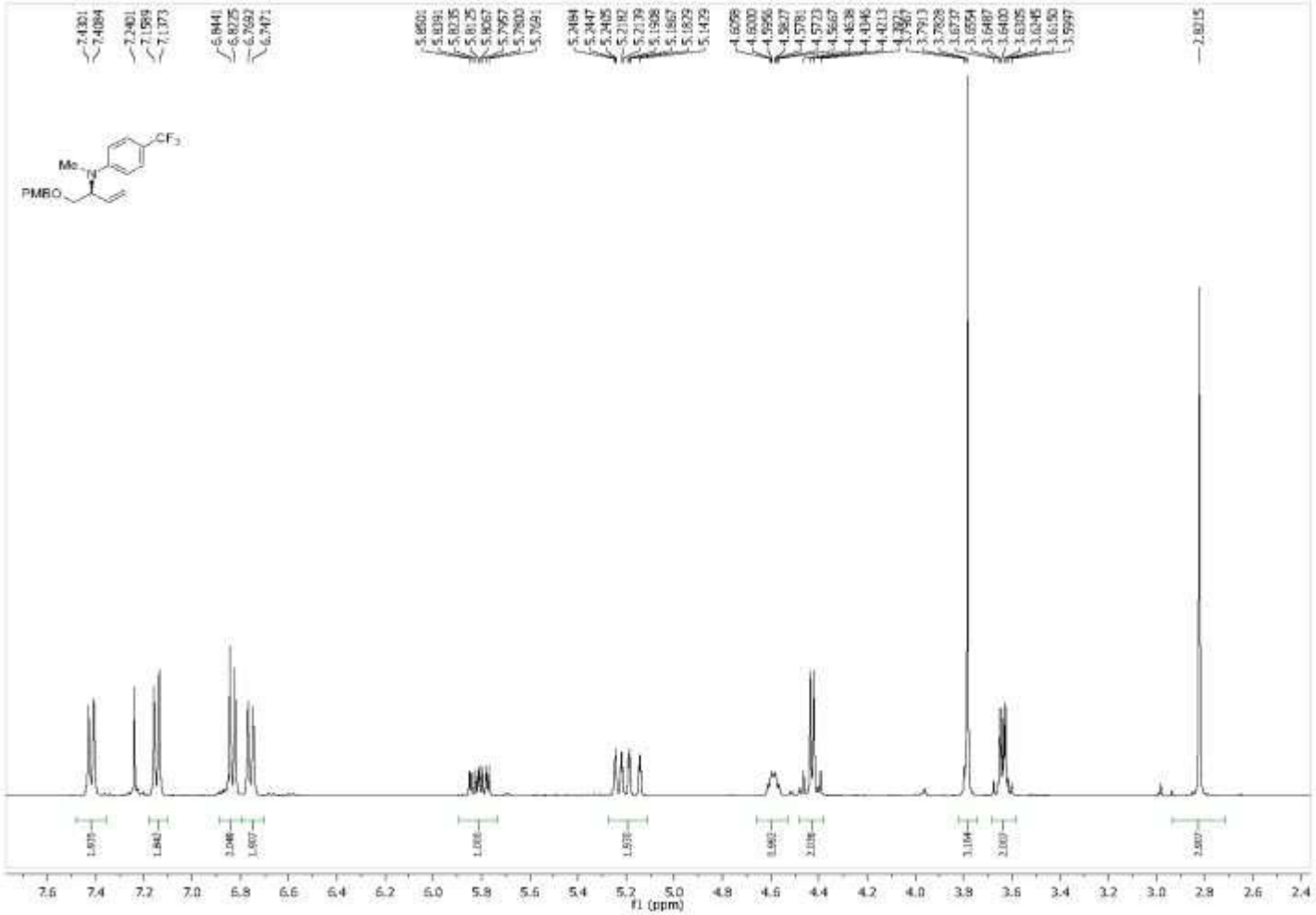

Figure A293 400 MHz 1H NMR ($CDCl_3$) Spectra of Compound **308r**

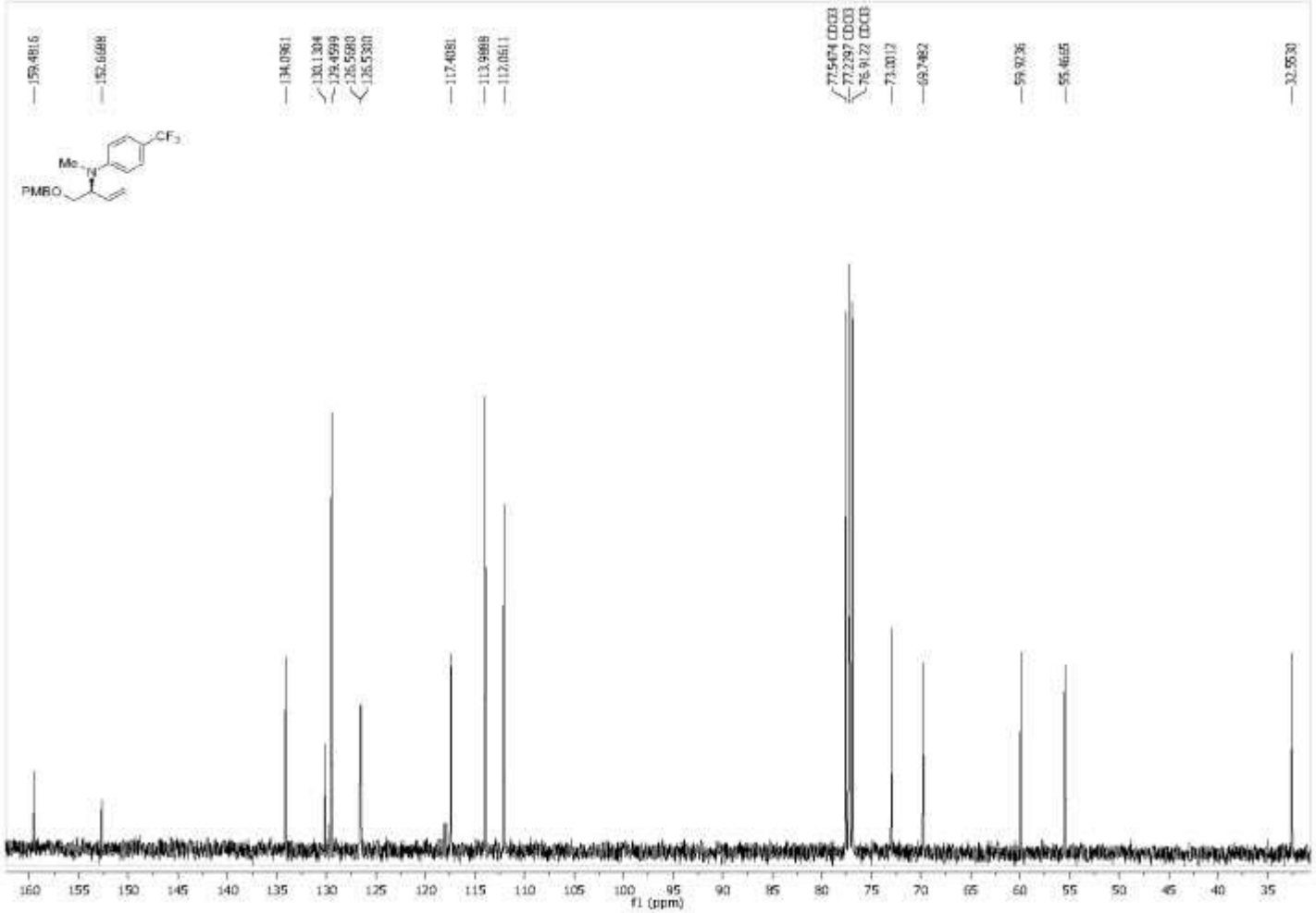

Figure A294 100 MHz 13C NMR ($CDCl_3$) Spectra of Compound **308r**

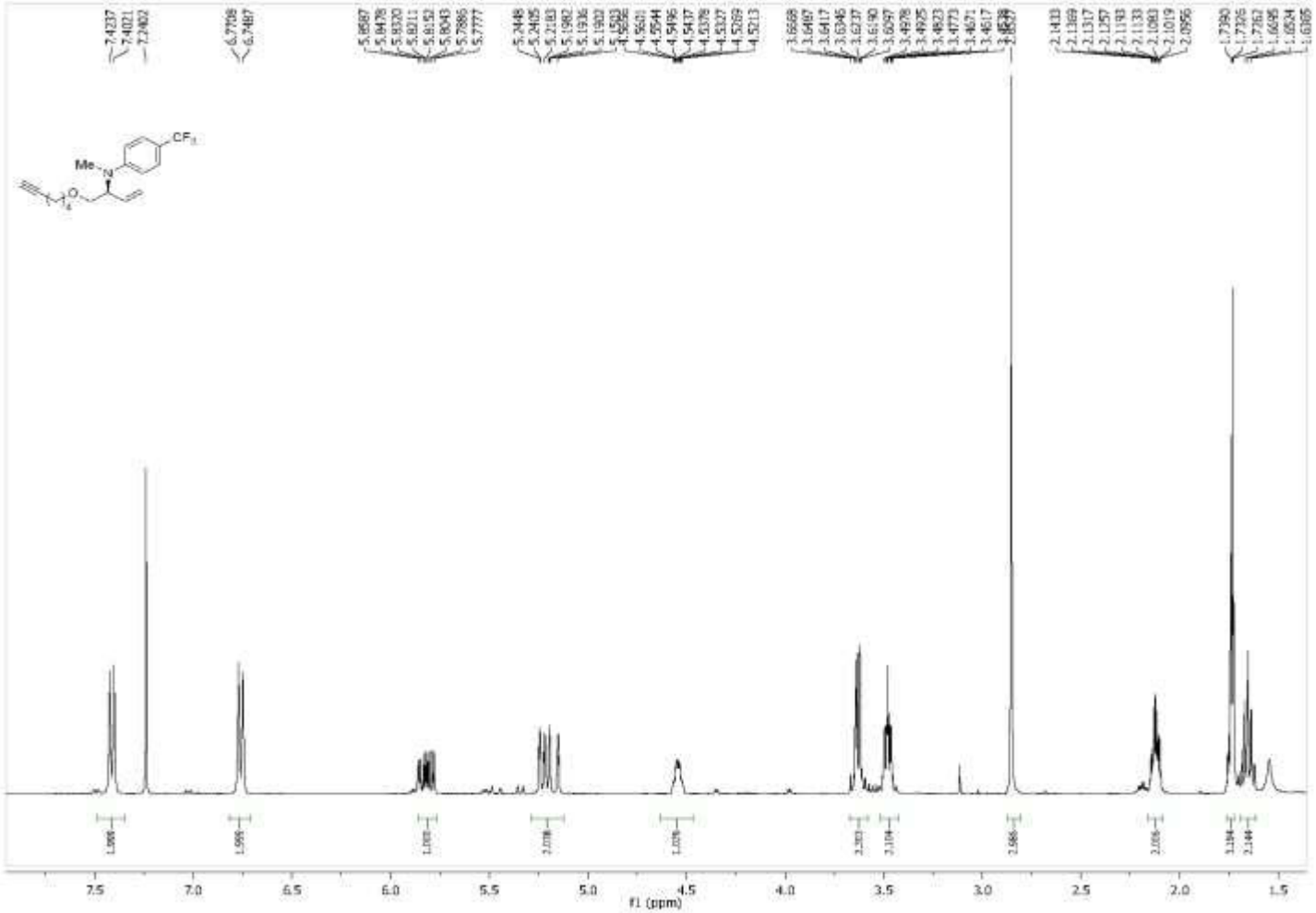

Figure A295 400 MHz 1H NMR ($CDCl_3$) Spectra of Compound **309r**

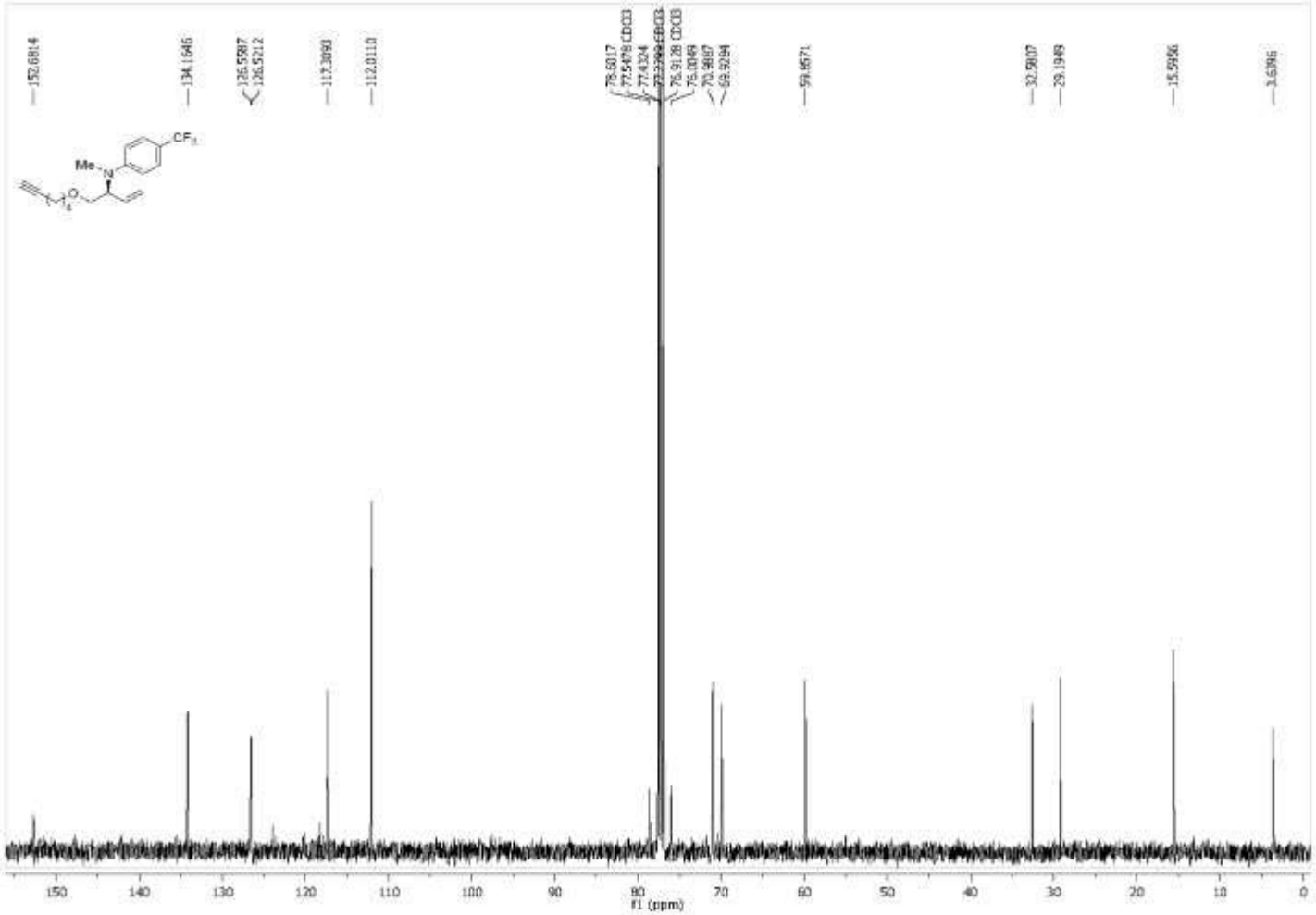

Figure A296 100 MHz 13C NMR ($CDCl_3$) Spectra of Compound **309r**

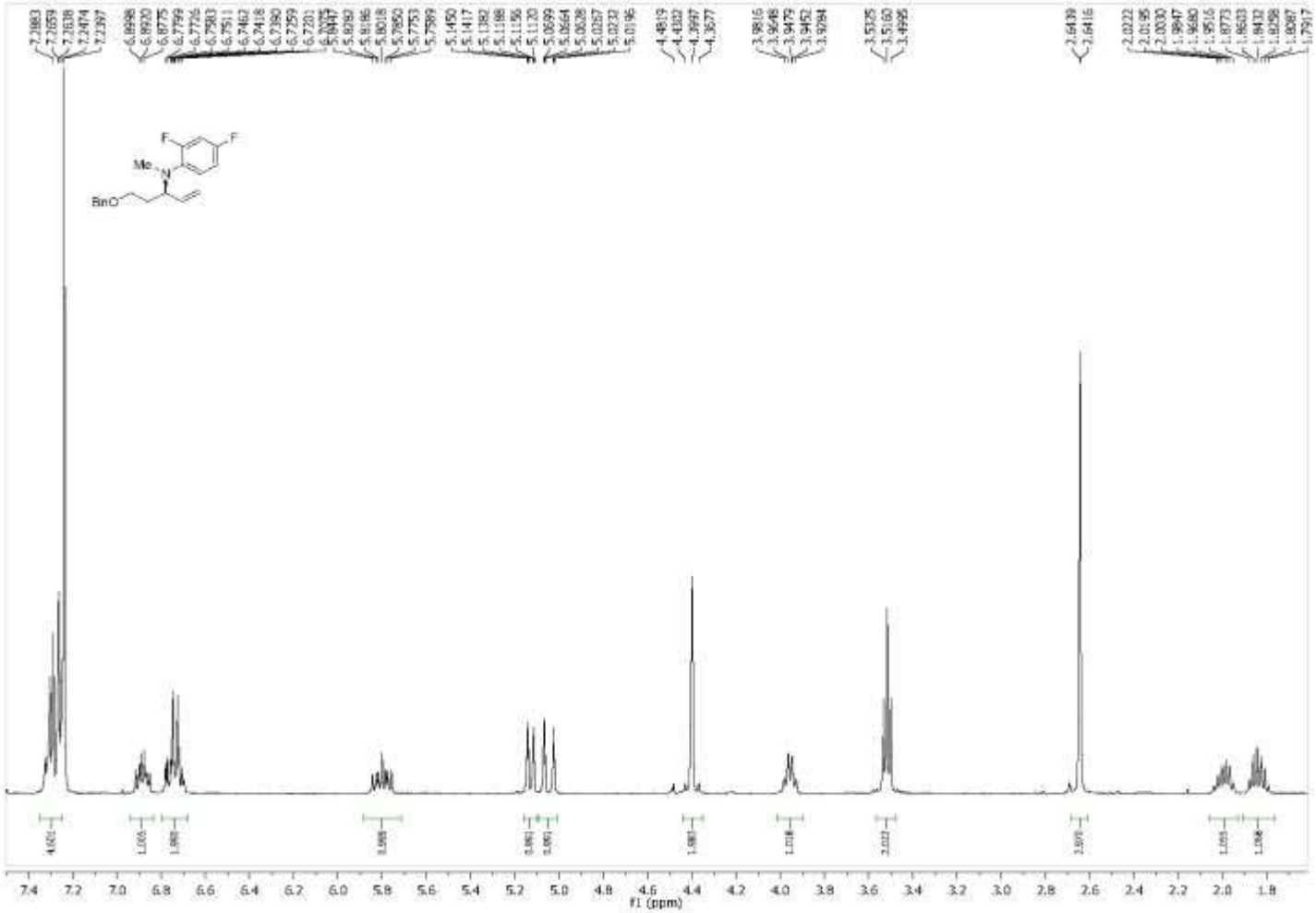

Figure A297 400 MHz 1H NMR ($CDCl_3$) Spectra of Compound **310t**

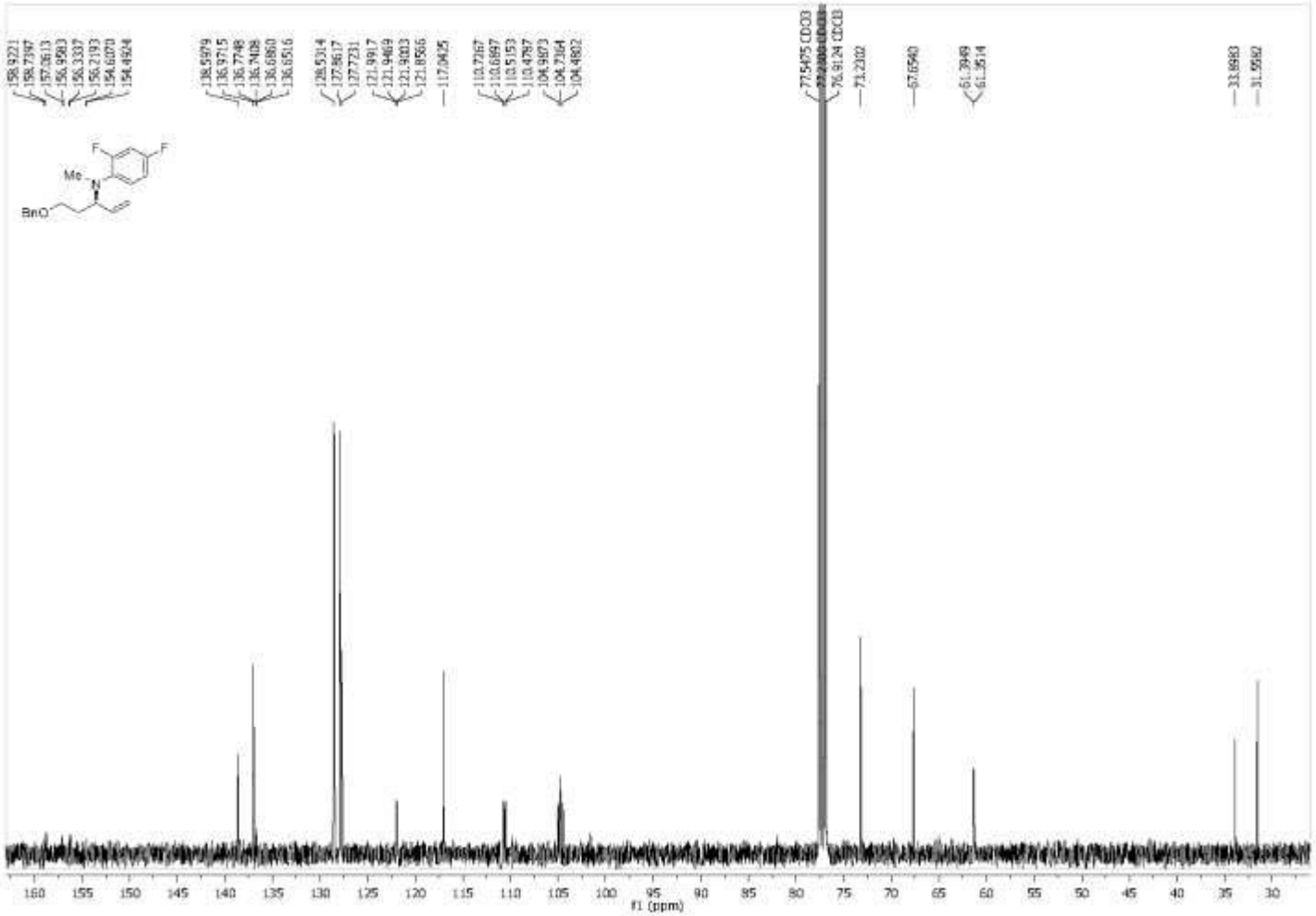

Figure A298 100 MHz 13C NMR ($CDCl_3$) Spectra of Compound **310t**

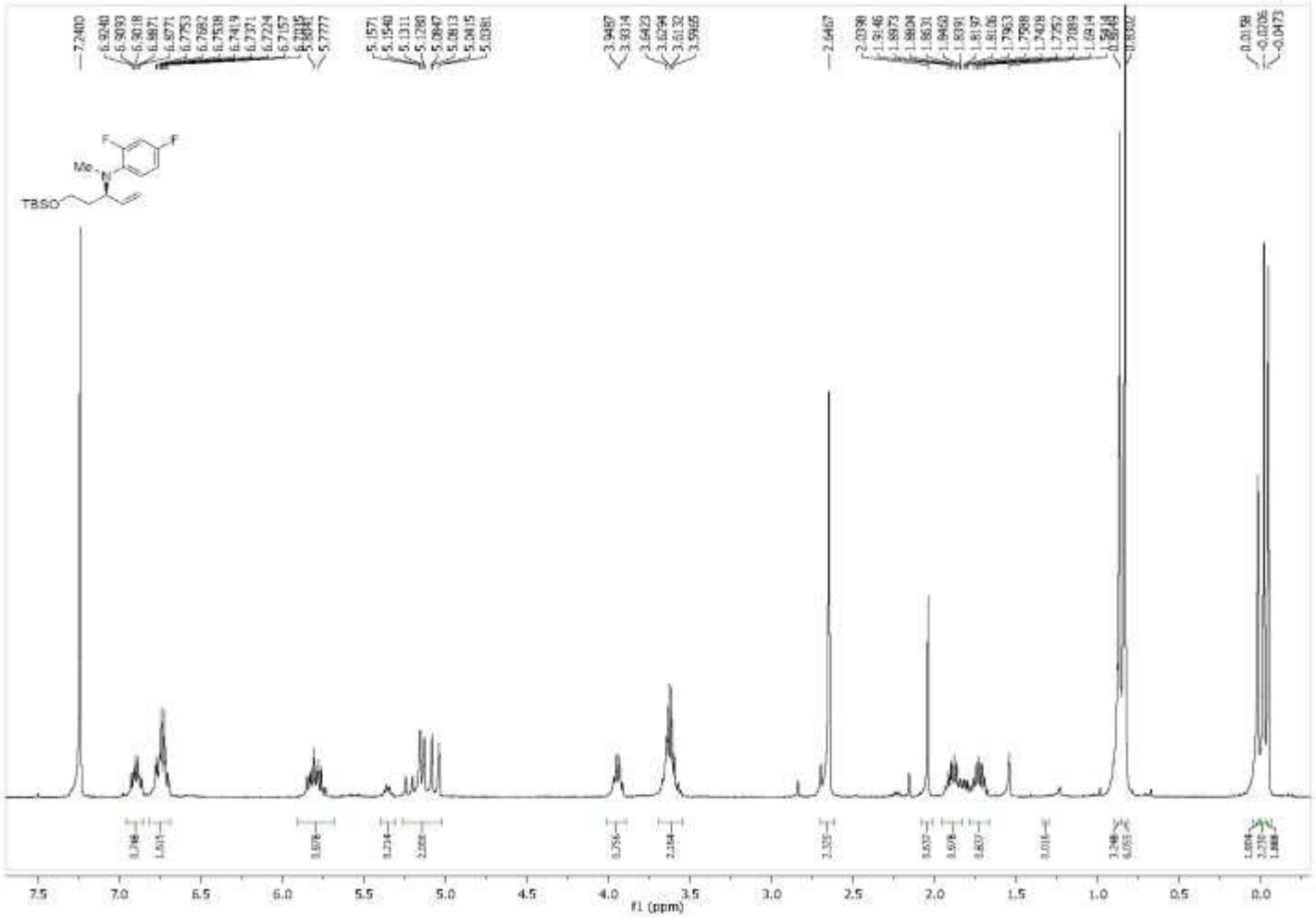

Figure A299 400 MHz 1H NMR ($CDCl_3$) Spectra of Compound **223t**

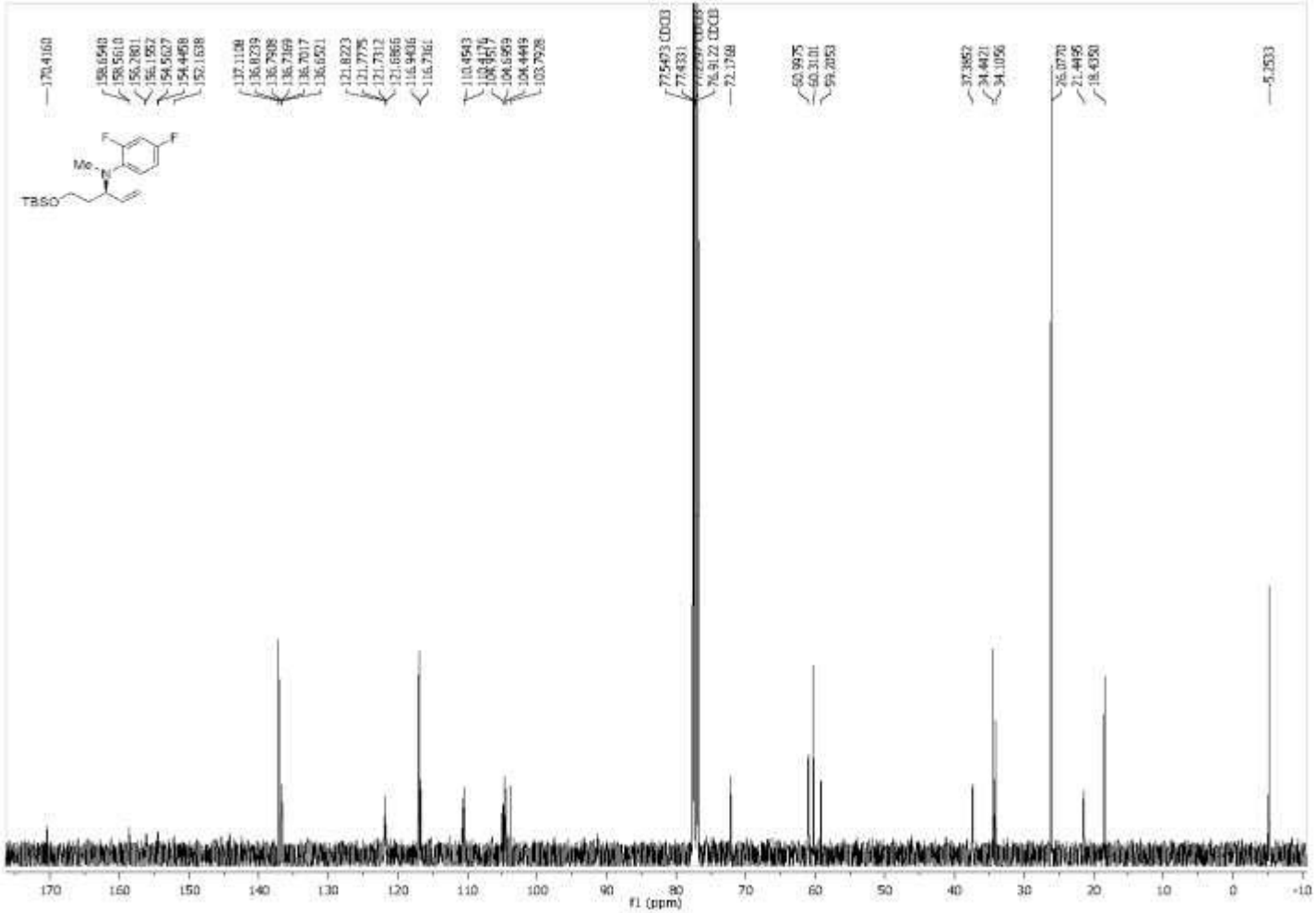

Figure A300 100 MHz 13C NMR ($CDCl_3$) Spectra of Compound **223t**

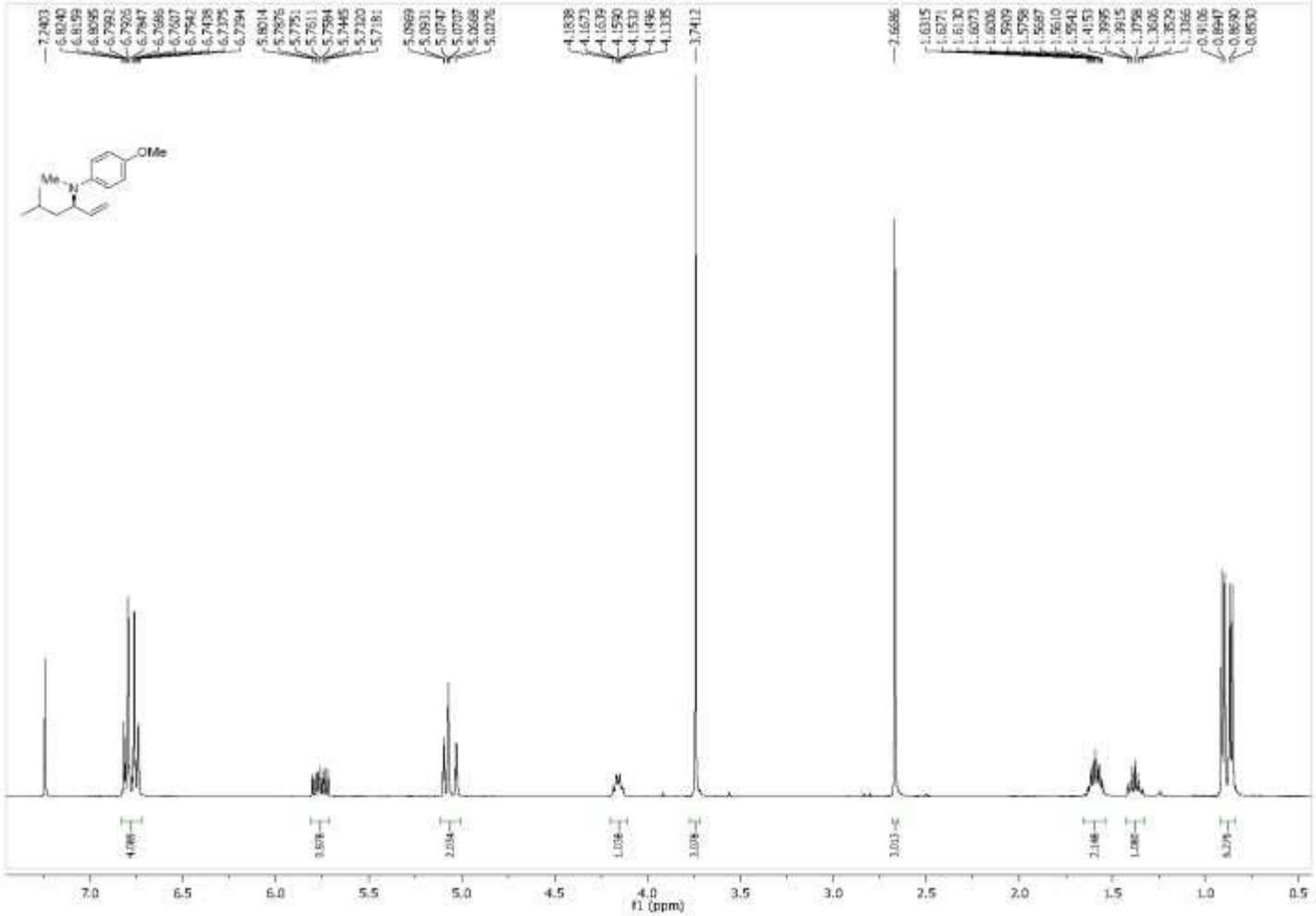

Figure A301 400 MHz 1H NMR ($CDCl_3$) Spectra of Compound **311q**

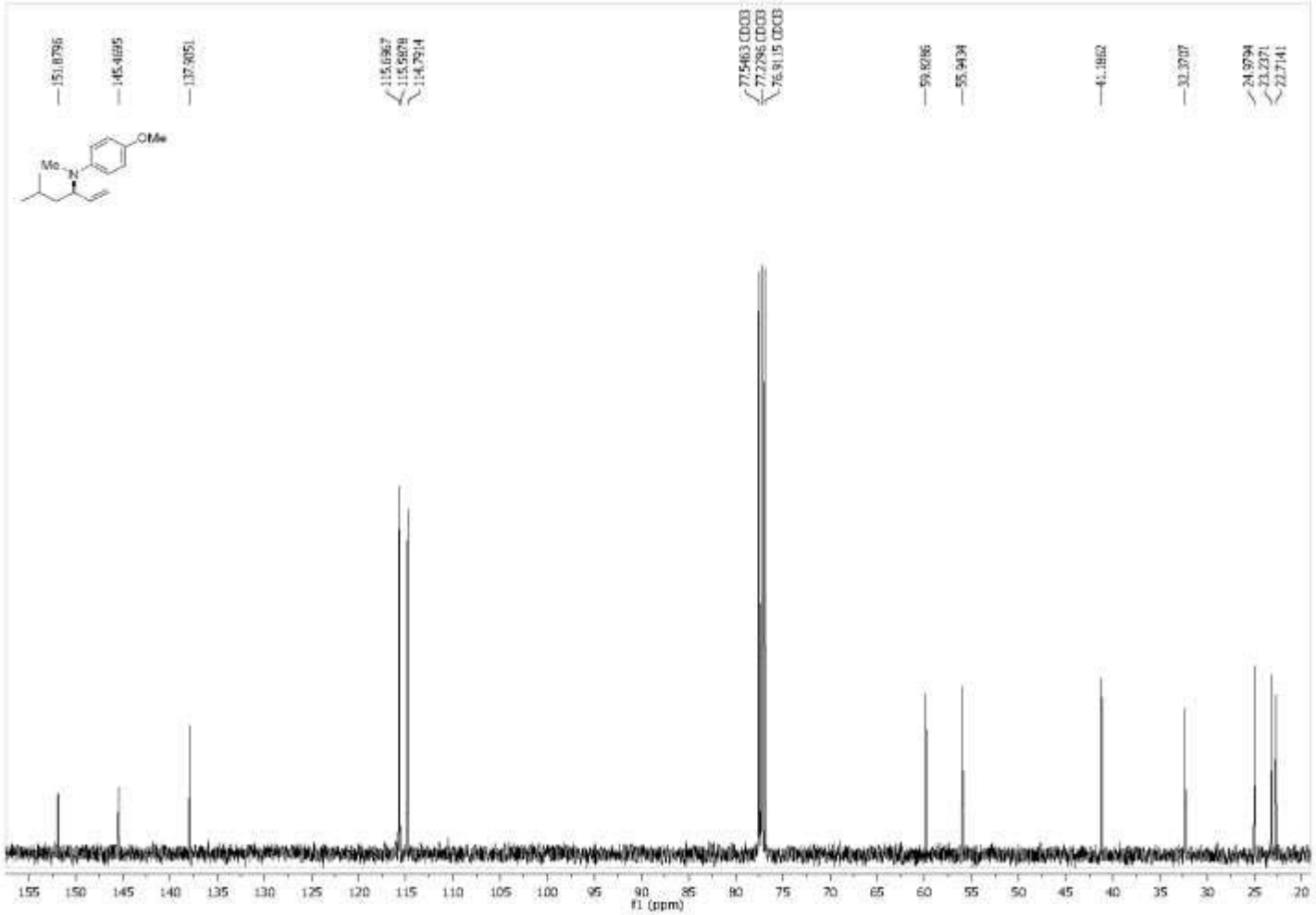

Figure A302 100 MHz 13C NMR ($CDCl_3$) Spectra of Compound **311q**

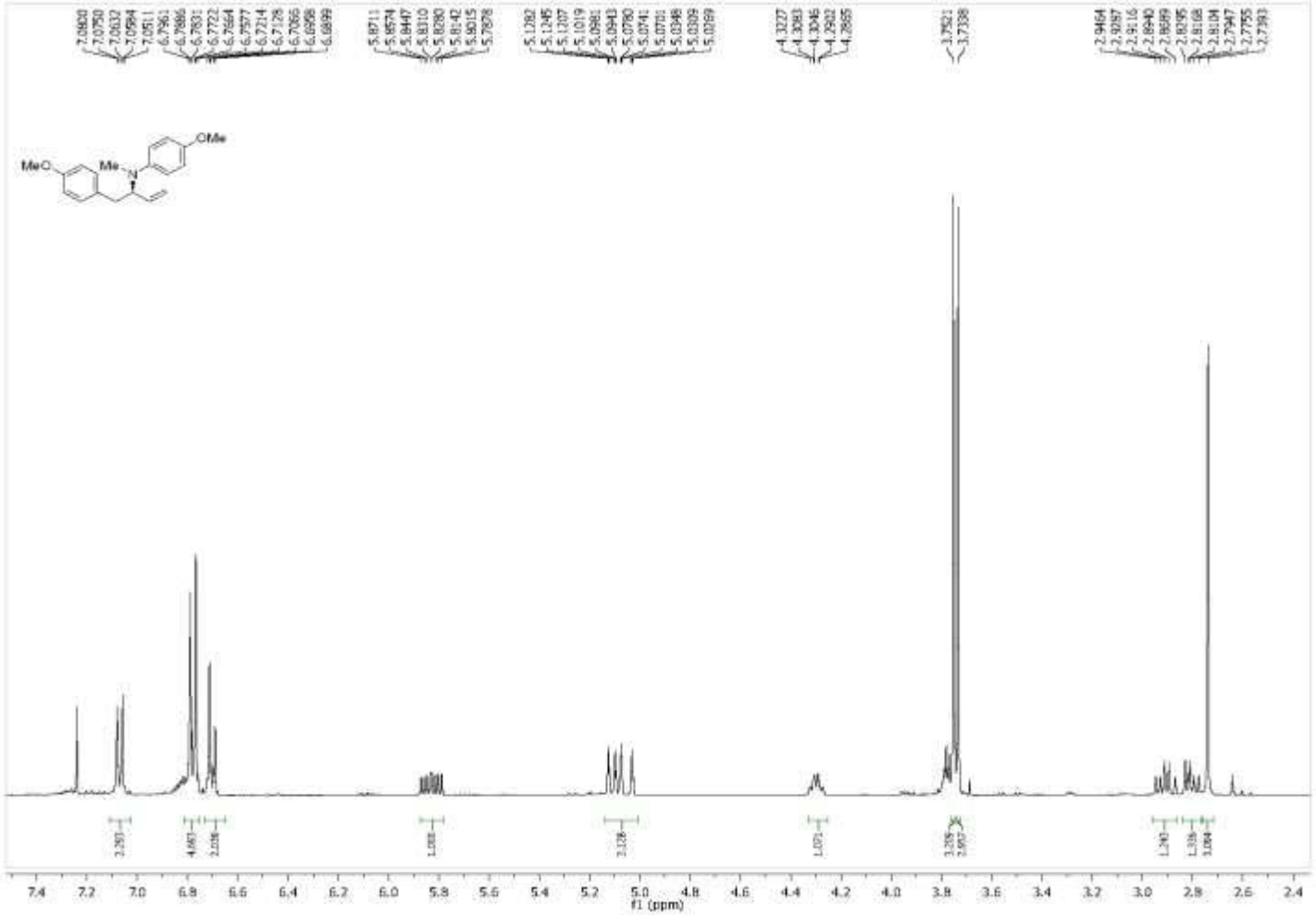

Figure A303 400 MHz 1H NMR ($CDCl_3$) Spectra of Compound **312q**

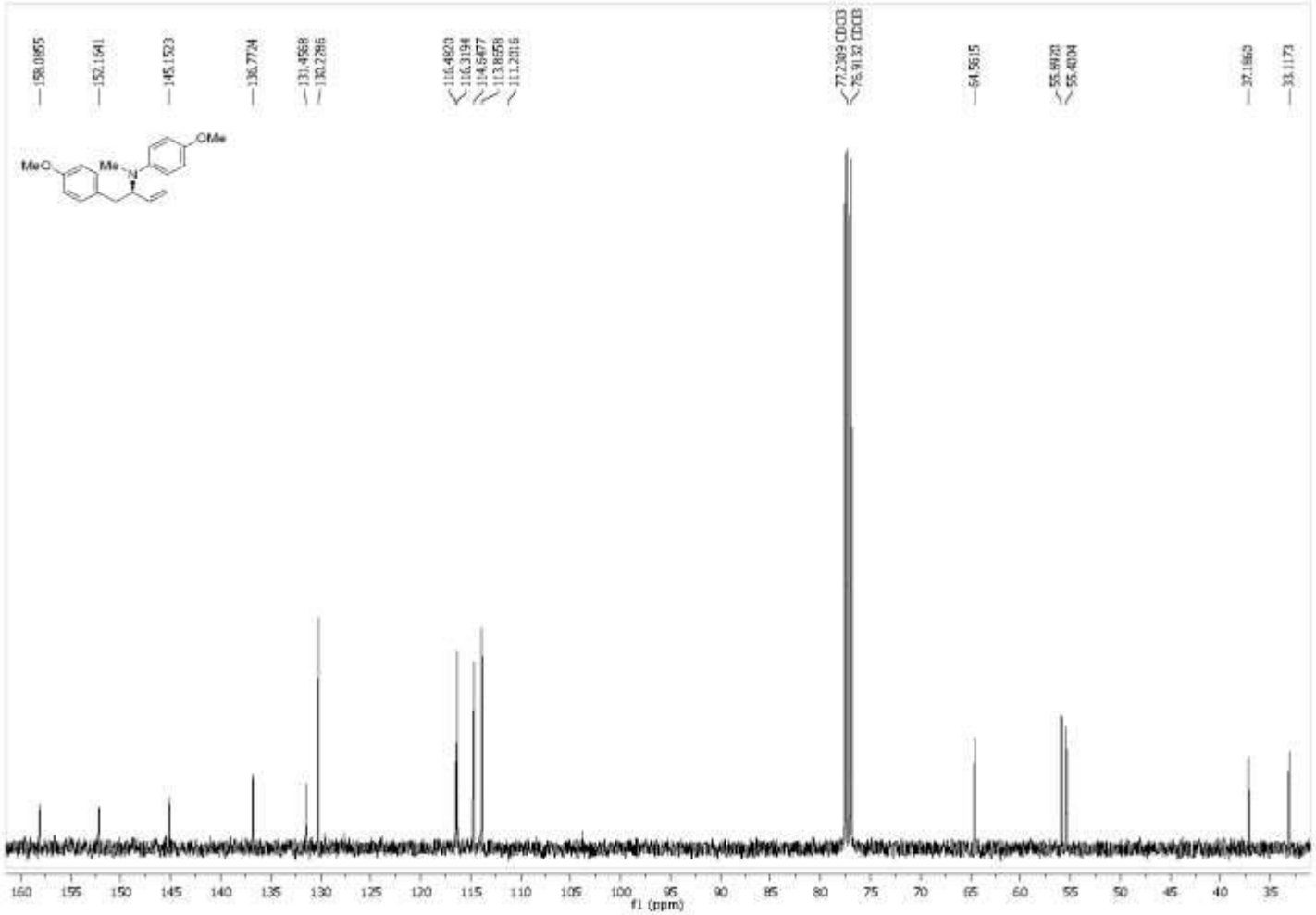

Figure A304 100 MHz 13C NMR ($CDCl_3$) Spectra of Compound **312q**

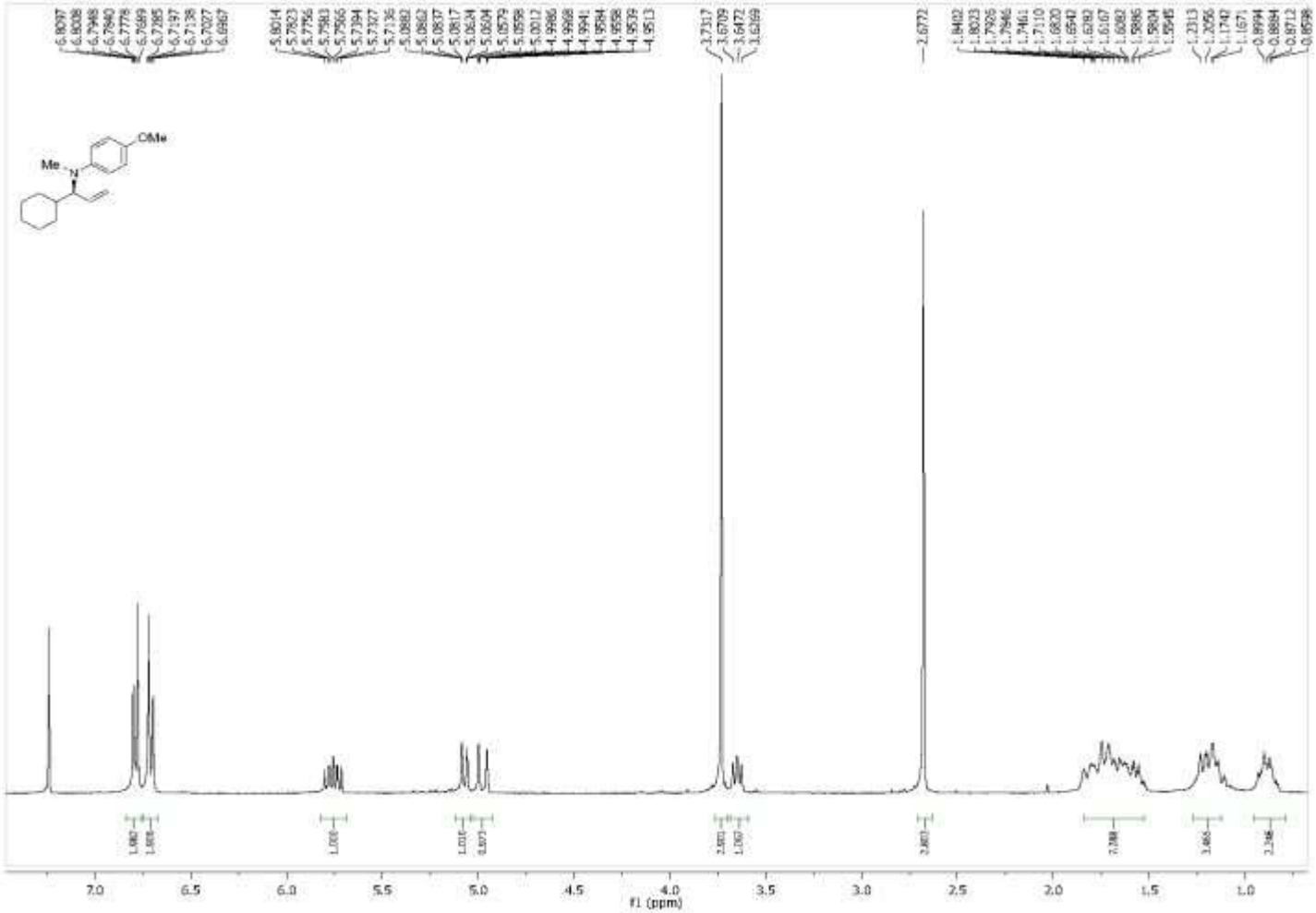

Figure A305 400 MHz 1H NMR ($CDCl_3$) Spectra of Compound **231q**

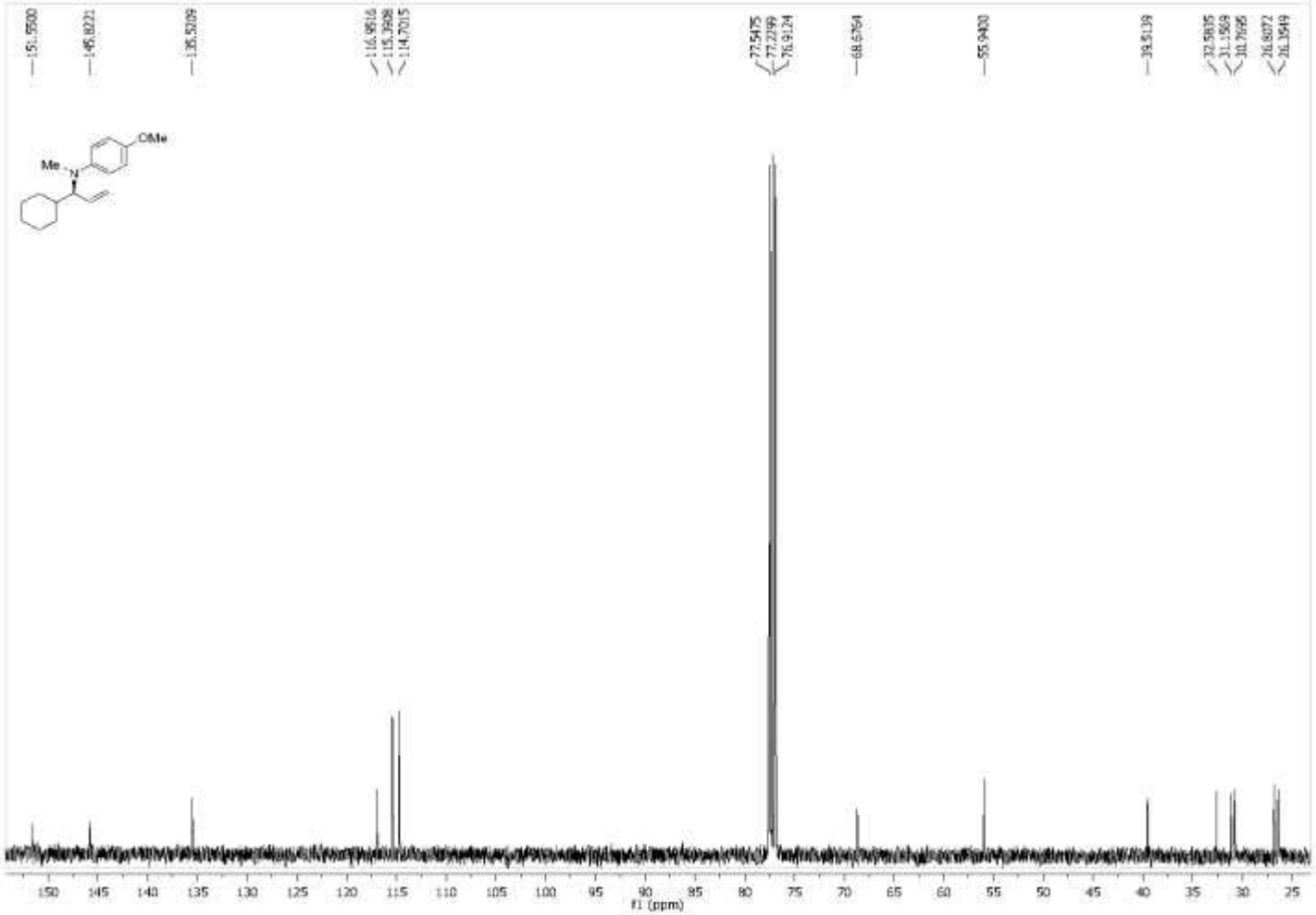

Figure A306 100 MHz 13C NMR ($CDCl_3$) Spectra of Compound **231q**

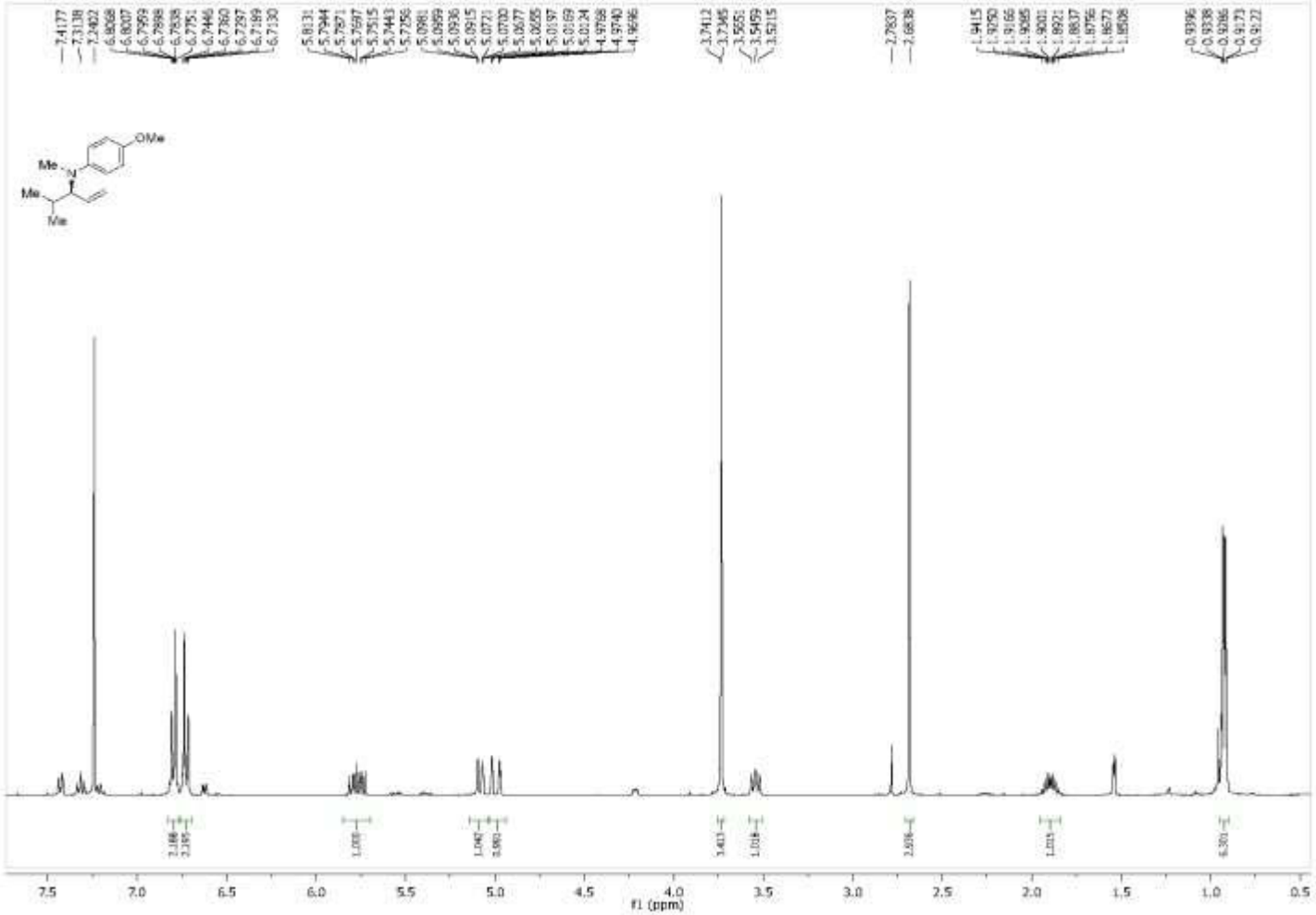

Figure A307 400 MHz 1H NMR ($CDCl_3$) Spectra of Compound **232q**

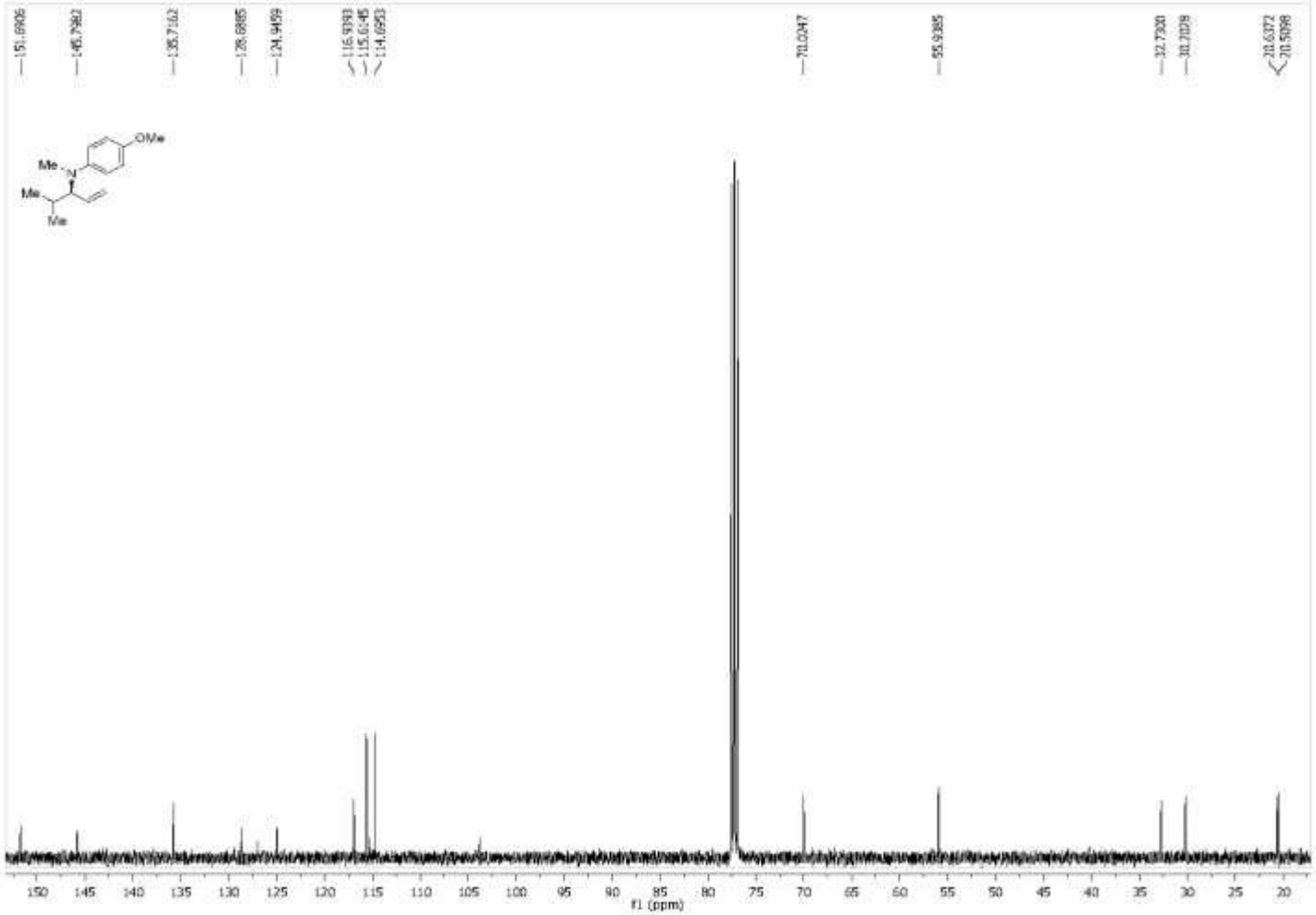

Figure A308 100 MHz 13C NMR ($CDCl_3$) Spectra of Compound **232q**

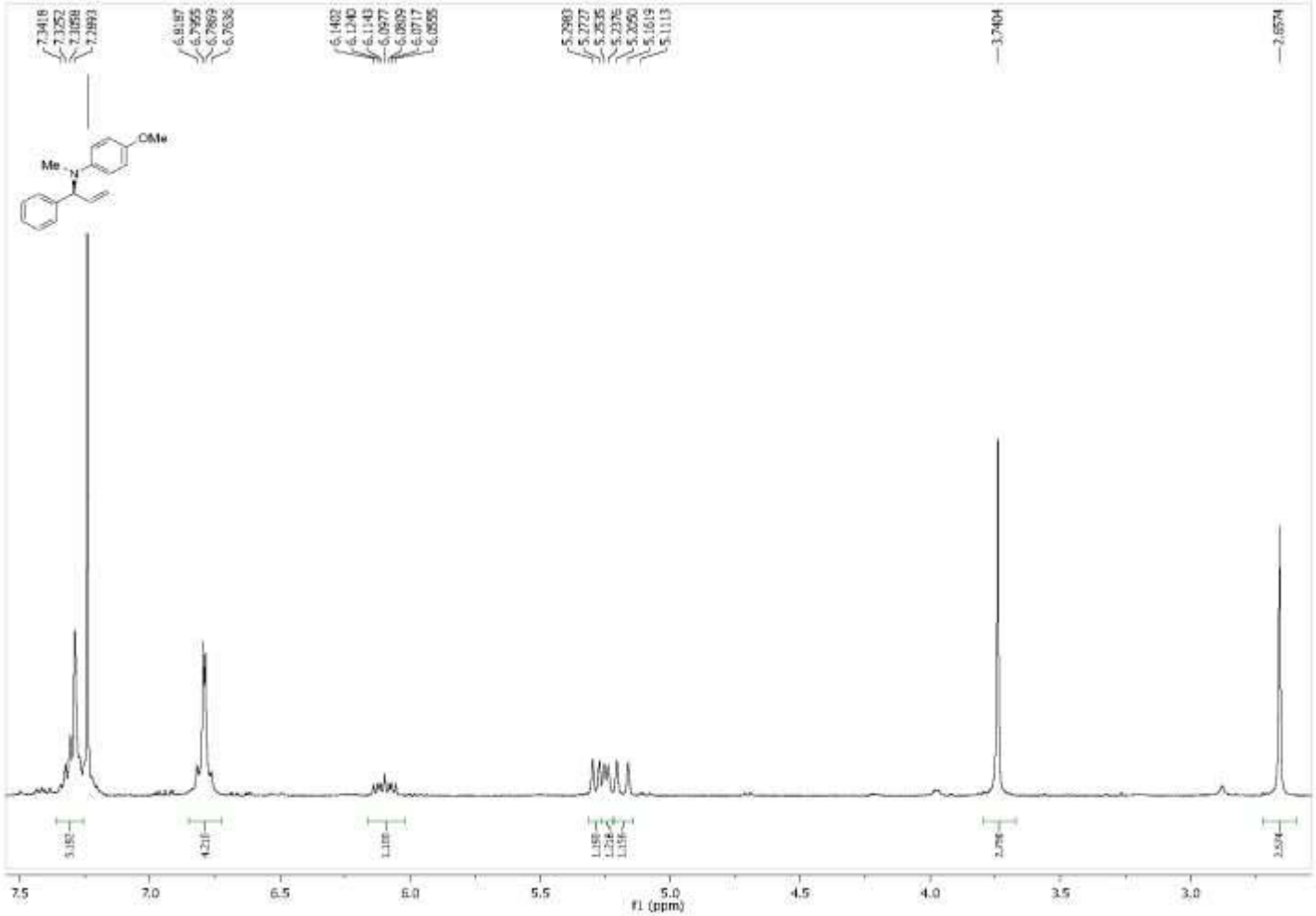

Figure A309 400 MHz 1H NMR ($CDCl_3$) Spectra of Compound **233q**

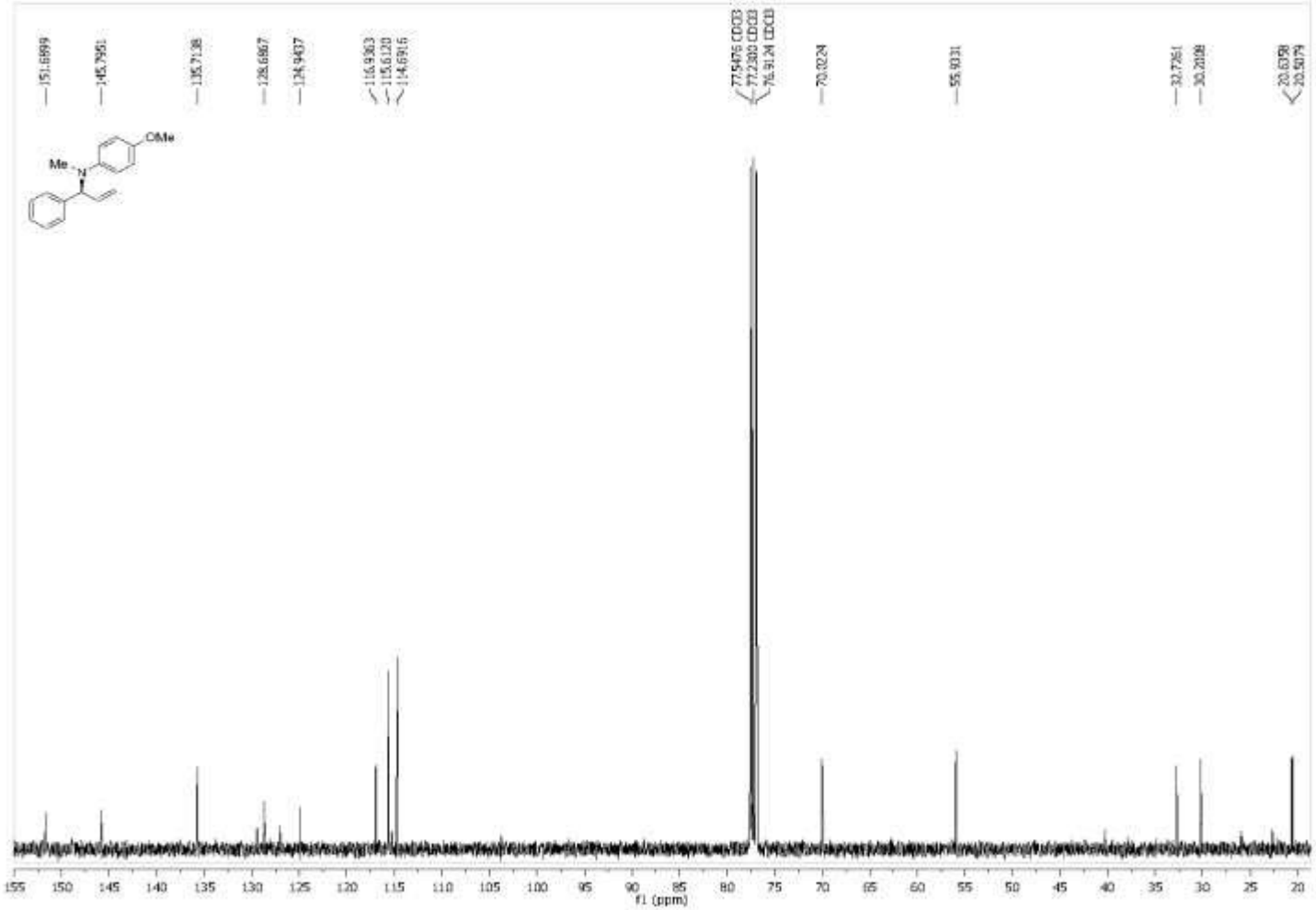

Figure A310 100 MHz 13C NMR ($CDCl_3$) Spectra of Compound **233q**

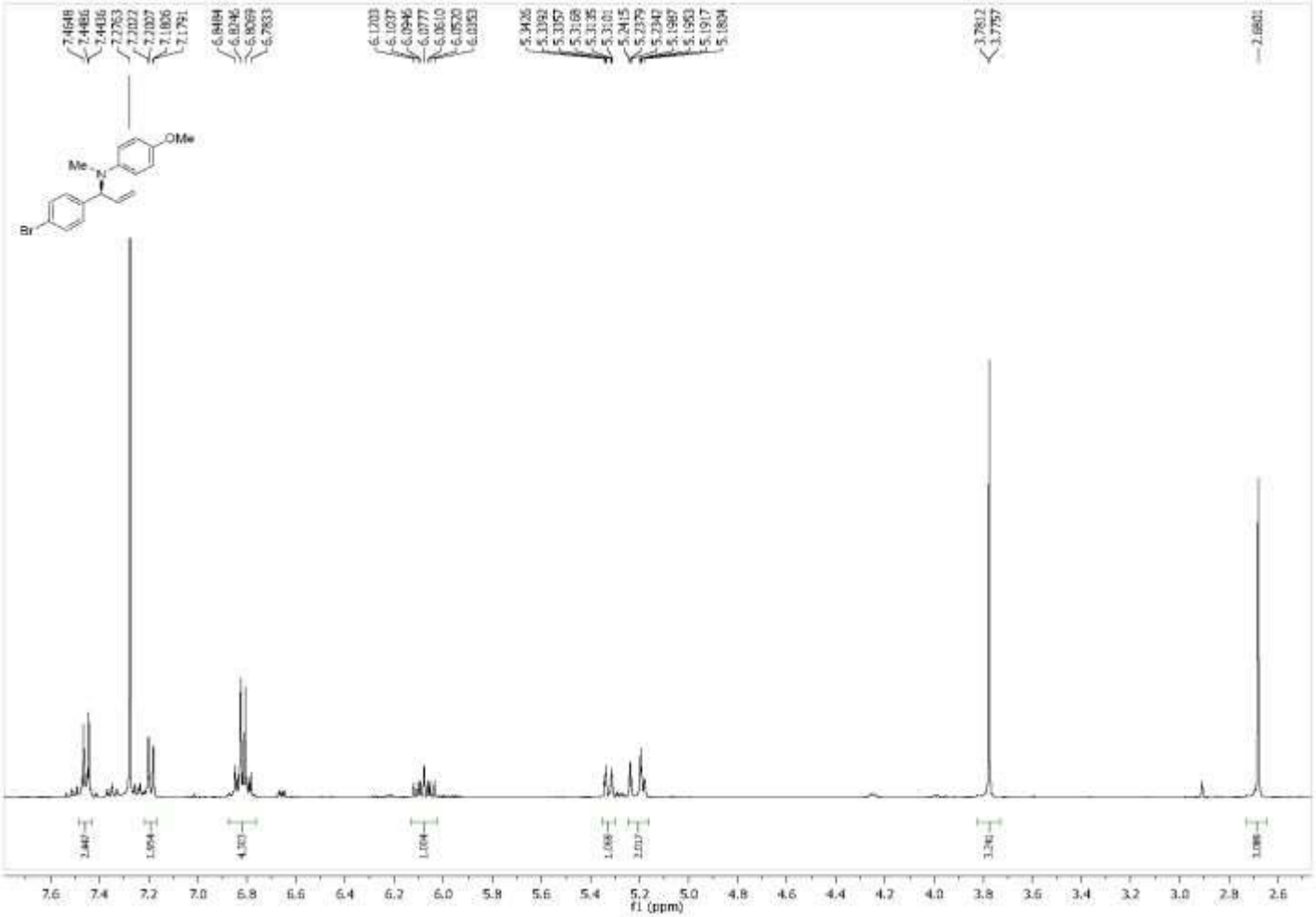

Figure A311 400 MHz 1H NMR ($CDCl_3$) Spectra of Compound **313q**

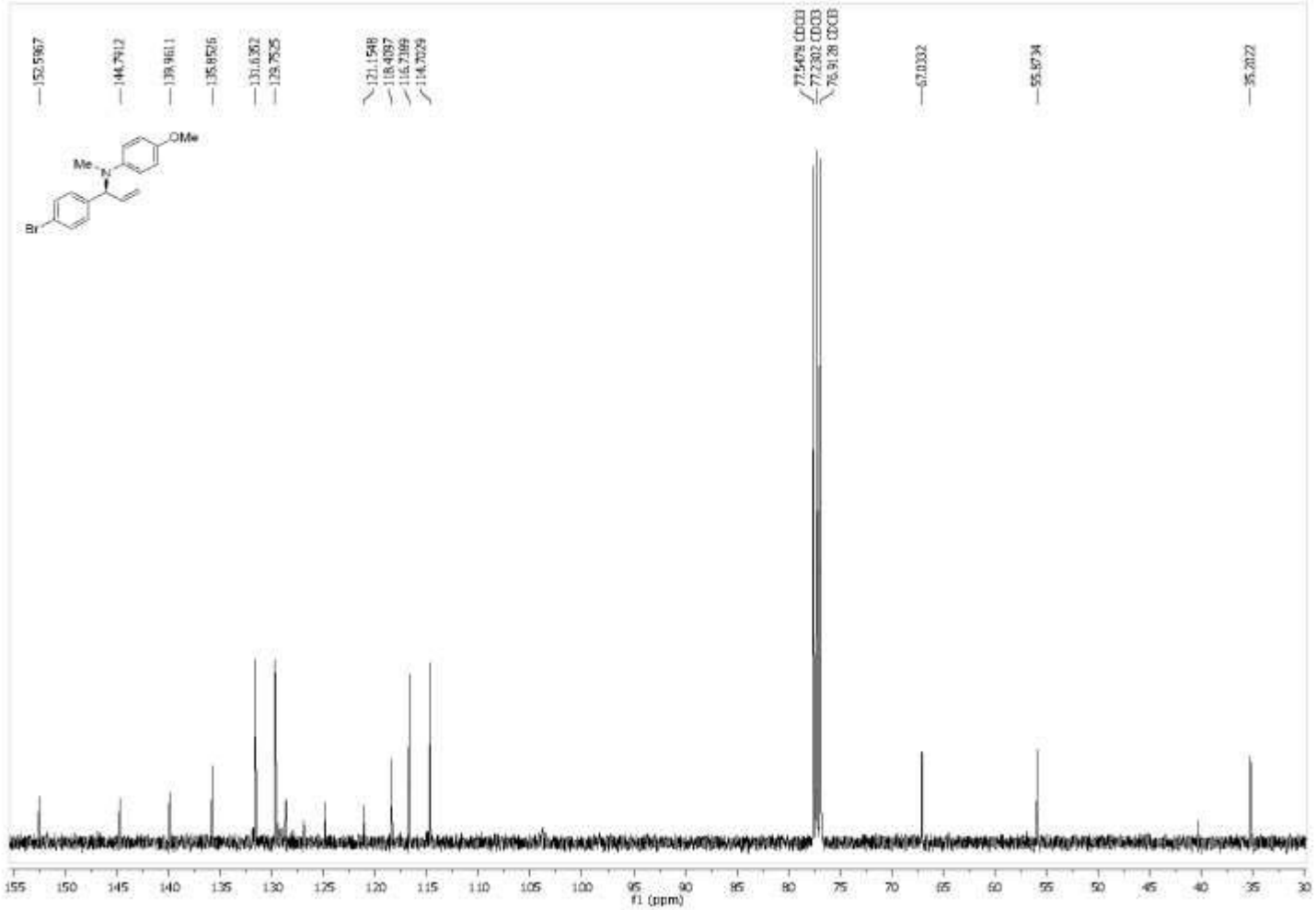

Figure A312 100 MHz 13C NMR ($CDCl_3$) Spectra of Compound **313q**

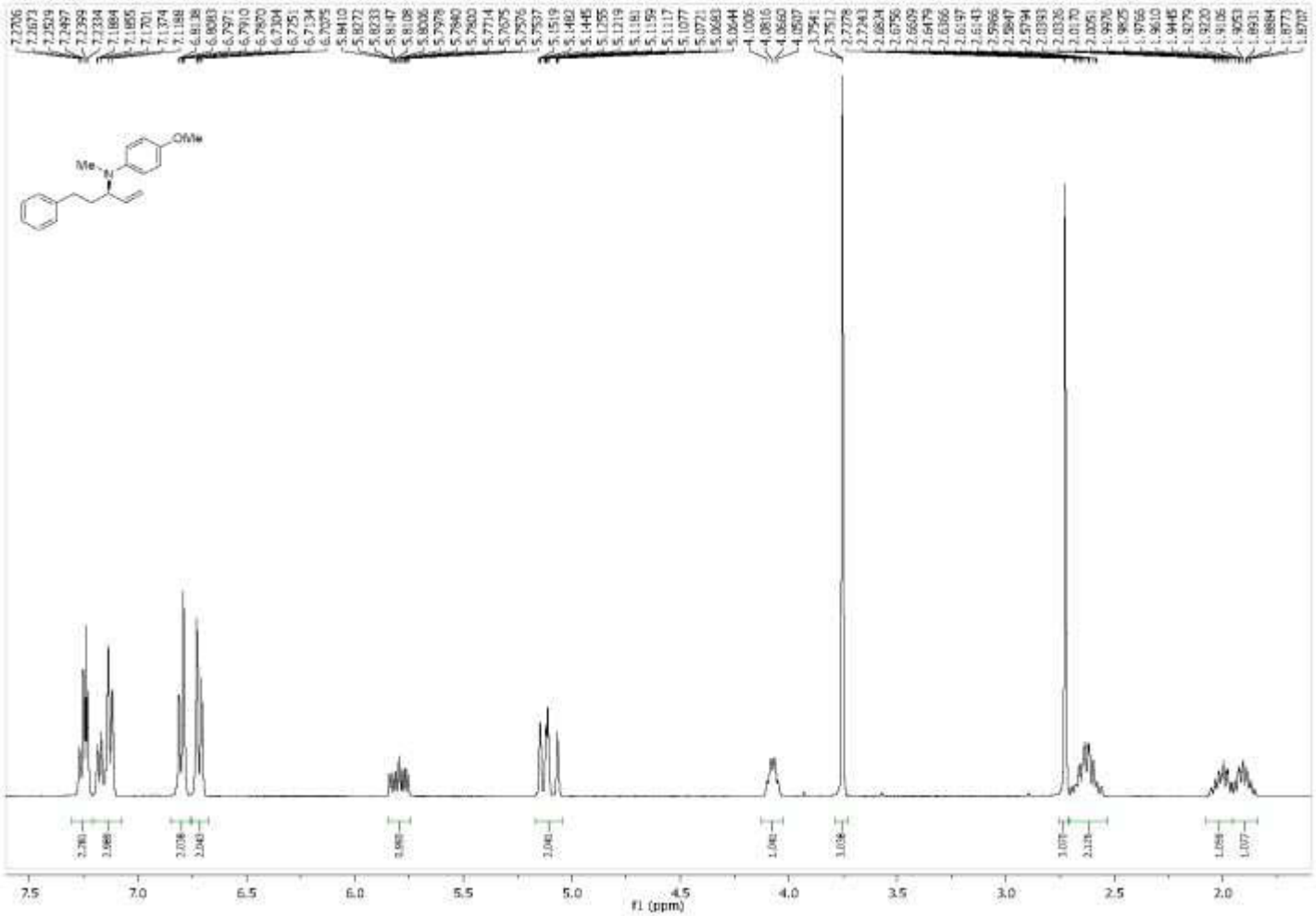

Figure A313 400 MHz 1H NMR ($CDCl_3$) Spectra of Compound **227q**

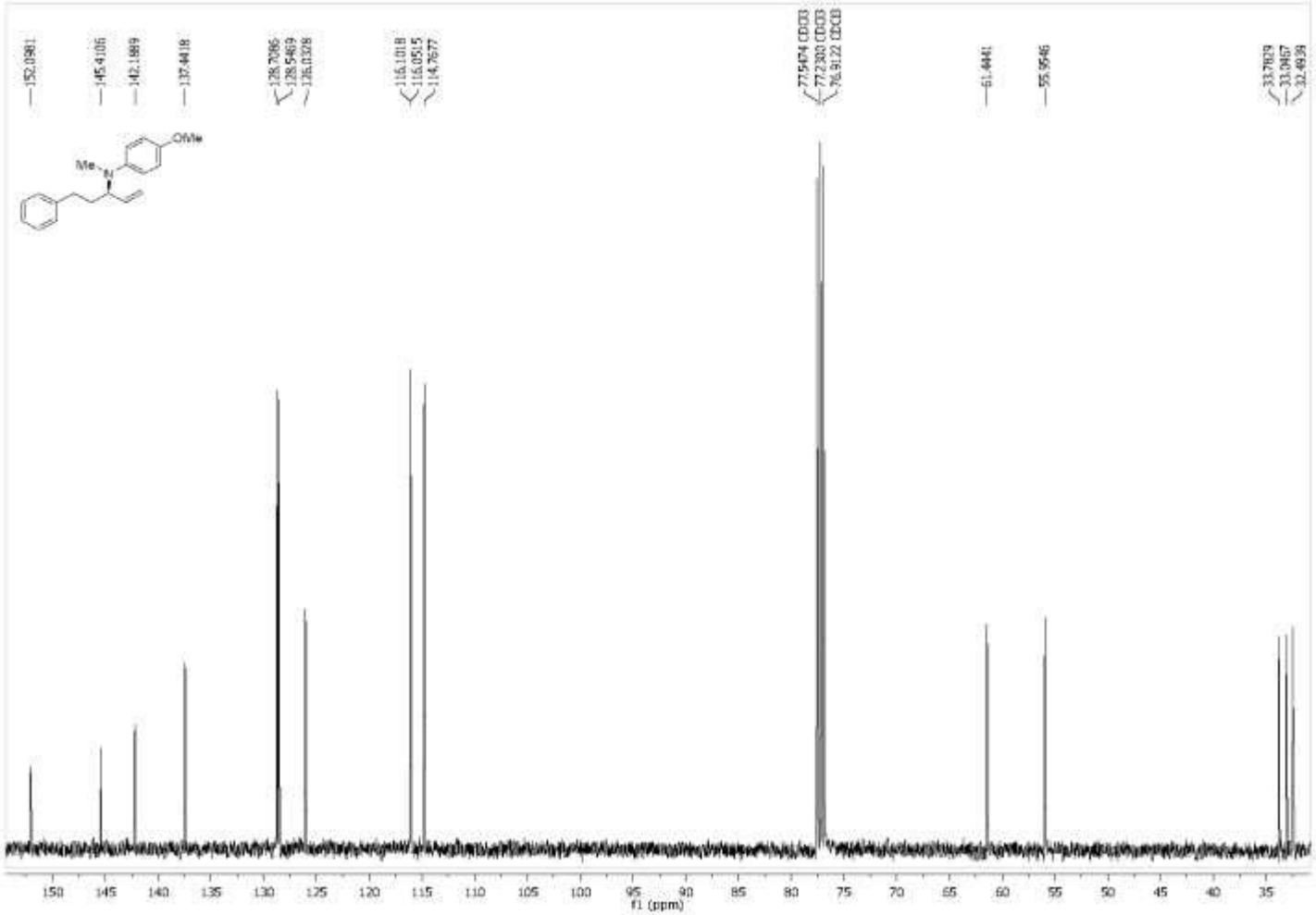

Figure A314 100 MHz 13C NMR ($CDCl_3$) Spectra of Compound **227q**

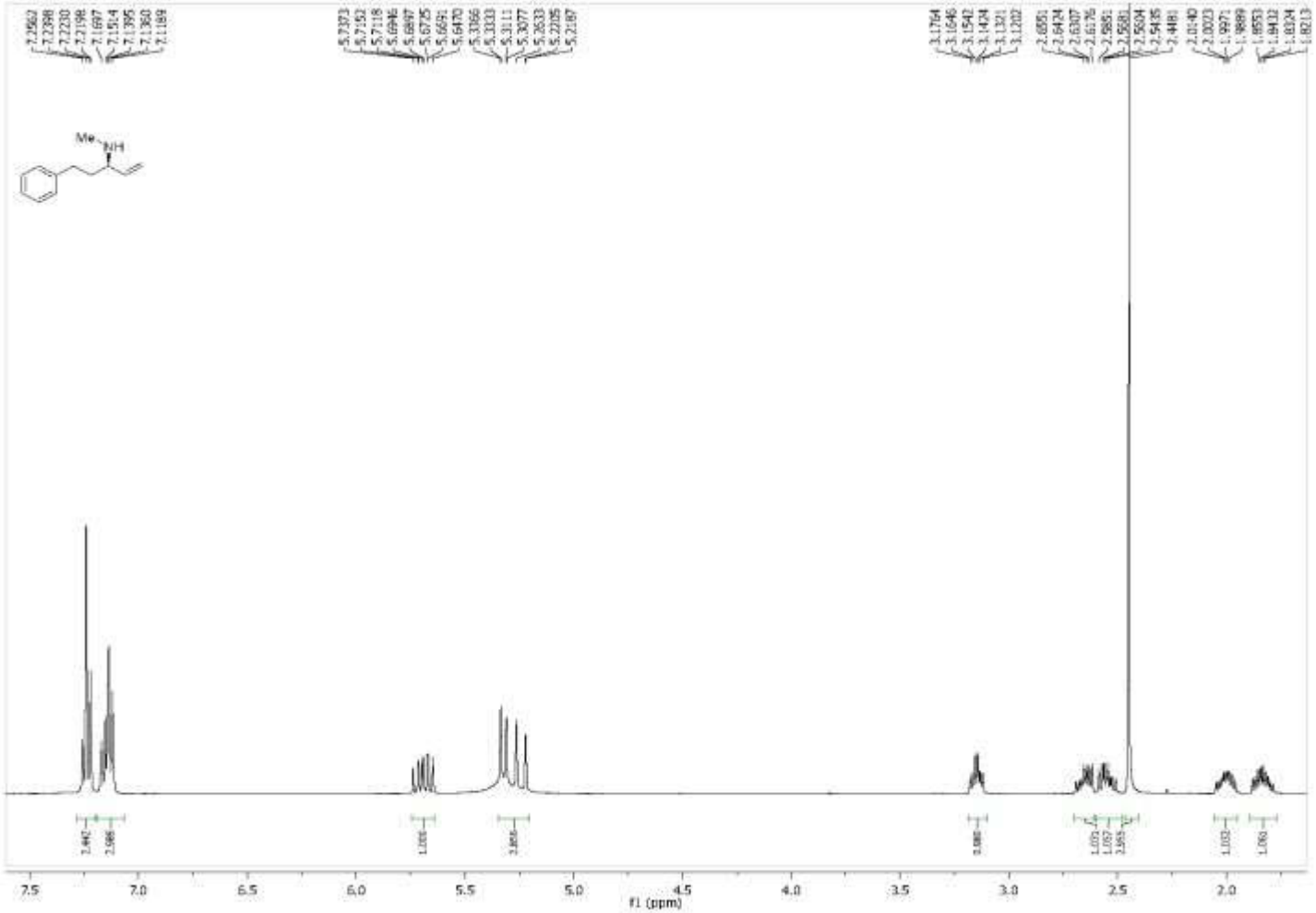

Figure A315 400 MHz 1H NMR ($CDCl_3$) Spectra of Compound **314**

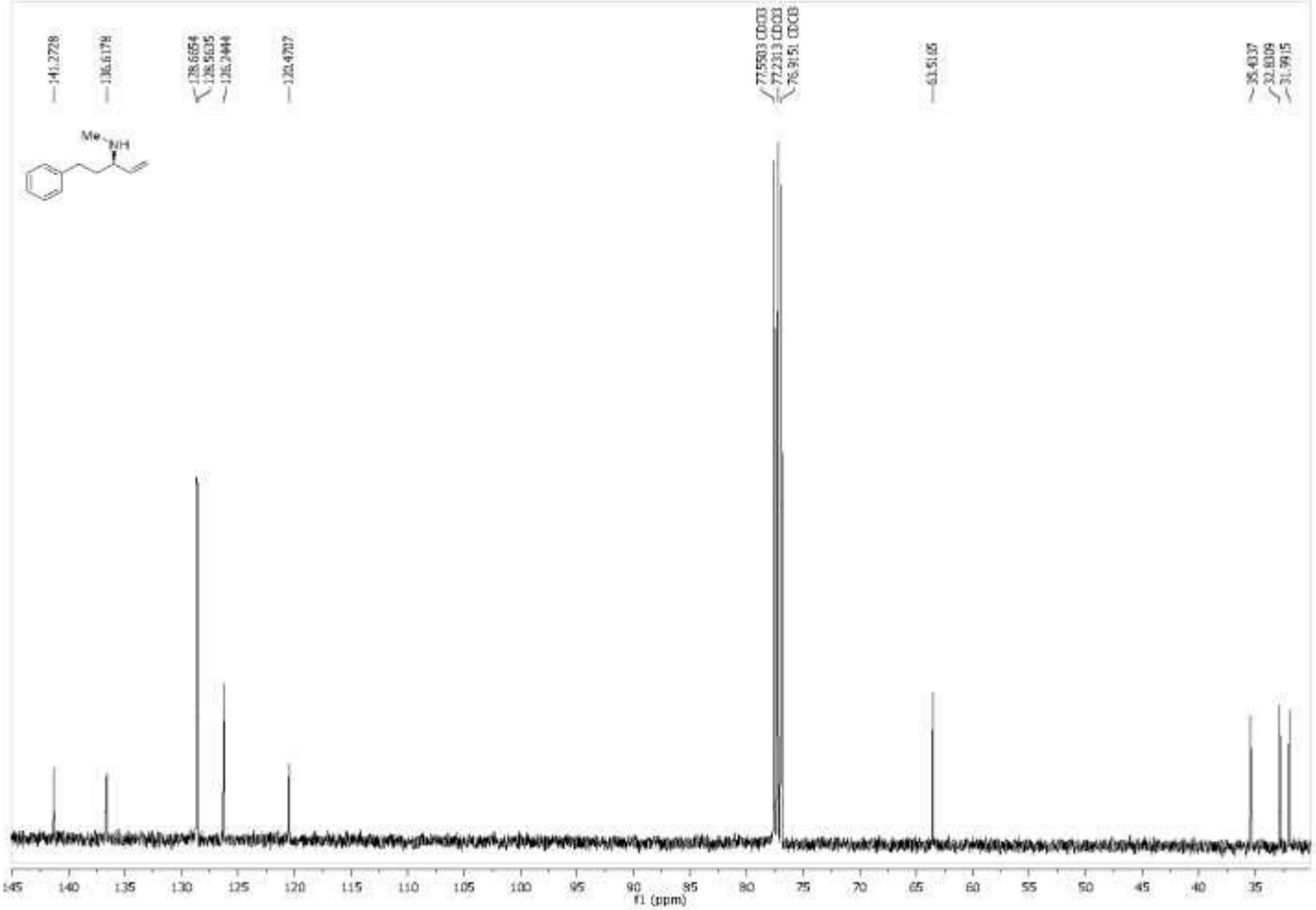

Figure A316 100 MHz 13C NMR ($CDCl_3$) Spectra of Compound **314**

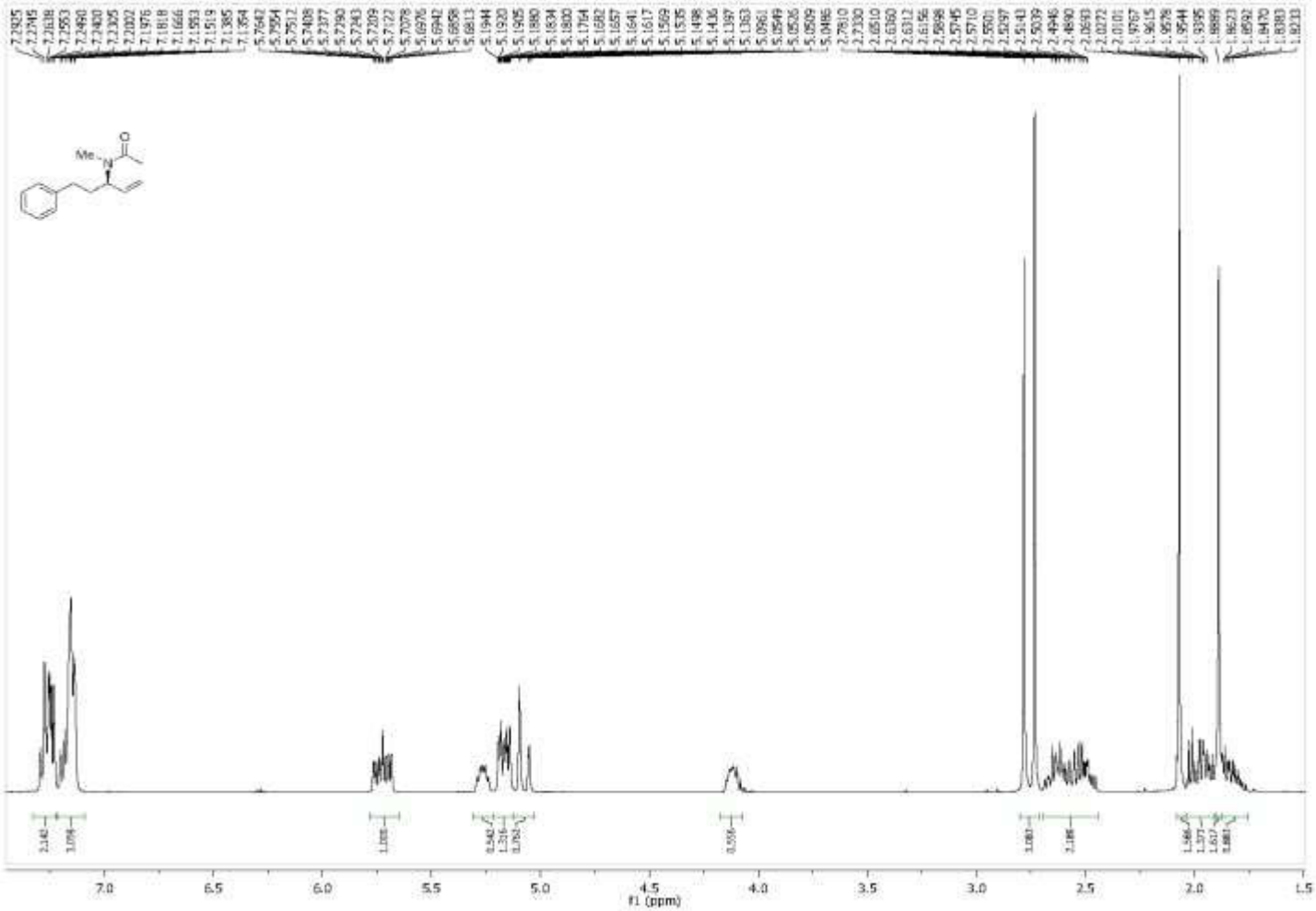

Figure A317 400 MHz 1H NMR ($CDCl_3$) Spectra of Compound **314-OAc**

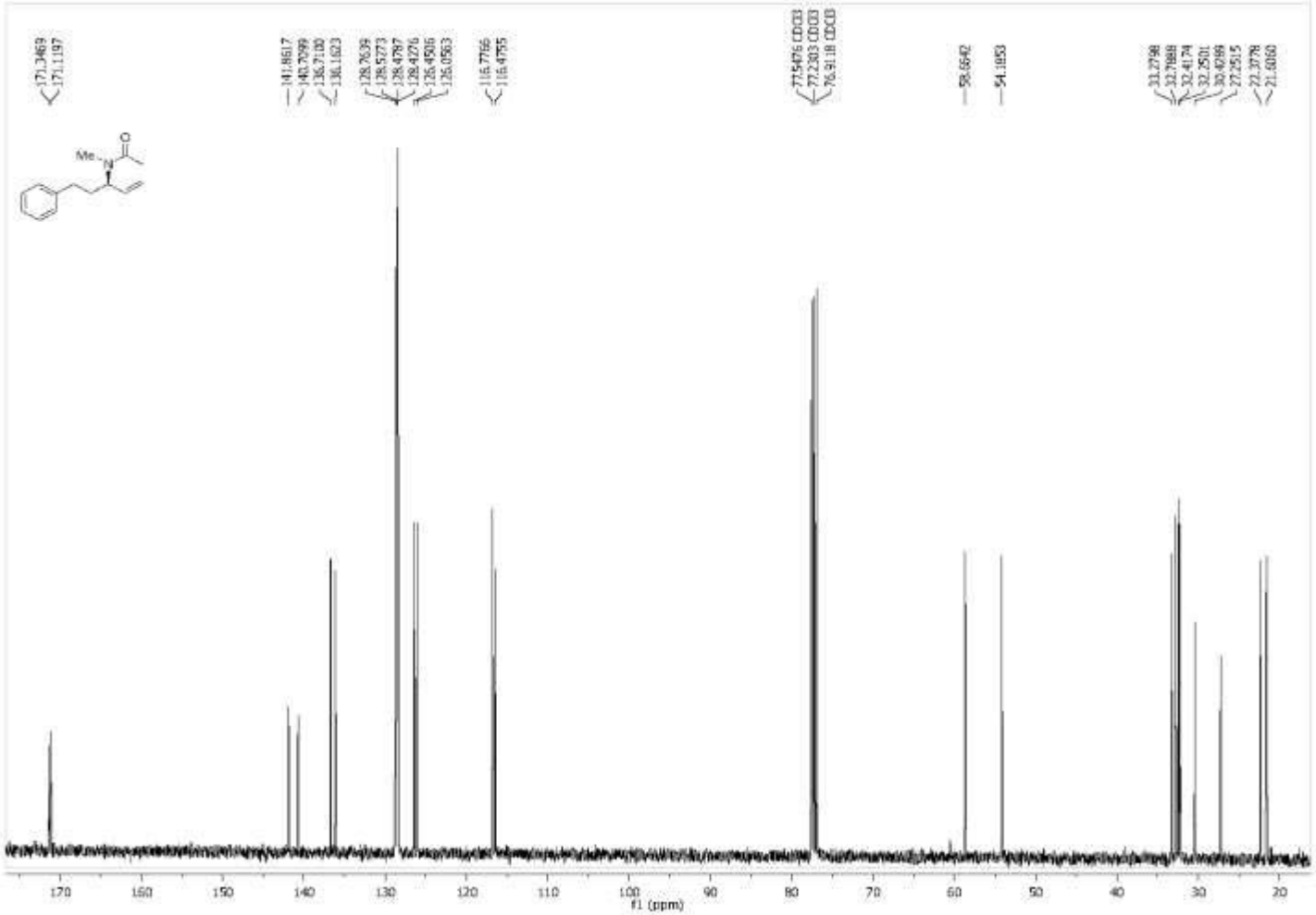

Figure A318 100 MHz 13C NMR ($CDCl_3$) Spectra of Compound **314-OAc**

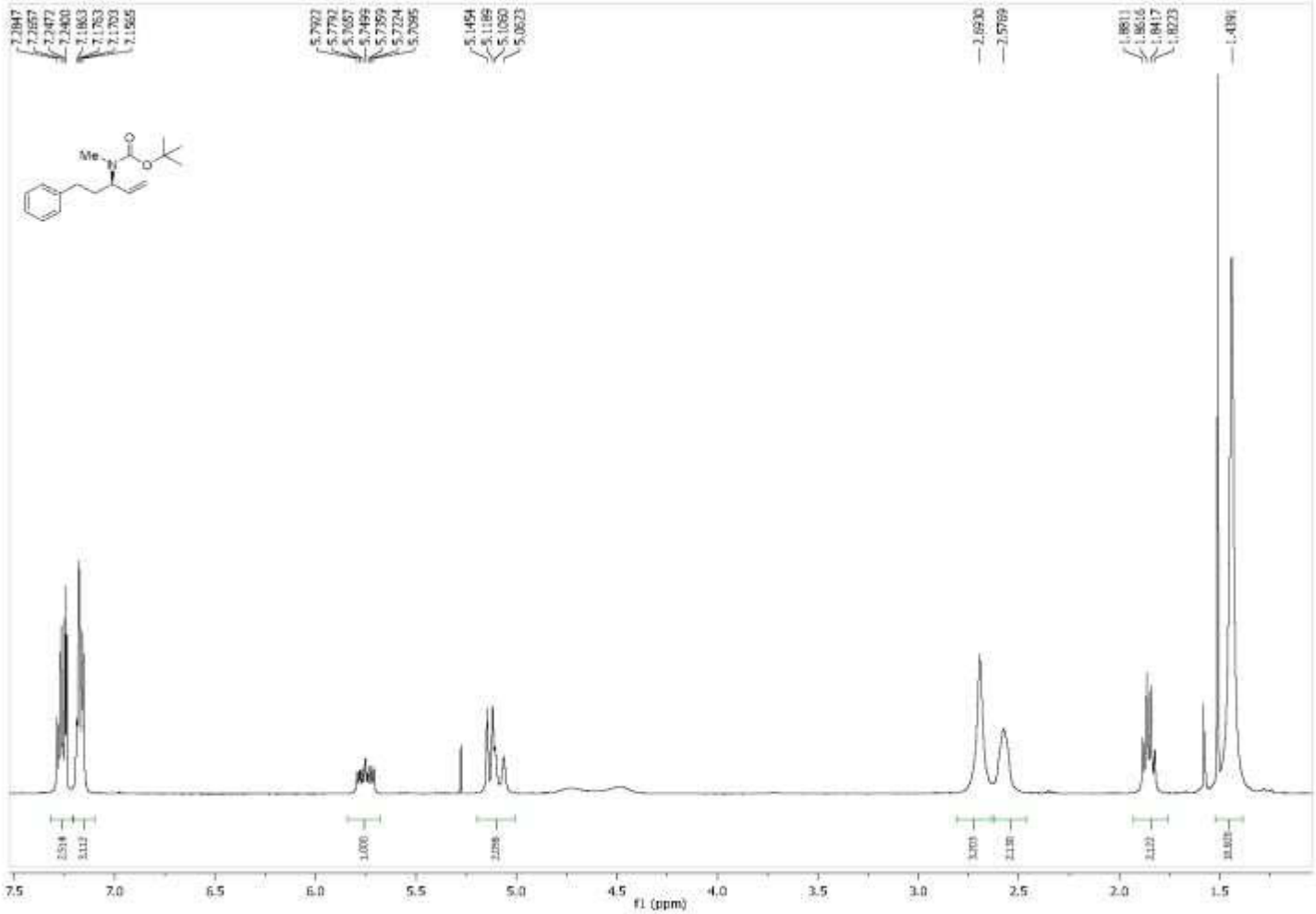

Figure A319 400 MHz 1H NMR ($CDCl_3$) Spectra of Compound **314-Boc**

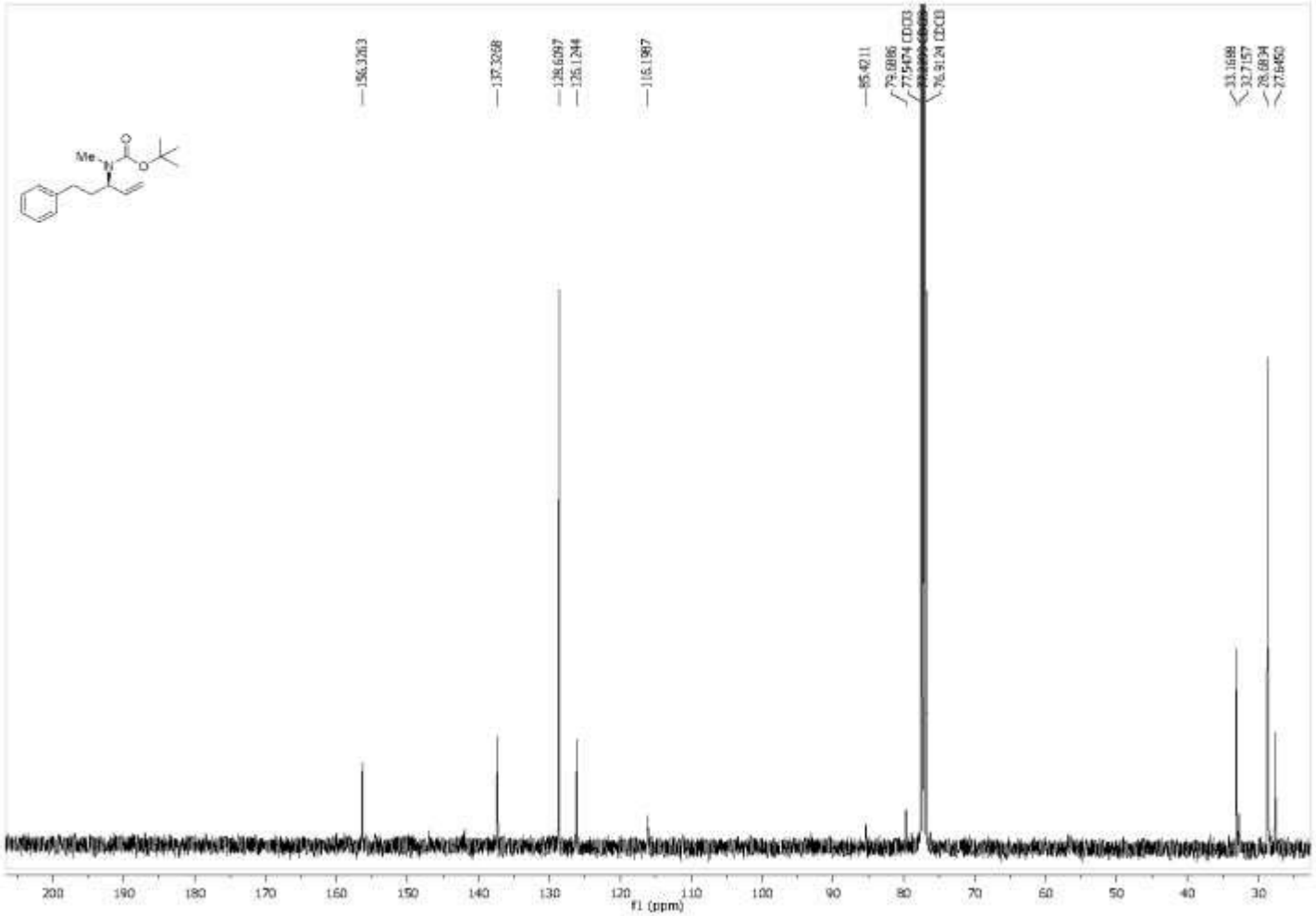

Figure A320 100 MHz 13C NMR ($CDCl_3$) Spectra of Compound **314-Boc**

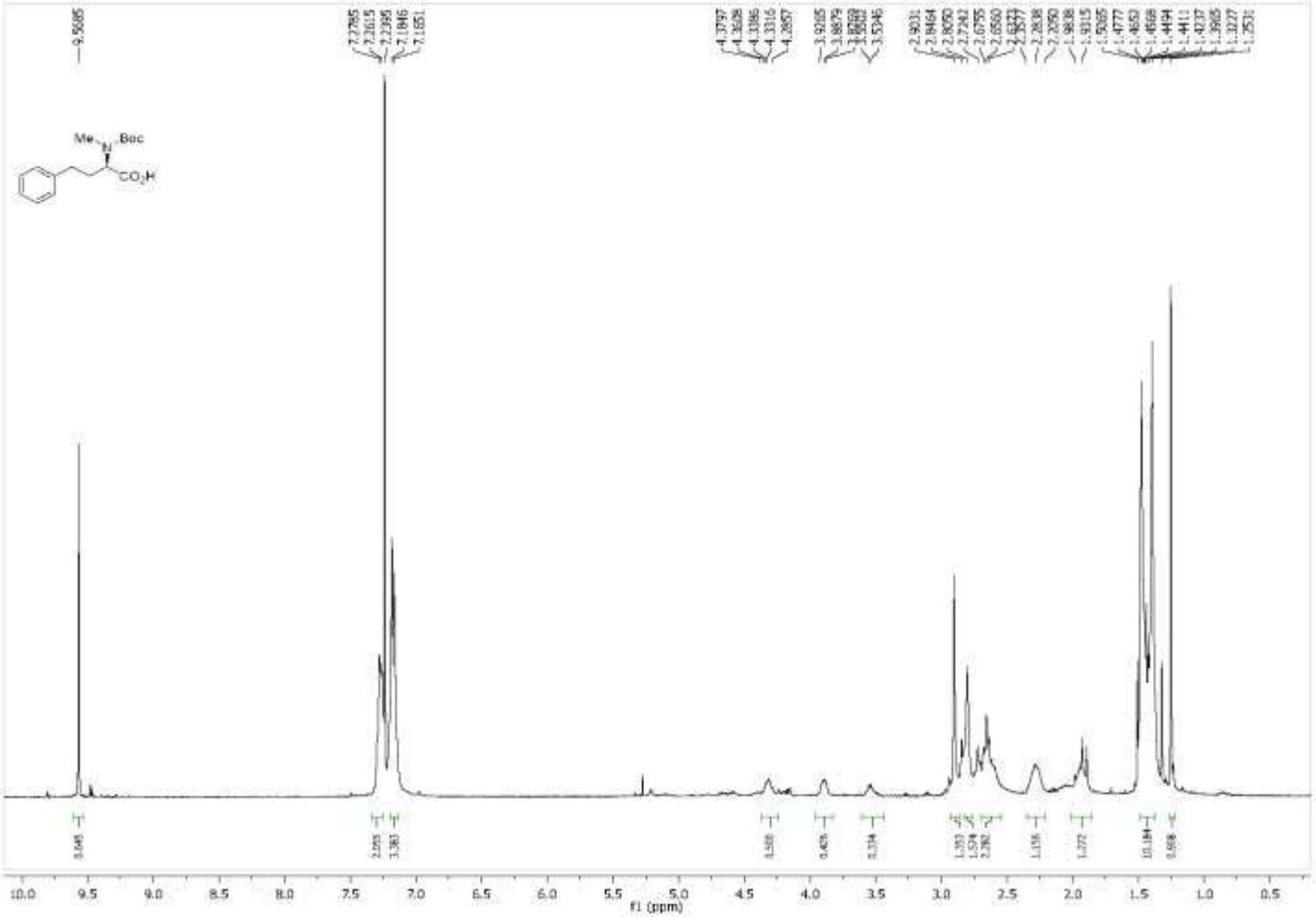

Figure A321 400 MHz 1H NMR ($CDCl_3$) Spectra of Compound **315**

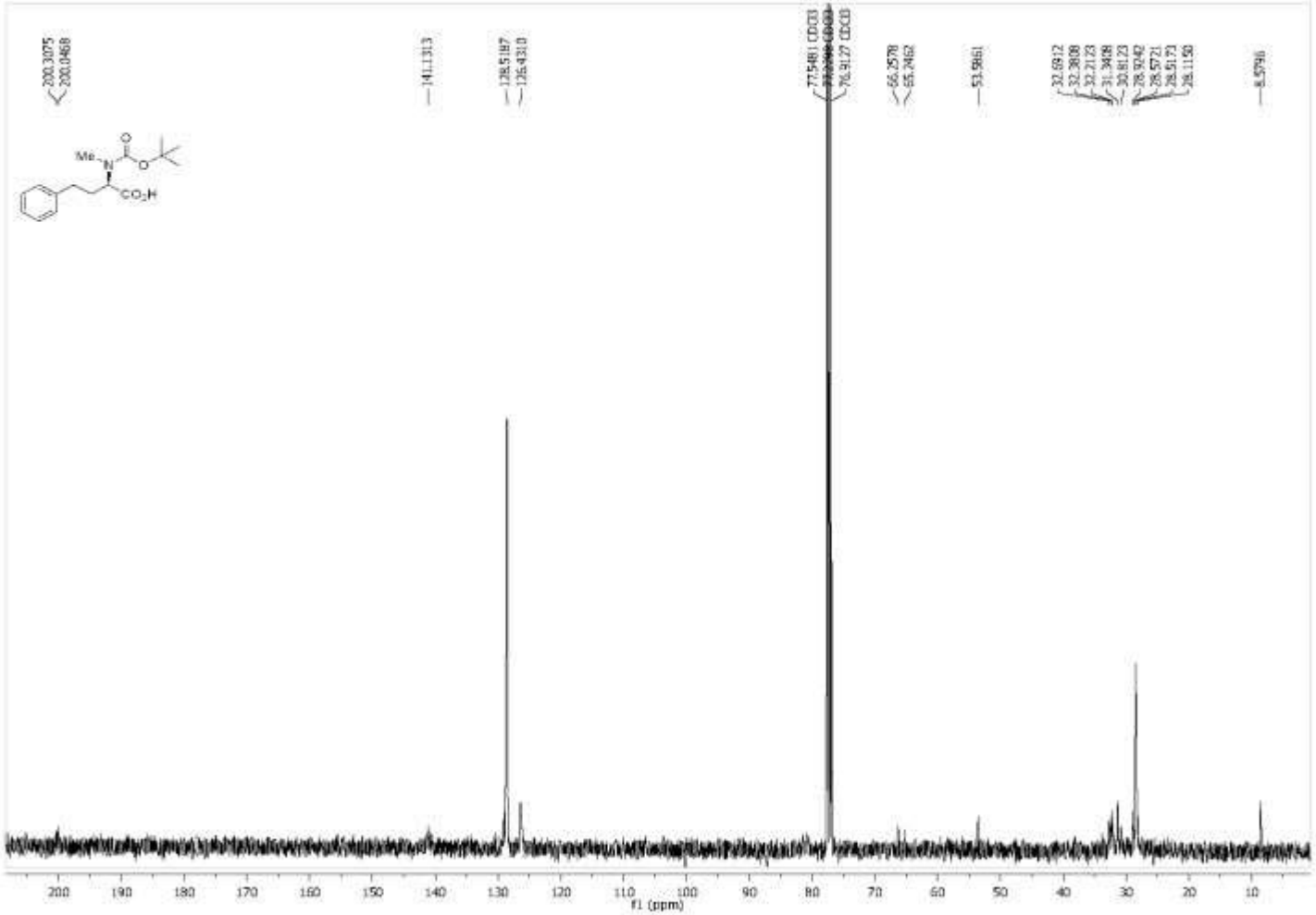

Figure A322 100 MHz 13C NMR ($CDCl_3$) Spectra of Compound **315**

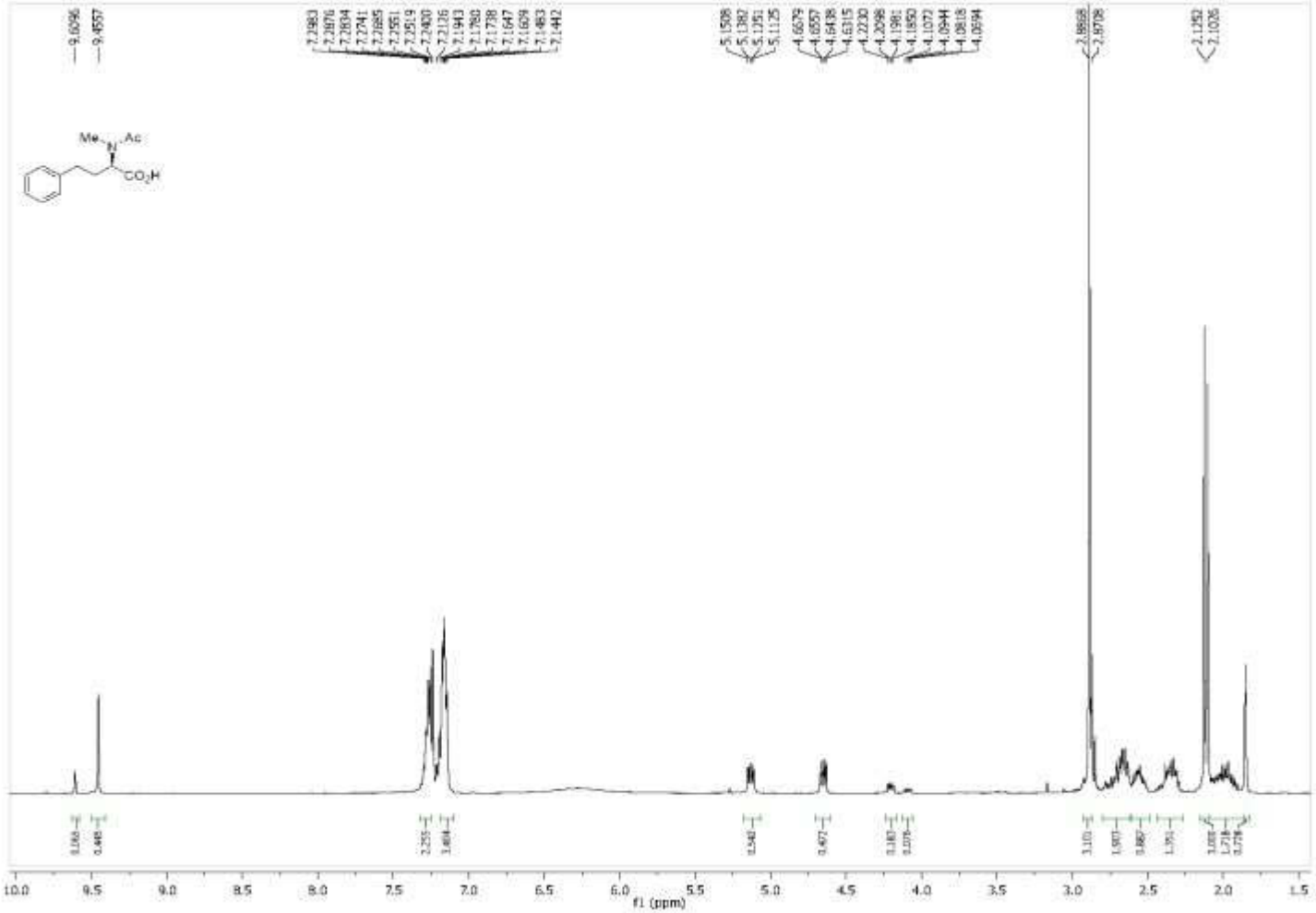

Figure A323 400 MHz 1H NMR ($CDCl_3$) Spectra of Compound **316**

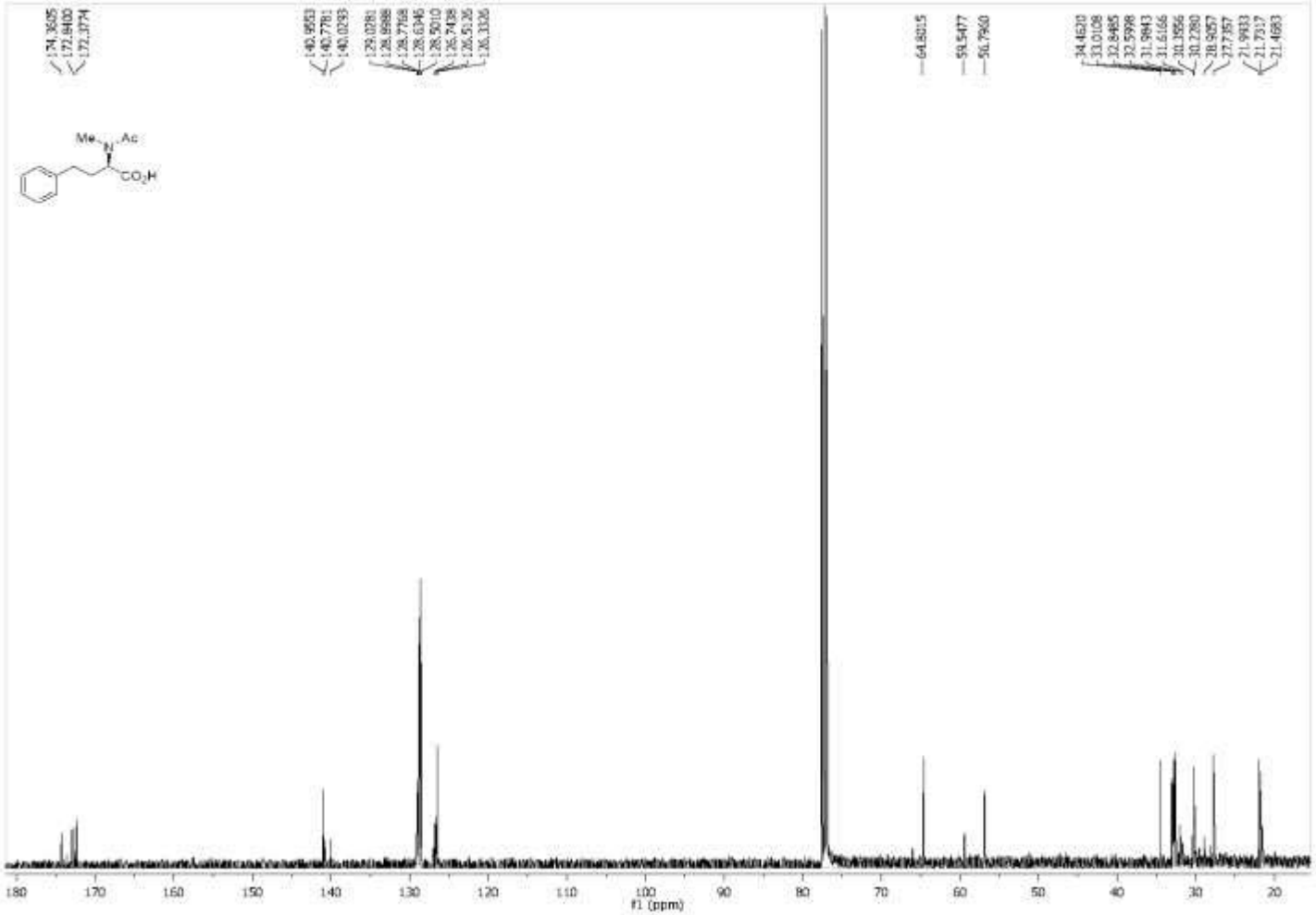

Figure A324 100 MHz 13C NMR ($CDCl_3$) Spectra of Compound **316**

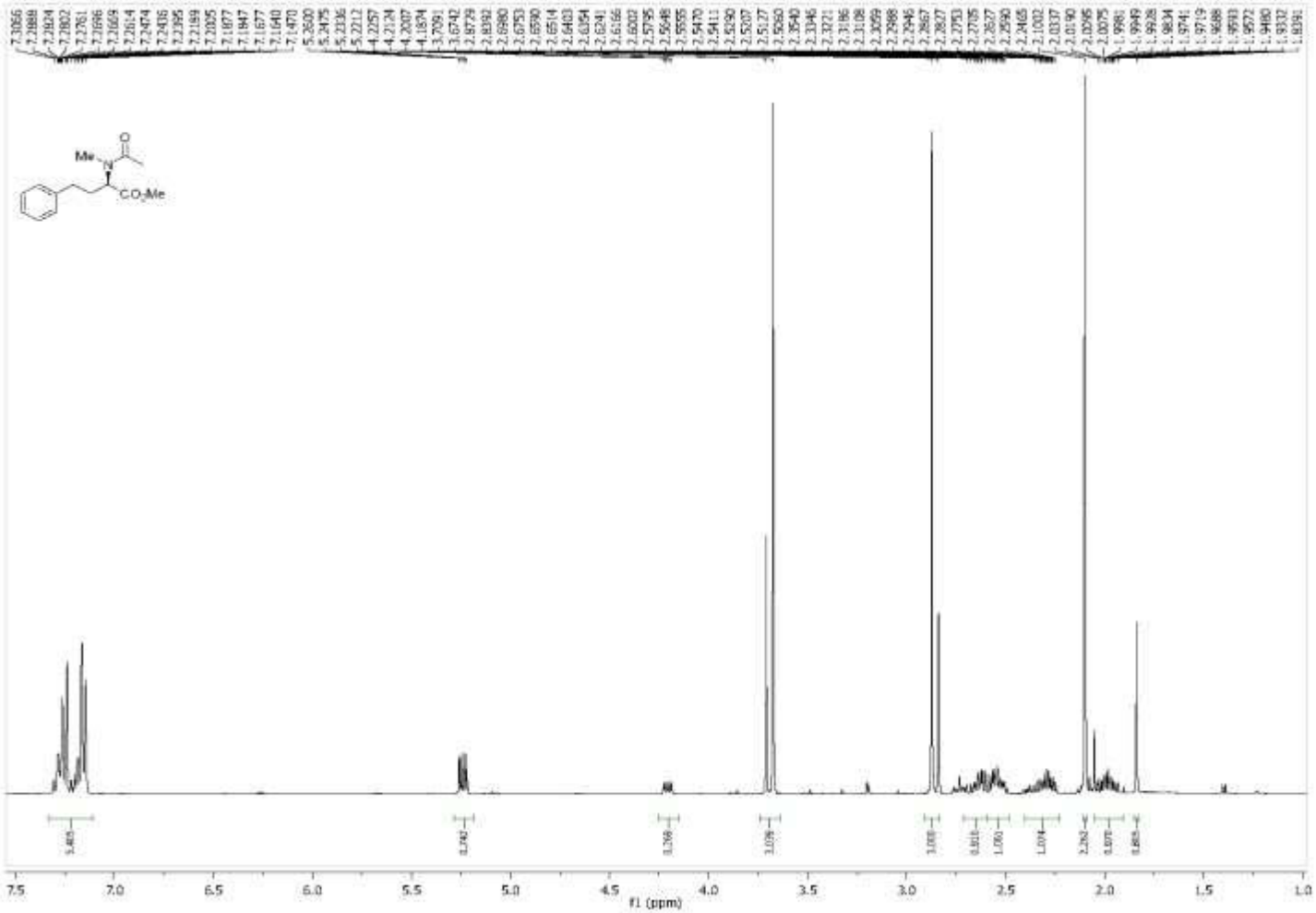

Figure A325 400 MHz 1H NMR ($CDCl_3$) Spectra of Compound **317**

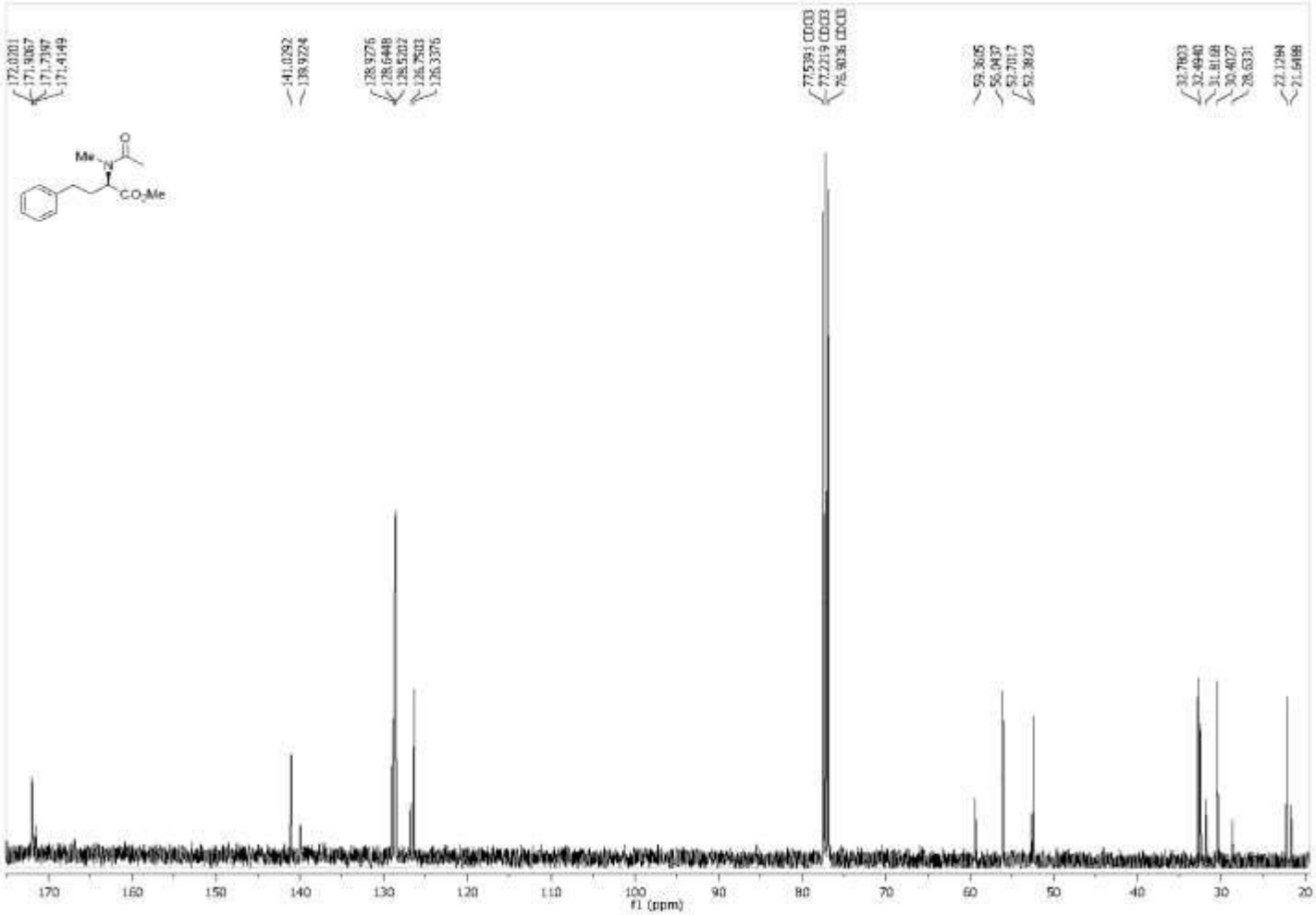

Figure A326 100 MHz 13C NMR ($CDCl_3$) Spectra of Compound **317**

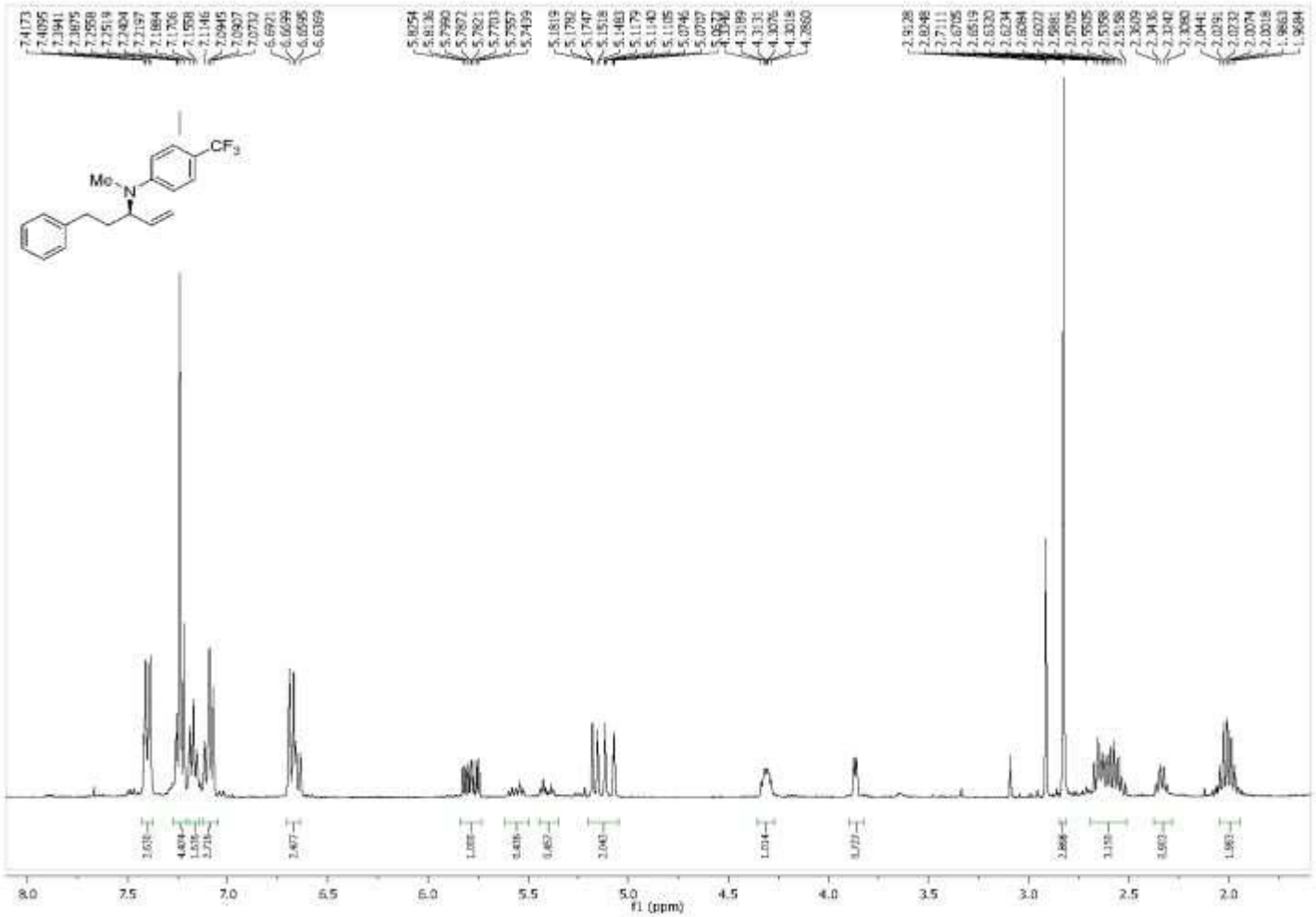

Figure A327 400 MHz 1H NMR ($CDCl_3$) Spectra of Compound **227r**

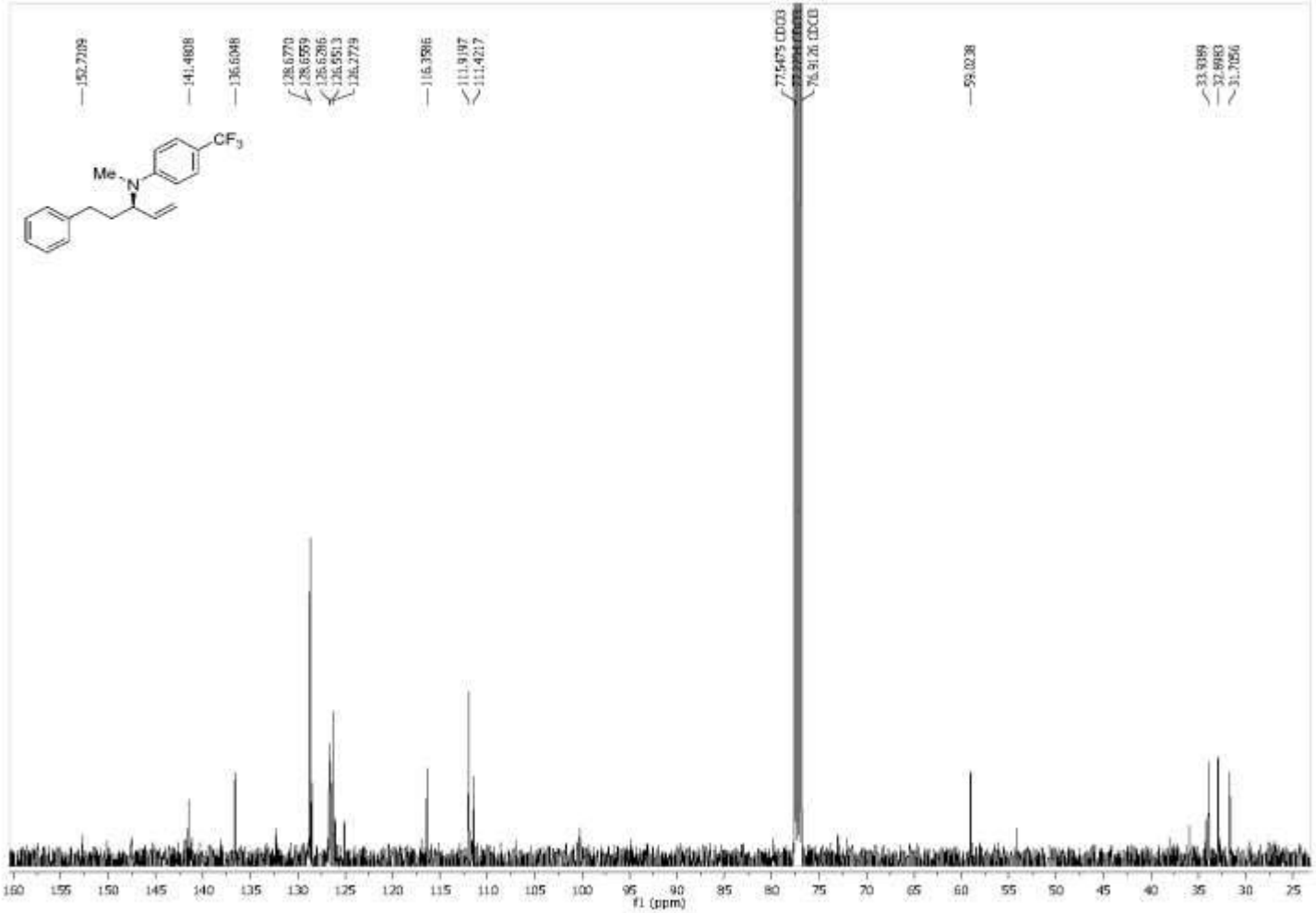

Figure A328 100 MHz 13C NMR ($CDCl_3$) Spectra of Compound **227r**

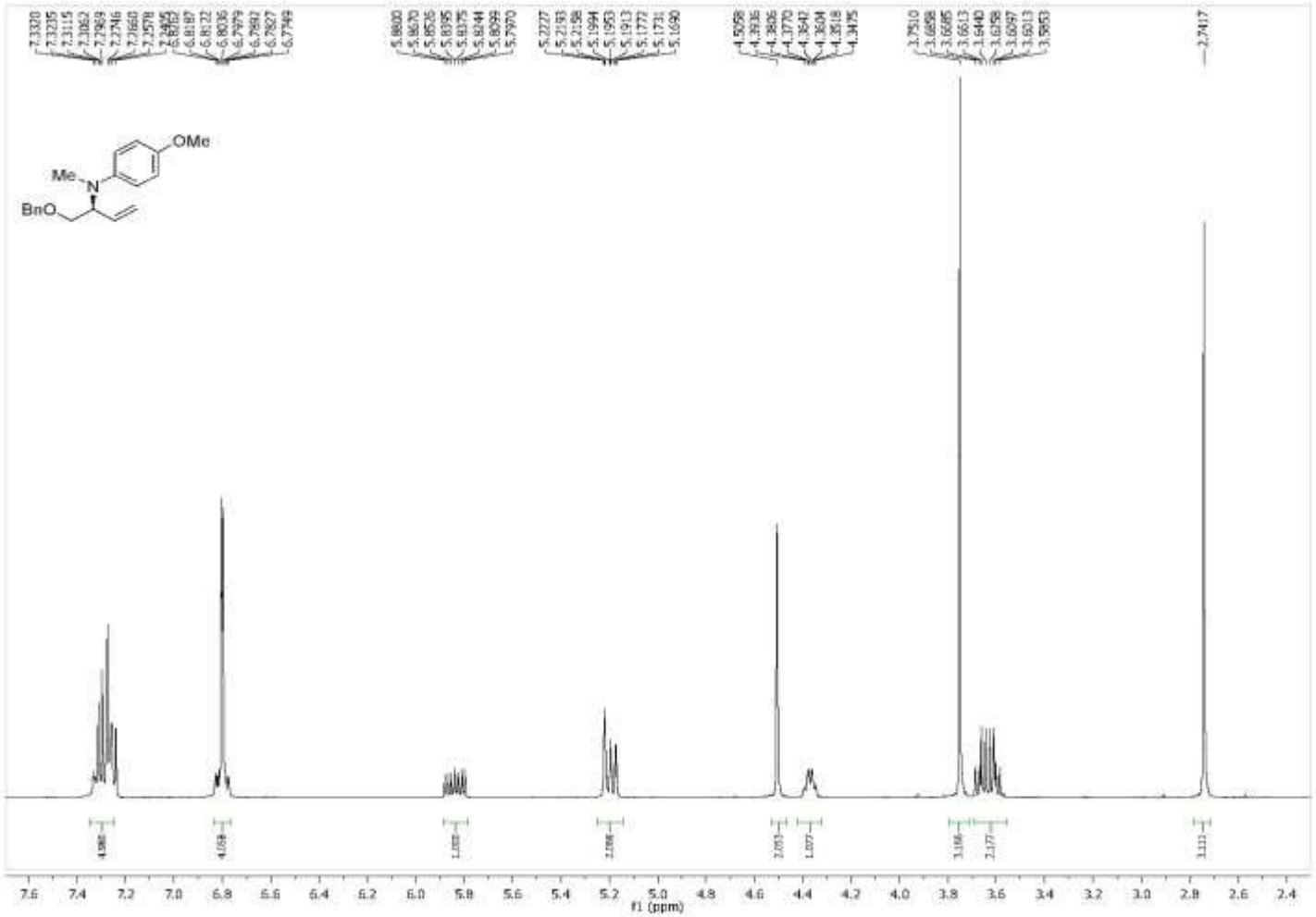

Figure A329 400 MHz 1H NMR ($CDCl_3$) Spectra of Compound **229q**

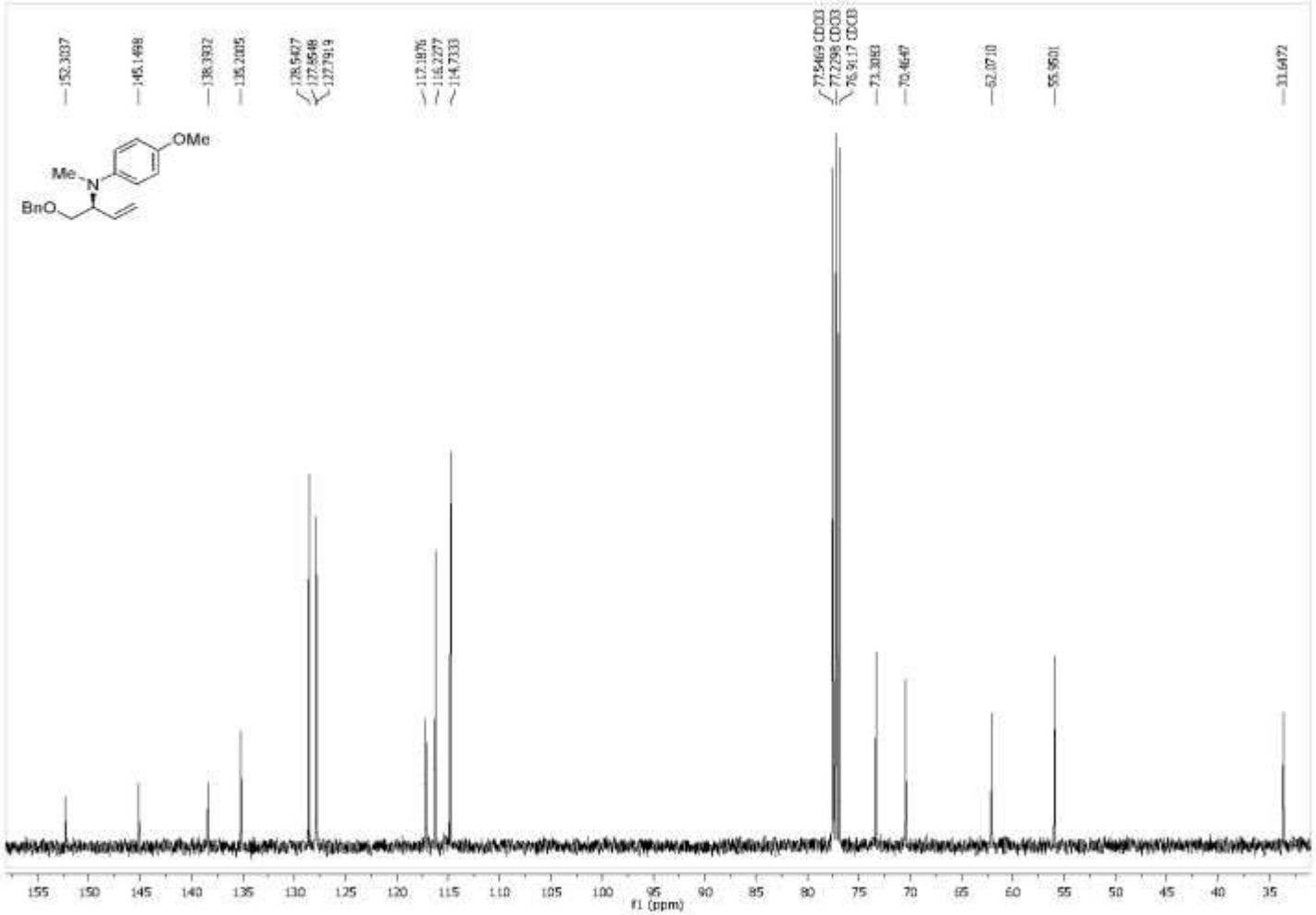

Figure A330 100 MHz 13C NMR ($CDCl_3$) Spectra of Compound **229q**

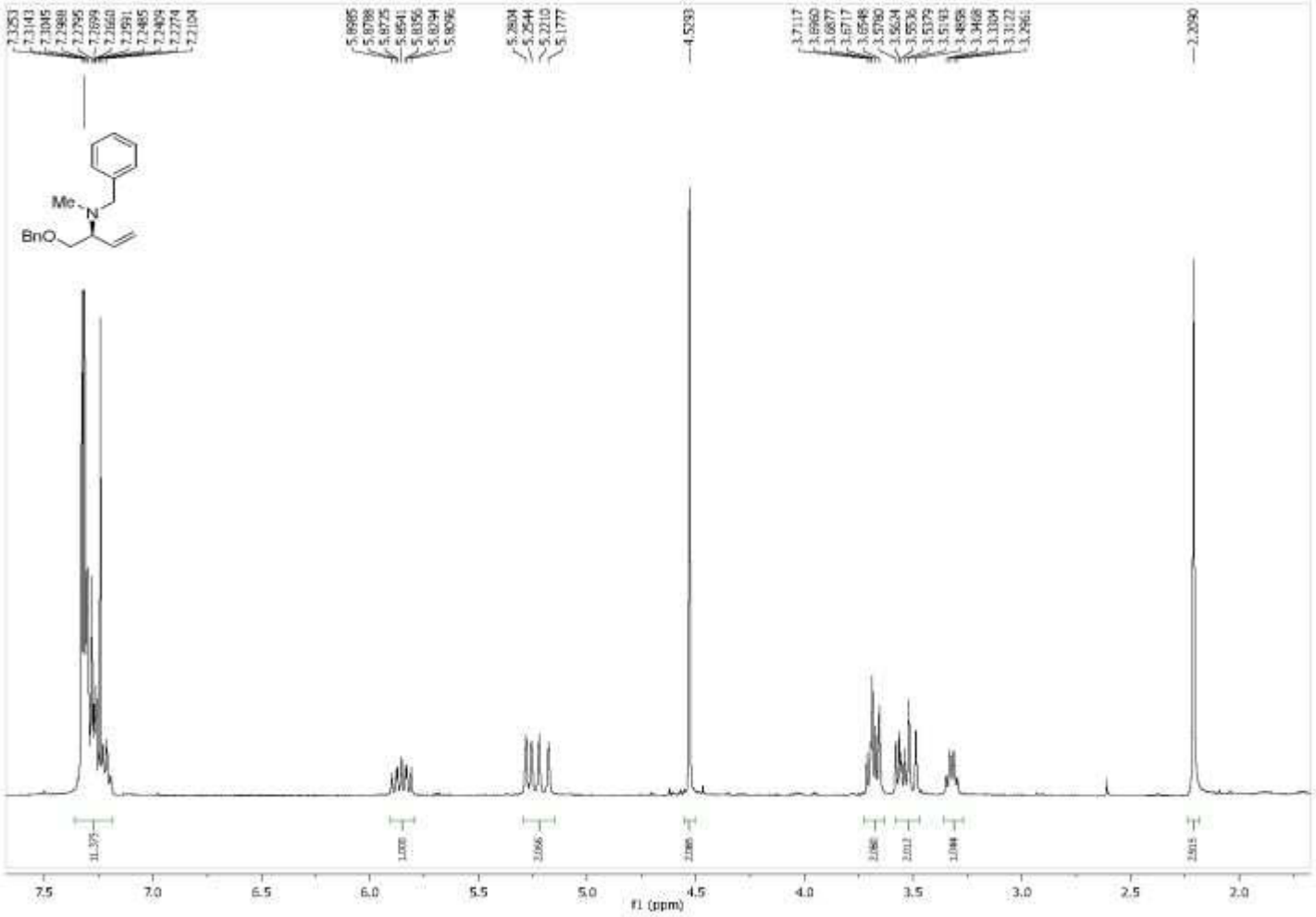

Figure A331 400 MHz 1H NMR ($CDCl_3$) Spectra of Compound **229y**

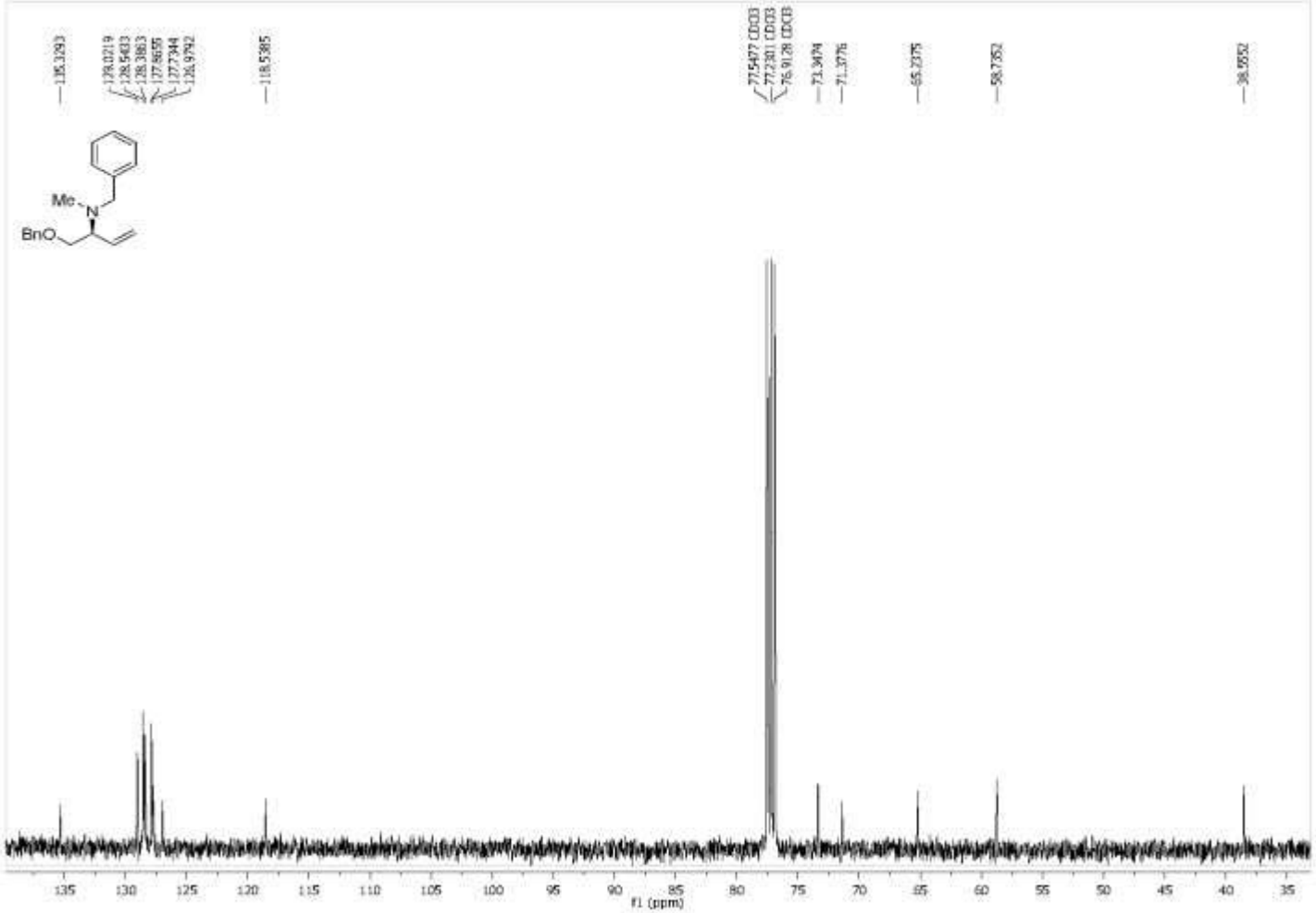

Figure A332 100 MHz 13C NMR ($CDCl_3$) Spectra of Compound **229y**

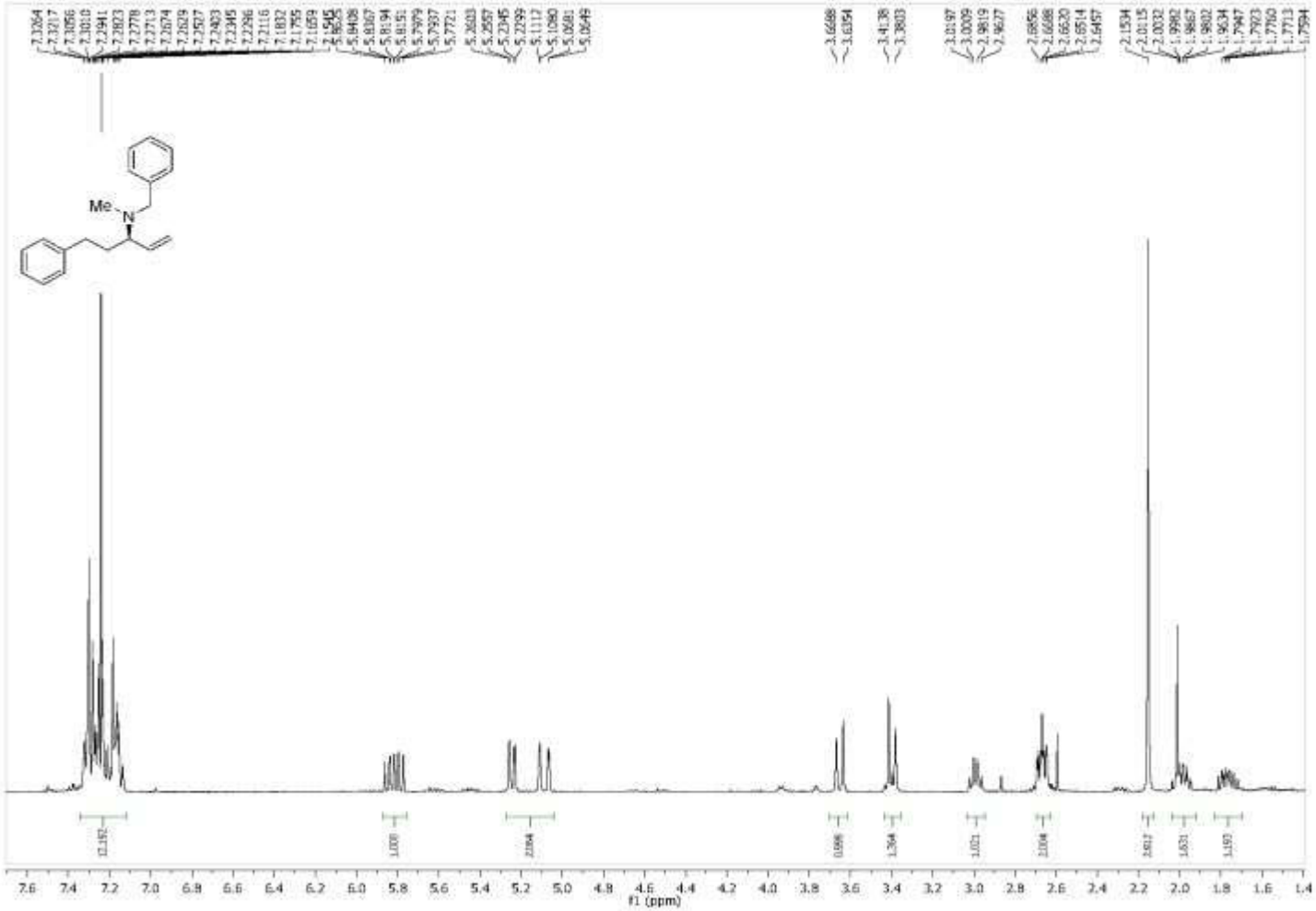

Figure A333 400 MHz 1H NMR ($CDCl_3$) Spectra of Compound **227y**

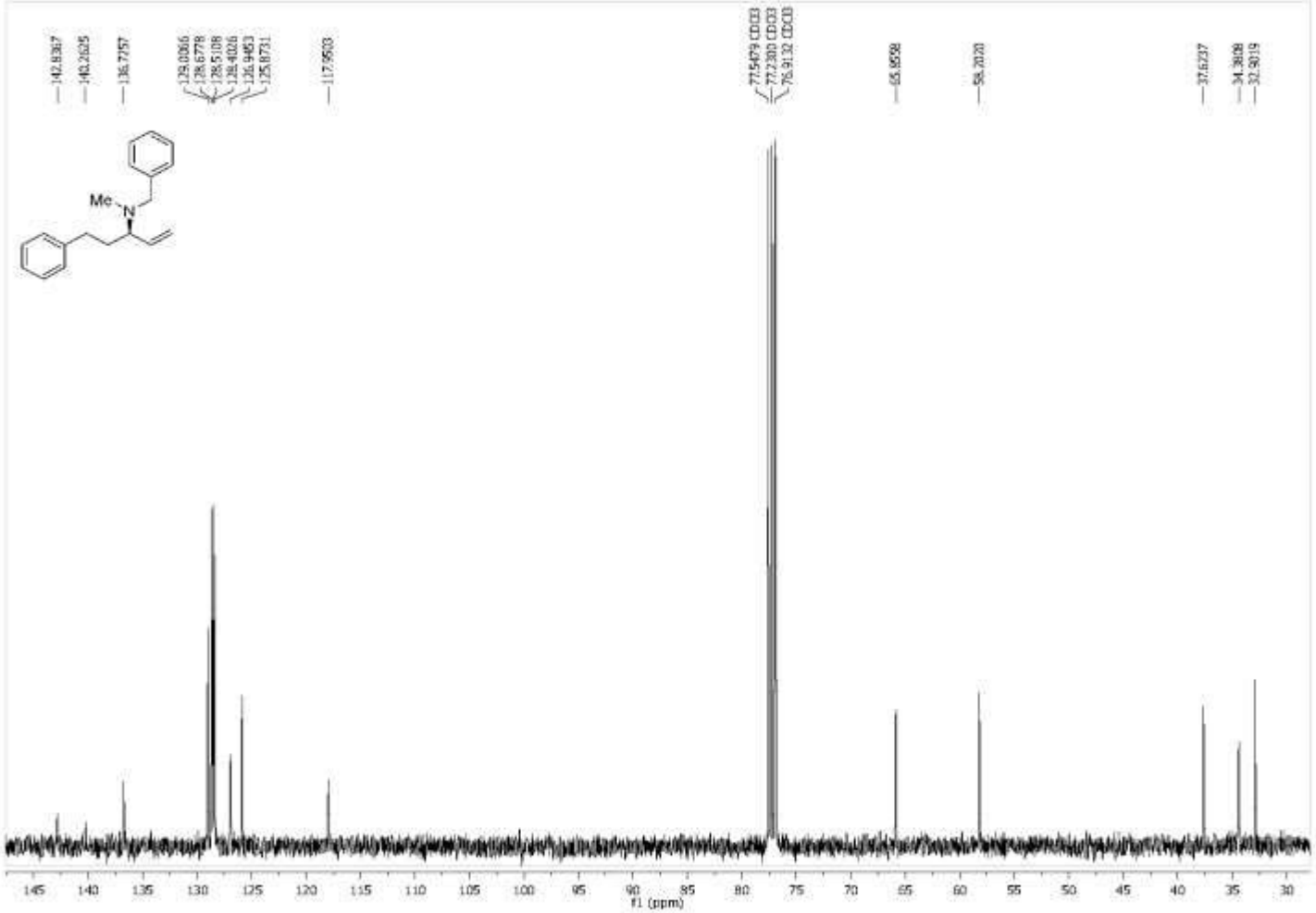

Figure A334 100 MHz 13C NMR ($CDCl_3$) Spectra of Compound **227y**

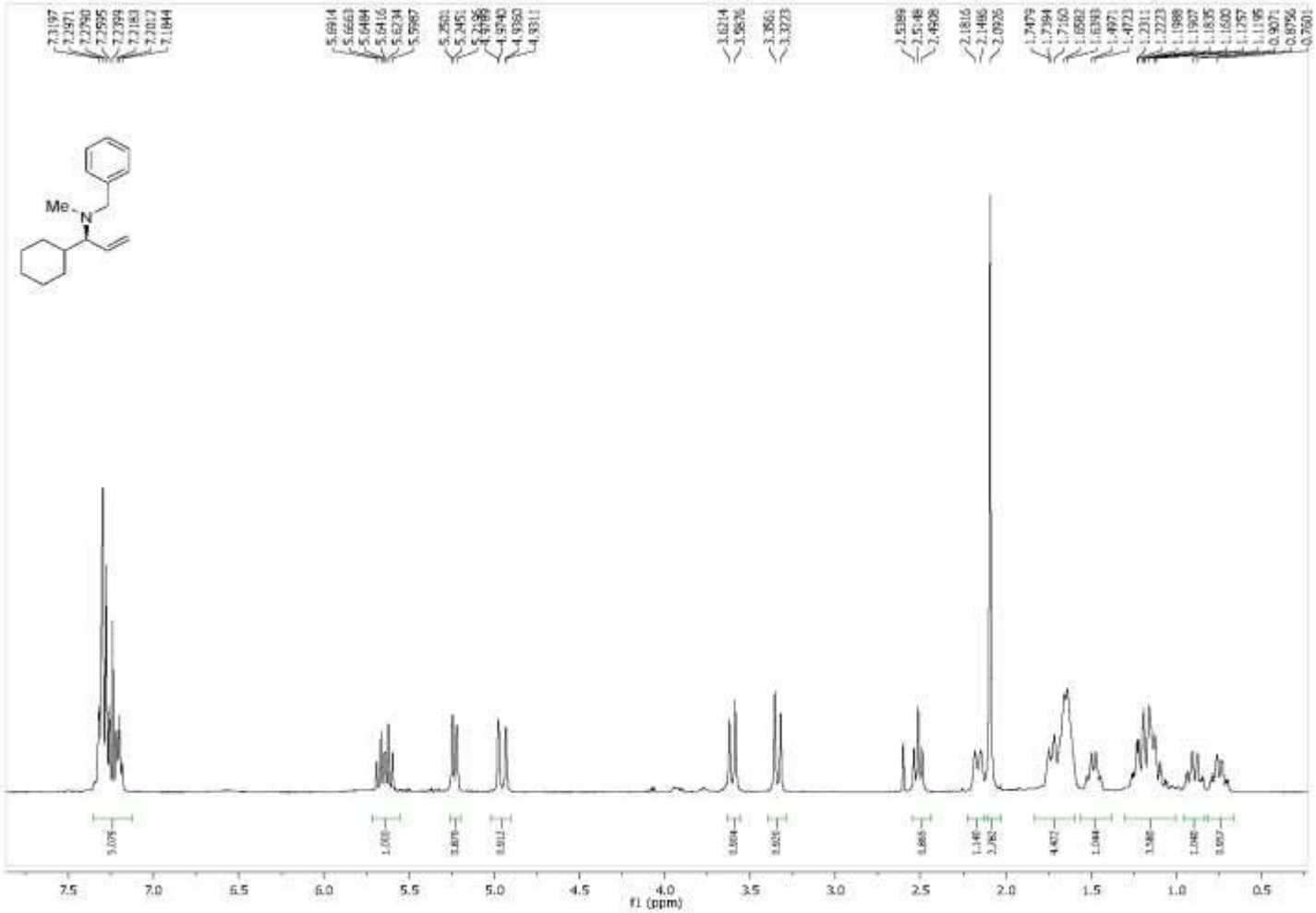

Figure A335 400 MHz 1H NMR ($CDCl_3$) Spectra of Compound **231y**

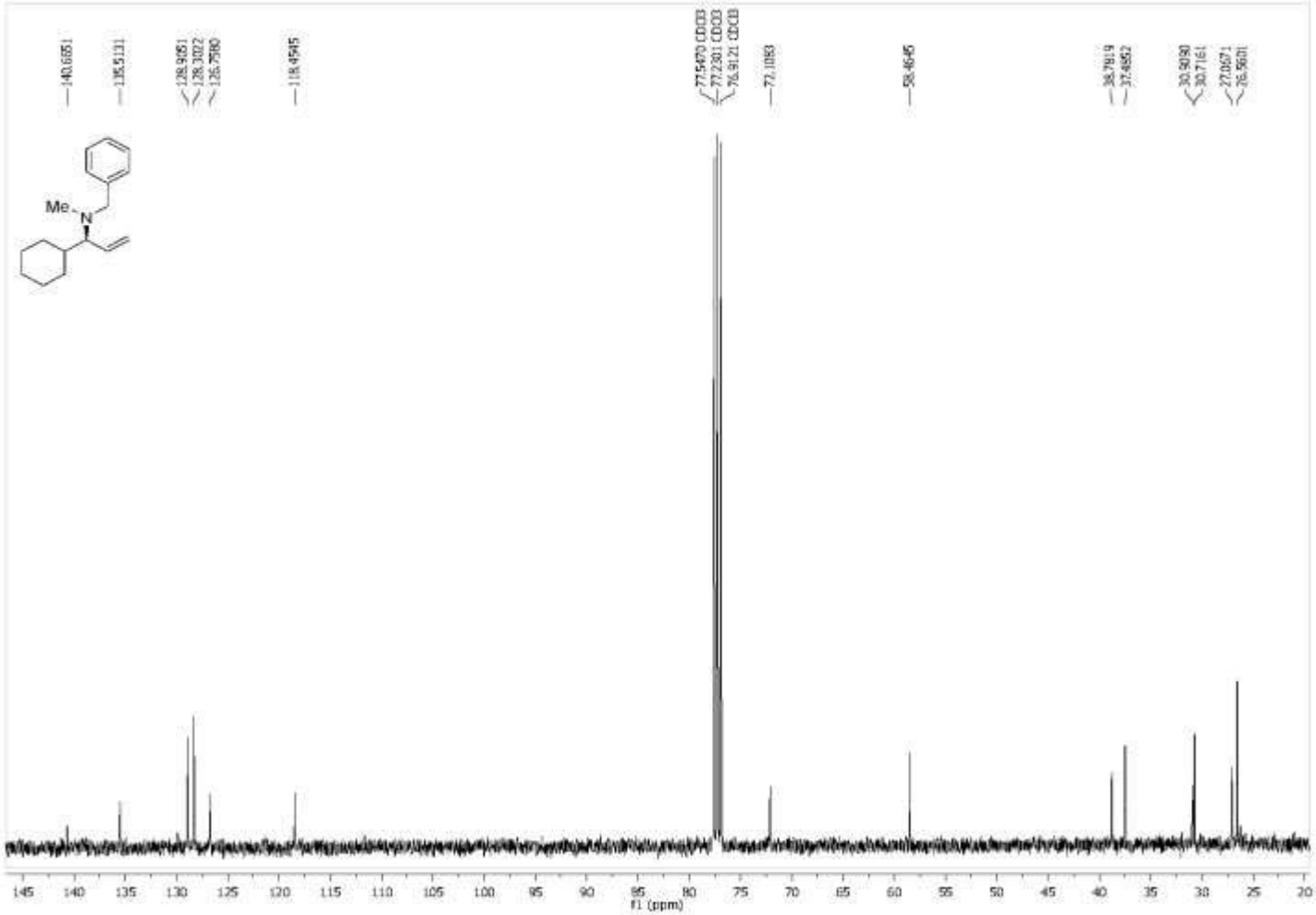

Figure A336 100 MHz 13C NMR ($CDCl_3$) Spectra of Compound **231y**

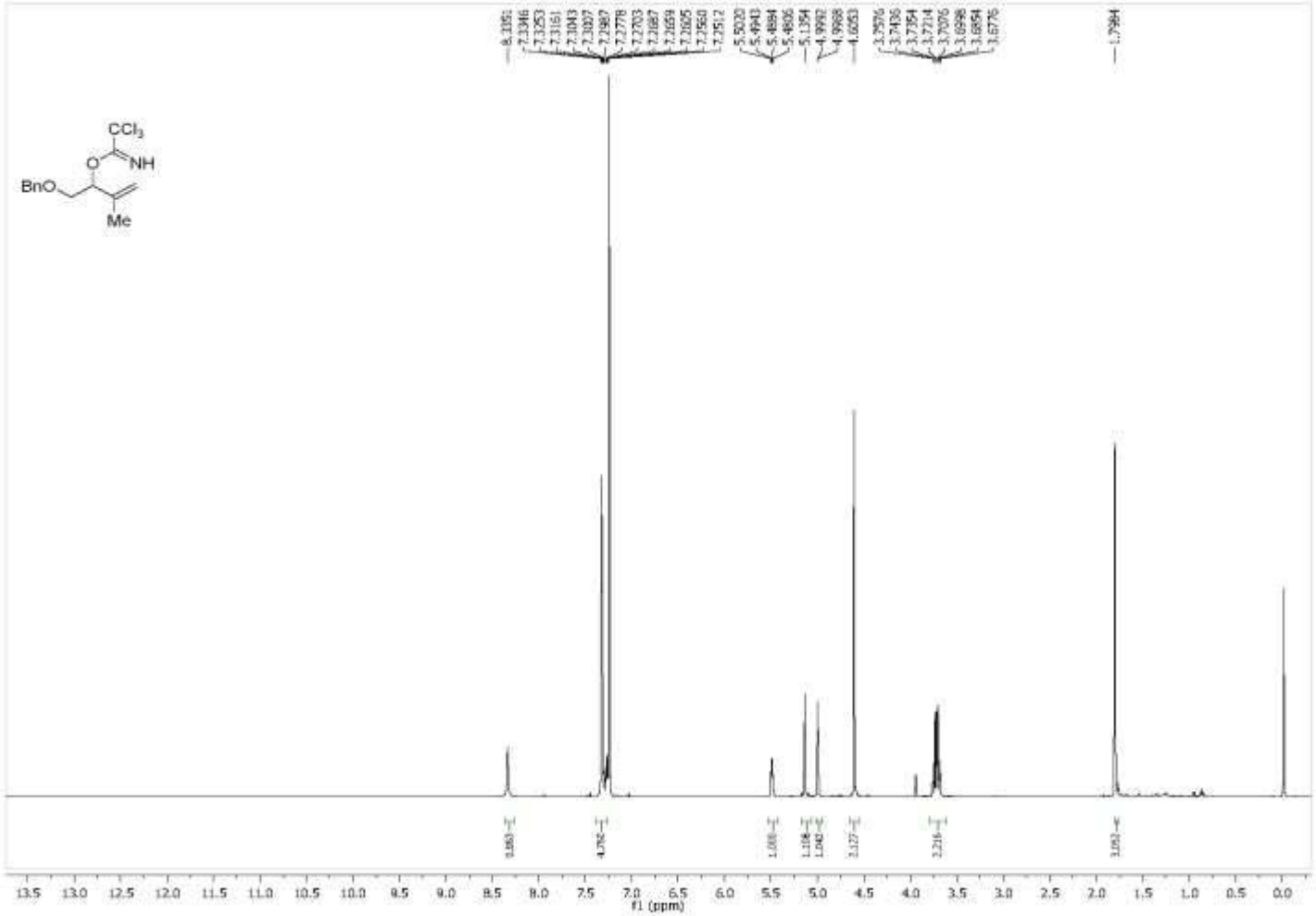

Figure A337 400 MHz 1H NMR ($CDCl_3$) Spectra of Compound **377**

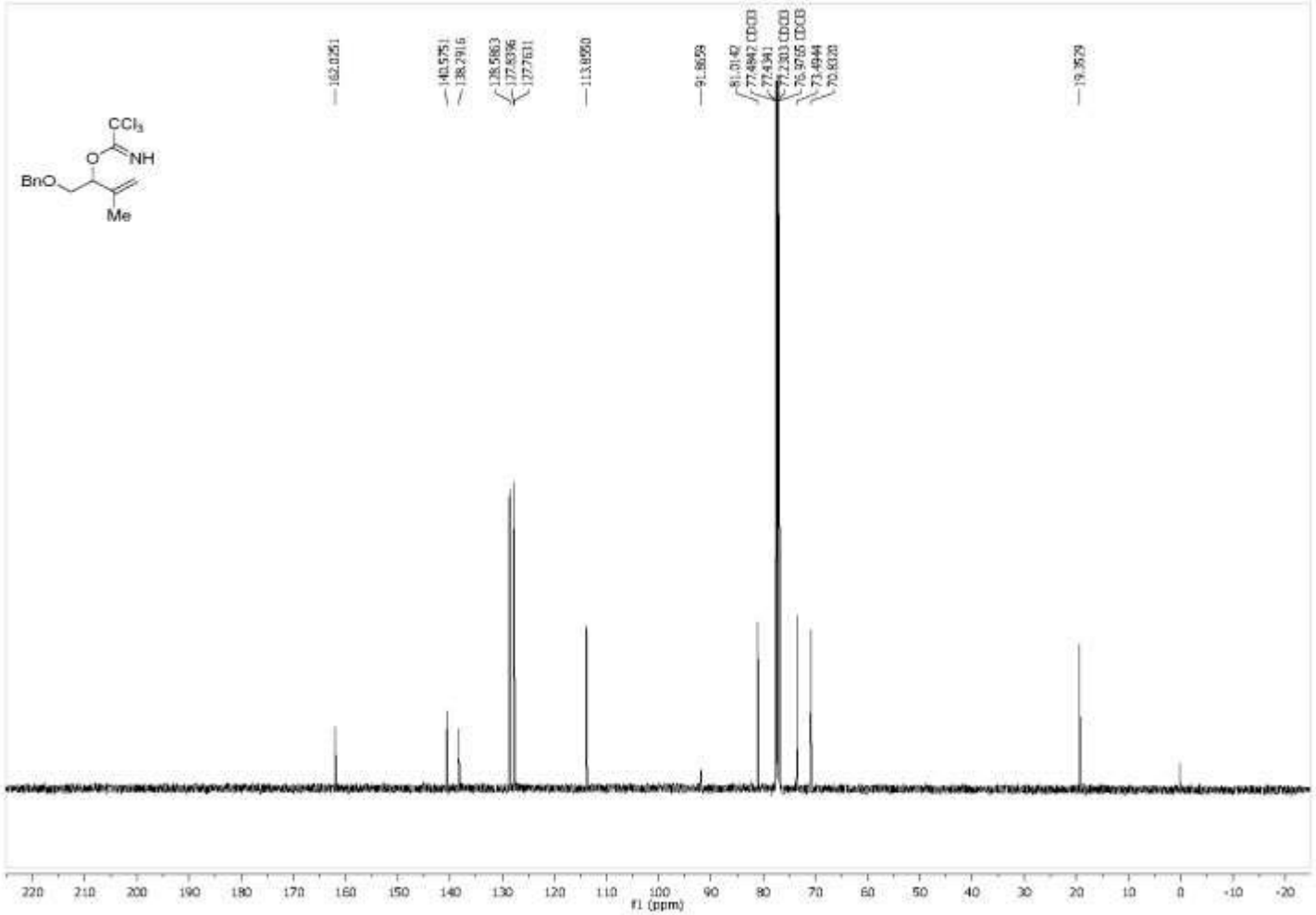

Figure A338 100 MHz 13C NMR ($CDCl_3$) Spectra of Compound **377**

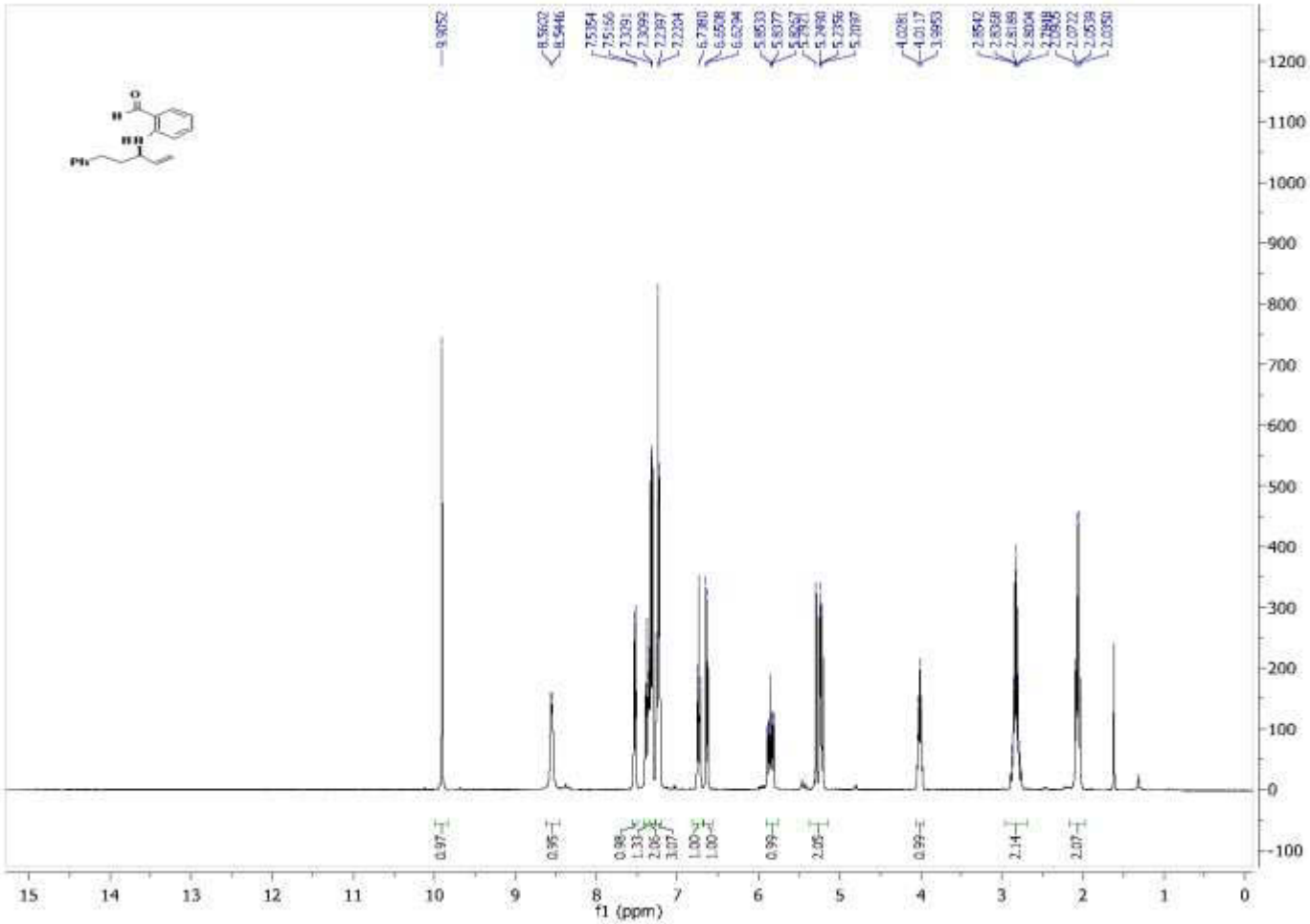

Figure A339 400 MHz 1H NMR ($CDCl_3$) Spectra of Compound **227z**

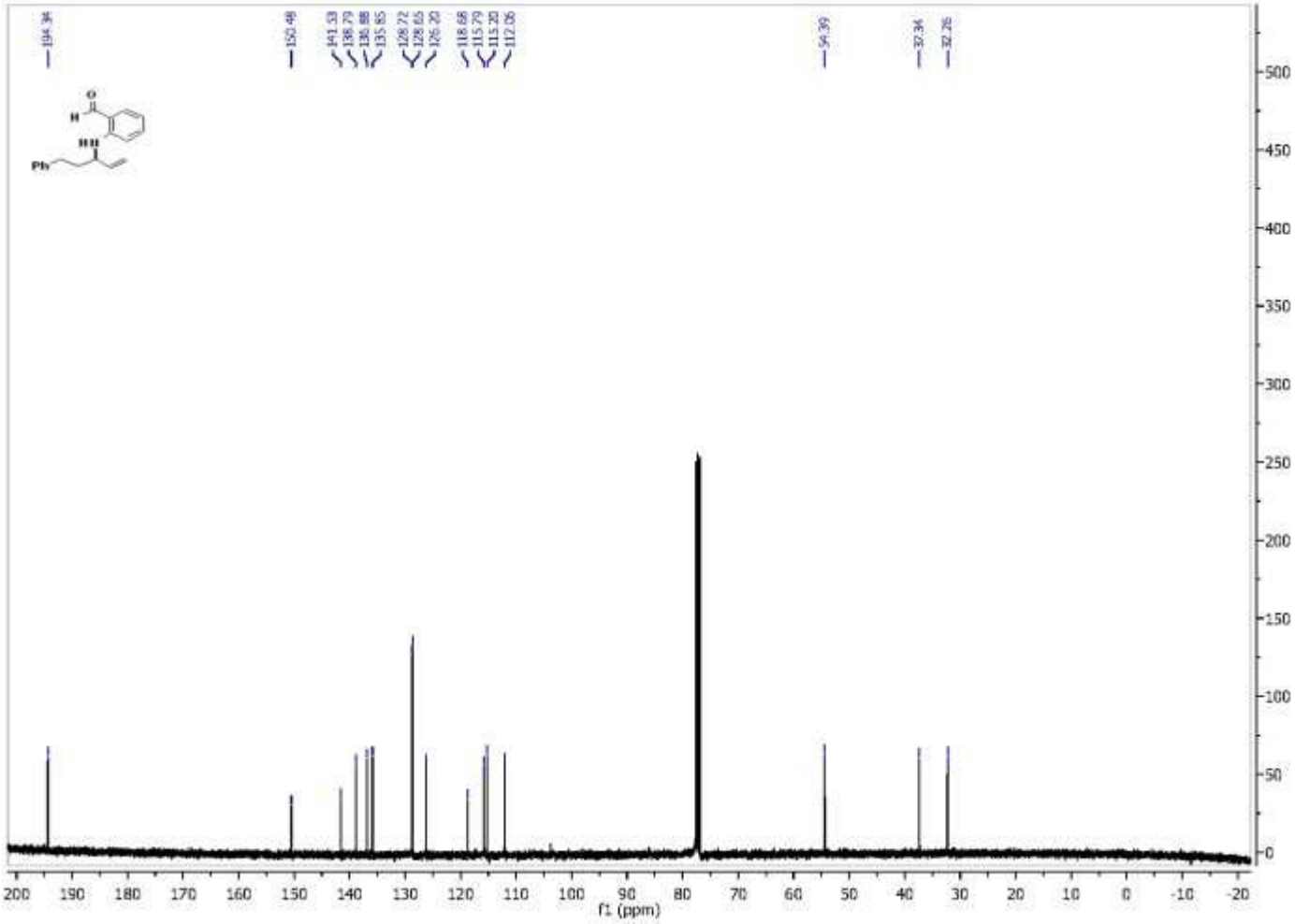

Figure A340 100 MHz 13C NMR ($CDCl_3$) Spectra of Compound **227z**

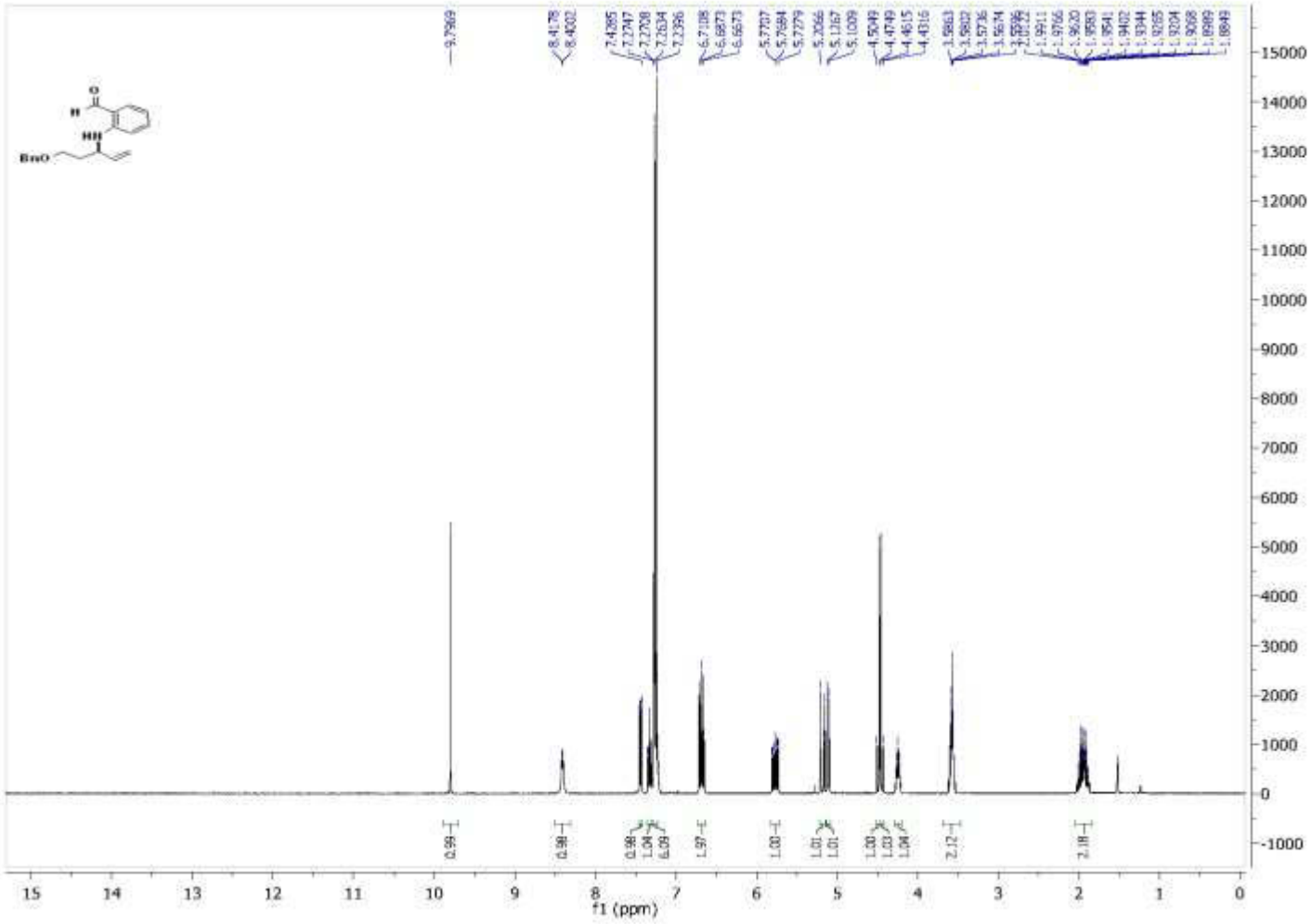

Figure A341 400 MHz 1H NMR ($CDCl_3$) Spectra of Compound **310z**

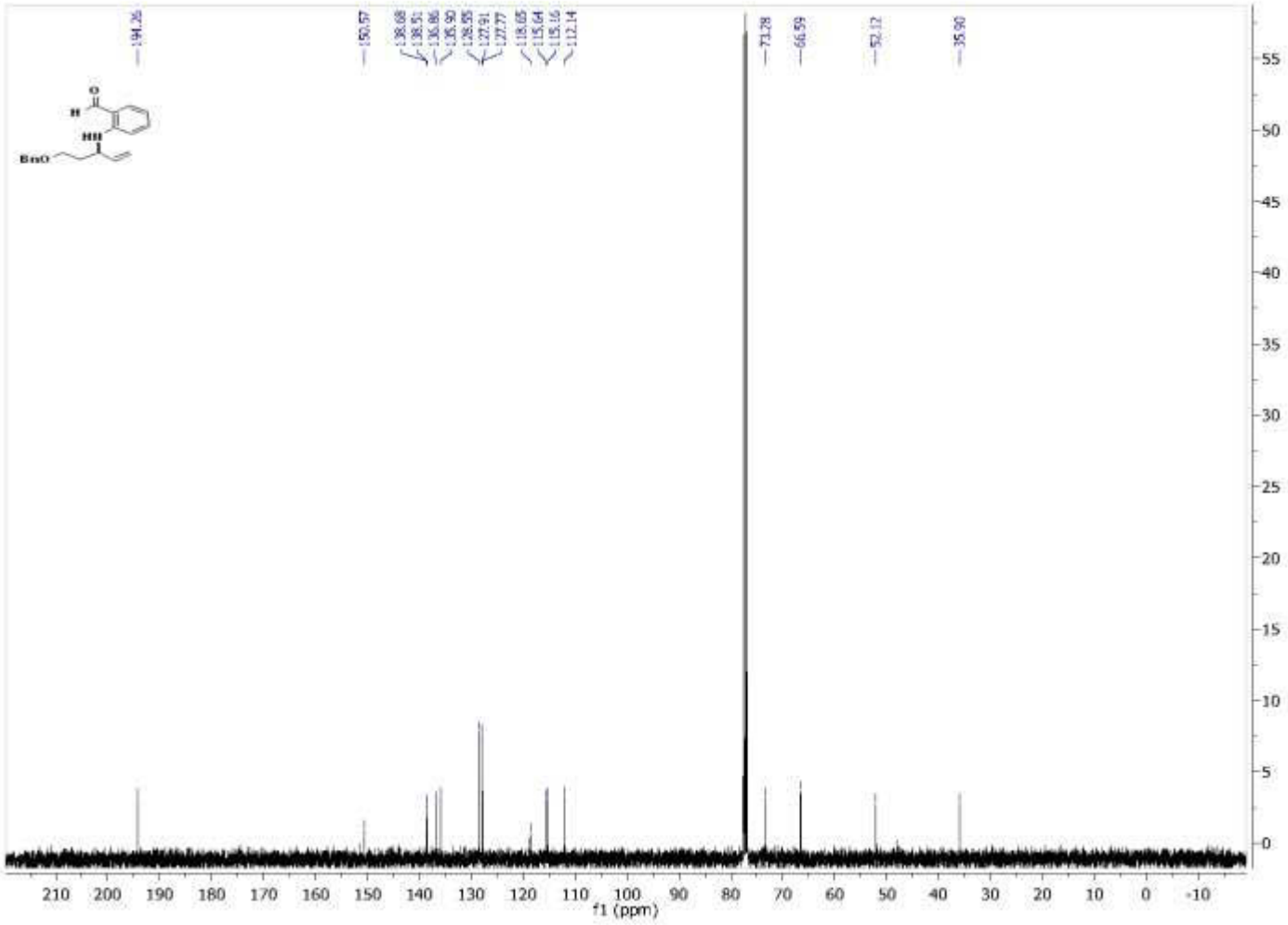

Figure A342 100 MHz 13C NMR ($CDCl_3$) Spectra of Compound **310z**

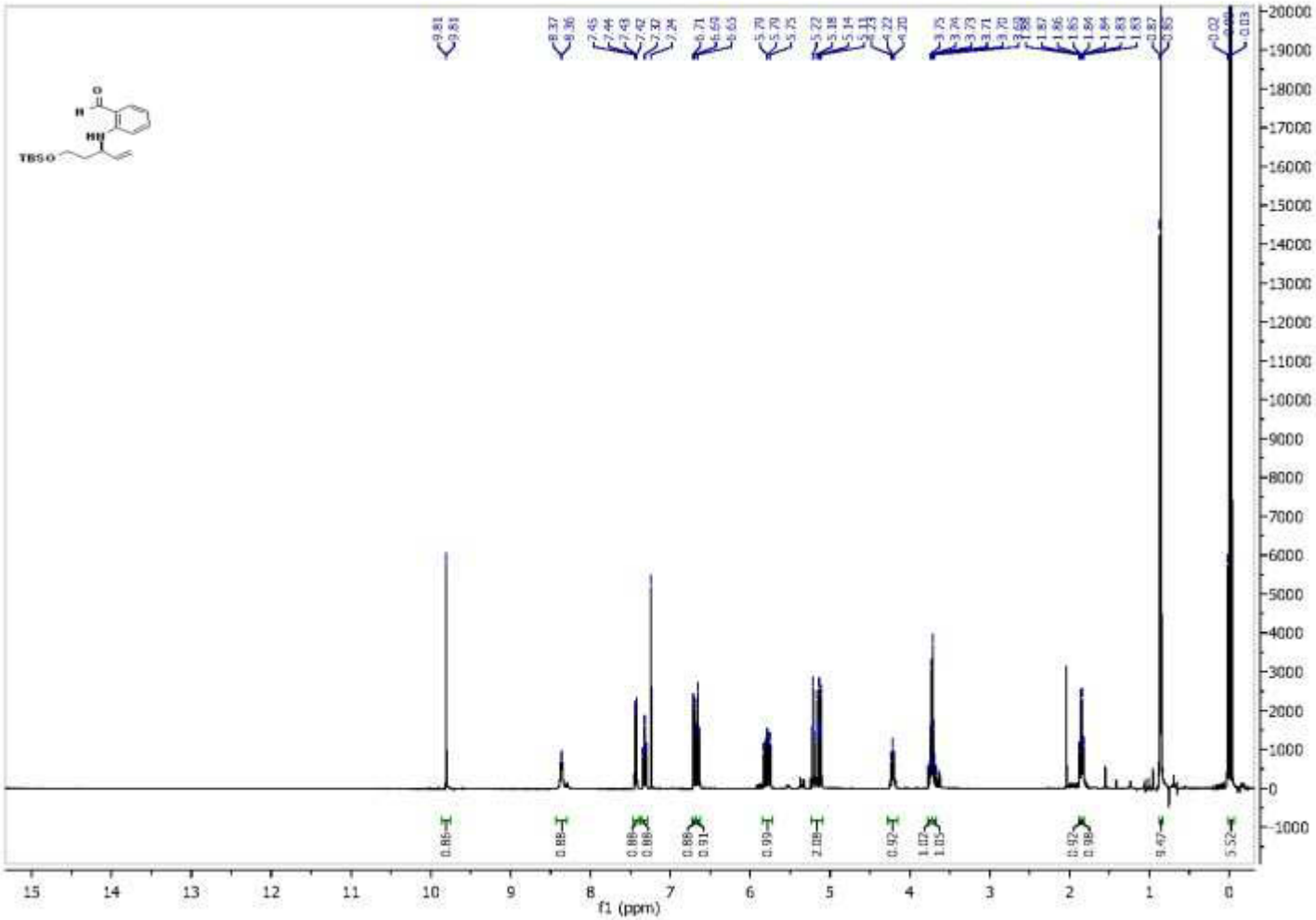

Figure A343 400 MHz 1H NMR ($CDCl_3$) Spectra of Compound **223z**

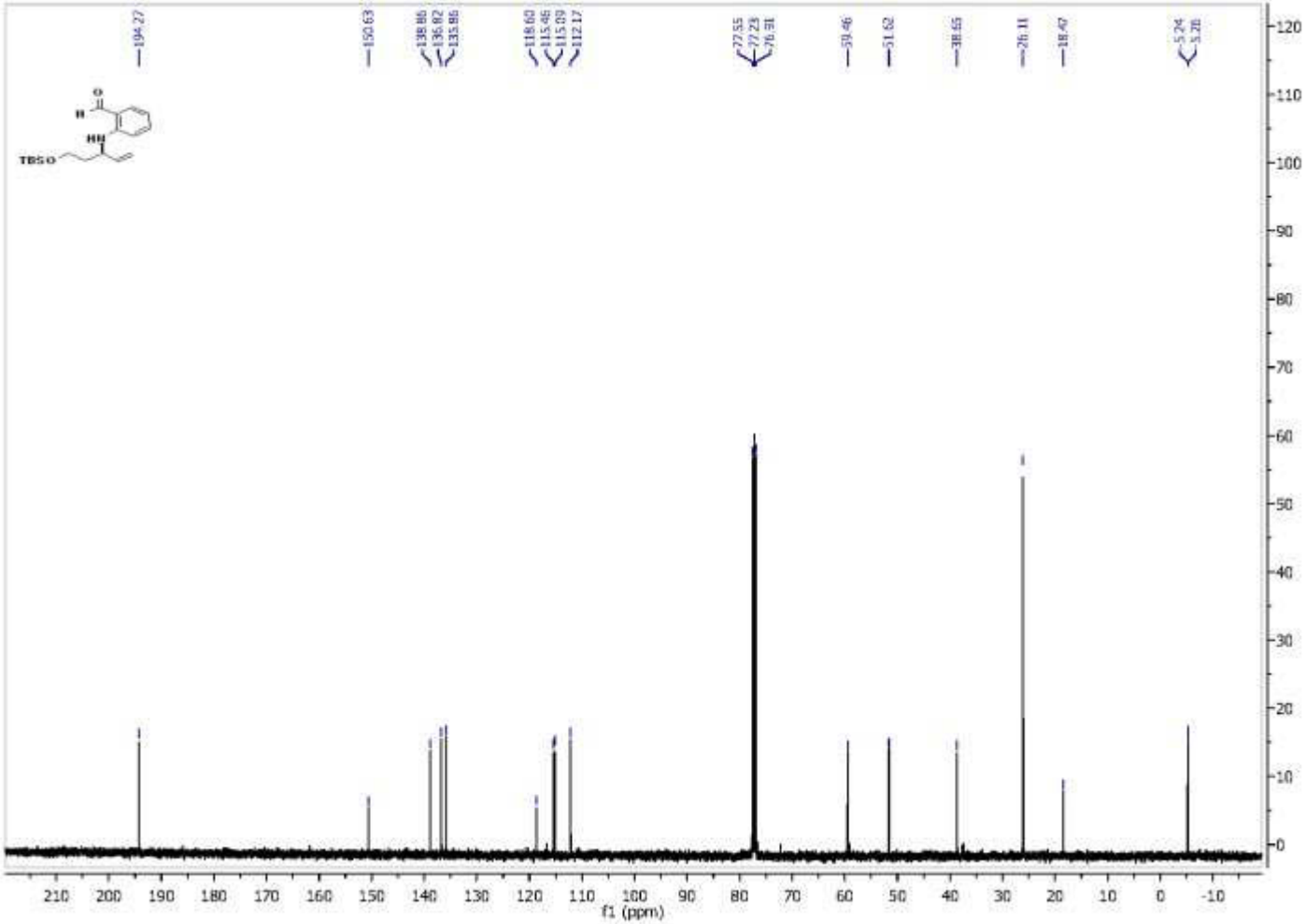

Figure A344 100 MHz 13C NMR ($CDCl_3$) Spectra of Compound **223z**

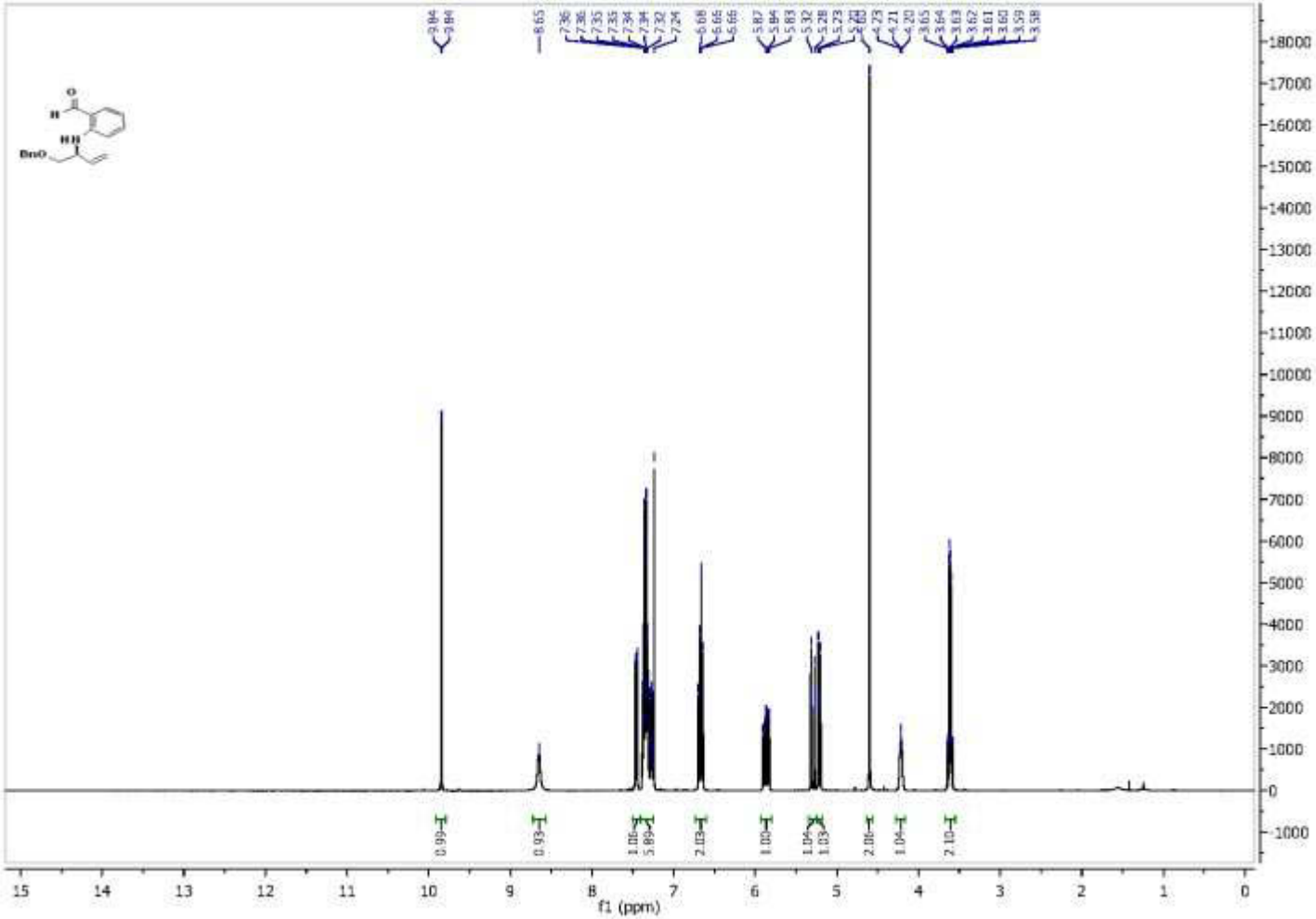

Figure A345 400 MHz 1H NMR ($CDCl_3$) Spectra of Compound **229z**

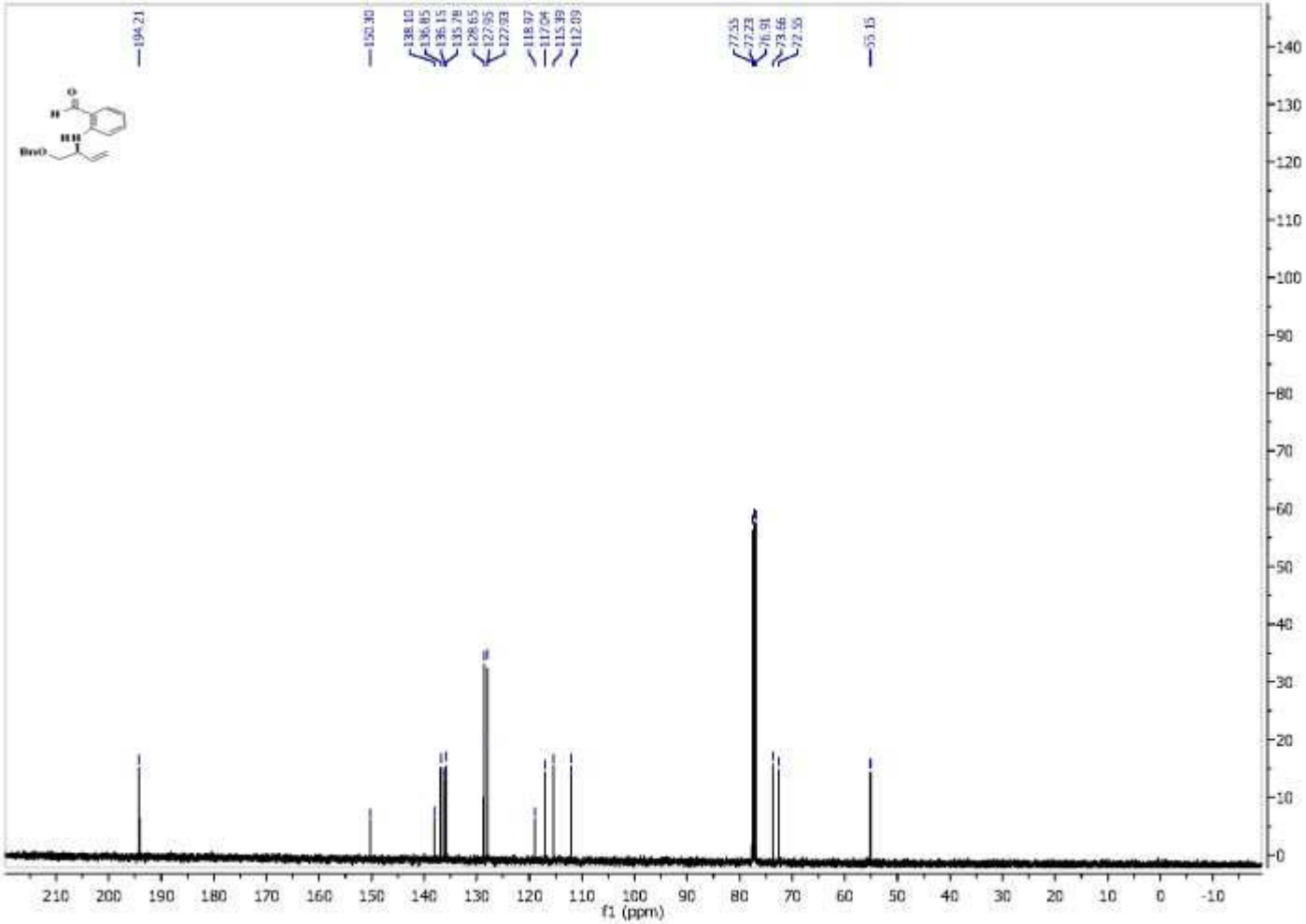

Figure A346 100 MHz 13C NMR ($CDCl_3$) Spectra of Compound **229z**

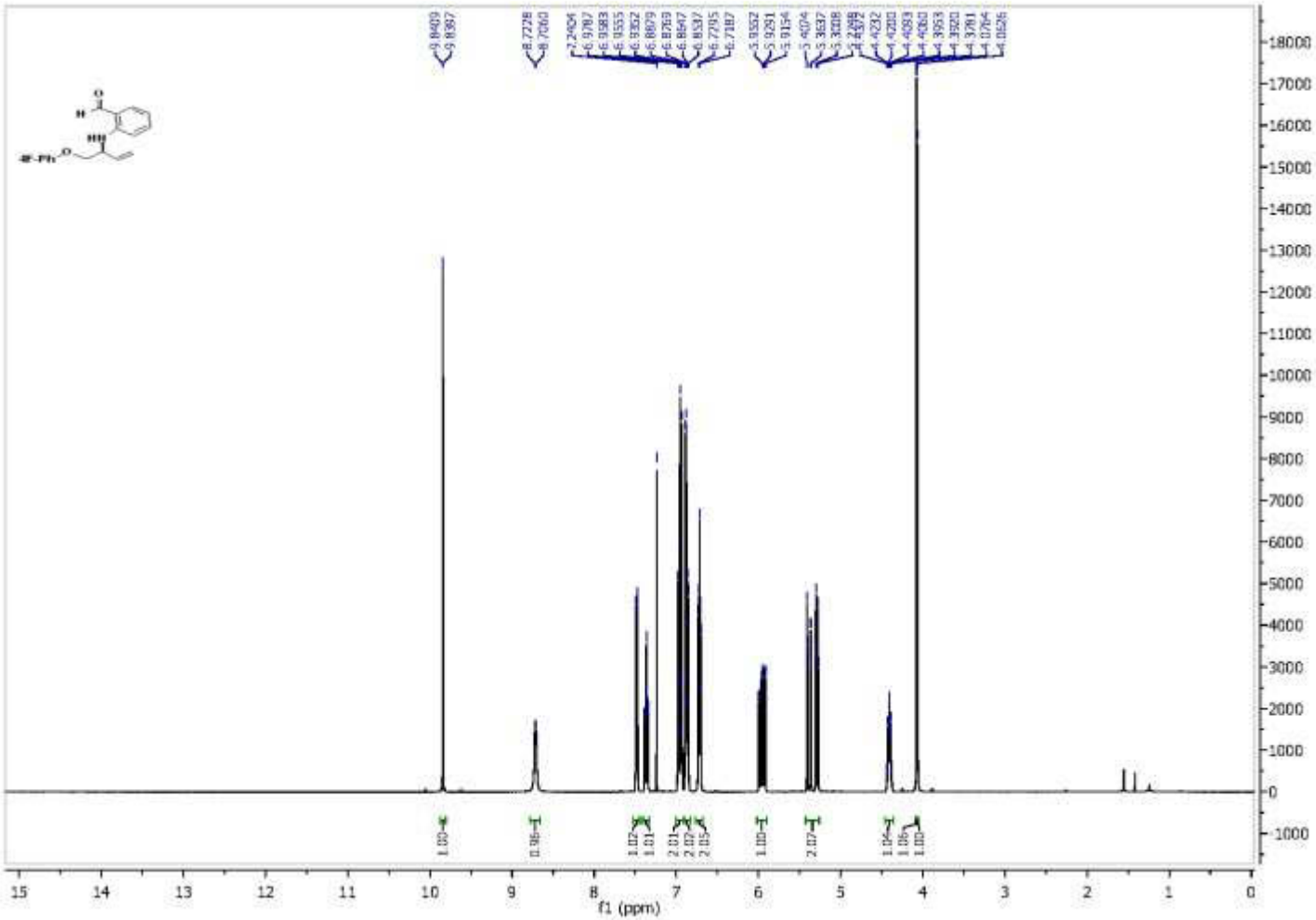

Figure A347 400 MHz 1H NMR ($CDCl_3$) Spectra of Compound **375z**

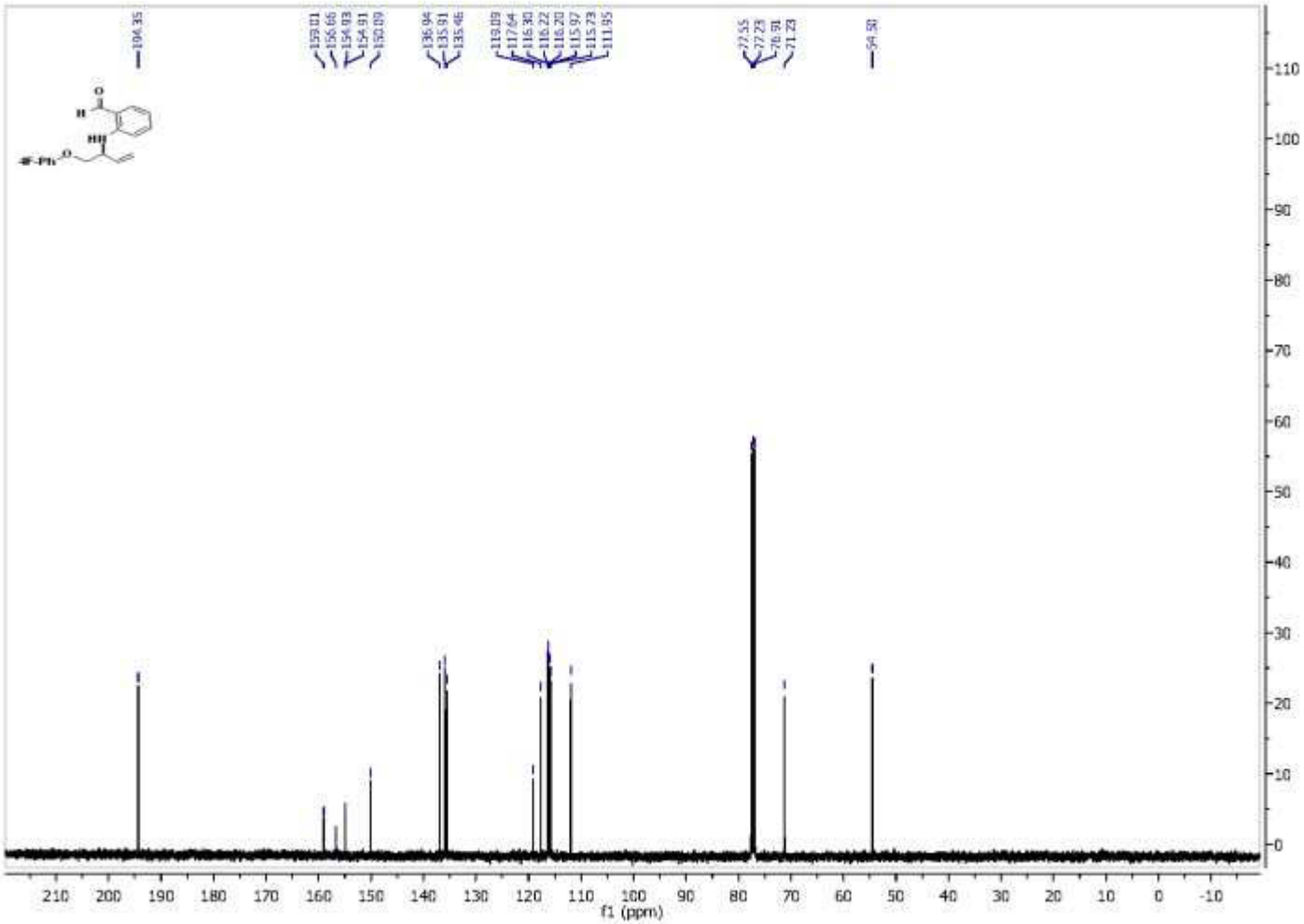

Figure A348 100 MHz 13C NMR ($CDCl_3$) Spectra of Compound **375z**

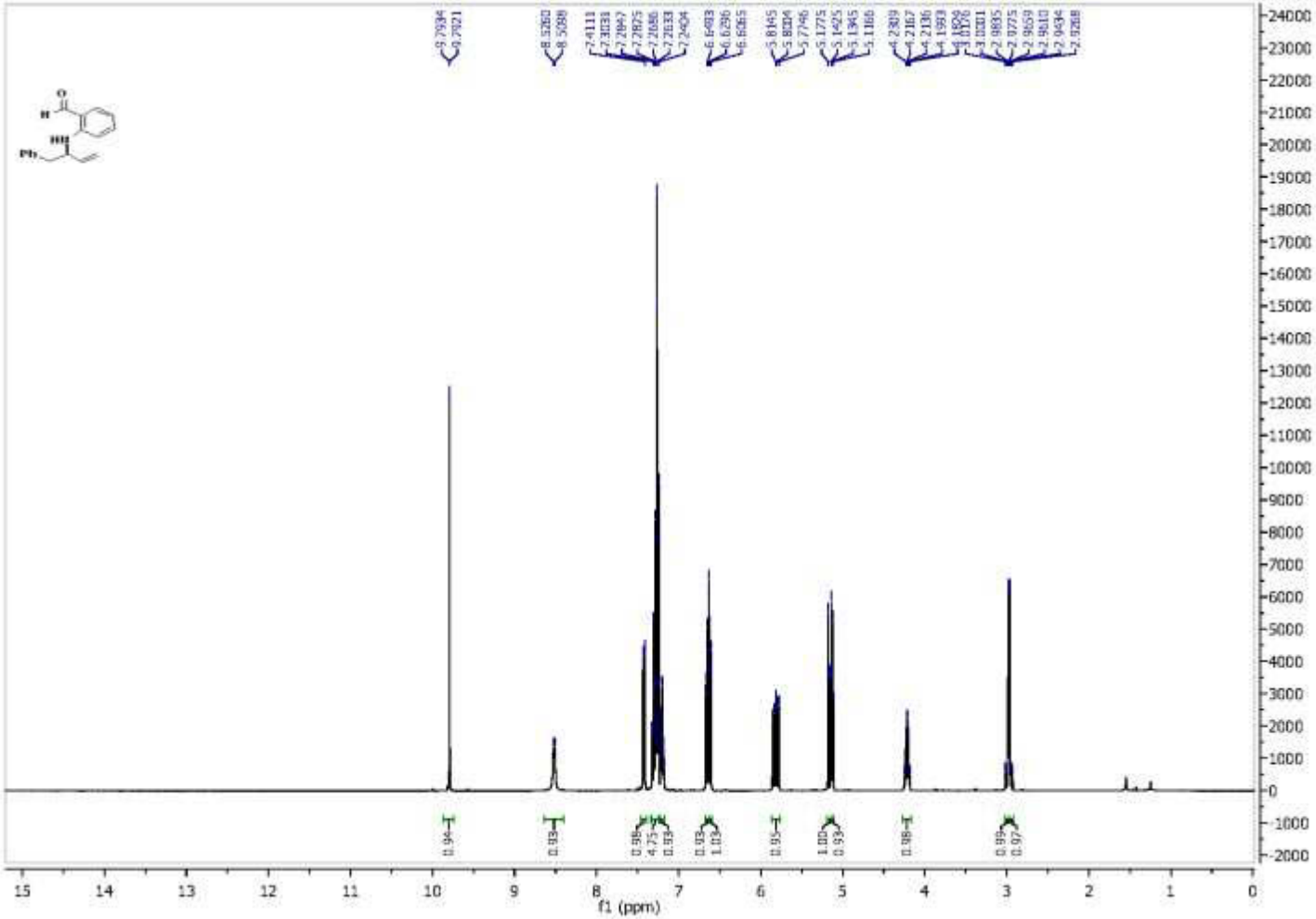

Figure A349 400 MHz 1H NMR ($CDCl_3$) Spectra of Compound **230z**

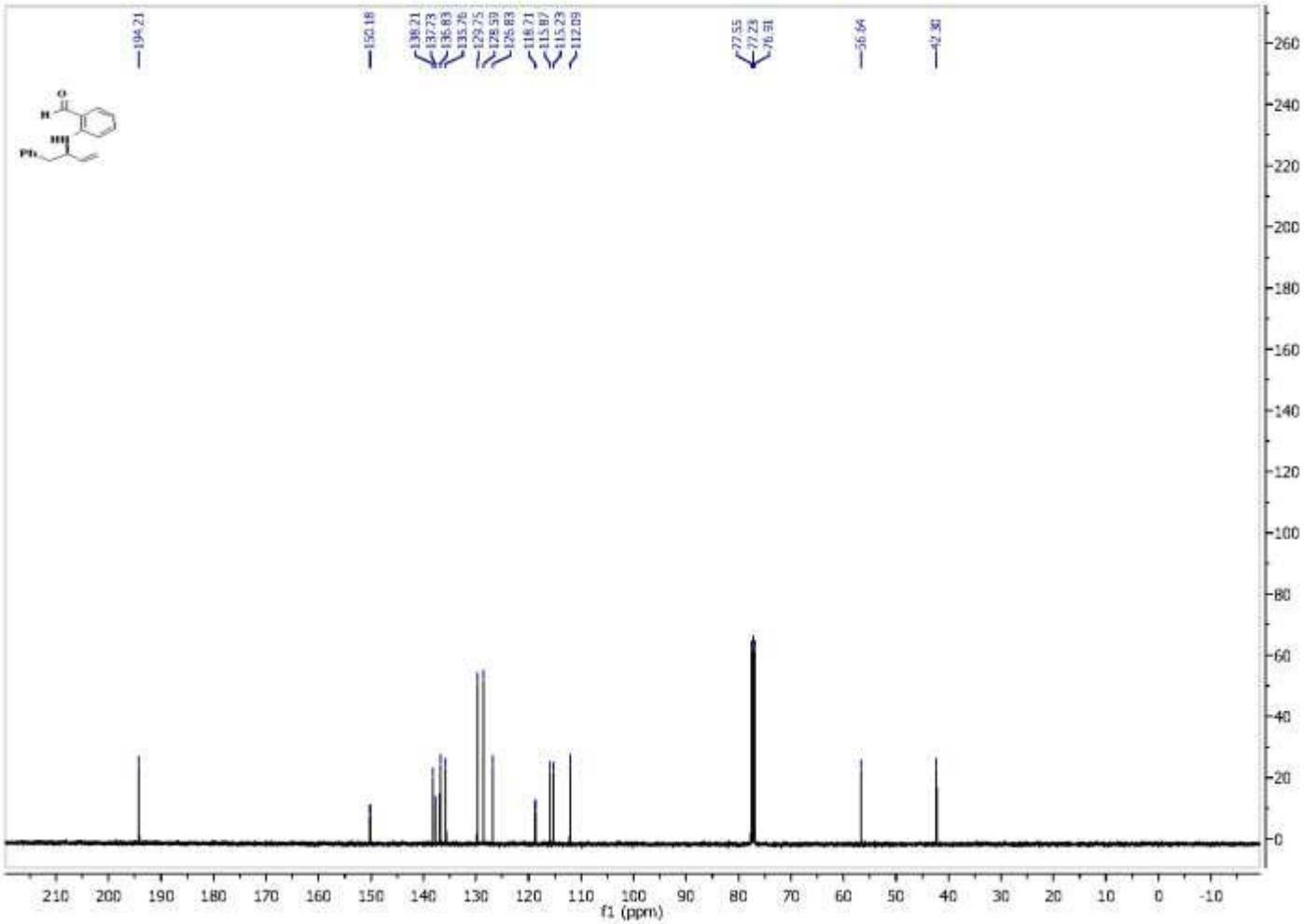

Figure A350 100 MHz 13C NMR ($CDCl_3$) Spectra of Compound **230z**

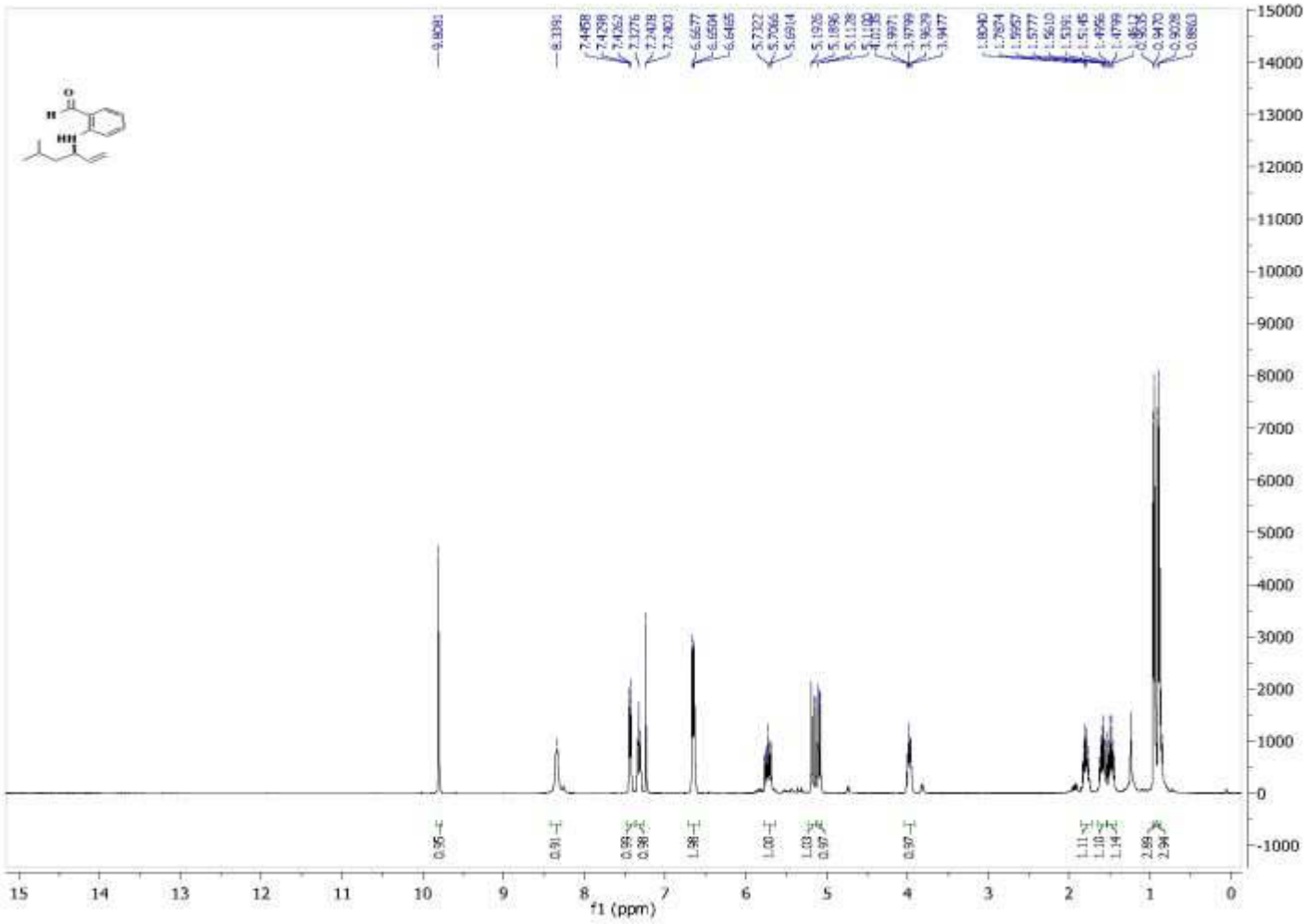

Figure A351 400 MHz 1H NMR ($CDCl_3$) Spectra of Compound **311z**

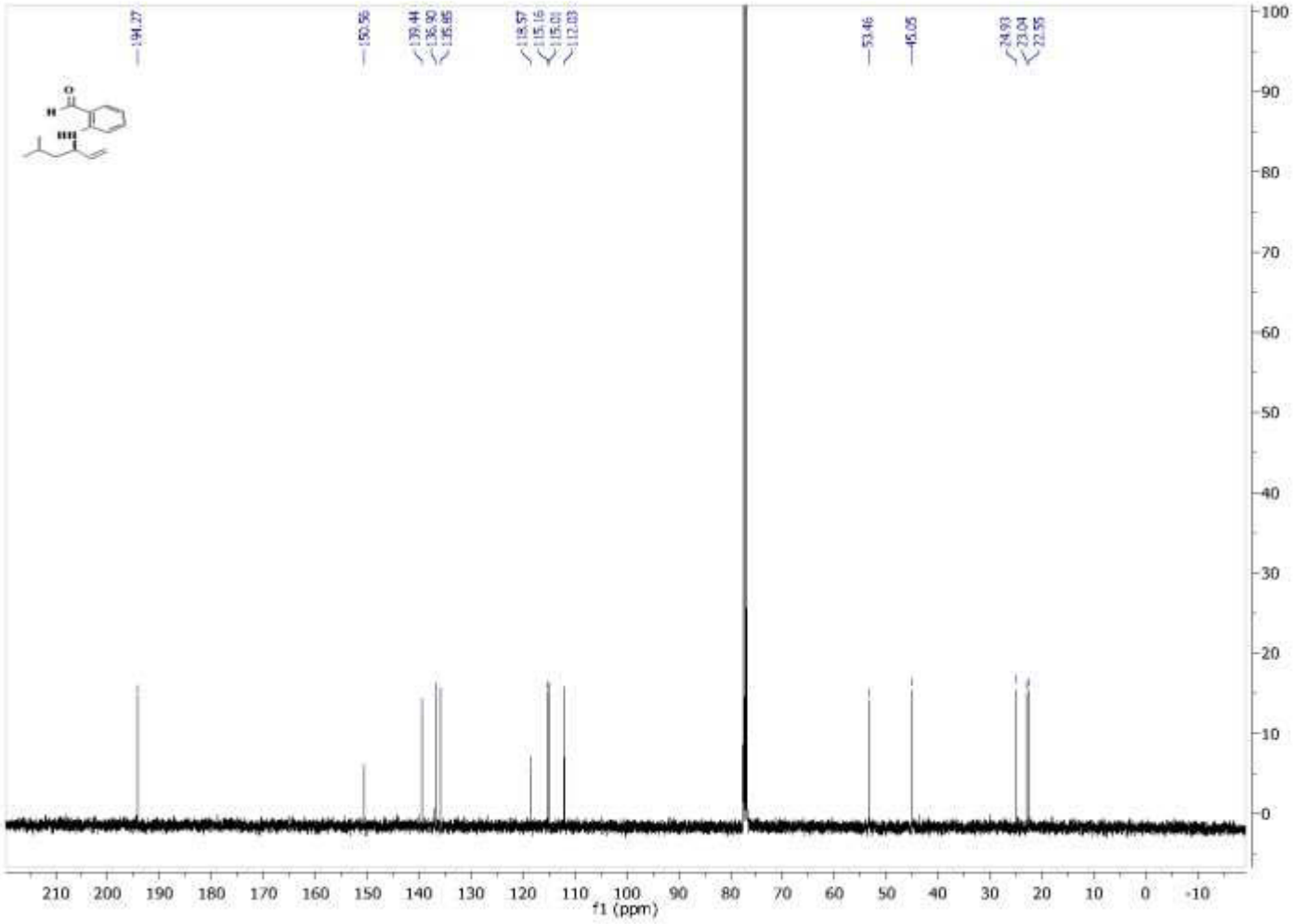

Figure A352 100 MHz 13C NMR ($CDCl_3$) Spectra of Compound **311z**

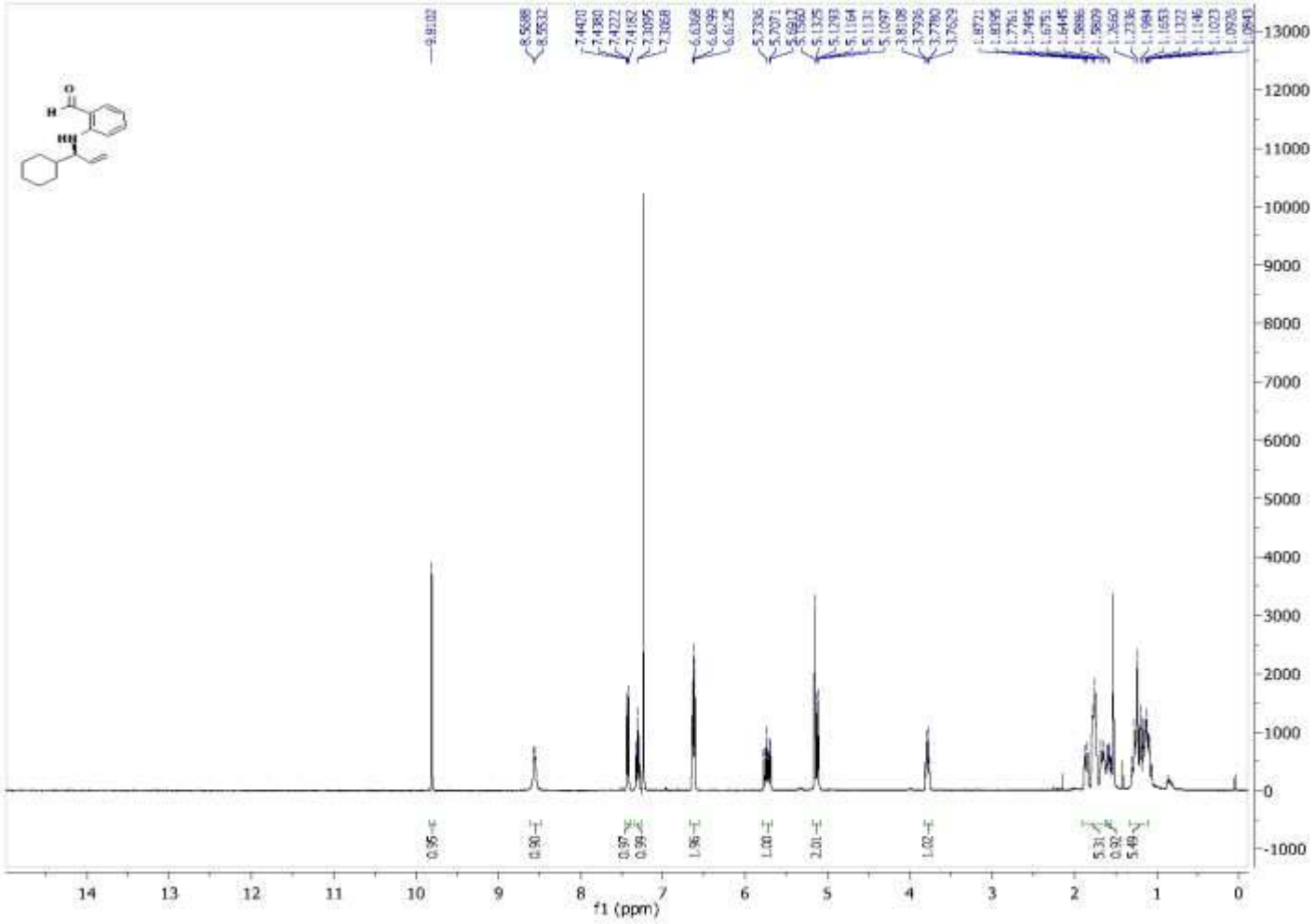

Figure A353 400 MHz 1H NMR ($CDCl_3$) Spectra of Compound **231z**

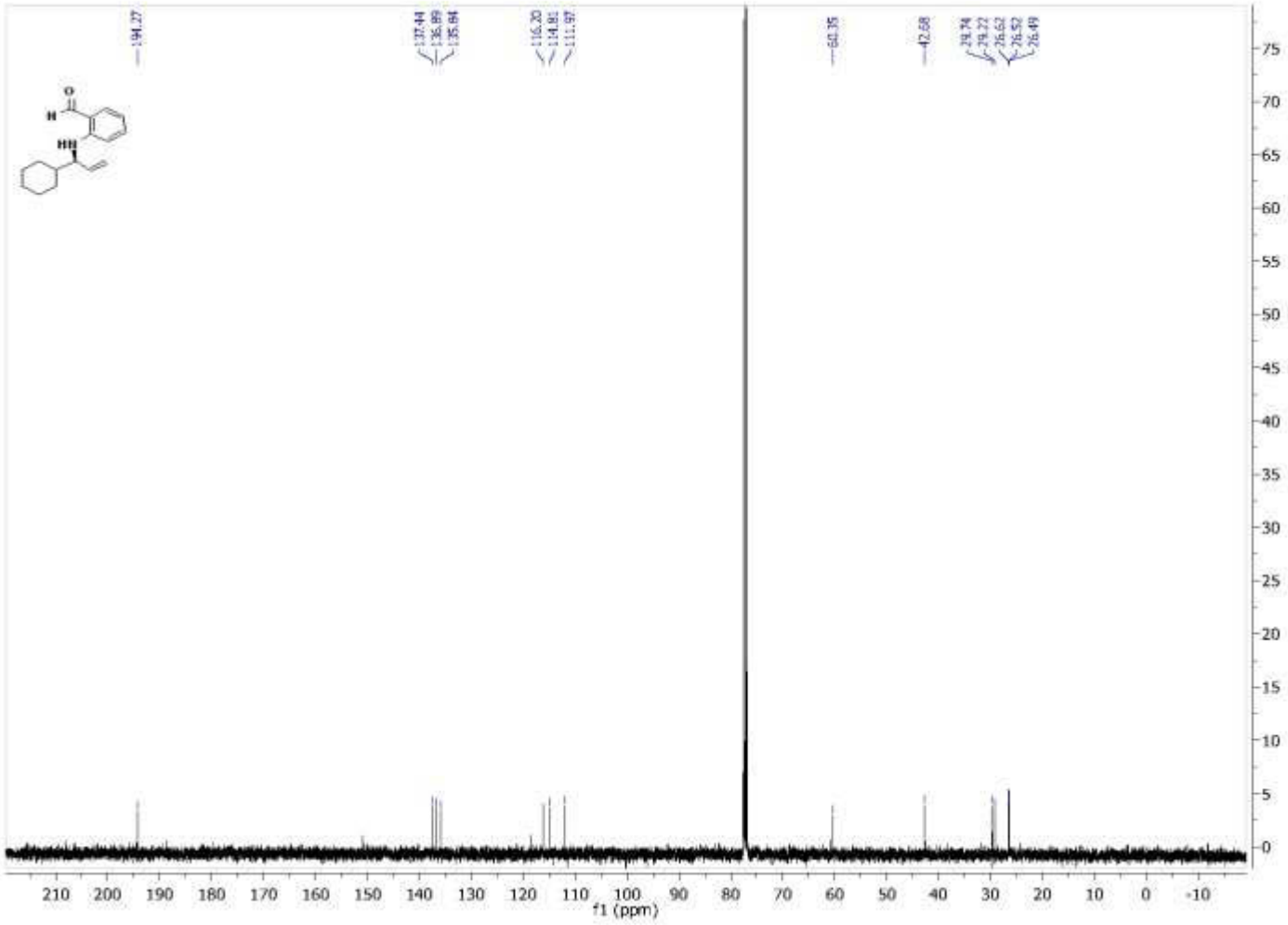

Figure A354 100 MHz 13C NMR ($CDCl_3$) Spectra of Compound **231z**

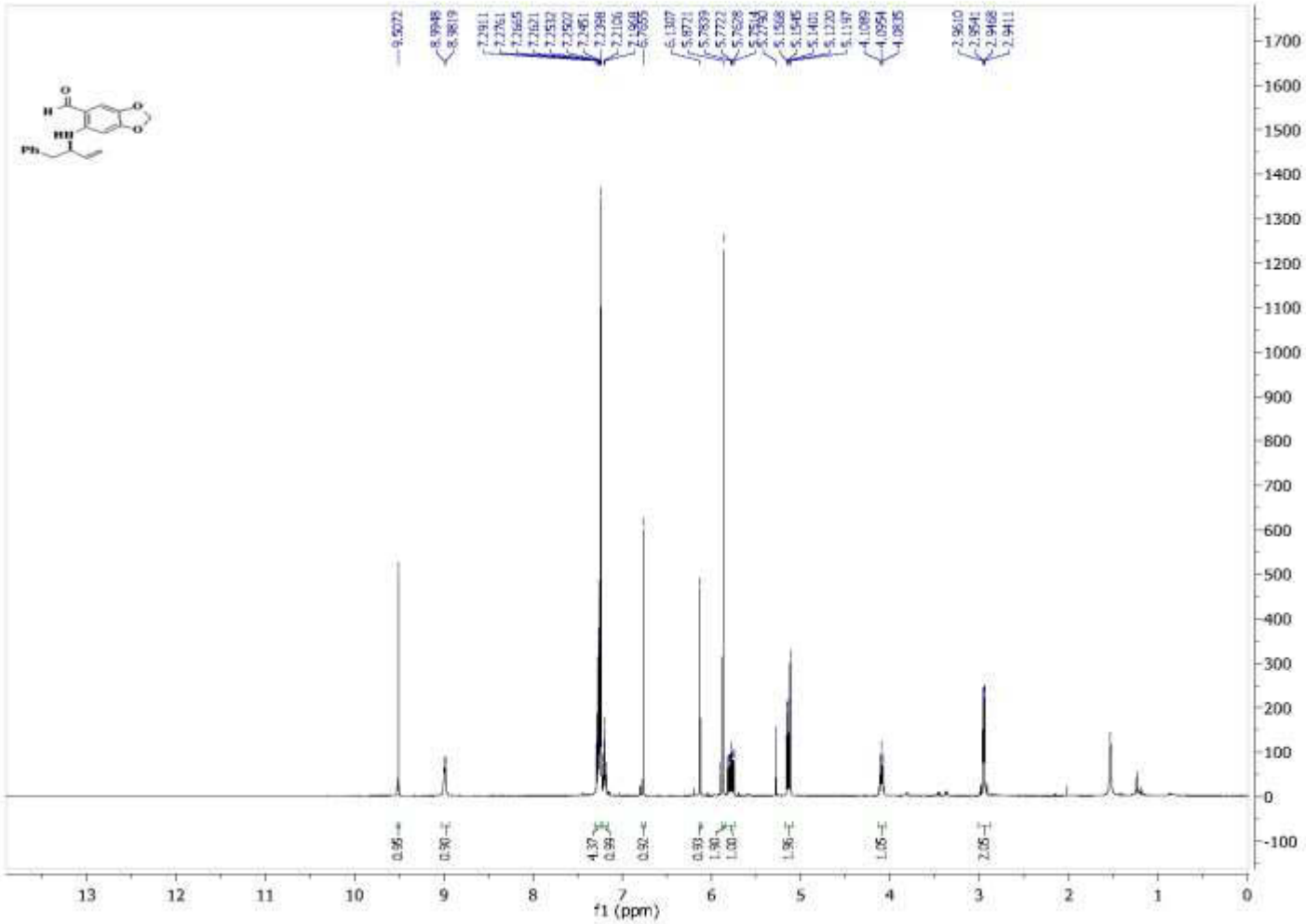

Figure A355 400 MHz 1H NMR ($CDCl_3$) Spectra of Compound **230za**

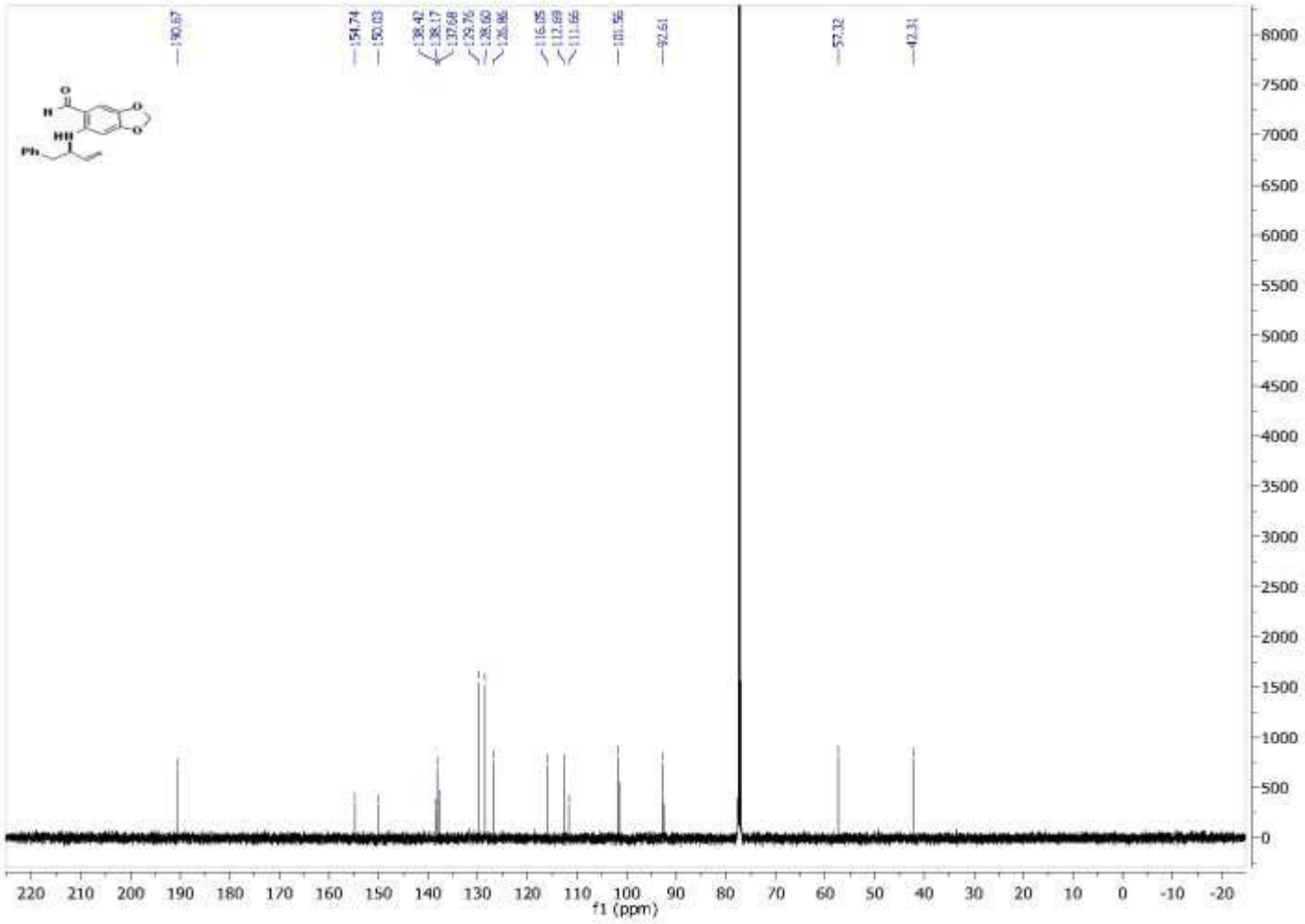

Figure A356 100 MHz 13C NMR ($CDCl_3$) Spectra of Compound **230za**

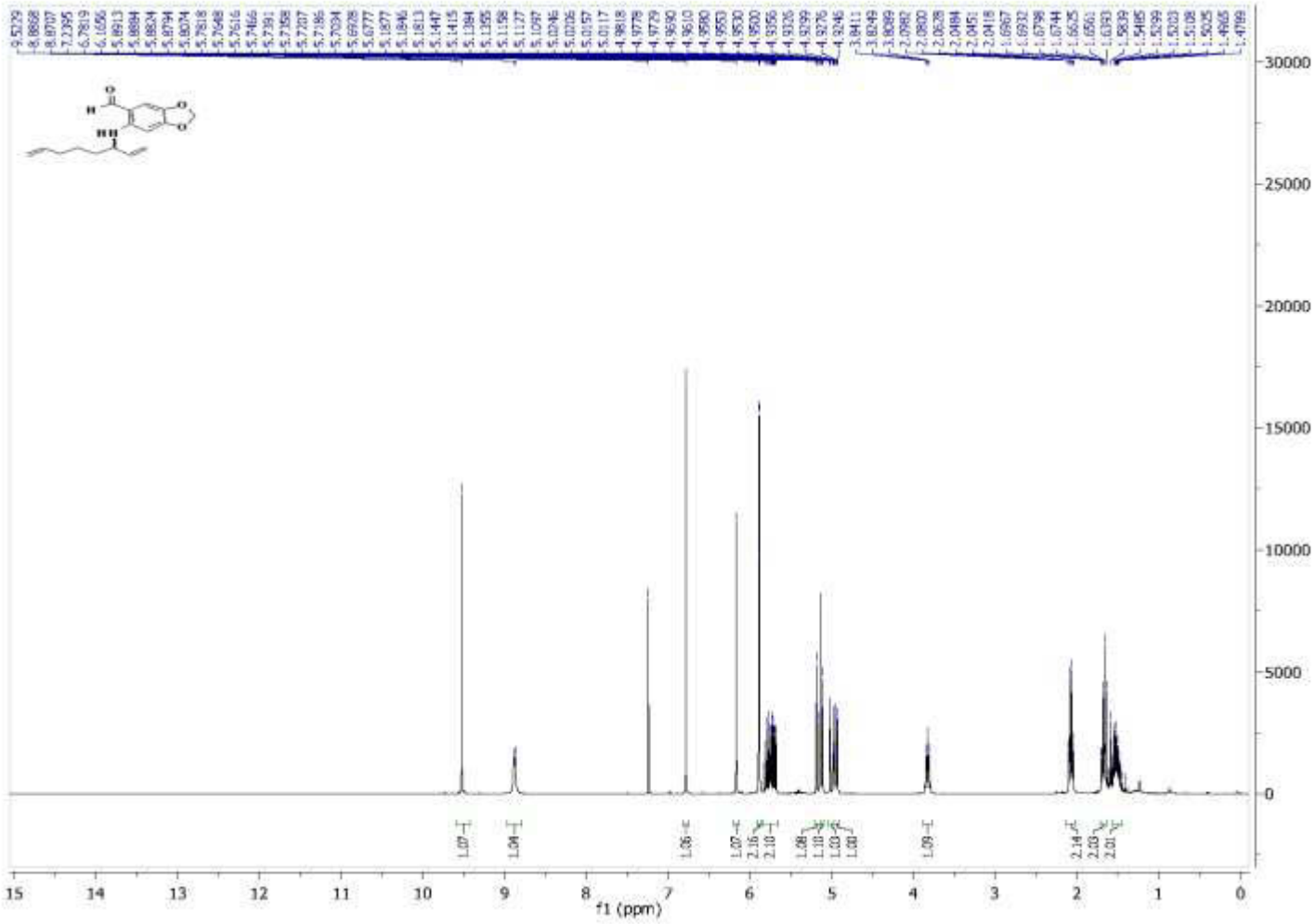

Figure A357 400 MHz 1H NMR ($CDCl_3$) Spectra of Compound **376za**

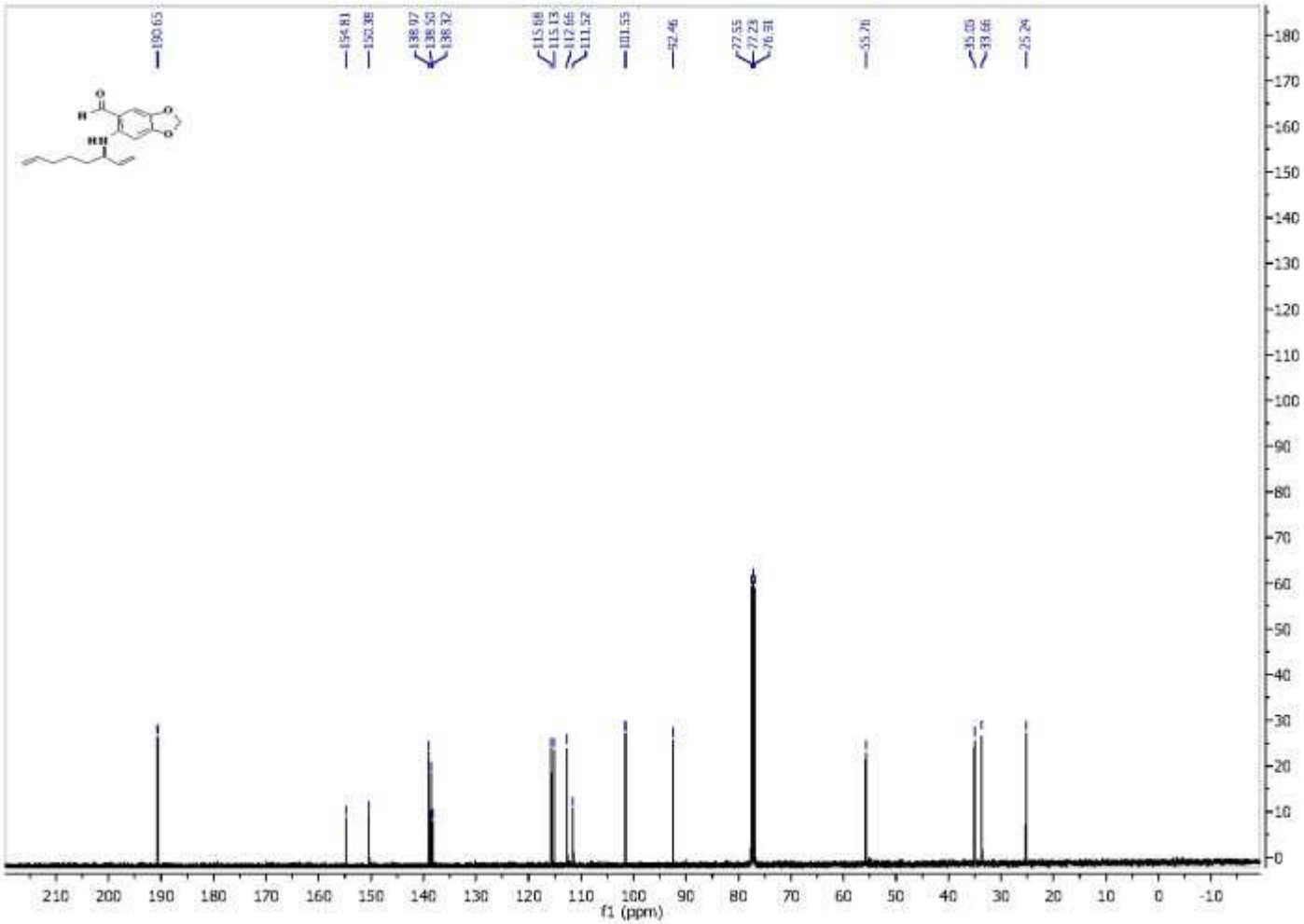

Figure A358 100 MHz 13C NMR ($CDCl_3$) Spectra of Compound **376za**

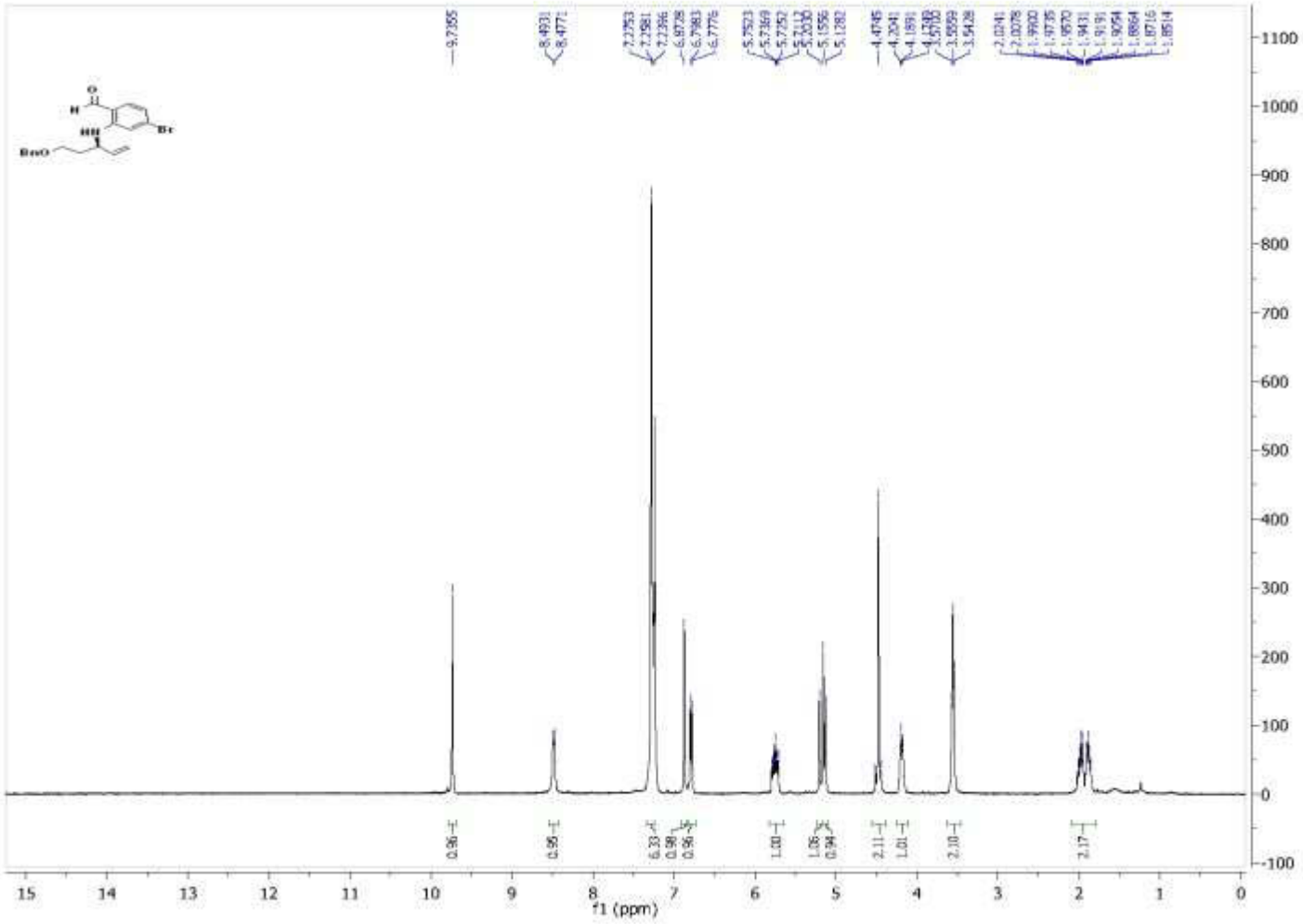

Figure A359 400 MHz 1H NMR ($CDCl_3$) Spectra of Compound **310zb**

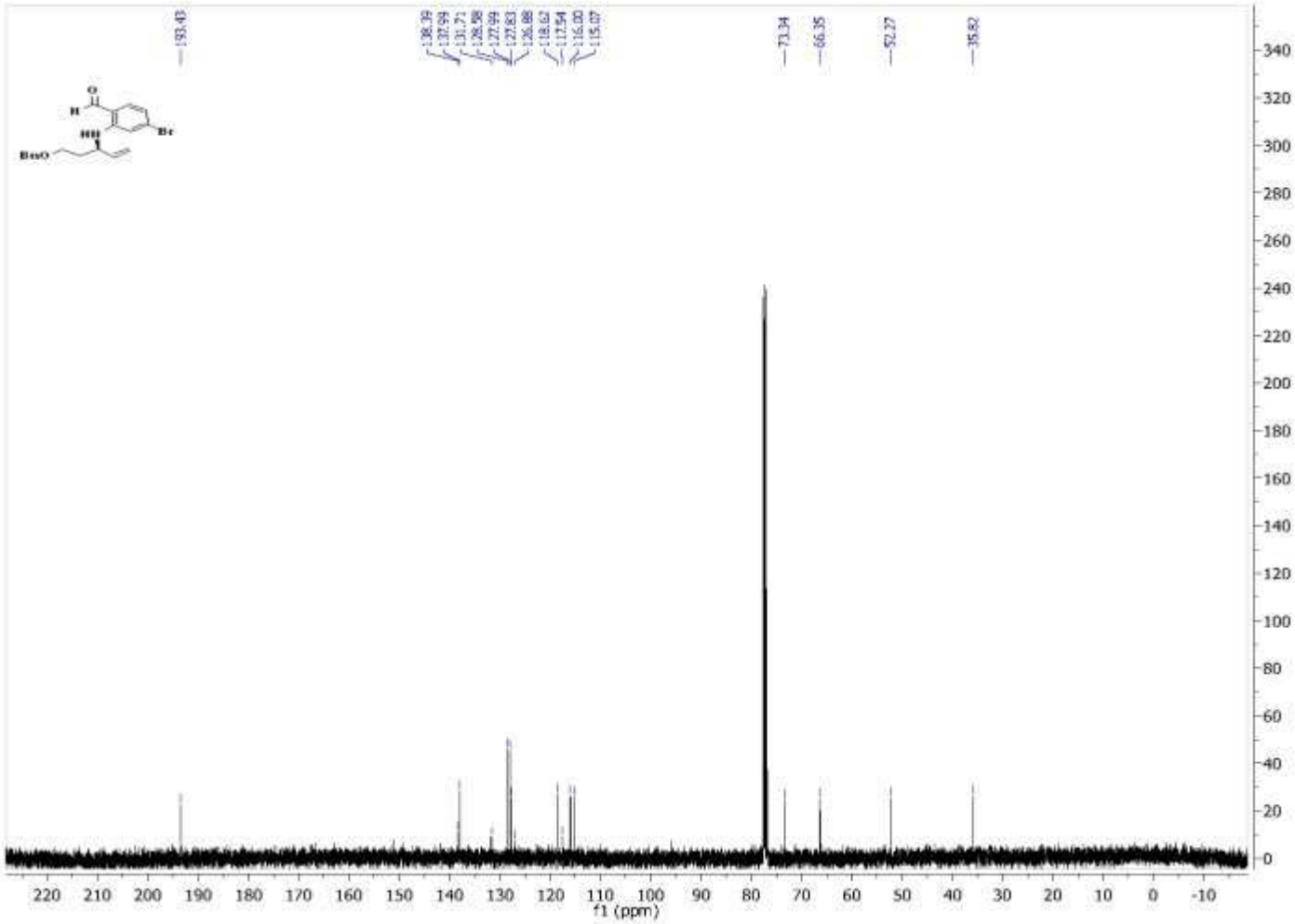

Figure A360 100 MHz 13C NMR ($CDCl_3$) Spectra of Compound **310zb**

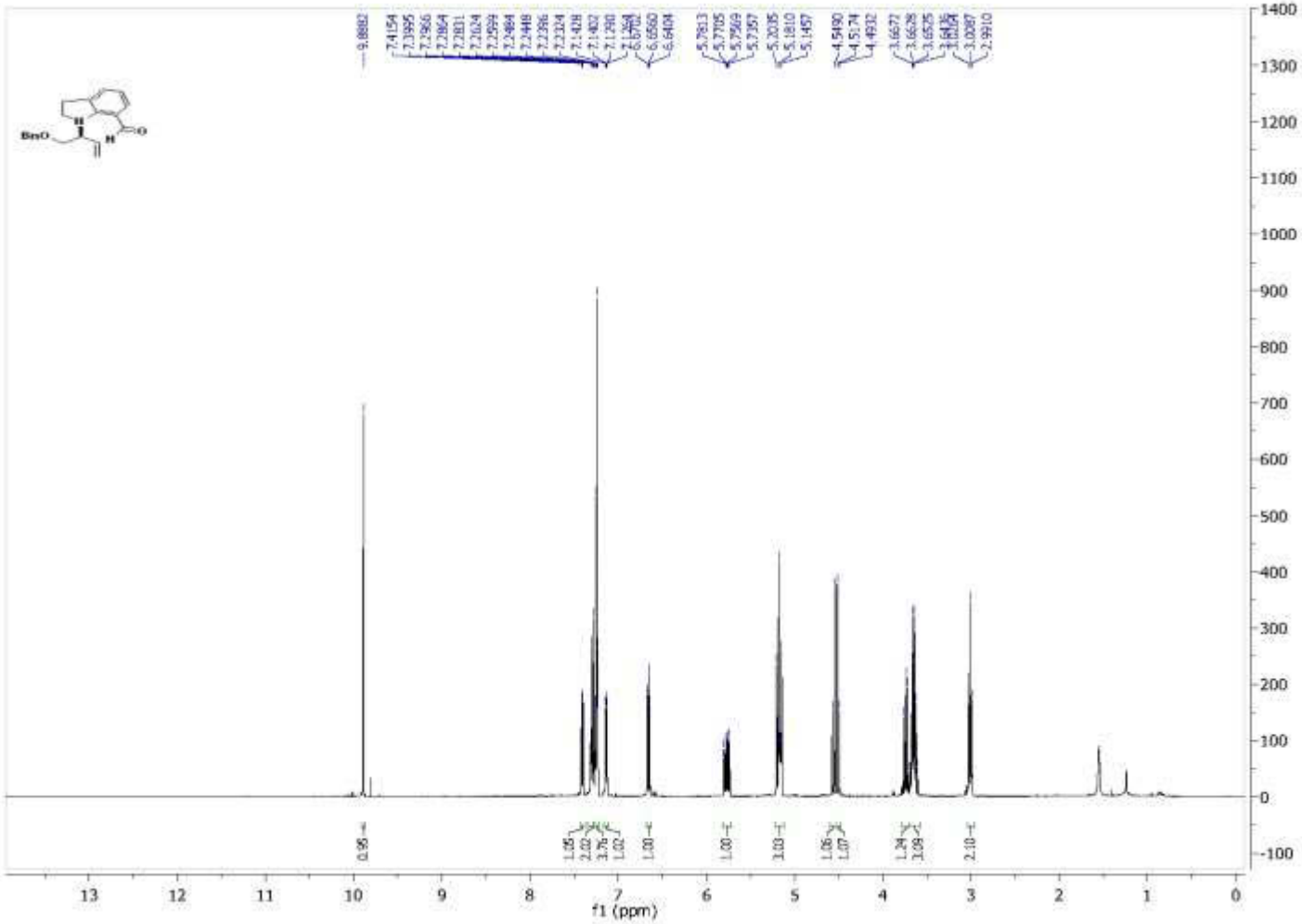

Figure A361 400 MHz 1H NMR ($CDCl_3$) Spectra of Compound **229zc**

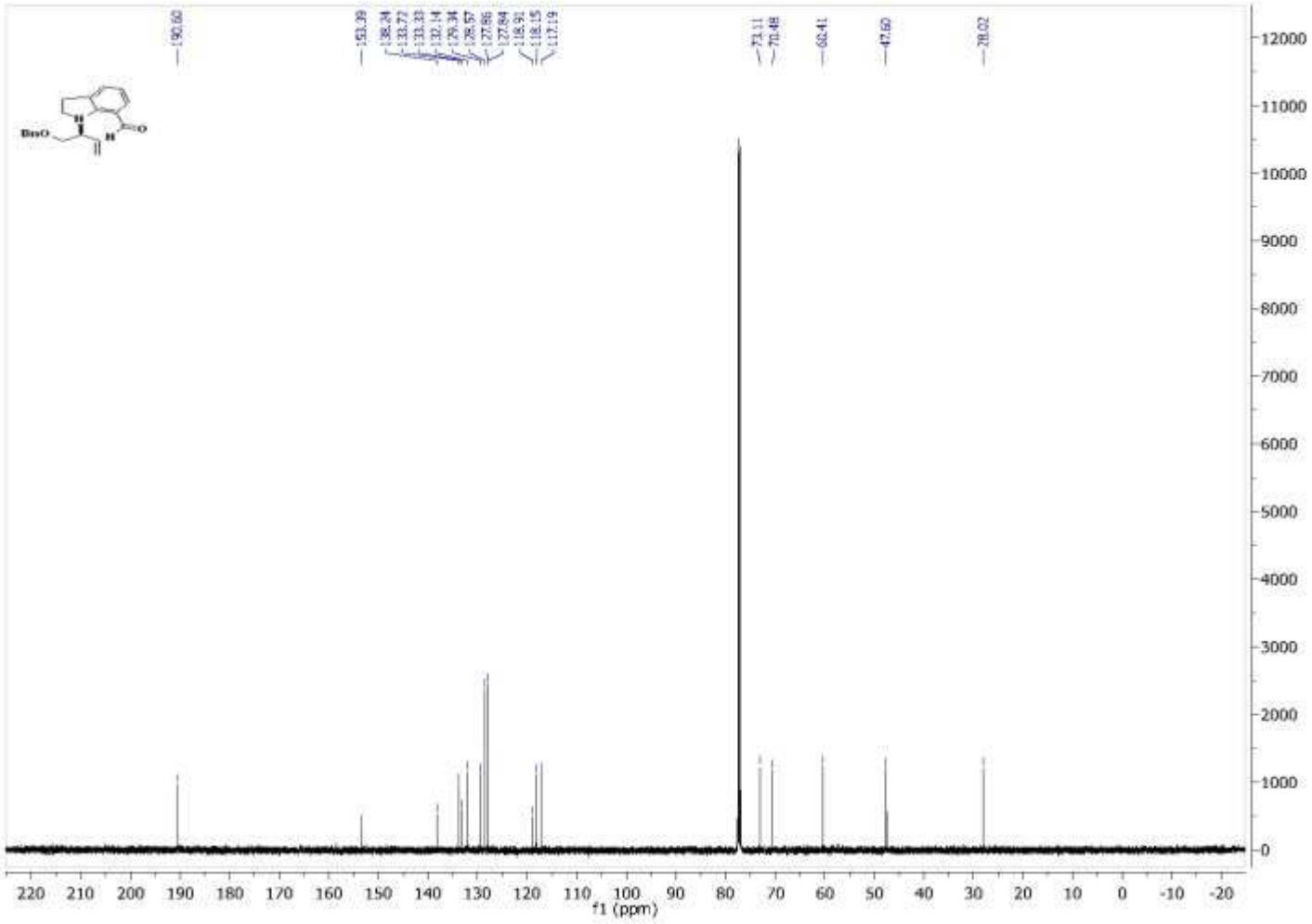

Figure A362 100 MHz 13C NMR ($CDCl_3$) Spectra of Compound **229zc**

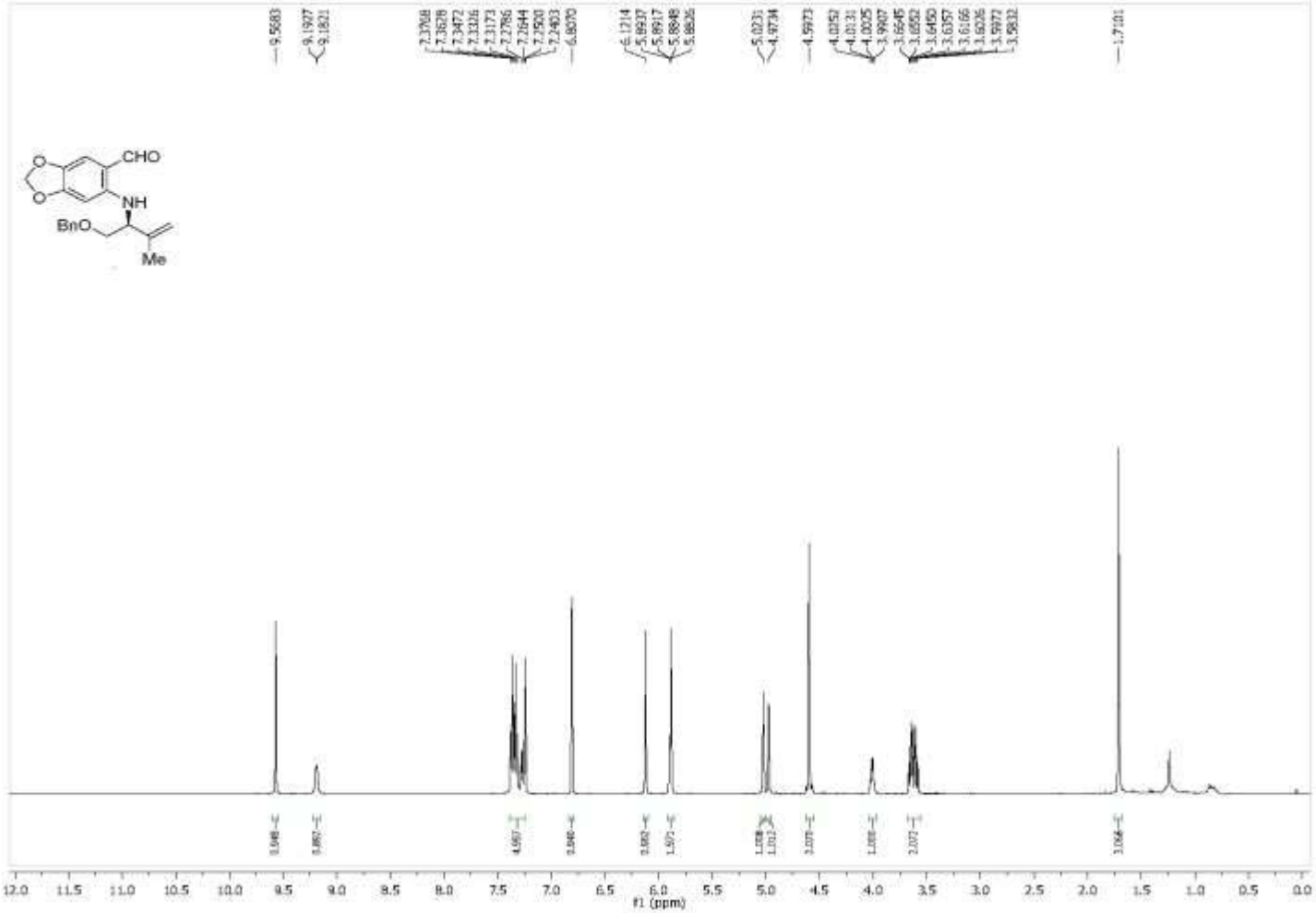

Figure A363 400 MHz 1H NMR ($CDCl_3$) Spectra of Compound **377za**

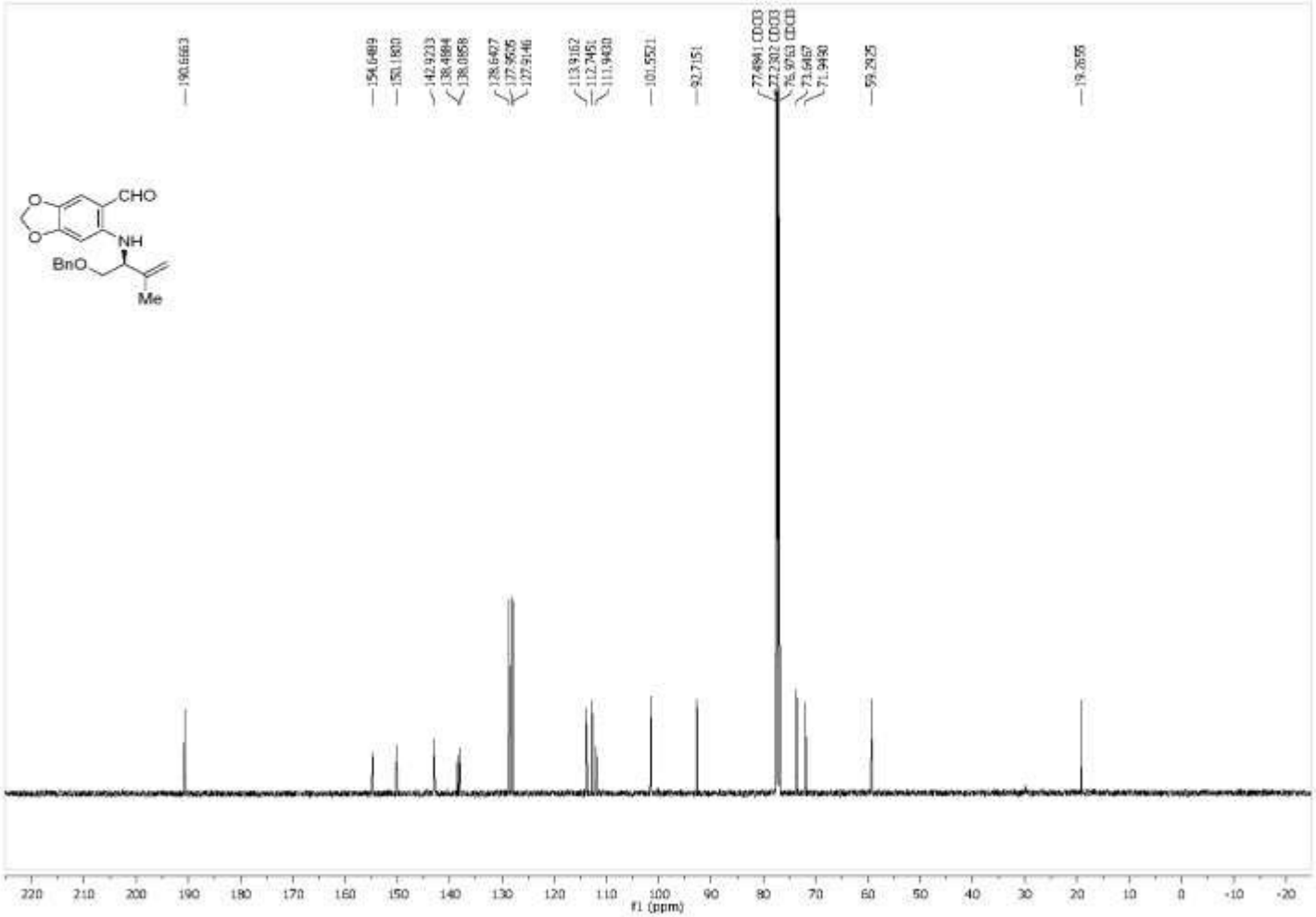

Figure A364 100 MHz 13C NMR ($CDCl_3$) Spectra of Compound **377za**

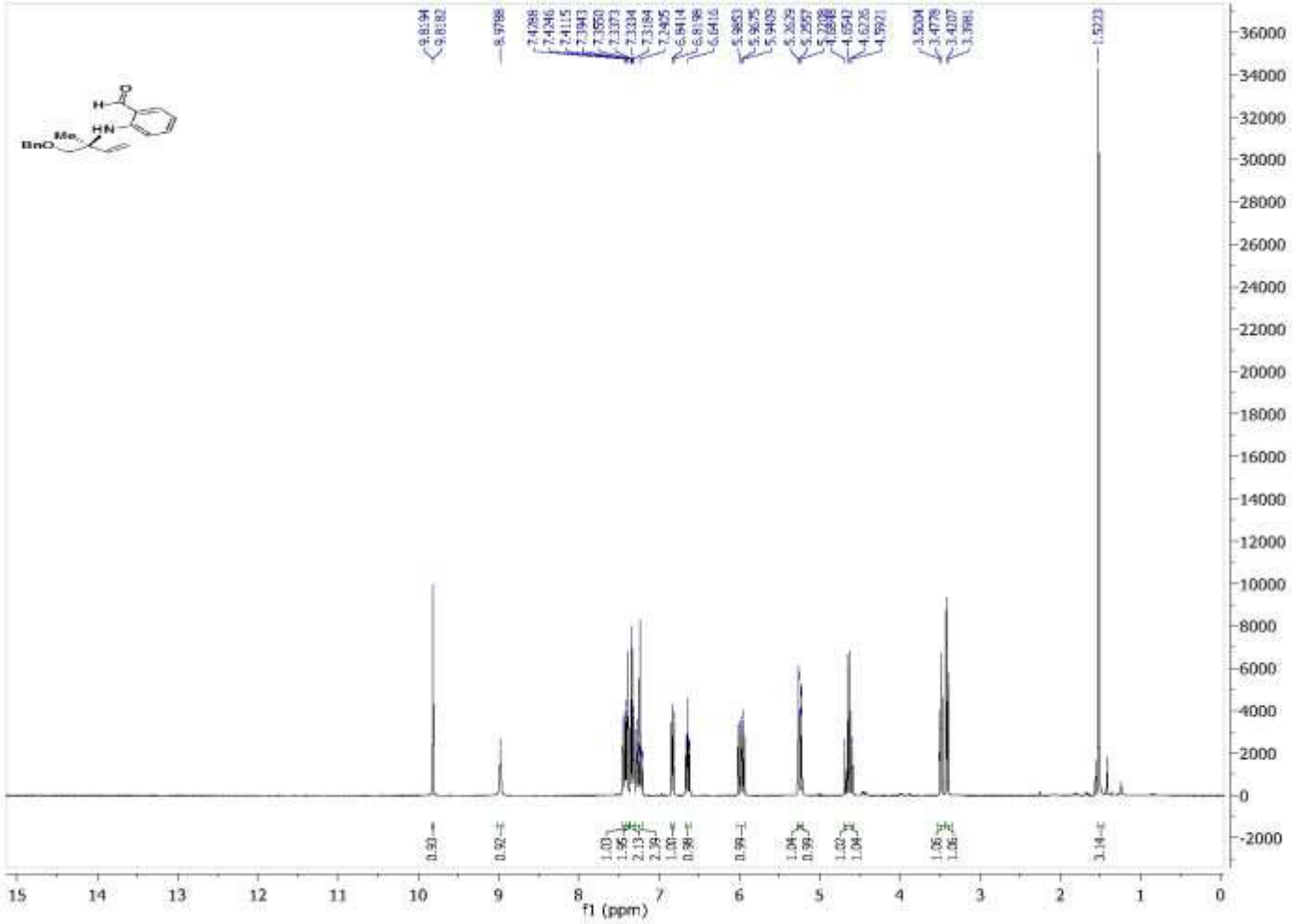

Figure A365 400 MHz 1H NMR ($CDCl_3$) Spectra of Compound **390**

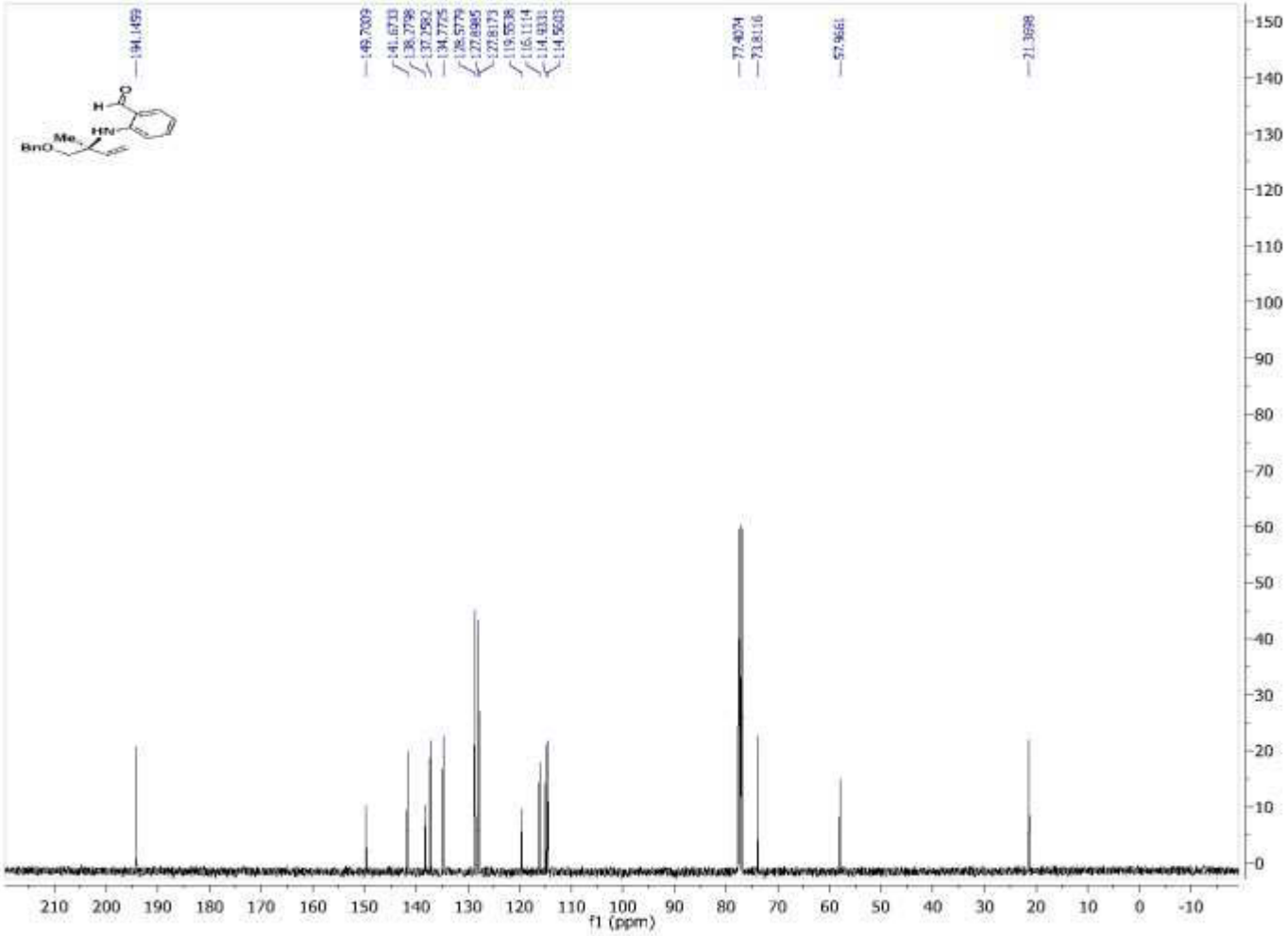

Figure A366 100 MHz 13C NMR ($CDCl_3$) Spectra of Compound **390**

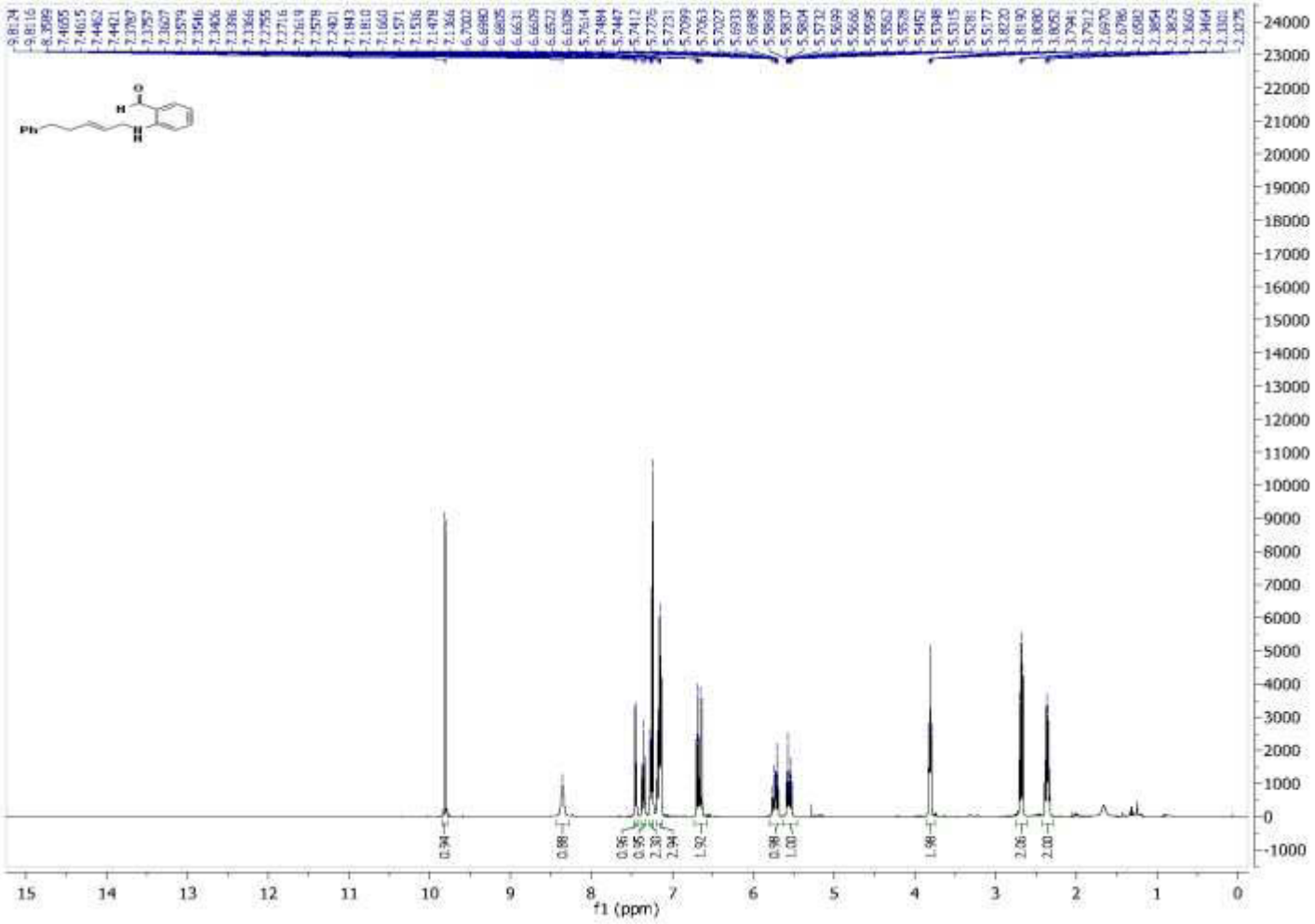

Figure A367 400 MHz 1H NMR ($CDCl_3$) Spectra of Compound **371**

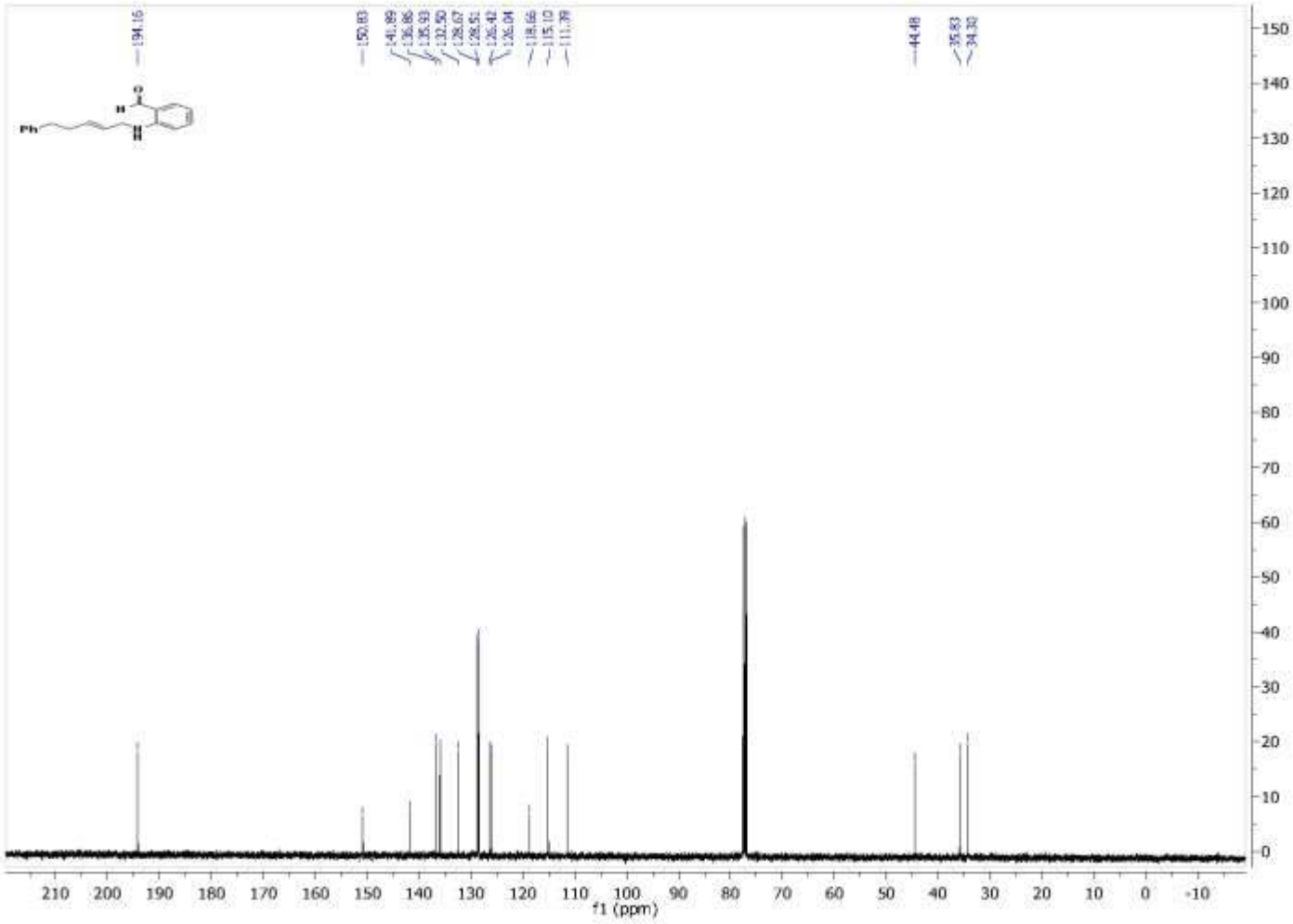

Figure A368 100 MHz 13C NMR ($CDCl_3$) Spectra of Compound **371**

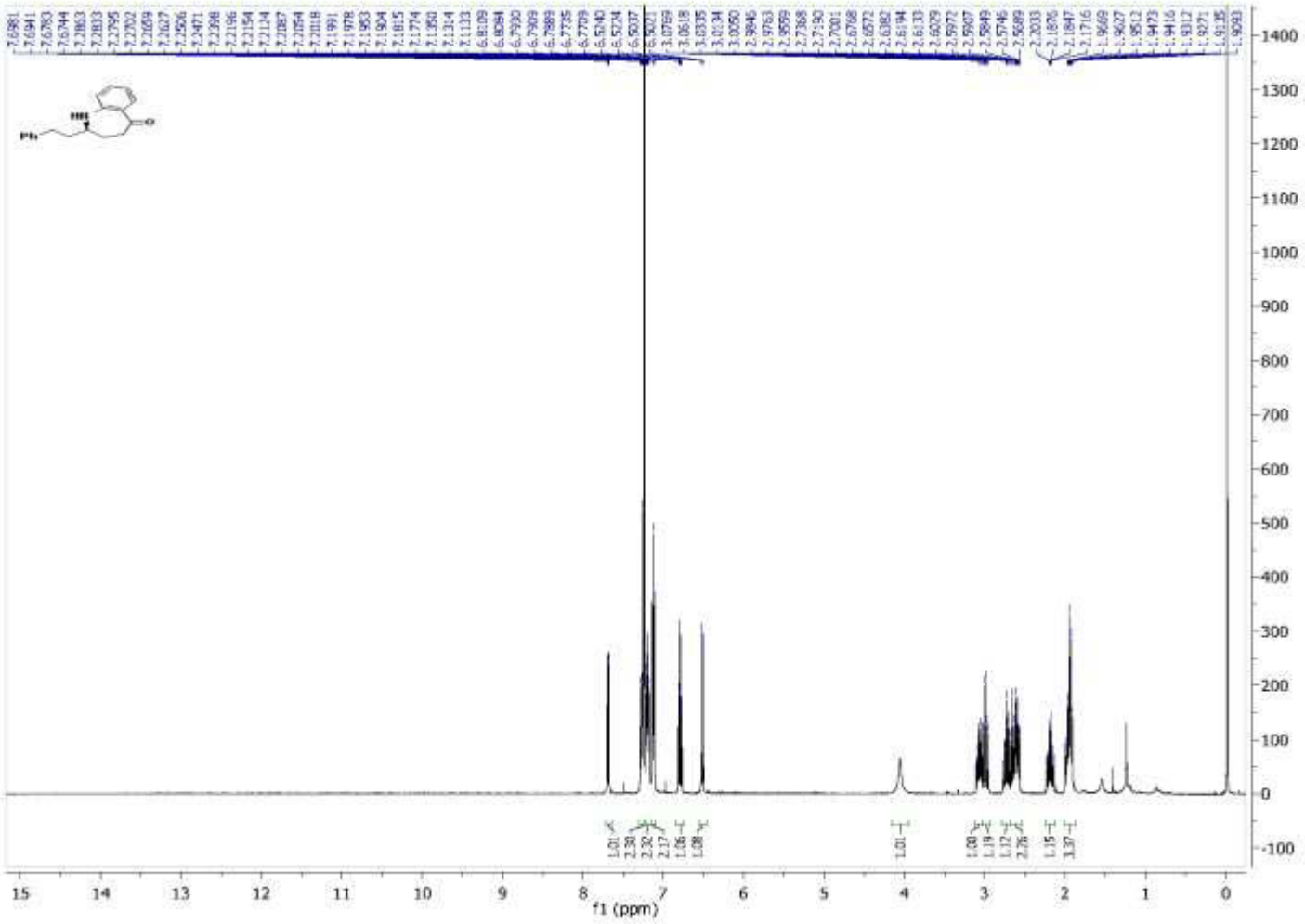

Figure A369 400 MHz 1H NMR ($CDCl_3$) Spectra of Compound **372**

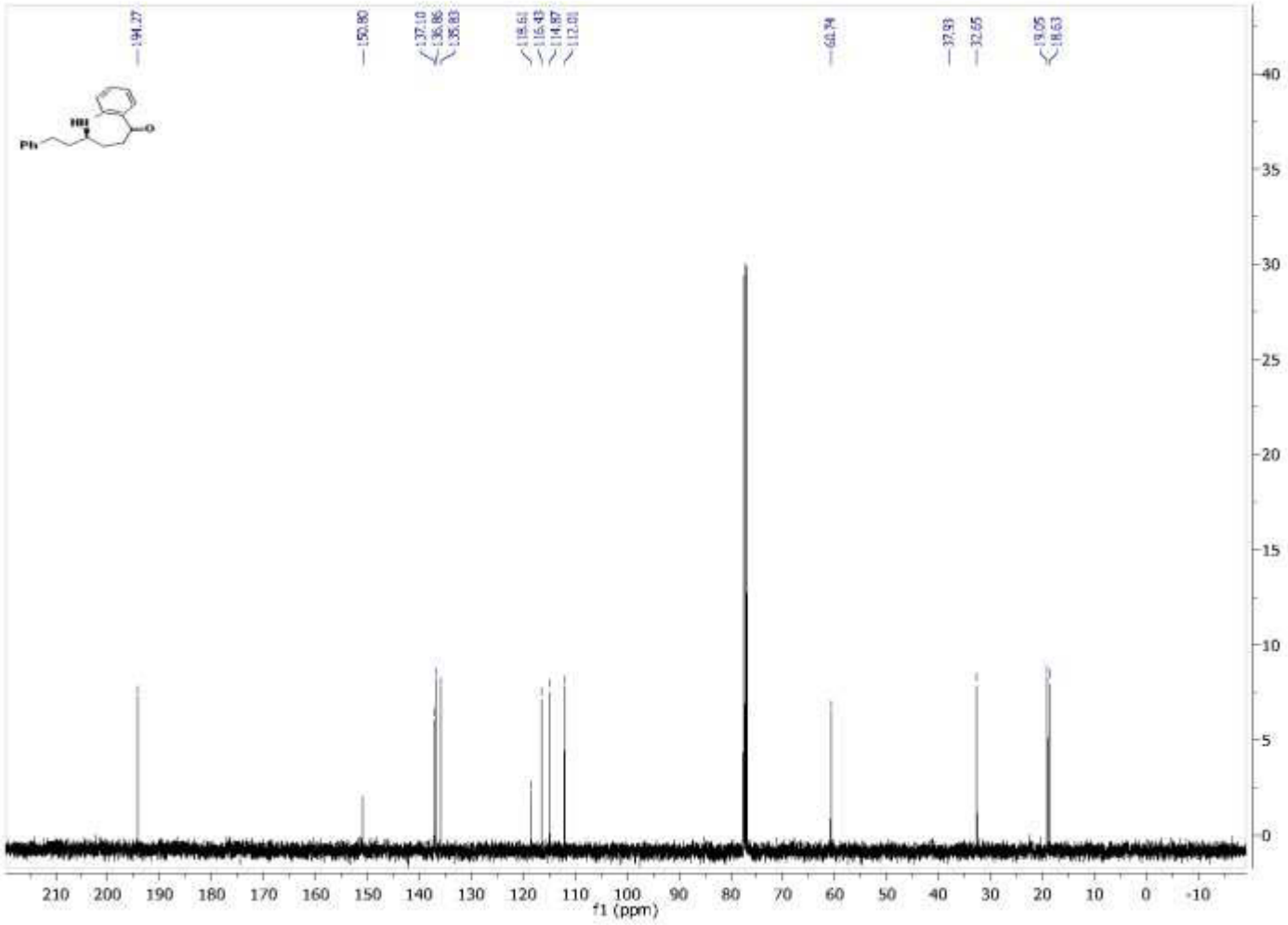

Figure A370 100 MHz 13C NMR ($CDCl_3$) Spectra of Compound **372**

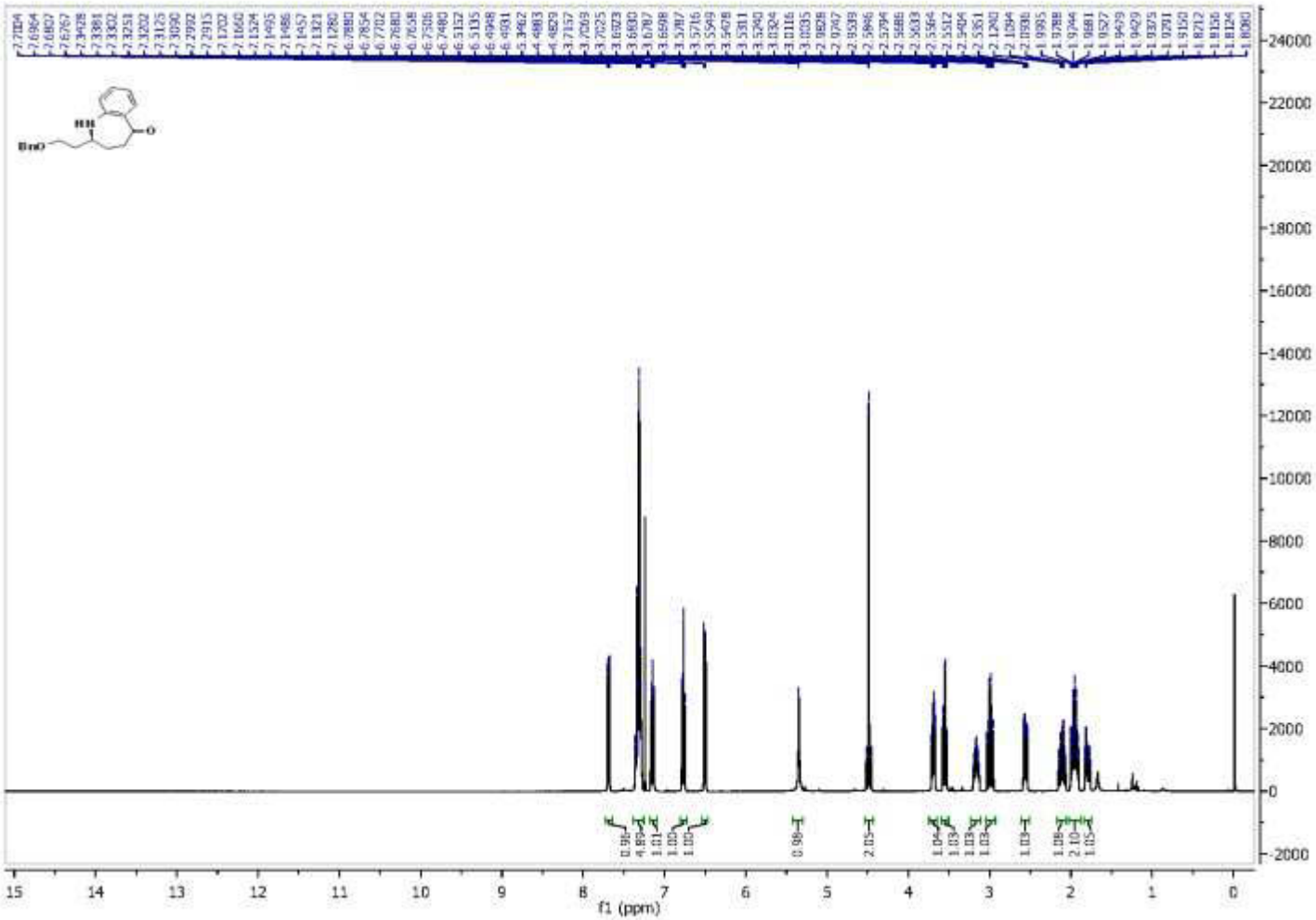

Figure A371 400 MHz 1H NMR ($CDCl_3$) Spectra of Compound **378**

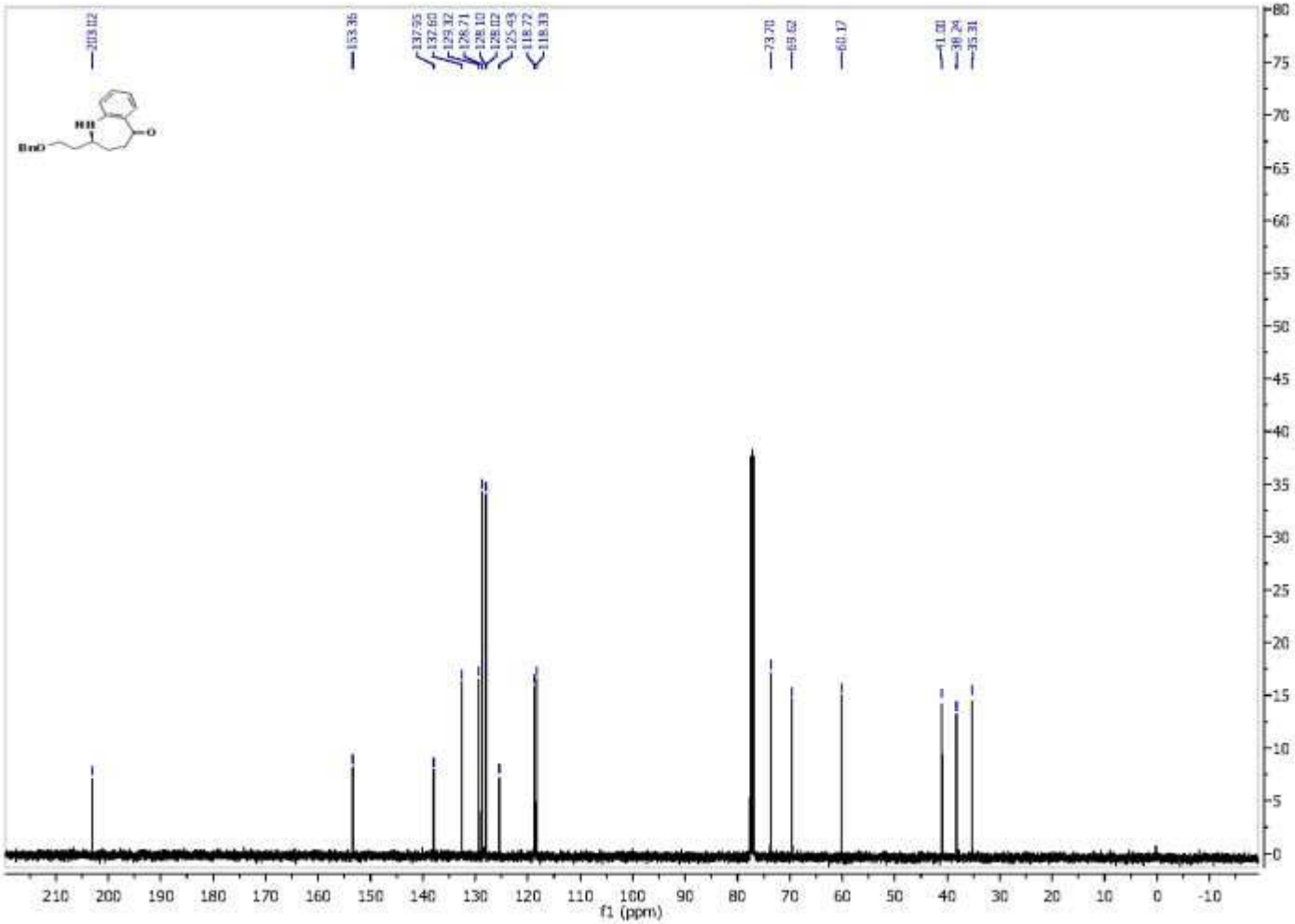

Figure A372 100 MHz 13C NMR ($CDCl_3$) Spectra of Compound **378**

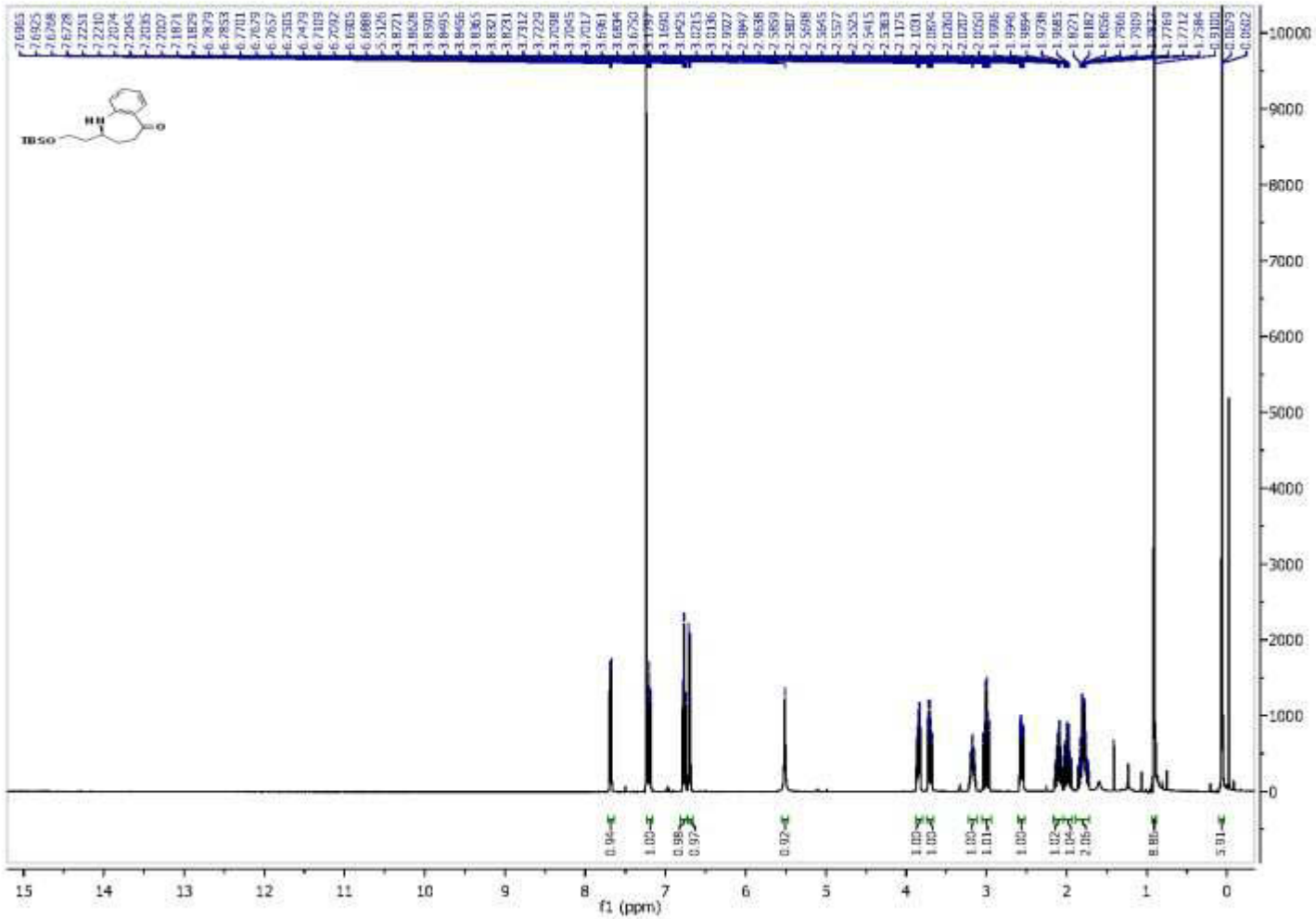

Figure A373 400 MHz 1H NMR ($CDCl_3$) Spectra of Compound **379**

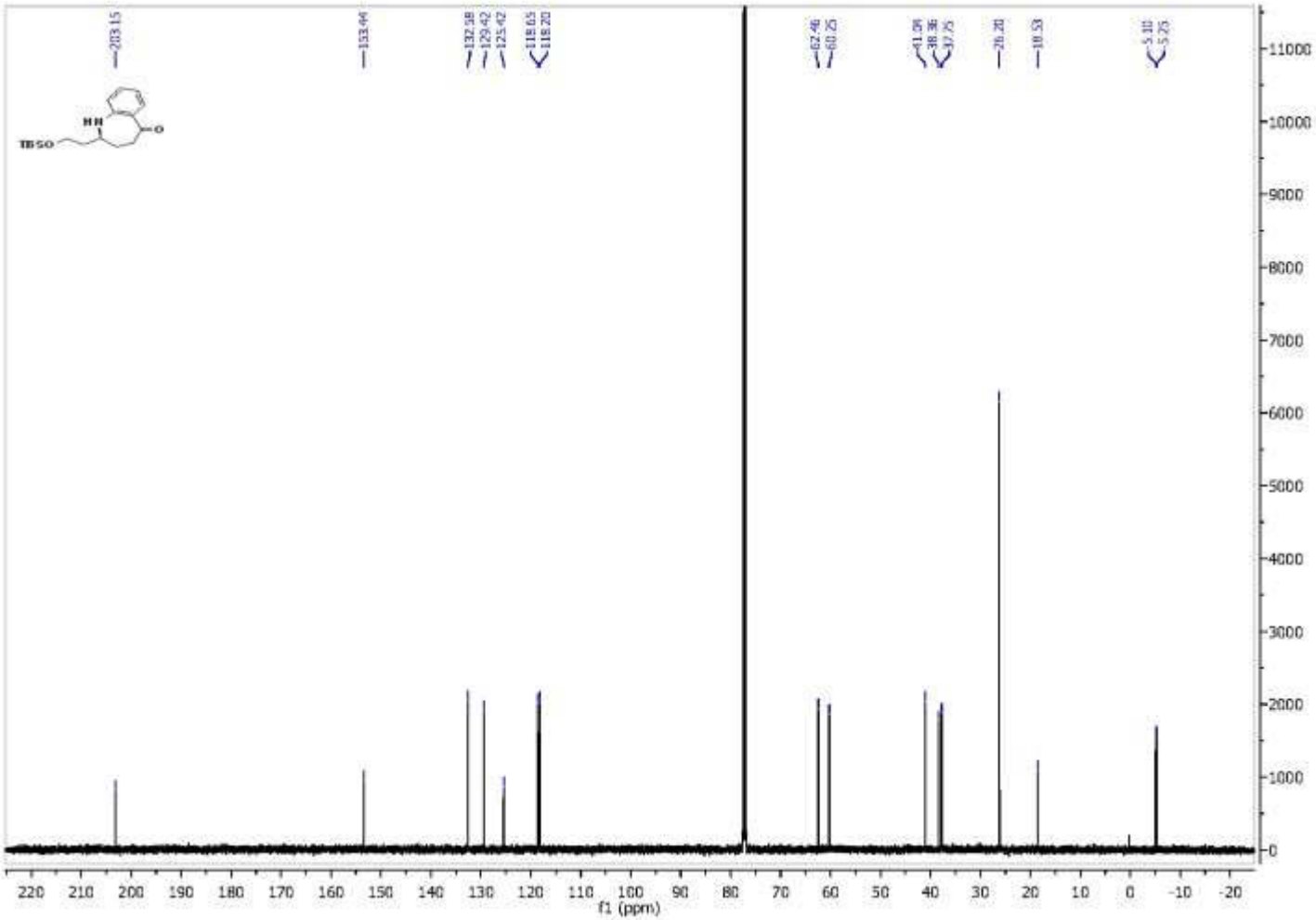

Figure A374 100 MHz 13C NMR ($CDCl_3$) Spectra of Compound **379**

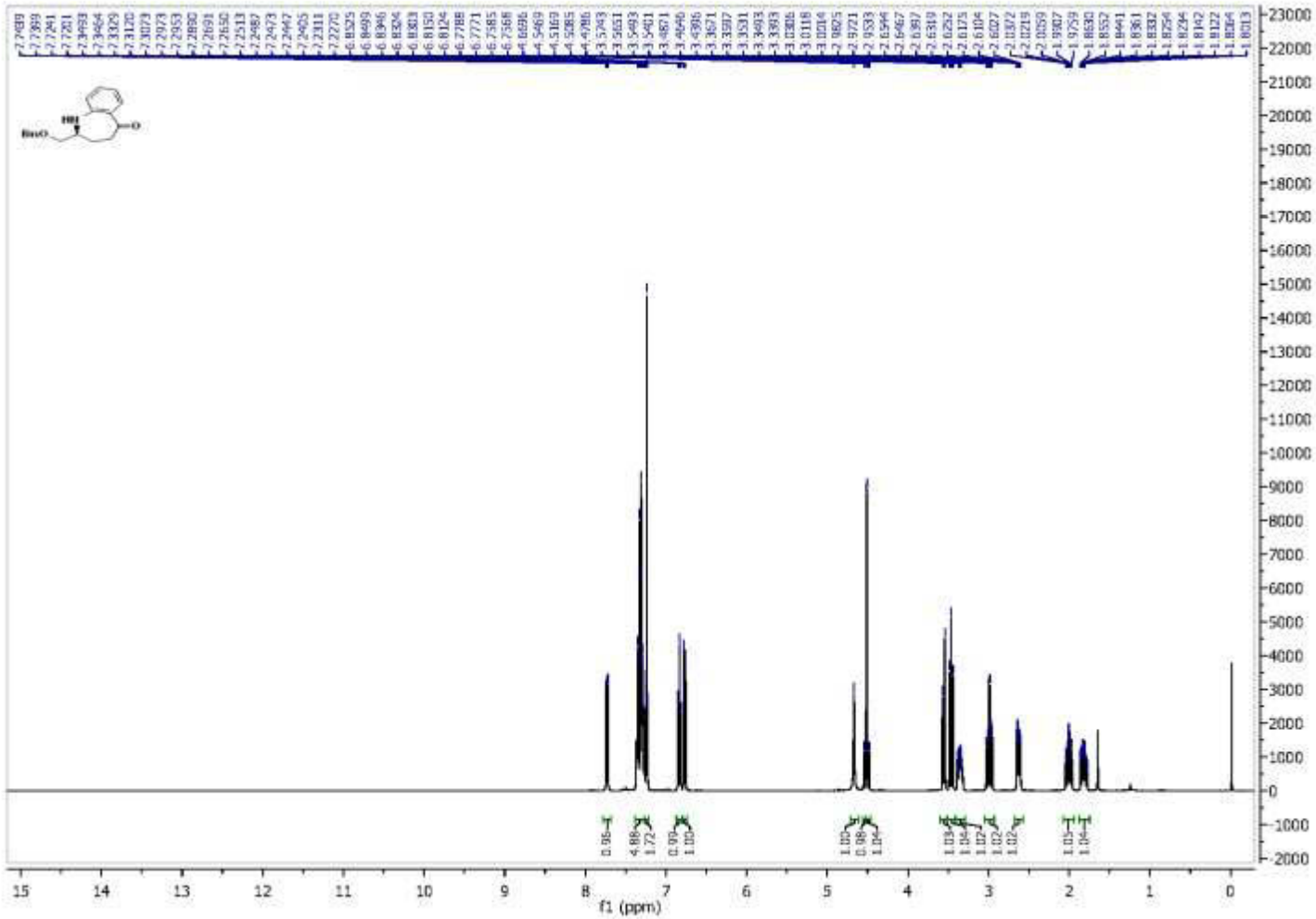

Figure A375 400 MHz 1H NMR ($CDCl_3$) Spectra of Compound **380**

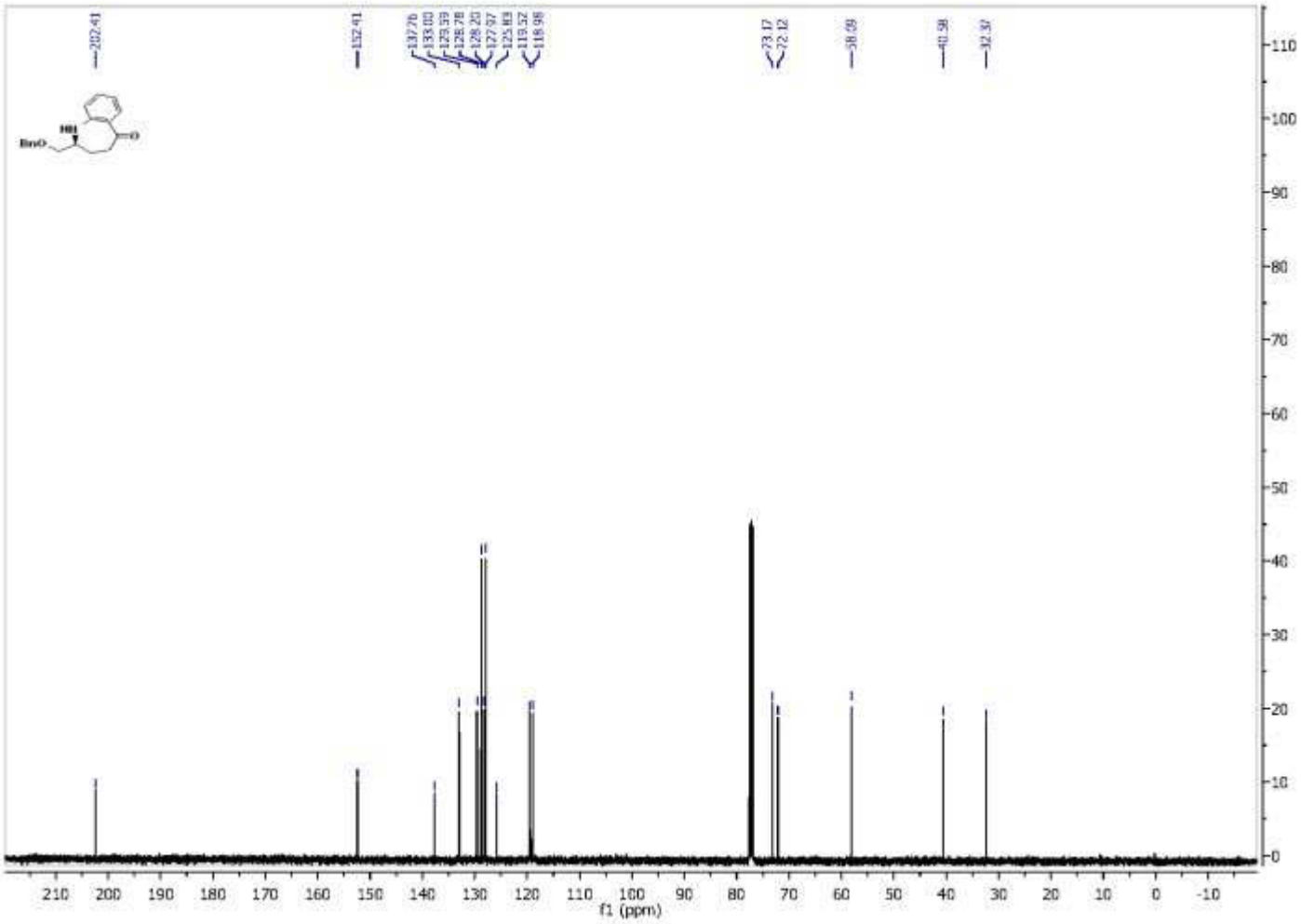

Figure A376 100 MHz 13C NMR ($CDCl_3$) Spectra of Compound **380**

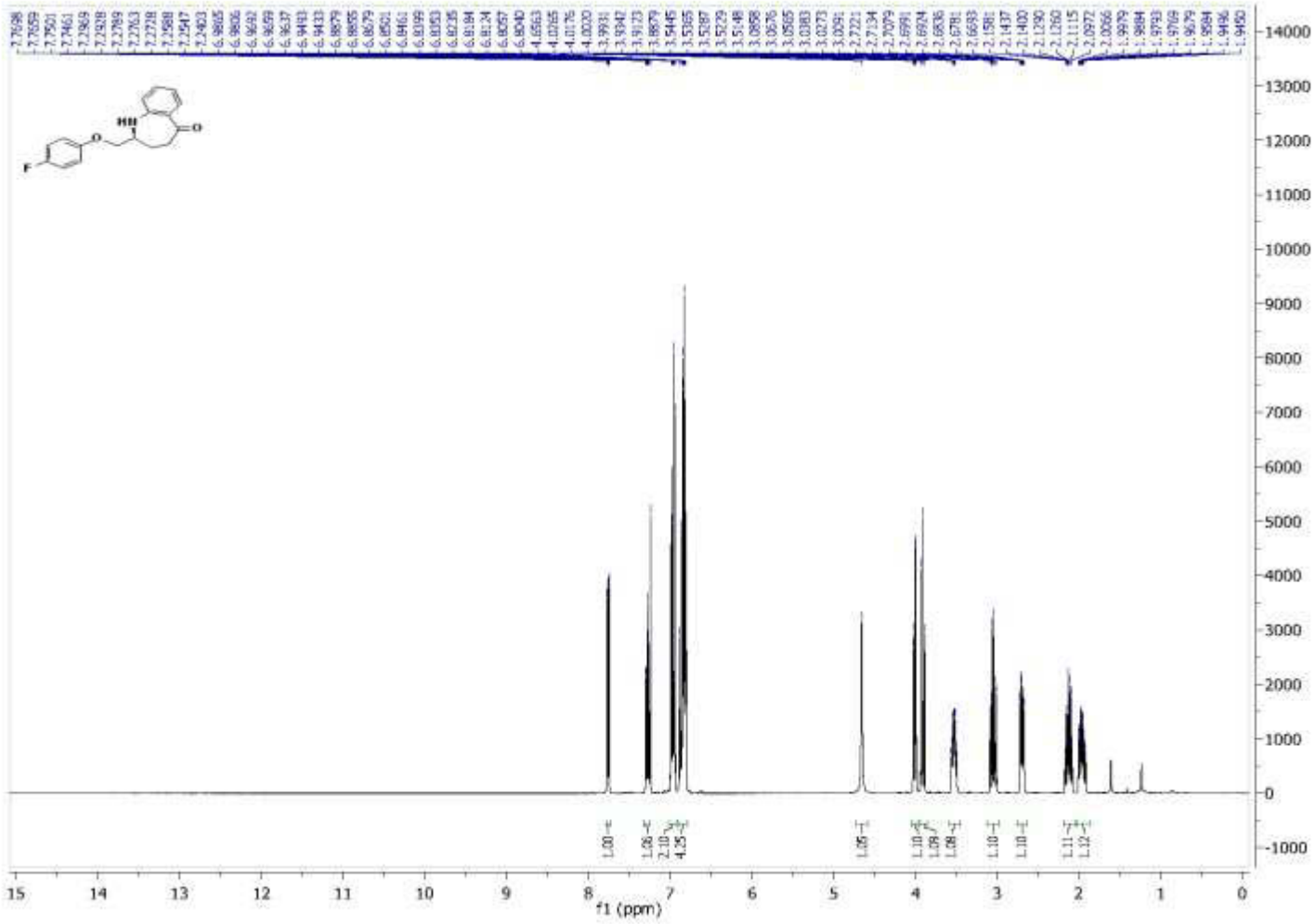

Figure A377 400 MHz 1H NMR ($CDCl_3$) Spectra of Compound **381**

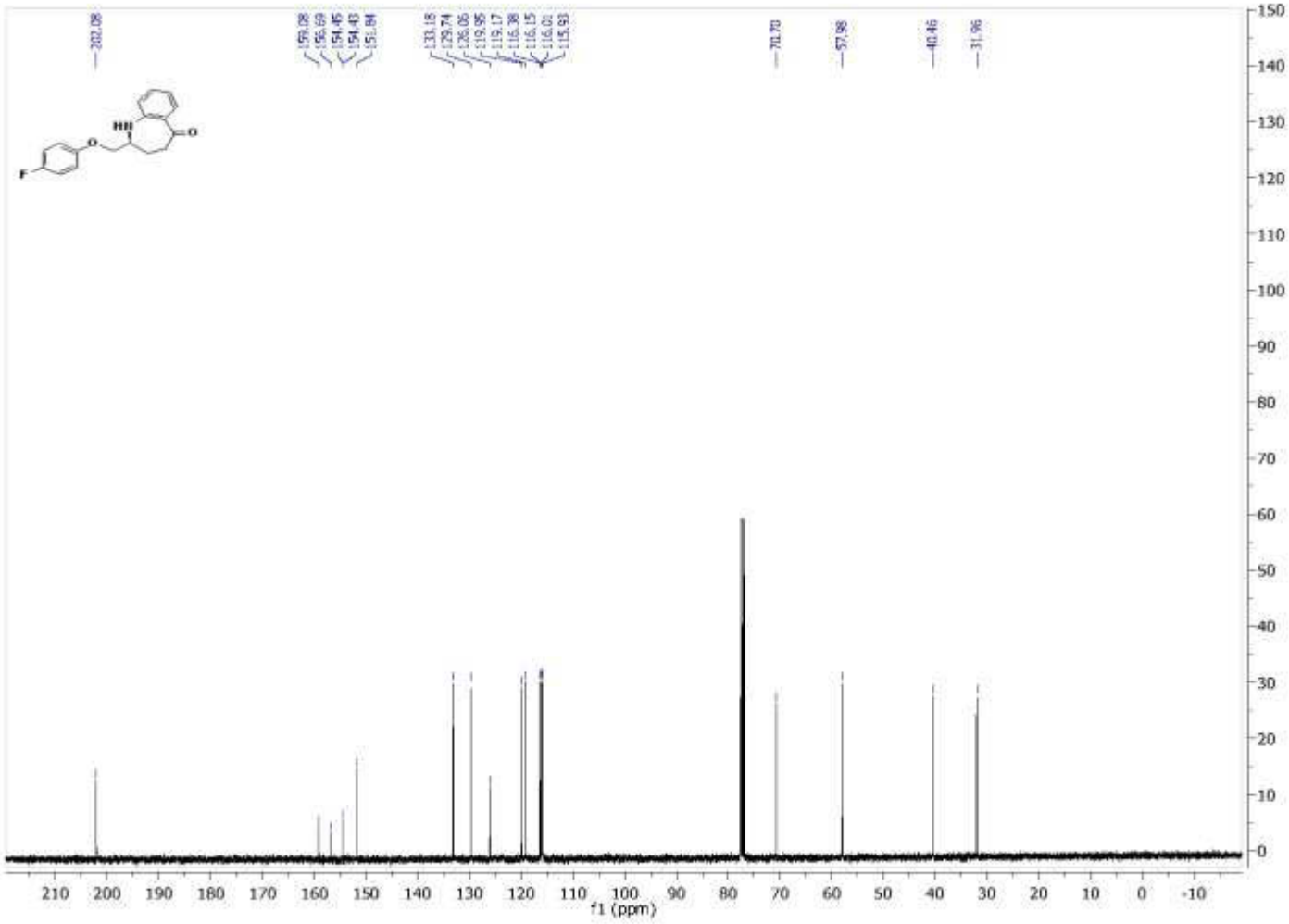

Figure A378 100 MHz 13C NMR ($CDCl_3$) Spectra of Compound **381**

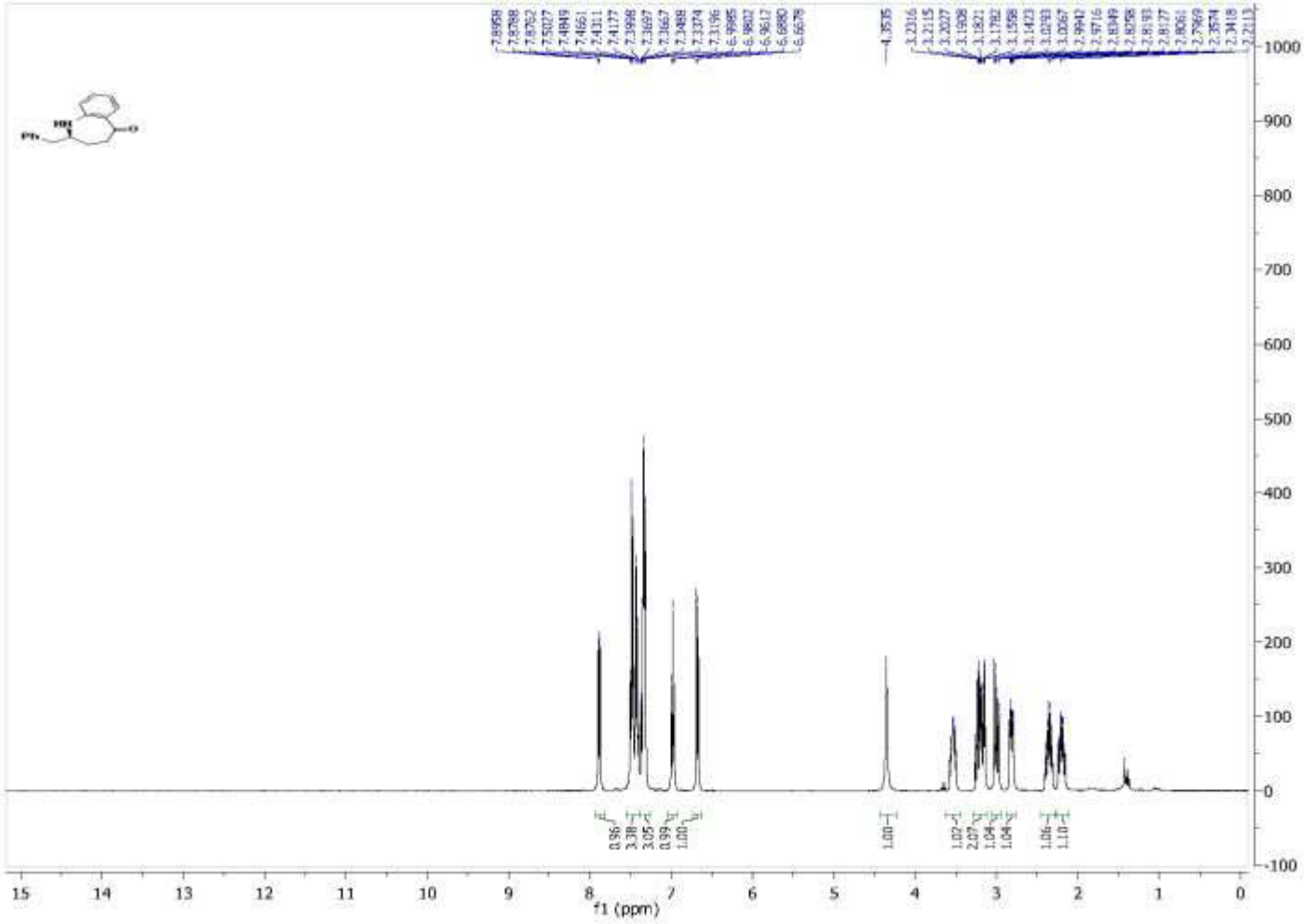

Figure A379 400 MHz 1H NMR ($CDCl_3$) Spectra of Compound **382**

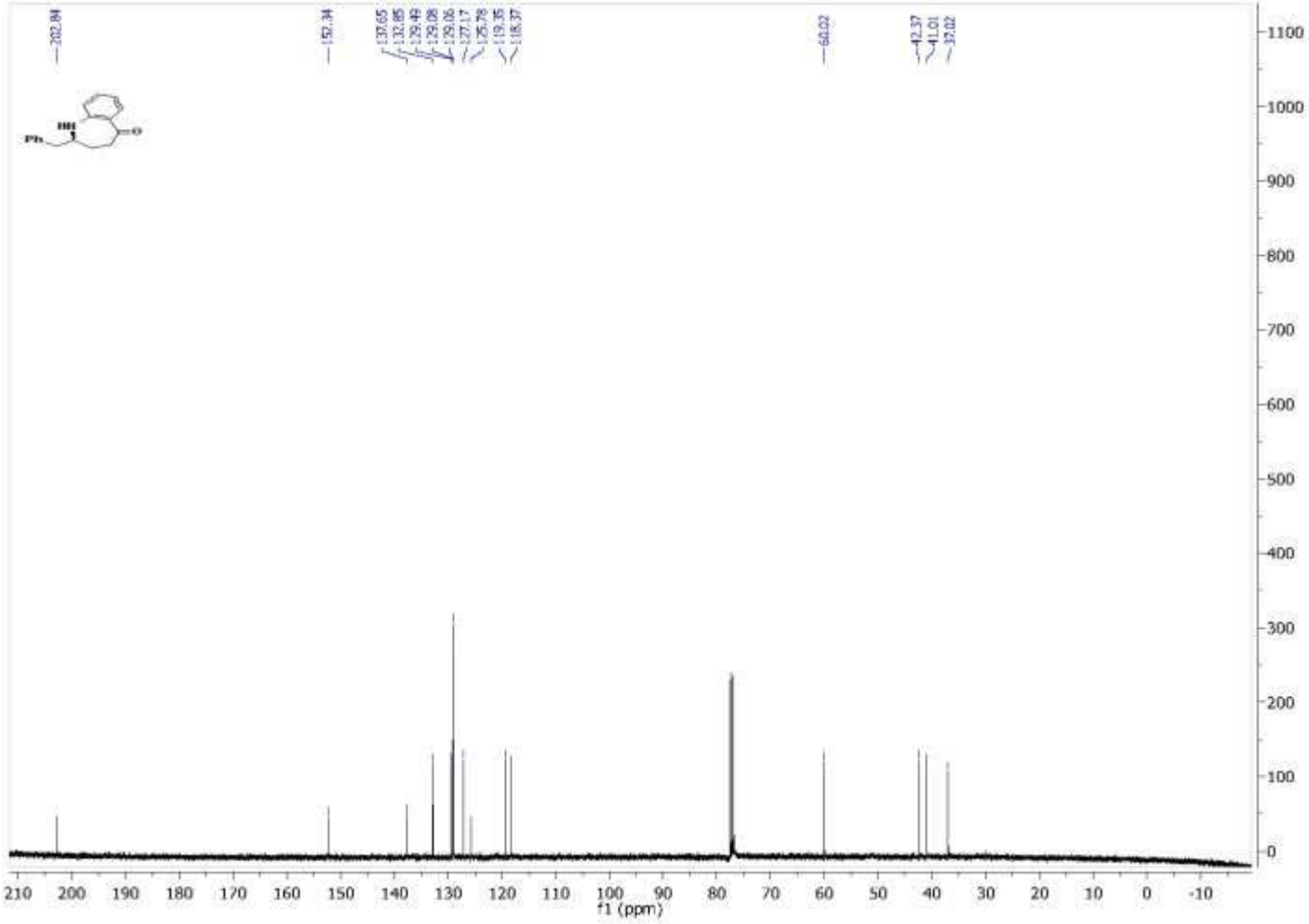

Figure A380 100 MHz 13C NMR ($CDCl_3$) Spectra of Compound **382**

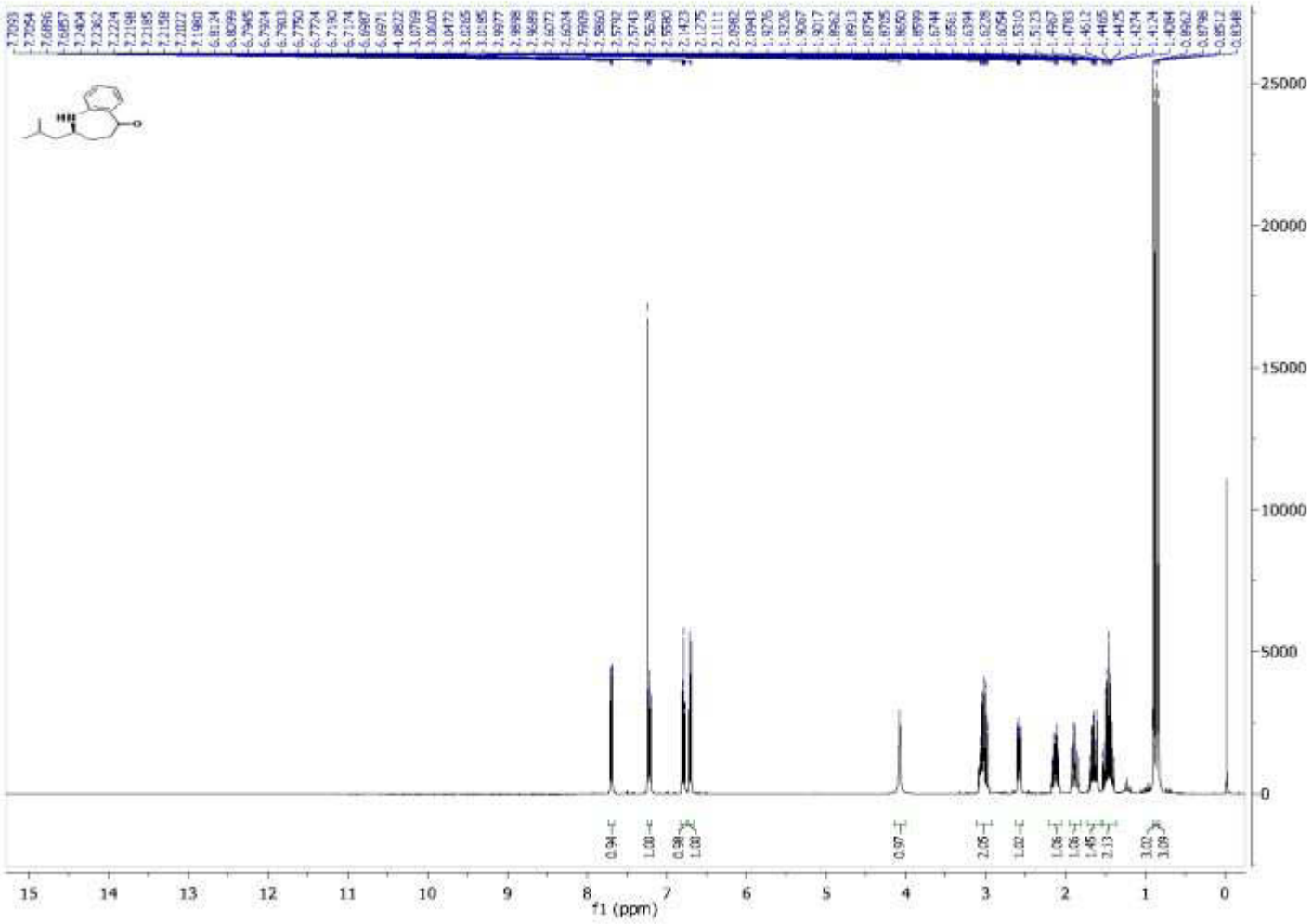

Figure A381 400 MHz 1H NMR ($CDCl_3$) Spectra of Compound **383**

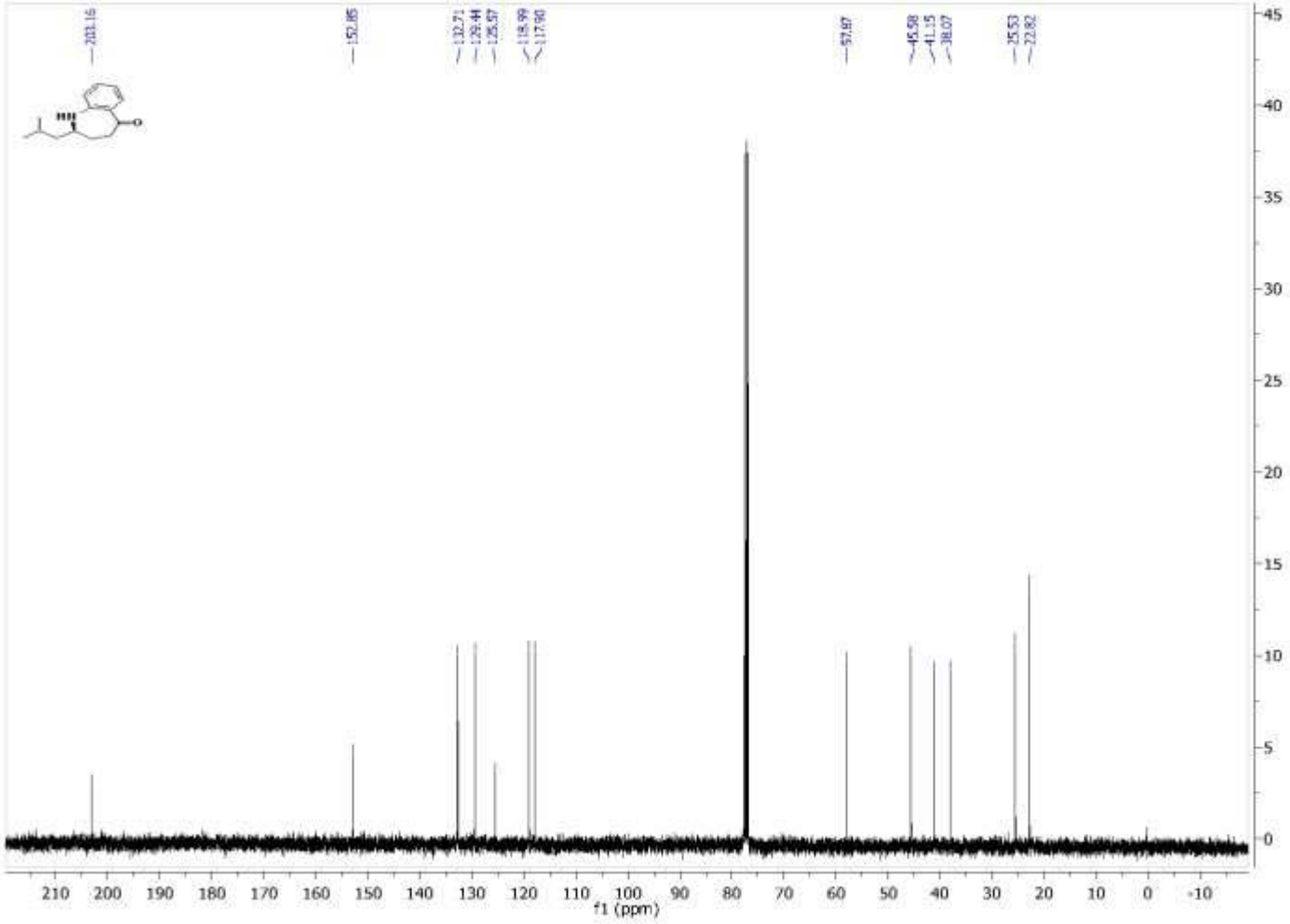

Figure A382 100 MHz 13C NMR ($CDCl_3$) Spectra of Compound **383**

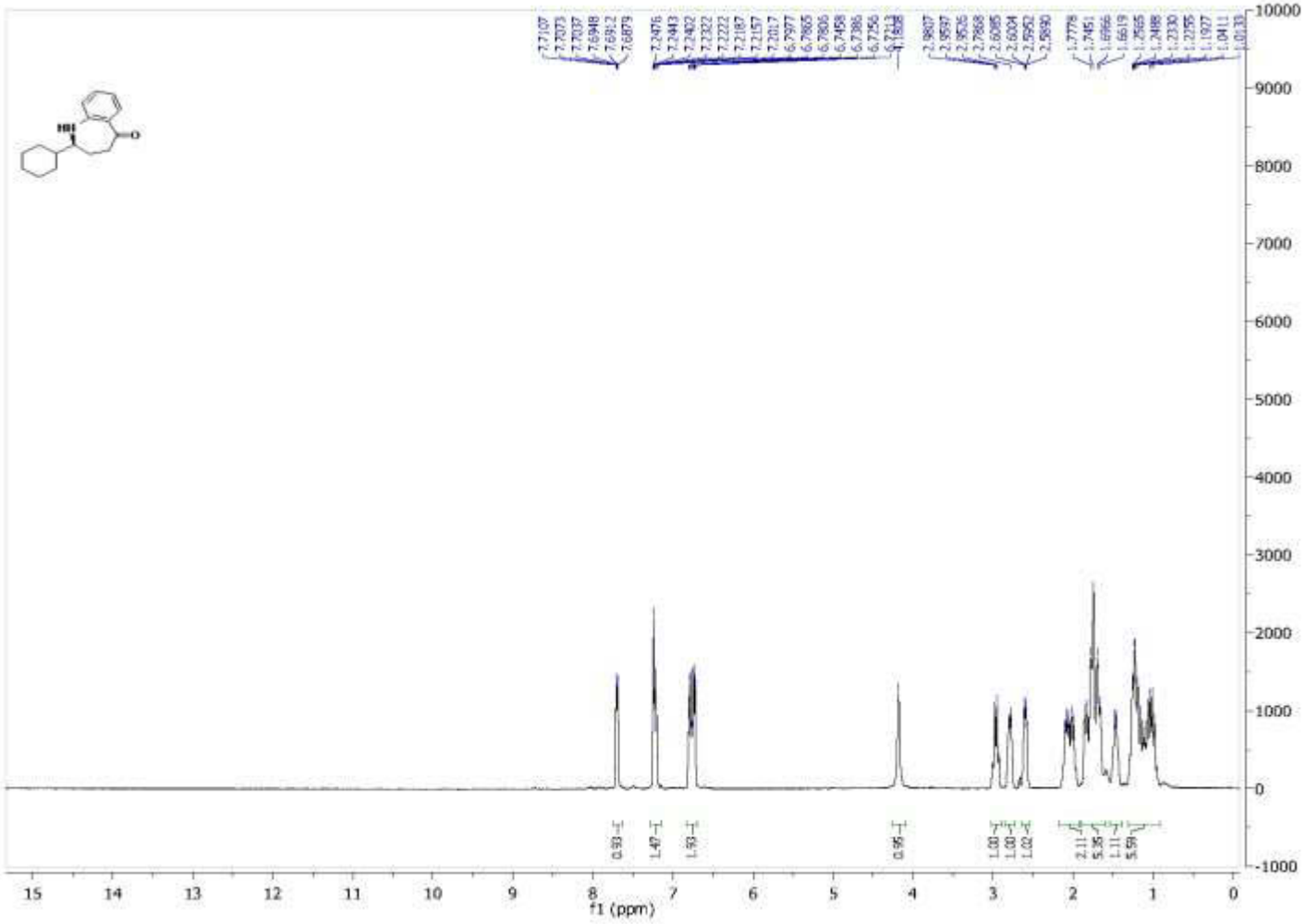

Figure A383 400 MHz 1H NMR ($CDCl_3$) Spectra of Compound **384**

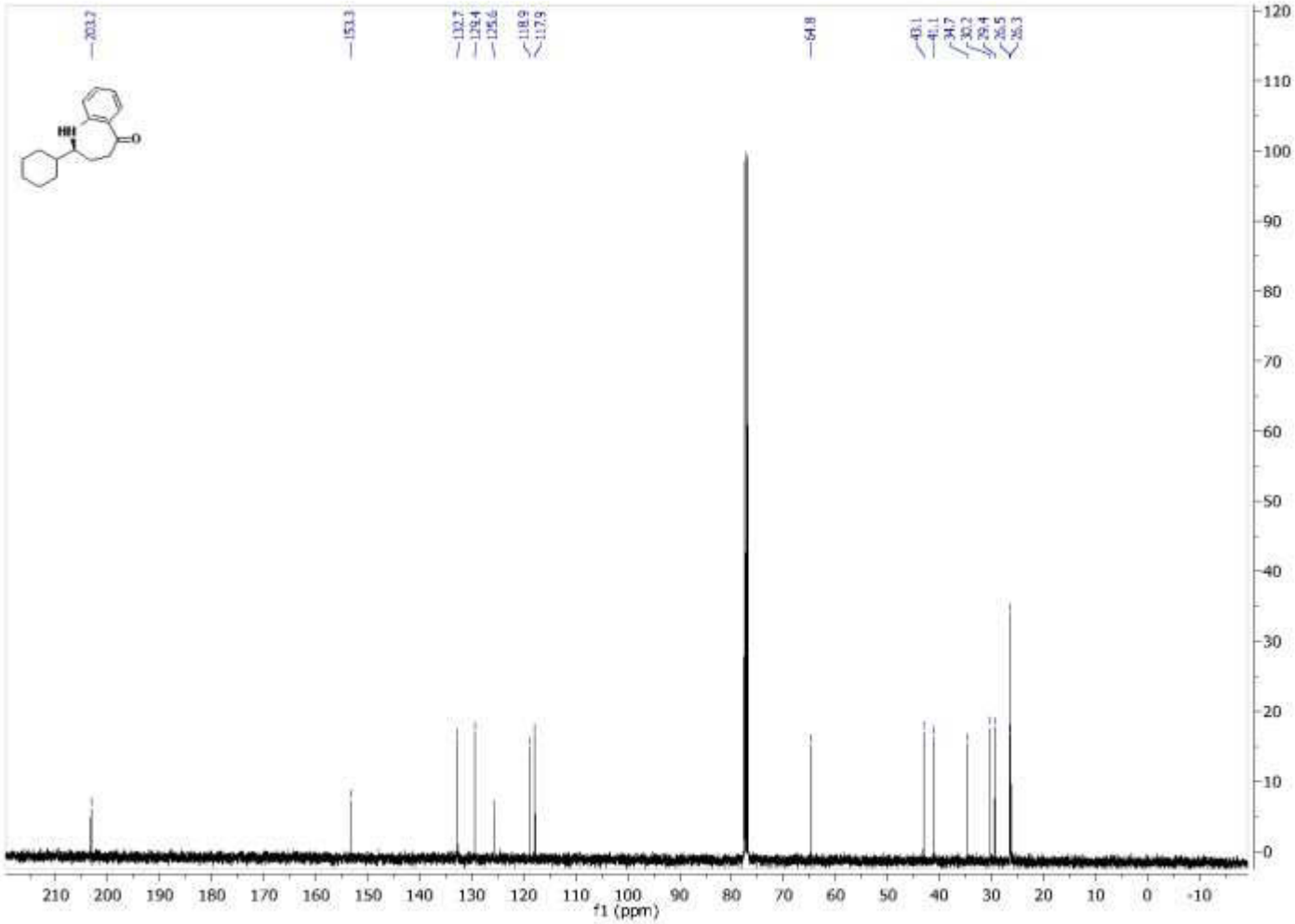

Figure A384 100 MHz 13C NMR ($CDCl_3$) Spectra of Compound **384**

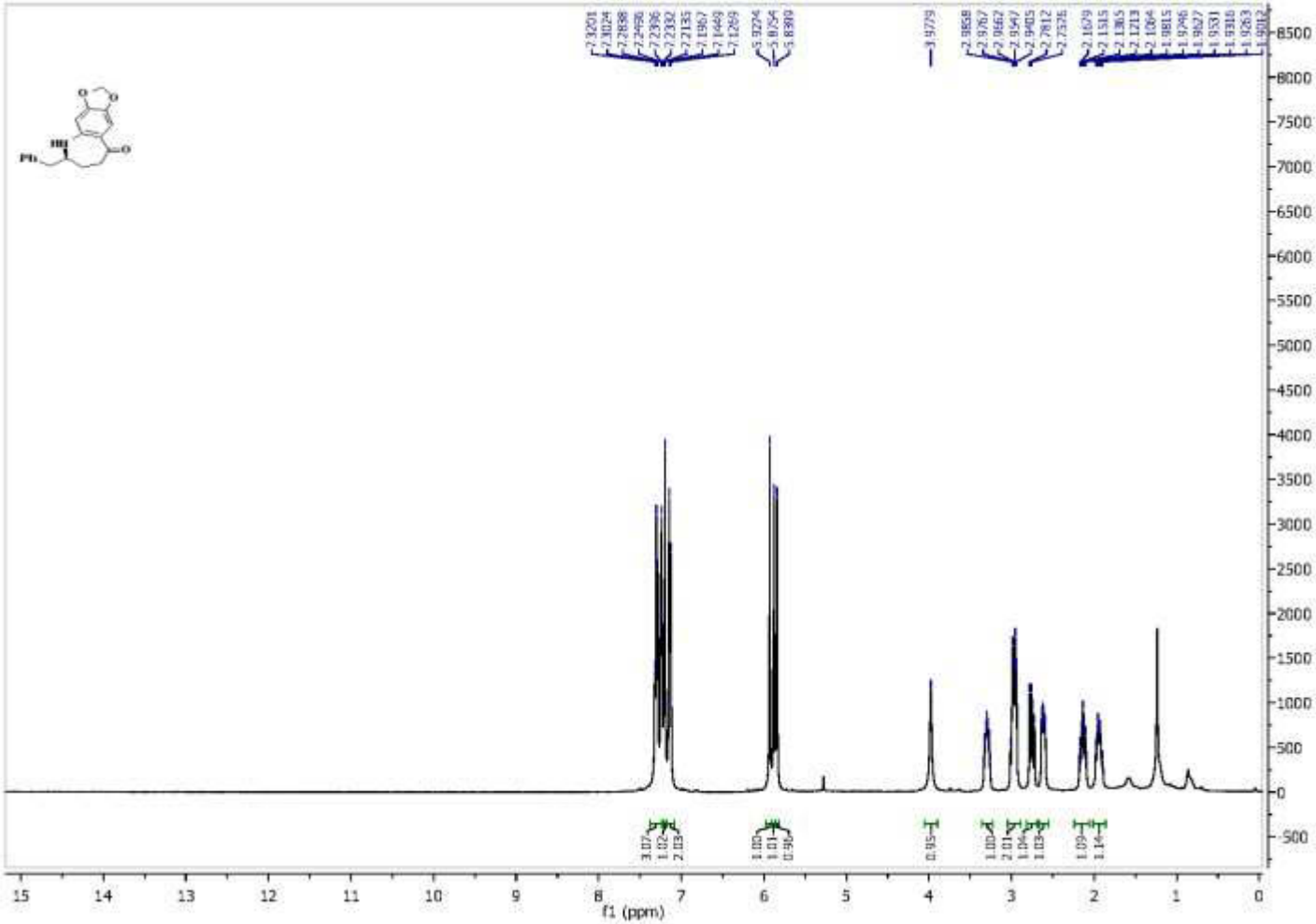

Figure A385 400 MHz 1H NMR ($CDCl_3$) Spectra of Compound **385**

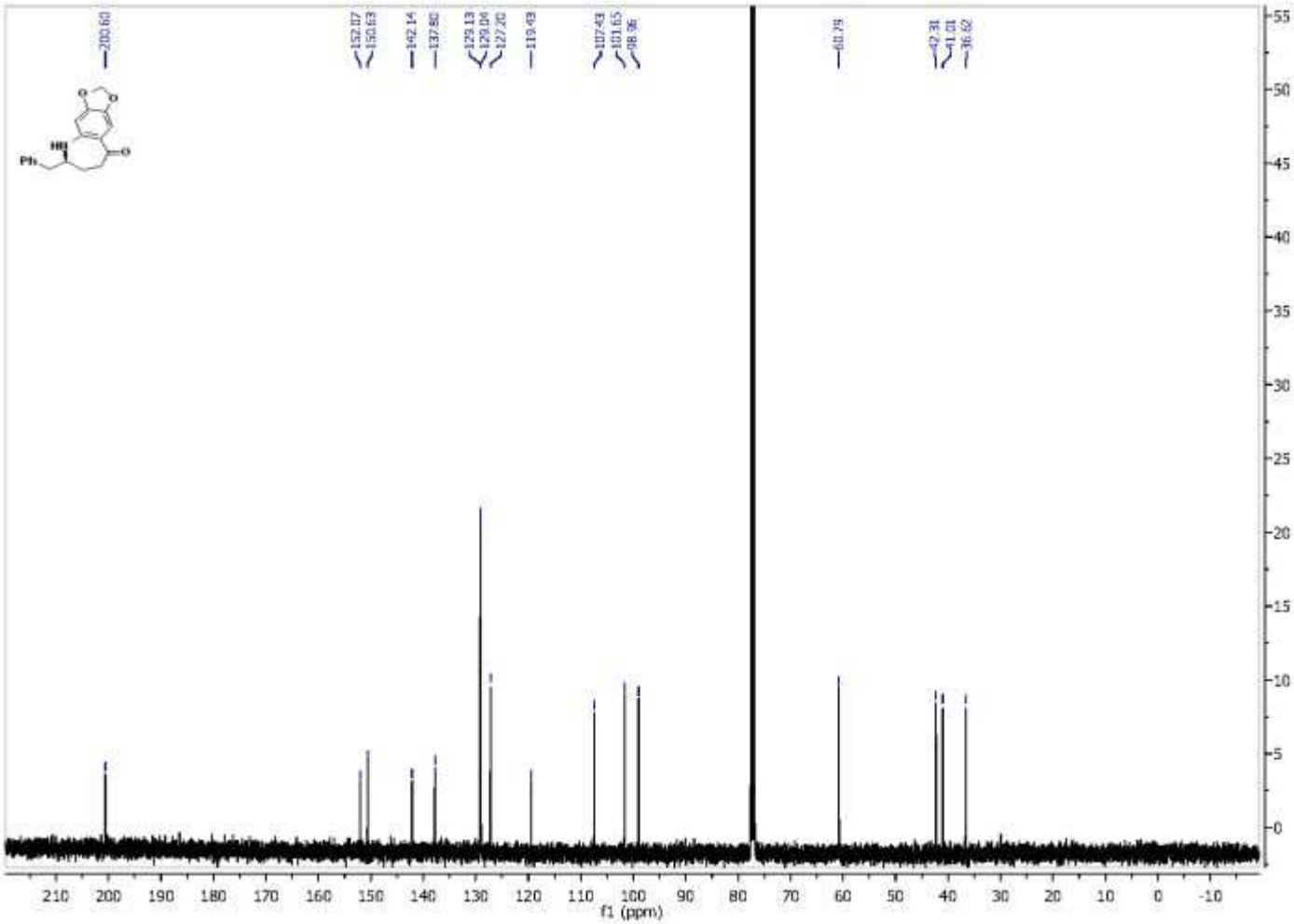

Figure A386 100 MHz 13C NMR ($CDCl_3$) Spectra of Compound **385**

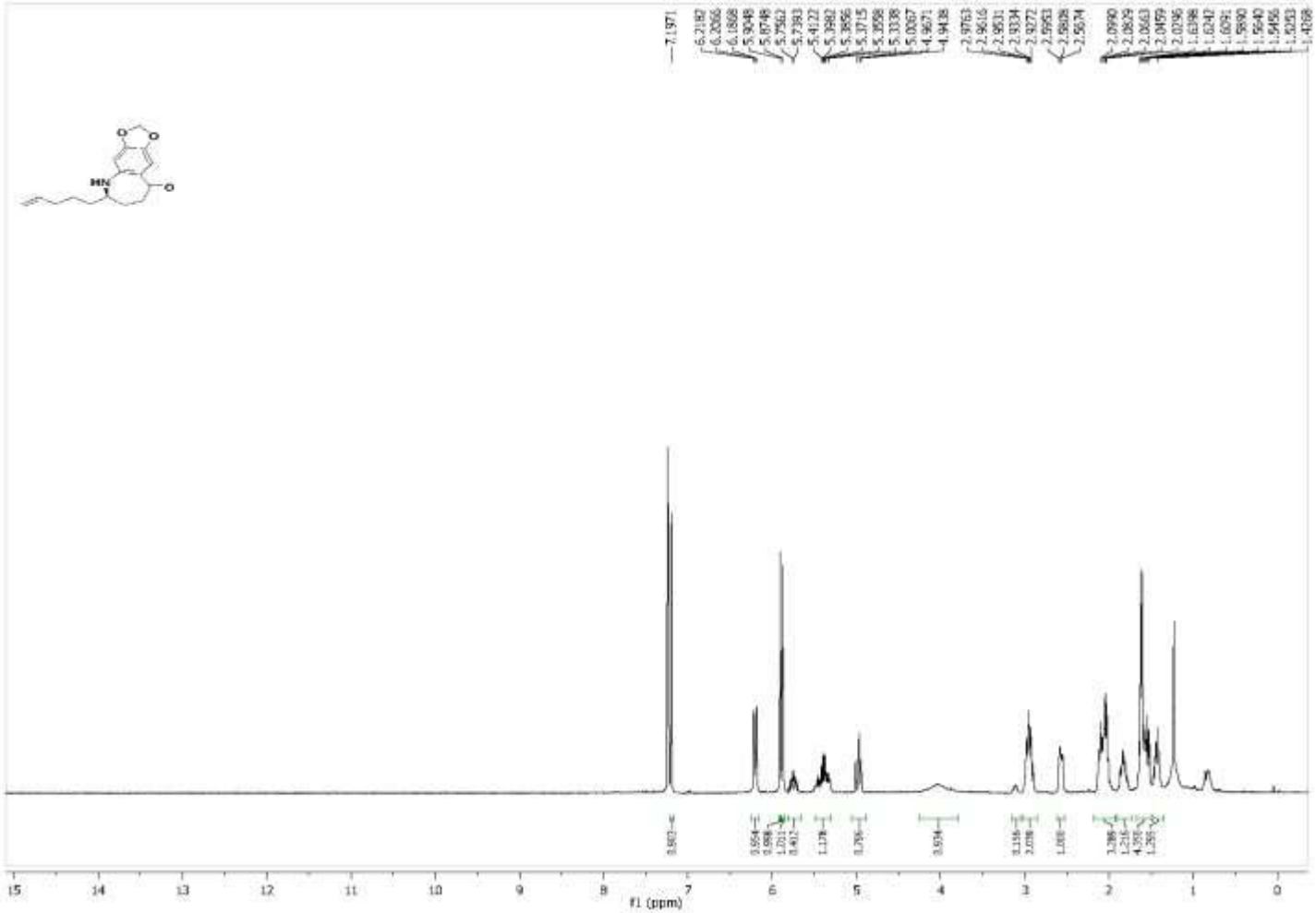

Figure A387 400 MHz 1H NMR ($CDCl_3$) Spectra of Compound **386**

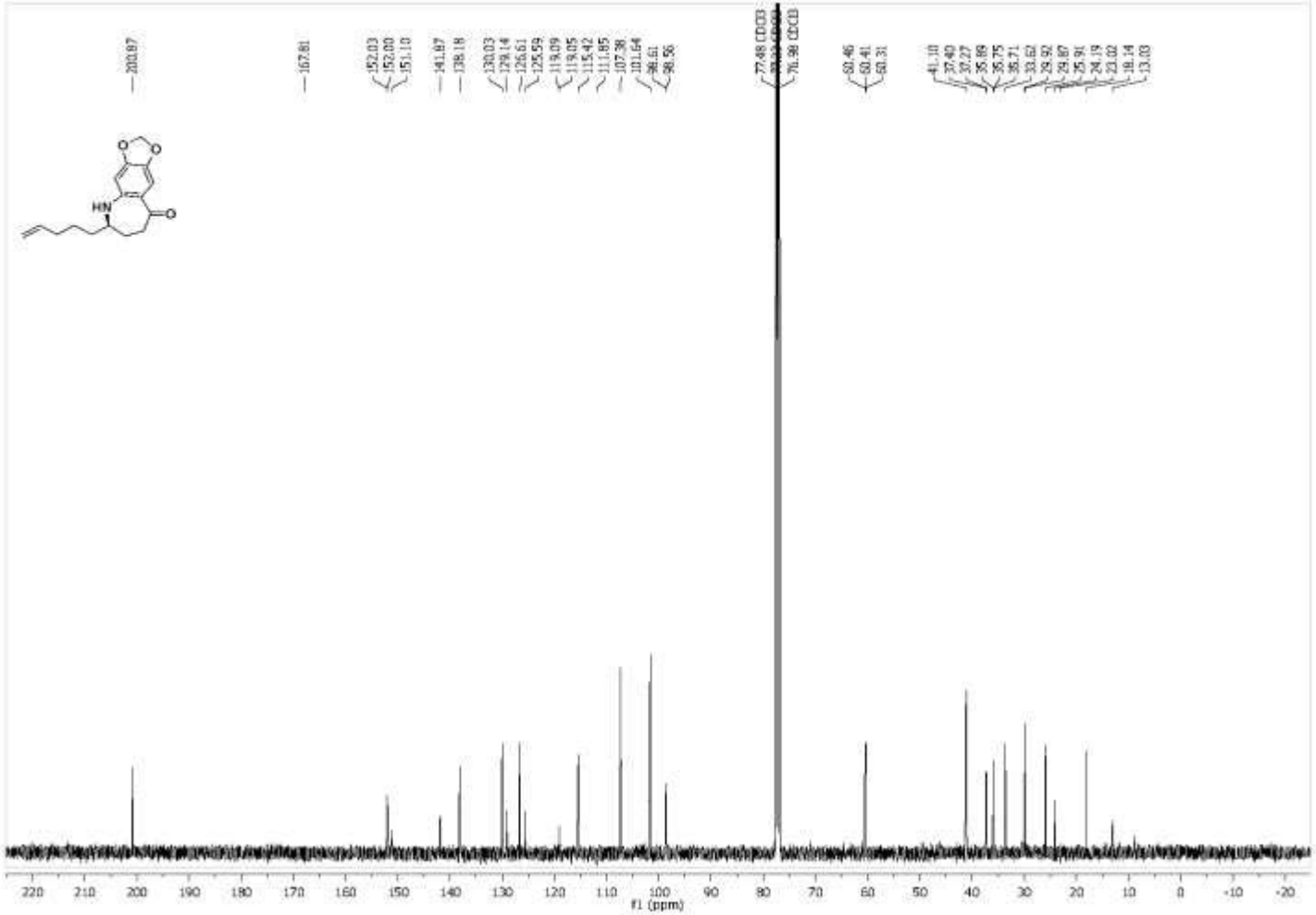

Figure A388 100 MHz 13C NMR ($CDCl_3$) Spectra of Compound **386**

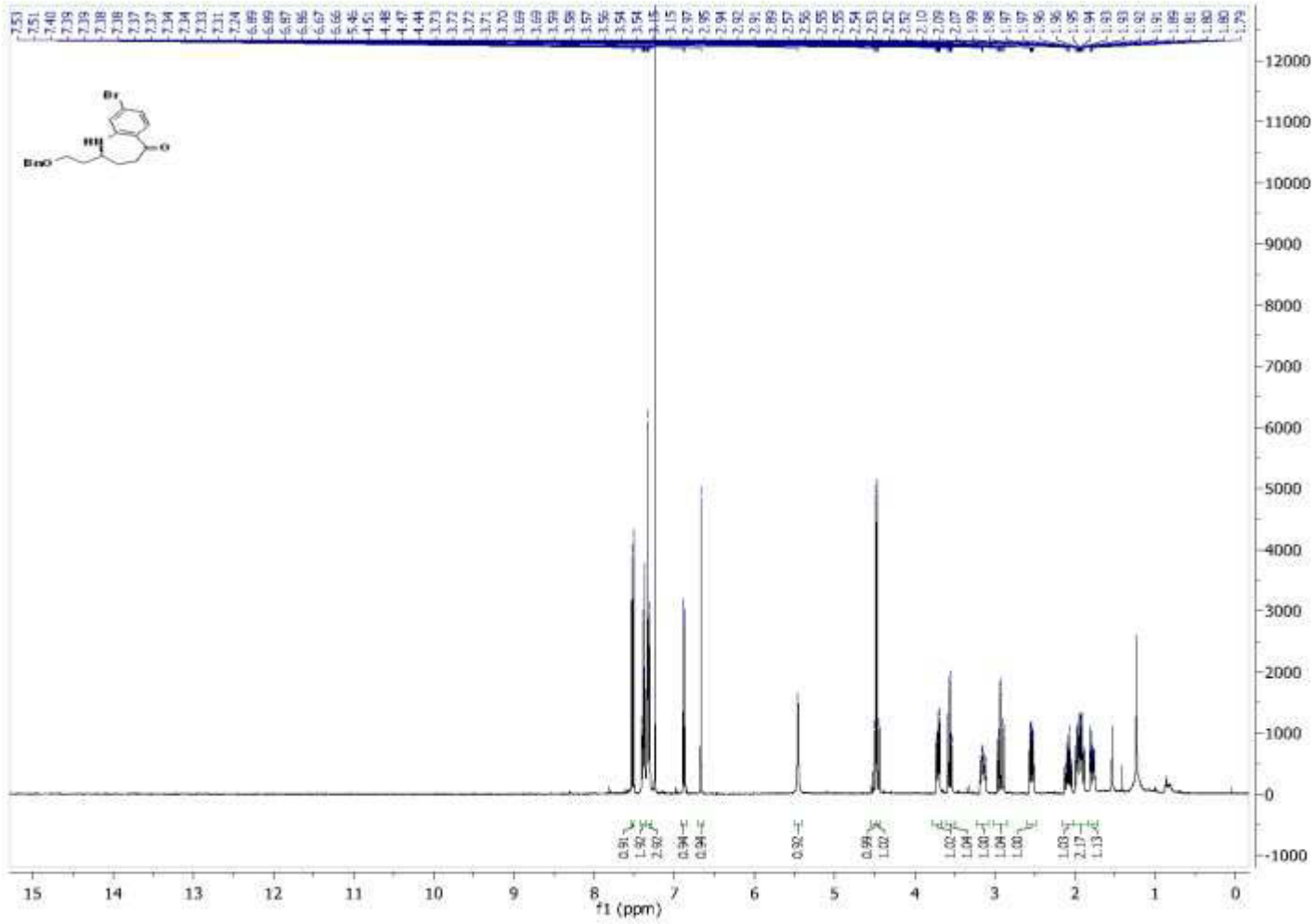

Figure A389 400 MHz 1H NMR ($CDCl_3$) Spectra of Compound **387**

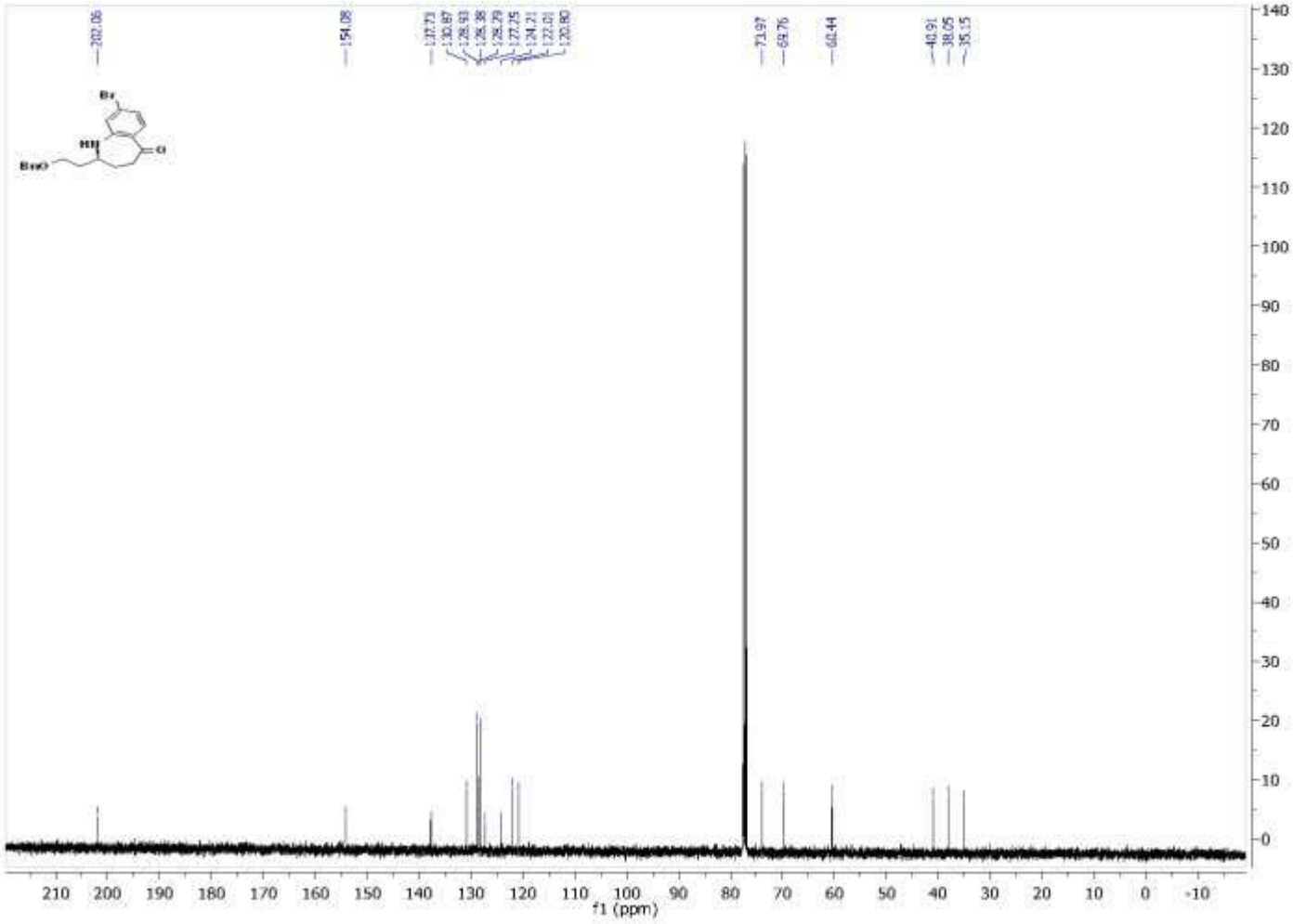

Figure A390 100 MHz 13C NMR ($CDCl_3$) Spectra of Compound **387**

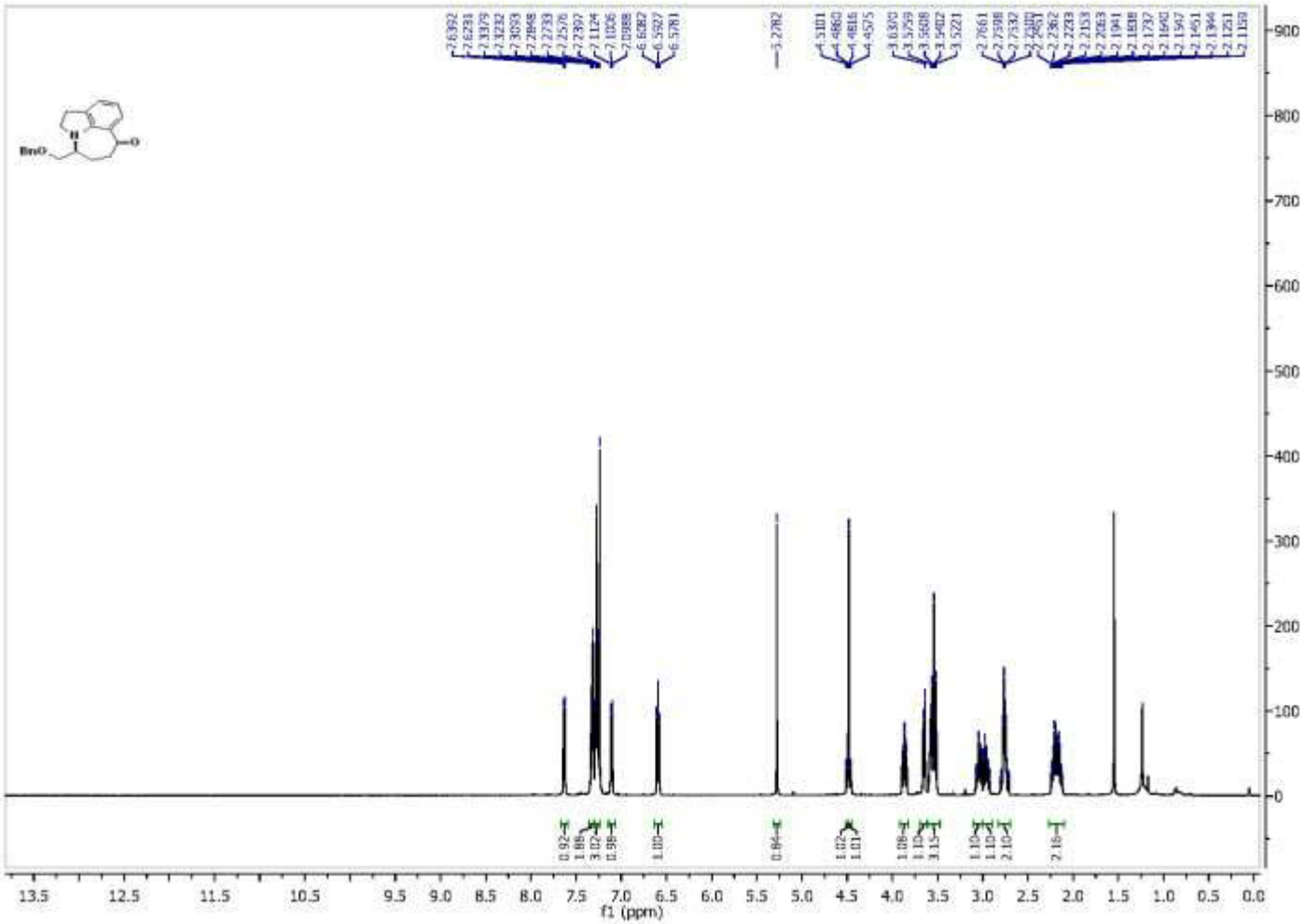

Figure A391 400 MHz 1H NMR ($CDCl_3$) Spectra of Compound **388**

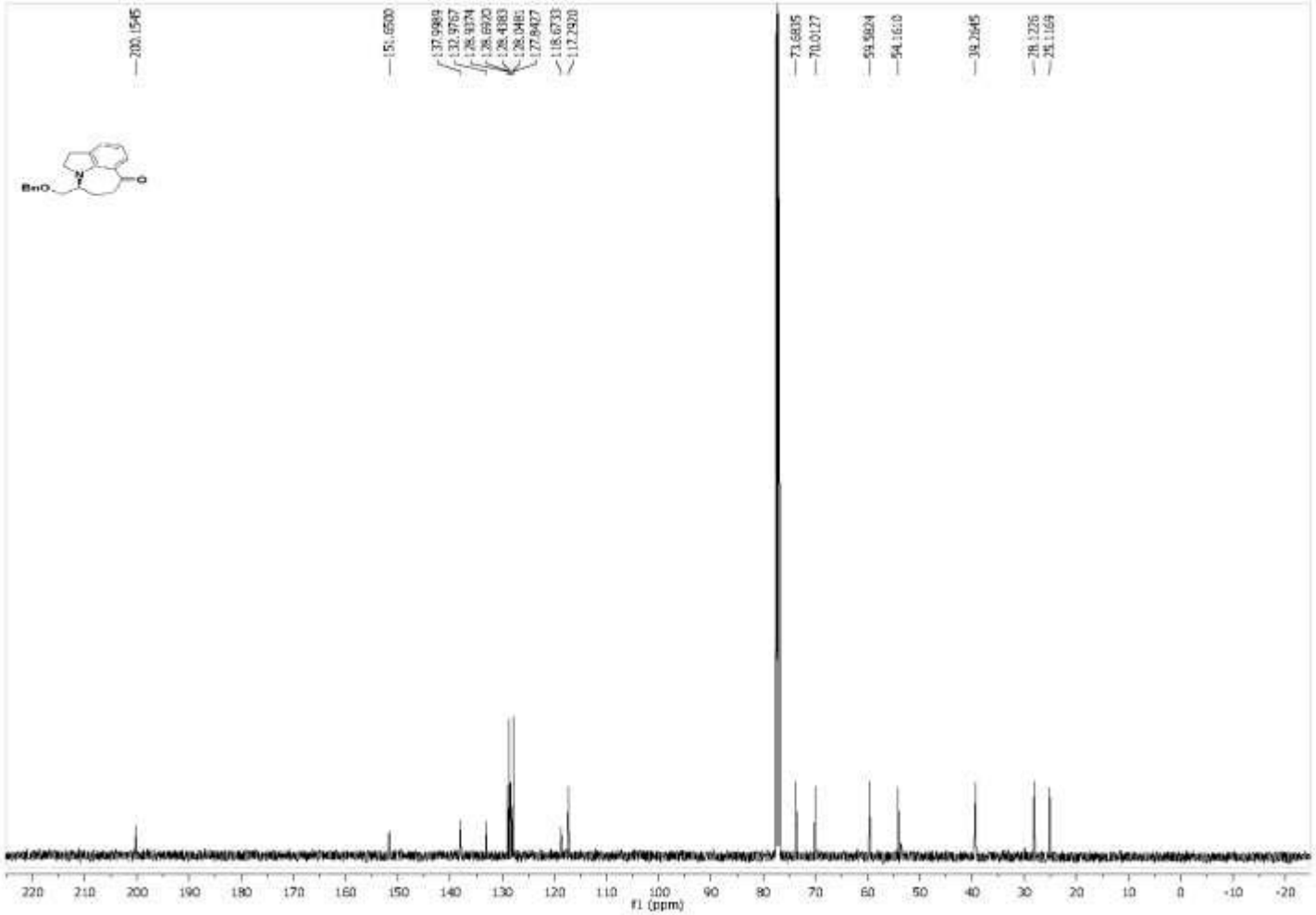

Figure A392 100 MHz 13C NMR ($CDCl_3$) Spectra of Compound **388**

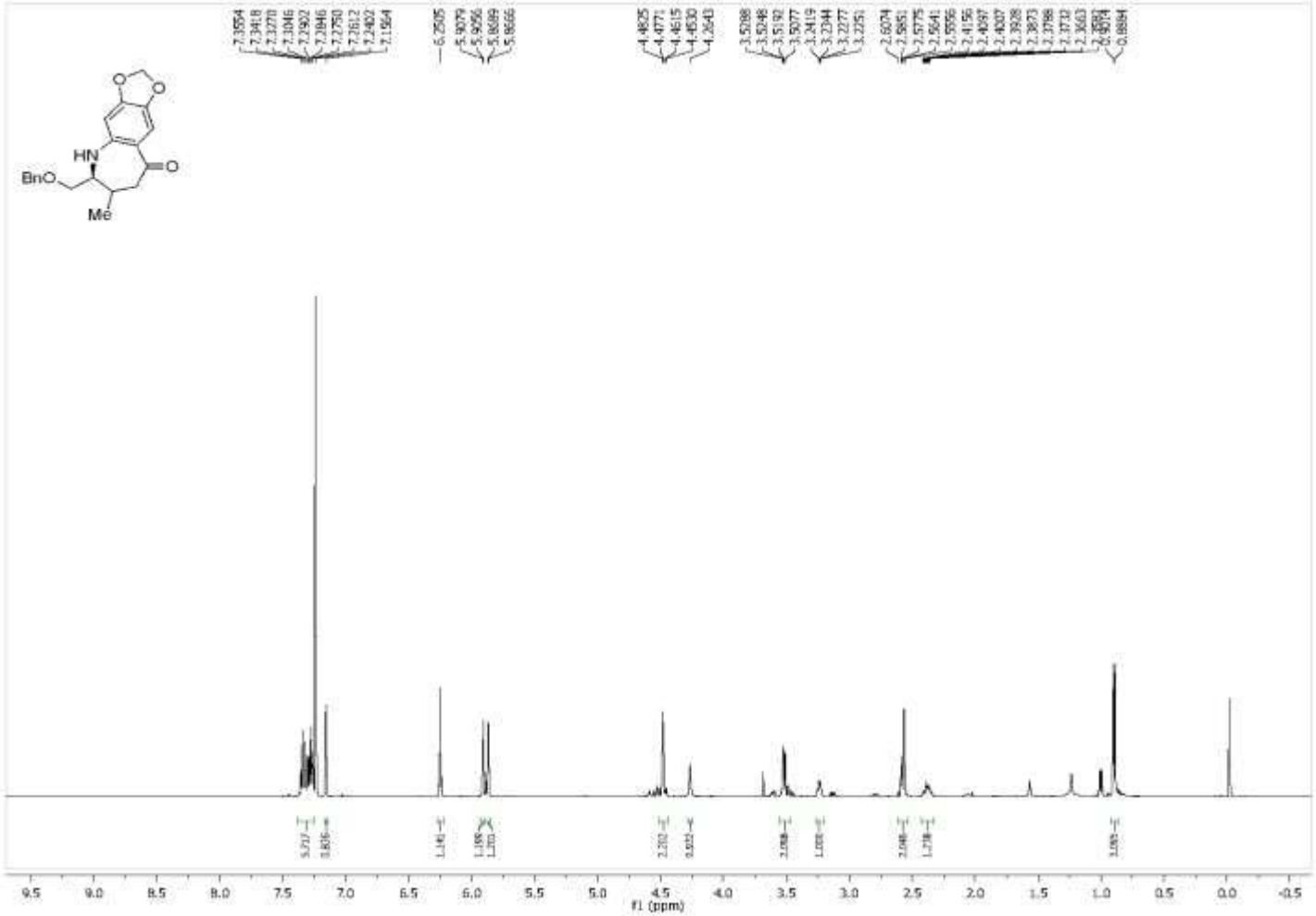

Figure A393 400 MHz 1H NMR ($CDCl_3$) Spectra of Compound **389**

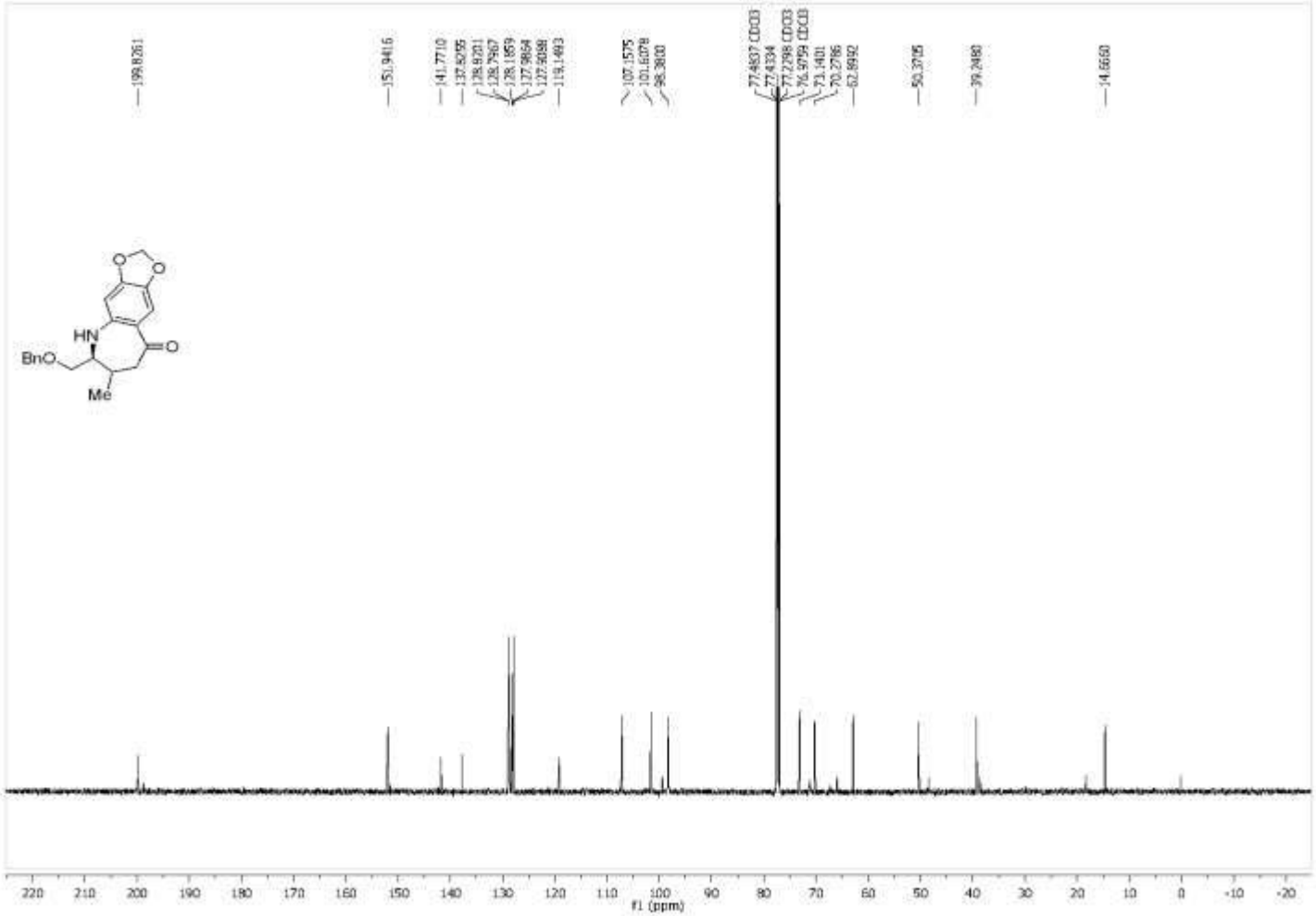

Figure A394 100 MHz 13C NMR ($CDCl_3$) Spectra of Compound **389**

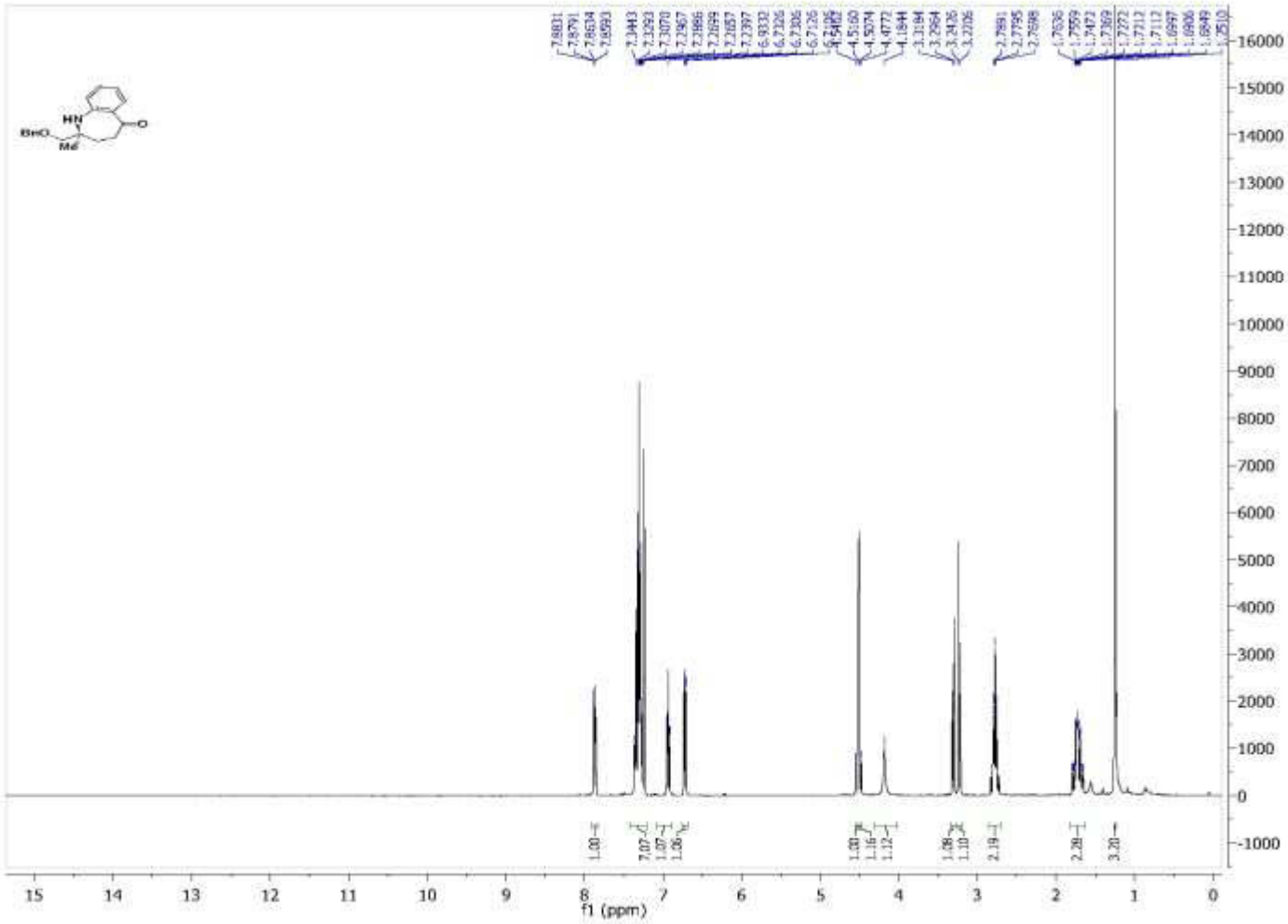

Figure A395 400 MHz 1H NMR ($CDCl_3$) Spectra of Compound **391**

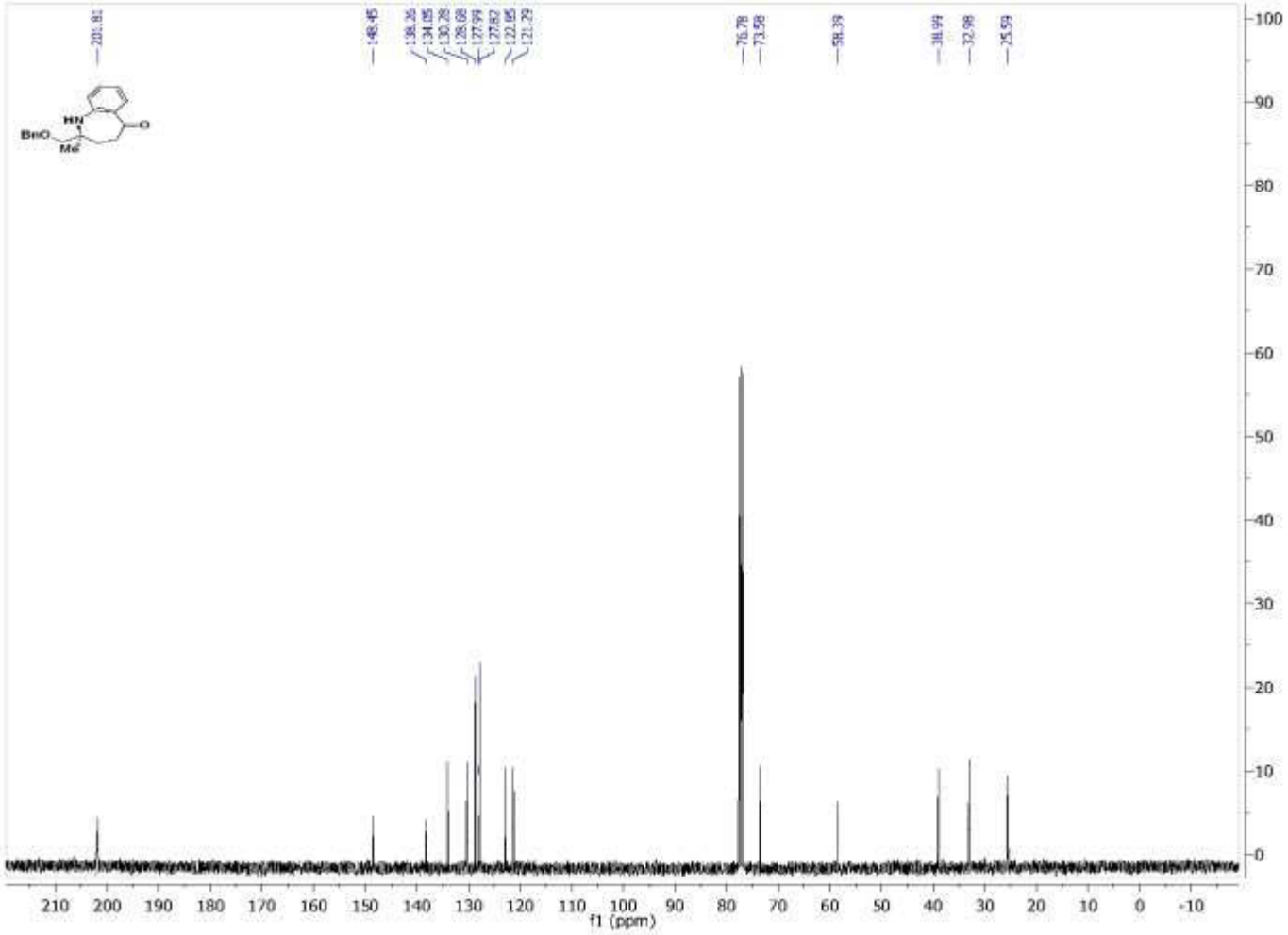

Figure A396 100 MHz 13C NMR ($CDCl_3$) Spectra of Compound **391**

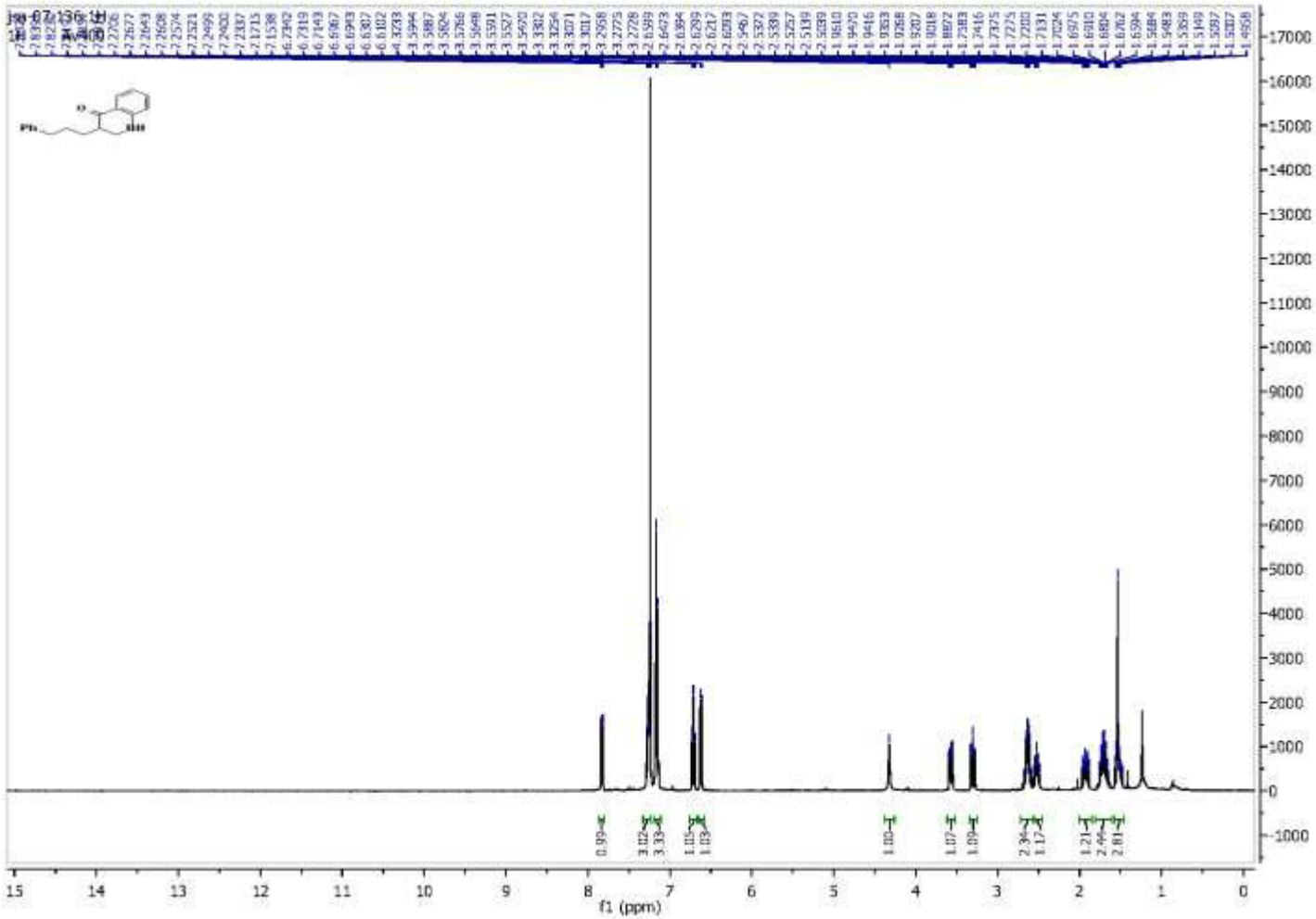

Figure A397 400 MHz 1H NMR ($CDCl_3$) Spectra of Compound **373**

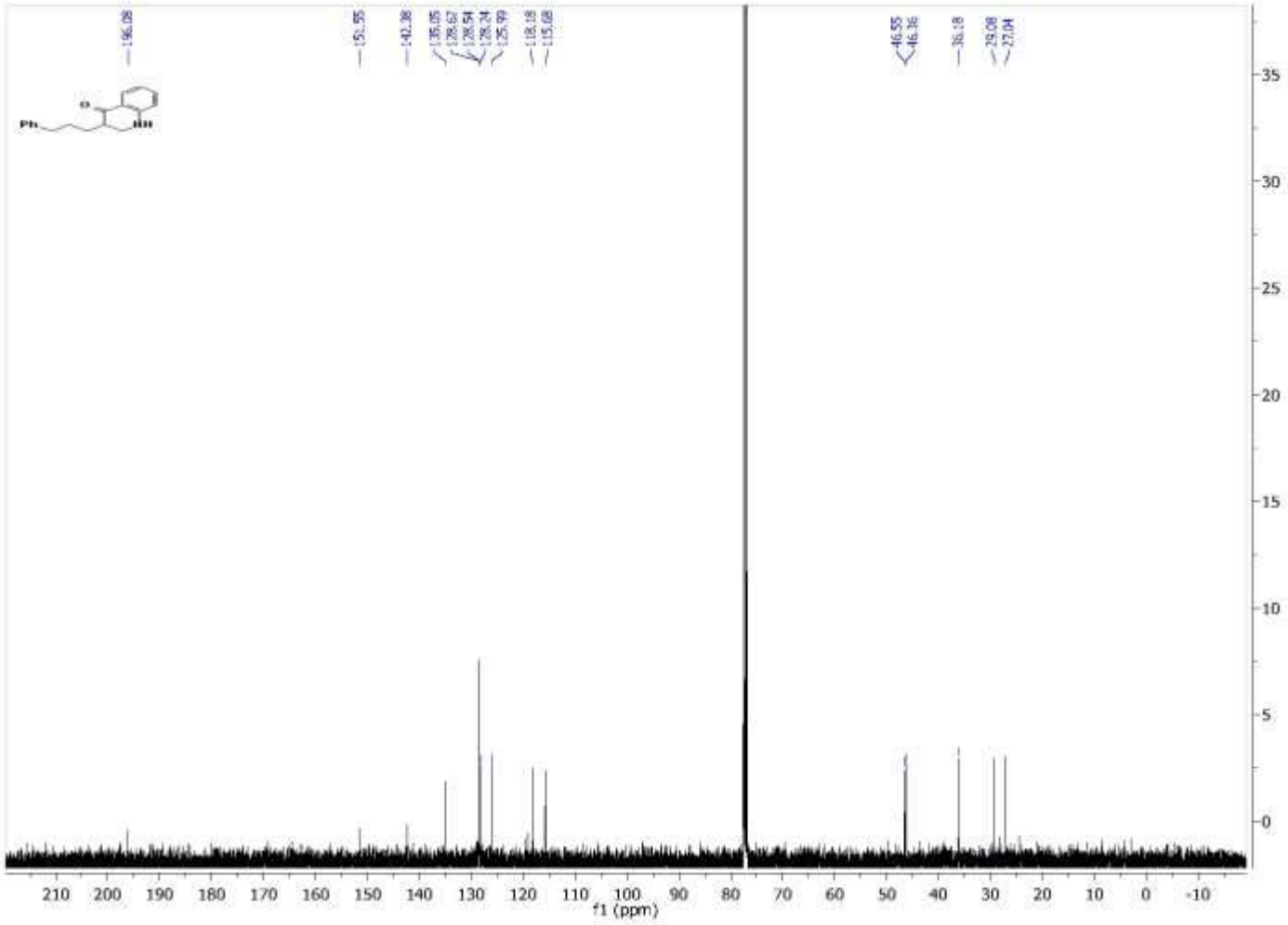

Figure A398 100 MHz 13C NMR ($CDCl_3$) Spectra of Compound **373**

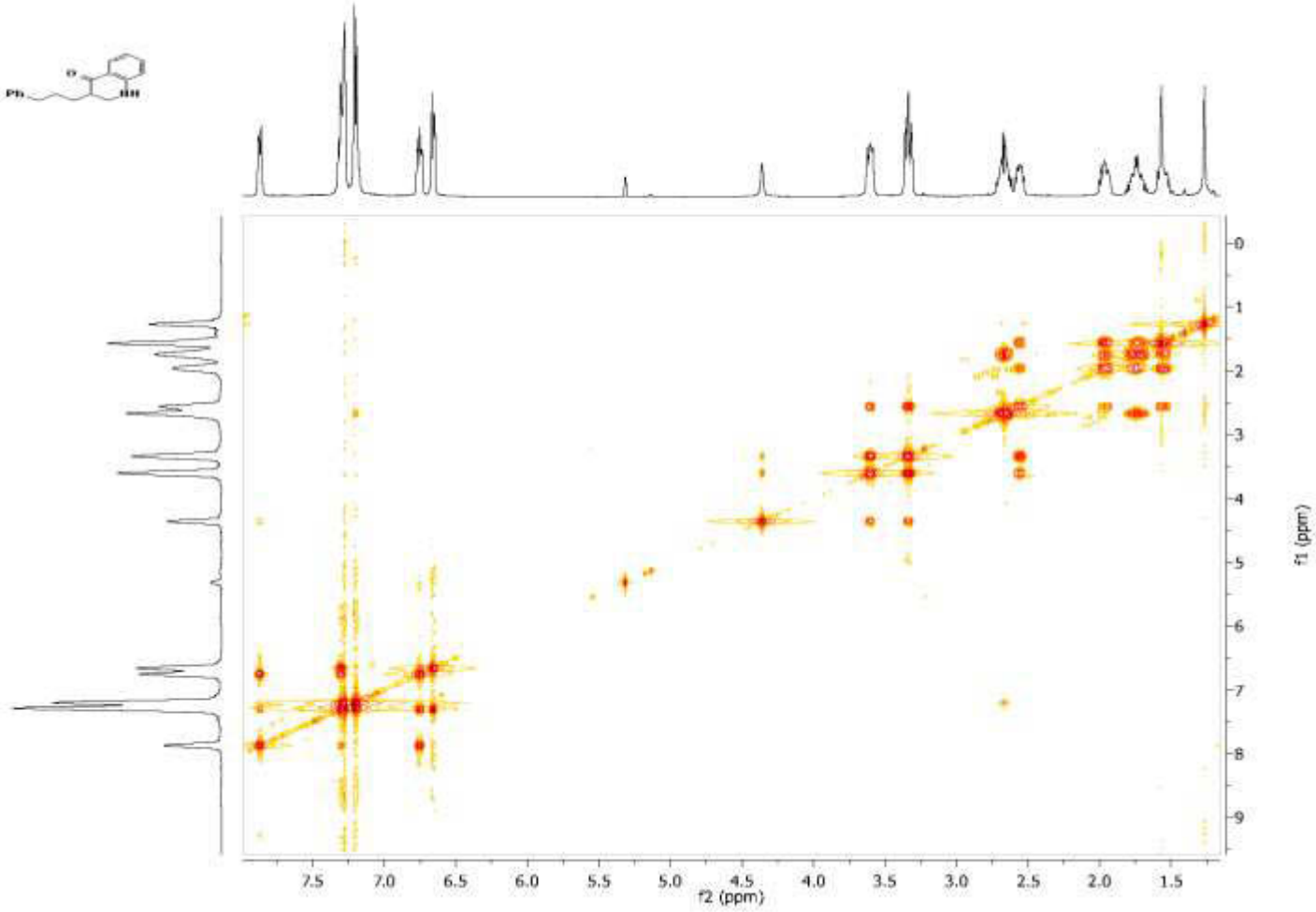

Figure A399 1H COSY NMR ($CDCl_3$) Spectra of Compound **373**

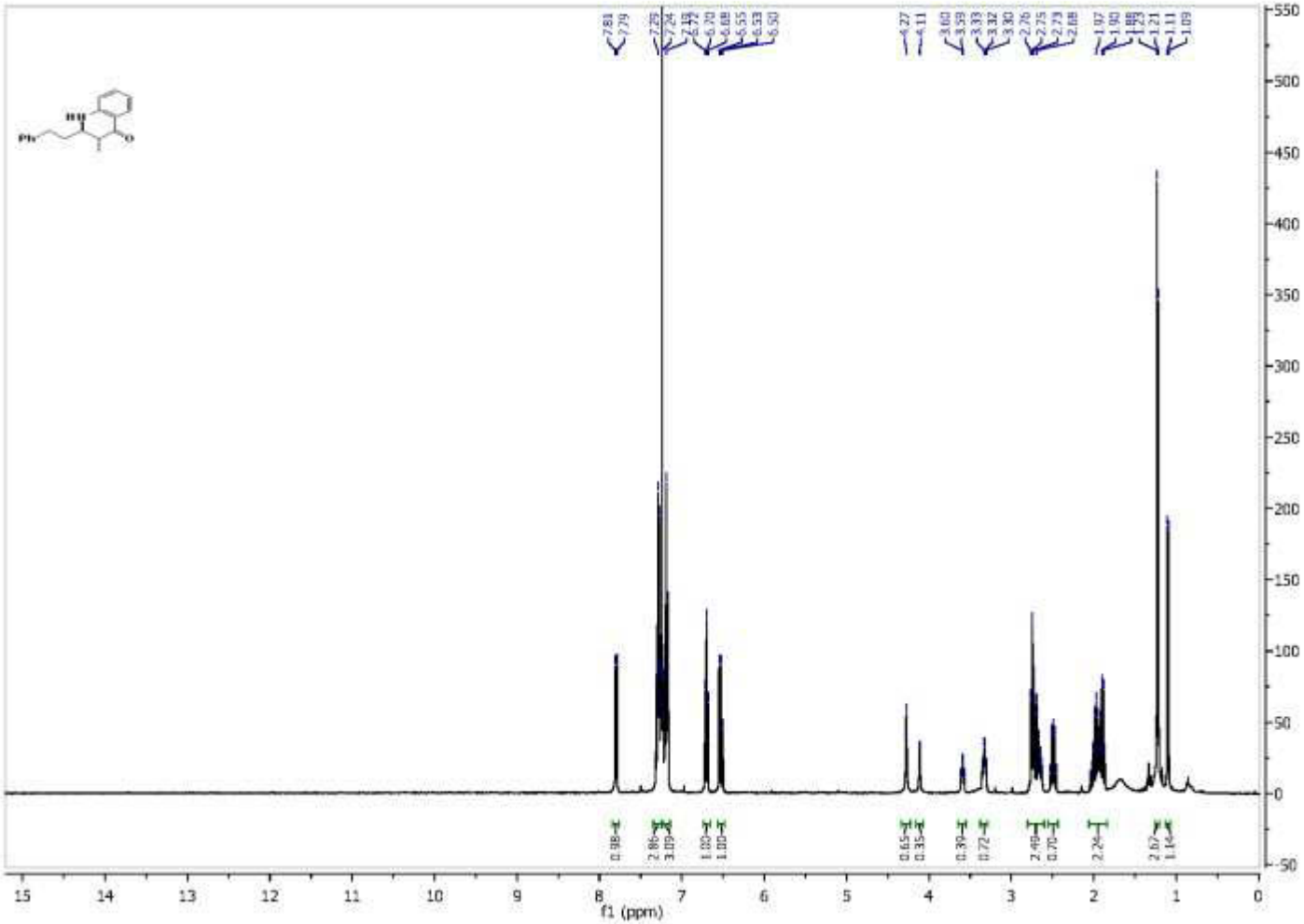

Figure A400 400 MHz 1H NMR ($CDCl_3$) Spectra of Compound **374**

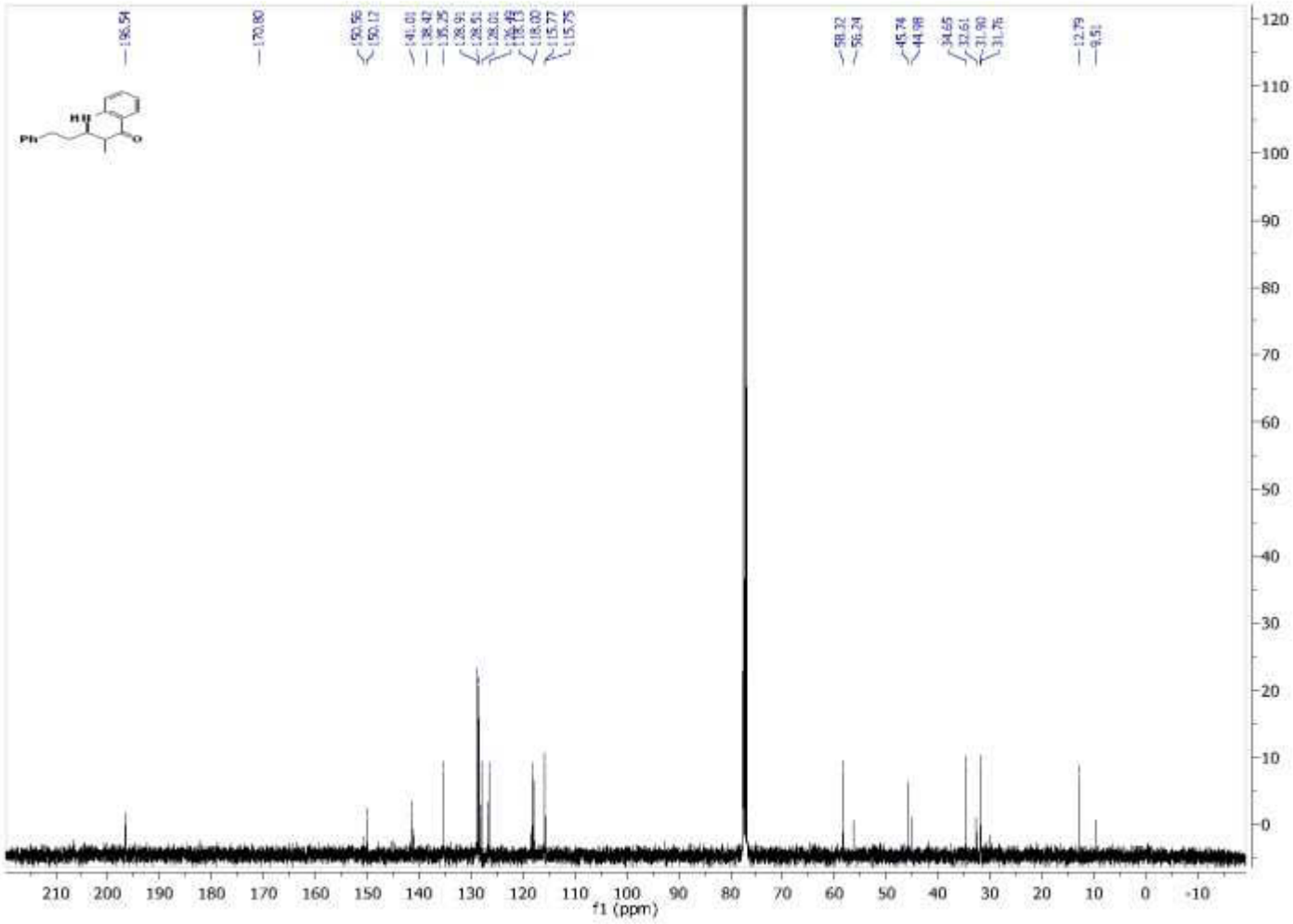

Figure A401 100 MHz 13C NMR ($CDCl_3$) Spectra of Compound **374**

APPENDIX B
X-RAY CRYSTALLOGRAPHIC DATA FOR TFA-SALT **152**

A colorless plate (0.38 x 0.28 x 0.06 mm) was isolated from the sample and mounted with grease on the tip of a nitrile polymer mount wrapped around a stainless steel pin epoxied to a brass pin and placed on the diffractometer with the long crystal dimension (unit cell b-axis) approximately parallel to the diffractometer phi axis.

Data for **152** were collected with a Nonius KappaCCD diffractometer (Mo K-alpha radiation, graphite monochromator) at 190(2) K (cold N_2 gas stream) using standard CCD techniques yielding 57173 data. Lorentz and polarization corrections were applied. A correction for absorption using the multi-scan technique was applied (T-max = 0.508, T-min = 0.868). Equivalent data were averaged yielding 9061 unique data (R-int = 0.022, 7601* F > 4*Sig(F), Friedel pairs not averaged). Based on a preliminary examination of the crystal, the space group P2(1) was assigned, no significant exceptions to the systematic absences (0k0, k=odd) were noted. The computer programs from the HKL package were used for data reduction.

The preliminary model of the structure was obtained using XS, a direct methods program. Least-squares refining of the model vs. the data was performed with XL computer program. Illustrations were made with the XP program and tables were made with the XCIF program. All are in the SHELXTL v6.1 package. Thermal ellipsoids shown in the illustrations are at the 50% level unless otherwise noted.

All non-hydrogen atoms (except minor component F atoms were refined with anisotropic thermal parameters.

The structure has two cation-anion pairs per asymmetric unit, the second pair is has primed atom labels.

The CF_3 groups of both anions were disordered by rotation about the C-CF_3 bond by approximately 180 degrees. The second orientation of the F atoms have 'A' appended.

The occupancies refined to 0.906(5):0.094(5) for F(1-3):F(1A-3A) and 0.862(5):0.138(5) for F(1'-3'):F(1A'-3A'). The C-F bonds were restrained to be the same and the F(1-3)-F(1-2) and F(1-3)A-F(1-3)A distances were restrained to be the same. The F1A, F2A and F3A atoms were constrained to have the same isotropic displacement parameter and the F1A', F2A' and F3A' atoms were constrained to have the same isotropic displacement parameter.

All H atoms were included with the riding model using the XL program default values.

No further restraints or constraints were imposed on the refinement model. Hydrogen bonding geometries are in Table B8.

Table B1 Crystal Data and Structure Refinement for **152**

Identification code	**152**
Empirical formula	C20 H21 Br F3 N O3
Formula weight	460.29
Temperature	190(2) K
Wavelength	0.71073 Å
Crystal system, space group	Monoclinic, P 21
Unit cell dimension	a = 11.7144(12) Å alpha = 90 deg. b = 8.8267(10) Å beta = 101.940(5) deg. c = 20.144(3) Å gamma = 90 deg.
Volume	2037.8(4) $Å^3$
Z, Calculated density	4, 1.500 Mg/m^3
Absorption coefficient	2.064 mm^{-1}
Crystal size	0.38 x 0.26 x 0.06 mm

Table B1 Continued

Theta range for data collection .....2.9 to 27.5 deg.

Limiting indices ..... -15<=h<=15, -11<=k<=11, -26<=l<=26

Reflections collected / unique.....57173 / 9061 [R(int) = 0.0217]

Completeness to theta = 27.50 ..... 99.7 %

Absorption correction .....Semi-empirical from equivalents

Max. and min. transmission .....0.8862 and 0.5077

Refinement method..... Full-matrix least-squares on F^2

Data / restraints / parameters..... 9061 / 139 / 530

Goodness-of-fit on F^2.....1.022

Final R indices [I>2sigma(I)] .....R1 = 0.0344, wR2 = 0.0744

R indices (all data) .....R1 = 0.0472, wR2 = 0.0795

Absolute structure parameter .....0.004(5)

Extinction coefficient.....0.0020(4)

Largest diff. peak and hole.....0.324 and -0.360 eÅ^{-3}

Table B2 Atomic coordinates (x 10^4) and equivalent isotropic displacement parameters (A^2 x 10^3) for **152**

	x	y	z	U(eq)
Br(1)	-488(1)	9675(1)	6863(1)	73(1)
O(1)	6189(2)	6411(2)	6339(1)	45(1)
N(1)	4041(2)	6462(3)	6660(1)	34(1)
C(1)	5424(2)	5209(3)	6099(2)	44(1)

Table B2 Continued

C(2)	4178(3)	5812(3)	5971(2)	40(1)
C(3)	4017(3)	7087(4)	5474(2)	49(1)
C(4)	3241(4)	7058(5)	4903(2)	76(1)
C(5)	3342(3)	4464(4)	5778(2)	56(1)
C(6)	7344(2)	5927(4)	6635(2)	46(1)
C(7)	8033(2)	5416(3)	6122(2)	39(1)
C(8)	8769(3)	4191(4)	6252(2)	47(1)
C(9)	9442(3)	3757(5)	5795(2)	66(1)
C(10)	9374(4)	4522(6)	5205(2)	80(1)
C(11)	8628(4)	5739(6)	5060(2)	80(1)
C(12)	7967(3)	6195(4)	5519(2)	57(1)
C(13)	2937(2)	7229(3)	6684(1)	33(1)
C(14)	1968(2)	6387(3)	6727(2)	40(1)
C(15)	936(3)	7116(3)	6771(2)	44(1)
C(16)	918(2)	8684(4)	6782(2)	44(1)
C(17)	1883(2)	9530(3)	6751(2)	42(1)
C(18)	2908(2)	8795(3)	6698(1)	39(1)
Br(1')	10772(1)	3472(1)	8062(1)	47(1)
O(1')	4071(2)	6611(2)	8751(1)	40(1)
N(1')	6239(2)	6359(2)	8484(1)	28(1)
C(1')	4921(2)	7672(3)	9071(2)	37(1)
C(2')	6108(2)	6885(3)	9194(1)	32(1)
C(3')	7025(2)	8056(3)	9455(2)	38(1)
C(4')	7773(3)	7979(4)	10038(2)	49(1)
C(5')	6137(3)	5493(3)	9644(2)	43(1)
C(6')	2976(2)	7262(4)	8456(2)	42(1)

Table B2 Continued

C(7')	2266(2)	7739(3)	8972(2)	38(1)
C(8')	1487(3)	8942(3)	8830(2)	49(1)
C(9')	773(3)	9291(5)	9289(2)	67(1)
C(10')	875(3)	8479(6)	9882(2)	71(1)
C(11')	1650(3)	7322(5)	10012(2)	64(1)
C(12')	2345(3)	6951(4)	9571(2)	49(1)
C(13')	7352(2)	5654(3)	8426(1)	28(1)
C(14')	7399(2)	4107(3)	8343(1)	31(1)
C(15')	8426(2)	3439(4)	8243(1)	33(1)
C(16')	9377(2)	4343(3)	8232(1)	33(1)
C(17')	9337(2)	5900(3)	8321(1)	37(1)
C(18')	8307(2)	6567(3)	8410(1)	32(1)
C(21)	6401(2)	9600(3)	7531(1)	36(1)
O(2)	5707(2)	8505(2)	7501(1)	39(1)
O(3)	7206(2)	9970(2)	7990(1)	54(1)
C(22)	6197(2)	10585(3)	6891(2)	41(1)
F(1)	7000(2)	11612(3)	6884(1)	74(1)
F(2)	5201(2)	11331(3)	6804(2)	94(1)
F(3)	6139(4)	9789(3)	6332(1)	106(1)
F(1A)	6049(15)	12024(10)	7038(7)	53(5)
F(2A)	5262(10)	10246(18)	6433(7)	53(5)
F(3A)	7064(10)	10562(19)	6577(7)	53(5)
C(21')	3831(2)	3309(3)	7666(2)	37(1)
O(2')	4562(2)	4357(2)	7666(1)	37(1)
O(3')	2950(2)	3005(2)	7244(1)	54(1)
C(22')	4077(2)	2293(3)	8294(2)	44(1)

Table B2 Continued

F(1')	3859(4)	3053(3)	8834(2)	99(1)
F(2')	5152(2)	1851(4)	8479(2)	98(1)
F(3')	3400(3)	1106(3)	8259(2)	92(1)
F(1A')	3234(8)	2154(16)	8612(6)	56(4)
F(2A')	5012(8)	2608(15)	8740(6)	56(4)
F(3A')	4258(12)	908(10)	8068(6)	56(4)

Note: U(eq) is defined as one third of the trace of the orthogonalized Uij tensor.

Table B3 Selected bond lengths [A] and angles [deg] for **152**

Br(1)-C(16)	1.901(3)
O(1)-C(1)	1.408(3)
O(1)-C(6)	1.426(3)
N(1)-C(13)	1.469(3)
N(1)-C(2)	1.541(4)
C(1)-C(2)	1.524(4)
C(2)-C(3)	1.492(5)
C(2)-C(5)	1.539(4)
C(3)-C(4)	1.310(5)
C(6)-C(7)	1.507(4)
C(7)-C(8)	1.374(4)
C(7)-C(12)	1.384(4)
C(8)-C(9)	1.383(5)
C(9)-C(10)	1.355(6)
C(10)-C(11)	1.377(7)
C(11)-C(12)	1.383(5)

Table B3 Continued

C(13)-C(14)	1.374(4)
C(13)-C(18)	1.384(4)
C(14)-C(15)	1.390(4)
C(15)-C(16)	1.385(5)
C(16)-C(17)	1.367(4)
C(17)-C(18)	1.387(4)
Br(1')-C(16')	1.900(2)
O(1')-C(6')	1.419(3)
O(1')-C(1')	1.421(3)
N(1')-C(13')	1.471(3)
N(1')-C(2')	1.542(3)
C(1')-C(2')	1.528(4)
C(2')-C(3')	1.504(4)
C(2')-C(5')	1.523(4)
C(3')-C(4')	1.314(4)
C(6')-C(7')	1.519(4)
C(7')-C(12')	1.379(5)
C(7')-C(8')	1.391(4)
C(8')-C(9')	1.403(5)
C(9')-C(10')	1.377(6)
C(10')-C(11')	1.356(6)
C(11')-C(12')	1.363(5)
C(13')-C(14')	1.378(4)
C(13')-C(18')	1.385(4)
C(14')-C(15')	1.393(4)
C(15')-C(16')	1.374(4)

Table B3 Continued

C(16')-C(17')	1.388(4)
C(17')-C(18')	1.387(4)
C(21)-O(3)	1.221(3)
C(21)-O(2)	1.257(3)
C(21)-C(22)	1.532(4)
C(22)-F(1)	1.309(3)
C(22)-F(3)	1.317(3)
C(22)-F(2)	1.319(3)
C(21')-O(3')	1.223(3)
C(21')-O(2')	1.261(3)
C(21')-C(22')	1.528(4)
C(22')-F(2')	1.296(3)
C(22')-F(3')	1.308(3)
C(22')-F(1')	1.348(4)
C(1)-O(1)-C(6)	113.5(2)
C(13)-N(1)-C(2)	117.2(2)
O(1)-C(1)-C(2)	108.3(2)
C(3)-C(2)-C(1)	111.1(3)
C(3)-C(2)-C(5)	115.3(3)
C(1)-C(2)-C(5)	108.1(3)
C(3)-C(2)-N(1)	107.6(2)
C(1)-C(2)-N(1)	104.6(2)
C(5)-C(2)-N(1)	109.6(2)
C(4)-C(3)-C(2)	122.9(3)
O(1)-C(6)-C(7)	113.6(2)

Table B3 Continued

C(8)-C(7)-C(12)	118.6(3)
C(8)-C(7)-C(6)	120.6(3)
C(12)-C(7)-C(6)	120.8(3)
C(7)-C(8)-C(9)	120.8(3)
C(10)-C(9)-C(8)	120.5(4)
C(9)-C(10)-C(11)	119.6(4)
C(10)-C(11)-C(12)	120.3(4)
C(11)-C(12)-C(7)	120.2(4)
C(14)-C(13)-C(18)	121.0(3)
C(14)-C(13)-N(1)	119.8(3)
C(18)-C(13)-N(1)	119.1(2)
C(13)-C(14)-C(15)	119.7(3)
C(16)-C(15)-C(14)	118.7(3)
C(17)-C(16)-C(15)	122.0(3)
C(17)-C(16)-Br(1)	119.5(2)
C(15)-C(16)-Br(1)	118.5(2)
C(16)-C(17)-C(18)	119.0(3)
C(13)-C(18)-C(17)	119.6(3)
C(6')-O(1')-C(1')	114.2(2)
C(13')-N(1')-C(2')	117.45(19)
O(1')-C(1')-C(2')	107.6(2)
C(3')-C(2')-C(5')	114.8(2)
C(3')-C(2')-C(1')	107.7(2)
C(5')-C(2')-C(1')	111.8(2)
C(3')-C(2')-N(1')	109.3(2)
C(5')-C(2')-N(1')	108.3(2)

Table B3 Continued

C(1')-C(2')-N(1')	104.4(2)
C(4')-C(3')-C(2')	124.9(3)
O(1')-C(6')-C(7')	113.7(2)
C(12')-C(7')-C(8')	119.1(3)
C(12')-C(7')-C(6')	120.8(3)
C(8')-C(7')-C(6')	120.0(3)
C(7')-C(8')-C(9')	119.2(3)
C(10')-C(9')-C(8')	120.1(3)
C(11')-C(10')-C(9')	119.6(3)
C(10')-C(11')-C(12')	121.4(4)
C(11')-C(12')-C(7')	120.6(4)
C(14')-C(13')-C(18')	121.4(2)
C(14')-C(13')-N(1')	119.1(2)
C(18')-C(13')-N(1')	119.3(2)
C(13')-C(14')-C(15')	119.6(3)
C(16')-C(15')-C(14')	119.0(3)
C(15')-C(16')-C(17')	121.5(3)
C(15')-C(16')-Br(1')	119.9(2)
C(17')-C(16')-Br(1')	118.5(2)
C(18')-C(17')-C(16')	119.4(2)
C(13')-C(18')-C(17')	118.9(2)
O(3)-C(21)-O(2)	129.3(3)
O(3)-C(21)-C(22)	116.6(2)
O(2)-C(21)-C(22)	114.1(2)
F(1)-C(22)-F(3)	105.7(3)
F(1)-C(22)-F(2)	105.7(2)

Table B3 Continued

F(3)-C(22)-F(2)	105.4(3)
F(1)-C(22)-C(21)	114.5(2)
F(3)-C(22)-C(21)	112.9(2)
F(2)-C(22)-C(21)	112.0(2)
O(3')-C(21')-O(2')	129.5(3)
O(3')-C(21')-C(22')	115.7(2)
O(2')-C(21')-C(22')	114.8(2)
F(2')-C(22')-F(3')	108.5(3)
F(2')-C(22')-F(1')	104.6(3)
F(3')-C(22')-F(1')	103.2(3)
F(1')-C(22')-C(21')	109.9(2)
F(2')-C(22')-C(21')	114.9(2)
F(3')-C(22')-C(21')	114.6(3)

Symmetry transformations used to generate equivalent atoms.

Table B4 Bond lengths [A] and angles [deg] for **152**

Br(1)-C(16)	1.901(3)
O(1)-C(1)	1.408(3)
O(1)-C(6)	1.426(3)
N(1)-C(13)	1.469(3)
N(1)-C(2)	1.541(4)
N(1)-H(1C)	0.9200
N(1)-H(1D)	0.9200
C(1)-C(2)	1.524(4)

Table B4 Continued

C(1)-H(1A)	0.9900
C(1)-H(1B)	0.9900
C(2)-C(3)	1.492(5)
C(2)-C(5)	1.539(4)
C(3)-C(4)	1.310(5)
C(3)-H(3)	0.9500
C(4)-H(4A)	0.9500
C(4)-H(4B)	0.9500
C(5)-H(5A)	0.9800
C(5)-H(5B)	0.9800
C(5)-H(5C)	0.9800
C(6)-C(7)	1.507(4)
C(6)-H(6A)	0.9900
C(6)-H(6B)	0.9900
C(7)-C(8)	1.374(4)
C(7)-C(12)	1.384(4)
C(8)-C(9)	1.383(5)
C(8)-H(8)	0.9500
C(9)-C(10)	1.355(6)
C(9)-H(9)	0.9500
C(10)-C(11)	1.377(7)
C(10)-H(10)	0.9500
C(11)-C(12)	1.383(5)
C(11)-H(11)	0.9500
C(12)-H(12)	0.9500
C(13)-C(14)	1.374(4)

Table B4 Continued

C(13)-C(18)	1.384(4)
C(14)-C(15)	1.390(4)
C(14)-H(14)	0.9500
C(15)-C(16)	1.385(5)
C(15)-H(15)	0.9500
C(16)-C(17)	1.367(4)
C(17)-C(18)	1.387(4)
C(17)-H(17)	0.9500
C(18)-H(18)	0.9500
Br(1')-C(16')	1.900(2)
O(1')-C(6')	1.419(3)
O(1')-C(1')	1.421(3)
N(1')-C(13')	1.471(3)
N(1')-C(2')	1.542(3)
N(1')-H(1C')	0.9200
N(1')-H(1D')	0.9200
C(1')-C(2')	1.528(4)
C(1')-H(1A')	0.9900
C(1')-H(1B')	0.9900
C(2')-C(3')	1.504(4)
C(2')-C(5')	1.523(4)
C(3')-C(4')	1.314(4)
C(3')-H(3')	0.9500
C(4')-H(4A')	0.9500
C(4')-H(4B')	0.9500
C(5')-H(5A')	0.9800

Table B4 Continued

C(5')-H(5B')	0.9800
C(5')-H(5C')	0.9800
C(6')-C(7')	1.519(4)
C(6')-H(6A')	0.9900
C(6')-H(6B')	0.9900
C(7')-C(12')	1.379(5)
C(7')-C(8')	1.391(4)
C(8')-C(9')	1.403(5)
C(8')-H(8')	0.9500
C(9')-C(10')	1.377(6)
C(9')-H(9')	0.9500
C(10')-C(11')	1.356(6)
C(10')-H(10')	0.9500
C(11')-C(12')	1.363(5)
C(11')-H(11')	0.9500
C(12')-H(12')	0.9500
C(13')-C(14')	1.378(4)
C(13')-C(18')	1.385(4)
C(14')-C(15')	1.393(4)
C(14')-H(14')	0.9500
C(15')-C(16')	1.374(4)
C(15')-H(15')	0.9500
C(16')-C(17')	1.388(4)
C(17')-C(18')	1.387(4)
C(17')-H(17')	0.9500
C(18')-H(18')	0.9500

Table B4 continued

C(21)-O(3)	1.221(3)
C(21)-O(2)	1.257(3)
C(21)-C(22)	1.532(4)
C(22)-F(3A)	1.303(7)
C(22)-F(1)	1.309(3)
C(22)-F(2A)	1.312(7)
C(22)-F(3)	1.317(3)
C(22)-F(2)	1.319(3)
C(22)-F(1A)	1.324(7)
C(21')-O(3')	1.223(3)
C(21')-O(2')	1.261(3)
C(21')-C(22')	1.528(4)
C(22')-F(1A')	1.290(6)
C(22')-F(2A')	1.295(6)
C(22')-F(2')	1.296(3)
C(22')-F(3')	1.308(3)
C(22')-F(3A')	1.336(6)
C(22')-F(1')	1.348(4)
C(1)-O(1)-C(6)	113.5(2)
C(13)-N(1)-C(2)	117.2(2)
C(13)-N(1)-H(1C)	108.0
C(2)-N(1)-H(1C)	108.0
C(13)-N(1)-H(1D)	108.0
C(2)-N(1)-H(1D)	108.0
H(1C)-N(1)-H(1D)	107.2

Table B4 Continued

O(1)-C(1)-C(2)	108.3(2)
O(1)-C(1)-H(1A)	110.0
C(2)-C(1)-H(1A)	110.0
O(1)-C(1)-H(1B)	110.0
C(2)-C(1)-H(1B)	110.0
H(1A)-C(1)-H(1B)	108.4
C(3)-C(2)-C(1)	111.1(3)
C(3)-C(2)-C(5)	115.3(3)
C(1)-C(2)-C(5)	108.1(3)
C(3)-C(2)-N(1)	107.6(2)
C(1)-C(2)-N(1)	104.6(2)
C(5)-C(2)-N(1)	109.6(2)
C(4)-C(3)-C(2)	122.9(3)
C(4)-C(3)-H(3)	118.6
C(2)-C(3)-H(3)	118.6
C(3)-C(4)-H(4A)	120.0
C(3)-C(4)-H(4B)	120.0
H(4A)-C(4)-H(4B)	120.0
C(2)-C(5)-H(5A)	109.5
C(2)-C(5)-H(5B)	109.5
H(5A)-C(5)-H(5B)	109.5
C(2)-C(5)-H(5C)	109.5
H(5A)-C(5)-H(5C)	109.5
H(5B)-C(5)-H(5C)	109.5
O(1)-C(6)-C(7)	113.6(2)
O(1)-C(6)-H(6A)	108.9

Table B4 Continued

C(7)-C(6)-H(6A)	108.9
O(1)-C(6)-H(6B)	108.9
C(7)-C(6)-H(6B)	108.9
H(6A)-C(6)-H(6B)	107.7
C(8)-C(7)-C(12)	118.6(3)
C(8)-C(7)-C(6)	120.6(3)
C(12)-C(7)-C(6)	120.8(3)
C(7)-C(8)-C(9)	120.8(3)
C(7)-C(8)-H(8)	119.6
C(9)-C(8)-H(8)	119.6
C(10)-C(9)-C(8)	120.5(4)
C(10)-C(9)-H(9)	119.8
C(8)-C(9)-H(9)	119.8
C(9)-C(10)-C(11)	119.6(4)
C(9)-C(10)-H(10)	120.2
C(11)-C(10)-H(10)	120.2
C(10)-C(11)-C(12)	120.3(4)
C(10)-C(11)-H(11)	119.8
C(12)-C(11)-H(11)	119.8
C(11)-C(12)-C(7)	120.2(4)
C(11)-C(12)-H(12)	119.9
C(7)-C(12)-H(12)	119.9
C(14)-C(13)-C(18)	121.0(3)
C(14)-C(13)-N(1)	119.8(3)
C(18)-C(13)-N(1)	119.1(2)
C(13)-C(14)-C(15)	119.7(3)

Table B4 Continued

C(13)-C(14)-H(14)	120.2
C(15)-C(14)-H(14)	120.2
C(16)-C(15)-C(14)	118.7(3)
C(16)-C(15)-H(15)	120.7
C(14)-C(15)-H(15)	120.7
C(17)-C(16)-C(15)	122.0(3)
C(17)-C(16)-Br(1)	119.5(2)
C(15)-C(16)-Br(1)	118.5(2)
C(16)-C(17)-C(18)	119.0(3)
C(16)-C(17)-H(17)	120.5
C(18)-C(17)-H(17)	120.5
C(13)-C(18)-C(17)	119.6(3)
C(13)-C(18)-H(18)	120.2
C(17)-C(18)-H(18)	120.2
C(6')-O(1')-C(1')	114.2(2)
C(13')-N(1')-C(2')	117.45(19)
C(13')-N(1')-H(1C')	107.9
C(2')-N(1')-H(1C')	107.9
C(13')-N(1')-H(1D')	107.9
C(2')-N(1')-H(1D')	107.9
H(1C')-N(1')-H(1D')	107.2
O(1')-C(1')-C(2')	107.6(2)
O(1')-C(1')-H(1A')	110.2
C(2')-C(1')-H(1A')	110.2
O(1')-C(1')-H(1B')	110.2
C(2')-C(1')-H(1B')	110.2

Table B4 Continued

H(1A')-C(1')-H(1B')	108.5
C(3')-C(2')-C(5')	114.8(2)
C(3')-C(2')-C(1')	107.7(2)
C(5')-C(2')-C(1')	111.8(2)
C(3')-C(2')-N(1')	109.3(2)
C(5')-C(2')-N(1')	108.3(2)
C(1')-C(2')-N(1')	104.4(2)
C(4')-C(3')-C(2')	124.9(3)
C(4')-C(3')-H(3')	117.5
C(2')-C(3')-H(3')	117.5
C(3')-C(4')-H(4A')	120.0
C(3')-C(4')-H(4B')	120.0
H(4A')-C(4')-H(4B')	120.0
C(2')-C(5')-H(5A')	109.5
C(2')-C(5')-H(5B')	109.5
H(5A')-C(5')-H(5B')	109.5
C(2')-C(5')-H(5C')	109.5
H(5A')-C(5')-H(5C')	109.5
H(5B')-C(5')-H(5C')	109.5
O(1')-C(6')-C(7')	113.7(2)
O(1')-C(6')-H(6A')	108.8
C(7')-C(6')-H(6A')	108.8
O(1')-C(6')-H(6B')	108.8
C(7')-C(6')-H(6B')	108.8
H(6A')-C(6')-H(6B')	107.7
C(12')-C(7')-C(8')	119.1(3)

Table B4 Continued

C(12')-C(7')-C(6')	120.8(3)
C(8')-C(7')-C(6')	120.0(3)
C(7')-C(8')-C(9')	119.2(3)
C(7')-C(8')-H(8')	120.4
C(9')-C(8')-H(8')	120.4
C(10')-C(9')-C(8')	120.1(3)
C(10')-C(9')-H(9')	120.0
C(8')-C(9')-H(9')	120.0
C(11')-C(10')-C(9')	119.6(3)
C(11')-C(10')-H(10')	120.2
C(9')-C(10')-H(10')	120.2
C(10')-C(11')-C(12')	121.4(4)
C(10')-C(11')-H(11')	119.3
C(12')-C(11')-H(11')	119.3
C(11')-C(12')-C(7')	120.6(4)
C(11')-C(12')-H(12')	119.7
C(7')-C(12')-H(12')	119.7
C(14')-C(13')-C(18')	121.4(2)
C(14')-C(13')-N(1')	119.1(2)
C(18')-C(13')-N(1')	119.3(2)
C(13')-C(14')-C(15')	119.6(3)
C(13')-C(14')-H(14')	120.2
C(15')-C(14')-H(14')	120.2
C(16')-C(15')-C(14')	119.0(3)
C(16')-C(15')-H(15')	120.5
C(14')-C(15')-H(15')	120.5

Table B4 Continued

C(15')-C(16')-C(17')	121.5(3)
C(15')-C(16')-Br(1')	119.9(2)
C(17')-C(16')-Br(1')	118.5(2)
C(18')-C(17')-C(16')	119.4(2)
C(18')-C(17')-H(17')	120.3
C(16')-C(17')-H(17')	120.3
C(13')-C(18')-C(17')	118.9(2)
C(13')-C(18')-H(18')	120.5
C(17')-C(18')-H(18')	120.5
O(3)-C(21)-O(2)	129.3(3)
O(3)-C(21)-C(22)	116.6(2)
O(2)-C(21)-C(22)	114.1(2)
F(1)-C(22)-F(3)	105.7(3)
F(1)-C(22)-F(2)	105.7(2)
F(3)-C(22)-F(2)	105.4(3)
F(3A)-C(22)-F(2A)	106.1(6)
F(3A)-C(22)-F(1A)	106.0(6)
F(2A)-C(22)-F(1A)	104.3(6)
F(1)-C(22)-C(21)	114.5(2)
F(3)-C(22)-C(21)	112.9(2)
F(2)-C(22)-C(21)	112.0(2)
F(2A)-C(22)-C(21)	115.1(7)
F(3A)-C(22)-C(21)	113.5(7)
F(1A)-C(22)-C(21)	111.1(7)
O(3')-C(21')-O(2')	129.5(3)
O(3')-C(21')-C(22')	115.7(2)

Table B4 Continued

O(2')-C(21')-C(22')	114.8(2)
F(2')-C(22')-F(3')	108.5(3)
F(2')-C(22')-F(1')	104.6(3)
F(3')-C(22')-F(1')	103.2(3)
F(1A')-C(22')-F(3A')	105.9(6)
F(2A')-C(22')-F(3A')	105.2(6)
F(1A')-C(22')-F(2A')	107.4(6)
F(1')-C(22')-C(21')	109.9(2)
F(2')-C(22')-C(21')	114.9(2)
F(3')-C(22')-C(21')	114.6(3)
F(3A')-C(22')-C(21')	105.8(6)
F(1A')-C(22')-C(21')	115.7(6)
F(2A')-C(22')-C(21')	115.9(6)

Symmetry transformations used to generate equivalent atoms.

Table B5 Anisotropic displacement parameters (A^2 x 10^3) for **152**
(The anisotropic displacement factor exponent takes the form:
-2 pi^2 [h^2 a*^2 U11 + ... + 2 h k a* b* U12])

	U11	U22	U33	U23	U13	U12
Br(1)	39(1)	55(1)	123(1)	-18(1)	12(1)	8(1)
O(1)	34(1)	41(1)	60(1)	-11(1)	11(1)	-1(1)
N(1)	31(1)	33(1)	37(1)	-3(1)	6(1)	-5(1)
C(1)	40(2)	40(2)	54(2)	-10(1)	15(1)	-1(1)
C(2)	41(2)	44(2)	37(2)	-8(1)	10(1)	-5(1)
C(3)	45(2)	61(2)	43(2)	-3(2)	10(1)	1(2)

Table B5 Continued

C(4)	79(3)	79(3)	65(2)	21(2)	1(2)	1(2)
C(5)	54(2)	62(2)	53(2)	-19(2)	11(2)	-15(2)
C(6)	34(2)	57(2)	45(2)	-4(1)	7(1)	3(1)
C(7)	31(1)	47(2)	37(2)	-3(1)	5(1)	-4(1)
C(8)	38(2)	48(2)	55(2)	-2(1)	6(1)	1(1)
C(9)	48(2)	67(3)	87(3)	-21(2)	22(2)	3(2)
C(10)	69(3)	95(3)	91(3)	-27(3)	49(2)	-11(3)
C(11)	96(3)	100(4)	54(2)	3(2)	37(2)	-20(3)
C(12)	65(2)	57(2)	53(2)	11(2)	19(2)	5(2)
C(13)	30(1)	35(2)	34(2)	-1(1)	2(1)	-1(1)
C(14)	34(1)	33(2)	51(2)	-6(1)	5(1)	-4(1)
C(15)	34(2)	39(2)	58(2)	-7(1)	7(1)	-7(1)
C(16)	32(1)	43(2)	53(2)	-7(2)	2(1)	3(1)
C(17)	42(2)	29(2)	52(2)	-2(1)	1(1)	-2(1)
C(18)	33(1)	40(2)	43(2)	-1(1)	5(1)	-7(1)
Br(1')	30(1)	52(1)	59(1)	-7(1)	9(1)	8(1)
O(1')	30(1)	35(1)	57(1)	-10(1)	13(1)	-4(1)
N(1')	26(1)	26(1)	34(1)	-1(1)	7(1)	-1(1)
C(1')	33(1)	31(1)	47(2)	-7(1)	11(1)	-1(1)
C(2')	34(1)	30(1)	33(1)	-3(1)	10(1)	3(1)
C(3')	34(1)	36(2)	44(2)	-8(1)	12(1)	0(1)
C(4')	42(2)	51(2)	51(2)	-14(1)	4(1)	3(1)
C(5')	45(2)	43(2)	42(2)	2(1)	15(1)	6(1)
C(6')	34(1)	48(2)	44(2)	-2(1)	8(1)	1(1)
C(7')	27(1)	37(2)	51(2)	-15(1)	10(1)	-7(1)
C(8')	32(2)	44(2)	67(2)	-11(1)	4(1)	-2(1)

Table B5 Continued

C(9')	28(2)	64(2)	105(3)	-36(2)	6(2)	5(2)
C(10')	44(2)	97(3)	82(3)	-36(3)	35(2)	-17(2)
C(11')	62(2)	74(3)	64(2)	-17(2)	32(2)	-26(2)
C(12')	48(2)	46(2)	56(2)	-8(2)	19(2)	-12(1)
C(13')	28(1)	29(1)	26(1)	-2(1)	6(1)	0(1)
C(14')	29(1)	29(1)	7(1)	-1(1)	8(1)	-6(1)
C(15')	35(1)	28(1)	36(1)	0(1)	7(1)	2(1)
C(16')	28(1)	37(2)	34(1)	-2(1)	7(1)	7(1)
C(17')	28(1)	39(2)	43(2)	-4(1)	8(1)	-7(1)
C(18')	32(1)	28(1)	36(1)	-3(1)	7(1)	-4(1)
C(21)	31(1)	28(1)	49(2)	0(1)	1(1)	1(1)
O(2)	40(1)	31(1)	47(1)	3(1)	10(1)	-7(1)
O(3)	50(1)	39(1)	66(2)	7(1)	-7(1)	-11(1)
C(22)	36(2)	32(2)	54(2)	3(1)	11(1)	-2(1)
F(1)	67(2)	70(2)	81(2)	26(1)	5(1)	-35(1)
F(2)	56(2)	92(2)	140(3)	75(2)	33(2)	32(1)
F(3)	226(4)	47(1)	47(1)	-2(1)	33(2)	-20(2)
C(21')	30(1)	26(1)	56(2)	-5(1)	14(1)	2(1)
O(2')	36(1)	29(1)	48(1)	-4(1)	11(1)	-7(1)
O(3')	36(1)	44(1)	77(2)	2(1)	-1(1)	-9(1)
C(22')	34(2)	36(2)	66(2)	4(1)	17(1)	-6(1)
F(1')	168(4)	71(2)	71(2)	4(1)	52(2)	-3(2)
F(2')	44(1)	111(3)	141(3)	83(2)	24(2)	18(2)
F(3')	95(2)	56(2)	115(2)	27(2)	-2(2)	-45(2)

Table B6 Hydrogen coordinates (x 10^4) and isotropic displacement parameters (A^2 x 10^3) for **152**

	x	y	z	U(eq)
H(1C)	4138	5680	6969	41
H(1D)	4639	7139	6803	41
H(1A)	5521	4384	6439	53
H(1B)	5598	4799	5674	53
H(3)	4498	7957	5576	59
H(4A)	2751	6199	4790	92
H(4B)	3169	7896	4601	92
H(5A)	3580	3875	5417	85
H(5B)	2546	4842	5618	85
H(5C)	3367	3818	6176	85
H(6A)	7299	5081	6951	55
H(6B)	7763	6773	6903	55
H(8)	8816	3634	6660	57
H(9)	9955	2917	5896	80
H(10)	9838	4221	4893	96
H(11)	8567	6266	4643	96
H(12)	7465	7047	5419	69
H(14)	2005	5312	6726	48
H(15)	255	6550	6794	53
H(17)	1853	10605	6766	51
H(18)	3585	9364	6672	47
H(1C')	5651	5678	8326	34
H(1D')	6120	7185	8200	34
H(1A')	4743	8011	9507	44
H(1B')	4924	8570	8777	44
H(3')	7067	8915	9177	45
H(4A')	7759	7137	10330	59
H(4B')	8328	8765	10168	59
H(5A')	6908	5016	9709	64
H(5B')	5539	4772	9427	64
H(5C')	5983	5797	10085	64
H(6A')	2519	6519	8141	50
H(6B')	3109	8160	8187	50
H(8')	1438	9520	8427	58
H(9')	220	10089	9191	80
H(10')	404	8728	10198	85
H(11')	1710	6757	10419	77
H(12')	2887	6143	9677	59
H(14')	6733	3500	8354	37
H(15')	8470	2374	8183	39

Table B6 Continued

H(17')	10008	6503	8320	44
H(18')	8258	7634	8460	38

Table B7 Torsion angles [deg] for **152**

C(6)-O(1)-C(1)-C(2)	165.3(2)
O(1)-C(1)-C(2)-C(3)	58.1(3)
O(1)-C(1)-C(2)-C(5)	-174.4(2)
O(1)-C(1)-C(2)-N(1)	-57.7(3)
C(13)-N(1)-C(2)-C(3)	57.7(3)
C(13)-N(1)-C(2)-C(1)	175.9(2)
C(13)-N(1)-C(2)-C(5)	-68.4(3)
C(1)-C(2)-C(3)-C(4)	121.7(4)
C(5)-C(2)-C(3)-C(4)	-1.7(5)
N(1)-C(2)-C(3)-C(4)	-124.3(4)
C(1)-O(1)-C(6)-C(7)	74.3(3)
O(1)-C(6)-C(7)-C(8)	-141.2(3)
O(1)-C(6)-C(7)-C(12)	40.7(4)
C(12)-C(7)-C(8)-C(9)	0.9(5)
C(6)-C(7)-C(8)-C(9)	-177.2(3)
C(7)-C(8)-C(9)-C(10)	-1.0(5)
C(8)-C(9)-C(10)-C(11)	-0.1(6)
C(9)-C(10)-C(11)-C(12)	1.1(7)
C(10)-C(11)-C(12)-C(7)	-1.2(6)
C(8)-C(7)-C(12)-C(11)	0.1(5)
C(6)-C(7)-C(12)-C(11)	178.3(3)

Table B7 Continued

C(2)-N(1)-C(13)-C(14)	80.2(3)
C(2)-N(1)-C(13)-C(18)	-103.0(3)
C(18)-C(13)-C(14)-C(15)	1.3(4)
N(1)-C(13)-C(14)-C(15)	178.0(3)
C(13)-C(14)-C(15)-C(16)	-1.0(5)
C(14)-C(15)-C(16)-C(17)	-0.1(5)
C(14)-C(15)-C(16)-Br(1)	-178.7(2)
C(15)-C(16)-C(17)-C(18)	0.9(5)
Br(1)-C(16)-C(17)-C(18)	179.5(2)
C(14)-C(13)-C(18)-C(17)	-0.5(4)
N(1)-C(13)-C(18)-C(17)	-177.2(2)
C(16)-C(17)-C(18)-C(13)	-0.6(4)
C(6')-O(1')-C(1')-C(2')	-165.5(2)
O(1')-C(1')-C(2')-C(3')	173.3(2)
O(1')-C(1')-C(2')-C(5')	-59.7(3)
O(1')-C(1')-C(2')-N(1')	57.2(3)
C(13')-N(1')-C(2')-C(3')	60.3(3)
C(13')-N(1')-C(2')-C(5')	-65.4(3)
C(13')-N(1')-C(2')-C(1')	175.4(2)
C(5')-C(2')-C(3')-C(4')	-3.5(4)
C(1')-C(2')-C(3')-C(4')	121.7(3)
N(1')-C(2')-C(3')-C(4')	-125.5(3)
C(1')-O(1')-C(6')-C(7')	-74.2(3)
O(1')-C(6')-C(7')-C(12')	-32.0(4)
O(1')-C(6')-C(7')-C(8')	150.9(3)
C(12')-C(7')-C(8')-C(9')	-2.0(4)

Table B7 Continued

C(6')-C(7')-C(8')-C(9')	175.1(3)
C(7')-C(8')-C(9')-C(10')	2.0(5)
C(8')-C(9')-C(10')-C(11')	-1.4(5)
C(9')-C(10')-C(11')-C(12')	0.7(6)
C(10')-C(11')-C(12')-C(7')	-0.8(5)
C(8')-C(7')-C(12')-C(11')	1.4(4)
C(6')-C(7')-C(12')-C(11')	-175.7(3)
C(2')-N(1')-C(13')-C(14')	105.0(3)
C(2')-N(1')-C(13')-C(18')	-79.3(3)
C(18')-C(13')-C(14')-C(15')	0.2(4)
N(1')-C(13')-C(14')-C(15')	175.8(2)
C(13')-C(14')-C(15')-C(16')	0.3(4)
C(14')-C(15')-C(16')-C(17')	0.3(4)
C(14')-C(15')-C(16')-Br(1')	-177.61(19)
C(15')-C(16')-C(17')-C(18')	-1.2(4)
Br(1')-C(16')-C(17')-C(18')	176.7(2)
C(14')-C(13')-C(18')-C(17')	-1.1(4)
N(1')-C(13')-C(18')-C(17')	-176.7(2)
C(16')-C(17')-C(18')-C(13')	1.6(4)
O(3)-C(21)-C(22)-F(3A)	63.6(9)
O(2)-C(21)-C(22)-F(3A)	-115.8(9)
O(3)-C(21)-C(22)-F(1)	7.4(4)
O(2)-C(21)-C(22)-F(1)	-172.0(3)
O(3)-C(21)-C(22)-F(2A)	-173.9(9)
O(2)-C(21)-C(22)-F(2A)	6.7(9)
O(3)-C(21)-C(22)-F(3)	128.4(3)

Table B7 Continued

O(2)-C(21)-C(22)-F(3)	-51.0(4)
O(3)-C(21)-C(22)-F(2)	-112.9(3)
O(2)-C(21)-C(22)-F(2)	67.7(3)
O(3)-C(21)-C(22)-F(1A)	-55.6(9)
O(2)-C(21)-C(22)-F(1A)	125.0(8)
O(3')-C(21')-C(22')-F(1A')	-53.2(7)
O(2')-C(21')-C(22')-F(1A')	125.8(7)
O(3')-C(21')-C(22')-F(2A')	179.7(7)
O(2')-C(21')-C(22')-F(2A')	-1.3(7)
O(3')-C(21')-C(22')-F(2')	135.2(3)
O(2')-C(21')-C(22')-F(2')	-45.8(4)
O(3')-C(21')-C(22')-F(3')	8.6(4)
O(2')-C(21')-C(22')-F(3')	-172.4(3)
O(3')-C(21')-C(22')-F(3A')	63.6(7)
O(2')-C(21')-C(22')-F(3A')	-117.4(6)
O(3')-C(21')-C(22')-F(1')	-107.1(3)
O(2')-C(21')-C(22')-F(1')	71.9(3)

Symmetry transformations used to generate equivalent atoms.

Table B8 Hydrogen bonds for **152** [A and deg.]

D-H...	A	d(D-H)	d(H...A)	d(D...A)	<(DHA)
N(1)-H(1C)	O(2')	0.92	1.81	2.723(3)	169
N(1)-H(1D)	O(2)	0.92	2.07	2.926(3)	155
N(1')-H(1C')	O(2')	0.92	2.01	2.891(3)	159
N(1')-H(1D')	O(2)	0.92	1.81	2.718(3)	167

Symmetry transformations used to generate equivalent atoms:

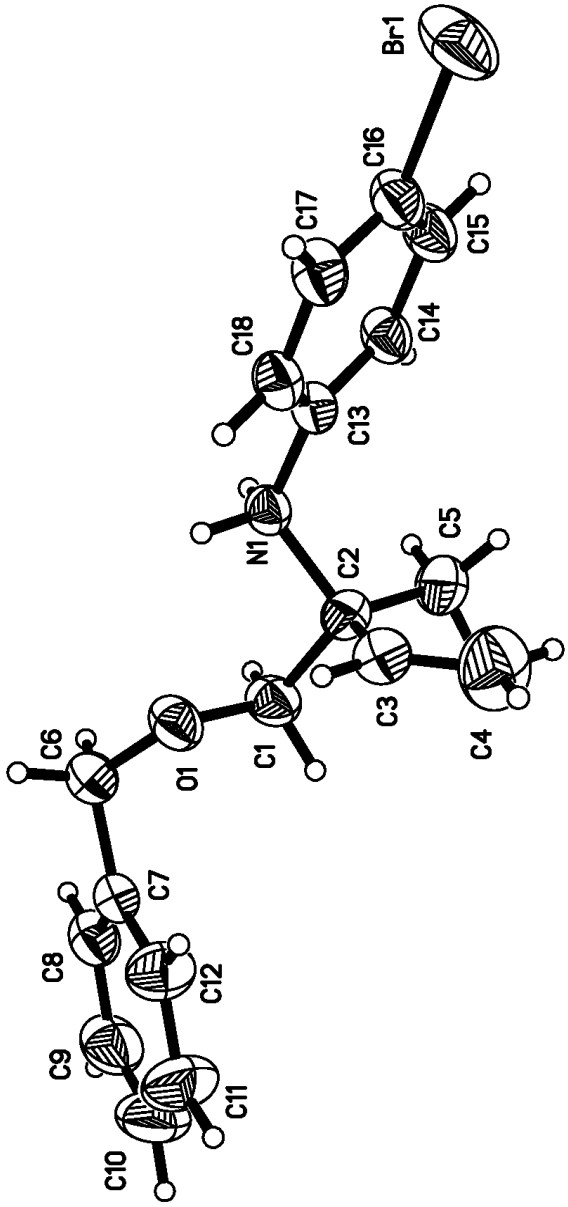

Figure B1 Monomer A **152** Structure

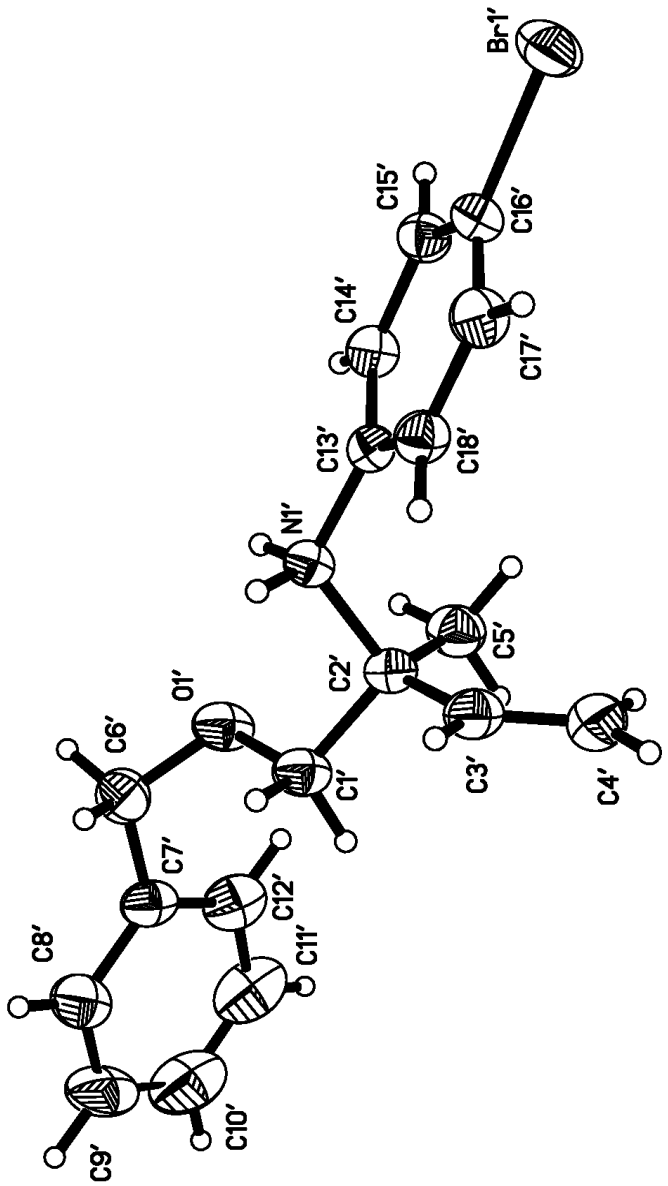

Figure B2 Monomer B **152** Structure

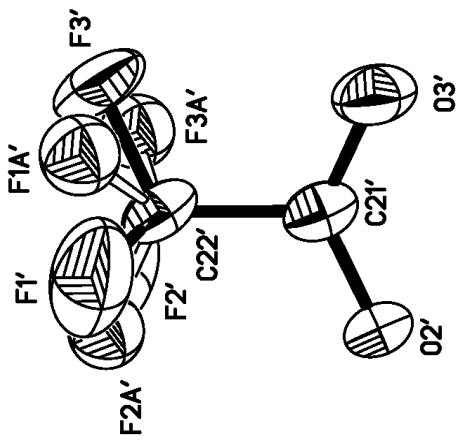

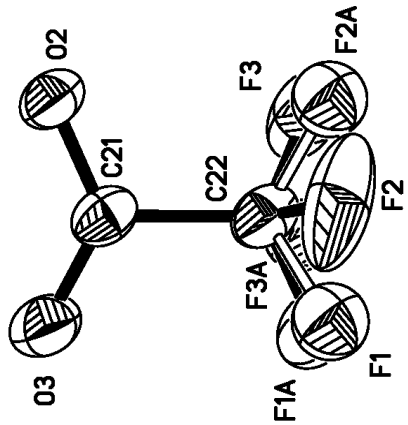

Figure B3 TFA-Salt Structures

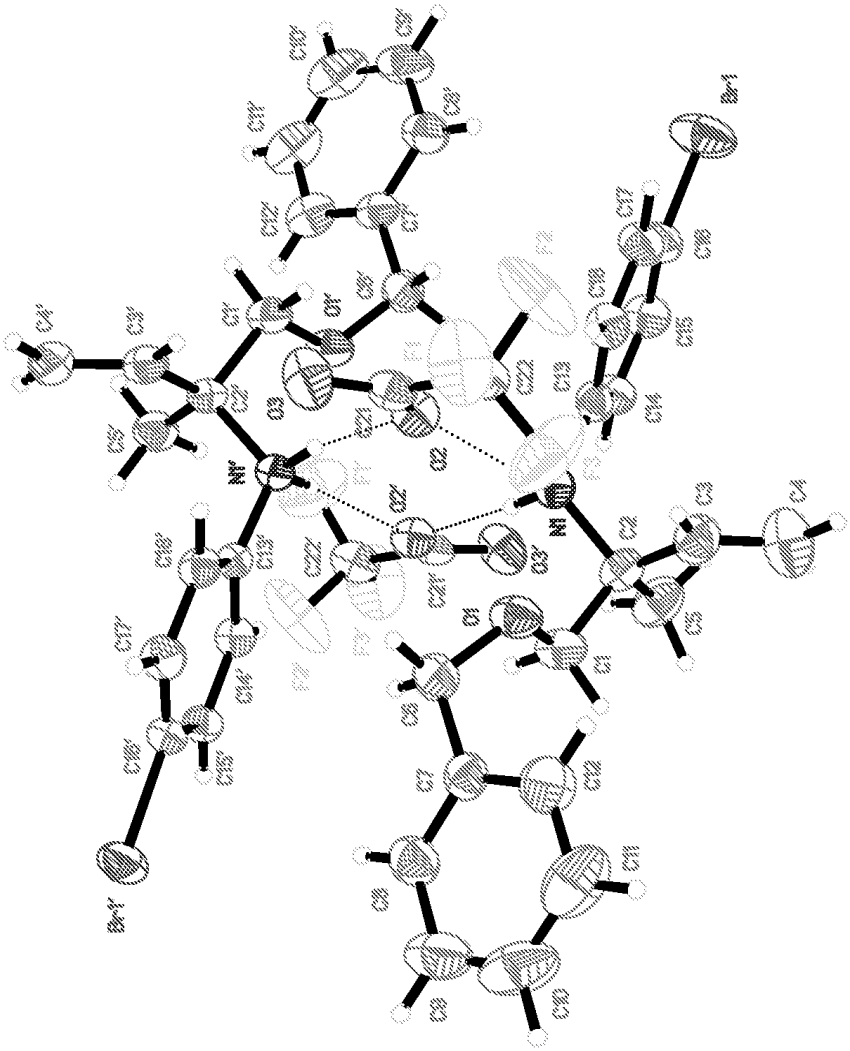

Figure B4 TFA-Salt Bridged Structural Dimer of **152**

Table B9 Observed and calculated structure factors for **152**

h k l 10Fo 10Fc 10s h k l 10Fo 10Fc 10s h k l 10Fo 10Fc 10s h k l 10Fo 10Fc 10s h k l 10Fo 10Fc 10s

1-11 0 0 11 1 7 -3 0 279 292 1 9 3 0 466 467 5 3 11 0 68 63 12 11 -7 1 100 91 14
2-11 0 68 68 14 8 -3 0 282 294 3 10 3 0 182 184 2 4 11 0 67 66 11 -12 -6 1 103 100 11
3-11 0 59 58 17 9 -3 0 493 489 4 11 3 0 78 77 5 -4-11 1 0 42 1 -11 -6 1 126 133 6
4-11 0 54 62 54 10 -3 0 170 170 3 12 3 0 50 59 11 -3-11 1 42 42 42 -10 -6 1 206 205 10
0-10 0 196 209 5 11 -3 0 76 54 6 13 3 0 61 84 10 -2-11 1 129 100 14 -9 -6 1 162 171 4
1-10 0 82 85 7 12 -3 0 69 72 31 14 3 0 77 58 12 -1-11 1 117 105 8 -8 -6 1 119 119 3
2-10 0 156 143 5 13 -3 0 72 82 11 0 4 0 586 584 3 0-11 1 138 137 7 -6 -6 1 287 279 2
3-10 0 0 35 1 14 -3 0 58 42 23 1 4 0 112 109 1 1-11 1 71 79 13 -5 -6 1 200 201 2
4-10 0 115 117 5 0 -2 0 352 351 2 2 4 0 223 215 1 2-11 1 83 71 11 -4 -6 1 596 583 2
5-10 0 49 47 17 1 -2 0 1699 1673 19 3 4 0 210 203 3 3-11 1 46 19 39 -3 -6 1 327 331 2
6-10 0 66 59 22 2 -2 0 831 846 3 4 4 0 468 459 2 4-11 1 0 15 1 -2 -6 1 372 370 1
7-10 0 115 107 10 3 -2 0 308 308 1 5 4 0 168 169 5 -7-10 1 89 85 15 -1 -6 1 83 78 1
1 -9 0 92 86 7 4 -2 0 164 160 1 6 4 0 314 319 2 -6-10 1 53 81 27 0 -6 1 132 142 1
2 -9 0 75 77 5 5 -2 0 783 768 4 7 4 0 137 139 1 -5-10 1 128 128 6 1 -6 1 209 214 1
3 -9 0 316 303 4 6 -2 0 439 443 2 8 4 0 59 56 4 -4-10 1 115 124 5 2 -6 1 449 438 3
4 -9 0 137 134 4 7 -2 0 337 336 2 9 4 0 65 70 4 -3-10 1 54 32 19 3 -6 1 346 351 1
5 -9 0 144 139 6 8 -2 0 483 481 3 10 4 0 175 173 2 -2-10 1 20 39 19 4 -6 1 456 452 2
6 -9 0 155 140 9 9 -2 0 110 105 3 11 4 0 238 252 3 -1-10 1 13 14 13 5 -6 1 264 268 1
7 -9 0 0 23 1 10 -2 0 491 486 4 12 4 0 238 243 4 0-10 1 28 23 27 6 -6 1 139 140 2
8 -9 0 84 68 18 11 -2 0 69 69 10 13 4 0 175 177 13 1-10 1 113 111 10 7 -6 1 221 218 2

Table B9 Continued

0 -8 0 350 352 5 12 -2 0 219 227 4 1 5 0 749 726 3 2-10 1 98 102 6
8 -6 1 137 136 6
1 -8 0 314 307 4 13 -2 0 257 260 9 2 5 0 184 185 2 3-10 1 122 141 5
9 -6 1 180 170 10
2 -8 0 234 234 2 14 -2 0 167 175 10 3 5 0 152 150 1 4-10 1 62 68 11
10 -6 1 176 169 5
3 -8 0 191 201 2 1 -1 0 54 81 14 4 5 0 522 528 4 5-10 1 67 62 16
11 -6 1 108 102 11
4 -8 0 93 90 3 2 -1 0 765 764 4 5 5 0 221 223 1 6-10 1 88 63 10 12
-6 1 36 36 35
5 -8 0 133 122 5 3 -1 0 758 777 4 6 5 0 91 95 2 7-10 1 86 67 13 -
13 -5 1 64 85 14
6 -8 0 189 197 8 4 -1 0 579 597 3 7 5 0 233 236 2 -9 -9 1 88 60 18 -
12 -5 1 65 24 17
7 -8 0 172 171 7 5 -1 0 578 601 3 8 5 0 272 277 2 -8 -9 1 13 43 12 -
11 -5 1 53 49 12
8 -8 0 204 203 9 6 -1 0 565 560 4 9 5 0 217 222 2 -7 -9 1 58 47 15 -
10 -5 1 191 182 4
9 -8 0 101 98 15 7 -1 0 271 278 2 10 5 0 193 188 2 -6 -9 1 55 85 14 -
9 -5 1 256 245 6
10 -8 0 124 99 14 8 -1 0 125 124 1 11 5 0 67 78 7 -5 -9 1 134 126 6
-8 -5 1 335 332 3
1 -7 0 241 246 2 9 -1 0 146 152 2 12 5 0 67 67 8 -4 -9 1 57 52 16 -
7 -5 1 227 214 5
2 -7 0 231 229 2 10 -1 0 236 230 4 13 5 0 116 101 9 -3 -9 1 128 117 4
-6 -5 1 90 89 4
3 -7 0 293 296 2 11 -1 0 174 181 11 0 6 0 449 468 5 -2 -9 1 55 45 7 -
5 -5 1 286 276 1
4 -7 0 277 273 2 12 -1 0 91 97 8 1 6 0 117 121 1 -1 -9 1 30 22 14 -
4 -5 1 475 463 2
5 -7 0 349 346 2 13 -1 0 125 126 6 2 6 0 216 219 2 0 -9 1 240 235 3
-3 -5 1 297 302 1
6 -7 0 154 153 2 14 -1 0 73 62 29 3 6 0 249 245 3 1 -9 1 96 89 4 -
2 -5 1 433 441 2
7 -7 0 170 156 4 2 0 0 352 348 2 4 6 0 201 196 1 2 -9 1 88 92 4 -
1 -5 1 796 789 7
8 -7 0 100 83 6 3 0 0 655 682 3 5 6 0 177 182 1 3 -9 1 82 78 4 0
-5 1 547 551 3
9 -7 0 78 82 18 4 0 0 424 447 2 6 6 0 234 228 3 4 -9 1 27 35 27 1
-5 1 505 507 7
10 -7 0 86 99 17 5 0 0 326 340 2 7 6 0 168 167 2 5 -9 1 104 106 8
2 -5 1 65 67 2
0 -6 0 478 484 4 6 0 0 835 831 5 8 6 0 180 182 2 6 -9 1 66 60 19 3
-5 1 88 92 2

Table B9 Continued

1 -6 0 92 95 1 7 0 0 577 551 3 9 6 0 158 162 2 7 -9 1 0 37 1 4 -5 1 136 140 2
2 -6 0 212 213 1 8 0 0 549 547 3 10 6 0 163 157 12 8 -9 1 25 54 25 5 -5 1 556 548 3
3 -6 0 245 242 1 9 0 0 748 749 4 11 6 0 150 141 4 9 -9 1 0 65 1 6 -5 1 214 205 1
4 -6 0 215 209 1 10 0 0 41 52 10 12 6 0 150 150 4 -10 -8 1 164 146 12 7 -5 1 506 505 3
5 -6 0 146 150 3 11 0 0 21 31 21 1 7 0 229 231 1 -9 -8 1 191 185 9 8 -5 1 183 174 2
6 -6 0 206 206 2 12 0 0 0 7 1 2 7 0 251 248 3 -8 -8 1 116 117 8 9 -5 1 149 155 6
7 -6 0 204 202 4 13 0 0 181 182 5 3 7 0 294 296 2 -7 -8 1 94 103 9 10 -5 1 152 155 3
8 -6 0 179 178 4 14 0 0 103 108 9 4 7 0 267 260 2 -6 -8 1 115 99 7 11 -5 1 113 127 11
9 -6 0 158 155 3 1 1 0 48 40 2 5 7 0 373 369 2 -5 -8 1 33 29 18 12 -5 1 84 88 13
10 -6 0 190 181 17 2 1 0 735 734 3 6 7 0 178 169 2 -4 -8 1 166 175 2 13 -5 1 147 133 10
11 -6 0 151 144 7 3 1 0 743 764 4 7 7 0 144 136 3 -3 -8 1 65 63 5 -14 -4 1 42 42 41
12 -6 0 149 141 9 4 1 0 582 603 4 8 7 0 99 100 3 -2 -8 1 97 92 4 -13 -4 1 112 112 7
1 -5 0 773 740 3 5 1 0 631 652 3 9 7 0 95 90 4 -1 -8 1 47 39 6 -12 -4 1 122 122 15
2 -5 0 168 167 1 6 1 0 503 500 4 10 7 0 90 88 4 0 -8 1 97 100 4 -11 -4 1 138 136 5
3 -5 0 149 144 2 7 1 0 288 296 3 11 7 0 108 102 11 1 -8 1 98 103 1 -10 -4 1 137 134 6
4 -5 0 533 533 2 8 1 0 121 114 2 0 8 0 335 331 5 2 -8 1 93 99 2 -9 -4 1 83 86 5
5 -5 0 238 237 1 9 1 0 164 171 2 1 8 0 309 311 6 3 -8 1 14 23 13 -8 -4 1 106 99 2
6 -5 0 78 74 2 10 1 0 199 196 3 2 8 0 240 237 14 4 -8 1 56 60 6 -7 -4 1 294 291 2
7 -5 0 251 256 8 11 1 0 160 157 4 3 8 0 188 195 3 5 -8 1 118 110 7 -6 -4 1 527 517 4
8 -5 0 249 256 2 12 1 0 126 121 6 4 8 0 93 87 5 6 -8 1 134 132 7 -5 -4 1 489 488 2
9 -5 0 226 232 8 13 1 0 129 108 6 5 8 0 132 128 3 7 -8 1 130 123 10 -4 -4 1 916 910 4
10 -5 0 203 207 5 14 1 0 82 69 11 6 8 0 181 185 4 8 -8 1 167 157 9 -3 -4 1 313 322 1

Table B9 Continued

11 -5 0 45 74 14 0 2 0 330 316 2 7 8 0 167 166 5 9 -8 1 122 98 9 -
2 -4 1 172 179 1
12 -5 0 57 63 20 1 2 0 1674 1670 11 8 8 0 219 204 2 10 -8 1 81 106 16
-1 -4 1 84 84 1
13 -5 0 71 84 18 2 2 0 835 853 5 9 8 0 106 97 4 -10 -7 1 0 45 1 0
-4 1 388 393 2
0 -4 0 594 584 4 3 2 0 311 315 1 10 8 0 97 98 4 -9 -7 1 137 132 10
1 -4 1 488 497 3
1 -4 0 119 116 1 4 2 0 161 158 1 1 9 0 84 85 6 -8 -7 1 18 37 17 2
-4 1 563 581 2
2 -4 0 237 229 1 5 2 0 790 779 4 2 9 0 123 117 9 -7 -7 1 340 336 4
3 -4 1 985 961 4
3 -4 0 205 200 1 6 2 0 457 460 2 3 9 0 309 296 2 -6 -7 1 65 67 3 4
-4 1 605 606 3
4 -4 0 443 434 2 7 2 0 353 352 3 4 9 0 142 140 3 -5 -7 1 330 335 2
5 -4 1 213 209 1
5 -4 0 175 171 1 8 2 0 482 478 3 5 9 0 137 130 10 -4 -7 1 171 170 1
6 -4 1 291 295 6
6 -4 0 313 318 2 9 2 0 137 139 2 6 9 0 137 140 3 -3 -7 1 157 155 1
7 -4 1 71 69 2
7 -4 0 124 127 2 10 2 0 478 475 3 7 9 0 27 34 9 -2 -7 1 117 110 6 8
-4 1 224 224 3
8 -4 0 54 51 5 11 2 0 123 117 4 8 9 0 56 71 6 -1 -7 1 195 204 5 9
-4 1 142 139 2
9 -4 0 93 92 2 12 2 0 214 220 6 9 9 0 0 6 1 0 -7 1 88 91 1 10 -
4 1 228 227 3
10 -4 0 194 179 4 13 2 0 254 253 6 0 10 0 183 196 8 1 -7 1 148 141 1
11 -4 1 148 140 7
11 -4 0 238 249 4 14 2 0 190 186 5 1 10 0 99 96 9 2 -7 1 175 178 1
12 -4 1 152 164 5
12 -4 0 227 229 4 1 3 0 486 504 2 2 10 0 141 137 6 3 -7 1 204 207 2
13 -4 1 92 73 7
13 -4 0 166 174 5 2 3 0 134 136 1 3 10 0 20 46 19 4 -7 1 358 353 2
-14 -3 1 46 47 25
1 -3 0 494 506 2 3 3 0 228 232 1 4 10 0 126 120 7 5 -7 1 114 115 2 -
13 -3 1 127 132 5
2 -3 0 129 128 1 4 3 0 270 275 2 5 10 0 28 38 17 6 -7 1 85 79 9 -
12 -3 1 78 89 7
3 -3 0 248 246 2 5 3 0 296 289 2 6 10 0 57 64 8 7 -7 1 176 171 6 -
11 -3 1 141 124 4
4 -3 0 228 231 2 6 3 0 349 365 2 7 10 0 113 108 11 8 -7 1 24 19 24 -
10 -3 1 107 102 6
5 -3 0 350 339 2 7 3 0 253 264 1 1 11 0 78 20 19 9 -7 1 51 36 17 -
9 -3 1 510 514 4

Table B9 Continued

6 -3 0 334 348 2 8 3 0 319 332 2 2 11 0 75 64 14 10 -7 1 152 158 13 -8 -3 1 212 209 2
-7 -3 1 443 446 2 -4 0 1 20 20 4 0 3 1 1332 1339 7 5 6 1 254 255 1 -3 11 1 46 49 46
-6 -3 1 237 236 1 -3 0 1 422 445 2 1 3 1 635 648 3 6 6 1 117 114 2 -2 11 1 118 104 10
-5 -3 1 524 508 2 -2 0 1 273 288 1 2 3 1 159 153 1 7 6 1 231 230 2 0 11 1 155 132 10
-4 -3 1 223 226 1 2 0 1 92 106 1 3 3 1 409 400 2 8 6 1 122 121 2 1 11 1 51 87 47
-3 -3 1 783 787 4 3 0 1 115 133 3 4 3 1 731 703 6 9 6 1 184 178 4 2 11 1 42 64 26
-2 -3 1 267 286 4 4 0 1 0 16 1 5 3 1 407 405 2 10 6 1 183 185 9 3 11 1 0 22 1
-1 -3 1 1029 1009 5 5 0 1 334 344 2 6 3 1 659 670 3 11 6 1 100 96 5 4 11 1 26 19 25
0 -3 1 1347 1346 6 6 0 1 424 448 2 7 3 1 371 371 2 12 6 1 26 35 25 -4-11 2 78 53 26
1 -3 1 628 635 2 7 0 1 466 465 5 8 3 1 231 235 2 -11 7 1 70 64 9 -3-11 2 44 69 23
2 -3 1 139 138 1 8 0 1 276 279 3 9 3 1 439 435 3 -10 7 1 45 43 15 -2-11 2 54 16 25
3 -3 1 393 383 2 9 0 1 678 686 4 10 3 1 116 109 3 -9 7 1 134 126 3 -1-11 2 42 13 41
4 -3 1 751 725 4 10 0 1 31 19 15 11 3 1 97 88 5 -8 7 1 43 52 8 0-11 2 53 34 19
6 -3 1 676 682 4 11 0 1 14 13 13 12 3 1 101 81 11 -7 7 1 347 343 2 1-11 2 100 94 20
7 -3 1 353 357 2 12 0 1 136 150 5 13 3 1 161 159 5 -6 7 1 57 45 5 2-11 2 60 43 21
8 -3 1 248 257 4 13 0 1 335 317 5 14 3 1 31 40 31 -5 7 1 299 298 2 3-11 2 74 59 9
9 -3 1 425 419 3 14 0 1 260 263 6 -14 4 1 54 48 16 -4 7 1 193 188 2 -7-10 2 110 105 12
10 -3 1 129 117 10 -14 1 1 122 107 7 -13 4 1 113 114 13 -3 7 1 156 153 1 -6-10 2 105 108 12
11 -3 1 110 109 5 -13 1 1 208 212 5 -12 4 1 119 121 5 -2 7 1 136 127 1 -5-10 2 127 139 9
12 -3 1 86 85 7 -12 1 1 274 276 3 -11 4 1 147 153 4 -1 7 1 175 186 3 -4-10 2 80 85 8
13 -3 1 158 156 6 -11 1 1 303 306 3 -10 4 1 108 111 3 0 7 1 110 121 3 -3-10 2 75 80 8
14 -3 1 56 47 19 -10 1 1 168 177 3 -9 4 1 96 92 2 1 7 1 155 146 1 -2-10 2 84 80 8

Table B9 Continued

-14 -2 1 125 129 6 -9 1 1 209 216 3 -8 4 1 105 109 3 2 7 1 169 166 2 -1-10 2 86 86 7
-13 -2 1 125 125 9 -8 1 1 144 150 2 -7 4 1 283 282 1 3 7 1 216 221 12 0-10 2 186 185 7
-12 -2 1 136 150 5 -7 1 1 326 326 2 -6 4 1 521 514 2 4 7 1 375 364 3 1-10 2 49 53 14
-11 -2 1 92 86 6 -6 1 1 626 630 5 -5 4 1 481 488 2 5 7 1 92 81 5 2-10 2 67 57 10
-10 -2 1 566 552 4 -5 1 1 513 517 2 -4 4 1 906 901 4 6 7 1 91 80 2 3-10 2 103 87 11
-9 -2 1 167 173 2 -4 1 1 576 590 3 -3 4 1 351 360 1 7 7 1 181 175 2 4-10 2 157 160 5
-8 -2 1 372 386 2 -3 1 1 879 892 4 -2 4 1 156 159 1 8 7 1 47 41 6 5-10 2 94 72 12
-7 -2 1 225 219 1 -2 1 1 283 305 2 -1 4 1 82 81 1 9 7 1 35 39 17 6-10 2 79 77 11
-6 -2 1 325 338 3 -1 1 1 452 489 8 0 4 1 358 363 2 10 7 1 155 159 4 -9 -9 2 61 64 29
-5 -2 1 542 544 3 1 1 1 127 125 1 1 4 1 489 503 2 11 7 1 100 92 5 -8 -9 2 96 92 13
-4 -2 1 850 840 4 2 1 1 1072 1093 5 2 4 1 602 617 3 -10 8 1 140 136 6 -7 -9 2 73 54 16
-3 -2 1 899 906 4 3 1 1 336 343 2 3 4 1 961 949 4 -9 8 1 194 194 4 -6 -9 2 180 184 8
-1 -2 1 923 939 3 4 1 1 296 301 2 4 4 1 566 573 2 -8 8 1 123 115 3 -5 -9 2 114 106 7
0 -2 1 1207 1208 12 5 1 1 561 569 3 5 4 1 236 235 2 -7 8 1 114 112 3 -4 -9 2 176 176 5
1 -2 1 1106 1106 7 6 1 1 200 196 2 6 4 1 288 290 1 -6 8 1 102 106 3 -3 -9 2 220 220 4
2 -2 1 173 185 1 7 1 1 199 189 5 7 4 1 60 63 3 -5 8 1 41 33 5 -2 -9 2 50 59 8
4 -2 1 996 968 5 8 1 1 221 227 2 8 4 1 223 228 2 -4 8 1 180 179 5 -1 -9 2 98 98 4
5 -2 1 737 727 4 9 1 1 248 252 4 9 4 1 164 169 2 -3 8 1 63 60 3 0 -9 2 315 316 4
6 -2 1 412 421 2 10 1 1 181 183 3 10 4 1 238 236 2 -2 8 1 104 102 6 1 -9 2 221 217 5
7 -2 1 286 276 2 11 1 1 186 190 5 11 4 1 136 125 4 -1 8 1 55 38 7 2 -9 2 120 114 7
8 -2 1 369 374 2 12 1 1 192 182 3 12 4 1 139 145 4 0 8 1 88 102 9 3 -9 2 260 258 5
9 -2 1 175 181 3 13 1 1 230 220 5 13 4 1 81 67 6 1 8 1 99 100 1 4 -9 2 75 73 7

Table B9 Continued

10 -2 1 375 376 8 14 1 1 43 40 35 -13 5 1 71 75 12 2 8 1 101 101 1 5 -9 2 97 75 8
11 -2 1 158 165 3 -14 2 1 110 124 14 -12 5 1 34 15 16 3 8 1 26 26 25 6 -9 2 0 33 1
12 -2 1 125 124 6 -13 2 1 126 131 8 -11 5 1 50 37 9 4 8 1 56 54 5 7 -9 2 115 93 12
13 -2 1 142 152 6 -12 2 1 156 154 4 -10 5 1 190 190 3 5 8 1 117 118 2 8 -9 2 106 118 16
14 -2 1 243 236 5 -11 2 1 126 133 4 -9 5 1 255 252 2 6 8 1 114 109 2 -9 -8 2 124 122 9
-14 -1 1 128 118 7 -10 2 1 546 539 4 -8 5 1 323 323 4 7 8 1 129 120 6 -8 -8 2 94 86 13
-13 -1 1 219 214 5 -9 2 1 154 160 2 -7 5 1 239 230 2 8 8 1 154 150 3 -7 -8 2 158 134 8
-12 -1 1 261 270 14 -8 2 1 372 390 4 -6 5 1 113 115 1 9 8 1 97 97 4 -6 -8 2 67 50 14
-11 -1 1 308 306 3 -7 2 1 212 214 1 -5 5 1 302 290 3 10 8 1 100 104 12 -5 -8 2 67 83 13
-10 -1 1 156 155 3 -6 2 1 316 328 2 -4 5 1 470 464 2 -9 9 1 53 62 7 -4 -8 2 159 169 2
-9 -1 1 195 204 3 -5 2 1 533 540 3 -3 5 1 307 312 2 -8 9 1 36 46 9 -3 -8 2 216 209 1
-8 -1 1 123 123 2 -4 2 1 832 829 4 -2 5 1 442 458 5 -7 9 1 50 46 9 -2 -8 2 283 281 3
-7 -1 1 348 350 2 -3 2 1 882 895 4 -1 5 1 771 774 8 -6 9 1 78 84 4 -1 -8 2 228 225 3
-6 -1 1 575 567 5 -2 2 1 341 343 1 0 5 1 550 563 3 -5 9 1 145 135 3 0 -8 2 297 295 2
-5 -1 1 564 579 7 -1 2 1 905 924 4 1 5 1 508 515 3 -4 9 1 33 30 20 1 -8 2 127 136 2
-4 -1 1 543 552 3 0 2 1 1209 1209 6 2 5 1 118 116 1 -3 9 1 125 112 12 2 -8 2 102 105 2
-3 -1 1 866 879 4 1 2 1 1113 1112 9 3 5 1 87 87 1 -2 9 1 66 60 6 3 -8 2 33 33 5
-2 -1 1 261 281 1 2 2 1 166 168 1 4 5 1 117 106 2 -1 9 1 27 38 27 4 -8 2 253 254 4
-1 -1 1 445 481 8 3 2 1 159 174 2 5 5 1 535 532 2 0 9 1 231 227 11 5 -8 2 167 167 4
1 -1 1 121 143 1 4 2 1 1002 975 4 6 5 1 246 241 2 1 9 1 105 100 7 6 -8 2 280 265 8
2 -1 1 1051 1070 5 5 2 1 732 726 3 7 5 1 504 502 3 2 9 1 95 94 2 7 -8 2 148 153 9
3 -1 1 367 375 2 6 2 1 409 417 5 8 5 1 192 178 4 3 9 1 62 65 4 8 -8 2 116 116 12

Table B9 Continued

4 -1 1 324 330 2 7 2 1 229 222 2 9 5 1 151 151 6 4 9 1 46 34 8 9 -8 2 25 49 25
5 -1 1 581 590 3 8 2 1 393 395 3 10 5 1 156 159 3 5 9 1 120 119 3 10 -8 2 78 64 23
6 -1 1 150 142 2 9 2 1 157 159 2 11 5 1 114 122 10 6 9 1 62 61 6 -9 -7 2 145 161 9
7 -1 1 194 181 2 10 2 1 393 389 3 12 5 1 78 92 6 7 9 1 0 26 1 -8 -7 2 138 141 10
8 -1 1 216 219 2 11 2 1 122 134 3 13 5 1 124 120 9 8 9 1 59 44 9 -7 -7 2 239 232 4
9 -1 1 280 281 5 12 2 1 137 133 4 -12 6 1 114 108 5 9 9 1 62 76 10 -6 -7 2 166 167 3
10 -1 1 157 163 3 13 2 1 151 158 9 -11 6 1 134 131 4 -7 10 1 76 75 6 -5 -7 2 370 370 2
11 -1 1 170 169 7 14 2 1 237 229 9 -10 6 1 223 212 3 -6 10 1 80 79 5 -4 -7 2 224 223 2
12 -1 1 192 189 5 -14 3 1 33 50 33 -9 6 1 153 157 2 -5 10 1 128 138 7 -3 -7 2 232 236 1
13 -1 1 226 214 4 -13 3 1 141 131 7 -8 6 1 127 123 8 -4 10 1 121 119 6 -2 -7 2 132 138 1
14 -1 1 50 53 21 -12 3 1 102 108 10 -7 6 1 250 256 5 -3 10 1 0 45 1 -1 -7 2 185 189 1
-15 0 1 248 247 6 -11 3 1 127 111 4 -6 6 1 263 252 2 -2 10 1 46 50 14 0 -7 2 301 297 2
-14 0 1 82 92 8 -10 3 1 107 100 3 -5 6 1 183 183 4 -1 10 1 18 15 18 1 -7 2 415 407 2
-13 0 1 54 43 11 -9 3 1 501 505 3 -4 6 1 584 578 3 0 10 1 0 15 1 2 -7 2 442 438 3
-12 0 1 232 234 4 -8 3 1 185 188 1 -3 6 1 344 347 2 1 10 1 81 100 8 3 -7 2 103 101 2
-11 0 1 123 128 3 -7 3 1 445 449 2 -2 6 1 363 361 2 2 10 1 125 121 11 4 -7 2 230 228 1
-10 0 1 129 128 3 -6 3 1 218 217 1 -1 6 1 85 77 1 3 10 1 115 128 6 5 -7 2 161 168 5
-9 0 1 552 577 5 -5 3 1 549 535 2 0 6 1 134 140 2 4 10 1 59 60 16 6 -7 2 95 100 9
-8 0 1 592 595 3 -4 3 1 193 183 1 1 6 1 228 235 2 5 10 1 79 76 29 7 -7 2 155 149 4
-7 0 1 221 241 1 -3 3 1 786 796 6 2 6 1 434 426 3 6 10 1 62 60 11 8 -7 2 118 113 5
-6 0 1 148 139 1 -2 3 1 295 313 7 3 6 1 351 357 2 7 10 1 70 76 7 9 -7 2 113 118 5
-5 0 1 108 122 3 -1 3 1 998 996 5 4 6 1 453 451 2 -4 11 1 0 28 1 10 -7 2 146 148 10

Table B9 Continued

11 -7 2 94 116 20 -7 -3 2 286 289 3 -7 0 2 65 74 2 -6 3 2 171 178 1
-1 6 2 253 252 2
-11 -6 2 108 104 9 -6 -3 2 166 172 4 -6 0 2 15 7 14 -5 3 2 418 432 2
0 6 2 378 384 2
-10 -6 2 135 132 6 -5 -3 2 427 441 2 -5 0 2 76 78 2 -4 3 2 298 301 3
1 6 2 132 145 16
-9 -6 2 195 188 8 -4 -3 2 312 313 1 -4 0 2 474 487 3 -3 3 2 469 473 2
2 6 2 199 201 2
-8 -6 2 151 150 7 -3 -3 2 462 466 2 -3 0 2 1536 1516 8 -2 3 2 391 402 6
3 6 2 207 209 1
-7 -6 2 91 92 10 -2 -3 2 367 379 3 -2 0 2 903 911 4 -1 3 2 154 159 2
4 6 2 315 302 2
-6 -6 2 159 161 2 -1 -3 2 171 180 2 1 0 2 280 279 9 0 3 2 325 330 2
5 6 2 322 318 4
-5 -6 2 350 356 2 0 -3 2 334 334 2 2 0 2 310 299 2 1 3 2 90 106 1
6 6 2 199 199 2
-4 -6 2 231 231 1 1 -3 2 64 68 3 3 0 2 423 419 2 2 3 2 49 49 2 7
6 2 108 105 2
-3 -6 2 355 366 1 2 -3 2 30 28 2 4 0 2 375 396 2 3 3 2 468 478 2 8
6 2 126 123 2
-2 -6 2 134 130 1 3 -3 2 488 493 2 5 0 2 959 948 5 4 3 2 613 606 3
9 6 2 232 227 5
-1 -6 2 246 249 1 4 -3 2 619 611 3 6 0 2 772 770 4 5 3 2 475 462 2
10 6 2 140 155 3
0 -6 2 399 395 2 5 -3 2 509 497 2 7 0 2 282 295 2 6 3 2 341 348 2
11 6 2 136 121 5
1 -6 2 121 121 1 6 -3 2 334 338 2 8 0 2 208 219 2 7 3 2 163 158 2
12 6 2 80 96 6
2 -6 2 193 192 1 7 -3 2 162 155 2 9 0 2 363 355 4 8 3 2 355 361 2 -
11 7 2 62 72 7
3 -6 2 212 214 4 8 -3 2 335 339 4 10 0 2 92 85 10 9 3 2 221 220 2 -
10 7 2 113 105 4
4 -6 2 330 318 1 9 -3 2 241 240 3 11 0 2 214 217 3 10 3 2 95 93 8 -
9 7 2 151 149 3
5 -6 2 317 313 2 10 -3 2 97 103 4 12 0 2 147 150 4 11 3 2 183 184 5
-8 7 2 152 149 3
6 -6 2 163 169 2 11 -3 2 171 178 5 13 0 2 113 117 7 12 3 2 130 135 5
-7 7 2 217 215 3
7 -6 2 107 101 4 12 -3 2 138 130 5 14 0 2 93 87 7 13 3 2 208 209 10
-6 7 2 190 190 3
8 -6 2 112 117 7 13 -3 2 237 222 12 -15 1 2 0 31 1 14 3 2 111 116 8
-5 7 2 389 386 2
9 -6 2 234 227 5 14 -3 2 109 109 7 -14 1 2 51 7 51 -14 4 2 136 141 13
-4 7 2 228 226 3

Table B9 Continued

10 -6 2 149 160 5 -14 -2 2 88 101 7 -13 1 2 160 158 5 -13 4 2 219 209 8 -3 7 2 222 224 2
11 -6 2 146 125 25 -13 -2 2 181 182 10 -12 1 2 192 187 3 -12 4 2 234 244 6 -2 7 2 144 147 3
12 -6 2 73 90 16 -12 -2 2 130 138 5 -11 1 2 326 331 3 -11 4 2 110 104 5 -1 7 2 173 170 6
-13 -5 2 104 82 12 -11 -2 2 106 99 7 -10 1 2 180 183 3 -10 4 2 89 97 4 0 7 2 316 311 2
-12 -5 2 122 130 10 -10 -2 2 304 305 4 -9 1 2 298 305 2 -9 4 2 95 103 3 1 7 2 415 409 5
-11 -5 2 200 192 4 -9 -2 2 216 211 3 -8 1 2 210 212 2 -8 4 2 262 253 4 2 7 2 422 425 3
-10 -5 2 245 236 4 -8 -2 2 330 333 2 -7 1 2 503 501 3 -7 4 2 294 295 2 3 7 2 120 115 15
-9 -5 2 289 283 4 -7 -2 2 244 252 3 -6 1 2 733 740 3 -6 4 2 363 367 2 4 7 2 205 201 6
-8 -5 2 292 287 3 -6 -2 2 153 165 1 -5 1 2 737 745 3 -5 4 2 269 271 1 5 7 2 174 173 1
-7 -5 2 125 124 2 -5 -2 2 362 369 2 -4 1 2 669 684 3 -4 4 2 319 296 1 6 7 2 108 116 2
-6 -5 2 60 62 3 -4 -2 2 347 352 3 -3 1 2 935 947 4 -3 4 2 223 218 4 7 7 2 127 129 2
-5 -5 2 173 171 4 -3 -2 2 1033 1053 5 -2 1 2 336 328 1 -2 4 2 192 199 2 8 7 2 98 102 9
-4 -5 2 635 631 3 -2 -2 2 1003 989 9 -1 1 2 101 97 3 -1 4 2 212 200 2 9 7 2 121 123 10
-3 -5 2 190 186 1 -1 -2 2 304 325 2 0 1 2 659 694 5 0 4 2 402 387 2 10 7 2 133 128 6
-2 -5 2 268 258 1 0 -2 2 682 691 3 1 1 2 1082 1094 6 1 4 2 160 166 1 11 7 2 138 128 4
-1 -5 2 70 46 4 1 -2 2 371 383 2 2 1 2 828 838 4 2 4 2 96 100 1 -10 8 2 129 135 5
0 -5 2 150 151 3 2 -2 2 582 582 3 3 1 2 1587 1576 8 3 4 2 232 231 1 -9 8 2 108 111 4
1 -5 2 284 286 1 3 -2 2 966 959 4 4 1 2 433 435 2 4 4 2 288 301 1 -8 8 2 68 74 5
2 -5 2 78 76 1 4 -2 2 447 453 3 5 1 2 541 550 3 5 4 2 53 53 3 -7 8 2 123 124 4
3 -5 2 262 248 1 6 -2 2 622 624 3 6 1 2 144 152 2 6 4 2 209 209 1 -6 8 2 50 53 4
4 -5 2 92 96 2 7 -2 2 336 331 3 7 1 2 290 288 2 7 4 2 53 54 3 -5 8 2 97 91 2
5 -5 2 451 448 2 8 -2 2 191 189 2 8 1 2 292 295 2 8 4 2 249 243 2 -4 8 2 164 165 4

Table B9 Continued

6 -5 2 116 112 4 9 -2 2 210 219 2 9 1 2 423 415 4 9 4 2 158 161 2 -3 8 2 233 223 5
7 -5 2 340 338 2 10 -2 2 211 205 7 10 1 2 317 315 3 10 4 2 292 282 3 -2 8 2 253 262 3
8 -5 2 58 56 4 11 -2 2 252 253 3 11 1 2 84 91 10 11 4 2 163 165 4 -1 8 2 237 233 3
9 -5 2 100 110 3 12 -2 2 201 195 5 12 1 2 87 101 5 12 4 2 180 179 3 0 8 2 306 300 2
10 -5 2 172 172 6 13 -2 2 122 119 7 13 1 2 51 45 18 13 4 2 95 99 5 1 8 2 120 127 3
11 -5 2 94 93 9 14 -2 2 63 58 13 14 1 2 46 57 46 -13 5 2 72 81 6 2 8 2 98 107 3
12 -5 2 119 125 10 -15 -1 2 39 39 38 -14 2 2 99 107 7 -12 5 2 140 137 9 3 8 2 33 20 33
13 -5 2 157 142 9 -14 -1 2 0 24 1 -13 2 2 165 176 7 -11 5 2 221 214 3 4 8 2 262 254 2
-14 -4 2 151 145 10 -13 -1 2 144 134 5 -12 2 2 116 118 4 -10 5 2 224 227 2 5 8 2 175 180 9
-13 -4 2 219 214 7 -12 -1 2 190 183 4 -11 2 2 74 75 6 -9 5 2 269 270 2 6 8 2 276 271 3
-12 -4 2 244 253 4 -11 -1 2 337 340 3 -10 2 2 322 327 3 -8 5 2 286 284 2 7 8 2 166 158 3
-11 -4 2 117 110 5 -10 -1 2 170 171 3 -9 2 2 195 196 2 -7 5 2 113 110 2 8 8 2 116 119 3
-10 -4 2 103 99 5 -9 -1 2 308 312 3 -8 2 2 320 326 4 -6 5 2 95 92 3 9 8 2 55 52 6
-9 -4 2 93 112 5 -8 -1 2 228 231 3 -7 2 2 236 239 2 -5 5 2 208 205 2 10 8 2 77 67 5
-8 -4 2 280 274 3 -7 -1 2 504 499 4 -6 2 2 151 163 1 -4 5 2 601 600 2 -9 9 2 65 58 5
-7 -4 2 285 287 2 -6 -1 2 750 757 4 -5 2 2 333 343 4 -3 5 2 198 197 2 -8 9 2 95 97 5
-6 -4 2 337 339 2 -5 -1 2 717 720 4 -4 2 2 413 416 3 -2 5 2 275 271 1 -7 9 2 83 75 5
-5 -4 2 263 270 1 -4 -1 2 694 710 3 -3 2 2 1033 1052 4 -1 5 2 75 54 1 -6 9 2 178 179 2
-4 -4 2 351 326 2 -3 -1 2 937 948 5 -2 2 2 984 971 6 0 5 2 144 146 2 -5 9 2 113 109 4
-3 -4 2 206 201 1 -2 -1 2 353 343 2 -1 2 2 287 307 1 1 5 2 283 286 2 -4 9 2 193 186 2
-2 -4 2 197 199 1 0 -1 2 656 712 8 0 2 2 700 722 3 2 5 2 42 35 3 -3 9 2 210 211 5
-1 -4 2 221 205 1 1 -1 2 1063 1070 5 1 2 2 368 381 4 3 5 2 272 260 1 -2 9 2 71 62 8

Table B9 Continued

0 -4 2 404 385 3 2 -1 2 825 834 4 2 2 2 591 597 3 4 5 2 90 87 1 -1 9 2 110 109 4
1 -4 2 158 159 1 3 -1 2 1581 1565 7 3 2 2 996 982 4 5 5 2 461 457 2 0 9 2 294 301 6
2 -4 2 108 111 1 4 -1 2 401 408 2 4 2 2 393 401 3 6 5 2 98 99 2 1 9 2 215 218 5
3 -4 2 209 202 2 5 -1 2 563 566 3 5 2 2 279 295 1 7 5 2 331 330 3 2 9 2 148 155 2
4 -4 2 280 291 1 6 -1 2 125 132 2 6 2 2 602 602 3 8 5 2 80 88 11 3 9 2 247 246 3
5 -4 2 30 27 12 7 -1 2 297 289 2 7 2 2 385 384 4 9 5 2 120 117 3 4 9 2 86 85 14
6 -4 2 217 216 1 8 -1 2 300 298 2 8 2 2 170 165 1 10 5 2 157 166 5 5 9 2 62 70 6
7 -4 2 41 57 4 9 -1 2 403 394 3 9 2 2 216 222 2 11 5 2 106 101 4 6 9 2 35 28 34
8 -4 2 263 258 2 10 -1 2 294 296 7 10 2 2 201 196 3 12 5 2 109 111 5 7 9 2 96 94 6
9 -4 2 130 141 5 11 -1 2 127 124 7 11 2 2 253 255 9 13 5 2 144 147 4 8 9 2 124 123 6
10 -4 2 312 294 7 12 -1 2 79 91 6 12 2 2 192 190 8 -12 6 2 145 138 6 -7 10 2 112 111 7
11 -4 2 144 149 7 13 -1 2 69 59 20 13 2 2 118 119 6 -11 6 2 122 124 5 -6 10 2 94 103 5
12 -4 2 190 175 7 14 -1 2 53 57 23 14 2 2 79 48 14 -10 6 2 116 117 4 -5 10 2 119 127 6
13 -4 2 72 91 17 -15 0 2 55 32 55 -14 3 2 35 20 34 -9 6 2 187 186 2 -4 10 2 101 83 7
-14 -3 2 46 26 17 -14 0 2 48 46 14 -13 3 2 138 130 6 -8 6 2 143 146 2 -3 10 2 87 82 8
-13 -3 2 151 129 6 -13 0 2 85 64 18 -12 3 2 194 195 5 -7 6 2 59 54 4 -2 10 2 82 77 12
-12 -3 2 195 209 6 -12 0 2 218 218 3 -11 3 2 296 292 3 -6 6 2 184 180 1 -1 10 2 107 105 6
-11 -3 2 284 273 5 -11 0 2 14 33 14 -10 3 2 275 282 2 -5 6 2 365 370 2 0 10 2 176 175 9
-10 -3 2 254 264 11 -10 0 2 128 124 3 -9 3 2 374 375 2 -4 6 2 229 228 3 1 10 2 76 64 11
-9 -3 2 358 366 6 -9 0 2 362 375 2 -8 3 2 205 211 2 -3 6 2 338 355 2 2 10 2 47 55 22
-8 -3 2 203 213 5 -8 0 2 554 540 3 -7 3 2 300 298 1 -2 6 2 154 152 2 3 10 2 85 82 4
4 10 2 164 159 5 10 -7 3 168 158 11 -7 -3 3 316 304 2 -7 0 3 96 86 2 -5 3 3 176 170 4

Table B9 Continued

5 10 2 74 76 7 11 -7 3 147 128 13 -6 -3 3 533 525 3 -6 0 3 36 29 3 -4 3 3 995 987 7
6 10 2 90 86 13 -11 -6 3 159 146 7 -5 -3 3 180 177 1 -5 0 3 301 310 2 -3 3 3 1124 1117 7
-4 11 2 70 64 14 -10 -6 3 164 167 6 -4 -3 3 994 982 5 -4 0 3 456 485 3 -2 3 3 360 372 3
-3 11 2 67 64 13 -9 -6 3 152 151 4 -3 -3 3 1139 1128 5 -3 0 3 219 208 1 -1 3 3 335 360 2
-2 11 2 22 15 21 -8 -6 3 49 49 8 -2 -3 3 359 372 3 -2 0 3 134 143 1 0 3 3 255 264 3
-1 11 2 45 8 44 -7 -6 3 87 79 3 -1 -3 3 283 307 1 -1 0 3 144 144 1 1 3 3 727 710 4
0 11 2 0 45 1 -6 -6 3 299 303 2 0 -3 3 243 253 4 1 0 3 31 21 1 2 3 3 502 494 4
1 11 2 48 91 48 -5 -6 3 178 175 2 1 -3 3 731 709 5 2 0 3 317 324 3 3 3 3 919 905 4
2 11 2 57 38 14 -4 -6 3 294 286 2 2 -3 3 532 518 3 3 0 3 11 24 11 4 3 3 588 602 3
3 11 2 67 58 16 -3 -6 3 235 244 1 3 -3 3 907 889 4 4 0 3 228 245 1 5 3 3 916 884 4
-4-11 3 43 36 43 -2 -6 3 54 54 1 4 -3 3 570 581 3 5 0 3 329 332 2 6 3 3 364 366 2
-3-11 3 117 107 18 -1 -6 3 178 175 3 5 -3 3 923 894 4 6 0 3 225 225 1 7 3 3 140 145 3
-2-11 3 101 91 9 0 -6 3 279 282 1 6 -3 3 379 379 2 7 0 3 117 118 3 8 3 3 193 196 2
-1-11 3 72 81 13 1 -6 3 284 290 1 7 -3 3 153 156 1 8 0 3 139 156 2 9 3 3 132 141 5
0-11 3 71 53 16 2 -6 3 327 328 2 8 -3 3 209 210 2 9 0 3 132 116 3 10 3 3 126 119 3
1-11 3 52 37 19 3 -6 3 210 208 1 9 -3 3 122 132 3 10 0 3 260 262 3 11 3 3 208 204 9
2-11 3 28 26 27 4 -6 3 258 255 1 10 -3 3 135 122 4 11 0 3 257 247 3 12 3 3 92 89 6
3-11 3 46 52 45 5 -6 3 133 139 1 11 -3 3 215 209 4 12 0 3 329 344 4 13 3 3 98 92 17
-7-10 3 60 66 22 6 -6 3 60 73 3 12 -3 3 98 87 11 13 0 3 162 159 9 -14 4 3 52 52 15
-6-10 3 94 68 11 7 -6 3 132 135 2 13 -3 3 60 76 18 14 0 3 208 214 5 -13 4 3 108 116 5
-5-10 3 98 86 10 8 -6 3 196 196 4 -14 -2 3 51 43 14 -15 1 3 168 165 7 -12 4 3 108 114 5
-4-10 3 0 19 1 9 -6 3 157 164 5 -13 -2 3 130 134 7 -14 1 3 239 230 5 -11 4 3 47 27 12

Table B9 Continued

-3-10 3 77 88 9 10 -6 3 108 110 7 -12 -2 3 210 204 12 -13 1 3 341 333 10 -10 4 3 115 120 3
-2-10 3 83 89 8 11 -6 3 124 121 6 -11 -2 3 206 193 4 -12 1 3 230 232 5 -9 4 3 137 144 3
-1-10 3 50 47 11 12 -6 3 40 33 40 -10 -2 3 145 163 4 -11 1 3 169 171 4 -8 4 3 289 289 2
0-10 3 113 108 6 -13 -5 3 0 25 1 -9 -2 3 234 237 3 -10 1 3 115 114 3 -7 4 3 397 401 4
1-10 3 121 121 6 -12 -5 3 109 100 5 -8 -2 3 324 319 2 -9 1 3 501 514 3 -6 4 3 438 451 3
2-10 3 87 78 7 -11 -5 3 132 131 5 -7 -2 3 346 354 4 -8 1 3 430 427 5 -5 4 3 219 225 2
3-10 3 143 139 5 -10 -5 3 203 201 3 -6 -2 3 174 190 3 -7 1 3 472 479 2 -4 4 3 746 745 3
4-10 3 67 47 13 -9 -5 3 324 323 7 -5 -2 3 404 403 3 -6 1 3 465 478 2 -3 4 3 135 132 2
5-10 3 74 76 10 -8 -5 3 155 151 3 -4 -2 3 980 959 5 -5 1 3 583 589 3 -2 4 3 102 110 1
6-10 3 9 29 8 -7 -5 3 85 86 3 -3 -2 3 282 297 2 -4 1 3 252 237 1 -1 4 3 493 498 2
-8 -9 3 115 129 11 -6 -5 3 211 205 2 -2 -2 3 534 526 5 -3 1 3 926 927 5 0 4 3 655 650 5
-7 -9 3 136 128 9 -5 -5 3 368 372 3 -1 -2 3 95 106 1 -2 1 3 294 308 2 1 4 3 1120 1119 7
-6 -9 3 61 72 16 -4 -5 3 463 452 2 0 -2 3 717 775 3 -1 1 3 306 311 2 2 4 3 619 635 3
-5 -9 3 109 75 9 -3 -5 3 704 694 3 1 -2 3 95 99 1 0 1 3 1263 1293 18 3 4 3 168 181 1
-4 -9 3 62 59 9 -2 -5 3 444 448 2 2 -2 3 854 830 4 1 1 3 1058 1060 5 4 4 3 355 360 2
-3 -9 3 164 170 5 -1 -5 3 592 584 3 3 -2 3 237 254 2 2 1 3 610 581 3 5 4 3 104 105 1
-2 -9 3 22 46 21 0 -5 3 207 213 2 4 -2 3 537 524 3 3 1 3 643 662 3 6 4 3 114 110 3
-1 -9 3 107 114 3 1 -5 3 52 43 2 6 -2 3 433 435 2 4 1 3 396 377 2 7 4 3 363 364 2
0 -9 3 69 57 5 2 -5 3 333 329 1 7 -2 3 317 318 2 5 1 3 194 191 2 8 4 3 351 346 2
1 -9 3 58 47 6 3 -5 3 218 228 4 8 -2 3 92 96 3 6 1 3 423 430 2 9 4 3 217 218 2
2 -9 3 33 11 32 4 -5 3 716 695 3 9 -2 3 327 324 3 7 1 3 317 310 2 10 4 3 340 338 3
3 -9 3 103 89 17 5 -5 3 504 494 2 10 -2 3 184 182 4 8 1 3 339 345 2 11 4 3 60 44 7

Table B9 Continued

4 -9 3 14 26 13 6 -5 3 304 301 2 11 -2 3 219 215 4 9 1 3 329 336 4 12 4 3 43 47 10
5 -9 3 71 55 9 7 -5 3 276 278 2 12 -2 3 124 101 18 10 1 3 383 383 5 13 4 3 67 54 13
6 -9 3 111 121 9 8 -5 3 76 71 3 13 -2 3 155 170 6 11 1 3 106 100 14 -13 5 3 36 18 21
7 -9 3 74 34 19 9 -5 3 32 36 15 14 -2 3 93 83 12 12 1 3 29 22 28 -12 5 3 105 93 4
8 -9 3 98 100 12 10 -5 3 189 190 4 -15 -1 3 162 164 7 13 1 3 108 112 8 -11 5 3 106 109 4
-8 -8 3 42 60 26 11 -5 3 88 104 8 -14 -1 3 228 229 5 14 1 3 73 62 11 -10 5 3 197 200 2
-7 -8 3 66 26 15 12 -5 3 114 110 10 -13 -1 3 351 345 5 -14 2 3 50 60 16 -9 5 3 341 339 2
-6 -8 3 113 112 9 -14 -4 3 44 54 43 -12 -1 3 224 231 4 -13 2 3 121 134 5 -8 5 3 152 151 2
-5 -8 3 89 86 8 -13 -4 3 103 106 6 -11 -1 3 172 177 11 -12 2 3 206 206 3 -7 5 3 77 78 2
-4 -8 3 179 192 2 -12 -4 3 99 110 7 -10 -1 3 97 102 8 -11 2 3 214 213 3 -6 5 3 192 183 3
-3 -8 3 62 55 3 -11 -4 3 52 36 20 -9 -1 3 516 529 4 -10 2 3 121 122 9 -5 5 3 369 380 6
-2 -8 3 134 147 5 -10 -4 3 102 108 4 -8 -1 3 412 412 2 -9 2 3 243 249 5 -4 5 3 455 447 4
-1 -8 3 52 50 2 -9 -4 3 108 113 3 -7 -1 3 469 474 3 -8 2 3 325 323 2 -3 5 3 673 672 5
0 -8 3 54 51 8 -8 -4 3 298 298 3 -6 -1 3 468 485 3 -7 2 3 342 351 2 -2 5 3 477 487 2
1 -8 3 61 62 13 -7 -4 3 396 405 5 -5 -1 3 587 589 3 -6 2 3 171 185 1 -1 5 3 568 572 3
2 -8 3 76 72 8 -6 -4 3 438 444 2 -4 -1 3 227 215 1 -5 2 3 479 482 3 0 5 3 199 210 1
3 -8 3 88 88 2 -5 -4 3 245 253 1 -3 -1 3 930 931 7 -4 2 3 920 912 4 1 5 3 51 42 3
4 -8 3 92 91 3 -4 -4 3 756 750 8 -2 -1 3 293 308 1 -3 2 3 295 309 1 2 5 3 337 332 2
5 -8 3 48 64 13 -3 -4 3 131 127 1 -1 -1 3 310 313 1 -2 2 3 546 537 5 3 5 3 206 221 1
6 -8 3 102 121 11 -2 -4 3 102 113 2 0 -1 3 1291 1307 8 0 2 3 707 768 3 4 5 3 718 697 3
7 -8 3 122 111 11 -1 -4 3 493 491 2 1 -1 3 1064 1063 7 2 2 3 839 817 6 5 5 3 483 480 2
8 -8 3 86 95 12 0 -4 3 653 639 3 2 -1 3 622 592 3 3 2 3 214 232 1 6 5 3 307 301 2

Table B9 Continued

9 -8 3 0 14 1 1 -4 3 1151 1133 5 3 -1 3 639 658 3 4 2 3 567 555 2 7 5 3 265 265 2
10 -8 3 45 42 44 2 -4 3 608 615 2 4 -1 3 424 407 4 5 2 3 279 273 2 8 5 3 91 94 3
-8 -7 3 143 140 4 3 -4 3 168 173 1 5 -1 3 138 139 2 6 2 3 454 455 5 9 5 3 46 49 6
-7 -7 3 278 279 3 4 -4 3 373 371 2 6 -1 3 432 437 2 7 2 3 304 303 2 10 5 3 184 180 3
-6 -7 3 213 218 4 5 -4 3 103 100 2 7 -1 3 326 317 2 8 2 3 92 96 2 11 5 3 102 94 4
-5 -7 3 255 253 2 6 -4 3 146 146 2 8 -1 3 360 360 3 9 2 3 340 337 2 12 5 3 123 112 5
-4 -7 3 192 189 5 7 -4 3 346 349 2 9 -1 3 327 326 3 10 2 3 188 187 4 -12 6 3 166 179 4
-3 -7 3 247 249 2 8 -4 3 337 334 3 10 -1 3 414 410 4 11 2 3 208 212 7 -11 6 3 125 132 4
-2 -7 3 162 159 8 9 -4 3 231 232 4 11 -1 3 107 112 6 12 2 3 108 102 5 -10 6 3 179 179 3
-1 -7 3 315 312 2 10 -4 3 338 326 13 12 -1 3 0 16 1 13 2 3 173 177 10 -9 6 3 144 139 4
0 -7 3 61 54 2 11 -4 3 66 59 8 13 -1 3 95 104 8 14 2 3 104 93 8 -8 6 3 72 72 3
1 -7 3 21 12 20 12 -4 3 18 49 17 14 -1 3 67 67 12 -14 3 3 87 84 10 -7 6 3 101 92 2
2 -7 3 138 138 2 13 -4 3 43 49 27 -15 0 3 154 150 7 -13 3 3 108 96 5 -6 6 3 308 310 2
3 -7 3 173 170 1 -14 -3 3 69 85 11 -14 0 3 67 79 15 -12 3 3 167 165 8 -5 6 3 196 188 2
4 -7 3 406 403 2 -13 -3 3 113 99 7 -13 0 3 223 219 5 -11 3 3 238 235 3 -4 6 3 281 270 1
5 -7 3 189 189 1 -12 -3 3 158 156 4 -12 0 3 397 385 6 -10 3 3 215 209 4 -3 6 3 244 254 6
6 -7 3 51 60 7 -11 -3 3 260 262 4 -11 0 3 68 80 22 -9 3 3 213 213 2 -2 6 3 75 74 5
7 -7 3 155 150 4 -10 -3 3 207 206 4 -10 0 3 256 261 3 -8 3 3 337 338 2 -1 6 3 176 174 2
8 -7 3 108 119 6 -9 -3 3 201 199 3 -9 0 3 166 171 2 -7 3 3 278 274 2 0 6 3 299 309 3
9 -7 3 105 104 14 -8 -3 3 319 322 5 -8 0 3 235 236 2 -6 3 3 544 540 2 1 6 3 261 267 5
2 6 3 330 335 2 6 10 3 0 22 1 -3 -6 4 256 252 2 4 -3 4 309 292 1 3 0 4 969 956 5
3 6 3 221 217 1 -4 11 3 76 57 24 -2 -6 4 189 192 4 5 -3 4 532 519 3 4 0 4 649 661 3

Table B9 Continued

4 6 3 252 255 2 -3 11 3 81 94 14 -1 -6 4 206 201 1 6 -3 4 224 222 2
5 0 4 472 481 2
5 6 3 131 134 8 -2 11 3 95 101 18 0 -6 4 97 87 1 7 -3 4 163 178 2 6
0 4 383 394 2
6 6 3 51 60 8 -1 11 3 83 78 18 1 -6 4 31 31 5 8 -3 4 169 171 4 7
0 4 92 104 2
7 6 3 121 122 2 0 11 3 37 49 36 2 -6 4 430 425 2 9 -3 4 99 100 9 8
0 4 159 159 5
8 6 3 216 210 2 1 11 3 0 36 1 3 -6 4 183 186 1 10 -3 4 143 133 6 9
0 4 228 225 3
9 6 3 161 154 3 2 11 3 13 36 12 4 -6 4 297 289 4 11 -3 4 184 190 4
10 0 4 17 29 16
10 6 3 103 106 5 3 11 3 71 57 15 5 -6 4 534 511 7 12 -3 4 104 110 6
11 0 4 179 175 5
11 6 3 123 121 4 -3-11 4 152 141 11 6 -6 4 191 194 2 13 -3 4 170 169 7
12 0 4 157 156 7
12 6 3 18 32 18 -2-11 4 110 96 31 7 -6 4 129 133 5 -14 -2 4 25 35 25
13 0 4 74 91 15
-12 7 3 39 29 12 -1-11 4 42 32 41 8 -6 4 137 150 5 -13 -2 4 49 26 17
14 0 4 42 41 42
-11 7 3 85 86 5 0-11 4 92 83 10 9 -6 4 173 159 12 -12 -2 4 71 66 8
-15 1 4 84 76 12
-10 7 3 125 121 4 1-11 4 48 60 18 10 -6 4 138 133 6 -11 -2 4 95 77 5
-14 1 4 93 104 7
-9 7 3 177 180 3 2-11 4 0 7 1 11 -6 4 87 92 12 -10 -2 4 208 225 5 -
13 1 4 221 226 4
-8 7 3 120 122 3 3-11 4 57 61 13 12 -6 4 101 101 9 -9 -2 4 379 383 7
-12 1 4 237 238 3
-7 7 3 294 293 2 -4-10 4 128 136 7 -13 -5 4 131 122 9 -8 -2 4 364 366 2
-11 1 4 31 17 31
-6 7 3 214 209 2 -3-10 4 112 106 7 -12 -5 4 197 195 4 -7 -2 4 190 194 5
-10 1 4 108 106 3
-5 7 3 230 225 1 -2-10 4 145 143 12 -11 -5 4 268 261 5 -6 -2 4 297 303 2
-9 1 4 468 469 3
-4 7 3 191 188 3 -1-10 4 23 41 23 -10 -5 4 192 199 4 -5 -2 4 551 557 5
-8 1 4 501 500 3
-3 7 3 257 255 9 0-10 4 41 27 41 -9 -5 4 212 212 5 -4 -2 4 224 224 3
-7 1 4 742 742 4
-2 7 3 154 148 7 1-10 4 26 29 25 -8 -5 4 91 88 4 -3 -2 4 645 643 3 -
6 1 4 341 336 2
-1 7 3 316 317 2 2-10 4 25 39 25 -7 -5 4 112 115 7 -2 -2 4 1021 1007 5
-5 1 4 817 809 4
0 7 3 42 41 6 3-10 4 90 80 19 -6 -5 4 247 257 2 -1 -2 4 554 529 3 -
4 1 4 112 104 1

Table B9 Continued

1 7 3 45 10 9 4-10 4 175 177 7 -5 -5 4 286 281 2 0 -2 4 691 703 3 -3 1 4 383 372 4
2 7 3 131 133 6 5-10 4 144 141 6 -4 -5 4 201 201 1 1 -2 4 571 559 4 -2 1 4 799 798 4
3 7 3 196 195 6 6-10 4 64 43 14 -3 -5 4 330 325 1 2 -2 4 364 368 1 -1 1 4 645 651 3
4 7 3 394 396 2 -6 -9 4 121 118 8 -2 -5 4 198 191 3 3 -2 4 281 292 1 0 1 4 2137 2172 24
5 7 3 191 188 1 -5 -9 4 109 108 8 -1 -5 4 100 107 3 4 -2 4 304 315 2 1 1 4 1816 1773 10
6 7 3 58 59 5 -4 -9 4 72 76 8 0 -5 4 99 92 2 5 -2 4 172 189 1 2 1 4 920 907 4
7 7 3 165 163 2 -3 -9 4 64 59 7 1 -5 4 111 114 1 6 -2 4 537 540 3 3 1 4 166 183 1
8 7 3 121 133 3 -2 -9 4 131 141 4 2 -5 4 120 125 1 7 -2 4 279 278 2 4 1 4 253 255 1
9 7 3 123 127 5 -1 -9 4 225 225 4 3 -5 4 69 70 1 8 -2 4 110 103 7 5 1 4 205 202 2
10 7 3 152 152 5 0 -9 4 290 290 4 4 -5 4 306 304 3 9 -2 4 302 292 3 6 1 4 725 704 8
11 7 3 111 121 6 1 -9 4 191 194 4 5 -5 4 104 107 1 10 -2 4 234 226 3 7 1 4 556 544 5
-10 8 3 135 144 3 2 -9 4 128 120 5 6 -5 4 237 238 5 11 -2 4 203 199 4 8 1 4 517 515 4
-9 8 3 105 113 4 3 -9 4 80 95 8 7 -5 4 43 44 5 12 -2 4 66 63 11 9 1 4 296 287 4
-8 8 3 78 72 4 4 -9 4 32 45 32 8 -5 4 136 141 8 13 -2 4 65 71 21 10 1 4 310 311 3
-7 8 3 11 31 11 5 -9 4 57 50 12 9 -5 4 77 78 10 14 -2 4 0 27 1 11 1 4 98 100 6
-6 8 3 111 117 3 6 -9 4 100 80 7 10 -5 4 172 168 8 -15 -1 4 63 61 16 12 1 4 91 92 5
-5 8 3 79 70 7 7 -9 4 57 80 13 11 -5 4 106 107 8 -14 -1 4 103 108 8 13 1 4 72 66 12
-4 8 3 191 195 1 8 -9 4 158 160 7 12 -5 4 148 147 7 -13 -1 4 196 207 12 14 1 4 94 108 9
-3 8 3 80 71 1 -7 -8 4 0 26 1 -14 -4 4 112 139 12 -12 -1 4 238 242 8 -14 2 4 35 44 34
-2 8 3 150 157 2 -6 -8 4 178 170 7 -13 -4 4 121 102 7 -11 -1 4 55 43 9 -13 2 4 59 27 14
-1 8 3 55 48 2 -5 -8 4 286 301 8 -12 -4 4 0 33 1 -10 -1 4 118 121 5 -12 2 4 76 71 6
0 8 3 51 45 3 -4 -8 4 100 106 3 -11 -4 4 125 138 5 -9 -1 4 444 455 4 -11 2 4 97 77 4

Table B9 Continued

1 8 3 74 71 3 -3 -8 4 236 235 6 -10 -4 4 160 146 4 -8 -1 4 483 487 3 -10 2 4 162 179 4
2 8 3 77 66 3 -2 -8 4 156 152 1 -8 -4 4 450 447 4 -7 -1 4 736 738 4 -9 2 4 392 389 2
3 8 3 76 80 8 -1 -8 4 113 110 5 -7 -4 4 291 295 3 -6 -1 4 328 328 2 -8 2 4 387 388 2
4 8 3 100 94 4 0 -8 4 208 212 3 -6 -4 4 369 371 2 -5 -1 4 821 814 4 -7 2 4 191 197 1
5 8 3 77 60 10 1 -8 4 247 241 4 -5 -4 4 90 94 2 -4 -1 4 136 134 1 -6 2 4 316 326 2
6 8 3 94 95 2 2 -8 4 135 127 4 -4 -4 4 374 357 2 -3 -1 4 391 383 5 -5 2 4 513 520 4
7 8 3 113 113 4 3 -8 4 312 306 3 -3 -4 4 276 271 1 -2 -1 4 788 786 4 -4 2 4 224 227 2
8 8 3 79 95 4 4 -8 4 258 257 4 -2 -4 4 233 226 1 -1 -1 4 651 656 3 -3 2 4 655 655 4
9 8 3 7 9 6 5 -8 4 120 110 4 -1 -4 4 136 128 2 0 -1 4 2137 2183 24 -2 2 4 1029 1025 9
10 8 3 49 48 9 6 -8 4 174 185 4 0 -4 4 266 249 4 1 -1 4 1796 1755 11 -1 2 4 530 507 2
-9 9 3 91 101 4 7 -8 4 43 47 27 1 -4 4 115 108 1 2 -1 4 917 902 4 0 2 4 690 708 3
-8 9 3 103 105 7 8 -8 4 0 27 1 2 -4 4 283 271 1 3 -1 4 183 200 1 1 2 4 573 561 3
-7 9 3 134 128 3 9 -8 4 54 35 23 3 -4 4 27 19 5 4 -1 4 242 242 3 3 2 4 299 303 3
-6 9 3 82 86 3 -8 -7 4 189 196 4 4 -4 4 266 264 1 5 -1 4 177 167 4 4 2 4 306 319 2
-5 9 3 78 63 2 -7 -7 4 185 176 3 5 -4 4 83 82 2 6 -1 4 744 722 6 5 2 4 193 208 1
-4 9 3 52 49 3 -6 -7 4 168 175 2 6 -4 4 206 208 2 7 -1 4 557 546 3 6 2 4 510 514 3
-3 9 3 157 163 4 -5 -7 4 62 56 2 7 -4 4 302 301 2 8 -1 4 495 492 3 7 2 4 273 271 2
-2 9 3 62 49 7 -4 -7 4 136 136 3 8 -4 4 267 261 3 9 -1 4 305 304 6 8 2 4 149 147 2
-1 9 3 110 120 5 -3 -7 4 107 104 2 9 -4 4 200 205 3 10 -1 4 290 291 4 9 2 4 274 263 2
0 9 3 65 55 2 -2 -7 4 383 384 2 10 -4 4 319 315 4 11 -1 4 96 86 8 10 2 4 231 224 3
1 9 3 44 50 3 -1 -7 4 392 380 2 11 -4 4 46 52 12 12 -1 4 64 77 11 11 2 4 190 195 3
2 9 3 29 1 28 0 -7 4 300 297 3 12 -4 4 29 23 28 13 -1 4 69 74 13 12 2 4 70 66 9

Table B9 Continued

3 9 3 89 86 7 1 -7 4 307 304 2 13 -4 4 0 28 1 14 -1 4 90 100 8 13 2 4 67 68 22
4 9 3 35 32 14 2 -7 4 178 183 2 -14 -3 4 104 90 16 -15 0 4 64 74 14 14 2 4 23 30 23
5 9 3 57 58 8 3 -7 4 150 149 2 -13 -3 4 270 283 6 -14 0 4 16 17 16 -14 3 4 91 95 8
6 9 3 117 124 4 4 -7 4 78 76 2 -12 -3 4 296 294 10 -13 0 4 0 15 1 -13 3 4 272 278 4
7 9 3 17 21 16 5 -7 4 182 191 2 -11 -3 4 280 287 4 -12 0 4 202 197 4 -12 3 4 294 295 4
8 9 3 97 92 5 6 -7 4 95 89 6 -10 -3 4 290 290 4 -11 0 4 44 43 29 -11 3 4 304 310 3
-7 10 3 62 55 26 7 -7 4 223 226 5 -9 -3 4 157 158 4 -10 0 4 190 189 3 -10 3 4 265 265 4
-6 10 3 55 72 51 8 -7 4 144 135 5 -8 -3 4 364 371 6 -9 0 4 111 116 2 -9 3 4 128 131 2
-5 10 3 91 86 11 9 -7 4 120 128 13 -7 -3 4 158 149 6 -8 0 4 157 161 2 -8 3 4 366 367 2
-4 10 3 75 33 13 10 -7 4 79 87 16 -6 -3 4 350 352 2 -7 0 4 134 130 1 -7 3 4 195 184 2
-3 10 3 92 93 11 11 -7 4 50 90 49 -5 -3 4 379 393 3 -6 0 4 269 272 2 -6 3 4 332 335 2
-2 10 3 83 83 17 -11 -6 4 75 82 13 -4 -3 4 372 373 5 -5 0 4 166 174 3 -5 3 4 354 374 4
-1 10 3 79 69 15 -10 -6 4 111 116 6 -3 -3 4 229 219 3 -4 0 4 937 929 5 -4 3 4 343 343 4
0 10 3 94 101 14 -9 -6 4 213 206 5 -2 -3 4 107 102 3 -3 0 4 1251 1251 7 -3 3 4 253 243 2
1 10 3 112 120 7 -8 -6 4 104 99 4 -1 -3 4 399 414 1 -2 0 4 667 656 4 -2 3 4 123 122 2
2 10 3 91 94 9 -7 -6 4 325 316 3 0 -3 4 562 569 5 -1 0 4 351 381 2 -1 3 4 426 442 3
3 10 3 132 132 6 -6 -6 4 31 17 7 1 -3 4 707 712 5 0 0 4 833 879 5 0 3 4 546 564 3
4 10 3 35 38 13 -5 -6 4 136 145 3 2 -3 4 301 304 1 1 0 4 609 618 3 1 3 4 677 684 5
5 10 3 86 75 11 -4 -6 4 691 662 4 3 -3 4 716 689 3 2 0 4 420 390 2 3 3 4 706 678 3
4 3 4 340 324 2 11 6 4 62 75 8 -2-11 5 46 48 45 -12 -5 5 115 118 5 -8 -2 5 131 134 4
5 3 4 531 525 5 12 6 4 116 115 6 -1-11 5 20 51 19 -11 -5 5 151 155 6 -7 -2 5 325 326 2
6 3 4 259 258 1 -12 7 4 71 58 7 0-11 5 19 20 18 -10 -5 5 129 140 4 -6 -2 5 448 439 3

Table B9 Continued

7 3 4 178 187 2 -11 7 4 111 115 4 1-11 5 91 113 9 -9 -5 5 237 245 4 -5 -2 5 543 543 4
8 3 4 188 187 2 -10 7 4 109 90 6 2-11 5 29 45 28 -8 -5 5 280 285 4 -4 -2 5 318 306 2
9 3 4 83 86 4 -9 7 4 145 143 5 -4-10 5 109 116 11 -7 -5 5 161 159 5 -3 -2 5 323 317 2
10 3 4 134 133 3 -8 7 4 195 197 2 -3-10 5 0 18 1 -6 -5 5 147 152 2 -2 -2 5 343 345 2
11 3 4 189 188 3 -7 7 4 177 172 2 -2-10 5 111 108 7 -5 -5 5 582 573 3 -1 -2 5 1487 1455 8
12 3 4 121 119 7 -6 7 4 159 160 4 -1-10 5 78 72 7 -4 -5 5 202 198 4 0 -2 5 487 509 3
13 3 4 158 170 14 -5 7 4 88 81 3 0-10 5 149 149 5 -3 -5 5 528 524 2 1 -2 5 762 767 6
-14 4 4 134 140 7 -4 7 4 126 126 1 1-10 5 53 51 14 -2 -5 5 361 357 2 2 -2 5 460 460 3
-13 4 4 101 92 6 -3 7 4 89 74 12 2-10 5 18 26 17 -1 -5 5 36 38 1 3 -2 5 220 209 1
-12 4 4 18 35 18 -2 7 4 373 383 3 3-10 5 44 56 16 0 -5 5 170 171 1 4 -2 5 476 467 3
-11 4 4 119 123 7 -1 7 4 389 388 6 4-10 5 62 67 12 1 -5 5 324 320 2 5 -2 5 398 398 2
-10 4 4 161 150 3 0 7 4 297 291 2 5-10 5 115 108 8 2 -5 5 390 395 5 6 -2 5 238 238 3
-9 4 4 218 226 2 1 7 4 302 300 4 6-10 5 30 29 29 3 -5 5 428 422 2 7 -2 5 328 330 2
-8 4 4 476 472 3 2 7 4 176 175 3 -5 -9 5 35 54 34 4 -5 5 693 677 3 8 -2 5 248 251 3
-7 4 4 285 290 6 3 7 4 158 156 4 -4 -9 5 138 126 6 5 -5 5 103 100 4 9 -2 5 102 94 5
-6 4 4 389 395 3 4 7 4 77 67 3 -3 -9 5 117 122 4 6 -5 5 273 268 2 10 -2 5 263 262 3
-5 4 4 102 103 2 5 7 4 198 201 4 -2 -9 5 30 39 17 7 -5 5 96 90 2 11 -2 5 150 145 9
-4 4 4 373 356 1 6 7 4 108 99 6 -1 -9 5 136 135 6 8 -5 5 204 212 5 12 -2 5 121 113 6
-3 4 4 256 256 5 7 7 4 201 209 2 0 -9 5 132 136 7 9 -5 5 103 98 4 13 -2 5 145 148 6
-2 4 4 231 220 1 8 7 4 130 119 5 1 -9 5 70 69 14 10 -5 5 185 182 7 -15 -1 5 165 170 8
-1 4 4 115 102 5 9 7 4 116 119 3 2 -9 5 33 52 33 11 -5 5 121 105 7 -14 -1 5 102 86 8
0 4 4 246 233 1 10 7 4 98 93 5 3 -9 5 74 60 9 12 -5 5 91 82 19 -13 -1 5 111 100 7

Table B9 Continued

1 4 4 114 108 1 11 7 4 84 88 7 4 -9 5 0 35 1 -14 -4 5 65 61 11 -12 -1 5 226 230 4
2 4 4 269 260 1 -10 8 4 68 70 6 5 -9 5 72 87 8 -13 -4 5 70 70 8 -11 -1 5 240 238 6
3 4 4 38 13 9 -9 8 4 52 66 7 6 -9 5 51 46 13 -12 -4 5 62 72 8 -10 -1 5 219 230 4
4 4 4 256 254 2 -8 8 4 92 86 4 7 -9 5 53 55 21 -11 -4 5 113 116 5 -9 -1 5 477 467 5
5 4 4 73 72 2 -7 8 4 37 39 9 8 -9 5 121 105 8 -10 -4 5 81 71 7 -8 -1 5 530 535 3
6 4 4 234 233 1 -6 8 4 165 164 3 -5 -8 5 130 128 6 -9 -4 5 234 242 3 -7 -1 5 405 407 2
7 4 4 277 276 2 -5 8 4 308 309 2 -4 -8 5 151 152 4 -8 -4 5 509 507 4 -6 -1 5 145 165 2
8 4 4 257 251 3 -4 8 4 129 126 5 -3 -8 5 79 79 3 -7 -4 5 363 360 2 -5 -1 5 450 431 2
9 4 4 226 221 3 -3 8 4 222 214 7 -2 -8 5 22 33 11 -6 -4 5 283 280 2 -4 -1 5 91 89 3
10 4 4 296 296 3 -2 8 4 183 181 7 -1 -8 5 74 82 2 -5 -4 5 86 74 2 -3 -1 5 707 718 4
11 4 4 69 62 12 -1 8 4 119 113 3 0 -8 5 126 126 3 -4 -4 5 107 101 1 -2 -1 5 520 509 3
12 4 4 32 26 28 0 8 4 210 210 2 1 -8 5 108 103 2 -3 -4 5 567 559 5 -1 -1 5 827 807 5
13 4 4 39 38 15 1 8 4 233 223 2 2 -8 5 44 40 22 -2 -4 5 668 663 3 0 -1 5 135 145 2
-13 5 4 138 130 4 2 8 4 164 164 2 3 -8 5 132 130 3 -1 -4 5 679 692 3 1 -1 5 324 335 2
-12 5 4 190 192 3 3 8 4 296 301 4 4 -8 5 143 138 5 0 -4 5 771 766 12 2 -1 5 289 277 1
-11 5 4 275 269 5 4 8 4 258 258 5 5 -8 5 94 99 6 1 -4 5 663 680 3 3 -1 5 296 303 3
-10 5 4 208 218 2 5 8 4 136 130 4 6 -8 5 52 45 17 2 -4 5 409 408 2 4 -1 5 342 342 4
-9 5 4 184 181 2 6 8 4 179 187 2 7 -8 5 0 36 1 3 -4 5 76 82 1 5 -1 5 181 180 2
-8 5 4 107 103 4 7 8 4 41 46 7 8 -8 5 0 45 1 4 -4 5 113 108 2 6 -1 5 516 501 7
-7 5 4 99 106 2 8 8 4 17 26 17 9 -8 5 61 19 14 5 -4 5 398 394 2 7 -1 5 275 268 2
-6 5 4 267 276 2 9 8 4 26 31 25 -7 -7 5 135 144 4 6 -4 5 412 401 2 8 -1 5 284 292 3
-5 5 4 307 299 3 -9 9 4 54 68 18 -6 -7 5 25 33 18 7 -4 5 548 543 7 9 -1 5 232 222 3

Table B9 Continued

-4 5 4 205 203 1 -8 9 4 170 172 4 -5 -7 5 136 148 2 8 -4 5 250 240 7
10 -1 5 204 199 4
-3 5 4 347 340 2 -7 9 4 113 118 7 -4 -7 5 479 475 7 9 -4 5 180 190 5
11 -1 5 97 101 6
-2 5 4 191 188 1 -6 9 4 131 126 2 -3 -7 5 265 257 5 10 -4 5 184 167 4
12 -1 5 124 129 6
-1 5 4 114 121 1 -5 9 4 102 105 2 -2 -7 5 54 44 3 11 -4 5 33 32 33
13 -1 5 79 78 12
0 5 4 114 102 4 -4 9 4 85 82 3 -1 -7 5 230 232 2 12 -4 5 104 103 14 -
15 0 5 223 225 7
1 5 4 121 122 1 -3 9 4 51 54 3 0 -7 5 84 94 5 13 -4 5 88 83 17 -14
0 5 180 180 10
2 5 4 113 118 2 -2 9 4 153 154 5 1 -7 5 82 82 2 -14 -3 5 78 76 11 -
13 0 5 217 219 5
3 5 4 50 54 3 -1 9 4 230 227 2 2 -7 5 186 191 1 -13 -3 5 85 93 9 -
12 0 5 353 349 5
4 5 4 290 288 2 0 9 4 281 273 2 3 -7 5 61 63 5 -12 -3 5 146 140 5 -
11 0 5 383 382 4
5 5 4 141 141 5 1 9 4 192 189 3 4 -7 5 179 189 3 -11 -3 5 154 156 4 -
10 0 5 179 174 3
6 5 4 275 270 5 2 9 4 141 137 3 5 -7 5 304 306 2 -10 -3 5 250 248 7
-9 0 5 244 241 3
7 5 4 68 61 3 3 9 4 74 85 5 6 -7 5 84 72 19 -9 -3 5 210 223 4 -8
0 5 117 115 3
8 5 4 113 120 5 4 9 4 53 47 11 7 -7 5 125 118 6 -8 -3 5 158 156 6 -
7 0 5 266 279 4
9 5 4 99 99 9 5 9 4 37 36 13 8 -7 5 83 70 8 -7 -3 5 100 98 2 -6 0
5 407 423 2
10 5 4 157 155 5 6 9 4 73 78 5 9 -7 5 129 130 13 -6 -3 5 606 604 3
-5 0 5 417 418 5
11 5 4 118 117 4 7 9 4 88 94 8 10 -7 5 118 104 16 -5 -3 5 283 279 2
-4 0 5 406 404 2
12 5 4 160 152 5 8 9 4 162 156 4 -11 -6 5 24 41 23 -4 -3 5 710 697 4
-3 0 5 300 308 2
-12 6 4 89 91 5 -7 10 4 36 41 36 -10 -6 5 85 98 6 -3 -3 5 343 348 2
-2 0 5 192 210 2
-11 6 4 78 81 6 -6 10 4 91 93 10 -9 -6 5 232 218 9 -2 -3 5 538 529 5
-1 0 5 79 103 1
-10 6 4 110 112 3 -5 10 4 73 87 8 -8 -6 5 167 156 8 -1 -3 5 180 184 1
0 0 5 24 24 5
-9 6 4 215 211 2 -4 10 4 140 128 7 -7 -6 5 340 327 4 0 -3 5 647 638 3
1 0 5 240 243 2
-8 6 4 78 71 4 -3 10 4 129 120 7 -6 -6 5 246 255 6 1 -3 5 222 213 1
2 0 5 132 127 1

Table B9 Continued

-7 6 4 324 318 2 -2 10 4 130 138 5 -5 -6 5 98 105 2 2 -3 5 986 975 12 3 0 5 167 170 1
-6 6 4 34 42 6 -1 10 4 24 52 23 -4 -6 5 308 305 2 3 -3 5 542 539 2 4 0 5 290 292 2
-5 6 4 150 160 2 0 10 4 54 21 28 -3 -6 5 205 209 1 4 -3 5 236 229 2 5 0 5 150 146 2
-4 6 4 666 644 6 1 10 4 24 24 14 -2 -6 5 199 198 1 5 -3 5 737 711 3 6 0 5 259 263 2
-3 6 4 284 281 3 2 10 4 68 62 4 -1 -6 5 435 434 2 6 -3 5 219 223 2 7 0 5 95 106 2
-2 6 4 188 191 1 3 10 4 83 80 5 0 -6 5 352 356 2 7 -3 5 35 45 18 8 0 5 65 66 6
-1 6 4 193 187 1 4 10 4 176 174 8 1 -6 5 282 280 1 8 -3 5 311 304 3 9 0 5 437 452 4
0 6 4 90 83 2 5 10 4 130 138 5 2 -6 5 253 251 2 9 -3 5 150 149 11 10 0 5 109 126 6
1 6 4 49 58 9 6 10 4 47 51 10 3 -6 5 260 261 1 10 -3 5 157 159 4 11 0 5 237 221 4
2 6 4 414 415 3 -4 11 4 0 21 1 4 -6 5 51 53 2 11 -3 5 150 145 4 12 0 5 160 167 4
3 6 4 194 196 1 -3 11 4 145 144 9 5 -6 5 361 347 3 12 -3 5 111 109 7 13 0 5 144 138 8
4 6 4 294 287 2 -2 11 4 85 87 18 6 -6 5 87 88 2 13 -3 5 37 68 27 14 0 5 51 67 27
5 6 4 522 503 3 -1 11 4 65 35 16 7 -6 5 178 178 2 -14 -2 5 137 132 6 -15 1 5 177 168 6
6 6 4 235 234 3 0 11 4 95 86 16 8 -6 5 212 213 7 -13 -2 5 149 154 5 -14 1 5 92 90 15
7 6 4 125 129 4 1 11 4 49 60 49 9 -6 5 100 103 9 -12 -2 5 204 204 4 -13 1 5 89 92 9
8 6 4 129 135 3 2 11 4 25 20 25 10 -6 5 15 23 14 -11 -2 5 167 167 4 -12 1 5 224 225 7
9 6 4 163 158 3 3 11 4 72 54 14 11 -6 5 144 148 6 -10 -2 5 195 211 6 -11 1 5 284 284 5
10 6 4 133 136 8 -3-11 5 109 77 21 -13 -5 5 60 58 20 -9 -2 5 363 347 4 -10 1 5 216 224 3
-9 1 5 436 430 3 -6 4 5 269 267 1 5 7 5 298 292 3 5 -9 6 104 102 6 -9 -4 6 339 338 4
-8 1 5 504 508 3 -5 4 5 101 85 1 6 7 5 81 79 3 6 -9 6 122 138 6 -8 -4 6 382 384 4
-7 1 5 418 421 2 -4 4 5 90 85 1 7 7 5 124 128 2 7 -9 6 31 43 31 -7 -4 6 222 207 2
-6 1 5 165 182 1 -3 4 5 561 558 2 8 7 5 61 63 10 -3 -8 6 202 204 6 -6 -4 6 150 145 2

Table B9 Continued

-5 1 5 448 433 2 -2 4 5 674 678 3 9 7 5 124 121 3 -2 -8 6 34 36 7 -5 -4 6 318 312 2
-4 1 5 121 125 4 -1 4 5 673 698 3 10 7 5 103 102 6 -1 -8 6 128 143 2 -4 -4 6 255 244 2
-3 1 5 675 689 4 0 4 5 740 738 9 -10 8 5 60 59 6 0 -8 6 207 214 4 -3 -4 6 362 352 2
-2 1 5 568 559 3 1 4 5 666 686 3 -9 8 5 79 79 5 1 -8 6 386 374 4 -2 -4 6 136 133 1
-1 1 5 795 778 8 2 4 5 404 412 2 -8 8 5 104 104 4 2 -8 6 213 218 3 -1 -4 6 435 423 2
0 1 5 116 120 2 3 4 5 87 90 3 -7 8 5 35 35 9 3 -8 6 231 226 4 0 -4 6 371 363 3
1 1 5 347 364 4 4 4 5 93 89 2 -6 8 5 225 223 7 4 -8 6 173 162 4 1 -4 6 162 160 1
2 1 5 299 284 1 5 4 5 417 410 2 -5 8 5 104 97 2 5 -8 6 65 62 8 2 -4 6 127 122 1
3 1 5 256 266 4 6 4 5 406 394 2 -4 8 5 172 161 4 6 -8 6 27 51 27 3 -4 6 201 185 1
4 1 5 342 342 2 7 4 5 567 560 3 -3 8 5 61 66 4 7 -8 6 67 93 11 4 -4 6 175 183 2
5 1 5 195 194 1 8 4 5 241 231 2 -2 8 5 36 29 8 8 -8 6 122 121 8 5 -4 6 220 220 4
6 1 5 531 513 3 9 4 5 164 164 2 -1 8 5 82 85 8 9 -8 6 81 107 12 6 -4 6 110 108 2
7 1 5 261 256 2 10 4 5 191 181 3 0 8 5 122 119 2 -7 -7 6 62 54 6 7 -4 6 393 381 3
8 1 5 270 276 2 11 4 5 24 25 23 1 8 5 118 111 2 -6 -7 6 107 112 3 8 -4 6 72 72 5
9 1 5 250 236 4 12 4 5 101 98 6 2 8 5 40 39 6 -5 -7 6 155 168 3 9 -4 6 149 153 3
10 1 5 192 200 4 13 4 5 80 83 9 3 8 5 124 121 5 -4 -7 6 192 193 2 10 -4 6 132 128 10
11 1 5 96 99 7 -13 5 5 51 45 11 4 8 5 143 145 13 -3 -7 6 148 151 2 11 -4 6 88 92 9
12 1 5 125 123 4 -12 5 5 114 124 4 5 8 5 108 115 4 -2 -7 6 485 477 4 12 -4 6 117 113 7
13 1 5 53 79 14 -11 5 5 151 149 3 6 8 5 25 29 12 -1 -7 6 217 225 4 -14 -3 6 96 111 9
-14 2 5 148 140 6 -10 5 5 100 110 4 7 8 5 33 34 9 0 -7 6 67 71 9 -13 -3 6 222 224 5
-13 2 5 145 153 4 -9 5 5 245 259 2 8 8 5 46 46 8 1 -7 6 287 292 5 -12 -3 6 171 159 4
-12 2 5 198 189 3 -8 5 5 264 265 2 9 8 5 37 19 36 2 -7 6 40 41 7 -11 -3 6 163 169 4

Table B9 Continued

-11 2 5 176 175 3 -7 5 5 191 193 2 -9 9 5 162 166 6 3 -7 6 47 55 5 -10 -3 6 172 168 8
-10 2 5 226 234 3 -6 5 5 171 168 2 -8 9 5 66 65 7 4 -7 6 179 178 4 -9 -3 6 137 149 3
-9 2 5 341 332 2 -5 5 5 547 546 3 -7 9 5 140 145 3 5 -7 6 353 344 3 -8 -3 6 262 262 9
-8 2 5 136 136 2 -4 5 5 213 205 3 -6 9 5 97 92 11 6 -7 6 158 157 3 -7 -3 6 308 312 3
-7 2 5 312 316 2 -3 5 5 531 535 2 -5 9 5 61 62 8 7 -7 6 151 144 4 -6 -3 6 268 268 2
-6 2 5 431 418 2 -2 5 5 350 350 2 -4 9 5 115 116 6 8 -7 6 128 138 4 -5 -3 6 414 417 3
-5 2 5 586 587 7 -1 5 5 31 30 2 -3 9 5 107 120 3 9 -7 6 64 70 10 -4 -3 6 486 479 2
-4 2 5 329 319 6 0 5 5 189 188 2 -2 9 5 21 29 21 10 -7 6 0 75 1 -3 -3 6 216 208 1
-3 2 5 311 304 2 1 5 5 319 313 2 -1 9 5 134 142 3 -11 -6 6 153 136 6 -2 -3 6 301 300 1
-2 2 5 350 351 2 2 5 5 382 388 3 0 9 5 132 135 3 -10 -6 6 181 180 5 -1 -3 6 394 402 3
-1 2 5 1461 1432 12 3 5 5 460 456 3 1 9 5 69 82 5 -9 -6 6 220 207 3 0 -3 6 362 375 2
0 2 5 577 608 4 4 5 5 682 669 3 2 9 5 33 42 13 -8 -6 6 200 191 3 1 -3 6 194 198 1
1 2 5 733 745 4 5 5 5 137 146 9 3 9 5 56 60 28 -7 -6 6 324 316 3 2 -3 6 130 128 1
2 2 5 460 463 2 6 5 5 242 234 2 4 9 5 50 38 14 -6 -6 6 92 97 3 3 -3 6 205 193 1
3 2 5 204 193 2 7 5 5 92 81 3 5 9 5 79 91 14 -5 -6 6 221 207 4 4 -3 6 328 324 2
4 2 5 454 445 2 8 5 5 195 198 3 6 9 5 28 42 28 -4 -6 6 220 216 1 5 -3 6 397 402 4
5 2 5 411 411 2 9 5 5 130 132 4 7 9 5 86 66 6 -3 -6 6 187 192 1 6 -3 6 131 129 5
6 2 5 278 277 4 10 5 5 189 185 3 8 9 5 88 95 6 -2 -6 6 153 146 1 7 -3 6 118 122 3
7 2 5 330 327 2 11 5 5 115 110 12 -7 10 5 10 58 9 -1 -6 6 224 231 2 8 -3 6 331 335 5
8 2 5 246 250 4 12 5 5 72 69 7 -6 10 5 27 13 26 0 -6 6 136 142 1 9 -3 6 108 110 3
9 2 5 122 118 3 -12 6 5 114 110 4 -5 10 5 67 59 14 1 -6 6 178 182 2 10 -3 6 99 94 5
10 2 5 253 260 3 -11 6 5 49 42 8 -4 10 5 104 105 7 2 -6 6 523 510 3 11 -3 6 114 117 8

Table B9 Continued

11 2 5 143 141 5 -10 6 5 97 101 4 -3 10 5 40 32 20 3 -6 6 66 69 2
12 -3 6 181 175 4
12 2 5 115 106 6 -9 6 5 222 216 2 -2 10 5 100 102 7 4 -6 6 184 179 1
13 -3 6 86 90 8
13 2 5 152 144 8 -8 6 5 174 170 2 -1 10 5 64 80 13 5 -6 6 261 268 1
-14 -2 6 47 32 16
-14 3 5 67 64 12 -7 6 5 324 322 3 0 10 5 138 141 3 6 -6 6 99 98 2 -
13 -2 6 105 98 7
-13 3 5 92 103 6 -6 6 5 267 275 2 1 10 5 53 61 6 7 -6 6 134 130 6 -
12 -2 6 175 192 4
-12 3 5 125 132 4 -5 6 5 68 67 2 2 10 5 33 32 13 8 -6 6 182 176 4 -
11 -2 6 242 246 4
-11 3 5 149 150 5 -4 6 5 287 283 2 3 10 5 56 60 7 9 -6 6 0 40 1 -
10 -2 6 306 312 8
-10 3 5 277 267 3 -3 6 5 217 217 1 4 10 5 64 61 27 10 -6 6 89 80 27
-9 -2 6 369 366 4
-9 3 5 239 251 7 -2 6 5 206 205 1 5 10 5 104 111 22 11 -6 6 97 102 9
-8 -2 6 180 182 4
-8 3 5 152 146 5 -1 6 5 426 426 3 6 10 5 0 38 1 -13 -5 6 116 107 10
-7 -2 6 213 215 2
-7 3 5 60 70 3 0 6 5 355 364 2 -3 11 5 58 68 15 -12 -5 6 209 202 5 -
6 -2 6 699 680 4
-6 3 5 610 615 3 1 6 5 263 266 2 -2 11 5 60 57 12 -11 -5 6 105 109 6
-5 -2 6 507 509 5
-5 3 5 267 268 7 2 6 5 265 265 2 -1 11 5 0 53 1 -10 -5 6 132 149 4 -
4 -2 6 361 359 5
-4 3 5 701 693 6 3 6 5 264 269 1 0 11 5 52 30 42 -9 -5 6 88 79 5 -
3 -2 6 783 782 7
-3 3 5 349 359 1 4 6 5 66 65 4 1 11 5 98 102 16 -8 -5 6 247 247 3 -
2 -2 6 289 296 5
-2 3 5 522 520 2 5 6 5 335 321 2 2 11 5 52 64 21 -6 -5 6 205 209 2
-1 -2 6 1047 1038 14
-1 3 5 190 198 1 6 6 5 103 105 4 -3-11 6 45 36 44 -5 -5 6 349 345 3
0 -2 6 562 575 3
0 3 5 633 631 3 7 6 5 184 181 4 -2-11 6 85 75 14 -4 -5 6 389 383 4
1 -2 6 738 755 5
1 3 5 307 300 2 8 6 5 221 228 3 -1-11 6 58 55 19 -3 -5 6 119 124 1
2 -2 6 401 418 2
2 3 5 956 947 6 9 6 5 114 104 7 0-11 6 109 100 19 -2 -5 6 146 146 1
3 -2 6 643 635 3
3 3 5 578 576 3 10 6 5 47 43 10 1-11 6 0 4 1 -1 -5 6 482 462 2 4
-2 6 448 441 2
4 3 5 147 142 2 11 6 5 139 144 4 -4-10 6 167 181 9 0 -5 6 168 163 5
5 -2 6 310 301 2

Table B9 Continued

5 3 5 705 688 9 -12 7 5 61 49 8 -3-10 6 93 90 8 1 -5 6 181 174 1 6 -2 6 56 56 3
6 3 5 246 245 2 -11 7 5 84 86 5 -2-10 6 38 53 22 2 -5 6 121 117 1 7 -2 6 203 205 2
7 3 5 62 67 4 -10 7 5 177 182 3 -1-10 6 37 47 36 3 -5 6 145 145 1 8 -2 6 324 324 3
8 3 5 303 294 2 -9 7 5 191 187 3 0-10 6 70 83 10 4 -5 6 326 322 2 9 -2 6 211 218 3
9 3 5 135 142 5 -8 7 5 161 157 2 1-10 6 148 141 5 5 -5 6 215 210 2 10 -2 6 195 192 4
10 3 5 188 182 3 -7 7 5 155 158 2 2-10 6 105 85 12 6 -5 6 109 111 4 11 -2 6 131 121 4
11 3 5 139 139 4 -6 7 5 53 51 5 3-10 6 61 70 10 7 -5 6 259 252 6 12 -2 6 98 105 8
12 3 5 108 104 5 -5 7 5 161 163 1 4-10 6 42 65 20 8 -5 6 126 118 4 13 -2 6 108 114 8
13 3 5 85 72 6 -4 7 5 478 473 2 5-10 6 88 86 8 9 -5 6 44 40 11 -15 -1 6 65 83 28
-14 4 5 45 51 22 -3 7 5 275 265 2 -3 -9 6 180 183 5 10 -5 6 209 201 5 -14 -1 6 74 71 8
-13 4 5 72 68 7 -2 7 5 59 53 4 -2 -9 6 87 83 8 11 -5 6 144 146 7 -13 -1 6 54 62 11
-12 4 5 64 70 7 -1 7 5 236 234 2 -1 -9 6 111 110 6 12 -5 6 100 89 11 -12 -1 6 205 214 9
-11 4 5 125 124 4 0 7 5 74 85 16 0 -9 6 217 210 4 -14 -4 6 0 38 1 -11 -1 6 190 188 4
-10 4 5 35 29 13 1 7 5 95 94 2 1 -9 6 164 160 5 -13 -4 6 80 86 9 -10 -1 6 122 131 7
-9 4 5 256 264 2 2 7 5 186 191 5 2 -9 6 49 49 19 -12 -4 6 142 147 5 -9 -1 6 185 184 9
-8 4 5 487 488 3 3 7 5 53 45 6 3 -9 6 23 11 22 -11 -4 6 320 304 8 -8 -1 6 370 366 5
-7 4 5 379 375 2 4 7 5 189 193 3 4 -9 6 154 149 5 -10 -4 6 274 276 6 -7 -1 6 363 370 2
-6 -1 6 187 190 5 -4 2 6 347 352 2 1 5 6 190 186 1 -1 9 6 141 143 8 -5 -6 7 451 440 2
-5 -1 6 336 330 4 -3 2 6 788 795 4 2 5 6 125 122 2 0 9 6 207 198 3 -4 -6 7 224 221 2
-4 -1 6 201 216 2 -2 2 6 280 288 4 3 5 6 130 127 1 1 9 6 159 159 3 -3 -6 7 474 467 2
-3 -1 6 72 82 3 -1 2 6 1022 1013 6 4 5 6 341 335 2 2 9 6 18 47 17 -2 -6 7 218 217 1
-2 -1 6 1279 1256 6 0 2 6 601 616 3 5 5 6 181 177 8 3 9 6 44 24 10 -1 -6 7 385 376 2

Table B9 Continued

-1 -1 6 293 303 1 1 2 6 719 739 5 6 5 6 130 134 2 4 9 6 132 142 6
0 -6 7 163 167 2
0 -1 6 699 729 4 2 2 6 400 419 2 7 5 6 277 267 2 5 9 6 108 103 4 1
-6 7 46 32 15
1 -1 6 1231 1247 6 3 2 6 657 652 3 8 5 6 105 107 3 6 9 6 127 134 4
2 -6 7 213 212 1
2 -1 6 125 123 1 4 2 6 474 468 2 9 5 6 34 34 15 7 9 6 59 59 25 3
-6 7 150 153 2
3 -1 6 437 440 2 5 2 6 305 298 2 10 5 6 200 197 3 -7 10 6 15 35 15
4 -6 7 259 259 2
4 -1 6 391 389 6 6 2 6 28 31 23 11 5 6 149 145 5 -6 10 6 51 16 19
5 -6 7 440 426 3
5 -1 6 387 388 2 7 2 6 221 223 6 12 5 6 91 85 6 -5 10 6 68 65 30 6
-6 7 171 179 4
6 -1 6 742 725 4 8 2 6 296 297 7 -12 6 6 125 121 5 -4 10 6 189 181 5
7 -6 7 143 134 4
7 -1 6 392 390 3 9 2 6 245 255 3 -11 6 6 159 146 3 -3 10 6 102 92 7
8 -6 7 89 88 5
8 -1 6 145 147 5 10 2 6 189 191 4 -10 6 6 182 179 5 -2 10 6 50 57 12
9 -6 7 71 91 6
9 -1 6 134 122 6 11 2 6 123 124 5 -9 6 6 209 200 6 -1 10 6 39 47 10
10 -6 7 72 82 12
10 -1 6 119 114 4 12 2 6 113 112 10 -8 6 6 186 185 2 0 10 6 52 70 7
11 -6 7 137 136 8
11 -1 6 195 208 4 13 2 6 107 117 6 -7 6 6 315 316 2 1 10 6 136 142 4
-13 -5 7 68 83 17
12 -1 6 168 171 5 -14 3 6 137 128 7 -6 6 6 63 66 2 2 10 6 102 96 4 -
12 -5 7 113 128 6
13 -1 6 93 102 11 -13 3 6 207 217 4 -5 6 6 254 248 1 3 10 6 75 66 6
-11 -5 7 74 84 22
-15 0 6 0 34 1 -12 3 6 157 150 4 -4 6 6 228 225 1 4 10 6 69 75 8 -
10 -5 7 62 69 9
-14 0 6 46 6 23 -11 3 6 155 165 7 -3 6 6 172 168 2 5 10 6 78 79 21
-9 -5 7 122 131 4
-13 0 6 78 77 10 -10 3 6 169 165 2 -2 6 6 137 130 1 -3 11 6 29 47 28
-8 -5 7 165 169 5
-12 0 6 159 166 8 -9 3 6 136 142 2 -1 6 6 227 231 2 -2 11 6 76 73 14
-7 -5 7 51 50 7
-11 0 6 276 282 4 -8 3 6 237 233 2 0 6 6 150 149 5 -1 11 6 32 62 32
-6 -5 7 263 273 2
-10 0 6 188 185 5 -7 3 6 298 302 4 1 6 6 182 188 2 0 11 6 101 95 16
-5 -5 7 541 525 7
-9 0 6 384 411 4 -6 3 6 255 256 1 2 6 6 503 497 3 1 11 6 30 16 29
-4 -5 7 366 368 6

Table B9 Continued

-8 0 6 46 47 4 -5 3 6 458 462 6 3 6 6 44 34 4 -2-11 7 45 41 15 -3 -5 7 222 228 1
-7 0 6 487 505 3 -4 3 6 453 446 3 4 6 6 199 198 2 -1-11 7 87 95 10 -2 -5 7 126 127 1
-6 0 6 561 562 3 -3 3 6 232 234 2 5 6 6 251 254 2 0-11 7 119 95 15 -1 -5 7 146 150 1
-5 0 6 1194 1157 6 -2 3 6 294 297 1 6 6 6 121 119 2 -4-10 7 57 52 20 0 -5 7 407 412 2
-4 0 6 723 739 4 -1 3 6 394 406 6 7 6 6 119 119 5 -3-10 7 57 67 27 1 -5 7 370 373 1
-3 0 6 187 184 3 0 3 6 365 379 4 8 6 6 173 168 3 -2-10 7 86 98 8 2 -5 7 451 449 2
-2 0 6 1024 998 5 1 3 6 188 195 1 9 6 6 23 28 23 -1-10 7 86 89 6 3 -5 7 326 329 2
-1 0 6 1201 1157 5 2 3 6 141 137 1 10 6 6 61 60 13 0-10 7 61 28 30 4 -5 7 335 329 2
0 0 6 1984 2010 12 3 3 6 226 214 1 11 6 6 102 102 5 1-10 7 30 27 30 5 -5 7 109 104 1
1 0 6 722 732 3 4 3 6 356 350 2 -12 7 6 45 60 16 2-10 7 46 10 14 6 -5 7 70 71 3
2 0 6 567 571 3 5 3 6 377 383 3 -11 7 6 95 98 10 3-10 7 24 48 24 7 -5 7 130 127 3
3 0 6 605 610 3 6 3 6 86 89 5 -10 7 6 91 88 18 4-10 7 0 32 1 8 -5 7 257 242 5
4 0 6 572 567 3 7 3 6 90 89 3 -9 7 6 126 131 4 5-10 7 85 79 20 9 -5 7 189 186 10
5 0 6 188 193 1 8 3 6 338 341 3 -8 7 6 91 93 5 -3 -9 7 92 88 12 10 -5 7 153 153 9
6 0 6 78 82 2 9 3 6 131 126 2 -7 7 6 56 47 4 -2 -9 7 71 87 8 11 -5 7 73 75 9
7 0 6 88 75 4 10 3 6 104 90 5 -6 7 6 88 91 4 -1 -9 7 96 110 7 -14 -4 7 33 40 32
8 0 6 419 424 3 11 3 6 125 126 4 -5 7 6 171 177 2 0 -9 7 28 31 28 -13 -4 7 50 60 14
9 0 6 431 417 4 12 3 6 178 172 4 -4 7 6 189 186 2 1 -9 7 97 99 7 -12 -4 7 51 30 14
10 0 6 160 163 4 13 3 6 85 90 8 -3 7 6 194 195 7 2 -9 7 93 87 8 -11 -4 7 263 260 14
11 0 6 189 174 5 -14 4 6 55 44 18 -2 7 6 459 454 3 3 -9 7 59 48 20 -10 -4 7 118 114 7
12 0 6 53 34 16 -13 4 6 82 88 10 -1 7 6 242 242 3 4 -9 7 71 61 24 -9 -4 7 245 242 4
13 0 6 23 11 22 -12 4 6 147 155 4 0 7 6 118 112 2 5 -9 7 76 68 16 -8 -4 7 261 260 3

Table B9 Continued

-15 1 6 88 89 9 -11 4 6 290 294 9 1 7 6 273 282 2 6 -9 7 64 61 40 -7 -4 7 241 236 3
-14 1 6 38 52 19 -10 4 6 318 319 3 2 7 6 42 45 6 7 -9 7 33 16 33 -6 -4 7 140 145 2
-13 1 6 83 83 7 -9 4 6 333 327 2 3 7 6 73 77 4 -3 -8 7 154 147 5 -5 -4 7 349 340 3
-12 1 6 204 207 4 -8 4 6 404 392 2 4 7 6 179 172 1 -2 -8 7 122 137 6 -4 -4 7 527 511 3
-11 1 6 164 158 4 -7 4 6 191 177 1 5 7 6 376 361 2 -1 -8 7 154 159 4 -3 -4 7 468 458 6
-10 1 6 148 147 7 -6 4 6 155 146 3 6 7 6 159 161 4 0 -8 7 113 116 4 -2 -4 7 661 652 3
-9 1 6 233 225 4 -5 4 6 335 330 1 7 7 6 143 144 3 1 -8 7 114 119 4 -1 -4 7 214 221 2
-8 1 6 367 362 2 -4 4 6 239 234 1 8 7 6 152 147 3 2 -8 7 84 78 4 0 -4 7 137 147 1
-7 1 6 350 357 2 -3 4 6 327 324 1 9 7 6 75 81 9 3 -8 7 79 74 20 1 -4 7 265 263 3
-6 1 6 155 151 3 -2 4 6 124 115 1 10 7 6 65 78 8 4 -8 7 36 46 21 2 -4 7 270 263 6
-5 1 6 305 300 2 -1 4 6 449 441 3 -10 8 6 71 58 19 5 -8 7 80 83 6 3 -4 7 392 397 2
-4 1 6 275 285 3 0 4 6 360 354 2 -9 8 6 55 60 17 6 -8 7 6 20 6 4 -4 7 508 501 2
-3 1 6 203 199 2 1 4 6 162 159 1 -8 8 6 121 122 3 7 -8 7 69 49 10 5 -4 7 538 525 3
-2 1 6 1272 1248 7 2 4 6 125 119 1 -7 8 6 129 131 3 8 -8 7 96 77 10 6 -4 7 244 237 3
0 1 6 714 745 4 3 4 6 190 178 2 -6 8 6 169 169 3 9 -8 7 79 73 13 7 -4 7 338 329 3
1 1 6 1211 1232 6 4 4 6 169 176 1 -5 8 6 303 310 3 -7 -7 7 71 50 9 8 -4 7 29 11 12
2 1 6 135 135 1 5 4 6 210 210 2 -4 8 6 148 147 1 -6 -7 7 130 126 3 9 -4 7 92 100 7
3 1 6 432 433 2 6 4 6 117 114 2 -3 8 6 200 192 3 -5 -7 7 96 102 3 10 -4 7 53 42 11
4 1 6 380 383 2 7 4 6 376 366 4 -2 8 6 46 42 19 -4 -7 7 310 303 6 11 -4 7 144 130 14
5 1 6 422 423 5 8 4 6 115 114 4 -1 8 6 124 131 2 -3 -7 7 297 290 6 12 -4 7 94 99 19
6 1 6 692 683 4 9 4 6 164 169 3 0 8 6 223 231 2 -2 -7 7 68 58 6 -14 -3 7 0 9 1
7 1 6 429 419 6 10 4 6 123 123 4 1 8 6 357 354 3 -1 -7 7 168 160 12 -13 -3 7 65 54 10

Table B9 Continued

8 1 6 160 158 2 11 4 6 97 95 5 2 8 6 213 224 2 0 -7 7 71 70 8 -12 -3 7 128 105 5
9 1 6 103 95 3 12 4 6 113 114 4 3 8 6 240 242 5 1 -7 7 185 184 3 -11 -3 7 208 205 4
10 1 6 98 94 5 -13 5 6 114 110 5 4 8 6 149 144 12 2 -7 7 199 204 3 -10 -3 7 92 82 5
11 1 6 182 188 5 -12 5 6 201 193 4 5 8 6 27 39 27 3 -7 7 93 98 4 -9 -3 7 93 90 4
12 1 6 159 169 7 -11 5 6 116 115 4 6 8 6 45 56 8 4 -7 7 117 125 7 -8 -3 7 217 217 6
13 1 6 113 110 7 -10 5 6 136 155 3 7 8 6 73 84 10 5 -7 7 148 139 3 -7 -3 7 353 360 2
-14 2 6 12 27 12 -9 5 6 106 101 3 8 8 6 121 118 4 6 -7 7 39 58 20 -6 -3 7 500 486 3
-13 2 6 100 84 7 -8 5 6 238 237 2 9 8 6 116 117 4 7 -7 7 84 90 9 -4 -3 7 241 245 1
-12 2 6 187 197 4 -7 5 6 160 159 2 -9 9 6 107 115 10 8 -7 7 143 137 5 -3 -3 7 578 546 3
-11 2 6 236 241 4 -6 5 6 212 212 5 -8 9 6 119 121 3 9 -7 7 38 47 28 -2 -3 7 309 290 2
-10 2 6 304 313 6 -5 5 6 375 370 2 -7 9 6 137 146 3 10 -7 7 0 52 1 -1 -3 7 727 725 4
-9 2 6 399 387 3 -4 5 6 395 395 2 -6 9 6 44 35 9 -10 -6 7 136 143 6 0 -3 7 541 545 4
-8 2 6 163 174 4 -3 5 6 97 99 1 -5 9 6 0 19 1 -9 -6 7 215 211 3 1 -3 7 739 736 6
-7 2 6 223 228 2 -2 5 6 156 161 1 -4 9 6 161 163 3 -8 -6 7 227 234 10 2 -3 7 717 712 4
-6 2 6 707 686 4 -1 5 6 453 444 2 -3 9 6 181 177 7 -7 -6 7 200 196 3 3 -3 7 100 102 1
-5 2 6 491 497 2 0 5 6 188 188 4 -2 9 6 76 83 8 -6 -6 7 114 118 3 4 -3 7 415 413 2
5 -3 7 111 116 2 7 0 7 148 141 2 9 3 7 195 194 5 -4 7 7 314 309 4 -2 -8 8 57 76 6
6 -3 7 67 73 3 8 0 7 348 350 3 10 3 7 194 185 3 -3 7 7 293 289 2 -1 -8 8 324 323 4
7 -3 7 142 135 2 9 0 7 404 388 3 11 3 7 120 122 12 -2 7 7 77 80 3 0 -8 8 261 263 3
8 -3 7 367 369 3 10 0 7 139 132 9 12 3 7 68 52 7 -1 7 7 184 178 2 1 -8 8 178 174 3
9 -3 7 190 195 10 11 0 7 113 132 7 -14 4 7 60 50 11 0 7 7 79 76 3 2 -8 8 206 193 3
10 -3 7 193 187 4 12 0 7 61 58 10 -13 4 7 79 63 14 1 7 7 164 171 2 3 -8 8 81 76 6

Table B9 Continued

11 -3 7 115 115 6 13 0 7 0 29 1 -12 4 7 39 21 34 2 7 7 204 211 2 4 -8 8 48 67 13
12 -3 7 58 60 11 -15 1 7 0 16 1 -11 4 7 256 256 4 3 7 7 61 70 4 5 -8 8 92 88 7
-14 -2 7 145 150 6 -14 1 7 94 89 9 -10 4 7 87 85 4 4 7 7 141 142 3 6 -8 8 122 123 5
-13 -2 7 160 164 4 -13 1 7 111 129 6 -9 4 7 251 243 3 5 7 7 125 126 4 7 -8 8 102 99 9
-12 -2 7 181 171 11 -12 1 7 356 343 4 -8 4 7 255 253 7 6 7 7 46 42 6 8 -8 8 104 107 10
-11 -2 7 168 169 4 -11 1 7 261 264 4 -7 4 7 256 251 2 7 7 7 64 71 4 -7 -7 8 83 89 7
-10 -2 7 183 190 4 -10 1 7 252 254 3 -6 4 7 143 147 3 8 7 7 132 125 3 -6 -7 8 72 68 5
-9 -2 7 326 320 3 -9 1 7 166 167 3 -5 4 7 347 336 1 9 7 7 38 46 14 -5 -7 8 293 295 10
-8 -2 7 345 347 3 -8 1 7 261 256 3 -4 4 7 528 520 3 10 7 7 41 48 14 -4 -7 8 361 357 3
-7 -2 7 373 365 4 -7 1 7 69 76 3 -3 4 7 476 470 2 -10 8 7 89 68 5 -3 -7 8 168 174 1
-6 -2 7 358 363 2 -6 1 7 189 180 2 -2 4 7 631 628 5 -9 8 7 155 166 3 -2 -7 8 125 125 4
-5 -2 7 652 641 6 -5 1 7 257 260 2 -1 4 7 274 278 2 -8 8 7 102 100 3 -1 -7 8 103 106 8
-4 -2 7 607 575 3 -4 1 7 315 315 2 0 4 7 122 134 1 -7 8 7 129 145 2 0 -7 8 100 102 5
-3 -2 7 806 776 4 -3 1 7 699 695 4 1 4 7 259 259 3 -6 8 7 173 172 6 1 -7 8 53 62 7
-2 -2 7 498 505 3 -2 1 7 425 418 2 2 4 7 254 250 1 -5 8 7 59 64 5 2 -7 8 231 232 3
-1 -2 7 423 428 2 -1 1 7 120 114 1 3 4 7 381 387 3 -4 8 7 110 111 1 3 -7 8 163 163 7
0 -2 7 404 413 4 0 1 7 236 234 2 4 4 7 532 525 3 -3 8 7 152 147 2 4 -7 8 229 229 11
1 -2 7 100 104 1 1 1 7 304 302 2 5 4 7 519 510 3 -2 8 7 132 138 2 5 -7 8 230 230 3
2 -2 7 133 137 3 2 1 7 415 415 2 6 4 7 294 287 4 -1 8 7 149 155 2 6 -7 8 150 153 3
3 -2 7 417 411 2 3 1 7 327 316 2 7 4 7 309 302 2 0 8 7 115 113 2 7 -7 8 96 93 9
4 -2 7 578 557 3 4 1 7 136 135 1 8 4 7 30 25 27 1 8 7 117 122 3 8 -7 8 78 59 12
5 -2 7 573 560 3 5 1 7 74 65 9 9 4 7 91 100 7 2 8 7 69 75 4 9 -7 8 38 66 25

Table B9 Continued

6 -2 7 257 250 2 6 1 7 275 274 4 10 4 7 53 41 9 3 8 7 78 81 5 -10 -6 8 172 177 5
7 -2 7 143 140 6 7 1 7 256 255 2 11 4 7 125 116 4 4 8 7 46 43 13 -9 -6 8 122 99 10
8 -2 7 176 176 5 8 1 7 53 55 8 12 4 7 99 88 7 5 8 7 83 90 12 -8 -6 8 230 230 8
9 -2 7 167 163 3 9 1 7 85 77 7 -13 5 7 40 76 39 6 8 7 31 24 11 -7 -6 8 63 61 5
10 -2 7 200 202 4 10 1 7 213 214 4 -12 5 7 140 140 4 7 8 7 59 51 5 -6 -6 8 115 95 4
11 -2 7 161 162 4 11 1 7 114 87 20 -11 5 7 78 82 5 8 8 7 68 74 5 -5 -6 8 134 129 4
12 -2 7 98 108 7 12 1 7 208 209 12 -10 5 7 50 63 8 9 8 7 86 82 5 -4 -6 8 409 396 2
13 -2 7 65 57 15 13 1 7 128 127 7 -9 5 7 131 147 2 -9 9 7 104 114 4 -3 -6 8 198 188 4
-15 -1 7 0 7 1 -14 2 7 153 159 6 -8 5 7 169 174 2 -8 9 7 103 93 4 -2 -6 8 116 118 2
-14 -1 7 84 87 12 -13 2 7 157 164 4 -7 5 7 30 28 13 -7 9 7 53 45 6 -1 -6 8 377 372 2
-13 -1 7 113 112 6 -12 2 7 168 169 4 -6 5 7 285 291 1 -6 9 7 0 17 1 0 -6 8 166 166 2
-12 -1 7 368 354 4 -11 2 7 158 163 6 -5 5 7 544 531 5 -5 9 7 125 124 3 1 -6 8 302 304 4
-11 -1 7 222 222 4 -10 2 7 179 182 4 -4 5 7 353 357 2 -4 9 7 95 96 4 2 -6 8 68 64 4
-10 -1 7 262 260 8 -9 2 7 325 319 2 -3 5 7 231 233 1 -3 9 7 105 103 5 3 -6 8 48 47 3
-9 -1 7 183 183 3 -8 2 7 386 381 2 -2 5 7 115 114 1 -2 9 7 88 86 4 4 -6 8 71 76 4
-8 -1 7 242 242 2 -7 2 7 331 320 4 -1 5 7 158 163 4 -1 9 7 117 110 4 5 -6 8 285 282 5
-7 -1 7 52 63 3 -6 2 7 338 344 2 0 5 7 409 415 2 0 9 7 35 44 11 6 -6 8 197 195 4
-6 -1 7 155 135 7 -5 2 7 667 662 7 1 5 7 390 392 2 1 9 7 94 91 5 7 -6 8 37 32 16
-5 -1 7 262 261 1 -4 2 7 607 579 3 2 5 7 431 435 2 2 9 7 100 95 4 8 -6 8 152 162 8
-4 -1 7 295 297 2 -3 2 7 795 765 8 3 5 7 333 338 2 3 9 7 46 46 9 9 -6 8 80 93 7
-3 -1 7 747 738 10 -2 2 7 520 528 3 4 5 7 322 320 2 4 9 7 47 56 12 10 -6 8 12 53 11
-2 -1 7 384 379 2 -1 2 7 389 396 2 5 5 7 118 110 2 5 9 7 72 69 7 -13 -5 8 88 94 10

Table B9 Continued

-1 -1 7 145 143 2 0 2 7 449 462 5 6 5 7 57 54 7 6 9 7 51 58 32 -12 -5 8 111 103 7
0 -1 7 254 258 2 1 2 7 91 95 1 7 5 7 92 93 3 7 9 7 29 28 28 -11 -5 8 66 71 15
1 -1 7 260 251 8 2 2 7 105 113 2 8 5 7 262 252 5 -6 10 7 49 46 9 -10 -5 8 147 152 4
2 -1 7 430 427 2 3 2 7 432 424 2 9 5 7 197 200 3 -5 10 7 79 78 8 -9 -5 8 267 270 6
3 -1 7 327 316 2 4 2 7 569 549 3 10 5 7 166 165 3 -4 10 7 56 57 14 -8 -5 8 241 239 4
4 -1 7 148 147 2 5 2 7 578 560 3 11 5 7 63 66 14 -3 10 7 52 50 6 -7 -5 8 346 337 8
5 -1 7 71 73 3 6 2 7 233 231 2 -12 6 7 72 74 8 -2 10 7 101 100 4 -6 -5 8 110 103 3
6 -1 7 251 250 1 7 2 7 125 128 2 -11 6 7 115 114 5 -1 10 7 84 87 4 -5 -5 8 324 323 3
7 -1 7 254 258 6 8 2 7 188 184 3 -10 6 7 136 141 3 0 10 7 35 22 14 -4 -5 8 212 217 5
8 -1 7 80 81 9 9 2 7 155 148 3 -9 6 7 215 217 4 1 10 7 31 28 15 -3 -5 8 117 117 1
9 -1 7 64 68 8 10 2 7 208 203 4 -8 6 7 233 239 4 2 10 7 33 15 17 -2 -5 8 296 294 2
10 -1 7 191 193 3 11 2 7 161 163 6 -7 6 7 198 195 2 3 10 7 28 44 28 -1 -5 8 143 139 1
11 -1 7 65 63 11 12 2 7 93 89 5 -6 6 7 131 133 1 4 10 7 53 38 11 0 -5 8 47 37 7
12 -1 7 214 209 7 13 2 7 50 62 17 -5 6 7 427 416 2 5 10 7 76 75 9 1 -5 8 170 168 1
13 -1 7 116 128 7 -14 3 7 28 20 27 -4 6 7 245 241 1 -2 11 7 56 48 17 2 -5 8 132 132 1
-15 0 7 213 214 6 -13 3 7 76 62 10 -3 6 7 449 448 4 -1 11 7 87 86 11 3 -5 8 49 47 7
-14 0 7 215 216 7 -12 3 7 130 104 6 -2 6 7 220 217 1 0 11 7 127 105 12 4 -5 8 388 372 2
-13 0 7 243 229 7 -11 3 7 189 191 4 -1 6 7 392 394 2 -4-10 8 0 11 1 5 -5 8 240 241 2
-12 0 7 176 196 5 -10 3 7 115 109 6 0 6 7 150 155 2 -3-10 8 101 96 14 6 -5 8 73 62 7
-11 0 7 136 132 5 -9 3 7 48 56 7 1 6 7 24 15 14 -2-10 8 52 39 19 7 -5 8 75 76 4
-10 0 7 39 38 10 -8 3 7 224 222 2 2 6 7 208 209 1 -1-10 8 57 47 15 8 -5 8 191 201 4
-9 0 7 431 425 4 -7 3 7 339 346 3 3 6 7 164 165 5 0-10 8 55 70 14 9 -5 8 139 138 4

Table B9 Continued

-8 0 7 461 470 3 -6 3 7 487 478 6 4 6 7 268 265 5 1-10 8 199 210 5 10 -5 8 128 132 8
-7 0 7 480 486 3 -5 3 7 174 176 1 5 6 7 441 428 2 2-10 8 81 76 17 11 -5 8 93 84 9
-6 0 7 413 409 2 -4 3 7 241 248 1 6 6 7 133 140 2 3-10 8 36 31 28 -14 -4 8 96 97 9
-5 0 7 485 473 2 -3 3 7 542 524 2 7 6 7 152 149 5 4-10 8 35 35 35 -13 -4 8 197 197 8
-4 0 7 341 363 2 -2 3 7 280 270 1 8 6 7 102 100 4 -3 -9 8 95 98 9 -12 -4 8 257 252 6
-3 0 7 194 195 1 -1 3 7 713 715 3 9 6 7 109 109 4 -2 -9 8 190 192 5 -11 -4 8 278 284 5
-2 0 7 331 334 2 0 3 7 562 572 3 10 6 7 82 91 10 -1 -9 8 44 10 18 -10 -4 8 174 172 3
-1 0 7 42 44 3 1 3 7 713 720 4 11 6 7 124 123 5 0 -9 8 59 45 16 -9 -4 8 127 128 4
0 0 7 22 17 13 2 3 7 709 709 4 -11 7 7 111 110 5 1 -9 8 54 45 11 -8 -4 8 203 202 6
1 0 7 158 167 3 3 3 7 126 135 4 -10 7 7 154 159 3 2 -9 8 130 127 8 -7 -4 8 219 221 4
2 0 7 36 34 2 4 3 7 406 405 2 -9 7 7 182 166 5 3 -9 8 64 67 13 -6 -4 8 201 193 2
3 0 7 174 183 1 5 3 7 122 128 1 -8 7 7 41 45 18 4 -9 8 161 160 5 -5 -4 8 341 334 2
4 0 7 67 57 4 6 3 7 64 75 3 -7 7 7 83 73 12 5 -9 8 166 156 9 -4 -4 8 363 358 2
5 0 7 27 32 9 7 3 7 132 132 2 -6 7 7 119 114 2 6 -9 8 71 78 10 -3 -4 8 322 310 2
6 0 7 151 141 2 8 3 7 374 370 3 -5 7 7 71 72 3 7 -9 8 38 36 38 -2 -4 8 139 140 3
-1 -4 8 141 142 8 4 -1 8 695 679 3 5 2 8 162 166 3 -12 6 8 83 69 7 2 10 8 94 91 5
0 -4 8 245 249 1 5 -1 8 256 258 1 6 2 8 282 285 4 -11 6 8 149 144 8 3 10 8 0 16 1
1 -4 8 231 231 1 6 -1 8 207 211 3 7 2 8 284 283 2 -10 6 8 189 187 3 4 10 8 31 39 31
2 -4 8 28 19 5 7 -1 8 167 167 4 8 2 8 264 259 2 -9 6 8 80 78 5 -4-10 9 0 55 1
3 -4 8 16 5 15 8 -1 8 39 35 4 9 2 8 219 216 3 -8 6 8 219 223 2 -3-10 9 50 62 49
4 -4 8 173 166 3 9 -1 8 148 151 2 10 2 8 118 114 5 -7 6 8 85 84 3 -2-10 9 0 26 1
5 -4 8 238 238 2 10 -1 8 74 75 7 11 2 8 98 98 6 -6 6 8 130 127 1 -1-10 9 0 38 1

Table B9 Continued

6 -4 8 98 107 2 11 -1 8 204 210 5 12 2 8 85 90 10 -5 6 8 116 113 3 0-10 9 59 63 14
7 -4 8 217 209 2 12 -1 8 108 110 7 -14 3 8 105 114 13 -4 6 8 434 417 2 1-10 9 118 109 9
8 -4 8 0 5 1 13 -1 8 78 70 20 -13 3 8 67 60 32 -3 6 8 168 158 2 2-10 9 8 38 8
9 -4 8 21 24 21 -15 0 8 76 72 13 -12 3 8 38 30 26 -2 6 8 118 111 2 3-10 9 70 80 23
10 -4 8 28 20 27 -14 0 8 23 34 22 -11 3 8 123 116 5 -1 6 8 364 364 2 4-10 9 19 45 18
11 -4 8 124 111 8 -13 0 8 84 68 9 -10 3 8 161 172 4 0 6 8 177 177 1 -3 -9 9 0 5 1
12 -4 8 78 81 10 -12 0 8 130 130 8 -9 3 8 292 301 3 1 6 8 305 308 4 -2 -9 9 0 39 1
-14 -3 8 110 119 11 -11 0 8 41 16 18 -8 3 8 369 370 3 2 6 8 49 42 2 -1 -9 9 20 33 20
-13 -3 8 57 42 20 -10 0 8 229 230 4 -7 3 8 337 336 2 3 6 8 71 66 2 0 -9 9 79 97 11
-12 -3 8 53 32 13 -9 0 8 398 395 4 -6 3 8 330 326 5 4 6 8 76 73 7 1 -9 9 141 160 4
-11 -3 8 85 94 6 -8 0 8 460 453 3 -5 3 8 118 111 2 5 6 8 277 270 2 2 -9 9 65 72 10
-10 -3 8 204 216 3 -7 0 8 496 494 3 -4 3 8 370 371 2 6 6 8 230 230 5 3 -9 9 41 5 18
-9 -3 8 282 292 3 -6 0 8 600 589 3 -3 3 8 171 172 1 7 6 8 68 50 16 4 -9 9 53 25 14
-8 -3 8 366 370 3 -5 0 8 784 750 4 -2 3 8 640 634 3 8 6 8 135 135 19 5 -9 9 85 78 8
-7 -3 8 318 320 2 -4 0 8 566 550 3 -1 3 8 247 226 5 9 6 8 89 92 5 6 -9 9 20 41 19
-6 -3 8 300 303 3 -3 0 8 120 99 1 0 3 8 445 444 2 10 6 8 59 51 8 -2 -8 9 74 88 14
-5 -3 8 138 130 3 -2 0 8 87 76 1 1 3 8 181 174 1 -11 7 8 67 74 7 -1 -8 9 173 171 4
-4 -3 8 366 367 2 -1 0 8 739 763 4 2 3 8 32 28 3 -10 7 8 126 125 4 0 -8 9 131 140 4
-3 -3 8 222 221 2 0 0 8 974 981 5 3 3 8 199 201 1 -9 7 8 45 50 10 1 -8 9 49 48 16
-2 -3 8 630 618 3 1 0 8 1195 1204 6 4 3 8 330 327 2 -8 7 8 136 129 3 2 -8 9 30 7 30
-1 -3 8 262 241 2 2 0 8 494 506 7 5 3 8 134 136 5 -7 7 8 89 80 4 3 -8 9 98 109 5
0 -3 8 438 439 2 3 0 8 779 757 4 6 3 8 132 133 2 -6 7 8 69 62 2 4 -8 9 99 101 6

Table B9 Continued

1 -3 8 190 186 1 4 0 8 70 61 2 7 3 8 75 70 3 -5 7 8 305 303 2 5 -8 9 94 114 6
2 -3 8 44 32 6 5 0 8 337 331 2 8 3 8 201 205 2 -4 7 8 365 358 2 6 -8 9 89 98 6
3 -3 8 183 187 1 6 0 8 258 263 2 9 3 8 98 91 4 -3 7 8 181 182 1 7 -8 9 40 56 30
4 -3 8 345 344 3 7 0 8 363 358 3 10 3 8 223 223 3 -2 7 8 110 106 3 8 -8 9 73 75 14
5 -3 8 103 108 1 8 0 8 450 439 5 11 3 8 93 81 4 -1 7 8 131 133 2 -7 -7 9 191 199 5
6 -3 8 148 149 2 9 0 8 362 348 4 12 3 8 56 49 12 0 7 8 94 97 3 -6 -7 9 260 230 5
7 -3 8 76 72 3 10 0 8 184 184 4 -14 4 8 94 100 11 1 7 8 84 82 2 -5 -7 9 68 68 12
8 -3 8 193 201 2 11 0 8 0 8 1 -13 4 8 211 195 13 2 7 8 218 224 2 -4 -7 9 147 144 2
9 -3 8 112 101 3 12 0 8 37 38 36 -12 4 8 254 252 4 3 7 8 160 157 2 -3 -7 9 111 121 2
10 -3 8 233 235 4 13 0 8 57 68 19 -11 4 8 274 286 4 4 7 8 214 214 1 -2 -7 9 175 183 4
11 -3 8 82 79 6 -15 1 8 51 67 21 -10 4 8 190 197 4 5 7 8 236 232 2 -1 -7 9 129 130 5
12 -3 8 51 49 14 -14 1 8 60 19 12 -9 4 8 146 145 5 6 7 8 165 167 2 0 -7 9 149 157 6
-14 -2 8 72 89 12 -13 1 8 120 96 6 -8 4 8 202 198 2 7 7 8 117 112 3 1 -7 9 191 194 6
-13 -2 8 147 158 5 -12 1 8 142 131 5 -7 4 8 247 241 2 8 7 8 48 56 10 2 -7 9 46 39 7
-12 -2 8 203 201 4 -11 1 8 88 74 7 -6 4 8 174 172 1 9 7 8 54 56 10 3 -7 9 82 95 5
-11 -2 8 208 220 6 -10 1 8 191 203 3 -5 4 8 347 345 2 -10 8 8 44 37 11 4 -7 9 60 69 6
-10 -2 8 178 179 4 -9 1 8 172 162 7 -4 4 8 330 326 2 -9 8 8 93 89 4 5 -7 9 100 106 5
-9 -2 8 260 268 3 -8 1 8 168 180 2 -3 4 8 338 327 1 -8 8 8 94 92 4 6 -7 9 84 86 5
-8 -2 8 258 258 3 -7 1 8 80 79 2 -2 4 8 163 162 1 -7 8 8 154 160 3 7 -7 9 27 26 26
-7 -2 8 278 277 2 -6 1 8 123 116 3 -1 4 8 144 142 1 -6 8 8 146 129 2 8 -7 9 35 27 34
-6 -2 8 282 279 3 -5 1 8 325 336 2 0 4 8 257 257 1 -5 8 8 42 43 6 9 -7 9 65 76 21
-5 -2 8 509 499 4 -4 1 8 523 515 5 1 4 8 235 238 2 -4 8 8 133 135 1 -10 -6 9 100 117 22

Table B9 Continued

-4 -2 8 376 372 2 -3 1 8 304 319 2 2 4 8 27 14 7 -3 8 8 36 31 36 -9 -6 9 180 176 4
-3 -2 8 416 416 2 -2 1 8 1026 998 5 3 4 8 13 6 13 -2 8 8 55 60 10 -8 -6 9 148 149 7
-2 -2 8 268 262 2 -1 1 8 209 216 2 4 4 8 158 150 2 -1 8 8 328 325 10 -7 -6 9 147 148 3
-1 -2 8 597 596 3 0 1 8 472 457 2 5 4 8 243 240 2 0 8 8 271 266 2 -6 -6 9 104 108 4
0 -2 8 161 176 2 1 1 8 312 323 2 6 4 8 126 130 2 1 8 8 172 171 3 -5 -6 9 178 178 2
1 -2 8 827 837 4 2 1 8 422 429 4 7 4 8 222 218 3 2 8 8 192 189 3 -4 -6 9 60 50 3
2 -2 8 315 316 2 3 1 8 391 398 3 8 4 8 24 20 23 3 8 8 77 62 5 -3 -6 9 466 463 10
3 -2 8 239 247 2 4 1 8 687 675 3 9 4 8 0 23 1 4 8 8 54 72 9 -2 -6 9 299 296 4
4 -2 8 154 153 2 5 1 8 258 268 2 10 4 8 0 7 1 5 8 8 91 97 5 -1 -6 9 63 62 6
5 -2 8 178 180 2 6 1 8 194 198 2 11 4 8 120 112 4 6 8 8 110 117 3 0 -6 9 153 149 1
6 -2 8 280 282 2 7 1 8 166 164 3 12 4 8 100 94 6 7 8 8 99 103 5 1 -6 9 113 114 1
7 -2 8 273 273 4 8 1 8 4 23 3 -13 5 8 100 99 6 8 8 8 106 106 3 2 -6 9 245 243 2
8 -2 8 261 260 2 9 1 8 153 156 7 -12 5 8 99 92 8 -8 9 8 46 44 12 3 -6 9 57 59 3
9 -2 8 198 206 3 10 1 8 97 110 7 -11 5 8 68 64 7 -7 9 8 0 22 1 4 -6 9 291 291 2
10 -2 8 104 106 7 11 1 8 178 179 7 -10 5 8 150 150 3 -6 9 8 63 65 5 5 -6 9 386 378 3
11 -2 8 102 99 5 12 1 8 96 110 7 -9 5 8 231 233 2 -5 9 8 109 105 5 6 -6 9 180 184 6
12 -2 8 77 79 11 13 1 8 65 72 13 -8 5 8 235 229 2 -4 9 8 215 214 4 7 -6 9 0 27 1
-15 -1 8 48 72 27 -14 2 8 70 87 13 -7 5 8 348 341 2 -3 9 8 121 104 13 8 -6 9 84 84 7
-14 -1 8 54 36 14 -13 2 8 155 164 15 -6 5 8 65 56 3 -2 9 8 190 190 7 9 -6 9 57 77 23
-13 -1 8 103 88 7 -12 2 8 213 216 15 -5 5 8 335 333 2 -1 9 8 0 22 1 10 -6 9 109 102 9
-12 -1 8 150 132 5 -11 2 8 208 224 4 -4 5 8 209 211 1 0 9 8 28 37 28 -13 -5 9 83 65 14
-11 -1 8 88 95 7 -10 2 8 169 164 3 -3 5 8 135 133 1 1 9 8 46 36 9 -12 -5 9 79 65 30

Table B9 Continued

-10 -1 8 206 217 6 -9 2 8 256 256 2 -2 5 8 275 271 1 2 9 8 156 140 4 -11 -5 9 52 66 10
-9 -1 8 203 198 7 -8 2 8 258 253 4 -1 5 8 142 137 2 3 9 8 50 63 9 -10 -5 9 67 67 7
-8 -1 8 185 190 2 -7 2 8 300 300 5 0 5 8 33 18 4 4 9 8 157 164 4 -9 -5 9 206 199 5
-7 -1 8 75 75 3 -6 2 8 282 276 2 1 5 8 162 160 1 5 9 8 154 157 4 -8 -5 9 263 265 4
-6 -1 8 117 114 3 -5 2 8 524 513 5 2 5 8 146 149 2 6 9 8 78 73 7 -7 -5 9 219 208 9
-5 -1 8 325 333 2 -4 2 8 373 372 6 3 5 8 73 72 2 7 9 8 0 29 1 -6 -5 9 295 300 3
-4 -1 8 511 504 3 -3 2 8 397 397 4 4 5 8 376 361 2 -6 10 8 63 72 9 -5 -5 9 112 110 2
-3 -1 8 343 359 3 -2 2 8 245 240 2 5 5 8 238 237 2 -5 10 8 76 75 5 -4 -5 9 217 212 2
-2 -1 8 1018 988 7 -1 2 8 587 589 3 6 5 8 83 70 3 -4 10 8 0 21 1 -3 -5 9 187 186 2
-1 -1 8 187 194 1 0 2 8 223 237 2 7 5 8 84 96 3 -3 10 8 101 99 7 -2 -5 9 357 359 2
0 -1 8 489 469 3 1 2 8 824 833 4 8 5 8 185 188 3 -2 10 8 31 32 17 -1 -5 9 349 357 3
1 -1 8 279 291 5 2 2 8 298 295 2 9 5 8 141 139 5 -1 10 8 50 54 9 0 -5 9 555 550 3
2 -1 8 437 446 2 3 2 8 240 250 1 10 5 8 123 122 4 0 10 8 65 69 8 1 -5 9 255 252 4
3 -1 8 376 382 2 4 2 8 155 154 1 11 5 8 86 81 18 1 10 8 205 203 4 2 -5 9 388 384 2
3 -5 9 195 189 2 12 -2 9 81 70 9 -11 2 9 99 98 5 -3 5 9 212 207 1 1 9 9 137 151 4
4 -5 9 205 202 4 -15 -1 9 125 137 7 -10 2 9 181 186 6 -2 5 9 342 346 2 2 9 9 78 74 5
5 -5 9 225 225 2 -14 -1 9 232 223 10 -9 2 9 290 296 6 -1 5 9 360 367 2 3 9 9 9 9 8
6 -5 9 222 226 2 -13 -1 9 233 235 5 -8 2 9 249 245 5 0 5 9 530 539 5 4 9 9 0 25 1
7 -5 9 183 187 2 -12 -1 9 300 311 6 -7 2 9 301 290 3 1 5 9 269 268 3 5 9 9 94 75 6
8 -5 9 229 234 4 -11 -1 9 263 257 9 -6 2 9 80 72 2 2 5 9 375 376 2 6 9 9 36 53 26
9 -5 9 75 66 8 -10 -1 9 175 172 3 -5 2 9 571 566 3 3 5 9 190 186 2 -6 10 9 89 94 17
10 -5 9 17 39 16 -9 -1 9 305 296 8 -4 2 9 205 187 4 4 5 9 183 183 2 -5 10 9 68 65 6

Table B9 Continued

11 -5 9 52 64 16 -8 -1 9 126 124 5 -3 2 9 273 268 2 5 5 9 213 215 2 -4 10 9 46 56 9
-14 -4 9 69 60 11 -7 -1 9 195 194 2 -2 2 9 511 517 3 6 5 9 228 240 8 -3 10 9 78 65 6
-13 -4 9 48 34 14 -6 -1 9 467 461 2 -1 2 9 191 186 1 7 5 9 170 166 2 -2 10 9 0 18 1
-12 -4 9 98 88 7 -5 -1 9 325 329 2 0 2 9 208 208 2 8 5 9 251 250 3 -1 10 9 38 38 14
-11 -4 9 127 141 8 -4 -1 9 349 347 2 1 2 9 160 162 1 9 5 9 69 64 7 0 10 9 65 59 9
-10 -4 9 72 88 6 -3 -1 9 676 659 4 2 2 9 331 325 5 10 5 9 65 40 10 1 10 9 124 118 5
-9 -4 9 102 109 4 -2 -1 9 64 50 5 3 2 9 389 385 2 11 5 9 57 59 25 2 10 9 9 30 8
-8 -4 9 245 257 3 -1 -1 9 612 609 3 4 2 9 454 447 2 -12 6 9 35 28 16 3 10 9 67 70 9
-7 -4 9 70 83 5 0 -1 9 538 527 3 5 2 9 274 266 2 -11 6 9 171 169 4 4 10 9 47 43 19
-6 -4 9 94 98 9 1 -1 9 334 331 2 6 2 9 219 218 2 -10 6 9 94 103 6 -4-10 10 84 98 16
-5 -4 9 554 526 6 2 -1 9 118 131 2 7 2 9 199 191 8 -9 6 9 197 196 3 -3-10 10 0 42 1
-4 -4 9 343 344 2 3 -1 9 170 161 4 8 2 9 191 185 3 -8 6 9 151 155 2 -2-10 10 86 71 13
-3 -4 9 367 356 2 4 -1 9 279 270 4 9 2 9 243 231 3 -7 6 9 134 137 2 -1-10 10 105 107 11
-2 -4 9 181 185 1 5 -1 9 63 69 2 10 2 9 94 89 4 -6 6 9 144 137 2 0-10 10 83 68 8
-1 -4 9 137 146 1 6 -1 9 211 212 2 11 2 9 121 119 14 -5 6 9 161 161 1 1-10 10 126 123 6
0 -4 9 167 166 1 7 -1 9 58 57 8 12 2 9 89 65 15 -4 6 9 70 62 6 2-10 10 44 37 24
1 -4 9 375 375 2 8 -1 9 206 206 3 -14 3 9 81 94 11 -3 6 9 458 458 4 3-10 10 23 22 23
2 -4 9 243 248 2 9 -1 9 198 201 3 -13 3 9 87 78 9 -2 6 9 307 307 3 -3 -9 10 77 61 17
3 -4 9 417 412 2 10 -1 9 58 69 10 -12 3 9 135 128 11 -1 6 9 67 70 4 -2 -9 10 40 83 40
4 -4 9 294 286 2 11 -1 9 61 42 11 -11 3 9 155 147 4 0 6 9 150 146 1 -1 -9 10 71 89 9
5 -4 9 372 369 2 12 -1 9 153 146 6 -10 3 9 142 131 4 1 6 9 134 131 3 0 -9 10 75 88 10
6 -4 9 147 147 2 -15 0 9 132 136 9 -9 3 9 126 120 3 2 6 9 246 246 2 1 -9 10 128 122 6

Table B9 Continued

7 -4 9 161 158 2 -14 0 9 97 79 9 -8 3 9 471 462 3 3 6 9 61 50 5 2 -9 10 155 146 5
8 -4 9 92 102 3 -13 0 9 62 32 13 -7 3 9 177 180 1 4 6 9 286 289 2 3 -9 10 47 71 16
9 -4 9 189 189 4 -12 0 9 0 21 1 -6 3 9 504 498 3 5 6 9 401 392 2 4 -9 10 97 83 6
10 -4 9 162 159 9 -11 0 9 208 226 4 -5 3 9 241 237 1 6 6 9 157 163 3 5 -9 10 105 105 9
11 -4 9 96 82 12 -10 0 9 144 150 4 -4 3 9 483 478 9 7 6 9 0 29 1 6 -9 10 60 50 13
-14 -3 9 105 95 15 -9 0 9 307 305 3 -3 3 9 138 125 5 8 6 9 78 81 5 -2 -8 10 124 156 10
-13 -3 9 52 51 17 -8 0 9 448 449 3 -2 3 9 677 670 3 9 6 9 69 66 9 -1 -8 10 247 259 6
-12 -3 9 137 140 5 -7 0 9 393 402 2 -1 3 9 694 699 4 10 6 9 103 95 6 0 -8 10 65 91 13
-11 -3 9 158 153 8 -6 0 9 130 129 2 0 3 9 475 481 3 -11 7 9 62 63 9 1 -8 10 141 146 5
-10 -3 9 121 121 4 -5 0 9 73 66 3 1 3 9 646 656 3 -10 7 9 59 54 7 2 -8 10 55 59 11
-9 -3 9 114 106 3 -4 0 9 102 103 2 2 3 9 158 160 1 -9 7 9 33 25 16 3 -8 10 61 62 11
-8 -3 9 469 469 4 -3 0 9 278 281 2 3 3 9 142 147 3 -8 7 9 173 177 3 4 -8 10 114 108 5
-6 -3 9 536 524 3 -2 0 9 234 233 3 4 3 9 256 250 3 -7 7 9 192 201 2 5 -8 10 158 156 4
-5 -3 9 216 211 2 -1 0 9 225 242 1 5 3 9 444 432 3 -6 7 9 247 231 3 6 -8 10 136 138 5
-4 -3 9 469 460 2 1 0 9 245 239 2 6 3 9 172 173 2 -5 7 9 66 61 3 7 -8 10 50 50 22
-3 -3 9 160 153 1 2 0 9 22 11 7 7 3 9 348 336 3 -4 7 9 121 118 4 -7 -7 10 162 159 6
-2 -3 9 682 664 3 3 0 9 468 462 3 8 3 9 225 225 3 -3 7 9 116 118 2 -6 -7 10 188 173 5
-1 -3 9 719 717 4 4 0 9 61 47 3 9 3 9 150 145 3 -2 7 9 170 175 1 -5 -7 10 215 220 5
0 -3 9 415 424 5 5 0 9 212 219 2 10 3 9 92 83 6 -1 7 9 146 141 4 -4 -7 10 125 130 3
1 -3 9 675 679 3 6 0 9 43 55 7 11 3 9 31 41 30 0 7 9 138 142 2 -3 -7 10 101 108 2
2 -3 9 160 161 3 7 0 9 137 135 2 12 3 9 52 61 21 1 7 9 199 201 2 -2 -7 10 18 23 18
3 -3 9 140 137 1 8 0 9 313 308 3 -14 4 9 28 62 28 2 7 9 67 54 5 -1 -7 10 145 146 8

Table B9 Continued

4 -3 9 252 246 2 9 0 9 189 192 3 -13 4 9 63 50 11 3 7 9 87 96 4 0 -7 10 87 82 4
5 -3 9 460 451 2 10 0 9 212 196 6 -12 4 9 103 85 7 4 7 9 63 74 5 1 -7 10 211 224 2
6 -3 9 159 159 4 11 0 9 67 74 32 -11 4 9 124 137 10 5 7 9 104 106 3 2 -7 10 315 312 4
7 -3 9 317 305 2 12 0 9 70 84 11 -10 4 9 47 58 9 6 7 9 76 87 4 3 -7 10 95 90 4
8 -3 9 253 252 2 -15 1 9 137 136 11 -9 4 9 104 104 3 7 7 9 27 35 17 4 -7 10 124 116 4
9 -3 9 125 129 4 -14 1 9 239 230 8 -8 4 9 257 260 3 8 7 9 37 27 13 5 -7 10 109 115 8
10 -3 9 79 79 6 -13 1 9 224 217 4 -7 4 9 113 111 3 9 7 9 75 82 17 6 -7 10 69 61 5
11 -3 9 31 46 31 -12 1 9 332 329 5 -6 4 9 106 106 2 -10 8 9 68 73 7 7 -7 10 60 64 17
12 -3 9 48 61 48 -11 1 9 243 236 4 -5 4 9 530 509 2 -9 8 9 193 197 9 8 -7 10 106 103 17
-14 -2 9 73 74 9 -10 1 9 199 195 4 -4 4 9 349 354 2 -8 8 9 150 146 3 9 -7 10 0 62 1
-13 -2 9 113 114 6 -9 1 9 308 307 4 -3 4 9 355 349 2 -7 8 9 87 87 5 -10 -6 10 41 68 17
-12 -2 9 41 60 40 -8 1 9 156 152 2 -2 4 9 196 196 1 -6 8 9 76 57 4 -9 -6 10 36 42 18
-11 -2 9 108 105 5 -7 1 9 219 217 2 -1 4 9 136 138 1 -5 8 9 69 77 3 -8 -6 10 168 172 3
-10 -2 9 200 192 8 -6 1 9 451 446 3 0 4 9 154 151 2 -4 8 9 85 83 2 -7 -6 10 131 126 8
-9 -2 9 286 292 3 -5 1 9 343 346 2 1 4 9 390 391 2 -3 8 9 157 155 3 -6 -6 10 275 280 8
-8 -2 9 239 239 10 -4 1 9 324 322 2 2 4 9 258 258 2 -2 8 9 71 67 18 -5 -6 10 129 126 2
-7 -2 9 323 312 2 -3 1 9 704 683 4 3 4 9 418 413 3 -1 8 9 176 176 3 -4 -6 10 532 512 4
-6 -2 9 119 119 4 -2 1 9 81 84 2 4 4 9 315 305 2 0 8 9 138 145 3 -2 -6 10 299 300 3
-5 -2 9 571 566 3 -1 1 9 598 594 3 5 4 9 351 347 3 1 8 9 59 49 7 -1 -6 10 204 208 2
-4 -2 9 200 187 4 0 1 9 512 506 2 6 4 9 166 158 5 2 8 9 0 2 1 0 -6 10 132 127 4
-3 -2 9 215 219 2 1 1 9 369 368 2 7 4 9 155 156 11 3 8 9 105 112 5 1 -6 10 199 197 3
-2 -2 9 538 548 3 2 1 9 125 135 1 8 4 9 71 80 9 4 8 9 95 96 5 2 -6 10 184 194 2

Table B9 Continued

-1 -2 9 169 159 5 3 1 9 168 162 2 9 4 9 189 185 3 5 8 9 100 110 3 3 -6 10 101 106 3
0 -2 9 234 236 2 4 1 9 283 271 2 10 4 9 188 181 7 6 8 9 77 93 4 4 -6 10 124 119 2
1 -2 9 112 111 2 5 1 9 26 33 6 11 4 9 92 85 9 7 8 9 73 68 4 5 -6 10 343 332 4
2 -2 9 362 352 4 6 1 9 187 189 1 -13 5 9 49 72 16 8 8 9 82 71 5 6 -6 10 106 94 5
3 -2 9 391 384 2 7 1 9 67 72 6 -12 5 9 80 78 15 -8 9 9 47 53 18 7 -6 10 137 129 5
4 -2 9 438 433 2 8 1 9 227 222 3 -11 5 9 57 64 11 -7 9 9 70 72 6 8 -6 10 41 44 15
5 -2 9 270 262 2 9 1 9 187 188 4 -10 5 9 65 65 6 -6 9 9 63 68 6 9 -6 10 55 47 16
6 -2 9 235 235 2 10 1 9 0 39 1 -9 5 9 212 210 2 -5 9 9 42 34 5 10 -6 10 0 20 1
7 -2 9 173 170 2 11 1 9 79 58 10 -8 5 9 262 266 3 -4 9 9 246 253 11 -12 -5 10 165 163 9
8 -2 9 194 193 2 12 1 9 153 149 6 -7 5 9 214 208 5 -3 9 9 17 25 17 -11 -5 10 191 189 4
9 -2 9 241 223 3 -14 2 9 64 72 10 -6 5 9 301 301 3 -2 9 9 27 35 26 -10 -5 10 232 227 4
10 -2 9 115 117 5 -13 2 9 103 106 6 -5 5 9 126 118 2 -1 9 9 0 30 1 -9 -5 10 231 230 9
11 -2 9 121 112 6 -12 2 9 65 71 11 -4 5 9 203 196 1 0 9 9 104 108 5 -8 -5 10 203 197 10
-7 -5 10 237 233 5 5 -2 10 269 270 2 11 1 10 71 78 12 -6 5 10 70 67 2 0 9 10 83 85 6
-6 -5 10 68 56 5 6 -2 10 406 404 3 12 1 10 56 66 27 -5 5 10 154 149 2 1 9 10 101 105 5
-5 -5 10 126 127 3 7 -2 10 316 319 3 -14 2 10 71 58 13 -4 5 10 163 143 5 2 9 10 153 156 4
-4 -5 10 142 129 2 8 -2 10 144 157 7 -13 2 10 170 157 7 -3 5 10 249 253 3 3 9 10 39 71 17
-3 -5 10 246 251 2 9 -2 10 113 111 5 -12 2 10 156 165 5 -2 5 10 103 100 1 4 9 10 85 83 7
-2 -5 10 124 128 3 10 -2 10 46 24 13 -11 2 10 63 58 7 -1 5 10 210 213 4 5 9 10 115 110 6
-1 -5 10 200 207 2 11 -2 10 91 91 8 -10 2 10 25 24 25 0 5 10 93 88 2 6 9 10 62 48 10
0 -5 10 70 66 3 12 -2 10 112 117 7 -9 2 10 386 370 6 1 5 10 61 55 8 -5 10 10 65 72 17
1 -5 10 73 74 3 -14 -1 10 89 81 9 -8 2 10 87 84 2 2 5 10 173 168 2 -4 10 10 79 91 17

Table B9 Continued

2 -5 10 180 175 2 -13 -1 10 46 15 15 -7 2 10 515 504 3 3 5 10 47 51 5 -3 10 10 64 49 11
3 -5 10 66 72 3 -12 -1 10 192 197 4 -6 2 10 230 239 5 4 5 10 124 118 2 -2 10 10 73 74 6
4 -5 10 121 118 2 -11 -1 10 103 101 6 -5 2 10 59 54 3 5 5 10 43 36 7 -1 10 10 98 100 6
5 -5 10 31 36 9 -10 -1 10 161 151 3 -4 2 10 216 216 1 6 5 10 52 50 15 0 10 10 100 87 5
6 -5 10 43 38 12 -9 -1 10 204 206 3 -3 2 10 354 350 2 7 5 10 145 143 3 1 10 10 119 116 5
7 -5 10 139 133 7 -8 -1 10 240 243 3 -2 2 10 225 241 1 8 5 10 151 148 4 2 10 10 47 35 17
8 -5 10 153 155 4 -7 -1 10 121 128 8 -1 2 10 411 417 3 9 5 10 32 7 16 3 10 10 0 20 1
9 -5 10 0 19 1 -6 -1 10 446 427 2 0 2 10 471 472 2 10 5 10 42 29 18 -4-10 11 0 43 1
10 -5 10 37 28 36 -5 -1 10 675 643 4 1 2 10 490 500 2 -12 6 10 60 43 10 -3-10 11 84 76 12
-13 -4 10 183 168 5 -4 -1 10 501 492 3 2 2 10 57 68 7 -11 6 10 170 159 4 -2-10 11 0 24 1
-12 -4 10 185 183 8 -3 -1 10 255 256 2 3 2 10 151 151 2 -10 6 10 56 63 7 -1-10 11 129 144 13
-11 -4 10 96 100 16 -2 -1 10 383 386 2 4 2 10 133 140 2 -9 6 10 59 47 7 0-10 11 58 57 24
-10 -4 10 58 60 9 -1 -1 10 460 456 3 5 2 10 250 253 2 -8 6 10 159 164 3 1-10 11 67 69 13
-9 -4 10 37 9 18 0 -1 10 501 489 4 6 2 10 419 415 3 -7 6 10 152 150 2 2-10 11 36 44 36
-8 -4 10 285 290 6 1 -1 10 805 790 4 7 2 10 276 280 2 -6 6 10 238 242 2 -3 -9 11 51 41 32
-6 -4 10 308 308 3 2 -1 10 316 328 2 8 2 10 174 175 3 -5 6 10 109 107 2 -2 -9 11 39 48 39
-5 -4 10 252 239 2 3 -1 10 234 233 3 9 2 10 130 117 3 -4 6 10 542 519 6 -1 -9 11 0 32 1
-4 -4 10 170 173 1 4 -1 10 462 446 3 10 2 10 30 43 29 -3 6 10 122 117 1 0 -9 11 68 59 12
-3 -4 10 112 112 2 5 -1 10 121 121 4 11 2 10 72 82 9 -2 6 10 286 294 4 1 -9 11 0 28 1
-2 -4 10 100 102 2 6 -1 10 126 118 2 12 2 10 115 116 17 -1 6 10 199 203 2 2 -9 11 66 73 14
-1 -4 10 170 180 4 7 -1 10 126 123 2 -14 3 10 33 22 33 0 6 10 144 140 2 3 -9 11 36 31 36
0 -4 10 272 270 2 8 -1 10 216 210 2 -13 3 10 158 163 6 1 6 10 194 197 1 4 -9 11 0 34 1

Table B9 Continued

1 -4 10 309 314 2 9 -1 10 238 229 4 -12 3 10 128 127 5 2 6 10 190 197 2 5 -9 11 50 52 16
2 -4 10 200 197 1 10 -1 10 176 175 4 -11 3 10 265 268 6 3 6 10 115 117 2 -2 -8 11 95 106 14
3 -4 10 249 247 2 11 -1 10 67 79 14 -10 3 10 259 268 4 4 6 10 130 125 3 -1 -8 11 80 65 15
4 -4 10 180 181 2 12 -1 10 69 61 13 -9 3 10 195 186 2 5 6 10 339 326 2 0 -8 11 66 53 11
5 -4 10 150 157 2 -14 0 10 53 54 24 -8 3 10 344 344 2 6 6 10 128 116 3 1 -8 11 77 95 9
6 -4 10 54 47 7 -13 0 10 44 48 14 -7 3 10 198 188 5 7 6 10 138 136 7 2 -8 11 67 75 9
7 -4 10 84 88 3 -12 0 10 56 75 14 -6 3 10 44 26 5 8 6 10 40 47 12 3 -8 11 102 103 6
8 -4 10 69 64 4 -11 0 10 91 119 10 -5 3 10 170 163 2 9 6 10 73 55 8 4 -8 11 70 61 8
9 -4 10 91 88 20 -10 0 10 67 66 5 -4 3 10 333 328 3 10 6 10 18 30 18 5 -8 11 53 50 12
10 -4 10 114 114 8 -9 0 10 62 46 6 -3 3 10 249 245 2 -11 7 10 32 42 32 6 -8 11 76 71 8
11 -4 10 57 58 15 -8 0 10 320 331 2 -2 3 10 458 461 3 -10 7 10 102 98 4 7 -8 11 27 26 26
-14 -3 10 25 25 24 -7 0 10 181 186 3 -1 3 10 258 257 1 -9 7 10 128 124 6 -7 -7 11 154 152 6
-13 -3 10 167 173 7 -6 0 10 170 162 2 0 3 10 146 153 1 -8 7 10 111 102 8 -6 -7 11 185 173 6
-12 -3 10 99 116 8 -5 0 10 43 50 6 1 3 10 118 125 1 -7 7 10 155 163 2 -5 -7 11 63 52 11
-11 -3 10 260 269 4 -4 0 10 534 512 3 2 3 10 305 301 2 -6 7 10 159 160 2 -4 -7 11 227 236 6
-10 -3 10 286 282 4 -3 0 10 158 137 1 3 3 10 104 106 2 -5 7 10 225 219 2 -3 -7 11 200 206 3
-9 -3 10 206 200 3 -2 0 10 575 573 3 4 3 10 132 135 2 -4 7 10 159 166 2 -2 -7 11 84 98 3
-8 -3 10 323 324 5 -1 0 10 274 287 2 5 3 10 249 239 2 -3 7 10 94 91 1 -1 -7 11 116 119 2
-7 -3 10 216 205 5 0 0 10 297 301 2 6 3 10 47 48 13 -2 7 10 36 28 19 0 -7 11 115 125 2
-6 -3 10 46 45 4 1 0 10 1185 1179 6 7 3 10 50 47 7 -1 7 10 135 136 3 1 -7 11 30 18 29
-5 -3 10 182 186 2 2 0 10 179 174 1 8 3 10 166 167 3 0 7 10 99 100 3 2 -7 11 47 34 10
-4 -3 10 326 318 5 3 0 10 23 25 9 9 3 10 135 128 5 1 7 10 213 218 1 3 -7 11 84 90 6

Table B9 Continued

-3 -3 10 269 263 2 4 0 10 432 423 3 10 3 10 91 99 11 2 7 10 306 303 3 4 -7 11 85 73 18
-2 -3 10 424 432 3 5 0 10 453 453 3 11 3 10 66 64 9 3 7 10 88 84 3 5 -7 11 198 199 3
-1 -3 10 271 275 6 6 0 10 260 257 2 -13 4 10 171 154 5 4 7 10 126 124 2 6 -7 11 49 71 13
0 -3 10 152 155 1 7 0 10 384 375 3 -12 4 10 177 192 4 5 7 10 90 97 3 7 -7 11 44 47 17
1 -3 10 132 140 2 8 0 10 211 207 7 -11 4 10 84 86 7 6 7 10 71 66 13 8 -7 11 41 50 41
2 -3 10 294 292 2 9 0 10 63 51 8 -10 4 10 53 64 16 7 7 10 53 49 7 -10 -6 11 92 88 10
3 -3 10 135 137 2 10 0 10 0 31 1 -9 4 10 23 14 21 8 7 10 93 95 9 -9 -6 11 133 137 7
4 -3 10 122 126 1 11 0 10 31 24 30 -8 4 10 316 314 2 9 7 10 54 53 24 -8 -6 11 63 73 7
5 -3 10 229 221 2 12 0 10 97 92 11 -7 4 10 248 241 2 -10 8 10 35 47 18 -7 -6 11 35 42 11
6 -3 10 48 51 4 -14 1 10 84 80 15 -6 4 10 308 306 2 -9 8 10 84 95 5 -6 -6 11 149 136 3
7 -3 10 67 74 6 -13 1 10 41 26 19 -5 4 10 279 270 2 -8 8 10 73 72 5 -5 -6 11 95 94 2
8 -3 10 169 173 5 -12 1 10 181 187 4 -4 4 10 160 162 1 -7 8 10 105 113 4 -4 -6 11 175 172 2
9 -3 10 126 117 4 -11 1 10 112 118 6 -3 4 10 113 113 1 -6 8 10 0 14 1 -3 -6 11 286 289 2
10 -3 10 111 112 5 -10 1 10 160 160 4 -2 4 10 116 110 1 -5 8 10 71 74 4 -2 -6 11 76 74 2
11 -3 10 37 59 30 -9 1 10 205 194 2 -1 4 10 160 162 1 -4 8 10 102 100 3 -1 -6 11 119 126 2
-14 -2 10 57 49 17 -8 1 10 234 231 2 0 4 10 243 241 1 -3 8 10 144 145 5 0 -6 11 53 58 15
-13 -2 10 150 142 21 -7 1 10 166 174 2 1 4 10 326 335 2 -2 8 10 143 150 3 1 -6 11 79 87 2
-12 -2 10 171 170 4 -6 1 10 433 415 2 2 4 10 190 188 3 -1 8 10 269 267 4 2 -6 11 274 273 5
-11 -2 10 40 50 18 -5 1 10 669 642 4 3 4 10 248 241 5 0 8 10 89 94 5 3 -6 11 212 217 2
-10 -2 10 53 42 7 -4 1 10 506 497 2 4 4 10 188 185 2 1 8 10 140 142 3 4 -6 11 44 39 8
-9 -2 10 367 362 3 -3 1 10 258 264 2 5 4 10 177 175 2 2 8 10 56 60 8 5 -6 11 151 150 3
-8 -2 10 95 94 4 -2 1 10 379 380 2 6 4 10 46 38 6 3 8 10 78 71 6 6 -6 11 46 8 13

Table B9 Continued

-7 -2 10 498 484 3 -1 1 10 445 438 3 7 4 10 84 86 6 4 8 10 83 84 5
7 -6 11 35 6 34
-6 -2 10 269 279 5 0 1 10 489 476 2 8 4 10 72 68 4 5 8 10 181 176 2
8 -6 11 99 103 9
-5 -2 10 95 88 2 1 1 10 825 820 7 9 4 10 85 85 8 6 8 10 136 140 3
9 -6 11 97 99 8
-4 -2 10 198 202 1 2 1 10 324 334 2 10 4 10 104 104 11 7 8 10 57 51 8
-12 -5 11 70 52 10
-3 -2 10 345 342 2 3 1 10 188 193 2 11 4 10 83 70 8 -8 9 10 82 78 15
-11 -5 11 66 67 10
-2 -2 10 247 259 2 4 1 10 482 461 3 -13 5 10 0 13 1 -7 9 10 105 108 5
-10 -5 11 139 147 4
-1 -2 10 419 425 2 5 1 10 107 113 2 -12 5 10 181 169 12 -6 9 10 27 32
13 -9 -5 11 144 143 4
0 -2 10 470 469 3 6 1 10 133 124 3 -11 5 10 171 173 4 -5 9 10 99 96 8
-8 -5 11 222 228 3
1 -2 10 496 503 3 7 1 10 153 145 3 -10 5 10 241 244 3 -4 9 10 179 176 10
-7 -5 11 58 69 8
2 -2 10 47 53 5 8 1 10 196 187 2 -9 5 10 228 219 2 -3 9 10 46 53 16
-6 -5 11 92 98 3
3 -2 10 151 152 1 9 1 10 246 240 3 -8 5 10 207 212 2 -2 9 10 84 82 5
-5 -5 11 322 319 3
4 -2 10 124 125 2 10 1 10 202 200 3 -7 5 10 242 235 1 -1 9 10 69 84 8
-4 -5 11 197 188 4
-3 -5 11 266 260 2 8 -2 11 158 157 3 -11 2 11 163 156 4 1 5 11 102 99 2
-1 10 11 161 148 4
-2 -5 11 321 326 3 9 -2 11 175 170 4 -10 2 11 137 150 5 2 5 11 94 96 4
0 10 11 54 43 12
-1 -5 11 282 288 3 10 -2 11 83 89 13 -9 2 11 240 227 3 3 5 11 226 228 2
1 10 11 73 75 10
0 -5 11 279 284 2 11 -2 11 0 52 1 -8 2 11 92 92 2 4 5 11 267 263 2
2 10 11 50 48 16
1 -5 11 101 103 2 -14 -1 11 189 185 7 -7 2 11 163 163 4 5 5 11 207 206 4
-4-10 12 75 76 23
2 -5 11 81 88 3 -13 -1 11 171 160 7 -6 2 11 283 274 2 6 5 11 186 170 2
-3-10 12 93 101 14
3 -5 11 242 239 2 -12 -1 11 110 102 7 -5 2 11 246 247 2 7 5 11 116 108 4
-2-10 12 89 92 17
4 -5 11 252 248 2 -11 -1 11 149 147 3 -4 2 11 184 178 2 8 5 11 92 80 4
-1-10 12 70 68 27
5 -5 11 200 198 2 -10 -1 11 42 39 9 -3 2 11 381 374 2 9 5 11 33 29 32
0-10 12 63 37 12
6 -5 11 196 186 5 -9 -1 11 365 366 6 -2 2 11 138 141 2 10 5 11 64 92 21
1-10 12 63 60 34

Table B9 Continued

7 -5 11 140 122 6 -8 -1 11 377 375 3 -1 2 11 53 53 2 -12 6 11 99 105 6 -3 -9 12 57 34 28
8 -5 11 80 77 18 -7 -1 11 353 349 3 0 2 11 439 437 3 -11 6 11 179 185 4 -2 -9 12 62 71 26
9 -5 11 0 25 1 -6 -1 11 279 274 2 1 2 11 401 400 2 -10 6 11 60 71 7 -1 -9 12 0 45 1
10 -5 11 87 80 10 -5 -1 11 257 248 3 2 2 11 276 283 2 -9 6 11 122 134 4 0 -9 12 98 127 15
-13 -4 11 92 69 9 -4 -1 11 230 224 4 3 2 11 146 146 2 -8 6 11 77 74 4 1 -9 12 168 158 6
-12 -4 11 99 87 7 -3 -1 11 465 463 3 4 2 11 96 92 4 -7 6 11 20 30 20 2 -9 12 150 158 8
-11 -4 11 140 149 4 -2 -1 11 287 289 3 5 2 11 194 191 4 -6 6 11 130 120 2 3 -9 12 12 33 12
-10 -4 11 67 63 12 -1 -1 11 398 398 3 6 2 11 131 132 3 -5 6 11 109 106 2 4 -9 12 0 25 1
-9 -4 11 188 192 3 0 -1 11 481 479 2 7 2 11 77 68 3 -4 6 11 181 176 4 -2 -8 12 135 115 11
-8 -4 11 261 275 4 1 -1 11 231 226 1 8 2 11 154 151 4 -3 6 11 293 294 4 -1 -8 12 53 36 32
-7 -4 11 281 276 7 2 -1 11 103 97 2 9 2 11 170 173 3 -2 6 11 89 84 5 0 -8 12 88 79 16
-6 -4 11 22 22 22 3 -1 11 77 85 4 10 2 11 84 71 7 -1 6 11 123 127 2 1 -8 12 77 87 19
-5 -4 11 559 550 4 4 -1 11 278 278 2 11 2 11 83 64 10 0 6 11 42 45 4 2 -8 12 85 93 7
-4 -4 11 156 162 2 5 -1 11 281 273 7 -14 3 11 94 102 14 1 6 11 66 79 8 3 -8 12 175 158 12
-3 -4 11 206 198 2 6 -1 11 184 183 2 -13 3 11 105 106 7 2 6 11 282 283 2 4 -8 12 103 106 6
-2 -4 11 13 6 12 7 -1 11 32 32 11 -12 3 11 131 121 6 3 6 11 194 199 2 5 -8 12 80 86 9
-1 -4 11 46 36 4 8 -1 11 41 43 9 -11 3 11 200 203 3 4 6 11 55 57 4 6 -8 12 76 72 10
0 -4 11 340 341 2 9 -1 11 202 196 4 -10 3 11 84 80 5 5 6 11 160 153 3 -6 -7 12 67 61 11
1 -4 11 667 670 4 10 -1 11 179 185 4 -9 3 11 136 134 4 6 6 11 13 7 13 -5 -7 12 37 24 36
2 -4 11 235 235 2 11 -1 11 79 84 7 -8 3 11 175 177 1 7 6 11 23 18 22 -4 -7 12 60 70 9
3 -4 11 287 280 2 12 -1 11 58 49 16 -7 3 11 179 177 2 8 6 11 109 101 5 -3 -7 12 67 78 9
4 -4 11 354 354 2 -14 0 11 67 70 24 -6 3 11 148 145 2 9 6 11 89 93 6 -2 -7 12 33 26 10

Table B9 Continued

5 -4 11 49 50 4 -13 0 11 99 97 17 -5 3 11 169 164 2 -11 7 11 32 28 25 -1 -7 12 199 205 2
6 -4 11 99 101 5 -12 0 11 261 263 6 -4 3 11 502 492 3 -10 7 11 94 111 6 0 -7 12 187 189 4
7 -4 11 146 142 2 -11 0 11 336 353 4 -3 3 11 354 339 3 -9 7 11 74 79 6 1 -7 12 151 163 4
8 -4 11 185 184 4 -10 0 11 271 259 4 -2 3 11 616 603 3 -8 7 11 216 219 12 2 -7 12 175 167 4
9 -4 11 120 128 5 -9 0 11 84 88 4 0 3 11 111 117 2 -7 7 11 143 142 3 3 -7 12 34 52 15
10 -4 11 171 160 8 -8 0 11 142 140 3 1 3 11 200 201 1 -6 7 11 185 185 2 4 -7 12 103 112 4
11 -4 11 64 68 12 -7 0 11 70 72 4 2 3 11 185 183 3 -5 7 11 56 54 4 5 -7 12 132 139 11
-14 -3 11 89 104 11 -6 0 11 257 257 2 3 3 11 84 99 2 -4 7 11 233 229 3 6 -7 12 115 130 5
-13 -3 11 61 81 11 -5 0 11 227 217 2 4 3 11 280 274 2 -3 7 11 202 204 2 7 -7 12 31 41 31
-12 -3 11 130 135 6 -4 0 11 214 220 1 5 3 11 435 427 3 -2 7 11 96 102 3 8 -7 12 102 98 14
-11 -3 11 182 195 4 -3 0 11 395 392 2 6 3 11 350 332 7 -1 7 11 122 118 2 -10 -6 12 86 112 10
-10 -3 11 73 71 7 -2 0 11 256 270 2 7 3 11 119 115 10 0 7 11 123 123 4 -9 -6 12 177 180 6
-9 -3 11 107 106 4 -1 0 11 27 23 6 8 3 11 56 62 5 1 7 11 22 9 15 -8 -6 12 126 127 6
-8 -3 11 192 196 4 1 0 11 247 241 2 9 3 11 54 72 16 2 7 11 39 36 4 -7 -6 12 224 232 4
-7 -3 11 147 146 3 2 0 11 109 117 3 10 3 11 52 45 24 3 7 11 92 96 2 -6 -6 12 144 146 6
-6 -3 11 161 166 2 3 0 11 110 106 2 11 3 11 100 107 16 4 7 11 75 73 4 -5 -6 12 64 61 6
-5 -3 11 179 169 4 4 0 11 132 125 2 -13 4 11 67 71 11 5 7 11 195 199 3 -4 -6 12 280 283 3
-4 -3 11 505 494 3 5 0 11 61 70 8 -12 4 11 89 80 7 6 7 11 64 72 14 -3 -6 12 257 266 12
-3 -3 11 350 335 2 6 0 11 45 52 8 -11 4 11 143 152 4 7 7 11 71 57 6 -2 -6 12 69 74 4
-2 -3 11 621 605 4 7 0 11 247 243 3 -10 4 11 75 71 7 8 7 11 55 55 9 -1 -6 12 54 51 4
-1 -3 11 88 91 2 8 0 11 35 29 4 -9 4 11 174 184 3 -9 8 11 71 70 8 0 -6 12 150 159 2
0 -3 11 120 133 2 9 0 11 13 11 13 -8 4 11 282 280 2 -8 8 11 116 113 5 1 -6 12 105 119 2

Table B9 Continued

1 -3 11 198 199 1 10 0 11 90 86 11 -7 4 11 289 281 2 -7 8 11 37 33 28
2 -6 12 127 132 3
2 -3 11 183 185 4 11 0 11 116 132 9 -6 4 11 77 72 3 -6 8 11 53 53 10
3 -6 12 92 100 7
3 -3 11 89 93 7 12 0 11 73 85 14 -5 4 11 552 541 3 -5 8 11 49 51 5
4 -6 12 111 126 4
4 -3 11 296 287 6 -14 1 11 191 192 5 -4 4 11 170 174 1 -4 8 11 149 145 3
5 -6 12 250 239 3
5 -3 11 447 441 4 -13 1 11 150 154 6 -3 4 11 199 192 1 -3 8 11 184 187 2
6 -6 12 91 97 6
6 -3 11 317 300 3 -12 1 11 123 122 5 -2 4 11 18 10 17 -2 8 11 134 120 4
7 -6 12 83 98 8
7 -3 11 105 104 2 -11 1 11 143 134 5 -1 4 11 76 69 2 -1 8 11 80 72 6
8 -6 12 55 58 14
8 -3 11 79 72 6 -10 1 11 35 21 14 0 4 11 309 309 1 0 8 11 49 55 10
9 -6 12 59 53 14
9 -3 11 70 73 8 -9 1 11 337 337 3 1 4 11 679 679 8 1 8 11 95 89 4 -
12 -5 12 139 138 9
10 -3 11 62 42 20 -8 1 11 375 365 3 2 4 11 249 248 2 2 8 11 79 78 5
-11 -5 12 177 173 5
11 -3 11 117 104 9 -7 1 11 369 367 7 3 4 11 307 305 5 3 8 11 92 101 5
-10 -5 12 162 142 5
-14 -2 11 56 24 12 -6 1 11 269 271 2 4 4 11 339 334 3 4 8 11 61 67 3
-9 -5 12 47 44 11
-13 -2 11 72 82 9 -5 1 11 280 270 2 5 4 11 60 55 18 5 8 11 52 46 5
-8 -5 12 160 158 6
-12 -2 11 190 187 4 -4 1 11 224 220 2 6 4 11 100 98 9 6 8 11 67 61 5
-7 -5 12 83 84 5
-11 -2 11 148 141 3 -3 1 11 455 452 3 7 4 11 145 140 2 7 8 11 0 17 1
-6 -5 12 110 110 4
-10 -2 11 140 143 5 -2 1 11 335 333 3 8 4 11 166 165 8 -8 9 11 61 79 7
-5 -5 12 111 117 6
-9 -2 11 227 225 3 -1 1 11 368 373 2 9 4 11 135 127 13 -7 9 11 89 84 5
-4 -5 12 330 317 3
-8 -2 11 123 118 3 0 1 11 467 462 2 10 4 11 176 176 5 -6 9 11 85 88 12
-3 -5 12 159 162 3
-7 -2 11 170 171 3 1 1 11 247 246 2 11 4 11 61 66 15 -5 9 11 50 38 22
-2 -5 12 166 167 2
-6 -2 11 281 276 4 2 1 11 94 91 2 -13 5 11 47 36 19 -4 9 11 51 41 50
-1 -5 12 39 25 5
-5 -2 11 225 212 5 3 1 11 48 59 4 -12 5 11 59 57 12 -3 9 11 47 31 47
0 -5 12 86 91 3
-4 -2 11 156 153 1 4 1 11 295 290 2 -11 5 11 70 62 9 -2 9 11 39 46 17
1 -5 12 74 58 4

Table B9 Continued

-3 -2 11 404 402 3 5 1 11 278 263 2 -10 5 11 130 132 4 -1 9 11 31 33 21
2 -5 12 127 130 5
-2 -2 11 153 154 3 6 1 11 174 173 4 -9 5 11 126 128 3 0 9 11 59 52 8
3 -5 12 127 128 4
-1 -2 11 84 87 4 7 1 11 25 15 5 -8 5 11 226 235 2 1 9 11 60 19 12
4 -5 12 135 132 2
0 -2 11 429 420 2 8 1 11 66 61 6 -7 5 11 55 51 3 2 9 11 81 76 9 5
-5 12 102 100 4
1 -2 11 397 395 3 9 1 11 205 197 3 -6 5 11 102 103 2 3 9 11 20 38 20
6 -5 12 77 69 6
2 -2 11 303 308 2 10 1 11 190 186 5 -5 5 11 310 305 1 4 9 11 65 40 12
7 -5 12 100 100 5
3 -2 11 146 145 2 11 1 11 90 78 8 -4 5 11 208 200 2 5 9 11 0 46 1
8 -5 12 32 41 31
4 -2 11 64 62 3 12 1 11 70 31 11 -3 5 11 264 263 3 -5 10 11 60 70 9
9 -5 12 47 35 27
5 -2 11 196 188 3 -14 2 11 0 29 1 -2 5 11 321 323 2 -4 10 11 7 31 6
10 -5 12 11 3 11
6 -2 11 121 120 3 -13 2 11 74 80 9 -1 5 11 287 285 2 -3 10 11 69 77 7
-13 -4 12 87 76 23
7 -2 11 77 76 3 -12 2 11 178 180 4 0 5 11 272 278 5 -2 10 11 0 27 1 -
12 -4 12 24 26 24
-11 -4 12 99 95 7 -1 -1 12 341 334 2 8 2 12 71 49 7 -2 6 12 101 92 2
-1 -7 13 110 112 6
-10 -4 12 120 121 5 0 -1 12 404 407 2 9 2 12 106 95 10 -1 6 12 39 42 4
0 -7 13 112 111 5
-9 -4 12 234 234 5 1 -1 12 711 708 3 10 2 12 52 70 17 0 6 12 148 150 5
1 -7 13 62 49 14
-8 -4 12 284 297 7 2 -1 12 357 358 4 11 2 12 88 78 10 1 6 12 119 122 6
2 -7 13 0 13 1
-7 -4 12 291 279 4 3 -1 12 196 194 1 -14 3 12 74 86 14 2 6 12 135 132 4
3 -7 13 82 90 8
-6 -4 12 141 139 3 4 -1 12 213 219 5 -13 3 12 110 116 6 3 6 12 119 126
3 4 -7 13 52 64 11
-5 -4 12 102 102 4 5 -1 12 93 98 4 -12 3 12 229 223 4 4 6 12 86 97 6
5 -7 13 124 136 4
-4 -4 12 43 41 7 6 -1 12 248 253 4 -11 3 12 219 207 4 5 6 12 237 231 3
6 -7 13 125 130 10
-3 -4 12 137 142 2 7 -1 12 217 217 3 -10 3 12 186 193 5 6 6 12 90 97 5
7 -7 13 81 21 25
-2 -4 12 110 116 4 8 -1 12 226 226 4 -9 3 12 103 106 6 7 6 12 108 110 5
-9 -6 13 60 38 12
-1 -4 12 250 255 2 9 -1 12 225 227 4 -8 3 12 123 120 3 8 6 12 55 58 21
-8 -6 13 132 127 7

Table B9 Continued

0 -4 12 136 129 3 10 -1 12 143 147 7 -7 3 12 86 83 3 9 6 12 45 54 12 -7 -6 13 168 159 6
1 -4 12 167 166 2 11 -1 12 125 123 5 -6 3 12 364 352 2 -11 7 12 53 41 11 -6 -6 13 227 214 4
2 -4 12 82 86 3 -14 0 12 22 8 21 -5 3 12 370 359 2 -10 7 12 65 60 14 -5 -6 13 107 107 9
3 -4 12 79 74 3 -13 0 12 45 44 32 -4 3 12 195 191 2 -9 7 12 102 89 6 -4 -6 13 147 156 5
4 -4 12 167 167 4 -12 0 12 167 173 4 -3 3 12 260 258 3 -8 7 12 103 98 4 -3 -6 13 61 53 5
5 -4 12 108 108 3 -11 0 12 103 125 12 -2 3 12 123 121 2 -7 7 12 108 112 3 -2 -6 13 165 173 4
6 -4 12 121 117 2 -10 0 12 118 99 4 -1 3 12 236 234 2 -6 7 12 65 57 5 -1 -6 13 133 147 4
7 -4 12 32 35 32 -9 0 12 28 22 15 0 3 12 307 313 5 -5 7 12 30 30 9 0 -6 13 144 150 2
8 -4 12 0 35 1 -8 0 12 33 17 10 1 3 12 160 161 1 -4 7 12 80 78 3 1 -6 13 256 262 2
9 -4 12 103 94 18 -7 0 12 0 8 1 2 3 12 141 144 2 -3 7 12 72 63 3 2 -6 13 66 61 6
10 -4 12 157 137 10 -6 0 12 70 62 5 3 3 12 123 135 3 -2 7 12 25 2 24 3 -6 13 71 68 6
-14 -3 12 83 71 11 -5 0 12 391 377 2 4 3 12 141 144 5 -1 7 12 198 195 2 4 -6 13 139 146 3
-13 -3 12 149 144 6 -4 0 12 363 362 2 5 3 12 227 233 2 0 7 12 189 190 3 5 -6 13 107 112 4
-12 -3 12 198 201 5 -3 0 12 337 337 2 6 3 12 103 98 4 1 7 12 156 161 5 6 -6 13 153 146 5
-11 -3 12 243 226 5 -2 0 12 319 308 2 7 3 12 171 177 3 2 7 12 183 174 2 7 -6 13 84 79 8
-10 -3 12 196 195 11 -1 0 12 329 329 2 8 3 12 115 122 6 3 7 12 30 32 10 8 -6 13 77 63 9
-9 -3 12 78 84 6 0 0 12 394 384 4 9 3 12 86 96 9 4 7 12 114 116 3 -12 -5 13 38 48 38
-8 -3 12 133 131 10 1 0 12 290 289 2 10 3 12 65 41 13 5 7 12 137 140 3 -11 -5 13 114 130 6
-7 -3 12 53 58 12 2 0 12 99 108 2 11 3 12 0 37 1 6 7 12 134 140 4 -10 -5 13 142 145 5
-6 -3 12 334 329 5 3 0 12 232 232 2 -13 4 12 78 85 9 7 7 12 0 34 1 -9 -5 13 81 88 9
-5 -3 12 360 347 3 4 0 12 443 429 5 -12 4 12 39 29 38 8 7 12 93 96 6 -8 -5 13 231 226 4
-4 -3 12 227 228 2 5 0 12 208 202 3 -11 4 12 115 110 6 -9 8 12 46 41 19 -7 -5 13 143 141 4

Table B9 Continued

-3 -3 12 251 246 2 6 0 12 194 195 3 -10 4 12 126 127 5 -8 8 12 29 36 29
-6 -5 13 173 171 13
-2 -3 12 129 131 2 7 0 12 93 98 4 -9 4 12 220 213 3 -7 8 12 49 54 8
-5 -5 13 370 359 8
-1 -3 12 217 218 2 8 0 12 81 75 7 -8 4 12 262 264 2 -6 8 12 70 82 6
-4 -5 13 230 229 7
0 -3 12 320 327 3 9 0 12 77 86 17 -7 4 12 278 275 3 -5 8 12 103 102 6
-3 -5 13 160 162 3
1 -3 12 152 148 1 10 0 12 100 101 14 -6 4 12 160 154 3 -4 8 12 255 256
4 -2 -5 13 280 283 3
2 -3 12 133 135 2 11 0 12 44 45 16 -5 4 12 120 117 5 -3 8 12 145 140 2
-1 -5 13 126 121 2
3 -3 12 137 144 4 -14 1 12 76 52 12 -4 4 12 53 44 4 -2 8 12 107 120 5
0 -5 13 73 81 3
4 -3 12 150 152 2 -13 1 12 84 93 8 -3 4 12 121 127 1 -1 8 12 0 15 1
1 -5 13 21 21 20
5 -3 12 242 241 3 -12 1 12 84 97 7 -2 4 12 111 108 2 0 8 12 73 77 7
2 -5 13 214 210 7
6 -3 12 124 123 3 -11 1 12 98 95 7 -1 4 12 248 251 2 1 8 12 84 83 4
3 -5 13 98 99 3
7 -3 12 152 156 4 -10 1 12 218 216 3 0 4 12 111 103 2 2 8 12 95 98 5
4 -5 13 230 229 2
8 -3 12 125 126 4 -9 1 12 125 126 3 1 4 12 184 177 7 3 8 12 174 168 4
5 -5 13 245 242 3
9 -3 12 80 88 13 -8 1 12 282 282 2 2 4 12 92 84 7 4 8 12 90 89 3 6
-5 13 83 79 8
10 -3 12 56 43 12 -7 1 12 239 234 2 3 4 12 81 88 4 5 8 12 85 88 4
7 -5 13 54 61 14
11 -3 12 1 33 1 -6 1 12 214 212 2 4 4 12 168 169 3 6 8 12 72 77 5
8 -5 13 81 70 11
-14 -2 12 89 86 10 -5 1 12 371 361 2 5 4 12 90 96 4 -7 9 12 99 113 5
9 -5 13 91 79 27
-13 -2 12 0 31 1 -4 1 12 547 539 3 6 4 12 118 121 6 -6 9 12 58 55 6
-13 -4 13 75 70 9
-12 -2 12 0 24 1 -3 1 12 224 216 2 7 4 12 17 37 16 -5 9 12 80 78 18
-12 -4 13 101 101 8
-11 -2 12 87 97 5 -2 1 12 155 161 3 8 4 12 24 37 24 -4 9 12 12 36 11
-11 -4 13 69 58 19
-10 -2 12 181 170 3 -1 1 12 328 319 2 9 4 12 110 99 7 -3 9 12 40 37 34
-10 -4 13 7 15 7
-9 -2 12 328 321 3 0 1 12 382 388 5 10 4 12 140 132 7 -2 9 12 77 83 7
-9 -4 13 164 162 5
-8 -2 12 175 176 3 1 1 12 705 707 3 -12 5 12 139 123 5 -1 9 12 30 28 29
-8 -4 13 208 205 4

Table B9 Continued

-7 -2 12 223 223 3 2 1 12 367 365 2 -11 5 12 191 194 7 0 9 12 102 118 6 -7 -4 13 117 105 4
-6 -2 12 271 268 4 3 1 12 204 204 4 -10 5 12 160 163 5 1 9 12 173 164 5 -6 -4 13 18 17 8
-5 -2 12 60 64 3 4 1 12 217 219 2 -9 5 12 56 46 5 2 9 12 147 153 6 -5 -4 13 190 190 5
-4 -2 12 246 255 2 5 1 12 81 85 4 -8 5 12 151 152 2 3 9 12 24 33 23 -4 -4 13 39 38 39
-3 -2 12 212 211 2 6 1 12 240 242 3 -7 5 12 103 102 6 4 9 12 37 21 36 -3 -4 13 56 61 5
-2 -2 12 374 368 7 7 1 12 258 253 3 -6 5 12 119 121 2 -4 10 12 86 74 8 -2 -4 13 270 266 3
-1 -2 12 256 263 2 8 1 12 209 201 3 -5 5 12 133 134 3 -3 10 12 92 104 6 -1 -4 13 201 201 2
0 -2 12 107 119 3 9 1 12 222 220 4 -4 5 12 346 329 5 -2 10 12 88 91 7 0 -4 13 385 396 3
1 -2 12 66 60 2 10 1 12 155 149 5 -3 5 12 143 146 7 -1 10 12 59 75 12 1 -4 13 247 242 2
2 -2 12 247 246 2 11 1 12 132 129 6 -2 5 12 178 175 2 0 10 12 20 38 20 2 -4 13 266 266 3
3 -2 12 189 192 2 -14 2 12 72 79 14 -1 5 12 45 41 4 1 10 12 54 59 13 3 -4 13 61 68 6
4 -2 12 284 286 4 -13 2 12 52 24 18 0 5 12 79 79 4 -3 -9 13 9 33 8 4 -4 13 122 122 2
5 -2 12 295 287 3 -12 2 12 0 19 1 1 5 12 78 74 5 -2 -9 13 80 85 20 5 -4 13 159 161 4
6 -2 12 96 92 4 -11 2 12 117 106 6 2 5 12 144 145 2 -1 -9 13 49 34 49 6 -4 13 239 228 3
7 -2 12 28 29 16 -10 2 12 146 140 4 3 5 12 123 119 2 0 -9 13 86 70 19 7 -4 13 91 95 13
8 -2 12 48 45 11 -9 2 12 336 332 3 4 5 12 135 129 7 1 -9 13 61 69 12 8 -4 13 127 118 7
9 -2 12 109 101 5 -8 2 12 172 166 2 5 5 12 90 90 4 2 -9 13 99 95 9 9 -4 13 103 101 10
10 -2 12 60 45 23 -7 2 12 217 215 2 6 5 12 98 85 13 3 -9 13 16 18 15 10 -4 13 59 42 19
11 -2 12 71 81 11 -6 2 12 255 249 2 7 5 12 105 109 10 -2 -8 13 69 52 20 -13 -3 13 0 38 1
-14 -1 12 49 42 17 -5 2 12 70 71 3 8 5 12 51 48 15 -1 -8 13 88 87 11 -12 -3 13 32 46 32
-13 -1 12 96 95 7 -4 2 12 248 252 2 9 5 12 15 24 14 0 -8 13 69 88 14 -11 -3 13 97 106 6
-12 -1 12 87 89 15 -3 2 12 188 185 2 10 5 12 0 9 1 1 -8 13 90 78 16 -10 -3 13 94 93 7

Table B9 Continued

-11 -1 12 84 82 5 -2 2 12 396 387 3 -12 6 12 91 89 6 2 -8 13 61 62 12
-9 -3 13 103 109 6
-10 -1 12 196 199 3 -1 2 12 229 233 2 -11 6 12 21 22 20 3 -8 13 44 16
44 -8 -3 13 178 178 7
-9 -1 12 117 118 7 0 2 12 124 136 1 -10 6 12 110 116 11 4 -8 13 19 15
19 -7 -3 13 165 160 4
-8 -1 12 278 281 3 1 2 12 71 71 3 -9 6 12 153 162 3 5 -8 13 69 58 15
-6 -3 13 163 168 5
-7 -1 12 239 241 3 2 2 12 256 256 2 -8 6 12 128 124 3 6 -8 13 84 70 23
-5 -3 13 108 113 4
-6 -1 12 218 220 2 3 2 12 208 211 2 -7 6 12 248 249 5 -6 -7 13 47 51 32
-4 -3 13 232 233 3
-5 -1 12 341 336 2 4 2 12 300 295 2 -6 6 12 111 112 2 -5 -7 13 48 54 20
-3 -3 13 487 471 3
-4 -1 12 537 529 3 5 2 12 272 271 3 -5 6 12 78 81 2 -4 -7 13 69 72 12
-2 -3 13 169 168 2
-3 -1 12 242 233 2 6 2 12 106 100 3 -4 6 12 282 279 2 -3 -7 13 248 257 6
-1 -3 13 36 43 12
-2 -1 12 122 121 2 7 2 12 0 8 1 -3 6 12 264 263 2 -2 -7 13 118 123 7
0 -3 13 109 113 2
1 -3 13 315 316 2 -14 1 13 92 80 9 -2 4 13 270 267 3 5 8 13 72 59 13
-7 -4 14 178 179 3
2 -3 13 108 105 4 -13 1 13 74 58 17 -1 4 13 225 223 4 6 8 13 51 80 25
-6 -4 14 36 37 11
3 -3 13 329 332 3 -12 1 13 19 20 19 0 4 13 367 378 2 -7 9 13 68 83 6
-5 -4 14 179 179 4
4 -3 13 217 213 2 -11 1 13 109 96 5 1 4 13 260 257 2 -6 9 13 33 42 32
-4 -4 14 191 184 7
5 -3 13 207 205 9 -10 1 13 140 134 3 2 4 13 268 265 5 -5 9 13 0 18 1
-3 -4 14 214 216 3
6 -3 13 240 230 3 -9 1 13 224 228 3 3 4 13 49 54 16 -4 9 13 53 51 13
-2 -4 14 136 137 4
7 -3 13 181 173 4 -8 1 13 222 223 3 4 4 13 113 118 3 -3 9 13 0 20 1
-1 -4 14 241 246 3
8 -3 13 41 35 17 -7 1 13 263 263 2 5 4 13 124 131 4 -2 9 13 72 77 8
0 -4 14 82 82 5
9 -3 13 116 116 5 -6 1 13 218 207 2 6 4 13 239 235 4 -1 9 13 0 24 1
1 -4 14 219 224 3
10 -3 13 111 115 15 -5 1 13 37 37 17 7 4 13 95 101 6 0 9 13 75 72 8
2 -4 14 96 103 4
-14 -2 13 112 115 7 -4 1 13 381 375 2 8 4 13 131 121 6 1 9 13 64 68 10
3 -4 14 88 89 5
-13 -2 13 169 162 5 -3 1 13 105 117 5 9 4 13 98 91 8 2 9 13 118 99 7
4 -4 14 32 41 10

Table B9 Continued

-12 -2 13 127 120 6 -2 1 13 252 252 4 10 4 13 36 45 36 3 9 13 0 15 1
5 -4 14 111 111 3
-11 -2 13 206 198 11 -1 1 13 180 186 2 -12 5 13 48 41 14 -3 -9 14 57 66
19 6 -4 14 43 18 13
-10 -2 13 172 174 3 0 1 13 93 97 2 -11 5 13 97 123 9 -2 -9 14 54 36 53
7 -4 14 0 19 1
-9 -2 13 72 79 6 1 1 13 123 118 3 -10 5 13 131 132 4 -1 -9 14 107 109 16
8 -4 14 75 72 12
-8 -2 13 235 234 6 2 1 13 114 110 2 -9 5 13 75 83 6 0 -9 14 123 117 13
9 -4 14 68 83 15
-7 -2 13 235 227 3 3 1 13 210 210 2 -8 5 13 232 236 3 1 -9 14 0 48 1
-13 -3 14 71 81 10
-6 -2 13 242 242 3 4 1 13 234 236 2 -7 5 13 131 136 3 2 -9 14 76 60 13
-12 -3 14 163 162 5
-5 -2 13 232 229 3 5 1 13 164 163 2 -6 5 13 192 189 8 -2 -8 14 46 40 30
-11 -3 14 94 95 8
-4 -2 13 278 273 2 6 1 13 107 104 4 -5 5 13 361 350 2 -1 -8 14 72 84 14
-10 -3 14 44 13 13
-3 -2 13 139 141 6 7 1 13 45 32 12 -4 5 13 231 226 4 0 -8 14 86 71 18
-9 -3 14 80 82 7
-2 -2 13 285 287 2 8 1 13 111 103 5 -3 5 13 165 160 6 1 -8 14 83 61 17
-8 -3 14 284 273 4
-1 -2 13 259 251 2 9 1 13 196 190 4 -2 5 13 295 290 5 2 -8 14 130 144
14 -7 -3 14 223 233 3
0 -2 13 345 344 5 10 1 13 158 155 10 -1 5 13 114 106 3 3 -8 14 75 79 10
-6 -3 14 220 216 2
1 -2 13 219 218 2 11 1 13 67 70 24 0 5 13 69 74 3 4 -8 14 69 52 14
-5 -3 14 241 247 4
2 -2 13 54 60 5 -14 2 13 99 112 23 1 5 13 36 39 4 5 -8 14 115 90 16
-4 -3 14 79 74 5
3 -2 13 124 122 3 -13 2 13 167 172 6 2 5 13 230 221 2 -6 -7 14 28 67 28
-3 -3 14 123 119 3
4 -2 13 150 147 3 -12 2 13 150 143 8 3 5 13 103 101 4 -5 -7 14 57 70 16
-2 -3 14 70 77 6
5 -2 13 177 180 8 -11 2 13 199 184 4 4 5 13 233 229 11 -4 -7 14 25 25 25
-1 -3 14 239 243 2
6 -2 13 161 172 3 -10 2 13 197 189 6 5 5 13 248 250 4 -3 -7 14 139 149 7
0 -3 14 179 177 6
7 -2 13 148 147 2 -9 2 13 92 100 4 6 5 13 90 78 6 -2 -7 14 62 62 14
1 -3 14 194 191 2
8 -2 13 117 104 11 -8 2 13 234 232 3 7 5 13 23 57 22 -1 -7 14 182 179 4
2 -3 14 191 198 6
9 -2 13 80 85 7 -7 2 13 221 224 2 8 5 13 68 77 10 0 -7 14 122 127 6
3 -3 14 143 146 3

Table B9 Continued

10 -2 13 46 49 45 -6 2 13 235 230 2 9 5 13 83 81 11 1 -7 14 91 102 7
4 -3 14 113 120 5
11 -2 13 49 31 48 -5 2 13 263 255 3 -11 6 13 29 41 29 2 -7 14 100 83 36
5 -3 14 176 183 9
-14 -1 13 107 93 10 -4 2 13 305 302 3 -10 6 13 110 117 11 3 -7 14 33 32
33 6 -3 14 181 193 5
-13 -1 13 56 54 14 -3 2 13 126 129 2 -9 6 13 49 39 9 4 -7 14 58 52 9
7 -3 14 86 98 6
-12 -1 13 50 18 17 -2 2 13 285 289 2 -8 6 13 112 121 5 5 -7 14 106 120
8 8 -3 14 59 63 9
-11 -1 13 84 82 7 -1 2 13 247 242 1 -7 6 13 173 167 2 6 -7 14 158 168
11 9 -3 14 57 56 15
-10 -1 13 151 142 4 0 2 13 366 361 5 -6 6 13 221 221 2 7 -7 14 75 53
26 10 -3 14 68 82 11
-9 -1 13 227 230 3 1 2 13 226 224 2 -5 6 13 99 98 2 -9 -6 14 122 118 9
-13 -2 14 57 54 27
-8 -1 13 233 236 6 2 2 13 38 41 5 -4 6 13 129 135 2 -8 -6 14 140 135 7
-12 -2 14 115 125 7
-7 -1 13 249 249 3 3 2 13 125 128 7 -3 6 13 58 60 3 -7 -6 14 124 113 7
-11 -2 14 181 179 5
-6 -1 13 242 236 5 4 2 13 156 150 2 -2 6 13 176 177 3 -6 -6 14 69 66 12
-10 -2 14 167 169 3
-5 -1 13 50 51 4 5 2 13 175 175 7 -1 6 13 133 139 6 -5 -6 14 87 95 9
-9 -2 14 178 179 4
-4 -1 13 390 380 2 6 2 13 131 134 4 0 6 13 145 144 3 -4 -6 14 101 113 8
-8 -2 14 173 167 4
-3 -1 13 131 141 2 7 2 13 154 152 3 1 6 13 270 272 2 -3 -6 14 189 189 4
-7 -2 14 84 89 5
-2 -1 13 255 254 2 8 2 13 106 106 5 2 6 13 70 68 5 -2 -6 14 109 117 4
-6 -2 14 47 45 5
-1 -1 13 178 179 2 9 2 13 96 101 9 3 6 13 52 56 14 -1 -6 14 75 83 4
-5 -2 14 134 140 2
0 -1 13 115 117 4 10 2 13 66 45 14 4 6 13 135 148 3 0 -6 14 0 24 1
-4 -2 14 496 485 5
1 -1 13 114 106 1 11 2 13 57 29 18 5 6 13 101 108 5 1 -6 14 108 124 10
-3 -2 14 99 100 6
2 -1 13 95 100 3 -13 3 13 46 30 18 6 6 13 116 123 5 2 -6 14 74 69 9
-2 -2 14 232 241 3
3 -1 13 224 223 2 -12 3 13 40 45 17 7 6 13 102 97 5 3 -6 14 115 108 4
-1 -2 14 87 91 2
4 -1 13 221 224 6 -11 3 13 92 103 6 8 6 13 48 57 13 4 -6 14 33 51 32
0 -2 14 127 128 2
5 -1 13 158 161 3 -10 3 13 60 72 7 -10 7 13 134 126 10 5 -6 14 53 43 8
1 -2 14 84 88 2

Table B9 Continued

6 -1 13 122 114 4 -9 3 13 95 91 5 -9 7 13 121 122 5 6 -6 14 105 119 19
2 -2 14 319 323 4
7 -1 13 0 26 1 -8 3 13 191 190 4 -8 7 13 153 151 3 7 -6 14 61 30 17
3 -2 14 56 69 5
8 -1 13 102 93 9 -7 3 13 144 137 3 -7 7 13 98 83 6 8 -6 14 75 80 12
4 -2 14 204 204 3
9 -1 13 184 182 6 -6 3 13 158 164 2 -6 7 13 62 59 5 -12 -5 14 115 92 11
5 -2 14 76 72 6
10 -1 13 149 151 13 -5 3 13 117 124 4 -5 7 13 46 52 8 -11 -5 14 113 101
11 6 -2 14 123 123 4
11 -1 13 67 69 17 -4 3 13 217 220 2 -4 7 13 39 48 7 -10 -5 14 90 84 7
7 -2 14 19 24 19
-14 0 13 210 210 14 -3 3 13 475 463 5 -3 7 13 257 258 2 -9 -5 14 0 36 1
8 -2 14 63 64 9
-13 0 13 151 152 5 -2 3 13 167 166 2 -2 7 13 125 125 3 -8 -5 14 106 112
5 9 -2 14 90 86 7
-12 0 13 262 268 5 -1 3 13 59 66 3 -1 7 13 120 122 2 -7 -5 14 164 165 5
10 -2 14 83 80 7
-11 0 13 221 226 5 0 3 13 95 101 2 0 7 13 123 118 6 -6 -5 14 196 196
4 -14 -1 14 55 55 16
-10 0 13 131 122 3 1 3 13 304 314 2 1 7 13 52 47 7 -5 -5 14 43 34 10
-13 -1 14 89 91 8
-9 0 13 58 59 11 2 3 13 117 112 2 2 7 13 39 20 7 -4 -5 14 213 213 3
-12 -1 14 136 137 5
-8 0 13 167 164 7 3 3 13 335 330 3 3 7 13 77 81 5 -3 -5 14 87 93 6 -
11 -1 14 93 75 8
-7 0 13 163 174 3 4 3 13 237 238 3 4 7 13 47 43 8 -2 -5 14 143 147 3
-10 -1 14 32 33 15
-6 0 13 288 280 3 5 3 13 180 179 3 5 7 13 129 141 3 -1 -5 14 86 90 5
-9 -1 14 137 147 5
-5 0 13 404 397 3 6 3 13 245 243 5 6 7 13 122 129 4 0 -5 14 109 117 3
-8 -1 14 157 161 3
-4 0 13 308 307 2 7 3 13 174 169 4 7 7 13 42 26 15 1 -5 14 204 203 4
-7 -1 14 328 327 10
-3 0 13 40 40 6 8 3 13 49 39 27 -9 8 13 57 31 21 2 -5 14 38 37 8 -
6 -1 14 126 124 6
-2 0 13 187 189 2 9 3 13 132 115 6 -8 8 13 28 28 27 3 -5 14 101 104 4
-5 -1 14 86 89 7
-1 0 13 258 256 2 10 3 13 97 110 11 -7 8 13 106 107 8 4 -5 14 142 148
3 -4 -1 14 66 66 3
1 0 13 75 78 2 -13 4 13 58 59 11 -6 8 13 82 79 5 5 -5 14 116 109 4 -
3 -1 14 391 389 3
2 0 13 97 96 2 -12 4 13 114 112 6 -5 8 13 127 122 3 6 -5 14 66 66 9
-2 -1 14 296 298 4

Table B9 Continued

3 0 13 166 177 3 -11 4 13 55 59 10 -4 8 13 25 20 15 7 -5 14 40 41 35 -1 -1 14 144 147 3
4 0 13 31 26 12 -10 4 13 47 24 13 -3 8 13 88 81 3 8 -5 14 0 11 1 0 -1 14 234 235 2
5 0 13 100 97 4 -9 4 13 167 164 4 -2 8 13 54 51 4 9 -5 14 0 40 1 1 -1 14 408 407 2
6 0 13 86 89 4 -8 4 13 224 218 3 -1 8 13 86 93 6 -13 -4 14 35 71 34 2 -1 14 250 250 2
7 0 13 30 31 30 -7 4 13 110 108 5 0 8 13 84 93 6 -12 -4 14 155 144 7 3 -1 14 86 85 5
8 0 13 31 29 31 -6 4 13 27 26 18 1 8 13 63 62 9 -11 -4 14 143 162 5 4 -1 14 157 162 3
9 0 13 79 94 10 -5 4 13 191 191 1 2 8 13 28 68 28 -10 -4 14 190 189 5 5 -1 14 167 167 3
10 0 13 0 9 1 -4 4 13 42 42 5 3 8 13 18 24 17 -9 -4 14 213 201 13 6 -1 14 182 181 8
11 0 13 92 111 7 -3 4 13 50 56 4 4 8 13 0 11 1 -8 -4 14 144 139 4 7 -1 14 254 254 4
8 -1 14 102 116 5 -3 3 14 106 107 2 -2 7 14 81 76 4 1 -5 15 149 150 3 -3 -1 15 243 243 4
9 -1 14 59 55 15 -2 3 14 101 103 2 -1 7 14 182 184 4 2 -5 15 146 155 4 -2 -1 15 164 174 2
10 -1 14 19 9 19 -1 3 14 237 241 2 0 7 14 138 130 3 3 -5 15 164 171 3 -1 -1 15 99 96 6
-14 0 14 47 38 17 0 3 14 156 155 3 1 7 14 86 88 4 4 -5 15 70 67 6 0 -1 15 137 138 3
-13 0 14 57 22 29 1 3 14 221 217 2 2 7 14 93 87 5 5 -5 15 81 72 8 1 -1 15 142 146 2
-12 0 14 70 64 11 2 3 14 185 189 2 3 7 14 42 34 7 6 -5 15 34 47 34 2 -1 15 243 235 3
-11 0 14 77 76 9 3 3 14 146 147 2 4 7 14 50 37 7 7 -5 15 64 60 15 3 -1 15 78 77 4
-10 0 14 174 155 3 4 3 14 123 133 3 5 7 14 114 122 4 8 -5 15 28 80 27 4 -1 15 102 95 9
-9 0 14 67 83 4 5 3 14 168 178 3 6 7 14 185 178 7 -12 -4 15 69 59 24 5 -1 15 32 39 15
-8 0 14 175 181 3 6 3 14 182 187 3 7 7 14 69 68 10 -11 -4 15 47 70 14 6 -1 15 26 37 26
-7 0 14 22 21 22 7 3 14 116 112 11 -8 8 14 49 43 13 -10 -4 15 97 93 6 7 -1 15 109 113 5
-6 0 14 454 447 4 8 3 14 62 54 10 -7 8 14 82 91 5 -9 -4 15 46 64 12 8 -1 15 72 78 9
-5 0 14 71 67 3 9 3 14 94 61 25 -6 8 14 103 102 7 -8 -4 15 196 187 4 9 -1 15 72 69 14

Table B9 Continued

-4 0 14 140 140 2 10 3 14 57 78 15 -5 8 14 94 89 5 -7 -4 15 66 64 8 10 -1 15 32 27 32
-3 0 14 420 413 5 -13 4 14 72 66 9 -4 8 14 188 183 3 -6 -4 15 99 93 6 -14 0 15 143 130 15
-2 0 14 15 18 14 -12 4 14 164 157 4 -3 8 14 65 66 8 -5 -4 15 4 27 3 -13 0 15 136 135 7
-1 0 14 293 301 4 -11 4 14 132 146 4 -2 8 14 48 42 5 -4 -4 15 334 328 8 -12 0 15 87 89 14
0 0 14 486 479 4 -10 4 14 195 191 4 -1 8 14 84 86 3 -3 -4 15 159 165 3 -11 0 15 64 40 9
1 0 14 489 476 3 -9 4 14 216 208 3 0 8 14 68 73 3 -2 -4 15 217 221 6 -10 0 15 62 44 6
2 0 14 257 260 2 -8 4 14 106 105 7 1 8 14 37 43 17 -1 -4 15 119 119 3 -9 0 15 74 74 4
3 0 14 284 279 4 -7 4 14 193 192 3 2 8 14 145 142 6 0 -4 15 190 193 3 -8 0 15 286 279 3
4 0 14 155 152 3 -6 4 14 51 37 5 3 8 14 83 80 10 1 -4 15 100 107 3 -7 0 15 281 288 4
5 0 14 138 132 6 -5 4 14 188 187 2 4 8 14 67 56 11 2 -4 15 56 63 5 -6 0 15 144 146 4
6 0 14 43 40 42 -4 4 14 162 158 2 5 8 14 57 81 19 3 -4 15 71 72 6 -5 0 15 229 228 6
7 0 14 116 111 5 -3 4 14 221 220 4 -6 9 14 58 74 12 4 -4 15 192 194 3 -4 0 15 0 7 1
8 0 14 90 100 5 -2 4 14 158 151 3 -5 9 14 30 19 30 5 -4 15 173 174 4 -3 0 15 92 85 4
9 0 14 145 147 5 -1 4 14 244 249 2 -4 9 14 0 13 1 6 -4 15 166 162 4 -2 0 15 44 45 6
10 0 14 132 120 6 0 4 14 87 87 2 -3 9 14 66 57 10 7 -4 15 105 92 11 -1 0 15 257 261 2
-14 1 14 71 70 12 1 4 14 223 231 2 -2 9 14 52 47 11 8 -4 15 15 39 15 1 0 15 122 126 3
-13 1 14 84 85 22 2 4 14 85 89 2 -1 9 14 109 104 5 9 -4 15 29 18 29 2 0 15 41 36 14
-12 1 14 147 146 18 3 4 14 89 87 4 0 9 14 134 124 5 -13 -3 15 16 14 15 3 0 15 93 88 4
-11 1 14 45 67 24 4 4 14 65 56 7 1 9 14 60 55 15 -12 -3 15 127 132 6 4 0 15 12 32 12
-10 1 14 33 19 33 5 4 14 104 105 6 2 9 14 60 57 13 -11 -3 15 85 92 9 5 0 15 104 99 5
-9 1 14 124 134 3 6 4 14 0 13 1 -3 -9 15 82 73 20 -10 -3 15 67 84 10 6 0 15 154 161 4
-8 1 14 153 159 3 7 4 14 0 15 1 -2 -9 15 90 101 14 -9 -3 15 102 97 6 7 0 15 119 129 5

Table B9 Continued

-7 1 14 344 340 3 8 4 14 60 67 13 -1 -9 15 88 62 21 -8 -3 15 91 83 6
8 0 15 78 94 7
-6 1 14 139 133 2 9 4 14 88 83 19 0 -9 15 46 20 45 -7 -3 15 242 241 3
9 0 15 19 28 18
-5 1 14 79 82 6 -12 5 14 95 84 8 1 -9 15 57 72 49 -6 -3 15 214 217 6
10 0 15 196 178 5
-4 1 14 87 82 3 -11 5 14 114 108 6 -2 -8 15 30 33 29 -5 -3 15 100 96 10
-13 1 15 92 103 7
-3 1 14 387 388 3 -10 5 14 96 84 5 -1 -8 15 46 67 45 -4 -3 15 73 76 6
-12 1 15 152 160 11
-2 1 14 299 301 2 -9 5 14 48 32 9 0 -8 15 87 91 16 -3 -3 15 201 205 4
-11 1 15 209 204 6
-1 1 14 155 162 2 -8 5 14 122 115 3 1 -8 15 57 41 32 -2 -3 15 151 154 3
-10 1 15 192 189 3
0 1 14 218 218 4 -7 5 14 141 144 4 2 -8 15 33 14 33 -1 -3 15 35 45 10
-9 1 15 244 235 3
1 1 14 400 394 5 -6 5 14 199 194 2 3 -8 15 44 21 30 0 -3 15 114 117 5
-8 1 15 209 207 3
2 1 14 255 257 2 -5 5 14 50 36 8 4 -8 15 0 25 1 1 -3 15 372 366 4 -
7 1 15 110 115 7
3 1 14 80 81 7 -4 5 14 223 224 5 -5 -7 15 47 51 23 2 -3 15 181 187 3
-6 1 15 79 88 4
4 1 14 156 164 5 -3 5 14 85 82 2 -4 -7 15 102 102 9 3 -3 15 210 210 3
-5 1 15 226 226 2
5 1 14 160 157 3 -2 5 14 142 145 2 -3 -7 15 97 93 9 4 -3 15 22 20 16
-4 1 15 329 325 3
6 1 14 202 200 8 -1 5 14 100 93 3 -2 -7 15 137 128 6 5 -3 15 24 58 23
-3 1 15 288 285 4
7 1 14 238 232 4 0 5 14 88 97 3 -1 -7 15 29 45 28 6 -3 15 75 90 6 -
2 1 15 157 168 2
8 1 14 121 120 5 1 5 14 201 200 2 0 -7 15 33 55 33 7 -3 15 94 93 6
-1 1 15 106 102 2
9 1 14 47 49 16 2 5 14 39 42 6 1 -7 15 68 73 23 8 -3 15 100 101 9
0 1 15 119 122 2
10 1 14 0 9 1 3 5 14 107 103 3 2 -7 15 33 27 33 9 -3 15 115 103 9
1 1 15 169 173 2
-13 2 14 42 59 18 4 5 14 135 150 4 3 -7 15 96 91 6 -13 -2 15 120 128
11 2 1 15 250 243 2
-12 2 14 88 106 7 5 5 14 104 107 6 4 -7 15 17 25 16 -12 -2 15 67 63 10
3 1 15 61 57 5
-11 2 14 195 198 4 6 5 14 71 65 15 5 -7 15 0 16 1 -11 -2 15 97 87 8
4 1 15 101 105 3
-10 2 14 123 132 13 7 5 14 51 46 14 6 -7 15 67 58 21 -10 -2 15 86 75 5
5 1 15 43 41 9

Table B9 Continued

-9 2 14 149 147 3 8 5 14 6 11 5 -9 -6 15 91 88 12 -9 -2 15 131 135 3
6 1 15 45 36 9
-8 2 14 179 173 3 9 5 14 39 37 38 -8 -6 15 141 136 8 -8 -2 15 221 216 3
7 1 15 124 128 4
-7 2 14 94 98 5 -11 6 14 93 84 6 -7 -6 15 161 158 7 -7 -2 15 181 182 3
8 1 15 65 68 10
-6 2 14 48 50 5 -10 6 14 123 122 6 -6 -6 15 82 81 11 -6 -2 15 165 163 2
9 1 15 57 64 11
-5 2 14 110 115 3 -9 6 14 107 106 7 -5 -6 15 79 77 8 -5 -2 15 152 151 4
10 1 15 0 22 1
-4 2 14 513 491 3 -8 6 14 148 142 3 -4 -6 15 134 131 6 -4 -2 15 52 47 8
-13 2 15 115 118 10
-3 2 14 90 88 4 -7 6 14 103 107 4 -3 -6 15 143 143 6 -3 -2 15 375 365 3
-12 2 15 65 75 11
-2 2 14 244 244 3 -6 6 14 58 56 4 -2 -6 15 166 169 6 -2 -2 15 178 181 3
-11 2 15 90 77 8
-1 2 14 65 71 2 -5 6 14 100 104 3 -1 -6 15 166 157 6 -1 -2 15 205 211 3
-10 2 15 63 68 7
0 2 14 136 131 3 -4 6 14 141 140 3 0 -6 15 168 164 4 0 -2 15 200 195 7
-9 2 15 134 138 7
1 2 14 102 105 2 -3 6 14 173 170 2 1 -6 15 51 68 15 1 -2 15 233 244 5
-8 2 15 212 209 6
2 2 14 310 318 2 -2 6 14 124 130 4 2 -6 15 60 34 12 2 -2 15 113 113 4
-7 2 15 173 171 2
3 2 14 86 86 4 -1 6 14 82 83 3 3 -6 15 57 52 27 3 -2 15 162 169 6 -
6 2 15 192 189 3
4 2 14 197 199 5 0 6 14 38 39 6 4 -6 15 144 137 4 4 -2 15 150 157 4
-5 2 15 132 135 2
5 2 14 86 83 4 1 6 14 112 123 2 5 -6 15 129 142 6 5 -2 15 203 207 3
-4 2 15 59 52 4
6 2 14 127 130 8 2 6 14 74 72 6 6 -6 15 144 155 7 6 -2 15 210 215 10
-3 2 15 366 353 3
7 2 14 36 37 15 3 6 14 102 98 3 7 -6 15 0 50 1 7 -2 15 112 114 5 -
2 2 15 190 191 2
8 2 14 76 76 7 4 6 14 40 31 9 -12 -5 15 0 79 1 8 -2 15 24 16 24 -1
2 15 202 203 3
9 2 14 87 92 8 5 6 14 65 54 11 -11 -5 15 157 143 8 9 -2 15 60 33 18
0 2 15 184 180 2
10 2 14 77 75 10 6 6 14 125 122 5 -10 -5 15 0 36 1 10 -2 15 43 49 22
1 2 15 245 250 3
-13 3 14 75 75 25 7 6 14 31 30 30 -9 -5 15 38 40 15 -13 -1 15 116 111 8
2 2 15 123 121 6
-12 3 14 174 163 4 8 6 14 81 77 12 -8 -5 15 0 37 1 -12 -1 15 148 154 6
3 2 15 147 149 2

Table B9 Continued

-11 3 14 104 101 12 -10 7 14 87 100 6 -7 -5 15 184 181 4 -11 -1 15 218 213 4 4 2 15 158 158 3
-10 3 14 10 12 10 -9 7 14 44 47 8 -6 -5 15 19 24 18 -10 -1 15 157 164 4 5 2 15 222 216 3
-9 3 14 84 83 8 -8 7 14 78 97 6 -5 -5 15 158 150 3 -9 -1 15 208 199 4 6 2 15 198 197 3
-8 3 14 301 297 3 -7 7 14 32 22 16 -4 -5 15 208 209 6 -8 -1 15 234 233 6 7 2 15 125 129 11
-7 3 14 248 254 3 -6 7 14 67 54 9 -3 -5 15 103 99 4 -7 -1 15 112 116 3 8 2 15 15 5 15
-6 3 14 214 211 3 -5 7 14 78 73 7 -2 -5 15 72 78 5 -6 -1 15 67 62 5 9 2 15 34 34 33
-5 3 14 229 229 3 -4 7 14 9 7 9 -1 -5 15 83 89 6 -5 -1 15 240 237 3 10 2 15 54 49 30
-4 3 14 69 63 5 -3 7 14 147 144 9 0 -5 15 151 152 3 -4 -1 15 341 344 3 -13 3 15 43 15 42
-12 3 15 120 123 14 -6 7 15 80 84 4 7 -5 16 30 27 29 6 -1 16 100 99 8 1 3 16 51 46 4
-11 3 15 105 98 6 -5 7 15 27 37 16 -12 -4 16 116 121 10 7 -1 16 71 64 8 2 3 16 81 86 3
-10 3 15 94 86 14 -4 7 15 93 81 5 -11 -4 16 121 126 6 8 -1 16 48 43 11 3 3 16 34 41 12
-9 3 15 92 82 5 -3 7 15 92 94 4 -10 -4 16 157 154 9 9 -1 16 69 85 9 4 3 16 109 116 3
-8 3 15 70 72 9 -2 7 15 130 128 3 -9 -4 16 99 110 7 -13 0 16 73 74 10 5 3 16 84 90 5
-7 3 15 244 241 3 -1 7 15 36 51 11 -8 -4 16 19 19 18 -12 0 16 81 73 7 6 3 16 60 76 8
-6 3 15 219 223 3 0 7 15 57 62 5 -7 -4 16 58 58 7 -11 0 16 114 105 5 7 3 16 25 21 25
-5 3 15 116 115 9 1 7 15 57 60 6 -6 -4 16 107 101 5 -10 0 16 101 106 5 8 3 16 0 26 1
-4 3 15 99 96 3 2 7 15 22 7 22 -5 -4 16 233 232 3 -9 0 16 202 210 3 9 3 16 35 46 35
-3 3 15 178 187 2 3 7 15 95 94 6 -4 -4 16 96 103 5 -8 0 16 193 213 3 -12 4 16 120 118 5
-2 3 15 154 158 2 4 7 15 35 26 34 -3 -4 16 200 189 6 -7 0 16 151 142 3 -11 4 16 111 118 6
-1 3 15 63 69 3 5 7 15 0 14 1 -2 -4 16 91 98 4 -6 0 16 149 151 3 -10 4 16 169 168 11
0 3 15 129 121 4 6 7 15 77 54 12 -1 -4 16 69 80 5 -5 0 16 123 123 3 -9 4 16 111 117 7
1 3 15 357 356 3 -8 8 15 78 77 12 0 -4 16 41 41 7 -4 0 16 503 495 4 -8 4 16 0 20 1

Table B9 Continued

2 3 15 199 202 2 -7 8 15 81 76 7 1 -4 16 96 98 4 -3 0 16 179 187 3 -
7 4 16 41 49 9
3 3 15 210 211 4 -6 8 15 70 81 6 2 -4 16 134 131 4 -2 0 16 22 29 21
-6 4 16 124 126 3
4 3 15 22 30 22 -5 8 15 130 124 4 3 -4 16 41 37 11 -1 0 16 82 80 9 -
5 4 16 252 246 3
5 3 15 46 53 7 -4 8 15 79 90 4 4 -4 16 19 31 18 0 0 16 333 329 4 -
4 4 16 106 100 3
6 3 15 106 102 11 -3 8 15 57 47 6 5 -4 16 0 8 1 1 0 16 396 381 3 -
3 4 16 184 188 2
7 3 15 95 95 7 -2 8 15 34 35 10 6 -4 16 61 61 14 2 0 16 341 337 3 -
2 4 16 90 97 8
8 3 15 92 80 13 -1 8 15 71 67 5 7 -4 16 69 47 43 3 0 16 177 180 3 -
1 4 16 83 80 4
9 3 15 115 100 8 0 8 15 102 95 3 8 -4 16 67 55 36 4 0 16 54 44 9 0
4 16 39 51 4
-12 4 15 77 53 9 1 8 15 38 36 8 -13 -3 16 35 51 35 5 0 16 0 5 1 1
4 16 97 109 6
-11 4 15 54 78 23 2 8 15 36 21 35 -12 -3 16 64 48 14 6 0 16 83 83 8
2 4 16 139 138 3
-10 4 15 89 86 7 3 8 15 42 25 20 -11 -3 16 119 120 6 7 0 16 144 149 4
3 4 16 40 41 5
-9 4 15 60 67 8 4 8 15 0 33 1 -10 -3 16 86 92 13 8 0 16 88 99 8 4
4 16 9 31 9
-8 4 15 176 177 6 -5 9 15 84 98 8 -9 -3 16 202 210 4 9 0 16 122 116 5
5 4 16 0 3 1
-7 4 15 83 73 10 -4 9 15 0 27 1 -8 -3 16 209 206 3 -13 1 16 0 15 1
6 4 16 61 60 12
-6 4 15 93 92 3 -3 9 15 75 75 9 -7 -3 16 142 143 4 -12 1 16 0 16 1
7 4 16 9 46 8
-5 4 15 26 30 12 -2 9 15 90 99 7 -6 -3 16 160 150 4 -11 1 16 38 63 38
8 4 16 48 54 14
-4 4 15 326 320 3 -1 9 15 84 73 8 -5 -3 16 31 19 31 -10 1 16 70 97 22
-11 5 16 9 14 9
-3 4 15 174 177 2 0 9 15 16 18 15 -4 -3 16 131 130 5 -9 1 16 46 53 11
-10 5 16 107 117 6
-2 4 15 228 224 2 1 9 15 62 64 14 -3 -3 16 231 226 3 -8 1 16 113 119 4
-9 5 16 76 90 7
-1 4 15 148 143 2 -3 -9 16 84 113 26 -2 -3 16 148 153 3 -7 1 16 124 126
4 -8 5 16 155 164 3
0 4 15 179 185 2 -2 -9 16 71 54 27 -1 -3 16 167 156 9 -6 1 16 145 149 4
-7 5 16 154 147 4
1 4 15 85 89 3 -1 -9 16 70 69 19 0 -3 16 177 182 6 -5 1 16 231 230 2
-6 5 16 82 77 4

Table B9 Continued

2 4 15 55 58 3 -2 -8 16 16 6 15 1 -3 16 41 34 30 -4 1 16 245 236 6 -5 5 16 57 60 6
3 4 15 82 76 3 -1 -8 16 0 37 1 2 -3 16 84 91 6 -3 1 16 127 135 3 -4 5 16 67 65 6
4 4 15 192 193 3 0 -8 16 85 109 22 3 -3 16 42 33 23 -2 1 16 66 62 4 -3 5 16 158 158 2
5 4 15 156 153 7 1 -8 16 60 79 25 4 -3 16 94 99 10 -1 1 16 232 226 5 -2 5 16 121 122 2
6 4 15 181 176 7 2 -8 16 118 110 10 5 -3 16 87 98 5 0 1 16 122 129 2 -1 5 16 69 68 2
7 4 15 99 98 7 3 -8 16 47 53 47 6 -3 16 63 79 8 1 1 16 201 193 2 0 5 16 117 116 13
8 4 15 53 43 14 -5 -7 16 47 10 28 7 -3 16 0 25 1 2 1 16 5 17 4 1 5 16 104 105 2
9 4 15 44 16 21 -4 -7 16 105 125 10 8 -3 16 56 20 19 3 1 16 151 159 3 2 5 16 34 18 8
-12 5 15 75 68 12 -3 -7 16 128 132 8 9 -3 16 47 47 46 4 1 16 187 191 3 3 5 16 90 95 10
-11 5 15 149 152 5 -2 -7 16 103 94 10 -13 -2 16 67 84 13 5 1 16 188 189 6 4 5 16 0 20 1
-10 5 15 49 47 16 -1 -7 16 61 69 21 -12 -2 16 105 108 7 6 1 16 99 106 6 5 5 16 122 114 6
-9 5 15 0 34 1 0 -7 16 0 25 1 -11 -2 16 138 137 6 7 1 16 62 52 11 6 5 16 74 75 9
-8 5 15 36 43 13 1 -7 16 0 7 1 -10 -2 16 75 89 10 8 1 16 37 46 18 7 5 16 0 24 1
-7 5 15 174 181 3 2 -7 16 111 100 9 -9 -2 16 88 80 5 9 1 16 83 82 9 -10 6 16 73 65 7
-6 5 15 54 38 6 3 -7 16 116 116 5 -8 -2 16 27 26 18 -13 2 16 95 87 18 -9 6 16 74 66 8
-5 5 15 147 142 2 4 -7 16 47 48 32 -7 -2 16 156 143 4 -12 2 16 109 110 6 -8 6 16 74 59 25
-4 5 15 207 207 2 5 -7 16 57 72 49 -6 -2 16 181 192 3 -11 2 16 147 149 4 -7 6 16 64 62 8
-3 5 15 117 110 3 -9 -6 16 92 66 12 -5 -2 16 207 210 14 -10 2 16 84 96 11 -6 6 16 130 132 3
-2 5 15 88 85 5 -8 -6 16 59 60 20 -4 -2 16 307 295 4 -9 2 16 84 77 6 -5 6 16 67 71 7
-1 5 15 97 97 1 -7 -6 16 67 65 15 -3 -2 16 43 3 16 -8 2 16 42 22 19 -4 6 16 187 188 3
0 5 15 133 134 10 -6 -6 16 138 145 8 -2 -2 16 67 69 5 -7 2 16 121 130 7 -3 6 16 126 123 3
1 5 15 153 158 4 -5 -6 16 70 64 14 -1 -2 16 79 72 5 -6 2 16 215 214 4 -2 6 16 20 23 19

Table B9 Continued

2 5 15 137 139 2 -4 -6 16 164 168 6 0 -2 16 301 294 3 -5 2 16 216 218 3 -1 6 16 16 19 16
3 5 15 174 191 4 -3 -6 16 110 114 9 1 -2 16 242 239 3 -4 2 16 317 301 3 0 6 16 168 175 3
4 5 15 70 72 8 -2 -6 16 0 8 1 2 -2 16 248 240 3 -3 2 16 31 24 30 1 6 16 55 51 7
5 5 15 77 70 12 -1 -6 16 22 38 21 3 -2 16 62 44 8 -2 2 16 80 82 4 2 6 16 69 68 7
6 5 15 24 40 23 0 -6 16 182 177 8 4 -2 16 63 75 8 -1 2 16 93 87 2 3 6 16 70 74 14
7 5 15 56 61 12 1 -6 16 36 26 26 5 -2 16 49 23 28 0 2 16 302 296 3 4 6 16 27 31 27
8 5 15 17 92 17 2 -6 16 59 66 12 6 -2 16 193 198 4 1 2 16 230 229 2 5 6 16 71 74 9
-11 6 15 33 38 32 3 -6 16 79 81 6 7 -2 16 78 89 7 2 2 16 247 243 3 6 6 16 111 118 14
-10 6 15 64 75 9 4 -6 16 32 30 32 8 -2 16 78 86 8 3 2 16 67 72 5 -9 7 16 66 57 10
-9 6 15 95 84 6 5 -6 16 76 76 12 9 -2 16 72 88 10 4 2 16 72 68 5 -8 7 16 30 42 30
-8 6 15 133 140 9 6 -6 16 107 114 18 -13 -1 16 40 26 19 5 2 16 53 22 11 -7 7 16 57 71 14
-7 6 15 173 164 3 -11 -5 16 32 18 32 -12 -1 16 18 16 18 6 2 16 176 183 4 -6 7 16 75 69 5
-6 6 15 83 83 4 -10 -5 16 102 104 9 -11 -1 16 72 60 13 7 2 16 103 109 6 -5 7 16 20 21 20
-5 6 15 87 81 4 -9 -5 16 109 106 10 -10 -1 16 81 94 6 8 2 16 88 87 6 -4 7 16 126 124 3
-4 6 15 123 129 3 -8 -5 16 169 176 4 -9 -1 16 81 85 11 9 2 16 82 84 11 -3 7 16 121 126 3
-3 6 15 136 135 3 -7 -5 16 145 144 9 -8 -1 16 137 136 3 -13 3 16 84 61 8 -2 7 16 112 106 3
-2 6 15 185 177 2 -6 -5 16 87 87 5 -7 -1 16 111 119 8 -12 3 16 49 53 16 -1 7 16 61 69 6
-1 6 15 163 159 3 -5 -5 16 79 77 6 -6 -1 16 161 161 3 -11 3 16 127 127 5 0 7 16 43 34 22
0 6 15 160 163 3 -4 -5 16 52 52 11 -5 -1 16 218 228 3 -10 3 16 40 63 17 1 7 16 0 11 1
1 6 15 62 53 4 -3 -5 16 178 172 8 -4 -1 16 245 246 5 -9 3 16 218 223 10 2 7 16 78 88 7
2 6 15 46 37 6 -2 -5 16 120 128 4 -3 -1 16 102 117 4 -8 3 16 185 188 9 3 7 16 134 128 4
3 6 15 35 48 9 -1 -5 16 70 69 15 -2 -1 16 111 114 11 -7 3 16 98 110 3 4 7 16 61 49 8

Table B9 Continued

4 6 15 145 148 3 0 -5 16 134 134 3 -1 -1 16 237 230 4 -6 3 16 159 149 3
5 7 16 54 60 10
5 6 15 136 149 5 1 -5 16 99 101 5 0 -1 16 106 121 4 -5 3 16 31 23 16
-7 8 16 122 130 7
6 6 15 119 136 6 2 -5 16 37 25 11 1 -1 16 202 195 3 -4 3 16 126 119 5
-6 8 16 47 30 12
7 6 15 46 52 20 3 -5 16 92 95 11 2 -1 16 44 32 8 -3 3 16 240 231 3 -
5 8 16 33 28 33
-9 7 15 79 72 5 4 -5 16 0 12 1 3 -1 16 157 158 3 -2 3 16 161 170 3 -
4 8 16 83 82 4
-8 7 15 57 33 8 5 -5 16 134 113 12 4 -1 16 158 163 3 -1 3 16 142 136 3
-3 8 16 70 69 5
-7 7 15 47 40 9 6 -5 16 78 82 9 5 -1 16 213 212 4 0 3 16 162 163 2
-2 8 16 0 14 1
-1 8 16 35 33 11 -3 -3 17 62 64 7 -5 1 17 261 256 3 -3 5 17 25 25 24
2 -5 18 60 40 13
0 8 16 98 108 4 -2 -3 17 58 66 8 -4 1 17 261 259 3 -2 5 17 74 78 4 3
-5 18 122 124 14
1 8 16 70 75 13 -1 -3 17 122 128 3 -3 1 17 84 82 4 -1 5 17 152 158 2
4 -5 18 91 102 10
2 8 16 111 106 8 0 -3 17 136 141 3 -2 1 17 171 169 3 0 5 17 54 62 7
5 -5 18 93 83 11
3 8 16 18 52 17 1 -3 17 138 137 5 -1 1 17 230 223 6 1 5 17 168 174 3
6 -5 18 29 39 28
-3 9 16 124 118 6 2 -3 17 189 194 4 0 1 17 303 290 4 2 5 17 63 68 8
-11 -4 18 83 73 17
-2 9 16 66 65 9 3 -3 17 53 52 9 1 1 17 124 112 2 3 5 17 73 68 7 -
10 -4 18 0 8 1
-1 9 16 69 60 10 4 -3 17 58 61 8 2 1 17 161 157 2 4 5 17 50 64 13
-9 -4 18 53 61 11
-2 -8 17 67 78 29 5 -3 17 70 83 7 3 1 17 18 45 17 5 5 17 79 88 9 -
8 -4 18 115 118 6
-1 -8 17 64 40 21 6 -3 17 136 129 5 4 1 17 59 69 7 6 5 17 96 91 8 -
7 -4 18 107 116 7
0 -8 17 74 82 18 7 -3 17 83 78 7 5 1 17 108 106 5 7 5 17 61 58 19 -
6 -4 18 135 130 5
1 -8 17 53 49 29 8 -3 17 57 60 47 6 1 17 39 22 18 -10 6 17 88 92 7 -
5 -4 18 103 97 9
2 -8 17 52 58 17 -13 -2 17 15 31 15 7 1 17 76 79 6 -9 6 17 72 85 7 -
4 -4 18 72 73 7
-4 -7 17 47 38 17 -12 -2 17 69 29 13 8 1 17 20 27 20 -8 6 17 141 140 6
-3 -4 18 66 68 7
-3 -7 17 84 84 11 -11 -2 17 74 74 9 9 1 17 39 31 29 -7 6 17 53 38 6
-2 -4 18 39 57 39

Table B9 Continued

-2 -7 17 33 31 33 -10 -2 17 42 69 17 -13 2 17 45 38 15 -6 6 17 33 46 14 -1 -4 18 108 113 5
-1 -7 17 46 23 17 -9 -2 17 80 82 14 -12 2 17 58 28 13 -5 6 17 32 8 31 0 -4 18 35 31 23
0 -7 17 82 73 8 -8 -2 17 165 162 4 -11 2 17 70 65 7 -4 6 17 45 63 24 1 -4 18 48 30 10
1 -7 17 63 86 42 -7 -2 17 111 113 6 -10 2 17 69 59 11 -3 6 17 206 191 5 2 -4 18 121 124 4
2 -7 17 9 31 9 -6 -2 17 98 101 3 -9 2 17 105 95 6 -2 6 17 180 178 6 3 -4 18 0 9 1
3 -7 17 30 49 30 -5 -2 17 114 123 6 -8 2 17 146 152 4 -1 6 17 33 18 15 4 -4 18 70 64 25
4 -7 17 65 35 34 -4 -2 17 191 192 5 -7 2 17 107 104 7 0 6 17 104 99 6 5 -4 18 0 24 1
-9 -6 17 88 99 14 -3 -2 17 249 250 3 -6 2 17 109 102 4 1 6 17 33 42 17 6 -4 18 76 91 14
-8 -6 17 127 136 10 -2 -2 17 239 235 4 -5 2 17 99 118 5 2 6 17 62 67 13 7 -4 18 31 29 30
-7 -6 17 0 30 1 -1 -2 17 147 147 3 -4 2 17 203 193 14 3 6 17 66 62 9 -12 -3 18 75 69 11
-6 -6 17 42 43 41 0 -2 17 147 141 4 -3 2 17 232 238 4 4 6 17 22 55 21 -11 -3 18 117 121 9
-5 -6 17 39 24 39 1 -2 17 28 30 27 -2 2 17 219 215 3 5 6 17 87 101 8 -10 -3 18 115 117 21
-4 -6 17 59 64 13 2 -2 17 58 67 8 -1 2 17 168 166 2 6 6 17 71 92 10 -9 -3 18 97 105 13
-3 -6 17 185 183 7 3 -2 17 122 128 10 0 2 17 149 150 4 -8 7 17 50 47 10 -8 -3 18 128 129 5
-2 -6 17 182 185 7 4 -2 17 115 111 5 1 2 17 19 16 17 -7 7 17 79 90 6 -7 -3 18 30 33 23
-1 -6 17 32 24 31 5 -2 17 121 112 6 2 2 17 39 46 7 -6 7 17 93 91 9 -6 -3 18 51 48 10
0 -6 17 81 93 9 6 -2 17 85 86 15 3 2 17 123 124 5 -5 7 17 102 102 6 -5 -3 18 111 110 7
1 -6 17 61 37 29 7 -2 17 42 62 18 4 2 17 110 118 4 -4 7 17 0 17 1 -4 -3 18 141 140 5
2 -6 17 66 68 11 8 -2 17 57 28 12 5 2 17 112 112 6 -3 7 17 67 75 14 -3 -3 18 104 95 14
3 -6 17 76 77 7 -13 -1 17 129 117 8 6 2 17 88 89 6 -2 7 17 45 34 8 -2 -3 18 191 205 14
4 -6 17 44 52 19 -12 -1 17 115 121 7 7 2 17 43 60 12 -1 7 17 20 20 19 -1 -3 18 42 31 8
5 -6 17 95 88 10 -11 -1 17 149 153 4 8 2 17 0 27 1 0 7 17 66 79 7 0 -3 18 17 10 17

Table B9 Continued

6 -6 17 84 89 17 -10 -1 17 106 107 5 -12 3 17 69 80 11 1 7 17 82 82 12 1 -3 18 79 79 6
-11 -5 17 65 51 17 -9 -1 17 106 99 4 -11 3 17 100 98 7 2 7 17 34 38 16 2 -3 18 168 169 5
-10 -5 17 36 46 35 -8 -1 17 154 154 3 -10 3 17 67 59 8 3 7 17 32 50 24 3 -3 18 98 100 10
-9 -5 17 13 50 12 -7 -1 17 154 160 3 -9 3 17 48 58 10 4 7 17 24 35 24 4 -3 18 53 54 10
-8 -5 17 47 65 19 -6 -1 17 150 154 10 -8 3 17 65 76 13 -6 8 17 50 43 10 5 -3 18 51 45 11
-7 -5 17 118 118 6 -5 -1 17 247 240 3 -7 3 17 228 229 3 -5 8 17 63 65 9 6 -3 18 0 36 1
-6 -5 17 58 53 10 -4 -1 17 237 231 4 -6 3 17 129 121 6 -4 8 17 108 107 4 7 -3 18 24 9 24
-5 -5 17 56 55 12 -3 -1 17 86 86 12 -5 3 17 79 78 4 -3 8 17 70 73 5 -12 -2 18 115 119 10
-4 -5 17 37 23 16 -2 -1 17 177 181 14 -4 3 17 117 115 3 -2 8 17 76 77 8 -11 -2 18 19 53 18
-3 -5 17 18 21 17 -1 -1 17 218 208 4 -3 3 17 58 70 5 -1 8 17 30 27 16 -10 -2 18 15 30 15
-2 -5 17 78 79 6 0 -1 17 328 313 4 -2 3 17 76 71 4 0 8 17 92 90 4 -9 -2 18 0 32 1
-1 -5 17 154 160 4 1 -1 17 108 102 4 -1 3 17 105 112 3 1 8 17 68 45 13 -8 -2 18 250 240 5
0 -5 17 61 58 6 2 -1 17 138 140 9 0 3 17 147 147 3 2 8 17 75 59 12 -7 -2 18 141 132 8
1 -5 17 175 177 5 3 -1 17 58 55 18 1 3 17 163 156 2 -2 -8 18 35 30 34 -6 -2 18 131 132 5
2 -5 17 79 72 19 4 -1 17 45 71 16 2 3 17 193 193 4 -1 -8 18 52 16 51 -5 -2 18 140 150 4
3 -5 17 31 60 30 5 -1 17 120 106 7 3 3 17 63 53 5 0 -8 18 58 87 54 -4 -2 18 30 23 29
4 -5 17 49 63 17 6 -1 17 43 42 42 4 3 17 55 63 7 -3 -7 18 116 110 10 -3 -2 18 110 114 4
5 -5 17 91 83 9 7 -1 17 80 78 7 5 3 17 68 69 5 -2 -7 18 57 59 21 -2 -2 18 218 214 7
6 -5 17 98 112 12 8 -1 17 34 37 33 6 3 17 142 132 4 -1 -7 18 54 63 31 -1 -2 18 100 101 5
7 -5 17 67 71 12 9 -1 17 56 40 34 7 3 17 80 81 9 0 -7 18 30 43 30 0 -2 18 158 164 3
-12 -4 17 0 32 1 -13 0 17 55 45 17 8 3 17 67 49 14 1 -7 18 79 84 9 1 -2 18 220 221 4
-11 -4 17 0 8 1 -12 0 17 54 3 13 -12 4 17 0 39 1 2 -7 18 0 26 1 2 -2 18 94 97 10

Table B9 Continued

-10 -4 17 165 171 6 -11 0 17 96 98 5 -11 4 17 0 20 1 3 -7 18 86 78 23
3 -2 18 73 75 17
-9 -4 17 38 52 38 -10 0 17 57 70 20 -10 4 17 168 167 10 -9 -6 18 59 71 58
4 -2 18 51 58 14
-8 -4 17 72 67 10 -9 0 17 143 137 3 -9 4 17 60 49 9 -8 -6 18 20 42 20
5 -2 18 75 76 7
-7 -4 17 62 66 9 -8 0 17 184 190 4 -8 4 17 48 62 9 -7 -6 18 65 50 14
6 -2 18 85 95 6
-6 -4 17 75 67 8 -7 0 17 103 103 8 -7 4 17 69 63 5 -6 -6 18 74 81 11
7 -2 18 107 109 7
-5 -4 17 139 143 5 -6 0 17 53 51 9 -6 4 17 48 71 8 -5 -6 18 69 63 12
8 -2 18 54 50 20
-4 -4 17 207 219 10 -5 0 17 33 19 12 -5 4 17 155 151 3 -4 -6 18 40 63 40
-12 -1 18 65 46 15
-3 -4 17 130 106 5 -4 0 17 180 187 13 -4 4 17 208 212 3 -3 -6 18 97 95 9
-11 -1 18 115 112 6
-2 -4 17 147 137 3 -3 0 17 42 23 16 -3 4 17 117 101 4 -2 -6 18 16 3 15
-10 -1 18 102 102 6
-1 -4 17 180 188 3 -2 0 17 253 251 4 -2 4 17 133 135 3 -1 -6 18 75 87 10
-9 -1 18 72 63 7
0 -4 17 52 49 19 -1 0 17 20 24 19 -1 4 17 179 185 8 0 -6 18 117 123 7
-8 -1 18 71 73 6
1 -4 17 146 151 3 1 0 17 104 102 6 0 4 17 54 51 6 1 -6 18 47 44 14
-7 -1 18 33 29 11
2 -4 17 89 95 5 2 0 17 314 300 3 1 4 17 148 149 3 2 -6 18 56 36 16
-6 -1 18 57 47 6
3 -4 17 125 120 4 3 0 17 22 11 21 2 4 17 111 114 3 3 -6 18 0 28 1 -
5 -1 18 76 80 7
4 -4 17 165 159 7 4 0 17 48 61 15 3 4 17 108 113 3 4 -6 18 30 33 29
-4 -1 18 102 101 6
5 -4 17 101 108 9 5 0 17 115 118 4 4 4 17 175 166 5 5 -6 18 70 82 24
-3 -1 18 229 223 6
6 -4 17 57 75 15 6 0 17 0 16 1 5 4 17 97 99 10 -10 -5 18 89 67 15 -
2 -1 18 113 113 11
7 -4 17 0 11 1 7 0 17 0 14 1 6 4 17 77 75 9 -9 -5 18 136 118 10 -1
-1 18 203 204 7
8 -4 17 41 30 29 8 0 17 105 91 7 7 4 17 0 14 1 -8 -5 18 105 122 20
0 -1 18 155 155 4
-12 -3 17 78 61 12 9 0 17 0 10 1 8 4 17 27 33 27 -7 -5 18 94 105 12
1 -1 18 192 193 4
-11 -3 17 111 102 11 -13 1 17 132 117 6 -11 5 17 57 53 28 -6 -5 18 46 48
30 2 -1 18 149 158 4
-10 -3 17 70 54 23 -12 1 17 131 130 6 -10 5 17 46 50 14 -5 -5 18 51 37
23 3 -1 18 142 140 2

Table B9 Continued

-9 -3 17 36 48 16 -11 1 17 147 143 4 -9 5 17 52 52 10 -4 -5 18 84 100 7
4 -1 18 141 137 4
-8 -3 17 46 62 11 -10 1 17 109 103 5 -8 5 17 71 70 6 -3 -5 18 131 144 4
5 -1 18 82 83 6
-7 -3 17 222 238 4 -9 1 17 106 104 3 -7 5 17 124 116 4 -2 -5 18 81 85 9
6 -1 18 0 45 1
-6 -3 17 113 99 5 -8 1 17 146 153 3 -6 5 17 59 43 6 -1 -5 18 81 84 12
7 -1 18 86 82 8
-5 -3 17 77 75 16 -7 1 17 155 165 4 -5 5 17 64 61 7 0 -5 18 85 84 12
8 -1 18 56 63 12
-4 -3 17 102 109 8 -6 1 17 125 131 4 -4 5 17 35 28 9 1 -5 18 63 85 42
-12 0 18 60 25 22
-11 0 18 60 35 9 -6 4 18 148 142 3 -5 -5 19 32 21 32 7 -1 19 0 34 1
-3 4 19 87 94 5
-10 0 18 81 82 5 -5 4 18 103 106 4 -4 -5 19 101 111 11 -12 0 19 109 90
9 -2 4 19 96 97 12
-9 0 18 25 8 25 -4 4 18 81 84 4 -3 -5 19 72 65 11 -11 0 19 183 173 10
-1 4 19 38 36 9
-8 0 18 44 67 11 -3 4 18 61 61 6 -2 -5 19 126 124 9 -10 0 19 90 98 6
0 4 19 62 72 5
-7 0 18 304 303 5 -2 4 18 52 53 6 -1 -5 19 49 54 25 -9 0 19 78 67 5
1 4 19 108 120 5
-6 0 18 66 72 4 -1 4 18 106 111 3 0 -5 19 135 130 6 -8 0 19 75 75 6
2 4 19 104 90 5
-5 0 18 75 69 6 0 4 18 48 53 5 1 -5 19 100 110 6 -7 0 19 0 19 1 3
4 19 44 56 27
-4 0 18 157 159 4 1 4 18 36 30 10 2 -5 19 39 26 39 -6 0 19 58 38 8
4 4 19 102 103 7
-3 0 18 369 374 5 2 4 18 116 121 8 3 -5 19 0 4 1 -5 0 19 79 89 12
5 4 19 40 33 39
-2 0 18 136 130 3 3 4 18 24 14 24 4 -5 19 90 115 8 -4 0 19 179 187 6
6 4 19 49 54 19
-1 0 18 163 163 3 4 4 18 36 62 28 5 -5 19 119 107 16 -3 0 19 96 92 7
-10 5 19 0 45 1
0 0 18 23 30 15 5 4 18 21 15 20 -11 -4 19 89 50 16 -2 0 19 161 151 7
-9 5 19 106 94 14
1 0 18 24 26 23 6 4 18 68 86 27 -10 -4 19 39 62 39 -1 0 19 0 12 1 -
8 5 19 91 88 5
2 0 18 353 345 3 7 4 18 45 41 23 -9 -4 19 62 43 47 1 0 19 79 84 4 -
7 5 19 102 100 5
3 0 18 33 32 33 -10 5 18 72 79 8 -8 -4 19 22 26 22 2 0 19 305 291 6
-6 5 19 89 105 5
4 0 18 85 92 10 -9 5 18 130 128 9 -7 -4 19 78 86 17 3 0 19 0 13 1 -
5 5 19 22 21 22

Table B9 Continued

5 0 18 66 61 13 -8 5 18 101 99 5 -6 -4 19 51 39 15 4 0 19 29 28 28 -4 5 19 102 112 10
6 0 18 84 103 8 -7 5 18 106 108 11 -5 -4 19 77 81 9 5 0 19 84 105 6 -3 5 19 81 72 7
7 0 18 72 83 21 -6 5 18 38 40 38 -4 -4 19 108 106 9 6 0 19 35 33 35 -2 5 19 135 120 5
8 0 18 45 59 14 -5 5 18 35 46 16 -3 -4 19 108 106 7 7 0 19 0 7 1 -1 5 19 71 52 10
-12 1 18 39 33 39 -4 5 18 107 105 4 -2 -4 19 103 98 5 -12 1 19 83 80 8 0 5 19 143 139 4
-11 1 18 127 116 10 -3 5 18 135 137 5 -1 -4 19 48 37 21 -11 1 19 49 69 15 1 5 19 92 98 5
-10 1 18 102 113 5 -2 5 18 84 82 5 0 -4 19 68 72 13 -10 1 19 0 22 1 2 5 19 0 28 1
-9 1 18 71 53 16 -1 5 18 91 97 5 1 -4 19 117 126 4 -9 1 19 0 31 1 3 5 19 43 11 15
-8 1 18 78 63 7 0 5 18 87 81 12 2 -4 19 95 92 7 -8 1 19 189 197 4 4 5 19 85 117 8
-7 1 18 36 28 13 1 5 18 90 95 5 3 -4 19 64 62 17 -7 1 19 149 159 5 5 5 19 116 114 7
-6 1 18 33 48 11 2 5 18 41 37 40 4 -4 19 90 90 11 -6 1 19 122 120 4 -8 6 19 63 63 9
-5 1 18 88 86 7 3 5 18 128 121 12 5 -4 19 55 29 15 -5 1 19 93 86 15 -7 6 19 60 51 28
-4 1 18 106 102 6 4 5 18 94 108 7 6 -4 19 34 50 33 -4 1 19 74 68 8 -6 6 19 91 96 9
-3 1 18 221 212 5 5 5 18 85 83 7 -11 -3 19 21 51 21 -3 1 19 55 48 13 -5 6 19 36 39 14
-2 1 18 108 104 3 6 5 18 0 38 1 -10 -3 19 97 99 7 -2 1 19 141 127 4 -4 6 19 77 77 7
-1 1 18 211 214 3 -9 6 18 59 75 17 -9 -3 19 34 33 30 -1 1 19 191 189 7 -3 6 19 48 13 11
0 1 18 135 147 4 -8 6 18 37 45 16 -8 -3 19 52 63 10 0 1 19 31 36 31 -2 6 19 90 84 6
1 1 18 190 194 3 -7 6 18 60 61 15 -7 -3 19 178 178 10 1 1 19 131 135 3 -1 6 19 94 88 5
2 1 18 183 181 3 -6 6 18 88 74 15 -6 -3 19 55 58 9 2 1 19 52 47 6 0 6 19 71 77 6
3 1 18 131 127 15 -5 6 18 54 49 22 -5 -3 19 118 104 8 3 1 19 32 18 21 1 6 19 31 35 31
4 1 18 138 143 4 -4 6 18 73 73 6 -4 -3 19 69 68 16 4 1 19 56 58 8 2 6 19 69 57 11
5 1 18 81 92 6 -3 6 18 111 96 4 -3 -3 19 238 230 4 5 1 19 112 113 5 3 6 19 33 41 33

Table B9 Continued

6 1 18 34 38 18 -2 6 18 29 16 28 -2 -3 19 55 61 11 6 1 19 49 46 11
4 6 19 45 19 22
7 1 18 72 77 9 -1 6 18 79 81 6 -1 -3 19 165 164 9 7 1 19 51 25 14 -
7 7 19 149 139 6
8 1 18 61 75 10 0 6 18 123 122 4 0 -3 19 103 97 4 -12 2 19 73 66 9
-6 7 19 36 14 17
-12 2 18 126 125 12 1 6 18 45 47 10 1 -3 19 68 57 7 -11 2 19 99 109 6
-5 7 19 189 174 4
-11 2 18 0 50 1 2 6 18 28 36 27 2 -3 19 34 33 16 -10 2 19 65 69 10
-4 7 19 48 42 19
-10 2 18 19 30 18 3 6 18 0 23 1 3 -3 19 87 78 16 -9 2 19 111 124 5
-3 7 19 77 86 7
-9 2 18 0 27 1 4 6 18 23 27 22 4 -3 19 90 76 7 -8 2 19 51 58 10 -
2 7 19 27 45 27
-8 2 18 256 248 4 5 6 18 70 75 9 5 -3 19 94 100 11 -7 2 19 49 52 18
-1 7 19 123 112 7
-7 2 18 134 136 4 -8 7 18 45 47 16 6 -3 19 116 117 10 -6 2 19 91 99 5
0 7 19 61 63 19
-6 2 18 150 149 5 -7 7 18 16 20 15 7 -3 19 43 60 43 -5 2 19 93 97 4
1 7 19 65 54 21
-5 2 18 122 129 5 -6 7 18 113 120 6 -12 -2 19 68 69 22 -4 2 19 133 127 4
2 7 19 63 40 12
-4 2 18 31 29 30 -5 7 18 83 80 5 -11 -2 19 111 104 7 -3 2 19 162 158 4
-2 -7 20 0 30 1
-3 2 18 123 127 4 -4 7 18 63 61 7 -10 -2 19 87 75 19 -2 2 19 50 53 6
-1 -7 20 80 43 23
-2 2 18 209 208 2 -3 7 18 105 98 4 -9 -2 19 100 100 12 -1 2 19 26 14 17
0 -7 20 37 56 36
-1 2 18 104 106 2 -2 7 18 63 61 10 -8 -2 19 83 74 8 0 2 19 37 25 6 -
8 -6 20 61 82 25
0 2 18 182 181 4 -1 7 18 57 68 8 -7 -2 19 58 54 9 1 2 19 63 61 4 -
7 -6 20 93 66 15
1 2 18 213 212 5 0 7 18 32 42 31 -6 -2 19 106 105 6 2 2 19 107 105 6
-6 -6 20 60 42 26
2 2 18 82 83 5 1 7 18 78 90 7 -5 -2 19 65 73 7 3 2 19 96 100 5 -5
-6 20 79 91 10
3 2 18 73 77 5 2 7 18 40 18 16 -4 -2 19 136 137 11 4 2 19 44 49 12
-4 -6 20 48 42 21
4 2 18 69 66 13 3 7 18 69 76 8 -3 -2 19 132 135 4 5 2 19 44 30 13 -
3 -6 20 90 96 12
5 2 18 84 87 10 -5 8 18 71 68 6 -2 -2 19 29 41 29 6 2 19 46 50 14 -
2 -6 20 54 72 23
6 2 18 74 81 7 -4 8 18 32 42 31 -1 -2 19 11 14 11 7 2 19 74 70 12 -
1 -6 20 98 94 15

Table B9 Continued

7 2 18 89 100 7 -3 8 18 48 32 8 0 -2 19 0 30 1 -11 3 19 37 46 23 0 -6 20 28 46 27
8 2 18 44 51 20 -2 8 18 32 29 18 1 -2 19 54 52 8 -10 3 19 98 98 7 1 -6 20 12 17 11
-12 3 18 63 61 11 -1 8 18 0 7 1 2 -2 19 109 103 5 -9 3 19 4 33 4 2 -6 20 24 15 23
-11 3 18 116 130 16 0 8 18 74 87 9 3 -2 19 101 103 5 -8 3 19 69 73 6 3 -6 20 43 60 28
-10 3 18 105 100 12 -2 -7 19 51 40 16 4 -2 19 30 36 30 -7 3 19 161 171 4 -9 -5 20 27 73 26
-9 3 18 100 95 5 -1 -7 19 96 101 10 5 -2 19 21 31 20 -6 3 19 71 75 6 -8 -5 20 32 43 32
-8 3 18 128 126 4 0 -7 19 55 61 15 6 -2 19 48 53 16 -5 3 19 95 93 4 -7 -5 20 40 61 40
-7 3 18 52 45 10 1 -7 19 54 56 54 7 -2 19 72 63 11 -4 3 19 72 62 5 -6 -5 20 77 75 12
-6 3 18 55 53 11 2 -7 19 47 44 47 -12 -1 19 67 75 10 -3 3 19 231 229 6 -5 -5 20 40 38 30
-5 3 18 90 96 11 -8 -6 19 0 64 1 -11 -1 19 79 77 12 -2 3 19 49 55 6 -4 -5 20 84 84 10
-4 3 18 140 143 4 -7 -6 19 36 51 35 -10 -1 19 45 28 17 -1 3 19 172 168 4 -3 -5 20 129 135 10
-3 3 18 107 100 4 -6 -6 19 78 91 16 -9 -1 19 19 31 18 0 3 19 110 104 2 -2 -5 20 40 39 24
-2 3 18 179 190 3 -5 -6 19 62 60 20 -8 -1 19 215 215 5 1 3 19 62 61 10 -1 -5 20 47 46 22
-1 3 18 29 37 28 -4 -6 19 89 82 13 -7 -1 19 143 148 3 2 3 19 21 30 20 0 -5 20 88 87 9
0 3 18 27 16 8 -3 -6 19 37 27 36 -6 -1 19 131 125 4 3 3 19 82 83 5 1 -5 20 97 94 12
1 3 18 90 89 5 -2 -6 19 81 88 12 -5 -1 19 100 101 6 4 3 19 47 60 16 2 -5 20 40 35 30
2 3 18 161 156 5 -1 -6 19 76 86 10 -4 -1 19 81 65 8 5 3 19 97 97 9 3 -5 20 17 51 16
3 3 18 115 106 5 0 -6 19 77 72 23 -3 -1 19 44 38 11 6 3 19 103 111 8 4 -5 20 33 67 32
4 3 18 42 50 15 1 -6 19 50 29 21 -2 -1 19 142 130 4 7 3 19 77 67 54 -10 -4 20 62 57 17
5 3 18 36 45 14 2 -6 19 68 69 9 -1 -1 19 201 199 6 -11 4 19 51 47 16 -9 -4 20 57 61 31
6 3 18 61 40 16 3 -6 19 46 42 27 0 -1 19 57 63 8 -10 4 19 66 66 10 -8 -4 20 94 104 8
7 3 18 34 15 33 4 -6 19 17 32 17 1 -1 19 139 140 3 -9 4 19 59 36 11 -7 -4 20 78 87 11

Table B9 Continued

-11 4 18 84 73 8 -10 -5 19 0 56 1 2 -1 19 30 39 29 -8 4 19 0 33 1 -6 -4 20 94 103 16
-10 4 18 27 8 27 -9 -5 19 78 89 18 3 -1 19 0 13 1 -7 4 19 77 80 10 -5 -4 20 32 46 31
-9 4 18 34 51 18 -8 -5 19 86 89 14 4 -1 19 40 57 13 -6 4 19 69 60 6 -4 -4 20 96 93 7
-8 4 18 108 122 8 -7 -5 19 94 97 13 5 -1 19 118 115 6 -5 4 19 75 74 9 -3 -4 20 79 73 9
-7 4 18 106 109 4 -6 -5 19 119 105 9 6 -1 19 58 54 10 -4 4 19 112 112 4 -2 -4 20 63 80 10
-1 -4 20 65 76 10 -6 1 20 88 83 5 -1 6 20 65 85 8 -2 -1 21 80 85 6 1 4 21 72 55 10
0 -4 20 137 134 4 -5 1 20 133 133 5 0 6 20 52 46 23 -1 -1 21 83 81 8 2 4 21 84 92 7
1 -4 20 27 53 27 -4 1 20 188 185 6 1 6 20 0 16 1 0 -1 21 42 25 22 3 4 21 38 62 38
2 -4 20 48 58 21 -3 1 20 91 119 9 2 6 20 0 8 1 1 -1 21 31 11 30 4 4 21 9 16 9
3 -4 20 55 56 16 -2 1 20 65 66 8 3 6 20 0 51 1 2 -1 21 0 58 1 -8 5 21 29 29 29
4 -4 20 81 80 11 -1 1 20 38 38 9 -5 7 20 95 89 7 3 -1 21 67 61 14 -7 5 21 44 45 17
5 -4 20 0 12 1 0 1 20 146 148 3 -4 7 20 64 53 31 4 -1 21 47 64 34 -6 5 21 0 39 1
-11 -3 20 98 86 10 1 1 20 172 176 4 -3 7 20 8 24 8 5 -1 21 29 37 28 -5 5 21 29 17 28
-10 -3 20 79 71 13 2 1 20 200 198 4 -2 7 20 0 22 1 6 -1 21 0 44 1 -4 5 21 109 109 5
-9 -3 20 53 48 16 3 1 20 91 80 6 -1 7 20 49 46 13 -11 0 21 104 93 17 -3 5 21 112 99 5
-8 -3 20 35 44 30 4 1 20 0 37 1 0 7 20 66 60 12 -10 0 21 61 53 17 -2 5 21 93 92 8
-7 -3 20 23 40 23 5 1 20 34 39 34 -6 -6 21 109 105 10 -9 0 21 57 42 21 -1 5 21 48 49 15
-6 -3 20 82 78 7 6 1 20 41 41 18 -5 -6 21 36 23 35 -8 0 21 40 67 17 0 5 21 65 59 9
-5 -3 20 154 151 5 7 1 20 48 61 17 -4 -6 21 55 57 29 -7 0 21 21 50 20 1 5 21 0 5 1
-4 -3 20 80 76 11 -11 2 20 10 28 9 -3 -6 21 18 18 17 -6 0 21 130 116 6 2 5 21 86 87 9
-3 -3 20 93 87 6 -10 2 20 66 45 9 -2 -6 21 59 17 24 -5 0 21 155 142 5 3 5 21 25 22 25
-2 -3 20 29 58 28 -9 2 20 55 38 10 -1 -6 21 73 56 11 -4 0 21 47 35 11 -6 6 21 97 105 5

Table B9 Continued

-1 -3 20 77 89 8 -8 2 20 113 118 4 0 -6 21 0 56 1 -3 0 21 139 128 6 -5 6 21 0 4 1
0 -3 20 33 37 18 -7 2 20 94 87 6 1 -6 21 66 69 14 -2 0 21 64 69 12 -4 6 21 65 51 64
1 -3 20 143 141 4 -6 2 20 115 109 6 -8 -5 21 0 36 1 -1 0 21 129 113 14 -3 6 21 0 23 1
2 -3 20 92 107 6 -5 2 20 56 67 13 -7 -5 21 55 48 29 1 0 21 36 24 35 -2 6 21 39 18 26
3 -3 20 67 76 8 -4 2 20 60 71 28 -6 -5 21 0 41 1 2 0 21 47 43 12 -1 6 21 58 57 11
4 -3 20 30 34 29 -3 2 20 86 91 6 -5 -5 21 0 25 1 3 0 21 57 72 9 0 6 21 35 47 34
5 -3 20 30 7 29 -2 2 20 121 117 4 -4 -5 21 114 108 11 4 0 21 48 67 15 1 6 21 84 76 25
6 -3 20 57 71 20 -1 2 20 70 64 18 -3 -5 21 94 87 13 5 0 21 63 62 11 -4 -6 22 105 98 17
-11 -2 20 36 31 36 0 2 20 42 56 18 -2 -5 21 80 98 11 6 0 21 0 23 1 -3 -6 22 71 28 20
-10 -2 20 80 61 11 1 2 20 28 30 28 -1 -5 21 53 58 19 -11 1 21 62 44 15 -2 -6 22 98 84 13
-9 -2 20 59 53 12 2 2 20 48 39 13 0 -5 21 72 53 9 -10 1 21 40 55 39 -1 -6 22 0 47 1
-8 -2 20 126 128 7 3 2 20 43 15 15 1 -5 21 0 3 1 -9 1 21 80 56 9 -7 -5 22 82 82 16
-7 -2 20 92 87 12 4 2 20 58 65 8 2 -5 21 74 79 26 -8 1 21 97 86 4 -6 -5 22 0 40 1
-6 -2 20 98 102 9 5 2 20 69 67 9 3 -5 21 3 24 3 -7 1 21 99 102 5 -5 -5 22 65 55 22
-5 -2 20 77 71 16 6 2 20 54 49 15 -9 -4 21 41 37 41 -6 1 21 72 63 8 -4 -5 22 18 11 17
-4 -2 20 68 77 9 -11 3 20 81 82 9 -8 -4 21 0 26 1 -5 1 21 49 48 22 -3 -5 22 58 41 16
-3 -2 20 86 78 6 -10 3 20 86 78 8 -7 -4 21 95 70 18 -4 1 21 74 82 11 -2 -5 22 0 29 1
-2 -2 20 119 123 9 -9 3 20 41 43 20 -6 -4 21 110 99 11 -3 1 21 78 83 8 -1 -5 22 54 62 54
-1 -2 20 66 82 16 -8 3 20 0 43 1 -5 -4 21 39 31 39 -2 1 21 95 86 11 0 -5 22 0 25 1
0 -2 20 67 76 8 -7 3 20 46 39 12 -4 -4 21 102 100 6 -1 1 21 87 91 7 1 -5 22 14 48 14
1 -2 20 53 38 12 -6 3 20 90 92 6 -3 -4 21 21 19 20 0 1 21 46 38 14 2 -5 22 40 34 40
2 -2 20 43 39 15 -5 3 20 147 151 3 -2 -4 21 0 0 1 1 1 21 0 7 1 -8 -4 22 57 63 29

Table B9 Continued

3 -2 20 0 26 1 -4 3 20 73 72 7 -1 -4 21 90 62 12 2 1 21 69 67 10 -7 -4 22 78 60 18
4 -2 20 50 56 9 -3 3 20 95 95 5 0 -4 21 44 50 43 3 1 21 66 66 9 -6 -4 22 0 20 1
5 -2 20 61 61 12 -2 3 20 65 54 15 1 -4 21 46 66 26 4 1 21 51 58 26 -5 -4 22 0 34 1
6 -2 20 28 44 28 -1 3 20 89 87 5 2 -4 21 86 86 8 5 1 21 0 39 1 -4 -4 22 0 38 1
-11 -1 20 124 120 16 0 3 20 48 43 8 3 -4 21 57 59 16 6 1 21 31 41 30 -3 -4 22 87 92 10
-10 -1 20 65 68 15 1 3 20 155 152 4 4 -4 21 31 16 31 -11 2 21 70 77 15 -2 -4 22 98 110 9
-9 -1 20 64 71 38 2 3 20 120 121 8 -10 -3 21 54 80 32 -10 2 21 80 77 7 -1 -4 22 15 26 15
-8 -1 20 51 68 15 3 3 20 81 70 7 -9 -3 21 78 70 19 -9 2 21 64 66 10 0 -4 22 55 42 15
-7 -1 20 86 86 9 4 3 20 38 30 29 -8 -3 21 56 44 12 -8 2 21 51 59 18 1 -4 22 39 16 38
-6 -1 20 77 72 12 5 3 20 0 8 1 -7 -3 21 57 56 12 -7 2 21 81 83 9 2 -4 22 64 48 14
-5 -1 20 142 137 6 6 3 20 68 68 19 -6 -3 21 77 77 7 -6 2 21 91 106 8 3 -4 22 86 75 10
-4 -1 20 172 177 8 -10 4 20 53 63 13 -5 -3 21 0 8 1 -5 2 21 97 92 8 -9 -3 22 57 57 11
-3 -1 20 100 109 5 -9 4 20 42 57 17 -4 -3 21 52 57 12 -4 2 21 99 100 6 -8 -3 22 68 66 11
-2 -1 20 66 63 7 -8 4 20 105 98 5 -3 -3 21 109 93 7 -3 2 21 47 72 9 -7 -3 22 88 88 14
-1 -1 20 65 53 14 -7 4 20 99 89 6 -2 -3 21 111 110 5 -2 2 21 20 56 19 -6 -3 22 68 68 10
0 -1 20 136 137 4 -6 4 20 90 91 8 -1 -3 21 136 130 6 -1 2 21 45 32 18 -5 -3 22 88 89 7
1 -1 20 183 185 4 -5 4 20 24 37 24 0 -3 21 80 70 8 0 2 21 134 135 4 -4 -3 22 58 54 22
2 -1 20 207 200 6 -4 4 20 93 90 6 1 -3 21 54 38 11 1 2 21 116 112 5 -3 -3 22 37 37 25
3 -1 20 79 79 7 -3 4 20 69 75 7 2 -3 21 49 80 49 2 2 21 169 157 4 -2 -3 22 60 68 16
4 -1 20 28 28 28 -2 4 20 86 78 10 3 -3 21 60 41 16 3 2 21 53 47 11 -1 -3 22 45 57 13
5 -1 20 32 40 31 -1 4 20 93 89 4 4 -3 21 49 40 49 4 2 21 40 27 19 0 -3 22 92 89 7
6 -1 20 47 41 15 0 4 20 115 117 6 5 -3 21 80 71 23 5 2 21 50 40 14 1 -3 22 35 47 34

Table B9 Continued

7 -1 20 40 57 29 1 4 20 27 42 27 -11 -2 21 83 74 15 -10 3 21 53 73 16 2 -3 22 0 30 1
-12 0 20 23 7 22 2 4 20 76 56 9 -10 -2 21 84 81 8 -9 3 21 48 63 48 3 -3 22 64 71 13
-11 0 20 40 9 20 3 4 20 59 54 9 -9 -2 21 82 61 10 -8 3 21 59 50 11 4 -3 22 73 37 15
-10 0 20 95 105 8 4 4 20 71 74 11 -8 -2 21 28 50 27 -7 3 21 37 55 17 -10 -2 22 80 65 13
-9 0 20 24 18 23 5 4 20 31 14 31 -7 -2 21 100 87 9 -6 3 21 64 85 10 -9 -2 22 34 35 33
-8 0 20 53 11 9 -9 5 20 94 77 6 -6 -2 21 108 103 9 -5 3 21 0 19 1 -8 -2 22 43 60 27
-7 0 20 39 27 9 -8 5 20 60 44 9 -5 -2 21 107 104 7 -4 3 21 45 45 12 -7 -2 22 25 34 25
-6 0 20 29 27 29 -7 5 20 65 63 8 -4 -2 21 98 88 9 -3 3 21 104 97 9 -6 -2 22 44 21 28
-5 0 20 81 97 8 -6 5 20 66 61 10 -3 -2 21 54 62 11 -2 3 21 89 97 5 -5 -2 22 107 104 10
-4 0 20 146 168 6 -5 5 20 63 53 8 -2 -2 21 44 65 21 -1 3 21 138 131 4 -4 -2 22 43 42 43
-3 0 20 36 43 36 -4 5 20 105 100 5 -1 -2 21 71 48 21 0 3 21 76 70 11 -3 -2 22 71 74 9
-2 0 20 34 20 11 -3 5 20 128 142 11 0 -2 21 144 134 4 1 3 21 48 44 27 -2 -2 22 87 92 7
-1 0 20 74 83 10 -2 5 20 49 49 8 1 -2 21 105 117 12 2 3 21 63 77 10 -1 -2 22 42 48 41
0 0 20 52 28 8 -1 5 20 63 39 11 2 -2 21 145 151 4 3 3 21 58 39 14 0 -2 22 65 46 10
1 0 20 62 79 6 0 5 20 77 84 13 3 -2 21 20 36 20 4 3 21 25 25 24 1 -2 22 58 67 10
2 0 20 12 29 11 1 5 20 88 97 8 4 -2 21 28 26 28 5 3 21 82 73 24 2 -2 22 0 25 1
3 0 20 79 63 13 2 5 20 57 50 11 5 -2 21 47 42 13 -9 4 21 59 39 18 3 -2 22 18 40 18
4 0 20 47 58 12 3 5 20 57 53 11 -11 -1 21 63 46 14 -8 4 21 27 18 27 4 -2 22 91 86 8
5 0 20 97 85 7 4 5 20 64 71 11 -10 -1 21 57 42 27 -7 4 21 84 71 22 -10 -1 22 46 33 31
6 0 20 56 48 12 -8 6 20 96 89 6 -9 -1 21 46 58 18 -6 4 21 99 95 5 -9 -1 22 45 34 36
7 0 20 0 27 1 -7 6 20 64 59 9 -8 -1 21 89 75 9 -5 4 21 55 34 10 -8 -1 22 8 42 8
-11 1 20 126 123 7 -6 6 20 19 45 19 -7 -1 21 121 114 6 -4 4 21 119 111 5 -7 -1 22 76 87 11

Table B9 Continued

-10 1 20 70 77 17 -5 6 20 79 79 8 -6 -1 21 64 69 36 -3 4 21 43 19 43 -6 -1 22 84 87 10
-9 1 20 71 73 8 -4 6 20 65 53 7 -5 -1 21 48 45 13 -2 4 21 14 10 13 -5 -1 22 0 19 1
-8 1 20 56 67 11 -3 6 20 102 85 6 -4 -1 21 68 75 25 -1 4 21 60 64 16 -4 -1 22 15 25 14
-7 1 20 82 84 5 -2 6 20 82 80 7 -3 -1 21 94 97 7 0 4 21 48 36 13 -3 -1 22 75 59 12
-2 -1 22 74 76 10 -4 4 22 63 37 18 1 -1 23 0 12 1 -4 -4 24 105 77 10 -4 3 24 0 23 1
-1 -1 22 88 79 10 -3 4 22 86 84 15 2 -1 23 51 43 16 -3 -4 24 75 27 18 -3 3 24 14 35 14
0 -1 22 0 16 1 -2 4 22 109 108 23 3 -1 23 72 71 8 -2 -4 24 0 23 1 -2 3 24 41 53 20
1 -1 22 95 89 10 -1 4 22 48 33 17 4 -1 23 0 9 1 -1 -4 24 12 36 11 -1 3 24 51 22 31
2 -1 22 116 118 12 0 4 22 0 41 1 -9 0 23 0 9 1 0 -4 24 73 65 16 0 3 24 113 110 8
3 -1 22 31 36 31 1 4 22 0 20 1 -8 0 23 62 57 12 -7 -3 24 53 47 40 1 3 24 71 19 13
4 -1 22 35 60 35 2 4 22 53 46 17 -7 0 23 85 85 7 -6 -3 24 64 54 17 -5 4 24 63 74 62
5 -1 22 34 51 33 3 4 22 77 72 9 -6 0 23 62 70 17 -5 -3 24 44 4 43 -4 4 24 92 79 8
-10 0 22 126 131 6 -7 5 22 85 86 6 -5 0 23 18 9 18 -4 -3 24 0 24 1 -3 4 24 0 30 1
-9 0 22 59 92 17 -6 5 22 42 45 17 -4 0 23 84 90 11 -3 -3 24 41 41 41 -2 4 24 34 26 33
-8 0 22 89 87 10 -5 5 22 55 42 10 -3 0 23 63 68 9 -2 -3 24 67 49 15 -1 4 24 35 34 34
-7 0 22 57 63 18 -4 5 22 50 17 27 -2 0 23 13 13 12 -1 -3 24 44 18 35 0 4 24 75 61 9
-6 0 22 0 11 1 -3 5 22 50 43 15 -1 0 23 48 61 20 0 -3 24 119 119 9 -5 -3 25 95 88 12
-5 0 22 68 61 11 -2 5 22 28 23 28 1 0 23 26 11 26 1 -3 24 61 13 19 -4 -3 25 0 57 1
-4 0 22 135 134 5 -1 5 22 61 59 19 2 0 23 51 23 39 -8 -2 24 0 32 1 -3 -3 25 49 38 49
-3 0 22 117 107 7 0 5 22 69 26 30 3 0 23 16 17 15 -7 -2 24 54 23 16 -2 -3 25 0 14 1
-2 0 22 57 47 10 1 5 22 33 41 32 4 0 23 28 10 27 -6 -2 24 90 71 14 -1 -3 25 0 30 1
-1 0 22 118 125 5 2 5 22 40 39 40 -9 1 23 96 111 8 -5 -2 24 60 39 11 -6 -2 25 55 19 21

Table B9 Continued

0 0 22 0 23 1 -4 6 22 112 110 6 -8 1 23 72 27 14 -4 -2 24 86 86 10 -5 -2 25 42 14 19
1 0 22 128 131 5 -3 6 22 57 32 57 -7 1 23 22 31 22 -3 -2 24 80 61 9 -4 -2 25 0 11 1
2 0 22 123 124 5 -2 6 22 62 72 14 -6 1 23 60 39 32 -2 -2 24 26 11 26 -3 -2 25 79 70 12
3 0 22 51 49 14 -1 6 22 55 54 11 -5 1 23 76 61 10 -1 -2 24 40 39 40 -2 -2 25 43 29 30
4 0 22 57 46 13 -5 -5 23 33 25 33 -4 1 23 41 62 41 0 -2 24 46 41 19 -1 -2 25 98 87 8
5 0 22 58 68 15 -4 -5 23 47 36 46 -3 1 23 124 125 7 1 -2 24 105 106 7 0 -2 25 42 16 20
-10 1 22 42 31 25 -3 -5 23 81 73 17 -2 1 23 48 51 13 2 -2 24 84 68 11 -7 -1 25 0 30 1
-9 1 22 21 27 20 -2 -5 23 31 19 31 -1 1 23 38 36 20 -8 -1 24 44 51 44 -6 -1 25 105 107 8
-8 1 22 32 34 32 -1 -5 23 30 47 29 0 1 23 70 66 8 -7 -1 24 59 54 13 -5 -1 25 55 47 16
-7 1 22 77 86 14 0 -5 23 32 31 31 1 1 23 23 20 22 -6 -1 24 75 75 14 -4 -1 25 50 28 30
-6 1 22 85 80 19 -7 -4 23 79 59 19 2 1 23 35 50 35 -5 -1 24 37 57 36 -3 -1 25 28 41 27
-5 1 22 5 3 5 -6 -4 23 22 73 21 3 1 23 71 70 8 -4 -1 24 66 69 11 -2 -1 25 23 32 22
-4 1 22 27 31 27 -5 -4 23 0 32 1 4 1 23 0 14 1 -3 -1 24 32 40 31 -1 -1 25 43 47 18
-3 1 22 73 63 14 -4 -4 23 84 50 17 -9 2 23 0 11 1 -2 -1 24 86 78 10 0 -1 25 96 83 7
-2 1 22 83 70 9 -3 -4 23 0 56 1 -8 2 23 115 117 12 -1 -1 24 68 54 9 1 -1 25 0 31 1
-1 1 22 92 88 7 -2 -4 23 60 52 26 -7 2 23 65 81 20 0 -1 24 36 33 36 -7 0 25 0 26 1
0 1 22 0 22 1 -1 -4 23 93 84 10 -6 2 23 52 75 52 1 -1 24 6 41 5 -6 0 25 72 82 10
1 1 22 84 75 7 0 -4 23 84 66 12 -5 2 23 43 46 12 2 -1 24 27 32 26 -5 0 25 39 41 38
2 1 22 111 113 8 1 -4 23 0 17 1 -4 2 23 11 37 11 -8 0 24 45 36 21 -4 0 25 61 33 16
3 1 22 39 38 38 2 -4 23 0 26 1 -3 2 23 83 92 8 -7 0 24 108 108 25 -3 0 25 48 50 24
4 1 22 25 56 25 -8 -3 23 35 7 34 -2 2 23 59 76 25 -6 0 24 50 27 14 -2 0 25 54 57 19
5 1 22 79 62 11 -7 -3 23 14 31 13 -1 2 23 58 54 10 -5 0 24 128 121 8 -1 0 25 22 12 22

Table B9 Continued

-10 2 22 69 72 15 -6 -3 23 0 12 1 0 2 23 54 48 12 -4 0 24 61 30 26 1 0 25 0 9 1
-9 2 22 34 21 34 -5 -3 23 45 7 19 1 2 23 50 53 12 -3 0 24 82 67 14 -7 1 25 61 38 15
-8 2 22 54 53 14 -4 -3 23 74 61 12 2 2 23 50 49 20 -2 0 24 33 19 32 -6 1 25 104 98 9
-7 2 22 38 37 37 -3 -3 23 51 64 21 3 2 23 0 13 1 -1 0 24 0 19 1 -5 1 25 57 50 17
-6 2 22 53 24 52 -2 -3 23 84 63 14 -8 3 23 44 14 44 0 0 24 65 64 11 -4 1 25 64 31 21
-5 2 22 108 104 6 -1 -3 23 67 63 16 -7 3 23 27 30 27 1 0 24 72 70 34 -3 1 25 42 40 41
-4 2 22 43 48 14 0 -3 23 59 19 58 -6 3 23 39 23 23 2 0 24 114 123 7 -2 1 25 0 35 1
-3 2 22 85 80 5 1 -3 23 19 28 18 -5 3 23 8 20 7 3 0 24 59 49 12 -1 1 25 57 45 12
-2 2 22 86 84 13 2 -3 23 77 70 11 -4 3 23 64 64 13 -8 1 24 31 36 31 0 1 25 95 82 7
-1 2 22 52 42 11 3 -3 23 38 37 37 -3 3 23 73 66 12 -7 1 24 60 51 23 1 1 25 0 19 1
0 2 22 42 47 14 -9 -2 23 0 21 1 -2 3 23 32 52 32 -6 1 24 84 80 11 -6 2 25 0 24 1
1 2 22 59 64 9 -8 -2 23 111 124 9 -1 3 23 76 64 9 -5 1 24 72 55 25 -5 2 25 28 10 28
2 2 22 39 37 19 -7 -2 23 77 85 10 0 3 23 24 26 23 -4 1 24 44 66 20 -4 2 25 0 17 1
3 2 22 57 52 16 -6 -2 23 75 72 9 1 3 23 42 35 21 -3 1 24 44 40 15 -3 2 25 81 77 11
4 2 22 69 78 12 -5 -2 23 46 54 16 2 3 23 86 63 9 -2 1 24 71 78 12 -2 2 25 0 14 1
-9 3 22 40 51 18 -4 -2 23 56 40 13 3 3 23 42 36 34 -1 1 24 58 50 19 -1 2 25 104 86 9
-8 3 22 71 75 8 -3 -2 23 87 92 8 -7 4 23 52 63 19 0 1 24 47 46 14 0 2 25 38 18 38
-7 3 22 96 83 7 -2 -2 23 86 81 12 -6 4 23 68 70 8 1 1 24 11 37 11 -5 3 25 89 83 9
-6 3 22 67 66 13 -1 -2 23 63 50 8 -5 4 23 30 36 29 2 1 24 26 34 26 -4 3 25 84 62 12
-5 3 22 105 99 8 0 -2 23 57 49 11 -4 4 23 47 52 21 -8 2 24 30 32 30 -3 3 25 34 44 33
-4 3 22 53 63 18 1 -2 23 63 61 10 -3 4 23 34 52 34 -7 2 24 0 28 1 -2 3 25 15 13 14
-3 3 22 45 36 13 2 -2 23 44 47 21 -2 4 23 52 60 16 -6 2 24 85 79 9 -1 3 25 51 31 19

Table B9 Continued

-2 3 22 68 71 11 3 -2 23 0 12 1 -1 4 23 80 76 10 -5 2 24 50 24 14 -4 -1 26 72 83 15
-1 3 22 9 47 9 -9 -1 23 91 93 8 0 4 23 76 76 9 -4 2 24 79 80 11 -3 -1 26 60 65 25
0 3 22 104 95 5 -8 -1 23 24 16 24 1 4 23 0 20 1 -3 2 24 75 68 22 -4 0 26 25 24 25
1 3 22 53 58 52 -7 -1 23 10 34 9 2 4 23 63 25 13 -2 2 24 32 15 31 -3 0 26 14 27 14
2 3 22 62 37 28 -6 -1 23 57 41 29 -5 5 23 44 18 43 -1 2 24 20 39 20 -2 0 26 48 34 20
3 3 22 85 67 8 -5 -1 23 32 46 32 -4 5 23 85 39 9 0 2 24 49 46 20 -4 1 26 104 90 9
4 3 22 29 36 29 -4 -1 23 78 59 10 -3 5 23 83 69 10 1 2 24 102 101 12 -3 1 26 75 59 22
-8 4 22 46 51 16 -3 -1 23 120 115 11 -2 5 23 57 28 15 2 2 24 92 78 14
-7 4 22 67 53 14 -2 -1 23 68 64 8 -1 5 23 25 47 24 -7 3 24 34 44 33
-6 4 22 19 19 19 -1 -1 23 69 38 12 0 5 23 0 34 1 -6 3 24 59 54 11
-5 4 22 35 40 35 0 -1 23 66 68 9 -5 -4 24 46 58 37 -5 3 24 34 5 33

BIBLIOGRAPHY

1. Overman, L. E. *Journal of the American Chemical Society* **1974,** *96*, 597-599.

2. Overman, L. E.; Carpenter, N. E., The Allylic Trihaloacetimidate Rearrangement. In *Organic Reactions*, John Wiley & Sons, Inc.: 2004.

3. (a) Schmidt, R. R.; Michel, J. *Angewandte Chemie International Edition in English* **1980,** *19*, 731-732; (b) Schmidt, R. R.; Michel, J. *Journal of Carbohydrate Chemistry* **1985,** *4*, 141-169; (c) Schmidt, R. R. *Angewandte Chemie International Edition in English* **1986,** *25*, 212-235; (d) Schmidt, R. R.; Kinzy, W., Anomeric-Oxygen Activation for Glycoside Synthesis: The Trichloroacetimidate Method. In *Advances in Carbohydrate Chemistry and Biochemistry*, Derek, H., Ed. Academic Press: 1994; Vol. Volume 50, pp 21-123; (e) Schmidt, R. R.; Jung, K.-H.; Ernst, B.; Hart, G. W.; Sinaý, P., Trichloroacetimidates. In *Carbohydrates in Chemistry and Biology*, Wiley-VCH Verlag GmbH: 2008; pp 5-59.

4. *The Chemistry of Amidines and Imidates*. John Wiley & Sons, Ltd.: New York, **1975**.

5. Roger, R.; Neilson, D. G. *Chemical Reviews* **1961,** *61*, 179-211.

6. Pinner, A., *Die Imidoather und ihre Derivative*. Oppenheim: Berlin, **1892**.

7. Cramer, F.; Pawelzik, K.; Baldauf, H. *Chemische Berichte* **1958,** *91*, 1049-54.

8. Schaefer, F. C.; Peters, G. A. *The Journal of Organic Chemistry* **1961,** *26*, 412-418.

9. (a) Ho Kang, S.; Bae Lee, S. *Chemical Communications* **1998**, 761-762; (b) Takahashi, T.; Tsukamoto, H.; Kurosaki, M.; Yamada, H. *Synlett* **1997,** *1997*, 1065-1066; (c) Ideguchi, T.; Yamada, T.; Shirahata, T.; Hirose, T.; Sugawara, A.; Kobayashi, Y.; Ōmura, S.; Sunazuka, T. *Journal of the American Chemical Society* **2013,** *135*, 12568-12571.

10. Overman, L. E. *Journal of the American Chemical Society* **1976,** *98*, 2901-10.

11. (a) Beier, B.; Schurrle, K.; Werbitzky, O.; Piepersberg, W. *Journal of the Chemical Society, Perkin Transactions 1* **1990**, 2255-2262; (b) Kakinuma, K.; Koudate, T.; Li, H.-Y.; Eguchi, T. *Tetrahedron Letters* **1991,** *32*, 5801-5804; (c) Hashmi, A. S. K.; Rudolph, M.; Schymura, S.; Visus, J.; Frey, W. *European Journal of Organic Chemistry* **2006**, 4905-4909.

12. Arnold, J. S.; Stone, R. F.; Nguyen, H. M. *Organic Letters* **2010,** *12*, 4580-4583.

13. Arnold, J. S.; Cizio, G. T.; Nguyen, H. M. *Organic Letters* **2011,** *13*, 5576-5579.

14. Allen, F. H.; Kennard, O.; Watson, D. G.; Brammer, L.; Orpen, A. G.; Taylor, R. *Journal of the Chemical Society, Perkin Transactions 2* **1987**, S1-S19.

15. (a) Iversen, T.; Bundle, D. R. *Journal of the Chemical Society, Chemical Communications* **1981**, 1240-1241; (b) Wessel, H.-P.; Iversen, T.; Bundle, D. R. *Journal of the Chemical Society, Perkin Transactions 1* **1985**, 2247-2250; (c)

Eckenberg, P.; Groth, U.; Huhn, T.; Richter, N.; Schmeck, C. *Tetrahedron* **1993,** *49*, 1619-1624.

16. Choi, Y. W.; Reckhow, D. A. *Bulletin of the Korean Chemical Society* **2004,** *25*, 900-906.

17. Overman, L. E. *Accounts of Chemical Research* **1980,** *13*, 218-224.

18. Schulenberg, J. W.; Archer, S., The Chapman Rearrangement. In *Organic Reactions*, John Wiley & Sons, Inc.: 2004.

19. Beak, P. *Accounts of Chemical Research* **1977,** *10*, 186-192.

20. Beak, P.; Lee, J.-K.; Zeigler, J. M. *The Journal of Organic Chemistry* **1978,** *43*, 1536-1538.

21. McDougal, P. G.; Iadonisi, A., Trichloroacetonitrile. In *Encyclopedia of Reagents for Organic Synthesis*, John Wiley & Sons, Ltd: 2001.

22. Cannon, J. S.; Kirsch, S. F.; Overman, L. E.; Sneddon, H. F. *Journal of the American Chemical Society* **2010,** *132*, 15192-15203.

23. Granik, V. G.; Pyatin, B. M.; Persianova, J. V.; Peresleni, E. M.; Kostyuchenko, N. P.; Glushkov, R. G.; Sheinker, Y. N. *Tetrahedron* **1970,** *26*, 4367-4373.

24. Liler, M. *Journal of the Chemical Society B: Physical Organic* **1969**, 385-389.

25. Mumm, O.; Moller, F. *Berichte der Deutschen Chemischen Gesellschaft B* **1937,** *70B*, 2214-27.

26. Cramer, F.; Baldauf, H. *Chemische Berichte* **1959,** *92*, 370-8.

27. Schenck, T. G.; Bosnich, B. *Journal of the American Chemical Society* **1985,** *107*, 2058-2066.

28. Metz, P.; Mues, C.; Schoop, A. *Tetrahedron* **1992,** *48*, 1071-1080.

29. Overman, L. E. *Angewandte Chemie International Edition in English* **1984,** *23*, 579-586.

30. Hollis, T. K.; Overman, L. E. *Journal of Organometallic Chemistry* **1999,** *576*, 290-299.

31. Uozumi , Y.; Kato, K.; Hayashi , T. *Tetrahedron: Asymmetry* **1998,** *9*, 1065-1072.

32. Calter, M.; Hollis, T. K.; Overman, L. E.; Ziller, J.; Zipp, G. G. *The Journal of Organic Chemistry* **1997,** *62*, 1449-1456.

33. Hollis, T. K.; Overman, L. E. *Tetrahedron Letters* **1997,** *38*, 8837-8840.

34. Cohen, F.; Overman, L. E. *Tetrahedron: Asymmetry* **1998,** *9*, 3213-3222.

35. Donde, Y.; Overman, L. E. *Journal of the American Chemical Society* **1999,** *121*, 2933-2934.

36. Anderson, C. E.; Donde, Y.; Douglas, C. J.; Overman, L. E. *The Journal of Organic Chemistry* **2004,** *70*, 648-657.

37. Anderson, C. E.; Overman, L. E. *Journal of the American Chemical Society* **2003,** *125*, 12412-12413.

38. Kirsch, S. F.; Overman, L. E.; Watson, M. P. *The Journal of Organic Chemistry* **2004,** *69*, 8101-8104.

39. Watson, M. P.; Overman, L. E.; Bergman, R. G. *Journal of the American Chemical Society* **2007,** *129*, 5031-5044.

40. (a) Haakansson, A. E.; Palmelund, A.; Holm, H.; Madsen, R. *Chemistry - A European Journal* **2006,** *12*, 3243-3253; (b) Bojstrup, M.; Fanefjord, M.; Lundt, I. *Organic & Biomolecular Chemistry* **2007,** *5*, 3164-3171; (c) Xu, C.; Wang, L.; Hao, X.; Wang, D. Z. *The Journal of Organic Chemistry* **2012,** *77*, 6307-6313; (d) Collett, N. D.; Carter, R. G. *Org. Lett.* **2011,** *13*, 4144-4147; (e) Singh, O. V.; Han, H. *Organic Letters* **2004,** *6*, 3067-3070; (f) Chida, N.; Takeoka, J.; Tsutsumi, N.; Ogawa, S. *Journal of the Chemical Society, Chemical Communications* **1995**, 793-794; (g) Danishefsky, S.; Lee, J. Y. *Journal of the American Chemical Society* **1989,** *111*, 4829-4837; (h) Kim, S.; Lee, T.; Lee, E.; Lee, J.; Fan, G.-j.; Lee, S. K.; Kim, D. *The Journal of Organic Chemistry* **2004,** *69*, 3144-3149; (i) Jiang, X.-Y.; Chu, L.; Wang, R.-W.; Qing, F.-L. *Tetrahedron Letters* **2012,** *53*, 6853-6857.

41. Mercer, G. J.; Yang, J.; McKay, M. J.; Nguyen, H. M. *Journal of the American Chemical Society* **2008,** *130*, 11210-11218.

42. Takano, S.; Akiyama, M.; Ogasawara, K. *Journal of the Chemical Society, Chemical Communications* **1984**, 770-771.

43. Mehmandoust, M.; Petit, Y.; Larchevêque, M. *Tetrahedron Letters* **1992,** *33*, 4313-4316.

44. Chen, Y. K.; Lurain, A. E.; Walsh, P. J. *Journal of the American Chemical Society* **2002,** *124*, 12225-12231.

45. Momose, T.; Hama, N.; Higashino, C.; Sato, H.; Chida, N. *Tetrahedron Letters* **2008,** *49*, 1376-1379.

46. Hama, N.; Matsuda, T.; Sato, T.; Chida, N. *Organic Letters* **2009,** *11*, 2687-2690.

47. Hama, N.; Aoki, T.; Miwa, S.; Yamazaki, M.; Sato, T.; Chida, N. *Organic Letters* **2011,** *13*, 616-619.

48. McGonagle, F. I.; Brown, L.; Cooke, A.; Sutherland, A. *Organic & Biomolecular Chemistry* **2010,** *8*, 3418-3425.

49. Ahmad, S.; Sutherland, A. *Organic & Biomolecular Chemistry* **2012,** *10*, 8251-8259.

50. Jamieson, A. G.; Sutherland, A. *Organic & Biomolecular Chemistry* **2005,** *3*, 735-736; Jaunzeme, I.; Jirgensons, A. *Tetrahedron* **2008,** *64*, 5794-5799.

51. Zaed, A. M.; Sutherland, A. *Organic & Biomolecular Chemistry* **2010,** *8*, 4394-4399.

52. Zaed, A. M.; Sutherland, A. *Organic & Biomolecular Chemistry* **2011,** *9*, 8030-8037.

53. Calder, E. D. D.; Zaed, A. M.; Sutherland, A. *Journal of Organic Chemistry* **2013,** *78*, 7223-7233.

54. Overman, L. E.; Clizbe, L. A. *Journal of the American Chemical Society* **1976,** *98*, 2352-2354.

55. Overman, L. E.; Clizbe, L. A.; Freerks, R. L.; Marlowe, C. K. *Journal of the American Chemical Society* **1981,** *103*, 2807-2815.

56. Overman, L. E.; Jessup, P. J. *Journal of the American Chemical Society* **1978,** *100*, 5179-5185.

57. Overman, L. E.; Fukaya, C. *Journal of the American Chemical Society* **1980,** *102*, 1454-1456.

58. Kobbelgaard, S.; Brandes, S.; Jørgensen, K. A. *Chemistry – A European Journal* **2008,** *14*, 1464-1471.

59. Çelebi-Ölüm, N.; Aviyente, V.; Houk, K. N. *The Journal of Organic Chemistry* **2009,** *74*, 6944-6952.

60. (a) Schmidt, U.; Respondek, M.; Lieberknecht, A.; Werner, J.; Fisher, P., *Synthesis*, **1989**; pp 256-261; (b) Bernet, B.; Vasella, A. *Tetrahedron Letters* **1983,** *24*, 5491-5494; (c) Hatakeyama, S.; Matsumoto, H.; Fukuyama, H.; Mukugi, Y.; Irie, H. *The Journal of Organic Chemistry* **1997,** *62*, 2275-2279; (d) Liu, D.-G.; Wang, B.; Lin, G.-Q. *The Journal of Organic Chemistry* **2000,** *65*, 9114-9119; (e) Hart, T. W.; Vacher, B. *Tetrahedron Letters* **1992,** *33*, 3009-3012.

61. (a) Pauls, H. W.; Fraser-Reid, B. *Can. J. Chem.* **1984**, 1532-1538; (b) Alonso, R. A.; Burgey, C. S.; Rao, B. V.; Vite, G. D.; Vollerthun, R.; Zottola, M. A.; Fraser-Reid, B. *Journal of the American Chemical Society* **1993,** *115*, 6666-6672.

62. Kang, S. H.; Jun, H.-S. *Chemical Communications (Cambridge)* **1998**, 1929-1930.

63. Kang, S. H.; Kim, C. M.; Youn, J.-H. *Tetrahedron Lett.* **1999,** *40*, 3581-3582.

64. (a) Brown, J. R.; Nishimura, Y.; Esko, J. D. *Bioorganic & Medicinal Chemistry Letters* **2006,** *16*, 532-536; (b) Matsushima, Y.; Kino, J. *Tetrahedron Letters* **2006,** *47*, 8777-8780; (c) Matsushima, Y.; Kino, J. *European Journal of Organic Chemistry* **2009**, 1619-1624; (d) Matsushima, Y.; Kino, J. *European Journal of Organic Chemistry* **2010**, 2206-2211.

65. (a) Nishimura, Y.; Satoh, T.; Adachi, H.; Kondo, S.; Takeuchi, T.; Azetaka, M.; Fukuyasu, H.; Iizuka, Y. *Journal of the American Chemical Society* **1996,** *118*, 3051-3052; (b) Nishimura, Y.; Satoh, T.; Adachi, H.; Kondo, S.; Takeuchi, T.; Azetaka, M.; Fukuyasu, H.; Iizuka, Y. *Journal of Medicinal Chemistry* **1997,** *40*, 2626-2633.

66. Maleckis, A.; Jaunzeme, I.; Jirgensons, A. *European Journal of Organic Chemistry* **2009**, 6407-6412.

67. Abdel-Rahman, Adel A. H.; Winterfeld, Gottfried A.; Takhi, M.; Schmidt, Richard R. *European Journal of Organic Chemistry* **2002,** *2002*, 713-717.
68. (a) Kirsch, S. F.; Overman, L. E. *The Journal of Organic Chemistry* **2005,** *70*, 2859-2861; (b) Overman, L. E.; Remarchuk, T. P. *Journal of the American Chemical Society* **2001,** *124*, 12-13.

69. Cannon, J. S.; Kirsch, S. F.; Overman, L. E. Catalytic Asymmetric Synthesis of Chiral Allylic Esters *NCBI NIH Public Access* [Online], **2005**.

70. Cannon, J. S.; Kirsch, S. F.; Overman, L. E. *Journal of the American Chemical Society* **2010,** *132*, 15185-15191.

71. Kirsch, S. F.; Overman, L. E. *Journal of the American Chemical Society* **2005,** *127*, 2866-2867.

72. Haug, T. T.; Kirsch, S. F. *Organic & Biomolecular Chemistry* **2010,** *8*, 991-993.

73. Jiao, P.; Swenson, D. C.; Gloer, J. B.; Wicklow, D. T. *Journal of Natural Products* **2006,** *69*, 636-639.

74. Binder, J. T.; Kirsch, S. F. *Chemical Communications (Cambridge, U. K.)* **2007**, 4164-4166.

75. Menz, H.; Kirsch, S. F. *Organic Letters* **2009,** *11*, 5634-5637.

76. Kirsch, S. F.; Klahn, P.; Menz, H. *Synthesis* **2011,** *2011*, 3592-3603.

77. Kirsch, S. F.; Overman, L. E.; White, N. S. *Organic Letters* **2007,** *9*, 911-913.

78. Lopez, F.; Ohmura, T.; Hartwig, J. F. *Journal of the American Chemical Society* **2003,** *125*, 3426-3427.

79. Shu, C.; Hartwig, J. F. *Angewandte Chemie International Edition* **2004,** *43*, 4794-4797.

80. Olson, A. C.; Overman, L. E.; Sneddon, H. F.; Ziller, J. W. *Advanced Synthesis & Catalysis* **2009,** *351*, 3186-3192.

81. Cannon, J. S.; Olson, A. C.; Overman, L. E.; Solomon, N. S. *Journal of Organic Chemistry* **2012,** *77*, 1961-1973.

82. Topczewski, J. J.; Tewson, T. J.; Nguyen, H. M. *Journal of the American Chemical Society* **2011,** *133*, 19318-19321.

83. Park, N. H.; Nguyen, H. M. *Organic Letters* **2009,** *11*, 2433-2436.

84. (a) Schuff, B. P.; Mercer, G. J.; Nguyen, H. M. *Organic Letters* **2007,** *9*, 3173-3176; (b) Yang, J.; Cooper-Vanosdell, C.; Mensah, E. A.; Nguyen, H. M. *The Journal of Organic Chemistry* **2008,** *73*, 794-800; (c) Mensah, E. A.; Azzarelli, J. M.; Nguyen, H. M. *The Journal of Organic Chemistry* **2009,** *74*, 1650-1657; (d) Mensah, E. A.; Yu, F.; Nguyen, H. M. *Journal of the American Chemical Society* **2010,** *132*, 14288-14302.

85. Bartels, B.; García-Yebra, C.; Rominger, F.; Helmchen, G. *European Journal of Inorganic Chemistry* **2002,** *2002*, 2569-2586.
86. Bartels, B.; García-Yebra, C.; Helmchen, G. *European Journal of Organic Chemistry* **2003,** *2003*, 1097-1103.

87. Trost, B. M.; Fandrick, D. R., *Aldrichimica Acta*, **2007**; Vol. *40*, pp 59-72.

88. Evans, P. A.; Leahy, D. K. *Journal of the American Chemical Society* **2000,** *122*, 5012-5013.

89. *Chiral Amine Synthesis*. Wiley-VCH: New York, NY, 2008.

90. Johannsen, M.; Jørgensen, K. A. *Chemical Reviews* **1998,** *98*, 1689-1708; Trost, B. M.; Crawley, M. L. *Chemical Reviews* **2003,** *103*, 2921-2944.

91. Trost, B. M.; Zhang, T.; Sieber, J. D. *Chemical Science* **2010,** *1*, 427-440.

92. Watson, I. D. G.; Yudin, A. K. *Journal of the American Chemical Society* **2005,** *127*, 17516-17529.

93. Dubovyk, I.; Watson, I. D. G.; Yudin, A. K. *Journal of the American Chemical Society* **2007,** *129*, 14172-14173.

94. Dubovyk, I.; Watson, I. D. G.; Yudin, A. K. *The Journal of Organic Chemistry* **2013,** *78*, 1559-1575.

95. Shu, C.; Leitner, A.; Hartwig, J. F. *Angewandte Chemie International Edition* **2004,** *43*, 4797-4800.

96. Evans, P. A.; Robinson, J. E.; Nelson, J. D. *Journal of the American Chemical Society* **1999,** *121*, 6761-6762.

97. Evans, P. A.; Robinson, J. E.; Moffett, K. K. *Organic Letters* **2001,** *3*, 3269-3271.

98. Evans, P. A.; Robinson, J. E. *Organic Letters* **1999,** *1*, 1929-1931.

99. Evans, P. A.; Nelson, J. D. *Journal of the American Chemical Society* **1998,** *120*, 5581-5582.

100. Takeuchi, R.; Ue, N.; Tanabe, K.; Yamashita, K.; Shiga, N. *Journal of the American Chemical Society* **2001,** *123*, 9525-9534.

101. (a) Trost, B. M.; Verhoeven, T. R. *Journal of the American Chemical Society* **1980,** *102*, 4730-4743; (b) Trost, B. M.; Lautens, M. *Journal of the American Chemical Society* **1987,** *109*, 1469-1478; (c) Takeuchi, R.; Kashio, M. *Journal of the American Chemical Society* **1998,** *120*, 8647-8655; (d) Trost, B. M.; Fraisse, P. L.; Ball, Z. T. *Angewandte Chemie International Edition* **2002,** *41*, 1059-1061.

102. Stanley, L. M.; Bai, C.; Ueda, M.; Hartwig, J. F. *Journal of the American Chemical Society* **2010,** *132*, 8918-8920.

103. Arnold, J. S.; Nguyen, H. M. *Journal of the American Chemical Society* **2012,** *134*, 8380-8383.

104. Arnold, J. S.; Nguyen, H. M. *Synthesis-Stuttgart* **2013,** *45*, 2101-2108.
105. (a) Cogan, D. A.; Ellman, J. A. *Journal of the American Chemical Society* **1999,** *121*, 268-269; (b) Riant, O.; Hannedouche, J. *Organic & Biomolecular Chemistry* **2007,** *5*, 873-888.

106. (a) Robak, M. T.; Herbage, M. A.; Ellman, J. A. *Chemical Reviews* **2010,** *110*, 3600-3740; (b) Spero, D. M.; Kapadia, S. R. *The Journal of Organic Chemistry* **1997,** *62*, 5537-5541.

107. Shintani, R.; Takeda, M.; Tsuji, T.; Hayashi, T. *Journal of the American Chemical Society* **2010,** *132*, 13168-13169.

108. Bloch, R. *Chemical Reviews* **1998,** *98*, 1407-1438.

109. (a) Fischer, D. F.; Barakat, A.; Xin, Z.-q.; Weiss, M. E.; Peters, R. *Chemistry – A European Journal* **2009,** *15*, 8722-8741; (b) Fischer, D. F.; Xin, Z.-q.; Peters, R. *Angewandte Chemie International Edition* **2007,** *46*, 7704-7707.

110. Iuliis, M. Z. D.; Watson, I. D. G.; Yudin, A. K.; Morris, R. H. *Canadian Journal of Chemistry* **2009,** *87*, 54-62.

111. Plietker, B. *Angewandte Chemie International Edition* **2006,** *45*, 6053-6056.

112. Yang, S.-C.; Hsu, Y.-C.; Gan, K.-H. *Tetrahedron* **2006,** *62*, 3949-3958.

113. (a) Baran, P. S.; Guerrero, C. A.; Corey, E. J. *Journal of the American Chemical Society* **2003,** *125*, 5628-5629; (b) Sugiyama, H.; Shioiri, T.; Yokokawa, F. *Tetrahedron Letters* **2002,** *43*, 3489-3492; (c) Sugiyama, H.; Yokokawa, F.; Aoyama, T.; Shioiri, T. *Tetrahedron Letters* **2001,** *42*, 7277-7280; (d) Della Sala, G.; Capozzo, D.; Izzo, I.; Giordano, A.; Iommazzo, A.; Spinella, A. *Tetrahedron Letters* **2002,** *43*, 8839-8841; (e) Roe, J. M.; Webster, R. A. B.; Ganesan, A. *Organic Letters* **2003,** *5*, 2825-2827.

114. Luzung, M. R.; Lewis, C. A.; Baran, P. S. *Angewandte Chemie International Edition* **2009,** *48*, 7025-7029.

115. (a) Castro, C. E.; Gaughan, E. J.; Owsley, D. C. *The Journal of Organic Chemistry* **1966,** *31*, 4071-4078; (b) Kamijo, S.; Jin, T.; Yamamoto, Y. *Angewandte Chemie International Edition* **2002,** *41*, 1780-1782; (c) Kamijo, S.; Yamamoto, Y. *Journal of the American Chemical Society* **2002,** *124*, 11940-11945; (d) Nair, R. N.; Lee, P. J.; Rheingold, A. L.; Grotjahn, D. B. *Chemistry – A European Journal* **2010,** *16*, 7992-7995.

116. (a) Enders, D.; Gottfried, K.; Raabe, G. *Advanced Synthesis & Catalysis* **2010,** *352*, 3147-3152; (b) Nugent, T. C.; El-Shazly, M. *Advanced Synthesis & Catalysis* **2010,** *352*, 753-819.

117. Vachal, P.; Jacobsen, E. N. *Organic Letters* **2000,** *2*, 867-870.

118. (a) Shibasaki, M.; Kanai, M. *Chemical Reviews* **2008,** *108*, 2853-2873; (b) Wada, R.; Shibuguchi, T.; Makino, S.; Oisaki, K.; Kanai, M.; Shibasaki, M. *Journal of the American Chemical Society* **2006,** *128*, 7687-7691; (c) Lauzon, C.; Charette, A. B.

Organic Letters **2006,** *8*, 2743-2745; (d) Suto, Y.; Kanai, M.; Shibasaki, M. *Journal of the American Chemical Society* **2007,** *129*, 500-501.

119. (a) Dong, Y.; Teesdale-Spittle, P.; Hoberg, J. O. *Tetrahedron Letters* **2005,** *46*, 353-355; (b) Stanley, L. M.; Hartwig, J. F. *Journal of the American Chemical Society* **2009,** *131*, 8971-8983.

120. Trost, B. M.; Machacek, M. R.; Aponick, A. *Accounts of Chemical Research* **2006,** *39*, 747-760.

121. Trost, B. M.; Machacek, M. R.; Tsui, H. C. *Journal of the American Chemical Society* **2005,** *127*, 7014-7024.

122. Vrieze, D. C.; Hoge, G. S.; Hoerter, P. Z.; Van Haitsma, J. T.; Samas, B. M. *Organic Letters* **2009,** *11*, 3140-3142.

123. You, S.-L.; Zhu, X.-Z.; Luo, Y.-M.; Hou, X.-L.; Dai, L.-X. *Journal of the American Chemical Society* **2001,** *123*, 7471-7472.

124. Lafrance, M.; Roggen, M.; Carreira, E. M. *Angewandte Chemie-International Edition* **2012,** *51*, 3470-3473.

125. Trost, B. M.; Bunt, R. C.; Lemoine, R. C.; Calkins, T. L. *Journal of the American Chemical Society* **2000,** *122*, 5968-5976.

126. Defieber, C.; Grützmacher, H.; Carreira, E. M. *Angewandte Chemie International Edition* **2008,** *47*, 4482-4502.

127. Wang, Z.-Q.; Feng, C.-G.; Xu, M.-H.; Lin, G.-Q. *Journal of the American Chemical Society* **2007,** *129*, 5336-5337.

128. Okamoto, K.; Hayashi, T.; Rawal, V. H. *Organic Letters* **2008,** *10*, 4387-4389.

129. Fischer, C.; Defieber, C.; Suzuki, T.; Carreira, E. M. *Journal of the American Chemical Society* **2004,** *126*, 1628-1629.

130. Tokunaga, N.; Otomaru, Y.; Okamoto, K.; Ueyama, K.; Shintani, R.; Hayashi, T. *Journal of the American Chemical Society* **2004,** *126*, 13584-13585.

131. Bodner, G. M.; Storhoff, B. N.; Doddrell, D.; Todd, L. J. *Journal of the Chemical Society D: Chemical Communications* **1970**, 1530-1531.

132. Cramer, R. *Journal of the American Chemical Society* **1967,** *89*, 4621-4626.

133. Aakermark, B.; Blomberg, M. R. A.; Glaser, J.; Oehrstroem, L.; Wahlberg, S.; Waernmark, K.; Zetterberg, K. *Journal of the American Chemical Society* **1994,** *116*, 3405-3413.

134. Arnold, J. S.; Cizio, G. T.; Heitz, D. R.; Nguyen, H. M. *Chemical Communications (Cambridge, U. K.)* **2012,** *48*, 11531-11533.

135. Nogle, L. M.; Okino, T.; Gerwick, W. H. *Journal of Natural Products* **2001,** *64*, 983-985.

136. (a) Aakermark, B.; Vitagliano, A. *Organometallics* **1985,** *4*, 1275-1283; (b) Helmchen, G.; Pfaltz, A. *Accounts of Chemical Research* **2000,** *33*, 336-345; (c) van Haaren, R. J.; Keeven, P. H.; van der Veen, L. A.; Goubitz, K.; van Strijdonck, G. P. F.; Oevering, H.; Reek, J. N. H.; Kamer, P. C. J.; van Leeuwen, P. W. N. M. *Inorganica Chimica Acta* **2002,** *327*, 108-115; (d) Hayashi, T.; Kawatsura, M.; Uozumi, Y. *Chemical Communications* **1997**, 561-562.

137. (a) Drouin, C.; Woo, J. C. S.; MacKay, B.; Lavigne, R. M. A. *Tetrahedron Letters* **2004,** *45*, 7197-7199; (b) Woo, J. C. S.; MacKay, D. B. *Tetrahedron Letters* **2003,** *44*, 2881-2883; (c) Kang, S. H.; Kang, S. Y.; Lee, H. S.; Buglass, A. J. *Chemical Reviews* **2005,** *105*, 4537-4558; (d) Shinada, T.; Oe, K.; Ohfune, Y. *Tetrahedron Letters* **2012,** *53*, 3250-3253; (e) Oe, K.; Shinada, T.; Ohfune, Y. *Tetrahedron Letters* **2008,** *49*, 7426-7429; (f) Ohfune, Y.; Shinada, T. *Bulletin of the Chemical Society of Japan* **2003,** *76*, 1115-1129; (g) Namba, K.; Shinada, T.; Teramoto, T.; Ohfune, Y. *Journal of the American Chemical Society* **2000,** *122*, 10708-10709; (h) Tran, K.; Lombardi, P. J.; Leighton, J. L. *Organic Letters* **2008,** *10*, 3165-3167.

138. Hashimoto, T.; Maruoka, K. *Organic & Biomolecular Chemistry* **2008,** *6*, 829-835.

139. Willis, M. C. *Chemical Reviews* **2009,** *110*, 725-748.

140. Fu, G. C. *Modern Rhodium-Catalyzed Organic Reactions* **2005**, 79-91.

141. Sakai, K.; Ide, J.; Oda, O.; Nakamura, N. *Tetrahedron Letters* **1972,** *13*, 1287-1290.

142. (a) Leung, J. C.; Krische, M. J. *Chemical Science* **2012,** *3*, 2202-2209; (b) Stemmler, R. T.; Bolm, C. *Advanced Synthesis & Catalysis* **2007,** *349*, 1185-1198; (c) Tsuji, J.; Ohno, K. *Tetrahedron Letters* **1965,** *6*, 3969-3971.

143. Jun, C. H.; Hong, J. B.; Lee, D. Y. *Synlett* **1999**, 1-12.

144. Jun, C. H.; Jo, E. A.; Park, J. W. *European Journal of Organic Chemistry* **2007**, 1869-1881.

145. Lochow, C. F.; Miller, R. G. *Journal of the American Chemical Society* **1976,** *98*, 1281-1283.

146. Fairlie, D. P.; Bosnich, B. *Organometallics* **1988,** *7*, 936-945.

147. Osborne, J. D.; Randell-Sly, H. E.; Currie, G. S.; Cowley, A. R.; Willis, M. C. *Journal of the American Chemical Society* **2008,** *130*, 17232-17233.

148. Larock, R. C.; Oertle, K.; Potter, G. F. *Journal of the American Chemical Society* **1980,** *102*, 190-197.

149. Sato, Y.; Oonishi, Y.; Mori, M. *Angewandte Chemie International Edition* **2002,** *41*, 1218-1221.

150. Aloise, A. D.; Layton, M. E.; Shair, M. D. *Journal of the American Chemical Society* **2000,** *122*, 12610-12611.

151. (a) Tanaka, K.; Fu, G. C. *Journal of the American Chemical Society* **2002,** *124*, 10296-10297; (b) Phan, D. H. T.; Kim, B.; Dong, V. M. *Journal of the American Chemical Society* **2009,** *131*, 15608; (c) Shen, Z.; Khan, H. A.; Dong, V. M. *Journal of the*

American Chemical Society **2008,** *130*, 2916-2917; (d) Shen, Z.; Khan, H. A.; Dong, V. M. *Journal of the American Chemical Society* **2008,** *130*, 2916-2917.

152. Coulter, M. M.; Dornan, P. K.; Dong, V. M. *Journal of the American Chemical Society* **2009,** *131*, 6932.

153. Shen, Z.; Dornan, P. K.; Khan, H. A.; Woo, T. K.; Dong, V. M. *Journal of the American Chemical Society* **2009,** *131*, 1077-1091.

154. Bendorf, H. D.; Colella, C. M.; Dixon, E. C.; Marchetti, M.; Matukonis, A. N.; Musselman, J. D.; Tiley, T. A. *Tetrahedron Letters* **2002,** *43*, 7031-7034.

155. Bendorf, H. D.; Ruhl, K. E.; Shurer, A. J.; Shaffer, J. B.; Duffin, T. O.; LaBarte, T. L.; Maddock, M. L.; Wheeler, O. W. *Tetrahedron Letters* **2012,** *53*, 1275-1277.

156. Khan, H. A.; Kou, K. G. M.; Dong, V. M. *Chemical Science* **2011,** *2*.

157. Suggs, J. W. *Journal of the American Chemical Society* **1979,** *101*, 489-489.

158. Beletskiy, E. V.; Sudheer, C.; Douglas, C. J. *Journal of Organic Chemistry* **2012,** *77*, 5884-5893.

159. Fustero, S.; Bartolome, A.; Sanz-Cervera, J.; Sanchez-Rosello, M.; Soler, J. C.; Arellano, C. R.; Fuentes, A. S. *Organic Letters* **2003**, *5*, 2523.